frontiers | Research Topics

Patterns, functions, and processes of alpine grassland ecosystems under global change.

Edited by
Jian Sun, Gao-Lin Wu, Junran Jimmy Li, Shiliang Liu, Nigussie Haregeweyn and Huakun Zhou

Published in
Frontiers in Plant Science

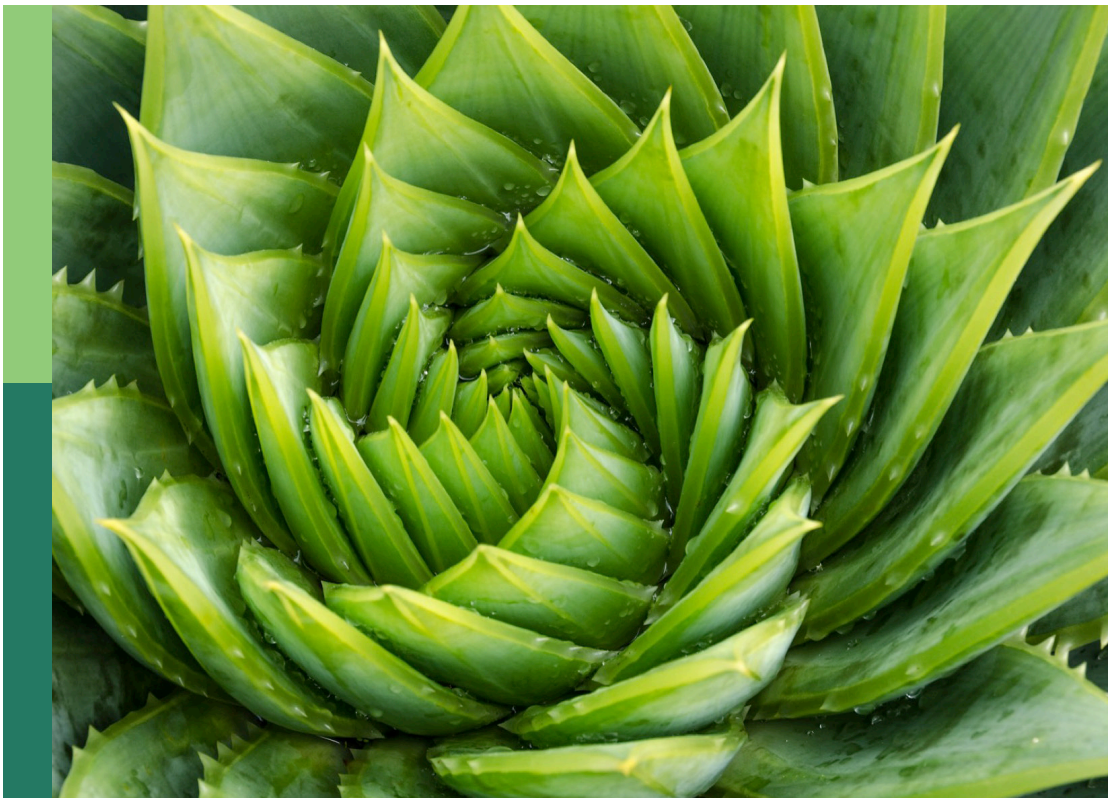

FRONTIERS EBOOK COPYRIGHT STATEMENT

The copyright in the text of individual articles in this ebook is the property of their respective authors or their respective institutions or funders. The copyright in graphics and images within each article may be subject to copyright of other parties. In both cases this is subject to a license granted to Frontiers.

The compilation of articles constituting this ebook is the property of Frontiers.

Each article within this ebook, and the ebook itself, are published under the most recent version of the Creative Commons CC-BY licence. The version current at the date of publication of this ebook is CC-BY 4.0. If the CC-BY licence is updated, the licence granted by Frontiers is automatically updated to the new version.

When exercising any right under the CC-BY licence, Frontiers must be attributed as the original publisher of the article or ebook, as applicable.

Authors have the responsibility of ensuring that any graphics or other materials which are the property of others may be included in the CC-BY licence, but this should be checked before relying on the CC-BY licence to reproduce those materials. Any copyright notices relating to those materials must be complied with.

Copyright and source acknowledgement notices may not be removed and must be displayed in any copy, derivative work or partial copy which includes the elements in question.

All copyright, and all rights therein, are protected by national and international copyright laws. The above represents a summary only. For further information please read Frontiers' Conditions for Website Use and Copyright Statement, and the applicable CC-BY licence.

ISSN 1664-8714
ISBN 978-2-8325-3057-3
DOI 10.3389/978-2-8325-3057-3

About Frontiers

Frontiers is more than just an open access publisher of scholarly articles: it is a pioneering approach to the world of academia, radically improving the way scholarly research is managed. The grand vision of Frontiers is a world where all people have an equal opportunity to seek, share and generate knowledge. Frontiers provides immediate and permanent online open access to all its publications, but this alone is not enough to realize our grand goals.

Frontiers journal series

The Frontiers journal series is a multi-tier and interdisciplinary set of open-access, online journals, promising a paradigm shift from the current review, selection and dissemination processes in academic publishing. All Frontiers journals are driven by researchers for researchers; therefore, they constitute a service to the scholarly community. At the same time, the *Frontiers journal series* operates on a revolutionary invention, the tiered publishing system, initially addressing specific communities of scholars, and gradually climbing up to broader public understanding, thus serving the interests of the lay society, too.

Dedication to quality

Each Frontiers article is a landmark of the highest quality, thanks to genuinely collaborative interactions between authors and review editors, who include some of the world's best academicians. Research must be certified by peers before entering a stream of knowledge that may eventually reach the public - and shape society; therefore, Frontiers only applies the most rigorous and unbiased reviews. Frontiers revolutionizes research publishing by freely delivering the most outstanding research, evaluated with no bias from both the academic and social point of view. By applying the most advanced information technologies, Frontiers is catapulting scholarly publishing into a new generation.

What are Frontiers Research Topics?

Frontiers Research Topics are very popular trademarks of the *Frontiers journals series*: they are collections of at least ten articles, all centered on a particular subject. With their unique mix of varied contributions from Original Research to Review Articles, Frontiers Research Topics unify the most influential researchers, the latest key findings and historical advances in a hot research area.

Find out more on how to host your own Frontiers Research Topic or contribute to one as an author by contacting the Frontiers editorial office: frontiersin.org/about/contact

Patterns, functions, and processes of alpine grassland ecosystems under global change.

Topic editors

Jian Sun — Institute of Tibetan Plateau Research, Chinese Academy of Sciences (CAS), China

Gao-Lin Wu — Northwest A&F University, China

Junran Jimmy Li — University of Tulsa, United States

Shiliang Liu — Beijing Normal University, China

Nigussie Haregeweyn — Tottori University, Japan

Huakun Zhou — Key Laboratory of Restoration Ecology in Cold Regions, Northwest Institute of Plateau Biology, Chinese Academy of Sciences (CAS), China

Citation

Sun, J., Wu, G.-L., Li, J. J., Liu, S., Haregeweyn, N., Zhou, H., eds. (2023). *Patterns, functions, and processes of alpine grassland ecosystems under global change*. Lausanne: Frontiers Media SA. doi: 10.3389/978-2-8325-3057-3

Table of contents

07 Editorial: Patterns, functions, and processes of alpine grassland ecosystems under global change
Jian Sun, Yingxin Wang, Shiliang Liu, Junran Li, Huakun Zhou, Gaolin Wu and Nigussie Haregeweyn

12 Plant and Soil Enzyme Activities Regulate CO_2 Efflux in Alpine Peatlands After 5 Years of Simulated Extreme Drought
Zhongqing Yan, Enze Kang, Kerou Zhang, Yong Li, Yanbin Hao, Haidong Wu, Meng Li, Xiaodong Zhang, Jinzhi Wang, Liang Yan and Xiaoming Kang

27 Plants and Microbes Mediate the Shift in Ecosystem Multifunctionality From Low to High Patterns Across Alpine Grasslands on the Tibetan Plateau
Yi Wang, Miao Liu, Youchao Chen, Tao Zeng, Xuyang Lu, Bin Yang, Yafeng Wang, Lin Zhang, Xiaowei Nie, Feipeng Xiao, Zhigang Zhang and Jian Sun

38 Effects of Plateau Pika Disturbance on the Spatial Heterogeneity of Vegetation in Alpine Meadows
Jie Li, Hao Hao Qi, Yuan Yuan Duan and Zheng Gang Guo

46 Applying Bayesian Belief Networks to Assess Alpine Grassland Degradation Risks: A Case Study in Northwest Sichuan, China
Shuang Zhou and Li Peng

62 The Mixed Addition of Biochar and Nitrogen Improves Soil Properties and Microbial Structure of Moderate–Severe Degraded Alpine Grassland in Qinghai-Tibet Plateau
Jinsheng Li, Yinquan Zhao, Xinqing Shao, Ding Huang, Jianying Shang, Hui Li, Yixuan He and Kesi Liu

77 Litter-Induced Reduction in Ecosystem Multifunctionality Is Mediated by Plant Diversity and Cover in an Alpine Meadow
Zhouwen Ma, Jing Wu, Lan Li, Qingping Zhou and Fujiang Hou

87 Distinguishing Stoichiometric Homeostasis of Soil Microbial Biomass in Alpine Grassland Ecosystems: Evidence From 5,000 km Belt Transect Across Qinghai–Tibet Plateau
Jihui Fan, Tianyuan Liu, Ying Liao, Yiying Li, Yan Yan and Xuyang Lu

99 Distinct Responses of Leaf Traits to Environment and Phylogeny Between Herbaceous and Woody Angiosperm Species in China
Nannan An, Nan Lu, Bojie Fu, Mengyu Wang and Nianpeng He

113 Effect of Nutrient Addition on the Productivity and Species Richness of Grassland Along With an Elevational Gradient in Tajikistan
Lian-Lian Fan, Okhonniyozov Mekrovar, Yao-Ming Li, Kai-Hui Li, Xue-Xi Ma and Jie-Fei Mao

122 Effects of Different Grazing Disturbances on the Plant Diversity and Ecological Functions of Alpine Grassland Ecosystem on the Qinghai-Tibetan Plateau
Wenlong Li, Chenli Liu, Wenying Wang, Huakun Zhou, Yating Xue, Jing Xu, Pengfei Xue and Hepiao Yan

135 Restoration of Degraded Grassland Significantly Improves Water Storage in Alpine Grasslands in the Qinghai-Tibet Plateau
Xiaowei Guo, Huakun Zhou, Licong Dai, Jing Li, Fawei Zhang, Yikang Li, Li Lin, Qian Li, Dawen Qian, Bo Fan, Yuting Lan, Mengke Si, Bencuo Li, Guangmin Cao, Yangong Du and Bin Wang

144 Phylogenetic Correlation and Symbiotic Network Explain the Interdependence Between Plants and Arbuscular Mycorrhizal Fungi in a Tibetan Alpine Meadow
Qiang Dong, Xin Guo, Keyu Chen, Shijie Ren, Muhammad Atif Muneer, Jing Zhang, Yaoming Li and Baoming Ji

155 Differential Responses of Plant Primary Productivity to Nutrient Addition in Natural and Restored Alpine Grasslands in the Qinghai Lake Basin
Chunli Li, Yonghui Li, Xinwei Li, Li Ma, Yuanming Xiao and Chunhui Zhang

168 The Change in Environmental Variables Linked to Climate Change Has a Stronger Effect on Aboveground Net Primary Productivity Than Does Phenological Change in Alpine Grasslands
Jiangwei Wang, Meng Li, Chengqun Yu and Gang Fu

178 Environmental Controls on Multi-Scale Dynamics of Net Carbon Dioxide Exchange From an Alpine Peatland on the Eastern Qinghai-Tibet Plateau
Hu Yao, Haijun Peng, Bing Hong, Qian Guo, Hanwei Ding, Yetang Hong, Yongxuan Zhu, Cheng Cai and Jinshu Chi

194 Spatiotemporal Dynamics of the Carbon Budget and the Response to Grazing in Qinghai Grasslands
Xiaotao Huang, Chunbo Chen, Buqing Yao, Zhen Ma and Huakun Zhou

205 A Meta-Analysis on Degraded Alpine Grassland Mediated by Climate Factors: Enlightenment for Ecological Restoration
Jiale Yu, Lingfan Wan, Guohua Liu, Keming Ma, Hao Cheng, Yu Shen, Yuqing Liu and Xukun Su

215 Assessing the Impact of Climate Change on Potential Distribution of *Meconopsis punicea* and Its Influence on Ecosystem Services Supply in the Southeastern Margin of Qinghai-Tibet Plateau
Ning Shi, Niyati Naudiyal, Jinniu Wang, Narayan Prasad Gaire, Yan Wu, Yanqiang Wei, Jiali He and Chunya Wang

232 Comparative Microbial Nitrogen Functional Gene Abundances in the Topsoil vs. Subsoil of Three Grassland Habitats in Northern China
Yuqing Liu, Qiaodong Chi, Hui Cheng, Huanxin Ding, Teng Wen, Jun Zhao, Xiaojuan Feng, Jinbo Zhang, Zucong Cai and Guohua Liu

245 Feedback and Trigger of Household Decision-Making to Ecological Protection Policies in Sanjiangyuan National Park
Xukun Su, Yu Shen, Shikui Dong, Yuqing Liu, Hao Cheng, Lingfan Wan and Guohua Liu

257 Dynamic Disturbance Analysis of Grasslands Using Neural Networks and Spatiotemporal Indices Fusion on the Qinghai-Tibet Plateau
Fengli Zou, Qingwu Hu, Haidong Li, Jie Lin, Yichuan Liu and Fulin Sun

273 Community Composition and Structure Affect Ecosystem and Canopy Water Use Efficiency Across Three Typical Alpine Ecosystems
Yuzhe Li, Xinyuan Zhang, Quanqin Shao, Jiangwen Fan, Zhi Chen, Jinwei Dong, Zhongmin Hu and Yue Zhan

287 The Complex Biodiversity-Ecosystem Function Relationships for the Qinghai-Tibetan Grassland Community
Wei Qi, Xiaomei Kang, Johannes M. H. Knops, Jiachang Jiang, A. Abuman and Guozhen Du

299 Specific Rhizobacteria Responsible in the Rhizosheath System of *Kengyilia hirsuta*
Youjun Chen, Chen Chen, Qingping Zhou, Jian Hu, Yingxia Lei and Wenhui Liu

309 Land Degradation Changes the Role of Above- and Belowground Competition in Regulating Plant Biomass Allocation in an Alpine Meadow
Yong Zhang, Qiuzhu Zheng, Xiaoxia Gao, Yandan Ma, Kemin Liang, Haitao Yue, Xiaoxia Huang, Kaiting Wu and Xiaorong Wang

319 Effects of Soil Physico-Chemical Properties on Plant Species Diversity Along an Elevation Gradient Over Alpine Grassland on the Qinghai-Tibetan Plateau, China
Wangya Han, Li Chen, Xukun Su, Dan Liu, Tiantian Jin, Songlin Shi, Tao Li and Guohua Liu

332 Synchronous Responses of Plant Functional Traits to Nitrogen Deposition From Dominant Species to Functional Groups and Whole Communities in Alpine Grasslands on the Qinghai-Tibetan Plateau
Shuai Li, Zhenzhen Zhao, Shikui Dong, Hao Shen, Yudan Xu, Jiannan Xiao, Xiaoxia Gao, Shengnan Wu and Paul Stufkens

342 Precipitation Alters the Effects of Temperature on the Ecosystem Multifunctionality in Alpine Meadows
Yunhe Ma, Lihua Tian, Guangpeng Qu, Ruicheng Li, Weiwei Wang and Jingxue Zhao

351 Leaf Stoichiometry of *Potentilla fruticosa* Across Elevations in China's Qilian Mountains
Yanyan Qin, Wei Liu, Xiaofang Zhang, Jan F. Adamowski and Asim Biswas

361 Differentiate Responses of Soil Microbial Community and Enzyme Activities to Nitrogen and Phosphorus Addition Rates in an Alpine Meadow
Hongbiao Zi, Lei Hu and Changting Wang

376 Ecosystem Coupling and Ecosystem Multifunctionality May Evaluate the Plant Succession Induced by Grazing in Alpine Meadow
Yingxin Wang, Zhe Wu, Zhaofeng Wang, Shenghua Chang, Yongqiang Qian, Jianmin Chu, Zhiqing Jia, Qingping Zhou and Fujiang Hou

389 Experimental Warming Has Not Affected the Changes in Soil Organic Carbon During the Growing Season in an Alpine Meadow Ecosystem on the Qinghai–Tibet Plateau
Yue Yang, Guoxi Shi, Yongjun Liu, Li Ma, Zhonghua Zhang, Shengjing Jiang, Jianbin Pan, Qi Zhang, Buqing Yao, Huakun Zhou and Huyuan Feng

403 The Plant Interspecific Association in the Revegetated Alpine Grasslands Determines the Productivity Stability of Plant Community Across Restoration Time on Qinghai–Tibetan Plateau
Shengnan Wu, Lu Wen, Shikui Dong, Xiaoxia Gao, Yudan Xu, Shuai Li, Quanming Dong and Kelly Wessell

412 Phosphorus Shapes Soil Microbial Community Composition and Network Properties During Grassland Expansion Into Shrubs in Tibetan Dry Valleys
Hanchang Zhou, Anzhou Ma, Xiaorong Zhou, Xianke Chen, Jiejie Zhang, Qinwei Zhang, Xiangning Qi, Guohua Liu and Guoqiang Zhuang

423 Context-Dependency in Relationships Between Herbaceous Plant Leaf Traits and Abiotic Factors
Zhenchao Zhang, Jian Sun, Miao Liu, Hua Shang, Jinniu Wang, Jinsong Wang, Huakun Zhou, Yong Li, Yi Wang and Wanjie Chen

436 Soil Moisture Variations in Response to Precipitation Across Different Vegetation Types on the Northeastern Qinghai-Tibet Plateau
Licong Dai, Ruiyu Fu, Xiaowei Guo, Yangong Du, Fawei Zhang and Guangmin Cao

447 Alpine Treeline Dynamics and the Special Exposure Effect in the Hengduan Mountains
Fuyan Zou, Chengyi Tu, Dongmei Liu, Chaoying Yang, Wenli Wang and Zhiming Zhang

frontiers | Frontiers in Plant Science

TYPE Editorial
PUBLISHED 12 October 2022
DOI 10.3389/fpls.2022.1048031

Check for updates

OPEN ACCESS

EDITED BY
Hannah Schneider,
Wageningen University and Research, Netherlands

REVIEWED BY
Wenbo Luo,
Northeast Normal University, China
Zhenchao Zhang,
Qingdao Agricultural University, China

*CORRESPONDENCE
Jian Sun
sunjian@itpcas.ac.cn

SPECIALTY SECTION
This article was submitted to Functional Plant Ecology, a section of the journal Frontiers in Plant Science

RECEIVED 19 September 2022
ACCEPTED 27 September 2022
PUBLISHED 12 October 2022

CITATION
Sun J, Wang Y, Liu S, Li J, Zhou H, Wu G and Haregeweyn N (2022) Editorial: Patterns, functions, and processes of alpine grassland ecosystems under global change. *Front. Plant Sci.* 13:1048031. doi: 10.3389/fpls.2022.1048031

COPYRIGHT
© 2022 Sun, Wang, Liu, Li, Zhou, Wu and Haregeweyn. This is an open-access article distributed under the terms of the Creative Commons Attribution License (CC BY). The use, distribution or reproduction in other forums is permitted, provided the original author(s) and the copyright owner(s) are credited and that the original publication in this journal is cited, in accordance with accepted academic practice. No use, distribution or reproduction is permitted which does not comply with these terms.

Editorial: Patterns, functions, and processes of alpine grassland ecosystems under global change

Jian Sun[1]*, Yingxin Wang[1], Shiliang Liu[2], Junran Li[3], Huakun Zhou[4], Gaolin Wu[5] and Nigussie Haregeweyn[6]

[1]State Key Laboratory of Earth System Resources and Environment of Tibetan Plateau, Institute of Tibetan Plateau Research, Chinese Academy of Sciences, Beijing, China, [2]State Key Laboratory of Water Environment Simulation, School of Environment, Beijing Normal University, Beijing, China, [3]Department of Geography, The University of Hong Kong, Hong Kong, Hong Kong SAR, China, [4]Key Laboratory of Restoration Ecology for Cold Regions in Qinghai, Northwest Institute of Plateau Biology, Chinese Academy of Sciences, Xining, China, [5]State Key Laboratory of Soil Erosion and Dryland Farming on the Loess Plateau, Institute of Soil and Water Conservation, Northwest A&F University, Yangling, China, [6]International Platform for Dryland Research and Education, Arid Land Research Center, Tottori University, Tottori, Japan

KEYWORDS

patterns, functions, processes, alpine grassland, global change

Editorial on the Research Topic:
Patterns, functions, and processes of alpine grassland ecosystems under global change

Alpine grassland on the Tibetan Plateau (TP) accounts for about 62% of the total area of the TP (Wang et al., 2022). These grassland ecosystems provide important ecological services and functions in pastoral production, biodiversity conservation, carbon storage, water resource regulation, cultural inheritance, tourism, and recreation etc. (Miehe et al., 2019; Sun et al., 2020; Wang et al., 2022). In the past serval decades, the alpine grassland on the TP has experienced rapid climate change and intensified human activities (He et al., 2021), the regulatory mechanisms and drivers are remained controversial.

Climate changes have been evident across the TP since the beginning of the 1970s (Yang et al., 2014). For instance, the mean annual air temperature has increased by about 0.4°C, which is twice that of the global average, however, a decrease in precipitation has been found in many other regions (Mountain Research Initiative EDW Working Group, 2015). Also, the degradation of permafrost has been accelerated as manifested by ground surface subsidence and thaw settlement of permafrost soils (Mu et al., 2020), and the total number of lakes increased from 868 in 1990 to 1207 in 2015, leading to the increase of total water surface area of the lakes at a rate of 383.5 km2 yr-1 (Sun et al., 2018). With the steady increase of human population and domestic livestock number (Wei et al., 2020), overgrazing has become a serious challenge with overstocking rates of 27–89% in the

alpine grassland (Wang et al., 2022). Currently, there are approximately 20 million yak and 50 million Tibetan sheep grazing in the alpine grassland, making it one of the regions with high grazing pressure worldwide (Wang et al., 2020). The interactions of soil, plant, animal, and grazing management affect the production and stability of grassland ecosystems, and also provide the driving force for the functions and services of the alpine grassland on the TP (Hodgkinson and Wang, 2020; Sun et al., 2022). For example, grazing exclusion has been widely adopted by the local and central government, predominantly through the use of fences, to restore the degraded alpine grasslands since 2003 (Sun et al., 2021). The total area of fences had increased up to 3.32 million hectares on the northern Tibetan Plateau (Sun et al., 2020).

In the past 20 years, numerous efforts have been done to explore the patterns, functions, and processes of alpine grassland ecosystems, including transect surveys, field observations, model simulation, comprehensive meta-analyses, and literature reviews. These studies have following characteristics: (i) with the improvement of testing methods, a diversity of technologies have been applied at the technical level such as remote sensing, model simulation, large-scale transect sampling survey, aerial filming, and long-term observation. Scales of these studies range from regional, landscape, ecosystem, and community to micro-molecular and genomic levels; (ii) the observation indexes have evolved from basic to comprehensive, which includes moisture, soil, biology, watershed, and climate; (iii) various factors such as the environmental, natural, human activities, and the impact of the whole habitat on alpine ecosystems were taken into account, and (iv) studies have evolved from trophic levels, food webs, and independent processes of ground and underground to the integration of above and below ground processes of the whole ecosystem. Despite remarkable knowledge gains, there are still some areas that require in-depth research, such as the driving mechanism of the impact of global change alpine ecosystems with new technologies and theories.

To advance our understandings of the patterns, functions, processes, and mechanisms of alpine grassland ecosystems responding to changing environments (e.g., dynamics of temperature and precipitation, nitrogen deposition and extreme weather events, grazing, fencing and ecological projects, etc.)., we organized a Special Issue (SI) entitled "Patterns, Functions, and Processes of Alpine Grassland Ecosystems under Global Change". This SI comprises 49 articles, sharing new ideas, techniques, and findings about this subject from field experiments, large-scale transect surveys, alongside remote sensing (Wang et al., 2022a; Zhang et al., 2022; Zou et al., 2022). These studies shed light on the future development of adaptive management practices for alpine grassland ecosystems under future environmental change.

The spatial-temporal patterns and drivers of alpine grassland ecosystem under the changing environment are the top priority for the grassland conservation. Due to the scale of the TP, remote sensing is critical for studies on the spatial and temporal heterogeneity of the grassland. Four papers in this SI discuss the spatial-temporal patterns and drivers of alpine grassland ecosystem under the changing environment based on patch, landscape or pixel based remote sensing observations. Zou et al. (2022) used neural networks and spatiotemporal indices fusion method to analyze the dynamic disturbance analysis of grasslands on the TP. Fan et al. (2021) carried out a 5,000 km belt transect investigation to distinguish stoichiometric homeostasis of soil microbial biomass in alpine grassland ecosystems. Huang et al. (2022) estimated the net ecosystem exchange (NEE) using the improved Biome-BGCMuSo model to characterize the spatiotemporal dynamics of the carbon budget. Shi et al. (2022) evaluated the effects of climate change on the distribution of Meconopsis punicea and ecosystem services supply.

Seven papers in this SI assess the variations of alpine ecosystem functions, and the response and feedback of ecological processes using long-term simulated experiments and large-scale transect surveys. Some of the studies used the entire TP as the study area and evaluated the complex biodiversity-ecosystem function relationships (Zhang et al., 2022; Qi et al., 2022), the effects of soil physico-chemical properties on plant species diversity (Han et al., 2022), the mechanism of plant communities on different EMF patterns (Wang et al., 2021), and on the canopy water use efficiency (Li et al., 2022b). Other studies investigated the impacts of human activities on ecosystems, especially alpine grasslands and meadows, with regard to overgrazing, rodent destroy, and grassland degradation. For example, Wang et al. (2022a)> indicated that climate change or the phenological change has stronger effects on ANPP. Li et al. (2021a) demonstrated that small semi-fossorial herbivores have an important impact on the spatial heterogeneity of vegetation.

Climate change and human activities dominate the recent changes in grassland patterns and processes on the TP, thus affecting the ecosystem functions and services. Many of the articles in this SI reveal the driving mechanism of the impact of climate change and human activities (Dai et al., 2022; Hua et al. (2022); Ma et al., 2022; Zuo et al., 2022) on alpine ecosystems with field observations and manipulative experiments combined with new experimental technologies (Chen et al., 2022; Qin et al., 2022; Zou et al., 2022). Experimental warming enhanced the pattern of the plant allometric growth and promoted migration of the soil stoichiometric characteristics to deep layers in Beiluhe (Xu et al., 2022). However, in Haibei, Yang et al. (2022) indicated that the warming treatment has not affected the changes in soil organic carbon. In addition, extreme drought can affect Re and Rs by altering plant and soil extracellular enzyme activities in alpine wetland (Yan et al., 2021). In alpine meadow, N and P addition significantly affect t plant communities (Ma et al.,

2021), soil microbial community and enzyme activities (Zi et al., 2022), and microbial functional genes (Xiao et al., 2022). In alpine steppe, N and P application led to an increase in aboveground biomass (Li et al., 2021b), and increased intensity of bacteria and fungi (Li et al., 2021c), also affected the plant functional traits (Li et al., 2022d). Meanwhile, grazing increased herbage respiration in summer, presumably through stimulation of gross photosynthesis (Yuan et al., 2022), and changed plant community composition and reduced stochasticity of soil microbial community assembly of alpine grasslands (Li et al., 2022a). Restoration of degraded grassland significantly improves shoot and root biomass (Zhang et al., 2022), plant interspecific associations (Wu et al., 2022), soil enzymatic activities (Wang et al., 2022b), and water storage (Guo et al., 2021).

Seven papers in this SI explored the mechanisms of alpine ecosystem dynamics using new analytical methods, e.g., artificial intelligence learning, network analysis (Zhou et al., 2022), Bayes analysis and other data mining methods (Zhou and Peng (2021). Dong et al. (2021) used phylogenetic correlation and symbiotic network to explain the interdependence between plants and arbuscular mycorrhizal fungi in alpine meadow. Also, the degradation of alpine meadows mediated by climatic factors and effects of different grazing regimes on the plant diversity, plant community traits and ecological functions were analyzed by using meta-analysis (Li et al., 2021d; Yu et al., 2022; Zhan et al., 2022). Wang et al. (2022c) highlighted that ecosystem coupling and ecosystem multifunctionality may be used to evaluate the plant succession induced by grazing.

It is well known that human activities and their feedbacks affect regional sustainable development, but relevant policy measures have rarely be evaluated at the household level. Hua et al. (2022) explored the views on grassland restoration programs on the Qinghai-Tibet Plateau. Also, feedback and trigger of household decision-making to ecological protection policies in Sanjiangyuan National Park were studied (Su et al., 2022).

Although some findings on the ecological system of TP may still be somewhat preliminary, all studies included in this SI have undoubtedly promoted our understanding of the patterns, functions, and processes of alpine grassland ecosystems in the context of global change. Some important questions remain unanswered, though. Further explorations need to focus on the following two aspects: (i) more long-term localized observations and manipulative experiments should be employed to reveal long-term change of coupling of plant-soil-livestock-human system and its driving mechanisms. Two TP-wide programs, namely, the Alpine Fence Observation Net (AFON) and the Alpine Climate Change Observation Net (ACON) were established in 2020 and 2022, respectively (Figure 1). The AFON contains 53 fenced observation sites in alpine meadow, alpine steppe and alpine desert steppe across the TP. Likewise, the ACON contains 23 study sites with the unified climate change experiment, such as warming (Open-top-chamber), N addition, removing the light and removing the plant functional group. (ii) special attentions must be drawn upon the ecological network of multiple trophic levels of alpine grassland and their responses to global change. There is a lack of empirical evidence in this respect. Encouragingly, with the advancement of science and technology, such as network analysis tools, access to internet in remote areas, molecular technologies (e.g., meta-genomics,

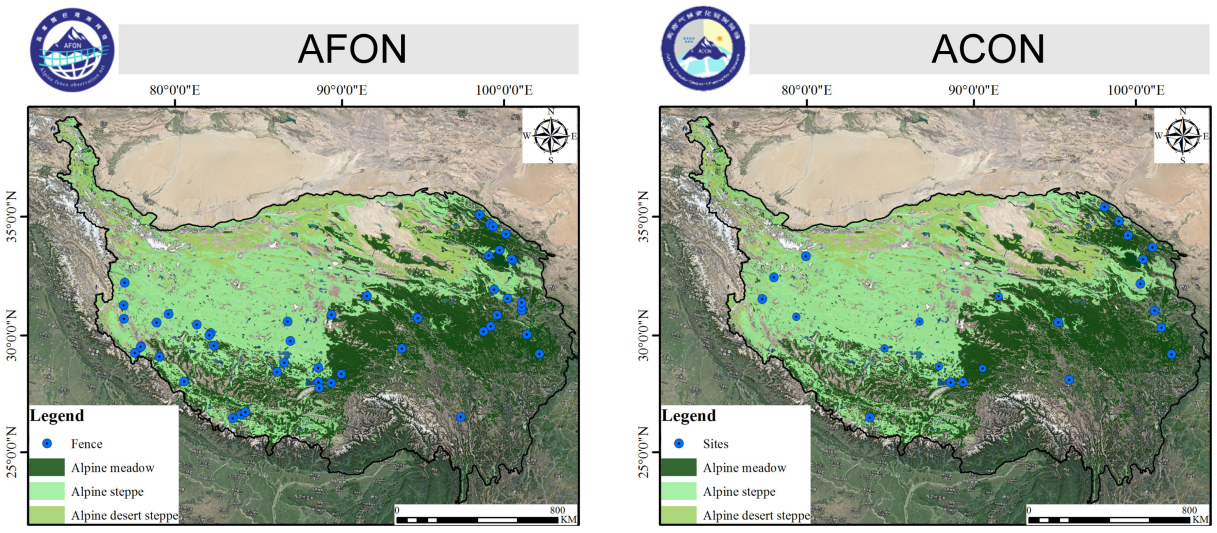

FIGURE 1
Locations of the Alpine Fence Observation Net (AFON) and the Alpine Climate Change Observation Net (ACON) on the TP. Both AFON and ACON are constructed by Prof. Sun' team at the Institute of Tibetan Plateau Research, Chinese Academy of Sciences.

and - metabolomics), the study of aboveground-belowground interactions of ecosystems is expected to make great progress in the near future.

Author contributions

JS, YW, SL, and JL drafted the story line of the editorial. SL, HZ, GW and NH refined the story line and contributed references and insights to the impact of the papers included in this editorial. All authors contributed to the article and approved the submitted version.

Funding

This work was supported by the National Natural Science Foundation of China (No. 41871040), the National Natural Science Foundation of China Joint Fund Project (U21A20186), the Joint Research Project of Three-River-Resource National Park Funded by the Chinese Academy of Sciences and Qinghai Provincial People's Government (LHZX-2020-08), Qinghai Natural Science Fund Innovation Team Project (2021-ZJ-902).

Acknowledgments

We thank all the authors who submitted their work to this Research Topics, the professional editorial staff at Frontiers in Plant Science for their support in creating this Research Topic, and the invaluable help of reviewers in manuscript evaluation.

Conflict of interest

The authors declare that the research was conducted in the absence of any commercial or financial relationships that could be construed as a potential conflict of interest.

Publisher's note

All claims expressed in this article are solely those of the authors and do not necessarily represent those of their affiliated organizations, or those of the publisher, the editors and the reviewers. Any product that may be evaluated in this article, or claim that may be made by its manufacturer, is not guaranteed or endorsed by the publisher.

References

Chen, Y., Chen, C., Zhou, Q., Hu, J., Lei, Y., and Liu, W. (2022). Specific rhizobacteria responsible in the rhizosheath system of kengyilia hirsuta. *Front. Plant Sci.* 12. doi: 10.3389/fpls.2021.785971

Dai, L., Fu, R., Guo, X., Du, Y., Zhang, F., and Cao, G. (2022). Soil moisture variations in response to precipitation across different vegetation types on the northeastern qinghai-Tibet plateau. *Front. Plant Sci.* 13. doi: 10.3389/fpls.2022.854152

Dong, Q., Guo, X., Chen, K., Ren, S., Muneer, M. A., Zhang, J., et al. (2021). Phylogenetic correlation and symbiotic network explain the interdependence between plants and arbuscular mycorrhizal fungi in a Tibetan alpine meadow. *Front. Plant Sci.* 12. doi: 10.3389/fpls.2021.804861

Fan, J., Liu, T., Liao, Y., Li, Y., Yan, Y., and Lu, X. (2021). Distinguishing stoichiometric homeostasis of soil microbial biomass in alpine grassland ecosystems: Evidence from 5,000 km belt transect across qinghai–Tibet plateau. *Front. Plant Sci.* 12. doi: 10.3389/fpls.2021.781695

Guo, X., Zhou, H., Dai, L., Li, J., Zhang, F., Li, Y., et al. (2021). Restoration of degraded grassland significantly improves water storage in alpine grasslands in the qinghai-Tibet plateau. *Front. Plant Sci.* 12. doi: 10.3389/fpls.2021.778656

Han, W., Chen, L., Su, X., Liu, D., Jin, T., Shi, S., et al. (2022). Effects of soil physico-chemical properties on plant species diversity along an elevation gradient over alpine grassland on the qinghai-Tibetan plateau, China. *Front. Plant Sci.* 13. doi: 10.3389/fpls.2022.822268

He, J. S., Dong, S., Shang, Z., Sundqvist, M. K., Wu, G., and Yang, Y. (2021). Above-belowground interactions in alpine ecosystems on the roof of the world. *Plant Soil.* 458 (1), 1–6. doi: 10.1007/s11104-020-04761-4

Hodgkinson, K. C., and Wang, D. L. (2020). Preventing rangeland degradation: a shared problem for Australia and China. *Rangeland. J.* 42 (5), 323–328. doi: 10.1071/RJ20068

Huang, X., Chen, C., Yao, B., Ma, Z., and Zhou, H. (2022). Spatiotemporal dynamics of the carbon budget and the response to grazing in qinghai grasslands. *Front. Plant Sci.* 12. doi: 10.3389/fpls.2021.775015

Hua, T., Zhao, W., and Pereira, P. (2022). Opinionated views on grassland restoration programs on the qinghai-Tibetan plateau. *Front. Plant Sci.* 13. doi: 10.3389/fpls.2022.861200

Li, Y., Dong, S., Gao, Q., Fan, C., Fayiah, M., Ganjurjav, H., et al. (2022a). Grazing changed plant community composition and reduced stochasticity of soil microbial community assembly of alpine grasslands on the qinghai-Tibetan plateau. *Front. Plant Sci.* 13. doi: 10.3389/fpls.2022.864085

Li, C., Li, Y., Li, X., Ma, L., Xiao, Y., and Zhang, C. (2021a). Differential responses of plant primary productivity to nutrient addition in natural and restored alpine grasslands in the qinghai lake basin. *Front. Plant Sci.* 12. doi: 10.3389/fpls.2021.792123

Li, W., Liu, C., Wang, W., Zhou, H., Xue, Y., Xu, J., et al. (2021b). Effects of different grazing disturbances on the plant diversity and ecological functions of alpine grassland ecosystem on the qinghai-Tibetan plateau. *Front. Plant Sci.* 12. doi: 10.3389/fpls.2021.765070

Li, J., Qi, H. H., Duan, Y. Y., and Guo, Z. G. (2021c). Effects of plateau pika disturbance on the spatial heterogeneity of vegetation in alpine meadows. *Front. Plant Sci.* 12. doi: 10.3389/fpls.2021.771058

Li, Y., Zhang, X., Shao, Q., Fan, J., Chen, Z., Dong, J., et al. (2022b). Community composition and structure affect ecosystem and canopy water use efficiency across three typical alpine ecosystems. *Front. Plant Sci.* 12. doi: 10.3389/fpls.2021.771424

Li, S., Zhao, Z., Dong, S., Shen, H., Xu, Y., Xiao, J., et al. (2022d). Synchronous responses of plant functional traits to nitrogen deposition from dominant species to functional groups and whole communities in alpine grasslands on the qinghai-Tibetan plateau. *Front. Plant Sci.* 13. doi: 10.3389/fpls.2022.827035

Li, J., Zhao, Y., Shao, X., Huang, D., Shang, J., Li, H., et al. (2021d). The mixed addition of biochar and nitrogen improves soil properties and microbial structure of moderate–severe degraded alpine grassland in qinghai-Tibet plateau. *Front. Plant Sci.* 12. doi: 10.3389/fpls.2021.765041

Liu, S., Sun, Y., Shi, F., Liu, Y., Wang, F., Dong, S., et al. (2022). Composition and diversity of soil microbial community associated with land use types in the agro–pastoral area in the upper yellow river basin. *Front. Plant Sci.* 13. doi: 10.3389/fpls.2022.819661

Ma, Y., Tian, L., Qu, G., Li, R., Wang, W., and Zhao, J. (2022). Precipitation alters the effects of temperature on the ecosystem multifunctionality in alpine meadows. *Front. Plant Sci.* 12. doi: 10.3389/fpls.2021.824296

Ma, Z., Wu, J., Li, L., Zhou, Q., and Hou, F. (2021). Litter-induced reduction in ecosystem multifunctionality is mediated by plant diversity and cover in an alpine meadow. *Front. Plant Sci.* 12. doi: 10.3389/fpls.2021.773804

Miehe, G., Schleuss, P. M., Seeber, E., Babel, W., Biermann, T., Braendle, M., et al. (2019). The kobresia pygmaea ecosystem of the Tibetan highlands–origin, functioning and degradation of the world's largest pastoral alpine ecosystem: Kobresia pastures of Tibet. *Sci. Total. Environ.* 648, 754–771. doi: 10.1016/j.scitotenv.2018.08.164

Mountain Research Initiative EDW Working Group (2015). Elevation-dependent warming in mountain regions of the world. *Nat. Clim. Change.* 5, 424–430. doi: 10.1038/nclimate2563

Mu, C., Abbott, B. W., Norris, A. J., Mu, M., Fan, C., Chen, X., et al. (2020). The status and stability of permafrost carbon on the Tibetan plateau. *Earth-Sci Rev.* 211, 103433. doi: 10.1016/j.earscirev.2020.103433

Qi, W., Kang, X., Knops, J. M. H., Jiang, J., Abuman, A., and Du, G. (2022). The complex biodiversity-ecosystem function relationships for the qinghai-Tibetan grassland community. *Front. Plant Sci.* 12. doi: 10.3389/fpls.2021.772503

Qin, Y., Liu, W., Zhang, X., Adamowski, J. F., and Biswas, A. (2022). Leaf stoichiometry of potentilla fruticosa across elevations in china's qilian mountains. *Front. Plant Sci.* 13. doi: 10.3389/fpls.2022.814059

Shi, N., Naudiyal, N., Wang, J., Gaire, N. P., Wu, Y., Wei, Y., et al. (2022). Assessing the impact of climate change on potential distribution of meconopsis punicea and its influence on ecosystem services supply in the southeastern margin of qinghai-Tibet plateau. *Front. Plant Sci.* 12. doi: 10.3389/fpls.2021.830119

Sun, J., Fu, B., Zhao, W., Liu, S., Liu, G., Zhou, H., et al. (2021). Optimizing grazing exclusion practices to achieve goal 15 of the sustainable development goals in the Tibetan plateau. *Sci. Bull.* 66, 1493–1496. doi: 10.75.249.4/handle/363003/60741

Sun, J., Liu, M., Fu, B., Kemp, D., Zhao, W., Liu, G., et al. (2020). Reconsidering the efficiency of grazing exclusion using fences on the Tibetan plateau. *Sci. Bull.* 65 (16), 1405–1414. doi: 10.1016/j.scib.2020.04.035

Sun, J., Wang, Y., Piao, S. L., Liu, M., Han, G. D., Li, J. R., et al. (2022). Toward a sustainable grassland ecosystem worldwide. *The Innovation*. 3(4), 100265. doi: 10.1016/j.xinn.2022.100265

Sun, J., Zhou, T. C., Liu, M., Chen, Y. C., Shang, H., Zhu, L. P., et al. (2018). Linkages of the dynamics of glaciers and lakes with the climate elements over the Tibetan Plateau. *Earth-Sci. Rev.* 185, 308–324. doi: 10.1016/j.earscirev.2018.06.012

Su, X., Shen, Y., Dong, S., Liu, Y., Cheng, H., Wan, L., et al. (2022). Feedback and trigger of household decision-making to ecological protection policies in sanjiangyuan national park. *Front. Plant Sci.* 12. doi: 10.3389/fpls.2021.827618

Wang, Y., Liu, M., Chen, Y., Zeng, T., Lu, X., Yang, B., et al. (2021). Plants and microbes mediate the shift in ecosystem multifunctionality from low to high patterns across alpine grasslands on the Tibetan plateau. *Front. Plant Sci.* 12. doi: 10.3389/fpls.2021.760599

Wang, J., Li, M., Yu, C., and Fu, G. (2022a). The change in environmental variables linked to climate change has a stronger effect on aboveground net primary productivity than does phenological change in alpine grasslands. *Front. Plant Sci.* 12. doi: 10.3389/fpls.2021.798633

Wang, Y. F., Lv, W. W., Xue, K., Wang, S. P., Zhang, L. R., et al. (2022). Grassland changes and adaptive management on the qinghai–Tibetan plateau. *Nat. Rev. Earth. Environ.* doi: 10.1038/s43017-022-00330-8

Wang, Y., Wu, Z., Wang, Z., Chang, S., Qian, Y., Chu, J., et al. (2022c). Ecosystem coupling and ecosystem multifunctionality may evaluate the plant succession induced by grazing in alpine meadow. *Front. Plant Sci.* 13. doi: 10.3389/fpls.2022.839920

Wang, Y., Zhang, X., Sun, Y., Chang, S., Wang, Z., Li, G., et al. (2020). Pika burrow and zokor mound density and their relationship with grazing management and sheep production in alpine meadow. *Ecosphere* 11 (5), e03088. doi: 10.1002/ecs2.3088

Wang, D., Zhou, H., Zuo, J., Chen, P., She, Y., Yao, B., et al. (2022b). Responses of soil microbial metabolic activity and community structure to different degraded and restored grassland gradients of the Tibetan plateau. *Front. Plant Sci.* 13. doi: 10.3389/fpls.2022.770315

Wei, D., Zhao, H., Zhang, J., Qi, Y., and Wang, X. (2020). Human activities alter response of alpine grasslands on Tibetan plateau to climate change. *J. Environ. Manage.* 262, 110335. doi: 10.1016/j.jenvman.2020.110335

Wu, S., Wen, L., Dong, S., Gao, X., Xu, Y., Li, S., et al. (2022). The plant interspecific association in the revegetated alpine grasslands determines the productivity stability of plant community across restoration time on qinghai–Tibetan plateau. *Front. Plant Sci.* 13. doi: 10.3389/fpls.2022.850854

Xiao, J., Dong, S., Shen, H., Li, S., Wessell, K., Liu, S., et al. (2022). N addition overwhelmed the effects of p addition on the soil c, n, and p cycling genes in alpine meadow of the qinghai-Tibetan plateau. *Front. Plant Sci.* 13. doi: 10.3389/fpls.2022.860590

Xu, M., Zhao, Z., Zhou, H., Ma, L., and Liu, X. (2022). Plant allometric growth enhanced by the change in soil stoichiometric characteristics with depth in an alpine meadow under climate warming. *Front. Plant Sci.* 13. doi: 10.3389/fpls.2022.860980

Yang, Y., Shi, G., Liu, Y., Ma, L., Zhang, Z., Jiang, S., et al. (2022). Experimental warming has not affected the changes in soil organic carbon during the growing season in an alpine meadow ecosystem on the qinghai–Tibet plateau. *Front. Plant Sci.* 13. doi: 10.3389/fpls.2022.847680

Yang, K., Wu, H., Qin, J., Lin, C., Tang, W., and Chen, Y. (2014). Recent climate changes over the Tibetan plateau and their impacts on energy and water cycle: A review. *Global. Planet. Change.* 112, 79–91. doi: 10.1016/j.gloplacha.2013.12.001

Yan, Z., Kang, E., Zhang, K., Li, Y., Hao, Y., Wu, H., et al. (2021). Plant and soil enzyme activities regulate CO_2 efflux in alpine peatlands after 5 years of simulated extreme drought. *Front. Plant Sci.* 12. doi: 10.3389/fpls.2021.756956

Yuan, H., Matthew, C., He, X. Z., Sun, Y., Liu, Y., Zhang, T., et al. (2022). Seasonal variation in soil and herbage CO_2 efflux for a sheep-grazed alpine meadow on the north-East qinghai Tibetan plateau and estimated net annual CO2 exchange. *Front. Plant Sci.* 13. doi: 10.3389/fpls.2022.860739

Yu, J., Wan, L., Liu, G., Ma, K., Cheng, H., Shen, Y., et al. (2022). A meta-analysis on degraded alpine grassland mediated by climate factors: Enlightenment for ecological restoration. *Front. Plant Sci.* 12. doi: 10.3389/fpls.2021.821954

Zhang, Z., Sun, J., Liu, M., Shang, H., Wang, J., Wang, J., et al. (2022). Context-dependency in relationships between herbaceous plant leaf traits and abiotic factors. *Front. Plant Sci.* 13. doi: 10.3389/fpls.2022.757077

Zhang, Y., Zheng, Q., Gao, X., Ma, Y., Liang, K., Yue, H., et al. (2022). Land degradation changes the role of aboveand belowground competition in regulating plant biomass allocation in an alpine meadow. *Front. Plant Sci.* 13. doi: 10.3389/fpls.2022.822594

Zhan, T., Zhao, W., Feng, S., and Hua, T. (2022). Plant community traits respond to grazing exclusion duration in alpine meadow and alpine steppe on the Tibetan plateau. *Front. Plant Sci.* 13. doi: 10.3389/fpls.2022.863246

Zhou, H., Ma, A., Zhou, X., Chen, X., Zhang, J., Zhang, Q., et al. (2022). Phosphorus shapes soil microbial community composition and network properties during grassland expansion into shrubs in Tibetan dry valleys. *Front. Plant Sci.* 13. doi: 10.3389/fpls.2022.848691

Zhou, S., and Peng, L. (2021). Applying Bayesian belief networks to assess alpine grassland degradation risks: A case study in Northwest sichuan, China. *Front. Plant Sci.* 12. doi: 10.3389/fpls.2021.773759

Zi, H., Hu, L., and Wang, C. (2022). Differentiate responses of soil microbial community and enzyme activities to nitrogen and phosphorus addition rates in an alpine meadow. *Front. Plant Sci.* 13. doi: 10.3389/fpls.2022.829381

Zou, F., Hu, Q., Li, H., Lin, J., Liu, Y., and Sun, F. (2022a). Dynamic disturbance analysis of grasslands using neural networks and spatiotemporal indices fusion on the qinghai-Tibet plateau. *Front. Plant Sci.* 12. doi: 10.3389/fpls.2021.760551

Zou, F., Tu, C., Liu, D., Yang, C., Wang, W., and Zhang, Z. (2022b). Alpine treeline dynamics and the special exposure effect in the hengduan mountains. *Front. Plant Sci.* 13. doi: 10.3389/fpls.2022.861231

Zuo, H., Shen, H., Dong, S., Wu, S., He, F., Zhang, R., et al. (2022). Effects of strong earthquake on plant species composition, diversity, and productivity of alpine grassland on qinghai-Tibetan plateau. *Front. Plant Sci.* 13. doi: 10.3389/fpls.2022.870613

frontiers in Plant Science

ORIGINAL RESEARCH
published: 14 October 2021
doi: 10.3389/fpls.2021.756956

Plant and Soil Enzyme Activities Regulate CO_2 Efflux in Alpine Peatlands After 5 Years of Simulated Extreme Drought

*Zhongqing Yan[1,2], Enze Kang[1,2], Kerou Zhang[1,2], Yong Li[1,2], Yanbin Hao[3], Haidong Wu[4], Meng Li[1,2], Xiaodong Zhang[1,2], Jinzhi Wang[1,2], Liang Yan[1,2] and Xiaoming Kang[1,2]**

[1] Beijing Key Laboratory of Wetland Services and Restoration, Institute of Wetland Research, Chinese Academy of Forestry, Beijing, China, [2] Sichuan Zoige Wetland Ecosystem Research Station, Tibetan Autonomous Prefecture of Aba, Zoige, China, [3] University of Chinese Academy of Sciences, Beijing, China, [4] Information Center of Ministry of Ecology and Environment, Beijing, China

Increasing attention has been given to the impact of extreme drought stress on ecosystem ecological processes. Ecosystem respiration (Re) and soil respiration (Rs) play a significant role in the regulation of the carbon (C) balance because they are two of the largest terrestrial C fluxes in the atmosphere. However, the responses of Re and Rs to extreme drought in alpine regions are still unclear, particularly with respect to the driver mechanism in plant and soil extracellular enzyme activities. In this study, we imposed three periods of extreme drought events based on field experiments on an alpine peatland: (1) early drought, in which the early stage of plant growth occurred from June 18 to July 20; (2) midterm drought, in which the peak growth period occurred from July 20 to August 23; and (3) late drought, in which the wilting period of plants occurred from August 23 to September 25. After 5 years of continuous extreme drought events, Re exhibited a consistent decreasing trend under the three periods of extreme drought, while Rs exhibited a non-significant decreasing trend in the early and midterm drought but increased significantly by 58.48% ($p < 0.05$) during the late drought compared with the ambient control. Plant coverage significantly increased by 79.3% ($p < 0.05$) in the early drought, and standing biomass significantly decreased by 18.33% ($p < 0.05$) in the midterm drought. Alkaline phosphatase, polyphenol oxidase, and peroxidase increased significantly by 76.46, 77.66, and 109.60% ($p < 0.05$), respectively, under late drought. Structural equation models demonstrated that soil water content (SWC), pH, plant coverage, plant standing biomass, soil β-D-cellobiosidase, and β-1,4-N-acetyl-glucosaminidase were crucial impact factors that eventually led to a decreasing trend in Re, and SWC, pH, β-1,4-glucosidase (BG), β-1,4-xylosidase (BX), polyphenol oxidase, soil organic carbon, microbial biomass carbon, and dissolved organic carbon were crucial impact factors that resulted in changes in Rs. Our results emphasize the key roles of plant and soil extracellular enzyme activities in regulating the different responses of Re and Rs under extreme drought events occurring at different plant growth stages.

Keywords: alpine peatland, extreme drought, ecosystem respiration, soil respiration, extracellular enzyme activities

OPEN ACCESS

Edited by:
Jian Sun,
Institute of Tibetan Plateau Research (CAS), China

Reviewed by:
Huai Chen,
Chengdu Institute of Biology, Chinese Academy of Sciences (CAS), China
Dashuan Tian,
Institute of Geographic Sciences and Natural Resources Research, Chinese Academy of Sciences (CAS), China

***Correspondence:**
Xiaoming Kang
xmkang@ucas.ac.cn

Specialty section:
This article was submitted to Functional Plant Ecology, a section of the journal Frontiers in Plant Science

Received: *11 August 2021*
Accepted: *13 September 2021*
Published: *14 October 2021*

Citation:
Yan Z, Kang E, Zhang K, Li Y, Hao Y, Wu H, Li M, Zhang X, Wang J, Yan L and Kang X (2021) Plant and Soil Enzyme Activities Regulate CO_2 Efflux in Alpine Peatlands After 5 Years of Simulated Extreme Drought. Front. Plant Sci. 12:756956. doi: 10.3389/fpls.2021.756956

INTRODUCTION

There are growing pieces of evidence that extreme drought events will occur more frequently and at greater intensity under the predicted climate change caused by a mass release of carbon dioxide (CO_2), (Dai, 2013; Asadieh and Krakauer, 2015). More extreme drought events affect the key processes of ecosystem functions, such as vegetation photosynthesis (Deng et al., 2021b), plant community composition (Zang et al., 2020), ecosystem water-use efficiency (Wang et al., 2021), and circulation of nutrients (Zhou et al., 2016; Schönbeck et al., 2020). Furthermore, drought has particularly severe effects on pools and fluxes (Hao et al., 2018) in terrestrial carbon (C) cycles (Schlesinger et al., 2016; Ren et al., 2017), which may cause positive C-climate feedback. A deeper understanding of the impact of these extreme drought events on C dynamics in natural ecosystems around the world is necessary (Deng et al., 2021a).

Ecosystem respiration and soil respiration (Rs) play a significant role in the maintenance of the functions and sustainability of terrestrial ecosystems (Chen et al., 2019; Zhou et al., 2019). Ecosystem respiration (Re) is the total sum of soil microbial, root, leaf, and stem respiration (Beer et al., 2010). Rs represents CO_2 released into the atmosphere from the soil surface, including that from autotrophic respiration of living roots and symbionts (Zhou et al., 2014), as well as microbial respiration in soil organic matter and plant litter decomposition (Bond-Lamberty and Thomson, 2010). Relevant results of field observations and modeling show that the annual variation in atmospheric CO_2 is strongly affected by the variation in Re and Rs caused by climate change (Kato et al., 2004). Therefore, small fluctuations in Re and Rs may induce remarkable variations in CO_2 concentrations in the atmosphere (Luo, 2007; Metcalfe et al., 2011). While Re and Rs are known to be controlled under multiple biotic and abiotic factors, understanding how Re and Rs respond to extreme drought and the driving mechanism is of great significance for predicting C-climate feedback over regional to global scales.

Plant productivity and species composition are critical to peatland ecosystem C sequestration and soil C input, and high-water levels and associated saturated soils play a key role in maintaining peatland vegetation composition and productivity (Bakker et al., 2007). Drought may lead to a decline in the water table, resulting in significant changes in the species competition level (Maestre et al., 2005), plant diversity, richness, evenness, coverage (Zeng et al., 2021), net primary productivity (Flanagan et al., 2013), litter yield, underground carbon distribution, and litter or secretion composition (Garssen et al., 2014). Changes in plant species composition and community structure may further affect the organic C pool of peatlands (De Deyn et al., 2008; Potvin et al., 2015). Re is divided into heterotrophic respiration generated by microbial decomposition residues and soil organic matter and plant autotrophic respiration or aboveground autotrophic respiration generated by a plant canopy and Rs. Different components may have different sensitivities to the same environmental factors (such as temperature and soil moisture), (Hu et al., 2015). Therefore, plant community changes after drought events may have a great impact on ecosystem C emissions, especially on Re and autotrophic respiration, but there is still a lack of relevant evidence on the specific influencing pathways.

It is well-known that soil extracellular enzyme activities (EEAs) provide a direct driving force for soil biogeochemical cycles, including C, nitrogen (N), and phosphorus (P) turnover (Burns et al., 2013). Full degradation in soil macromolecular organic matter depends on the synergistic effect among various soil extracellular enzymes, such as cellulose hydrolase and phenol oxidase, which can accelerate the decomposition of soil C (Freeman et al., 2004; Baldrian, 2009). Climate changes markedly alter soil EEAs *via* direct and indirect methods and in turn, modulate soil nutrient cycles (Henry, 2012; Wang et al., 2017a; Su et al., 2020). The activities of C-, N-, and P-acquisition enzymes have been proven to decrease significantly in the middle and late stages of the growing season under extreme drought (Gao et al., 2021). Water, oxygen, temperature, and pH interact to affect the activity of phenol oxidase, and the mineralization and output of peatland C are complex and sensitive to changes in environmental conditions (Laiho, 2006). Fenner et al. (2005), using microcosms, reported that simulated drought increased respiration, phenol oxidase, and β-glucosidase activities and decreased the concentration of phenolic. Few studies have explored the linkage between soil EEAs and ecological processes (Dominguez et al., 2017), which is a central focus in climate change ecology. Cellulose and lignin are the two most effluent soil organic matter (SOM) compounds. Meanwhile, microbial-mediated decomposition in the aforementioned substances is an important source of Re and Rs (Carreiro et al., 2000; Chen et al., 2018). The key role played by cellulase and lignase in mediating SOM decomposition reveals that extreme drought possibly affects Re and Rs *via* impacts on EEAs, but direct evidence of their contributions is still lacking.

Zoige peatlands cover an area of approximately 5,091 km^2 of the Qinghai-Tibetan Plateau, and the corresponding peat C stock was reported to be 0.477 Pg (0.206–0.672 Pg), accounting for 88% of the total C storage of the Qinghai-Tibetan Plateau (0.543 Pg C), (Chen et al., 2014). The Zoige peatlands are major C sources of CO_2 emissions due to the large C pool, potentially causing positive feedback to extreme drought. Thus, the Zoige peatlands provide a proper site for investigating extreme drought-induced variations in C emissions and the correlation of plants and EEAs with C emissions during extreme drought. The research tested Re and Rs responses after 5 years of simulated extreme drought events and relevant potential mechanisms. The study mainly answers three questions as follows: (i) What about experimental extreme drought impacts on Re and Rs dynamics? (ii) Do soil EEAs change significantly after extreme drought events? (iii) How do plants and soil EEAs regulate Re and Rs changes under extreme drought?

MATERIALS AND METHODS

Study Area Experimental Design

The peatland investigated in this research is at an altitude of 3,430 m. The study area is situated on the Zoige Plateau

(33°47′56.61″N, 102°57′28.43″E) of the northeastern Qinghai-Tibet Plateau. Due to the unique climatic and hydrological conditions of the region, the largest alpine peatlands worldwide have been discovered across the region (Ma et al., 2016). The average annual temperature ranges from −1 to 3.3°C, and the average annual precipitation is between 650 and 750 mm. The region has a long frost period (October to April) and a relatively short growing season (May to September), (Kang et al., 2016). The relevant average peat profile thickness across the region is approximately 1.39 m, and the maximum thickness can reach 10 m (Chen et al., 2014). The soil organic carbon (SOC) content fell between 179.36 and 276.41 $g{\cdot}kg^{-1}$. Soil pH was between 6.8 and 7.2. The dominant plant species are *Koeleria tibetica*, *Carex meyeriana*, *Carex muliensis*, *Blysmus sinocompressus*, *Eriophorum gracile*, and *Carex secbrirostris*.

We have collected precipitation statistics for the region for the past 5 decades (China Meteorological Data Service Center) and focused on one extreme drought event, not long-term drought, so fitting a Gumbel I distribution to the ∼50-year local weather data. Daily precipitation ≤3 mm indicates an absence of precipitation. According to the definition of extreme climate (Hoover and Rogers, 2016), meteorological drought is defined as the number of consecutive days of precipitation deficiency compared with a long-term average (Mishra and Singh, 2010; Sheffield and Wood, 2012), and invalid precipitation lasting for 32 days is considered an extreme drought event for this region. The artificial extreme drought event simulation started in June 2014, and precipitation was prevented by transparent awning, which was 2.5 m in length, 2.5 m in width, and 1.8 m in height. The light transmittance of the shielding material is over 90%. Each treatment consisted of three plots (each plot was 2 m × 2 m), a total of 12 plots were established, and replicates had random distribution throughout the field. A 1-m-deep aluminum plate was inserted at the edge of the plot to prevent the horizontal flow of water. For more detailed information, refer to Kang et al. (2018) and Yan et al. (2020). After 5 years of continuous extreme drought event stress once a year, the experiment in 2019 included the control treatment (CK), which was exposed to ambient precipitation throughout the entire experiment and different periods of extreme drought events for approximately 32 days during the growing season. The three extreme drought treatments of different periods were imposed on June 18 to July 20 (ED: early drought), July 20 to August 23 (MD: midterm drought), and August 23 to September 25 (LD: late drought).

Measurements of CO_2 Fluxes

Ecosystem respiration and soil respiration were measured approximately one time a week between 10:00 and 15:00 (local time) from June 18 to September 25, 2019. The square aluminum frame (0.5 m × 0.5 m) was placed in the soil on every plot at 2-or 3-cm depth, providing a certain flat base between the soil surface and the CO_2 sampling chamber. The experiment assessed Re using a 0.125-m^3 opaque chamber (0.5 m × 0.5 m × 0.5 m) fixed onto a microportable greenhouse gas analyzer (GLA131, ABB, Canada), covering all vegetation within the aluminum frame. During the measurements, the air inside the chamber was mixed by two small fans. A previous study showed that this method can be successfully applied to the measurement of CO_2 flux in alpine meadows (Chen et al., 2016). The CO_2 concentration was recorded continuously for 120 s after the steady state was reached (steady-state conditions were typically achieved in the range of 10 to 30 s). Increases in air temperature were <0.2°C inside the chamber within measurement intervals (Xia et al., 2009). Polyvinylchloride (PVC) collars 20 cm in diameter and 10-cm high were placed in soil at 2-or 3-cm depth near the aluminum frames, which were used in Rs measurements. To eliminate the effects of plant respiration, live plants within soil collars were interrupted on the soil surface. A soil CO_2 flux chamber (SC-12, LICA, China) attached to an infrared gas analyzer (PS-9000, LICA, China) was placed on each collar and then moved to the next collar after the automatic Rs measurement was completed.

Re ($mg{\cdot}m^{-2}{\cdot}h^{-1}$) can be calculated by a linear slope, which represents variations in gas concentration over time, which can be given by (Mastepanov et al., 2008).

$$Re = \frac{dc}{dt}\frac{M}{V_0}\frac{P}{P_0}\frac{T_0}{T}H \tag{1}$$

dc/dt indicates the gas concentration slope with time ($ppm{\cdot}h^{-1}$); M suggests the molar mass for gas to be calculated ($g{\cdot}mol^{-1}$); P implies the atmospheric pressure of the sampling site (Pa); P_0, V_0, and T_0 represent the standard atmospheric pressure (101,325 Pa), standard molar volume (22.41 $m^3{\cdot}mol^{-1}$), and absolute temperature in standard atmospheric pressure; and T and H represent the absolute temperature (°C) and effective height (m) inside the chamber, respectively.

Rs ($mg{\cdot}m^{-2}{\cdot}h$) is also calculated by the linear slope, which represents the change in gas concentration over time, which can be given by

$$Rs = \frac{10VP_0(1-\frac{W_0}{1000})}{RS(T_0+273.15)}\frac{\partial C'}{\partial t}43.2 \tag{2}$$

V indicates the volume inside the air chamber; P_0 means the standard atmospheric pressure (101,325 Pa), W_0 is the initial water vapor value; R is a constant (8.314); S is the gas measurement area; T_0 is the measured temperature during sampling; and $\partial C'/\partial t$ suggests the gas concentration slope over time ($ppm{\cdot}h^{-1}$).

Plant and Soil Characteristics

Plant and soil samples (0–10 cm) of every plot were gathered on July 20, August 23, and September 25, 2019, at the end of each extreme drought event. Standing biomass (SBM) samples were gathered using a square frame (0.5 m × 0.5 m) near the aluminum frames, followed by drying at 65°C for 72 h prior to weighing. At the same time, the vegetation coverage and species number in different treatment plots were recorded. Soil samples collected from the five cores were stored in separate insulated bags and instantly delivered to the laboratory using ice boxes. Overall, fresh field soils fell into three subsamples, following screening *via* a 2-mm sieve for soil physical and chemical properties and soil EEA analysis. Altogether, 18 soil samples were investigated for each indicator. The soil water content (SWC)

could be assessed *via* aTDR 300 moisture meter (Spectrum, USA) on site. Soil pH could be assessed through a pH electrode (PB-10, Sartorius, Germany) within a 1:2.5 soil-to-deionized water mixture. SOC, as well as total N (TN) concentrations, could be assessed through the C/N analyzer (Elementar, Vario Max CN, Germany) through dry combustion of samples (100-mesh). Microbial biomass C (MBC), microbial biomass N (MBN), and microbial biomass phosphorus (MBP), (Chen et al., 2016) were determined by an elemental TOC analyzer (LiquiTOC II, Germany), using the chloroform fumigation method. Dissolved organic carbon (DOC) was calculated for soil water extracts. A fresh sample of 15 g was placed in 150 ml of ultrapure water, oscillated at 15°C for 24 h, screened using a prebaked 0.7-mm glass fiber filter (GF/F, Whatman, UK), and then analyzed by an elemental TOC analyzer (LiquiTOC II, Germany). Soil NH_4^+ and NO_3^- concentrations were determined by an auto analyzer (SEAL-AA3, Germany) from 2-mol L^{-1} KCl extracts. Total phosphorus (TP) was measured using a flow injection auto analyzer, followed by digestion through H_2SO_4-$HClO_4$ (Huang et al., 2011). Available phosphorus (AP) was measured using molybdenum blue colorimetry with a spectrophotometer (TAS-990, Persee, Beijing).

Monitoring Changes in Soil Enzyme Activities Under Extreme Drought

In this study, a total of seven soil hydrolases were determined to be engaged with C-, N-, and P-acquisition (**Table 1**). Soil hydrolases in α-1,4-glucosidase (AG), β-1,4-glucosidase (BG), β-1,4-xylosidase (BX), β-D-cellobiosidase (CB), β-1,4-N-acetyl-glucosaminidase (NAG), leucine amino peptidase (LAP), and alkaline phosphatase (ALP) were determined using a fluorescence method (Jackson et al., 2013). The first step was to add 50-μl, 200-mM substrate solution into every sample well, a 50-ml acetate buffer, 200-ml sample suspension to blank wells, 50-ml substrate solution, and a 200-ml acetate buffer into negative control wells. Then, quench standard wells accepted 50 ml of the standard, which is 10-mM 7-amino-4-methyl coumarin in LAP and 4-methylumbelliferone in other soil hydrolases, with 200 ml of the sample suspension. The reference standard wells accepted 50 ml of the standard and 200 ml of an acetate buffer. For every blank, negative control, and quench standard, there were eight replicate wells. Then, microplates needed to be cultivated in darkness at 20°C for 3 h. When the incubation period terminated, each well received a 10-ml aliquot of 1-M NaOH for stopping the reaction. Finally, fluorescence was assessed with a microplate fluorometer, containing 365-nm excitation and 450-nm emission filters.

Soil oxidases of polyphenol oxidase (PPO) and peroxidase (PEO) were assessed spectrophotometrically with the substrate L-3,4-dihydroxyphenylalanine (DOPA), (Pind et al., 1994; Sinsabaugh, 2010). Every sample accepted 50 ml of 25-mM DOPA and 50 ml of 25-mM DOPA with 10 ml of 0.3% H_2O_2 in PPO and PEO measurements. Negative control wells received 200 ml of an acetate buffer as well as 50 ml of DOPA solution for PPO, and blank wells included 200 ml of sample suspension and 50 ml of the acetate buffer. For PEO, an extra 10 ml of H_2O_2 needed to be inserted into the negative control and blank wells. Altogether, 16 replicate sample wells were applied in every measurement, and eight replicate wells were adopted for the blank and control. Microplates were cultivated in darkness at 20°C for 18 h. The activity could be quantified by assessing the absorbance at 450 nm with a microplate spectrophotometer. The activity in soil hydrolases and oxidases was indicated by units of nmol g^{-1} soil h^{-1} upon correction in the negative control as well as quenching.

Statistical Analyses

Repeated measures analysis of variance was adopted to compare the impacts exerted by extreme drought, sampling time, and their interactions on Re and Rs. Independent sample *t*-tests were conducted to determine how extreme drought treatment affected vegetation, soil characteristics, and soil EEAs. Significant differences were evaluated at the $p < 0.05$ level. The structural equation model (SEM) could be used separately to determine the impacts of different variables on Re and Rs under extreme drought. The maximum likelihood estimation approach was employed for fitting data. The model showed fine fitting effects if $0.05 < p \leq 1.00$ in a chi-square (χ^2) test, comparative fit index (CFI) ≥ 0.95, and root mean square error of approximation (RMSEA) ≤ 0.05. Statistical analysis was performed with SPSS 22.0 (SPSS, Chicago, IL, USA); SEM analysis was performed with IBM SPSS Amos 24.0 (SPSS, Chicago, IL, USA). The figures were generated with OriginPro (Origin lab Corporation) and Adobe Illustrator CC (Adobe Inc.).

RESULTS

Meteorological Conditions, Vegetation, and Soil Variables

There was seasonal variation in the mean daily air temperature during the three extreme drought events, ranging from 2.8 to 16.1°C (**Figure 1**). The mean daily air temperature was highest on July 28 during the MD treatment and lowest on September 24 during the LD treatment. The mean daily air temperatures for the ED, MD, and LD treatments were 11.15, 11.89, and 9.10°C, respectively. There was also seasonal variation in daily precipitation during the three extreme drought events, ranging from 0 to 56.6°C. Daily precipitation was highest on August 21 during the MD treatment. The total precipitation for the ED, MD, and LD treatments was 150, 196.5, and 117.8 mm, respectively. The precipitation during the LD treatment was < that during the ED and MD.

The SBM decreased by 0.68, 18.33, and 2.38% compared with the control under the ED, MD, and LD treatments, respectively, and reached a significant level ($p < 0.05$) after MD (**Table 2**). Plant coverage increased by 79.31, 17.24, and 34.48% compared with the control under the ED, MD, and LD treatments, respectively, and reached a significant level ($p < 0.05$) under the ED treatment. The number of plant species showed no significant differences in treatments in 2019, decreased by 5.56% in the

TABLE 1 | Description of soil extracellular enzymes in this study.

Extracellular enzyme	EC	Type	Targets
α-1,4-glucosidase	3.2.1.20	C-acquisition hydrolysis	Starch and disaccharides
β-1,4-glucosidase	3.2.1.21	C-acquisition hydrolysis	Cellulose
β-1,4-xylosidase	3.2.1.37	C-acquisition hydrolysis	Hemicellulose
β-D-cellobiosidase	3.2.1.91	C-acquisition hydrolysis	Cellulose
β-1,4-N-acetyl-glucosaminidase	3.1.6.1	N-acquisition hydrolysis	Chitin
Leucine amino peptidase	3.4.11.1	N-acquisition hydrolysis	Protein
Alkaline phosphatase	3.1.3.1	P-acquisition hydrolysis	Organic phosphorus
Polyphenol oxidase	1.10.3.1	Recalcitrant C oxidation	Lignin
Peroxidase	1.11.1.7	Recalcitrant C oxidation	Lignin

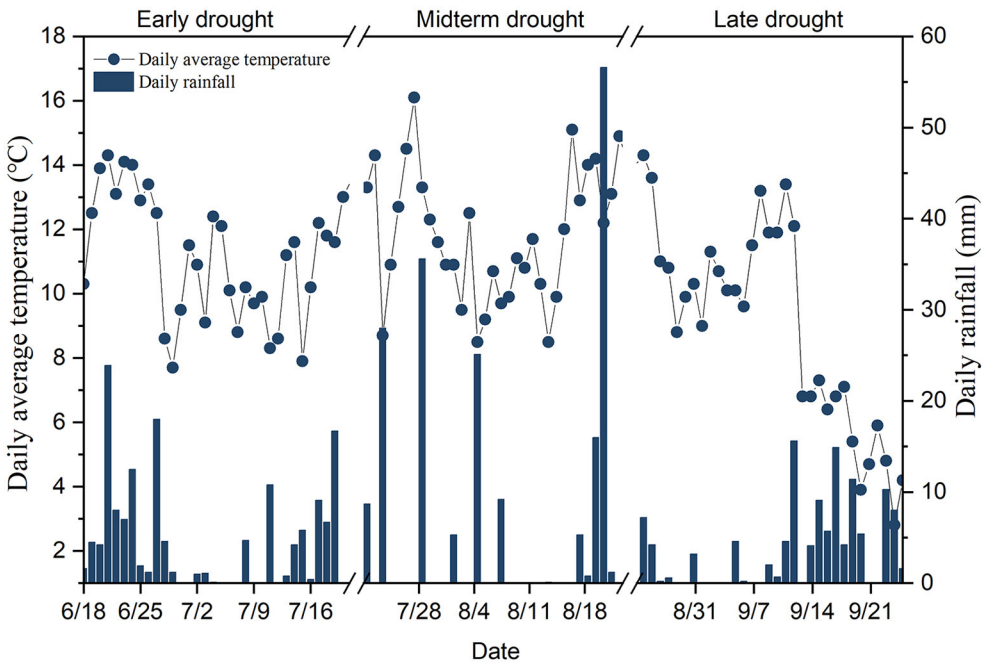

FIGURE 1 | Average daily temperature and precipitation of experiments in 2019.

ED treatment, and increased by 5.56% under both MD and LD treatments in contrast to the control.

The soil water content decreased by 9.42, 3.87, and 4.21% compared with the control under the ED, MD, and LD treatments, respectively, and reached a significant level ($p < 0.05$) during the ED treatment (**Table 2**). Soil pH, DOC, and TN increased by 1.29, 2.25, and 5.29% under the ED treatment, by 1.73, 17.70, and 29.83% under the MD treatment, and by 1.28, 1.10, and 4.54% under the LD treatment, respectively. SOC decreased by 5.49, 9.42, and 3.44% under the ED, MD, and LD treatments, respectively. MBC and MBP decreased by 2.31 and 6.61% under ED treatment, decreased by 13.18 and 8.79% under MD treatment, and increased by 0.30 and 0.58% under LD treatment, respectively. NH_4^+, MBN, and AP decreased by 5.53, 2.55, and 17.37% under the ED treatment, increased by 0.31, 5.18, and 21.34% under the MD treatment, and increased by 0.43, 2.29, and 32.61% under the LD treatment, respectively. NO_3^- decreased by 25.35 and 5.90% under the ED and MD treatments, respectively, but increased by 5.04% under the LD treatment. TP increased by 14.36 and 4.65% under ED and MD treatments, respectively, and decreased by 18.72% under LD treatment.

Effects of Extreme Drought on Re and Rs Dynamics

Ecosystem respiration and soil respiration showed similar seasonal patterns in the control and three different periods of the extreme drought treatments in 2019 (**Figures 2A,C**). The Re ranged from 410.51 to 1286.49 $mg \cdot m^{-2} \cdot h^{-1}$ in the growing season and reached its highest values at the end of July; additionally, when the growing season began and terminated, Re was lower than that at the other sampling times. The seasonal mean Re decreased by 8.46 (874.10 $mg \cdot m^{-2} \cdot h^{-1}$), 14.59 (942.41

TABLE 2 | Plant and soil characteristics in the control period and different periods of extreme drought in 2019.

Variables	Early drought		Midterm drought		Late drought	
	CK	ED	CK	MD	CK	LD
SBM (g m^{-2})	351.77 ± 16.00a	349.4 ± 9.99a	351.44 ± 15.68a	287.04 ± 9.26b	350.77 ± 16.73a	342.41 ± 24.58a
Coverage (%)	48.33 ± 8.33a	86.67 ± 3.33b	48.33 ± 8.33a	56.67 ± 8.33a	48.33 ± 8.33a	65 ± 8.66a
Species no.	6 ± 0a	5.67 ± 0.67a	6 ± 0a	6.33 ± 0.88a	6 ± 0a	6.33 ± 0.58a
SWC (%)	60.13 ± 0.33a	54.47 ± 1.88b	61.7 ± 0.8a	59.37 ± 1.55a	69.63 ± 0.5a	66.7 ± 1.45a
pH	7.73 ± 0.07a	7.83 ± 0.03a	7.73 ± 0.03a	7.87 ± 0.09a	7.8 ± 0.06a	7.9 ± 0.06a
SOC (g kg^{-1})	215.42 ± 19.75a	203.59 ± 28.56a	241.2 ± 6.59a	218.48 ± 21.01a	257 ± 13.18a	248.16 ± 13.14a
DOC (mg kg^{-1})	293.93 ± 14.86a	300.55 ± 12.98a	305.49 ± 78.29a	359.57 ± 72.99a	374.89 ± 14.72a	379 ± 22.8a
MBC (mg kg^{-1})	394.69 ± 59.35a	385.56 ± 53.63a	441.9 ± 4.54a	383.66 ± 55.62a	444.78 ± 11.14a	446.11 ± 7.09a
TN (g kg^{-1})	15.51 ± 0.48a	16.33 ± 0.15a	17.43 ± 6.37a	22.63 ± 3.45a	25.7 ± 1.85a	26.87 ± 2.87a
NH_4^+ (mg kg^{-1})	11.69 ± 0.17a	11.05 ± 0.79a	11.91 ± 0.11a	11.95 ± 0.36a	12.4 ± 0.33a	12.45 ± 0.22a
NO_3^- (mg kg^{-1})	6.36 ± 0.77a	4.75 ± 1.38a	6.55 ± 0.31a	6.17 ± 0.15a	6.55 ± 0.35a	6.88 ± 1.22a
MBN (mg kg^{-1})	73.41 ± 1.49a	71.54 ± 1.36a	70.39 ± 1.94a	74.03 ± 1.7a	73.4 ± 1.77a	75.08 ± 0.22a
TP (g kg^{-1})	1.3 ± 0.06a	1.49 ± 0.11a	1.43 ± 0.03a	1.5 ± 0.05a	1.46 ± 0.08a	1.19 ± 0.29a
AP (mg kg^{-1})	40.5 ± 2.32a	33.46 ± 9.64a	23.9 ± 5.1a	29 ± 5.67a	43.03 ± 4.6a	57.06 ± 3.98a
MBP (mg kg^{-1})	34.15 ± 6.97a	31.9 ± 6.65a	39 ± 0.79a	35.57 ± 3.05a	39.5 ± 1.93a	39.73 ± 1.23a

SBM, standing biomass; Species No., number of species; SWC, average soil water content during each extreme-drought period; SOC, soil organic carbon; DOC, dissolved organic carbon; MBC, microbial biomass carbon; TN, soil total nitrogen; MBN, microbial biomass nitrogen; TP, soil total phosphorus; AP, available phosphorus; MBP, microbial biomass phosphorus; ED, early drought; MD, midterm drought; LD, late drought; CK, the ambient control treatment corresponding to each stage of extreme-drought treatment. Different letters indicate a remarkable difference between the control and extreme drought treatments ($p < 0.05$). Relevant data are indicated by the mean ± standard error ($n = 3$).

mg·m^{-2}·h^{-1}), and 7.03% (908.48 mg·m^{-2}·h^{-1}) during the ED, MD, and LD treatments, respectively, in contrast to the control (**Figures 2A,B**). Rs ranged from 57.34 to 257.17 mg·m^{-2}·h^{-1} during the growing season, reaching its highest value until mid-July. The seasonal mean Rs decreased by 29.38 (121.09 mg·m^{-2}·h^{-1}) and 4.62% (173.12 mg·m^{-2}·h^{-1}) under the ED and MD treatments, respectively, but increased significantly ($p < 0.05$) by 58.48% (147.66 mg·m^{-2}·h^{-1}) under the LD treatment (**Figures 2C,D**).

Generally, Re and Rs were significantly influenced by the sampling date during 2019 (**Table 3**) in the different periods of the three extreme drought treatments, and no remarkable interactions were found between the sampling date and drought treatment. Notably, Rs increased remarkably under the LD treatment ($p < 0.05$).

Effects of Extreme Drought on Soil EEAs

In various extreme drought periods, the soil EEAs showed different trends (**Figure 3**): BG, ALP, and PPO had the highest activities among all soil enzymes (**Figures 3B,F,H**); their ranges of variation were 587.27–2108.84 nmol g^{-1} h^{-1}, 1152.80–2082.92 nmol g^{-1} h^{-1} and 46443.52–11560.30 nmol g^{-1} h^{-1}, respectively. AG and PPO increased by 7.61 (644.54 nmol g^{-1} h^{-1}) and 17.08% (76136.08 nmol g^{-1} h^{-1}) in the ED treatment, 10.31 (721.09 nmol g^{-1} h^{-1}) and 22.95% (57101.98 nmol g^{-1} h^{-1}) in the MD treatment, and 25.49 (636.92 nmol g^{-1} h^{-1}) and 77.66% (115660.30 nmol g^{-1} h^{-1}) in the LD treatment, respectively, compared with CK (**Figures 3A,H**). BG and LAP increased by 40.95 (1620.24 nmol g^{-1} h^{-1}) and 3.59% (234.89 nmol g^{-1} h^{-1}) in the ED treatment, increased by 15.15 (2108.84 nmol g^{-1} h^{-1}) and 19.80% (505.80 nmol g^{-1} h^{-1}) in the MD treatment, and decreased by 6.51 (587.27 nmol g^{-1} h^{-1}) and 7.08% (454.78 nmol g^{-1} h^{-1}) in the LD treatment, respectively, compared with CK (**Figures 3B,F**). CB, NAG, and ALP decreased by 26.01 (228.08 nmol g^{-1} h^{-1}), 27.19 (474.34 nmol g^{-1} h^{-1}), and 29.03% (1478.25 nmol g^{-1} h^{-1}) in the ED treatment, decreased by 38.86 (451.10 nmol g^{-1} h^{-1}), 23.36 (1085.05 nmol g^{-1} h^{-1}), and 13.23% (1779.06 nmol g^{-1} h^{-1}) in the MD treatment, and increased by 181.18 (243.18 nmol g^{-1} h^{-1}), 63.78 (565.34 nmol g^{-1} h^{-1}), and 76.46% (2034.22 nmol g^{-1} h^{-1}) in the LD treatment, respectively, compared with CK (**Figures 3D,E,G**). BX and PEO decreased by 35.72 (278.78 nmol g^{-1} h^{-1}) and 8.76% (106366.50 nmol g^{-1} h^{-1}) in the ED treatment, decreased by 41.85 (480.47 nmol g^{-1} h^{-1}) and 30.83% (66000.25 nmol g^{-1} h^{-1}) in the MD treatment, and decreased by 41.85 (480.47 nmol g^{-1} h^{-1}) and 109.60% (138704.20 nmol g^{-1} h^{-1}) in the LD treatment, respectively, compared with CK (**Figures 3C,I**). In the LD treatment, ALP, PPO, and PEO seemed remarkable ($p < 0.05$) > their counterparts in the control.

Impact of Pathways of Extreme Drought on Re and Rs

An SEM was used to predict the effects of extreme drought on Re (**Figure 4**), with SWC, pH, NAG, CB, plant coverage, and standing biomass (SBM) as the variables ($\chi^2 = 4.985$, d$f = 5$, $P = 0.418$; CFI = 1.000; RMSEA = 0.000). The final model explained 73% of the variance in Re, 3% of that in SBM, 43% of that in coverage, and 26% of that in soil hydrolases (NAG and CB). SWC generated prominent direct negative effects on plant coverage (−0.57), and coverage generated prominent direct negative effects on Re (−0.68). pH (0.32), soil hydrolases (0.72), and SBM (0.44) generated an obvious direct positive effect on

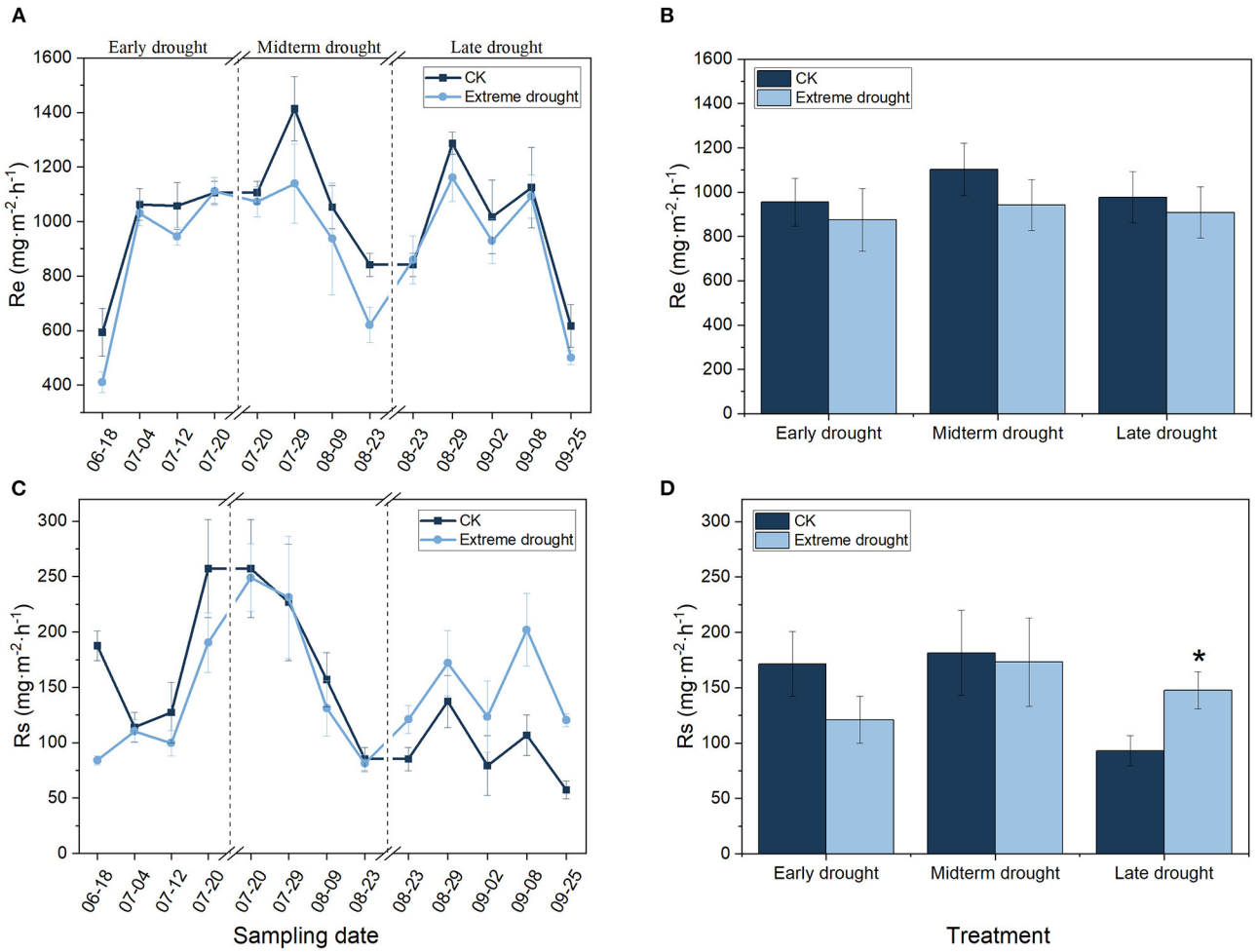

FIGURE 2 | Seasonal variations in Re **(A,B)** and Rs **(C,D)** in the growing season of 2019 for different periods of extreme drought treatments ($n = 3$; bars indicate SE). Significance: $^{*}p < 0.05$.

TABLE 3 | The effects of different periods of extreme drought treatment, sampling time, and relevant interactions on ecosystem respiration (Re) and soil respiration (Rs) in 2019.

Variance source	Early drought			Midterm drought			Late drought		
	df	Re	Rs	df	Re	Rs	df	Re	Rs
Treatment (T)	1	2.674	6.413	1	2.741	0.113	1	0.733	7.79*
Date (D)	4	53.092***	13.615***	4	11.006**	8.96**	4	22.58***	5.20**
T × D	4	1.194	2.358	4	0.62	0.15	4	0.321	0.841

*Significance: ***, $p < 0.001$; **, $p < 0.01$; *, $p < 0.05$. Re, ecosystem respiration; Rs, soil respiration.*

Re. These results implied that a decrease in SWC due to extreme drought resulted in a decrease in Re through plant coverage in the growing season, while the increase in pH, soil hydrolases, and SBM could result in an increase in Re. The final variation in Re is under the combined influence of the above factors.

The final SEM for predicting the direct and indirect impacts exerted by drought on Rs included the following variables (**Figure 5**): SWC, pH, SOC, DOC, MBC, BX, BG, and PPO ($\chi^2 = 7.992$, $df = 11$, $P = 0.714$, CFI = 1.000, RMSEA = 0.000). The final model explained 65% of the variance in Rs, 51% of that in SOC, 60% of that in DOC, 60% of that in MBC, 34% of that in PPO, and 66% of that in soil C-acquisition hydrolases (BG and BX). SEM demonstrated that SWC had a significant direct negative effect (−0.51) on soil C-acquisition hydrolases and a significant direct positive effect on SOC (0.48). Soil pH showed an obvious direct negative impact on SOC (−0.53) and a significant direct positive effect on PPO (0.68). PPO showed an obvious direct negative impact on soil C-acquisition hydrolases

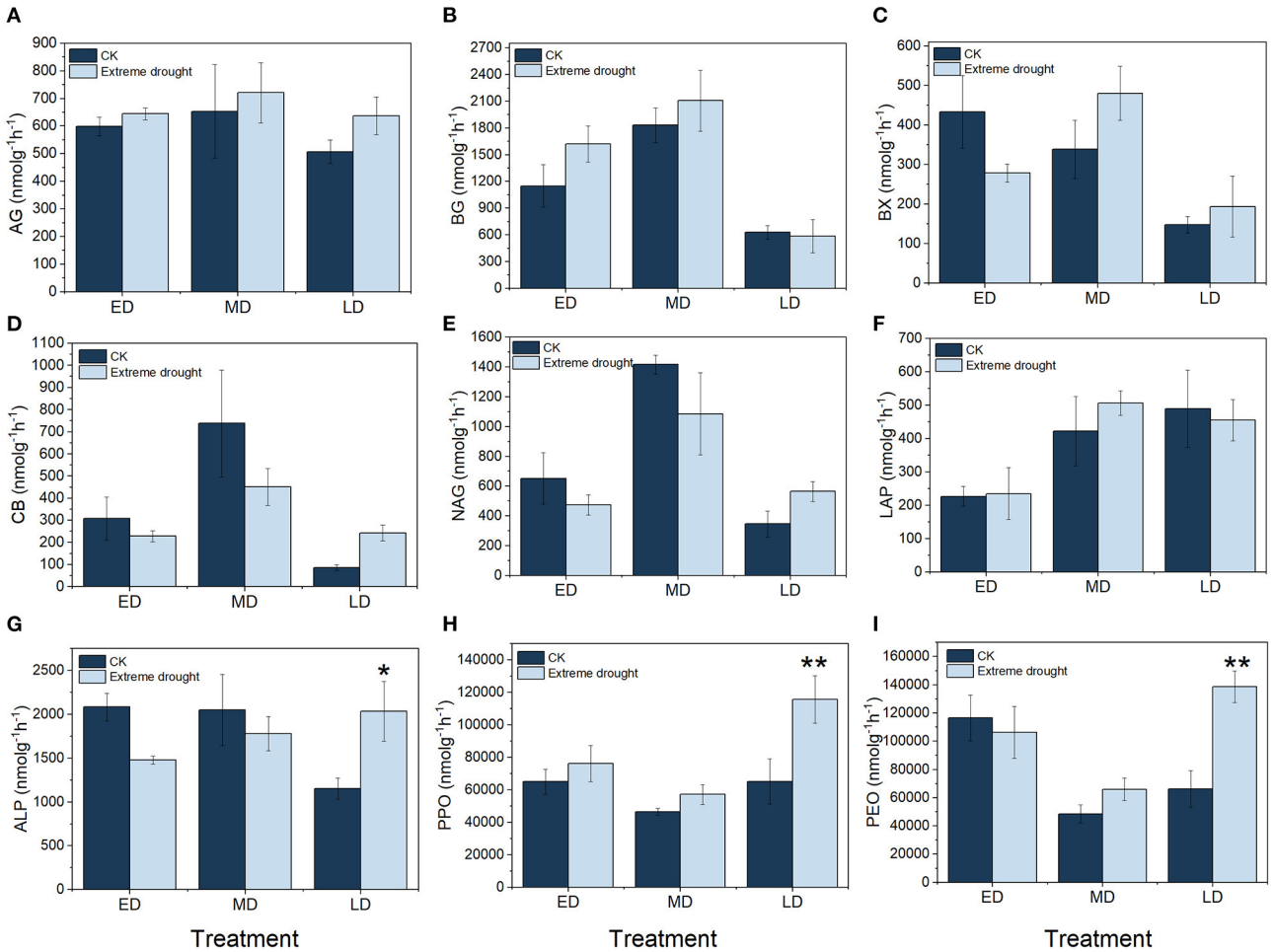

FIGURE 3 | Soil enzyme activities of C-acquisition **(A–D,H,I)**, N-acquisition **(E,F)** and P-acquisition **(G)** resulting from different treatments. ED, early drought; MD, midterm drought; LD, late drought; CK, the ambient control treatment corresponding to each stage of extreme drought treatment. AG, α-1,4-glucosidase; BG, β-1,4-glucosidase; BX, β-1,4-xylosidase; CB, cellobiosidase; NAG, β-1,4-N-acetyl-glucosaminidase; LAP, leucine amino peptidase; ALP, alkaline phosphatase; PPO, polyphenol oxidase; PEO, peroxidase; **, $p < 0.01$; *, $p < 0.05$. Relevant data are indicated by the mean ± standard error ($n = 3$; bars indicate SE).

(−0.56), and soil C-acquisition hydrolases showed an obvious direct positive impact on Rs (0.92), but the other soil indexes showed no significant direct influences. These results indicated that a decrease in SWC due to extreme drought resulted in an increase in soil C-acquisition hydrolases, while an increase in pH also increased PPO activity and then resulted in a decrease in soil C-acquisition hydrolases. Their synthesis led to a variation in soil C-acquisition hydrolases and then regulated Rs changes.

DISCUSSION

Different Responses of Re and Rs to Extreme Drought

Our results revealed that Re had a non-significant decreasing trend (**Figures 2A,B**) under early, midterm, and late extreme drought in the growing season compared with the ambient control, which may be explained by Bhanja and Wang (2021), which found SWC to be the least influential factor in respiration estimation. Re can be divided into several subcomponents, including heterotrophic respiration and above-and belowground plant autotrophic respiration (Sagar et al., 2019). These components respond to extreme drought in complex ways, and plant autotrophic respiration accounts for a high proportion of Re. Drought induces changes in plant biodiversity, richness, evenness, coverage, and standing biomass (Ma et al., 2020; Zeng et al., 2021). Therefore, vegetation conditions must be taken into account when estimating Re from peatlands, especially in future extreme drought conditions. In our study, after 5 years of extreme drought, despite some changes in plant biomass and coverage, the rewet after the end of extreme drought every year may be conducive to vegetation restoration, which likely caused the lower but not significant Re under early, midterm, and late drought compared with ambient conditions.

In the past 3 decades, as the second continental carbon flux, Rs has been the main way for carbon dioxide absorbed by terrestrial plants to return to the atmosphere, increasing the

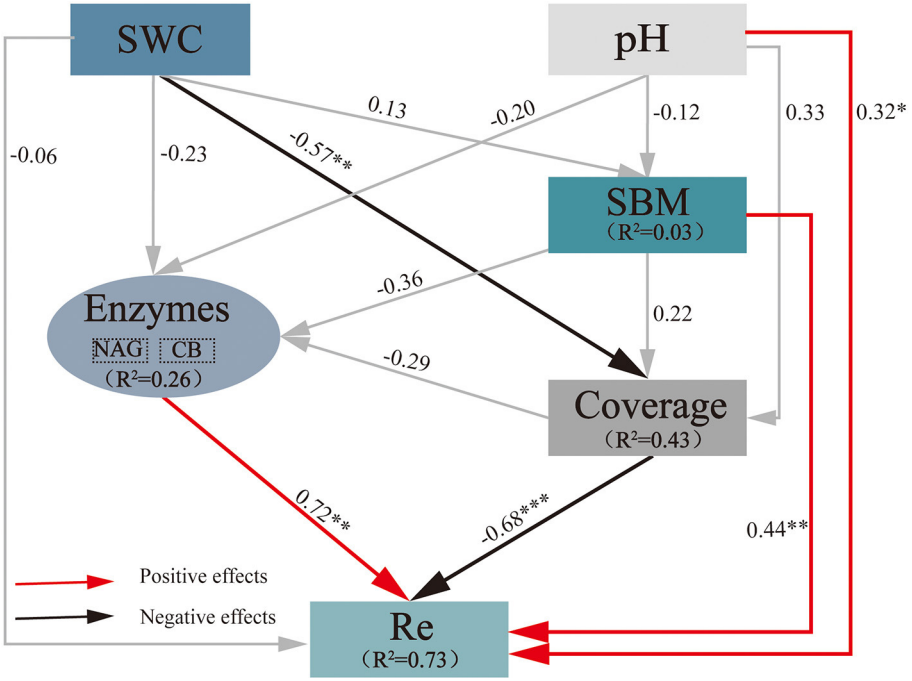

FIGURE 4 | Impacts of selected drivers on Re under extreme drought calculated by the SEM of path analysis based on data collected in 2019. The values on the arrows are normalized path coefficients, and the asterisks after the numbers indicate remarkable correlations (*$p < 0.05$, **$p < 0.01$, and ***$p < 0.001$). The rectangle R^2 value represents the ratio of variance explained by relationships with other variables. SWC, soil water content; SBM, standing biomass; NAG, β-1,4-N-acetyl-glucosaminidase; Re, ecosystem respiration.

positive feedback of climate warming (Bond-Lamberty et al., 2018). As identified by several studies, Rs was mainly affected by soil temperature and moisture (Carey et al., 2016; Yu et al., 2021). Increased water stress caused by drought may lead to reduced C synthesis for photosynthesis, which reduces substrate availability and microbial activity, thus impeding microbial and plant root respiration, thereby affecting Rs (Davidson et al., 2012; Fuchslueger et al., 2014). However, other points of view have indicated that extreme drought may lead to restricted root growth as well as soil organic matter-related microbial decomposition, with significant decreases in Rs (Sheik et al., 2011). Liu et al. (2016) suggested that an increase in precipitation also leads to an increase in Rs across arid regions, and the relevant excitation rate possibly decreases as climate humidity increases. Our results revealed that Rs increased significantly under late drought ($p < 0.05$) but decreased not significantly under early and midterm drought (**Figures 2C,D**). The responses of Rs diverged in response to drought in different stages of the growing season because autotrophic and heterotrophic Rs respond asymmetrically to drought (Huang et al., 2018). More detailed process analysis is necessary to reveal the mechanisms.

Both Re and RS are generally classified into heterotrophic and autotrophic respiration source components (Zhou et al., 2019). Under the continuous input of plant-derived C, soil constitutes the largest terrestrial C pool, which plays a decisive role in the global C cycle (Witzgall et al., 2021). Therefore, these results have implications for ecosystem function and climate change adaptation. If precipitation pattern change in the region leads to extreme drought events in the late period of the growing season, rather than the early or midterm period, then a significant increase in Rs could disrupt the balance of soil-atmosphere CO_2 exchange, resulting in a loss of soil C pools and triggering C-climate positive feedback. These results provide new insights into assessing the risks and benefits of extreme drought in alpine peatlands. In the future, a better understanding of the source components of Re and Rs will help to understand their overall response during different periods of extreme drought events.

Effects of Extreme Drought on Soil Enzyme Activities

Previous studies have compared the effects of drought on soil EEAs, but the results are controversial. A meta-analysis indicated that a decrease in precipitation caused a prominent decrease in soil microbial biomass and oxidoreductase activity by 11.61 and 10.99%, respectively, while C-acquisition hydrolase activity increased by 25.79% (Ren et al., 2017). Geisseler et al. (2011) suggested that, under dry conditions, soil EEAs significantly increased. According to Freeman et al. (2004), drought in peatlands increases oxygen and oxidase activity, resulting in low abundance of phenolic materials, which can further stimulate BG and BX activities. Plant standing biomass and soil substrates are considered to affect the response of C-acquisition EEAs to extreme drought (Beier et al., 2012; Steinauer et al., 2015). Therefore, in different extreme drought periods, the difference

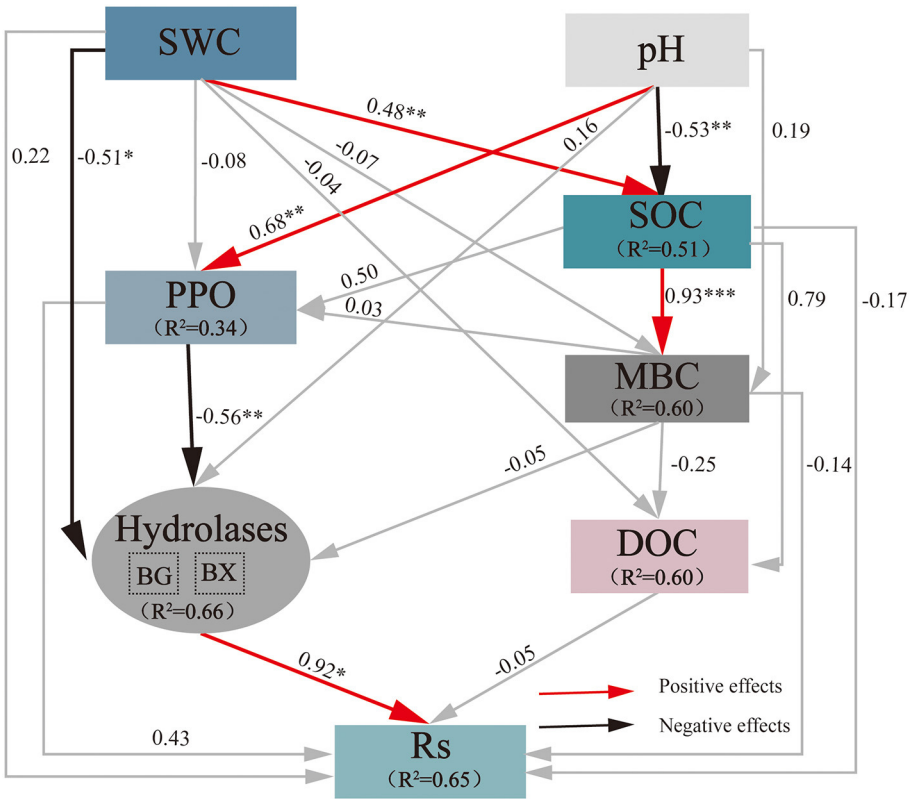

FIGURE 5 | Impacts of selected drivers on Rs under extreme drought calculated by the SEM of path analysis based on data collected in 2019. The values on the arrows are normalized path coefficients, and the asterisks after the numbers indicate remarkable correlations (*$p < 0.05$, **$p < 0.01$, and ***$p < 0.001$). The rectangle R^2 value represents the ratio of variance explained by relationships with other variables. SWC, soil water content; SOC, soil organic carbon; MBC, microbial biomass carbon; DOC, dissolved organic carbon; BG, β-1,4-glucosidase; Rs, soil respiration.

in plant coverage may also cause different changes in soil C-, N-, and P-acquisition EEAs (Baldrian, 2009; Baldrian et al., 2013; Bowles et al., 2014). Our results showed that, in an alpine peatland, the effects of extreme drought on soil EEAs were not uniform when comparing the early, midterm, and late periods of the growing season. Extreme drought that occurred during the plant-wilting period remarkably promoted soil oxidoreductase activity by 77.66 (PPO) and 109.60% (PEO) and increased P-acquisition hydrolase (ALP) activity by 76.46%. In contrast, extreme drought did not affect C-acquisition hydrolase (AG, BG, BX, and CB) or N-acquisition hydrolase (NAG and LAP) activities. The significant increase in soil oxidoreductase activity typically involved in recalcitrant C turnover under late drought in this study is in line with many studies (Li et al., 2020; Su et al., 2020) that have found that drought accelerated the degradation and C loss of peatlands (Zeng et al., 2021).

Due to the difference in SWC and its impacts on soil microbial biomass and plant productivity, the response of soil EEAs to drought showed divergence at different periods of extreme drought. The reduction in SWC and SBM was not the highest in the late-drought treatment of 2019, while the MBC was increased compared with the control treatment, which signified changes in plant and microbial competition, thereby facilitating microbial physiological activity and promoting the secretion of soil extracellular enzymes by a range of bacteria and fungi (Falade et al., 2017). During the early and midterm drought periods, the soil DOC was lower than that during the late-drought period, which showed that there were seasonal differences in the C turnover rate in different periods. In addition, a decline in the soil extractable C supply was caused by extreme drought through their indirect impact on plant growth (Zhou et al., 2019), therefore resulting in different changes in soil EEAs. Massive SOC storage was locked up in peatlands, probably because of the high stabilized oxidative enzyme activity induced by higher soil moisture and anaerobic environments (Freeman et al., 2001), while the high-potential activity of oxidative enzymes accelerated the degradation of phenolic compounds and thereby, increased decomposition potentials (Sinsabaugh, 2010). In our study, a decline in SOC under early, midterm, and late drought was observed; in particular, the increased oxidase activities under the late-drought period may be linked to large amounts of soil C loss and threaten the C-sink function of peatlands in the future.

Impact of Pathways of Extreme Drought on Alpine Peatland CO_2 Efflux

Previous studies have suggested that drought may have a significant impact on the underground C dynamics of overwhelming terrestrial ecosystems (Suseela et al., 2014), which

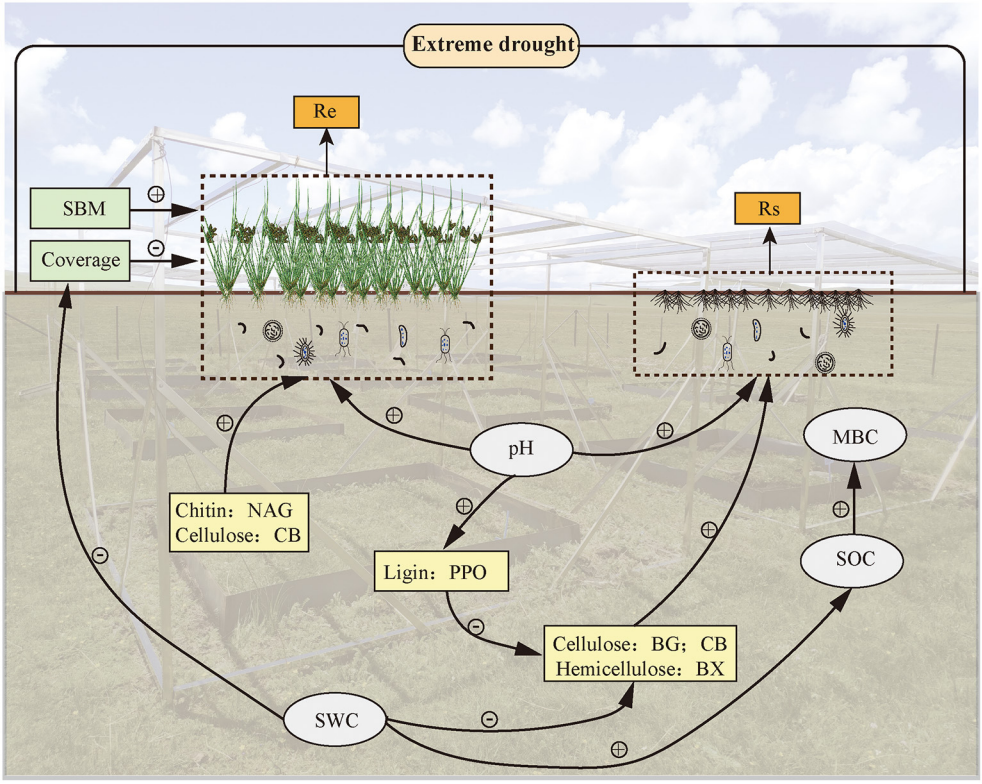

FIGURE 6 | A conceptual framework outlining the direct effects of soil EEAs, soil physicochemical properties, and plant variables on ecosystem C dynamics under extreme-drought conditions.

implied that extreme drought could alter the decomposition of SOM with corresponding consequences for Re. Here, with a field-manipulative extreme drought experiment using different influencing factors, an obvious positive correlation of soil hydrolases, including C-acquisition (CB) and N-acquisition (NAG), with Re (**Figure 4**) could be found, and this correlation should mainly come from the effect of soil hydrolases on the decomposition of SOM (Collins et al., 2008; Sinsabaugh, 2010). Because the autotrophic respiration of aboveground plants accounts for a large proportion of Re, we also observed that Re is significantly positively correlated with SBM and negatively correlated with plant coverage (**Figure 4**). Previous studies have shown that drought causes species to adapt to low-humidity habitats to replace species adapted to flooded habitats of different peatland types (Weltzin et al., 2000; Bakker et al., 2007). In the peatland of the Qinghai-Tibetan Plateau, the SBM decreased and remained unchanged in the 1st and 2nd years after the water table decreased and began to increase in the 3rd year. The increase in primary productivity is mainly due to the transformation of dominant aquatic plants into mesophytes (Cao et al., 2017; Wang et al., 2017b), and the duration of groundwater-level reduction has a great impact on the composition of the plant community. In this study, after the annual extreme drought event, there was still a rewet period to promote the restoration of vegetation, which was the same as the conclusion of short-term drought in the previous 2 years of the above studies. However, the change in vegetation community led to the increase in vegetation coverage, so SBM and plant coverage had different effects on ecosystem respiration, and plant coverage showed a significant and negative correlation with SWC (**Figure 4**). Although different periods of extreme drought did not cause significant changes in Re, under a series of complex influencing factors, Re showed a consistent downward trend in the early, midterm, and late extreme drought compared to the ambient control. It is worth noting that the investigation of the vegetation community should be strengthened, and different components of Re responses to extreme-drought events should be explored to reveal the multiple sources of Re variations.

The rate-limiting procedure of soil organic matter decomposition is catalyzed by soil extracellular enzymes; the activity of which plays a key role in determining Rs (Chen et al., 2018). Oxidative enzymes promote the oxidation and degradation of refractory compounds, containing phenols (Sinsabaugh, 2010), namely, PPO and PEO (Martinez et al., 2005). As a major component in the plant cell wall, the cellulose and hemicellulose hydrolase process has been primarily catalyzed by hydrolytic enzymes, such as BG, BX, and CB (Jian et al., 2016; Chen et al., 2017). This result conformed to former findings, the breakdown in organic matter and the release of CO_2 from biogeochemical cascades by stimulating cellulose

(BG) and hemicellulose (BX) hydrolase (**Figure 5**). Although oxidase activities are often considered to be uncorrelated with hydrolase activities (Sinsabaugh, 2010), the "enzymatic latch" hypothesis proposed by Freeman et al. (2001) showed that hydrolytic enzyme activities inhibited by phenolic compounds accumulate in peat because of the protection from degradation by oxidative enzymes. Our results do not support the concept of the "enzymatic latch" because PPO was significantly negatively correlated with soil hydrolase (BG and BX) (**Figure 5**). Recent studies have raised similar challenges for the "enzymatic latch" (Urbanova and Hajek, 2021). The reason may be that the peat microbial community seems to adapt to the natural high-phenol concentration, which is characteristic of other non-oceanic northern peatlands. In addition, we found that PPO activities showed a significant and positive correlation with soil pH, and similar results were also observed by Wu et al. (2021). Additionally, the negative relationships of soil hydrolase activities with SWC indicated that extreme drought may have the potential to stimulate soil hydrolases.

To take a closer look at driving forces in regulating ecosystem CO_2 release, we analyzed the influence of Re and Rs on changes in plants and soil EEAs during extreme drought (**Figure 6**). At present, the characterization of soil organic matter decomposition under soil EEAs regulation is lacking in the model prediction of ecosystem C dynamics (Davidson and Janssens, 2006; Wieder et al., 2013; Luo et al., 2016). However, we found that extreme drought-induced changes in soil hydrolases, as well as oxidases, possibly stimulate a continuous increase in Rs at the end of plant growth under repeated extreme drought conditions, which suggests the need to integrate enzymatic decomposition with soil biogeochemical models, and the mechanisms that regulate the effects in different periods remain to be elucidated. Furthermore, soil extracellular enzymes that are mainly produced by microorganisms play an important role in the decomposition of SOM, which also shows the importance of soil microorganisms in soil C turnover (Van Bodegom et al., 2005; Fenner and Freeman, 2011).

CONCLUSION

In the current study, the responses of the factors we measured to extreme drought were inconsistent; Re, Rs, and soil EEAs exhibited no significant change in the early and midterm drought periods of the growing season compared with the ambient control, while plant coverage significantly increased in the early drought and SBM significantly decreased in the midterm drought. The activities of soil oxidases and P-acquisition enzymes, as well as Rs, were significantly enhanced under late drought. The results of the structural equation model suggested that SWC, pH, NAG, CB, plant coverage, and SBM were the main forcing variables affecting Re dynamics, and SWC, pH, SOC, DOC, MBC, BX, BG, and PPO were the main forcing variables affecting Rs dynamics. Overall, this study provides experimental evidence that extreme drought occurring during the plant-withering period increased Rs, which altered the CO_2 balance between the soil and atmosphere in alpine peatlands. The regulation of plants and soil EEAs during Re and Rs changes suggested their important roles in the process of determining alpine ecosystem C emissions. The above findings help gain insights into C-climate feedback under future climate change and provide scientific evidence to maintain the functions and sustainability of the alpine peatland ecosystem. In future research, it is necessary to investigate and explain the impact mechanisms of the species composition of vegetation, as well as the resistance and resilience of alpine peatland ecosystem functions to extreme drought events.

DATA AVAILABILITY STATEMENT

The raw data supporting the conclusions of this article will be made available by the authors, without undue reservation.

AUTHOR CONTRIBUTIONS

ZY, YL, YH, and XK: contributed to the conception and the design of the study. EK and HW: organized the database. ZY and KZ: performed the statistical analysis. ZY and XK: wrote the first draft of the manuscript. ML, XZ, JW, and LY wrote sections of the manuscript. All the authors contributed to manuscript revision and read and approved the submitted version.

FUNDING

This study was supported by the National Non-profit Institute Research Grant (CAFYBB2019SY030), the National Natural Science Foundation of China (32171597 and 42041005), and the National Non-profit Institute Research Grant (CAFYBB2020ZA004).

REFERENCES

Asadieh, B., and Krakauer, N. Y. (2015). Global trends in extreme precipitation: climate models vs. observations. *Hydrol. Earth Syst. Sci.* 19, 877–891. doi: 10.5194/hess-19-877-2015

Bakker, C., van Bodegom, P. M., Nelissen, H. J. M., Aerts, R., and Ernst, W. H. O. (2007). Preference of wet dune species for waterlogged conditions can be explained by adaptations and specific recruitment requirements. *Aquat. Bot.* 86, 37–45. doi: 10.1016/j.aquabot.2006.08.005

Baldrian, P. (2009). Microbial enzyme-catalyzed processes in soils and their analysis. *Plant Soil Environ.* 55, 370–378. doi: 10.17221/134/2009-PSE

Baldrian, P., Snajdr, J., Merhautova, V., Dobiasova, P., Cajthaml, T., and Valaskova, V. (2013). Responses of the extracellular enzyme activities in hardwood forest to soil temperature and seasonality and the potential effects of climate change. *Soil Biol. Biochem.* 56, 60–68. doi: 10.1016/j.soilbio.2012.01.020

Beer, C., Reichstein, M., Tomelleri, E., Ciais, P., Jung, M., Carvalhais, N., et al. (2010). Terrestrial gross carbon dioxide uptake: global distribution and covariation with climate. *Science* 329, 834–838. doi: 10.1126/science.1184984

Beier, C., Beierkuhnlein, C., Wohlgemuth, T., Penuelas, J., Emmett, B., Korner, C., et al. (2012). Precipitation manipulation experiments–challenges and recommendations for the future. *Ecol. Lett.* 15, 899–911. doi: 10.1111/j.1461-0248.2012.01793.x

Bhanja, S. N., and Wang, J. Y. (2021). Influence of environmental factors on autotrophic, soil and ecosystem respirations in Canadian boreal forest. *Ecol. Indic.* 125:107517. doi: 10.1016/j.ecolind.2021.107517

Bond-Lamberty, B., Bailey, V. L., Chen, M., Gough, C. M., and Vargas, R. (2018). Globally rising soil heterotrophic respiration over recent decades. *Nature* 560:80. doi: 10.1038/s41586-018-0358-x

Bond-Lamberty, B., and Thomson, A. (2010). Temperature-associated increases in the global soil respiration record. *Nature* 464, 579–582. doi: 10.1038/nature08930

Bowles, T. M., Acosta-Martinez, V., Calderon, F., and Jackson, L. E. (2014). Soil enzyme activities, microbial communities, and carbon and nitrogen availability in organic agroecosystems across an intensively managed agricultural landscape. *Soil Biol. Biochem.* 68, 252–262. doi: 10.1016/j.soilbio.2013.10.004

Burns, R. G., DeForest, J. L., Marxsen, J., Sinsabaugh, R. L., Stromberger, M. E., Wallenstein, M. D., et al. (2013). Soil enzymes in a changing environment: current knowledge and future directions. *Soil Biol. Biochem.* 58, 216–234. doi: 10.1016/j.soilbio.2012.11.009

Cao, R., Wei, X., Yang, Y. H. S., Xi, X. Q., and Wu, X. W. (2017). The effect of water table decline on plant biomass and species composition in the Zoige peatland: a four-year *in situ* field experiment. *Agric. Ecosyst. Environ.* 247, 389–395. doi: 10.1016/j.agee.2017.07.008

Carey, J. C., Tang, J., Templer, P. H., Kroeger, K. D., Crowther, T. W., Burton, A. J., et al. (2016). Temperature response of soil respiration largely unaltered with experimental warming. *Proc. Natl. Acad. Sci. U.S.A.* 113, 13797–13802. doi: 10.1073/pnas.1605365113

Carreiro, M. M., Sinsabaugh, R. L., Repert, D. A., and Parkhurst, D. F. (2000). Microbial enzyme shifts explain litter decay responses to simulated nitrogen deposition. *Ecology* 81, 2359–2365. doi: 10.1890/0012-9658(2000)0812359:MESELD2.0.CO;2

Chen, H., Yang, G., Peng, C. H., Zhang, Y., Zhu, D., Zhu, Q. A., et al. (2014). The carbon stock of alpine peatlands on the Qinghai-Tibetan Plateau during the Holocene and their future fate. *Quat. Sci. Rev.* 95, 151–158. doi: 10.1016/j.quascirev.2014.05.003

Chen, J., Luo, Y. Q., Garcia-Palacios, P., Cao, J. J., Dacal, M., Zhou, X. H., et al. (2018). Differential responses of carbon-degrading enzyme activities to warming: implications for soil respiration. *Glob. Change Biol.* 24, 4816–4826. doi: 10.1111/gcb.14394

Chen, J., Luo, Y. Q., Li, J. W., Zhou, X. H., Cao, J. J., Wang, R. W., et al. (2017). Costimulation of soil glycosidase activity and soil respiration by nitrogen addition. *Glob. Change Biol.* 23, 1328–1337. doi: 10.1111/gcb.13402

Chen, J., Luo, Y. Q., Xia, J. Y., Shi, Z., Jiang, L. F., Niu, S. L., et al. (2016). Differential responses of ecosystem respiration components to experimental warming in a meadow grassland on the Tibetan Plateau. *Agric. For. Meteorol.* 220, 21–29. doi: 10.1016/j.agrformet.2016.01.010

Chen, J., Zhang, Y., Luo, Y., Zhou, X., Jiang, Y., Zhao, J., et al. (2019). Contrasting responses after fires of the source components of soil respiration and ecosystem respiration. *Eur. J. Soil Sci.* 70, 616–629. doi: 10.1111/ejss.12786

Collins, S. L., Sinsabaugh, R. L., Crenshaw, C., Green, L., Porras-Alfaro, A., Stursova, M., et al. (2008). Pulse dynamics and microbial processes in aridland ecosystems. *J. Ecol.* 96, 413–420. doi: 10.1111/j.1365-2745.2008.01362.x

Dai, A. G. (2013). Increasing drought under global warming in observations and models. *Nat. Clim. Change* 3, 52–58. doi: 10.1038/nclimate1633

Davidson, E. A., and Janssens, I. A. (2006). Temperature sensitivity of soil carbon decomposition and feedbacks to climate change. *Nature* 440, 165–173. doi: 10.1038/nature04514

Davidson, E. A., Samanta, S., Caramori, S. S., and Savage, K. (2012). The Dual Arrhenius and Michaelis-Menten kinetics model for decomposition of soil organic matter at hourly to seasonal time scales. *Glob. Change Biol.* 18, 371–384. doi: 10.1111/j.1365-2486.2011.02546.x

De Deyn, G. B., Cornelissen, J. H. C., and Bardgett, R. D. (2008). Plant functional traits and soil carbon sequestration in contrasting biomes. *Ecol. Lett.* 11, 516–531. doi: 10.1111/j.1461-0248.2008.01164.x

Deng, L., Peng, C. H., Kim, D. G., Li, J. W., Liu, Y. L., Hai, X. Y., et al. (2021a). Drought effects on soil carbon and nitrogen dynamics in global natural ecosystems. *Earth Sci. Rev.* 214:103501. doi: 10.1016/j.earscirev.2020.103501

Deng, Y., Wang, X. H., Wang, K., Ciais, P., Tang, S. C., Jin, L., et al. (2021b). Responses of vegetation greenness and carbon cycle to extreme droughts in China. *Agric. For. Meteorol.* 298–299:108307. doi: 10.1016/j.agrformet.2020.108307

Dominguez, M. T., Holthof, E., Smith, A. R., Koller, E., and Emmett, B. A. (2017). Contrasting response of summer soil respiration and enzyme activities to long-term warming and drought in a wet shrubland (NE Wales, UK). *Agric. Ecosyst. Environ. Appl. Soil Ecol.* 110, 151–155. doi: 10.1016/j.apsoil.2016.11.003

Falade, A. O., Eyisi, O. A. L., Mabinya, L. V., Nwodo, U. U., and Okoh, A. I. (2017). Peroxidase production and ligninolytic potentials of fresh water bacteria Raoultella ornithinolytica and Ensifer adhaerens. *Biotech. Rep.* 16, 12–17. doi: 10.1016/j.btre.2017.10.001

Fenner, N., and Freeman, C. (2011). Drought-induced carbon loss in peatlands. *Nat. Geosci.* 4, 895–900. doi: 10.1038/ngeo1323

Fenner, N., Freeman, C., Reynolds, B. (2005). Hydrological effects on the diversity of phenolic degrading bacteria in a peatland: implications for carbon cycling. *Soil Biol. Biochem.* 37, 1277–1287. doi: 10.1016/j.soilbio.2004.11.024

Flanagan, L. B., Sharp, E. J., and Letts, M. G. (2013). Response of plant biomass and soil respiration to experimental warming and precipitation manipulation in a northern great plains grassland. *Agric. For. Meteorol.* 173, 40–52. doi: 10.1016/j.agrformet.2013.01.002

Freeman, C., Ostle, N., and Kang, H. (2001). An enzymic "latch" on a global carbon store–a shortage of oxygen locks up carbon in peatlands by restraining a single enzyme. *Nature* 409:149. doi: 10.1038/35051650

Freeman, C., Ostle, N. J., Fenner, N., and Kang, H. (2004). A regulatory role for phenol oxidase during decomposition in peatlands. *Soil Biol. Biochem.* 36, 1663–1667. doi: 10.1016/j.soilbio.2004.07.012

Fuchslueger, L., Bahn, M., Fritz, K., Hasibeder, R., and Richter, A. (2014). Experimental drought reduces the transfer of recently fixed plant carbon to soil microbes and alters the bacterial community composition in a mountain meadow. *New Phytol.* 201, 916–927. doi: 10.1111/nph.12569

Gao, W. L., Reed, S. C., Munson, S. M., Rui, Y. C., Fan, W. Y., Zheng, Z. Z., et al. (2021). Responses of soil extracellular enzyme activities and bacterial community composition to seasonal stages of drought in a semiarid grassland. *Geoderma* 401:115327. doi: 10.1016/j.geoderma.2021.115327

Garssen, A. G., Verhoeven, J. T. A., and Soons, M. B. (2014). Effects of climate-induced increases in summer drought on riparian plant species: a meta-analysis. *Freshw. Biol.* 59, 1052–1063. doi: 10.1111/fwb.12328

Geisseler, D., Horwath, W. R., and Scow, K. M. (2011). Soil moisture and plant residue addition interact in their effect on extracellular enzyme activity. *Pedobiologia* 54, 71–78. doi: 10.1016/j.pedobi.2010.10.001

Hao, Y. B., Zhang, H., Biederman, J. A., Li, L. F., Cui, X. Y., Xue, K., et al. (2018). Seasonal timing regulates extreme drought impacts on CO_2 and H_2O exchanges over semiarid steppes in Inner Mongolia, China. *Agric. Ecosyst. Environ.* 266, 153–166. doi: 10.1016/j.agee.2018.06.010

Henry, H. A. L. (2012). Soil extracellular enzyme dynamics in a changing climate. *Soil Biol. Biochem.* 47, 53–59. doi: 10.1016/j.soilbio.2011.12.026

Hoover, D. L., and Rogers, B. M. (2016). Not all droughts are created equal: the impacts of interannual drought pattern and magnitude on grassland carbon cycling. *Glob. Change Biol.* 22, 1809–1820. doi: 10.1111/gcb.13161

Hu, Q. W., Wu, Q., Yao, B., and Xu, X. L. (2015). Ecosystem respiration and its components from a Carex meadow of Poyang Lake during the drawdown period. *Atmo. Environ.* 100, 124–132. doi: 10.1016/j.atmosenv.2014.10.047

Huang, S. D., Ye, G. F., Lin, J., Chen, K. T., Xu, X., Ruan, H. H., et al. (2018). Autotrophic and heterotrophic soil respiration responds asymmetrically to drought in a subtropical forest in the Southeast China. *Soil Boil. Biochem.* 123, 242–249. doi: 10.1016/j.soilbio.2018.04.029

Huang, Z. Q., Clinton, P. W., Baisden, W. T., and Davis, M. R. (2011). Long-term nitrogen additions increased surface soil carbon concentration in a forest plantation despite elevated decomposition. *Soil Biol. Biochem.* 43, 302–307. doi: 10.1016/j.soilbio.2010.10.015

Jackson, C. R., Tyler, H. L., and Millar, J. J. (2013). Determination of microbial extracellular enzyme activity in waters, soils, and sediments using high throughput microplate assays. *J. Vis. Exp.* 80:50399. doi: 10.3791/50399

Jian, S. Y., Li, J. W., Chen, J., Wang, G. S., Mayes, M. A., Dzantor, K. E., et al. (2016). Soil extracellular enzyme activities, soil carbon and nitrogen storage under nitrogen fertilization: a meta-analysis. *Soil Biol. Biochem.* 101, 32–43. doi: 10.1016/j.soilbio.2016.07.003

Kang, X. M., Hao, Y. B., Cui, X. Y., Chen, H., Huang, S. X., Du, Y. G., et al. (2016). Variability and changes in climate, phenology, and gross primary production of an alpine wetland ecosystem. *Remote Sens*. 8:391. doi: 10.3390/rs8050391

Kang, X. M., Yan, L., Cui, L. J., Zhang, X. D., Hao, Y. B., Wu, H. D., et al. (2018). Reduced carbon dioxide sink and methane source under extreme drought condition in an alpine peatland. *Sustainability* 10:4285. doi: 10.3390/su10114285

Kato, T., Tang, Y. H., Gu, S., Cui, X. Y., Hirota, M., Du, M. Y., et al. (2004). Carbon dioxide exchange between the atmosphere and an alpine meadow ecosystem on the Qinghai-Tibetan Plateau, China. *Agric. For. Meteorol.* 124, 121–134. doi: 10.1016/j.agrformet.2003.12.008

Laiho, R. (2006). Decomposition in peatlands: reconciling seemingly contrasting results on the impacts of lowered water levels. *Soil Biol. Biochem.* 38, 2011–2024. doi: 10.1016/j.soilbio.2006.02.017

Li, T., Ge, L. M., Huang, J. J., Yuan, X., Peng, C. H., Wang, S. Z., et al. (2020). Contrasting responses of soil exoenzymatic interactions and the dissociated carbon transformation to short-and long-term drainage in a minerotrophic peatland. *Geoderma* 377:114585. doi: 10.1016/j.geoderma.2020.114585

Liu, L. L., Wang, X., Lajeunesse, M. J., Miao, G. F., Piao, S. L., Wan, S. Q., et al. (2016). A cross-biome synthesis of soil respiration and its determinants under simulated precipitation changes. *Glob. Change Biol.* 22, 1394–1405. doi: 10.1111/gcb.13156

Luo, Y. Q. (2007). Terrestrial carbon-cycle feedback to climate warming. *Annu. Rev. Ecol. Evol. Syst.* 38, 683–712. doi: 10.1146/annurev.ecolsys.38.091206.095808

Luo, Y. Q., Ahlstrom, A., Allison, S. D., Batjes, N. H., Brovkin, V., Carvalhais, N., et al. (2016). Toward more realistic projections of soil carbon dynamics by Earth system models. *Global Biogeochem. Cycles* 30, 40–56. doi: 10.1002/2015GB005239

Ma, K., Liu, J. G., Balkovic, J., Skalsky, R., Azevedo, L. B., and Kraxner, F. (2016). Changes in soil organic carbon stocks of wetlands on China's Zoige plateau from 1980 to 2010. *Ecol. Model.* 327, 18–28. doi: 10.1016/j.ecolmodel.2016.01.009

Ma, W. W., Li, G., Wu, J. H., Xu, G. R., and Wu, J. Q. (2020). Respiration and CH_4 fluxes in Tibetan peatlands are influenced by vegetation degradation. *CATENA* 195:104789. doi: 10.1016/j.catena.2020.104789

Maestre, F. T., Valladares, F., and Reynolds, J. F. (2005). Is the change of plant–plant interactions with abiotic stress predictable? A meta-analysis of field results in arid environments. *J. Ecol.* 93, 748–757. doi: 10.1111/j.1365-2745.2005.01017.x

Martinez, A. T., Speranza, M., Ruiz-Duenas, F. J., Ferreira, P., Camarero, S., Guillen, F., et al. (2005). Biodegradation of lignocellulosics: microbial chemical, and enzymatic aspects of the fungal attack of lignin. *Int. Microbiol.* 8, 195–204.

Mastepanov, M., Sigsgaard, C., Dlugokencky, E. J., Houweling, S., Strom, L., Tamstorf, M. P., et al. (2008). Large tundra methane burst during onset of freezing. *Nature* 456, 628–658. doi: 10.1038/nature07464

Metcalfe, D. B., Fisher, R. A., and Wardle, D. A. (2011). Plant communities as drivers of soil respiration: pathways, mechanisms, and significance for global change. *Biogeosciences* 8, 2047–2061. doi: 10.5194/bg-8-2047-2011

Mishra, A. K., and Singh, V. P. (2010). A review of drought concepts. *J. Hydrol.* 391, 202–216. doi: 10.1016/j.jhydrol.2010.07.012

Pind, A., Freeman, C., and Lock, M. A. (1994). Enzymatic degradation of phenolic materials in peatlands-measurement of phenol oxidase activity. *Plant Soil* 159, 227–231. doi: 10.1007/BF00009285

Potvin, L. R., Kane, E. S., Chimner, R. A., Kolka, R. K., and Lilleskov, E. A. (2015). Effects of water table position and plant functional group on plant community, aboveground production, and peat properties in a peatland mesocosm experiment (PEATcosm). *Plant Soil* 387, 277–294. doi: 10.1007/s11104-014-2301-8

Ren, C. J., Zhao, F. Z., Shi, Z., Chen, J., Han, X. H., Yang, G. H., et al. (2017). Differential responses of soil microbial biomass and carbon-degrading enzyme activities to altered precipitation. *Soil Biol. Biochem.* 115, 1–10. doi: 10.1016/j.soilbio.2017.08.002

Sagar, R., Li, G. Y., Singh, J. S., and Wan,. S. (2019). Carbon fluxes and species diversity in grazed and fenced typical steppe grassland of inner Mongolia, China. *J. Plant Ecol.* 12, 10–22. doi: 10.1093/jpe/rtx052

Schlesinger, W. H., Dietze, M. C., Jackson, R. B., Phillips, R. P., Rhoades, C. C., Rustad, L. E., et al. (2016). Forest biogeochemistry in response to drought. *Glob. Change Biol.* 22, 2318–2328. doi: 10.1111/gcb.13105

Schönbeck, L., Gessler, A., Schaub, M., Rigling, A., Hoch, G., Kahmen, A., et al. (2020). Soil nutrients and lowered source:sink ratio mitigate effects of mild but not of extreme drought in trees. *Environ. Exp. Bot.* 169:103905. doi: 10.1016/j.envexpbot.2019.103905

Sheffield, J., and Wood, E. F. (2012). *Drought: Past Problems and Future Scenarios*. London: Routledge Press. doi: 10.4324/9781849775250

Sheik, C. S., Beasley, W. H., Elshahed, M. S., Zhou, X. H., Luo, Y. Q., and Krumholz, L. R. (2011). Effect of warming and drought on grassland microbial communities. *ISME J.* 5, 1692–1700. doi: 10.1038/ismej.2011.32

Sinsabaugh, R. L. (2010). Phenol oxidase, peroxidase and organic matter dynamics of soil. *Soil Biol. Biochem.* 42, 391–404. doi: 10.1016/j.soilbio.2009.10.014

Steinauer, K., Tilman, D., Wragg, P. D., Cesarz, S., Cowles, J. M., Pritsch, K., et al. (2015). Plant diversity effects on soil microbial functions and enzymes are stronger than warming in a grassland experiment. *Ecology* 96, 99–112. doi: 10.1890/14-0088.1

Su, X. L., Su, X., Zhou, G. Y., Du, Z. G., Yang, S. C., Ni, M. Y., et al. (2020). Drought accelerated recalcitrant carbon loss by changing soil aggregation and microbial communities in a subtropical forest. *Soil Biol. Biochem.* 148:107898. doi: 10.1016/j.soilbio.2020.107898

Suseela, V., Tharayil, N., Xing, B. S., and Dukes, J. S. (2014). Warming alters potential enzyme activity but precipitation regulates chemical transformations in grass litter exposed to simulated climatic changes. *Soil Biol. Biochem.* 75, 102–112. doi: 10.1016/j.soilbio.2014.03.022

Urbanova, Z., and Hajek, T. S. (2021). Revisiting the concept of "enzymic latch" on carbon in peatlands. *Sci. Total Environ.* 779:146384. doi: 10.1016/j.scitotenv.2021.146384

Van Bodegom, P. M., Broekman, R., Van Dijk, J., Bakker, C., and Aerts, R. (2005). Ferrous iron stimulates phenol oxidase activity and organic matter decomposition in waterlogged wetlands. *Biogeochemistry* 76, 69–83. 10533–005–2053-x. doi: 10.1007/s10533-005-2053-x

Wang, H., Yu, L. F., Zhang, Z. H., Liu, W., Chen, L. T., Cao, G. M., et al. (2017a). Molecular mechanisms of water table lowering and nitrogen deposition in affecting greenhouse gas emissions from a Tibetan alpine wetland. *Glob. Change Biol.* 23, 815–829. doi: 10.1111/gcb.13467

Wang, M., Ding, Z., Wu, C. Y., Song, L. S., Ma, M. G., Yu, P. J., et al. (2021). Divergent responses of ecosystem water-use efficiency to extreme seasonal droughts in Southwest China. *Sci. Total Environ.* 760:143427. doi: 10.1016/j.scitotenv.2020.143427

Wang, Y. H., Yan, D. H., Wang, J. F., Ding, Y., and Song, X. S. (2017b). Effects of elevated CO_2 and drought on plant physiology, soil carbon and soil enzyme activities. *Pedosphere* 27, 846–855. doi: 10.1016/S1002-0160(17)60458-2

Weltzin, J. F., Pastor, J., Harth, C., Bridgham, S. D., Updegraff, K., and Chapin, C. T. (2000). Response of bog and fen plant communities to warming and water-table manipulations. *Ecology* 81, 3464–3478. doi: 10.1890/0012-9658(2000)0813464:ROBAFP2.0.CO;2

Wieder, W. R., Bonan, G. B., and Allison, S. D. (2013). Global soil carbon projections are improved by modeling microbial processes. *Nat. Clim. Change* 3, 909–912. doi: 10.1038/nclimate1951

Witzgall, K., Vidal, A., Schubert, D. I., Höschen, C., Schweizer, S. A., Buegger, F., et al. (2021). Particulate organic matter as a functional soil component for persistent soil organic carbon. *Nat. Commun.* 12, 4115. doi: 10.1038/s41467-021-24192-8

Wu, G. H., Chen, Z. H., Jiang, D. Q., Jiang, N., Jiang, H., and Chen, L. J. (2021). Oxidases and hydrolases mediate soil organic matter accumulation in chernozem of northeastern China. *Geoderma* 403:115206. doi: 10.1016/j.geoderma.2021.115206

Xia, J. Y., Niu, S. L., and Wan, S. Q. (2009). Response of ecosystem carbon exchange to warming and nitrogen addition during two hydrologically contrasting growing seasons in a temperate steppe. *Glob. Change Biol.* 15, 1544–1556. doi: 10.1111/j.1365-2486.2008.01807.x

Yan, Z. Q., Li, Y., Wu, H. D., Zhang, K. R., Hao, Y. B., Wang, J. Z., et al. (2020). Different responses of soil hydrolases and oxidases to extreme drought in an alpine peatland on the Qinghai-Tibet Plateau, China. *Eur. J. Soil Biol.* 99:103195. doi: 10.1016/j.ejsobi.2020.103195

Yu, H. Y., Liu, X. D., Ma, Q. H., Yin, Z. T., Wang, Y. H., Xu, Z. Z., et al. (2021). Climatic warming enhances soil respiration resilience in an arid ecosystem. *Sci. Total Environ.* 756:144005. doi: 10.1016/j.scitotenv.2020.144005

Zang, Y. X., Min, X. J., de Dios, V. R., Ma, J. Y., and Sun, W. (2020). Extreme drought affects the productivity, but not the composition, of a desert plant

community in Central Asia differentially across microtopographies. *Sci. Total Environ*. 717:137251. doi: 10.1016/j.scitotenv.2020.137251

Zeng, J., Chen, H., Bai, Y. P., Dong, F. Q., Peng, C. H., Yan, F., et al. (2021). Water table drawdown increases plant biodiversity and soil polyphenol in the Zoige Plateau. *Ecol. Indic*. 121:107118. doi: 10.1016/j.ecolind.2020.107118

Zhou, G., Luo, Q., Chen, Y., Hu, J., He, M., Gao, J., et al. (2019). Interactive effects of grazing and global change factors on soil and ecosystem respiration in grassland ecosystems: a global synthesis. *J. Appl. Ecol*. 56, 2007–2019. doi: 10.1111/1365-2664.13443

Zhou, L. Y., Zhou, X. H., Zhang, B. C., Lu, M., Luo, Y. Q., and Liu, L. L. (2014). Different responses of soil respiration and its components to nitrogen addition among biomes: a meta-analysis. *Glob. Change Biol*. 20, 2332–2343. doi: 10.1111/gcb.12490

Zhou, X. H., Zhou, L. Y., Nie, Y. Y., Fu, Y. L., Du, Z. G., Shao, J. J., et al. (2016). Similar responses of soil carbon storage to drought and irrigation in terrestrial ecosystems but with contrasting mechanisms: a meta-analysis. *Agric. Ecosyst. Environ*. 228, 70–81. doi: 10.1016/j.agee.2016.04.030

Conflict of Interest: The authors declare that the research was conducted in the absence of any commercial or financial relationships that could be construed as a potential conflict of interest.

Publisher's Note: All claims expressed in this article are solely those of the authors and do not necessarily represent those of their affiliated organizations, or those of the publisher, the editors and the reviewers. Any product that may be evaluated in this article, or claim that may be made by its manufacturer, is not guaranteed or endorsed by the publisher.

Copyright © 2021 Yan, Kang, Zhang, Li, Hao, Wu, Li, Zhang, Wang, Yan and Kang. This is an open-access article distributed under the terms of the Creative Commons Attribution License (CC BY). The use, distribution or reproduction in other forums is permitted, provided the original author(s) and the copyright owner(s) are credited and that the original publication in this journal is cited, in accordance with accepted academic practice. No use, distribution or reproduction is permitted which does not comply with these terms.

frontiers in Plant Science

ORIGINAL RESEARCH
published: 15 October 2021
doi: 10.3389/fpls.2021.760599

Plants and Microbes Mediate the Shift in Ecosystem Multifunctionality From Low to High Patterns Across Alpine Grasslands on the Tibetan Plateau

Yi Wang[1,2,3], Miao Liu[4], Youchao Chen[5], Tao Zeng[6], Xuyang Lu[7], Bin Yang[8], Yafeng Wang[3], Lin Zhang[3], Xiaowei Nie[3], Feipeng Xiao[1], Zhigang Zhang[1]* and Jian Sun[3]*

[1]College of Management Science and Engineering, Guangxi University of Finance and Economics, Nanning, China, [2]School of Life Sciences and School of Ecology, State Key Laboratory of Biological Control, Sun Yat-sen University, Guangzhou, China, [3]State Key Laboratory of Tibetan Plateau Earth System, Resources and Environment (TPESRE), Institute of Tibetan Plateau Research, Chinese Academy of Sciences, Beijing, China, [4]College of Grassland Science and Technology, China Agricultural University, Beijing, China, [5]Key Laboratory of Aquatic Botany and Watershed Ecology, Wuhan Botanical Garden, Chinese Academy of Sciences, Wuhan, China, [6]College of Earth Sciences, Chengdu University of Technology, Chengdu, China, [7]Key Laboratory of Mountain Surface Processes and Ecological Regulation, Institute of Mountain Hazards and Environment, Chinese Academy of Sciences, Chengdu, China, [8]Natural Resources Comprehensive Survey Command Center, China Geological Survey, Beijing, China

OPEN ACCESS

Edited by:
Shiliang Liu,
Beijing Normal University, China

Reviewed by:
Su Xukun,
Research Center for Eco-Environmental Sciences, Chinese Academy of Sciences (CAS), China
Jin Hua Li,
Lanzhou University, China
Zhanhuan Shang,
Lanzhou University, China

***Correspondence:**
Feipeng Xiao
xiaofeipeng01@126.com
Zhigang Zhang
tozzg@163.com

Specialty section:
This article was submitted to Functional Plant Ecology, a section of the journal Frontiers in Plant Science

Received: *18 August 2021*
Accepted: *24 September 2021*
Published: *15 October 2021*

Citation:
Wang Y, Liu M, Chen Y, Zeng T, Lu X, Yang B, Wang Y, Zhang L, Nie X, Xiao F, Zhang Z and Sun J (2021) Plants and Microbes Mediate the Shift in Ecosystem Multifunctionality From Low to High Patterns Across Alpine Grasslands on the Tibetan Plateau. Front. Plant Sci. 12:760599. doi: 10.3389/fpls.2021.760599

Both plant communities and soil microbes have been reported to be correlated with ecosystem multifunctionality (EMF) in terrestrial ecosystems. However, the process and mechanism of aboveground and belowground communities on different EMF patterns are not clear. In order to explore different response patterns and mechanisms of EMF, we divided EMF into low (<0) and high patterns (>0). We found that there were contrasting patterns of low and high EMF in the alpine grassland ecosystem on the Tibetan Plateau. Specifically, compared with low EMF, environmental factors showed higher sensitivity to high EMF. Soil properties are critical factors that mediate the impact of community functions on low EMF based on the change of partial correlation coefficients from 0 to 0.24. In addition, plant community functions and microbial biomass may mediate the shift of EMF from low to high patterns through the driving role of climate across the alpine grassland ecosystem. Our findings will be vital to clarify the mechanism for the stability properties of grassland communities and ecosystems under ongoing and future climate change.

Keywords: ecosystem multifunctionality, alpine grassland, plant community, microbial biomass, Tibetan Plateau

INTRODUCTION

Recently, due to the reduction of global biodiversity, researchers have paid considerable attention to the linkages between biodiversity and ecosystem functioning (Maestre et al., 2012; Wang et al., 2020a). Hence, ecosystem multifunctionality (EMF), which represents the simultaneous provision of multiple ecosystem functions, such as productivity, carbon storage, and the accumulation of nutrients, has been proposed as a reliable indicator to reflect the effects of ecosystem services

and functioning (Xu et al., 2013; Jing et al., 2015). Currently, plant biodiversity has been considered to play a key role in regulating the performance of ecosystems (Hector and Hooper, 2002; Hector and Bagchi, 2007; Zavaleta et al., 2010; Sun et al., 2020a). For example, compared with low plant community diversity, higher plant community diversity could maintain higher soil moisture, which may restrain the adverse effects of drought or warming on soil microbes and retain high EMF (Milcu et al., 2010; Zavaleta et al., 2010). But taking grassland EMF patterns seriously is far from straightforward due to the unknown of the belowground community.

Soil microbial communities drive most biogeochemical processes and play a vital role in driving the cycling of carbon and nitrogen and their interactions (Chapin et al., 2008; Xu et al., 2013; Zhang et al., 2021). In general, an increased substrate for soil microbes results in more microbial biomass and a more abundant microbial community (Eisenhauer et al., 2010). The amount of microbial biomass carbon and nitrogen plays a major role in regulating the process of decomposition and sequestration of soil carbon, as well as nitrogen immobilization, which may further affect EMF in terrestrial ecosystems (Lange et al., 2015). However, most studies examining the EMF come from single investigations at plot scale (Tilman et al., 1997; Hillebrand and Matthiessen, 2009; Mori et al., 2016; Gross et al., 2017). Few studies have examined the influences of soil microbes on the patterns of EMF at a large regional scale due to high spatial heterogeneities in soil microbial properties and limitations of sampling and measuring methods (Joergensen et al., 2011; Schmidt et al., 2011).

Grasslands, covering approximately 40% of the Earth's land, are sensitive to climate change and anthropogenic disturbance (Tilman et al., 2006; Reid et al., 2014), which could lead to a loss of above- and belowground biodiversity and a reduction in EMF (Hector and Bagchi, 2007; Mcsherry and Ritchie, 2013; Zhou et al., 2017). Previous studies have highlighted the effects of climate (Jing et al., 2015), plant communities (Diaz et al., 2007; Jing et al., 2015), soil microbes (Bonkowski and Roy, 2005), and mycorrhizal fungi (van der Heijden et al., 1998; Maherali and Klironomos, 2007) on the EMF. For abiotic drivers, several studies have shown that climate change and anthropogenic activities reduce the microbial abundance and the overall diversity of soil organisms (Helgason et al., 1998; De Vries et al., 2013; Wagg et al., 2014; Wang et al., 2019) and have concluded that the reduced biodiversity in soils may influence the EMF by impairing ecosystem functions such as the cycling of resources between above- and belowground communities (van der Heijden et al., 2008; Wall et al., 2010). Academics have revealed that precipitation is the main factor affecting the dynamics of vegetation in alpine grasslands, especially in arid areas (Hu et al., 2010), which may further regulate the ecosystem process and EMF. Additionally, the air temperature may be another driver in environmental geochemistry cycles and soil nutrient availability for plant growth (Zhou et al., 2020), which, to some extent, may contribute to EMF. For biotic drivers, sustaining EMF in grassland ecosystems requires both biodiversity assemblages and higher species richness (Zavaleta et al., 2010). In contrast, high EMF may require suitable environmental conditions. In addition, the complex interactions between soil factors and complex food webs can shape diversity within one trophic group or may change the microbial abundance, diversity, and EMF (Hunt and Wall, 2002; Duffy et al., 2007). However, most of these studies are more concerned that high above- and belowground biodiversity and fertile habitats may lead to high EMF. It is still far from clear how plant and soil microbial factors work better at different EMF levels, especially which factors critically mediate the transformation from lower to higher EMF across grassland ecosystems.

To fill these knowledge gaps, we selected alpine grasslands on the Tibetan Plateau as the study area and analyzed data from 115 sites distributed along an extensive water–heat gradient (**Figure 1**). The Tibetan Plateau is the highest and most extensive highland on Earth with an extraordinarily sensitive ecosystem about alpine grasslands to climate change (Sun et al., 2020b). Particularly, the plateau has natural water–heat gradients from southeast to northwest, making it an ideal region to explore EMF patterns along with climate gradients (Yang et al., 2010a). Under the influence of hydrothermal patterns, different alpine grassland types are formed as alpine meadow, steppe, and desert steppe, and plants may lead to a series of differences in habitat conditions and community characteristics in the process of long-term adaptation to climatic conditions (Zhou et al., 2020). Therefore, under the climate gradient, a suite of adaptation and regulation processes of above- and belowground communities will eventually lead to the difference of EMF. Besides, based on these special environmental conditions, more comprehensive climate, plant, and soil factors were involved in our study to investigate the interacting effects of changing climate and ecosystem functions on the different levels of EMF. Hence, we aimed to examine how climatic factors, plant communities, soil properties, and microbial factors influenced EMF, and explore: (1) the different response patterns of EMF to environmental factors, and (2) highlight the underlying mechanisms of plants and microbes mediate the EMF patterns.

MATERIALS AND METHODS

Study Area and Sampling

We collected plant and soil samples from 115 sites over a wide area ($2.3 \times 10^6 km^2$) on the Tibetan Plateau (80–105°E, 27–37°N; **Figure 1**) during the growing season of 2015. The sites covered two main vegetation types on the plateau, i.e., alpine meadow and alpine steppe. Random plots (10 m × 10 m) were set up within an area with less human disturbance. Plant and soil samples were taken across a large area along a transect running from the northwest region of Sichuan Province (32°52'N, 102°25'E), to mid-Qinghai Province (34°52'N, 98°2'E), and finally to northern Tibet (33°24'N, 88°34'E) for the obvious water–heat gradients. The sites ranged in elevation from 3,030 to 5,000 m.

Plant Measurement

Before soil sampling, we counted the numbers of species and calculated the relative abundance of each species. Species richness (SR) was defined according to the number of species.

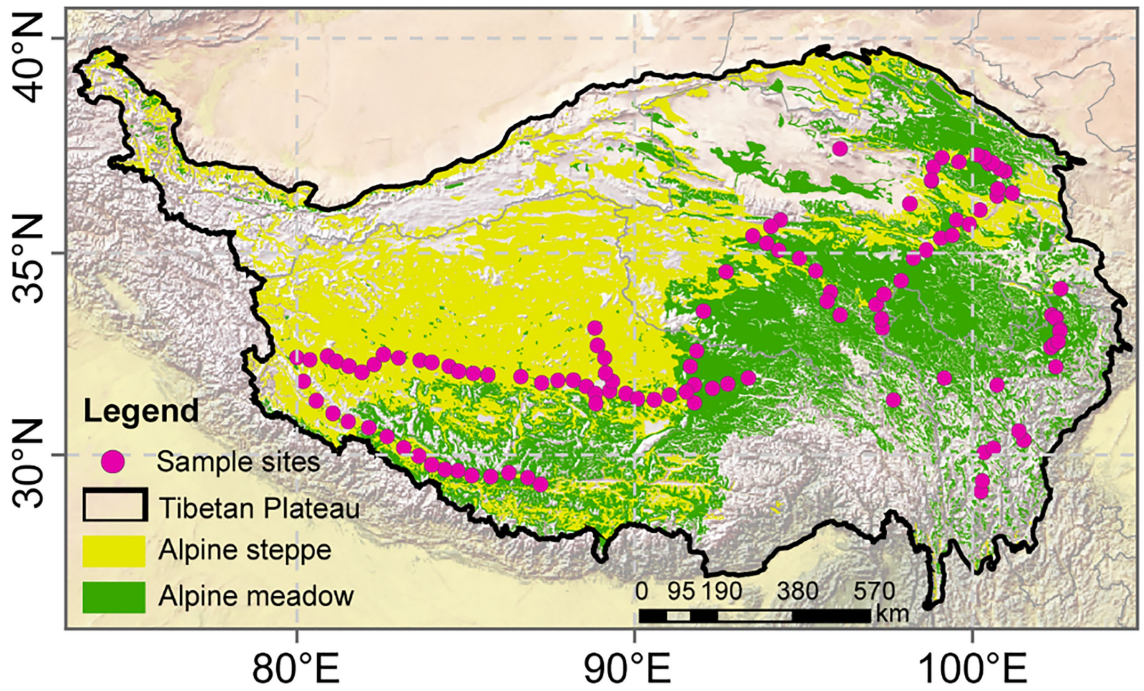

FIGURE 1 | Vegetation map of the Tibetan Plateau grasslands and location of sampling sites in 2015.

We harvested all standing plants in three quadrats (50 cm × 50 cm) to measure the aboveground biomass (AGB). Then, we ground part of the aboveground plant to a fine powder on a ball mill and analyzed plant nutrients. In addition, we collected 1,035 soil samples (0–10, 10–20, and 20–30 cm; 3 samples per site) from the sites for the determination of soil physicochemical properties, and the sum of the root biomass at each depth was treated as the belowground biomass (BGB). The biomass samples were dried at 65°C to constant mass and weighed to the nearest 0.01 g in the laboratory. We collected four plant traits: plant height (H), leaf nitrogen content (LN), leaf phosphorus content (LP), and leaf dry matter content (LDMC), which are known to be the key factors for acquiring sources and determining species abundance in grasslands (Ansquer et al., 2009). The plant height was calculated as the mean value of random individuals. We quantified functional diversity using community-weighted mean (CWM) values (Diaz et al., 2007), which were calculated as:

$$CWM = \sum p_i \times trait_i \quad (1)$$

where p_i is the relative abundance of species i in the community and $trait_i$ represents the trait value of species i (Lavorel et al., 2007).

Physiochemical Data Measurements

For plant nutrients, LN was determined by combustion on a Vario MACRO cube elemental analyzer (Elementar Analysensysteme Gmb H, Germany; Lu et al., 2015). LP was measured with the molybdate colorimetric test (Sommers and Nelson, 1972). For soil properties, soil water content (SWC) and soil bulk density (SBD) were tested using a drying method (Yao, 2006); soil organic carbon content (SOC) and soil total nitrogen content (STN) were determined by combustion on a Vario MACRO cube elemental analyzer (Lu et al., 2015); and soil total phosphorus content (STP) was measured with the molybdate colorimetric test after perchloric acid digestion (Sommers and Nelson, 1972). Soil available nitrogen content (SAN) was determined from the alkali hydrolyzable fraction, and soil available phosphorus content (SAP) was measured by the Olsen method (Sun et al., 2018). For soil microbial factors, the determination of microbial biomass carbon content (MBC) and nitrogen content (MBN) was performed with the chloroform–K_2SO_4 extraction method (Vance et al., 1987).

Climate and Phenological Data

For each of the sites, we compiled annual mean temperature (AMT) and annual total precipitation (ATP) from the National Meteorological Bureau of China database.[1] The ATP and AMT raster databases at a resolution of 1 km were spatially interpolated by Anusplin 4.2 (Centre for Resource and 220 Environmental Studies, Australian National University, Canberra). Our sites in AMT ranged from −2.4 to 6.8°C, and those in ATP ranged from 143 to 860 mm. The aridity index (AI) was calculated according to the method of Sun et al. (2020b). Phenological data stemming from the Global Inventory Modelling and Mapping Studies (Gonsamo et al., 2018), phenology features of the start of the growing season, and the peak of the growing season in 2015 were determined through simple linear regression analysis. Then, the start of the growing season and the peak

[1]http://data.cma.cn/

of the growing season were calculated using the derivatives of the fitted Fourier model (Sun et al., 2020b). Ultimately, the length of growing season accumulation (GSL) was calculated by the difference between the above two parameters.

Ecosystem Multifunctionality

Several variables were used to assess ecosystem functions by plant nutrients: (1) LN, (2) LP; plant productivity: (3) AGB, (4) BGB; soil properties: (5) SWC, (6) SOC, (7) STN, (8) STP, (9) SAN, (10) SAP; microbe: (11) MBC, (12) MBN. Considering the feature direct and interpretable measure to synthesize the multiple functions simultaneously, we adopted the average approach and used the EMF index (Maestre et al., 2012).

$$EMF = \sum_{j}^{n} Z_{ij} / n \quad (2)$$

Z_{ij} is the Z-score of ecosystem function j of plot i, and n is the number of ecosystem functions. We calculated the Z-scores for each of the ecosystem functions evaluated (Maestre et al., 2012):

$$Z_{ij} = \left(x_{ij} - \lambda_j\right) / \delta_j \quad (3)$$

x_{ij} is the value of ecosystem function j of plot i, λ_j is the mean value of ecosystem function j across all sites, and δ_j is the standard deviation of ecosystem function j across all sites. Notably, in this study, EMF indices above 0 are defined as high EMF, and those below 0 are defined as low EMF.

Statistical Analyses

First, we evaluated the relationships between effect factors and EMF using SPSS version 25.0 (SPSS, Inc., Chicago, IL, USA). Meanwhile, we conducted the box figure connected with the difference of EMF and environmental factors with Analysis of Variances, performed using the "*ggplot2*" and "*aov*" function in the base package of R version 3.6.0 (R Development Core Team). Second, a general linear model was utilized to explore the relationship of environmental factors and EMF under low and high EMF conditions by the packages "*ggplot2*" in R software. Partial correlations were adopted to judge main control elements by the packages "*plspm*," "*Hmisc*," "*ppcor*," and "*igraph*" in R software. Ultimately, we used the structural equation model (SEM) to determine the direct and indirect effects of climate, productivity, community functions, and soil microbes on EMF, which includes a synthesis of factor analysis, path analysis, and maximum likelihood analysis (Doncaster, 2007). We eliminated nonsignificant pathways and state variables and simplified the primary model based on regression weight estimates. Each model was fitted with the root mean square error of approximation (RMSEA; the model has an acceptable fit when $0.00 \leq \text{RMSEA} \leq 0.05$). Moreover, the Akaike information criterion, a criterion for the goodness of fit of SEM, was also used to select the most appropriate model. All the models were developed with AMOS 21 software (IBM SPSS Inc.).

RESULTS

Patterns of EMF

We found a high correlation coefficient of SAN ($r = 0.90$), STN ($r = 0.90$), MBN ($r = 0.89$), MBC ($r = 0.88$), SOC ($r = 0.88$), and SWC ($r = 0.86$) with EMF ($p < 0.01$; **Figure 2A**). Besides, EMF showed significantly negative correlation with SBD ($r = -0.86$, $p < 0.01$), CWM_LN ($r = -0.32$, $p < 0.01$), and AMT ($r = -0.21$, $p < 0.05$; **Figure 2A**). There was a significant difference between low EMF (mean value −0.44) and high EMF (mean value 0.66; $p < 0.01$; **Figure 2B**). Except GSL and AMT, all environmental factors showed significant difference ($p < 0.01$) under low EMF and high EMF conditions (**Figure 2B**).

Different Response of EMF to Environmental Factors

By the fitted lines between EMF and effect factors, eight variables, including AI, AGB, BGB, CWM_LDMC, STN, and MBN, showed a higher slope and R-square with high EMF. In particular, the slope of AI, AGB, SWC, and MBN with high EMF was more than twice the slope of low EMF (0.008–0.016, 0.001–0.003, 0.603–3.482, and 0.002–0.004). Other factors such as ATP, SR, CWM_LP, CWM_H, and STP expressed an opposite relationship of different EMFs (**Figure 3**; **Table 1**).

All environmental factors were divided into five potential variables, i.e., climate, productivity, community functions, soil properties, and soil microbe, under low EMF and high EMF conditions. For climate, positive weights were expressed by ATP (0.46) and AI (0.42) under low EMF conditions, but negative weights were expressed with the weight value of −0.38 and −0.61 under high EMF conditions, respectively (**Figures 4A,F**). However, productivity and soil microbe showed similar characteristics across different patterns (**Figures 4B,E,G,J**). CWM_H has a negative weight (−0.14) to community functions under low EMF conditions, but for a positive weight (0.23) under high EMF conditions (**Figures 4C,H**). Except for SBD, other factors have a positive contribution to the group of soil properties under different patterns (**Figures 4D,I**).

According to the partial correlations among potential variables and low EMF, soil properties contributed most to low EMF. Particularly, after eliminating their influence, the partial correlation coefficients of soil microbe decreased from 0.37 to 0.07, and productivity decreased from 0.29 to −0.21 (**Figure 5A**). It was highlighted that community functions showed a huge increase from 0 to 0.24 after eliminating the influence from soil properties (**Figure 5A**). Additionally, no matter which potential variables are excluded, there is a negative correlation between climate and low EMF (**Figure 5A**). In high EMF conditions, soil microbe contributed most to EMF, which resulted in a reduction of partial correlation coefficients about climate (from 0.51 to 0.12), productivity (from 0.57 to 0.30), community functions (from 0.46 to 0.12), and soil properties (from 0.89 to 0.74; **Figure 5B**).

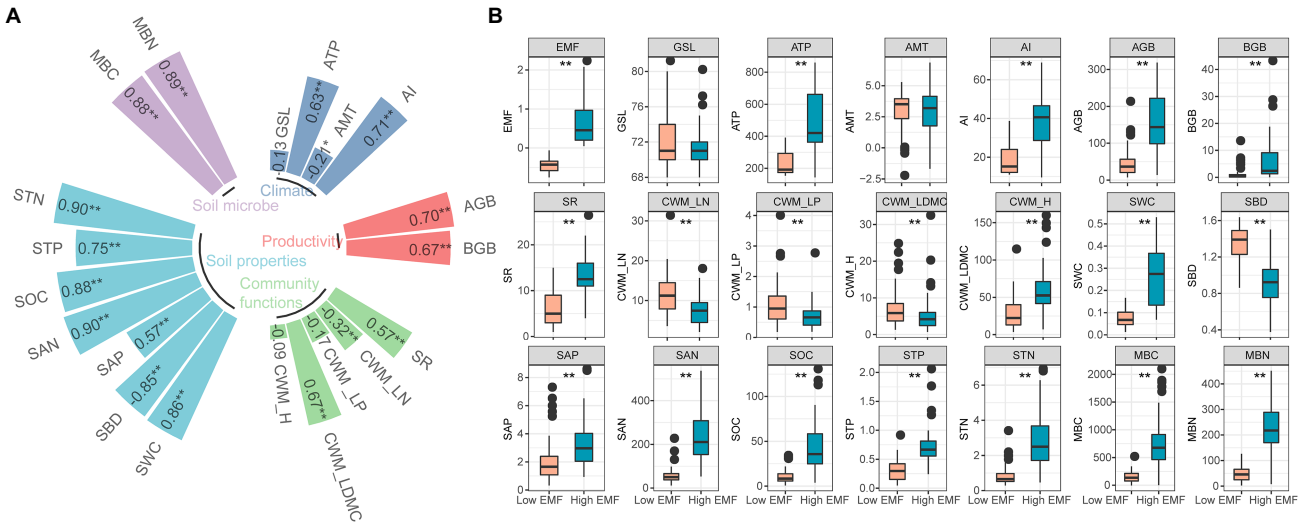

FIGURE 2 | Characteristics of ecosystem multifunctionality and environmental factors. **(A)** Relationship among ecosystem multifunctionality and climate, productivity, community functions, soil properties, soil microbial factors, and the value in the square represents the value of the correlation coefficient between each factor with ecosystem multifunctionality. * and ** show the significant correlations at 0.05 and 0.01 levels. **(B)** Difference of low and high ecosystem multifunctionality combined with environmental factors. Statistical significance between low and high ecosystem multifunctionality conditions was assessed by one-way ANOVA analysis. $^{**}p < 0.01$. EMF, ecosystem multifunctionality; GSL, start of growing season to the peak of growing season; ATP, annual total precipitation (mm); AMT, annual mean temperature (°C); AI, aridity index; AGB, aboveground biomass ($g\,m^{-2}$); BGB, belowground biomass ($g\,m^{-2}$); SR, species richness; CWM_LN, community-weighted mean value of leaf nitrogen; CWM_LP, community-weighted mean value of leaf phosphorus; CWM_LDMC, community-weighted mean value of leaf dry matter content; CWM_H, community-weighted mean value of plant height; SWC, soil water content (%); SBD, soil bulk density ($g\,cm^{-3}$); SAP, soil available phosphorus content ($mg\,kg^{-1}$); SAN, soil available nitrogen content ($mg\,kg^{-1}$); SOC, soil organic carbon content ($g\,kg^{-1}$); STP, soil total phosphorus content (%); MBC, microbial biomass carbon content ($mg\,kg^{-1}$); MBN, microbial biomass nitrogen content ($mg\,kg^{-1}$).

SEM Mining the EMF Links to Environmental Factors

Path analyses demonstrated that climate generated significant negative effects on productivity, soil properties, and soil microbe with the standard total effects of −0.65, −0.25, and −0.36, respectively, under low EMF conditions (**Figure 6A**). EMF was determined by productivity, community functions, soil microbe, and soil properties with standard total effect values of 0.22, 0.48, 0.19, and 0.69, respectively (**Figure 6A**). In contrast, climate exerted significant positive effects on productivity, community functions, soil microbe, and soil properties with the standard total effects of 0.34, 0.35, 0.46, and 0.32, respectively, under high EMF conditions (**Figure 6B**). There were significant positive effects of productivity, soil microbe, and soil properties on EMF (effect coefficients are 0.28, 0.38, and 0.61, respectively; **Figure 6B**). Nevertheless, community functions had significant negative effects on high EMF with an effect coefficient of −0.21 (**Figure 6B**).

DISCUSSION

Drivers of Low and High EMF Patterns

The relationship between EMF and its drivers may reflect the differences in the life histories of habitats, which are closely tied to above- and belowground communities (Jing et al., 2015). Our results emphasized that the abiotic and biotic environmental factors influenced EMF on the Tibetan Plateau (**Figure 2**). For the influence of climate, our results highlighted the important role of precipitation under low EMF conditions (**Figures 2, 3**; **Table 1**). Meanwhile, the AI index, which could reflect functions that drive the responses of plant nutrients to soils, plants, and eutrophication (Anderson et al., 2018), was positively correlated with high EMF with a higher slope than with low EMF (**Figure 3**). The plant biomass and species richness of alpine grassland generally increased from northwestern to southeastern Tibetan Plateau, which was closely related to the water–heat pattern (Zong et al., 2019; Sun et al., 2020b), and connected with the higher sensitivity response of low EMF. As for community functions, productivity, and soil properties, for example, AGB, CWM_LDMC, and SOC shaped EMF with higher sensitivity response under high EMF conditions (**Figure 3**; **Table 1**). Previous studies reported similar results on the relationships between biomass, soil nutrients, and EMF (Jing et al., 2015), which showed that, through the driving role of precipitation and soil moisture, higher water availability contributes to higher primary productivity and higher nutrient availability (Ma et al., 2010; Yang et al., 2010b; Sun et al., 2021b), leading to an increase in EMF. Besides, the role of soil microbial factors in driving different EMF patterns may be reflected by high correlations and sensitivity (**Figures 2, 3**). In grassland ecosystems, heterotrophic microbes usually accommodate with the suitable nutrient environment, which can promote

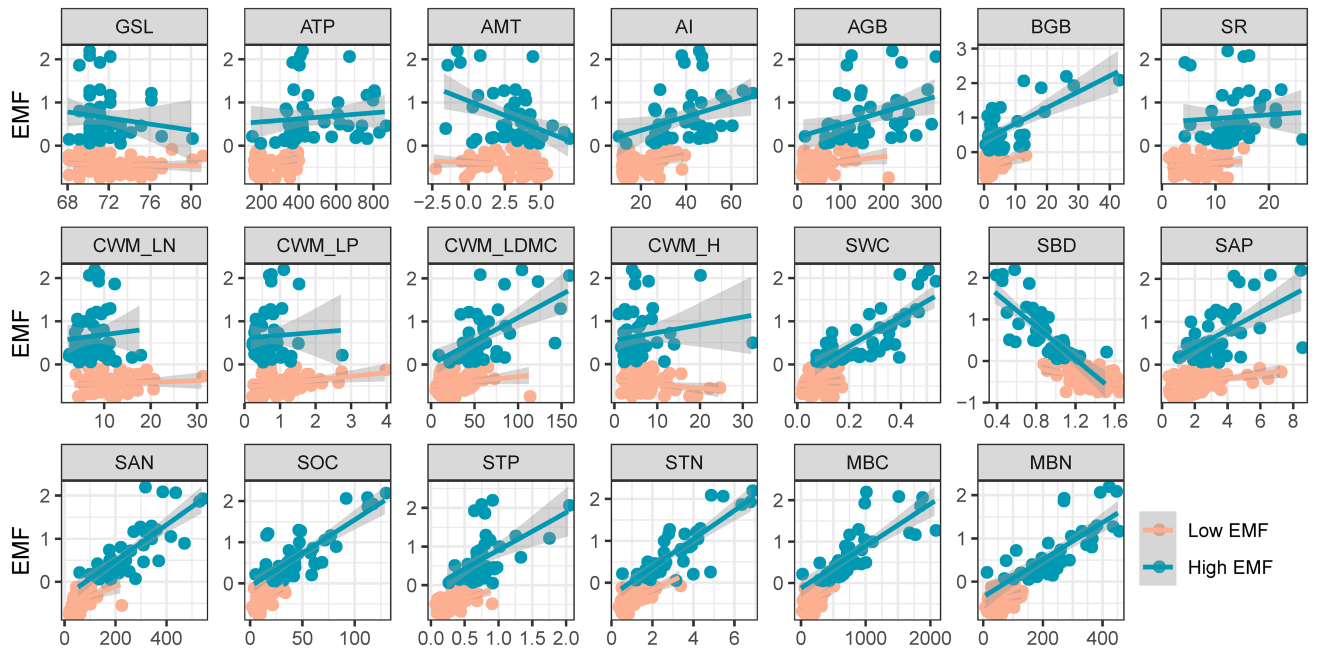

FIGURE 3 | Relationship among low and high ecosystem multifunctionality and effect factors. EMF, ecosystem multifunctionality; GSL, start of growing season to the peak of growing season; ATP, annual total precipitation (mm); AMT, annual mean temperature (°C); AI, aridity index; AGB, aboveground biomass ($g\,m^{-2}$); BGB, belowground biomass ($g\,m^{-2}$); SR, species richness; CWM_LN, community-weighted mean value of leaf nitrogen; CWM_LP, community-weighted mean value of leaf phosphorus; CWM_LDMC, community-weighted mean value of leaf dry matter content; CWM_H, community-weighted mean value of plant height; SWC, soil water content (%); SBD, soil bulk density ($g\,cm^{-3}$); SAP, soil available phosphorus content ($mg\,kg^{-1}$); SAN, soil available nitrogen content ($mg\,kg^{-1}$); SOC, soil organic carbon content ($g\,kg^{-1}$); STP, soil total phosphorus content (%); MBC, microbial biomass carbon content ($mg\,kg^{-1}$); MBN, microbial biomass nitrogen content ($mg\,kg^{-1}$). Red and green lines are the fitted lines from ordinary least squares regressions. Shaded areas show the 95% CI of the fit.

TABLE 1 | Results of the general linear regressions among low and high ecosystem multifunctionality (low EMF and high EMF) and influencing factors.

Observed variables	Low EMF				High EMF			
	R^2	*p*	Slope	Intercept	R^2	*p*	Slope	Intercept
GSL	0.004	$p > 0.05$	−0.037	−0.170	0.018	$p > 0.05$	−0.035	3.165
ATP	0.120	$p < 0.01$	0.001	−0.627	0.010	$p > 0.05$	0.000	0.482
AMT	0.017	$p > 0.05$	−0.015	−0.394	0.190	$p < 0.01$	−0.134	1.035
AI	0.100	$p < 0.01$	0.008	−0.584	0.120	$p < 0.05$	0.016	0.037
AGB	0.060	$p < 0.05$	0.001	−0.495	0.130	$p < 0.01$	0.003	0.197
BGB	0.120	$p < 0.01$	0.032	−0.473	0.430	$p < 0.01$	0.046	0.364
SR	0.020	$p > 0.05$	0.008	−0.487	0.010	$p > 0.05$	0.009	0.543
CWM_LN	0.007	$p > 0.05$	0.003	−0.475	0.006	$p > 0.05$	0.014	0.552
CWM_LP	0.087	$p < 0.05$	0.085	−0.528	0.002	$p > 0.05$	0.066	0.610
CWM_LDMC	0.050	$p > 0.05$	0.002	−0.496	0.320	$p < 0.01$	0.011	0.004
CWM_H	0.058	$p < 0.05$	−0.009	−0.371	0.026	$p > 0.05$	0.018	0.556
SWC	0.017	$p > 0.05$	0.603	−0.483	0.569	$p < 0.01$	3.482	−0.276
SBD	0.2395	$p < 0.01$	−0.493	0.229	0.604	$p < 0.01$	−1.956	2.390
SAP	0.182	$p < 0.01$	0.055	−0.546	0.339	$p < 0.01$	0.206	−0.015
SAN	0.168	$p < 0.01$	0.002	−0.569	0.634	$p < 0.01$	0.004	−0.346
SOC	0.360	$p < 0.01$	0.017	−0.611	0.630	$p < 0.01$	0.016	−0.078
STP	0.256	$p < 0.01$	0.516	−0.602	0.274	$p < 0.01$	0.969	−0.060
STN	0.430	$p < 0.01$	0.229	−0.630	0.690	$p < 0.01$	0.338	−0.306
MBC	0.210	$p < 0.01$	0.001	−0.572	0.600	$p < 0.01$	0.001	−0.122
MBN	0.090	$p < 0.05$	0.002	−0.532	0.570	$p < 0.01$	0.004	−0.351

GSL, the start of the growing season to the peak of the growing season; ATP, annual total precipitation; AMT, annual mean temperature; AI, aridity index; AGB, aboveground biomass; BGB, belowground biomass; SR, species richness; CWM_LN, community-weighted mean value of leaf nitrogen; CWM_LP, community-weighted mean value of leaf phosphorus; CWM_LDMC, community-weighted mean value of leaf dry matter content; CWM_H, community-weighted mean value of plant height; SWC, soil water content; SBD, soil bulk density; SAP, soil available phosphorus; SAN, soil available nitrogen; SOC, soil organic carbon; STP, soil total phosphorus; SAN; MBC, microbial biomass carbon; MBN, microbial biomass nitrogen.

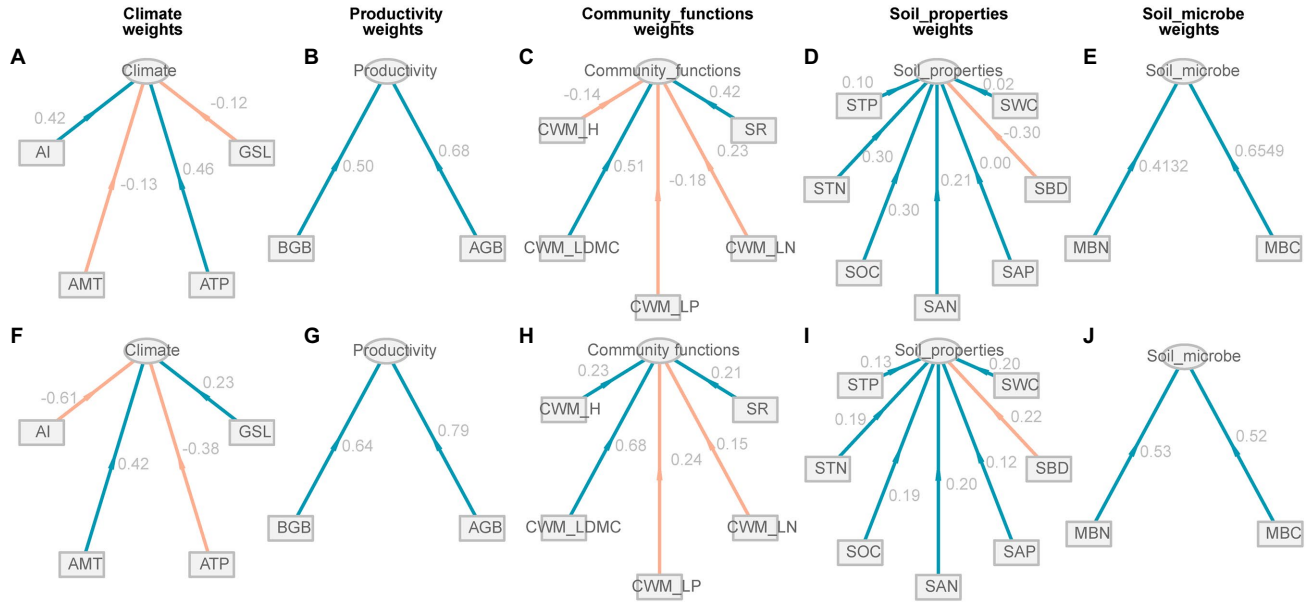

FIGURE 4 | Relationship between observed variables and potential variables of climate, productivity, community functions, soil properties, and soil microbial factors. **(A–E)** Low ecosystem multifunctionality conditions. **(F–J)** High ecosystem multifunctionality conditions. The value next to the line represents the path coefficient between observed variables and potential variables. Red lines represent the negative weights, and green lines represent the positive weights. GSL, the start of growing season to the peak of growing season; ATP, annual total precipitation; AMT, annual mean temperature; AI, aridity index; AGB, aboveground biomass; BGB, belowground biomass; SR, species richness; CWM_LN, community-weighted mean value of leaf nitrogen; CWM_LP, community-weighted mean value of leaf phosphorus; CWM_LDMC, community-weighted mean value of leaf dry matter content; CWM_H, community-weighted mean value of plant height; SWC, soil water content; SBD, soil bulk density; SAP, soil available phosphorus; SAN, soil available nitrogen; SOC, soil organic carbon; STP, soil total phosphorus; MBC, microbial biomass carbon; MBN, microbial biomass nitrogen.

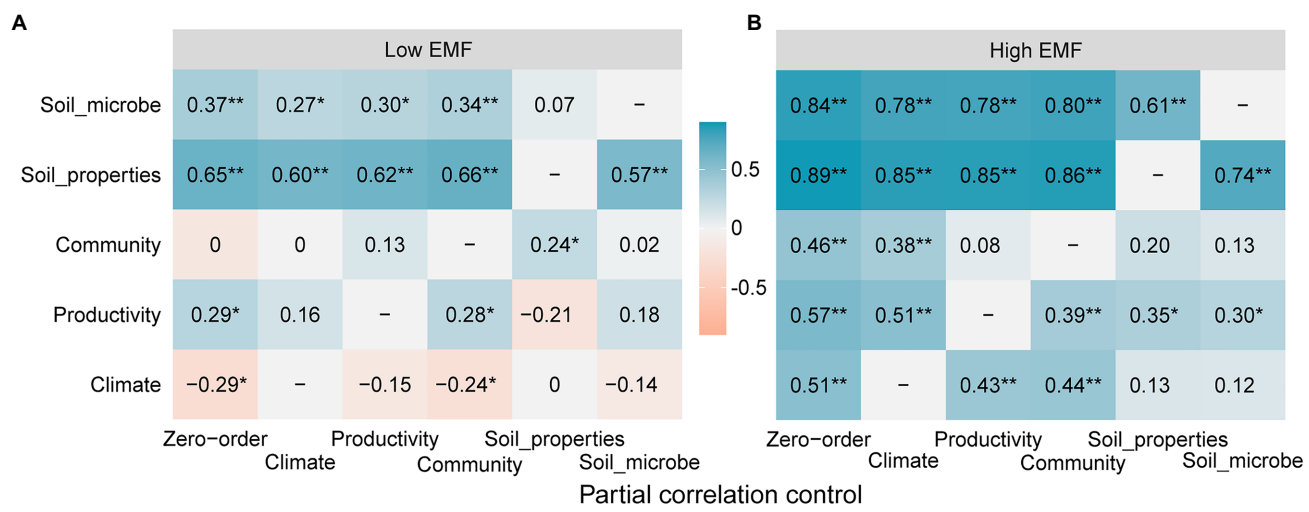

FIGURE 5 | Partial correlations among potential variables of climate, productivity, community functions, soil properties, soil microbial factors, and ecosystem multifunctionality (EMF) under **(A)** low EMF and **(B)** high EMF conditions, respectively. The value in the square represents the value of the correlation coefficient between potential variables from ordinate and ecosystem multifunctionality after eliminating the influence of abscissa variables. Zero-order represents the correlation coefficient between potential variables and EMF. * and ** show the significant correlations at 0.05 and 0.01 levels.

a series of biochemical reactions belowground, and are more sensitive to the variability of soil nutrients (Sistla and Schimel, 2012). In addition, the change of microbial metabolic characteristics is affected by the synergistic effect of plants and soil. Under the facilitation of soil carbon and nitrogen, soil microbial diversity increases, which shows the effect of microbial biomass on high EMF (Wang et al., 2021). To illustrate the mechanism deeply, how the belowground community affects the different EMFs needs to be further explored.

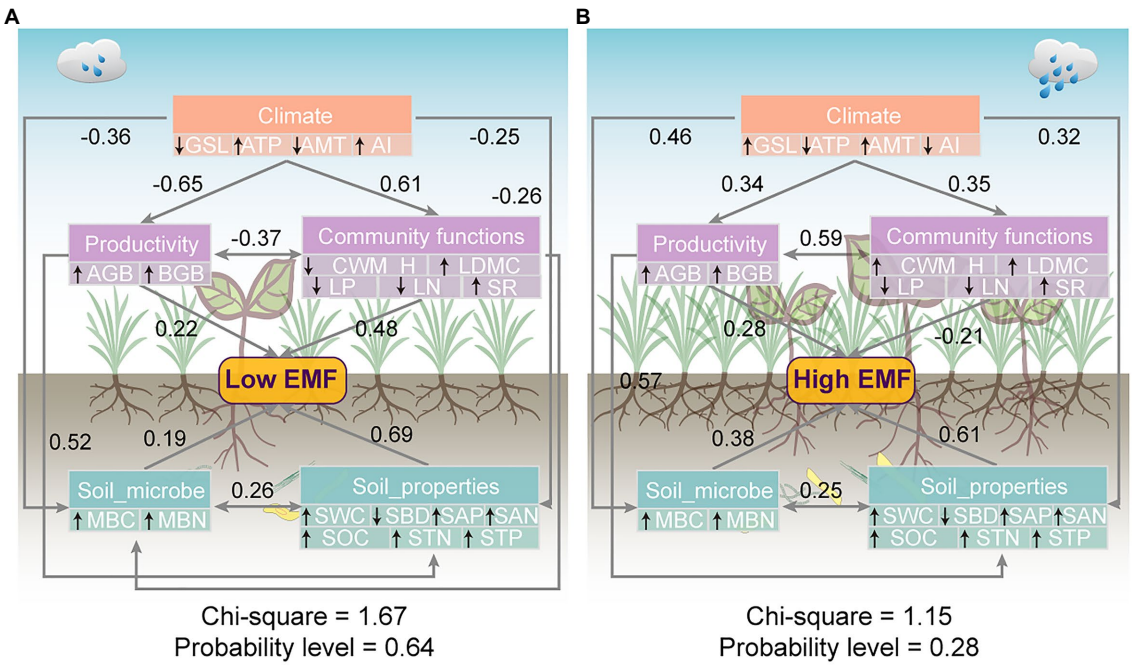

FIGURE 6 | Mechanisms for the patterns of **(A)** low ecosystem multifunctionality and **(B)** high ecosystem multifunctionality. Structure equation model examining the standard total effects of climate, productivity, community functions, soil properties, and soil microbial factors on EMF. Given are the standardized total path coefficients. Gray arrows represent significantly paths ($p < 0.05$). Black arrows pointing up or down in double-layer rectangles represent the positive or negative relationships between the observed variables and potential variables.

Mechanism of Low EMF

In our study, the partial correlation of community functions showed a shift on low EMF (**Figure 4**). Through the driver of the climate, SEM indicated a higher effect coefficient of community functions (0.48) on low EMF than soil microbes (0.19; **Figure 6A**). The key drivers of climatic factors such as ATP have been proven to shape the positive relationship between biodiversity and EMF (Ma et al., 2010). On the one hand, low EMF environments are usually accompanied by drought, the increase in precipitation could increase species richness and further induces the increase in EMF (Xu et al., 2018). On the other hand, researchers revealed that precipitation amendment had indirect positive effects on community functions and may play a key role in improving ecosystem stability (Falster and Westoby, 2003). Hence, our results showed high weights of CWM_LDMC (0.51) and SR (0.42), which led to low EMF (**Figures 4, 6A**). A previous study revealed that by increasing CWM_H, a vital trait that impacts plant carbon sequestration capacity, community productivity could have an indirect positive effect on EMF (Moles et al., 2009). However, our results showed a negative effect of plant height on low EMF, which is related to the hydraulic limitation hypothesis that with increasing plant height, the difficulty in supplying leaves with water and nutrition also increases (Moles et al., 2009), especially under poor environmental conditions. Moreover, productivity has direct effects (0.22) on low EMF (**Figure 6A**), which indicates that the positive effects of productivity, especially belowground productivity, on multifunctionality may be the main mediated function through increased community traits under a relatively suitable environment. Consequently, our results showed that under the low EMF environment, the primary task of the plant community may be to survive (Wang et al., 2020b).

Several studies have demonstrated that soil microbial communities play a key role in driving the resistance of EMF (Bunge et al., 2006; Wagg et al., 2014; Delgadobaquerizo et al., 2017). However, in this study, our results suggested that soil microbes had minor effects at EMF within low patterns (0.19; **Figure 6**) on the Tibetan Plateau scale. Consistent with several other studies in grassland ecosystems, an increase in soil nitrogen availability could increase plant community productivity and EMF (Jing et al., 2015; Demalach et al., 2017). Nitrogen is imperative for the production of structural proteins as building portions of plant tissues (Gan et al., 2010). Accordingly, nitrogen has been proven to accelerate net carbon sequestration and contribute to increased community plant productivity across grassland ecosystems (Niu et al., 2010; Xu et al., 2018), further improving low EMF. Nevertheless, the biochemical processes of the ecosystem are often limited by the availability of organic carbon, especially in arid and semiarid habitats (Bapiri et al., 2010; Liu et al., 2020). Hence, the availability of soil nutrients may be the main explanation for the low effects of microbial factors on low EMF (**Figure 6A**). Summarily, based on the above driven by climate factors, the plant community plays a more crucial role in low EMF.

Mechanism of High EMF

In contrast to the low EMF pattern, our findings suggest that AMT showed stronger positive effects on high EMF than precipitation, with weight values of 0.43 (**Figures 4, 6**). Due to sufficient precipitation conditions, especially in an alpine meadow,

the increase in temperature could promote community diversity and soil nutrient accumulation (Sun and Wang, 2016). For community functions, plant traits can reflect the adaptability of plants to environmental changes and the nutrient utilization efficiency of plants (Thompson et al., 1997). However, in this study, community functions showed negative effects on high EMF with a path coefficient of −0.21 (**Figure 6A**), which may be linked with low leaf nutrient turnover in higher soil nutrient environments (Sun et al., 2021a). Previous studies identified specific microbial taxa that are probably major drivers of EMF, which is also supported by many experiments showing that the total abundance of microbes controls particular functions (Delgadobaquerizo et al., 2017). As highlighted, MBC and MBN were indicators of nutrient availability that included quickly available sources for microbial activity and were strongly linked to the activity of the soil microbial community (Bastida et al., 2016). Therefore, it is possible that under low EMF conditions, the activity of microorganisms is limited by soil nutrients, while under high EMF conditions, microorganisms can play an important and positive role, and the final results of SEM show an effect of microbe groups on high EMF (**Figure 6**). In addition, high EMF is often connected with high plant diversity, and higher levels of carbon inputs to the soil linked to more diverse plant communities result in more active, more abundant, and more diverse soil microbial communities (Lange et al., 2015). Therefore, when the soil resources are sufficient to maintain the growth of plants, the increase in microorganism activity and biomass plays a major role in maintaining high EMF.

Importance and Uncertainties

Most of the regions in the world are undergoing climate warming and species diversity loss, especially on the Tibetan Plateau (Rockstrom et al., 2009; Zhou et al., 2017). Increasing efforts have been conducted to explore the internal mechanism and consequences for ecosystem stability (Jing et al., 2015). Three main aspects of our study distinguish it from the few previous studies on this topic. First, few studies have considered the shifting role of plant community functions and microbe factors, which could change the effects of several factors on EMF, and our study examines both reliability and sensitivity over a wide range. Second, we compare the response of EMF to abiotic and biotic factors under high and low EMF patterns. Third, our study builds a model for above- and belowground and demonstrates that plant and microbial factors mediate the shift of EMF from low to high patterns under the influence of precipitation.

Although the level of high and low EMF is distinguished, the high and low conditions of EMF are only a relative concept due to the method of measurement of the standards. Besides, due to the limitation of data, we used only MBC and MBN to represent microbial factors, which might not fully reflect microbial indicators.

CONCLUSION

Our work indicates that high EMF may show a higher sensitivity response to climate, productivity, community functions, soil properties, and soil microbial factors. Moreover, our results suggest that plants and microbes mediated the shift of low to high EMF through the comprehensive effect of climate and environmental factors. As climate change and biodiversity of above- and belowground are lost from ecosystems, predicting how ecosystems will function in the future will require more experiments and observations.

DATA AVAILABILITY STATEMENT

The original contributions presented in the study are included in the article/supplementary material, further inquiries can be directed to the corresponding authors.

AUTHOR CONTRIBUTIONS

YiW, FX, and ZZ: conceptualization and software. YiW and ML: methodology, investigation, and writing – original draft preparation. ML: validation and data curation. YiW: formal analysis and resources. YiW, ML, YC, TZ, XL, BY, YaW, LZ, XN, FX, ZZ, and JS: writing – review and editing. All authors contributed to the article and approved the submitted version.

FUNDING

This research was supported by "Construction Project of Characteristic Specialty and Experimental Training Teaching Base (Center) of Guangxi Undergraduate Colleges and Universities in 2018-2020 [Guijiao Higher Education (2018) 52]," Second Tibetan Plateau Scientific Expedition and Research (No. 2019QZKK0405), and National Natural Science Foundation of China (No. 31901198).

REFERENCES

Anderson, T. M., Griffith, D. M., Grace, J. B., Lind, E. M., Adler, P. B., Biederman, L. A., et al. (2018). Herbivory and eutrophication mediate grassland plant nutrient responses across a global climatic gradient. *Ecology* 99, 822–831. doi: 10.1002/ecy.2175

Ansquer, P., Duru, M., Theau, J. P., and Cruz, P. (2009). Functional traits as indicators of fodder provision over a short time scale in species-rich grasslands. *Ann. Bot.* 103, 117–126. doi: 10.1093/aob/mcn215

Bapiri, A., Bååth, E., and Rousk, J. (2010). Drying-rewetting cycles affect fungal and bacterial growth differently in an arable soil. *Microb. Ecol.* 60, 419–428. doi: 10.1007/s00248-010-9723-5

Bastida, F., Torres, I. F., Moreno, J. L., Baldrian, P., Ondono, S., Ruiznavarro, A., et al. (2016). The active microbial diversity drives ecosystem multifunctionality and is physiologically related to carbon availability in mediterranean semi-arid soils. *Mol. Ecol.* 25, 4660–4673. doi: 10.1111/mec.13783

Bonkowski, M., and Roy, J. (2005). Soil microbial diversity and soil functioning affect competition among grasses in experimental microcosms. *Oecologia* 143, 232–240. doi: 10.1007/s00442-004-1790-1

Bunge, J., Epstein, S. S., and Peterson, D. G. (2006). Comment on "computational improvements reveal great bacterial diversity and high metal toxicity in soil". *Science* 313:918. doi: 10.1126/science.1121225

Chapin, F. S., Randerson, J. T., Mcguire, A. D., Foley, J. A., and Field, C. B. (2008). Changing feedbacks in the climate–biosphere system. *Front. Ecol. Environ.* 6, 313–320. doi: 10.1890/080005

De Vries, F. T., Thebault, E., Liiri, M., Birkhofer, K., Tsiafouli, M. A., Bjornlund, L., et al. (2013). Soil food web properties explain ecosystem services across European land use systems. *Proc. Natl. Acad. Sci. U. S. A.* 110, 14296–14301. doi: 10.1073/pnas.1305198110

Delgadobaquerizo, M., Eldridge, D. J., Ochoa, V., Gozalo, B., Singh, B. K., and Maestre, F. T. (2017). Soil microbial communities drive the resistance of ecosystem multifunctionality to global change in drylands across the globe. *Ecol. Lett.* 20, 1295–1305. doi: 10.1111/ele.12826

Demalach, N., Zaady, E., and Kadmon, R. (2017). Contrasting effects of water and nutrient additions on grassland communities: A global meta-analysis. *Glob. Ecol. Biogeogr.* 26, 983–992. doi: 10.1111/geb.12603

Diaz, S., Lavorel, S., De Bello, F., Quetier, F., Grigulis, K., and Robson, T. M. (2007). Incorporating plant functional diversity effects in ecosystem service assessments. *Proc. Natl. Acad. Sci. U. S. A.* 104, 20684–20689. doi: 10.1073/pnas.0704716104

Doncaster, C. P. (2007). Structural equation modeling and natural systems. *Fish Fish.* 8, 368–369. doi: 10.1111/j.1467-2979.2007.00260.x

Duffy, J. E., Cardinale, B. J., Mcintyre, P. B., Thebault, E., and Loreau, M. (2007). The functional role of biodiversity in ecosystems: incorporating trophic complexity. *Ecol. Lett.* 10, 522–538. doi: 10.1111/j.1461-0248.2007.01037.x

Eisenhauer, N., Beler, H., Engels, C., Gleixner, G., Habekost, M., Milcu, A., et al. (2010). Plant diversity effects on soil microorganisms support the singular hypothesis. *Ecology* 91, 485–496. doi: 10.1890/08-2338.1

Falster, D. S., and Westoby, M. (2003). Plant height and evolutionary games. *Trends Ecol. Evol.* 18, 337–343. doi: 10.1016/S0169-5347(03)00061-2

Gan, Y., Campbell, C. A., Janzen, H. H., Lemke, R. L., Basnyat, P., and Mcdonald, C. L. (2010). Nitrogen accumulation in plant tissues and roots and N mineralization under oilseeds, pulses, and spring wheat. *Plant Soil* 332, 451–461. doi: 10.1007/s11104-010-0312-7

Gonsamo, A., Chen, J. M., and Ooi, Y. W. (2018). Peak season plant activity shift towards spring is reflected by increasing carbon uptake by extra-tropical ecosystems. *Glob. Chang. Biol.* 25, 2117–2128. doi: 10.1111/gcb.14001

Gross, N., Bagoussepinguet, Y. L., Liancourt, P., Berdugo, M., Gotelli, N. J., and Maestre, F. T. (2017). Functional trait diversity maximizes ecosystem multifunctionality. *Nat. Ecol. Evol.* 1:132. doi: 10.1038/s41559-017-0132

Hector, A., and Bagchi, R. (2007). Biodiversity and ecosystem multifunctionality. *Nature* 448, 188–190. doi: 10.1038/nature05947

Hector, A., and Hooper, R. (2002). Darwin and the first ecological experiment. *Science* 295, 639–640. doi: 10.1126/science.1064815

Helgason, T., Daniell, T. J., Husband, R., Fitter, A. H., and Young, J. P. W. (1998). Ploughing up the wood-wide web? *Nature* 394:431. doi: 10.1038/28764

Hillebrand, H., and Matthiessen, B. (2009). Biodiversity in a complex world: consolidation and progress in functional biodiversity research. *Ecol. Lett.* 12, 1405–1419. doi: 10.1111/j.1461-0248.2009.01388.x

Hu, Z. M., Yu, G. R., Fan, J. W., Zhong, H. P., Wang, S. Q., and Li, S. G. (2010). Precipitation-use efficiency along a 4500-km grassland transect. *Glob. Ecol. Biogeogr.* 19, 842–851. doi: 10.1111/j.1466-8238.2010.00564.x

Hunt, H. W., and Wall, D. H. (2002). Modelling the effects of loss of soil biodiversity on ecosystem function. *Glob. Chang. Biol.* 8, 33–50. doi: 10.1046/j.1365-2486.2002.00425.x

Jing, X., Sanders, N. J., Shi, Y., Chu, H., Classen, A. T., Zhao, K., et al. (2015). The links between ecosystem multifunctionality and above- and belowground biodiversity are mediated by climate. *Nat. Commun.* 6:8159. doi: 10.1038/ncomms9159

Joergensen, R. G., Wu, J., and Brookes, P. C. (2011). Measuring soil microbial biomass using an automated procedure. *Soil Biol. Biochem.* 43, 873–876. doi: 10.1016/j.soilbio.2010.09.024

Lange, M., Eisenhauer, N., Sierra, C. A., Bessler, H., Engels, C., Griffiths, R. I., et al. (2015). Plant diversity increases soil microbial activity and soil carbon storage. *Nat. Commun.* 6:6707. doi: 10.1038/ncomms7707

Lavorel, S., Grigulis, K., McIntyre, S., Williams, N. S. G., Garden, D., Dorrough, J., et al. (2007). Assessing functional diversity in the field – methodology matters. *Funct. Ecol.* 22, 134–147. doi: 10.1111/j.1365-2435.2007.01339.x

Liu, M., Wang, Y., Sun, J., Zhang, Z., Xua, X., Zhou, H., et al. (2020). Shift in nurse effect from facilitation to competition with increasing size of Salix cupularis canopy in a desertified alpine meadow on the Tibetan plateau. *Catena* 195:104757. doi: 10.1016/j.catena.2020.104757

Lu, X. Y., Yan, Y., Sun, J., Zhang, X. K., Chen, Y. C., Wang, X. D., et al. (2015). Carbon, nitrogen, and phosphorus storage in alpine grassland ecosystems of Tibet: effects of grazing exclusion. *Ecol. Evol.* 5, 4492–4504. doi: 10.1002/ece3.1732

Ma, W., He, J., Yang, Y., Wang, X., Liang, C., Anwar, M., et al. (2010). Environmental factors covary with plant diversity–productivity relationships among Chinese grassland sites. *Glob. Ecol. Biogeogr.* 19, 233–243. doi: 10.1111/j.1466-8238.2009.00508.x

Maestre, F. T., Quero, J. L., Gotelli, N. J., Escudero, A., Ochoa, V., Delgado-Baquerizo, M., et al. (2012). Plant species richness and ecosystem multifunctionality in global drylands. *Science* 335, 214–218. doi: 10.1126/science.1215442

Maherali, H., and Klironomos, J. N. (2007). Influence of phylogeny on fungal community assembly and ecosystem functioning. *Science* 316, 1746–1748. doi: 10.1126/science.1143082

Mcsherry, M. E., and Ritchie, M. E. (2013). Effects of grazing on grassland soil carbon: a global review. *Glob. Chang. Biol.* 19, 1347–1357. doi: 10.1111/gcb.12144

Milcu, A., Thebault, E., Scheu, S., and Eisenhauer, N. (2010). Plant diversity enhances the reliability of belowground processes. *Soil Biol. Biochem.* 42, 2102–2110. doi: 10.1016/j.soilbio.2010.08.005

Moles, A. T., Warton, D. I., Warman, L., Swenson, N. G., Laffan, S. W., Zanne, A. E., et al. (2009). Global patterns in plant height. *J. Ecol.* 97, 923–932. doi: 10.1111/j.1365-2745.2009.01526.x

Mori, A., Isbell, F., Fujii, S., Makoto, K., Matsuoka, S., and Osono, T. (2016). Low multifunctional redundancy of soil fungal diversity at multiple scales. *Ecol. Lett.* 19, 249–259. doi: 10.1111/ele.12560

Niu, S., Wu, M., Han, Y., Xia, J., Zhang, Z., Yang, H., et al. (2010). Nitrogen effects on net ecosystem carbon exchange in a temperate steppe. *Glob. Chang. Biol.* 16, 144–155. doi: 10.1111/j.1365-2486.2009.01894.x

Reid, R. S., Fernández-Giménez, M. E., and Galvin, K. A. (2014). Dynamics and resilience of rangelands and pastoral peoples around the globe. *Annu. Rev. Environ. Resour.* 39, 217–242. doi: 10.1146/annurev-environ-020713-163329

Rockstrom, J., Steffen, W., Noone, K. J., Persson, A., Chapin, F. S., Lambin, E. F., et al. (2009). A safe operating space for humanity. *Nature* 461, 472–475. doi: 10.1038/461472a

Schmidt, M. W. I., Torn, M. S., Abiven, S., Dittmar, T., Guggenberger, G., Janssens, I. A., et al. (2011). Persistence of soil organic matter as an ecosystem property. *Nature* 478, 49–56. doi: 10.1038/nature10386

Sistla, S. A., and Schimel, J. P. (2012). Stoichiometric flexibility as a regulator of carbon and nutrient cycling in terrestrial ecosystems under change. *New Phytol.* 196, 68–78. doi: 10.1111/j.1469-8137.2012.04234.x

Sommers, L. E., and Nelson, D. W. (1972). Determination of total phosphorus in soils: A rapid perchloric acid digestion procedure. *Soil Sci. Soc. Am. J.* 36, 902–904. doi: 10.2136/sssaj1972.03615995003600060020x

Sun, J., Liu, M., Fu, B. F., David, K., Zhao, W., Liu, G., et al. (2020a). Reconsidering the efficiency of grazing exclusion using fences on the Tibetan Plateau. *Sci. Bull.* 65, 1405–1414. doi: 10.1016/j.scib.2020.04.035

Sun, J., Ma, B., and Lu, X. (2018). Grazing enhances soil nutrient effects: trade-offs between aboveground and belowground biomass in alpine grasslands of the Tibetan Plateau. *Land Degrad. Dev.* 29, 337–348. doi: 10.1002/ldr.2822

Sun, J., and Wang, H. (2016). Soil nitrogen and carbon determine the trade-off of the above- and below-ground biomass across alpine grasslands, Tibetan plateau. *Ecol. Indic.* 60, 1070–1076. doi: 10.1016/j.ecolind.2015.08.038

Sun, J., Wang, Y., and Liu, G. H. (2021a). Linkages of aboveground plant carbon accumulation rate with ecosystem multifunctionality in alpine grassland, Qingzang Plateau. *Chin. J. Plant Ecol.* 45, 496–506. doi: 10.17521/cjpe.2020.0180

Sun, J., Zhan, T., Liu, M., Zhang, Z., Wang, Y., Liu, S. L., et al. (2021b). Verification of the biomass transfer hypothesis under moderate grazing across the Tibetan plateau: a meta-analysis. *Plant Soil* 458, 139–150. doi: 10.1007/s11104-019-04380-8

Sun, J., Zhou, T., Liu, M., Chen, Y., Liu, G., Xu, M., et al. (2020b). Water and heat availability are drivers of the aboveground plant carbon accumulation rate in alpine grasslands on the Tibetan Plateau. *Glob. Ecol. Biogeogr.* 29, 50–64. doi: 10.1111/geb.13006

Thompson, K., Parkinson, J., Band, S. R., and Spencer, R. E. (1997). A comparative study of leaf nutrient concentrations in a regional herbaceous flora. *New Phytol.* 136, 679–689. doi: 10.1046/j.1469-8137.1997.00787.x

Tilman, D., Knops, J. M. H., Wedin, D. A., Reich, P. B., Ritchie, M. E., and Siemann, E. (1997). The influence of functional diversity and composition on ecosystem processes. *Science* 277, 1300–1302. doi: 10.1126/science.277.5330.1300

Tilman, D., Reich, P. B., and Knops, J. (2006). Biodiversity and ecosystem stability in a decade-long grassland experiment. *Nature* 441, 629–632. doi: 10.1038/nature04742

van der Heijden, M. G. A., Bardgett, R. D., and van Straalen, N. M. (2008). The unseen majority: soil microbes as drivers of plant diversity and productivity in terrestrial ecosystems. *Ecol. Lett.* 11, 296–310. doi: 10.1111/j.1461-0248.2007.01139.x

van der Heijden, M. G. A., Klironomos, J. N., Ursic, M., Moutoglis, P., Streitwolfengel, R., Boller, T., et al. (1998). Mycorrhizal fungal diversity determines plant biodiversity, ecosystem variability and productivity. *Nature* 396, 69–72. doi: 10.1038/23932

Vance, E. D., Brookes, P. C., and Jenkinson, D. S. (1987). An extraction method for measuring soil microbial biomass C. *Soil Biol. Biochem.* 19, 703–707. doi: 10.1016/0038-0717(87)90052-6

Wagg, C., Bender, S. F., Widmer, F., and Van der Heijden, M. G. A. (2014). Soil biodiversity and soil community composition determine ecosystem multifunctionality. *Proc. Natl. Acad. Sci. U. S. A.* 111, 5266–5270. doi: 10.1073/pnas.1320054111

Wall, D. H., Bardgett, R. D., and Kelly, E. F. (2010). Biodiversity in the dark. *Nat. Geosci.* 3, 297–298. doi: 10.1038/ngeo860

Wang, X., Li, F. Y., Wang, Y., Liu, X., Cheng, J., Zhang, J., et al. (2020a). High ecosystem multifunctionality under moderate grazing is associated with high plant but low bacterial diversity in a semi-arid steppe grassland. *Plant Soil* 448, 265–276. doi: 10.1007/s11104-020-04430-6

Wang, Y., Ni, G., Hou, Y., Wang, Q., and Huang, Q. (2020b). Plant–soil feedbacks under resource limitation may not contribute to the invasion by annual Asteraceae plants. *Oecologia* 194, 165–176. doi: 10.1007/s00442-020-04756-z

Wang, Y., Sun, J., Liu, M., Zeng, T., and Zhou, H. (2019). Precipitation-use efficiency may explain net primary productivity allocation under different precipitation conditions across global grassland ecosystems. *Glob. Ecol. Conserv.* 20:e00713. doi: 10.1016/j.gecco.2019.e00713

Wang, Y., Sun, J., Ye, C. C., and Zeng, T. (2021). Climatic factors drive the aboveground ecosystem functions of alpine grassland via soil microbial biomass nitrogen on Qingzang Plateau. *Chin. J. Plant Ecol.* 45, 434–443. doi: 10.17521/cjpe.2020.0204

Xu, Z., Li, M., Zimmermann, N. E., Li, S., Li, H., Ren, H., et al. (2018). Plant functional diversity modulates global environmental change effects on grassland productivity. *J. Ecol.* 106, 1941–1951. doi: 10.1111/1365-2745.12951

Xu, X., Thornton, P. E., and Post, W. M. (2013). A global analysis of soil microbial biomass carbon, nitrogen and phosphorus in terrestrial ecosystems. *Glob. Ecol. Biogeogr.* 22, 737–749. doi: 10.1111/geb.12029

Yang, Y., Fang, J., Fay, P. A., Bell, J. E., and Ji, C. (2010a). Rain use efficiency across a precipitation gradient on the Tibetan Plateau. *Geophys. Res. Lett.* 37, 78–82. doi: 10.1029/2010GL043920

Yang, Y., Fang, J., Ma, W., Smith, P., Mohammat, A., Wang, S., et al. (2010b). Soil carbon stock and its changes in northern China's grasslands from 1980s to 2000s. *Glob. Chang. Biol.* 16, 3036–3047. doi: 10.1111/j.1365-2486.2009.02123.x

Yao, K. Y. (2006). "Determination of soil microbial activities and character," in *Soil Microbial Ecology Expreimental Technology*. eds. K. Y. Yao and C. Y. Huang (Beijing: Science Press), 24–191.

Zavaleta, E. S., Pasari, J. R., Hulvey, K. B., and Tilman, G. D. (2010). Sustaining multiple ecosystem functions in grassland communities requires higher biodiversity. *Proc. Natl. Acad. Sci. U. S. A.* 107, 1443–1446. doi: 10.1073/pnas.0906829107

Zhang, R., Wang, Z., Niu, S., Tian, D., Wu, Q., Gao, X., et al. (2021). Diversity of plant and soil microbes mediates the response of ecosystem multifunctionality to grazing disturbance. *Sci. Total Environ.* 776:145730. doi: 10.1016/j.scitotenv.2021.145730

Zhou, T., Liu, M., Sun, J., Li, Y., Shi, P., Tsunekawa, A., et al. (2020). The patterns and mechanisms of precipitation use efficiency in alpine grasslands on the Tibetan Plateau. *Agric. Ecosyst. Environ.* 292:106833. doi: 10.1016/j.agee.2020.106833

Zhou, G., Zhou, X., He, Y., Shao, J., Hu, Z., Liu, R., et al. (2017). Grazing intensity significantly affects belowground carbon and nitrogen cycling in grassland ecosystems: a meta-analysis. *Glob. Chang. Biol.* 23, 1167–1179. doi: 10.1111/gcb.13431

Zong, N., Zhao, G., and Shi, P. (2019). Different sensitivity and threshold in response to nitrogen addition in four alpine grasslands along a precipitation transect on the Northern Tibetan Plateau. *Ecol. Evol.* 9, 9782–9793. doi: 10.1002/ece3.5514

Conflict of Interest: The authors declare that the research was conducted in the absence of any commercial or financial relationships that could be construed as a potential conflict of interest.

Publisher's Note: All claims expressed in this article are solely those of the authors and do not necessarily represent those of their affiliated organizations, or those of the publisher, the editors and the reviewers. Any product that may be evaluated in this article, or claim that may be made by its manufacturer, is not guaranteed or endorsed by the publisher.

Copyright © 2021 Wang, Liu, Chen, Zeng, Lu, Yang, Wang, Zhang, Nie, Xiao, Zhang and Sun. This is an open-access article distributed under the terms of the Creative Commons Attribution License (CC BY). The use, distribution or reproduction in other forums is permitted, provided the original author(s) and the copyright owner(s) are credited and that the original publication in this journal is cited, in accordance with accepted academic practice. No use, distribution or reproduction is permitted which does not comply with these terms.

frontiers in Plant Science

ORIGINAL RESEARCH
published: 03 November 2021
doi: 10.3389/fpls.2021.771058

Effects of Plateau Pika Disturbance on the Spatial Heterogeneity of Vegetation in Alpine Meadows

*Jie Li, Hao Hao Qi, Yuan Yuan Duan and Zheng Gang Guo**

State Key Laboratory of Grassland Agro-Ecosystems, Key Laboratory of Grassland Livestock Industry Innovation, Ministry of Agriculture and Rural Affairs, Engineering Research Center of Grassland Industry, Ministry of Education, College of Pastoral Agriculture Science and Technology, Lanzhou University, Lanzhou, China

Herbivory is one of the important factors that influence spatial heterogeneity of vegetation in grasslands. In this study, we focused on plateau pika (*Ochotona curzoniae*) to investigate the effects of the presence of small semi-fossorial herbivores and their disturbance intensity on the spatial heterogeneity of vegetation in alpine meadows across three sites in the Qinghai-Tibetan Plateau. A random stratified paired sampling method was used to collect vegetation data, and plant species richness at both fine and coarse scales were used to estimate the spatial heterogeneity of vegetation. This study showed that the presence of plateau pikas led to higher spatial heterogeneity of vegetation in alpine meadows, which increased linearly as the disturbance intensities of plateau pikas increased. The findings of this study demonstrate that small semi-fossorial herbivores have an important impact on the spatial heterogeneity of vegetation, and present a possible approach for estimating the effect of the presence of a small semi-fossorial herbivore and its disturbance intensity on the spatial heterogeneity of vegetation in grasslands.

Keywords: *Ochotona curzoniae*, disturbance intensity, spatial heterogeneity of vegetation, Qinghai-Tibetan Plateau, alpine meadows

OPEN ACCESS

Edited by:
Jian Sun,
Institute of Tibetan Plateau Research, Chinese Academy of Sciences (CAS), China

Reviewed by:
Jiapeng Qu,
Northwest Institute of Plateau Biology, Chinese Academy of Sciences (CAS), China
Xiaojun Yu,
Gansu Agricultural University, China

****Correspondence:***
Zheng Gang Guo
guozhg@lzu.edu.cn

Specialty section:
This article was submitted to Functional Plant Ecology, a section of the journal Frontiers in Plant Science

Received: *05 September 2021*
Accepted: *08 October 2021*
Published: *03 November 2021*

Citation:
Li J, Qi HH, Duan YY and Guo ZG (2021) Effects of Plateau Pika Disturbance on the Spatial Heterogeneity of Vegetation in Alpine Meadows. Front. Plant Sci. 12:771058. doi: 10.3389/fpls.2021.771058

INTRODUCTION

Spatial heterogeneity of vegetation is an important proxy for gaining insight into grassland plant productivity since it is usually positive related to plant productivity in grasslands (Bai et al., 2007; Otieno et al., 2011; Song et al., 2020). The spatial heterogeneity of vegetation is usually estimated by non-spatial statistics and spatially explicit metrics (Kolasa and Rollo, 1991; Adler et al., 2001). In contrast to non-spatial statistics, spatially explicit metrics, containing many parameters of grassland plant communities (Bangert and Slobodchikoff, 2006; Bloor et al., 2020), are considered to predict the spatial heterogeneity of vegetation because a parameter value of grassland plant communities can be used to reasonably predict another parameter value in the same area (Adler et al., 2001). Although there are many parameters in spatially explicit metrics to estimate spatial heterogeneity of vegetation in grasslands, plant species richness is widely applied to estimate the spatial heterogeneity of vegetation in grasslands (Questad and Foster, 2007; Case et al., 2013; Lindtner et al., 2020). The plant species richness is closely related to the plant community structure and community productivity in grasslands (Hector et al., 1999; Tilman et al., 2006; Pang et al., 2021) and varies at different spatial scales in the field (Dumbrell et al., 2008). However, plant species

richness is affected by biotic factors (Adler and Lauenroth, 2000; Altesor et al., 2005; Pang et al., 2021), which have an important impact on the spatial heterogeneity of vegetation in grasslands (Jones et al., 2008; Yoshihara et al., 2009).

Herbivores are considered as important biotic factors that influence the spatial heterogeneity of vegetation in grasslands (Jones et al., 1997; Adler and Lauenroth, 2000; Davidson et al., 2012; Wei et al., 2019). Large herbivore grazing has been verified to increase the spatial heterogeneity of vegetation in grasslands (Adler and Lauenroth, 2000; Adler et al., 2001; Song et al., 2020; Michaels et al., 2021). In addition to large herbivores, many kinds of small semi-fossorial herbivores inhabit grasslands (Bagchi et al., 2006; Questad and Foster, 2007; Lindtner et al., 2020; Wei et al., 2020) and these small semi-fossorial herbivores often cause extensive disturbance to grassland vegetation and soil (Hobbs and Huenneke, 1992; Liu et al., 2017; Smith et al., 2019). They often modify the interspecies relationships among plants through selective feeding behavior and induce several fertilizer islands through redistribution of soil nutrients (Case et al., 2013; Liu et al., 2013; Yurkewycz et al., 2014; Yu et al., 2017). This enables some plants to reconstruct their niche (Jones et al., 2008), and consequently develop new and different plant assemblages (Milton et al., 1997; Questad and Foster, 2007; Scherrer et al., 2019), compared to areas where small semi-fossorial herbivores are absent. Thus, small semi-fossorial herbivores often lead to differences in grassland vegetation based on the presence/absence of semi-fossorial herbivores (Wilson and Smith, 2015; Wang et al., 2018). Lindtner et al. (2020) used plant species richness at fine scale (average species number of many subplots with the size of 1 × 1 m) and coarse scales (total number of plant species in that subplots) to estimate the spatial heterogeneity of vegetation in grasslands, and found that the spatial heterogeneity of vegetation in grasslands increased with increasing disturbance intensity of European ground squirrel (*Spermophilus citellus*) in the United States. However, this study did not use grasslands without European ground squirrel as a reference area for comparison. Further, whether the presence of small semi-fossorial influences the spatial heterogeneity of vegetation in grasslands is not well documented. Therefore, more studies are needed to investigate the effect of small semi-fossorial herbivores on the spatial heterogeneity of vegetation in grasslands, which can determine the relationship between small semi-fossorial herbivores and the spatial heterogeneity of vegetation in grasslands.

Plateau pika (*Ochotona curzoniae*) is a small, social semi-fossorial herbivore native to alpine grasslands in Asia (Fan et al., 1999; Davidson et al., 2012), particularly in the alpine meadows on the Qinghai-Tibetan Plateau (Smith et al., 2019). This small semi-fossorial herbivore often disturbs the alpine meadow through excretion of feces and urine (Fan et al., 1999), selectively consuming plants (Liu et al., 2013), producing bare soil patches (Pang et al., 2020), and aerating the soil (Wilson and Smith, 2015; Yu et al., 2017; Pang et al., 2021). This often leads to discrete mosaics of vegetated surfaces and bare soil patches over a range of different spatial scales in the alpine meadows (Wilson and Smith, 2015; Zhao et al., 2021). At a large spatial scale, the plateau pikas are distributed territorially and patchily on alpine meadows (Pang et al., 2020), because they prefer to live in low and open habitats to avoid predators (Fan et al., 1999; Zhang et al., 2020). Once the plateau pikas occupy a given suitable area, their activities often enable alpine meadows in that area to further degrade (Liu et al., 2013). In reality, some alpine meadows are low and open and are a potential habitat for the species, but are not inhabited by them (Fan et al., 1999), because the diffusion of plateau pikas is a gradual process (Wang et al., 2020). Thus, selecting the potential habitats for plateau pikas as reference areas is a possible way to test whether the presence of plateau pikas influences the spatial heterogeneity of vegetation in grasslands.

Plateau pikas have been found to live in various habitats with different soil types, topographies, microclimates, and vegetation types on the Qinghai-Tibetan Plateau (Smith and Foggin, 1999; Guo et al., 2012). If field surveys are conducted at only one site with similar environmental conditions, there will be uncertainty regarding the changes in the spatial heterogeneity of vegetation resulting from the presence of plateau pikas singly or in combination with environmental factors. Thus, multiple sites are necessary to identify the general pattern of the presence of plateau pikas influencing the spatial heterogeneity of vegetation in alpine meadows. In this study, we used the plateau pika as an example study animal to examine the effect of the presence of small semi-fossorial herbivores on the spatial heterogeneity of vegetation in grasslands across three sites. Specifically, this study hypothesized that: (1) the presence of plateau pikas will lead to higher spatial heterogeneity of vegetation in grasslands, and (2) the spatial heterogeneity of vegetation in grasslands will increase as the disturbance intensity of plateau pikas increases, which will provide useful information for quantify the relationship between small semi-fossorial herbivores and grassland plant productivity.

MATERIALS AND METHODS

Study Site Description

Three survey sites with different environmental conditions were selected to examine the effects of plateau pikas and their disturbance intensity on the spatial heterogeneity of vegetation in alpine grasslands on the Qinghai-Tibetan Plateau. These sites were located at Heimahe (99°41′ E, 36°21′ N) in Gonghe County, Xihai Town (100°37′ E, 36°51′ N) in Haiyan County, Qinghai Province, and at Gahai town (102°10′ E, 34°16′ N) in Luqu County, Gansu province (**Figure 1**). The three survey sites range in elevation from 3,000 to 4,650 m and in average annual precipitation from 250 to 800 mm, and experience a similar cold, humid continental plateau climate (**Table 1**). The soils at the three survey sites were classified into alpine meadow soils based on the Chinese Soil Classification System, similar to Cambisols in the world reference base (WRB) soil classification system. The main alpine grasslands in the study site are alpine meadows dominated by sedges (Liu et al., 2017), and these alpine meadows have been contracted to farm households. Each household has managed alpine meadows by classifying it into warm grazing areas and cold grazing areas; cold grazing areas were fenced from mid-April to early October and the fence was opened to yaks and Tibetan sheep for grazing from mid-October to early April in the last few decades. The plateau pika are the only small semi-fossorial

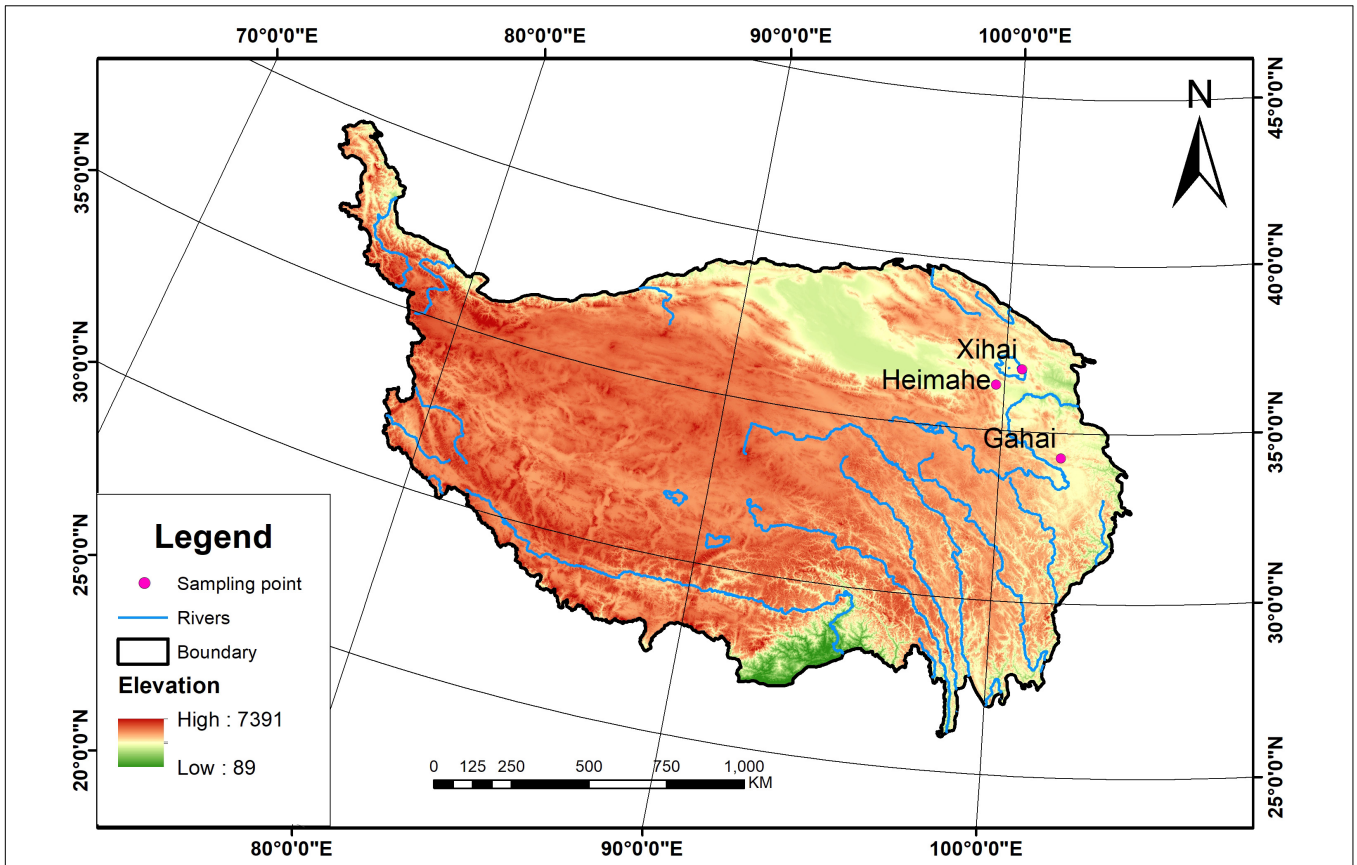

FIGURE 1 | The three survey sites in the Qinghai-Tibetan Plateau.

TABLE 1 | Description of the study areas at Gonghe, Haiyan, and Luqu.

Location	Elevation (m)	MAT (°C)	MAP (mm)	Dominant species	Main associate species
Gonghe	3,750	4.1	250–500	*Kobresia pygmaea*	*Elymus nutans* *Poa pratensis* *Anemone obtusiloba*
Haiyan	3,270	1.5	300–500	*K. humilis*	*P. pratensis* *Leontopodium nanum* *Potentilla bifurca*
Luqu	3,550	2.3	600–800	*K. pygmaea*	*E. nutans* *P. pratensis* *A. obtusiloba*

MAT is the mean annual temperature; MAP is the mean annual precipitation.

herbivores at the surveyed sites, although there are many small herbivores throughout the counties.

Experimental Design

The survey areas at each site were selected in the cold grazing areas that were relatively flat. In this study, a random stratified and paired design was used to select the plots. At each survey area, we randomly selected the first disturbed plot where plateau pikas were visible or the active burrow entrances were found, and then selected the second disturbed plot along the road. The distance between two disturbed plots was greater than 3 km. In a similar fashion, 10 disturbed plots were finally selected at each survey site. Because the average area of the plateau pika's home range has been reported as 1,262.5 m^2, the plot size was designed as 35 m × 35 m, which was approximately equivalent to the home range (Fan et al., 1999). Following this, a paired adjacent undisturbed plot, without visible plateau pikas or active burrow entrance, was selected for each disturbed plot. To ensure that the undisturbed plot was a true reference area, the distance between the paired plots was maintained at 500–1,000 m, which ensures avoiding the overlap between disturbed and undisturbed plots. To ensure that each disturbed plot had a paired undisturbed

plot to the extent possible, each paired plot was placed on the same alpine meadow, which ensured that each paired plot had no obvious differences in soil type, topography, microclimate, and vegetation composition. In total, this study surveyed 30 paired plots across three sites, consisting of 30 each of disturbed and undisturbed plots. Each paired plot was managed as a single unit. The active burrow entrances at each disturbed plot were used to estimate the disturbance intensity of the plateau pikas. The disturbance intensity of plateau pikas was possibly different among the 30 disturbed plots, which was helpful for identifying a general pattern of plateau pika disturbance in relation to the spatial heterogeneity of vegetation.

Field Survey and Sampling

Plateau pikas disturb alpine meadows mostly in August (Wang et al., 2018), and field surveys were conducted in early August 2020. First, the active burrow entrance at each disturbed plot was estimated by the "plugging tunnels method," in which the burrow entrances were plugged with dry hay for 3 days, and the number of plugs that were cleared by the plateau pikas to allow access to the meadow surface was recorded (Zhang et al., 2020). The average number of burrow entrances with cleared plugs in 3 days was considered as the disturbance density of plateau pikas. Second, five subplots with a W pattern were arranged in each plot. The size of the subplot was 1 × 1 m and the distance between the two subplots was approximately 8 m. The subplots in the disturbed plots were shifted slightly to avoid bare soil patches, if needed. All vascular plant species in each subplot were identified.

Estimation of Spatial Heterogeneity of Vegetation

Lindtner et al. (2020) proposed that the spatial heterogeneity of vegetation was estimated by $\beta = \gamma/\alpha - 1$, where β represents the spatial heterogeneity of vegetation, γ represents the plant species richness at a coarse scale, and α is the plant species richness at a fine scale. The plant species richness at fine scale was calculated by the average value of five subplots in a plot, and the plant species richness at coarse scale was calculated by the total number of plant species in all five subplots of a plot.

Statistical Analysis

All analyses were performed using R version 4.0.2 (R Core Team, 2020). A linear mixed model (LMM) with the function "lmer" from the lme4 package was used to examine the effects of the presence of plateau pikas on the spatial heterogeneity of vegetation across the three sites, in which paired design nested within each site (proceeding nested design analysis) was included as a random factor. To test the general pattern, a paired-samples *t*-test was used to examine the effect of the presence of plateau pikas on the spatial heterogeneity of vegetation at each site.

To clarify the responses of spatial heterogeneity of vegetation to the disturbance intensity of plateau pikas, a linear model (LM) was used to construct the regression models, describing relationships of spatial heterogeneity of vegetation with disturbance intensity of plateau pikas, in which the disturbance intensity of plateau pikas was considered to be the fixed factor.

RESULTS

Effect of the Presence of Plateau Pikas on Spatial Heterogeneity of Vegetation Resource

Accounting for an overall scale effect, the spatial heterogeneity of vegetation was higher in the presence of plateau pikas than in their absence (spatial heterogeneity of vegetation: $F = 139.198$, $P < 0.001$) (**Figure 2**). Accounting for individual site effects, the spatial heterogeneity of vegetation in the presence of plateau pikas was higher than that in their absence at each site, similar to the results from the three sites together. These results presented a general pattern regarding the spatial heterogeneity of vegetation in relation to the presence of plateau pikas.

Effect of Disturbance Intensity of Plateau Pikas on Spatial Heterogeneity of Vegetation

An analysis of the data from the three sites or an individual site suggested that there was a linear increase in the spatial heterogeneity of vegetation with the increase in disturbance intensity of plateau pikas (**Figure 3**). This indicated that there was a general pattern of disturbance intensity of plateau pikas influencing the spatial heterogeneity of vegetation.

DISCUSSION

Herbivory is one of the important biotic factors that induce the spatial heterogeneity of vegetation in grasslands (Adler and Lauenroth, 2000; Adler et al., 2001; Bangert and Slobodchikoff, 2006; Case et al., 2013), and optimal spatial heterogeneity of vegetation is acknowledged as an effective approach to maintain grassland ecosystem functions such as plant species richness and productivity (Jones et al., 1997; Bakker et al., 2006; Davidson et al., 2012; Song et al., 2020). Previous studies have shown that the spatial heterogeneity of vegetation is different between fine and coarse scales in the presence of small semi-fossorial herbivores, such as prairie voles (*Microtus ochrogaster*) (Questad and Foster, 2007) and Siberian marmots (*Marmota sibirica*) (Yoshihara et al., 2009), whereas these studies did not consider the areas without these animals as true reference areas for comparison. In this study, we select areas without plateau pikas as reference areas to examine the effect of the presence of plateau pikas on the spatial heterogeneity of vegetation across three sites, in an attempt to identify a general pattern concerning the spatial heterogeneity of vegetation in relation to the presence of a small semi-fossorial herbivore and its disturbance intensity.

We found a higher spatial heterogeneity of vegetation in the presence of plateau pikas than in their absence, which indicates that the presence of plateau pikas leads to higher spatial heterogeneity of vegetation, in agreement with the first hypothesis. The higher spatial heterogeneity of vegetation is caused by the following reasons. First, plateau pikas prefer to clip tall plants near the active burrow entrance to monitor predators (Liu et al., 2009; Zhang et al., 2020), which increases

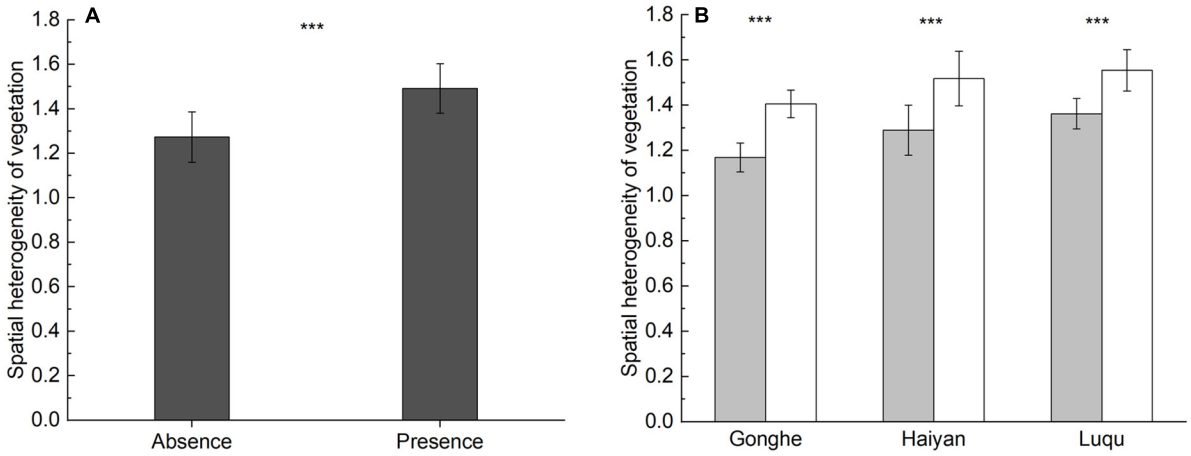

FIGURE 2 | Spatial heterogeneity of vegetation (mean ± standard error) in the presence or absence of plateau pika when the data from three sites was analyzed together **(A)** and in each site **(B)**. The statistics were based on the generalized linear mixed models (GLMMs) and the paired-samples *t*-test, with the paired plots nested within sites as random factors. "***" indicates significant differences at $P < 0.001$.

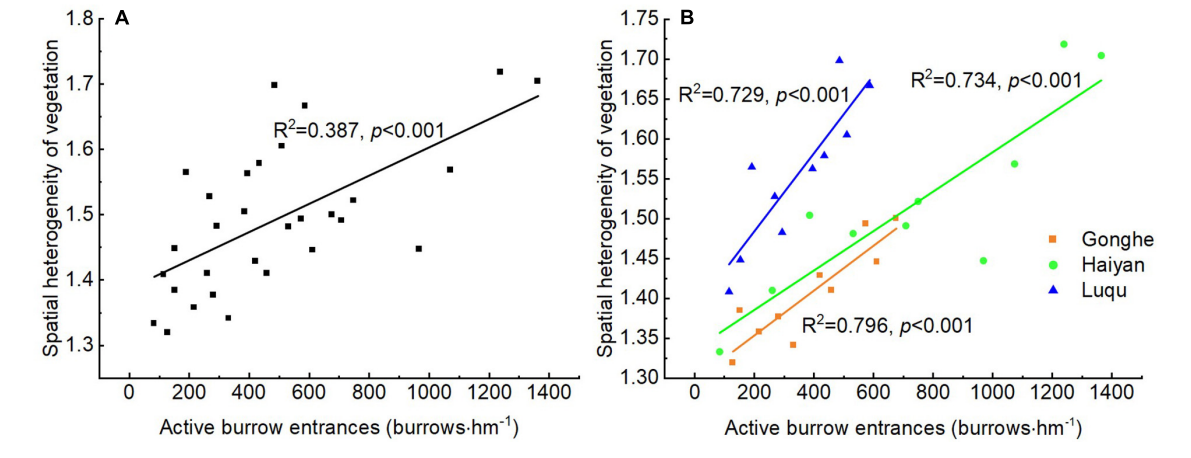

FIGURE 3 | Relationship between spatial heterogeneity of vegetation and the disturbance intensity of plateau pikas across three sites **(A)** and in each site **(B)** based on linear models (LMs).

light availability for short plant species and rare plants (Borer et al., 2014; Zhang et al., 2020), and forms new and various plant assemblages near the active burrow entrance, resulting in more spatial heterogeneity of vegetation at multiple spatial scales (Milton et al., 1997; Questad and Foster, 2007). Second, plateau pikas prefer graminoids as food throughout their home range (Liu et al., 2017), which alters the existing interspecific and intraspecific relationships among plants because graminoids are often dominant plants (Pang and Guo, 2018). This usually divides the areas with plateau pikas into alpine meadows dominated by strongly competitive dominant species and other alpine meadows dominated by disturbance-dependent species (Yoshihara et al., 2009; Kelemen et al., 2019), contributing to an increase in spatial heterogeneity of vegetation. Third, the presence of plateau pikas is beneficial to seed dispersal (Dobson et al., 1998). Some dispersed species cannot survive in a given habitat due to their weak competitive ability (Zhang et al., 2020), while others can survive in that habitat when they disperse and colonize (Wang et al., 2018, 2020), which develops more different plant communities in the presence of plateau pikas, increasing the spatial heterogeneity of vegetation. Fourth, plateau pikas often create a "spatiotemporal mosaic" of vegetated surface and bare soil patches (Pang et al., 2020), and these soil patches can provide suitable habitats for seeds of opportunistic plants for emergence and colonization (Bochet, 2015). The bare soil patches are similar to mounds created by small subterranean mammals, which can further increase the spatial heterogeneity of vegetation (Jones et al., 2008; Case et al., 2013). These four processes result in a higher spatial heterogeneity of vegetation in the presence of plateau pikas, indicating that the presence of plateau pikas is beneficial to plant productivity in alpine meadows since the spatial heterogeneity of vegetation is positive related to grassland plant productivity (Bai et al., 2007; Otieno et al., 2011; Song et al., 2020).

This study also found that the spatial heterogeneity of vegetation showed a linear increasing trend as the disturbance intensity of plateau pikas increased, which is consistent with the second hypothesis. This is similar to the relationships recorded between the spatial heterogeneity of vegetation and the disturbance intensity of European ground squirrels (Lindtner et al., 2020). In this case, three mechanisms can be used to explain the spatial heterogeneity of vegetation in relation to the disturbance intensity of plateau pikas. First, clipping behavior by plateau pikas near active burrow entrance increases as the disturbance intensity of plateau pikas increases (Liu et al., 2009). This provides more selectivity for the colonization of different species and develops more plant assemblages with unique features, contributing to an increase in spatial heterogeneity of vegetation. Second, more bare soil patches are accompanied by an increase in disturbance intensity of plateau pikas (Yu et al., 2017; Smith et al., 2019; Pang et al., 2020), which forms more diverse fertilizer islands and provides favorable conditions for the invasion and colonization of pioneer species, resulting in more diversification of species assemblages and an increase in spatial heterogeneity of vegetation. Third, graminoids consumed by plateau pikas become more frequent as the disturbance intensity of plateau pikas increases (Pang and Guo, 2017; Wei et al., 2020), which further decreases the dominance degree of dominant graminoids in the plateau pika home range. This leads to reconstruction of plants in the plateau pika home range, forming more unique plant communities at the microhabitat scale (Scherrer et al., 2019), contributing to an increase in the spatial heterogeneity of vegetation in the plateau pika home range (Yoshihara et al., 2009), which implies that the plant productivity in alpine meadows can increase as the disturbance intensity of plateau pikas increase. Although 30 disturbed plots, containing different disturbance intensity, is used to identify the general pattern concerning the effect of disturbance intensities on spatial heterogeneity of vegetation, some previous studies have verified that higher disturbance intensity of plateau pikas often results in higher unpalatable plant biomass (mainly consisting of forbs) and less palatable plant biomass (Zhang et al., 2020; Pang et al., 2021) and contributes to degradation of alpine meadows (Liu et al., 2013; Wilson and Smith, 2015). This implies that the contribution of higher disturbance intensity to degradation of alpine meadows is to deteriorate grazing quality of alpine meadows due to low palatable plant biomass (Sun et al., 2015; Wei et al., 2020). Consequently, how to manage plateau pika in alpine meadows is dependent on the operation targets of alpine meadows (Guo et al., 2012). If alpine meadows are operated to exert the ecological and social functions (Guo et al., 2003), the disturbance intensity of plateau pikas can be maintained at a relative higher level. However, alpine meadows are used to graze livestock, plateau pikas had better maintain their low disturbance intensity since palatable plant biomass in alpine meadows firstly increase, than then decrease as the disturbance intensity of plateau pikas increases (Pang and Guo, 2018). Therefore, further studies are necessary to quantify the disturbance intensity threshold of plateau pikas, in which the spatial heterogeneity of vegetation is positive related to palatable plant productivity in alpine meadows.

The data of this study come from three sites that range in elevation from 3,270 to 3,750 m (**Table 1**) and annual precipitation from 250 to 800 mm, and the results are conclusive. The findings of this study not only indicate that the presence of plateau pikas can lead to higher spatial heterogeneity of vegetation, but also confirms the response of the spatial heterogeneity of vegetation to disturbance intensity of European ground squirrels (Lindtner et al., 2020). Overall, the findings of this study concur with previous findings of the effect of small semi-fossorial herbivores on the spatial heterogeneity of vegetation.

CONCLUSION

The plateau pika was employed as an example animal species to investigate the responses of the spatial heterogeneity of vegetation to the presence and the variation in disturbance intensity of a small semi-fossorial mammal across three sites. This study found that the presence of plateau pikas relates to higher spatial heterogeneity of vegetation in alpine meadows. Further, we found a general pattern regarding the effect of disturbance intensity of plateau pika on spatial heterogeneity of vegetation, which can be described by a linear model. These results suggest that the plateau pika is an important biotic factor that alters the spatial heterogeneity of vegetation in alpine meadows. Further, we present a possible approach to estimate the effects of the presence and disturbance intensity of a small semi-fossorial herbivore on the spatial heterogeneity of vegetation in grasslands.

DATA AVAILABILITY STATEMENT

The original contributions presented in the study are included in the article/supplementary material, further inquiries can be directed to the corresponding author.

AUTHOR CONTRIBUTIONS

JL conceived the idea, performed the experiment, analyzed the data, originally drafted, and edited the manuscript. HQ and YD performed the experiment. ZG conceived the idea, found the funding acquisition, supervised the experiment, and polished and edited the manuscript. All authors read and approved the final manuscript.

FUNDING

This work was supported by the National Natural Science Foundation of China (32171675), The Open Project of State Key Laboratory of Plateau Ecology and Agriculture, Qinghai University, The Science and Technology Project of Gansu Province (21JR7RA489), The "Top Innovative Talents" training project of the Key Laboratory of Grassland Livestock Industry Innovation, Ministry of Agriculture and Rural Affairs (CMSYS2020-4 and CMSYS2020-21), and the 111 Project (B12002).

ACKNOWLEDGMENTS

The authors would like to thank Xiao Pan Pang, Jing Zhang, Qian Wang, Huan Yang, Ding Yang, Ying Ying Chen, Fu Yun Qiao, Di Gang Zhi, and Gan Lin Feng from Lanzhou University for the contributions made to this study through their field assistance and laboratory analysis.

REFERENCES

Adler, P. B., and Lauenroth, W. K. (2000). Livestock exclusion increases the spatial heterogeneity of vegetation in Colorado shortgrass steppe. *Appl. Veg. Sci.* 3, 213–222. doi: 10.2307/1479000

Adler, P., Raff, D., and Lauenroth, W. (2001). The effect of grazing on the spatial heterogeneity of vegetation. *Oecologia* 128, 465–479. doi: 10.1007/s004420100737

Altesor, A., Oesterheld, M., Leoni, E., Lezama, F., and Rodríguez, C. (2005). Effect of grazing on community structure and productivity of a Uruguayan grassland. *Plant Ecol.* 179, 83–91. doi: 10.1007/s11258-004-5800-5

Bagchi, S., Namgail, T., and Ritchie, M. E. (2006). Small mammalian herbivores as mediators of plant community dynamics in the high-altitude arid rangelands of Trans-Himalaya. *Biol. Conserv.* 127, 438–442. doi: 10.1016/j.biocon.2005.09.003

Bai, Y., Wu, J., Pan, Q., Huang, J., Wang, Q., Li, F., et al. (2007). Positive linear relationship between productivity and diversity: evidence from the Eurasian Steppe. *J. Appl. Ecol.* 44, 1023–1034. doi: 10.1111/j.1365-2664.2007.01351.x

Bakker, E. S., Ritchie, M. E., Olff, H., Milchunas, D. G., and Knops, J. M. (2006). Herbivore impact on grassland plant diversity depends on habitat productivity and herbivore size. *Ecol. Lett.* 9, 780–788. doi: 10.1111/j.1461-0248.2006.00925.x

Bangert, R. K., and Slobodchikoff, C. N. (2006). Conservation of prairie dog ecosystem engineering may support arthropod beta and gamma diversity. *J. Arid Environ.* 67, 100–115. doi: 10.1016/j.jaridenv.2006.01.015

Bloor, J. M., Tardif, A., and Pottier, J. (2020). Spatial heterogeneity of vegetation structure, plant n pools and soil N content in relation to grassland management. *Agronomy* 10:716. doi: 10.3390/agronomy10050716

Bochet, E. (2015). The fate of seeds in the soil: a review of the influence of overland flow on seed removal and its consequences for the vegetation of arid and semiarid patchy ecosystems. *Soil* 1, 131–146. doi: 10.5194/soil-1-131-2015

Borer, E. T., Seabloom, E. W., Gruner, D. S., Harpole, W. S., Hillebrand, H., Lind, E. M., et al. (2014). Herbivores and nutrients control grassland plant diversity via light limitation. *Nature* 508, 517–520. doi: 10.1038/nature13144

Case, M. F., Halpern, C. B., and Levin, S. A. (2013). Contributions of gopher mound and casting disturbances to plant community structure in a Cascade Range meadow complex. *Botany* 91, 555–561. doi: 10.1139/cjb-2013-0023

Davidson, A. D., Detling, J. K., and Brown, J. H. (2012). Ecological roles and conservation challenges of social, burrowing, herbivorous mammals in the world's grasslands. *Front. Ecol. Environ.* 10, 477–486. doi: 10.1890/110054

Dobson, F. S., Smith, A. T., and Gao, W. X. (1998). Social and ecological influences on dispersal and philopatry in the plateau pika (*Ochotona curzoniae*). *Behav. Ecol.* 9, 622–635. doi: 10.1093/beheco/9.6.622

Dumbrell, A. J., Clark, E. J., Frost, G. A., Randell, T. E., Pitchford, J. W., and Hill, J. K. (2008). Changes in species diversity following habitat disturbance are dependent on spatial scale: theoretical and empirical evidence. *J. Appl. Ecol.* 45, 1531–1539. doi: 10.1111/j.1365-2664.2008.01533.x

Fan, N., Zhou, W., Wei, W., Wang, Q., and Jiang, Y. (1999). "Rodent pest management in the Qinghai-Tibet alpine meadow ecosystem," in *Ecologically-Based Rodent Management*, eds G. R. Singleton, L. A. Hinds, H. Leirs, and Z. Zhang (Canberra, ACT: Australian Centre International Agricultural Research), 285–304.

Guo, Z. G., Li, X. F., Liu, X. Y., and Zhou, X. R. (2012). Response of alpine meadow communities to burrow density changes of plateau pika (*Ochotona curzoniae*) in the Qinghai-Tibet Plateau. *Acta Ecol. Sin.* 32, 44–49. doi: 10.1016/j.chnaes.2011.12.002

Guo, Z. G., Liang, T. G., and Zhang, Z. H. (2003). Classification management for grassland in Gansu Province, China. *N. Zeal. J. Agric. Res.* 46, 123–131. doi: 10.1080/00288233.2003.9513538

Hector, A., Schmid, B., Beierkuhnlein, C., Caldeira, M. C., Diemer, M., Dimitrakopoulos, P. G., et al. (1999). Plant diversity and productivity experiments in European grasslands. *Science* 286, 1123–1127. doi: 10.1126/science.286.5442.1123

Hobbs, R. J., and Huenneke, L. F. (1992). Disturbance, diversity, and invasion: implications for conservation. *Conserv. Biol.* 6, 324–337. doi: 10.1046/j.1523-1739.1992.06030324.x

Jones, C. C., Halpern, C. B., and Niederer, J. (2008). Plant succession on gopher mounds in western Cascade meadows: consequences for species diversity and heterogeneity. *Am. Midland Nat.* 159, 275–286. doi: 10.1674/0003-0031(2008)159[275:PSOGMI]2.0.CO;2

Jones, C. G., Lawton, J. H., and Shachak, M. (1997). Positive and negative effects of organisms as physical ecosystem engineers. *Ecology* 78, 1946–1957. doi: 10.1890/0012-9658(1997)078[1946:PANEOO]2.0.CO;2

Kelemen, A., Tölgyesi, C., Valkó, O., Deák, B., Miglécz, T., Fekete, R., et al. (2019). Density-dependent plant–plant interactions triggered by grazing. *Front. Plant Sci.* 10:876. doi: 10.3389/fpls.2019.00876

Kolasa, J., and Rollo, C. D. (1991). "Introduction: the heterogeneity of heterogeneity: a glossary," in *Ecological Heterogeneity*, eds J. Kolasa and S. T. A. Pickett (New York, N Y: Springer), 1–23. 07/978-1-4612-3062-5_1 doi: 10.1007/978-1-4612-3062-5_1

Lindtner, P., Svitok, M., Ujházy, K., and Kubovčík, V. (2020). Disturbances by the European ground squirrel enhance diversity and spatial heterogeneity of plant communities in temperate grassland. *Biodivers. Conserv.* 29, 853–867. doi: 10.1007/s10531-019-01914-5

Liu, W., Zhang, Y., Wang, X., Zhao, J. Z., Xu, Q. M., and Zhou, L. (2009). The relationship of the harvesting behavior of plateau pikas with the plant community. *Acta Theriol. Sin.* 29, 40–49.

Liu, Y. S., Fan, J. W., Harris, W., Shao, Q. Q., Zhou, Y. C., and Wang, N. (2013). Effects of plateau pika (*Ochotona curzoniae*) on net ecosystem carbon exchange of grassland in the Three Rivers Headwaters region, Qinghai-Tibet, China. *Plant Soil* 366, 491–504. doi: 10.1007/s11104-012-1442-x

Liu, Y. S., Fan, J. W., Shi, Z. J., Yang, X. H., and Harris, W. (2017). Relationships between plateau pika (*Ochotona curzoniae*) densities and biomass and biodiversity indices of alpine meadow steppe on the Qinghai–Tibet Plateau China. *Ecol. Eng.* 102, 509–518. doi: 10.1016/j.ecoleng.2017.02.026

Michaels, J., Batzer, E., Harrison, S., and Eviner, V. T. (2021). Grazing affects vegetation diversity and heterogeneity in California vernal pools. *Ecology* 102:e03295. doi: 10.1002/ecy.3295

Milton, S. J., Dean, W. R. J., and Klotz, S. (1997). Effects of small-scale animal disturbances on plant assemblages of set-aside land in Central Germany. *J. Veg. Sci.* 8, 45–54. doi: 10.2307/3237241

Otieno, D. O., K'Otuto, G. O., Jákli, B., Schröttle, P., Maina, J. N., Jung, E., et al. (2011). Spatial heterogeneity in ecosystem structure and productivity in a moist Kenyan savanna. *Plant Ecol.* 212, 769–783. doi: 10.1007/s11258-010-9863-1

Pang, X. P., and Guo, Z. G. (2017). Plateau pika disturbances alter plant productivity and soil nutrients in alpine meadows of the Qinghai-Tibetan Plateau, China. *Rangeland J.* 39, 133–144. doi: 10.1071/RJ16093

Pang, X. P., and Guo, Z. G. (2018). Effects of plateau pika disturbance levels on the plant diversity and biomass of an alpine meadow. *Grassland Sci.* 64, 159–166. doi: 10.1111/grs.12199

Pang, X. P., Wang, Q., and Guo, Z. G. (2021). The impact of the plateau pika on the relationship between plant aboveground biomass and plant species richness. *Land Degrad. Dev.* 32, 1205–1212. doi: 10.1002/ldr.3790

Pang, X. P., Wang, Q., Zhang, J., Xu, H. P., Zhang, W. N., Wang, J., et al. (2020). Responses of soil inorganic and organic carbon stocks of alpine meadows to the disturbance by plateau pikas. *Eur. J. Soil Sci.* 71, 706–715. doi: 10.1111/ejss.12895

Questad, E. J., and Foster, B. L. (2007). Vole disturbances and plant diversity in a grassland metacommunity. *Oecologia* 153, 341–351. doi: 10.1007/s00442-007-0734-y

R Core Team (2020). *R: A Language and Environment for Statistical Computing*. Vienna: R Foundation for Statistical Computing.

Scherrer, D., Mod, H. K., Pottier, J., Litsios-Dubuis, A., Pellissier, L., Vittoz, P., et al. (2019). Disentangling the processes driving plant assemblages in mountain grasslands across spatial scales and environmental gradients. *J. Ecol.* 107, 265–278. doi: 10.1111/1365-2745.13037

Smith, A. T., and Foggin, J. M. (1999). The plateau pika (*Ochotona curzoniae*) is a keystone species for biodiversity on the Tibetan plateau. *Anim. Conserv.* 2, 235–240. doi: 10.1111/j.1469-1795.1999.tb00069.x

Smith, A. T., Wilson, M. C., and Hogan, B. W. (2019). Functional-trait ecology of the plateau pika (*Ochotona curzoniae*) in the Qinghai-Tibetan Plateau ecosystem. *Integr. Zool.* 14, 87–103. doi: 10.1111/1749-4877.12300

Song, S., Zhu, J., Zheng, T., Tang, Z., Zhang, F., Ji, C., et al. (2020). Long-term grazing exclusion reduces species diversity but increases community heterogeneity in an alpine grassland. *Front. Ecol. Evol.* 8:66. doi: 10.3389/fevo.2020.00066

Sun, F. D., Chen, W. Y., Liu, L., Liu, W., Cai, Y. M., and Smith, P. (2015). Effects of plateau pika activities on seasonal plant biomass and soil properties in the alpine meadow ecosystems of the Tibetan Plateau. *Grassland Sci.* 61, 195–203. doi: 10.1111/grs.12101

Tilman, D., Reich, P. B., and Knops, J. M. (2006). Biodiversity and ecosystem stability in a decade-long grassland experiment. *Nature* 441, 629–632. doi: 10.1038/nature04742

Wang, Q., Guo, Z. G., Pang, X. P., Zhang, J., and Yang, H. (2020). Effects of small-herbivore disturbance on the clonal growth of two perennial graminoids in alpine meadows. *Alpine Bot.* 130, 115–127. doi: 10.1007/s00035-020-00240-9

Wang, Q., Yu, C., Pang, X. P., Jin, S. H., Zhang, J., and Guo, Z. G. (2018). The disturbance and disturbance intensity of small and semi-fossorial herbivores alter the belowground bud density of graminoids in alpine meadows. *Ecol. Eng.* 113, 35–42. doi: 10.1016/j.ecoleng.2018.01.003

Wei, W. R., He, J. D., and Zheng, Q. Y. (2020). Plateau pikas (*Ochotona curzoniae*) at low densities have no destructive effect on winter pasture in alpine meadows. *Rangeland J.* 42, 55–61. doi: 10.1071/RJ19042

Wei, W. R., Knops, J. M., and Zhang, W. (2019). The impact of plateau pikas (*Ochotona curzoniae*) on alpine grassland vegetation and soil is not uniform within the home range of pika families. *Plant Ecol. Divers.* 12, 417–426. doi: 10.1080/17550874.2019.1628113

Wilson, M. C., and Smith, A. T. (2015). The pika and the watershed: the impact of small mammal poisoning on the ecohydrology of the Qinghai-Tibetan Plateau. *Ambio* 44, 16–22. doi: 10.1007/s13280-014-0568-x

Yoshihara, Y., Ohkuro, T., Bayarbaatar, B., and Takeuchi, K. (2009). Effects of disturbance by Siberian marmots (*Marmota sibirica*) on spatial heterogeneity of vegetation at multiple spatial scales. *Grassland Sci.* 55, 89–95. doi: 10.1111/j.1744-697X.2009.00143.x

Yu, C., Zhang, J., Pang, X. P., Wang, Q., Zhou, Y. P., and Guo, Z. G. (2017). Soil disturbance and disturbance intensity: response of soil nutrient concentrations of alpine meadow to plateau pika bioturbation in the Qinghai-Tibetan Plateau, China. *Geoderma* 307, 98–106. doi: 10.1016/j.geoderma.2017.07.041

Yurkewycz, R. P., Bishop, J. G., Crisafulli, C. M., Harrison, J. A., and Gill, R. A. (2014). Gopher mounds decrease nutrient cycling rates and increase adjacent vegetation in volcanic primary succession. *Oecologia* 176, 1135–1150. doi: 10.1007/s00442-014-3075-7

Zhang, W. N., Wang, Q., Zhang, J., Pang, X. P., Xu, H. P., Wang, J., et al. (2020). Clipping by Plateau Pikas and impacts to plant community. *Rangeland Ecol. Manag.* 73, 368–374. doi: 10.1016/j.rama.2020.01.010

Zhao, J., Tian, L., Wei, H., Zhang, T., Bai, Y., Li, R., et al. (2021). Impact of plateau pika (*Ochotona curzoniae*) burrowing-induced microtopography on ecosystem respiration of the alpine meadow and steppe on the Tibetan plateau. *Plant Soil* 458, 217–230. doi: 10.1007/s11104-019-04122-w

Conflict of Interest: The authors declare that the research was conducted in the absence of any commercial or financial relationships that could be construed as a potential conflict of interest.

Publisher's Note: All claims expressed in this article are solely those of the authors and do not necessarily represent those of their affiliated organizations, or those of the publisher, the editors and the reviewers. Any product that may be evaluated in this article, or claim that may be made by its manufacturer, is not guaranteed or endorsed by the publisher.

Copyright © 2021 Li, Qi, Duan and Guo. This is an open-access article distributed under the terms of the Creative Commons Attribution License (CC BY). The use, distribution or reproduction in other forums is permitted, provided the original author(s) and the copyright owner(s) are credited and that the original publication in this journal is cited, in accordance with accepted academic practice. No use, distribution or reproduction is permitted which does not comply with these terms.

frontiers in Plant Science

ORIGINAL RESEARCH
published: 04 November 2021
doi: 10.3389/fpls.2021.773759

Applying Bayesian Belief Networks to Assess Alpine Grassland Degradation Risks: A Case Study in Northwest Sichuan, China

Shuang Zhou[1,2] *and Li Peng*[3]*

[1] Research Center for Mountain Development, Institute of Mountain Hazards and Environment, Chinese Academy of Sciences, Chengdu, China, [2] College of Resources and Environment, University of Chinese Academy of Sciences, Beijing, China, [3] College of Geography and Resources, Sichuan Normal University, Chengdu, China

OPEN ACCESS

Edited by:
Jian Sun,
Institute of Tibetan Plateau Research, Chinese Academy of Sciences (CAS), China

Reviewed by:
Jiangbo Gao,
Institute of Geographic Sciences and Natural Resources Research, Chinese Academy of Sciences (CAS), China
Dongsheng Zhao,
Institute of Geographic Sciences and Natural Resources Research, Chinese Academy of Sciences (CAS), China

***Correspondence:**
Li Peng
pengli@imde.ac.cn

Specialty section:
This article was submitted to Functional Plant Ecology, a section of the journal Frontiers in Plant Science

Received: *10 September 2021*
Accepted: *15 October 2021*
Published: *04 November 2021*

Citation:
Zhou S and Peng L (2021) Applying Bayesian Belief Networks to Assess Alpine Grassland Degradation Risks: A Case Study in Northwest Sichuan, China. Front. Plant Sci. 12:773759. doi: 10.3389/fpls.2021.773759

Grasslands are crucial components of ecosystems. In recent years, owing to certain natural and socio-economic factors, alpine grassland ecosystems have experienced significant degradation. This study integrated the frequency ratio model (FR) and Bayesian belief networks (BBN) for grassland degradation risk assessment to mitigate several issues found in previous studies. Firstly, the identification of non-encroached degraded grasslands and shrub-encroached grasslands could help stakeholders more accurately understand the status of different types of alpine grassland degradation. In addition, the index discretization method based on the FR model can more accurately ascertain the relationship between grassland degradation and driving factors to improve the accuracy of results. On this basis, the application of BBN not only effectively expresses the complex causal relationships among various variables in the process of grassland degradation, but also solves the problem of identifying key factors and assessing grassland degradation risks under uncertain conditions caused by a lack of information. The obtained result showed that the accuracies based on the confusion matrix of the slope of NDVI change (NDVIs), shrub-encroached grasslands, and grassland degradation indicators in the BBN model were 85.27, 88.99, and 74.37%, respectively. The areas under the curve based on the ROC curve of NDVIs, shrub-encroached grasslands, and grassland degradation were 75.39% ($P < 0.05$), 66.57% ($P < 0.05$), and 66.11% ($P < 0.05$), respectively. Therefore, this model could be used to infer the probability of grassland degradation risk. The results obtained using the model showed that the area with a higher probability of degradation ($P > 30\%$) was 2.22 million ha (15.94%), with 1.742 million ha (78.46%) based on NDVIs and 0.478 million ha (21.54%) based on shrub-encroached grasslands. Moreover, the higher probability of grassland degradation risk was mainly distributed in regions with lower vegetation coverage, lower temperatures, less potential evapotranspiration, and higher soil sand content. Our research can provide guidance for decision-makers when formulating scientific measures for alpine grassland restoration.

Keywords: Bayesian belief networks, alpine grassland degradation, frequency ratio model, NDVI, risk assessment

INTRODUCTION

Grasslands cover approximately 40% of the global area, and have significant effects on the production, daily life of humans, and ecology (Zong et al., 2021). However, these grasslands are currently degrading owing to the influence of human activity and climatic changes on grassland ecosystems. As a typical ecologically vulnerable area, alpine grasslands have significantly changed in terms of plant productivity and diversity, soil properties, and vegetation community. This has resulted in extensive degradation (Zhang et al., 2018; Miehe et al., 2019). Alpine grassland degradation has become an ecological and environmental issue that is of global concern (Seddon et al., 2016; Zhang et al., 2018). Take the Qinghai-Tibet Plateau as an example, whose coverage area of alpine grassland is 128.78 million ha (Liu et al., 2021). However, nearly 50% of the grasslands have been degraded owing to the interference of livestock husbandry and climatic changes (Teng et al., 2020). To relieve the ecological environmental pressure caused by alpine grassland degradation, the government of China (GOC) has implemented a plan to turn grazing land back into grassland and implement a policy of grassland ecological compensation. Although grassland vegetation is improving overall, intensive grassland degradation is occurring in local areas (Zhou et al., 2020; Wang Z. et al., 2021). Further, alpine grassland ecosystems are complex systems, making it difficult to solve all degradation problems through policy instruments alone. Hence, recognising and predicting grassland degradation patterns from the dual perspective of nature and humanity is imperative.

Previous studies on grassland degradation assessment are mainly based on remote sensing technology and parameter assessment systems (Gao et al., 2006; Feng et al., 2009; Lang et al., 2021). When using this method, indexes for grassland degradation are always uncertain, and most index parameters are set according to the subjective experience of researchers, resulting in the results being unreliable. Some scholars have detected grassland degradation using alarm signals (Lin et al., 2015; Han et al., 2018). However, this method had a small observation scope, and can only ascertain grassland degradation, without understanding its driving forces. In addition, previous studies do not take into consideration probability due to the complexity of grassland degradation mechanisms, the uncertainty of risk driving factors, and approaches limitations (Fleskens and Stringer, 2014; Farber, 2015). In fact, grassland degradation is influenced by multiple factors and the degradation trend should be a probability event. This risk assessment is determined by scientific cause and effect relationships where cause and effect are understood and predictable (although uncertainty is not quite zero) (French, 2015).

Therefore, an effective method for grassland degradation risk assessment – which can not only express the uncertainty of grassland degradation, but also understand the quantitative inference of grassland degradation risk probabilities according to the relationship between grassland degradation and driving factors – is required. As a method to measure the probability of risk occurrence, Bayesian belief networks (BBN) have been widely applied in accident risk assessment (Zywiec et al., 2021) and health risk prediction (Orak, 2020). Recently, the application of BBN to ecological environments is gradually increasing, including for decision support (Dang et al., 2019) and risk assessment (Plomaritis et al., 2018). BBN integrates several continuous variables (e.g., precipitation) and discrete variables (e.g., soil texture) through qualitative and quantitative analysis to construct an independent model (Zhu et al., 2020). Moreover, BBN inherits various data sources (e.g., expert knowledge, historical data, and empirical data) and transforms qualitative causality into a quantitative inference model based on probability calculations (Kerebel et al., 2019). The uncertainty of factors can be effectively solved because the uncertainty of the factor is transferred to the target variable through the conditional probability distribution table in the BBN model (Calder et al., 2019). Therefore, BBN not only can be used to assess the grassland degradation risk, but can also act as a decision support tool for stakeholders to make scientific measures.

The grassland of the Northwest Sichuan Plateau is located along the northeast edges of the Qinghai-Tibet Plateau, which is one of the five typical vulnerable grassland ecological regions in China. In this region, the grassland area is 13.93 million ha, accounting for more than 50% of the total area of the region, and has a high ecological value in terms of water conservation, soil and water conservation, and biodiversity protection. However, the ecosystem of local grasslands is becoming more and more vulnerable owing to the interference of humans and natural factors, which influences ecosystem services and the development of livestock husbandry (Li et al., 2020).

In this study, a quantitative grassland degradation risk assessment of the Northwest Sichuan Plateau was carried out by integrating the frequency ratio model (FR) model and BBN model. (1) The degradation pattern of grasslands in the study period was identified based on land use data and the normalized difference vegetation index (NDVI). (2) The driving risk factors of grassland degradation were discretized using the FR model and the BBN model structure was established according to knowledge regarding the grassland degradation and driving factors. (3) The importance of driving factors was identified based on a sensitivity analysis of the BBN model. (4) The probability of grassland degradation risk occurrence in each grid was predicted. On one hand, research conclusions can acquire objective and integrated grassland degradation states in the Northwest Sichuan Plateau. On the other hand, this study can assist decision-makers to formulate grassland restoration measures to maintain sustainable development in the region.

MATERIALS AND METHODS

Study Area

With a total area of approximately 13.93 million ha, the alpine grasslands of the Northwest Sichuan Plateau – located along the southeast edges of the Qinghai-Tibet Plateau (97°34′ – 104°43′E, 27°96′ – 34°31′N), is home to two prefecture-level cities (Ganzi Tibetan Autonomous Region and Aba Tibetan and Qiang Autonomous Prefecture) and 31 counties (districts) (**Figure 1**). In 2018, the population was about 2.14 million, which

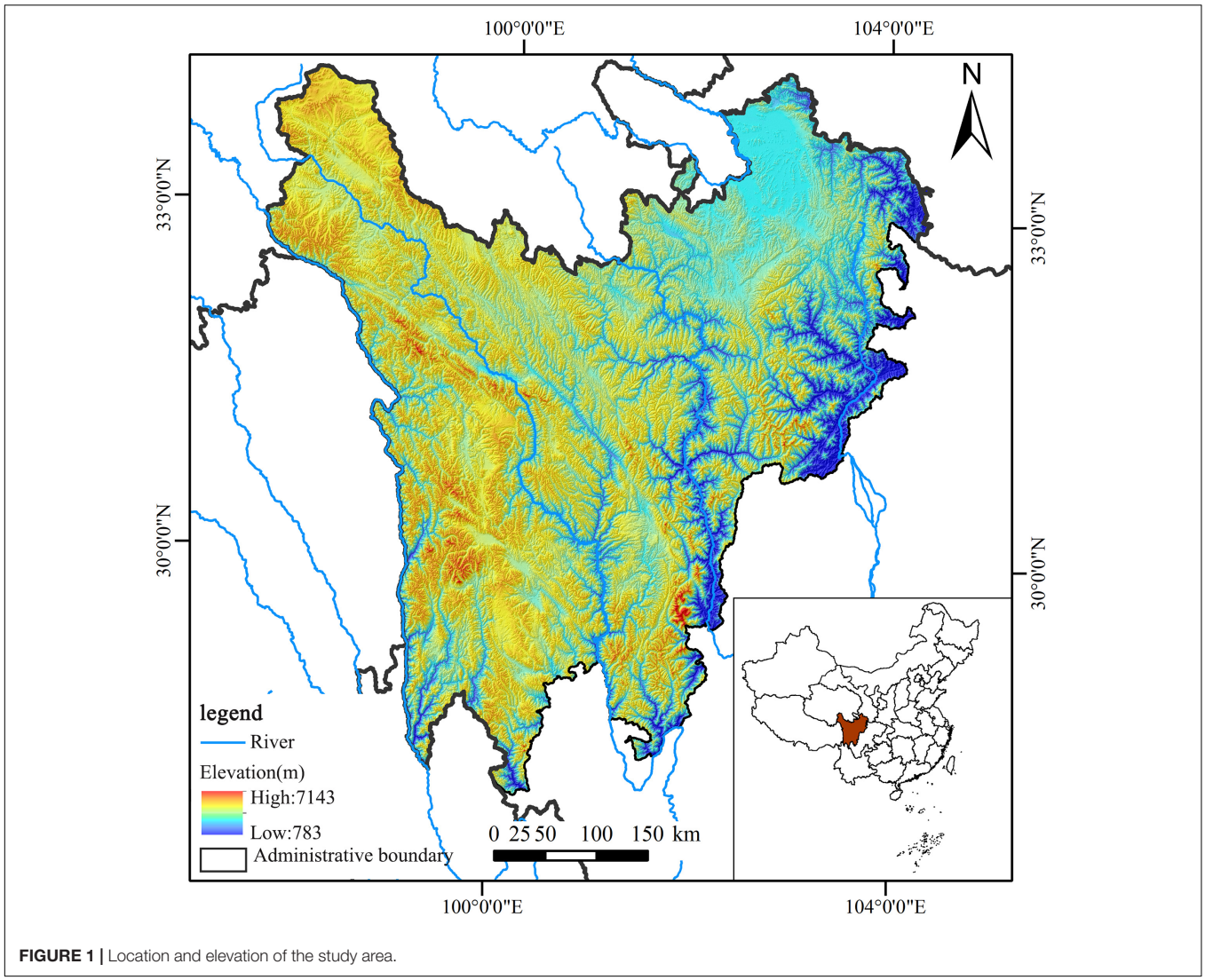

FIGURE 1 | Location and elevation of the study area.

only accounted for 2.6% of the total population of the Sichuan Province. In the region, the terrain lifts gradually from the east to the west, and the elevation ranges between 783 and 7,143 m. Grasslands are the major land-use type in the Northwest Sichuan Plateau, which accounts for 59.92% of the total area. Moreover, a large area comprises an ecological reserve, which plays an important role in water conservation, water–soil conservation, and biodiversity protection in China.

Owing to the high sensitivity and vulnerability of alpine grasslands, ecological functions in local areas are degrading in response to human activities and climate change. In particular, there has been a significant increase in grassland degradation and insect attacks. The area of grassland degradation, desertification, and salinization has reached 9.39 km^2, which accounts for 6.96% of the national value in China. Further, about 45% of the counties suffer from livestock overloading in the summer, which causes over-grazing in grasslands. Considering the ecological concerns and existing grassland degradation, the alpine grasslands of the Northwest Sichuan Plateau were chosen for grassland degradation risk assessment, which aims to help stakeholders recognize important spaces and allocate resources reasonably.

Data Collection

In this study, eight datasets were used, as follows. (1) Land use and land cover (LULC) data in 2005 and 2018, with spatial resolution of 30 m, from the Resource and Environmental Science Data Center of the Chinese Academy of Sciences[1]; (2) Digital elevation model (Elevation) data from SRTM90m were provided by the Resource and Environmental Science Data Center of the Chinese Academy of Sciences (see text footnote 1); (3) Nighttime light data was published on the Harvard Dataverse[2], with a spatial resolution of 500 m; (4) Geographic information data, including administrative boundaries, administrative centres, traffic network elements, and river basin datasets, were taken from the National

[1]http://www.resdc.cn/

[2]https://doi.org/10.7910/DVN/YGIVCD

Geomatics Center of China[3]; (5) Meteorological data from 2005 to 2018, including the precipitation, temperature, and potential evapotranspiration (ET_0), were obtained from China's meteorological data sharing service system[4]; (6) the MOD13Q1 NDVI from 2005 to 2018, with a spatial resolution of 250 m, was obtained from the United States Geological Survey[5]; (7) Soil texture data were taken from the 1:1,000,000 soil dataset of the National Tibetan Plateau Data Center[6]; and (8) the livestock numbers were provided by the local governmental department. In total, 18 potential factors affecting grassland degradation were selected (**Table 1**), and the spatial distribution of the indicators are shown in **Supplementary Figure 1**.

Methods

Concept of Bayesian Belief Networks

Bayesian belief networks is supported by a flexible network structure that can perform bottom-up reasoning or diagnostic analysis, along with top-down reasoning or predictive analysis (Rusek et al., 2021). They consist of nodes, which represent the random variables, and arrows, which represent the cause–effect relationship between variables. All variables in the BBN model are discretised into a limited number of states, and the causal relationship between a parent node X and a child node Y is quantified through a conditional probability table (CPT). For those nodes without a parent, the CPT transitions into a probability distribution with several possible states. These probabilities can be obtained through observational data, professional knowledge, or empirical observation (Kabir et al., 2015; Abebe et al., 2018). The primary advantage of using BBNs is that they reach probabilistic inferences or update their beliefs by integrating qualitative and quantitative data using the conditional probability theorem (Bicking et al., 2019) (Eq. 1). In the BBN model, the joint probability distribution (JPD) of related variables is obtained by multiplying the CPT of all nodes, as shown in Eq. 2. The JPD enables a BBN to effectively calculate the conditional probability of events based on the introduction of evidence variables. In the context of risk prediction, for example, the BBN can forecast the conditional probability of grassland degradation given information on evidence variables in each grid.

$$\mathbf{P}\,(\boldsymbol{B}|\boldsymbol{A}) \;=\; \frac{\boldsymbol{P}\,(\boldsymbol{A}|\boldsymbol{B}) \;\times\; \boldsymbol{P}\,(\boldsymbol{B})}{\boldsymbol{P}\,(\boldsymbol{A})} \tag{1}$$

Equation 1 indicates that the posterior probability of an event B based on the data or evidence A is observed in terms of the prior probability of B $P\,(B)$, the conditional probability of A given B $P\,(A \mid B)$, and the prior or marginal probability of A $P\,(A)$.

$$\mathbf{P}\,(\boldsymbol{X}_1, \boldsymbol{X}_2, \ldots, \boldsymbol{X}_\mathbf{n}) \;=\; \prod_{\boldsymbol{i}=\mathbf{1}}^{\boldsymbol{n}} \boldsymbol{P}\left(\boldsymbol{X}_\boldsymbol{i} \;\middle|\; \boldsymbol{parent}\,(\boldsymbol{X}_\boldsymbol{i})\right) \tag{2}$$

Equation 2 is a formal representation of probability theory to calculate the JPD over a set of related variables.

The construction of a BBN model includes model design and parameterization, model validation, and risk probability inference. The Genie and MATLAB software were used to construct the BBN model and infer the risk probability of grassland degradation. The design and application of the BBN model for the case study are presented in **Figure 2**.

Establish the Grassland Degradation Risk Inference Model

For macro-scale research, the characterization of grassland degradation based on NDVI is a commonly used method. NDVI is an important indicator of vegetation coverage, with which it has a significant linear relationship (Zhao et al., 2021). Therefore, for each grassland grid, the slope value of NDVI (NDVIs) from 2005 to 2018 could be used to indicate the trend of grassland change, and NDVIs values less than 0 could be regarded as grassland degradation. However, it is worth noting that NDVIs values lower than 0 do not indicate grassland degradation, because shrub-encroached grasslands in alpine regions are an important form of grassland degradation and do not necessarily lead to a reduction in NDVI (Fraser et al., 2014; May et al., 2020). Therefore, to more comprehensively identify the pattern of grassland degradation, we defined grassland degradation as non-encroached degraded

[3]https://www.openstreetmap.org/
[4]http://data.cma.cn/
[5]https://www.usgs.gov/
[6]http://data.tpdc.ac.cn/

TABLE 1 | Potential factors affecting grassland degradation.

Factors	Description	
Topographic	Elevation	Elevation (m)
	Slope	Slope (°)
Soil	Clay	Proportion of clay (%)
	Sand	Proportion of sand (%)
	Silt	Proportion of silt (%)
Climatic	Tm	Mean value of annual temperature (2005–2018) (°C)
	Ts	Slope of annual temperature change (2005–2018) (/)
	ETm	Mean value of annual potential evapotranspiration (2005–2018) (mm)
	ETs	Slope of annual potential evapotranspiration change (2005–2018) (/)
	Pm	Mean value of annual precipitation (2005–2018) (mm)
	Ps	Slope of annual precipitation change (2005–2018) (/)
Social and economic	Livestock	Mean value of the number of livestock (2005–2018) (cow unit)
	NTLm	Mean value of annual nighttime light (2005–2018) (/)
	NTLs	Slope of annual nighttime light change (2005–2018) (/)
	DW	Distance between each grid and its nearest water body (m)
	DR	Distance between each grid and its nearest road (m)
	DD/DC	Distance between each grid and its nearest administrative centre (m)
Others	NDVIm	Mean value of annual normalized difference vegetation index (2005–2018) (/)

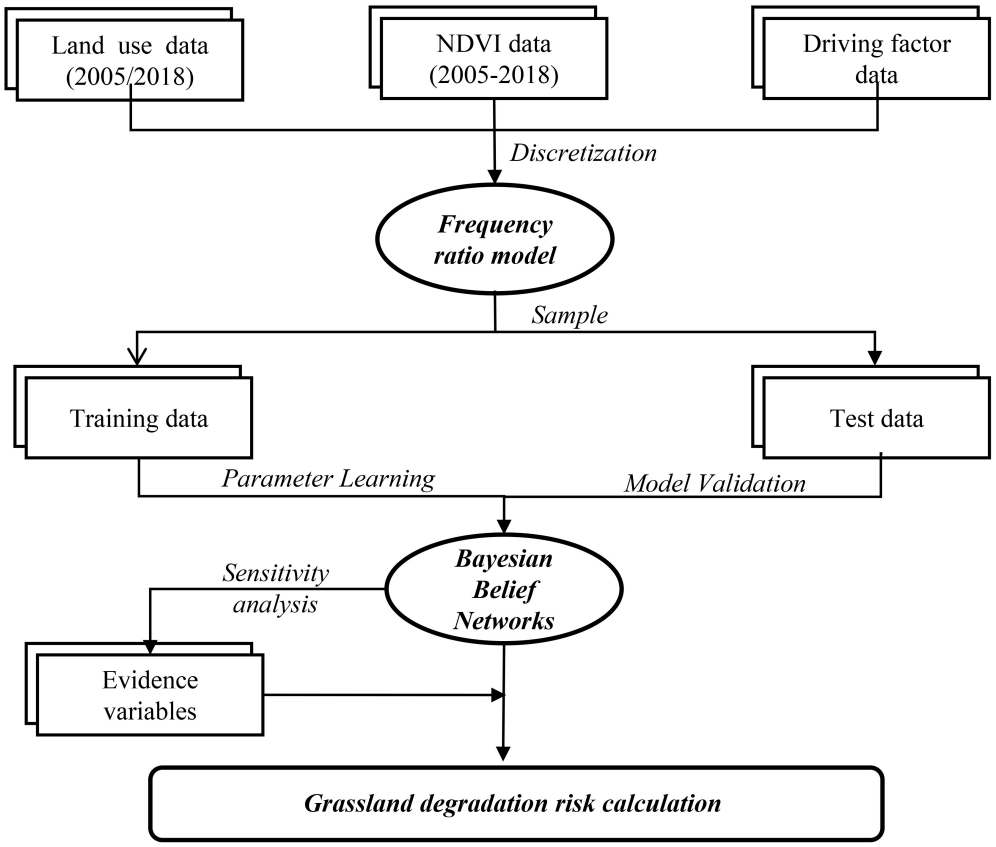

FIGURE 2 | Design and application framework of the BBN model.

grasslands with negative slope values of NDVIs (NDVIs < 0) and shrub-encroached grasslands.

Taking into account the non-stationarity of ecological processes, the diversity and incompleteness of data, and the complex relationships among factors, we selected 18 potential factors based on previous research results (Kane et al., 2017; Chen et al., 2020). The Pearson correlation coefficient was used to identify the correlation and intensity between potential factors and NDVIs or shrub-encroached grasslands. The results are shown in **Figure 3**, where the red pixels represent a positive correlation between two variables, blue pixels represent a negative correlation between two variables, and the flatter the ellipse, the larger the absolute value of the correlation coefficient. The results indicate that the selected potential factors had impacts on grassland degradation, other than NTLs, NTLm, and DD/DC. Therefore, NTLs, NTLm, and DD/DC were removed, because including them had no significant effect on the prediction results. In combination with the aforementioned analysis results, expert judgment, and historical data, the BBN-based grassland degradation risk model is constructed as shown in **Figure 4**.

Model Parameterization and Validation

First, the scientific division of driving factor states is the premise of the BBN model inference. As an efficient probabilistic method, the FR model can provide a more reliable prior knowledge for the BBN model of grassland degradation by calculating the frequency ratio of grassland degradation and impact factors in each interval. The larger the FR value, the higher the probability of grassland degradation (Yang et al., 2021). In this study, the FR not only characterizes the proportion of the area where grassland degradation occurs, but also explores the possibility of grassland degradation occurring (or not occurring)under given conditions. Thus, the intervals with similar frequency ratios can be merged to realize the scientific division of indicator factor status. It can be calculated as follows:

$$\mathrm{FR} = \frac{\boldsymbol{a}/\boldsymbol{b}(\%)}{\boldsymbol{c}/\boldsymbol{d}(\%)} \tag{3}$$

where a is the number of each factor's grassland degradation, b is the number of total grassland degradation, c is the number of pixels in a given factor, and d is the total number of pixels in the study area.

Then, a case file was generated, which included 124,517 observations, with each row representing a sample. The case file was randomly divided into two partitions: a training set (n = 99,614; 80%) for model development, and a testing set (n = 24,903; 20%) for accuracy. Given the link structures, the training dataset was entered into the model as evidence to calculate the CPTs of each node in the BBN model.

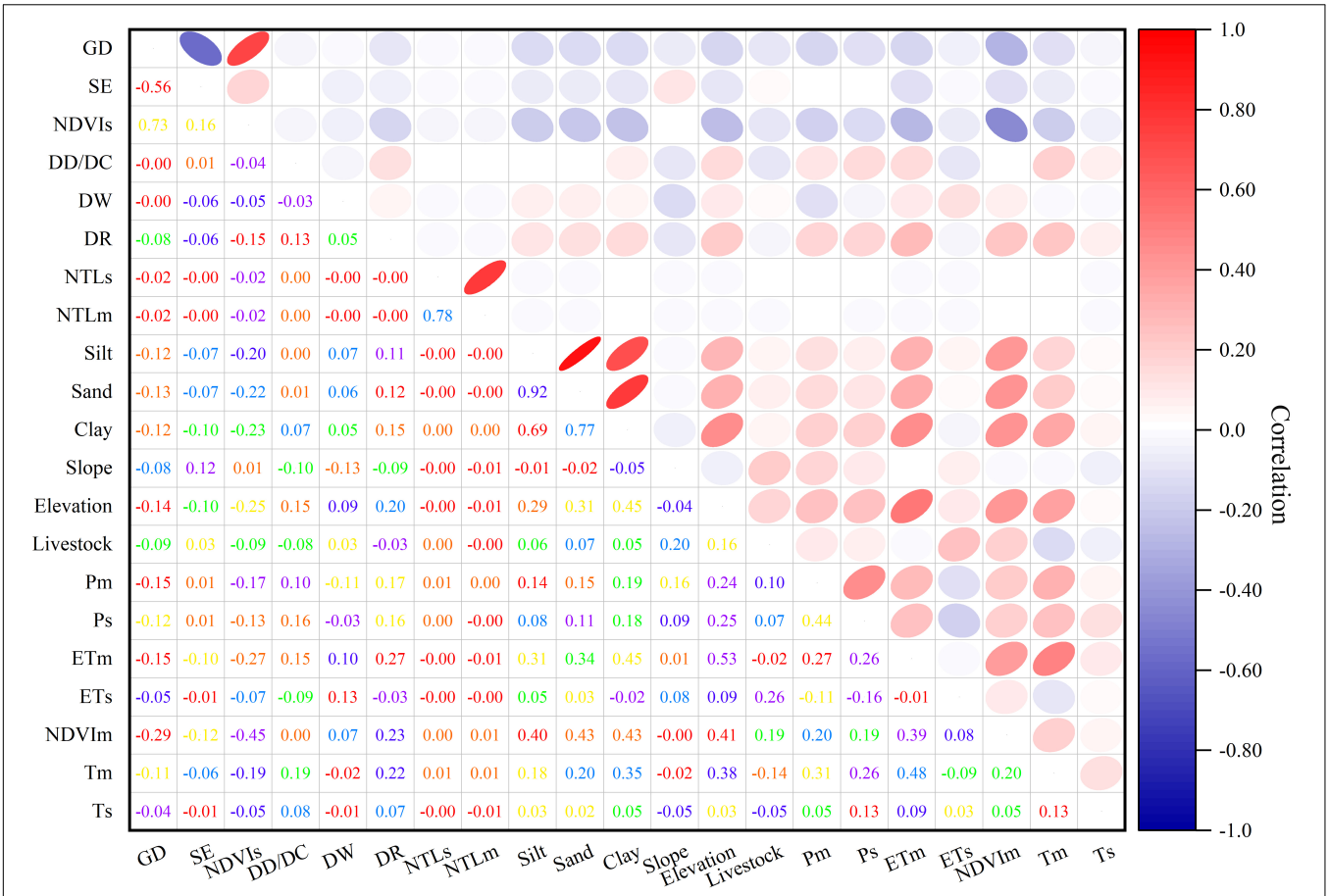

FIGURE 3 | Correlation matrix between the selected variables for grassland degradation. GD, grassland degradation; NDVIs, slope of NDVI change; SE, shrub-encroached grasslands.

Finally, to evaluate the accuracy of the BBN model predictions, a confusion matrix and receiver operating characteristic (ROC) curve were calculated using the testing set. The confusion matrix is a useful tool to ascertain the level of prediction accuracy by comparing the number of true values against the number of predicted values (Deng et al., 2016). The ROC curve can effectively measure the judgment ability of the model. If the model has good judgment ability, the ROC curve will be located above the diagonal of the coordinate axis, and the corresponding AUC will be greater than 0.5 (Anderson, 2019).

Grassland Degradation Risk Calculation

Through the evaluated BBN model, it is convenient to infer the probability of the target nodes in different combination states of evidence variables. The evidence variables with a significant contribution to grassland degradation were chosen through sensitivity analysis. Variance of belief (VB) – based on variance reduction – and mutual information (MI) – based on entropy reduction – are often used as sensitivity analysis indicators to quantitatively evaluate whether network nodes sensitively perceive changes in other nodes (Shi et al., 2020). Therefore, this study used the VB and MI to assess the sensitivity of input variables relative to the target variables. VB and MI are calculated as follows:

$$\mathrm{VB} = \mathbf{V}(S) - V(S|I) = \sum_{s} P(s) \times (s\text{-}E(S))^2 - \sum_{s} P(s|I) \times (s\text{-}E(S|I))^2 \quad (4)$$

$$\mathbf{MI} = H(S) - H(S|I) = \sum_{s}\sum_{i} P(s,i) log_2 \left(\frac{P(s,i)}{P(s) \times P(i)}\right) \quad (5)$$

where S is the target variable, I is another variable, and s and i represent the states of S and I, respectively. The larger the value of VB and MI, the stronger influence of the driving factor on the target variable.

According to the results of the sensitivity analysis, we selected six driving factors with the highest sensitivity to target variable changes as the evidence variables. The CPT and probability distribution of each node in the BBN model can infer the CPT of the target variable under given conditions (Hao et al., 2018). Therefore, by integrating the evidence variables of each grid into

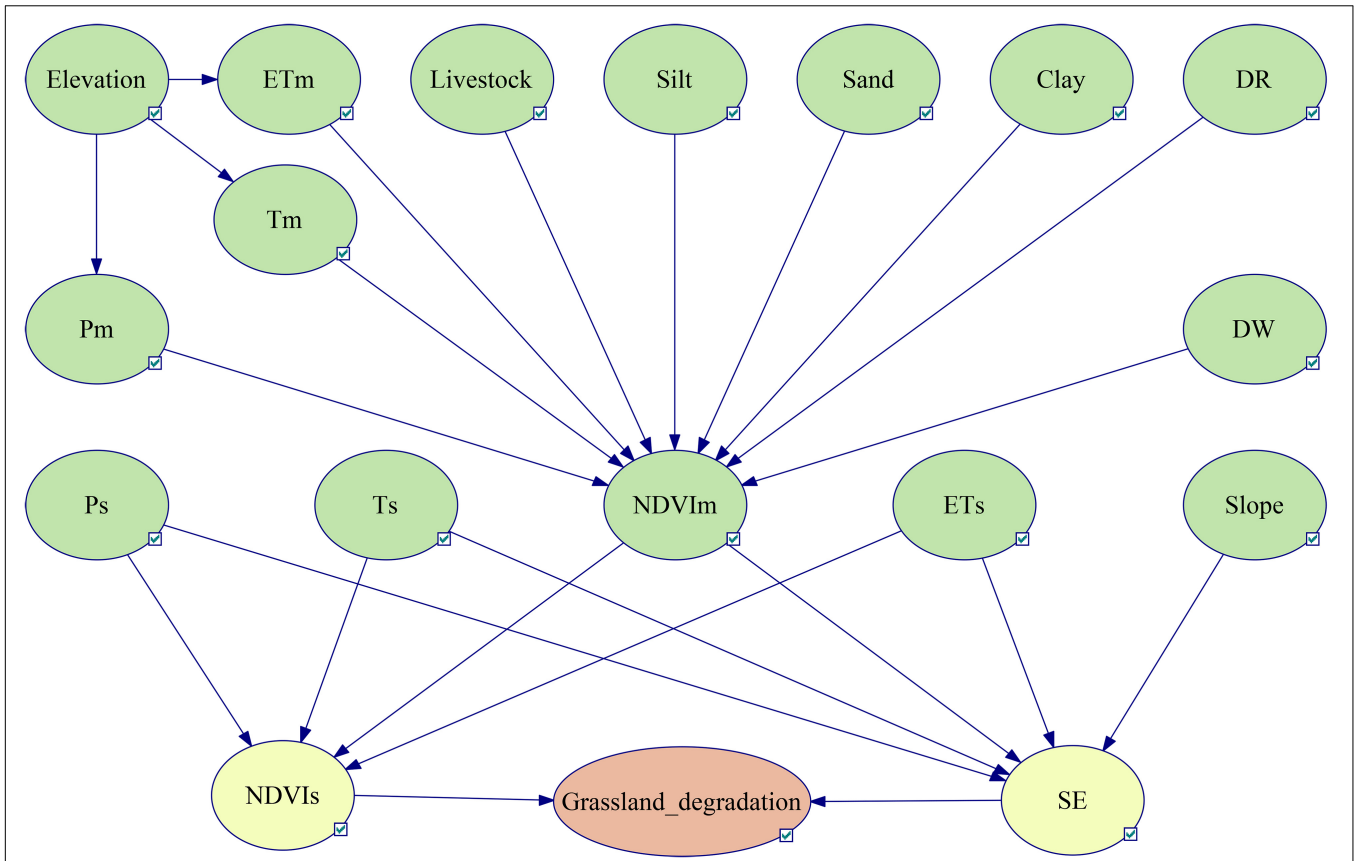

FIGURE 4 | Bayesian conceptual network of grassland degradation risk inference. NDVIs, slope of NDVI change; SE, shrub-encroached grasslands.

the established BBN model, we can obtain the potential grassland degradation risk in the grid.

RESULTS

Grassland Degradation Pattern

The dynamic variation trend of NDVI in each grid from 2005 to 2018 was calculated (**Figure 5A**). According to statistical results, the area of NDVIs less than 0 was 2.433 million ha, with 11.39% attributed to significantly decreased areas and 88.61% to non-significantly increased areas. In view of the spatial distribution, these areas are mainly distributed in Shiqu County, Songpan County, Daocheng County, and the junction of Maerkang County, Li County, and Xiaojin County. Based on land use data (**Supplementary Figure 2**) in 2005 and 2018, shrub-encroached grasslands were recognized, as shown in **Figure 5B**. The results showed that shrub-encroached grasslands covered an area of 1.689 million ha, and the areas of the degraded grids were larger in Daofu County, Songpan County, and Wenchuan County. Overall, the grassland degradation appeared in scattered areas and in a wide range. According to the results of the overlay analysis of shrub-encroached grasslands and NDVIs, a spatially intersecting area of 1.357 million ha was identified. This meant that the 1.553 million ha of degraded grasslands had been identified through shrub-encroached grasslands, which offset the shortcomings of grassland degradation recognition based on NDVIs only.

Driving Factors Analysis

The FR model was used to identify the relationship between screened driving factors and grassland degradation, and then the driving factors were discretized based on similar frequency ratios (**Figure 6**). For the soil silt content, the class with a soil silt content of less than 10% had the highest FR value, indicating that grassland degradation has the highest probability of occurrence. The results of soil sand content and soil silt content showed that most grassland degradation occurred at values >80% and <10%, respectively. The livestock results indicated that the >600,000 class had a higher FR value than the other classes, which indicated a high probability of grassland degradation. For Tm and Ts, the classes of −0.01 −0.03 and <−4°C, respectively, had a higher grassland degradation occurrence. The highest FR value of ETs, ETm, Ps, and Pm belonged to the −0.2−0.1 class, <400 mm, <−6, and >1,040 mm, respectively. Interestingly, some factors exhibited obvious spatial variations in terms of the FR results. For example, the FR results for the >5,000 m class of elevation and the >25° class of slope were greater than those of the other classes, indicating that the grassland degradation occurred close to high altitudes and high slopes. Regarding the DR and

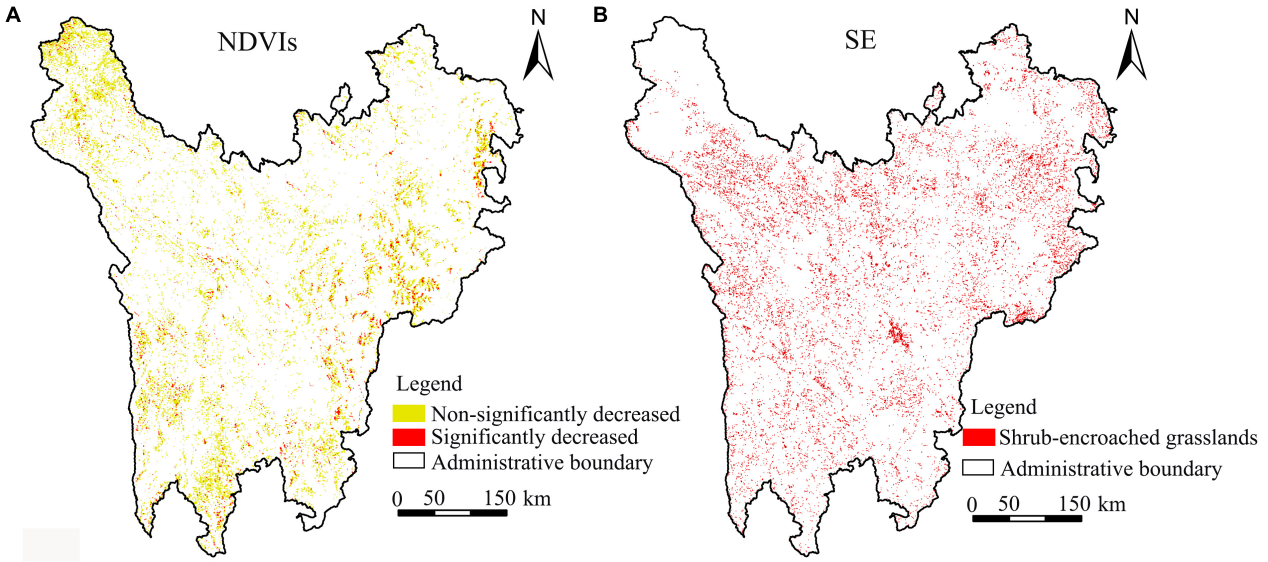

FIGURE 5 | Grassland degradation from 2005 to 2018. **(A)** NDVIs, slope of NDVI change. **(B)** SE, shrub-encroached grasslands.

DW factors, grassland degradation occurred more easily in areas 5,000–20,000 m away from roads and areas more than 7,500 m away from rivers. The FR value of NDVIm decreased with increases in vegetation coverage, which was not only consistent with prior knowledge of grassland degradation, but also verified the reliability of the experimental dataset. Based on the above analysis, the screened driving factors were classified according to the FR value. The results of the aforementioned classes can be found in **Supplementary Table 1**.

Parameter Learning and Model Validation

Based on the above discretization results regarding variables related to grassland degradation, 80% of the training set was selected randomly for the parameterization of the BBN model (**Figure 7**). According to the parameterization results, 31.58% of grassland grids were experiencing degradation trends, indicating that the severity of grassland degradation in the study area requires the attention of stakeholders. Furthermore, in comparison to the grid number of shrub-encroached grasslands (10.58%), the grid number of non-encroached degraded grasslands (NDVI <0) caused by human activities and climatic changes is higher (22.51%).

The NDVIs, shrub-encroached grasslands, and grassland degradation were predicted by entering the test set into the BBN model. The precision of the BBN model was evaluated based on the confusion matrix and ROC curve. The results of the confusion matrix showed that the prediction accuracy of NDVIs, shrub-encroached grasslands, and grassland degradation was 85.27, 88.99, and 74.37%, respectively. The AUCs based on the ROC curve of NDVIs, shrub-encroached grasslands, and grassland degradation were 75.39% ($P < 0.05$), 66.57% ($P < 0.05$), and 66.11% ($P < 0.05$), respectively (**Figure 8**). This made it clear that the model accuracy met the criterion for grassland degradation risk assessment.

Sensitivity Analysis of the Target Variables

Nodes of NDVIs, shrub-encroached grasslands, and grassland degradation were chosen as target variables for sensitivity analysis. **Figure 9** showed that the ratio of VB and MI exhibited a linear relationship; the higher value of MI, the higher value of VB. A high value of the ratio of VB and MI indicates the significant influence of the node on the target node. With respect to the nodes of grassland degradation and NDVIs, the variables of NDVIm, sand, silt, clay, ETm, and Tm had a high sensitivity (VB > 0.1%), indicating that they made significant contributions to grassland degradation. Therefore, significant attention should be paid to controlling the vegetation coverage, soil texture, and climatic factors in the grassland degradation regions in the future. For nodes of shrub-encroached grasslands, the higher sensitivity of NDVIm (VB = 0.179%) and Ps (VB = 0.106%) indicated that vegetation coverage and precipitation have significant influences on grassland degradation.

Heat maps showed the probability relationship between the state of the target variables and the influencing factors (**Figure 10**). The reddest pixels indicated that the factor has the highest conditional probability under the states of the given target variables. The bluest pixels indicated that the factor has the lowest conditional probability under the state of the given target variables. For example, the optimal combination of factors that had significant influences on grassland degradation was as follows: {NDVIm = Low, sand = Low, silt = Low, clay = Medium, ETm = Medium, Tm = Lowest}. For NDVIs, the probability of grassland degradation was relatively high when the optimal combination of factors was as follows: {NDVIm = Medium, sand = Low, silt = Low, clay = Medium, ETm = Medium, Tm = Lowest}. The probability of shrub-encroached grasslands in grids was relatively high when the grid was {NDVIm = Low, Ps = Low, slope = High, Ts = Highest, ETs = Medium, ETm = Low}. Therefore, attention should be paid to regions

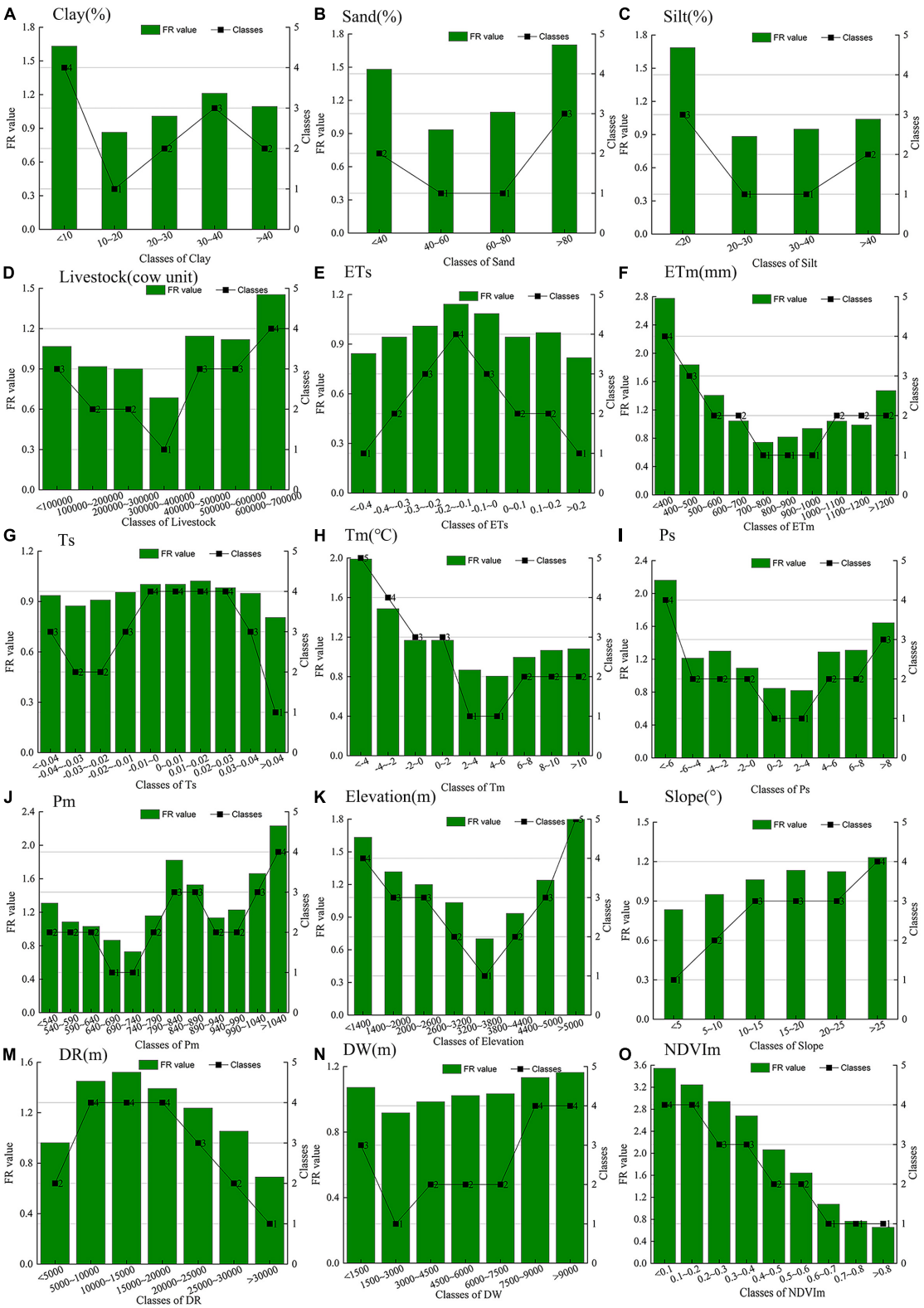

FIGURE 6 | Relationship between the grass degradation and the conditioning factors. **(A)** Clay. Proportion of clay. **(B)** Sand (%). Proportion of sand. **(C)** Silt (%). Proportion of silt. **(D)** Lm (cow unit). Mean value of the number of livestock. **(E)** Ts. Slope of annual temperature change. **(F)** Tm (°C). Mean value of annual temperature. **(G)** ETs. Slope of annual potential evapotranspiration change. **(H)** ETm (mm). Mean value of annual potential evapotranspiration. **(I)** Ps. Slope of annual precipitation. **(J)** Pm (mm). Mean value of annual precipitation. **(K)** DEM (m). Elevation. **(L)** Slope (°). Slope. **(M)** DR (m). The distance between each grid and its nearest road. **(N)** DW (°). The distance between each grid and its nearest water body. **(O)** NDVIm. Mean value of annual normalized difference vegetation index.

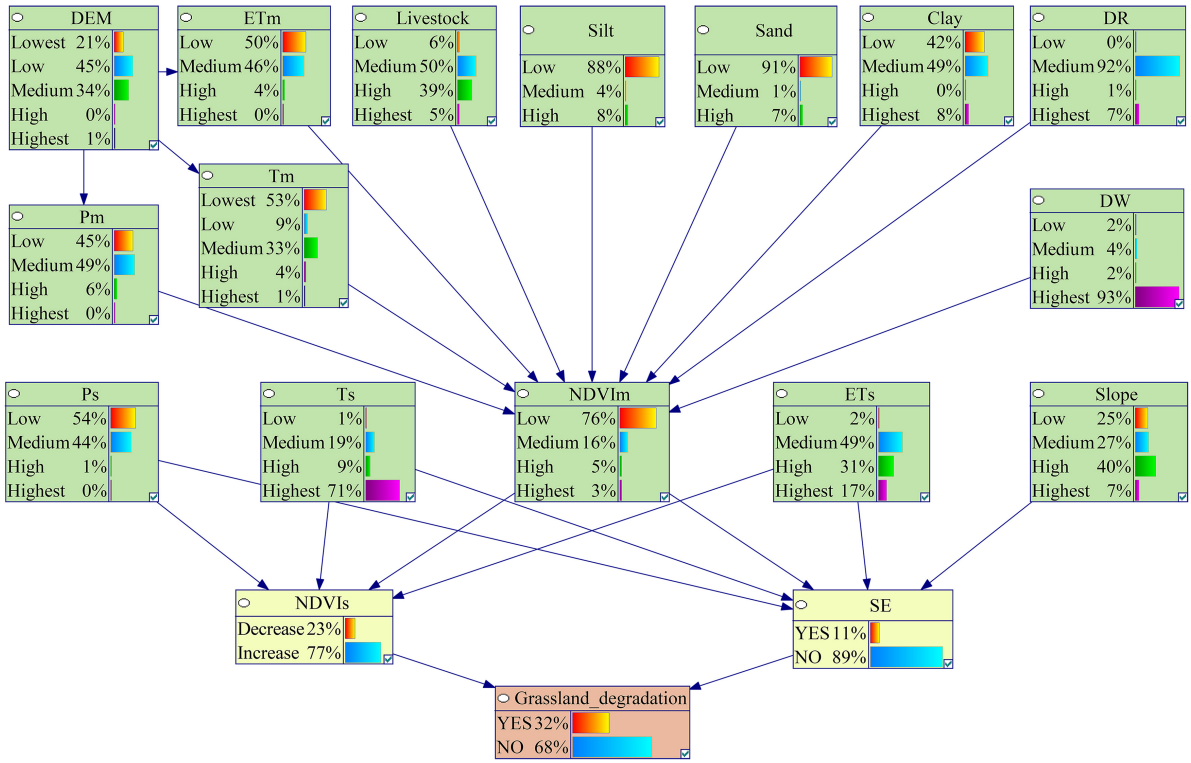

FIGURE 7 | Results of parameter learning in the BBN model. NDVIs, slope of NDVI change; SE, shrub-encroached grasslands.

in the factor state combination that met the above conditions in the next stage.

Grassland Degradation Risk Probability Calculation

Based on the sensitivity analysis results (**Figure 9**) and corresponding principles, the evidence variables for NDVIs, shrub-encroached grasslands, and grassland degradation were chosen to infer the probability of the land degradation risks for each grid unit. These were NDVIm, sand, silt, clay, ETm, and Tm in NDVIs index and grassland degradation index. In the shrub-encroached grasslands index, these variables were NDVIm, Ps, slope, Ts, ETs, and ETm.

Figure 11 showed the probability of the degradation risk identified by NDVIs and shrub-encroached grasslands indicators in each grid according to the selected evidence variables. The results showed that the probability ranges of the degradation risk of NDVIs and shrub-encroached grasslands in the study area were 10.15–78.88% and 0.69–83.33%, respectively. According to grading results of the risks, the area of high-risk grassland degradation ($P > 30\%$) predicted by NDVIs is 1.742 million ha, which accounted for 12.51% of the total study area. Moreover, these regions were primarily distributed in Shiqu County and the junction areas of Li County, Xiaojin County, and Wenchuan County, corresponding to areas with the "low" state of NDVIm, sand, and silt; the "medium" state of clay and ETm; and the "lowest" state of Tm. The area of high-risk grassland degradation ($P > 30\%$) predicted by shrub-encroached grasslands is 0.636 million ha, which accounted for 4.57% of the total area, and these regions were mainly distributed in Mao County and Luding County, corresponding to areas with a "low" state of NDVIm, Ps, and ETm; "high" state of slope; "highest" state of Ts; and "medium" state of ETs, as expected.

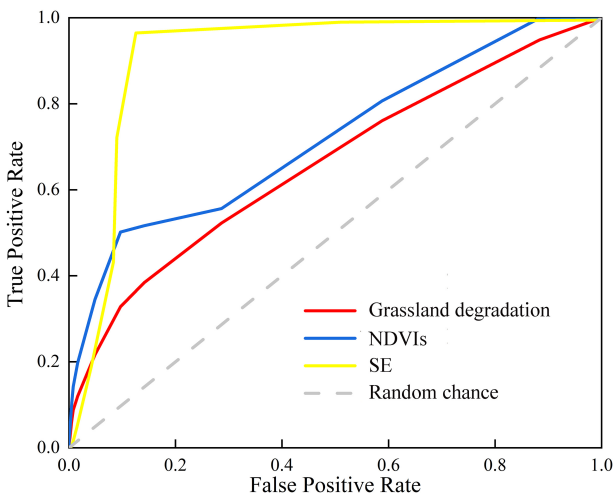

FIGURE 8 | ROC curve of NDVIs, shrub-encroached grasslands, and grassland degradation. NDVIs, slope of NDVI change; SE, shrub-encroached grasslands.

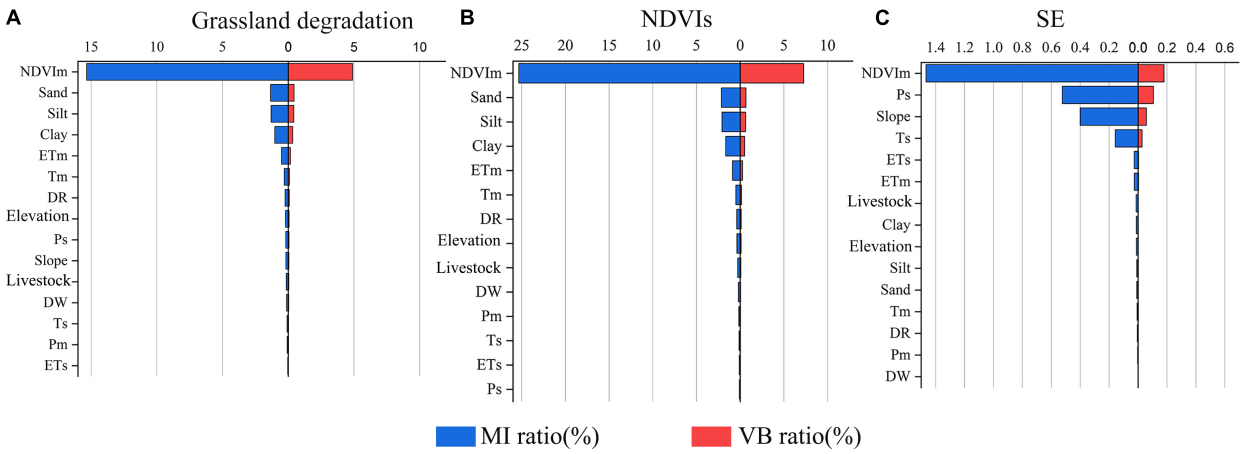

FIGURE 9 | Sensitivity analysis of all driving factors. **(A)** Grassland degradation. **(B)** NDVIs, slope of NDVI change. **(C)** SE, shrub-encroached grasslands.

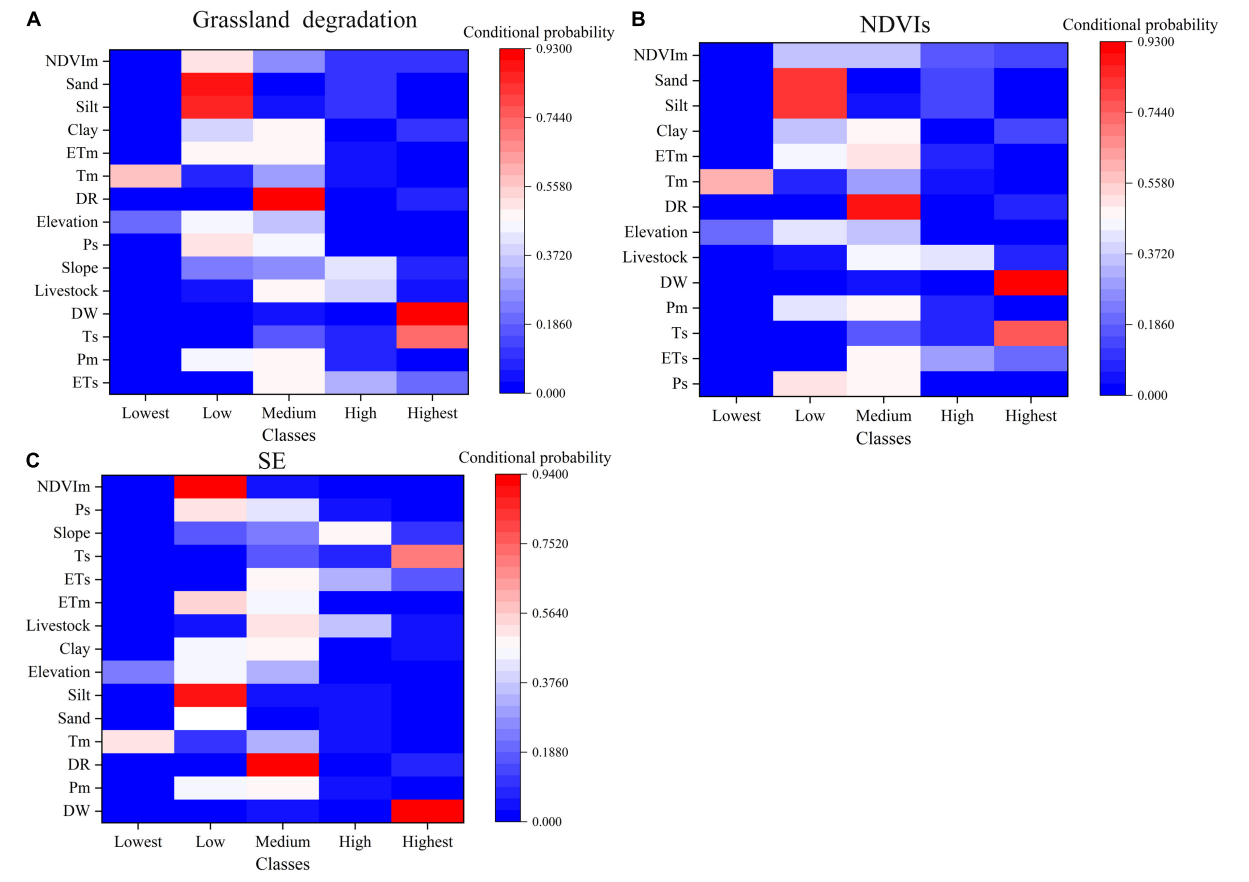

FIGURE 10 | Heat maps showing the conditional probabilities driving NDVIs, SE, and grassland degradation. **(A)** Grassland degradation. **(B)** NDVIs, slope of NDVI change. **(C)** SE, shrub-encroached grasslands.

The result of grassland degradation risk in each grid was predicted by the selected evidence variables, as shown in **Figure 12**. The risk probability values were about 21.65–87.15%. The region of high-risk grassland degradation (P > 30%) covered 2.22 million ha, accounting for 15.94% of the total study area. By comparing the high-risk degradation probabilities identified by NDVIs and shrub-encroached grasslands indicators in grids, it was found that the degradation area based on NDVIs was 1.742 million ha (78.46%) and the degradation area based on shrub-encroached grasslands was 0.478 million

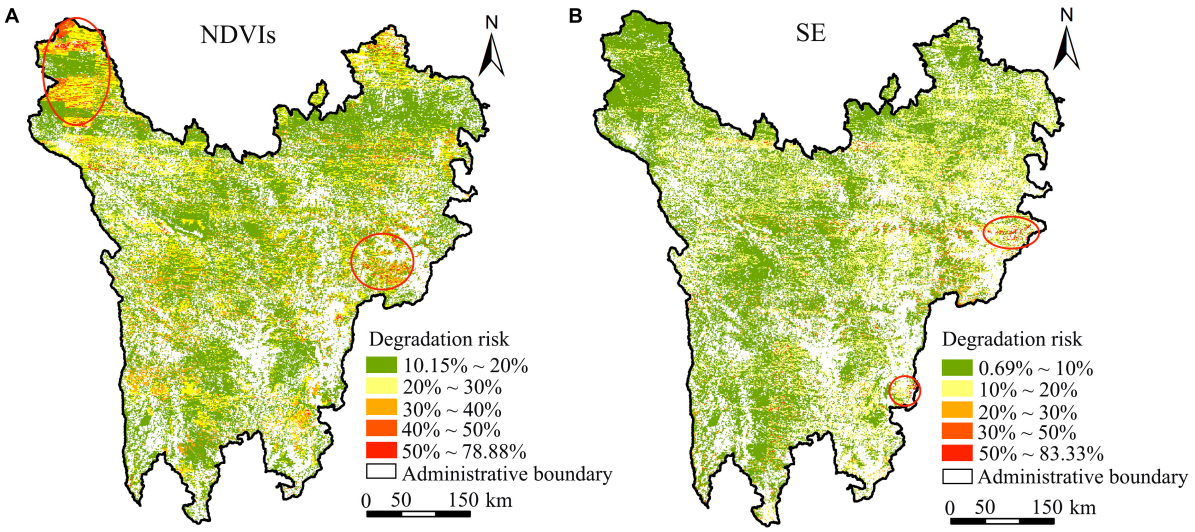

FIGURE 11 | Inference probability of grassland degradation risks based on NDVIs and SE. **(A)** NDVIs, slope of NDVI change. **(B)** SE, shrub-encroached grasslands.

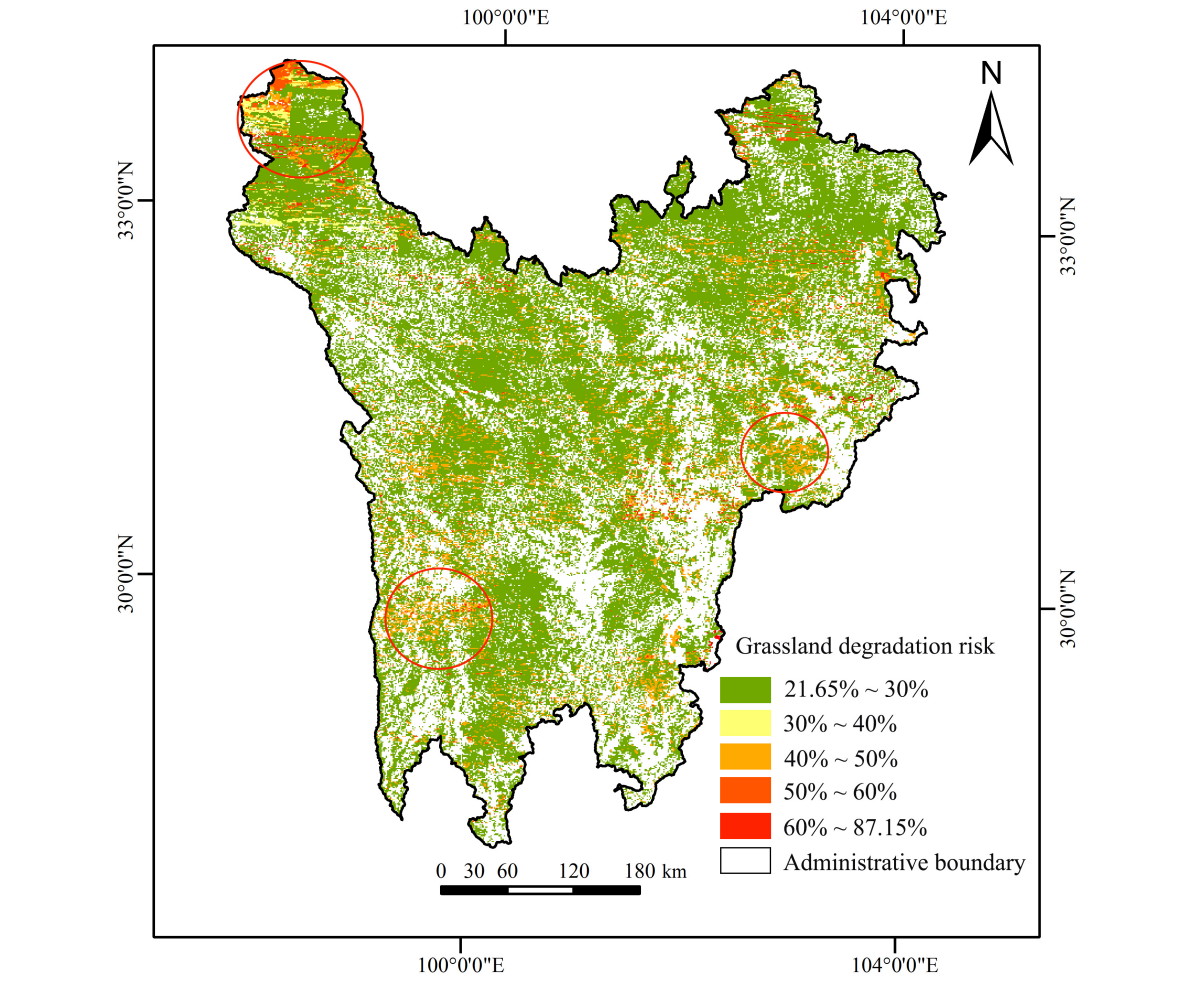

FIGURE 12 | Distribution of grassland degradation risk.

ha (21.54%). In terms of spatial distribution, regions with high-risk grassland degradation were quite scattered; however, they were clustered in local areas (e.g., the junction area of Shiqu County, Batang County, and Litang County, and the junction area of Li County, Wenchuan County, and Xiaojin County). It can be seen from **Table 2** and **Supplementary Table 1** that the grassland degradation mainly occurred in regions with lower vegetation coverage, higher soil sand content, lower soil clay and silt content, lower temperature, as well as less potential evapotranspiration, indicating that natural factors had stronger influences on vegetation degradation than human factors. Moreover, although this study chose 30% as the threshold for recognising high grassland degradation risks, there is uncertainty in terms of grassland degradation owing to the inherent nature of probability. As a result, regions with grassland degradation risk probabilities lower than 30% could have degraded, and regions with probabilities higher than 30% could have experienced no degradation. For example, grids with the highest degradation probability (87.15%) could also have no degradation.

DISCUSSION

In this study, alpine grassland degradation in Northwest Sichuan Plateau was assessed by integrating the FR model and the BBN model. First, the driving factors of grassland degradation were discretized using the FR model. Then, a BBN model was established to identify the driving factors of grassland degradation and quantitatively evaluate the probability of degradation risks.

For the grassland degradation analysis, NDVIs and shrub-encroached grasslands were chosen as the grassland degradation index. In previous studies, most alpine grassland degradation on the macro scale was based on NDVIs, and the effects of shrub-encroached grasslands in alpine regions were ignored (which are one of the most important forms of alpine grassland degradation), resulting in missing degradation grids (Chen et al., 2020). To offset the limitations of recognition based on NDVIs only, grassland degradation was identified herein by combining shrub-encroached grasslands and the slope of NDVI change, which could realize the complete characterization of macro-scaled grassland degradation, and is conducive to understanding the states of different dominant degradation types.

TABLE 2 | Comparison of evidence variables in different states in high-risk areas.

Indicator	Classes of evidence variable				
	Lowest	Low	Medium	High	Highest
NDVIm	–	49.8%	36.3%	11.8%	2.1%
Sand	–	41.1%	4.3%	54.6%	–
Silt	–	39.4%	4.3%	56.3%	–
Clay	–	0.9%	30.4%	0.1%	68.6%
ETm	–	0.2%	47.9%	51.8%	0.1%
Tm	32.9%	0.2%	48.4%	8.4%	10.1%

Furthermore, states of driving factors of NDVIs and shrub-encroached grasslands were divided by calculating the frequency ratios of different intervals of driving factors and combining intervals with similar frequency ratios (De Santana et al., 2021). The FR method obtains a prior probability, and then the BBN model is used to infer the posterior probability of the event. Compared with the node classification method based on the characteristics of the node itself in the previous studies (Dai et al., 2021; Sakib et al., 2021), the FR method is graded the driving factors based on the importance of each attribute interval of the factor to the susceptibility of the event, which is more scientific. Therefore, as the premise of the BBN model interference, the FR model can provide a relatively reliable prior probability.

In the process of grassland degradation risk assessment, the model structure and parameterization are the key steps of BBN modelling. In this study, the grassland degradation risk assessment model was constructed by integrating correlation analysis, expert experience, and previous research conclusions, which were effectively used to determine the complex causal relationships among variables during grassland degradation (Carriger and Parker, 2021). In comparison to previous grassland degradation risk assessment methods, the BBN-based grassland degradation risk assessment model was based on the relationship between grassland degradation and driving forces, which could deduce the uncertainty of grassland degradation that was caused by insufficient and incomplete relevant information or knowledge (Luu et al., 2009). Furthermore, the model could be applied to reassess the grassland degradation risk when new information or data from nodes were updated or replaced, helping decision-makers formulate appropriate management measures (Dai et al., 2021). Hence, the BBN method showed better reliability and practicability. According to the results of grassland degradation risk probability in the BBN model, the potential degradation risk in most regions in the study area was maintained at a low level (21.65–30%). However, local regions still had relatively high degradation risk probabilities, which primarily include the grassland restoration regions that decision-makers need to focus on in the future. In terms of the probability of degradation risks, it must be noted that the degradation risk in the BBN model is a concept of probability, which means that it is inherently uncertain (Rohmer, 2020). In other words, places with the lowest degradation probability (21.65%) could also experience degradation, and those with the highest degradation probability (87.15%) could experience no degradation. For this reason, the Bayesian results must be understood in terms of probability.

The sensitivity analysis results of target variables help us recognize the influence of factors on grassland degradation, facilitating the formulation of scientific and effective ecological restoration measures (Hao et al., 2018). The results showed that the vegetation coverage, soil texture, and climatic factors of grids influence grassland degradation significantly, while terrain and human activity-related factors had relatively smaller effects in the study area. This could be because of the low levels of human activity due to a small population in the study area; this caused grassland degradation to be mainly affected by natural factors (Gang et al., 2014; Wang et al., 2017). However, it is worth

noting that the IPCC report clearly stated that human activities significantly affect climate change, so that grass degradation related to climate change is indirectly affected by human activities (Intergovernmental Panel on Climate Change, 2021). In addition, the probability correlations between grassland degradation and important driving factors showed that the highest probability of grassland degradation occurred when the state combination of driving factors met the following conditions: {NDVIm = Low, sand = Low, silt = Low, clay = Medium, ETm = Medium, Tm = Lowest}. This was consistent with geographic features in high-risk regions predicted by the BBN model. Therefore, the grassland restoration measures in the future should pay keen attention to regions with low vegetation coverage, high soil sand content, less potential evapotranspiration, and low temperatures. Moreover, the probability of grassland degradation was relatively low in regions with high vegetation coverage, high soil clay content, high temperature, and high potential evapotranspiration. Based on previous studies, there is evidence that human activities can improve the status of the above factors to a certain extent, such as the Returning Grazing Land to Grassland Project can increase the vegetation coverage (Shao et al., 2016); fertilization or soil amendments can improve soil properties (Wang X. et al., 2021). The findings from this study provide a reference basis for the restoration of grassland ecosystems.

Overall, the BBN method used in this study is most suitable in the situation characterised by large uncertainties, long time frames, and the influence of socio-economic and biophysical changes. However, in addition to the impact of the driving factor status, the temporal and spatial scale along with the data update rate will also affect the accuracy of grassland degradation risk assessment. To improve the accuracy of the assessment and the reliability of grassland ecosystem restoration decisions, on the basis of ensuring the timeliness and accuracy of the data, other potential influencing factors should also be identified; this should be followed by the optimization of the BBN model should improve the accuracy of grassland degradation risk inferences.

CONCLUSION

In this study, we use the alpine grassland of Northwest Sichuan Plateau as an example to predict the grassland degradation risk probability. We also propose suggestions for the scientific and reasonable restoration of grassland ecosystems, elucidating the advantages of using this method. The results regarding the grassland degradation pattern indicated that the area of grassland degradation characterized by NDVIs is 2.433 million ha, with 11.39% in significantly decreased areas and 88.61% in non-significantly increased areas. The grassland degradation area characterized by shrub-encroached grasslands was 1.6886 million ha. Moreover, overlapping results of shrub-encroached grasslands and NDVIs less than 0 indicated a spatial intersection of 1.357 million ha. In other words, a total of 1.553 million ha of grassland degradation was recognized through shrub-encroached grasslands. In the BBN model, the prediction accuracy based on the confusion matrix of NDVIs, shrub-encroached grasslands, and grassland degradation was 85.27, 88.99, and 74.37%, respectively. The area under the curves based on the ROC curve of NDVIs, shrub-encroached grasslands, and grassland degradation were 75.39% ($P < 0.05$), 66.57% ($P < 0.05$), and 66.11% ($P < 0.05$), respectively. This proved that the proposed BBN model met the requirements and could be used to predict the grassland degradation risk probability. According to model inference results, the area of high degradation risk probability ($P > 30\%$) was 2.22 million ha (15.94%), with 1.742 million ha (78.46%) characterized by NDVIs and 0.478 ha (21.54%) characterized by shrub-encroached grasslands. Furthermore, the sensitivity analysis indicated that grassland degradation had a relatively high sensitivity to NDVIm, sand, silt, clay, ETm, and Tm, and regions with low vegetation coverage, high soil sand content, less evapotranspiration and low potential temperature could easily experience grassland degradation. Such regions included the junction area of Shiqu County, Batang County, and Litang County, and the junction area of Li County, Wenchuan County, and Xiaojin County.

Identifying and quantifying the complex relationships between driving factors and grassland degradation is crucial for grassland degradation assessment; the BBN method not only provides an effective solution to solve this problem, but assists stakeholders in formulating scientific decisions on grassland ecosystem restoration. Therefore, the BBN model could be used as a decision-support instrument for restoring grassland ecosystems, along with maintaining regional ecological safety and sustainable development.

DATA AVAILABILITY STATEMENT

The datasets presented in this study can be found in online repositories. The names of the repository/repositories and accession number(s) can be found in the article/**Supplementary Material**.

AUTHOR CONTRIBUTIONS

SZ and LP: conceive the ideas. SZ: methodology, investigation, formal analysis, software, data curation, visualization, and writing – original draft. LP: methodology, formal analysis, project administration, supervision, writing, review, and editing. Both authors read, commented on, and approved this version of the manuscript.

FUNDING

This work was supported by the National Natural Science Foundation of China (42071222 and 41930651).

SUPPLEMENTARY MATERIAL

The Supplementary Material for this article can be found online at: https://www.frontiersin.org/articles/10.3389/fpls.2021.773759/full#supplementary-material

REFERENCES

Abebe, Y., Kabir, G., and Tesfamariam, S. (2018). Assessing urban areas vulnerability to pluvial flooding using GIS applications and Bayesian Belief Network model. *J. Clean Prod.* 174, 1629–1641. doi: 10.1016/j.jclepro.2017.11.066

Anderson, B. (2019). Using Bayesian networks to perform reject inference. *Expert Syst. Appl.* 137, 349–356. doi: 10.1016/j.eswa.2019.07.011

Bicking, S., Burkhard, B., Kruse, M., and Müller, F. (2019). Bayesian belief network-based assessment of nutrient regulating ecosystem services in Northern Germany. *PLoS One* 14:e0216053. doi: 10.1371/journal.pone.0216053

Calder, R. S. D., Shi, C., Mason, S. A., Olander, L. P., and Borsuk, M. E. (2019). Forecasting ecosystem services to guide coastal wetland rehabilitation decisions. *Ecosyst. Serv.* 39:101007. doi: 10.1016/j.ecoser.2019.101007

Carriger, J. F., and Parker, R. A. (2021). Conceptual Bayesian networks for contaminated site ecological risk assessment and remediation support. *J. Environ. Manage.* 278:111478. doi: 10.1016/j.jenvman.2020.111478

Chen, Y., Wang, W., Guan, Y., Liu, F., Zhang, Y., Du, J., et al. (2020). An integrated approach for risk assessment of rangeland degradation: a case study in Burqin County, Xinjiang, China. *Ecol. Indic.* 113:106203. doi: 10.1016/j.ecolind.2020.106203

Dai, L., Han, Q., de Vries, B., and Wang, Y. (2021). Applying Bayesian belief network to explore key determinants for nature-based solutions' acceptance of local stakeholders. *J. Clean Prod.* 310:127480. doi: 10.1016/j.jclepro.2021.127480

Dang, K. B., Windhorst, W., Burkhard, B., and Müller, F. (2019). A Bayesian belief network – based approach to link ecosystem functions with rice provisioning ecosystem services. *Ecol. Indic.* 100, 30–44. doi: 10.1016/j.ecolind.2018.04.055

De Santana, R. O., Delgado, R. C., and Schiavetti, A. (2021). Modeling susceptibility to forest fires in the Central Corridor of the Atlantic Forest using the frequency ratio method. *J. Environ. Manage.* 296:113343. doi: 10.1016/j.jenvman.2021.113343

Deng, X., Liu, Q., Deng, Y., and Mahadevan, S. (2016). An improved method to construct basic probability assignment based on the confusion matrix for classification problem. *Inf. Sci.* 340-341, 250–261. doi: 10.1016/j.ins.2016.01.033

Farber, D. A. (2015). Coping with uncertainty: cost-benefit analysis, the precautionary principle, and climate chang. *Washingt. Law Rev.* 54, 23–46. doi: 10.1525/sp.2007.54.1.23

Feng, Y., Lu, Q., Tokola, T., Liu, H., and Wang, X. (2009). Assessment of grassland degradation in Guinan country, Qinghai Province, China, in the past 30 years. *Land Degrad. Dev.* 20, 55–68. doi: 10.1002/ldr.877

Fleskens, L., and Stringer, L. C. (2014). Land management and policy responses to mitigrate desertification and land degradation. *Land Degrad. Dev.* 25, 1–4. doi: 10.1002/ldr.2272

Fraser, R. H., Lantz, T. C., Olthof, I., Kokelj, S. V., and Sims, R. A. (2014). Warming-induced shrub expansion and Lichen decline in the Western Canadian Arctic. *Ecosystems* 17, 1151–1168. doi: 10.1007/s10021-014-9783-3

French, S. (2015). Cynefin: uncertainty, small worlds and scenarios. *J. Oper. Res. Soc.* 66, 1635–1645. doi: 10.1057/jors.2015.21

Gang, C., Zhou, W., Chen, Y., Wang, Z., Sun, Z., Li, J., et al. (2014). Quantitative assessment of the contributions of climate change and human activities on global grassland degradation. *Environ. Earth Sci.* 72, 4273–4282. doi: 10.1007/s12665-014-3322-6

Gao, Q., Li, Y. E., Wan, Y., Lin, E., Xiong, W., Jiangcun, W., et al. (2006). Grassland degradation in Northern Tibet based on remote sensing data. *J. Geogr. Sci.* 16, 165–173. doi: 10.1007/s11442-006-0204-1

Han, D., Wang, G., Xue, B., Liu, T., A, Y., and Xu, X. (2018). Evaluation of semiarid grassland degradation in North China from multiple perspectives. *Ecol. Eng.* 112, 41–50. doi: 10.1016/j.ecoleng.2017.12.011

Hao, L., Xiao, Z., Yan, Z., Yang, X., and Zhang, K. (2018). Risk assessment of forest landscape degradation using Bayesian network modeling in the Miyun Reservoir catchment (China) with emphasis on the Beijing-Tianjin sandstorm source control program. *Land Degrad. Dev.* 29, 3876–3885. doi: 10.1002/ldr.3133

Intergovernmental Panel on Climate Change (2021). *AR6 Synthesis Report*. Available online at: https://www.ipcc.ch/report/sixth-assessment-report-cycle (accessed September 29, 2021).

Kabir, G., Tesfamariam, S., Francisque, A., and Sadiq, R. (2015). Evaluating risk of water mains failure using a Bayesian belief network model. *Eur. J. Oper. Res.* 240, 220–234. doi: 10.1016/j.ejor.2014.06.033

Kane, K., Debinski, D. M., Anderson, C., Scasta, J. D., Engle, D. M., and Miller, J. R. (2017). Using regional climate projections to guide grassland community restoration in the face of climate change. *Front. Plant Sci.* 8:730. doi: 10.3389/fpls.2017.00730

Kerebel, A., Gélinas, N., Déry, S., Voigt, B., and Munson, A. (2019). Landscape aesthetic modelling using Bayesian networks: conceptual framework and participatory indicator weighting. *Landsc. Urban Plan.* 185, 258–271. doi: 10.1016/j.landurbplan.2019.02.001

Lang, Y., Yang, X., and Cai, H. (2021). Assessing the degradation of grassland ecosystems based on the advanced local net production scaling method—the case of Inner Mongolia, China. *Land Degrad. Dev.* 32, 559–572. doi: 10.1002/ldr.3741

Li, M., Qing, W., and Songtao, S. (2020). Response of soil aggregate stability and distribution of organic carbon to alpine grassland degradation in Northwest Sichuan. *Geoderma Reg.* 22:e00309. doi: 10.1016/j.geodrs.2020.e00309

Lin, L., Li, Y. K., Xu, X. L., Zhang, F. W., Du, Y. G., Liu, S. L., et al. (2015). Predicting parameters of degradation succession processes of Tibetan Kobresia grasslands. *Solid Earth* 6, 1237–1246. doi: 10.5194/se-6-1237-2015

Liu, W., Mo, X., Liu, S., Lin, Z., and Lv, C. (2021). Attributing the changes of grass growth, water consumed and water use efficiency over the Tibetan Plateau. *J. Hydrol.* 598:126464. doi: 10.1016/j.jhydrol.2021.126464

Luu, V. T., Kim, S.-Y., Tuan, N. V., and Ogunlana, S. O. (2009). Quantifying schedule risk in construction projects using Bayesian belief networks. *Int. J. Proj. Manag.* 27, 39–50. doi: 10.1016/j.ijproman.2008.03.003

May, J. L., Hollister, R. D., Betway, K. R., Harris, J. A., Tweedie, C. E., Welker, J. M., et al. (2020). NDVI changes show warming increases the length of the green season at Tundra communities in Northern Alaska: a fine-scale analysis. *Front. Plant Sci.* 11:1174. doi: 10.3389/fpls.2020.01174

Miehe, G., Schleuss, P.-M., Seeber, E., Babel, W., Biermann, T., Braendle, M., et al. (2019). The Kobresia pygmaea ecosystem of the Tibetan highlands – origin, functioning and degradation of the world's largest pastoral alpine ecosystem: Kobresia pastures of Tibet. *Sci. Total Environ.* 648, 754–771. doi: 10.1016/j.scitotenv.2018.08.164

Orak, N. H. (2020). A Hybrid Bayesian network framework for risk assessment of arsenic exposure and adverse reproductive outcomes. *Ecotox. Environ. Saf.* 192:110270. doi: 10.1016/j.ecoenv.2020.110270

Plomaritis, T. A., Costas, S., and Ferreira, Ó (2018). Use of a Bayesian network for coastal hazards, impact and disaster risk reduction assessment at a coastal barrier (Ria Formosa, Portugal). *Coast. Eng.* 134, 134–147. doi: 10.1016/j.coastaleng.2017.07.003

Rohmer, J. (2020). Uncertainties in conditional probability tables of discrete Bayesian belief networks: a comprehensive review. *Eng. Appl. Artif. Intell.* 88:103384. doi: 10.1016/j.engappai.2019.103384

Rusek, J., Tajduś, K., Firek, K., and Jędrzejczyk, A. (2021). Score-based Bayesian belief network structure learning in damage risk modelling of mining areas building development. *J. Clean Prod.* 296:126528. doi: 10.1016/j.jclepro.2021.126528

Sakib, N., Ibne Hossain, N. U., Nur, F., Talluri, S., Jaradat, R., and Lawrence, J. M. (2021). An assessment of probabilistic disaster in the oil and gas supply chain leveraging Bayesian belief network. *Int. J. Prod. Econ.* 235:108107. doi: 10.1016/j.ijpe.2021.108107

Seddon, A. W. R., Macias-Fauria, M., Long, P. R., Benz, D., and Willis, K. J. (2016). Sensitivity of global terrestrial ecosystems to climate variability. *Nature* 531, 229–232. doi: 10.1038/nature16986

Shao, H., Sun, X., Wang, H., Zhang, X., Xiang, Z., Tan, R., et al. (2016). A method to the impact assessment of the returning grazing land to grassland project on regional eco-environmental vulnerability. *Environ. Impact Assess. Rev.* 56, 155–167. doi: 10.1016/j.eiar.2015.10.006

Shi, H., Luo, G., Zheng, H., Chen, C., Bai, J., Liu, T., et al. (2020). Coupling the water-energy-food-ecology nexus into a Bayesian network for water resources analysis and management in the Syr Darya River basin. *J. Hydrol.* 581:124387. doi: 10.1016/j.jhydrol.2019.124387

Teng, Y., Zhan, J., Agyemang, F. B., and Sun, Y. (2020). The effects of degradation on alpine grassland resilience: a study based on meta-analysis data. *Glob. Ecol. Conserv.* 24:e01336. doi: 10.1016/j.gecco.2020.e01336

Wang, X., Li, X., Dou, F., Sun, W., Chen, K., Wen, Y., et al. (2021). Elucidating the impact of three metallic nanoagrichemicals and their bulk and ionic counterparts on the chemical properties of bulk and rhizosphere soils in rice paddies. *Environ. Pollut.* 290:118005. doi: 10.1016/j.envpol.2021.118005

Wang, Z., Deng, X., Song, W., Li, Z., and Chen, J. (2017). What is the main cause of grassland degradation? A case study of grassland ecosystem service in the middle-south Inner Mongolia. *Catena* 150, 100–107. doi: 10.1016/j.catena.2016.11.014

Wang, Z., Li, X., Ji, B., Struik, P. C., Jin, K., and Tang, S. (2021). Coupling between the responses of plants, soil, and microorganisms following grazing exclusion in an overgrazed grassland. *Front. Plant Sci.* 12:640789. doi: 10.3389/fpls.2021.640789

Yang, X., Liu, R., Yang, M., Chen, J., Liu, T., Yang, Y., et al. (2021). Incorporating landslide spatial information and correlated features among conditioning factors for landslide susceptibility mapping. *Remote Sens.* 13:2166. doi: 10.3390/rs13163339

Zhang, G., Biradar, C. M., Xiao, X., Dong, J., Zhou, Y., Qin, Y., et al. (2018). Exacerbated grassland degradation and desertification in Central Asia during 2000–2014. *Ecol. Appl.* 28, 442–456. doi: 10.1002/eap.1660

Zhao, Y., Feng, Q., and Lu, A. (2021). Spatiotemporal variation in vegetation coverage and its driving factors in the Guanzhong Basin, NW China. *Ecol. Inform.* 64:101371. doi: 10.1016/j.ecoinf.2021.101371

Zhou, W., Li, J., and Yue, T. (2020). "Grassland degradation remote sensing monitoring and driving factors quantitative assessment in China from 1982 to 2010," in *Remote Sensing Monitoring and Evaluation of Degraded Grassland in China: Accounting of Grassland Carbon Source and Carbon Sink*, eds W. Zhou, J. Li, and T. Yue (Singapore: Springer Singapore), 105–123.

Zhu, W., Gao, Y., Zhang, H., and Liu, L. (2020). Optimization of the land use pattern in Horqin Sandy Land by using the CLUMondo model and Bayesian belief network. *Sci. Total Environ.* 739:139929. doi: 10.1016/j.scitotenv.2020.139929

Zong, N., Shi, P., Zheng, L., Zhou, T., Cong, N., Hou, G., et al. (2021). Restoration effects of fertilization and grazing exclusion on different degraded alpine grasslands: evidence from a 10-year experiment. *Ecol. Eng.* 170:106361. doi: 10.1016/j.ecoleng.2021.106361

Zywiec, W. J., Mazzuchi, T. A., and Sarkani, S. (2021). Analysis of process criticality accident risk using a metamodel-driven Bayesian network. *Reliab. Eng. Syst. Saf.* 207:107322. doi: 10.1016/j.ress.2020.107322

Conflict of Interest: The authors declare that the research was conducted in the absence of any commercial or financial relationships that could be construed as a potential conflict of interest.

Publisher's Note: All claims expressed in this article are solely those of the authors and do not necessarily represent those of their affiliated organizations, or those of the publisher, the editors and the reviewers. Any product that may be evaluated in this article, or claim that may be made by its manufacturer, is not guaranteed or endorsed by the publisher.

Copyright © 2021 Zhou and Peng. This is an open-access article distributed under the terms of the Creative Commons Attribution License (CC BY). The use, distribution or reproduction in other forums is permitted, provided the original author(s) and the copyright owner(s) are credited and that the original publication in this journal is cited, in accordance with accepted academic practice. No use, distribution or reproduction is permitted which does not comply with these terms.

frontiers in Plant Science

ORIGINAL RESEARCH
published: 22 November 2021
doi: 10.3389/fpls.2021.765041

The Mixed Addition of Biochar and Nitrogen Improves Soil Properties and Microbial Structure of Moderate–Severe Degraded Alpine Grassland in Qinghai-Tibet Plateau

Jinsheng Li[1†], Yinquan Zhao[2†], Xinqing Shao[1], Ding Huang[1], Jianying Shang[3], Hui Li[1], Yixuan He[1] and Kesi Liu[1,4,5]*

[1] College of Grassland Science and Technology, China Agricultural University, Beijing, China, [2] College of Tourism and Urban Planning, Chengdu University of Technology, Chengdu, China, [3] College of Land Science and Technology, China Agricultural University, Beijing, China, [4] Key Laboratory of Restoration Ecology of Cold Area in Qinghai Province, Northwest Institute of Plateau Biology, Chinese Academy of Sciences, Xining, China, [5] National Field Station of Grassland Ecosystem, Guyuan, China

OPEN ACCESS

Edited by:
Jian Sun,
Institute of Tibetan Plateau Research, Chinese Academy of Sciences (CAS), China

Reviewed by:
Gang Fu,
Institute of Geographic Sciences and Natural Resources Research, Chinese Academy of Sciences (CAS), China
Yanhong Lou,
Shandong Agricultural University, China
Ben Niu,
Institute of Geographic Sciences and Natural Resources Research, Chinese Academy of Sciences (CAS), China

***Correspondence:**
Kesi Liu
kliu@cau.edu.cn

[†] These authors have contributed equally to this work

Specialty section:
This article was submitted to Functional Plant Ecology, a section of the journal Frontiers in Plant Science

Received: 26 August 2021
Accepted: 18 October 2021
Published: 22 November 2021

Citation:
Li J, Zhao Y, Shao X, Huang D, Shang J, Li H, He Y and Liu K (2021) The Mixed Addition of Biochar and Nitrogen Improves Soil Properties and Microbial Structure of Moderate–Severe Degraded Alpine Grassland in Qinghai-Tibet Plateau. Front. Plant Sci. 12:765041. doi: 10.3389/fpls.2021.765041

The degradation of the grassland system has severely threatened the safety of the ecological environment and animal husbandry. The supplement of key substances lost due to degradation is widely used to accelerate the restoration of the degraded grassland ecosystem. In this study, we investigated the effects of biochar and nitrogen addition on soil properties and microorganisms of degraded alpine grassland. The experimental treatments consisted of the control without any addition, only nitrogen addition (10 gN/m^2), only biochar addition (4.00 kg/m^2 biochar), and the mixed addition of biochar and nitrogen (4.00 kg/m^2 biochar and 10 gN/m^2 nitrogen, respectively). Adding N alone did not significantly change the pH, total organic carbon (TOC), total nitrogen (TN), microbial biomass (MB), and the composition proportion of microbes of the soil, but increased the contents of soil water content (SWC), NH_4^+-N, NO_3^--N, available phosphorus (AP), and the biomass of bacteria and fungi. The addition of biochar or the mixture of biochar and nitrogen increased the contents of pH, TOC, TN, MB, SWC, NH_4^+-N, NO_3^--N, AP, bacteria, and fungi in the soil and changed the structure of the soil microbial community. The increasing intensity of AP, bacteria, and fungi under the addition of biochar or the mixture of biochar and nitrogen was significantly greater than that under N addition alone. These results indicated that the separated addition of nitrogen and biochar and the mixed addition of biochar and nitrogen all improved the soil condition of the moderate–severe degraded alpine grassland, but the mixed addition of biochar and nitrogen could be a better strategy to remediate the degraded alpine grassland.

Keywords: alpine grassland, degradation, biochar, soil physicochemical property, microbial community

Abbreviations: TOC, total organic carbon; TN, total nitrogen; SWC, soil water content; EC, electrical conductivity; AP, available phosphorus; C/N, ratio of carbon to nitrogen; F/B, fungi:bacteria; GP/GN, Gram-positive:Gram-negative; MB:TOC, microbial biomass:total organic carbon; MB:TN, microbial biomass:total nitrogen; Gn, Gram-negative bacteria; Ab, Actinobacteria; Gp, Gram-positive bacteria; Sf, saprotrophic fungi; Ef, ectomycorrhizal fungi; Mb, methanotrophic bacteria; An, anaerobic bacteria; Am, arbuscular mycorrhizal fungi.

INTRODUCTION

The alpine grassland ecosystem in the Qinghai-Tibet Plateau is a unique ecosystem formed in a high-altitude environment, accounting for 50.9% areas of the Qinghai-Tibet Plateau and 44% areas of China grasslands (Piao et al., 2012). As the main ecosystem of the Qinghai-Tibet Plateau, alpine grassland is not only the basis of local animal husbandry but also has a variety of ecological functions, such as water conservation, soil erosion control, biodiversity maintenance, and carbon sequestration (Feng et al., 2009; Li et al., 2014; Sun et al., 2019). However, due to harsh climate, short growth period, weak resistance, and poor resilience, the alpine grassland ecosystem is relatively fragile (Feng et al., 2009; Liu et al., 2018). Due to unreasonable grazing utilization, grasslands on the Qinghai-Tibet Plateau underwent a large area of degradation between the end of the 19th century and the beginning of the 20th century (Yao et al., 2016; Li et al., 2020). The degradation of alpine grassland leads to the decline of grassland vegetation, the deterioration of soil habitat, the decrease of grassland productivity and ecological functions, and finally the serious imbalance of the whole ecosystem (Yao et al., 2016; Peng et al., 2018).

The deterioration of soil habitat caused by grassland degradation is mainly due to the destruction of soil structure and the sharp loss of soil nutrients, especially soil nitrogen and carbon, which destroy the soil biological system and the growth environment of plant roots (Liu et al., 2020; Sun et al., 2020; Wu et al., 2021). For example, a study in the Qinghai-Tibet Plateau found that the nitrogen content in the soil decreased by 49% after the degradation of grassland (Dong et al., 2012). Nitrogen is an essential nutrient for plant growth and microbial development and thus limits the productivity of natural grassland ecosystems (Wang D. et al., 2020). The reduction of soil nitrogen not only restricts the growth of aboveground vegetation (Li et al., 2020) but also reduces the microorganisms in the soil due to the lack of necessary nutrients (Che et al., 2019). In view of the lack of soil nitrogen after grassland degradation, nitrogen fertilizer application is a conventional method to increase soil nutrients. Nitrogen application can increase the content of available nitrogen and total organic carbon (TOC; Luo et al., 2011), improve the utilization efficiency of nitrogen and carbon by microorganisms (Li et al., 2018), and increase the productivity of the ecosystem (Somleva et al., 2002). In the Qinghai-Tibet Plateau, previous studies found that adding nitrogen not only changes the composition of soil nitrogen but also has a positive effect on aboveground vegetation (Fu and Shen, 2016, 2017). However, in the degraded grassland, the soil generally has high bulk density, low porosity, low organic matter, and unstable aggregate structure (Ma et al., 2020; Zhang et al., 2020). These traits make soil difficult to retain the introduced nutrients and result in the loss of nutrients and the decrease of utilization efficiency (Yagüe et al., 2016; Zhang et al., 2018).

Biochar is a highly aromatic and carbon-rich substance formed by high-temperature pyrolysis and carbonization of biomass under oxygen-limited or anaerobic conditions (Woolf et al., 2010). As biochar has porous, large specific surface area, strong adsorption capacity, rich carbon content, and other properties, it is widely used in agricultural land as an excellent soil improvement material (Butnan et al., 2017; El-Naggar et al., 2018; Muhammad et al., 2018). The bulk density of biochar is around 0.08–0.5 g/cm^3, smaller than that of soil (1.0–1.7 g/cm^3), and therefore, the biochar application significantly decreases the bulk density of the soil (Wahi et al., 2017). In addition, the porous structure of biochar increases soil porosity, improves soil permeability, promotes crop root development (Sadaf et al., 2017), and enhances the stability of soil aggregates (Lu et al., 2014). Meanwhile, the porous structure and surface polar functional groups of biochar enhance the adsorption of soil nutrients, thereby significantly reducing the leaching of soil nutrients (Gul and Whalen, 2016; Oliveira et al., 2017). Soil microbial biomass (MB), activity, and diversity have also been improved to different degrees after biochar application (Farrell et al., 2013; Zhang et al., 2018).

Numerous studies on the application of biochar and nitrogen to soil have been reported up to date (Oram et al., 2014; Sadaf et al., 2017; Wahi et al., 2017; Yu et al., 2018) with results showing good performance in the improvement of farmland degraded soil (Sadaf et al., 2017; Wahi et al., 2017; Li et al., 2019). However, there are few studies on using the combination of biochar and nitrogen to restore degraded grasslands, and the detailed effects need to be evaluated through empirical research. Compared with croplands, the plant diversity and the system complexity of grasslands are much higher. These differences might lead to different effects of biochar and nitrogen fertilizer on soil physicochemical properties and microorganisms of grasslands. Taking into account the ecological importance of the Qinghai-Tibet Plateau and the urgency of restoring its degradation, we took the degraded alpine grassland of the Qinghai-Tibet Plateau as the research object and used biochar and nitrogen fertilizer as additives to explore the effects of biochar and nitrogen fertilizer addition on soil physicochemical properties and microorganisms in different soil layers (0–10 and 10–20 cm) of degraded alpine grassland. We hypothesized that: (1) although grasslands were different from cropland, the addition of biochar and nitrogen fertilizer could significantly improve the soil physicochemical properties and soil microbial composition of the moderate–severe degraded grassland; (2) the improvement effect of the mixed application of biochar and nitrogen fertilizer might be better than that of biochar or nitrogen application alone.

MATERIALS AND METHODS

Study Site

The experimental site was located in the northeast of Senduo town, Guinan county, Qinghai province (36°35′N, 101°42′E, 3220 m a.s.l.). Region climate is a typical plateau continental climate with a 2.3°C annual average temperature and 403.80 mm annual average precipitation. The annual sunshine hours are 2,738 h, and the annual evaporation is 1,378.5 mm. The main plant species in the experimental grassland include *Poa crymophila, Cleistogenes squarrosa, Carex tristachya*, *Elymus nutans. Griseb, Ligularia Cass, Stipa krylovii* Roshev., *Oxytropis*

TABLE 1 | Variation of soil pH, electrical conductivity (EC), and soil water content (SWC) in the 0–20 cm soil layers under different treatments in 2017, 2018, and 2019.

Parameter	Year	Layer (cm)	CK	N	C	C + N
pH	2017	0–10	7.12 ± 0.06 aB	7.31 ± 0.09 aA	7.36 ± 0.15 aB	7.25 ± 0.05 aC
	2018		7.55 ± 0.04 bA	8.00 ± 0.6 abA	8.22 ± 0.26 aA	8.43 ± 0.24 aA
	2019		7.28 ± 0.27 bAB	7.66 ± 0.08 abA	7.75 ± 0.06 aA	7.78 ± 0.21 aB
	2017	10–20	7.24 ± 0.13 aA	7.35 ± 0.21 aB	7.31 ± 0.10 aC	7.38 ± 0.09 aB
	2018		7.48 ± 0.11 bA	8.26 ± 0.28 aA	8.44 ± 0.10 aA	8.42 ± 0.25 aA
	2019		7.49 ± 0.06 bA	8.25 ± 0.28 aA	7.81 ± 0.14 abB	7.99 ± 0.23 abA
EC (us/cm)	2017	0–10	362.76 ± 56.72 bB	430 ± 22.52 abA	502 ± 25.53 aA	483.67 ± 46.19 aA
	2018		574.09 ± 34.95 aA	129.79 ± 50.7 cB	302.58 ± 38.66 bB	297.92 ± 18.98 bB
	2019		209.80 ± 25.97 aC	109.79 ± 50.7 bB	220.73 ± 33.03 aB	222.93 ± 33.39 aB
	2017	10–20	324.91 ± 13.73 bB	423 ± 26.89 aA	419 ± 19.67 aA	411.33 ± 45.8 aA
	2018		605.27 ± 121.87 aA	107.65 ± 9.52 cB	282.62 ± 19 bB	342.53 ± 79.77 abA
	2019		197.53 ± 17.65 aB	97.65 ± 9.52 bB	198.33 ± 28.29 aB	195.2 ± 7.7 aB
SWC (%)	2017	0–10	24.52 ± 1.13 aA	24.85 ± 1.12 aB	24.35 ± 1.01 aB	25.76 ± 1.59 aAB
	2018		18.82 ± 0.47 bB	30.87 ± 3.26 aA	30.69 ± 2.22 aA	30.84 ± 3.06 aA
	2019		16.46 ± 1.24 bB	23.54 ± 0.63 aB	27.01 ± 3.26 aB	25.43 ± 0.75 aB
	2017	10–20	21.14 ± 0.87 aA	22.68 ± 2.34 aAB	21.89 ± 1.02 aB	21.25 ± 0.48 aB
	2018		19.85 ± 0.62 bA	25.85 ± 1.49 aA	27.31 ± 0.92 aA	28.61 ± 1.90 aA
	2019		16.08 ± 1.00 cB	19.01 ± 2.13 bB	20.55 ± 1.21 abB	25.85 ± 1.49 aA

Values are means ± SE, lowercase letters indicate differences between different treatments in the same year ($P < 0.05$), and uppercase letters indicate differences between different years in the same treatment ($P < 0.05$).

kansuensis Bunge, and *Stellera chamaejasme* Linn. The soil type is chernozem.

Experimental Design and Soil Sampling

According to the national standard "Parameters of degradation, sandification and salification of rangelands (GB19377-2003)," alpine grasslands with 40–60% coverage and less than 10 plant species were defined as the moderate–severe degraded alpine grasslands and were selected as the research object in the middle of July 2016. The whole experimental area was fenced off from grazing disturbance in March 2017. Biochar and nitrogen fertilizer was applied in May 3, 2017. Experimental biochar was made from corn straw by pyrolysis at 550°C for 1 h. Within biochar, organic carbon was 508.9 g/kg, total nitrogen (TN) was 10.2 g/kg, total phosphorus was 80.95 g/kg, electrical conductivity was 1,595 μs/cm, and pH was 8.96. The nitrogen fertilizer used for the application was urea.

Four treatments were established, including control (without any addition, CK), biochar addition alone (2%, 4.00 kg/m^2, C; the initial soil bulk density in the experimental plots was 1 g/cm^3, and the percentage was the ratio of biochar weight to the dry weight of soil in the 20 cm soil surface layer), nitrogen addition alone (22 g m^{-2}, urea, N), and the mixed addition of biochar and nitrogen (4.00 kg biochar/m^2 and 22 g urea/m^2, C + N). The amount of biochar and nitrogen application was the regular amount in agricultural practices. The experimental design was a complete random block design with three blocks. Each experimental plot was 2 m length × 2 m width. A buffer zone of 1.5 m width was set between each plot, and a 3 m width buffer strip was set between each block. The buffer zones were without any processing.

In the process of biochar and nitrogen addition, the combined method of hole application and surface application was adopted to reduce the damage to grassland and accelerate the transport of biochar particles and nitrogen in the soil. Sixteen holes (20 cm depth) were drilled in each plot with a diameter of 3.5 cm soil auger, and there was a spacing of 50 cm among holes. According to the treatment design, the mixture of biochar and nitrogen or biochar was first filled into the holes, and the remaining was evenly sprayed on the surface of the plot through the surface application. For the N treatment plot, half of the nitrogen was added to the hole and the other half was evenly sprayed on the surface through the surface application. The appropriate amount of original soil was used to cover the surface application thinly and then gently tramped to prevent the surface application from being blown away by the wind. The addition of biochar and nitrogen was conducted only in 2017.

Soil samples were collected from each plot during the peak growing period of plants (late July) in 2017, 2018, and 2019. In each plot, three sampling points were randomly selected. At each sampling point, a soil auger with a diameter of 3.5 cm was used to take soil samples from 0 to 10 cm and 10 to 20 cm depth, respectively. If we met the borehole of fertilization addition when we took soil samples, a new sample site was picked. Three soil samples from the same layer within the same sampling plot were combined into one composite sample and then separated into three parts. One part was placed into an aluminum box for soil water content (SWC) determination, one part was put in a kraft paper bag and dried at 65°C for soil physicochemical analysis, and the third part was put in a ziplock bag stored in the 0°C cooler and quickly sent back to the laboratory to store at −20°C refrigerator for soil microorganism analysis.

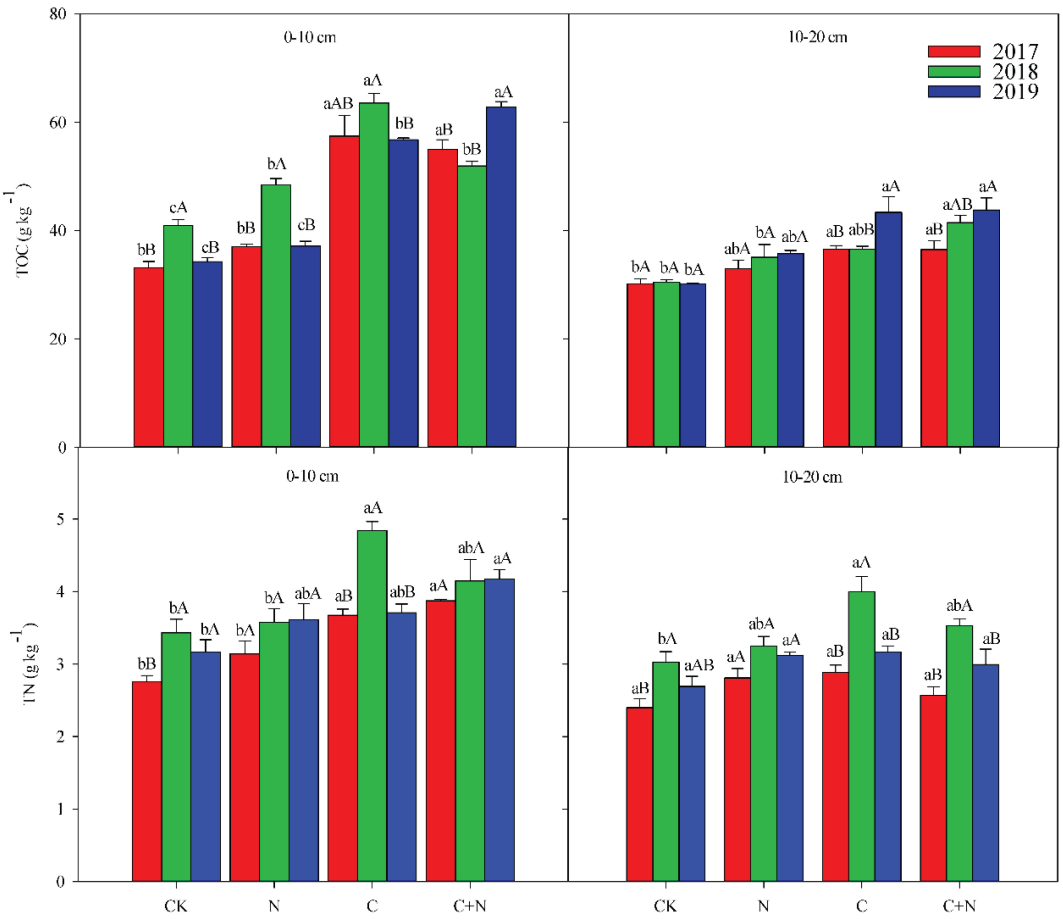

FIGURE 1 | Effects of different treatments on soil total organic carbon (TOC) and soil total nitrogen (TN) in 0–20 cm soil layers in 2017, 2018, and 2019. Error bars represent standard errors of the mean values, and different lowercase letters over the bars indicate differences among different treatments in the same year at $P < 0.05$. Different uppercase letters over the bars indicate differences among different years in the same treatment at $P < 0.05$.

Soil Physicochemical Properties Analysis

Soil physicochemical analysis included the determination of SWC, pH, electrical conductivity (EC), TOC, TN, nitrate–nitrogen (NO_3^--N), ammonium nitrogen (NH_4^+-N), and available phosphorus (AP). SWC was calculated as follows: SWC = (W2 − W3) × 100 / (W3 − W1), where W1 was the weight of the aluminum box, W2 was the weight of the initial soil sample with the aluminum box, and W3 was the weight of the dried soil sample with the aluminum box. Soil pH and EC values were determined by the acidity meter and conductivity meter (METTLER TOLEDO, Switzerland), respectively. TOC and TN were measured by Fisher 2000 elemental analyzer (Thermo Fisher Scientific, Italy). NH_4^+-N and NO_3^--N were determined by a flow autoanalyzer (FIA Compact, Germany). AP was measured by the sodium bicarbonate extraction molybdenum antimony anti-colorimetric method (Jinghua, China).

Soil Microorganism Analysis

Phospholipid fatty acid (PLFA) analysis was used to determine the main microorganisms of the soil. The method described by Bligh and Dyer (1959) and modified by White et al. (1979) was used to extract lipids from 8 g of freeze-dried soil using a single-phase mixture of chloroform, methanol, and phosphate buffer (1:2:0.8). Silicic acid column chromatography removed neutral lipids and other impurities from crude extracts. Then, the purified products were saponified to get fatty acids. A moderate methyl ester method was used to methylate fatty acids to obtain phospholipid fatty acid methyl esters (FAMEs). The FAMEs were analyzed *via* gas chromatography (Agilent 6850, United States) with Sherlock MIDI software (Newark, DE, United States).

The total PLFA concentration was used to determine the total MB for both the identified (phospholipid fatty acid composition, biomass, and activity). The bacterial PLFA markers include i14:0, 14:0, a15:0, i15:0, 15:0, i16:0, 16:0, 16:1w7, a17:0, i17:0, iso17:1, 17:0, 18:1 w5, 18:1 w7, 18:0, cy17:0, and cy19:0. The abundance of the PLFAs 18:2ω6c and 18:1ω9c indicates the presence of fungal biomass. Actinomycetes are predicted by the PLFAs 10Me17:0, 10Me17:0, and 10Me18:0. The PLFAs 16:1ω7, cy17:0, and cy19:0 are considered to be markers of Gram-negative bacteria (Gn). The PLFAs i14:0, a15:0, i15:0, i16:0, i17:0, and a17:0 are considered to be markers of Gram-positive bacteria

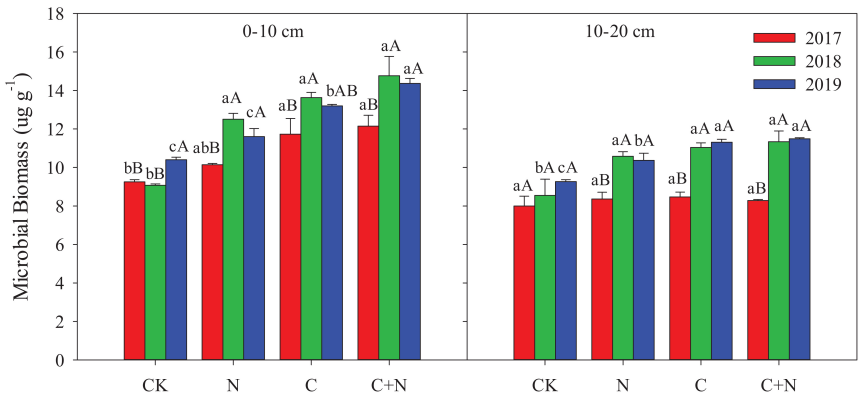

FIGURE 2 | Effects of different treatments on bacteria and fungi in 0–20 cm soil layers in 2017, 2018, and 2019. Error bars represent standard errors of the mean values, and different lowercase letters over the bars indicate differences among different treatments in the same year at $P < 0.05$. Different uppercase letters over the bars indicate differences among different years in the same treatment at $P < 0.05$.

(Gp) (Frostegard and Baath, 1996; Evgrafova et al., 2008; Djukic et al., 2010). Individual PLFA markers are as follows: 15:0iso is a marker of Gram-positive bacteria, 16:1w7c is a marker of Gram-negative bacteria, 16:10 methyl is a marker of anaerobic bacteria (Ab), 16:1w5c is a marker of arbuscular mycorrhizal fungi (Am), 18:1w7c is a marker of methanotrophic bacteria (Mb), 18:1w9c is a marker of ectomycorrhizal fungi (Ef), 18:2w6,9c is a marker of saprotrophic fungi (Sf), and 19:0 cyclo is a marker of anaerobic bacteria (An) (Sundh et al., 2000; Smith et al., 2015; Li et al., 2020).

Statistical Analysis

One-way ANOVA and Tukey's *post hoc* test (with a confidence of 95%) were used to analyze the differences between treatments in different years. Soil property and PLFA measurements were

TABLE 2 | Variation of soil ammonia-nitrogen (NH_4^+-N), nitrate-nitrogen (NO_3^--N), available phosphorus (AP), and the ratio of carbon to nitrogen (C/N) in the 0–20 cm soil layers under different treatments in 2017, 2018, and 2019.

Parameter	Year	Layer (cm)	CK	N	C	C + N
NH_4^+-N (mg/kg)	2017	0–10	17.5 ± 0.25 aC	18.12 ± 1.81 aB	11.74 ± 0.11 bC	16.8 ± 1.13 aC
	2018		35.05 ± 4.49 bA	78.83 ± 9.53 aA	70.37 ± 8.26 aA	66.64 ± 3.67 aA
	2019		26.13 ± 1.47 cB	48.83 ± 9.53 aB	48.35 ± 2.90 bB	45.38 ± 2.07 cB
	2017	10–20	16.71 ± 1.84 aB	11.38 ± 1.78 bB	9.65 ± 0.53 bB	9.39 ± 0.66 bB
	2018		22.17 ± 1.61 bA	36.52 ± 5.21 aA	34.56 ± 3.3 aA	41.96 ± 6.94 aA
	2019		14.64 ± 2.59 bB	20.53 ± 5.21 aB	36.06 ± 3.11 aA	36.50 ± 5.52 bB
NO_3^--N (mg/kg)	2017	0–10	7.57 ± 1.91 bA	18.5 ± 1.95 aB	21.62 ± 1.54 aB	21.76 ± 1.89 aB
	2018		4.97 ± 0.85 bA	9.57 ± 1.78 aC	5.77 ± 1.33 bC	9.09 ± 0.18 aC
	2019		8.96 ± 2.11 bA	26.57 ± 1.78 bA	31.7 ± 6.39 aA	36.73 ± 2.84 aA
	2017	10–20	7.18 ± 1.33 bAB	8.72 ± 0.56 bB	13.29 ± 1.36 aA	12.89 ± 2.44 aA
	2018		4.94 ± 0.97 cB	11.16 ± 0.7 aA	8.01 ± 1.61 bB	8.87 ± 0.98 bB
	2019		11.09 ± 3.66 aA	12.66 ± 0.7 aA	13.79 ± 1.36 aA	13.22 ± 1.67 aA
AP (mg/kg)	2017	0–10	2.58 ± 0.29 bA	2.62 ± 0.5 bA	4.19 ± 0.52 aA	4.63 ± 0.12 aA
	2018		3.02 ± 0.29 bA	3.10 ± 0.26 bA	4.37 ± 0.09 aA	4.42 ± 0.37 aA
	2019		1.57 ± 0.21 bB	3.10 ± 0.26 aA	3.31 ± 0.12 aA	3.49 ± 0.49 aA
	2017	10–20	1.79 ± 0.16 cA	2.24 ± 0.23 bcA	3.12 ± 0.3 aA	2.64 ± 0.2 abAB
	2018		1.89 ± 0.44 cA	2.24 ± 0.05 bcA	2.72 ± 0.15 abAB	3.16 ± 0.35 aA
	2019		1.49 ± 0.03 bA	2.14 ± 0.07 aA	2.37 ± 0.29 aB	2.20 ± 0.12 aB
C/N	2017	0–10	12.02 ± 0.6 bA	12.09 ± 1.16 bA	15.63 ± 1.66 aA	14.21 ± 0.7 abA
	2018		12.02 ± 1.69 abA	10.36 ± 1.35 bA	13.13 ± 0.72 aA	13.67 ± 1.16 aA
	2019		10.85 ± 0.7 bA	9.29 ± 1.24 bA	15.34 ± 0.71 aA	15.22 ± 1.19 aA
	2017	10–20	12.68 ± 1.69 bA	11.80 ± 1.42 bA	12.73 ± 1.09 bA	14.27 ± 1.74 aA
	2018		10.08 ± 0.58 abA	9.81 ± 0.99 bA	9.22 ± 1.00 bB	11.76 ± 0.58 aB
	2019		10.03 ± 0.97 abA	10.33 ± 0.84 bA	13.67 ± 1.22 aA	11.78 ± 1.86 bB

Values are means ± SE, lowercase letters indicate differences between different treatments in the same year ($P < 0.05$), and uppercase letters indicate differences between different years in the same treatment ($P < 0.05$).

indicated by the mean of three replicates with the standard error (SE) of the mean. Principal component analysis (PCA) was used to compare and analyze the structure of the soil microbe community, which was indicated by the composition of PLFAs. The relationships between soil physicochemical properties and special microorganisms were analyzed using redundant analysis (RDA). The correlation of soil physicochemical was analyzed using Pearson's correlation, and the Mantel test was used to explore the relationship between different microbial communities and environmental factors in different treatments. Procrustes analysis of the correlation between soil physicochemical properties and microbial community was based on the PCA (Bray–Curtis) results of different treatments. All analyses were performed in R3.3.3. Effects were considered to be significant if $P < 0.05$.

RESULTS

Changes of Soil Physicochemical Properties in Moderate–Severe Degraded Alpine Grassland

In the 0–10 cm soil layer, pH had no significant change among treatments in 2017, but pH was significantly higher in the treatments of biochar application than that in CK in 2018 and 2019. In the 10–20 cm soil layer, pH was significantly higher in treatments with additives than that in CK (**Table 1**). In the first experimental year (2017), EC in the 0–20 cm soil layer was much higher in the treatments of N addition, biochar addition, and the mixed addition of nitrogen and biochar than that in CK. In the third year (2019), EC within the treatments of biochar addition dropped to a similar value to that in CK, but EC in the treatment with N addition dropped to a value smaller than that in CK (**Table 1**). SWC in the 0–20 cm soil layer did not change significantly among different treatments in 2017, but was significantly higher in the treatments with additives than that in CK in 2018 and 2019 (**Table 1**). SWC in the 10–20 cm soil layer showed a similar trend in the surface layer.

The addition of biochar and nitrogen significantly changed TOC and TN in the 0–20 cm soil layer (**Figure 1**). Compared with CK, the addition of nitrogen alone had no significant effect on the TOC in the 0–10 cm soil layer, but the addition of biochar and the mixed addition of biochar and nitrogen significantly increased the TOC in the topsoil (0–10 cm). In the third experimental year (2019), TOC in the 0–10 cm soil layer reached 62.79 g/kg in the treatment of the mixed addition of biochar and nitrogen. In the 10–20 cm soil layer, the addition of N alone did not increase the TOC compared with CK, but the addition of biochar significantly increased the TOC and showed an upward trend year by year (**Figure 1**). In the

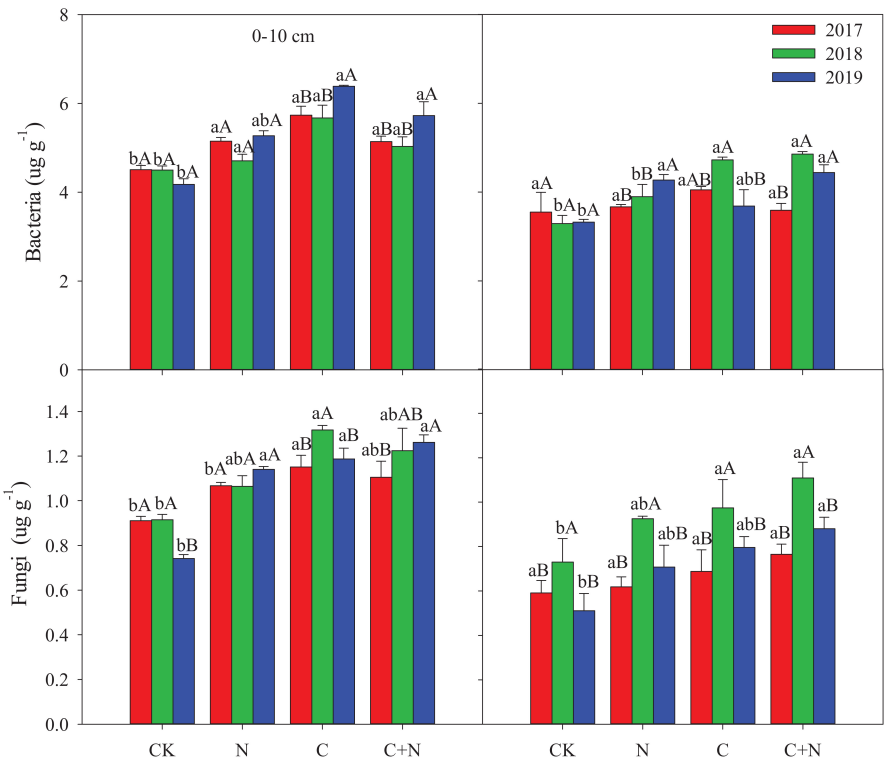

FIGURE 3 | Effects of different treatments on microbial biomass in 0–20 cm soil layers in 2017, 2018, and 2019. Error bars represent standard errors of the mean values, and different lowercase letters over the bars indicate differences among different treatments in the same year at $P < 0.05$. Different uppercase letters over the bars indicate differences among different years in the same treatment at $P < 0.05$.

third experimental year (2019), the TOC increased by 43.58 and 45.07% in the treatments of biochar addition and the mixed addition of nitrogen and biochar, respectively, compared with CK (**Figure 1**). TN in the topsoil (0–10 cm) increased significantly under the treatments of biochar addition and the mixed addition of nitrogen and biochar. Compared with nitrogen addition alone, the addition of biochar and the mixed addition of nitrogen and biochar resulted in higher TN accumulation in the topsoil (**Figure 1**). Ratio of carbon to nitrogen (C/N) in the 0–20 cm soil layer was higher in the treatments with biochar addition than that in CK, but C/N in the treatment with nitrogen addition alone showed no significant difference with CK (**Table 2**).

NH_4^+-N in the 0–10 cm soil layer had no significant difference among treatments in the first year (2017), but was significantly greater in the treatments with additives in the second and third years (2018 and 2019, respectively) than that in CK (**Table 2**). Within the same treatment, NH_4^+-N increased first and then decreased with the increase of experimental years (**Table 2**). In the 10–20 cm soil layer, the changes of NH_4^+-N in each treatment or between treatments were similar to that in the topsoil. Different from the changing trend of NH_4^+-N, NO_3^--N in the 0–10 cm soil layer was significantly greater in the treatments with additives than that in CK. Within the same treatment, NO_3^--N first decreased and then increased with the increase of the experimental year. The maximum value appeared in the third year (2019). In the 10–20 cm soil layer, NO_3^--N was greater in the treatments with additives than that in CK in the first 2 years (2017 and 2018), but in the third experimental year (2019), NO_3^--N had no significant difference between CK and the treatments with additives (**Table 2**). Compared with CK, AP in the 0–20 cm soil layer increased in the treatments with additives. Among these treatments, the addition of biochar and the mixed addition of biochar and nitrogen had a stronger effect on AP increase. AP in the third experimental year (2019) was relatively lower than that in 2017 and 2018 (**Table 2**).

Changes of Soil Microorganisms in the Moderate–Severe Degraded Alpine Grassland

Compared with CK, the N addition alone had no significant effect on the MB in the 0–10 cm soil layer, but the addition of biochar and the mixed addition of biochar and nitrogen increased the MB (**Figure 2**). With the increase of experimental year, the MB showed a certain upward trend in the treatments with additives, especially in the treatment of the mixed addition of biochar and nitrogen. The MB increased from 12.15 μg/g in 2017 to 14.37 μg/g in 2019 in the treatment of the mixed addition of

TABLE 3 | Fungi:bacteria (F/B), Gram-positive:Gram-negative (GP/GN), microbial biomass:total organic carbon (MB:TOC), and microbial biomass:total nitrogen (MB:TN) in 0–20 cm soil layers under different treatments in 2017, 2018, and 2019.

Parameter	Year	Layer (cm)	CK	N	C	C + N
F/B	2017	0–10	0.18 ± 0.01 bA	0.21 ± 0 aA	0.22 ± 0.02 aB	0.22 ± 0.04 aA
	2018		0.20 ± 0.01 aA	0.20 ± 0.01 aA	0.25 ± 0.01 aA	0.22 ± 0.01 aA
	2019		0.17 ± 0.01 aA	0.19 ± 0.02 aA	0.21 ± 0.01 aB	0.20 ± 0.01 aA
	2017	10–20	0.17 ± 0.01 bB	0.17 ± 0.01 bA	0.21 ± 0.07 aB	0.18 ± 0.04 bB
	2018		0.22 ± 0.03 bA	0.19 ± 0.01 bA	0.28 ± 0.05 bA	0.31 ± 0.15 aA
	2019		0.18 ± 0.02 aB	0.16 ± 0.03 abA	0.26 ± 0.01 abA	0.25 ± 0.04 bA
GP/GN	2017	0–10	1.44 ± 0.14 aAB	1.36 ± 0.11 aA	1.37 ± 0.04 aA	1.46 ± 0.05 aA
	2018		1.55 ± 0.06 aA	1.40 ± 0.24 abA	1.41 ± 0.2 abA	1.33 ± 0.01 bB
	2019		1.29 ± 0.06 aB	1.28 ± 0.04 aB	1.13 ± 0.01 bB	1.27 ± 0.02 aB
	2017	10–20	1.12 ± 0.23 aA	1.17 ± 0.02 aA	1.24 ± 0.10 aA	1.23 ± 0.15 aA
	2018		1.19 ± 0.04 bA	1.20 ± 0.13 bA	1.23 ± 0.20 bA	1.56 ± 0.13 aA
	2019		1.11 ± 0.10 aA	1.15 ± 0.05 aA	1.12 ± 0.06 aA	1.07 ± 0.01 aB
MB:TOC	2017	0–10	0.28 ± 0.01 aA	0.27 ± 0.00 aA	0.21 ± 0.02 bA	0.22 ± 0.02 bA
	2018		0.22 ± 0.01 bB	0.26 ± 0.01 abA	0.21 ± 0.01 bA	0.23 ± 0.03 bA
	2019		0.31 ± 0.01 aA	0.31 ± 0.03 aA	0.22 ± 0.00 bA	0.23 ± 0.01 bA
	2017	10–20	0.27 ± 0.04 aA	0.25 ± 0.01 aA	0.23 ± 0.01 aB	0.23 ± 0.01 aA
	2018		0.28 ± 0.04 aA	0.31 ± 0.04 aA	0.30 ± 0.01 aA	0.27 ± 0.01 aA
	2019		0.31 ± 0.00 aA	0.29 ± 0.01 aA	0.26 ± 0.03 aAB	0.26 ± 0.02 aA
MB:TN	2017	0–10	3.36 ± 0.11 aA	3.25 ± 0.22 aA	3.20 ± 0.39 aA	3.14 ± 0.22 aB
	2018		2.65 ± 0.19 bB	3.14 ± 0.4 abA	2.82 ± 0.05 bB	3.89 ± 0.46 aA
	2019		3.35 ± 0.25 aA	2.91 ± 0.38 bA	3.57 ± 0.17 aA	3.48 ± 0.11 abA
	2017	10–20	3.34 ± 0.16 aA	2.98 ± 0.14 aA	2.94 ± 0.20 aAB	3.24 ± 0.23 aA
	2018		2.84 ± 0.45 aA	2.98 ± 0.32 aA	2.78 ± 0.24 aB	3.22 ± 0.23 aA
	2019		3.50 ± 0.27 abA	2.91 ± 0.19 bA	3.58 ± 0.2 abA	3.89 ± 0.42 aA

Values are means ± SE, lowercase letters indicate differences between different treatments in the same year ($P < 0.05$), and uppercase letters indicate differences between different years in the same treatment ($P < 0.05$).

biochar and nitrogen. In the 10–20 cm soil layer, the MB had no significant difference among treatments in the first experimental year (2017), but the treatments with additives had higher MB in the second and third years (2018 and 2019, respectively) than CK (**Figure 2**). For the same treatment, MB increased with the increase of experimental year.

Bacteria biomass in the topsoil (0–10 cm) increased in the treatments with additives compared with CK, and the increased intensity was greater in the addition of biochar and the mixed addition of biochar and nitrogen than that in the nitrogen addition alone. In the 10–20 cm soil layer, treatments with additives had a higher bacterial biomass than CK in the second and third experimental years (2018 and 2019, respectively), and the mixed addition of biochar and nitrogen reached the highest value (**Figure 3**). Similar to the changes of bacteria, fungi in the 0–10 cm soil layer was significantly greater in the treatments with additives than that in CK, and the increased intensity was greater in the addition of biochar and the mixed addition of biochar and nitrogen than that in the nitrogen addition. In the 10–20 cm soil layer, fungi had no significant difference among treatments in the first experimental year (2017), but the treatments with additives increased the relative content of fungi of this layer compared with CK in the second and third experimental years (**Figure 3**). The fungi:bacteria (F/B) in the 0–10 cm soil layer was greater in the treatments with additives than that in CK. In the 10–20 cm soil layer, the N addition alone did not have a significant effect on the F/B, but the F/B increased in the treatment of biochar addition alone and the mixed addition of biochar and nitrogen (**Table 3**). Compared with CK, MB:TOC in the 0–10 cm soil layer decreased in the treatments of biochar addition alone and the mixed addition of biochar and nitrogen, but had no change in the treatment of N addition alone.

In PCA, the first two axes explained the variation of 78.23% in the 0–10 cm soil layer (**Figure 4A**) and 75.35% in the 10–20 cm soil layer (**Figure 4C**), respectively. The dispersion degree of the treatments among different years in the coordinate axis was greater in the 0–10 cm soil layer than that in the 10–20 cm soil layer, and the dispersion degree of different treatments increased with the increase of experimental year. It indicated that the addition of biochar and nitrogen had a significant impact on the microbial community structure of the topsoil, and the degree of influence became greater with the increase of residence time in soil, especially for the treatment of biochar addition alone and the mixed addition of biochar and nitrogen (**Figures 4A,C**). Compared with CK, biochar addition alone significantly increased the relative content of 16.1w5c, cy17.0, cy19.0, 10Me18.0, 18.1w7, and 18.1w9c, the mixed addition of biochar and nitrogen significantly increased the relative content of i14.0, i15.0, a15.0, 10Me16.0, 16.1w7, i16.0, i17.0, 10Me17.0, cy17.0, and 18.1w9c, but the nitrogen addition alone did not

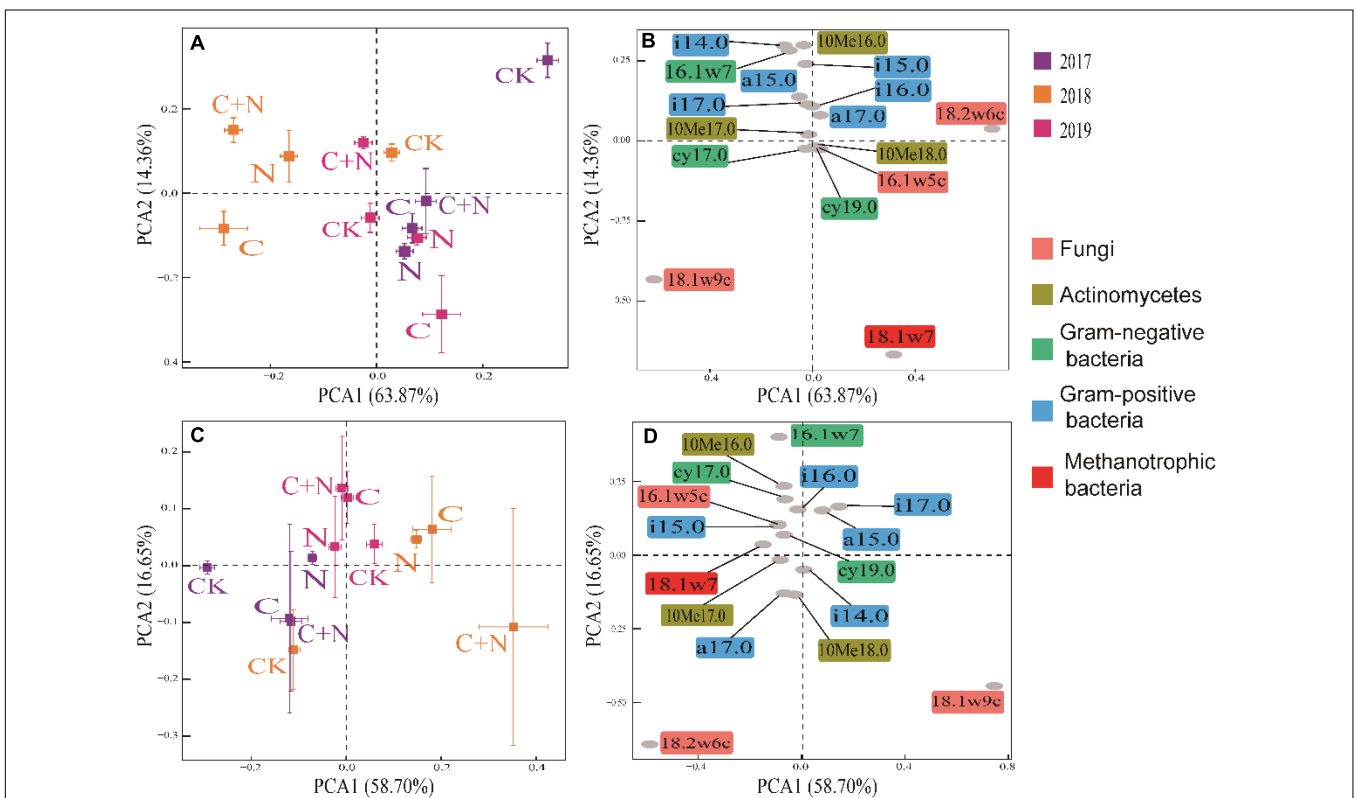

FIGURE 4 | Principal component analysis (PCA) of soil microbial community within different soil layers under different treatments in 2017, 2018, and 2019. **(A)** Treatment coordinates of 0–10 cm soil layer; **(B)** soil microorganism coordinates of 0–10 cm soil layer; **(C)** treatment coordinates of 10–20 cm soil layer; and **(D)** soil microorganism coordinates of 10–20 cm soil layer.

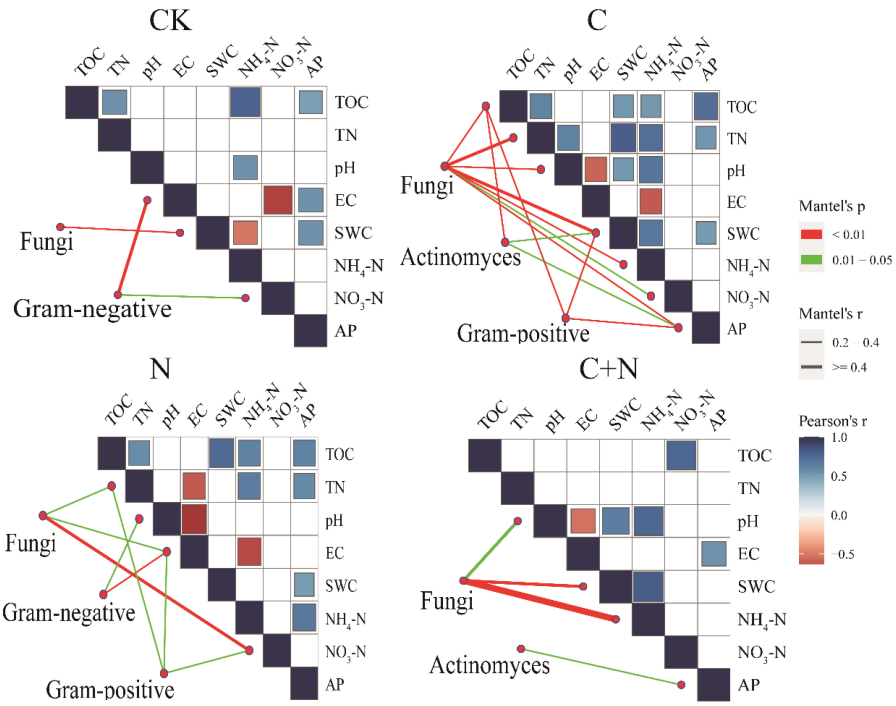

FIGURE 5 | Pairwise comparisons between environmental factors and microbial communities in the 0–10 cm and 10–20 cm soil layers by partial Mantel tests for different treatments. The color gradients denote Spearman's correlation coefficients; line edge width corresponds to the Mantel's *r* statistic for the corresponding distance correlations, and edge color denotes the statistical significance based on 9,999 permutations.

cause the significant change of soil microbial community in the topsoil (0–10 cm) (**Figures 4A,B**). In the deep soil (10–20 cm), the differences of microbial community structure among treatments were mainly reflected in experimental years, and the treatments of biochar addition alone and the mixed addition had figured prominently. Compared with CK, the relative contents of i14.0, a17.0, 10Me18.0, and 18.1w9c in 2017 were greater in the treatments of biochar addition alone and the mixed addition; the relative contents of a15.0, i17.0, and 18.1w9c were greater in 2018; and the relative contents of other microorganisms, except for i14.0, a17.0, 10Me18.0, and 18.1w9c, were greater in 2019 (**Figures 4C,D**). Among these microorganisms, 18.1w9c, 18.2w6c, and 18.1w7 had greater contributions (**Figure 4**).

The Interaction Between Microorganisms and Soil Properties

Different treatments showed various interactions between microorganisms and soil physicochemical properties. In CK, the interactions between microorganisms and soil physicochemical properties were weak, and only fungi and SWC, Gram-negative, EC, and NO_3^--N had a strong interaction (**Figure 5**). In the treatment of nitrogen addition alone, fungi had significant interactions with TN, EC, and NO_3^--N (**Figure 5**). In the treatment of biochar addition alone, most soil physicochemical properties showed significant positive correlations, and interactions between soil factors and fungi, actinomyces, and Gram-positive had improved. Especially, fungi had a significant interaction with most of the soil factors (**Figure 5**). In the treatment of the mixed addition, fungi showed significant correlations with pH, SWC, and NH_4^+-N (**Figure 5**). The Procrustes analysis further verified the potential relationship between soil factors and microbial community under different treatments (**Figure 6**). It showed that the *P*-values of different treatments in the Procrustes analysis were all less than 0.05, and the performance of M^2 was C (M^2 = 0.383) < C+N (M^2 = 0.575) < N (M^2 = 0.673) < CK (M^2 = 0.726) (**Figure 6**). It indicated that the consistency of the relationship between soil factors and microbial community was greater in the treatment of biochar addition alone and the mixed addition than that in the treatment of nitrogen addition alone and CK, and the biochar addition alone and the mixed addition had greater improving effect on the interaction between microorganisms and main soil physicochemical properties.

Focused on the relationship between soil physicochemical properties and specific microbes, RDA found that NO_3^--N, EC, and pH in the topsoil (0–10 cm) had a greater effect on specific microbial community structures. Ef and Gn had a positive correlation with most of the soil properties. Sf had a positive correlation with EC, and Mb had a positive correlation with NO_3^--N. With the increase of experimental year, the sensitivity of microorganisms to soil properties significantly increased in the treatments of biochar addition alone and the mixed addition (**Figure 7A**). In the 10–20 cm soil layer, EC, AP, and pH had a greater effect on specific microbial community structures (**Figure 7B**). Ef had a positive correlation with most of the soil

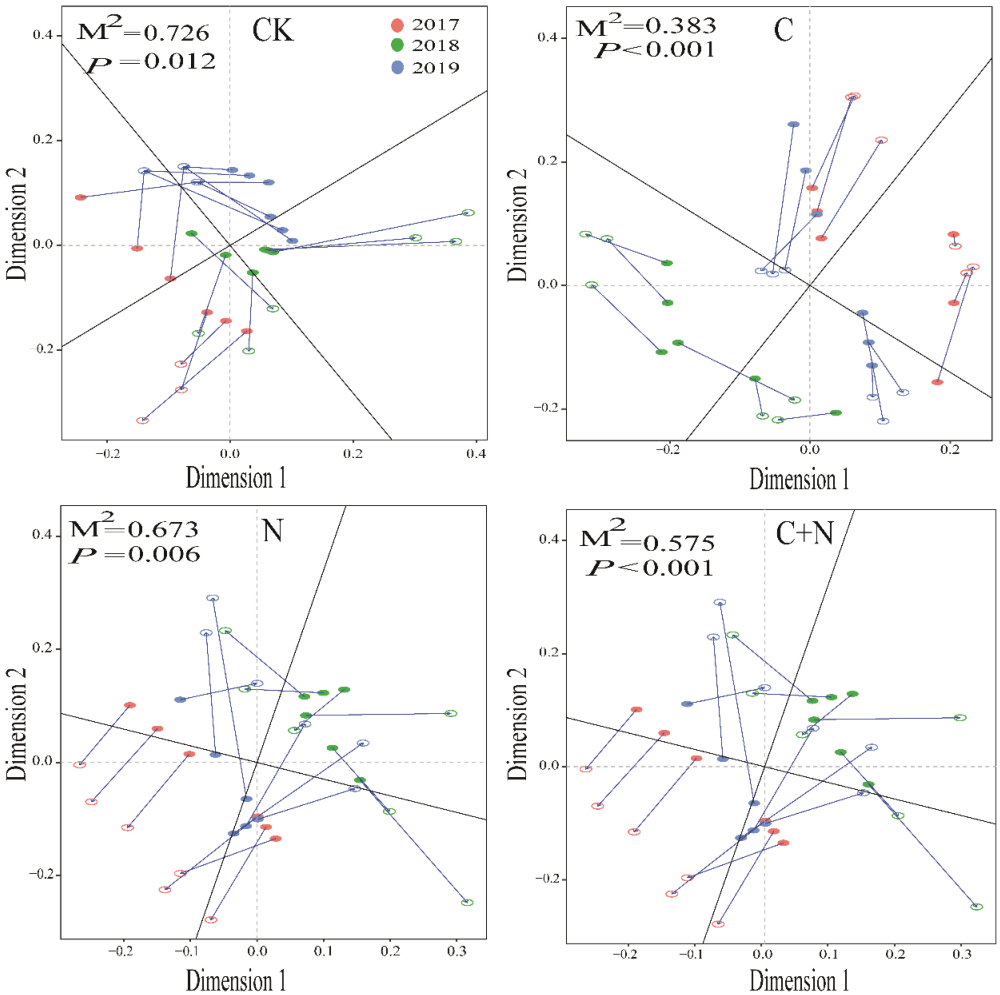

FIGURE 6 | Procrustes analysis of the correlation between soil physicochemical properties and microbial community based on the PCA (Bray–Curtis) results of different treatments.

properties. Sf had a positive correlation with EC, and Mb had a positive correlation with NO_3^--N.

DISCUSSION

Responses of Soil Physicochemical Properties to the Addition of Biochar or Nitrogen

When additives were added to the soil, it generally changed the physicochemical properties of the soil to some extent. In this study, soil TOC and TN significantly increased after the addition of biochar and the mixed addition of biochar and nitrogen, and the amplitude of increase was greater in the 0–10 cm soil layer than that in the 10–20 cm soil layer. Moreover, TOC and TN continuously increased with the increase of residence time of additives in soil (**Figure 1**). The accumulation of TOC in soil was probably associated with the unique properties of biochar. On the one hand, biochar has the capacity of strong adsorption to adsorb small organic molecules in the soil. These small organic molecules can polymerize to form organic matter under the catalysis, and then the soil organic carbon increases (Muhammad et al., 2018). On the other hand, biochar contains a large amount of organic carbon with an aromatic structure, which is considered as the recalcitrant carbon pool. Therefore, biochar addition increases the accumulation of soil organic carbon (Chen et al., 2018). In addition, MB also increased significantly after biochar addition (**Figure 2**). The increase of microorganisms can accelerate the decomposition of organic matter and lead to the increase of organic carbon (Pietikainen et al., 2000). The unique properties of biochar also promoted the increase of TN in soil. A study found that the cation exchange capacity of biochar increased as the residence time of biochar in the soil increased, then the holding capacity of nutrients was strengthened, and the leaching of soil nutrients decreased (Jiang et al., 2019), and therefore, the accumulation of nitrogen in the 0–20 cm soil layer increased. Biochar addition increased the contents of trace

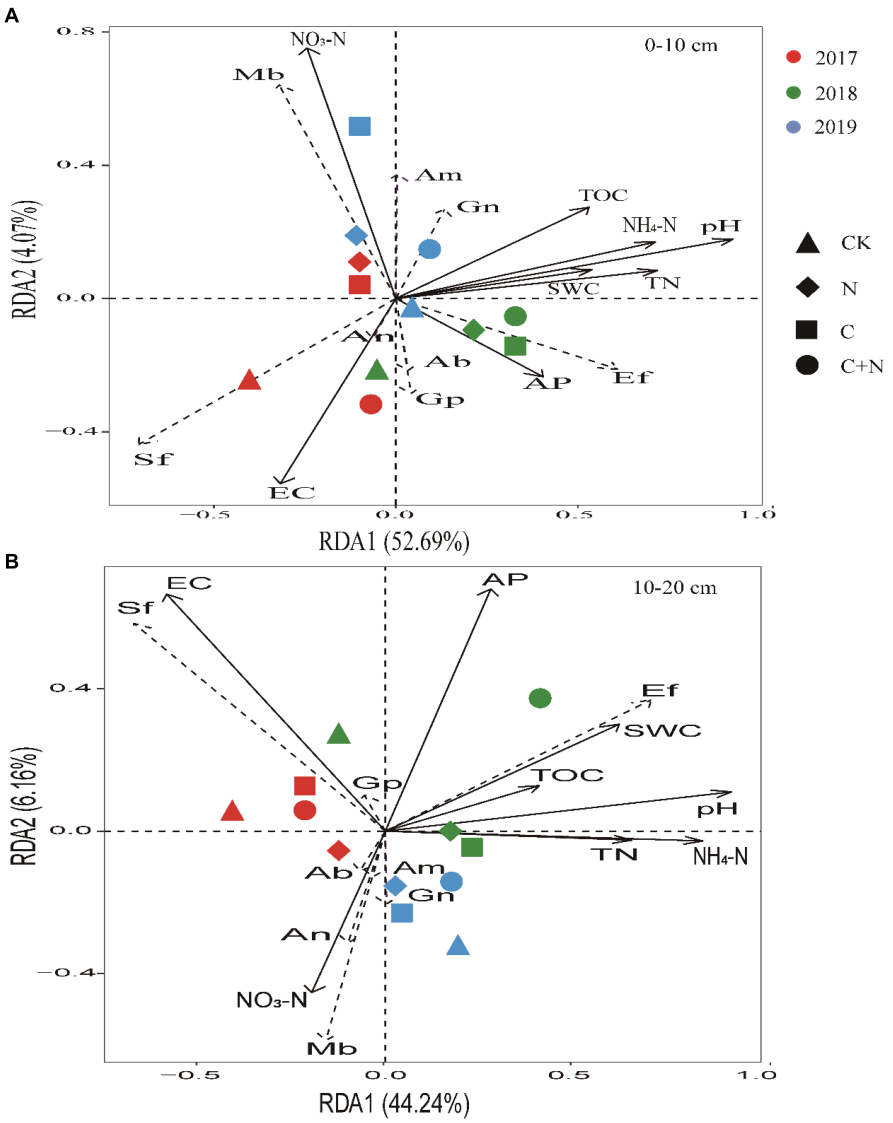

FIGURE 7 | Redundancy analysis (RDA) ordination biplot of soil physicochemical properties and microbes in 0–10 cm soil layer **(A)** and 10–20 cm soil layer **(B)**. Soil physicochemical properties were represented by black lines, and microorganism indicators were represented by dashed lines. TOC, total organic carbon; TN, total nitrogen; AP, available phosphorus; NO_3^--N, soil nitrate–nitrogen; NH_4^+-N, soil ammonia–nitrogen; EC, electrical conductivity; SWC, soil water content. Gn, Gram-negative bacteria; Ab, Actinobacteria; Gp, Gram-positive bacteria; Sf, saprotrophic fungi; Ef, ectomycorrhizal fungi; Mb, methanotrophic bacteria; An, anaerobic bacteria; Am, arbuscular mycorrhizal fungi.

elements, boron and manganese, related to nitrogenase activity in the soil and then improved the efficiency of nitrogen fixation (Quilliam et al., 2012). However, TOC and TN had no significant change under the treatment of nitrogen addition alone in this study. It indicated that this application method and the amount of nitrogen fertilizer did not cause an impact on soil TOC and TN of the moderate–severe degraded alpine grassland in this short-term.

The addition of biochar and nitrogen fertilizer significantly changed the content of available nitrogen NH_4^+-N and NO_3^--N in the soil, and the effect increased with the increase of application time (**Table 1**). As seen from the research results, NO_3^--N in soil was lower in 2018 than that in 2017 and 2019. This might be related to the higher soil pH and SWC in 2018 (**Table 1**). High water content causes soil hypoxia (Chen et al., 1997). Together with high pH, it strengthened the denitrification in the soil, and thereby accelerated the consumption of NO_3^--N and decreased the content of NO_3^--N. In addition, biochar has relatively high CEC, which can not only increase the adsorption of NH_4^+ but also reduce the conversion to NO_3^- (Ye et al., 2020). In general, the contents of available nitrogen NH_4^+-N and NO_3^--N were greater in the treatments of biochar addition alone and the mixed addition. It indicated that biochar addition increased the availability of nitrogen in degraded alpine grassland. Polyporous structure and strong adsorption properties of biochar also increase the absorption of phosphorus

and promote the increase of soil water-holding capacity, thus increasing AP and SWC (Han et al., 2016; Reed et al., 2017). The results of this study were consistent with this finding (**Tables 1**, **2**).

Biochar is alkaline because it forms a certain amount of carbonate during the process of preparation (Fan et al., 2018). When biochar is applied to the soil, the soil pH generally increases. The change of pH in this study verified the trend. However, the long-term excessive application of N fertilizer will lead to a decrease in pH (Fu and Shen, 2017). In this study, nitrogen fertilizer is not used excessively, so the pH had no significant change in the treatment of nitrogen addition alone. The ratio of total soil carbon to nitrogen is an important indicator to evaluate the composition and quality of soil organic matter (Fang et al., 2019). In this study, C/N increased significantly in the treatments of biochar addition alone and the mixed addition and was higher than the global average of grassland soil (11.8) (Wang X. G. et al., 2020). It indicated that biochar addition makes soil carbon be supplemented.

Response of Soil Microorganisms to the Addition of Biochar or Nitrogen

Total MB, bacteria, and fungi in the 0–20 cm soil layer significantly increased under the addition of biochar and the mixed addition of biochar and nitrogen and increased with the increase of application time (**Figures 2**, **3**). These changes were probably attributed to the improvement of soil properties (i.e., soil bulk density, water content, and soil nutrients) after biochar input. This improvement can provide suitable habitat for the growth and reproduction of microorganisms (Zhu et al., 2017). Furthermore, the porosity structure of biochar can absorb nutrient substrates for the growth and metabolism of microorganisms (Pietikainen et al., 2000). Nitrogen addition directly provides nutrients for the growth and reproduction of soil microorganisms (Ma et al., 2020).

Fungi:bacteria had significant differences among treatments (**Table 3**), but Gram-positive:Gram-negative (GP/GN) had no change. It indicated that the addition of biochar and nitrogen caused an asynchronous increase of soil bacteria and fungi and tends to increase more fungi. This finding was consistent with the findings of Zong and Fu (2021), who found that the fungal community is sensitive to soil degradation and varied in different degraded alpine grasslands. MB:TOC was greater in the treatments of biochar addition alone and the mixed addition of biochar and nitrogen, but MB:TN had no significant change among treatments (**Table 3**). It showed that additives with biochar were more likely to cause changes in the structure of the soil microbial community, but only nitrogen addition had a relatively weak effect. In the first year of the study, the community structure of soil microorganisms changed slightly, and the amplitude of change was greater in the surface soil (0–10 cm) than that in the deep soil (10–20 cm). In the second and third experimental years, different additive treatments caused different changes in the microbial communities. This response was probably associated with the way of "hole application" and "surface application." This addition method might result in an insufficient mixture of the added materials with the soil in the first year and required some time to expand the added materials into the deep soil. Therefore, the difference among treatments mainly occurred in the second and third experimental years. Under the treatment of biochar addition alone, 18.1w9c and 18.2w6c had significant changes. Under the treatment of the mixed addition of biochar and nitrogen, bacteria, 16.1w5c, 18.1w9c, and 18.2w6c had significant changes. Biochar input increased the accumulation of nutrients (**Figure 1** and **Table 1**), but biochar is rich in organic carbon and lacks other nutrients, and its input may cause the imbalance of nutrients for microbial growth over a period of time (Jenkins et al., 2017). Fungi, the main decomposer of the soil, can release extracellular enzymes to effectively degrade the stubborn organic matter components (DeForest and Snell, 2020). The input of biochar with porosity structure provides a good habitat for fungi (Zhu et al., 2017) and promotes the reproduction of fungi to ensure the accumulation of nutrients required for vegetation and microbial growth (Zhang et al., 2018). Nitrogen fertilizer, as the most direct nutrient substance, can directly provide nutrients for the growth of microorganisms (Li et al., 2018) and accelerate their reproduction (Zhao Z. B. et al., 2019).

In Procrustes analysis, the smaller value of M^2 means the better consistency between environmental factors and microbial community structure (Zhao R. et al., 2019). In this study, the values of M^2 in the treatments of biochar addition alone and the mixed addition were relatively higher (**Figure 7**). This further proved that the addition of biochar and the mixed addition improved soil microbial community and physicochemical properties at the same time. As for the addition of nitrogen alone, it produced similar results to CK. It was probably due to the volatilization or leaching of nitrogen as nitrogen was added alone (Zhu et al., 2018). This difference indirectly proved that the mixed addition of nitrogen and biochar could enhance the utilization efficiency of nitrogen fertilizer. In a degraded grassland, nitrogen is an important limiting factor for the development of soil microorganisms (Liu et al., 2020). Nitrogen input could decrease the high C/N and promote the activity of decomposers.

Biochar input could provide organic matter and absorb nutrients for the utilization of microorganisms. Also, the addition of nitrogen can quickly make up for the shortcomings of insufficient soil nutrients and stimulate the growth of microorganisms, and the addition of biochar can improve the utilization efficiency of nitrogen fertilizer and provide a good habitat for microorganisms. This was the important reason why the mixed addition of biochar and nitrogen caused higher improvement effects for the moderate–severe degraded alpine grassland.

CONCLUSION

Compared with nitrogen addition alone, the addition of biochar alone and the mixed addition of biochar and nitrogen had a greater improvement effect on the soil physicochemical properties and microorganisms of the vegetation growth layer (0–20 cm). In the 0–20 cm soil layer, TOC, TN, NO_3^--N, NH_4^+-N, AP, SWC, and MB increased significantly after the addition of biochar and the mixed addition of biochar and

nitrogen. As for specific microbes, the relative content of 16.1w5c, 18.1w9c, 18.2w6c, and bacteria increased significantly as well. Moreover, the biochar addition alone or the mixed addition of biochar and nitrogen changed the structure of the microbial community and the relationships between microorganisms and soil physicochemical properties. The mixed addition of biochar and nitrogen produced the superposition effect and made it superior to the biochar addition alone in some aspects. These findings indicated that the application of biochar in the moderate–severe degraded alpine grassland could improve soil properties and microbial community structure, and the mixed addition of biochar and nitrogen had a stronger improvement effect on the soil system of moderate–severe degraded alpine grassland.

DATA AVAILABILITY STATEMENT

The original contributions presented in the study are included in the article/supplementary material, further inquiries can be directed to the corresponding author.

AUTHOR CONTRIBUTIONS

JL, YZ, and KL contributed to conception and design of the study. YZ, HL, and YH organized the database. JL performed the statistical analysis. JL and YZ wrote the first draft of the manuscript. XS, DH, JS, and KL wrote sections of the manuscript. All authors contributed to manuscript revision, read, and approved the submitted version.

FUNDING

This research was supported by the National Key Research and Development Program (2016YFC0501902 and 2018YFF0213405).

ACKNOWLEDGMENTS

We gratefully acknowledge Ruiqi Wang, Ning Li, Chan An, and Zhao Tianci for their assistance in the field.

REFERENCES

Bligh, E. G., and Dyer, W. J. (1959). A rapid method of total lipid extraction and purification. *Can. J. Physiol. Pharm.* 37, 911–918. doi: 10.1139/y59-099

Butnan, S., Deenik, J. L., Toomsan, B., and Vityakon, P. (2017). Biochar properties affecting carbon stability in soils contrasting in texture and mineralogy. *Agric. Nat. Resour.* 51, 492–498. doi: 10.1016/j.anres.2018.03.002

Che, R., Wang, Y., Li, K., Xu, Z., Hu, J., Wang, F., et al. (2019). Degraded patch formation significantly changed microbial community composition in alpine meadow soils. *Soil Till. Res.* 195:104426. doi: 10.1016/j.still.2019.104426

Chen, H., Ma, J., Wei, J., Gong, X., Yu, X., Guo, H., et al. (2018). Biochar increases plant growth and alters microbial communities *via* regulating the moisture and temperature of green roof substrates. *Sci. Total Environ.* 635, 333–342. doi: 10.1016/j.scitotenv.2018.04.127

Chen, J., Xuan, J., Du, C., and Xie, J. (1997). Effect of potassium nutrition of rice on rhizosphere redox status. *Plant Soil* 188, 131–137. doi: 10.1023/A:1004264411323

DeForest, J. L., and Snell, R. S. (2020). Tree growth response to shifting soil nutrient economy depends on mycorrhizal associations. *New Phytol.* 225, 2557–2566. doi: 10.1111/nph.16299

Djukic, I., Zehetner, F., Mentler, A., and Gerzabek, M. H. (2010). Microbial community composition and activity in different Alpine vegetation zones. *Soil Biol. Biochem.* 42, 155–161. doi: 10.1016/j.soilbio.2009.10.006

Dong, S. K., Wen, L., Li, Y. Y., Wang, X. X., Zhu, L., and Li, X. Y. (2012). Soil-quality effects of grassland degradation and restoration on the qinghai-tibetan plateau. *Soil Sci. Soc. Am. J.* 76, 2256–2264. doi: 10.2136/sssaj2012.0092

El-Naggar, A., Lee, S. S., Awad, Y. M., Yang, X., Ryu, C., Rizwan, M., et al. (2018). Influence of soil properties and feedstocks on biochar potential for carbon mineralization and improvement of infertile soils. *Geoderma* 332, 100–108. doi: 10.1016/j.geoderma.2018.06.017

Evgrafova, S. Y., Santruckova, H., Shibistova, O. B., Elhottova, D., Cerna, B., Zrazhevskaya, G. K., et al. (2008). Phospholipid fatty acid composition of microorganisms in pine forest soils of Central Siberia. *Biol. Bull.* 35, 452–458. doi: 10.1134/s1062359008050038

Fan, Q., Cui, L., Quan, G., Wang, S., Sun, J., Han, X., et al. (2018). Effects of wet oxidation process on biochar surface in acid and alkaline soil environments. *Materials* 11:2362. doi: 10.3390/ma11122362

Fang, Z., Li, D. D., Jiao, F., Yao, J., and Du, H. T. (2019). The latitudinal patterns of leaf and soil C:N:P stoichiometry in the loess plateau of China. *Front. Plant Sci.* 10:85. doi: 10.3389/fpls.2019.00085

Farrell, M., Kuhn, T. K., Macdonald, L. M., Maddern, T. M., Murphy, D. V., Hall, P. A., et al. (2013). Microbial utilisation of biochar-derived carbon. *Sci. Total Environ.* 465, 288–297. doi: 10.1016/j.scitotenv.2013.03.090

Feng, R., Long, R., Shang, Z., Ma, Y., Dong, S., and Wang, Y. (2009). Establishment of Elymus natans improves soil quality of a heavily degraded alpine meadow in Qinghai-Tibetan Plateau, China. *Plant Soil* 327, 403–411. doi: 10.1007/s11104-009-0065-3

Frostegard, A., and Baath, E. (1996). The use of phospholipid fatty acid analysis to estimate bacterial and fungal biomass in soil. *Biol. Fert. Soils* 22, 59–65. doi: 10.1007/BF00384433

Fu, G., and Shen, Z. X. (2016). Response of Alpine plants to nitrogen addition on the tibetan plateau: a meta-analysis. *J. Plant Growth Regul.* 35, 974–979. doi: 10.1007/s00344-016-9595-0

Fu, G., and Shen, Z. X. (2017). Response of Alpine soils to nitrogen addition on the tibetan plateau: a meta-analysis. *Appl. Soil Ecol.* 114, 99–104. doi: 10.1016/j.apsoil.2017.03.008

Gul, S., and Whalen, J. K. (2016). Biochemical cycling of nitrogen and phosphorus in biochar-amended soils. *Soil Biol. Biochem.* 103, 1–15. doi: 10.1016/j.soilbio.2016.08.001

Han, F., Ren, L., and Zhang, X. C. (2016). Effect of biochar on the soil nutrients about different grasslands in the Loess Plateau. *Catena* 137, 554–562. doi: 10.1016/j.catena.2015.11.002

Jenkins, J. R., Viger, M., Arnold, E. C., Harris, Z. M., Ventura, M., Miglietta, F., et al. (2017). Biochar alters the soil microbiome and soil function: results of next-generation amplicon sequencing across Europe. *GCB Bioenergy* 9, 591–612. doi: 10.1111/gcbb.12371

Jiang, X., Tan, X., Cheng, J., Haddix, M. L., and Cotrufo, M. F. (2019). Interactions between aged biochar, fresh low molecular weight carbon and soil organic carbon after 3.5 years soil-biochar incubations. *Geoderma* 333, 99–107. doi: 10.1016/j.geoderma.2018.07.016

Li, J., Shao, X., Huang, D., Shang, J., Liu, K., Zhang, Q., et al. (2020). The addition of organic carbon and nitrogen accelerates the restoration of soil system of degraded alpine grassland in Qinghai-Tibet Plateau. *Ecol. Eng.* 158:106084. doi: 10.1016/j.ecoleng.2020.106084

Li, S., Wang, S., and Shangguan, Z. (2019). Combined biochar and nitrogen fertilization at appropriate rates could balance the leaching and availability of soil inorganic nitrogen. *Agric. Ecosyst. Environ.* 276, 21–30. doi: 10.1016/j.agee.2019.02.013

Li, Y. Y., Dong, S. K., Wen, L., Wang, X. X., and Wu, Y. (2014). Soil carbon and nitrogen pools and their relationship to plant and

soil dynamics of degraded and artificially restored grasslands of the Qinghai–Tibetan Plateau. *Geoderma* 213, 178–184. doi: 10.1007/s11368-018-2192-z

Li, Y., Pan, F., and Yao, H. (2018). Response of symbiotic and asymbiotic nitrogen-fixing microorganisms to nitrogen fertilizer application. *J. Soil Sediment* 19, 1948–1958. doi: 10.1016/j.geoderma.2013.08.022

Liu, S., Zamanian, K., Schleuss, P.-M., Zarebanadkouki, M., and Kuzyakov, Y. (2018). Degradation of Tibetan grasslands: consequences for carbon and nutrient cycles. *Agric. Ecosyst. Environ.* 252, 93–104. doi: 10.1016/j.agee.2017.10.011

Liu, X., Wang, Z., Zheng, K., Han, C., Li, L., Sheng, H., et al. (2020). Changes in soil carbon and nitrogen stocks following degradation of alpine grasslands on the Qinghai-Tibetan Plateau: a meta-analysis. *Land Degrad. Dev.* 32, 1262–1273. doi: 10.1002/ldr.3796

Lu, S. G., Sun, F. F., and Zong, Y. T. (2014). Effect of rice husk biochar and coal fly ash on some physical properties of expansive clayey soil (Vertisol). *Catena* 114, 37–44. doi: 10.1016/j.catena.2013.10.014

Luo, Y., Durenkamp, M., De Nobili, M., Lin, Q., and Brookes, P. C. (2011). Short term soil priming effects and the mineralisation of biochar following its incorporation to soils of different pH. *Soil Biol. Biochem.* 43, 2304–2314. doi: 10.1016/j.soilbio.2011.07.020

Ma, W., Li, J., Gao, Y., Xing, F., Sun, S., Zhang, T., et al. (2020). Responses of soil extracellular enzyme activities and microbial community properties to interaction between nitrogen addition and increased precipitation in a semi-arid grassland ecosystem. *Sci. Total Environ.* 703, 134691. doi: 10.1016/j.scitotenv.2019.134691

Muhammad, N., Hussain, M., Ullah, W., Khan, T. A., Ali, S., Akbar, A., et al. (2018). Biochar for sustainable soil and environment: a comprehensive review. *Arab. J. Geosci.* 11:731. doi: 10.1007/s12517-018-4074-5

Oliveira, F. R., Patel, A. K., Jaisi, D. P., Adhikari, S., Lu, H., and Khanal, S. K. (2017). Environmental application of biochar: current status and perspectives. *Bioresour. Technol.* 246, 110–122. doi: 10.1016/j.biortech.2017.08.122

Oram, N. J., van de Voorde, T. F. J., Ouwehand, G.-J., Bezemer, T. M., Mommer, L., Jeffery, S., et al. (2014). Soil amendment with biochar increases the competitive ability of legumes *via* increased potassium availability. *Agric. Ecosyst. Environ.* 191, 92–98. doi: 10.1016/j.agee.2014.03.031

Peng, F., Xue, X., You, Q., Huang, C., Dong, S., Liao, J., et al. (2018). Changes of soil properties regulate the soil organic carbon loss with grassland degradation on the Qinghai-Tibet Plateau. *Ecol. Indic.* 93, 572–580. doi: 10.1016/j.ecolind.2018.05.047

Piao, S., Tan, K., Nan, H., Ciais, P., Fang, J., Wang, T., et al. (2012). Impacts of climate and CO2 changes on the vegetation growth and carbon balance of Qinghai–Tibetan grasslands over the past five decades. *Global. Planet. Change* 98-99, 73–80. doi: 10.1016/j.gloplacha.2012.08.009

Pietikainen, J., Kiikkila, O., and Fritze, H. (2000). Charcoal as a habitat for microbes and its effect on the microbial community of the underlying humus. *Oikos* 89, 231–242. doi: 10.1034/j.1600-0706.2000.890203.x

Quilliam, R. S., DeLuca, T. H., and Jones, D. L. (2012). Biochar application reduces nodulation but increases nitrogenase activity in clover. *Plant Soil* 366, 83–92. doi: 10.1007/s11104-012-1411-4

Reed, E. Y., Chadwick, D. R., Hill, P. W., and Jones, D. L. (2017). Critical comparison of the impact of biochar and wood ash on soil organic matter cycling and grassland productivity. *Soil Biol. Biochem.* 110, 134–142. doi: 10.1016/j.soilbio.2017.03.012

Sadaf, J., Shah, G. A., Shahzad, K., Ali, N., Shahid, M., Ali, S., et al. (2017). Improvements in wheat productivity and soil quality can accomplish by co-application of biochars and chemical fertilizers. *Sci. Total Environ.* 607-608, 715–724. doi: 10.1016/j.scitotenv.2017.06.178

Smith, A. P., Marin-Spiotta, E., and Balser, T. (2015). Successional and seasonal variations in soil and litter microbial community structure and function during tropical postagricultural forest regeneration: a multiyear study. *Glob. Chang Biol.* 21, 3532–3547. doi: 10.1111/gcb.12947

Somleva, M., Tomaszewski, Z., and Conger, B. (2002). Agrobacterium-mediated genetic transformation of switchgrass. *Crop Sci.* 42, 2080–2087. doi: 10.2135/cropsci2002.2080

Sun, J., Hou, G., Liu, M., Fu, G., Zhan, T., Zhou, H., et al. (2019). Effects of climatic and grazing changes on desertification of alpine grasslands. *Northern Tibet. Ecol. Indic.* 107:105647. doi: 10.1016/j.ecolind.2019.105647

Sun, L., Li, J., Wang, Q., Zhang, Y., Xu, Z., Wang, R., et al. (2020). The effects of eight years of conservation tillage on the soil physicochemical properties and bacterial communities in a rain-fed agroecosystem of the loess plateau, China. *Land Degrad. Dev.* 31, 2475–2489. doi: 10.1002/ldr.3619

Sundh, I., Borjesson, G., and Tunlid, A. (2000). Methane oxidation and phospholipid fatty acid composition in a podzolic soil profile. *Soil Biol. Biochem.* 32, 1025–1028. doi: 10.1016/S0038-0717(99)00220-5

Wahi, R., Zuhaidi, N. F. Q. A., Yusof, Y., Jamel, J., Kanakaraju, D., and Ngaini, Z. (2017). Chemically treated microwave-derived biochar: an overview. *Biomass Bioenerg* 107, 411–421. doi: 10.1016/j.biombioe.2017.08.007

Wang, D., Huang, X., Qiao, N., Geng, Q., Liu, Y., Song, H., et al. (2020). Effects of mowing and fertilization on soil quality in a semiarid grassland of North China. *Land Degrad. Dev.* 32, 1656–1666. doi: 10.1002/ldr.3783

Wang, X. G., Lü, X. T., Zhang, H. Y., Dijkstra, F. A., Jiang, Y. G., Wang, X. B., et al. (2020). Changes in soil C:N:P stoichiometry along an aridity gradient in drylands of northern China. *Geoderma* 361:114087. doi: 10.1016/j.geoderma.2019.114087

White, D., Davis, W., Nickels, J., King, J., and Bobbie, R. (1979). Determination of the sedimentary microbial biomass by extractible lipid phosphate. *Oecologia* 40, 51–62. doi: 10.1007/BF00388810

Woolf, D., Amonette, J. E., Street-Perrott, F. A., Lehmann, J., and Joseph, S. (2010). Sustainable biochar to mitigate global climate change. *Nat. commun.* 1, 56. doi: 10.1038/ncomms1053

Wu, Y., Xu, N., Wang, H., Li, J., Zhong, H., Dong, H., et al. (2021). Variations in the diversity of the soil microbial community and structure under various categories of degraded wetland in Sanjiang Plain, northeastern China. *Land Degrad. Dev.* 32, 2143–2156. doi: 10.1002/ldr.3872

Yagüe, M. R., Domingo-Olivé, F., Bosch-Serra, ÀD., Poch, R. M., and Boixadera, J. (2016). Dairy cattle manure effects on soil quality: porosity, earthworms, aggregates and soil organic carbon fractions. *Land Degrad. Dev.* 27, 1753–1762. doi: 10.1002/ldr.2477

Yao, Z., Zhao, C., Yang, K., Liu, W., Li, Y., You, J., et al. (2016). Alpine grassland degradation in the Qilian Mountains, China — a case study in damaying grassland. *Catena* 137, 494–500. doi: 10.1016/j.catena.2015.09.021

Ye, Z., Liu, L., Tan, Z., Zhang, L., and Huang, Q. (2020). Effects of pyrolysis conditions on migration and distribution of biochar nitrogen in the soil-plant-atmosphere system. *Sci. Total Environ.* 723:138006. doi: 10.1016/j.scitotenv.2020.138006

Yu, L., Yu, M., Lu, X., Tang, C., Liu, X., Brookes, P. C., et al. (2018). Combined application of biochar and nitrogen fertilizer benefits nitrogen retention in the rhizosphere of soybean by increasing microbial biomass but not altering microbial community structure. *Sci. Total Environ.* 640-641, 1221–1230. doi: 10.1016/j.scitotenv.2018.06.018

Zhang, L., Jing, Y., Xiang, Y., Zhang, R., and Lu, H. (2018). Responses of soil microbial community structure changes and activities to biochar addition: a meta-analysis. *Sci. Total Environ.* 643, 926–935. doi: 10.1016/j.scitotenv.2018.06.231

Zhang, N., Zhong, B., Zhao, C., Wang, E., Wang, Y., Chen, D., et al. (2020). Change of soil physicochemical properties, bacterial community and aggregation during desertification of grasslands in the Tibetan Plateau. *Eur. J. Soil Sci.* 72, 274–288. doi: 10.1111/ejss.12939

Zhao, R., Feng, J., Liu, J., Fu, W., Li, X., and Li, B. (2019). Deciphering of microbial community and antibiotic resistance genes in activated sludge reactors under high selective pressure of different antibiotics. *Water Res.* 151, 388–402. doi: 10.1016/j.watres.2018.12.034

Zhao, Z. B., He, J. Z., Geisen, S., Han, L. L., Wang, J. T., Shen, J. P., et al. (2019). Protist communities are more sensitive to nitrogen fertilization than other microorganisms in diverse agricultural soils. *Microbiome* 7:33. doi: 10.1186/s40168-019-0647-0

Zhu, C., Tian, G., Luo, G., Kong, Y., Guo, J., Wang, M., et al. (2018). N-fertilizer-driven association between the arbuscular mycorrhizal fungal community and

diazotrophic community impacts wheat yield. *Agric. Ecosyst. Environ.* 254, 191–201. doi: 10.1016/j.agee.2017.11.029

Zhu, L. X., Xiao, Q., Shen, Y. F., and Li, S. Q. (2017). Microbial functional diversity responses to 2 years since biochar application in silt-loam soils on the Loess Plateau. *Ecotox. Environ. Saf.* 144, 578–584. doi: 10.1016/j.ecoenv.2017.06.075

Zong, N., and Fu, G. (2021). Variations in species and function diversity of soil fungal community along a desertification gradient in an alpine steppe. *Ecol. Indic.* 131:108197. doi: 10.1016/j.ecolind.2021.108197

Conflict of Interest: The authors declare that the research was conducted in the absence of any commercial or financial relationships that could be construed as a potential conflict of interest.

Publisher's Note: All claims expressed in this article are solely those of the authors and do not necessarily represent those of their affiliated organizations, or those of the publisher, the editors and the reviewers. Any product that may be evaluated in this article, or claim that may be made by its manufacturer, is not guaranteed or endorsed by the publisher.

Copyright © 2021 Li, Zhao, Shao, Huang, Shang, Li, He and Liu. This is an open-access article distributed under the terms of the Creative Commons Attribution License (CC BY). The use, distribution or reproduction in other forums is permitted, provided the original author(s) and the copyright owner(s) are credited and that the original publication in this journal is cited, in accordance with accepted academic practice. No use, distribution or reproduction is permitted which does not comply with these terms.

frontiers in Plant Science

ORIGINAL RESEARCH
published: 25 November 2021
doi: 10.3389/fpls.2021.773804

Litter-Induced Reduction in Ecosystem Multifunctionality Is Mediated by Plant Diversity and Cover in an Alpine Meadow

*Zhouwen Ma[1], Jing Wu[1], Lan Li[1], Qingping Zhou[2] and Fujiang Hou[1]**

[1]State Key Laboratory of Grassland Agro-Ecosystems, Key Laboratory of Grassland Livestock Industry Innovation, Ministry of Agriculture and Rural Affairs, College of Pastoral Agriculture Science and Technology, Lanzhou University, Lanzhou, China, [2]Institute of Qinghai-Tibet Plateau, Southwest Minzu University, Chengdu, China

OPEN ACCESS

Edited by:
Jian Sun,
Institute of Tibetan Plateau Research, Chinese Academy of Sciences (CAS), China

Reviewed by:
Fei Peng,
Northwest Institute of Eco-Environment and Resources, Chinese Academy of Sciences (CAS), China
Pedro Manuel Villa,
Universidade Federal de Viçosa, Brazil

***Correspondence:**
Fujiang Hou
cyhoufj@lzu.edu.cn

Specialty section:
This article was submitted to Functional Plant Ecology, a section of the journal Frontiers in Plant Science

Received: 10 September 2021
Accepted: 04 November 2021
Published: 25 November 2021

Citation:
Ma Z, Wu J, Li L, Zhou Q and Hou F (2021) Litter-Induced Reduction in Ecosystem Multifunctionality Is Mediated by Plant Diversity and Cover in an Alpine Meadow. Front. Plant Sci. 12:773804. doi: 10.3389/fpls.2021.773804

Litter has been shown to alter the structure and functions of grassland ecosystems, and a knowledge of the effects of litter is essential for understanding the dynamics of ecosystem multifunctionality. However, relatively little is known about the effects of plant litter on ecosystem multifunctionality in alpine meadows. A three-year field experiment was conducted to explore how litter manipulation affects ecosystem multifunctionality. The plant litter treatments that were applied consisted of a range of litter mass levels and three dominant plant species, in an alpine meadow on the Qinghai-Tibet Plateau. The results showed that litter mass manipulation had a negative effect on ecosystem multifunctionality and most individual ecosystem functions (species richness, plant cover, and above-ground biomass) but had a positive effect on plant functional group evenness. In particular, the study found that low or medium amounts of litter ($\leq$200 g m^{-2}) were beneficial in maintaining a high level of ecosystem multifunctionality. Furthermore, a structural equation model revealed that ecosystem multifunctionality was driven by indirect effects of litter mass manipulation on plant functional group evenness, plant cover, and species richness. These results suggest that litter-induced effects may be a major factor in determining grassland ecosystem multifunctionality, and they indicate the potential importance of grassland management strategies that regulate the dynamics of litter accumulation.

Keywords: alpine meadow, ecosystem multifunctionality, litter, plant diversity, plant functional composition

INTRODUCTION

Ecosystem multifunctionality is an important manifestation of the value of the ecosystems. It indicates the ability of an ecosystem to simultaneously maintain both above- and below-ground multiple ecological functions or services (Hector and Bagchi, 2007; Zavaleta et al., 2010) and critical for accurately evaluating multi-dimensional spatial pattern and implementing sustainable management (Song et al., 2020a). An understanding of how ecosystem multifunctionality is related to biotic attributes of ecological communities as the focus of attention (Manning et al., 2018). Biodiversity and optimal population allocation are key determinants of ecosystem multifunctionality in natural grassland (Liu et al., 2021) and are driven in particular by plant

community functional characteristics (Zhang et al., 2021) and soil microbial communities (Jing et al., 2015). Therefore, further research is needed to explore the key contributions of different biotic factors (e.g., plant litter) in driving ecosystem functioning, which in turn will enable improved grassland management strategies and maintain high levels of ecosystem multifunctionality.

Previous studies have shown that the ecological effects of ecosystem multifunctionality are mainly linked to biodiversity factors (Lefcheck et al., 2015). In particular, species richness and evenness are strongly and positively related to ecosystem multifunctionality (Li et al., 2017). In addition, plant cover has a critical role in sustaining ecosystem multifunctionality (Soliveres et al., 2014). Plant functional composition plays an important part in vegetation dynamics. Shifts in plant functional composition can determine the plant diversity, and this in turn affects ecosystem multifunctionality (Maestre et al., 2012a). Therefore, there is a need to examine the effect of such ecological functions on the ecosystem multifunctionality of alpine meadows with plant litter feedback.

In the diverse ecosystem of grassland, plant litter dynamics are considered to be one of the main factors that can influence ecosystem functions. Multiple plant litter feedbacks occur in terrestrial ecosystems, and they contribute to community functioning (Mariotte et al., 2016; Che et al., 2018). The complex interactions of litter with plant–soil communities are well documented (Eppinga et al., 2011; Veen et al., 2019). Plant litter may promote plant strategies that favor resource allocation for particular modules and thereby drive dynamics that optimize plant functional composition (Kaproth et al., 2013). Litter accumulation influences plant functional composition and diversity directly or indirectly by altering soil microclimate and species recruitment in terrestrial ecosystems (Fang et al., 2012; Yuan et al., 2016). The effects of litter quantity or allelopathic compounds that may favor vegetative growth are also widely recognized mechanisms that lead to altered above- and below-ground ecological functions (Elgersma et al., 2012; Mariotte et al., 2016). Therefore, plant litter may strongly influence ecosystem multifunctionality through physical or chemical drivers.

Meta-analytical studies have shown that a litter mass of less than 200 g m^{-2} has a more positive effect on the ecological functioning of plant community (e.g., plant establishment, species richness, and above-ground biomass; Xiong and Nilsson, 1999), and increased seedling survival has been reported where litter accumulation is low (<250 g m^{-2}) in grassland ecosystems (Loydi et al., 2013). These responses were dependent on the type of litter, with forbs litter having a stronger chemical effect on vegetation than grass litter (Xiong and Nilsson, 1999). It has been reported that the physical barrier created by litter can both reduce light availability and alter the temperature in the soil environment, thereby influencing the composition and productivity of plant communities (Weltzin et al., 2005). The resulting variation would amplify the effects of plant litter on ecosystem multifunctionality. However, to date, little evidence has been found for a relationship between plant litter and ecosystem multifunctionality in alpine meadows, and the role of litter feedback pathways as drivers of ecosystem multifunctionality is unclear.

The Qinghai-Tibet Plateau (QTP), often referred to as the "Roof of the World," is the largest and highest plateau (altitude > 4,000 m) in the world, with the most extensive biodiversity history (Myers et al., 2000). Alpine meadows represent the largest ecosystem (accounting for more than 60% of the eco-region of the QTP) and provide a number of important functions and services (Chen et al., 2013). Intensive livestock grazing is one of the main causes of grassland degradation, which in turn affects ecosystem functions (Dong et al., 2013). Although the vegetation on the QTP is generally dominated by several graminoid species, an increasing number of noxious forbs have been rapidly spreading in many areas of the plateau (Tang et al., 2015). Grazing exclusion and moderate grazing have been proposed and subsequently implemented in order to mitigate the degradation of ecosystem functions in alpine meadows, which would be likely to alter both the botanical composition and the productivity of this ecosystem. This would lead to heterogeneity of plant litter accumulation, including an increase in litter mass and changes in litter species composition (Hu et al., 2016; Zou et al., 2016), which would in turn have an impact on litter feedback mechanisms. Therefore, an understanding of such mechanisms is important for elucidating the ecosystem multifunctionality of ecological communities.

In this paper, we describe a three-year litter manipulation experiment designed to investigate three perennial grassland species, consisting of two graminoids (*Elymus nutans* and *Kobresia setchwanensis*) and one noxious forb (*Ligularia virgaurea*), and five litter mass levels, in an alpine meadow grassland on the QTP. These three species are all widely used indicator species in alpine meadows and represent different plant functional groups. The study attempted to explore the regulatory effects of litter manipulation on ecosystem multifunctionality, as the findings would have important implications for ecological conservation and sustainable management of grassland. Previous studies have shown that impacts of litter manipulation can decrease the species richness and species evenness (Lamb, 2008), and promote the transformation in plant functional composition (Amatangelo et al., 2008). These factors are important determinants of ecosystem multifunctionality (Maestre et al., 2012a). Therefore, we hypothesized that litter mass, litter species, and their interaction can significantly alter plant functional composition, species richness, plant functional group evenness, and plant cover, and further influence ecosystem multifunctionality. Based on previous studies on the effects of litter on plant community ecosystem functions, we predicted the net effect of litter addition would result a reduction of ecosystem multifunctionality and that the effect of *L. virgaurea* litter treatment would be stronger. Finally, we constructed the piecewise structural equation models to determine the relative importance and pathways of various drivers regulating the variations in ecosystem multifunctionality. The aims of the study were as follows: (1) to investigate the effects of litter manipulation on ecosystem multifunctionality; (2) to identify the mechanism that drives those effects; and

(3) to determine the response of the key mechanisms of ecosystem multifunctionality to litter manipulation.

MATERIALS AND METHODS

Study Site

The experiment site was conducted at an alpine meadow, located in Hongyuan county, Sichuan province, China (31°47' N, 102°33' E, 3,500 m a.s.l.) at the eastern Tibetan Plateau. This region climate is continental monsoon with a mean annual temperature of 1.5°C and annual precipitation 747 mm (1961–2013) with approximately 80% concentrated in growing season (May–September). The vegetation in alpine meadow dominated by graminoids, such as *E. nutans*, *Carex thibetica*, and *K. setchwanensis*, and perennial forbs, such as *Anemone rivularis*, *Anemone trullifolia*, *Saussurea hieracioides*, *L. virgaurea*, and legumes, is rare. The soil type in this study site is Mat Cry-gelic Cambisol.

Experimental Design

To determine the effects of the litter of dominant plant species on ecosystem multifunctionality, we conducted a field experiment using a randomized block design in an enclosed area in 2017. Treatments consisted of a range of litter mass levels (0, 100, 200, 400, and 600 g m^{-2}) for three individual plant species (*E. nutans*, *K. setchwanensis*, and *L. virgaurea*). Each treatment was applied to four 2×2 m plots, which were divided randomly into blocks. The individual plots were separated by a buffer zone of >1 m. Plant litter was collected from the vicinity of the study site and then air-dried. All standing above-ground dead plant material was removed from the experimental plots in late April each year, and then, the collected litter from the three plant species (clipped into fragments approximately 1 cm in length) was distributed evenly by hand. Subsamples of the litter from each plant species had previously been oven-dried at 65°C to a constant mass to allow calculation of the moisture correction factor and were then weighed so that the initial litter mass could be estimated.

Plant Community Surveys

Plant above-ground biomass was estimated by clipping plant material above the soil surface in randomly selected 0.5×0.5 m quadrats within in each plot. Samples were collected from mid-June to August each year. All plant samples were classified according to their functional group (grasses, sedges, forbs, or legumes). Above-ground plant samples were oven-dried at 65°C to a constant weight and were then weighed to calculate the plant above-ground biomass of the different functional groups and the plant community. At the time when above-ground biomass samples were collected, plant height and canopy cover were measured in a permanent quadrat (0.5×0.5 m) that had been established in each plot. Plant cover was estimated as the percentage of the surface area covered by all plant species present in the quadrat. Plant species richness and below-ground biomass were measured in each plot in mid-August (the peak of the growing season, with maximum species richness). Species richness was recorded as the total number of species detected in the quadrats. At the same time, soil samples were collected in each plot within the 0–10 cm soil layer, the moisture content, total carbon, and total nitrogen were measured.

Assessment of Plant Functional Group Evenness and Composition, and Community Biomass Stability

The plant functional group evenness index was calculated as: $E = \left(-\sum_{i=1}^{S} P_i \times \log P_i \right) / \ln S$, where P_i is the relative above-ground biomass of plant functional group i in the community and S the number of plant functional groups (Andruschkewitsch et al., 2014). The proportion of above-ground biomass for each of the functional groups was used to calculate the changes in plant functional composition that had resulted from the litter treatments. These changes were expressed as a percentage, namely, $(B_i/B_s) \times 100$, where B_i is the above-ground biomass of functional group i and B_s is the community above-ground biomass of all species present in the quadrat. Legumes accounted for only 3.2% of the plant community biomass and were therefore grouped with forbs. As in previous studies, the plant community biomass stability was quantified as the ratio of the mean community above-ground biomass to its temporal standard deviation in each plot (Hautier et al., 2014).

Assessment of Ecosystem Multifunctionality

Ten key ecosystem functions were selected, including both plant community functions (above- and below-ground biomass, species richness, functional group evenness, cover, and community biomass stability) and soil nutrient resources (moisture content, total carbon, total nitrogen, and carbon/nitrogen ratio), which together reflect ecosystem multifunctionality. The ecosystem multifunctionality was calculated using an averaging approach as described by Maestre et al. (2012b). We standardized each function by Z-score transformation observed in each plot and took the mean value across all functions in order to evaluate ecosystem multifunctionality at the plot level. Then, the average ecosystem multifunctionality values inverted around the 0 mean were converted to positive values by adding a constant (+1) to all values for further analysis. By doing this, the general difference among plant litter treatments in overall ecosystem functioning could be more easily assessed.

Statistical Analysis

Key ecosystem functions and plant functional composition were analyzed with a repeated-measurements model using species, mass, date and interaction as fixed effects, and unit nested within blocks as random effects. The effects of litter manipulation on ecosystem multifunctionality were assessed with a linear mixed-effects model using litter species and litter mass as fixed effects, and plot as random effects. These analyses were performed

using the "predictmeans" and "lme 4" packages in R 4.1.0 (R Core Team, 2021). In addition, we used piecewise structural equation modeling (SEM) to investigate the direct and indirect effects of plant community functional characteristics and litter manipulation on ecosystem multifunctionality. The model assumed that litter mass, litter species, and their interaction alter species richness, plant functional group evenness, and plant cover *via* changes in plant functional composition (extracting the first component scores from the principal component analysis conducted for proportion of above-ground biomass of three functional groups) and that they ultimately influence ecosystem multifunctionality. This was based on an *a priori* conceptual model of hypothetical relationships that include all of the different cascading pathways and all possible pathways (**Supplementary Figure 1**). We simplified the initial model by sequentially eliminating the non-significant pathways until the final optimal model was obtained. And the direct, indirect, and total effects of predictor variables on response variable in the conceptual model were calculated, respectively (Ali et al., 2019). Data were standardized by z transformation and used in the analysis, incorporating random effects in the plot. The d-separation tests, Fisher's *C* statistic, and Akaike information criteria (AIC) were used to assess the goodness-of-fit of the model (Shipley, 2013). SEM analyses were performed using the "piecewiseSEM" package (Lefcheck, 2016) in R version 4.1.0 (R Core Team, 2021).

RESULTS

Ecosystem Multifunctionality

Ecosystem multifunctionality decreased significantly with increasing litter mass (bivariate regressions: $R^2 = 0.29$, $p < 0.001$). Litter species or interaction effect (species × mass) had no significant effect on ecosystem multifunctionality ($p > 0.05$; **Figures 1A,B**). The ecosystem multifunctionality for 400 and 600 g m^{-2} litter treatments was significantly lower than that for the control and 100 g m^{-2} treatments.

Plant Above-Ground Biomass and Cover

Over the study period, above-ground biomass of community and plant cover decreased linearly with increasing litter mass (**Figures 2A,C**). Litter species treatment had a significant effect on above-ground biomass of community (**Figure 2B**), whereas plant cover showed a non-significant response to litter species treatment (**Figure 2D**). The above-ground biomass of community and plant cover was significantly lower for 400 and 600 g m^{-2} treatments compared with the other treatments ($p < 0.001$). The plant community above-ground biomass was significantly higher for *E. nutans* and *K. setchwanensis* litter treatments than for the *L. virgaurea* litter treatment ($p < 0.001$).

Plant Diversity

Litter manipulation had marked effects on both species richness and plant functional group evenness, but the interaction effect (species × mass) was not statistically significant (**Figures 2E–H**). Species richness was significantly lower for the 600 g m^{-2} litter treatment compared with the control ($p < 0.05$) and was significantly higher for the *K. setchwanensis* litter treatment than for the *L. virgaurea* litter treatment ($p < 0.05$). There was greater plant functional group evenness for the 400 and 600 g m^{-2} litter treatments and for the *L. virgaurea* litter treatment ($p < 0.001$).

Plant Functional Composition

Both litter mass and litter species had a significant impact on plant functional composition. The effect of the litter mass × species interaction on plant functional composition was not statistically significant (**Figures 3A,B**). For the 200 g m^{-2} litter treatment, the proportion of forbs biomass was highest and the proportion of grasses biomass was lowest. The 400 g m^{-2} and 600 g m^{-2} litter treatments significantly decreased the proportion of forbs biomass compared with the 100 and 200 g m^{-2} treatments ($p < 0.001$). In contrast, the 400 g m^{-2} and 600 g m^{-2} treatments significantly increased the proportion of grasses biomass compared with the 200 g m^{-2} treatment ($p < 0.01$) and the proportion of sedges biomass compared with the 100 g m^{-2} treatment ($p < 0.01$). The proportion of forbs biomass was significantly lower for the *L. virgaurea* treatment than for the *K. setchwanensis* and *E. nutans* treatments ($p < 0.001$), but the opposite result was obtained for the proportion of sedges biomass ($p < 0.001$). Litter species had no significant effect on the proportion of grasses biomass ($p > 0.05$).

Drivers of the Litter Manipulation Effect on Ecosystem Multifunctionality

In contrast to our hypothesis (**Supplementary Figure 1**), the final SEM predicted that only the litter mass has a significant impact on ecosystem multifunctionality (**Figure 4; Supplementary Table 1**). The SEM indicated that the litter mass response explained 64.4% of the variance in ecosystem multifunctionality. The positive and direct effects on ecosystem multifunctionality were mainly due to plant cover (path coefficient = 0.79; $p < 0.001$), and to a lesser extent to plant functional group evenness (path coefficient = 0.43; $p < 0.001$) and species richness (path coefficient = 0.29; $p < 0.05$; **Figure 4**). The SEM also indicated that the best predictor of ecosystem multifunctionality was plant cover and that it was directly influenced by litter mass (path coefficient = −0.81) and indirectly affected by plant functional composition (path coefficient = −0.17). Plant functional group evenness was indirectly affected by litter mass through plant functional composition (path coefficient = 0.93), and species richness was directly affected by litter mass (path coefficient = −0.53).

DISCUSSION

Factors that contribute to ecosystem multifunctionality across biotic communities, such as ecosystem biodiversity and above-ground community composition, have been well studied in many terrestrial ecosystems (Jing et al., 2015; Xu et al., 2021).

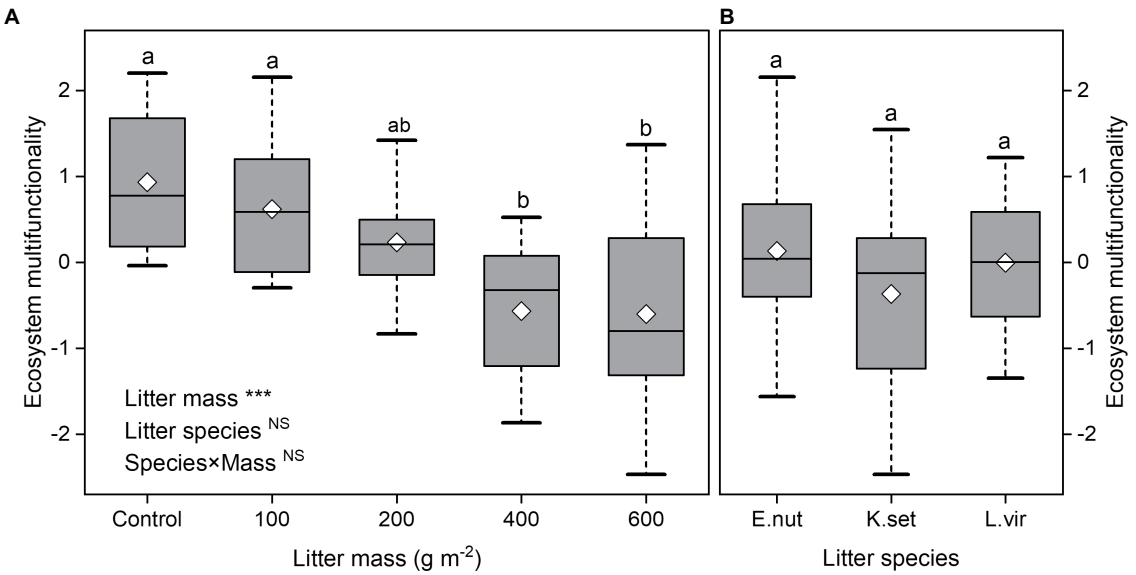

FIGURE 1 | Effects of litter mass **(A)** and species **(B)** on ecosystem multifunctionality. Lowercase letters indicate significant differences at $p < 0.05$ (***$p < 0.001$; NS, not significant). Box plots show midline, mean; box edges, first quartile and third quartile; and whiskers, minimum and maximum. *E. nut*, *E. nutans*; *K. set*, *K. setchwanensis*; *L. vir*, *L. virgaurea*.

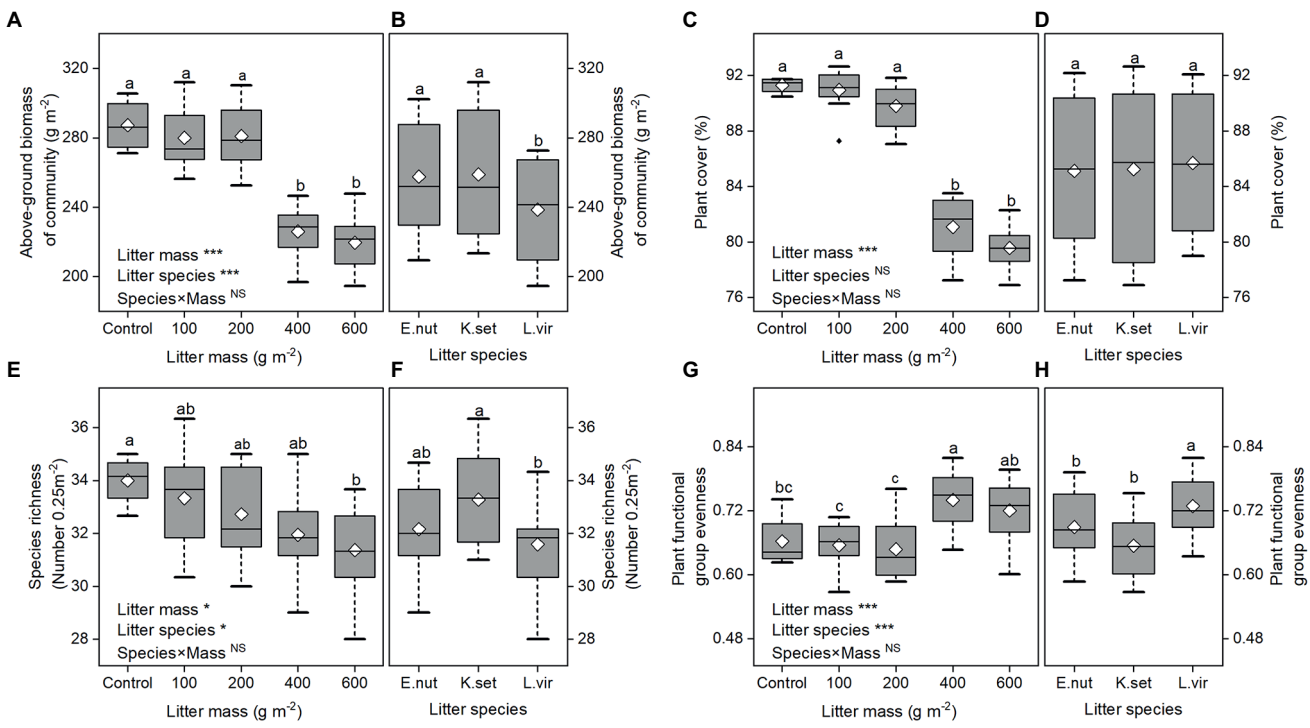

FIGURE 2 | Effects of litter mass and species on plant communities. Above-ground biomass of community **(A,B)**, plant cover **(C,D)**, species richness **(E,F)**, and plant functional group evenness **(G,H)**. Lowercase letters indicate significant differences at $p < 0.05$ (*$p < 0.05$ and ***$p < 0.001$; NS, not significant). Box plots show midline, mean; box edges, first quartile and third quartile; and whiskers, minimum and maximum. *E. nut*, *E. nutans*; *K. set*, *K. setchwanensis*; *L. vir*, *L. virgaurea*.

However, little is known about how plant diversity and most individual ecosystem functions under litter feedbacks directly or indirectly influence ecosystem multifunctionality, particularly when the litter mass of different plant litter species is quantitatively manipulated. The present study has shown that ecosystem multifunctionality decreases in response to increasing litter

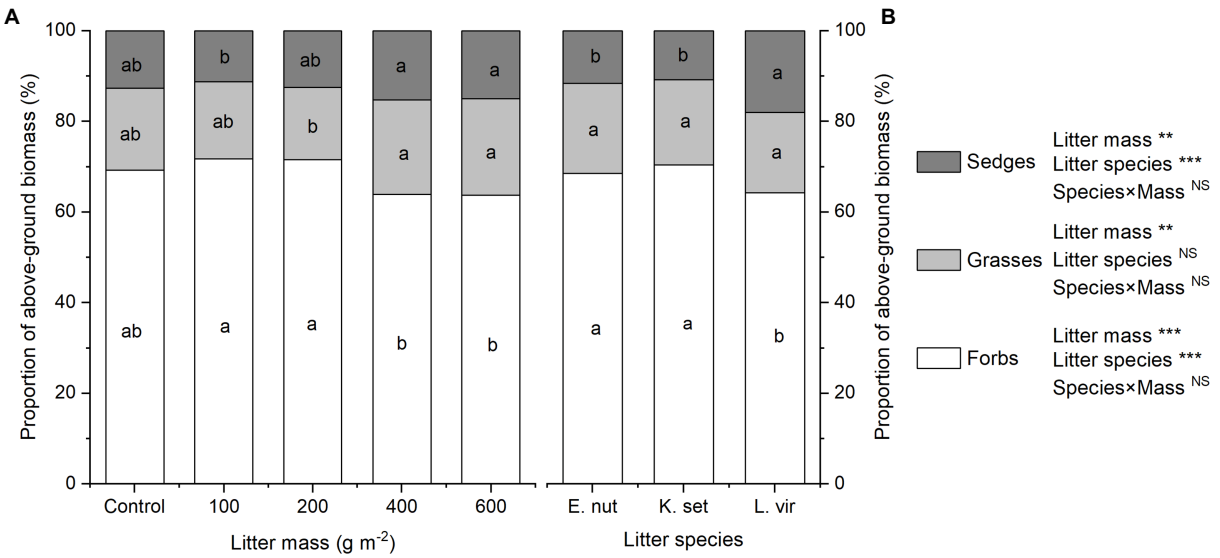

FIGURE 3 | Effects of litter mass **(A)** and species **(B)** on plant functional composition. Summarized into proportion of above-ground biomass of forbs, grasses, and sedges. Lowercase letters indicate significant differences at $p < 0.05$ (**$p < 0.01$ and ***$p < 0.001$; NS, not significant). *E. nut*, *E. nutans*; *K. set*, *K. setchwanensis*; *L. vir*, *L. virgaurea*.

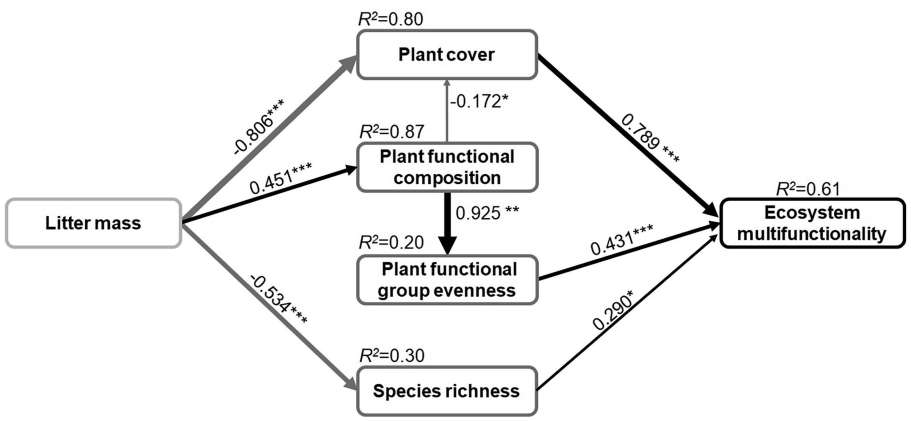

FIGURE 4 | The path analysis result of piecewise structural equation model showing the direct and indirect causal relationships of litter manipulation and plant community properties effects on ecosystem multifunctionality. The black and gray solid arrows indicate that the positive and negative effect is significant, respectively (*$p < 0.05$, **$p < 0.01$, and ***$p < 0.001$). Arrow width and the associated number indicate the strength of the effect and the standard path coefficients, respectively. R^2 values represent the proportion of variance explained for each dependent variable. Fisher's $C = 14.82$, value of $p = 0.39$, and AIC = 60.82.

mass (**Figure 1A**). Moreover, plant cover and plant functional group evenness played a more important role than species richness in mediating the response of ecosystem multifunctionality to litter manipulation in an alpine meadow (**Figure 4**). However, the results also indicated potentially positive effects of low and medium amounts of litter accumulation ($\leq$200 g m^{-2}) in maintaining ecosystem multifunctionality. Litter mass rather than litter species determined ecosystem multifunctionality under litter manipulation (**Figure 1**). These findings show that, in alpine grasslands, plant litter has a significant effect on most above-ground individual functions (**Figure 2**; Ma et al., 2021) and may be the primary driver of ecosystem multifunctionality.

Plant Cover in the Response of Ecosystem Multifunctionality to Litter Manipulation

The plant cover was found in the present study to be the strongest indicator of litter effects on the ecosystem multifunctionality in an alpine meadow. Plant cover was particularly sensitive to litter manipulation and likely decreased through both the overspread of undecomposed litter and changes in functional group composition, thereby decreasing the ecosystem multifunctionality (**Figure 4**). Consistent with the findings of previous studies, plant cover positively influences the ecosystem multifunctionality (Soliveres et al., 2014). Likewise, Maestre and Escudero (2009) emphasized that plant cover was expected to affect ecosystem multifunctionality, as it largely

modulated the effects of the soil variable. The physical and chemical effects of the higher litter mass inhibiting plant growth (Weltzin et al., 2005) or drastically increased the cover of functional groups (Wang et al., 2010), and thus indirectly reducing the vegetation cover. Limitation of light availability might also be the main reason for the reduction of plant cover under the litter manipulation (Deutsch et al., 2010).

Plant Diversity in the Response of Ecosystem Multifunctionality to Litter Manipulation

Our study revealed that the litter mass manipulation significantly impacted the species richness and plant functional group evenness, thus impacting the ecosystem multifunctionality (**Figure 4**). The finding that has also been observed in several previous studies, where the species richness modulated by community attributes (e.g., spatial pattern; Maestre et al., 2012a) or climate (Jing et al., 2015) altered ecosystem multifunctionality, and the same direction as evenness effects (Lembrechts et al., 2018). In contrast, Soliveres et al. (2014) have reported no effect of species richness or evenness on ecosystem multifunctionality. Specifically, the SEM identified that the effect of plant functional group evenness on ecosystem multifunctionality was indirect, by altering the plant functional composition under litter mass treatment (**Figure 4**). The possible explanation is that the reduction in dominant functional groups creates conditions that are more favorable for the establishment of seedlings of rare functional groups (Liu et al., 2018), and thus increases plant functional group evenness. Consistent with this, Letts et al. (2015) reported that the increased functional evenness that results from the presence of larger amounts of litter is most probably attributable to an increase in nutrient availability. In the present study, higher litter mass also had a negative effect on species richness (**Figure 2E**), where increases in litter quantity have directly influenced species recruitment as a result of the effects of light limitation (Mariotte et al., 2016) or poor soil aeration (Cheng et al., 2011).

Plant Functional Composition in the Response of Ecosystem Multifunctionality to Litter Manipulation

The SEM also identified the plant functional composition was key indirect driver of ecosystem multifunctionality, which can be attributed to the plant diversity and plant cover that are determined by the transformation of plant functional groups (**Figure 4**). In particular, the substantial reductions in the proportion of above-ground biomass of forbs may be the main reason impacting ecosystem multifunctionality, and to a lesser extent by an increase in that of grasses and sedges. This can be attributed to the approximately more than 60% of above-ground biomass of forbs in the experimental community (**Figure 3A**). Other studies have also previously observed that the plant functional composition contribute more to the ecosystem multifunctionality, probably because the more proportion of grass and sedge is more likely to improve soil nutrient (Xu et al., 2021) and below-ground biomass (Song et al., 2020b).

In our study, the dynamics of plant functional composition may be related to its ability to withstand various environmental perturbations. Plant litter may promote plant strategies that favor resource allocation for particular modules and may thereby drive dynamics that optimize vegetation composition (Kaproth et al., 2013). For example, Liu et al. (2018) found that shallow-rooted forbs were more sensitive to experimental manipulations than were deep-rooted grasses. In addition, the amount of litter can significantly affect photosynthetically active radiation (Zhang et al., 2019) and allelochemical content (Loydi et al., 2015), and thus increase the dominance of grass and sedge species. The observed reductions in the proportion of above-ground biomass of grasses were probably due to the vertical structure of grasses and their rhizome propagation characteristics in the plant community (Mao et al., 2015). Our findings are consistent with those of other studies that have been conducted in annual grassland (Amatangelo et al., 2008).

In particular, we still found that litter species of *L. virgaurea* had a stronger effect on above-ground biomass, plant diversity, and plant functional composition (**Figures 2B,F,H, 3B**). It is probably because litter species of *L. virgaurea* decomposes more quickly, affecting nutrient dynamics and driving effects that are attributable to phytotoxic compounds (Liang, 2013; Saito et al., 2015).

Implications for Ecosystem Management and Sustainability Based on Multifunctionality

Overall, our results have important implications for maintaining ecosystem multifunctionality in alpine meadows located on the QTP. Although grazing exclusion has been proposed and implemented for the mitigation of degraded grasslands, not all of the degradation of ecosystem functions has been mitigated (Zou et al., 2016; Sun et al., 2020). Our findings support the hypothesis that high levels of litter accumulation have a negative impact on ecosystem multifunctionality. In addition, the present study found that low and medium levels of litter accumulation ($\leq$200 g m^{-2}) were potentially beneficial for maintaining optimal ecosystem multifunctionality. Therefore, moderate grazing disturbance (e.g., low grazing intensity) is needed in order to achieve optimal litter accumulation levels and maximize the sustainability of ecosystem multifunctionality (Ren et al., 2018; Zhang et al., 2021). The results of our study increase our understanding of how litter manipulation can regulate ecosystem multifunctionality and will help to raise awareness of how ecosystem functions respond to such litter accumulation dynamics. These research findings therefore have important implications for achieving sustainable ecosystem multifunctionality in relation to litter accumulation dynamics and heterogeneity in the alpine meadows of the QTP region. They also suggest that ecosystem multifunctionality will be reduced under unsuitable grassland management regimes. Therefore, it is vitally important to optimize grassland management so as to minimize the negative impact of litter on the sustainable development of ecosystem multifunctionality.

CONCLUSION

This study has demonstrated that litter mass manipulation involving the application of high levels of litter significantly reduces ecosystem multifunctionality in an alpine meadow on the QTP. Ecosystem multifunctionality reaches a critical threshold after treatment with a litter mass of 200 g m^{-2}. Our findings highlight the potential role of plant diversity (species richness and plant functional group evenness) and plant cover in maintaining ecosystem multifunctionality under litter feedbacks, and the likely dependence on the dynamics of plant functional composition. Litter-induced feedback has fundamental implications for optimizing ecosystem multifunctionality while simultaneously maintaining biodiversity and ecological functions. In addition, it is suggested that appropriate grassland management measures need to regulate the accumulation of plant litter, which has a better driving and maintenance effect on the regulation of ecosystem multifunctionality in alpine meadows.

DATA AVAILABILITY STATEMENT

The original contributions presented in the study are included in the article/**Supplementary Material**, further inquiries can be directed to the corresponding author.

AUTHOR CONTRIBUTIONS

FH conceived the ideas and designed the experiment. ZM and JW conducted the field experiment and collected the data. FH, ZM, and LL performed all the statistical analyses and modeling. FH and ZM led the writing of the manuscript. All authors revised the manuscript and contributed critically to the drafts and gave final approval for publication.

FUNDING

This research was supported by the Second Tibetan Plateau Scientific Expedition: Grassland Ecosystem and Ecological Animal Husbandry (2019QZKK0302), the National Natural Science Foundation of China (31672472), the Program for Innovative Research Team of Ministry of Education (IRT17R50), the Technological Support for Grassland Ecological Management and Restoration and the Pastoral Livestock Industry in Gansu Province, China (GARS-08), and "Lanzhou City's Scientific Research Funding Subsidy to Lanzhou University".

ACKNOWLEDGMENTS

We thank the staff of the Qinghai-Tibet Plateau Research Base of Southwest Minzu University.

SUPPLEMENTARY MATERIAL

The Supplementary Material for this article can be found online at: https://www.frontiersin.org/articles/10.3389/fpls.2021.773804/full#supplementary-material

REFERENCES

Ali, A., Lin, S. L., He, J. K., Kong, F. M., Yu, J. H., and Jiang, H. S. (2019). Elucidating space, climate, edaphic and biodiversity effects on aboveground biomass in tropical forests. *Land Degrad. Dev.* 30, 918–927. doi: 10.1002/ldr.3278

Amatangelo, K. L., Dukes, J. S., and Field, C. B. (2008). Responses of a California annual grassland to litter manipulation. *J. Veg. Sci.* 19, 605–612. doi: 10.3170/2008-8-18415

Andruschkewitsch, M., Wachendorf, C., Sradnick, A., Hensgen, F., Joergensen, R. G., and Wachendorf, M. (2014). Soil substrate utilization pattern and relation of functional evenness of plant groups and soil microbial community in five low mountain NATURA 2000. *Plant Soil* 383, 275–289. doi: 10.1007/s11104-014-2167-9

Che, R. X., Qin, J. L., Tahmasbian, I., Wang, F., Zhou, S. T., Xu, Z. H., et al. (2018). Litter amendment rather than phosphorus can dramatically change inorganic nitrogen pools in a degraded grassland soil by affecting nitrogen-cycling microbes. *Soil Biol. Biochem.* 120, 145–152. doi: 10.1016/j.soilbio.2018.02.006

Chen, H., Zhu, Q., Peng, C. H., Wu, N., Wang, Y. F., Fang, X. Q., et al. (2013). The impacts of climate change and human activities on biogeochemical cycles on the Qinghai-Tibetan Plateau. *Glob. Chang. Biol.* 19, 2940–2955. doi: 10.1111/gcb.12277

Cheng, J., Cheng, J. M., Hu, T. M., Shao, H. B., and Zhang, J. M. (2011). Dynamic changes of *Stipa bungeana* steppe species diversity as better indicators for soil quality and sustainable utilization mode in Yunwu mountain nature reserve, Ningxia, China. *Clean Soil Air Water* 40, 127–133. doi: 10.1002/clen.201000438

Deutsch, E. S., Bork, E. W., and Willms, W. D. (2010). Soil moisture and plant growth responses to litter and defoliation impacts in parkland grasslands. *Agric. Ecosyst. Environ.* 135, 1–9. doi: 10.1016/j.agee.2009.08.002

Dong, Q. M., Zhao, X. Q., Wu, G. L., Shi, J. J., and Ren, G. H. (2013). A review of formation mechanism and restoration measures of "black-soil-type" degraded grassland in the Qinghai-Tibetan Plateau. *Environ. Earth Sci.* 70, 2359–2370. doi: 10.1007/s12665-013-2338-7

Elgersma, K. J., Yu, S., Vor, T., and Ehrenfeld, J. G. (2012). Microbial-mediated feedbacks of leaf litter on invasive plant growth and interspecific competition. *Plant Soil* 356, 341–355. doi: 10.1007/s11104-011-1117-z

Eppinga, M. B., Kaproth, M. A., Collins, A. R., and Molofsky, J. (2011). Litter feedbacks, evolutionary change and exotic plant invasion. *J. Ecol.* 99, 503–514. doi: 10.1111/j.1365-2745.2010.01781.x

Fang, Y., Xun, F., Bai, W. M., Zhang, W. H., and Li, L. H. (2012). Long-term nitrogen addition leads to loss of species richness due to litter accumulation and soil acidification in a temperate steppe. *PLoS One* 7:e47369. doi: 10.1371/journal.pone.0047369

Hautier, Y., Seabloom, E. W., Borer, E. T., Adler, P. B., Harpole, W. S., Hillebrand, H., et al. (2014). Eutrophication weakens stabilizing effects of diversity in natural grasslands. *Nature* 508, 521–525. doi: 10.1038/nature13014

Hector, A., and Bagchi, R. (2007). Biodiversity and ecosystem multifunctionality. *Nature* 448, 188–190. doi: 10.1038/nature05947

Hu, J., He, G. Y., Yin, X., Li, L. P., Chen, H., Yan, J., et al. (2016). Effect of grazing on soil nematode in alpine meadow on east edge of the Tibetan Plateau and its mechanism. *Acta Pedol. Sin.* 53, 1506–1516. doi: 10.11766/trxb201512190508

Jing, X., Sanders, N. J., Shi, Y., Chu, H. Y., Classen, A. T., Zhao, K., et al. (2015). The links between ecosystem multifunctionality and above- and belowground biodiversity are mediated by climate. *Nat. Commun.* 6:8159. doi: 10.1038/ncomms9159

Kaproth, M. A., Eppinga, M. B., and Molofsky, J. (2013). Leaf litter variation influences invasion dynamics in the invasive wetland grass *Phalaris arundinacea*. *Biol. Invasions* 15, 1819–1832. doi: 10.1007/s10530-013-0411-5

Lamb, E. G. (2008). Direct and indirect control of grassland community structure by litter, resources, and biomass. *Ecology* 89, 216–225. doi: 10.1890/07-0393.1

Lefcheck, J. S. (2016). PIECEWISESEM: piecewise structural equation modelling in R for ecology, evolution, and systematics. *Methods Ecol. Evol.* 7:573579. doi: 10.1111/2041-210X.12512

Lefcheck, J. S., Byrnes, J. E. K., Isbell, F., Gamfeldt, L., Griffin, J. N., Eisenhauer, N., et al. (2015). Biodiversity enhances ecosystem multifunctionality across trophic levels and habitats. *Nat. Commun.* 6:6936. doi: 10.1038/ncomms7936

Lembrechts, J. J., De Boeck, H. J., Liao, J. B., Milbau, A., and Nijs, I. (2018). Effects of species evenness can be derived from species richness - ecosystem functioning relationships. *Oikos* 127, 337–344. doi: 10.1111/oik.04786

Letts, B., Lamb, E. G., Mischkolz, J. M., and Romo, J. T. (2015). Litter accumulation drives grassland plant community composition and functional diversity via leaf traits. *Plant Ecol.* 216, 357–370. doi: 10.1007/s11258-014-0436-6

Li, J. P., Zheng, Z. R., Xie, H. T., Zhao, N. X., and Gao, Y. B. (2017). Heterogeneous microcommunities and ecosystem multifunctionality in seminatural grasslands under three management modes. *Ecol. Evol.* 7, 14–25. doi: 10.1002/ece3.2604

Liang, D. F. (2013). The additive and non-additive effects of the mixed litter decomposition and N, P release in an alpine meadow. master's thesis. Lanzhou: Lanzhou University.

Liu, H. Y., Mi, Z. R., Lin, L., Wang, Y. H., Zhang, Z. H., Zhang, F. W., et al. (2018). Shifting plant species composition in response to climate change stabilizes grassland primary production. *Proc. Natl. Acad. Sci. U. S. A.* 115, 4051–4056. doi: 10.1073/pnas.1700299114

Liu, X. C., Shi, X. M., and Zhang, S. T. (2021). Soil abiotic properties and plant functional diversity co-regulate the impacts of nitrogen addition on ecosystem multifunctionality in an alpine meadow. *Sci. Total Environ.* 780:146476. doi: 10.1016/j.scitotenv.2021.146476

Loydi, A., Donath, T. W., Eckstein, R. L., and Otte, A. (2015). Non-native species litter reduces germination and growth of resident forbs and grasses: allelopathic, osmotic or mechanical effects? *Biol. Invasions* 17, 581–595. doi: 10.1007/s10530-014-0750-x

Loydi, A., Eckstein, R. L., Otte, A., Donath, T. W., and Gómez-Aparicio, L. (2013). Effects of litter on seedling establishment in natural and semi-natural grasslands: a meta-analysis. *J. Ecol.* 101, 454–464. doi: 10.1111/1365-2745.12033

Ma, Z. W., Zeng, Y. F., Wu, J., Zhou, Q. P., and Hou, F. J. (2021). Plant litter influences the temporal stability of plant community biomass in an alpine meadow by altering the stability and asynchrony of plant functional groups. *Funct. Ecol.* doi: 10.1111/1365-2435.13935 [Epub ahead of print]

Maestre, F. T., Castillo-Monroy, A. P., Bowker, M. A., and Ochoa-Hueso, R. (2012a). Species richness effects on ecosystem multifunctionality depend on evenness, composition and spatial pattern. *J. Ecol.* 100, 317–330. doi: 10.1111/j.1365-2745.2011.01918.x

Maestre, F. T., and Escudero, A. (2009). Is the patch size distribution of vegetation a suitable indicator of desertification processes? *Ecology* 90, 1729–1735. doi: 10.1890/08-2096.1

Maestre, F. T., Quero, J. L., Gotelli, N. J., Adrián, E., Victori, O., Manuel, D. B., et al. (2012b). Plant species richness and ecosystem multifunctionality in global drylands. *Science* 335, 214–218. doi: 10.1126/science.1215442

Manning, P., van der Plas, F., Soliveres, S., Allan, E., Maestre, F. T., Mace, G., et al. (2018). Redefining ecosystem multifunctionality. *Nat. Ecol. Evol.* 2, 427–436. doi: 10.1038/s41559-017-0461-7

Mao, S. J., Wu, Q. H., Li, H. Q., Zhang, F. W., and Li, Y. N. (2015). Effects of grazing intensity on species diversity and biomass in alpine-cold forb meadow on the Tibet Plateau. *J. Glaciol. Geocryol.* 37, 1372–1380. doi: 10.7522/j.isnn.1000-0240.2015.0151

Mariotte, P., Spotswood, E. N., Farrer, E. C., Suding, K. N., and Fraser, L. (2016). Positive litter feedbacks of an introduced species reduce native diversity and promote invasion in Californian grasslands. *Appl. Veg. Sci.* 20, 28–39. doi: 10.1111/avsc.12291

Myers, N., Mittermeier, R. A., Mittermeier, C. G., da Fonseca, G. A. B., and Kent, J. (2000). Biodiversity hotspots for conservation priorities. *Nature* 403, 853–858. doi: 10.1038/35002501

R Core Team (2021). *R: A Language and Environment for Statistical Computing.* R Foundation for Statistical Computing. Available at: https://www.R-project.org/

Ren, H. Y., Eviner, V. T., Gui, W. Y., Wilson, G. W. T., Cobb, A. B., Yang, G. E., et al. (2018). Livestock grazing regulates ecosystem multifunctionality in semiarid grassland. *Funct. Ecol.* 32, 2790–2800. doi: 10.1111/1365-2435.13215

Saito, Y., Iga, S., Nakashima, K., Okamoto, Y., Gong, X., Kuroda, C., et al. (2015). Terpenoids from *Ligularia virgaurea* collected in China: the first example of two bakkane derivatives with an anhydride-type ring C and nineteen new chemical constituents. *Tetrahedron* 71, 8428–8435. doi: 10.1016/j.tet.2015.09.011

Shipley, B. (2013). The AIC model selection method applied to path analytic models compared using a d-separation test. *Ecology* 94, 560–564. doi: 10.1890/12-0976.1

Soliveres, S., Maestre, F. T., Eldridge, D. J., Delgado-Baquerizo, M., Quero, J. L., Bowker, M. A., et al. (2014). Plant diversity and ecosystem multifunctionality peak at intermediate levels of woody cover in global drylands. *Glob. Ecol. Biogeogr.* 23, 1408–1416. doi: 10.1111/geb.12215

Song, M. H., Li, M., Huo, J. J., Wu, L., and Zhang, X. Z. (2020a). Multifunctionality and thresholds of alpine grassland on the Tibetan Plateau. *J. Resour. Ecol.* 11, 263–271. doi: 10.5814/j.issn.1674-764x.2020.03.003

Song, M. H., Zhu, J. F., Li, Y. K., Zhou, H. K., Xu, X. L., Cao, G. M., et al. (2020b). Shifts in functional compositions predict desired multifunctionality along fragmentation intensities in an alpine grassland. *Ecol. Indic.* 112:106095. doi: 10.1016/j.ecolind.2020.106095

Sun, J., Liu, M., Fu, B. J., Kemp, D., Zhao, W. W., Liu, G. H., et al. (2020). Reconsidering the efficiency of grazing exclusion using fences on the Tibetan Plateau. *Sci. Bull.* 65, 1405–1414. doi: 10.1016/j.scib.2020.04.035

Tang, L., Dong, S. K., Sherman, R., Liu, S. L., Liu, Q. R., Wang, X. X., et al. (2015). Changes in vegetation composition and plant diversity with rangeland degradation in the alpine region of Qinghai-Tibet Plateau. *Rangel. J.* 37, 107–115. doi: 10.1071/RJ14077

Veen, C., Fry, E. L., ten Hooven, F. C., Kardol, P., Morrien, E., and De Long, J. R. (2019). The role of plant litter in driving plant-soil feedbacks. *Front. Environ. Sci.* 7:168. doi: 10.3389/fenvs.2019.00168

Wang, C. T., Long, R. J., Wang, Q. L., Liu, W., Jing, Z. C., and Zhang, L. (2010). Fertilization and litter effects on the functional group biomass, species diversity of plants, microbial biomass, and enzyme activity of two alpine meadow communities. *Plant Soil* 331, 377–389. doi: 10.1007/s11104-009-0259-8

Weltzin, J. F., Keller, J. K., Bridgham, S. D., Pastor, J., Allen, P. B., and Chen, J. (2005). Litter controls plant community composition in a northern fen. *Oikos* 110, 537–546. doi: 10.1111/j.0030-1299.2005.13718.x

Xiong, S. J., and Nilsson, C. (1999). The effects of plant litter on vegetation: a meta-analysis. *J. Ecol.* 87, 984–994. doi: 10.1046/j.1365-2745.1999.00414.x

Xu, Y. D., Dong, S. K., Gao, X. X., Yang, M. Y., Li, S., Shen, H., et al. (2021). Aboveground community composition and soil moisture play determining roles in restoring ecosystem multifunctionality of alpine steppe on Qinghai-Tibetan Plateau. *Agric. Ecosyst. Environ.* 305:107163. doi: 10.1016/j.agee.2020.107163

Yuan, J. L., Liang, D. F., and Zhang, S. T. (2016). Litter and its interaction with standing vegetation affect seedling recruitment in Tibetan alpine grasslands. *Plant Ecol. Divers.* 9, 89–95. doi: 10.1080/17550874.2015.1073400

Zavaleta, E. S., Pasari, J. R., Hulvey, K. B., and Tilman, G. D. G. (2010). Sustaining multiple ecosystem functions in grassland communities requires higher biodiversity. *Proc. Natl. Acad. Sci. U. S. A.* 107, 1443–1446. doi: 10.1073/pnas.0906829107

Zhang, R. Y., Wang, Z. W., Niu, S. L., Tian, D. S., Wu, Q., Gao, X. F., et al. (2021). Diversity of plant and soil microbes mediates the response of ecosystem multifunctionality to grazing disturbance. *Sci. Total Environ.* 776:145730. doi: 10.1016/j.scitotenv.2021.145730

Zhang, A., Wang, D., and Wan, S. Q. (2019). Litter addition decreases plant diversity by suppressing seeding in a semiarid grassland, Northern China. *Ecol. Evol.* 9, 9907–9915. doi: 10.1002/ece3.5532

Zou, J. R., Luo, C. Y., Xu, X. L., Zhao, N., Zhao, L., and Zhao, X. Q. (2016). Relationship of plant diversity with litter and soil available nitrogen in an alpine meadow under a 9-year grazing exclusion. *Ecol. Res.* 31, 841–851. doi: 10.1007/s11284-016-1394-3

Conflict of Interest: The authors declare that the research was conducted in the absence of any commercial or financial relationships that could be construed as a potential conflict of interest.

Publisher's Note: All claims expressed in this article are solely those of the authors and do not necessarily represent those of their affiliated organizations, or those of the publisher, the editors and the reviewers. Any product that may

be evaluated in this article, or claim that may be made by its manufacturer, is not guaranteed or endorsed by the publisher.

Copyright © 2021 Ma, Wu, Li, Zhou and Hou. This is an open-access article distributed under the terms of the Creative Commons Attribution License (CC BY). The use, distribution or reproduction in other forums is permitted, provided the original author(s) and the copyright owner(s) are credited and that the original publication in this journal is cited, in accordance with accepted academic practice. No use, distribution or reproduction is permitted which does not comply with these terms.

frontiers in Plant Science

ORIGINAL RESEARCH
published: 02 December 2021
doi: 10.3389/fpls.2021.781695

Distinguishing Stoichiometric Homeostasis of Soil Microbial Biomass in Alpine Grassland Ecosystems: Evidence From 5,000 km Belt Transect Across Qinghai–Tibet Plateau

Jihui Fan[1], Tianyuan Liu[2,3], Ying Liao[1,3], Yiying Li[1,3], Yan Yan[1] and Xuyang Lu[1]*

[1] *Institute of Mountain Hazards and Environment, Chinese Academy of Sciences, Chengdu, China,* [2] *Key Laboratory of Ecosystem Network Observation and Modelling, Synthesis Research Centre of Chinese Ecosystem Research Network, Institute of Geographic Sciences and Natural Resources Research, Chinese Academy of Sciences, Beijing, China,* [3] *College of Resources and Environment, University of Chinese Academy of Sciences, Beijing, China*

OPEN ACCESS

Edited by:
Jian Sun,
Institute of Tibetan Plateau Research, Chinese Academy of Sciences (CAS), China

Reviewed by:
Su Xukun,
Research Center for Eco-Environmental Sciences, Chinese Academy of Sciences (CAS), China
Dima Chen,
China Three Gorges University, China
Lei Deng,
Northwest A&F University, China

***Correspondence:**
Yan Yan
yy@imde.ac.cn

Specialty section:
This article was submitted to Functional Plant Ecology, a section of the journal Frontiers in Plant Science

Received: *23 September 2021*
Accepted: *28 October 2021*
Published: *02 December 2021*

Citation:
Fan J, Liu T, Liao Y, Li Y, Yan Y and Lu X (2021) Distinguishing Stoichiometric Homeostasis of Soil Microbial Biomass in Alpine Grassland Ecosystems: Evidence From 5,000 km Belt Transect Across Qinghai–Tibet Plateau. Front. Plant Sci. 12:781695. doi: 10.3389/fpls.2021.781695

The biogeographic characteristics of soil microbial biomass stoichiometry homeostasis and also its mechanisms are commonly thought to be key factors for the survival strategies and resource utilization of soil microbes under extreme habitat. In this work, we conducted a 5,000-km transect filed survey in alpine grassland across Qinghai–Tibet Plateau in 2015 to measure soil microbial biomass carbon (MBC) and nitrogen (MBN) across alpine steppe and meadow. Based on the differences of climate and soil conditions between alpine steppe and meadow, the variation coefficient was calculated to investigate the homeostatic degree of MBC to MBN. Furthermore, the "trade-off" model was utilized to deeply distinguish the homeostasis degree of MBC/MBN between alpine steppe and meadow, and the regression analysis was used to explore the variability of trade-off in response to environmental factors in the alpine grassland. The results showed that the coefficient of variation (CV) of MBC/MBN in alpine meadow (CV = 0.4) was lower than alpine steppe (CV = 0.7). According to the trade-off model, microbial turnover activity of soil N relative to soil C increased rapidly and then decreased slightly with soil organic carbon (SOC), soil total nitrogen (STN), and soil water content across alpine meadow. Nevertheless, in alpine steppe, SOC/STN had a positive effect on microbial turnover of soil N. These results suggested that water, heat, and soil nutrients availability were the key factors affecting the C:N stoichiometry homeostasis of soil microbial biomass in Qinghai–Tibet Plateau (QTP)'s alpine grassland. Since the difference of survival strategy of the trade-off demands between soil C and N resulting in different patterns and mechanism, the stoichiometry homeostasis of soil microbial biomass was more stable in alpine meadow than in alpine steppe.

Keywords: Qinghai–Tibet Plateau (QTP), alpine grassland, soil microbe, stoichiometric homeostasis, trade-off

INTRODUCTION

Ecological stoichiometry focuses on the balance and limitation of energy and multiple chemical elements in various ecosystems (Agren and Weih, 2020; Zhang et al., 2020), involving competition, herbivory, mutualism, food webs, and biogeochemistry (Sterner and Elser, 2002; Zhou et al., 2021). This theory can be quantified to research on the relationship between biology and environment, biological interaction, and biogeochemical cycle during the process of energy flow and material cycle (Crous et al., 2019; Wang et al., 2021; Zhou et al., 2021). The scales ranged from genes to biosphere (Wang et al., 2015; Cherif et al., 2017; Tian et al., 2018) and can be unified (Zeng and Chen, 2005) to reveal ecological structure, function, process, and stability (Fang et al., 2019; Li et al., 2021; Wang et al., 2021). Numerous studies have demonstrated the stoichiometric homeostasis among various living organisms (Elser et al., 2000; Sterner and Elser, 2002), but with large variations among ecological studies (McGroddy et al., 2004; Elser et al., 2010; Giordano, 2013).

The homeostasis of biological stoichiometry emphasizes that living organisms can maintain relatively stable and balanced state of its multiple elements' composition in the changing environment (Sterner and Elser, 2002). The theory of stoichiometry and its homeostasis reflect the requirements for constructure and metabolism of organisms (Michaels, 2003; Allen and Gillooly, 2009). The Redfield ratio, which describes the proportions of elements equal to 106 atoms of C per 16 atoms of N per 1 atom of P for marine organisms in ocean water (Redfield, 1958). Nevertheless, the biological characteristics of stoichiometric homeostasis might change with different ontogenetic stages (Wang et al., 2021), stoichiometric variation of their diet (Hood and Sterner, 2010; Wang et al., 2018), and various types of species (e.g., weak homeostasis of phototrophs is opposite to strong homeostasis of heterotrophs) (Sterner and Elser, 2002). Furthermore, stoichiometric homeostasis reflects biological adaptation by biochemical and physiological adjustments of multiple elements that respond to living environment (Elser et al., 2010; Li et al., 2021). It can be an indicator of ecosystem dynamics (Guo et al., 2017) and the organism's ability to maintain consistent or stable state (Meunier et al., 2014) facing environmental fluctuations. Consequently, there have existed various geographical scales of its research including individual (Abail and Whalen, 2018), population (Andersen et al., 2004), community (Fanin et al., 2017), ecosystem (Yu et al., 2010; Wang et al., 2021), national (Zhang et al., 2018), and global (Galbraith and Martiny, 2015) scale, and it has been also explored in forest (Bai et al., 2019), wetland (Julian et al., 2020), grassland (Yu et al., 2011; Dijkstra et al., 2012), and aquatic (Gong et al., 2018) ecosystems.

However, the relationship of stoichiometric homeostasis with biogeochemical processes in the soil which is the main place for the life activity (Chapin et al., 2011) and ecosystem exchange of material and energy (Li et al., 2004) remains limited (Wang et al., 2014; Feng and Bao, 2017). Particularly, soil microorganism is the main component of soil biology and the core indicator of material cycling and energy flow in the soil ecosystem (Pascual et al., 2000; Rogers and Tate, 2001). Moreover, soil microorganisms are very sensitive to changes of environmental factors so that it can reflect the changes of soil quality status and ecosystem function earlier (Caravaca et al., 2003; Chapin et al., 2011). Previous studies have focused on the C:N:P atomic ratio of soil microbial biomass across global scale and found that the ratio is relatively consistent, with the value of 60:7:1 (Cleveland and Liptzin, 2007) or 42:6:1 (Xu et al., 2013), and C:N ratios of microbes vary from 8:1 to 12:1, which is also relatively consistent (Wright and Coleman, 2000). Further, elementary ratios might vary significantly in different habitats (McGroddy et al., 2004). Meanwhile, soil microbes can adjust their stoichiometry of elements when the supply of multiple resources is imbalanced (Fanin et al., 2017). These studies improved our understanding about stoichiometric homeostasis of soil microbes, but the stoichiometry homeostasis characteristics of soil microbial communities in the extreme habitat (such as alpine ecosystem), which is extremely sensitive to environmental changes, or not (Chapin et al., 2008), is largely unknown.

Qinghai–Tibet Plateau (QTP) is the amplifier to respond global change (Liu et al., 2019) due to its unique alpine climate and harsh environment (Sun et al., 2019). QTP's ecosystem is dominated by alpine grasslands (alpine meadow and steppe) which cover more than 60% of QTP area (Wu et al., 2011). Notably, the spatial distribution of water, nutrient, and heat availability over the QTP is heterogeneous. For instance, there is a decreasing gradient of the precipitation and soil nutrient content from the southeast to the northwest of QTP (Yang et al., 2008; Tan et al., 2010; Zhou et al., 2020), and alpine meadow and steppe are separately distributed at the relatively humid and arid circumstance (Qin et al., 2018; Zhou et al., 2020). All these characteristics imply that soil microorganisms may take various strategies to adjust their homeostasis to adapt to sensitive and heterogeneous habitats of alpine grasslands on QTP.

Here, we conducted a belt-transect survey across alpine meadow and steppe (5,000 km) across QTP, with measurements of soil microbial biomass carbon (MBC) and nitrogen (MBN). These data, together with climatic and edaphic other factors, were used to test the overarching hypothesis that the stoichiometric homeostasis of soil microorganisms is moderated by soil nutrient, availability, and also hydrothermal condition. Furthermore, we untangle the underlying mechanisms on how water, heat, and nutrient availability mediate stoichiometric homeostasis of soil microbes to adapt alpine habitat.

MATERIALS AND METHODS

Study Area

Our sampling sites covered Qinghai–Tibet Plateau, which is viewed as the "Third Pole" and "Asia's water tower" (average elevation is about 4,000 m) (Sun et al., 2019; Xiong et al., 2019), including the areas of the south of Xinjiang province, the east of Gansu, the northwest of Sichuan province, Qinghai province, and Tibet Autonomous Region (**Figure 1**). Most regions of the plateau are covered by alpine grasslands, which mainly consist of alpine meadow and steppe (He et al., 2008; Wu et al., 2011),

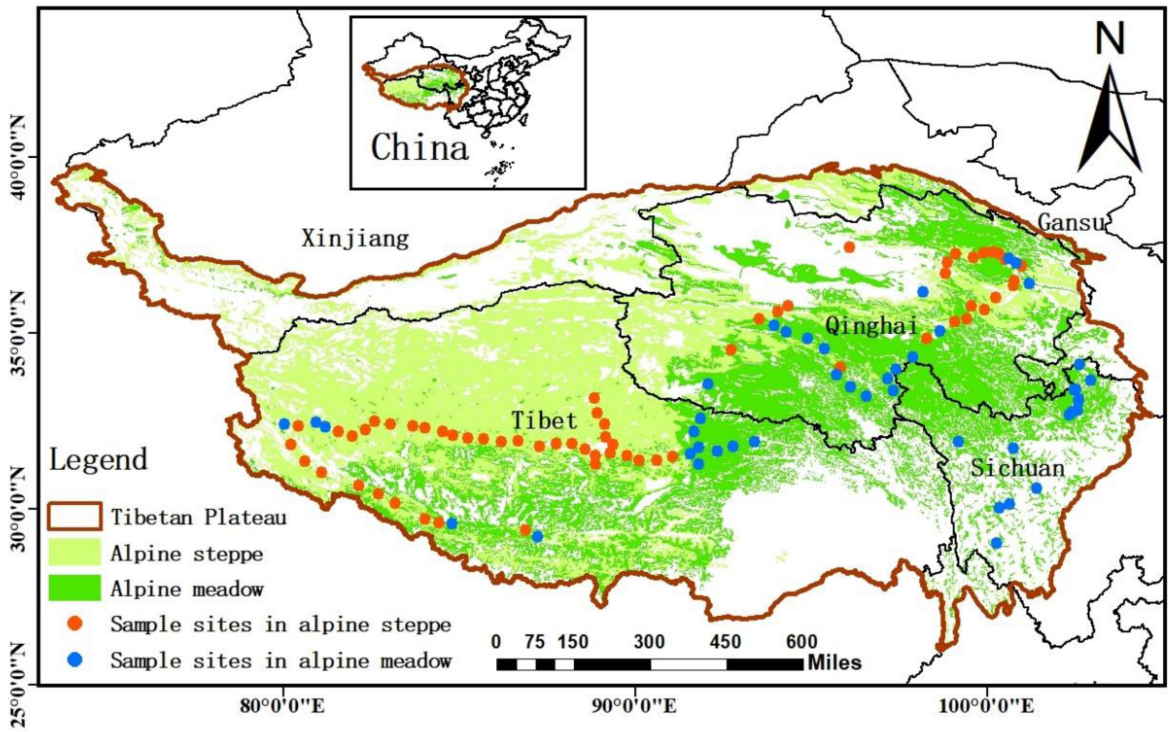

FIGURE 1 | The study area and sample sites. The sample sites (108 sites) were natural zonal grasslands across Qinghai–Tibet Plateau, including alpine meadow and alpine steppe grasslands.

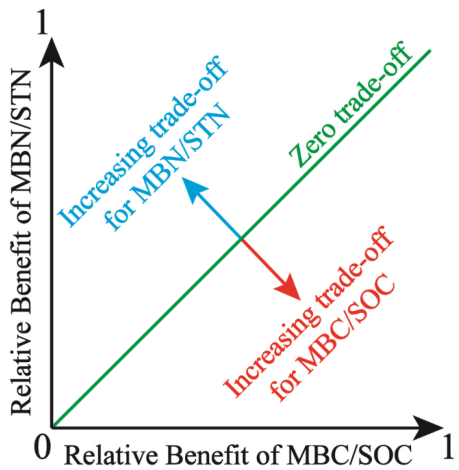

FIGURE 2 | Illustration of the trade-off between microbial entropy carbon (MBC/SOC) and microbial entropy nitrogen (MBN/STN), and the trade-off is calculated as the root mean square error (RMSE) of the individual benefits and increases with distance from the 1:1 line, in which the benefit of MBC/SOC equals the benefit of MBN/STN.

and the grassland ecosystem in this area is very sensitive to the changes of the external environment (Jacobsen et al., 2012). In the sites, the annual mean precipitation decreased from 1,000 to 100 mm from southeast to northwest of QTP, and the annual mean temperature ranged from −5°C in north-western QTP to 20°C in southern QTP during the study period (Sun et al., 2020). The natural gradients and unique combination of water and heat availability across QTP result in various changeable habitats for soil microbes. Therefore, we aimed to detect the changes of microbial homeostasis along the 5,000 km belt-transect survey on the regional scale of QTP.

Soil and Microbial Properties

For this research, 324 plots from 108 sites (three plots from each site) were sampled from July to August in 2015 the Qinghai–Tibet Plateau, and the selected sample plots along the transect must be natural alpine grasslands and as far away as possible from the interference of human activities. At each site (size of 10 m × 10 m), three paired plots (size of 50 cm × 50 cm) were sorted to obtain the soil samples after the grass above the ground was harvested. Soil samples were excavated by a standard 5-cm-diameter soil auger (at depths of 0–30 cm) in each quadrat. In the laboratory, soil samples were air-dried and sieved through 2-mm mesh as well as ground into fine powder with a ball mill (NM200, Retsch, Haan, Germany).

We used the drying and potentiometric method to measure soil water content (SWC) and the soil pH value (pH), respectively. One subsample was oven-dried at 105°C to a constant weight for measuring soil bulk density (SBD). A vario MACRO cube elemental analyzer (Elementar Analysensysteme GmbH, Germany) was used to measure soil organic carbon (SOC) and soil total nitrogen (STN) (Lu et al., 2015), and the ratio of SOC to STN was expressed as SOC/STN. We obtained SOM by the

potassium dichromate oxidation method determining SOC, with universal conversion factor 1.724 (Chen et al., 2018). Moreover, we used the chloroform fumigation method with a universal conversion factor of 0.45 and 0.54 to obtain (MBC) (Joergensen, 1996) and (MBN) (Joergensen and Mueller, 1996), respectively. MBC/MBN was the ratio of MBC to MBN. Furthermore, microbial entropy carbon (MBC/SOC) and microbial entropy nitrogen (MBN/STN), respectively, represent the biologically active fraction (MBC and MBN) and turnover activity of soil C and N pool, reflecting the activity degree of microbial demand for soil C and N resources to form microbial C and N elements (Srivastava and Singh, 1991; Wu et al., 2019).

Climate Database

We collected the climatic data (daily precipitation and temperature) of 2015 through the Meteorology Information Centre of the Chinese National Bureau of Meteorology[1], and the data from January to December was calculated to obtain the mean annual temperature (°C) (MAT) and the mean annual precipitation (mm) (MAP) by the average method. Moreover, climatic raster databases were spatially interpolated by the Anusplin 4.2 (Centre for Resource and Environmental Studies, Australian National University, Canberra) with 1 km resolution. The climatic data (MAP and MAT) of our sample sites was extracted from the raster climatic database by ArcGIS 10.2 (ESRI, Inc., Redlands, CA, United States). Additionally, aridity index (AI), an important aridity measure of meteorological factor was calculated (De Martonne, 1926):

$$AI = \frac{MAP}{MAT + 10}$$

Calculation of the Coefficient of Variation and Trade-Off Model

We used the coefficient of variation (CV) to indicate the stability of MBC, MBN, and MBC/MBN in alpine grasslands. CV is the SD divided by the mean value (MN) for the variable (MBC, MBN, or MBC/MBN):

$$CV = \frac{SD}{MN} \times 100\%$$

Bradford and D'Amato (2012) established the model for trade-off among individual benefits, which is suitable for living strategies and choices of soil microbes among multiple demand goals (MBC/SOC and MBN/STN). The trade-off model was calculated using the below equations:

$$\begin{cases} Trade-off = \frac{Benefit_{(MBN/STN)} - Benefit_{(MBC/SOC)}}{\sqrt{2}} \\ Benefit_{(MBC/SOC)} = \frac{(MBC/SOC)_{Obs} - (MBC/SOC)_{Min}}{(MBC/SOC)_{Max} - (MBC/SOC)_{Min}} \\ Benefit_{(MBN/STN)} = \frac{(MBN/STN)_{Obs} - (MBN/STN)_{Min}}{(MBN/STN)_{Max} - (MBN/STN)_{Min}} \end{cases}$$

where $(MBC/SOC)_{Obs}$ and $(MBN/STN)_{Obs}$ are the observed values of MBC/SOC and MBN/STN, respectively. $(MBC/SOC)_{Max}$ (maximum) and $(MBC/SOC)_{Min}$ (minimum)

[1]http://data.cma.cn/

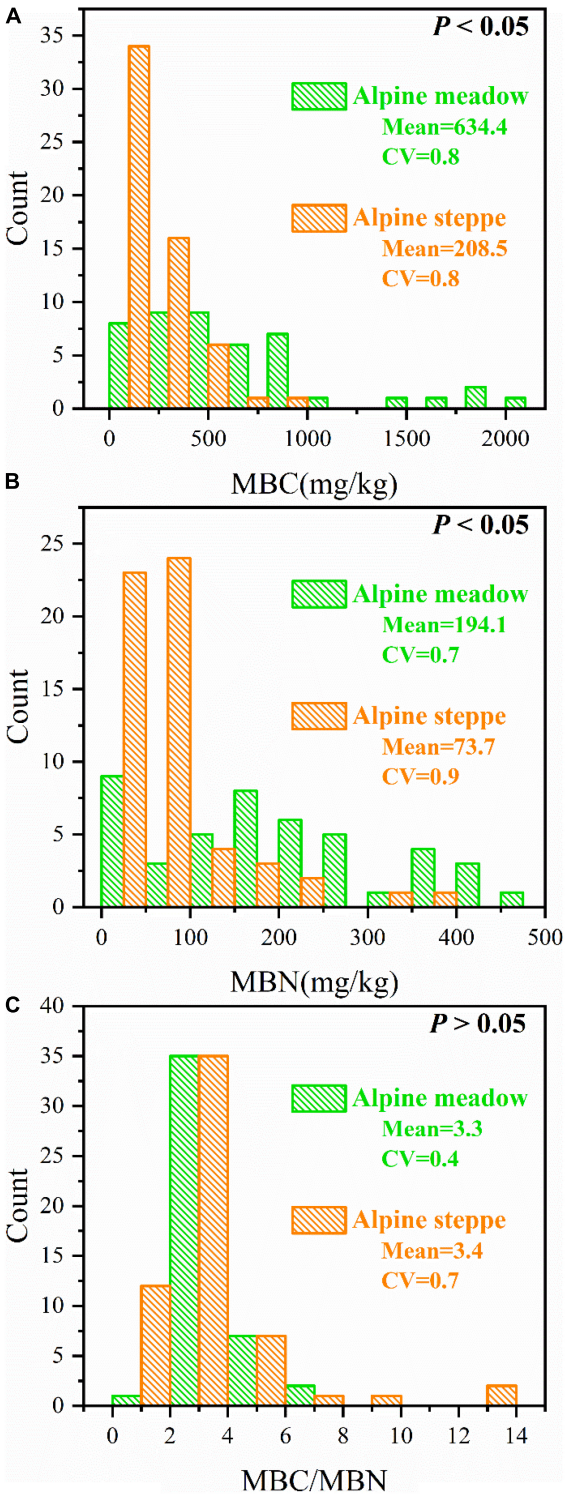

FIGURE 3 | Count distributions of **(A)** soil microbial biomass carbon (MBC), **(B)** soil microbial biomass nitrogen (MBN), and **(C)** the ratio of soil microbial biomass carbon to nitrogen (MBC/MBN) across alpine steppe and meadow. "Mean" and "CV" represent the average values and coefficients of variation of MBC, MBN, and MBC/MBN, respectively. And *P*-values indicate level of significant differences of MBC, MBN, and MBC/MBN between alpine steppe and alpine meadow.

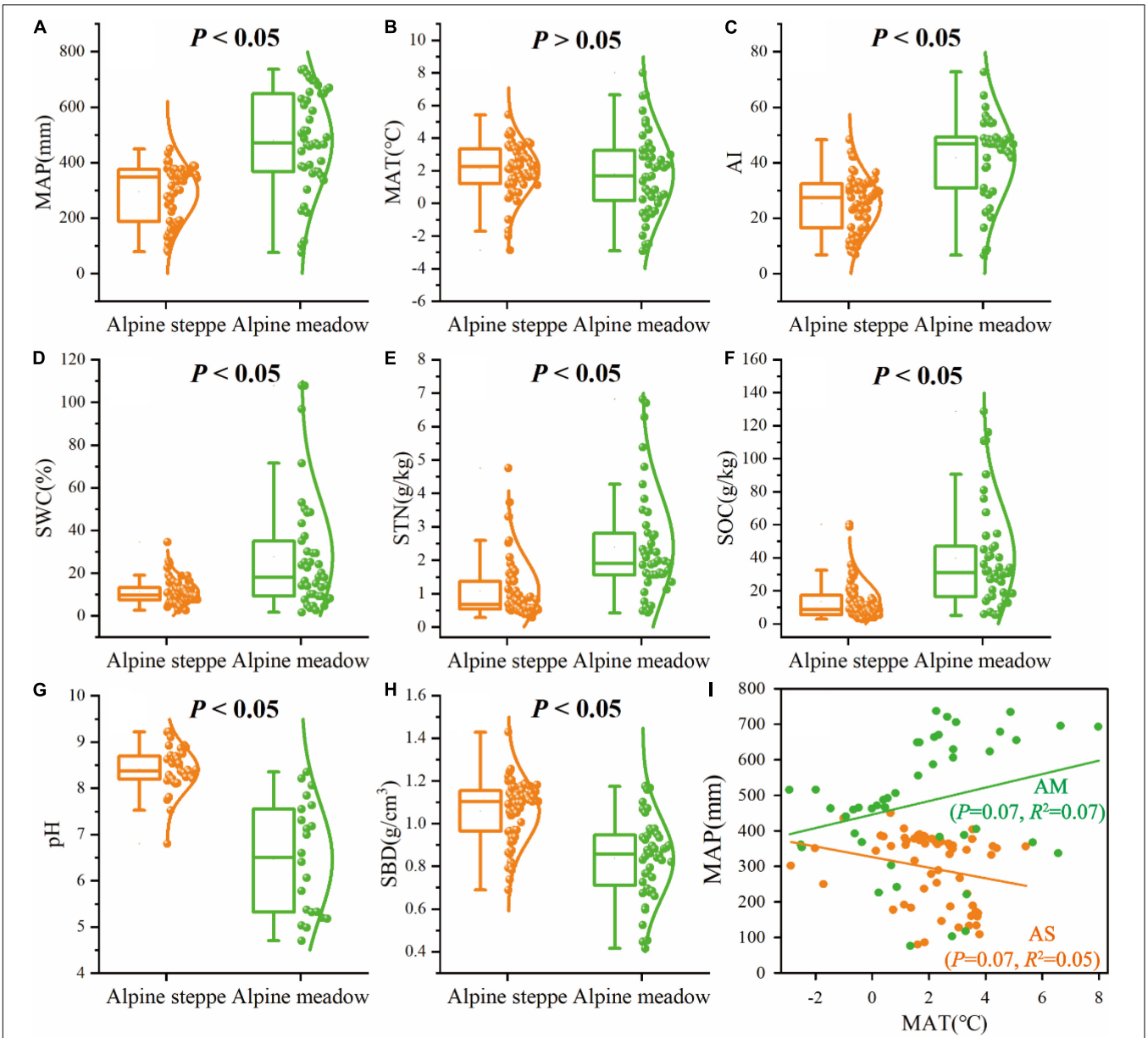

FIGURE 4 | Box-and-whisker plots showing changes in the **(A)** mean annual precipitation (MAP), **(B)** mean annual temperature (MAT), **(C)** aridity index (AI), **(D)** soil water content (SWC), **(E)** soil total nitrogen (STN), **(F)** soil organic carbon (SOC), **(G)** soil pH (pH), and **(H)** soil bulk density (SBD) in alpine steppe (AS) and alpine meadow (AM), *P*-values indicate level of significant differences between alpine steppe and alpine meadow. **(I)** The relationships between MAP and MAT across alpine steppe (AS) and alpine meadow (AM).

TABLE 1 | Correlations between the ratio of soil microbial biomass carbon to nitrogen (MBC/MBN) and environmental factors in alpine steppe and meadow; environmental factors include mean annual precipitation (MAP), mean annual temperature (MAT), aridity index (AI), soil organic carbon (SOC), soil total nitrogen (STN), the ratio of SOC to STN (SOC/STN), soil pH (pH), soil bulk density (SBD), soil water content (SWC), and soil organic matter (SOM).

MBC/MBN	Items	MAP	MAT	AI	SOC	STN	SOC/STN	pH	SBD	SWC	SOM
Alpine steppe	Pearson Correlation	0.128	0.046	0.121	−0.019	−0.024	0.004	0.110	−0.057	−0.248	−0.049
	Sig. (2-tailed)	0.317	0.719	0.345	0.888	0.860	0.978	0.519	0.658	0.062	0.714
Alpine meadow	Pearson Correlation	0.128	−0.072	0.141	0.077	0.107	−0.115	0.009	−0.180	0.207	0.027
	Sig. (2-tailed)	0.402	0.638	0.357	0.623	0.495	0.462	0.970	0.243	0.194	0.864

are calculated from the entire population of MBC/SOC, the same is also true for MBN/STN. Benefit$_{(MBC/SOC)}$ or Benefit$_{(MBN/STN)}$ is the magnitude of benefit for individual management objective (MBC/SOC or MBN/STN), being defined as the relative deviation from the mean for a given observation. Moreover, the trade-off between MBC/SOC and MBN/STN reflects soil microbial trade-off strategies about comprehensive demands for soil C and N resources. Specifically, the overall benefit toward MBN/STN is more with higher trade-off value, which implies that soil microbes tend to the turnover of soil N more, which indicates that microbes demand more soil N resource (Chapin et al., 2011). Further, the root mean square error (RMSE) of the Benefit$_{(MBC/SOC)}$ or Benefit$_{(MBN/STN)}$ was used to quantify the magnitude of the trade-off between MBC/SOC and MBN/STN. The RMSE approximates the average deviation from the mean Benefit$_{(MBC/SOC)}$ or the mean Benefit$_{(MBN/STN)}$. In two dimensions, the RMSE is the distance from the "1:1 line" of the "zero trade-off" (Bradford and D'Amato, 2012), and the trade-off model is expressed as the conceptual graph (**Figure 2**).

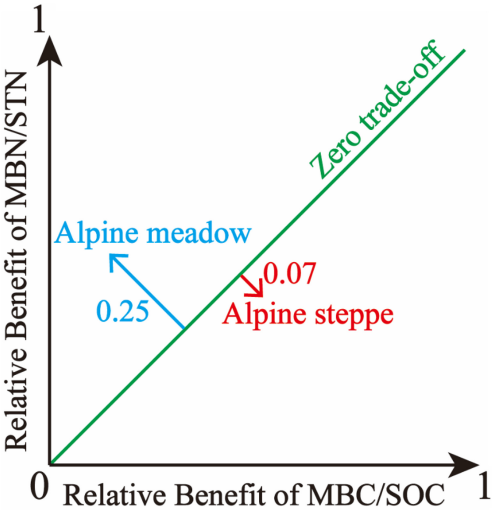

FIGURE 5 | The illustration of overall benefit between microbial entropy carbon (MBC/SOC) and microbial entropy nitrogen (MBN/STN) in alpine steppe and alpine meadow.

Statistic Analysis

The figure of our study area and sample sites was created using ArcGIS 10.2 (ESRI, Inc., Redlands, CA, United States). The one-way ANOVA was used to detect the differences in microbial properties (MBC, MBN, and MBC/MBN), soil properties (SOC, STN, SBD, pH, and SWC), and climatic characteristics (MAP, MAT, and AI) between alpine meadow and steppe. The correlation coefficients were calculated to reveal the relationships between MBC/MBN and environmental factors (MAP, MAT, AI, SOC, STN, SOC/STN, pH, SBD, SWC, and SOM) in alpine meadow and steppe. The above two methods were analyzed by SPSS 19.0 software (SPSS Inc., Chicago, IL, United States). Moreover, SigmaPlot for Windows version 14.0 (Systat Software, Inc., Chicago, IL, United States) were used to generate the relationships of trade-off with environmental factors (MAP, MAT, AI, SOC, STN, SOC/STN, pH, SBD, and SWC) in various grasslands. A linear piecewise quantile regression (LPQR) was used to evaluate the response of trade-off to SOC, STN, and SWC across alpine meadow for the plausible estimation of responses to a given variable (Ruppert et al., 2012). The segment function is calculated as follows:

$$t1 = \min(t)$$

$$t3 = \max(t)$$

$$f1(t) = \frac{y1 * (T1 - t) + y2 * (t - t1)}{T1 - t1}$$

$$f2(t) = \frac{y2 * (T2 - t) + y3 * (t - T1)}{T2 - T1}$$

$$f3(t) = \frac{y3 * (t3 - t) + y4 * (t - T2)}{t3 - T2}$$

$$f = if\left(t \leq T1,\ f1(t), if\left(t \leq T2, f2(t), regionf(t)\right)\right)$$

RESULTS

Variations of Climatic, Soil, and Microbial Variations

MBC and MBN were entirely different ($P < 0.05$, **Figures 3A,B**), but MBC/MBN was not significantly different ($P > 0.05$, **Figure 3C**) between alpine meadow and steppe.

The boxplots exhibited significant ($P < 0.05$) differences of MAP, AI, SWC, STN, SOC, pH, and SBD between alpine meadow and steppe (**Figure 4**). For the mean values of climate (MAP, AI) and soil (SWC, STN, SOC, SBD) variables, MAP ranged from 295.24 to 480.16 mm (**Figure 4A**), AI ranged from 25.18 to 41.80 (**Figure 4C**), SWC ranged from 11.21 to 27.67% (**Figure 4D**), STN ranged from 1.08 to 2.38 g/kg (**Figure 4E**), SOC ranged from 13.47 to 39.64 g/kg (**Figure 4F**), and SBD ranged from 1.06 to 0.84 g/cm^3 (**Figure 4H**) from alpine steppe to meadow based on regional study of QTP. MAP was negatively correlated with MAT ($R^2 = 0.05$, $P = 0.07$) in alpine steppe, but was positively correlated with MAT ($R^2 = 0.07$, $P = 0.07$) across alpine meadow (**Figure 4I**).

Homeostatic Analysis of Soil Microbial Biomass Carbon and Nitrogen

The variation coefficient of MBC/MBN in alpine meadow (CV = 0.4) was lower than alpine steppe (CV = 0.7) (**Figure 3**). Moreover, MBC/MBN was non-significantly ($P > 0.05$) correlated to all environmental factors, and the correlation

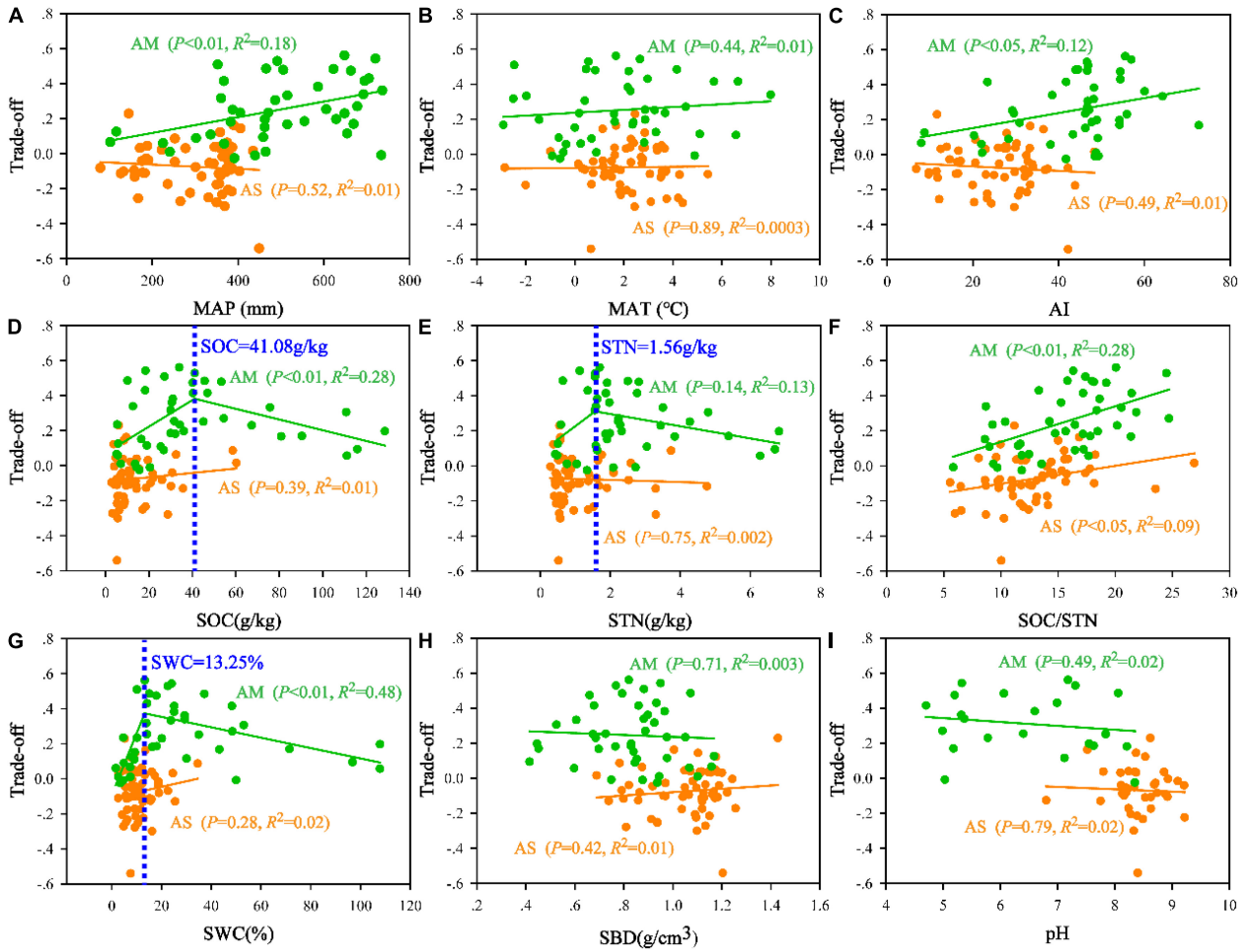

FIGURE 6 | Relationships of the trade-off with **(A)** mean annual precipitation (MAP), **(B)** mean annual temperature (MAT), **(C)** aridity index (AI), **(D)** soil organic carbon (SOC), **(E)** soil total nitrogen (STN), **(F)** the ratio of SOC to STN (SOC/STN), **(G)** soil water content (SWC), **(H)** soil bulk density (SBD), and **(I)** soil pH (pH) in alpine steppe (AS) and alpine meadow (AM).

coefficients ranged between −0.248 and 0.207 in alpine steppe and meadow (**Table 1**) across regional scale of QTP.

Trade-Off Between Microbial Biomass Carbon/Soil Organic Carbon and Microbial Biomass Nitrogen/Soil Total Nitrogen

Based on the trade-off model, the overall benefit was 0.25 toward MBN/STN in alpine meadows and 0.07 toward MBC/SOC in alpine steppes (**Figure 5**). Moreover, trade-off was positively correlated with MAP (R^2 = 0.18, P < 0.01, **Figure 6A**), AI (R^2 = 0.12, P < 0.05, **Figure 6C**), and SOC/STN (R^2 = 0.28, P < 0.01, **Figure 6F**) in alpine meadows. Trade-off demonstrated unimodality relationships with SOC (R^2 = 0.28, P < 0.01, **Figure 6D**), STN (R^2 = 0.13, P = 0.14, **Figure 6E**), and SWC (R^2 = 0.48, P < 0.01, **Figure 6G**) across alpine meadows ecosystem scale, and all trends of the trade-off were increased and then decreased with increasing SOC, STN, and SWC with the inflection points of 41.08 g/kg (**Figure 6D**), 1.56 g/kg (**Figure 6E**), and 13.25% (**Figure 6G**), respectively. In terms of alpine steppes, trade-off was positively correlated with SOC/STN (R^2 = 0.09, P < 0.05, **Figure 6F**). Trade-off was not significantly (P > 0.05) correlated with MAT, SBD and soil pH across alpine meadows and steppes (**Figures 6B,H,I**).

DISCUSSION

More Stable C:N Homeostasis of Microbial Biomass in Alpine Meadows Than Alpine Steppes on the Ecosystem Scale

MBC/MBN almost had no correlation with climate and soil factors in alpine grassland ecosystems (**Table 1**), indicating that soil microbial biomass stoichiometry was relatively homeostatic meeting the changing environments (Sterner and Elser, 2002; Persson et al., 2010) across both types of grassland. Furthermore,

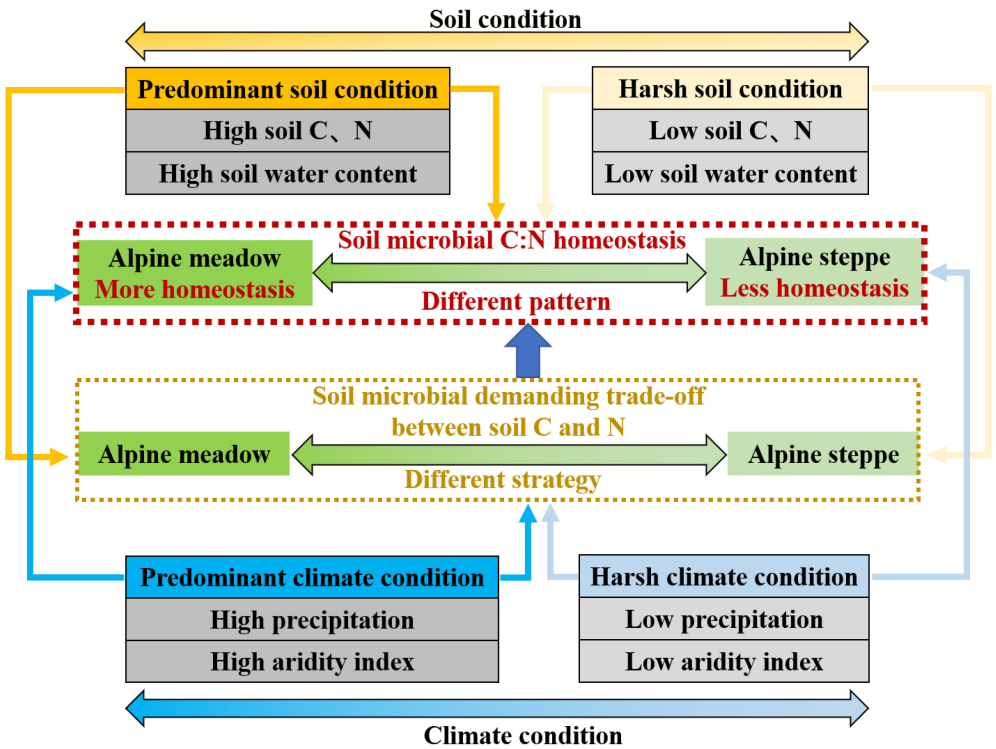

FIGURE 7 | Conceptual model of soil microbial biomass stoichiometry C:N homeostasis in arid (alpine steppe) and humid (alpine meadow) environments. Soil microbes tend to be less homeostatic in their C:N stoichiometry under harsh climate (low precipitation and aridity index) and soil (low soil C and N and low soil water content) condition in alpine steppe. Conversely, soil microbial C:N stoichiometry is more homeostatic under better climate (high precipitation and aridity index) and soil (high soil C and N and high soil water content) condition in alpine meadow. Furthermore, demanding trade-off of soil microbial strategy between soil C and N responding to climate and soil factors is different, leading to different homeostasis pattern of soil microbes between alpine meadow and steppe.

the variation coefficient of MBC/MBN in alpine meadow was lower than steppe (**Figure 3C**), indicating that stoichiometric homeostasis of soil microbes in alpine meadow is relatively more stable than steppe based on ecosystem scale. Indicators related to water (e.g., MAP, AI, and SWC) and nutrient (SOC and STN) availability in alpine meadow were significantly higher than those in alpine steppe (**Figures 4A,C–F**), which were vital factors determining different degree of microbial homeostasis. In arid condition (alpine steppe), it is well documented that soil microorganisms could not support constant compound synthesis and their activities of growth, mineralization, and decomposition are constrained with limited soil nutrient and water availability in drought–cold terrestrial ecosystem (Chapin et al., 2011; Kuzyakov and Xu, 2013). Consequently, soil microbes are flexible in their stoichiometry and it is energetically expensive for microbes to maintain the stoichiometric homeostasis under lower water and nutrient availability across alpine steppe (Sterner and Elser, 2002; Mooshammer et al., 2014b). On the contrary, in humid environments (alpine meadow), microbial decomposition and mineralization would be enhanced, and microbes can promote the turnover of soil nutrient. Then it is easier for microbes to balance the uptake of multiple elements under higher water and nutrient availability across alpine meadow (Vandecar et al., 2009; Delgado-Baquerizo et al., 2013; Jilling et al., 2018).

Generally, soil microbes consistently display some changes in body elemental composition in response to variation of soil resources they depend on (Hood and Sterner, 2010; Wang et al., 2018) based on regional scale across QTP in our study. It has been found that the elemental composition between soil resource and soil microbes would be more imbalanced and the growth and utilization efficiency of microorganisms are also lower with worse soil quality. Soil microbes might take non-homeostatic strategy to adjust their element use efficiencies and elemental composition to adapt to harsher environment (Mooshammer et al., 2014b). Given the fact that soil MBC and nitrogen are directly derived from the conversion of soil organic matter and they are very sensitive to variable soil condition (Chapin et al., 2011), soil microbes are likely to be more flexible in their MBC/MBN due to lower soil nutrient availability and harsher climate condition in alpine steppe relative to alpine meadow (**Figure 7**).

Using Trade-Off Model to Distinguish Microbial C:N Stoichiometry Homeostasis

Different homeostatic patterns of soil microbial biomass stoichiometry between alpine meadow and steppe reflected that soil microbes respond to the resource they require differently in different habitats (Sterner and Elser, 2002). It

has been well documented that the strength of stoichiometric homeostasis is highly relevant to the ecological strategy and adaptability of the organism (Frost et al., 2005; Jeyasingh et al., 2009; Yu et al., 2011), and homeostasis has the ability for consumers (soil microbes) to approach nutritional targets (such as intake or growth) that maximize the fitness in a variable environment region (Raubenheimer et al., 2012; Sperfeld et al., 2017). Therefore, we infer that microbial survival and adaptation strategy of demanding soil C and N resources to form their specific elementary composition of C and N is different in arid (alpine steppe) and humid (alpine meadow) habitat.

Based on the trade-off model (**Figure 2**), the overall benefit was, respectively, toward MBN/STN and MBC/SOC across alpine meadow and steppe, respectively (**Figure 5**), indicating that soil microbes tended to the turnover of soil C and N on the ecosystem scale of alpine meadow and steppe, respectively. Furthermore, the trade-off increased with increasing MAP and AI across alpine meadow (**Figures 6A,C**), indicating that microbial activity increases with more water availability (Mooshammer et al., 2014a) because soil C is richer than soil N for soil microorganisms in alpine ecosystem (Chen et al., 2016). Nevertheless, the increasing water availability (MAP and AI) did not enhance microbial activity in alpine steppe (**Figures 6A,C**), and that was because of the negative interaction between MAT and MAP (**Figure 4I**). This indicated that water and heat availability were not synchronous, constraining activities of microbial growth (Melillo et al., 2002; Fierer et al., 2007; Niu et al., 2008). The trade-off increased with increasing SOC and SWC across alpine steppe (**Figures 6D,G**), which revealed that the limited soil resource intensified the microbial fight for obtaining SOC and SWC. Moreover, SOC/STN had a positive effect on the trade-off across alpine steppe and meadow (**Figure 6F**) because STN would become a more restrictive nutrient for soil microbes with increasing SOC/STN. According to the law of minimum, organisms respond more strongly to limiting factors, thus soil microbes tended to require more soil N resources to form their own N element with relatively less STN (Chapin et al., 2011).

Notably, as for soil microbes in alpine meadow, the trade-off increased with increasing water and soil properties when SOC, STN, and SWC were lower than the threshold levels of 41.08 g/kg, 1.56 g/kg, and 13.25%, respectively, but decreased when SOC, STN, and SWC were higher than these threshold levels (**Figures 6D,E,G**), indicating microbial activity for demanding soil nutrient and moisture had weakened with relatively more soil available resources. Moreover, such threshold values for the limitations of water and nutrient availability identified in this study will become a powerful tool for exploring the physiological basis about the trade-off of microbial life history and critical thresholds of alpine ecosystems (Sutherland et al., 2013).

These results suggest that water, heat, and nutrient availability induce changes in microbial trade-off by mediating microbial activity and nutrient turnover (Papanikolaou et al., 2010; Moyano et al., 2013; Serna-Chavez et al., 2013) based on regional study across QTP's alpine grasslands. Soil microbial strategy of demanding trade-off between soil C and N in response to soil and climate factors was different between alpine steppe and meadow, leading to different variability of soil microbial biomass stoichiometry homeostasis (**Figure 7**). For soil microbes, stoichiometric homeostatic regulation reflects underlying biochemical allocations and trade-off when they respond to surrounding environments (Hessen et al., 2004) on the QTP's regional-scale study.

CONCLUSION

The soil microbial biomass stoichiometry homeostasis in alpine steppe was relatively less stable than alpine meadow across the regional scale of QTP's grasslands due to higher water, heat, and nutrient availability in alpine meadow than that in steppe. Meanwhile, the quantified trade-off model is an ideal interpretation to further distinguish stoichiometric homeostasis of soil microbes between alpine steppe and meadow. Based on the trade-off model, soil microbes tended to the turnover of soil C and N across alpine meadow and steppe, respectively. Furthermore, the trade-off significantly increased with increasing SOC/STN, MAP, and AI, and had unimodal relationships with SOC, STN, and SWC across the alpine meadow. In alpine steppe, water (MAP and AI) and nutrient (STN) availability had no remarkable effects on the trade-off. Nevertheless, further studies should be devoted to analyze biogeographic characteristics of homeostasis of the plant on the QTP-regional scale and reveal the effect of biological homeostasis to indicate the structure, function, and stability of alpine ecosystem.

DATA AVAILABILITY STATEMENT

The original contributions presented in the study are included in the article/supplementary material, further inquiries can be directed to the corresponding author.

AUTHOR CONTRIBUTIONS

JF and YY designed the experiment. TL, YL, and YYL sampled and analyzed the data. JF, TL, and YY were involved in drafting the original manuscript. JF and XL were involved in editing and revising the manuscript. All authors read and approved the final manuscript.

FUNDING

This study was supported by the National Natural Science Foundation of China (Nos. 41871072, 1871040, and 41877338).

ACKNOWLEDGMENTS

The authors would like to thank the National Qinghai–Tibet Plateau Data Center (http://data.tpdc.ac.cn) and National Meteorological Information Centre (http://data.cma.cn/data) providing the geographic data and meteorological data.

REFERENCES

Abail, Z., and Whalen, J. K. (2018). Selective ingestion contributes to the stoichiometric homeostasis in tissues of the endogeic earthworm Aporrectodea turgida. *Soil Biol. Biochem.* 119, 121–127. doi: 10.1016/j.soilbio.2018.01.014

Agren, G. I., and Weih, M. (2020). Multi-dimensional plant element stoichiometry-looking beyond carbon, nitrogen, and phosphorus. *Front. Plant Sci.* 11:23. doi: 10.3389/fpls.2020.00023

Allen, A. P., and Gillooly, J. F. (2009). Towards an integration of ecological stoichiometry and the metabolic theory of ecology to better understand nutrient cycling. *Ecol. Lett.* 12, 369–384. doi: 10.1111/j.1461-0248.2009.01302.x

Andersen, T., Elser, J. J., and Hessen, D. O. (2004). Stoichiometry and population dynamics. *Ecol. Lett.* 7, 884–900. doi: 10.1111/j.1461-0248.2004.00646.x

Bai, X. J., Wang, B. R., An, S. S., Zeng, Q. C., and Zhang, H. X. (2019). Response of forest species to C:N:P in the plant-litter-soil system and stoichiometric homeostasis of plant tissues during afforestation on the Loess Plateau, China. *Catena* 183:104186. doi: 10.1016/j.catena.2019.104186

Bradford, J. B., and D'Amato, A. W. (2012). Recognizing trade-offs in multi-objective land management. *Front. Ecol. Environ.* 10, 210–216. doi: 10.1890/110031

Caravaca, F., Alguacil, M. M., Figueroa, D., Barea, J. M., and Roldan, A. (2003). Re-establishment of Retama sphaerocarpa as a target species for reclamation of soil physical and biological properties in a semi-arid Mediterranean area. *Forest Ecol. Manag.* 182, 49–58. doi: 10.1016/s0378-1127(03)00067-7

Chapin, F. S., Matson, P. A., and Mooney, H. A. (2011). *Principles of Terrestrial Ecosystem Ecology*. New York: Springer.

Chapin, F. S., Randerson, J. T., McGuire, A. D., Foley, J. A., and Field, C. B. (2008). Changing feedbacks in the climate-biosphere system. *Front. Ecol. Environ.* 6, 313–320. doi: 10.1890/080005

Chen, L., Liu, L., Mao, C., Qin, S., Wang, J., Liu, F., et al. (2018). Nitrogen availability regulates topsoil carbon dynamics after permafrost thaw by altering microbial metabolic efficiency. *Nat. Commun.* 9:3951. doi: 10.1038/s41467-018-06232-y

Chen, Y. L., Chen, L. Y., Peng, Y. F., Ding, J. Z., Li, F., Yang, G. B., et al. (2016). Linking microbial C:N:P stoichiometry to microbial community and abiotic factors along a 3500-km grassland transect on the Tibetan Plateau. *Global Ecol. Biogeogr.* 25, 1416–1427. doi: 10.1111/geb.12500

Cherif, M., Faithfull, C., Guo, J. W., Meunier, C. L., Sitters, J., Uszko, W., et al. (2017). An operational framework for the advancement of a molecule-to-biosphere stoichiometry theory. *Front. Mar. Sci.* 4:286. doi: 10.3389/fmars.2017.00286

Cleveland, C. C., and Liptzin, D. (2007). C:N:P stoichiometry in soil: is there a "Redfield ratio" for the microbial biomass? *Biogeochemistry* 85, 235–252. doi: 10.1007/s10533-007-9132-0

Crous, K. Y., Wujeska-Klause, A., Jiang, M. K., Medlyn, B. E., and Ellsworth, D. S. (2019). Nitrogen and Phosphorus Retranslocation of Leaves and Stemwood in a Mature *Eucalyptus* Forest Exposed to 5 Years of Elevated CO2. *Front. Plant Sci.* 10:664. doi: 10.3389/fpls.2019.00664

De Martonne, E. (1926). *Une nouvelle function climatologique: L'indice d'aridite*. Paris: Gauthier-Villars.

Delgado-Baquerizo, M., Maestre, F. T., Gallardol, A., Bowker, M. A., Wallenstein, M. D., Luis Quero, J., et al. (2013). Decoupling of soil nutrient cycles as a function of aridity in global drylands. *Nature* 502, 672–676. doi: 10.1038/nature12670

Dijkstra, F. A., Pendall, E., Morgan, J. A., Blumenthal, D. M., Carrillo, Y., Lecain, D. R., et al. (2012). Climate change alters stoichiometry of phosphorus and nitrogen in a semiarid grassland. *New Phytol.* 196, 807–815. doi: 10.1111/j.1469-8137.2012.04349.x

Elser, J. J., Fagan, W. F., Kerkhoff, A. J., Swenson, N. G., and Enquist, B. J. (2010). Biological stoichiometry of plant production: metabolism, scaling and ecological response to global change. *New Phytol.* 186, 593–608. doi: 10.1111/j.1469-8137.2010.03214.x

Elser, J. J., Sterner, R. W., Gorokhova, E., Fagan, W. F., Markow, T. A., Cotner, J. B., et al. (2000). Biological stoichiometry from genes to ecosystems. *Ecol. Lett.* 3, 540–550. doi: 10.1046/j.1461-0248.2000.00185.x

Fang, Z., Li, D. D., Jiao, F., Yao, J., and Du, H. T. (2019). The Latitudinal Patterns of Leaf and Soil C:N:P Stoichiometry in the Loess Plateau of China. *Front. Plant Sci.* 10:85. doi: 10.3389/fpls.2019.00085

Fanin, N., Fromin, N., Barantal, S., and Hattenschwiler, S. (2017). Stoichiometric plasticity of microbial communities is similar between litter and soil in a tropical rainforest. *Sci. Rep.* 7:7. doi: 10.1038/s41598-017-12609-8

Feng, D. F., and Bao, W. K. (2017). Review of the temporal and spatial patterns of soil C:N:P stoichiometry and its driving factors. *Chin. J. Appl. Environ. Biol.* 23, 400–408. doi: 10.3724/SP.J.1145.2016.04018

Fierer, N., Bradford, M. A., and Jackson, R. B. (2007). Toward an ecological classification of soil bacteria. *Ecology* 88, 1354–1364. doi: 10.1890/05-1839

Frost, P. C., Evans-White, M. A., Finkel, Z. V., Jensen, T. C., and Matzek, V. (2005). Are you what you eat? Physiological constraints on organismal stoichiometry in an elementally imbalanced world. *Oikos* 109, 18–28. doi: 10.1111/j.0030-1299.2005.14049.x

Galbraith, E. D., and Martiny, A. C. (2015). A simple nutrient-dependence mechanism for predicting the stoichiometry of marine ecosystems. *Proc. Natl. Acad. Sci. U. S. A.* 112, 8199–8204. doi: 10.1073/pnas.1423917112

Giordano, M. (2013). Homeostasis: an underestimated focal point of-ecology and evolution. *Plant Sci.* 211, 92–101. doi: 10.1016/j.plantsci.2013.07.008

Gong, X. S., Xu, Z. Y., Lu, W., Tian, Y. Q., Liu, Y. H., Wang, Z. X., et al. (2018). Spatial patterns of leaf carbon, nitrogen, and phosphorus stoichiometry of aquatic macrophytes in the arid zone of northwestern China. *Front. Plant Sci.* 9:1398. doi: 10.3389/fpls.2018.01398

Guo, Y. P., Yang, X., Schob, C., Jiang, Y. X., and Tang, Z. Y. (2017). Legume shrubs are more nitrogen-homeostatic than non-legume shrubs. *Front. Plant Sci.* 8:1662. doi: 10.3389/fpls.2017.01662

He, J. S., Wang, L., Flynn, D. F. B., Wang, X. P., Ma, W. H., and Fang, J. Y. (2008). Leaf nitrogen : phosphorus stoichiometry across Chinese grassland biomes. *Oecologia* 155, 301–310. doi: 10.1007/s00442-007-0912-y

Hessen, D. O., Agren, G. I., Anderson, T. R., Elser, J. J., and De Ruiter, P. C. (2004). Carbon, sequestration in ecosystems: the role of stoichiometry. *Ecology* 85, 1179–1192. doi: 10.1890/02-0251

Hood, J. M., and Sterner, R. W. (2010). Diet mixing: do animals integrate growth or resources across temporal heterogeneity? *Am. Nat.* 176, 651–663. doi: 10.1086/656489

Jacobsen, D., Milner, A. M., Brown, L. E., and Dangles, O. (2012). Biodiversity under threat in glacier-fed river systems. *Nat. Clim. Change* 2, 361–364. doi: 10.1038/nclimate1435

Jeyasingh, P. D., Weider, L. J., and Sterner, R. W. (2009). Genetically-based trade-offs in response to stoichiometric food quality influence competition in a keystone aquatic herbivore. *Ecol. Lett.* 12, 1229–1237. doi: 10.1111/j.1461-0248.2009.01368.x

Jilling, A., Keiluweit, M., Contosta, A. R., Frey, S., Schimel, J., Schnecker, J., et al. (2018). Minerals in the rhizosphere: overlooked mediators of soil nitrogen availability to plants and microbes. *Biogeochemistry* 139, 103–122. doi: 10.1007/s10533-018-0459-5

Joergensen, R. G. (1996). The fumigation-extraction method to estimate soil microbial biomass: calibration of the k(EC) value. *Soil Biol. Biochem.* 28, 25–31. doi: 10.1016/0038-0717(95)00102-6

Joergensen, R. G., and Mueller, T. (1996). The fumigation-extraction method to estimate soil microbial biomass: calibration of the k(EN) value. *Soil Biol. Biochem.* 28, 33–37. doi: 10.1016/0038-0717(95)00101-8

Julian, P., Gerber, S., Bhomia, R. K., King, J., Osborne, T. Z., and Wright, A. L. (2020). Understanding stoichiometric mechanisms of nutrient retention in wetland macrophytes: stoichiometric homeostasis along a nutrient gradient in a subtropical wetland. *Oecologia* 193, 969–980. doi: 10.1007/s00442-020-04722-9

Kuzyakov, Y., and Xu, X. L. (2013). Competition between roots and microorganisms for nitrogen: mechanisms and ecological relevance. *New Phytol.* 198, 656–669. doi: 10.1111/nph.12235

Li, T., Sun, J. K., and Fu, Z. Y. (2021). Halophytes differ in their adaptation to soil environment in the yellow river delta: effects of water source, soil depth, and nutrient stoichiometry. *Front. Plant Sci.* 12:675921. doi: 10.3389/fpls.2021.675921

Li, Y. M., Hu, J. C., Wang, S. L., and Wang, S. J. (2004). Function and application of soil microorganisms in forest ecosystem. *Chin. J. Appl. Ecol.* 15, 1943–1946.

Liu, B. Y., Sun, J., Liu, M., Zeng, T., and Zhu, J. T. (2019). The aridity index governs the variation of vegetation characteristics in alpine grassland, Northern Tibet Plateau. *Peerj* 7, 1–17. doi: 10.7717/peerj.7272

Lu, X., Yan, Y., Sun, J., Zhang, X., Chen, Y., Wang, X., et al. (2015). Carbon, nitrogen, and phosphorus storage in alpine grassland ecosystems of Tibet: effects of grazing exclusion. *Ecol. Evol.* 5, 4492–4504. doi: 10.1002/ece3.1732

McGroddy, M. E., Daufresne, T., and Hedin, L. O. (2004). Scaling of C:N:P stoichiometry in forests worldwide: implications of terrestrial redfield-type ratios. *Ecology* 85, 2390–2401. doi: 10.1890/03-0351

Melillo, J. M., Steudler, P. A., Aber, J. D., Newkirk, K., Lux, H., Bowles, F. P., et al. (2002). Soil warming and carbon-cycle feedbacks to the climate system. *Science* 298, 2173–2176. doi: 10.1126/science.1074153

Meunier, C. L., Malzahn, A. M., and Boersma, M. (2014). A new approach to homeostatic regulation: towards a unified view of physiological and ecological concepts. *PLoS One* 9:e107737. doi: 10.1371/journal.pone.0107737

Michaels, A. F. (2003). The ratios of life. *Science* 300, 906–907.

Mooshammer, M., Wanek, W., Zechmeister-Boltenstern, S., and Richter, A. (2014b). Stoichiometric imbalances between terrestrial decomposer communities and their resources: mechanisms and implications of microbial adaptations to their resources. *Front. Microbiol.* 5:22. doi: 10.3389/fmicb.2014.00022

Mooshammer, M., Wanek, W., Haemmerle, I., Fuchslueger, L., Hofhansl, F., Knoltsch, A., et al. (2014a). Adjustment of microbial nitrogen use efficiency to carbon : nitrogen imbalances regulates soil nitrogen cycling. *Nat. Commun.* 5, 1–7. doi: 10.1038/ncomms4694

Moyano, F. E., Manzoni, S., and Chenu, C. (2013). Responses of soil heterotrophic respiration to moisture availability: an exploration of processes and models. *Soil Biol. Biochem.* 59, 72–85. doi: 10.1016/j.soilbio.2013.01.002

Niu, S. L., Wu, M. Y., Han, Y., Xia, J. Y., Li, L. H., and Wan, S. Q. (2008). Water-mediated responses of ecosystem carbon fluxes to climatic change in a temperate steppe. *New Phytol.* 177, 209–219. doi: 10.1111/j.1469-8137.2007.02237.x

Papanikolaou, N., Britton, A. J., Helliwell, R. C., and Johnson, D. (2010). Nitrogen deposition, vegetation burning and climate warming act independently on microbial community structure and enzyme activity associated with decomposing litter in low-alpine heath. *Global Change Biol.* 16, 3120–3132. doi: 10.1111/j.1365-2486.2010.02196.x

Pascual, J. A., Garcia, C., Hernandez, T., Moreno, J. L., and Ros, M. (2000). Soil microbial activity as a biomarker of degradation and remediation processes. *Soil Biol. Biochem.* 32, 1877–1883. doi: 10.1016/s0038-0717(00)00161-9

Persson, J., Fink, P., Goto, A., Hood, J. M., Jonas, J., and Kato, S. (2010). To be or not to be what you eat: regulation of stoichiometric homeostasis among autotrophs and heterotrophs. *Oikos* 119, 741–751. doi: 10.1111/j.1600-0706.2009.18545.x

Qin, X. J., Sun, J., and Wang, X. D. (2018). Plant coverage is more sensitive than species diversity in indicating the dynamics of the above-ground biomass along a precipitation gradient on the Tibetan Plateau. *Ecol. Indic.* 84, 507–514. doi: 10.1016/j.ecolind.2017.09.013

Raubenheimer, D., Simpson, S. J., and Tait, A. H. (2012). Match and mismatch: conservation physiology, nutritional ecology and the timescales of biological adaptation. *Philos. Trans. R. Soc. Lond. B Biol. Sci.* 367, 1628–1646. doi: 10.1098/rstb.2012.0007

Redfield, A. C. (1958). The biological control of chemical factors in the environment. *Am. Sci.* 46, 205–221.

Rogers, B. F., and Tate, R. L. (2001). Temporal analysis of the soil microbial community along a toposequence in Pineland soils. *Soil Biol. Biochem.* 33, 1389–1401. doi: 10.1016/s0038-0717(01)00044-x

Ruppert, J. C., Holm, A., Miehe, S., Muldavin, E., Snyman, H. A., Wesche, K., et al. (2012). Meta-analysis of ANPP and rain-use efficiency confirms indicative value for degradation and supports non-linear response along precipitation gradients in drylands. *J. Veg. Sci.* 23, 1035–1050. doi: 10.1111/j.1654-1103.2012.01420.x

Serna-Chavez, H. M., Fierer, N., and vanBodegom, P. M. (2013). Global drivers and patterns of microbial abundance in soil. *Global Ecol. Biogeogr.* 22, 1162–1172. doi: 10.1111/geb.12070

Sperfeld, E., Wagner, N. D., Halvorson, H. M., Malishev, M., and Raubenheimer, D. (2017). Bridging ecological stoichiometry and nutritional geometry with homeostasis concepts and integrative models of organism nutrition. *Funct. Ecol.* 31, 286–296. doi: 10.1111/1365-2435.12707

Srivastava, S. C., and Singh, J. S. (1991). Microbial-C, microbial-N and microbial-P in dry tropical forest soils - effects of alternate land-uses and nutrient flux. *Soil Biol. Biochem.* 23, 117–124. doi: 10.1016/0038-0717(91)90122-z

Sterner, R. W., and Elser, J. J. (2002). *Ecological Stoichiometry: The Biology of Elements from Molecules to the Biosphere*. Princeton: Princeton University Press.

Sun, J., Liu, B. Y., You, Y., Li, W. P., Liu, M., Shang, H., et al. (2019). Solar radiation regulates the leaf nitrogen and phosphorus stoichiometry across alpine meadows of the Tibetan Plateau. *Agric. Forest Meteorol.* 271, 92–101. doi: 10.1016/j.agrformet.2019.02.041

Sun, J., Zhou, T. C., Liu, M., Chen, Y. C., Liu, G. H., Xu, M., et al. (2020). Water and heat availability are drivers of the aboveground plant carbon accumulation rate in alpine grasslands on the Tibetan Plateau. *Global Ecol. Biogeogr.* 29, 50–64. doi: 10.1111/geb.13006

Sutherland, W. J., Freckleton, R. P., Godfray, H. C. J., Beissinger, S. R., Benton, T., Cameron, D. D., et al. (2013). Identification of 100 fundamental ecological questions. *J. Ecol.* 101, 58–67. doi: 10.1111/1365-2745.12025

Tan, K., Ciais, P., Piao, S. L., Wu, X. P., Tang, Y. H., Vuichard, N., et al. (2010). Application of the ORCHIDEE global vegetation model to evaluate biomass and soil carbon stocks of Qinghai-Tibetan grasslands. *Global Biogeochem. Cyc.* 24, 1–12. doi: 10.1029/2009GB003530

Tian, D., Yan, Z. B., Niklas, K. J., Han, W. X., Kattge, J., Reich, P. B., et al. (2018). Global leaf nitrogen and phosphorus stoichiometry and their scaling exponent. *Natl. Sci. Rev.* 5, 728–739. doi: 10.1093/nsr/nwx142

Vandecar, K. L., Lawrence, D., Wood, T., Oberbauer, S. F., Das, R., Tully, K., et al. (2009). Biotic and abiotic controls on diurnal fluctuations in labile soil phosphorus of a wet tropical forest. *Ecology* 90, 2547–2555. doi: 10.1890/08-1516.1

Wang, H., Li, H., Zhang, Z., Muehlbauer, J. D., He, Q., Xu, X., et al. (2014). Linking stoichiometric homeostasis of microorganisms with soil phosphorus dynamics in wetlands subjected to microcosm warming. *PLoS One* 9:e85575. doi: 10.1371/journal.pone.0085575

Wang, H., Lu, Z. X., and Raghavan, A. (2018). Weak dynamical threshold for the "strict homeostasis" assumption in ecological stoichiometry. *Ecol. Model* 384, 233–240. doi: 10.1016/j.ecolmodel.2018.06.027

Wang, K., Wang, G. G., Song, L. N., Zhang, R. S., Yan, T., and Li, Y. H. (2021). Linkages between nutrient resorption and ecological stoichiometry and homeostasis along a chronosequence of mongolian pine plantations. *Front. Plant Sci.* 12:692683. doi: 10.3389/fpls.2021.692683

Wang, Z. N., Lu, J. Y., Yang, M., Yang, H. M., and Zhang, Q. P. (2015). Stoichiometric characteristics of carbon, nitrogen, and phosphorus in leaves of differently aged lucerne (*Medicago sativa*) Stands. *Front. Plant Sci.* 6:692683. doi: 10.3389/fpls.2015.01062

Wright, C. J., and Coleman, D. C. (2000). Cross-site comparison of soil microbial biomass, soil nutrient status, and nematode trophic groups. *Pedobiologia* 44, 2–23. doi: 10.1078/s0031-4056(04)70024-4

Wu, X. Z., Liu, B. R., Yan, X., Liu, R. T., and An, H. (2019). Response of soil microbial biomass and microbial entropy to desertification in desert grassland. *Chin. J. Appl. Ecol.* 30, 2691–2698. doi: 10.13287/j.1001-9332.201908.009

Wu, Y. B., Wu, J., Deng, Y. C., Tan, H. C., Du, Y. G., Gu, S., et al. (2011). Comprehensive assessments of root biomass and production in a Kobresia humilis meadow on the Qinghai-Tibetan Plateau. *Plant Soil* 338, 497–510. doi: 10.1007/s11104-010-0562-4

Xiong, J., Yong, Z., Wang, Z., Cheng, W., Li, Y., Zhang, H., et al. (2019). Spatial and Temporal Patterns of the Extreme Precipitation across the Tibetan Plateau (1986-2015). *Water* 11, 1–24. doi: 10.3390/w11071453

Xu, X. F., Thornton, P. E., and Post, W. M. (2013). A global analysis of soil microbial biomass carbon, nitrogen and phosphorus in terrestrial ecosystems. *Global Ecol. Biogeogr.* 22, 737–749. doi: 10.1111/geb.12029

Yang, Y. H., Fang, J. Y., Tang, Y. H., Ji, C. J., Zheng, C. Y., He, J. S., et al. (2008). Storage, patterns and controls of soil organic carbon in the Tibetan grasslands. *Global Change Biol.* 14, 1592–1599. doi: 10.1111/j.1365-2486.2008.01591.x

Yu, Q., Chen, Q. S., Elser, J. J., He, N. P., Wu, H. H., Zhang, G. M., et al. (2010). Linking stoichiometric homoeostasis with ecosystem structure, functioning and stability. *Ecol. Lett.* 13, 1390–1399. doi: 10.1111/j.1461-0248.2010.01532.x

Yu, Q., Elser, J. J., He, N., Wu, H., Chen, Q., Zhang, G., et al. (2011). Stoichiometric homeostasis of vascular plants in the Inner Mongolia grassland. *Oecologia* 166, 1–10. doi: 10.1007/s00442-010-1902-z

Zeng, D. H., and Chen, G. S. (2005). Ecological stoichiometry: a science to explore the complexity of living systems. *Chin. J. Plant Ecol.* 29, 1007–1019. doi: 10.17521/cjpe.2005.0120

Zhang, J., Wang, Y. Z., and Cai, C. T. (2020). Multielemental stoichiometry in plant organs: a case study with the alpine herb Gentiana rigescens across southwest China. *Front. Plant Sci.* 11:441. doi: 10.3389/fpls.2020.00441

Zhang, J. H., Zhao, N., Liu, C. C., Yang, H., Li, M. L., Yu, G. R., et al. (2018). C:N:P stoichiometry in China's forests: from organs to ecosystems. *Funct. Ecol.* 32, 50–60. doi: 10.1111/1365-2435.12979

Zhou, T. C., Sun, J., Liu, M., Shi, P. L., Zhang, X. B., Sun, W., et al. (2020). Coupling between plant nitrogen and phosphorus along water and heat gradients in alpine grassland. *Sci. Total Environ.* 701, 1–9. doi: 10.1016/j.scitotenv.2019.13466

Zhou, Y., Jiao, L., Qin, H. J., and Li, F. (2021). Effect of Environmental Stress on the Nutrient Stoichiometry of the Clonal Plant *Phragmites australis* in Inland Riparian Wetlands of Northwest China. *Front. Plant Sci.* 12:705319. doi: 10.3389/fpls.2021.705319

Conflict of Interest: The authors declare that the research was conducted in the absence of any commercial or financial relationships that could be construed as a potential conflict of interest.

Publisher's Note: All claims expressed in this article are solely those of the authors and do not necessarily represent those of their affiliated organizations, or those of the publisher, the editors and the reviewers. Any product that may be evaluated in this article, or claim that may be made by its manufacturer, is not guaranteed or endorsed by the publisher.

Copyright © 2021 Fan, Liu, Liao, Li, Yan and Lu. This is an open-access article distributed under the terms of the Creative Commons Attribution License (CC BY). The use, distribution or reproduction in other forums is permitted, provided the original author(s) and the copyright owner(s) are credited and that the original publication in this journal is cited, in accordance with accepted academic practice. No use, distribution or reproduction is permitted which does not comply with these terms.

frontiers in Plant Science

ORIGINAL RESEARCH
published: 07 December 2021
doi: 10.3389/fpls.2021.799401

Distinct Responses of Leaf Traits to Environment and Phylogeny Between Herbaceous and Woody Angiosperm Species in China

Nannan An[1,2], *Nan Lu*[1,2]*, *Bojie Fu*[1,2,3], *Mengyu Wang*[1,2] and *Nianpeng He*[2,4]

[1] State Key Laboratory of Urban and Regional Ecology, Research Center for Eco-Environmental Sciences, Chinese Academy of Sciences, Beijing, China, [2] University of Chinese Academy of Sciences, Beijing, China, [3] Faculty of Geographical Science, Beijing Normal University, Beijing, China, [4] Key Laboratory of Ecosystem Network Observation and Modeling, Institute of Geographic Sciences and Natural Resources Research, Chinese Academy of Sciences, Beijing, China

Leaf traits play key roles in plant resource acquisition and ecosystem processes; however, whether the effects of environment and phylogeny on leaf traits differ between herbaceous and woody species remains unclear. To address this, in this study, we collected data for five key leaf traits from 1,819 angiosperm species across 530 sites in China. The leaf traits included specific leaf area, leaf dry matter content, leaf area, leaf N concentration, and leaf P concentration, all of which are closely related to trade-offs between resource uptake and leaf construction. We quantified the relative contributions of environment variables and phylogeny to leaf trait variation for all species, as well as for herbaceous and woody species separately. We found that environmental factors explained most of the variation (44.4–65.5%) in leaf traits (compared with 3.9–23.3% for phylogeny). Climate variability and seasonality variables, in particular, mean temperature of the warmest and coldest seasons of a year (MTWM/MTWQ and MTCM/MTCQ) and mean precipitation in the wettest and driest seasons of a year (MPWM/MPWQ and MPDM/MPDQ), were more important drivers of leaf trait variation than mean annual temperature (MAT) and mean annual precipitation (MAP). Furthermore, the responses of leaf traits to environment variables and phylogeny differed between herbaceous and woody species. Our study demonstrated the different effects of environment variables and phylogeny on leaf traits among different plant growth forms, which is expected to advance the understanding of plant adaptive strategies and trait evolution under different environmental conditions.

Keywords: angiosperm species, climate variability and seasonality, functional biogeography, leaf traits, phylogeny, plant growth form

OPEN ACCESS

Edited by:
Jian Sun,
Institute of Tibetan Plateau Research, Chinese Academy of Sciences (CAS), China

Reviewed by:
Yanjun Du,
Hainan University, China
Yafeng Wang,
Nanjing Forestry University, China

***Correspondence:**
Nan Lu
nanlv@rcees.ac.cn

Specialty section:
This article was submitted to Functional Plant Ecology, a section of the journal Frontiers in Plant Science

Received: *21 October 2021*
Accepted: *16 November 2021*
Published: *07 December 2021*

Citation:
An N, Lu N, Fu B, Wang M and He N (2021) Distinct Responses of Leaf Traits to Environment and Phylogeny Between Herbaceous and Woody Angiosperm Species in China. Front. Plant Sci. 12:799401. doi: 10.3389/fpls.2021.799401

INTRODUCTION

Leaf traits play multifaceted roles in plant resource acquisition (Wilson et al., 1999; Diaz et al., 2004), environmental adaptation (Reich and Oleksyn, 2004; Ordoñez et al., 2009), and ecosystem functions (Lavorel and Garnier, 2002; Ali et al., 2017). Leaf traits are highly variable across plant growth forms, phylogenetic groups, and environmental gradients, and reflect distinct plant

responses to evolutionary history and environmental changes. Identifying the primary factors that influence leaf trait variation is helpful for understanding how plant assemblages drive community structures and ecosystem processes in response to global environmental change.

Climate and soil are important factors influencing interspecific variation in leaf traits and can affect both plant adaptive strategies and ecosystem functions (Wright et al., 2005a; Ordoñez et al., 2009; Maire et al., 2015). Plants in wetter, warmer, and more fertile conditions are characterized by greater specific leaf area (SLA) and leaf N concentration (LNC) but lower leaf dry matter content (LDMC), which can allow for faster resource uptake and lower construction costs by the leaves (Simpson et al., 2016; Delpiano et al., 2020). Regarding climate variables, some studies have suggested that climate variability and seasonality variables influence the variation in plant functional traits to a greater extent than annual temperature and precipitation averages (Moles et al., 2009; Shiono et al., 2015; Wright et al., 2017; Wang et al., 2019). Climate variability and seasonality variables generally refer to the temporal variability and fluctuations in temperature and precipitation, which can affect plant phenology, rate of photosynthesis, and the length of the growing season (Kikuzawa et al., 2013; Ernakovich et al., 2014). Similarly, phylogeny has also been suggested to have an important effect on leaf traits, some of which leaf traits [e.g., SLA, LNC, and leaf P concentration (LPC)] show significant phylogenetic conservatism among species (Kerkhoff et al., 2006; Stock and Verboom, 2012; Yang et al., 2016). Results concerning the relative importance of environment variables and phylogeny on leaf trait variation among different studies have been inconsistent. For instance, Li et al. (2021) suggested that LNC was more strongly influenced by environment variables than phylogeny in Southwest China, whereas He et al. (2010) reported that phylogeny and environment explained approximately equal proportions of the variation in LNC in grasslands in China. Determining the relative contributions of environment and phylogeny to leaf trait variation is important for advancing our understanding of plant adaptive strategies to environmental change.

Leaf traits have also been found to differ significantly among plant growth forms (Kerkhoff et al., 2006; Santiago and Wright, 2007). Relative to woody species, herbaceous species have greater SLA and LNC but lower LDMC, reflecting the pursual of a more resource-acquisitive strategy (Wright et al., 2005b; Rossatto and Franco, 2017). Diaz et al. (2016) also showed that herbaceous and woody plant groups represent two almost independent hotspots in the global spectrum of plant form and function. These observations suggest that the responses of leaf traits to environment variables and phylogeny may differ between herbaceous and woody species. In general, woody species have longer lifespans and higher phylogenetic conservatism, and thus tend to have more consistent functional similarity among lineages that share the same habitat when compared with herbaceous species (Lanfear et al., 2013; Flores et al., 2014). Additionally, some studies have demonstrated that the relationships between leaf traits and climate are dependent on plant growth form (Šímová et al., 2018; Gong et al., 2020). However, studies on the effects of environment variables and phylogeny on leaf traits have focused on woody species (Asner and Martin, 2016; Yang et al., 2016; de la Riva et al., 2017), herbaceous species (He et al., 2010), or the two in combination (Valverde-Barrantes et al., 2017; Yang et al., 2018), which may obscure leaf trait-environment relationships and different evolutionary processes among the two plant growth forms. Accordingly, an extensive comparative analysis of the effects of environment variables and phylogeny on leaf trait variation between herbaceous and woody species is critical for understanding plant responses to both external environments and evolutionary history (Cornwell et al., 2014).

Although several studies have reported on leaf trait-environment relationships or phylogenetic effects on leaf traits across different spatial scales (Ordoñez et al., 2009; Flores et al., 2014; Maire et al., 2015; Valverde-Barrantes et al., 2017; Šímová et al., 2018), none have investigated the combined effects of environment variables and phylogeny on leaf traits at a national level in China. Selective pressures can vary across spatial scales (Albert et al., 2010), and different traits may have different sensitivities to the same pressures (Messier et al., 2010). Importantly, China has large-scale climate gradients and biome types, ranging from tropical rainforests to deserts, that cover almost all global vegetation types (Fang et al., 2020). These represent ideal conditions for determining the relative contributions of environment variables and phylogeny to leaf traits for different plant growth forms.

In this study, we sought to determine the relative contributions of environment variables and phylogeny to leaf trait variation as well as identify how they differ between herbaceous and woody species in China. For this, we collected data for five key leaf traits from 1,819 terrestrial angiosperm species from 530 sampling sites in China, covering almost all major seed plant lineages and biome types. The leaf traits included SLA, LDMC, leaf area (LA), LNC, and LPC, all of which are closely associated with the leaf economics spectrum (LES), plant growth rate, and resource acquisition (Reich and Oleksyn, 2004; Wright et al., 2005a, 2017).

MATERIALS AND METHODS

Leaf Trait Data Collection

Leaf trait data (**Table 1**) were collected from three sources, namely, the TRY database (Kattge et al., 2011), the China Plant Traits Database[1] (Wang et al., 2018), and published literature (a list of the data sources is presented in **Supplementary Appendix A**). The following criteria were used to ensure data quality and comparability: first, to minimize the effects of management disturbance, plant leaves were collected only from natural terrestrial ecosystems (excluding croplands, greenhouses, and laboratories); second, to reduce the confounding effects of ontogeny (Mason and Donovan, 2015), leaves were collected from healthy and mature plant individuals, while leaves in particular life stages (e.g., leaves from seedlings and expanding leaves) were excluded; third, leaves were sampled and measured

[1]http://onlinelibrary.wiley.com/doi/10.1002/ecy.2091/suppinfo

according to the handbook for standardized measurement of plant functional traits (Perez-Harguindeguy et al., 2013); fourth, because plant ecological strategies may differ between native species and non-native species, leaves were collected only from the former (van Kleunen et al., 2010). Leaf samples were mostly collected during the peak of the growing season (June–August). In addition, when data for one species were collected from multiple sites, trait values for each site–species combination were recorded. When a species was reported at the same sampling site in more than one study, the mean of the trait values reported in these studies was used. Where leaf traits were presented only in figures, the trait values were extracted using GetData software (GetData Software Company, Kogarah, NSW, Australia). The geographical coordinates of the sampling sites were also recorded to obtain the corresponding environmental data.

Species name and taxonomic nomenclature were standardized and corrected according to the *Flora of China*[2] (Wu et al., 1994-2013) and an automated phylogeny assembly tool SoTree v2.0 in the DarwinTree platform[3] (Meng et al., 2015). A total of 1,819 species from 147 families and 730 genera were collected in this study.

Climate Data

Twenty climate variables were considered and divided into four groups, as follows (**Supplementary Table 1**):

1) *Light indicator group*: The variable included was mean annual sunlight (MASL).
2) *Temperature indicator group*: In addition to mean annual temperature (MAT), variables related to temperature variability and seasonality were also collected, that is, mean growing season temperature (GST); mean diurnal range (MDR); mean annual range of temperature (MTAR); mean temperature of the warmest month of a year (MTWM); mean temperature of the warmest quarter of a year (MTWQ); mean temperature of the coldest month of a year (MTCM); mean temperature of the coldest quarter of a year (MTCQ); and active accumulated temperature above 0°C (AA0).
3) *Precipitation indicator group*: In addition to mean annual precipitation (MAP), variables related to precipitation variability and seasonality were also collected, namely, mean growing season precipitation (GSP); mean annual range of precipitation (MPAR); mean precipitation of the wettest month of a year (MPWM); mean precipitation of the wettest quarter of a year (MPWQ); mean precipitation of the driest month of a year (MPDM); and mean precipitation of the driest quarter of a year (MPDQ).
4) *Aridity indicator group*: Variables included potential evapotranspiration (PET), actual evapotranspiration (AET), and aridity index (AI, the ratio between MAP and AET).

Excluding AA0, AET, AI, and PET, the above-mentioned climate variables were collected between 1990 and 2015 by 824 national meteorological stations and interpolated to a 1 km × 1 km grid with elevation as a covariate using the interpolation software ANUSPLIN (Hancock and Hutchinson, 2006). Values for the AA0 were obtained from the Data Center for Resources and Environmental Sciences, Chinese Academy of Sciences, with a spatial resolution of 500 m.[4] AET-, AI- and PET-related data were extracted from the CGIAR-CSI GeoPortal dataset and were collected between 1950 and 2000 (Trabucco and Zomer, 2009).[5] All climate variables were resampled to 1 km. Notably, the MAT and MAP from the original literature agreed well with the values in our interpolated dataset (all R^2 values were >0.95, $p < 0.05$). Consequently, the interpolated data were used in subsequent analyses.

Soil Data

Data for a total of 17 soil variables were collected and divided into two groups, as follows (**Supplementary Table 1**):

1) *Physical indicator group*: Variables included the percentage of sand fraction (SAND), percentage of silt fraction (SILT), percentage of clay fraction (CLAY), and bulk density (BD).
2) *Chemical indicator group*: Variables included pH, soil organic matter (SOM), soil organic carbon (SOC), soil total N (STN), soil total P (STP), soil total K (STK), clay cation exchange capacity (CCEC), soil cation exchange capacity (SCEC), base saturation (BS), total exchangeable bases (TEB), calcium carbonate content ($CaCO_3$), exchangeable sodium percentage (ESP), and electrical conductivity (EC).

Data for SOM, STN, STP, and STK were extracted from the National Earth System Science Data Sharing Infrastructure, National Science & Technology Infrastructure of China,[6] and the spatial resolution was 1 km. The remaining variables were obtained from the Harmonized World Soil Database v1.2[7] (FAO et al., 2012).

Data Analysis

Before analysis, leaf trait data were $\log_{10}$-transformed to meet the approximate normality and homogeneity of the residuals. Climate and soil variables were subjected to Yeo-Johnson transformation to reduce skewness and allow for the normalized transformation of non-positive values using the "*bestNormalize*" R package (Peterson and Cavanaugh, 2019; **Supplementary Table 2**).

A phylogenetic tree was constructed based on the published phylogenetic tree of Chinese vascular plants developed by Chen et al. (2016) and updated by Hu et al. (2020). As the largest and most up-to-date species-level phylogeny of Chinese vascular plants, this phylogeny was based on sequences of chloroplast and mitochondrial genes and covered 95.7% of genera native to China. This phylogenetic tree in this study was constructed via SoTree v2.0 tool in the DarwinTree platform

[2]http://www.iplant.cn/frps

[3]http://www.darwintree.cn/flora-sotree-v2/index.shtml

[4]http://www.resdc.cn

[5]http://www.csi.cgiar.org

[6]http://www.geodata.cn

[7]http://webarchive.iiasa.ac.at/Research/LUC/External-World-soil-database/HTML/

TABLE 1 | Description of the five leaf traits evaluated.

Leaf trait	Abbreviation	Unit	Functional role	References
Specific leaf area	SLA	$m^2\ kg^{-1}$	Light capture, plant growth rate, and ecological strategy	Reich et al., 1991; Wright et al., 2004
Leaf dry matter content	LDMC	$g\ g^{-1}$	Resistance to herbivory and drought and leaf litter decomposition	Pakeman et al., 2010; Yang et al., 2018
Leaf area	LA	cm^2	Light interception and leaf energy balance related to photosynthesis, respiration, and evaporation	Wright et al., 2017; Yang et al., 2018
Leaf N concentration	LNC	$mg\ g^{-1}$	Leaf metabolic activity, plant growth rate, and nutrient cycling	Reich and Oleksyn, 2004; Wright et al., 2004
Leaf P concentration	LPC	$mg\ g^{-1}$	Leaf metabolic activity, plant growth rate, and nutrient cycling	Reich and Oleksyn, 2004; Wright et al., 2004

(see text footnote 3). All 1,819 species were included in this phylogenetic tree (**Supplementary Figure 1**). The phylogenetic tree was visualized in Interactive Tree of Life (iTOL)[8] (Letunic and Bork, 2019). Given that the incorporation of phylogenetic information in further statistical analysis required fully resolved phylogenetic trees, polytomies within the phylogeny were resolved using the "multi2di" function in the "*ape*" R package (Paradis and Schliep, 2019).

Pagel's λ (Pagel, 1999) was calculated to examine the phylogenetic signals of the leaf traits. A λ value close to zero indicates a weak phylogenetic signal for a given trait, while a value close to one suggests a strong phylogenetic signal (Freckleton et al., 2002). This analysis was performed using the "*phytools*" R package (Revell, 2012).

To consider the phylogenetic effect among species, a phylogenetic linear mixed model (PLMM) was used to examine the relationship between leaf traits and climate and soil variables using residual maximum likelihood (REML) estimation. This approach offers a flexible framework that includes the phylogenetic relationships among species to reduce the variance in the estimated regression or correlation coefficients (Rohlf, 2006; Chamberlain et al., 2012) and overcomes the limitation of phylogenetic generalized least squares that allows a specific species to correspond to only one observation. In the model, each climate and soil variable was treated as a fixed effect, species was treated as a random effect and the distance matrix among species was treated as a covariance. The sums of squares explained by fixed effects and their significance were estimated using the "r.squaredGLMM" function and "Anova" function in the "*lme4qtl*" R package, respectively (Ziyatdinov et al., 2018).

The PLMM was further used to partition the individual contributions of environment variables and phylogeny to the variation in leaf traits for all species as well as herbaceous and woody plant groups, respectively. The phylogenetic effect was defined as a hierarchically nested structure "clade/order/family." The phylogenetic clades were classified into the following seven groups according to Angiosperm Phylogeny Group IV (APG IV) classification (APG, 2016): basal angiosperms, chloranthales, magnoliids, monocots, basal eudicots, superrosids, and superasterids (Hu et al., 2020). Basal eudicots indicated unranked eudicot species, i.e., species that were not included in the superrosids and superasterids clades. The overall random term within the variance components model was "environment + [clade/order/family]," and no fixed factor was defined. The variation in leaf traits due to climate and soil was assigned to the "environment" component in the regression models (Watanabe et al., 2007; Zhao et al., 2016). Given the large number of environmental factors involved and their collinearity (**Supplementary Figures 2, 3**), a principal component analysis (PCA) was performed to reduce the number of dimensions of less important environmental factors. Thus, the first three principal components accounted for 72.2% of the total variance and were used in the models to represent the "environment" component (**Supplementary Table 3**). In addition, the interactive effects of environment variables and phylogenetic structure were labeled as "overlap."

All above-mentioned analyses were performed using R 3.4.3 (R Core Team, 2017). The significance of differences in leaf traits among plant growth forms and phylogenetic clades were examined using one-way ANOVA with Tukey's *post hoc* tests in SPSS software v17 (SPSS Inc., Chicago, IL, United States).

RESULTS

Leaf Trait Variation

Our dataset comprised 1,819 terrestrial angiosperm species from 530 sampling sites (**Figure 1**). The five leaf traits showed large variability across species (**Figure 2**). LA showed the largest variation (more than 1000-fold), varying from 0.003 to 1085.61 cm^2. SLA varied by more than 90-fold among species, ranging from 0.83 to 75.14 $m^2\ kg^{-1}$. For leaf nutrient traits, differences of up to 60-fold for LNC (range: 0.09 to 60.10 $mg\ g^{-1}$) and 70-fold for LPC (range: 0.11 to 7.74 $mg\ g^{-1}$) were detected. Significant differences were observed between herbaceous and woody plant groups ($p < 0.05$). Herbaceous species had smaller LA, greater SLA, and higher LNC, and lower LDMC and LPC compared with woody species.

Phylogenetic Signals of the Leaf Traits

The five leaf traits displayed significant phylogenetic signals for all species as well as herbaceous and woody species (**Table 2**). Generally, the phylogenetic signals of LNC and LPC were relatively lower than SLA, LDMC, and LA. Also, the five leaf traits

[8]https://itol.embl.de/

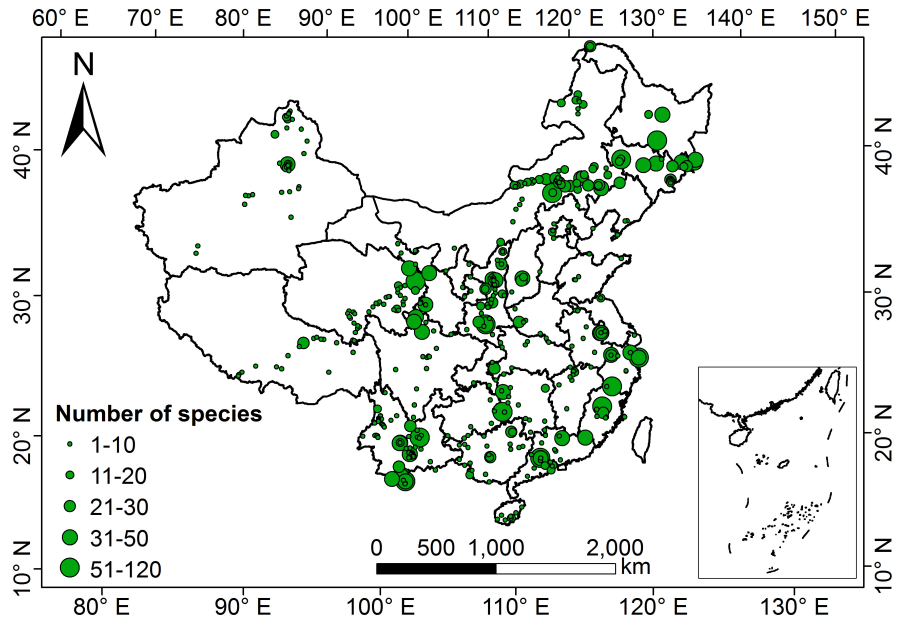

FIGURE 1 | Geographical distribution of sampling sites in China. The size of the green dots on the map indicates the relative number of species measurements.

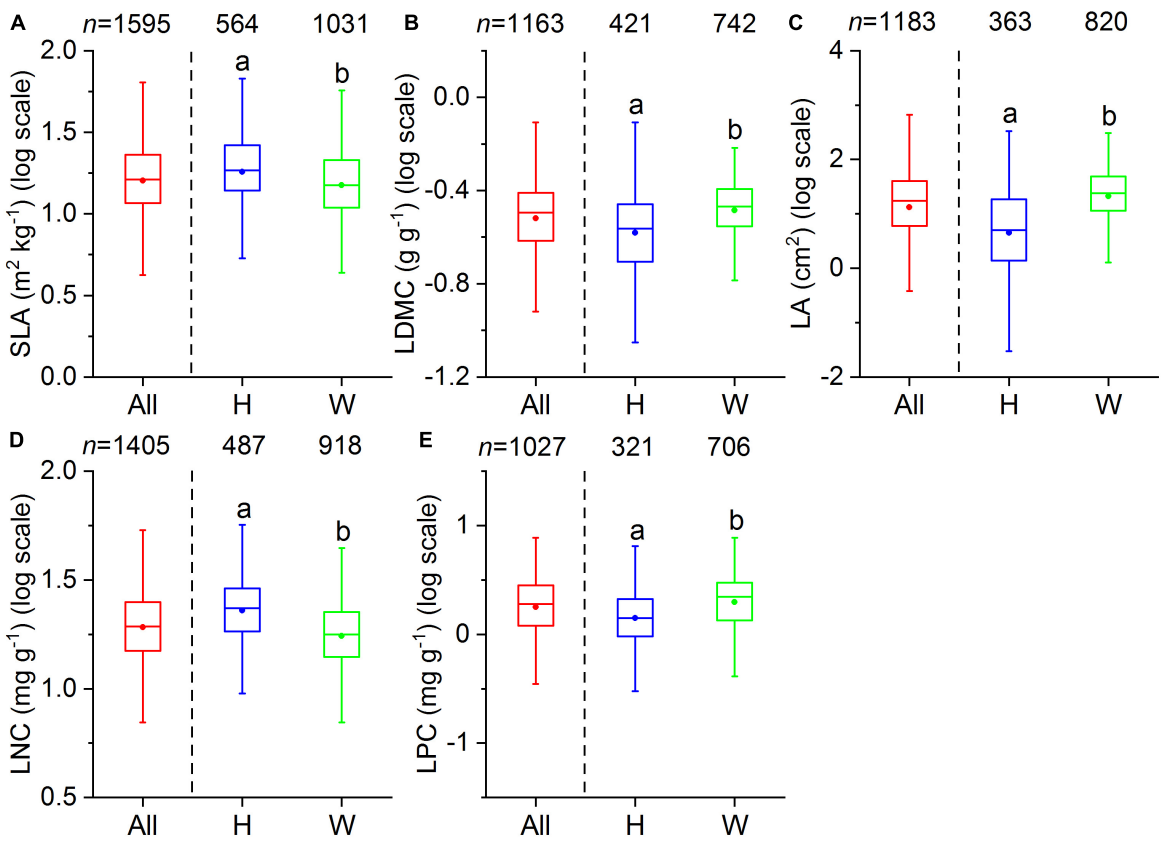

FIGURE 2 | Boxplots of leaf traits for all species (All), herbaceous species (H), and woody species (W). The number above each box indicates the total number of species per group. The bottom and top of the boxplots indicate the first and third quartile, the two whiskers correspond to the 1.5 times of the outliers, and the solid dots within the boxes are the mean values. Different lowercase letters indicate significant differences between herbaceous and woody species ($p < 0.05$). **(A)** SLA, specific leaf area; **(B)** LDMC, leaf dry matter content; **(C)** LA, leaf area; **(D)** LNC, leaf N concentration; **(E)** LPC, leaf P concentration.

TABLE 2 | Phylogenetic signals of the leaf traits evaluated.

	All species		Herbaceous species		Woody species	
	Pagel's λ	*p*	Pagel's λ	*p*	Pagel's λ	*p*
SLA	0.680	<0.001	0.660	<0.001	0.752	<0.001
LDMC	0.788	<0.001	0.770	<0.001	0.668	<0.001
LA	0.839	<0.001	0.656	<0.001	0.781	<0.001
LNC	0.646	<0.001	0.449	<0.001	0.616	<0.001
LPC	0.610	<0.001	0.353	0.03	0.556	<0.001

The leaf trait values are log_{10}-transformed.
SLA, specific leaf area; LDMC, leaf dry matter content; LA, leaf area; LNC, leaf N concentration; LPC, leaf P concentration.

showed significant differences among different phylogenetic clades ($p < 0.05$, **Table 3**). The early-diverged clades (e.g., magnoliids) had larger leaves, smaller SLA, and lower LNC, but higher LDMC than the late-diverged clades (e.g., superasterids and superrosids).

Relationships Between Leaf Traits and Climate and Soil Variables

Specific leaf area was strongly related to MTCM, MTCQ, and PET ($R = -0.118$, -0.114, and -0.118, respectively, all $p < 0.001$) (**Figure 3A**). The relationships between LDMC and most climate variables were significant but weak ($|R| < 0.11$). LA showed strong associations with precipitation indices and had the closest relationships with MPWM and MPWQ ($R = 0.138$ and 0.158, respectively, both $p < 0.001$). LNC was significantly related to most climate variables and showed the strongest correlations with MPDM and MPDQ ($R = -0.200$ and -0.245, respectively, both $p < 0.001$). LPC was most strongly linked to MTWM and MTWQ ($R = 0.219$ and 0.214, respectively, both $p < 0.001$). Most soil variables, especially those associated with soil fertility, showed weak or insignificant associations with leaf traits (**Figure 4A**); however, LDMC was significantly and negatively correlated with pH, $CaCO_3$, and EC ($R = -0.126$, -0.205 and -0.230, respectively, both $p < 0.001$).

The relationships between leaf traits and environment variables showed large variation between herbaceous and woody species. SLA of woody species was more strongly related to MTCM and MTCQ ($R = -0.130$ and -0.126, respectively, both $p < 0.001$) compared with that from herbaceous species (**Figures 3B,C**). LDMC and LPC were closely related to MTWM and MTWQ for both herbaceous and woody species. LA of herbaceous species was more strongly influenced by precipitation indices than temperature indices, especially MAP, GSP, MPWM, and MPWQ (both $R > 0.150$, both $p < 0.001$).The LNC of herbaceous species displayed the closest links to MTWM and MTWQ ($R = -0.237$ and -0.239, respectively, both $p < 0.001$), whereas that from woody species was more strongly related to precipitation indices than temperature indices, especially MPDM and MPDQ ($R = -0.182$ and -0.210, respectively, both $p < 0.001$). Among the soil fertility variables, the LNC of herbaceous species showed strong associations with SOM and STN ($R = 0.202$ and 0.205, respectively, both $p < 0.001$) (**Figure 4B**). LDMC for the woody species and LNC for the herbaceous species were negatively correlated with $CaCO_3$ and EC (both $R < -0.20$, all $p < 0.001$) (**Figures 4B,C**).

The Relative Contributions of Environment Variables and Phylogeny to Leaf Traits

Analysis of the PLMM results showed that environment variables explained most of the variation in leaf traits, accounting for 44.4–65.5% of the total variation (**Figure 5A**). Meanwhile, phylogeny had only weak effects on leaf traits, explaining 3.9–23.3% of the total variation. The effects of phylogeny were mainly observed at the family level, especially for LDMC (17.4%), LNC (10.1%), and SLA (7.2%).

Similarly, environment variables were primary sources of variation in leaf traits for both herbaceous and woody species, accounting for 32.9–75.3 and 34.4–60.9% of the total variation for herbaceous and woody species, respectively (**Figures 5B,C**). Phylogeny also had weak effects on leaf traits for both herbaceous and woody species (1.1–22.9 vs 1.8–16.8%, respectively). In addition, the effects of environment variables and phylogeny on herbaceous and woody species differed among leaf traits. SLA, LA, and LNC for herbaceous species were less influenced by phylogenetic structure compared with woody species. However,

TABLE 3 | Differences in the five leaf traits among phylogenetic clades.

Phylogenetic clade	SLA	LDMC	LA	LNC	LPC
Basal angiosperms*	22.37 ± 11.46	0.23 ± 0.04	63.81 ± 48.42	13.45 ± 4.91	1.95 ± 1.48
Chloranthales*	44.14 ± 5.61	0.14 ± 0.05	9.48 ± 6.21	29.77	4.80
Magnoliids	14.82 ± 7.46a	0.38 ± 0.10a	76.60 ± 152.20a	17.46 ± 5.44a	2.44 ± 1.29a
Monocots	19.94 ± 10.06bc	0.33 ± 0.13b	34.32 ± 110.63b	21.44 ± 7.12b	1.62 ± 0.99b
Basal eudicots	21.70 ± 12.57b	0.29 ± 0.08c	33.38 ± 45.41b	23.05 ± 8.86b	1.65 ± 0.86bc
Superrosids	18.83 ± 11.21c	0.35 ± 0.10ab	38.72 ± 60.43b	21.46 ± 8.01b	2.27 ± 1.15a
Superasterids	18.53 ± 10.16bc	0.28 ± 0.10c	30.57 ± 48.04b	20.17 ± 9.23b	2.06 ± 1.16ac
p-Value	<0.001	<0.001	<0.001	<0.001	<0.001

Letters indicate significant differences among phylogenetic clades ($p < 0.05$).
**Basal angiosperms and chloranthales is not included in ANOVA analyses due to few species ($n < 5$).*
SLA, specific leaf area; LDMC, leaf dry matter content; LA, leaf area; LNC, leaf N concentration; LPC, leaf P concentration.

LDMC and LPC of woody species were more influenced by environment variables than those of herbaceous species.

DISCUSSION

The Effects of Environment Variables on Leaf Traits

Identifying the relationships between leaf traits and the environment variables is helpful for better understanding the impacts of environmental filtering on trait value selection and paleoclimate reconstruction (Peppe et al., 2011; Van Bodegom et al., 2012). Our results showed that environment variables explained the largest proportion of the variation in leaf traits, which was inconsistent with the results of a study by Yang et al. (2018), where the authors reported that environment variables exerted relatively weak effects on SLA and LDMC. A possible explanation for this discrepancy may be that Yang et al. (2018) sampled only a limited number of sites at each biome in eastern and southwestern China, which may have influenced the values for responses of leaf traits to environmental conditions. In particular, our study revealed that climate variability and seasonality variables were more important than MAT and MAP as drivers of leaf trait variation. This result highlighted the importance of climate variability and seasonality variables in regulating the variation in plant functional traits (Moles et al., 2009; Shiono et al., 2015; Wright et al., 2017). For instance, precipitation in the wettest season (i.e., MPWM and MPWQ) was the factor that most (positively) influenced LA variation. A smaller LA could be an adaptative strategy to decrease water loss *via* reducing the surface area for transpiration under dry environmental conditions (Picotte et al., 2007; Du et al., 2019). In the present study, temperature in the warmest season (i.e., MTWM and MTWQ) accounted for the greatest proportion of LNC variation among herbaceous species, and species growing in areas with lower MTWM/MTWQ tended to have higher LNC. This may be related to the fact that species with higher LNC generally have higher rates of photosynthetic C fixation, which would thus offset the lower rates of biochemical reactions observed in cold climates (McGroddy et al., 2004; Reich and Oleksyn, 2004). However, for woody species, precipitation in the driest season (i.e., MPDM and MPDQ) was an important factor for the variation in LNC, and negative relationships were found between the two. A higher LNC can enhance the exploitation of light availability, thereby maximizing the photosynthetic rate under conditions of low precipitation (Cunningham et al., 1999; Wright et al., 2003; Santiago et al., 2004). Overall, these findings identified climate variability and seasonality variables as critical links between resource conditions and plant adaptive strategies, thereby contributing our understanding of leaf trait-climate relationships under future global changes.

In contrast to previously reported results (Ordoñez et al., 2009; Pakeman, 2013; Gong et al., 2020), we found only weak correlations between leaf traits and soil fertility variables. The weakness of these correlations may be partially related to the complexity of soil fertility-mediated regulation on leaf traits, such as the interactive effects among soil nutrients, soil-climate interactions, or differences in the type and magnitude of nutrient limitation (Greenwood et al., 2004; Fujita et al., 2013; Simpson et al., 2016). However, we found strong and negative relationships between LDMC and pH or $CaCO_3$. This indicated that plants tended to invest more in dry matter in nutrient-poor environments, which can enable plants to have high construction costs and longer lifespans (Hodgson et al., 2011; Jager et al., 2015; Maire et al., 2015). Strong and negative relationships were also observed between LDMC and EC, in contrast to the positive or no correlations reported by other studies (Wang et al., 2015; De Battisti et al., 2020). This discrepancy may be attributable to differences in species composition between our and previous studies that may have resulted in heterogeneous responses to soil salinity. For instance, our study comprised a large number of species, whereas other studies examined only one species or relatively few halophyte species (Wang et al., 2015; De Battisti et al., 2020).

In addition, we found that environment variables explained most of variation in leaf traits for both herbaceous and woody species. However, the strength of environmental effects on herbaceous and woody species varied among leaf traits. For example, LDMC, LA, and LPC for woody species were more influenced by environment variables compared with herbaceous species, which is consistent with a previous study reporting that LPC was more environmentally constrained than phylogenetic effect in shrubland biomes (Yang et al., 2016). This reflected that woody and herbaceous species have different ecological strategies to cope with changing environments, especially fluctuating and seasonally inhospitable climates (Zanne et al., 2014; Qian et al., 2017). Compared with herbaceous plants, woody plants generally with larger plant sizes and higher investment in tissue construction and maintenance (e.g., higher LDMC) expose in climate, which can facilitate adaptation to unfavorable environments (Ricklefs and Latham, 1992; Wang et al., 2020; Zhou et al., 2020). Further studies that explore which leaf traits strongly respond to climate conditions for different plant growth forms could improve our understanding of the effects of climate changes on ecosystem functions.

The Effects of Phylogeny on Leaf Traits

Our results demonstrated that phylogeny had a weak effect on leaf trait variation, which was in contrast to recent studies that have reported phylogeny as the most important contributor to the variance in leaf traits (Valverde-Barrantes et al., 2017; Yang et al., 2018). We attributed this inconsistency to the different evolutionary processes associated with the different taxa and phylogenetic scales studied (Figueroa and Smith, 2020; Valverde-Barrantes et al., 2020). The weak effects of phylogeny were indicative of evolutionary lability during seed plant diversification, resulting in considerable trait distinctiveness across lineages (Cornwell et al., 2014; Amaral et al., 2021). Furthermore, most of the phylogenetic effects on leaf traits were observed at the family level, which is consistent with the findings of previous studies (Yang et al., 2018; Zhang et al., 2019). This result is also in line with evidence indicating that plant functional traits are conserved at the family level

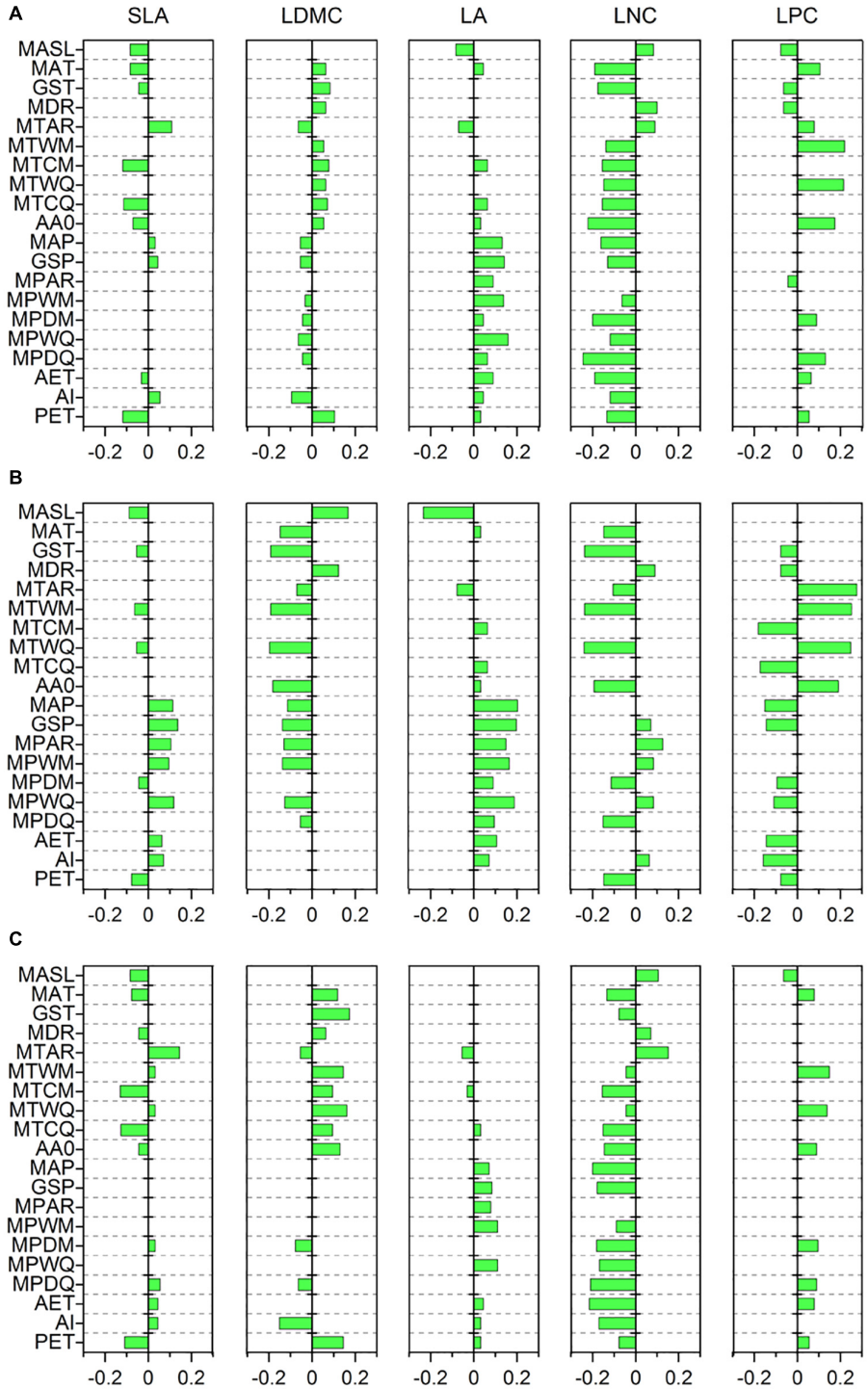

FIGURE 3 | Correlations of leaf traits with climate variables based on a phylogenetic linear mixed model (PLMM). Significant correlations between leaf traits and climate variables are shown ($p < 0.05$). Positive values represent positive correlations between leaf traits and climate variables, while negative values represent negative correlations between them. **(A)** All species; **(B)** herbaceous species; **(C)** woody species. SLA, specific leaf area; LDMC, leaf dry matter content; LA, leaf area; LNC, leaf N concentration; LPC, leaf P concentration; MASL, mean annual sunlight; MAT, mean annual temperature; GST, mean growing season temperature; MDR, mean diurnal range; MTAR, mean annual range of temperature; MTWM, mean temperature of the warmest month of a year; MTCM, mean temperature of the coldest month of a year; MTWQ, mean temperature of the warmest quarter of a year; MTCQ, mean temperature of the coldest quarter of a year; AA0, active accumulated temperature above 0°C; MAP, mean annual precipitation; GSP, mean growing season precipitation; MPAR, mean annual range of precipitation; MPWM, mean precipitation of the wettest month of a year; MPDM, mean precipitation of the driest month of a year; MPWQ, mean precipitation of the wettest quarter of a year; MPDQ, mean precipitation of the driest quarter of a year; AET, actual evapotranspiration; AI, aridity index; PET, potential evapotranspiration.

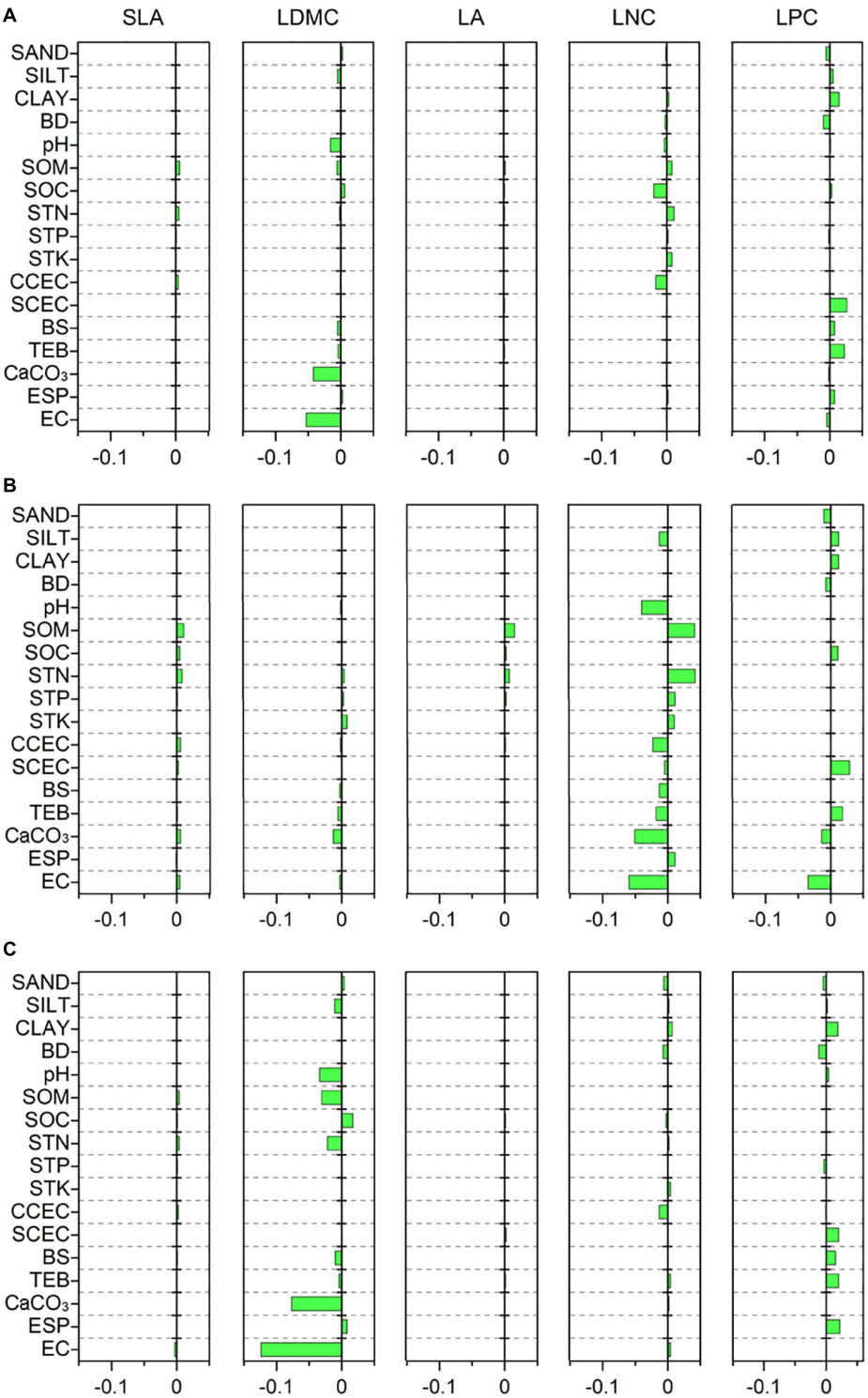

FIGURE 4 | Correlations of leaf traits with soil variables based on a phylogenetic linear mixed model (PLMM). Significant correlations between leaf traits and soil variables are shown ($p < 0.05$). Positive values represent positive correlations between leaf traits and soil variables, while negative values represent negative correlations between them. **(A)** All species; **(B)** herbaceous species; **(C)** woody species. SLA, specific leaf area; LDMC, leaf dry matter content; LA, leaf area; LNC, leaf N concentration; LPC, leaf P concentration; SAND, percentage of sand fraction; SILT, percentage of silt fraction; CLAY, percentage of clay fraction; BD, bulk density; SOM, soil organic matter; SOC, soil organic carbon; STN, soil total N; STP, soil total P; STK, soil total K; CCEC, clay cation exchange capacity; SCEC, soil cation exchange capacity; BS, base saturation; TEB, total exchangeable bases; $CaCO_3$, calcium carbonate content; ESP, exchangeable sodium percentage; EC, electrical conductivity.

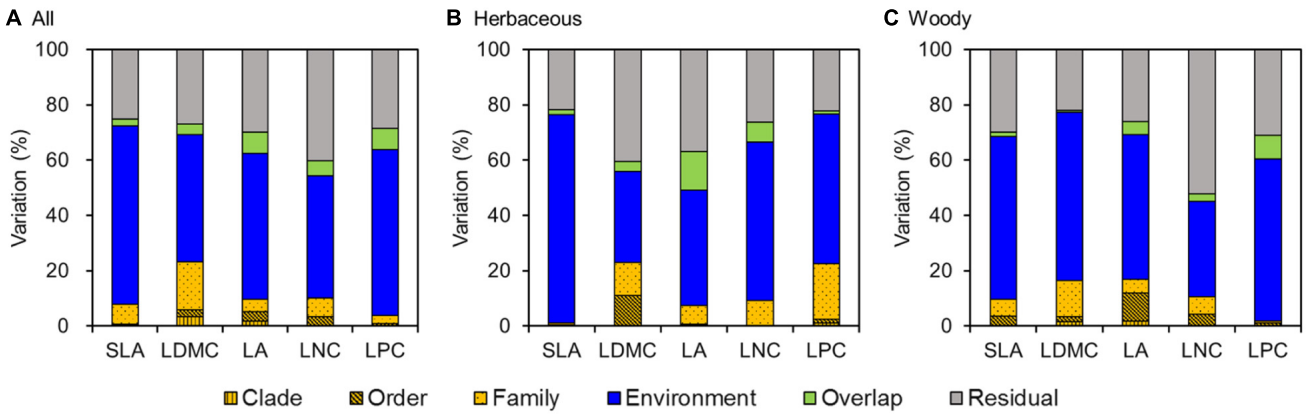

FIGURE 5 | Variance partitioning for leaf traits using a phylogenetic linear mixed model (PLMM) for **(A)** all species, **(B)** herbaceous species, and **(C)** woody species. SLA, specific leaf area; LDMC, leaf dry matter content; LA, leaf area; LNC, leaf N concentration; LPC, leaf P concentration.

(Kerkhoff et al., 2006; Qian and Zhang, 2016), suggesting that different patterns of geographic distribution of various families reflect their adaptations to specific geographical and climatic contexts (Cornwell et al., 2014).

We found that phylogenetic effects on herbaceous and woody species also differed among leaf traits. SLA, LA, and LNC for herbaceous species were less influenced by phylogeny compared with woody species. This result is consistent with the study of Flores et al. (2014) who found that leaf mass per area of herbaceous species showed lower phylogenetic conservatism than that of woody species, and also partly supported previous studies suggesting that herbaceous plants have higher evolutionary rate, phylogenetic turnover and lower phylogenetic conservatism compared with woody plants (Smith and Donoghue, 2008; Smith and Beaulieu, 2009; Hawkins et al., 2011). However, LDMC and LPC for herbaceous were more influenced by phylogenetic effects compared with woody species in this present study, which supported the above-mentioned results in which these traits were more environmentally constrained. The different responses of leaf traits to phylogeny between herbaceous and woody species may result from differences in evolutionary processes (e.g., evolutionary rate and stabilizing selection) (Flores et al., 2014; Zhou et al., 2018; Wang et al., 2020).

The Interactive Effects of Environment Variables and Phylogeny on Leaf Traits

In the present study, we detected interactive effects of environment variables and phylogeny on leaf traits, indicating that phylogenetic structure across lineages is mediated by environmental filtering (Crisp et al., 2009; Gagnon et al., 2019). For instance, Proteaceae with lower LNC for a given SLA were found to be more frequent in infertile soils, suggesting that they are associated with a slow return position on the LES (Cornwell et al., 2014; Delgado et al., 2018). Major evolutionary lineages that were restricted to specific environmental conditions may reflect their preferred environmental regimes (Sanchez-Martinez et al., 2020). Therefore, further studies on distinctive plant lineage-trait combinations under different environmental contexts are helpful for elucidating the shifts in plant trait syndromes under changing environmental conditions.

Uncertainties and Research Directions

In our study, we used a large leaf trait dataset to elucidate the relative importance of environment variables and phylogeny on leaf traits between herbaceous and woody species in China; however, some uncertainties remain. First, the limited number of species evaluated from habitats in northwestern China, i.e., deserts and alpine tundra, may have biased the interpretation of leaf trait variation and their relationships with environmental factors. Future studies should include a greater number of species from this area of China to test the generality of our results. Second, we used a species-level phylogenetic tree of Chinese vascular plants that was based on a variety of molecular sequences (Chen et al., 2016; Hu et al., 2020). Some studies have demonstrated that phylogenies representing different levels of phylogenetic resolution (i.e., family, genus, and species) may result in some bias in quantification of phylogenetic structure (Molina-Venegas and Roquet, 2014; Qian and Jin, 2021). Further studies in developing phylogenies well resolved at the genus or species level with more species and gene markers will help for better understanding the geographical patterns of plant traits at the large scale (Janssens et al., 2020). Third, our measures of soil variables were represented by the large-scale estimations of soil properties, which may not reflect the high heterogeneity of soil properties at multiple spatial scales and may introduce some uncertainties regarding the correlations between leaf traits and soil variables. Finally, we did not consider the interactive effects of climate and soil on leaf trait variation. The geographical patterns of leaf traits in a given climate may depend on the level of soil fertility (Ordoñez et al., 2009; Simpson et al., 2016). Future studies that determine the effects of climate-soil interactions on leaf trait variation should

improve our understanding of plant community responses to environmental change.

CONCLUSION

Our study provided a comprehensive analysis of how environment variables and phylogeny contribute to the variation in key leaf traits between herbaceous and woody plant species in China. Environment variables explained most of the variation in leaf traits, whereas phylogeny had only a weak effect. Our study highlighted the importance of climate variability and seasonality variables in determining leaf trait variation, providing important information regarding ecological adaptations used by plants to cope with seasonal and fluctuating climatic conditions. Furthermore, the responses of leaf traits to environment variables and phylogeny were different between herbaceous and woody species, suggesting that shifts in plant growth form are important factors in predicting changes in plant traits and ecosystem functions under future climate change.

DATA AVAILABILITY STATEMENT

The raw data supporting the conclusions of this article will be made available by the authors, without undue reservation.

AUTHOR CONTRIBUTIONS

NA conceived the ideas and collected the data. NA and NL led the writing of the manuscript. All authors contributed critically to the drafts and gave the final approval for publication.

FUNDING

This work was supported by the National Key R&D Program of China (2017YFA0604702) and the International Partnership Program of Chinese Academy of Sciences (121311KYSB20170004).

ACKNOWLEDGMENTS

We thank Shuang Zhang for the assistance in statistical analyses.

SUPPLEMENTARY MATERIAL

The Supplementary Material for this article can be found online at: https://www.frontiersin.org/articles/10.3389/fpls.2021.799401/full#supplementary-material

REFERENCES

Albert, C. H., Thuiller, W., Yoccoz, N. G., Soudant, A., Boucher, F., Saccone, P., et al. (2010). Intraspecific functional variability: extent, structure and sources of variation. *J. Ecol.* 98, 604–613. doi: 10.1111/j.1365-2745.2010.01651.x

Ali, A., Yan, E. R., Chang, S. X., Cheng, J. Y., and Liu, X. Y. (2017). Community-weighted mean of leaf traits and divergence of wood traits predict aboveground biomass in secondary subtropical forests. *Sci. Total Environ.* 574, 654–662. doi: 10.1016/j.scitotenv.2016.09.022

Amaral, E. J., Franco, A. C., Rivera, V. L., and Munhoz, C. B. R. (2021). Environment, phylogeny, and photosynthetic pathway as determinants of leaf traits in savanna and forest graminoid species in central Brazil. *Oecologia* 197, 1–11. doi: 10.1007/s00442-021-04923-w

APG (2016). An update of the Angiosperm Phylogeny Group classification for the orders and families of flowering plants: APG IV. *Bon. J. Linn. Soc.* 181, 1–20. doi: 10.1111/boj.12385

Asner, G. P., and Martin, R. E. (2016). Convergent elevation trends in canopy chemical traits of tropical forests. *Global Change Biol.* 22, 2216–2227. doi: 10.1111/gcb.13164

Chamberlain, S. A., Hovick, S. M., Dibble, C. J., Rasmussen, N. L., Van Allen, B. G., Maitner, B. S., et al. (2012). Does phylogeny matter? Assessing the impact of phylogenetic information in ecological meta-analysis. *Ecol. Lett.* 15, 627–636. doi: 10.1111/j.1461-0248.2012.01776.x

Chen, Z. D., Yang, T., Lin, L., Lu, L. M., Li, H. L., Sun, M., et al. (2016). Tree of life for the genera of Chinese vascular plants. *J. Syst. Evol.* 54, 277–306. doi: 10.1111/jse.12219

Cornwell, W. K., Westoby, M., Falster, D. S., FitzJohn, R. G., O'Meara, B. C., Pennell, M. W., et al. (2014). Functional distinctiveness of major plant lineages. *J. Ecol.* 102, 345–356. doi: 10.1111/1365-2745.12208

Crisp, M. D., Arroyo, M. T., Cook, L. G., Gandolfo, M. A., Jordan, G. J., McGlone, M. S., et al. (2009). Phylogenetic biome conservatism on a global scale. *Nature* 458, 754–756. doi: 10.1038/nature07764

Cunningham, S. A., Summerhayes, B., and Westoby, M. (1999). Evolutionary divergences in leaf structure and chemistry, comparing rainfall and soil nutrient gradients. *Ecol. Monog.* 69, 569–588.

De Battisti, D., Fowler, M. S., Jenkins, S. R., Skov, M. W., Bouma, T. J., Neyland, P. J., et al. (2020). Multiple trait dimensions mediate stress gradient effects on plant biomass allocation, with implications for coastal ecosystem services. *J. Ecol.* 108, 1227–1240. doi: 10.1111/1365-2745.13393

de la Riva, E. G., Villar, R., Pérez-Ramos, I. M., Quero, J. L., Matías, L., Poorter, L., et al. (2017). Relationships between leaf mass per area and nutrient concentrations in 98 Mediterranean woody species are determined by phylogeny, habitat and leaf habit. *Trees* 32, 497–510. doi: 10.1007/s00468-017-1646-z

Delgado, M., Valle, S., Reyes-Diaz, M., Barra, P. J., and Zuniga-Feest, A. (2018). Nutrient use efficiency of southern south America Proteaceae Species. Are there general patterns in the Proteaceae family? *Front. Plant Sci.* 9:883. doi: 10.3389/fpls.2018.00883

Delpiano, C. A., Prieto, I., Loayza, A. P., Carvajal, D. E., and Squeo, F. A. (2020). Different responses of leaf and root traits to changes in soil nutrient availability do not converge into a community-level plant economics spectrum. *Plant Soil* 450, 463–478. doi: 10.1007/s11104-020-04515-2

Diaz, S., Hodgson, J. G., Thompson, K., Cabido, M., Cornelissen, J. H. C., Jalili, A., et al. (2004). The plant traits that drive ecosystems: evidence from three continents. *J. Veg. Sci.* 15, 295–304. doi: 10.1111/j.1654-1103.2004.tb02266.x

Diaz, S., Kattge, J., Cornelissen, J. H., Wright, I. J., Lavorel, S., Dray, S., et al. (2016). The global spectrum of plant form and function. *Nature* 529, 167–171. doi: 10.1038/nature16489

Du, L., Liu, H., Guan, W., Li, J., and Li, J. (2019). Drought affects the coordination of belowground and aboveground resource-related traits in Solidago canadensis in China. *Ecol. Evol.* 9, 9948–9960. doi: 10.1002/ece3.5536

Ernakovich, J. G., Hopping, K. A., Berdanier, A. B., Simpson, R. T., Kachergis, E. J., Steltzer, H., et al. (2014). Predicted responses of arctic and alpine ecosystems to altered seasonality under climate change. *Global Change Biol.* 20, 3256–3269. doi: 10.1111/gcb.12568

Fang, J. Y., Guo, K., Wang, G. H., Tang, Z. Y., Xie, Z. Q., Shen, Z. H., et al. (2020). Vegetation classification system and classification of vegetation types used for the compilation of vegetation of China. *Chin. J. Plant Ecol.* 44, 96–110.

FAO, IIASA, ISRIC, ISSCAS, and JRC (2012). *Harmonized World Soil Database (Version 1.2)*. Rome: FAO.

Figueroa, H., and Smith, S. A. (2020). A targeted phylogenetic approach helps explain New World functional diversity patterns of two eudicot lineages. *J. Biogeogr.* 48, 202–215. doi: 10.1111/jbi.13993

Flores, O., Garnier, E., Wright, I. J., Reich, P. B., Pierce, S., Diaz, S., et al. (2014). An evolutionary perspective on leaf economics: phylogenetics of leaf mass per area in vascular plants. *Ecol. Evol.* 4, 2799–2811. doi: 10.1002/ece3.1087

Freckleton, R. P., Harvey, P. H., and Pagel, M. (2002). Phylogenetic analysis and comparative data: a test and review of evidence. *Am. Nat.* 160, 712–726. doi: 10.1086/343873

Fujita, Y., van Bodegom, P. M., and Witte, J. P. M. (2013). Relationships between nutrient-related plant traits and combinations of soil N and P fertility measures. *PLoS One* 8:e83735. doi: 10.1371/journal.pone.0083735

Gagnon, E., Ringelberg, J. J., Bruneau, A., Lewis, G. P., and Hughes, C. E. (2019). Global succulent biome phylogenetic conservatism across the pantropical Caesalpinia Group (Leguminosae). *New Phytol.* 222, 1994–2008. doi: 10.1111/nph.15633

Gong, H. D., Cui, Q. J., and Gao, J. (2020). Latitudinal, soil and climate effects on key leaf traits in northeastern China. *Glob. Ecol. Conserv.* 22:e00904. doi: 10.1016/j.gecco.2020.e00904

Greenwood, D. R., Wilf, P., Wing, S. L., and Christophel, D. C. (2004). Paleotemperature estimation using leaf-margin analysis: is Australia different? *Palaios* 19, 129–142. doi: 10.1669/0883-13512004019<0129:peulai<2.0.co;2

Hancock, P. A., and Hutchinson, M. F. (2006). Spatial interpolation of large climate data sets using bivariate thin plate smoothing splines. *Environ. Modell. Softw.* 21, 1684–1694. doi: 10.1016/j.envsoft.2005.08.005

Hawkins, B. A., Rodríguez, M. Á, and Weller, S. G. (2011). Global angiosperm family richness revisited: linking ecology and evolution to climate. *J. Biogeogr.* 38, 1253–1266. doi: 10.1111/j.1365-2699.2011.02490.x

He, J. S., Wang, X. P., Schmid, B., Flynn, D. F. B., Li, X. F., Reich, P. B., et al. (2010). Taxonomic identity, phylogeny, climate and soil fertility as drivers of leaf traits across Chinese grassland biomes. *J. Plant Res.* 123, 551–561. doi: 10.1007/s10265-009-0294-9

Hodgson, J. G., Montserrat-Marti, G., Charles, M., Jones, G., Wilson, P., Shipley, B., et al. (2011). Is leaf dry matter content a better predictor of soil fertility than specific leaf area? *Ann. Bot.* 108, 1337–1345. doi: 10.1093/aob/mcr225

Hu, H. H., Liu, B., Liang, Y. S., Ye, J. F., Saqib, S., Meng, Z., et al. (2020). An updated Chinese vascular plant tree of life: phylogenetic diversity hotspots revisited. *J. Syst. Evol.* 58, 663–672. doi: 10.1111/jse.12642

Jager, M. M., Richardson, S. J., Bellingham, P. J., Clearwater, M. J., Laughlin, D. C., and De Deyn, G. (2015). Soil fertility induces coordinated responses of multiple independent functional traits. *J. Ecol.* 103, 374–385. doi: 10.1111/1365-2745.12366

Janssens, S. B., Couvreur, T. L. P., Mertens, A., Dauby, G., Dagallier, L. M. J., Vanden Abeele, S., et al. (2020). A large-scale species level dated angiosperm phylogeny for evolutionary and ecological analyses. *Biodivers. Data J.* 8:e39677. doi: 10.3897/BDJ.8.e39677

Kattge, J., Diaz, S., Lavorel, S., Prentice, C., Leadley, P., Bonisch, G., et al. (2011). TRY – a global database of plant traits. *Global Change Biol.* 17, 2905–2935. doi: 10.1111/j.1365-2486.2011.02451.x

Kerkhoff, A. J., Fagan, W. F., Elser, J. J., and Enquist, B. J. (2006). Phylogenetic and growth form variation in the scaling of nitrogen and phosphorus in the seed plants. *Am. Nat.* 168, E103–E122. doi: 10.1086/507879

Kikuzawa, K., Onoda, Y., Wright, I. J., and Reich, P. B. (2013). Mechanisms underlying global temperature-related patterns in leaf longevity. *Global Ecol. Biogeogr.* 22, 982–993. doi: 10.1111/geb.12042

Lanfear, R., Ho, S. Y., Jonathan Davies, T., Moles, A. T., Aarssen, L., Swenson, N. G., et al. (2013). Taller plants have lower rates of molecular evolution. *Nat. Commun.* 4:1879. doi: 10.1038/ncomms2836

Lavorel, S., and Garnier, E. (2002). Predicting changes in community composition and ecosystem functioning from plant traits: revisiting the Holy Grail. *Funct. Ecol.* 16, 545–556. doi: 10.1046/j.1365-2435.2002.00664.x

Letunic, I., and Bork, P. (2019). Interactive Tree Of Life (iTOL) v4: recent updates and new developments. *Nucleic Acids Res.* 47, W256–W259. doi: 10.1093/nar/gkz239

Li, Y. Q., He, W., Wu, J., Zhao, P., Chen, T., Zhu, L. W., et al. (2021). Leaf stoichiometry is synergistically-driven by climate, site, soil characteristics and phylogeny in karst areas, Southwest China. *Biogeochemistry* 155, 283–301. doi: 10.1007/s10533-021-00826-3

Maire, V., Wright, I. J., Prentice, I. C., Batjes, N. H., Bhaskar, R., van Bodegom, P. M., et al. (2015). Global effects of soil and climate on leaf photosynthetic traits and rates. *Global Ecol. Biogeogr.* 24, 706–717. doi: 10.1111/geb.12296

Mason, C. M., and Donovan, L. A. (2015). Does investment in leaf defenses drive changes in leaf economic strategy? A focus on whole-plant ontogeny. *Oecologia* 177, 1053–1066. doi: 10.1007/s00442-014-3177-2

McGroddy, M. E., Daufresne, T., and Hedin, L. O. (2004). Scaling of C:N:P stoichiometry in forests worldwide: implications of terrestrial redfield-type ratios. *Ecology* 85, 2390–2401. doi: 10.1890/03-0351

Meng, Z., Li, J. H., Yang, T., Lin, L., and Chen, Z. D. (2015). "SoTree: an automated phylogeny assembly tool for ecologists from big tree," in *Proceedings of the 2015 IEEE International Conference on Smart City*, Chengdu, 792–797.

Messier, J., McGill, B. J., and Lechowicz, M. J. (2010). How do traits vary across ecological scales? A case for trait-based ecology. *Ecol. Lett.* 13, 838–848. doi: 10.1111/j.1461-0248.2010.01476.x

Moles, A. T., Warton, D. I., Warman, L., Swenson, N. G., Laffan, S. W., Zanne, A. E., et al. (2009). Global patterns in plant height. *J. Ecol.* 97, 923–932. doi: 10.1111/j.1365-2745.2009.01526.x

Molina-Venegas, R., and Roquet, C. (2014). Directional biases in phylogenetic structure quantification: a Mediterranean case study. *Ecography* 37, 572–580. doi: 10.1111/j.1600-0587.2013.00442.x

Ordoñez, J. C., van Bodegom, P. M., Witte, J.-P. M., Wright, I. J., Reich, P. B., and Aerts, R. (2009). A global study of relationships between leaf traits, climate and soil measures of nutrient fertility. *Global Ecol. Biogeogr.* 18, 137–149. doi: 10.1111/j.1466-8238.2008.00441.x

Pagel, M. (1999). Inferring the historical patterns of biological evolution. *Nature* 401, 877–884. doi: 10.1038/44766

Pakeman, R. J. (2013). Intra-specific leaf trait variation: management and fertility matter more than the climate at continental scales. *Folia Geobot.* 48, 355–371. doi: 10.1007/s12224-013-9168-y

Pakeman, R. J., Eastwood, A., and Scobie, A. (2010). Leaf dry matter content as a predictor of grassland litter decomposition: a test of the 'mass ratio hypothesis'. *Plant Soil* 342, 49–57. doi: 10.1007/s11104-010-0664-z

Paradis, E., and Schliep, K. (2019). ape 5.0: an environment for modern phylogenetics and evolutionary analyses in R. *Bioinformatics* 35, 526–528. doi: 10.1093/bioinformatics/bty633

Peppe, D. J., Royer, D. L., Cariglino, B., Oliver, S. Y., Newman, S., Leight, E., et al. (2011). Sensitivity of leaf size and shape to climate: global patterns and paleoclimatic applications. *New Phytol.* 190, 724–739. doi: 10.1111/j.1469-8137.2010.03615.x

Perez-Harguindeguy, N., Diaz, S., Garnier, E., Lavorel, S., Poorter, H., Jaureguiberry, P., et al. (2013). New handbook for standardised measurement of plant functional traits worldwide. *Aust. Bot.* 61, 167–234. doi: 10.1071/bt12225

Peterson, R. A., and Cavanaugh, J. E. (2019). Ordered quantile normalization: a semiparametric transformation built for the cross-validation era. *J. Appl. Stat.* 47, 2312–2327. doi: 10.1080/02664763.2019.1630372

Picotte, J. J., Rosenthal, D. M., Rhode, J. M., and Cruzan, M. B. (2007). Plastic responses to temporal variation in moisture availability: consequences for water use efficiency and plant performance. *Oecologia* 153, 821–832. doi: 10.1007/s00442-007-0794-z

Qian, H., and Jin, Y. (2021). Are phylogenies resolved at the genus level appropriate for studies on phylogenetic structure of species assemblages? *Plant Divers.* 43, 255–263. doi: 10.1016/j.pld.2020.11.005

Qian, H., and Zhang, J. (2016). Are phylogenies derived from family-level supertrees robust for studies on macroecological patterns along environmental gradients? *J. Syst. Evol.* 54, 29–36. doi: 10.1111/jse.12161

Qian, H., Jin, Y., and Ricklefs, R. E. (2017). Phylogenetic diversity anomaly in angiosperms between eastern Asia and eastern North America. *Proc. Natl. Acad. Sci. U.S.A.* 114, 11452–11457. doi: 10.1073/pnas.1703985114

R Core Team (2017). *R: A Language and Environment for Statistical Computing*. Vienna: R Foundation for Statistical Computing.

Reich, P. B., and Oleksyn, J. (2004). Global patterns of plant leaf N and P in relation to temperature and latitude. *Proc. Natl. Acad. Sci. U.S.A.* 101, 11001–11006. doi: 10.1073/pnas.0403588101

Reich, P. B., Uhl, C., Walters, M. B., and Ellsworth, D. S. (1991). Leaf life-span as a determinant of leaf structure and function among 23 Amazonian tree species. *Oecologia* 86, 16–24. doi: 10.1007/BF00317383

Revell, L. J. (2012). Phytools: an R package for phylogenetic comparative biology (and other things). *Methods Ecol. Evol.* 3, 217–223. doi: 10.1111/j.2041-210X.2011.00169.x

Ricklefs, R. E., and Latham, R. E. (1992). Intercontinental correlation of geographical ranges suggests stasis in ecological traits of relict genera of temperate perennial herbs. *Am. Nat.* 139, 1305–1321. doi: 10.1086/285388

Rohlf, F. J. (2006). A comment on phylogenetic correction. *Evolution* 60, 1509–1515. doi: 10.1111/j.0014-3820.2006.tb01229.x

Rossatto, D. R., and Franco, A. C. (2017). Expanding our understanding of leaf functional syndromes in savanna systems: the role of plant growth form. *Oecologia* 183, 953–962. doi: 10.1007/s00442-017-3815-6

Sanchez-Martinez, P., Martinez-Vilalta, J., Dexter, K. G., Segovia, R. A., and Mencuccini, M. (2020). Adaptation and coordinated evolution of plant hydraulic traits. *Ecol. Lett.* 23, 1599–1610. doi: 10.1111/ele.13584

Santiago, L. S., and Wright, S. J. (2007). Leaf functional traits of tropical forest plants in relation to growth form. *Funct. Ecol.* 21, 19–27. doi: 10.1111/j.1365-2435.2006.01218.x

Santiago, L. S., Kitajima, K., Wright, S. J., and Mulkey, S. S. (2004). Coordinated changes in photosynthesis, water relations and leaf nutritional traits of canopy trees along a precipitation gradient in lowland tropical forest. *Oecologia* 139, 495–502. doi: 10.1007/s00442-004-1542-2

Shiono, T., Kusumoto, B., Maeshiro, R., Fujii, S.-J., Götzenberger, L., de Bello, F., et al. (2015). Climatic drivers of trait assembly in woody plants in Japan. *J. Biogeogr.* 42, 1176–1186. doi: 10.1111/jbi.12503

Šímová, I., Violle, C., Svenning, J.-C., Kattge, J., Engemann, K., Sandel, B., et al. (2018). Spatial patterns and climate relationships of major plant traits in the New World differ between woody and herbaceous species. *J. Biogeogr.* 45, 895–916. doi: 10.1111/jbi.13171

Simpson, A. H., Richardson, S. J., and Laughlin, D. C. (2016). Soil-climate interactions explain variation in foliar, stem, root and reproductive traits across temperate forests. *Global Ecol. Biogeogr.* 25, 964–978. doi: 10.1111/geb.12457

Smith, S. A., and Beaulieu, J. M. (2009). Life history influences rates of climatic niche evolution in flowering plants. *Proc. R. Soc. Lond. B Biol. Sci.* 276, 4345–4352. doi: 10.1098/rspb.2009.1176

Smith, S. A., and Donoghue, M. J. (2008). Rates of molecular evolution are linked to life history in flowering plants. *Science* 322, 86–89. doi: 10.1126/science.1163197

Stock, W. D., and Verboom, G. A. (2012). Phylogenetic ecology of foliar N and P concentrations and N:P ratios across mediterranean-type ecosystems. *Global Ecol. Biogeogr.* 21, 1147–1156. doi: 10.1111/j.1466-8238.2011.00752.x

Trabucco, A., and Zomer, R. J. (2009). *Global Aridity Index (Global-Aridity) and Global Potential Evapo-Transpiration (Global-PET) Geospatial Database. CGIAR Consortium for Spatial Information*. Available online at: http://www.csi.cgiar.org

Valverde-Barrantes, O. J., Freschet, G. T., Roumet, C., and Blackwood, C. B. (2017). A worldview of root traits: the influence of ancestry, growth form, climate and mycorrhizal association on the functional trait variation of fine-root tissues in seed plants. *New Phytol.* 215, 1562–1573. doi: 10.1111/nph.14571

Valverde-Barrantes, O. J., Maherali, H., Baraloto, C., and Blackwood, C. B. (2020). Independent evolutionary changes in fine-root traits among main clades during the diversification of seed plants. *New Phytol.* 228, 541–553. doi: 10.1111/nph.16729

Van Bodegom, P. M., Douma, J. C., Witte, J. P. M., Ordoñez, J. C., Bartholomeus, R. P., and Aerts, R. (2012). Going beyond limitations of plant functional types when predicting global ecosystem-atmosphere fluxes: exploring the merits of traits-based approaches. *Global Ecol. Biogeogr.* 21, 625–636. doi: 10.1111/j.1466-8238.2011.00717.x

van Kleunen, M., Weber, E., and Fischer, M. (2010). A meta-analysis of trait differences between invasive and non-invasive plant species. *Ecol. Lett.* 13, 235–245. doi: 10.1111/j.1461-0248.2009.01418.x

Wang, H., Harrison, S. P., Prentice, I. C., Yang, Y. Z., Bai, F., Togashi, H. F., et al. (2018). The China plant trait database: toward a comprehensive regional compilation of functional traits for land plants. *Ecology* 99:500. doi: 10.1002/ecy.2091

Wang, L. L., Zhao, G. X., Li, M., Zhang, M. T., Zhang, L. F., Zhang, X. F., et al. (2015). C:N:P stoichiometry and leaf traits of halophytes in an arid saline environment, northwest China. *PLoS One* 10:e0119935. doi: 10.1371/journal.pone.0119935

Wang, Y. F., Case, B., Rossi, S., Dawadi, B., Liang, E. Y., and Ellison, A. M. (2019). Frost controls spring phenology of juvenile Smith fir along elevational gradients on the southeastern Tibetan Plateau. *Int. J. Biometeorol.* 63, 963–972. doi: 10.1007/s00484-019-01710-4

Wang, Y. Y., Lyu, T., Luo, A., Li, Y. Q., Liu, Y. P., Freckleton, R. P., et al. (2020). Spatial patterns and drivers of angiosperm sexual systems in China differ between woody and herbaceous species. *Front. Plant Sci.* 11:10. doi: 10.3389/fpls.2020.01222

Watanabe, T., Broadley, M. R., Jansen, S., White, P. J., Takada, J., Satake, K., et al. (2007). Evolutionary control of leaf element composition in plants. *New Phytol.* 174, 516–523. doi: 10.1111/j.1469-8137.2007.02078.x

Wilson, P. J., Thompson, K., and Hodgson, J. G. (1999). Specific leaf area and leaf dry matter content as alternative predictors of plant strategies. *New Phytol.* 143, 155–162. doi: 10.1046/j.1469-8137.1999.00427.x

Wright, I. J., Dong, N., Maire, V., Prentice, I. C., Westoby, M., Diaz, S., et al. (2017). Global climatic drivers of leaf size. *Science* 357, 917–921. doi: 10.1126/science.aal4760

Wright, I. J., Reich, P. B., and Westoby, M. (2003). Least-cost input mixtures of water and nitrogen for photosynthesis. *Am. Nat.* 161, 98–111. doi: 10.1086/344920

Wright, I. J., Reich, P. B., Cornelissen, J. H. C., Falster, D. S., Groom, P. K., Hikosaka, K., et al. (2005a). Modulation of leaf economic traits and trait relationships by climate. *Global Ecol. Biogeogr.* 14, 411–421. doi: 10.1111/j.1466-822x.2005.00172.x

Wright, I. J., Reich, P. B., Cornelissen, J. H., Falster, D. S., Garnier, E., Hikosaka, K., et al. (2005b). Assessing the generality of global leaf trait relationships. *New Phytol.* 166, 485–496. doi: 10.1111/j.1469-8137.2005.01349.x

Wright, I. J., Reich, P. B., Westoby, M., Ackerly, D. D., Baruch, Z., Bongers, F., et al. (2004). The worldwide leaf economics spectrum. *Nature* 428, 821–827. doi: 10.1038/nature02403

Wu, Z. Y., Raven, P., and Hong, D. Y. (1994-2013). *Flora of China, Beijing*. St. Louis: Missouri Botanical Garden Press.

Yang, X., Chi, X. L., Ji, C. J., Liu, H. Y., Ma, W. H., Mohhammat, A., et al. (2016). Variations of leaf N and P concentrations in shrubland biomes across northern China: phylogeny, climate, and soil. *Biogeosciences* 13, 4429–4438. doi: 10.5194/bg-13-4429-2016

Yang, Y. Z., Wang, H., Harrison, S. P., Prentice, I. C., Wright, I. J., Peng, C. H., et al. (2018). Quantifying leaf-trait covariation and its controls across climates and biomes. *New Phytol.* 221, 155–168. doi: 10.1111/nph.15422

Zanne, A. E., Tank, D. C., Cornwell, W. K., Eastman, J. M., Smith, S. A., FitzJohn, R. G., et al. (2014). Three keys to the radiation of angiosperms into freezing environments. *Nature* 506, 89–92. doi: 10.1038/nature12872

Zhang, H., Zeng, Z. X., Zou, Z. G., and Zeng, F. P. (2019). Climate, life form and family jointly control variation of leaf traits. *Plants (Basel)* 8, 286. doi: 10.3390/plants8080286

Zhao, N., Yu, G. R., He, N. P., Wang, Q. F., Guo, D. L., Zhang, X. Y., et al. (2016). Coordinated pattern of multi-element variability in leaves and roots across Chinese forest biomes. *Global Ecol. Biogeogr.* 25, 359–367. doi: 10.1111/geb.12427

Zhou, Y. D., Boru, B. H., Wang, S. W., and Wang, Q. F. (2020). Species richness and phylogenetic diversity of different growth forms of angiosperms across a biodiversity hotspot in the horn of Africa. *J. Syst. Evol.* 59, 141–150. doi: 10.1111/jse.12559

Zhou, Y. D., Chen, S. C., Hu, G. W., Mwachala, G., Yan, X., and Wang, Q. F. (2018). Species richness and phylogenetic diversity of seed plants across vegetation zones of Mount Kenya, East Africa. *Ecol. Evol.* 8, 8930–8939. doi: 10.1002/ece3.4428

Ziyatdinov, A., Vazquez-Santiago, M., Brunel, H., Martinez-Perez, A., Aschard, H., and Soria, J. M. (2018). lme4qtl: linear mixed models with flexible covariance structure for genetic studies of related individuals. *BMC Bioinformatics* 19:68. doi: 10.1186/s12859-018-2057-x

Conflict of Interest: The authors declare that the research was conducted in the absence of any commercial or financial relationships that could be construed as a potential conflict of interest.

Publisher's Note: All claims expressed in this article are solely those of the authors and do not necessarily represent those of their affiliated organizations, or those of the publisher, the editors and the reviewers. Any product that may be evaluated in this article, or claim that may be made by its manufacturer, is not guaranteed or endorsed by the publisher.

Copyright © 2021 An, Lu, Fu, Wang and He. This is an open-access article distributed under the terms of the Creative Commons Attribution License (CC BY). The use, distribution or reproduction in other forums is permitted, provided the original author(s) and the copyright owner(s) are credited and that the original publication in this journal is cited, in accordance with accepted academic practice. No use, distribution or reproduction is permitted which does not comply with these terms.

frontiers in Plant Science

ORIGINAL RESEARCH
published: 10 December 2021
doi: 10.3389/fpls.2021.765077

Effect of Nutrient Addition on the Productivity and Species Richness of Grassland Along With an Elevational Gradient in Tajikistan

*Lian-Lian Fan[1,2,3], Okhonniyozov Mekrovar[1,2,3], Yao-Ming Li[1,2,3], Kai-Hui Li[1,2,3], Xue-Xi Ma[1,2] and Jie-Fei Mao[1,2,3]**

[1] State Key Laboratory of Desert and Oasis Ecology, Xinjiang Institute of Ecology and Geography, Chinese Academy of Sciences, Urumqi, China, [2] Research Center for Ecology and Environment of Central Asia, Chinese Academy of Sciences, Urumqi, China, [3] University of Chinese Academy of Sciences, Beijing, China

OPEN ACCESS

Edited by:
Huakun Zhou,
Key Laboratory of Restoration Ecology in Cold Regions, Northwest Institute of Plateau Biology, Chinese Academy of Sciences (CAS), China

Reviewed by:
Jianshuang Wu,
Institute of Environment and Sustainable Development in Agriculture, Chinese Academy of Agricultural Sciences (CAAS), China
Hui Fu,
Hunan Agricultural University, China

***Correspondence:**
Jie-Fei Mao
mjf@ms.xjb.ac.cn

Specialty section:
This article was submitted to Functional Plant Ecology, a section of the journal Frontiers in Plant Science

Received: 26 August 2021
Accepted: 11 November 2021
Published: 10 December 2021

Citation:
Fan L-L, Mekrovar O, Li Y-M, Li K-H, Ma X-X and Mao J-F (2021) Effect of Nutrient Addition on the Productivity and Species Richness of Grassland Along With an Elevational Gradient in Tajikistan. Front. Plant Sci. 12:765077. doi: 10.3389/fpls.2021.765077

Grasslands provide key resource for the millions of people who are dependent on livestock in Tajikistan. Productivity and species richness (SR) are important characteristics of grassland ecosystems and are greatly affected by nutrient inputs. The effect that climate change might have on these characteristics remains unclear. Here, an *in situ* nitrogen (N) and phosphorus (P) fertilization experiment was conducted at four sites along with an elevational gradient (650, 1,100, 1,250, and 2,000 m) in western Tajikistan over 2 years (2018 and 2019) to examine the influences of nutrient availability and climate change on aboveground biomass (AGB) and SR; precipitation and temperature were also considered to analyze the responses. It demonstrated that enrichment with N, P, and their combinations significantly increased AGB along with an elevational gradient ($p < 0.05$). AGB increased as the concentrations of nutrients added increased. The maximum AGB, which was 2-fold higher compared with control, was observed when 90 kg N ha^{-1} $year^{-1}$ and 30 kg P ha^{-1} $year^{-1}$ were added. In addition, nitrogen addition alone stimulated greater AGB than P addition, although no significant difference was observed between these two treatments. Enrichment with N, P, and their combination had no significant effect on SR; however, SR significantly changed at different elevation. Elevation had direct effect on precipitation and temperature, which, in turn, resulted in variation in AGB and SR. Moreover, both nutrient and elevation had significant effect on AGB and SR, but there was no interaction effect of them. AGB and SR interacted with significant negative correlation. In the high-elevation area, plants grew better in the warmer year (2018); this indicates that grasslands in high mountain areas in Tajikistan might have higher productivity as the climate warms, which will positively affect the economic development of the country.

Keywords: climate change, meteorological factor, nutrient addition, above-ground biomass (AGB), Central Asia

INTRODUCTION

Grasslands are important terrestrial ecosystems, accounting for almost 30% of the land area of earth (Bi et al., 2020). They are important providers of various ecosystem services including the production of livestock forage and biodiversity conservation. Currently, grassland ecosystems have experienced severe changes, for example, the decline of grassland productivity and the loss of species diversity, as both climate change and anthropogenic activities have contributed to dynamic variations in these ecosystems (Jiang et al., 2015; Su et al., 2021). Plant productivity and species richness (SR) are both fundamental properties of grassland and those two properties can reflect the structure and function of grassland ecosystems (Tilman et al., 2006; Wu et al., 2020). However, the degree to which these two properties might change under climate change remains unclear.

Nitrogen (N) and phosphorus (P) play vital roles in plant development and are the most important limiting nutrients in various grasslands (Fay et al., 2015). Climate change and human activities have greatly exacerbated grassland degradation. Fertilization is the primary means for improving the productivity of grassland systems (Ineichen et al., 2020). The effect of nitrogen and phosphorus application on the productivity and diversity of grassland ecosystems has been examined by previous studies and the results of these studies are variable (Alhamad et al., 2012; Harpole et al., 2017; Soons et al., 2017). Increase in nitrogen is known to significantly increase the above-ground biomass (AGB) and reduce the species diversity (Zhao et al., 2019; Gao et al., 2021). However, some studies have shown that although nitrogen addition reduced the species diversity, it increased the functional richness (Niu et al., 2014; Mao et al., 2017). Enrichment with phosphorus fertilizer has been shown to have either increased or no effect on ecosystem productivity and species diversity (Menge and Field, 2007; Gao et al., 2021). The effect of phosphorus fertilizer on ecosystems can also be regulated by nitrogen fertilizer (Bracken et al., 2015).

Tajikistan is a mountainous country located in the region of Central Asia, where the grasslands are widely distributed. The main grassland distribution ranges about from 300 to 4,000 m, resulting in different microclimate and grassland types (Zhang et al., 2014). Grasslands are an important resource supporting the economy of Tajikistan. However, the rapid increase in the human population during the last three decades has greatly increased the demand for dairy products and meat; consequently, the overgrazing and overuse of grasslands have resulted in serious grassland degradation (Han et al., 2016). As fertilization is commonly used to improve grassland quality (Ineichen et al., 2020), understanding how fertilization affects grassland productivity and diversity is essential for managing grassland and ensuring the sustainable development and utilization of grassland resources. Meanwhile, the vegetation in this arid area is sensitive to variation in climate, as changes in vegetation in this region are correlated with annual precipitation and temperature fluctuation (Yin et al., 2016). Therefore, in this study, we explored the impacts of nutrient (N and P) addition along with an elevational gradient in western Tajikistan on aboveground biomass and SR in 2018 and 2019. Furthermore, precipitation and temperature were also considered to analyze the responses.

MATERIALS AND METHODS

Study Area Description

This study was conducted in Tajikistan (total area: 1.431×10^3 km^2), which covers a latitudinal range of 36°40′ to 41°04′N and a longitudinal range of 67°22′ to 75°13′E (**Figure 1**). Tajikistan is known as "the country of mountains" and its mountainous area accounts for about 93% of the total land area (Hafiz, 2008). The area of natural grassland in Tajikistan is 3.6895 million hm^2 and the distribution of plant communities shows obvious zonal characteristics (Zhang et al., 2014). Depending on vegetation composition, altitude, and utilization, Tajikistan has more than 10 pasture types, which are important resources for the economic development (Ahmadov, 2012). This study was conducted at four sites varying in elevation. The study area experiences a continental climate. The patterns of temperature change at the four sites are similar (**Figure 2**). The annual average temperature increases from January, peaks in July, and then decreases. The distribution of precipitation is similar among the four experimental sites (**Figures 2E–H**). Most precipitation is concentrated in winter and spring; summer and autumn are the dry seasons. In **Table 1**, the annual total precipitation increased with elevation: 172.6 mm in Tabakchi (650 m) in 2018 compared with 1,290.00 and 692.9 mm in Luchob (1,250 m) and Ziddi (2,000 m), respectively.

Experimental Design

Our *in situ* field experiments were conducted in West Tajikistan from 2018 to 2019. Experiments were conducted at four sites (**Figure 1**) along with an elevational gradient: Tabakchi (650 m), Blakhi (1,110 m), Luchob (1,250 m), and Ziddi site (2,000 m) to examine the effect of nutrient (N and P) addition on the productivity and the SR of pasture ecosystems. At each site, four blocks (20 m × 3 m) were setup at each site with a 1-m wide buffer zone between the blocks. Each block was further divided into 20 plots for different nutrition treatment (**Figure 1**). The size of each plot was 3 m × 3 m with 1 m wide buffer zones between the plots. Five nutrition treatments were conducted in each block and the four replicates of each five treatments were randomly assigned: CK—control; N3—addition 30 kg Nha^{-1} year^{-1}, P3—addition 30 kg Pha^{-1} year^{-1}, N3P3—addition 30 kg Nha^{-1} year^{-1} and 30 kg Pha^{-1} year^{-1}, and N9P3—addition 90 kg Nha^{-1} year^{-1} and 30 kg Pha^{-1} year^{-1}. Nutrient addition was added *via* a single application after snow melting. Stainless steel sheets were used to prevent water infiltration between treatments, 40 cm of the sheets were inserted into the ground and 10 cm of the sheets were left above ground. The meteorological data were obtained from the metrological station near the experimental sites.

Plant Sampling

In 2018 and 2019, the name and number of plant species were recorded in each 1 m × 1 m quadrats under different nutrient treatments along with an elevational gradient each year during

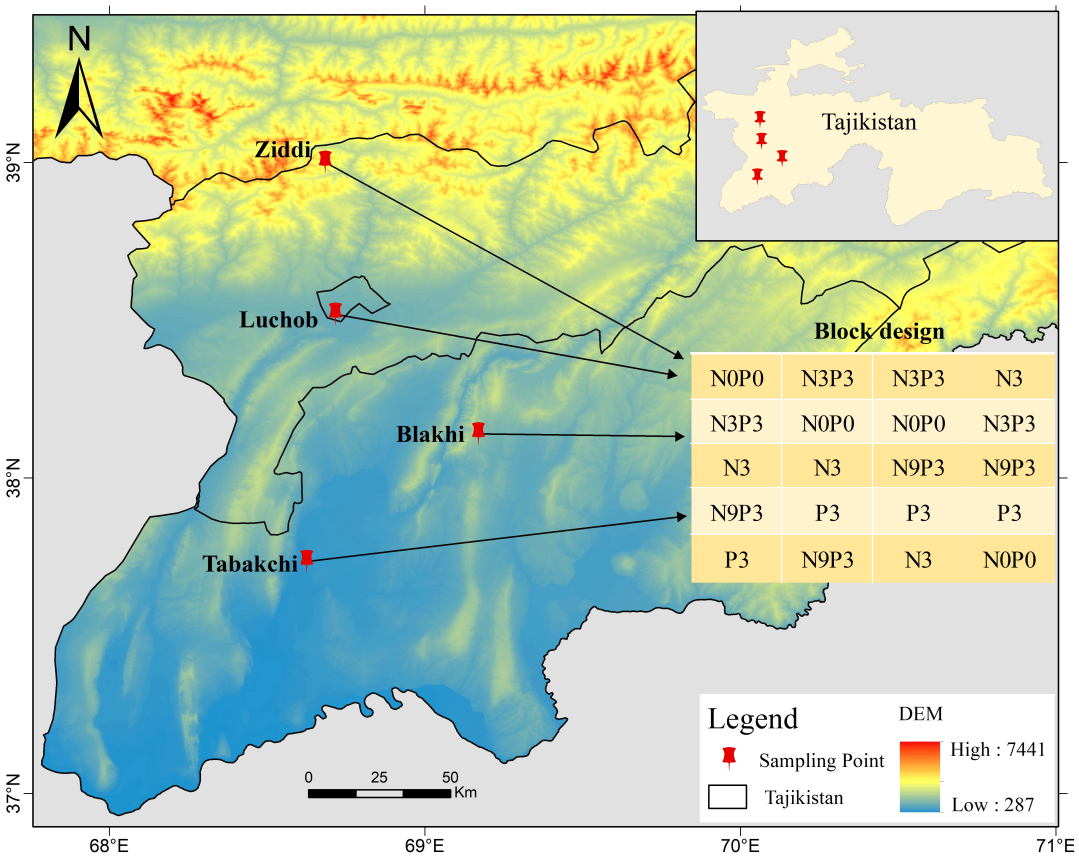

FIGURE 1 | Map of the study area and the experimental design. N0P0–the control; N3—addition of 30 kg N $ha^{-1}year^{-1}$, P3—addition of 30 kg P $ha^{-1}year^{-1}$, N3P3—addition of 30 kg N $ha^{-1}year^{-1}$ and 30 kg P $ha^{-1}year^{-1}$, N9P3—addition of 90 kg N $ha^{-1}year^{-1}$ and 30 kg P $ha^{-1}year^{-1}$. The fertilizer was added *via* a single application. The Shuttle Radar Topographic Mission (SRTM) 30 m digital elevation model (DEM) dataset was obtained from USGS (https://glovis.usgs.gov/).

the peak of the growing season. Above-ground plants were harvested at the end of the growth period in 1 m × 1 m quadrats. AGB was determined by oven drying at 68°C until a constant weight was achieved. Total SR was recorded by noting all the plant species present within 1 m × 1 m quadrats.

Statistical Analysis

A linear mixed-effects models were used to analyze the effect of different nutrition addition treatments on plant AGB and SR along with an elevational gradient, with nutrient and elevation as independent variable and years as a random factor. Structural equation modeling (SEM) was used to evaluate and quantify the effects of elevation, precipitation, temperature, and nutrient addition on plant AGB. The SEM was fit using the "lavaan" package in R version 3.3.2 (R Core Team, 2016). The model was considered to be a good fit based on the following criteria: an insignificant ($p > 0.05$) chi-square test statistic, chi-square/df < 3, root mean square error of approximation (RMSEA) < 0.05, goodness of fit index (GFI) > 0.95, and standardized root mean square residual (SRMR) < 0.09 (Liu et al., 2020). The Tukey's *post hoc* test following the one-way ANOVA was used to compare the differences of mean values at $p < 0.05$. All the statistical analyses were conducted in R version 3.3.2 (R Core Team, 2016). Origin 2015 software (Origin Lab, Northampton, MA, United States) was used to prepare figures.

RESULTS

Above-Ground Biomass and Species Richness Under Different Nutrition Addition Treatment Along With an Elevational Gradient

In both 2018 and 2019, the addition of nutrients greatly increased AGB as the elevation increased (**Figures 3A,B** and **Table 2**; $p < 0.05$). AGB was higher under N addition than under P addition; however, no significant differences were observed between these treatments. AGB was higher under nutrient addition compared with the control and the maximum AGB was observed under N9P3. Nutrient addition significantly increased AGB 2-fold at Tabakchi and Ziddi relative to the control; AGB at these sites ranged from 37.65 to 99.50 g/m^2 and from 451.30 to 918.86 g/m^2, respectively. The effect of nutrient addition on species diversity did not significantly differ at these two sites. However, elevation had a significant effect on species

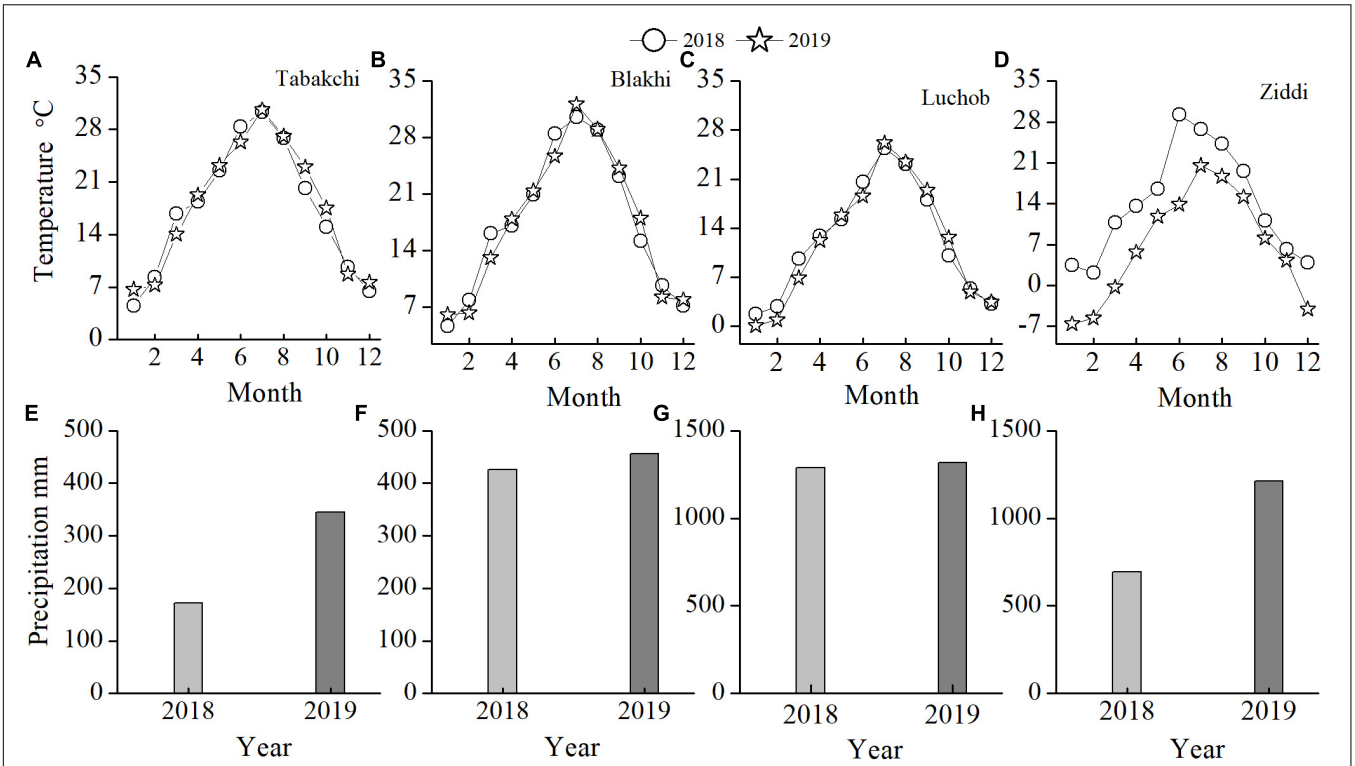

FIGURE 2 | The average monthly temperature **(A–G)** and monthly precipitation **(E–H)** in the four experimental sites.

diversity (**Figures 3C,D** and **Table 2**). SR was lowest at Luchob (6 species/m^2) (**Figures 3C,D**). There was no interaction effect between nutrients and elevations and they independently affected AGB and SR (**Table 2**).

Influence of Elevation P and T on Aboveground Biomass and Species Richness

The SEM analysis showed that elevation had significant ($p < 0.01$) positive direct and indirect effects on plant AGB and SR. Elevation had direct effects on annual total precipitation and annual average temperature, but positive direct effect on precipitation and negative direct effect on temperature. Annual total precipitation and annual average temperature were significant negatively correlated ($p < 0.01$). Nutrient addition had positive direct effect on plant AGB, but nutrient addition had no significant direct effect on SR ($p > 0.05$). AGB and SR had negative correlation (**Figure 4**). AGB was observed higher in 2018 (more precipitation) at lower and middle elevation areas (**Figures 5A,B**). Contrary to expectations, it showed the opposite result at the high elevation (Ziddi). In the warm year (2018), AGB at higher elevation was more than in the cold year (2019) though with less precipitation (**Figures 5A,B**). SR had no significant between years at Tabakchi and Blakhi. However, SR had significant difference between years at Luchob and Ziddi with higher SR in 2018 (**Figure 5C**).

TABLE 1 | The location of the four experimental sites and the total precipitation and annual average temperature among the four sites.

Site	Latitude	Longitude	Altitude (m)	TP (mm)		AAT (°C)	
				2018	2019	2018	2019
Tabakchi	37°51.55′°N	68°57.56′°E	650	172.60	344.50	17.28	17.60
Blakhi	38°14.05′°N	69°17.02′°E	1,100	426.30	456.70	17.51	17.51
Luchob	38°39.91′°N	68°39.38′°E	1,250	1,290.00	1,317.80	12.35	12.05
Ziddi	39°02.19′°N	68°49.37′°E	2,000	692.90	1,211.90	13.96	6.77

TP, total precipitation; AAT, annual average temperature.

DISCUSSION

Effect of Nutrients on the Grass Aboveground Biomass and Species Richness

Nitrogen and phosphorus are two limiting nutrients that regulate the development of grassland ecosystems (Fay et al., 2015). Nitrogen and phosphorus addition significantly increased the AGB as the elevation increased and AGB increased as the concentrations of nutrients applied to the soil increased. These results are consistent with previous studies in grassland ecosystems showing that nitrogen and phosphorus additions stimulated primary production (Li et al., 2015; Zhao et al., 2019). Moreover, our findings indicated that nutrient addition was more effective at promoting plant growth compared to the control. The effect was enhanced by the increased precipitation at the

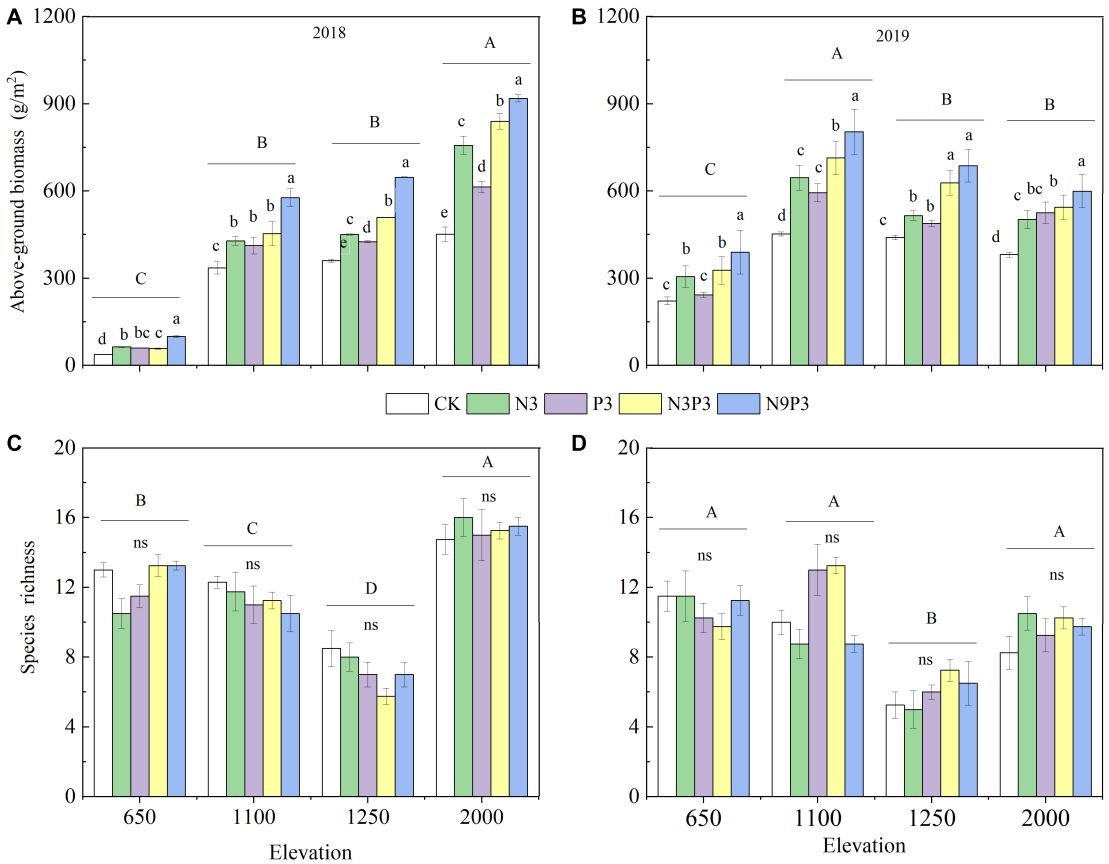

FIGURE 3 | Changes in the above-ground biomass **(A,B)** and species richness **(C,D)** changing under different nutrient treatments at different elevations in 2018 (left) and 2019 (right). Within each panel, groups with the same capital letters above them are not significantly different at $p < 0.05$ (Duncan's test). Within each group of five bars, bars sharing the different letters are significantly different from each other at $p < 0.05$. Letters are not presented when none of the five bars differs significantly from any of the others (Duncan's test), ns means that differences are not significant. The data were showed as mean ± SE.

middle to lower elevations (Tabqichi, Blakhi, and Luchob). The AGB was higher in 2019 than in 2018 in the nutrient addition treatments because precipitation was higher in 2019 compared with 2018 (**Figures 3A,B** and **Table 1**). Other studies have shown that increase in water promotes nutrient availability and increases primary productivity (Yang et al., 2011; Fan et al., 2013). A global scale experiment of nutrient addition in grasslands has shown that N addition increases biomass to a greater degree than P addition. The addition of both N and P was more beneficial for biomass increasing than adding only one of these two elements (Fay et al., 2015). It is in an agreement with our 2-year nutrient fertilizer experiment. The amount of the AGB with adding only nitrogen was higher than that adding only phosphorus. Combined NP enrichment was more beneficial for the plant growth than either along nitrogen or phosphorus addition. Furthermore, the AGB showed a positive response to nutrient concentration, especially to the nitrogen. These results indicated that nitrogen is more likely to be the limiting nutrient for biomass production in Tajikistan grassland as the elevation increases and the effect of phosphorus addition on the plant growth was regulated by nitrogen nutrient.

Species diversity plays an important role in maintaining the structure of ecosystems (Hautier et al., 2020). Increase in nitrogen is thought to significantly increase the AGB and reduces the species diversity (Humbert et al., 2016). Several meta-analyses have shown that nitrogen enrichment generally reduced plant SR in terrestrial ecosystems, especially in grassland ecosystems (Soons et al., 2017; Yue et al., 2020). However, the results of this study were not fully consistent with the results of these previous studies. Nitrogen, phosphorus, or their combinations addition did not increase or decrease SR, but SR exhibited significant responses within elevations. Among with an elevational gradient,

TABLE 2 | Summary of the linear mixed-effects models relating fixed factor (N, E) and random factor (Y) for the grassland above-ground biomass and species richness.

Source	AGB		SR	
	F	*P*	*F*	*P*
N	14.971	0.000***	0.2684	0.898
E	156.448	0.000***	125.5307	0.000***
N × E	1.281	0.237	1.071	0.389

*N means different nutrient addition and E means different elevation, N × E means the interaction. ***Significant difference at p < 0.001 level.*

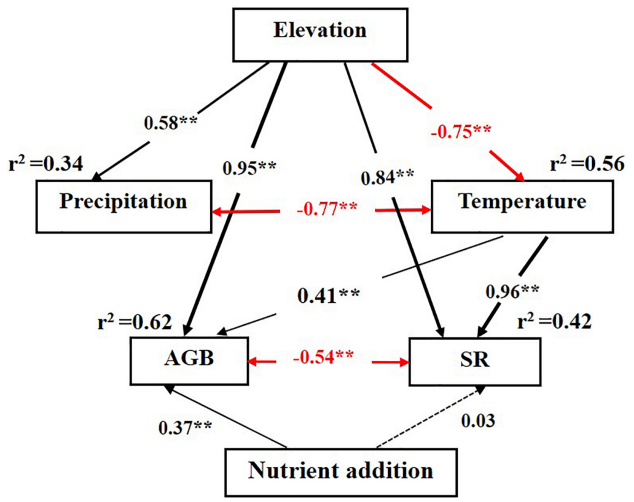

FIGURE 4 | Structural equation model for the effect of environmental factors and nutrient inputs on the plant above-ground biomass. Red and black arrows indicate positive and negative relationships, respectively. Single-headed arrows represent causal relationships and two-headed arrows indicate correlation. Dotted arrows represent non-significant paths ($p > 0.05$). Values adjacent to arrows indicate standardized path coefficients. The proportion of variance explained (r^2) appears alongside response variable in the model. Significance levels are denoted with $^{**}p < 0.01$.

SR showed significant different with Lucholb that had the lowest SR. The reason for that might be explained by short-term nutrient addition. Long-term experiments may be necessary for characterizing the effect of nutrient addition on species diversity. The previous study found that the greater increase in plant productivity with long-term nitrogen addition, the greater decline in plant diversity, and vice versa (Yue et al., 2020). This study conducted nutrient addition for 2 years; the SR to nutrient availability may be not so sensitive, which needs to take longer time fertilizer experiment to analyze the response. Overall, nutrient limitation often increases with increasing elevation (Johnson et al., 2000), but some recent observational studies suggested that the relative importance of different limiting nutrients changes with elevation (Fisher et al., 2013; Sundqvist et al., 2014). In this study, though both nutrient and elevation had significant effect on the AGB or SR, there was no interaction effect of them on the AGB or SR and they independently affected AGB and SR (**Table 2**).

Changes in Biomass and Diversity Driven by Environmental Variables

Precipitation and temperature are considered to be the major limiting factors in arid and semiarid region and high latitude ecosystems and these systems are, therefore, predicted to be particularly sensitive to climate change (IPCC, 2014). Most previous studies have found productivity to be linearly correlated with mean annual precipitation (Hu et al., 2007; Mowll et al., 2015), as the amount of precipitation largely determines the productivity of the grassland ecosystem (Esteban and Osvaldo, 2000; Bai et al., 2004). Other studies indicated that declining temperatures associated with increasing elevation can directly influence ecosystem properties (Bahram et al., 2012; Sundqvist et al., 2014). Our study area spans different elevations, so there are differences in rainfall and temperature. Through the SEM analysis, we can know that annual total precipitation and annual average temperature variation were directly significantly affected *via* elevational gradient, with positive on precipitation and negative on temperature. Meantime, precipitation and temperature were negatively correlated (**Figure 4**). Therefore, consistent with previous studies, the AGB and SR were affected not only by elevation, but also by annual total precipitation and annual average temperature (**Figure 5**). Different effects of precipitation and temperature can be observed at different elevations correlated with the vegetation. In this study, vegetation changed from desert grassland to mountain grassland from the south to the north experimental site and correspondingly, the AGB increased. Specifically, the AGB in desert grassland was more sensitive to variation of precipitation, which can be more than quadrupled in 2019 (the year with more precipitation) compared with 2018. Besides precipitation, annual average temperature also had a significant positive relationship with the grassland AGB. Generally, warming had a negative indirect effect on plant productivity because of increased soil drought associated with higher evapotranspiration and temperature (Dulamsuren et al., 2013). Nevertheless, in our high-elevation experimental site Ziddi, the year (2018) with higher temperature had the higher AGB compared with the year with relative lower temperature (2019). This result indicated that warming might be beneficial for the plant growth. Since global warming is an indisputable fact (IPCC, 2014), the grassland in high mountain areas in Tajikistan may have higher productivity in the future based on current warming trends and this would have a positive effect on the economic development of Tajikistan.

Productivity and diversity are two major properties of ecosystems and environmental factors can affect the productivity; the variation will lead to the change of diversity simultaneously and vice versa (Gross and Cardinale, 2007; Wang et al., 2019). In arid areas, water largely determines the plant growth, thus competition among plants is mainly access to water resources (Mu et al., 2021). When precipitation increases, the rapid growth of some species will further lead to the competition for light, which may lead to the decrease in diversity. Therefore, the relationship between growth ability and species diversity is mainly caused by the competition of resources (Miki, 2009). The competition for water and light, thus, provides the best explanation of our finding.

CONCLUSION

The AGB and SR in this mountainous arid community were largely affected by nutrient availability and elevation. Nutrient enrichment was beneficial for the plant growth. The AGB increased with the more nutrient concentration along with an elevational gradients and the maximum increment of the AGB can be quadrupled compared with CK. Nitrogen adding alone was more beneficial for accumulation of the AGB compared with

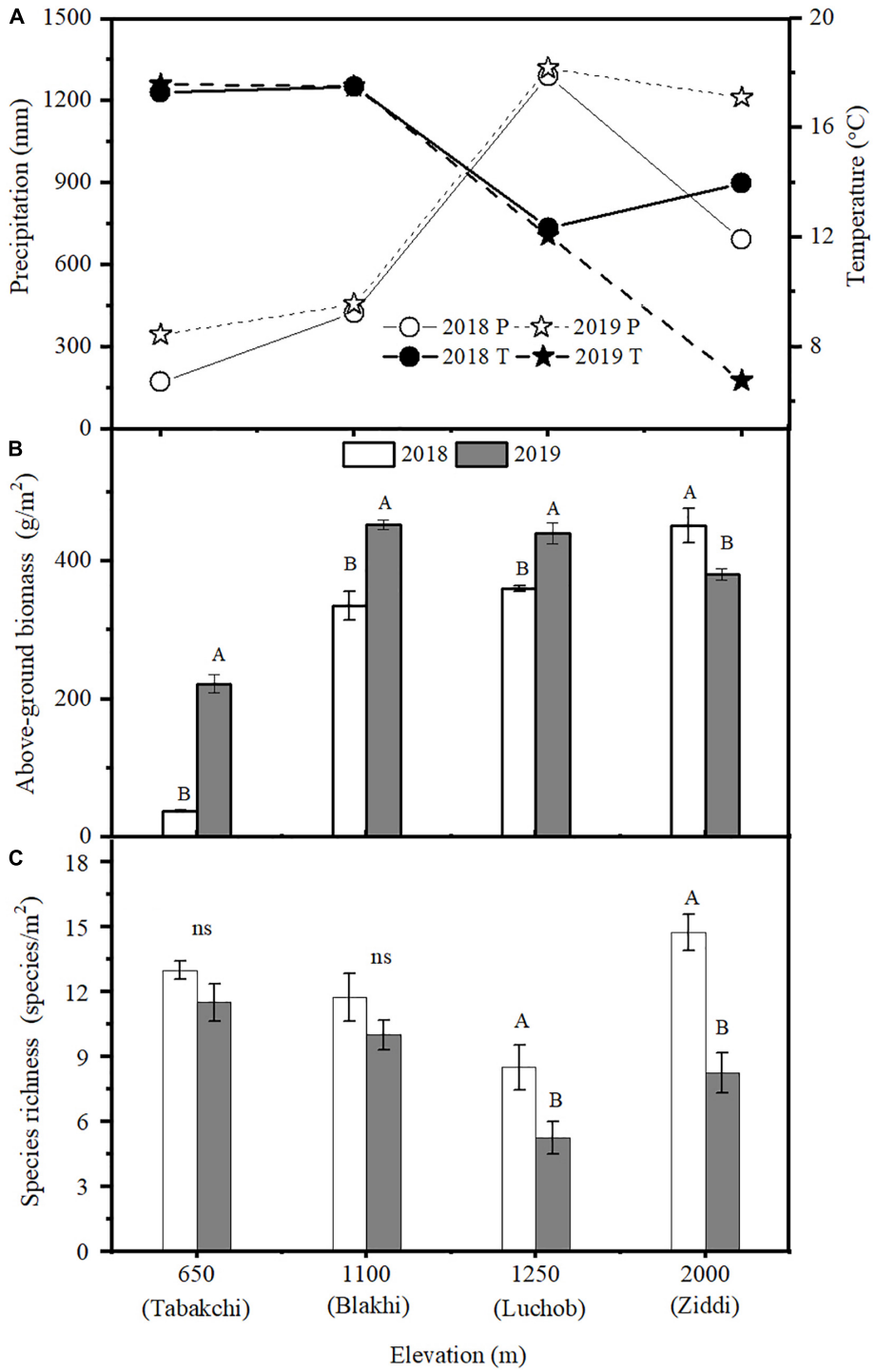

FIGURE 5 | Annual total precipitation and annual average temperature at different elevations **(A)**, the average above-ground biomass **(B)**, and species richness **(C)** in 2018 and 2019. Data of the control treatment were used (mean ± SE). Different capital letters indicate significant difference between years at the same elevation ($p < 0.05$), ns, no significant difference.

phosphorus adding. Enrichment with N, P, and their combination had no significant effect on SR; however, SR significantly changed at different elevation. Moreover, both nutrient and elevation had significant effect on the AGB and SR, but there was no interaction effect of them. The AGB and SR interacted with significant negative correlation. Elevation had direct effect on

precipitation and temperature, which, in turn, caused variation in the AGB and SR.

DATA AVAILABILITY STATEMENT

The original contributions presented in the study are included in the article/supplementary material, further inquiries can be directed to the corresponding authors.

AUTHOR CONTRIBUTIONS

Y-ML and J-FM conceived the study. L-LF conducted the experiments, analyzed the data, and drafted the manuscript. OM, K-HL, and X-XM performed the experiments. All authors showed in the article contributed to study conceptualization, read, and approved the final version of this manuscript.

FUNDING

This study was supported by the Strategic Priority Research Program of the Chinese Academy of Sciences (XDA20020101), the "West Light" Talent Program of the Chinese Academy of Sciences (2019-XBQNXZ-B-005), and National Natural Science Foundation of China (42077327). Strategic Priority Research Program of the Chinese Academy of Sciences (XDA2005010304).

ACKNOWLEDGMENTS

This study was conducted in Tajikistan and we thank all the staffs at the Research Center for Ecology and Environment of Central Asia (Dushanbe subcenter) for their great and effective assistance. A special thanks to A. A. Madaminov for his field work and comments. We also thank TopEdit (www.topeditsci.com) for linguistic assistance during the preparation of this manuscript.

REFERENCES

Ahmadov, H. M. (2012). Influence of over-grazing on biodiversity and productivity of the pasture on high mountain zone Tajikistan. *J. Acad. Soil Sci.* 2, 33–42, (In Russia).

Alhamad, N. M., Alrababah, A. M., and Gharaibeh, A. M. (2012). Impact of burning and fertilization on dry Mediterranean grassland productivity and diversity. *Acta Oecol.* 40, 19–26. doi: 10.1016/j.actao.2012.02.005

Bahram, M., Põlme, S., Kõljalg, U., Zarre, S., and Tedersoo, L. (2012). Regional and local patterns of ectomycorrhizal fungal diversity and community structure along an altitudinal gradient in the Hyrcanian forests of northern Iran. *New Phytol.* 193, 465–473. doi: 10.1111/j.1469-8137.2011.03927.x

Bai, Y. F., Han, X., Wu, J., Chen, Z., and Li, L. (2004). Ecosystem stability and compensatory effects in the Inner Mongolia grassland. *Nature* 431, 181–184. doi: 10.1038/nature02850

Bi, X., Li, B., Zhang, L. X., and Nan, B. (2020). Response of grassland productivity to climate change and anthropogenic activities in arid regions of Central Asia. *PeerJ* 8:e9797. doi: 10.7717/peerj.9797

Bracken, M. E. S., Hillebrand, H., Borer, E. T., Seabloom, E. W., Cebrian, J., Cleland, E. E., et al. (2015). Signatures of nutrient limitation and co-limitation: responses of autotroph internal nutrient concentrations to nitrogen and phosphorus additions. *Oikos* 124, 113–121. doi: 10.1111/oik.01215

Dulamsuren, C., Wommelsdorf, T., Zhao, F. J., Xue, Y. Q., Zhumadilov, B. Z., Leuschner, C., et al. (2013). Increased summer temperatures reduce the growth and regeneration of *Larix sibirica* in southern boreal forests of Eastern Kazakhstan. *Ecosystems* 16, 1536–1549. doi: 10.1007/s10021-013-9700-1

Esteban, G. J., and Osvaldo, E. S. (2000). Controls of Grass and shrub aboveground production in the patagonian steppe. *Ecol. Appl.* 10, 541–549. doi: 10.2307/2641113

Fan, L. L., Li, Y., Tang, L. S., and Ma, J. (2013). Combined effects of snow depth and nitrogen addition on ephemeral growth at the southern edge of the Gurbantunggut Desert, China. *J. Arid Land.* 5, 500–510. doi: 10.1007/s40333-013-0185-8

Fay, P. A., Prober, S., Harpole, W. S., Knops, J. M. H., Bakker, J. D., Borer, E. T., et al. (2015). Grassland productivity limited by multiple nutrients. *Nat. Plants* 1:15080. doi: 10.1038/nplants.2015.80

Fisher, J. B., Malhi, Y., Torres, I. C., Metcalfe, D. B., van de Weg, M. J., Meir, P., et al. (2013). Nutrient limitation in rainforests and cloud forests along a 3,000-m elevation gradient in the Peruvian Andes. *Oecologia* 172, 889–902. doi: 10.1007/s00442-012-2522-6

Gao, L. M., Su, J., Chen, C., Tian, Q., and Shen, Y. X. (2021). Increases in forage legume biomass as a response to nitrogen input depend on temperature, soil characters and planting system: a meta-analysis. *Grass For. Sci.* 76, 309–319. doi: 10.1111/gfs.12511

Gross, K., and Cardinale, B. (2007). Does species richness drive community production or vice versa? reconciling historical and contemporary paradigms in competitive communities. *Am. Natur.* 170, 207–220. doi: 10.1086/518950

Hafiz, M. (2008). State of plant genetic resources for food and agriculture (pgrfa) in the Republic of Tajikistan. *Count. Rep.* 8, 4–10.

Han, Q. F., Luo, G. P., Li, C. F., Shakir, A., Wu, M., and Saidov, A. (2016). Simulated grazing effects on carbon emission in Central Asia. *Agricult. For. Meteorol.* 216, 203–214. doi: 10.1016/j.agrformet.2015.10.007

Harpole, W. S., Sullivan, L. L., Lind, E. M., Firn, J., Adler, P. B., Borer, E. T., et al. (2017). Out of the shadows: multiple nutrient limitations drive relationships among biomass, light and plant diversity. *Funct. Ecol.* 31, 1839–1846. doi: 10.1111/1365-2435.12967

Hautier, Y., Zhang, P., Loreau, M., Wilcox, K. R., Seabloom, E. W., Borer, E. T., et al. (2020). General destabilizing effects of eutrophication on grassland productivity at multiple spatial scales. *Nat. Commun.* 11:1234567890. doi: 10.1038/s41467-020-19252-4

Hu, Z., Fan, J., Zhong, H., and Yu, G. (2007). Spatiotemporal dynamics of aboveground primary productivity along a precipitation gradient in Chinese temperate grassland. *Sci. China Ser. D Earth Sci.* 50, 754–764. doi: 10.1007/s11430-007-0010-3

Humbert, J., Dwyer, A., Andrey, A., and Arlettaz, A. (2016). Impacts of nitrogen addition on plant biodiversity in mountain grasslands depend on dose, application duration and climate: a systematic review. *Glob. Change Biol.* 22, 110–120. doi: 10.1111/gcb.12986

Ineichen, S., Marquardt, S., Kreuzer, M., and Reidy, B. (2020). Forage quality of species-rich mountain grasslands subjected to zero, PK and NPK mineral fertilization for decades. *Grass Forage Sci.* 75, 385–397. doi: 10.1111/gfs.12488

IPCC (2014). *Climate Change 2014: Synthesis Report: Contribution of Working Groups I, II and III to the Fifth Assessment Report of the Intergovernmental Panel on Climate Change*. Geneva: IPCC.

Jiang, W. G., Yuan, L. H., Wang, W. J., Cao, R., Zhang, Y. F., and Shen, W. M. (2015). Spatio-temporal analysis of vegetation variation in the yellow river basin. *Ecol. Indicat.* 51, 117–126. doi: 10.1016/j.ecolind.2014.07.031

Johnson, C. E., Driscoll, C. T., Siccama, T. G., and Likens, G. E. (2000). Element fluxes and landscape position in a northern hardwood forest watershed ecosystem. *Ecosystems* 3, 159–184. doi: 10.1007/s100210000017

Li, K. H., Liu, X. J., Song, L., Gong, Y. M., Lu, C., Yue, P., et al. (2015). Response of alpine grassland to elevated nitrogen deposition and water supply in China. *Oecologia* 177, 65–72. doi: 10.1007/s00442-014-3122-4

Liu, X., Lamb, E. G., and Zhang, S. (2020). Nitrogen addition impacts on soil microbial stoichiometry are driven by changes in plant resource stoichiometry not by the composition of main microbial groups in an alpine meadow. *Biol. Fertil. Soils* 56:1423. doi: 10.1007/s00374-019-01423-1

Mao, W., Felton, A. J., and Zhang, T. H. (2017). Linking changes to intraspecific trait diversity to community functional diversity and biomass in response to snow and nitrogen addition within an inner mongolian grassland. *Front. Plant Sci.* 8:339. doi: 10.3389/fpls.2017.00339

Menge, D. N. L., and Field, C. B. (2007). Simulated global changes alter phosphorus demand in annual grassland. *Glob. Change Biol.* 13, 2582–2591. doi: 10.1111/j.1365-2486.2007.01456.x

Miki, T. (2009). A new graphical model for untangling complex relationships among environment, biodiversity, and ecosystem functioning. *Ecol. Res.* 24, 937–941. doi: 10.1007/s11284-008-0552-7

Mowll, W., Blumenthal, D. M., Cherwin, K., Smith, A., Symstad, A. J., Vermeire, L. T., et al. (2015). Climatic controls of aboveground net primary production in semi-arid grasslands along a latitudinal gradient portend low sensitivity to warming. *Oecologia* 177, 959–969. doi: 10.1007/s00442-015-3232-7

Mu, X. H., Huang, G., Li, Y., Zheng, X. J., Xu, G. Q., Wu, X., et al. (2021). Population dynamics and life history response to precipitation changes for a desert ephemeral plant with biseasonal germination. *Front. Plant Sci.* 12:625475. doi: 10.3389/fpls.2021.625475

Niu, K. C., Choler, P., Bello, F. D., Mirotchnickg, N., Du, J., and Sun, S. (2014). Fertilization decreases species diversity but increases functional diversity: a three-year experiment in a Tibetan alpine meadow. *Agricult. Ecosyst. Environ.* 182, 106–122. doi: 10.1016/j.agee.2013.07.015

R Core Team (2016). *R: A Language and Environment for Statistical Computing*. Vienna: R Foundation for Statistical Computing. Available online at: https://www.r-project.org/

Soons, M. B., Hefting, M. M., Dorland, E., Lamers, L. P. M., Versteeg, C., and Bobbink, R. (2017). Nitrogen effects on plant species richness in herbaceous communities are more widespread and stronger than those of phosphorus. *Biol. Conserv.* 212(Pt B), 390–397. doi: 10.1016/j.biocon.2016.12.006

Su, Y., Ma, X. F., Le, J. J., Li, K. H., Han, W. X., and Liu, X. J. (2021). Decoupling of nitrogen and phosphorus in dominant grass species in response to long-term nitrogen addition in an Alpine Grassland in Central Asia. *Plant Ecol.* 9, 1–14. doi: 10.1007/s11258-020-01103-3

Sundqvist, M. K., Liu, Z. F., Giesler, R., and Wardle, D. (2014). Plant and microbial responses to nitrogen and phosphorus addition across an elevational gradient in subarctic tundra. *Ecology* 95, 1819–1835. doi: 10.1890/13-0869.1

Tilman, D., Reich, P. B., and Knops, J. M. H. (2006). Biodiversity and ecosystem stability in a decade-long grassland experiment. *Nature* 441, 629–632. doi: 10.1038/nature04742

Wang, Z., Chiarucci, A., and Arratia, J. F. (2019). Integrative models explain the relationships between species richness and productivity in plant communities. *Sci. Rep.* 9:13730. doi: 10.1038/s41598-019-50016-3

Wu, Q., Ren, H. Y., Wang, Z. W., Li, Z. G., Liu, Y. H., Wang, Z., et al. (2020). Additive negative effects of decadal warming and nitrogen addition on grassland community stability. *J. Ecol.* 108:13363. doi: 10.1111/1365-2745.13363

Yang, H., Li, Y., Wu, M., and Zhang, Z. (2011). Plant community responses to nitrogen addition and increased precipitation: the importance of water availability and species traits. *Glob. Change Biol.* 17, 2936–2944. doi: 10.1111/j.1365-2486.2011.02423.x

Yin, G., Hu, Z. Y., Chen, X., and Tashpolat, Y. (2016). Vegetation dynamics and its response to climate change in Central Asia. *J. Arid Land* 8, 375–388. doi: 10.1007/s40333-016-0043-6

Yue, K., Jarvie, S., Senior, A. M., Meerbeek, K. V., Peng, Y., Ni, X., et al. (2020). Changes in plant diversity and its relationship with productivity in response to nitrogen addition, warming and increased rainfall. *Oikos* 129, 939–952. doi: 10.1111/oik.07006

Zhang, L. P., Li, X. S., and Ding, A. Y. (2014). The status and conservation of grassland resources in Tajikistan. *Grass Feed. Livestock* 1, 26–28, (In Chinese).

Zhao, Y. N., Yang, B., Li, M. X., Xiao, R. Q., Rao, K. Y., Wang, J. Q., et al. (2019). Community composition, structure and productivity in response to nitrogen and phosphorus additions in a temperate meadow. *Sci. Total Environ.* 654, 863–871. doi: 10.1016/j.scitotenv.2018.11.155

Conflict of Interest: The authors declare that the research was conducted in the absence of any commercial or financial relationships that could be construed as a potential conflict of interest.

Publisher's Note: All claims expressed in this article are solely those of the authors and do not necessarily represent those of their affiliated organizations, or those of the publisher, the editors and the reviewers. Any product that may be evaluated in this article, or claim that may be made by its manufacturer, is not guaranteed or endorsed by the publisher.

Copyright © 2021 Fan, Mekrovar, Li, Li, Ma and Mao. This is an open-access article distributed under the terms of the Creative Commons Attribution License (CC BY). The use, distribution or reproduction in other forums is permitted, provided the original author(s) and the copyright owner(s) are credited and that the original publication in this journal is cited, in accordance with accepted academic practice. No use, distribution or reproduction is permitted which does not comply with these terms.

frontiers in Plant Science

ORIGINAL RESEARCH
published: 13 December 2021
doi: 10.3389/fpls.2021.765070

Effects of Different Grazing Disturbances on the Plant Diversity and Ecological Functions of Alpine Grassland Ecosystem on the Qinghai-Tibetan Plateau

Wenlong Li[1], Chenli Liu[1], Wenying Wang[2]*, Huakun Zhou[3], Yating Xue[4], Jing Xu[5], Pengfei Xue[1] and Hepiao Yan[1]*

[1] State Key Laboratory of Grassland Agro-Ecosystems, Key Laboratory of Grassland Livestock Industry Innovation, College of Pastoral Agriculture Science and Technology, Lanzhou University, Lanzhou, China, [2] Department of Life Sciences, Qinghai Normal University, Xining, China, [3] Key Laboratory of Cold Regions Restoration Ecology, Qinghai Province, Northwest Institute of Plateau Biology, Chinese Academy of Sciences, Xining, China, [4] College of Resources and Environment, Chengdu University of Information Technology, Chengdu, China, [5] School of Agriculture and Forestry Economic and Management, Lanzhou University of Finance and Economics, Lanzhou, China

Grazing is one of the main human disturbance factors in alpine grassland on the Qinghai-Tibet Plateau (QTP), which can directly or indirectly influence the community structures and ecological functions of grassland ecosystems. However, despite extensive field grazing experiments, there is currently no consensus on how different grazing management approaches affect alpine grassland diversity, soil carbon (C), and nitrogen (N). Here, we conducted a meta-analysis of 70 peer-reviewed publications to evaluate the general response of 11 variables related to alpine grassland ecosystems plant diversity and ecological functions to grazing. Overall, the results showed that grazing significantly increased the species richness, Shannon–Wiener index, and Pielou evenness index values by 9.89% (95% CI: 2.75–17.09%), 7.28% (95% CI: 1.68–13.62%), and 3.74% (95% CI: 1.40–6.52%), respectively. Aboveground biomass (AGB) and belowground biomass (BGB) decreased, respectively, by 41.91% (95% CI: −50.91 to −32.88%) and 17.68% (95% CI: −26.94 to −8.52%). Soil organic carbon (SOC), soil total nitrogen (TN), soil C:N ratio, and soil moisture decreased by 13.06% (95% CI: −15.88 to −10.15%), 12.62% (95% CI: −13.35 to −8.61%), 3.27% (95% CI: −4.25 to −2.09%), and 20.75% (95% CI: −27.89 to −13.61%), respectively, whereas, soil bulk density and soil pH increased by 17.46% (95% CI: 11.88–24.53%) and 2.24% (95% CI: 1.01–3.64%), respectively. Specifically, moderate grazing, long-durations (>5 years), and winter grazing contributed to increases in the species richness, Shannon–Wiener index, and Pielou evenness index. However, AGB, BGB, SOC, TN, and soil C:N ratios showed a decrease with enhanced grazing intensity. The response ratio of SOC was positively associated with AGB and BGB but was negatively related to the Shannon–Wiener index and Pielou evenness index. Furthermore, the effects of grazing on plant diversity, AGB, BGB, SOC, and TN in alpine grassland varied with grazing

OPEN ACCESS

Edited by:
Gang Fu,
Institute of Geographic Sciences and Natural Resources Research, Chinese Academy of Sciences (CAS), China

Reviewed by:
Wenming Bai,
State Key Laboratory of Vegetation and Environmental Change, Institute of Botany, Chinese Academy of Sciences (CAS), China
Yangong Du,
Northwest Institute of Plateau Biology, Chinese Academy of Sciences (CAS), China
Zhi-Cong Dai,
Jiangsu University, China

***Correspondence:**
Chenli Liu
liuchl18@lzu.edu.cn
Wenying Wang
wangwy0106@163.com

Specialty section:
This article was submitted to Functional Plant Ecology, a section of the journal Frontiers in Plant Science

Received: *26 August 2021*
Accepted: *18 November 2021*
Published: *13 December 2021*

Citation:
Li W, Liu C, Wang W, Zhou H, Xue Y, Xu J, Xue P and Yan H (2021) Effects of Different Grazing Disturbances on the Plant Diversity and Ecological Functions of Alpine Grassland Ecosystem on the Qinghai-Tibetan Plateau. Front. Plant Sci. 12:765070. doi: 10.3389/fpls.2021.765070

duration, grazing season, livestock type, and grassland type. The findings suggest that grazing should synthesize other appropriate grazing patterns, such as seasonal and rotation grazing, and, furthermore, additional research on grazing management of alpine grassland on the QTP is needed in the future.

Keywords: grazing management, alpine grassland, species richness, biomass, meta-analysis, Qinghai-Tibet Plateau

INTRODUCTION

Grassland is an important component of terrestrial ecosystems, accounting for approximately 20% of the total global land surface (Scurlock and Hall, 1998). Grasslands play vital roles not only in supporting living and grazing conditions but also in mitigating the effects of both local and global climate change (Zhang et al., 2015; Ren et al., 2016; Yan et al., 2020). Among them, the alpine grassland on the Qinghai-Tibet Plateau (QTP) is the highest elevation grassland ecosystem in the world, at an average elevation of over 4,000 m, with over 85% of the QTP covered by alpine grasslands (Li et al., 2013; Liu X. et al., 2021). As one of the main pastoral areas in China, the QTP is abundant in grassland resources with alpine meadow, alpine steppe, and alpine desert steppe types, which occupy 47.05, 30.98, and 7.41% of the total plateau area, respectively (Tian et al., 2014; Li et al., 2018). However, because of human overuse and climate change, the alpine grassland has degraded seriously in recent decades, resulting in a loss of biodiversity and the degradation of ecosystem functions (Li et al., 2017; Liu et al., 2018). Among the factors affecting alpine grassland, grazing is regarded as one of the most important, especially overgrazing, which can lead to grassland degradation (McSherry and Ritchie, 2013). In order to mitigate further deterioration and degradation of grassland, the Chinese government has correspondingly implemented ecological restoration programs, such as the Returning Grazing Land of Grassland initiative (Zhang et al., 2015; Xiong et al., 2016). The main purpose of these programs is to reverse the negative effects of overgrazing and rebuild the ecological functions of degraded grassland areas. Since then, grazing management has become a widely effective strategy to help prevent grassland degradation and maintain sustainable grazing on the QTP (Lu et al., 2017; Liu X. et al., 2021).

To date, a number of experimental studies have been conducted to examine and clarify the impact of different grazing management strategies on plant diversity and the soil properties of alpine grassland. The outcomes of these studies are not consistent – for example, the results of Wu J. S. et al. (2014) showed that grazing reduced species diversity, whereas, Xiong et al. (2014) found that grazing for 6 years enhanced the species diversity of alpine grassland areas compared to non-grazing. Zou et al. (2016) also concluded that the plant diversity in grazing alpine grassland increased significantly compared to diversity in areas with fences. Furthermore, previous studies have generally found that grazing reduced grassland biomass (Lin et al., 2011; Zhao et al., 2016), while a few studies showed that grazing increased biomass (Niu et al., 2009). Different studies have also reported marked differences in the effects of grazing on soil properties in alpine grassland. Some studies have reported that grazing had negative effects on soil carbon (C) and nitrogen (N) levels (Sun et al., 2011; Shi et al., 2013; Li H. Q. et al., 2016), while other studies found that grazing had no significant effect on either of these parameters (Lu X. Y. et al., 2015). In addition, many previous studies have demonstrated that heavy grazing (HG) reduces plant diversity, plant biomass, and soil organic carbon (SOC) content in alpine grassland (Sun et al., 2011; Dlamini et al., 2016; Sun Y. et al., 2018) and that moderate grazing (MG) might help to balance the competing factors of species diversity protection and biomass production (Li et al., 2011). However, the results of these studies are controversial and inconclusive due to differences in grazing intensity, grazing duration, grassland types, and environmental factors between individual studies (Li et al., 2017; He et al., 2020). Consequently, to better understand the effects of differences in grazing on plant diversity and soil properties of alpine grassland on the QTP, it is urgent to conduct a systematic and comprehensive analysis based on published literature.

Meta-analysis provides a robust, quantitative, scientific, and comprehensive statistical approach to integrating information from individual studies (Hedges et al., 1999; Gurevitch et al., 2018) and several publications have synthesized the effects of grazing on grassland ecosystems at global and national scales. For example, Gao and Carmel (2020) performed a global meta-analysis and found that grazing significantly increased plant richness compared to grazing exclusion. In contrast, Herrero-Jauregui and Oesterheld (2018) reported that species richness significantly decreased as grazing intensity increased on a global scale. Zhou et al. (2017) and Byrnes et al. (2018) conducted global meta-analyses, which indicated that grazing significantly decreased belowground C and N levels in grassland ecosystems. Furthermore, Yan et al. (2013) found that, compared to the global average value, grazing had a greater negative effect on grassland total biomass in China.

However, an area-specific synthesis of the effects of grazing on alpine grassland on the QTP is still lacking and, in particular, the results of such an analysis may not be consistent outcomes of meta-analysis on a global and national scale. In terms of recent meta-analysis studies, both Yan et al. (2020) and Liu C. et al. (2021) showed that grazing significantly decreased the biomass or SOC of alpine grasslands on the QTP. However, a comprehensive analysis of the response of plant communities and soil properties of alpine grassland on the QTP to different grazing patterns remains unclear. Given these uncertainties, it is thus necessary to integrate the available data from the study area to analyze how grazing affects alpine grassland on the QTP.

In this study, we compiled data from 70 peer-reviewed studies and conducted a meta-analysis to quantitatively assess the impact of grazing on alpine grassland plant diversity indices, plant biomass, and soil properties on the QTP. Specifically, our principal objectives were (a) to evaluate the magnitude and direction (i.e., positive or negative change) of grazing disturbance on plant diversity, biomass, and soil properties in alpine grassland; (b) to examine how differences in grazing intensity, grazing duration, grazing season, livestock type, and grassland type regulate these response variables; and (c) to understand the effects of grazing disturbances on interactions between plant diversity and biomass and soil properties. These findings could provide new perspective for the formulation of grazing management strategies in alpine grasslands on the QTP.

MATERIALS AND METHODS

Data Collection and Compilation

To identify we searched peer-reviewed papers published before January 2020 using the ISI Web of Science[1] and China National Knowledge Infrastructure.[2] The following keywords and combinations were used for retrieval: "grazing" OR "fencing" AND "alpine grassland" OR "alpine meadow" OR "alpine steppe" OR "soil carbon" OR "soil nitrogen" OR "diversity" OR "biomass" AND "Tibet" OR "Tibetan Plateau" OR "Qinghai-Tibetan Plateau." To avoid bias in publication selection, the papers were chosen based on the following criteria: (1) all study results were from field experiments and must be carried out in the alpine grassland of the QTP; (2) there was at least one group of grazing treatment and a control group (i.e., non-grazing); (3) the experiment must contain at least one pair of target variables; (4) the grazing and control experiments both need to be carried out under similar environmental conditions, including slope, aspect, orientation, and position; (5) grazing intensity, duration, season, and livestock type need to be clearly described; and (6) the mean, standard deviation (SD) or standard error (SE), and sample size of each variable in the treatment and control group were clearly reported in the paper. Based on these criteria, a total of 70 published papers were selected for this study (**Figure 1** and **Supplementary Text 1**).

The compiled database included three categories, comprising a total of 11 variables, as follows: (1) plant diversity – because different indices represent different aspects of species diversity, we used the common indicators of species richness, the Shannon–Wiener index, and the Pielou evenness index; (2) plant biomass, including aboveground biomass (AGB) and belowground biomass (BGB); and (3) soil properties, including SOC, soil total nitrogen (TN), soil C:N ratio, soil bulk density (BD), soil moisture (SM), and soil pH. Note that we selected BGB data in a depth range between 0 and 30 cm because more than 80% of grassland biomass and soil nutrients are concentrated in surface soil at depths of 0–30 cm (Yu et al., 2019). To detail the impact of grazing on grassland, referring to the previous studies of He et al. (2020) and Liu C. et al. (2021), based on the original papers' data collection, the grazing levels were classified divided into light grazing (LG), MG, HG, and free grazing (FG). In addition, we also evaluated the influence of different grazing durations [short-term grazing (≤2 years), medium-term grazing (2–5 years), and long-term grazing (>5 years)] (Liu C. et al., 2021), grazing seasons (winter season, summer season, and annual grazing), and livestock types (yak, Tibetan sheep, mixed yak, and Tibetan sheep). The grassland types in each study were classified into the alpine meadow, alpine steppe, and alpine desert steppe, which are the three main grassland types on the QTP (**Figure 1**). All raw data were extracted from the studies' text, tables, and graphics. If data were presented graphically, we used the GetData Graph Digitizer to extract data (ver 2.26, Russian Federation[3]). For each of the selected papers, we recorded the journal name, study site, latitude, longitude, elevation, MAT, and MAP (**Supplementary Text 1**). In cases where the MAT and MAP were not reported in the paper, the data were extracted from the global climate database[4] using the study location's corresponding latitude and longitude information (Zhou et al., 2017).

Meta-Analysis

The data were analyzed by adopting a meta-analysis method based on Hedges et al. (1999) and Luo et al. (2006). A natural logarithm of the calculated response ratio (*RR*) was used as the effective amount to indicate the effect of grazing on the grassland-related variables. The *RR* was calculated using Eq. 1:

$$RR = \ln(\overline{X_t}/\overline{X_c}) = \ln(\overline{X_t}) - \ln(\overline{X_c}) \quad (1)$$

where $\overline{X_t}$ and $\overline{X_c}$ are the mean values in the grazing treatment group and control group (non-grazing), respectively. The variance (v) of *RR* was estimated using Eq. 2:

$$v = \frac{S_t^2}{n_t \overline{X_t}^2} + \frac{S_c^2}{n_c \overline{X_c}^2} \quad (2)$$

where n_t and n_c represent the sample sizes of the grazing treatment and the control (non-grazing) groups, respectively, and S_t and S_c are the SD of the variable of interest in the grazing treatment and control group, respectively. In order to obtain lower variability and higher accuracy, the weighted response ratio (RR_{++}) was used to improve the statistical accuracy, with the weight factor (w) of the effect value (*RR*) of each study given by the inverse of its variance ($w = 1/v$). The mean response ratio (RR_{++}) was calculated from each pair of control and grazing treatments, based on individual *RR* values (Zhou et al., 2017). The equation for calculating the weighted *RR* is shown in Eq. 3:

$$RR_{++} = \frac{\sum_{i=1}^{m}\sum_{j=1}^{k} w_{ij} RR_{ij}}{\sum_{i=1}^{m}\sum_{j=1}^{k} w_{ij}} \quad (3)$$

where w_{ij} is the weight factor for each group. The m and k values are the number of datasets and data points in each

[1] http://apps.webofknowledge.com

[2] http://www.cnki.net

[3] http://www.getdata-graph-digitizer.com

[4] http://www.worldclim.org

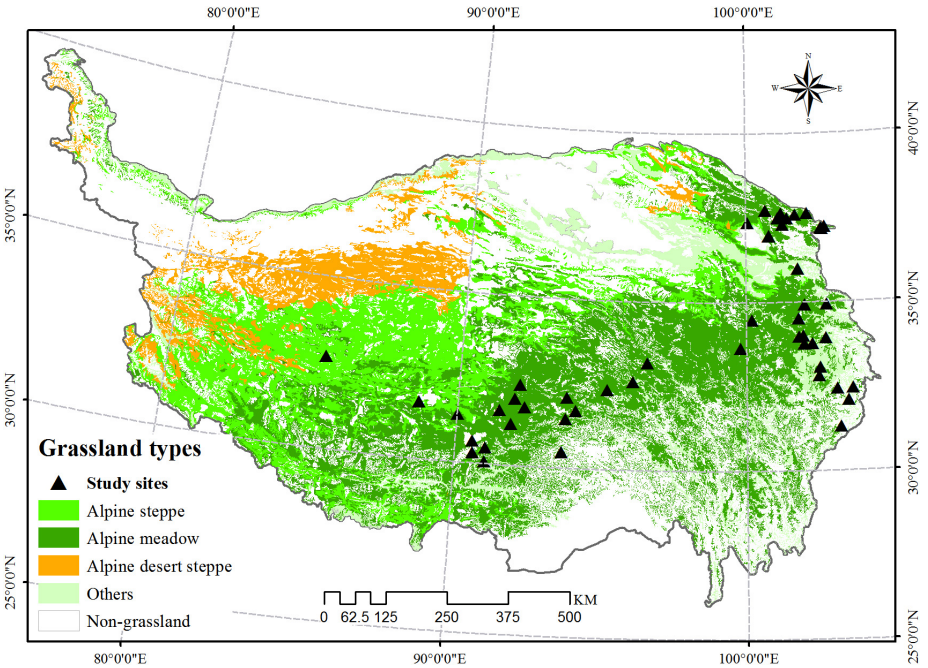

FIGURE 1 | The distribution of grazing experiments selected in this meta-analysis on the QTP. The geographical location of field studies was mapped in ArcGIS 10.2 (https://www.esri.com/).

category group, respectively. The effect of grazing was considered significant if the 95% confidence interval (CI) values of RR_{++} for a he CI is given by Eq. 4:

$$95\%CI = RR_{++} \pm 1.96S(RR_{++}) \quad (4)$$

The overall SE (S) was calculated using the equation given in Eq. 5:

$$S(RR_{++}) = \sqrt{\frac{1}{\sum_{i=1}^{m}\sum_{j=1}^{k} w_{ij}}} \quad (5)$$

We applied the random-effects model to calculate the mean effect size for each study, which used the bootstrapping method to obtain the lowest and highest values to derive the bootstrap 95% confidence interval (95% CI) based on 5,000 iterations (Janssens et al., 2010; Zhou et al., 2018). As noted above, instances where the 95% CI of RR_{++} did not overlap with zero indicated cases where grazing had a significant impact on the selected variables. In contrast, if the 95% CI overlapped with zero, it was assumed that there was no significant difference in the variable under various grazing conditions. The percentage change of the variable was then calculated with the following equation, given in Eq. 6:

$$Change\ (\%) = (e^{RR_{++}} - 1) \times 100\% \quad (6)$$

To further examine the effects of categorical classes, the total heterogeneity (Q_T) was composed of within-group heterogeneity (Q_W) and between-group heterogeneity (Q_B) (Ren et al., 2018). To establish whether there was a distinct difference among different treatments within the same group, if the probability value of Q_B was lower than 0.05, the response rates were interpreted to be significantly different among the various subgroups (Li Y. et al., 2016). The publication bias (**Supplementary Text 1**) was tested using Rosenthal's fail-safe number method in the meta-analysis (Rosenberg et al., 2000; Møller and Jennions, 2001; Rosenberg, 2005). If the fail-safe number is larger than $5n + 10$ (where n is the number of observations used in the analysis), then the result is considered to be a robust and reliable estimate of the true effect (Ren et al., 2016; Zheng et al., 2019). In addition to the above methods, we also performed Pearson's correlation analysis to explore the relationships between the *RR* of plants and soils under grazing and the relationships between these response variables and MAT and MAP. All meta-analyses were calculated using METAWIN 2.1 software (Hedges et al., 1999; Rosenberg et al., 2000) and the plots were made using SIGMAPLOT 11.0 software (Systat Software Inc., San Jose, CA, United States).

RESULTS

Effects on Grassland Plant Diversity

Across all the observations compiled in this study, our meta-analysis showed that grazing significantly increased all the grassland diversity indices: the species richness, Shannon–Wiener index, and the Pielou evenness index increased on average by 9.89% (95% CI: 2.75–17.09%), 7.28% (95% CI: 1.68–13.62%), and 3.74% (95% CI: 1.40–6.52%), respectively (**Figure 2**). Among the different grazing intensities, MG had the largest impact on both species richness and the Shannon–Wiener index, increasing these values by 18.79% (95% CI: 2.08–38.65%)

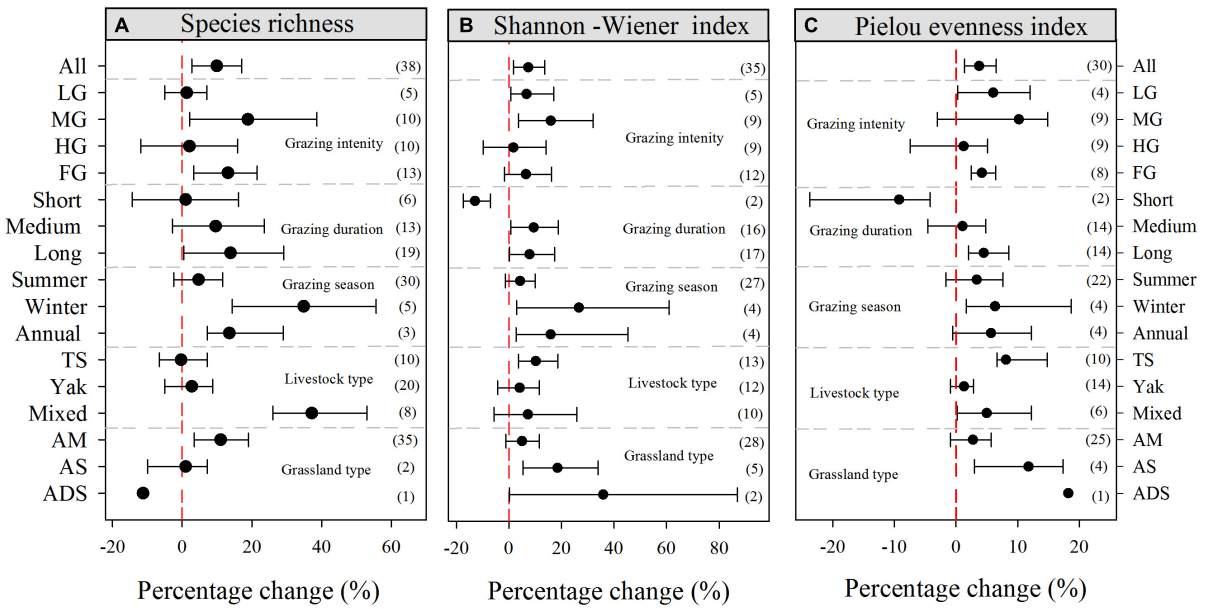

FIGURE 2 | Percentage changes in **(A)** species richness, **(B)** Shannon–Wiener index, and **(C)** Pielou evenness index in response to grazing. The variables are categorized into different groups by grazing intensity, grazing duration, grazing season, livestock type, and grassland type. The error bars represent the bootstrap 95% CI. Data on the right-hand side of each panel represents the sample sizes of observations. LG, light grazing; MG, moderate grazing; HG, heavy grazing; FG, free grazing; TS, Tibetan sheep; AM, alpine meadow; AS, alpine steppe; ADS, alpine desert steppe.

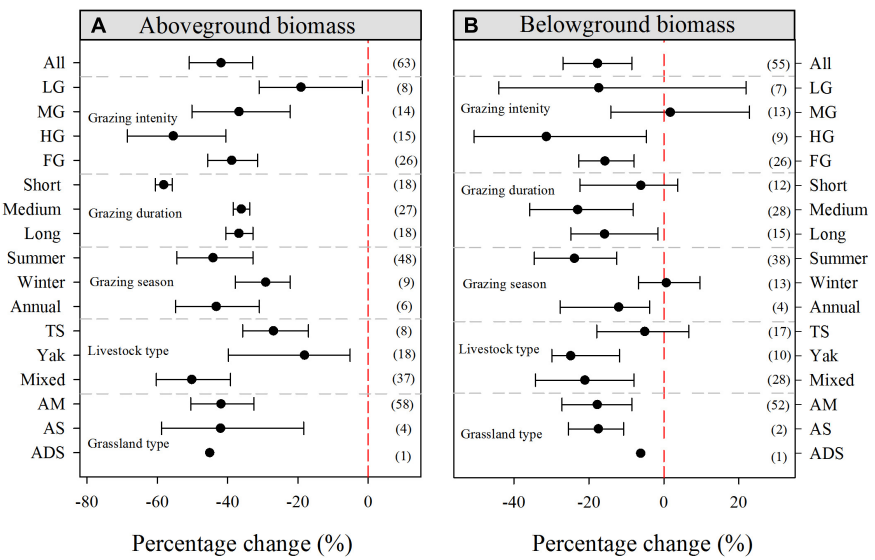

FIGURE 3 | Percentage changes in **(A)** aboveground biomass and **(B)** belowground biomass in response to grazing. The variables are categorized into different groups by grazing intensity, grazing duration, grazing season, livestock type, and grassland type. The error bars represent the bootstrap 95% CI. Data on the right-hand side of each panel represents the sample sizes of observations. LG, light grazing; MG, moderate grazing; HG, heavy grazing; FG, free grazing; TS, Tibetan sheep; AM, alpine meadow; AS, alpine steppe; ADS, alpine desert steppe.

and 15.89% (95% CI: 3.68–32.04%), respectively; however, it did not significantly affect the Pielou evenness index (**Figure 2**). Furthermore, FG had positive effects on species richness (13.10%, 95% CI: 3.38–21.47%) and the Pielou evenness index (4.17%, 95% CI: 2.45–6.44%). For the experimental duration, short and medium grazing durations did not significantly increase species richness compared to non-grazing, however, long-duration grazing increased species richness by 13.83% (95% CI: 0.47–29.16%). In contrast, short-duration grazing significantly reduced both the Shannon–Wiener index and Pielou evenness index, with decreases of 12.95% (95% CI: −17.33 to −6.99%) and 9.23% (95% CI: −23.67 to −4.18%), respectively. In

terms of the grazing season, winter grazing contributed to increased species richness (34.84%, 95% CI: 14.32–55.66%), Shannon–Wiener index (26.58%, 95% CI: 2.95–60.91%), and Pielou evenness index (6.31%, 95% CI: 1.67–18.67%). With respect to livestock type, grazing by Tibetan sheep significantly increased the Shannon–Wiener index and Pielou evenness index by 10.20% (95% CI: 3.63–18.55%) and 8.07% (95% CI: 6.66–14.83%), respectively (**Figure 2**). Grazing in an alpine meadow environment significantly increased species richness by 11.02% (95% CI: 3.50–19.08%), whereas it had no significant effect on either the Shannon–Wiener index or Pielou evenness index. In contrast, both the Shannon–Wiener index and Pielou evenness index significantly increased after grazing in an alpine steppe environment (**Figure 2**).

Effects on Grassland Biomass

The overall responses of the selected grassland plant biomass indices to grazing are presented in **Figure 3**. On average, grazing significantly decreased the AGB and BGB by 41.91% (95% CI: −50.91 to −32.88%) and 17.68% (95% CI: −26.94 to −8.52%), respectively. In detail, all grazing intensities had significant negative effects on AGB, however, only heavy and FG significantly decreased BGB (**Figure 3**). In terms of grazing duration, short grazing duration had the greatest impact on AGB, with a decrease of 58.19% (95% CI: −60.53 to −55.71%), but did not affect BGB. Similarly, both medium and long grazing durations had significantly negative effects on the AGB and BGB parameters. Regarding different grazing seasons, winter grazing had less impact on AGB than summer and annual grazing, while it had no significant effect on BGB. Grazing by different livestock types showed different magnitudes of biomass changes, with mixed grazing showing the greatest reduction in AGB compared with yak and Tibetan sheep grazing. Furthermore, grazing significantly decreased both AGB and BGB in alpine meadow and alpine steppe environments (**Figure 3**). In short, grazing significantly reduced AGB, however, the values for BGB differed due to different grazing management strategies.

Effects on Grassland Soil C, N, and Related Variables

Averaged across all studies, grazing significantly decreased SOC (13.06%, 95% CI: −13.06 to −10.15%), TN (12.62%, 95% CI: −17.35 to −8.61%), the C:N ratio (3.27%, 95% CI: −4.25 to −2.09%), and SM (20.75%, 95% CI: −27.89 to −13.61%). However, on average, grazing increased soil BD by 17.46% (95% CI: 11.88–24.53%) and soil pH by 2.24% (95% CI: 1.01–3.64%) (**Figure 4**). Specifically, with increasing intensity, grazing had an increasingly negative impact on SOC, TN, C:N ratio, and SM, whereas, it had a positive effect on both soil BD and pH. Regarding grazing duration, long grazing durations had the greatest impact on SOC (−24.90%, 95% CI: −31.32 to −17.38%), TN (−18.52%, 95% CI: −27.69 to −8.12%), and C:N ratio (−4.10%, 95% CI: −5.64 to −3.48%). Moreover, all grazing durations significantly increased soil BD and soil pH, whereas they significantly decreased SM; on average, SM decreased more with increased grazing duration. In terms of grazing season, all grazing seasons significantly reduced the SOC, TN, and SM parameters, but increased soil BD. When grouped by livestock type, the greatest reductions in SOC, TN, and C:N ratio occurred with mixed livestock grazing, with decreases of 17.63% (95% CI: −23.59 to −12.08%), 21.85% (95% CI: −33.40 to −12.44%), and 3.30% (95% CI: −6.49 to −1.23%), respectively. However, Tibetan sheep grazing had the most significant impact on soil BD (+34.76%, 95% CI: 20.73–51.65%), SM (−29.61%, 95% CI: −44.57 to −11.45%), and soil pH (+8.49%, 95% CI: 2.92–13.68%). Additionally, in terms of environment, based on the limited number of observations ($n < 20$), grazing had no significant effect on the SOC, TN, or SM variables in alpine steppe and alpine desert steppe settings. However, the opposite result was identified for meadow grassland, where grazing significantly reduced SOC, TN, C:N ratio, and SM, but both soil BD and pH were significantly increased (**Figure 4**).

Plant Diversity and Biomass Relationship With Soil Properties Under Grazing

As shown above, grazing affected the relationship between plant communities and soil properties in alpine grassland. In order to quantify this relationship, we used Pearson's correlation analysis to investigate the *RR* of plant diversity, biomass, and soil environmental factors (**Table 1**). The results showed that the *RR* of SOC was significantly negatively correlated with both the Shannon–Wiener index and the Pielou evenness index, however, it was significantly positively correlated with AGB and BGB. In contrast, the *RR* of species richness showed no significant correlation with SOC and TN ($p > 0.05$). In addition, the relationships between the *RR* of the Shannon–Wiener index, Pielou evenness index, AGB, and BGB all had a significant negative correlation with BD (**Table 1**).

In addition, we also investigated the relationship between the *RR* and climate factors. Specifically, our analysis indicated that there was no significant correlation between the *RR* of plant diversity and MAT or MAP (**Table 2**). Similarly, no significant relationships were observed between the *RR* values of AGB, BGB, SOC, and TN and climate. The *RR* of the soil C:N ratio, SM, and soil pH were all significantly negatively correlated with MAT ($p < 0.05$), however, they were not significantly correlated with MAP. The *RR* of BD declined with increasing MAP ($p < 0.05$), however, it was not significantly correlated with MAT (**Table 2**).

DISCUSSION

Response of Grassland Plant Diversity to Grazing

Our findings indicate that grazing significantly increases species richness, the Shannon–Wiener index, and the Pielou evenness index in alpine grassland on the QTP, consistent with the results of a meta-analysis by Lu et al. (2017) located in alpine grassland. These outcomes may be explained by grazing reducing plant height, cover, dominance, and litter, increasing light availability, enhancing the niche of grassland communities, promoting the coexistence of species, and improving plant species diversity in

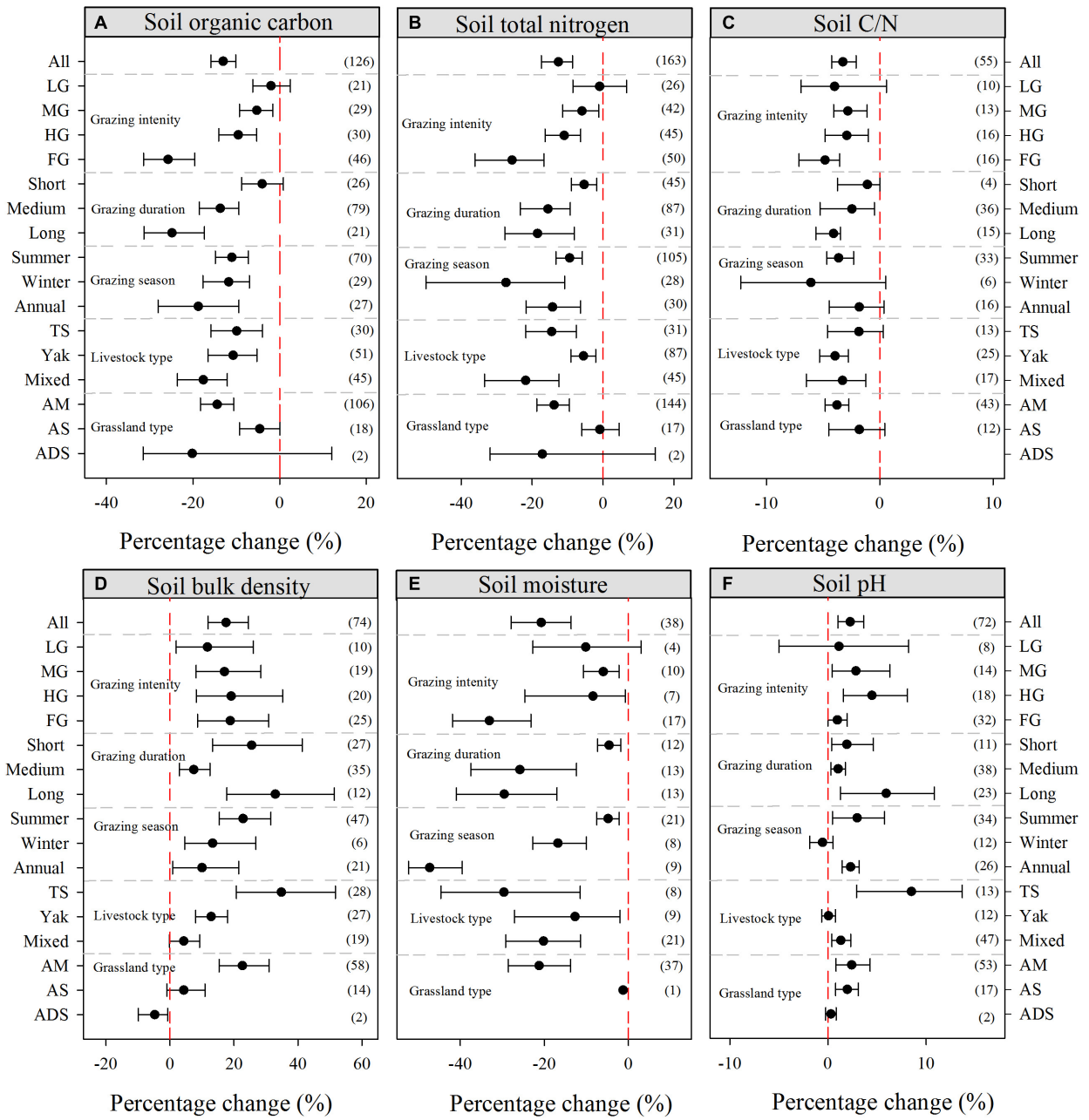

FIGURE 4 | Percentage changes in soil organic carbon **(A)**, soil total nitrogen **(B)**, soil C:N ratio **(C)**, soil bulk density **(D)**, soil moisture **(E)**, and soil pH **(F)** in response to grazing. The variables are categorized into different groups by grazing intensity, grazing duration, grazing season, livestock type, and grassland type. The error bars represent the bootstrap 95% CI. Data on the right-hand side of each panel represents the sample sizes of observations. LG, light grazing; MG, moderate grazing; HG, heavy grazing; FG, free grazing; TS, Tibetan sheep; AM, alpine meadow; AS, alpine steppe; ADS, alpine desert steppe.

alpine grassland (Ren et al., 2016; Segre et al., 2016). In addition, Gao and Carmel (2020) also found that grazing significantly increased plant richness compared to grazing exclusion scenarios, based on a global meta-analysis. However, our analysis of different subgroups found notable differences – in particular, moderate and FG remarkably increased species richness, whereas, the effect was not significant in areas of light and HG. Two possible explanations have been proposed for these patterns: (1) LG has more dominant species in the grassland community to a certain extent, thus preventing the establishment of other invasive species (Ganjurjav et al., 2015); or (2) MG reduces the dominance of certain species and promotes an increase in short-statured species, thus facilitating species coexistence, while HG may eliminate some grazing-intolerant species and reduce species diversity. Additionally, Sun et al. (2021) also found that MG increased the species richness in alpine grassland,

TABLE 1 | Pearson's correlation coefficients (R^2) between the response ratio (*RR*) of plant and soil.

Variables	Species richness	Shannon–Wiener index	Pielou evenness index	AGB	BGB
SOC	0.01 (5)	−0.78* (5)	−0.83* (5)	0.27* (19)	0.33** (36)
TN	0.13 (16)	−0.45* (10)	−0.33 (10)	0.05 (26)	0.12* (37)
C:N ratio	–	–	–	0.04 (5)	0.87* (5)
BD	−0.45 (6)	−0.76* (6)	−0.64* (7)	−0.31** (30)	−0.20* (24)
SM	–	−0.34 (6)	−0.34 (6)	0.08 (17)	−0.37* (14)
Soil pH	0.48 (4)	0.14 (5)	0.06 (7)	−0.03 (21)	−0.01 (8)

*$p < 0.05$; **$p < 0.01$. The symbol "–" indicates no data available. Values in parentheses indicate the sample size of observations.*

TABLE 2 | Pearson's correlation coefficients (R^2) between response variables, mean annual temperature (MAT), and mean annual precipitation (MAP).

Variables	*n*	MAT			MAP		
		Intercept	Slope	R^2	Intercept	Slope	R^2
Species richness	38	0.07	0.01	0.03	−0.04	2.E-04	0.02
Shannon–Wiener index	34	0.09	0.01	0.04	0.21	−2.E-04	0.05
Pielou evenness index	30	0.03	6.E-03	0.04	0.122	−2.E-04	0.035
AGB	63	−0.51	−0.02	9.E-03	−0.71	3.E-04	8.E-03
BGB	55	−0.12	−0.04	0.04	−0.10	−8.E-05	6.E-04
SOC	126	−0.16	0.02	0.03	−0.18	4.E-05	6.E-04
TN	163	−0.15	0.01	3.E-03	−0.22	1.E-04	4.E-03
C:N ratio	55	−0.05	−0.03	0.08*	0.05	−2.E-04	0.06
BD	74	0.17	0.01	0.02	0.52	−6.E-04	0.18*
SM	38	−0.25	−0.06	0.19*	0.21	−8.E−04	0.08
Soil pH	72	0.04	−0.01	0.15*	0.04	−4.E-05	0.01

*$p < 0.05$. *n*, indicates the sample size of observations.*

consistent with the predictions of the intermediate disturbance hypothesis, which further supports our meta-analysis results. Light, moderate, and FG significantly increased the Shannon–Wiener index and Pielou evenness index, whereas HG did not affect them. This change may be due to the decrease of dominant species in alpine grassland after grazing, which ultimately affected the plant Shannon–Wiener index and Pielou evenness index (Zhou et al., 2006; Li et al., 2013).

Notably, long-term (>5 years) grazing durations increased species diversity compared to non-grazing, however, the effects of short- and medium-duration grazing on species diversity were not significant. This may be potentially associated with the succession of alpine grassland vegetation: long-term non-grazing has led to dominant species which are more robust and, as a result, some less competitive species have gradually decreased or disappeared from plant communities because of competition, light resource, or nutrient availability (Yan and Lu, 2015; Liu et al., 2020). This result is consistent with a China scale meta-analysis performed by Xiong et al. (2016) that found that short-term grazing exclusion (<5 years) remarkably increased species richness. In addition, our results show that long-term grazing also increased the Shannon–Wiener index and Pielou evenness index. This finding is similar to that of Xiong et al. (2014), who reported that both the Shannon–Wiener index and Pielou evenness index were significantly lower in the grazing excluded plots than in the adjacent grazing plots at all sites. Moreover, our synthesis indicates that winter grazing significantly increased species richness, the Shannon–Wiener index, and Pielou evenness index, perhaps because winter grazing may reduce the accumulation of grassland litter and increase the sunshine exposure of the ground surface, thus leading to an increase in the emergence rate and number of seed species (Zou et al., 2016). In terms of livestock type, yak and Tibetan sheep are the dominant species grazing on the QTP (Cheng et al., 2016). Our meta-analysis indicated that yak grazing had no significant impact on plant diversity indices, but mixed grazing significantly increased species richness and the Pielou evenness index. It is worth noting that the effects of Tibetan sheep grazing on the Shannon–Wiener index and Pielou evenness index were more pronounced than the effects of yak and mixed grazing. This was presumably because there are differences between Tibetan sheep and yak in size and habit, including feeding and trampling behaviors (Cai et al., 2014). The increase of species richness was most pronounced in the alpine meadow environment under grazing, which could be attributed to the different components of different alpine grassland types.

Response of Grassland Biomass to Grazing

Livestock grazing significantly decreased both AGB and BGB in the alpine grasslands of QTP (**Figure 3**), a finding that is supported by outcomes of many previous synthesis studies (Lu et al., 2017; Sun et al., 2021). In addition, Hao and He (2019)

and Jiang et al. (2020) also found that grazing reduced AGB and BGB through China-scale meta-analysis. Among the different grazing intensities, HG yielded the most significant reductions in AGB and BGB by 55.43% (95% CI: −68.49 to −40.51%) and 31.35% (95% CI: −50.60 to −4.60%), respectively (**Figure 3**). This may occur because, as the destruction of soil increase as grazing pressure increases, SOC and soil nutrients decrease, and, thus, soil BD and soil pH also increase (Wiesmeier et al., 2012; Liu C. et al., 2021). Furthermore, we also found that SOC was significantly positively correlated with AGB and BGB under grazing (**Table 1**). However, light and MG intensities had no significant effect on BGB, which was consistent with meta-analysis on global scales (Tang et al., 2019). In addition, Yan et al. (2013), who performed a meta-analysis in China, found that light and MG did not have significant effects on grassland BGB at depths of 0–30 cm. Compared with medium and long durations of grazing, the short-duration (<2 years) grazing decreased AGB, while there was no significant change in BGB. This result is in agreement with the findings of Hao and He (2019) and may be due to the impact of short-term grazing on BGB having a certain lag effect. For different grazing seasons, grazing significantly decreased AGB and BGB, however, winter had no significant effect on BGB, which might be due to the following reasons. Firstly, summer is the growing season for alpine grassland on the QTP and grazing livestock may inhibit the normal growth of grassland by eating and trampling the plants. Secondly, the majority of grassland species stopped growing above ground in winter, however, their underground roots did not stop growing. The effect of mixed grazing on AGB was greater than that of yak or Tibetan sheep grazing, whereas, yak grazing had the greatest impact on BGB. This phenomenon might be related to the different living habits of yak and Tibetan sheep, including differences in their eating, walking, resting, and excretion habits (Cai et al., 2014). Overall, for all three grassland types, grazing reduced grassland AGB and BGB, which is consistent with findings of previous studies (Yan and Lu, 2015; Zhao et al., 2016; Chen et al., 2018).

Response of Soil C, N, and Related Variables to Grazing

Soil C and N are materials that store energy and limit plant productivity in grassland ecosystems (Song et al., 2017). Overall, our meta-analysis indicated that grazing significantly reduced SOC, TN, and the C:N ratio in alpine grasslands, which is in accordance with the outcomes of several other studies (Lu et al., 2017; Hao and He, 2019; Zhan et al., 2020; Liu C. et al., 2021). This effect may be attributed to a decrease in grassland biomass and litter after grazing, which, in turn, leads to a decrease in the soil nutrient input (Zhou et al., 2017). With increased grazing intensity, only LG did not have a significant impact on SOC, TN, and the C:N ratio. Dong et al. (2012) and Tang et al. (2019) indicated that TN and SOC exhibited downward trends with increasing grazing intensity. These findings imply that the turnover of plant materials and excreta disruption of soil hastened the loss of soil C and N under different grazing pressures (Wu et al., 2010; Dong et al., 2012). It should be noted that the SOC, TN, and C:N ratio changed more significantly with long-durations of grazing, whereas short-duration grazing had the least effect on them. As shown in a previous study, long-term grazing reduced the input of soil organic matter in grassland (Zhang et al., 2018). Likewise, Zhou et al. (2017) also demonstrated a negative linear relationship between grazing duration and soil carbon and nitrogen from a global perspective. All grazing seasons exhibited a significant reduction in SOC and TN, however, winter and annual grazing did not change the C:N ratio (**Figure 4**). This was consistent with the findings of Wang et al. (2018), presumably because livestock feeding reduced the ability of the aboveground organic matter to return to the soil. Compared to yak and Tibetan sheep grazing, mixed grazing had the greatest impact on SOC, TN, and the C:N ratio in alpine grassland, which is consistent with the finding of a recent meta-analysis (Liu C. et al., 2021). This may be due to different foraging selectivity between Tibetan sheep and yak, leading to changes in the input and output of C and N by grazing. In terms of grassland types, our results indicated that grazing significantly decreased SOC, TN, and the C:N ratio in alpine meadow environments, but the results were opposite to those in alpine steppe and alpine desert steppe settings. These different results may be due to environmental factors (such as climatic conditions and soil properties) of grassland types (Sun et al., 2013). Furthermore, Yang et al. (2009) found that the plant biomass of alpine meadows on the QTP is typically higher than that of alpine grasslands and alpine desert grasslands.

Our synthesis also showed that grazing significantly increased soil BD and soil pH, but significantly decreased SM. This finding is in agreement with previous meta-analyses based on the QTP and at larger scales across China (Hao and He, 2019; Liu C. et al., 2021; Sun et al., 2021). In addition, Zheng et al. (2012) and Lu X. et al. (2015) found that grazing increased the soil BD, which led to a decrease in SM and an increase in the soil pH of alpine grasslands. We speculate that the following reasons could explain these results. Firstly, these outcomes may be attributed to frequent trampling of the soil during grazing, which leads to deterioration and consolidation of the soil structure and has a negative impact on SM (Davidson et al., 2017; Liu C. et al., 2021). Secondly, this is likely due to was likely because of the accumulation of excreta and urine from grazing livestock (Dong et al., 2012; Yang et al., 2016). Furthermore, long-duration grazing significantly increased soil pH; this effect is likely related to grazing having an additive effect on soil trampling. With respect to different grazing seasons, summer grazing had minimal effects on SM, which was likely due to precipitation on the QTP was mainly concentrated in summer, and the soil was moist. The effect of Tibetan sheep grazing on soil BD and pH was greater than that of mixed grazing, which is in agreement with a previous study (Xiao et al., 2018). Grazing significantly increased both the soil BD and pH of alpine grassland, based on our analysis of a number of studies in alpine steppe and desert steppe environments. Grazing significantly reduced soil BD in the alpine desert steppe but did not change the soil BD in the alpine steppe environment, possibly because soil properties and climatic conditions varied with grassland type.

Regulating Mechanisms of the Grazing on Plant Community and Soil Properties

Overall, grazing is one of the most important factors affecting and regulating the vegetation and soil of the alpine grassland on the QTP (Yang et al., 2018). We found that the *RR* of SOC was negatively correlated with the Shannon–Wiener index and Pielou evenness index with increasing grazing interference. This change may be due to differences in the structure and function of vegetation communities, which cause different feedback mechanisms between them (Wardle et al., 2004). Our results also show that the *RR* of AGB and BGB were significantly positively correlated with SOC and TN, respectively (**Table 1**); this finding is likely because the soil C and N mainly come from grassland biomass and litter decomposition (Sun J. et al., 2018). Livestock can also increase soil hardness and pH by trampling, in addition to inhibiting the growth of grassland plants; this corresponds well with our correlation analysis, which indicates that the *RR* of soil BD and pH are negatively correlated with AGB and BGB, respectively (**Table 1**), consistent with the finding of Hao and He (2019). In addition, the effects of climate change will also affect the growth of alpine grassland vegetation on the QTP (Wu J. et al., 2014). In this study, we found that each plant diversity index was not significantly correlated with MAT or MAP under grazing (**Table 2**). This result may indicate that grazing disturbance is the main cause of changes in grassland species diversity (Collins and Barber, 1985). Suitable temperature and rainfall also help to increase soil microbial activity and accelerate soil organic matter mineralization (Ghee et al., 2013); however, our results indicate that SOC and TN are not significantly correlated with climate under grazing, potentially because grazing decreases biomass and litter, resulting in less soil organic matter and nutrients. The *RR* of the C:N ratio exhibited a negative correlation with MAT, indicating that MAT plays an important role in C:N ratio regulation (Klaminder et al., 2009). Furthermore, our results showed that the *RR* of SM and soil pH had a significant negative correlation with MAT under grazing, largely resulting from increases in soil evaporation and soil temperature by caused grazing (Wolf et al., 2010).

CONCLUSION

Grazing is an important form of alpine grassland resources utilization on the QTP. Understanding the effects of various grazing type and extent on plant diversity and ecological functions in alpine grassland could provide a reference for grassland management practices. Our meta-analysis revealed that MG intensity significantly increased species richness, Shannon–Wiener index, and Pielou evenness index, indicating that MG intensity may be an effective management approach for improving the species diversity of alpine grassland on the QTP. In addition, long-duration (>5 years), winter, and mixed grazing could help to enhance grassland diversity. However, there was a greater decrease of AGB, SOC, and TN with increasing grazing intensity, among which light and MG had less impact on biomass and soil quality. Given these outcomes, this study indicates that grazing should be chosen according to local environmental conditions, in order to realize the sustainable utilization, biodiversity, and environmental protection of alpine grassland on the QTP.

DATA AVAILABILITY STATEMENT

The datasets presented in this study can be found in online repositories. The names of the repository/repositories and accession number(s) can be found in the article/ **Supplementary Material**.

AUTHOR CONTRIBUTIONS

WL: conceptualization, writing – review and editing, supervision, and funding acquisition. CL: conceptualization, writing – original draft, methodology, validation, investigation, software, and formal analysis. WW and HZ: supervision and funding acquisition. YX: funding acquisition. JX: supervision. PX and HY: data collect and supervision. All authors have read and agreed to the published version of the manuscript.

FUNDING

This work was supported by the National Natural Science Foundation of China (41471450), the Earmarked Fund for China Agriculture Research System (CARS-34), the Fundamental Research Funds for the Central Universities (lzujbky-2021-ct11), Qilian Mountain National Park Mountain Vertical Belt Monitoring Plot Construction Project "Investigation and Testing of Ecosystems of Typical Forests, Shrubs, Grasslands and Meadows in the Vertical Distribution Belt of Haibei Area of National Park" (QHXH-2021-017), and Muli Duowei Gongma Wetland Protection and Restoration Project (2021).

SUPPLEMENTARY MATERIAL

The Supplementary Material for this article can be found online at: https://www.frontiersin.org/articles/10.3389/fpls.2021.765070/full#supplementary-material

REFERENCES

Byrnes, R. C., Eastburn, D. J., Tate, K. W., and Roche, L. M. (2018). A Global Meta-Analysis of Grazing Impacts on Soil Health Indicators. *J. Environ. Qual.* 47, 758–765. doi: 10.2134/jeq2017.08.0313

Cai, Y. J., Wang, X. D., Tian, L. L., Zhao, H., Lu, X. Y., and Yan, Y. (2014). The impact of excretal returns from yak and Tibetan sheep dung on nitrous oxide emissions in an alpine steppe on the Qinghai-Tibetan Plateau. *Soil Biol. Biochem.* 76, 90–99. doi: 10.1016/j.soilbio.2014.05.008

Chen, J., Luo, Y. Q., Xia, J. Y., Zhou, X. H., Niu, S. L., Shelton, S., et al. (2018). Divergent responses of ecosystem respiration components to livestock exclusion on the Qinghai Tibetan Plateau. *Land Degrad. Dev.* 29, 1726–1737. doi: 10.1002/ldr.2981

Cheng, Y., Cai, Y. J., and Wang, S. Q. (2016). Yak and Tibetan sheep dung return enhance soil N supply and retention in two alpine grasslands in the Qinghai-Tibetan Plateau. *Biol. Fertil. Soils* 52, 413–422. doi: 10.1007/s00374-016-1088-6

Collins, S. L., and Barber, S. C. (1985). EFFECTS OF DISTURBANCE ON DIVERSITY IN MIXED-GRASS PRAIRIE. *Vegetatio* 64, 87–94. doi: 10.1007/BF00044784

Davidson, K. E., Fowler, M. S., Skov, M. W., Doerr, S. H., Beaumont, N., and Griffin, J. N. (2017). Livestock grazing alters multiple ecosystem properties and services in salt marshes: a meta-analysis. *J. Appl. Ecol.* 54, 1395–1405. doi: 10.1111/1365-2664.12892

Dlamini, P., Chivenge, P., and Chaplot, V. (2016). Overgrazing decreases soil organic carbon stocks the most under dry climates and low soil pH: A meta-analysis shows. *Agric. Ecosyst. Environ.* 221, 258–269. doi: 10.1016/j.agee.2016.01.026

Dong, Q. M., Zhao, X. Q., Wu, G. L., Shi, J. J., Wang, Y. L., and Sheng, L. (2012). Response of soil properties to yak grazing intensity in a Kobresia parva-meadow on the Qinghai-Tibetan Plateau, China. *J. Soil Sci. Plant Nutr.* 12, 535–546. doi: 10.4067/S0718-95162012005000014

Ganjurjav, H., Duan, M. J., Wan, Y. F., Zhang, W. N., Gao, Q. Z., Li, Y., et al. (2015). Effects of grazing by large herbivores on plant diversity and productivity of semi-arid alpine steppe on the Qinghai-Tibetan Plateau. *Rangel. J.* 37, 389–397. doi: 10.1071/RJ14127

Gao, J., and Carmel, Y. (2020). A global meta-analysis of grazing effects on plant richness. *Agricult. Ecosyst. Environ.* 302:107072. doi: 10.1016/j.agee.2020.107072

Ghee, C., Neilson, R., Hallett, P. D., Robinson, D., and Paterson, E. (2013). Priming of soil organic matter mineralisation is intrinsically insensitive to temperature. *Soil Biol. Biochem.* 66, 20–28. doi: 10.1016/j.soilbio.2013.06.020

Gurevitch, J., Koricheva, J., Nakagawa, S., and Stewart, G. (2018). Meta-analysis and the science of research synthesis. *Nature* 555, 175–182. doi: 10.1038/nature25753

Hao, Y. Q., and He, Z. W. (2019). Effects of grazing patterns on grassland biomass and soil environments in China: A meta-analysis. *PLoS One* 14:15. doi: 10.1371/journal.pone.0215223

He, M., Zhou, G. Y., Yuan, T. F., van Groenigen, K. J., Shao, J. J., and Zhou, X. H. (2020). Grazing intensity significantly changes the C : N : P stoichiometry in grassland ecosystems. *Glob. Ecol. Biogeogr.* 29, 355–369. doi: 10.1111/geb.13028

Hedges, L. V., Gurevitch, J., and Curtis, P. S. (1999). The meta-analysis of response ratios in experimental ecology. *Ecology* 80, 1150–1156. doi: 10.1890/0012-9658(1999)080[1150:TMAORR]2.0.CO;2

Herrero-Jauregui, C., and Oesterheld, M. (2018). Effects of grazing intensity on plant richness and diversity: a meta-analysis. *Oikos* 127, 757–766. doi: 10.1017/S1751731111002618

Janssens, I. A., Dieleman, W., Luyssaert, S., Subke, J. A., Reichstein, M., Ceulemans, R., et al. (2010). Reduction of forest soil respiration in response to nitrogen deposition. *Nat. Geosci.* 3, 315–322. doi: 10.1038/ngeo844

Jiang, Z. Y., Hu, Z. M., Lai, D. Y. F., Han, D. R., Wang, M., Liu, M., et al. (2020). Light grazing facilitates carbon accumulation in subsoil in Chinese grasslands: A meta-analysis. *Glob. Change Biol.* 26, 7186–7197. doi: 10.1111/gcb.15326

Klaminder, J., Yoo, K., and Giesler, R. (2009). Soil carbon accumulation in the dry tundra: Important role played by precipitation. *J. Geophys. Res. Biogeosci.* 9:114. doi: 10.1029/2009JG000947

Li, C., Wulf, H., Schmid, B., He, J. S., and Schaepman, M. E. (2018). Estimating Plant Traits of Alpine Grasslands on the Qinghai-Tibetan Plateau Using Remote Sensing. *IEEE J. Select. Top. Appl. Earth Observat. Remote Sens.* 11, 2263–2275. doi: 10.1109/JSTARS.2018.2824901

Li, H. Q., Zhang, F. W., Mao, S. J., Zhu, J. B., Yang, Y. S., He, H. D., et al. (2016). Effects of Grazing Exclusion on Soil Properties in Maqin Alpine Meadow, Tibetan Plateau, China. *Pol. J. Environ. Stud.* 25, 1583–1587. doi: 10.15244/pjoes/62099

Li, Y., Niu, S. L., and Yu, G. R. (2016). Aggravated phosphorus limitation on biomass production under increasing nitrogen loading: a meta-analysis. *Glob. Change Biol.* 22, 934–943. doi: 10.1111/gcb.13125

Li, W., Cao, W. X., Wang, J. L., Li, X. L., Xu, C. L., and Shi, S. L. (2017). Effects of grazing regime on vegetation structure, productivity, soil quality, carbon and nitrogen storage of alpine meadow on the Qinghai-Tibetan Plateau. *Ecol. Engin.* 98, 123–133. doi: 10.1016/j.ecoleng.2016.10.026

Li, W., Huang, H. Z., Zhang, Z. N., and Wu, G. L. (2011). Effects of grazing on the soil properties and C and N storage in relation to biomass allocation in an alpine meadow. *J. Soil Sci. Plant Nutr.* 11, 27–39. doi: 10.4067/S0718-95162011000400003

Li, W., Tian, F. P., Ren, Z. W., Huang, H. Z., and Zhang, Z. N. (2013). Effects of grazing and fertilization on the relationship between species abundance and functional traits in an alpine meadow community on the Tibetan Plateau. *Nordic J. Bot.* 31, 247–255. doi: 10.1111/j.1756-1051.2012.01511.x

Lin, X. W., Zhang, Z. H., Wang, S. P., Hu, Y. G., Xu, G. P., Luo, C. Y., et al. (2011). Response of ecosystem respiration to warming and grazing during the growing seasons in the alpine meadow on the Tibetan plateau. *Agric. For. Meteorol.* 151, 792–802. doi: 10.1016/j.agrformet.2011.01.009

Liu, C., Li, W., Xu, J., Wei, W., Xue, P., and Yan, H. (2021). Response of soil nutrients and stoichiometry to grazing management in alpine grassland on the Qinghai-Tibet Plateau. *Soil Tillage Res.* 206:104822. doi: 10.1016/j.still.2020.104822

Liu, X., Wang, Z. Q., Zheng, K., Han, C. L., Li, L. H., Sheng, H. Y., et al. (2021). Changes in soil carbon and nitrogen stocks following degradation of alpine grasslands on the Qinghai-Tibetan Plateau: A meta-analysis. *Land Degrad. Dev.* 32, 1262–1273. doi: 10.1002/ldr.3796

Liu, S. B., Zamanian, K., Schleuss, P. M., Zarebanadkouki, M., and Kuzyakov, Y. (2018). Degradation of Tibetan grasslands: Consequences for carbon and nutrient cycles. *Agric. Ecosyst. Environ.* 252, 93–104. doi: 10.1016/j.agee.2017.10.011

Liu, X., Ma, Z. W., Huang, X. T., and Li, L. H. (2020). How does grazing exclusion influence plant productivity and community structure in alpine grasslands of the Qinghai-Tibetan Plateau? *Global Ecol. Conservat.* 23:e01066. doi: 10.1016/j.gecco.2020.e01066

Lu, X., Yan, Y., Sun, J., Zhang, X., Chen, Y., Wang, X., et al. (2015). Short-term grazing exclusion has no impact on soil properties and nutrients of degraded alpine grassland in Tibet, China. *Solid Earth* 6, 1195–1205. doi: 10.5194/se-6-1195-2015

Lu, X. Y., Yan, Y., Sun, J., Zhang, X. K., Chen, Y. C., Wang, X. D., et al. (2015). Carbon, nitrogen, and phosphorus storage in alpine grassland ecosystems of Tibet: effects of grazing exclusion. *Ecol. Evol.* 5, 4492–4504. doi: 10.1002/ece3.1732

Lu, X. Y., Kelsey, K. C., Yan, Y., Sun, J., Wang, X. D., Cheng, G. W., et al. (2017). Effects of grazing on ecosystem structure and function of alpine grasslands in Qinghai-Tibetan Plateau: a synthesis. *Ecosphere* 8:e01656. doi: 10.1002/ecs2.1656

Luo, Y. Q., Hui, D. F., and Zhang, D. Q. (2006). Elevated CO2 stimulates net accumulations of carbon and nitrogen in land ecosystems: A meta-analysis. *Ecology* 87, 53–63. doi: 10.1890/04-1724

McSherry, M. E., and Ritchie, M. E. (2013). Effects of grazing on grassland soil carbon: a global review. *Glob. Change Biol.* 19, 1347–1357. doi: 10.1111/gcb.12144

Møller, A. P., and Jennions, M. D. (2001). Testing and adjusting for publication bias. *Trends Ecol. Evol.* 16, 580–586. doi: 10.1111/j.0006-341x.2000.00455.x

Niu, K. C., Choler, P., Zhao, B. B., and Du, G. Z. (2009). The allometry of reproductive biomass in response to land use in Tibetan alpine grasslands. *Funct. Ecol.* 23, 274–283. doi: 10.1111/j.1365-2435.2008.01502.x

Ren, C. J., Chen, J., Lu, X. J., Doughty, R., Zhao, F. Z., Zhong, Z. K., et al. (2018). Responses of soil total microbial biomass and community compositions to rainfall reductions. *Soil Biol. Biochem.* 116, 4–10. doi: 10.1016/j.soilbio.2017.09.028

Ren, Y., Lü, Y., and Fu, B. (2016). Quantifying the impacts of grassland restoration on biodiversity and ecosystem services in China: A meta-analysis. *Ecol. Engin.* 95, 542–550. doi: 10.1016/j.ecoleng.2016.06.082

Rosenberg, M. S. (2005). The file-drawer problem revisited: A general weighted method for calculating fail-safe numbers in meta-analysis. *Evolution* 59, 464–468. doi: 10.1111/j.0014-3820.2005.tb01004.x

Rosenberg, M. S., Adams, D. C., and Gurevitch, J. (2000). *MetaWin: Statistical Software for Meta-Analysis*. Sunderland, MA: Sinauer Associates.

Scurlock, J. M. O., and Hall, D. O. (1998). The global carbon sink: a grassland perspective. *Glob. Change Biol.* 4, 229–233. doi: 10.1046/j.1365-2486.1998.00151.x

Segre, H., DeMalach, N., Henkin, Z., and Kadmon, R. (2016). Quantifying Competitive Exclusion and Competitive Release in Ecological Communities: A Conceptual Framework and a Case Study. *PLoS One* 11:14. doi: 10.1371/journal.pone.0160798

Shi, X. M., Li, X. G., Li, C. T., Zhao, Y., Shang, Z. H., and Ma, Q. F. (2013). Grazing exclusion decreases soil organic C storage at an alpine grassland of the Qinghai-Tibetan Plateau. *Ecol. Engin.* 57, 183–187. doi: 10.1016/j.ecoleng.2013.04.032

Song, Y., Zou, Y. C., Wang, G. P., and Yu, X. F. (2017). Altered soil carbon and nitrogen cycles due to the freeze-thaw effect: A meta-analysis. *Soil Biol. Biochem.* 109, 35–49. doi: 10.1016/j.soilbio.2017.01.020

Sun, D. S., Wesche, K., Chen, D. D., Zhang, S. H., Wu, G. L., Du, G. Z., et al. (2011). Grazing depresses soil carbon storage through changing plant biomass and composition in a Tibetan alpine meadow. *Plant Soil Environ.* 57, 271–278. doi: 10.17221/7/2011-PSE

Sun, J., Cheng, G. W., and Li, W. P. (2013). Meta-analysis of relationships between environmental factors and aboveground biomass in the alpine grassland on the Tibetan Plateau. *Biogeosciences* 10, 1707–1715. doi: 10.1371/journal.pone.0081986

Sun, J., Ma, B. B., and Lu, X. Y. (2018). Grazing enhances soil nutrient effects: Trade-offs between aboveground and belowground biomass in alpine grasslands of the Tibetan Plateau. *Land Degrad. Dev.* 29, 337–348. doi: 10.1002/ldr.2822

Sun, Y., He, X. Z., Hou, F. J., Wang, Z. F., and Chang, S. H. (2018). Grazing increases litter decomposition rate but decreases nitrogen release rate in an alpine meadow. *Biogeosciences* 15, 4233–4243. doi: 10.5194/bg-15-4233-2018

Sun, J., Zhan, T. Y., Liu, M., Zhang, Z. C., Wang, Y., Liu, S. L., et al. (2021). Verification of the biomass transfer hypothesis under moderate grazing across the Tibetan plateau: a meta-analysis. *Plant Soil* 458, 139–150. doi: 10.1007/s11104-019-04380-8

Tang, S. M., Wang, K., Xiang, Y. Z., Tian, D. S., Wang, J. S., Liu, Y. S., et al. (2019). Heavy grazing reduces grassland soil greenhouse gas fluxes: A global meta-analysis. *Sci. Total Environ.* 654, 1218–1224. doi: 10.1016/j.scitotenv.2018.11.082

Tian, L., Zhang, Y. J., and Zhu, J. T. (2014). Decreased surface albedo driven by denser vegetation on the Tibetan Plateau. *Environ. Res. Lett.* 9:11. doi: 10.1088/1748-9326/9/10/104001

Wang, Y. X., Hodgkinson, K. C., Hou, F. J., Wang, Z. F., and Chang, S. H. (2018). An evaluation of government-recommended stocking systems for sustaining pastoral businesses and ecosystems of the Alpine Meadows of the Qinghai-Tibetan Plateau. *Ecol. Evol.* 8, 4252–4264. doi: 10.1002/ece3.3960

Wardle, D. A., Bardgett, R. D., Klironomos, J. N., Setala, H., van der Putten, W. H., and Wall, D. H. (2004). Ecological linkages between aboveground and belowground biota. *Science* 304, 1629–1633. doi: 10.1126/science.1094875

Wiesmeier, M., Steffens, M., Mueller, C. W., Kolbl, A., Reszkowska, A., Peth, S., et al. (2012). Aggregate stability and physical protection of soil organic carbon in semi-arid steppe soils. *Eur. J. Soil Sci.* 63, 22–31. doi: 10.1111/j.1365-2389.2011.01418.x

Wolf, B., Zheng, X. H., Brueggemann, N., Chen, W. W., Dannenmann, M., Han, X. G., et al. (2010). Grazing-induced reduction of natural nitrous oxide release from continental steppe. *Nature* 464, 881–884. doi: 10.1038/nature08931

Wu, G. L., Liu, Z. H., Zhang, L., Chen, J. M., and Hu, T. M. (2010). Long-term fencing improved soil properties and soil organic carbon storage in an alpine swamp meadow of western China. *Plant Soil* 332, 331–337. doi: 10.1007/s11104-010-0299-0

Wu, J., Zhang, X., Shen, Z., Shi, P., Yu, C., and Chen, B. (2014). Effects of livestock exclusion and climate change on aboveground biomass accumulation in alpine pastures across the Northern Tibetan Plateau. *Chin. Sci. Bull.* 59, 4332–4340. doi: 10.1007/s11434-014-0362-y

Wu, J. S., Shen, Z. X., Shi, P. L., Zhou, Y. T., and Zhang, X. Z. (2014). Effects of Grazing Exclusion on Plant Functional Group Diversity Alpine Grasslands along a Precipitation Gradient on the Northern Tibetan Plateau. *Arct. Antarct. Alp. Res.* 46, 419–429. doi: 10.1657/1938-4246-46.2.419

Xiao, H., Peng, Z., Xu, C. L., Zhang, D. G., Chai, J. L., Pan, T. T., et al. (2018). Yak and Tibetan sheep trampling inhibit reproductive and photosynthetic traits of Medicago ruthenica var. inschanica. *Environ. Monit. Assess.* 16:190. doi: 10.1007/s10661-018-6896-8

Xiong, D., Shi, P., Zhang, X., and Zou, C. B. (2016). Effects of grazing exclusion on carbon sequestration and plant diversity in grasslands of China—A meta-analysis. *Ecol. Engin.* 94, 647–655. doi: 10.1016/j.ecoleng.2016.06.124

Xiong, D. P., Shi, P. L., Sun, Y. L., Wu, J. S., and Zhang, X. Z. (2014). Effects of grazing exclusion on plant productivity and soil carbon, nitrogen storage in alpine meadows in northern Tibet. *China. Chin. Geogr. Sci.* 24, 488–498. doi: 10.1007/s11769-014-0697-y

Yan, L., Li, Y., Wang, L., Zhang, X. D., Wang, J. Z., Wu, H. D., et al. (2020). Grazing significantly increases root shoot ratio but decreases soil organic carbon in Qinghai-Tibetan Plateau grasslands: A hierarchical meta-analysis. *Land Degrad. Dev.* 10:16. doi: 10.1002/ldr.3606

Yan, L., Zhou, G., and Zhang, F. (2013). Effects of different grazing intensities on grassland production in China: a meta-analysis. *PLoS One* 8:e81466. doi: 10.1371/journal.pone.0081466

Yan, Y., and Lu, X. Y. (2015). Is grazing exclusion effective in restoring vegetation in degraded alpine grasslands in Tibet, China? *PeerJ* 3:16. doi: 10.7717/peerj.1020

Yang, Y. H., Fang, J. Y., Pan, Y. D., and Ji, C. J. (2009). Aboveground biomass in Tibetan grasslands. *J. Arid. Environ.* 73, 91–95. doi: 10.1016/j.jaridenv.2008.09.027

Yang, Z., Xiong, W., Xu, Y., Jiang, L., Zhu, E., Zhan, W., et al. (2016). Soil properties and species composition under different grazing intensity in an alpine meadow on the eastern Tibetan Plateau, China. *Environ. Monit Assess* 188:678. doi: 10.1007/s10661-016-5663-y

Yang, Z. N., Zhu, Q. A., Zhan, W., Xu, Y. Y., Zhu, E. X., Gao, Y. H., et al. (2018). The linkage between vegetation and soil nutrients and their variation under different grazing intensities in an alpine meadow on the eastern Qinghai-Tibetan Plateau. *Ecol. Engin.* 110, 128–136. doi: 10.1016/j.ecoleng.2017.11.001

Yu, L., Chen, Y., Sun, W., and Huang, Y. (2019). Effects of grazing exclusion on soil carbon dynamics in alpine grasslands of the Tibetan Plateau. *Geoderma* 353, 133–143. doi: 10.1016/j.geoderma.2019.06.036

Zhan, T. Y., Zhang, Z. C., Sun, J., Liu, M., Zhang, X. B., Peng, F., et al. (2020). Meta-analysis demonstrating that moderate grazing can improve the soil quality across China's grassland ecosystems. *Appl. Soil Ecol.* 6:147. doi: 10.1016/j.apsoil.2019.103438

Zhang, B., Thomas, B. W., Beck, R., Liu, K., Zhao, M. L., and Hao, X. Y. (2018). Labile soil organic matter in response to long-term cattle grazing on sloped rough fescue grassland in the foothills of the Rocky Mountains, Alberta. *Geoderma* 318, 9–15. doi: 10.1016/j.geoderma.2017.12.019

Zhang, Y., Gao, Q., Dong, S., Liu, S., Wang, X., Su, X., et al. (2015). Effects of grazing and climate warming on plant diversity, productivity and living state in the alpine rangelands and cultivated grasslands of the Qinghai-Tibetan Plateau. *Rangel. J.* 37, 57–65. doi: 10.1071/RJ14080

Zhao, J. X., Li, X., Li, R. C., Tian, L. H., and Zhang, T. (2016). Effect of grazing exclusion on ecosystem respiration among three different alpine grasslands on the central Tibetan Plateau. *Ecol. Engin.* 94, 599–607. doi: 10.1016/j.ecoleng.2016.06.112

Zheng, H., Ying, H., Yin, Y., Wang, Y., He, G., Bian, Q., et al. (2019). Irrigation leads to greater maize yield at higher water productivity and lower environmental costs: a global meta-analysis. *Agricult. Ecosyst. Environ.* 273, 62–69. doi: 10.1016/j.agee.2018.12.009

Zheng, Y., Yang, W., Sun, X., Wang, S. P., Rui, Y. C., Luo, C. Y., et al. (2012). Methanotrophic community structure and activity under warming and grazing of alpine meadow on the Tibetan Plateau. *Appl. Microbiol. Biotechnol.* 93, 2193–2203. doi: 10.1007/s00253-011-3535-5

Zhou, G., Zhou, X., He, Y., Shao, J., Hu, Z., Liu, R., et al. (2017). Grazing intensity significantly affects belowground carbon and nitrogen cycling in grassland ecosystems: a meta-analysis. *Glob. Chang Biol.* 23, 1167–1179. doi: 10.1111/gcb.13431

Zhou, G., Zhou, X., Nie, Y., Bai, S. H., Zhou, L., Shao, J., et al. (2018). Drought-induced changes in root biomass largely result from altered root morphological traits: Evidence from a synthesis of global field trials. *Plant Cell Environ.* 41, 2589–2599. doi: 10.1111/pce.13356

Zhou, H. K., Tang, Y. H., Zhao, X. Q., and Zhou, L. (2006). Long-term grazing alters species composition and biomass of a shrub meadow on the Qinghai-Tibet

Plateau. *Pak. J. Bot.* 38, 1055–1069. doi: 10.1111/j.1744-7909.2008.00676.x

Zou, J. R., Luo, C. Y., Xu, X. L., Zhao, N., Zhao, L., and Zhao, X. Q. (2016). Relationship of plant diversity with litter and soil available nitrogen in an alpine meadow under a 9-year grazing exclusion. *Ecol. Res.* 31, 841–851. doi: 10.1007/s11284-016-1394-3

Conflict of Interest: The authors declare that the research was conducted in the absence of any commercial or financial relationships that could be construed as a potential conflict of interest.

The reviewer YD declared a shared affiliation, with no collaboration, with one of the authors HZ to the handling editor at the time of the review.

Publisher's Note: All claims expressed in this article are solely those of the authors and do not necessarily represent those of their affiliated organizations, or those of the publisher, the editors and the reviewers. Any product that may be evaluated in this article, or claim that may be made by its manufacturer, is not guaranteed or endorsed by the publisher.

Copyright © 2021 Li, Liu, Wang, Zhou, Xue, Xu, Xue and Yan. This is an open-access article distributed under the terms of the Creative Commons Attribution License (CC BY). The use, distribution or reproduction in other forums is permitted, provided the original author(s) and the copyright owner(s) are credited and that the original publication in this journal is cited, in accordance with accepted academic practice. No use, distribution or reproduction is permitted which does not comply with these terms.

frontiers in Plant Science

ORIGINAL RESEARCH
published: 16 December 2021
doi: 10.3389/fpls.2021.778656

Restoration of Degraded Grassland Significantly Improves Water Storage in Alpine Grasslands in the Qinghai-Tibet Plateau

Xiaowei Guo[1], Huakun Zhou[1], Licong Dai[2], Jing Li[1], Fawei Zhang[1], Yikang Li[1], Li Lin[1], Qian Li[1], Dawen Qian[1], Bo Fan[1], Yuting Lan[1], Mengke Si[1], Bencuo Li[1], Guangmin Cao[1], Yangong Du[1] and Bin Wang[1,3]**

[1]Key Laboratory of Adaptation and Evolution of Plateau Biota, Northwest Institute of Plateau Biology, Chinese Academy of Sciences, Xining, China, [2]College of Ecology and Environment, Hainan University, Haikou, China, [3]New South Wales Department of Primary Industries, Wagga Wagga Agricultural Institute, Wagga Wagga, NSW, Australia

OPEN ACCESS

Edited by:
Yu Liu,
Northwest A&F University, China

Reviewed by:
Yanfu Bai,
Lanzhou University, China
Daorui Han,
South China Normal University, China

***Correspondence:**
Yangong Du
duyangong@163.com
Bin Wang
bin.a.wang@dpi.nsw.gov.au

Specialty section:
This article was submitted to Functional Plant Ecology, a section of the journal Frontiers in Plant Science

Received: *17 September 2021*
Accepted: *25 November 2021*
Published: *16 December 2021*

Citation:
Guo X, Zhou H, Dai L, Li J, Zhang F, Li Y, Lin L, Li Q, Qian D, Fan B, Lan Y, Si M, Li B, Cao G, Du Y and Wang B (2021) Restoration of Degraded Grassland Significantly Improves Water Storage in Alpine Grasslands in the Qinghai-Tibet Plateau. Front. Plant Sci. 12:778656. doi: 10.3389/fpls.2021.778656

Alpine grassland has very important water conservation function. Grassland degradation seriously affects the water conservation function; moreover, there is little understanding of the change of water state during grassland restoration. Our study aims to bridge this gap and improve our understanding of changes in soil moisture during the restoration process. In this study, the water storage, vegetation, and meteorology of a non-degradation grassland (grazing intensity of 7.5 sheep/ha) and a severely degraded grassland (grazing intensity of 12–18 sheep/ha) were monitored in the Qinghai-Tibet Plateau for seven consecutive years. We used correlation, stepwise regression, and the boosted regression trees (BRT) model analyses, five environmental factors were considered to be the most important factors affecting water storage. The severely degraded grassland recovered by light grazing treatment for 7 years, with increases in biomass, litter, and vegetation cover, and a soil-water storage capacity 41.9% higher in 2018 compared to that in 2012. This increase in soil-water storage was primarily due to the increase in surface soil moisture content. The key factors that influenced water storage were listed in a decreasing order: air temperature, litter, soil heat flux, precipitation, and wind speed. Their percentage contributions to soil-water storage were 50.52, 24.02, 10.86, 7.82, and 6.77%, respectively. Current and future climate change threatens soil-water conservation in alpine grasslands; however, grassland restoration is an effective solution to improve the soil-water retention capacity in degraded grassland soils.

Keywords: alpine grasslands, degraded grassland restoration, grass litter, Qinghai-Tibet plateau, soil-water storage

INTRODUCTION

The Qinghai-Tibet Plateau (QTP) plays a critical role in regional sustainable development and water resource conservation. This plateau is home to many rivers in China and Southeast Asia, and plays a key role in ensuring water security (Wang and Fu, 2004). In this region, the alpine grasslands contribute significantly to water conservation *via* the water retention.

The alpine grassland covers an area of 1.5×10^8 ha and accounts for 50.9% of the total area of the QTP. Therefore, alpine meadow is the most representative vegetation on the QTP. However, 30 % of the alpine grasslands are now severely degraded, due to the combined influence of climate change and human disturbance (Dai et al., 2021). Since the 1970s, grassland degeneration of the QTP has been recognized by many researchers, policy makers, and managers (Dong et al., 2020), degeneration severely threatens ecological security at regional and global scales. Additionally, the field surveys of grassland vegetation carried out at the beginning of this century demonstrated the alpine grasslands have indeed degraded, compared with those in the 1980s (Yang et al., 2006). Between 1992 and 2002, grassland degradation in the central and northwestern of the QTP was very serious, and degradation is more severe at high altitudes (4300–4600 m above sea level; Fassnacht et al., 2015). The degradation of plateau vegetation has a severe impact not only on China, but also global ecological security.

The water conservation function of alpine grassland is strongly affected by climate change and overgrazing. Evapotranspiration in grassland ecosystems is being continuously enhanced due to global warming, which reduces the water conservation capacity of grassland soil (Guo et al., 2020). However, the impact of climate change on grassland water conservation is slow and indirect. Conversely, the impact of grazing is not, and grazing can lead to serious grassland degradation within only three to 5 years (Mipam et al., 2019). Grassland degradation is the main reason for reducing the soil-water conservation function of grassland on the QTP (Dai et al., 2020). Even in the serious degraded grasslands that have been reclaimed into artificial grasslands, there is no significant improvement in water conservation function (Shen et al., 2020). The soil saturated moisture capacity, the capillary moisture capacity, and the field moisture capacity increase under light grazing, while these values drop sharply under heavy grazing. The saturation point and field capacity in moderately degraded grasslands increase by 17.1 and 5.8%, respectively, compared to less degraded grasslands (Zhao et al., 2011). However, the saturated moisture capacity, capillary moisture capacity, and field moisture capacity of the grassland decrease sharply in severely or extremely degraded grasslands (Kruemmelbein et al., 2009). The soil-water conservation function in degraded grassland has reduced by 18.3–27.8% on the QTP (Jiang et al., 2016), and therefore, moderate grazing of alpine grasslands is paramount to maintaining the water conservation function of alpine grassland.

Previous studies on grassland degradation and its effects on water conservation function have predominantly focused on spatial, rather than temporal data coverage; for example, comparing the water conservation function of grasslands with different degrees of degradation across different sites. However, alpine grassland vegetation and soil conditions vary geographically (Wang et al., 2016), and preclude complete explanations for changes in soil-water storage capacity. Our study monitored the same site of degraded alpine grassland for a period of 7 years, while the meadow was being restored through reduced grazing pressure, and postponing autumn grazing to give the seeds time to mature. The collected long-term dataset can be used to investigate the factors that are responsible for changes in soil-water capacity. The restoration of degraded grasslands can improve the vegetation condition, soil particle size, soil macro-aggregates, and organic matter content of the grassland, and these attributes in turn can lead to an improvement in the soil-water storage. Based on seven consecutive years of grassland moisture monitoring, we hypothesize that the restoration of degraded grasslands in the QTP will act to increase their soil-water storage capacity. We propose that the main reason for this change is the change of vegetation characteristics.

MATERIALS AND METHODS

Site Description and Experimental Design

This study was carried out in the Haibei National Field Research Station in the alpine grassland ecosystem (N37.6109°, E101.3142°, 3200 m above sea level), located in the northeastern region of the QTP. Seasonally, frozen ground is well developed in this region, which is characterized by a plateau continental monsoon climate. The mean annual air temperature is −1.70°C and the yearly precipitation is 570 mm, 80% of which occurs from May to September (Chen et al., 2008). The vegetation type is typical alpine meadow.

Our study observed the soil moisture content in the two plots selected during the growing seasons from 2012 to 2018. Two flat winter grassland plots along were selected, one with a native grassland (NG; N37.6109°, E101.3142°, 3212 m above sea level) and were another with a severely degraded grassland (SDG; N37.7003°, E101.5828°, 3268 m above sea level). The two plots were 2.8 km apart. They have been lightly grazed since 2012, with a grazing intensity of 7.5 sheep/ha, the difference between the two plots was caused by different previous grazing pressures. The SDG plot owned by a farmer was heavily grazed for 10 years with a rough estimate grazing intensity about 12–18 sheep/ha. Conversely, the SDG plot was gradually restored, the NG plot was operated by the Haibei National Field Research Station, and its grazing intensity had never changed. Due to a reduction in the grazing intensity from 2012 to 2018, detailed information about the two plots was provided in **Table 1**. Based on our field investigation, the soil in both plots was classified as Mat Cry-gelic Cambisols, which is rich in organic matter in the surface layer, because some plant roots in alpine grassland have surface accumulation. There are a lot of dead roots in the soil surface. The QTP has a relatively cold climate and the decomposition of organic matter is relatively slow, so the soil surface organic matter is relatively high.

Data Collection

Daily meteorological data including relative humidity, wind speed, net radiation, soil temperature, and mean air temperature were obtained from a meteorological station between 2012 and 2018. Precipitation data were obtained

TABLE 1 | Characteristics in the plots studied from 2012 to 2018.

Year	2012		2018	
Site	**NG†**	**SDG**	**NG**	**SDG**
Exposed soil coverage (%)	1 ± 1.0‡	21.8 ± 5.9	1 ± 1.0	8.9 ± 3.2
Total biomass (gm^{-2})	183.6 ± 32.8	4.4 ± 2.2	181.6 ± 22.9	126.5 ± 31.6
Organic matter (g/kg)	162.1 ± 22.1	145.8 ± 8.7	189.8 ± 34.9	158.6 ± 28.7
total nitrogen (g/kg)	7.6 ± 0.7	6.9 ± 0.4	8.6 ± 1.2	8.1 ± 0.9
Available phosphorus (mg/kg)	9.1 ± 0.4	7.4 ± 1.0	15.7 ± 1.6	12.8 ± 1.4
Nitrate nitrogen (mg/kg)	12.8 ± 2.2	5.4 ± 1.4	18.8 ± 3.7	17.8 ± 4.8
Ammoniacal nitrogen (mg/kg)	13.4 ± 1.7	12.7 ± 3.8	16.9 ± 3.0	15.5 ± 3.0
Dominant species composition and plant community description	Two-layer canopy. Upper canopy: *Stipa aliena*, *Helictotrichon tibeticum,* and *Elymus nutans*. Lower canopy: *Kobresia humilis, Scirpus distigmaticus, Poa crymophila,* and *Dracocephalum heterophyllum*	One-layer-canopy. *Elsholtzia calycocarpa, Ajania tenuifolia, Polygonum sibiricum, Ligularia virgaurea, and Potentilla anserine.*	Two-layer canopy. Upper canopy: *Stipa aliena, Helictotrichon tibeticum*, and *Elymus nutans*. Lower canopy: *Kobresia humilis, Scirpus distigmaticus, Poa crymophila,* and *Dracocephalum heterophyllum*	Two-layer canopy. Upper canopy: *Stipa aliena, Helictotrichon tibeticum,* and Elymus nutans. Lower canopy: *Kobresia humilis, Scirpus distigmaticus, Poa crymophila,* and *Dracocephalum heterophyllum*

†*NG, native grassland; SCG, severely degraded grassland.*
‡*Mean ± SE of three replicates were presented.*

by collecting precipitation manually. Soil moisture was measured from 2012 to 2014 using the drying and weighing method, oven drying for 24 h, then calculating the difference between dry weight and wet weight. Soil moisture was automatically measured by the soil monitoring system (A755; Campbell, United States; **Figure 1**). The probe type of soil moisture automatic observation system is Hydra Probe (America, Campbell), which was set at the soil depth of 5 cm, 10 cm, 15 cm, 20 cm, 30 cm, and 50 cm. This probe can quickly and continuously measure soil moisture, temperature, and electrical conductivity every hour. Time Domain Reflectometry (TDR) is the principle of soil moisture measurement in this study, because the dielectric constant of liquid is much higher than soil. The dielectric constants were calculated from the pulse velocity, and the relationship between dielectric constant and soil-water storage could be described by a third-order polynomial (Nadler, 1991; White et al., 1994).

The plant community was surveyed every month in the growing season using a grid method of quadrat survey procedure (0.5 m × 0.5 m). Vegetation coverage was calculated based on the occurrence within the 100 points. The above-ground biomass and grass litter were obtained by a standard harvesting method, then quickly brought back to the laboratory and dried at 75°C for 24 h before weighing.

Daily soil-water storage, expressed as mm, was defined as the actual soil-water content in a soil sample of a given thickness under natural conditions, is calculated as follow (Guo et al., 2020):

$$W = F \times H \times SD \times 10 \quad (1)$$

where W is the soil-water storage (mm), F is the bulk density of soil (g/cm^3), H is the thickness of the soil (cm), and SD is the soil moisture content (%).

Statistical Analysis

The significance of differences in soil-water storage, soil moisture content, and soil temperature between the different soil layers was analyzed using ANOVA and POST-HOC tests (LSD method). All differences were tested for significance at $p < 0.05$ level with SPSS 20.0 (SPSS Inc., Chicago, IL, United States). There are some disadvantages to examine the individual effects of environmental variables on soil-water storage solely based on the coefficients of independent variables, in a multiple regression analysis, which cannot split the individual contribution rate of each factor. The boosted regression trees (BRT) model was adopted to quantitatively evaluate the relative influence of environmental variables on soil-water storage. The BRT model was conducted with R software version 4.1.1.

RESULTS

Soil-Water Storage in the Two Plots

From 2012 to 2018, there was no significant change in the soil-water storage capacity of NG. However, the soil-water storage capacity of the degraded grassland plot increased every year due to the decrease in grazing pressure. The soil-water storage in the degraded grassland plot in 2017 and 2018 was significantly higher than in 2012 and 2013 ($p < 0.05$; **Figure 2**); in 2018, it was 41.9% higher than in 2012. The annual difference of soil-water storage was significant from 2012 to 2018 ($p < 0.05$), especially in the degraded grassland plot. The soil-water storage in NG was significantly higher than that in the degraded grassland plot in the years 2012, 2013, 2014, and 2015 ($p < 0.05$) but showed no significant differences in the years 2016, 2017, and 2018. Soil-water storage in the growing season changed periodically every

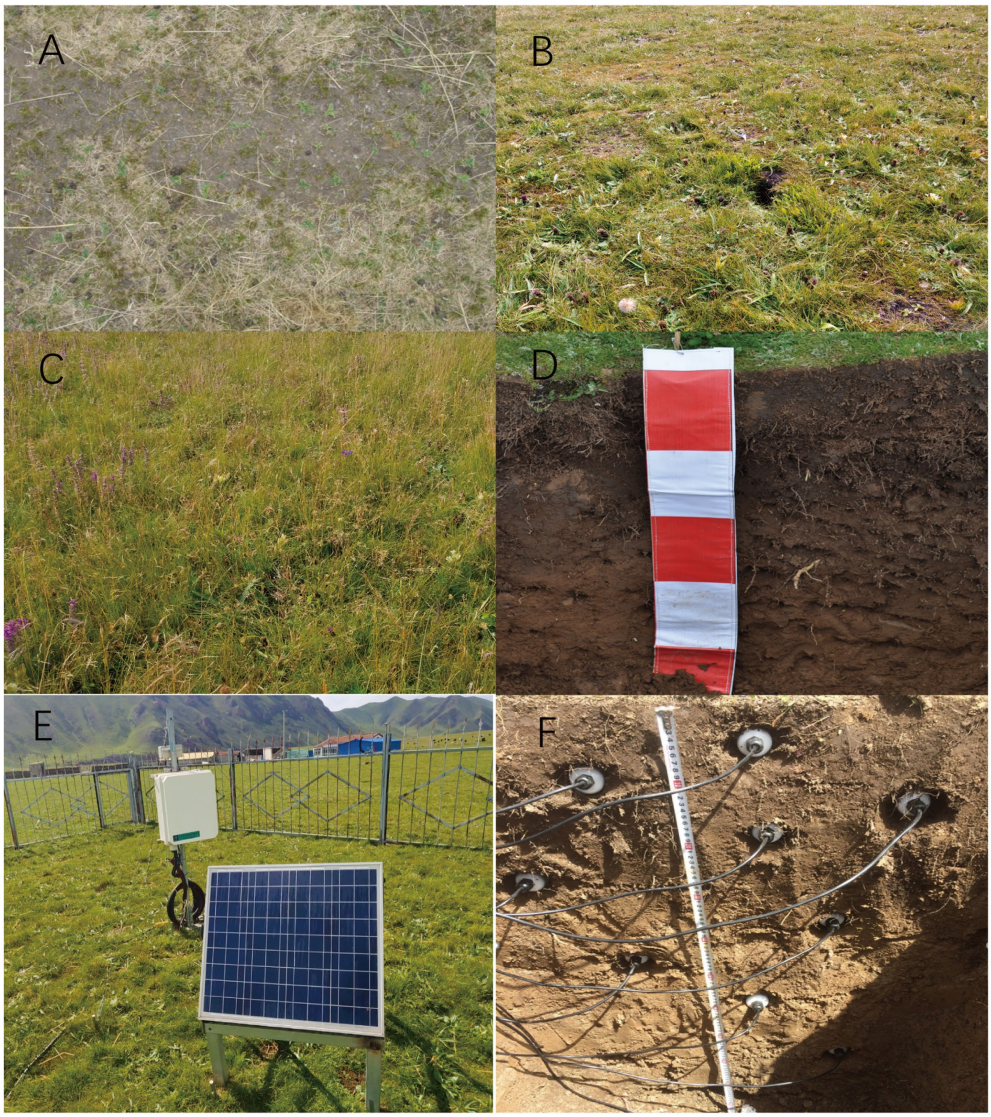

FIGURE 1 | The experiment plots and the soil moisture monitoring system. *Surface vegetation photograph of SDG in 2008 **(A)** and 2018 **(B)**, Surface vegetation photograph of NG in 2018 **(C)**, the Soil profile photograph **(D)**, the soil moisture monitoring system **(E)** and Hydra Probe **(F)**.

year, with a double peak (mid-May and mid- to late-August) and single valley observed in each change curve. The minimum value usually occurred in mid-August.

Changes in the Environmental Characteristics at the SDG Plot

The SDG plot was gradually restored from 2012 to 2018 due to the reduction of grazing pressure. The degenerative state of this area improved from a severe to light degradation status over this time, and its above-ground biomass, vegetation cover, and litter showed increasing trends (**Figure 3**). The above-ground biomass increased by 38.4% in 2018 compared to that in 2012. The bulk density of degraded grassland was higher than that of native grassland in each soil layer (**Table 2**).

A one-way ANOVA and POST-HOC tests (LSD method) showed that the biomass in the degraded grassland in 2018 was significantly higher than that in 2012 and 2013 ($p < 0.05$). The biomass increased year by year in 2016, 2017, and 2018, but it did not reach a significant level. Also, the vegetation covers of the degraded alpine grassland increased and was 83.8 ± 4.2%, 83.2 ± 6.9%, 84 ± 5.3%, 85.7 ± 6.2%, 89.8 ± 5.1%, 88.6 ± 4.7%, and 89.1 ± 3.9%, respectively, from 2012 to 2018. However, the ANOVA results showed that there was no significant difference in vegetation cover between these years. The amount of litter was the vegetation parameter that showed the largest variation. The litter density in the degraded grassland in 2016, 2017, and 2018 was significantly higher than that in 2012 and 2013 ($p < 0.05$) by POST-HOC tests (LSD method). The density of litter in 2018 had increased 3.7 times than that in 2012.

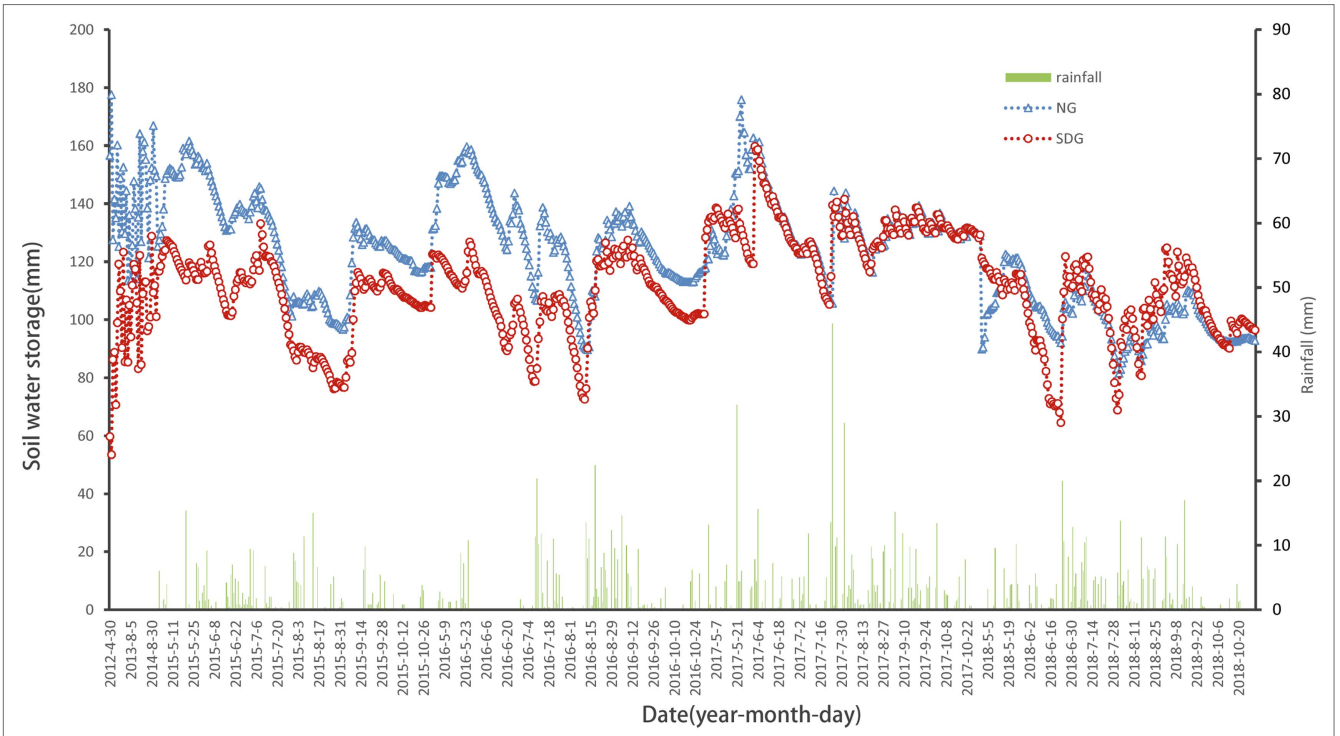

FIGURE 2 | Changes in grassland water storage during the growing season. *Due to the lack of data, the precipitation data began on May 1, 2014.

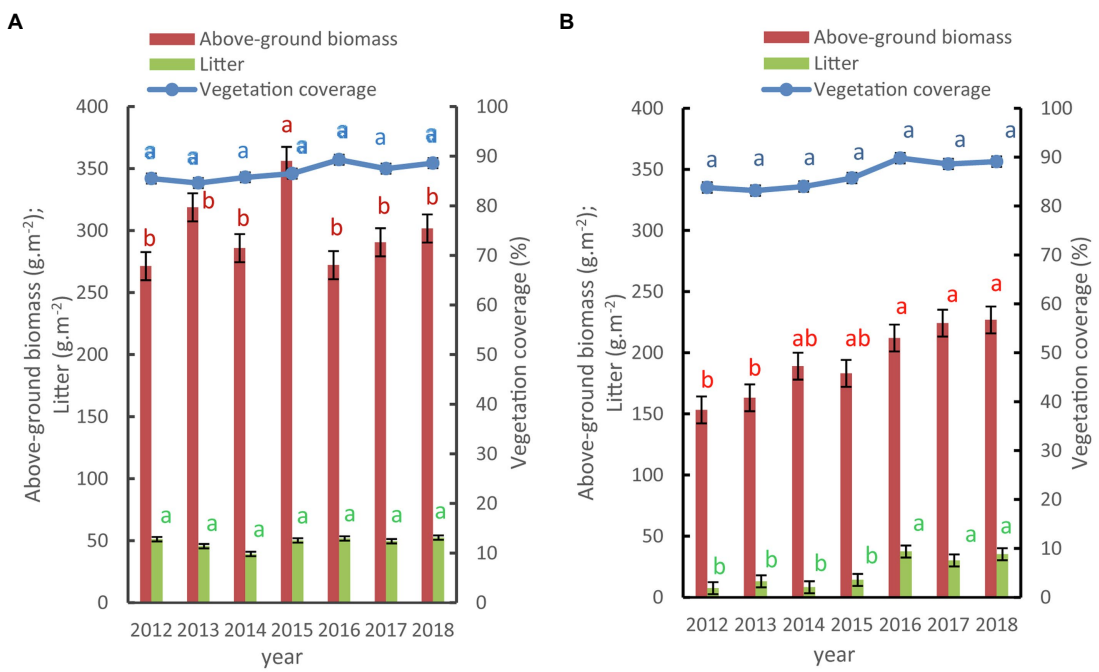

FIGURE 3 | Changes in the vegetation characteristics of the severely degraded grassland plot. *vegetation characteristic from 2012 to 2018 at NG **(A)** and SDG **(B)**.

Soil-water storage in SDG increased every year. We compared the soil moisture content at the same soil depths from 2015 to 2018 and found that the main reason for the increase in soil-water storage was an increase in surface soil moisture

content (**Figure 4**). The POST-HOC tests (LSD method) showed that the soil moisture content at the 5 cm and 10 cm depths increased significantly ($p < 0.01$), while the soil moisture at the 30 cm and 40 cm depths did not show any obvious changes. The soil moisture content in 5 cm and 10 cm increased by 61.2 and 46.3%, respectively, in 2018 compared with 2015.

We wanted to identify the key factors affecting soil-water storage in alpine grasslands. We conducted a correlation analysis among soil-water storage and 16 environmental factors including above-ground biomass, vegetation cover, litter, root biomass, wind speed, air temperature, humidity, atmospheric pressure, precipitation, total radiation, reflected radiation, ultraviolet radiation, net radiation, effective radiation, and soil heat flux. The results showed that wind speed, precipitation, underground, and litter showed a positive correlation with soil-water storage ($p < 0.05$). Conversely, air temperature, net radiation, soil heat flux, and vegetation cover were negatively correlated with soil-water storage ($p < 0.05$).

A stepwise regression analysis and a dominance analysis were conducted to further understand how these eight factors jointly affect soil-water storage. The stepwise regression equation obtained was as follows:

TABLE 2 | The soil bulk density of NG and SDG in 2018.

Year	Soil bulk density in NG (g/cm^3)	Soil bulk density in SDG (g/cm^3)
0–10 cm	0.71 ± 0.05	0.75 ± 0.01
10–20 cm	0.86 ± 0.06	0.94 ± 0.08
20–30 cm	0.95 ± 0.04	1.13 ± 0.06
30–40 cm	1.19 ± 0.07	1.41 ± 0.11
40–50 cm	1.44 ± 0.01	1.47 ± 0.04

Soil-water storage = 0.048 L +0.439 precipitation +2.247 wind speed − 2.409 air temperature + 5.679 soil heat flux ($r^2 = 0.176$, $p < 0.01$).

We conducted a dominance analysis using the BRT model, and the top five important factors that influenced water storage were listed in a decreasing order: air temperature, litter, soil heat flux, precipitation, and wind speed (**Figure 5**). Their relative contributions to soil-water storage were 50.52, 24.02, 10.86, 7.82, and 6.77%, respectively. Based on the BRT model analysis, we found that the role of climate factors in determining soil-water storage was greater than that of vegetation factors. Air temperature and litter together explained 74.5% of the total variation, which were two key factors controlling the soil-water storage of grassland.

DISCUSSION

Soil-Water Storage in Alpine Grasslands

The soil-water storage capacity in alpine grasslands experienced obvious fluctuations during the growing season, where the typical curve illustrates two peaks and a single valley (**Figure 2**). The two peaks occur at mid-May and early September, coinciding with the beginning and end of the growing season, and the minimum value of soil-water storage occurs at early August. Other ecosystems generally show a fluctuation characterized by a single peak and valley (Oudin et al., 2008; Ren et al., 2019). This difference is attributed to the combined impacts of permafrost thawing, rising temperatures, and transpiration from vegetation. The soil in alpine grasslands is mostly comprised of seasonally frozen soil, which forms in early November and disappears completely by mid-May of the following year, with a maximum

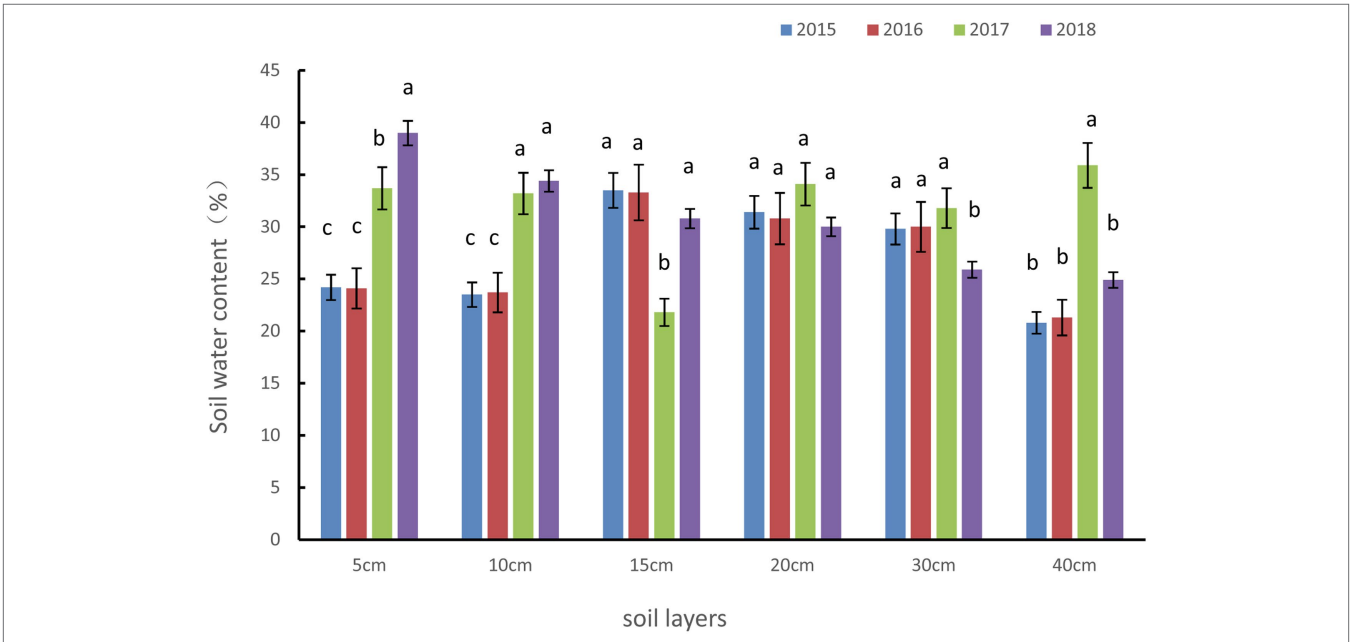

FIGURE 4 | Changes in the soil moisture content at different soil depths in the severely degraded grassland.

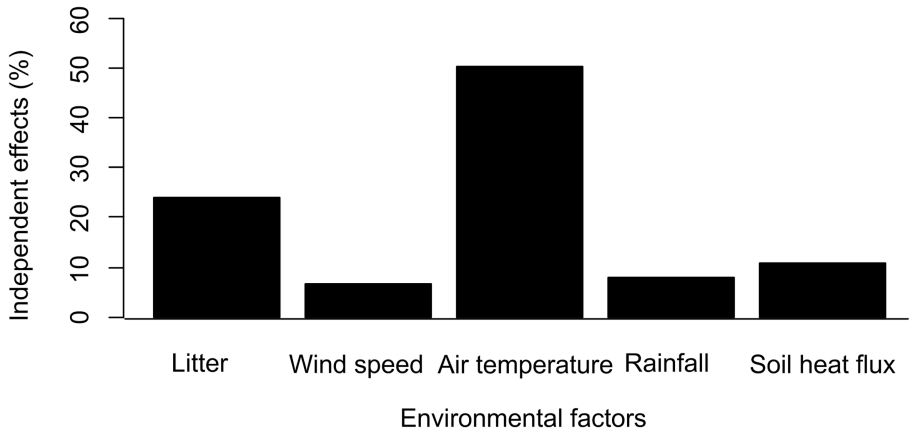

FIGURE 5 | Independent effects of environmental factors on soil-water storage.

depth of 2 m (Zhang et al., 2019). The thawing of seasonally frozen soil in mid-May was the reason for the first peak in soil-water storage; the plant water consumption in the growing season makes the grassland water storage appear the lowest value at early August. Therefore, we imply that the effect of precipitation on soil-water storage is not as large as that of vegetation transpiration consumption. Vegetation transpiration in alpine grasslands accounts for 68.6–73.9% of the total evapotranspiration (Hongqin et al., 2018). By early September, some alpine grassland plants have withered, reducing the vegetation transpiration, and leading to a second peak in soil-water storage.

Soil-water storage showed a strong relationship with surface soil moisture content (depths at 5 cm and 10 cm), but at a depth of 40 cm, the soil moisture content did not fluctuate significantly throughout the growing season. This illustrates the dependence of soil-water storage on surface vegetation and environmental conditions. During the restoration of the degraded grassland, biomass and litter will increase to reduce soil evaporation. In our seven-year study, the soil-water storage capacity of the degraded grassland increased every year, as it was being gradually restored. Vegetation transpiration in alpine meadows during the peak of the growing season does not support soil-water storage, while moderate grazing leads to a reduction in transpiration. Therefore, reducing grazing on well-grown grasslands can protect soil moisture, and banning grazing is not considered a promising management strategy to improve the soil-water storage capacity in these grasslands. Several previous studies have shown that grazing bans can lead to an increase in plant growth and the disappearance of sedge plants. Therefore, in our study site, we recommend a grazing intensity of 8.5 sheep/ha to restore soil water.

Factors Influencing Grassland Water Storage

Soil-water storage in a grassland is distinctly affected in two specific ways by the state of the vegetation in the grassland. Firstly, above-ground vegetation stores part of the water on the grass by intercepting rainfall and condensing dew, effectively regulating and increasing soil moisture. At the same time, the surface vegetation decreases raindrop splash impact, indirectly increasing infiltration capacity. For example, Lin et al. (2015) reported that the soil-water storage capacity of different vegetation types was significantly different at the same site. Secondly, vegetation transpiration contributes to significant losses in soil moisture. The average transpiration in alpine grasslands for our study was 379.35 mm, which was 2.16 times greater than the evaporation from surface soil. Heavy grazing reduced the protection of vegetation and litter; then, we think that the grassland soil is getting drier and drier.

In our study, the lowest amount of soil-water storage occurs in late July or early August, this time period is consistent with the time of maximum transpiration for grassland vegetation. The above-ground biomass was not considered as the main control factor in the BRT model. This was because, although an increase in vegetation can promote plant transpiration, it increases the amount of litter as well. In our study, the quantity of litter was the second key factor (24.02%) influencing grassland water storage. It can be inferred that grass litter regulates the water utilization of grassland by absorbing precipitation and increasing dew condensation, an increase in the quantity of litter will improve the water permeability and retention capacity of soil (Yu et al., 2012). Therefore, the restoration of water conservation in degraded grasslands should begin with the addition of surface litters.

Soil bulk density increased gradually under the trampling action of grazing cattle and sheep (Bilotta et al., 2007), short-term grazing affects the surface soil, resulting in the reduction of soil porosity; therefore, the soil moisture content also decreases gradually with grassland degradation. In addition, the total carbon, organic matter, and total nitrogen, which are closely related to the water holding capacity of grassland, also show a decreasing trend after grassland degradation (Zhao et al., 2007). As a result, the water absorbing matter in soil decreases, and such negative feedback further exacerbates the decline of grassland water conservation function. With different grazing gradients, the soil-water storage is influenced in the following order: lightly grazed grassland > native grassland

> moderately grazed grassland > heavily grazed grassland (Guo et al., 2020). Additionally, the adsorption of water by living roots is an important factor affecting grassland soil-water storage. Damage to the root systems in alpine grasslands can result in the decrease of soil moisture content by 22–50% (Chunxia et al., 2007). With the restoration of degraded grassland, the vegetation roots and root exudates gradually increase, as well as the litter and above-ground biomass (Huang et al., 2019). This combination results in an increase in plant residue. During our study, the restoration of the degraded grassland increased grassland soil-water storage by 40.5%. We found that the primary factor influencing the increase of grassland soil-water storage was the quantity of litter, which was caused by an increase in the above-ground biomass. Therefore, it can be inferred that the improvement of water storage in the degraded grassland was mainly due to the improvement of vegetation conditions.

Changes in environmental conditions include global warming, precipitation changes, and soil environment changes, all of which have important consequences to grassland soil-water storage. Air temperature was significantly and negatively correlated with soil-water storage, because higher temperatures increase soil evaporation and transpiration of vegetation, as well as affecting the composition of plant communities. Liu et al. (2018) found that higher temperatures are beneficial to the growth of gramineous plants in alpine grasslands. The transpiration in gramineous plants is obviously higher than that in sedge plants; therefore, temperature increase has a negative influence on soil-water storage. Among all the environmental factors studied, temperature had the greatest effect on grassland water storage. We imply that any increase in temperature will further reduce soil-water storage in the alpine grasslands of the QTP. The average annual temperature has increased by 1.5–2.8°C since 1960 (Wu and Tang, 2017); therefore, further intensification of global warming will have a profound impact on soil-water storage in alpine grasslands.

The direct sources of soil water in alpine grasslands include precipitation, groundwater, and dew. Precipitation is one of the direct sources of soil water, and we found a positive correlation between precipitation and soil-water storage. For example, in the study of Zhang et al. (2017), for every 1 mm increase in precipitation, the soil-water infiltration depth increases by 0.79–1.06 cm. However, precipitation infiltration is not dependent only on precipitation size and duration. In addition, soil moisture, biological crust, and topography play an important role in precipitation infiltration. Heavy grazing causes extensive changes in the grassland soil environment. It will thicken the mattic epipedon of alpine grasslands. The soil biological crusts under heavy grazing will die and become hard, and the soil total porosity will decrease continuously. These effects lead to a reduction in the soil-water holding capacity in alpine grassland. Precipitation infiltration is a complicated biophysiological process affected by a soil type, vegetation, and atmospheric precipitation. In our study, only 7.82% of the variation of soil-water storage was explained by growing season atmospheric precipitation.

Also, wind speed was another main factor affecting grassland soil-water storage, explaining 6.77% of the variation in soil-water storage. Unfortunately, there are very few studies on the effects of wind speed on grassland soil-water storage. Dai et al. (2019) reported that wind speed is the most important factor affecting the groundwater level in the QTP because wind can promote melting ice, snow, and frozen soil that be used to replenish soil moisture. The annual average wind speed in the QTP has considerably decreased over the timescale of our study, which has, in turn, a profound effect on the soil-water storage in the alpine grasslands. Further study is needed to improve our understanding of the relationship between wind speed and soil-water storage.

CONCLUSION

We found that restoration of degraded grassland significantly improved grassland vegetation and soil-water storage. The above-ground biomass and soil-water storage increased by 38.4 and 41.9% from severe degradation stage to moderate degradation stage, respectively. Temperature and litters were the most important environmental factors determining grassland soil-water storage. Therefore, for improved grassland management, we suggest that increasing the amount of litter is a good option to promote water recovery in the degraded grassland.

DATA AVAILABILITY STATEMENT

Publicly available datasets were analyzed in this study. This data can be found at: Data can be applied from Haibei station website: http://hbg.cern.ac.cn/.

AUTHOR CONTRIBUTIONS

XG: conceptualization, writing – original draft preparation, and project administration. GC: methodology and resources. QL: validation. LD: formal analysis. DQ: investigation and data curation. YD: writing – review and editing. All authors have read and agreed to the published version of the manuscript.

FUNDING

This work was supported by the Natural Science Foundation of China (41730752 and 31700395), the Natural Science Foundation of Qinghai (2020-ZJ-916), and Qinghai innovation platform construction project (2017-ZJ-Y20). The funders had no role in study design, data collection and analysis, decision to publish, or preparation of the manuscript.

ACKNOWLEDGMENTS

We thank the Haibei National Field Research Station for providing the experimental platform and meteorological data. Bernie Dominiak reviewed an early version of the manuscript.

REFERENCES

Bilotta, G. S., Brazier, R. E., and Haygarth, P. M. (2007). The impacts of grazing animals on the quality of soils, vegetation, and surface waters in intensively managed grasslands. *Adv. Agro.* 94, 237–280. doi: 10.1016/S0065-2113(06)94006-1

Chen, J., Yamamura, Y., Hori, Y., Shiyomi, M., Yasuda, T., Zhou, H.-K., et al. (2008). Small-scale species richness and its spatial variation in an alpine meadow on the Qinghai-Tibet plateau. *Ecol. Res.* 23, 657–663. doi: 10.1007/s11284-007-0423-7

Chunxia, L. U., Ge, Y. U., Gaodi, X. I. E., and Yu, X. (2007). Wind tunnel simulation and assessment of soil moisture conservation of alpine grassland in Qinghai-Tibet plateau. *Ecol. Environ.* 16, 1289–1293. doi: 10.1016/j.ecolecon.2012.10.015

Dai, L., Guo, X., Du, Y., Zhang, F., Ke, X., Cao, Y., et al. (2019). The Response of Shallow Groundwater Levels to Soil Freeze–Thaw Process on the Qinghai-Tibet Plateau. *Groundwater* 57:602–611.

Dai, L., Fu, R., Guo, X., Du, Y., Lin, L., Zhang, F., et al. (2021). Long-term grazing exclusion greatly improve carbon and nitrogen store in an alpine meadow on the northern Qinghai-Tibet plateau. *Catena* 197:104955. doi: 10.1016/j.catena.2020.104955

Dai, L., Guo, X., Ke, X., Du, Y., Mang, F., and Cao, G. (2020). The variation in soil water retention of alpine shrub meadow under different degrees of degradation on northeastern Qinghai-Tibetan plateau. *Plant Soil* 458, 231–244. doi: 10.1007/s11104-020-04522-3

Dong, S., Shang, Z., Gao, J., and Boone, R. B. (2020). Enhancing sustainability of grassland ecosystems through ecological restoration and grazing management in an era of climate change on Qinghai-Tibetan plateau. *Agri. Eco. Environ.* 287:106684. doi: 10.1016/j.agee.2019.106684

Fassnacht, F. E., Li, L., and Fritz, A. (2015). Mapping degraded grassland on the eastern Tibetan plateau with multi-temporal Landsat 8 data - where do the severely degraded areas occur? *Int. J. Appl. Earth Obs. Geoinf.* 42, 115–127. doi: 10.1016/j.jag.2015.06.005

Guo, X., Dai, L., Li, Q., Qian, D., Cao, G., Zhou, H., et al. (2020). Light grazing significantly reduces soil water storage in alpine grasslands on the Qinghai-Tibet plateau. *Sustainability* 6:2523. doi: 10.3390/su12062523

Hongqin, L., Fawei, Z., Wenying, W., Yikang, L., Li, L., Junbang, W., et al. (2018). The strongest EI event stimulated ecosystem respiration, not evapotranspiration, over a humid alpine meadow on the Qinghai-Tibetan plateau. *Ecol. Indic.* 91, 562–569. doi: 10.1016/j.ecolind.2018.04.039

Huang, Z., Sun, L., Liu, Y., Liu, Y.-F., Lopez-Vicente, M., Wei, X.-H., et al. (2019). Alfalfa planting significantly improved alpine soil water infiltrability in the Qinghai-Tibetan plateau. *Agri. Eco. Environ.* 285:106606. doi: 10.1016/j.agee.2019.106606

Jiang, C., Li, D., Wang, D., and Zhang, L. (2016). Quantification and assessment of changes in ecosystem service in the Three-River headwaters region, China as a result of climate variability and land cover change. *Ecol. Indic.* 66, 199–211. doi: 10.1016/j.ecolind.2016.01.051

Kruemmelbein, J., Peth, S., Zhao, Y., and Horn, R. (2009). Grazing-induced alterations of soil hydraulic properties and functions in Inner Mongolia, PR China. *J. Plant Nutr. Soil Sci.* 172, 769–776. doi: 10.1002/jpln.200800218

Lin, L., Li, Y. K., Xu, X. L., Zhang, F. W., Du, Y. G., Liu, S. L., et al. (2015). Predicting parameters of degradation succession processes of Tibetan Kobresia grasslands. *Solid Earth* 6, 1237–1246. doi: 10.5194/se-6-1237-2015

Liu, H., Mi, Z., Lin, L., Wang, Y., Zhang, Z., Zhang, F., et al. (2018). Shifting plant species composition in response to climate change stabilizes grassland primary production. *Proc. National Acad. Sci. U. S. A.* 115, 4051–4056. doi: 10.1073/pnas.1700299114

Mipam, T. D., Zhong, L. L., Liu, J. Q., Miehe, G., and Tian, L. M. (2019). Productive overcompensation of alpine meadows in response to yak grazing in the eastern Qinghai-Tibet plateau. *Front. Plant Sci.* 10:925. doi: 10.3389/fpls.2019.00925

Nadler, A. (1991). Soil electrical conductivity and soil salinity: new formulations and calibrations. *Soil Sci. Soc. Am. J.* 55, 294–295. doi: 10.2136/sssaj1991.03615995005500010053x

Oudin, L., Andréassian, V., Lerat, J., and Michel, C. (2008). Has land cover a significant impact on mean annual streamflow? An international assessment using 1508 catchments. *J. Hydrol.* 357, 303–316. doi: 10.1016/j.jhydrol.2008.05.021

Ren, A., Sun, M., Xue, L., Deng, Y., Wang, P., Lei, M., et al. (2019). Spatio-temporal dynamics in soil water storage reveals effects of nitrogen inputs on soil water consumption at different growth stages of winter wheat. *Agric. Water Manag.* 216, 379–389. doi: 10.1016/j.agwat.2019.01.023

Shen, M.-S., Zhang, J.-J., Zhang, S.-H., Zhang, H.-B., Sun, R.-X., and Zhang, Y.-Z. (2020). Seasonal variations in the influence of vegetation cover on soil water on the loess hillslope. *J. Mt. Sci.* 17, 2148–2160. doi: 10.1007/s11629-019-5942-5

Wang, X., and Fu, X. (2004). Sustainable management of alpine meadows on the Tibetan plateau: problems overlooked and suggestions for change. *Ambio* 33, 169–171. doi: 10.1579/0044-7447-33.3.169

Wang, M., Wang, S., Wu, L., Xu, D., Lin, Q., Hu, Y., et al. (2016). Evaluating the lingering effect of livestock grazing on functional potentials of microbial communities in Tibetan grassland soils. *Plant Soil* 407, 385–399. doi: 10.1007/s11104-016-2897-y

White, I., Knight, J. H., Zegelin, S. J., and Topp, G. C. (1994). Considerations on the use of time-domain reflectometry (TDR) for measuring soil water content. *Eur. J. Soil Sci.* 45, 503–508. doi: 10.1111/j.1365-2389.1994.tb00536.x

Wu, C., and Tang, D. (2017). Change of temperature in The Tibetan plateau in the context of global warming in recent 50 years. *Res. Soil Water Cons.* 24, 262–272. doi: 10.13869/j.cnki.rswc.2017.06.040

Yang, J., Ding, Y., and Chen, R. (2006). Spatial and temporal of variations of alpine vegetation cover in the source regions of the Yangtze and yellow Rivers of the Tibetan plateau from 1982 to 2001. *Environ. Geol.* 50, 313–322. doi: 10.1007/s00254-006-0210-8

Yu, K., Pypker, T. G., Keim, R. F., Chen, N., Yang, Y., Guo, S., et al. (2012). Canopy rainfall storage capacity as affected by sub-alpine grassland degradation in the Qinghai-Tibetan plateau, China. *Hydrol. Process.* 26, 3114–3123. doi: 10.1002/hyp.8377

Zhang, F., Li, H., Li, Y., Guo, X., Dai, L., Lin, L., et al. (2019). Strong seasonal connectivity between shallow groundwater and soil frost in a humid alpine meadow, northeastern Qinghai-Tibetan plateau. *J. Hydrol.* 574, 926–935. doi: 10.1016/j.jhydrol.2019.05.008

Zhang, B., Tan, X., Wang, S., Chen, M., Chen, S., Ren, T., et al. (2017). Asymmetric sensitivity of ecosystem carbon and water processes in response to precipitation change in a semi-arid steppe. *Funct. Ecol.* 31, 1301–1311. doi: 10.1111/1365-2435.12836

Zhao, Y., Peth, S., Krummelbein, J., Horn, R., Wang, Z., Steffens, M., et al. (2007). Spatial variability of soil properties affected by grazing intensity in Inner Mongolia grassland. *Ecol. Model.* 205, 241–254. doi: 10.1016/j.ecolmodel.2007.02.019

Zhao, Y., Peth, S., Reszkowska, A., Gan, L., Kruemmelbein, J., Peng, X., et al. (2011). Response of soil moisture and temperature to grazing intensity in a Leymus chinensis steppe, Inner Mongolia. *Plant Soil* 340, 89–102. doi: 10.1007/s11104-010-0460-9

Conflict of Interest: The authors declare that the research was conducted in the absence of any commercial or financial relationships that could be construed as a potential conflict of interest.

Publisher's Note: All claims expressed in this article are solely those of the authors and do not necessarily represent those of their affiliated organizations, or those of the publisher, the editors and the reviewers. Any product that may be evaluated in this article, or claim that may be made by its manufacturer, is not guaranteed or endorsed by the publisher.

Copyright © 2021 Guo, Zhou, Dai, Li, Zhang, Li, Lin, Li, Qian, Fan, Lan, Si, Li, Cao, Du and Wang. This is an open-access article distributed under the terms of the Creative Commons Attribution License (CC BY). The use, distribution or reproduction in other forums is permitted, provided the original author(s) and the copyright owner(s) are credited and that the original publication in this journal is cited, in accordance with accepted academic practice. No use, distribution or reproduction is permitted which does not comply with these terms.

frontiers in Plant Science

ORIGINAL RESEARCH
published: 17 December 2021
doi: 10.3389/fpls.2021.804861

Phylogenetic Correlation and Symbiotic Network Explain the Interdependence Between Plants and Arbuscular Mycorrhizal Fungi in a Tibetan Alpine Meadow

Qiang Dong[1], Xin Guo[1], Keyu Chen[1], Shijie Ren[1], Muhammad Atif Muneer[2], Jing Zhang[1], Yaoming Li[1] and Baoming Ji[1]**

[1] School of Grassland Science, Beijing Forestry University, Beijing, China, [2] College of Resources and Environment, International Magnesium Institute, Fujian Agriculture and Forestry University, Fuzhou, China

OPEN ACCESS

Edited by:
Jian Sun,
Institute of Tibetan Plateau Research, Chinese Academy of Sciences (CAS), China

Reviewed by:
Yonglong Wang,
Baotou Teachers' College, China
Yongjun Liu,
Lanzhou University, China

***Correspondence:**
Yaoming Li
yaomingli@bjfu.edu.cn
Baoming Ji
baomingji@bjfu.edu.cn

Specialty section:
This article was submitted to Functional Plant Ecology, a section of the journal Frontiers in Plant Science

Received: 29 October 2021
Accepted: 24 November 2021
Published: 17 December 2021

Citation:
Dong Q, Guo X, Chen K, Ren S, Muneer MA, Zhang J, Li Y and Ji B (2021) Phylogenetic Correlation and Symbiotic Network Explain the Interdependence Between Plants and Arbuscular Mycorrhizal Fungi in a Tibetan Alpine Meadow. Front. Plant Sci. 12:804861. doi: 10.3389/fpls.2021.804861

Plants and arbuscular mycorrhizal fungi (AMF) can form complex symbiotic networks based on functional trait selection, contributing to the maintenance of ecosystem biodiversity and stability. However, the selectivity of host plants on AMF and the characteristics of plant-AMF networks remain unclear in Tibetan alpine meadows. In this study, we studied the AMF communities in 69 root samples from 23 plant species in a Tibetan alpine meadow using Illumina-MiSeq sequencing of the 18S rRNA gene. The results showed a significant positive correlation between the phylogenetic distances of plant species and the taxonomic dissimilarity of their AMF community. The plant-AMF network was characterized by high connectance, high nestedness, anti-modularity, and anti-specialization, and the phylogenetic signal from plants was stronger than that from AMF. The high connected and nested plant-AMF network potentially promoted the interdependence and stability of the plant-AMF symbioses in Tibetan alpine meadows. This study emphasizes that plant phylogeny and plant-AMF networks play an important role in the coevolution of host plants and their mycorrhizal partners and enhance our understanding of the interactions between aboveground and belowground communities.

Keywords: arbuscular mycorrhizal fungi, plant species, host selectivity, symbiotic network, phylogenetic distance, community dissimilarity, Tibetan alpine meadow

INTRODUCTION

Arbuscular mycorrhizal fungi (AMF) are an ancient root symbiotic group, whose origin is consistent with the first appearance of terrestrial plants, and generally considered to be the result of coevolution of fungi and plants (Bonfante and Genre, 2008; Walder and van der Heijden, 2015; Genre et al., 2020). As a key component of the underground biological community, AMF can form a symbiotic relationship with most terrestrial plant species and can increase the absorption of phosphorus and nitrogen for plants (Wang and Qiu, 2006; Smith and Read, 2008; Zhang et al., 2021). At the same time, plants provide photosynthetic carbon products to AMF (Bever et al., 2009; Kiers et al., 2011; Wipf et al., 2019). The combination of AMF and plants improves the

adaptability of plants and AMF symbionts (Blackwell, 2000; Chen et al., 2018; Tedersoo et al., 2020). Furthermore, the plant-AMF symbioses are not formed stochastically but are dependent on their functional traits (Bever et al., 2009; Kiers et al., 2011). Both plant hosts and AMF have been shown to preferentially allocate resources to higher-quality partners (Ji and Bever, 2016), inducing reciprocal shifts in each assemblage, ultimately affecting the partner selection in the mycorrhizal symbiosis (Werner and Kiers, 2015). Due to the simultaneous processes of coevolution, niche differentiation, and niche conservatism, the closely related plants tend to interact with similar AMF species (i.e., phylogenetic signal in the interaction) (Gomez et al., 2010; Sargent et al., 2011). However, negative correlations between the phylogenetic distance of plants and AMF community distance were also reported in three locations of the northern Great Plains of the United States (Reinhart and Anacker, 2014). In addition, the specificity of the interactions between the plant and AMF changed with community succession (Montesinos-Navarro et al., 2012a). These contrasting findings indicate the complexity of plant and AMF interactions.

Many studies have shown that phylogenetic relatedness affects the mycorrhizal symbiotic network structure, which could answer the question of how coevolution explained species assemblages (Barberan et al., 2012; Chagnon et al., 2012; Montesinos-Navarro et al., 2012b; Chen et al., 2017; Goberna et al., 2019). The network is increasingly used to study co-occurrence patterns in plant and AMF symbioses, providing insights for biological interactions (Barberan et al., 2012; Chagnon et al., 2012; Chen et al., 2017; Gao et al., 2019). The AMF communities of 166 root samples from 17 woody plants in subtropical forests of China showed that the woody plant-AMF network was highly interconnected and nested but in anti-modular and anti-specialized manners (Chen et al., 2017). Most of the studies on the plant-fungus symbiotic network focused on temperate and tropical ecosystems, and the research objects were mainly woody plant-AMF symbiotic interactions. However, herbaceous plant-AMF network characteristics in the alpine ecosystems remain poorly understood.

As the Third Pole on the earth, the Tibetan Plateau is a unique geographic unit with great biodiversity and critical ecosystem functions and is experiencing striking climate warming (Bai-ping et al., 2002; Duan et al., 2006; Qiu, 2008). Alpine meadow is a typical vegetation type, accounting for approximately 40% of the total grassland area on the Tibetan Plateau (Miehe et al., 2008; Wang et al., 2016). The importance of AMF in plant succession on the Tibetan plateau has been well documented (Liu et al., 2011; Gai et al., 2012; Li et al., 2015). However, most of the studies focused on the effects of altitude gradients (Liu et al., 2011; Gai et al., 2012; Li et al., 2014), precipitation (Zhang et al., 2016), and vegetation types (Gai et al., 2009; Gao and Guo, 2010; Xu et al., 2017) on AMF community composition. The selectivity of the interactions between the plant and AMF and their network properties in Tibetan alpine meadows remains unclear.

In this study, to explore the selectivity in the plant-AMF interactions and clarify the maintenance mechanism of symbiosis, 23 species of common herbs in a Tibetan alpine meadow were selected. Illumina-MiSeq sequencing was used to characterize AMF communities living in each plant root to address the following questions: (1) How is the selectivity in the plant-AMF interactions in Tibetan alpine meadow? and (2) What are the characteristics of the plant-AMF network in Tibetan alpine meadows?

MATERIALS AND METHODS

Site and Sampling

The study site is located at the Naqu Alpine Grassland Ecosystem National Field Scientific Observation and Research Station (Kaima Station) of Tibetan Plateau Research of Chinese Academy of Sciences (31°16′N, 92°06′E, 4453 m a.s.l). This region is a typical alpine meadow ecosystem, where the mean annual temperature is −2.1°C, the mean annual rainfall is 406 mm, and most of the precipitation was concentrated from June to September. Summers are short and cool, and winters are long and severely cold (Cui et al., 2017). The plant community is dominated by *Kobresia Pygmaea* and *Kobresia Humilis*, and the *Carex moorcroftii*, *Stipa purpurea*, *Poa tibetica*, *Potentilla bifurca*, and *Heteropappus semiprostratus* (Hs) are companion species.

In mid-August 2018, 23 representative plant species (**Figure 1**) were selected based on a vegetation survey in the alpine meadow of Naqu county. Notably, 23 sampling sites were randomly chosen for plant sampling around the Kaima Station, which was at least 50 m away from each other to avoid interactions among plant species. Then, three 0.5 × 0.5 m^2 quadrats were randomly selected in each sampling site, and three plant individuals in each quadrat were collected and pooled as one composite sample. Finally, 207 plant individuals of 69 samples (i.e., 23 plant species × 3 replicates) belonging to 11 families and 20 genera (**Figure 1**, according to the genetic relationship of species) were collected in this study. Plant roots were carefully separated from aboveground parts and soil, packaged in plastic bags, refrigerated and transported to the laboratory, and stored at −2°C for colonization determination and DNA extraction.

Plant Phylogenetic Tree

Based on Zanne phylogeny as the backbone (Zanne et al., 2014), the phylogenetic tree of plant species was constructed using Phylomatic (V.3)[1]. The phylogenetic distance of plant species was calculated using R software 3.1.1 with the package "picante" (V.1.8.2) (Kembel et al., 2010).

Arbuscular Mycorrhizal Fungi Colonization

The plant roots were washed carefully and cut into 1 cm length. Approximately, 100 root segments of each sample were cleared in 10% KOH at 90°C for 90 min, then acidified in 2% HCl at room temperature for 10 min, and stained with 0.05% Trypan blue at 90°C for 10 min. Finally, the dyed root segments were randomly selected and measured for the

[1]http://phylodiversity.Net/phylomatic/

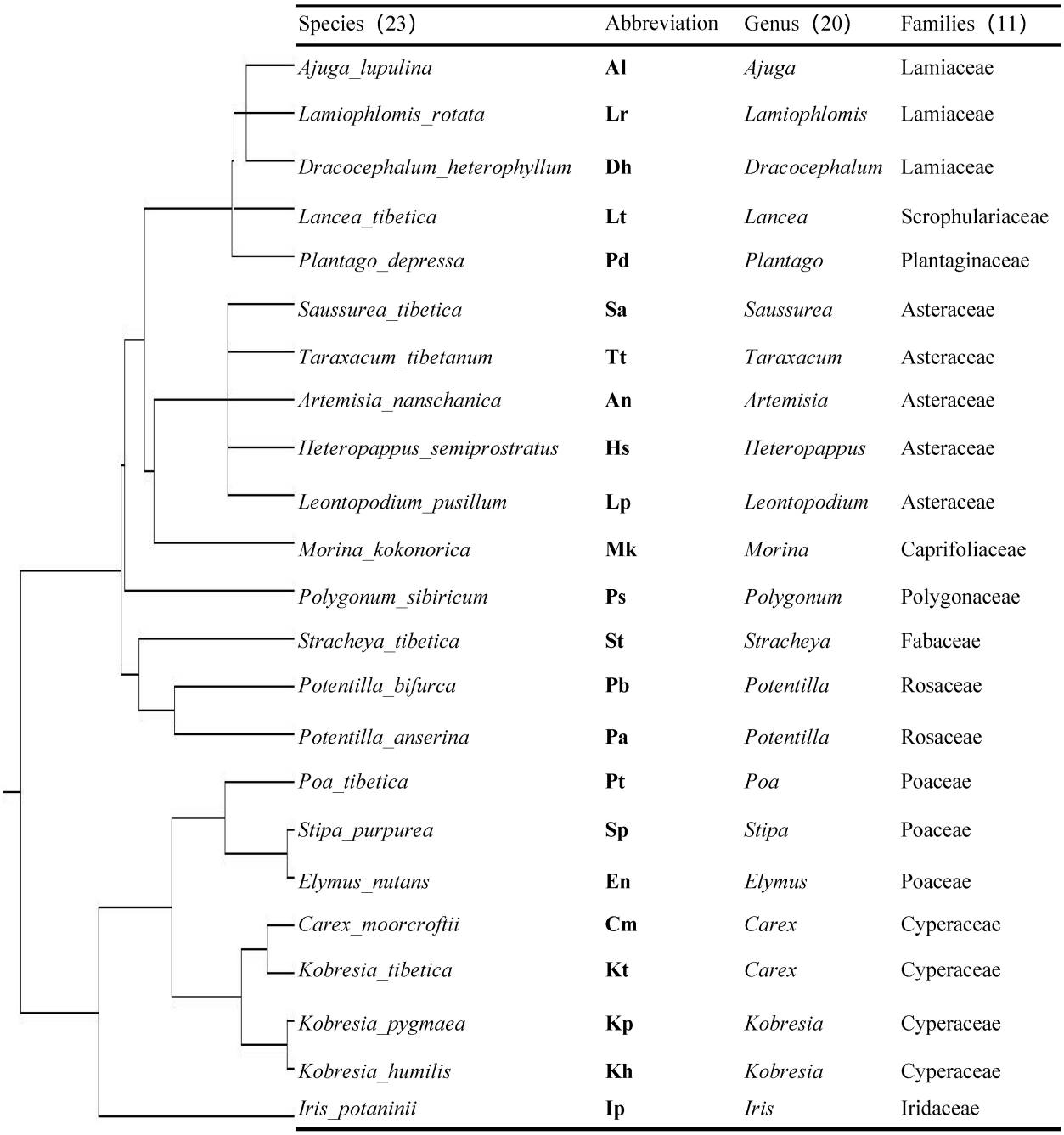

Species (23)	Abbreviation	Genus (20)	Families (11)
Ajuga_lupulina	**Al**	*Ajuga*	Lamiaceae
Lamiophlomis_rotata	**Lr**	*Lamiophlomis*	Lamiaceae
Dracocephalum_heterophyllum	**Dh**	*Dracocephalum*	Lamiaceae
Lancea_tibetica	**Lt**	*Lancea*	Scrophulariaceae
Plantago_depressa	**Pd**	*Plantago*	Plantaginaceae
Saussurea_tibetica	**Sa**	*Saussurea*	Asteraceae
Taraxacum_tibetanum	**Tt**	*Taraxacum*	Asteraceae
Artemisia_nanschanica	**An**	*Artemisia*	Asteraceae
Heteropappus_semiprostratus	**Hs**	*Heteropappus*	Asteraceae
Leontopodium_pusillum	**Lp**	*Leontopodium*	Asteraceae
Morina_kokonorica	**Mk**	*Morina*	Caprifoliaceae
Polygonum_sibiricum	**Ps**	*Polygonum*	Polygonaceae
Stracheya_tibetica	**St**	*Stracheya*	Fabaceae
Potentilla_bifurca	**Pb**	*Potentilla*	Rosaceae
Potentilla_anserina	**Pa**	*Potentilla*	Rosaceae
Poa_tibetica	**Pt**	*Poa*	Poaceae
Stipa_purpurea	**Sp**	*Stipa*	Poaceae
Elymus_nutans	**En**	*Elymus*	Poaceae
Carex_moorcroftii	**Cm**	*Carex*	Cyperaceae
Kobresia_tibetica	**Kt**	*Carex*	Cyperaceae
Kobresia_pygmaea	**Kp**	*Kobresia*	Cyperaceae
Kobresia_humilis	**Kh**	*Kobresia*	Cyperaceae
Iris_potaninii	**Ip**	*Iris*	Iridaceae

FIGURE 1 | Phylogenetic tree of 23 plants species constructed using Phylomatic. The detailed information of the 23 plant species is shown including their abbreviation, genus, and families.

mycorrhizal colonization by the magnified intersections method at 200 × microscopes (McGonigle et al., 1990).

DNA Extraction and Polymerase Chain Reaction

Total DNA was extracted from a 0.05 g (freeze-dried) subsample of fine roots using a PowerPlant DNA Isolation Kit (MoBio Laboratories, United States) following the instructions of manufacturer. A NanoDrop 8000 Ultramicro UV spectrophotometer (NanoDrop Technologies, Wilmington, DE, United States) was used to determine the quantity and purity of DNA samples. A two-step polymerase chain reaction (PCR) was performed to amplify the 18S ribosomal RNA (rRNA) gene. The primers used in the first PCR were NS31 (TTGGAGGGCAAGTCTGGTGCC) and AML2 (GAACCCAAACACTTTGGTTTCC) and the second PCR amplification with the primers AMV4.5NF

(AAGCTCGTAGTTGAATTTCG) and AMDGR (CCCAA CTATCCCTATTAATCAT) (Lumini et al., 2010; Van Geel et al., 2014). The PCR products were purified with an agarose gel DNA purification kit (AP-GX-250G; Axygen, United States) and quantified using a NanoDrop 8000. The purified products were pooled in equimolar amounts and then sequenced on the Illumina-MiSeq platform (Shanghai Magigene Inc., Shanghai, China).

Bioinformatics Analysis

We used the Quantitative Insights Into Microbial Ecology (QIIME) and the UPARSE pipeline to treat raw sequences as described previously (Caporaso et al., 2010; Edgar, 2013). Sequence quality control was conducted with QIIME, and the obtained high-quality sequences were imported into a Usearch (vision 11). Then, the Usearch was used for dereplication and merging of paired-end reads. The singletons were removed, and the chimeras were detected and removed using the *de novo* approach. The operational taxonomic units (OTUs) were clustered at 97% similarity. The representative sequences of OTUs were uploaded to the National Center for Biotechnology Information (NCBI) and MarrjAM[2] database for taxonomy identification. Non-AMF reads were removed from the OTU table. Then, the OTU table was rarefied to a sequencing depth of 5,000 reads per sample, resulting in 345,000 AMF reads for all samples (i.e., 69 samples × 5,000 reads = 345,000 AMF reads). The rarefaction curves of each sample tended to be flat, indicating adequate sequencing depth (**Supplementary Figure 1**). Alpha diversity metrics (richness and Shannon-Wiener) were calculated using the rarefied OTU table. The phylogenetic tree of AMF OTUs was constructed according to Neighbor-Joining using MEGA 7.0 software (**Supplementary Figure 2**). The sequences obtained in this study have been submitted to the GenBank database (PRJNA 748864).

Statistical Analysis

Analysis of variance (ANOVA) test and Tukey's honestly (HSD) significant difference test ($P < 0.05$) were used for the pairwise comparisons of the diversity of AMF in different plant species. We tested for host-plant species effects on AMF community dissimilarity using Permutational ANOVA (PERMANOVA) using the "adonis" function in the R package "vegan" (V.2.5.7) with 999 permutations. Mantel tests were used to examine the correlation between AMF community dissimilarity matrix (Bray-Curtis and Unifrac distance) and plant phylogenetic distance matrix, and the relationship between pairwise AMF community dissimilarity distances and plant phylogenetic distances was tested by linear regressions. To better explain the plant-AMF symbiotic network, the plant-AMF visualization matrix at the species level was established. For a given paired plant-OTU sample, the association frequency (i.e., 0, 1, 2, or 3) was defined as the number of plant root samples with AMF OTUs observed (Toju et al., 2016), which reflected the selectivity of plant-AMF association. The association frequency matrix was represented by the heat map using TBtools software (v.0.6655) (Chen et al., 2020).

[2]http://maarjam.botany.ut.ee

The species-level matrix was used to calculate the network indexes, such as connectance, nestedness, modularity, specialization, and checkerboard score. The ecological meaning of these indexes can be found in the **Supplementary Material**.

With network analysis and null model comparison, we could infer the non-randomness constructional laws of biological communities (Ulrich and Gotelli, 2007). The result of the network structure index was stable using the random test. First, random values of 1,000 randomly arranged samples of the null model matrix were generated, and then the *t*-test ($P < 0.05$) was used to test the significant difference between the observed values and the random values based on the null model. Based on the association frequency matrix and random matrix, weighted connectance, H_2', weighted nestedness metric based on the overlap and decreasing fill (WNODF), and checkerboard score index were calculated using "bipartite" package "networklevel" command in R (Dormann et al., 2013). For the modular analysis, the association frequency matrix and random matrix were the outputs from R, and then the data were analyzed using the MODULAR program. The estimated generalized least squares method (EGLS) was used to assess the phylogenetic signals of plant-AMF. The analysis fitted the phylogenetic variance-covariance matrix to the plant-AMF association frequency matrix (Ives and Godfray, 2006; Montesinos-Navarro et al., 2012b). Using the EGLS method, we calculated the independent phylogenetic signals of the plant (*d*plant) and AMF (*d*AMF) on association frequency matrix, assessed the overall intensity of the two phylogenetic signals combined with the mean square error (MSE) value, and regarded the model of minimizing MSE as the best fit. The MSE full model (MSEd), the MSE derived under the assumption of no phylogenetic signal (i.e., a star phylogeny, MSEstar), and maximum phylogenetic signal (i.e., Brownian motion evolution, MSEb) were calculated according to the description of Chen et al. (2017).

RESULTS

Arbuscular Mycorrhizal Fungi Colonization, Diversity, and Community Composition of Different Plant Species

The sequences annotated as AMF were grouped into 121 OTUs, covering 3 orders, 6 families, and 9 genera (**Supplementary Figure 3** and **Supplementary Table 1**). *Glomus* was the dominant genus (181013 sequences corresponding to 52.5% of the total sequences and 84 OTUs corresponding to 69.4% of the total OTUs), followed by *Claroideoglomus* and *Rhizophagus* (**Supplementary Table 1**).

Arbuscular mycorrhizal fungi colonization was significantly different ($F = 9.14$, $P < 0.001$) among the 23 plant species (**Figure 2A**). The colonization of Hs was the lowest (18.3 ± 3.0%) and *Lancea tibetica* (Lt) was the highest (90.0 ± 2.7%). Significant differences in the Shannon-Wiener index were found among the AMF community hosted by different plant species (**Figure 2B**; $F = 3.07$, $P = 0.001$), but no significant differences were found in OTU richness (**Figure 2C**; $F = 1.55$, $P = 0.10$). *Elymus*

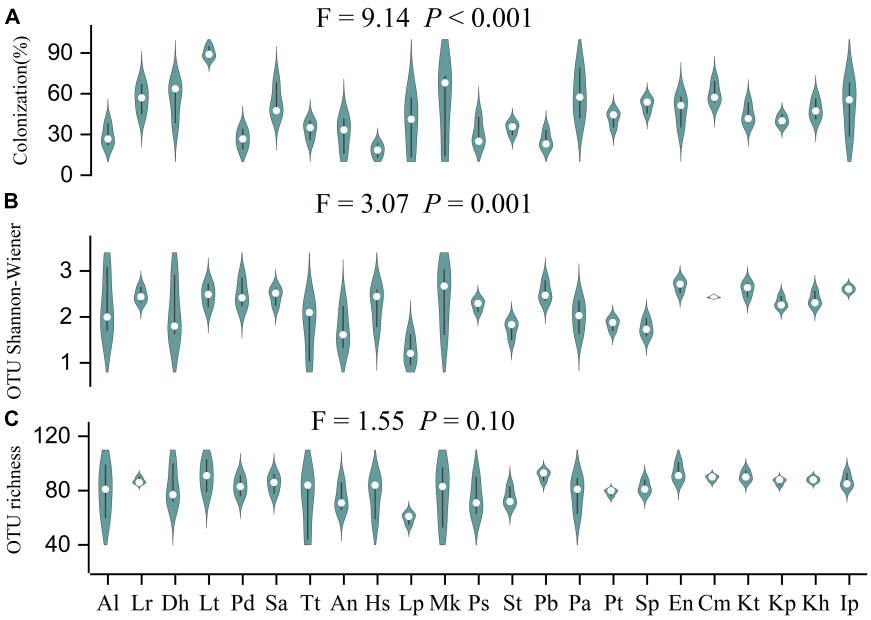

FIGURE 2 | Differences in Arbuscular mycorrhizal fungi (AMF) colonization **(A)**; OTU Shannon-Wiener diversity index **(B)**; and OTU richness **(C)** of 23 plant roots. Al: *Ajuga lupulina*; Lr: *Lamiophlomis rotata*; Dh: *Dracocephalum heterophyllum*; Lt: *Lancea tibetica*; Pd: *Plantago depressa*; Sa: *Saussurea tibetica*; Tt: *Taraxacum tibetanum*; An: *Artemisia nanschanica*; Hs: *Heteropappus semiprostratus*; Lp: *Leontopodium pusillum*; Mk: *Morina kokonorica*; Ps: *Polygonum sibiricum*; St: *Stracheya tibetica*; Pb: *Potentilla bifurca*; Pa: *Potentilla anserina*; Pt: *Poa tibetica*; Sp: *Stipa purpurea*; En: *Elymus nutans*; Cm: *Carex moorcroftii*; Kt: *Kobresia tibetica*; Kp: *Kobresia pygmaea*; Kh: *Kobresia humilis*; Ip: *Iris potaninii*.

nutans (En) of Poace had the highest AMF richness and Shannon-Wiener index, while *Leontopodium Pusillum* (Lp) of Asteraceae showed the lowest diversity. For example, *Glomus* and *Rhizophagus* were more enriched in *Potentilla bifurca* (Pb) and Lp root separately relative to other species, respectively (**Figure 3**). PERMANOVA showed that taxonomic composition was significantly different (**Figure 4A**; $F = 2.81$, $P = 0.001$), but not phylogenetic composition (**Figure 4B**; $F = 1.38$, $P = 0.18$) of AMF communities varied among plant species.

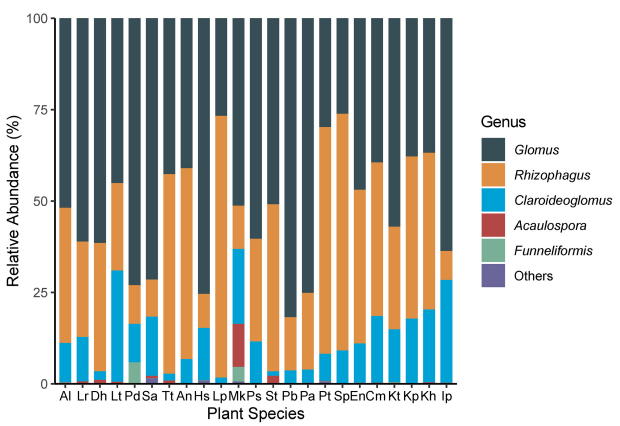

FIGURE 3 | Composition of AMF genera in roots of 23 plant roots. Al: *Ajuga lupulina*; Lr: *Lamiophlomis rotata*; Dh: *Dracocephalum heterophyllum*; Lt: *Lancea tibetica*; Pd: *Plantago depressa*; Sa: *Saussurea tibetica*; Tt: *Taraxacum tibetanum*; An: *Artemisia nanschanica*; Hs: *Heteropappus semiprostratus*; Lp: *Leontopodium pusillum*; Mk: *Morina kokonorica*; Ps: *Polygonum sibiricum*; St: *Stracheya tibetica*; Pb: *Potentilla bifurca*; Pa: *Potentilla anserina*; Pt: *Poa tibetica*; Sp: *Stipa purpurea*; En: *Elymus nutans*; Cm: *Carex moorcroftii*; Kt: *Kobresia tibetica*; Kp: *Kobresia pygmaea*; Kh: *Kobresia humilis*; Ip: *Iris potaninii*.

Phylogenetic Correlations Between Plants and Arbuscular Mycorrhizal Fungi

The result of linear fitting and mantel test showed that there was a significant positive correlation between the plant interspecies phylogenetic distance and the corresponding AMF taxonomic community dissimilarity (**Figure 5A**; $R^2 = 0.13$, $P < 0.001$; $r = 0.36$, $P = 0.001$), meaning that closely related plant species in phylogenetic trees tend to have more similar AMF community compositions. The result of linear fitting between the plant interspecies phylogenetic distance and corresponding AMF phylogenetic community dissimilarity was the same as above, but the mantel test was not significant (**Figure 5B**; $R^2 = 0.01$, $P = 0.03$; $r = 0.03$, $P = 0.26$).

Characteristics of Plant-AMF Network

The heat map of the plant-AMF incidence matrix showed that the symbiotic network relationship between the plant and AMF was established (**Figure 6**). Compared with the predicted value of the null model, the characteristics of the plant-AMF network, such as high connectance, high nestedness, anti-modularity, and anti-specialization, were obtained (**Figures 7A–D**). The observed values of weighted connectance and WNODF were significantly higher than the predicted values ($P < 0.001$). The values of

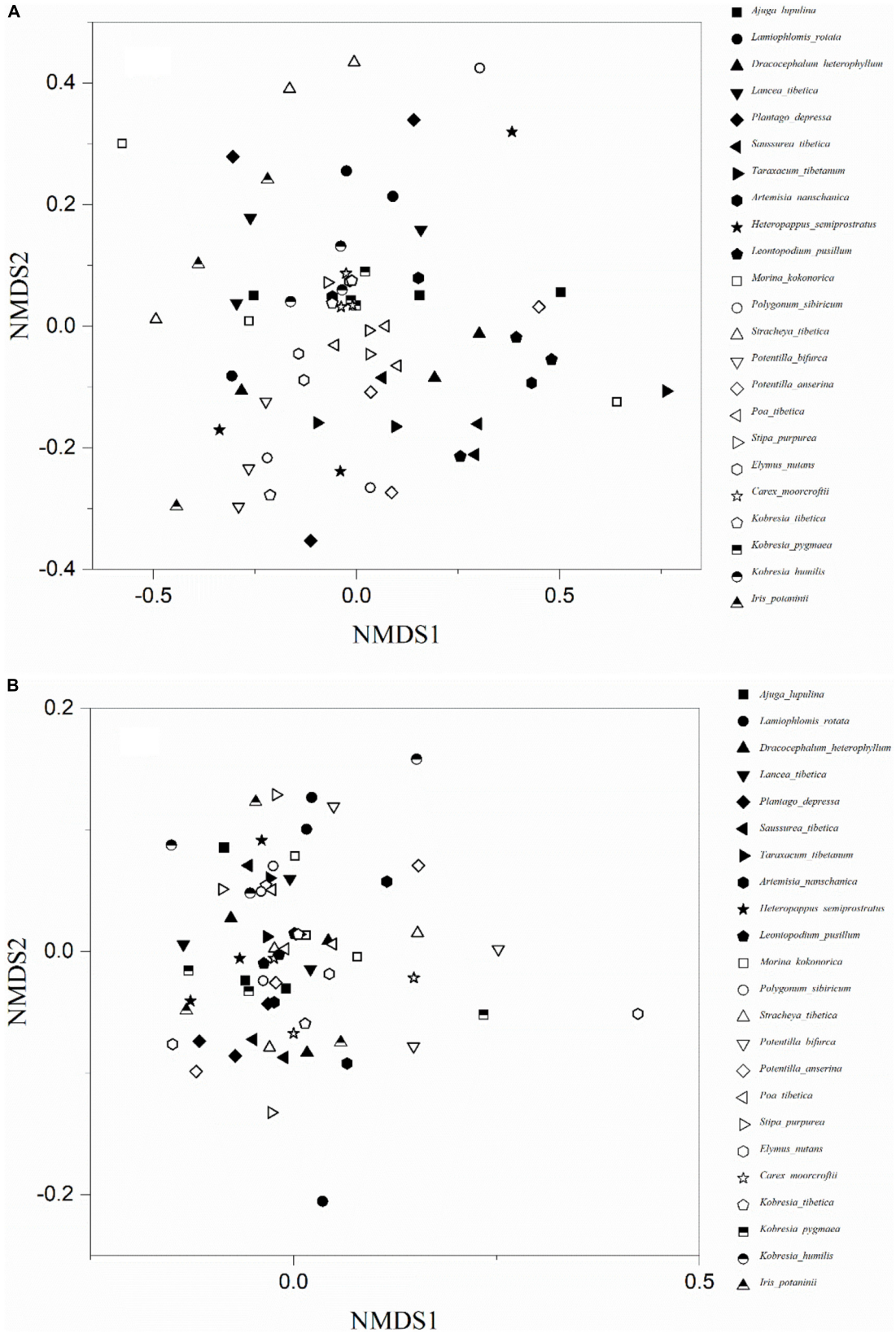

FIGURE 4 | The non-metric multidimensional scaling (NMDS) ordinations of AMF taxonomic **(A)** and phylogenetic **(B)** community composition of 23 plant roots.

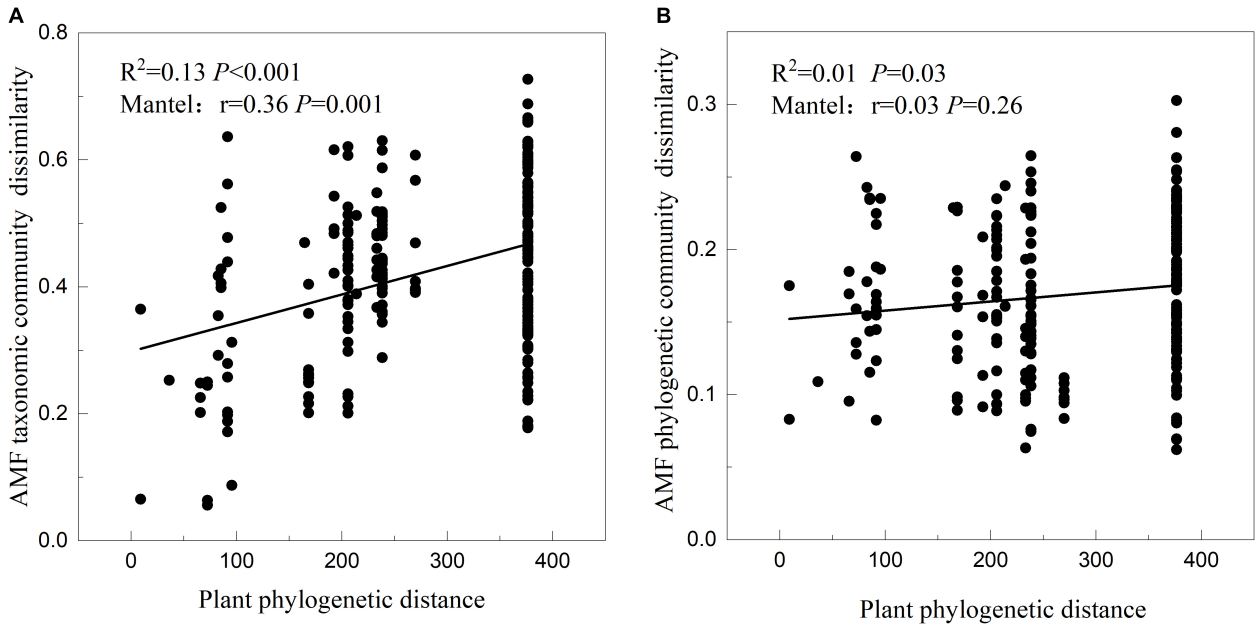

FIGURE 5 | Relationships between the phylogenetic distance of 23 plant species and their corresponding AMF taxonomic **(A)** and phylogenetic **(B)** community dissimilarity tested by linear regression and mantel test.

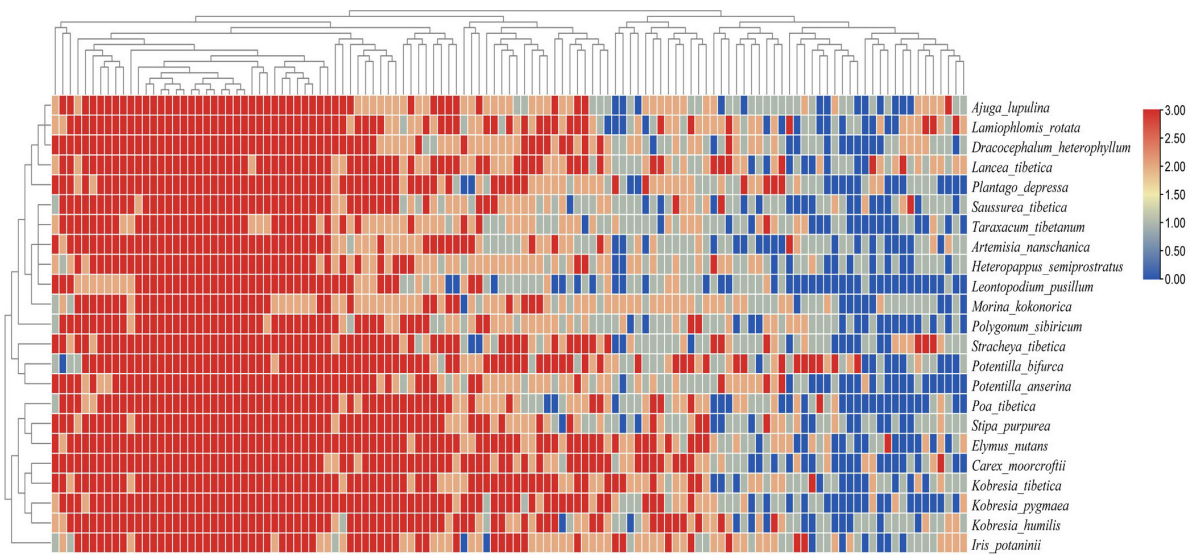

FIGURE 6 | Heat map of plant-AMF association frequency matrix combined with the phylogenetic tree. Different shades of color denote the association frequency between different plant species and AMF OTUs, and blue denotes an absence of association.

H_2' and modularity were both significantly lower than the observed values ($P < 0.001$). The results of the checkerboard score analysis showed that the observed values of plants and AMF communities were significantly lower than the expected values based on the null model ($P < 0.001$), but the checkerboard score (**Figures 7E,F**; fungus: 0.51, plant: 0.37) showed that the competition intensity of AMF was higher than that of plant species. The plant-AMF association frequency matrix showed that the phylogenetic signals of the plant species and AMF OTUs had significant effects on the plant-AMF network structure, and the phylogenetic signals from the plant were stronger than that from AMF (**Table 1**).

DISCUSSION

There were 121 AMF molecular species detected from plant roots in this study, indicating diverse AMF species in Tibetan

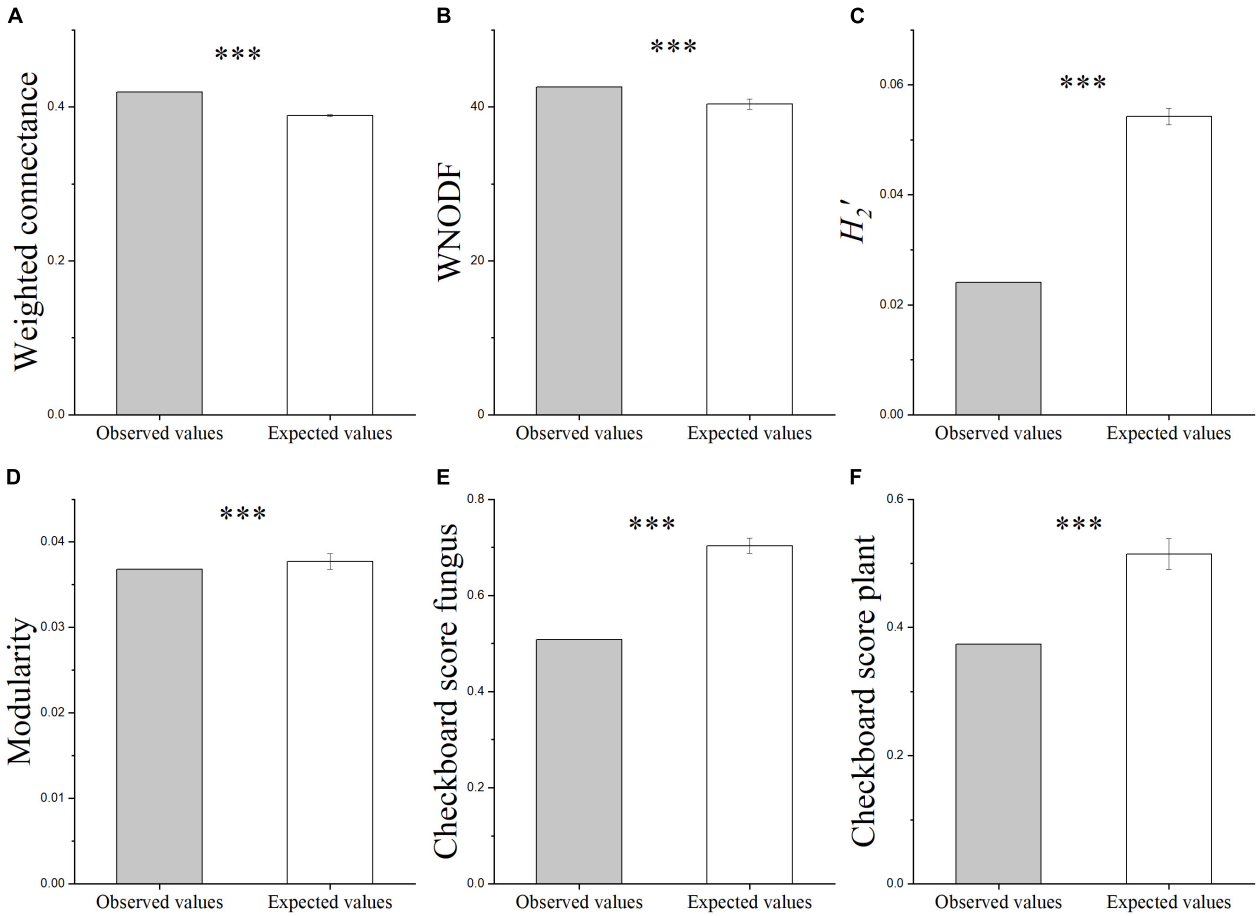

FIGURE 7 | The characteristics of different plant-AMF networks. Weight connectance **(A)**, WNODF **(B)**, H_2' **(C)**, modularity **(D)**, checkerboard score fungus [**(E)**, degree of avoiding overlapping of plants in the fungal community], and checkerboard score plant [**(F)**, degree of avoiding overlapping of fungi in the plant community]. Asterisks indicate significant differences between the observed and expected values according to the *t*-test (***$P < 0.001$; bars indicate SE).

TABLE 1 | Phylogenetic signals of plant-AMF based on incidence matrix frequency.

MSEd	MSEstar	MSEb	*d*plant (95% CI)	*d*AMF(95% CI)
0.26	0.32	0.46	0.41(0.36–0.45)	0.08(0.06–0.11)

MSEd, mean-squared error (MSE) calculated for the full model; MSEstar, MSE calculated for a "star" phylogeny; MSEb, MSE calculated for a Brownian evolution model; d, the intensity of plant (dplant) and AMF (dAMF) phylogenetic signals.

alpine meadow, in concordance with the previous studies (Gai et al., 2009, 2012; Liu et al., 2011; Zhang et al., 2016). At the same time, it was consistent with previous studies (Gai et al., 2012; Li et al., 2014) that Cyperaceae plants which were considered unable or not easy to form mycorrhizal fungi also had high AMF colonization (**Figure 2A**; 40.4–60.2%) and diversity (**Figures 2B,C**; Shannon-Wiener: 2.31–2.60; richness: 86.67–90.67). These findings suggest the potential ecological importance of AMF for plant growth in the alpine meadow. To survive in the harsh environment of the alpine meadow, plants might choose AMF species to improve their ability to absorb nitrogen and phosphorus or the stress-resistance ability (Bever, 2002). It has been found that some AMF species with strong cold resistance ability could survive, thus affecting the growth of host plants and community dynamics (Deepika and Kothamasi, 2015; Bauer et al., 2017).

Furthermore, this study found a significant positive correlation between plant phylogenetic distance and AMF community dissimilarity. Thus, the selectivity existed in the plant-AMF interactions, so that closely phylogenetic-related plant species select similar AMF communities (**Figure 5**). This plant-AMF selectivity has been well documented in previous studies (Vandenkoornhuyse et al., 2003; Horn et al., 2014; Veresoglou and Rillig, 2014; Chagnon et al., 2015; Deepika and Kothamasi, 2015). The different AMF communities in the rhizosphere of different plant species may be achieved by preferentially allocating plant carbon to the most beneficial fungal partners (Bever et al., 2009; Kiers et al., 2011). The construction of the plant-AMF community was to maximize the functional matching between partners (Thompson, 2005). Plants with similar traits preferentially hosted similar AMF and, likewise, phylogenetically related AMF (assumed to have similar functional traits) interacted with similar plants. No

doubt that the plant phylogeny was used to map the mycorrhizal information to examine evolutionary patterns (Wang and Qiu, 2006), but the complex symbiotic relationships between plants and AMF cannot be fully explained by plant phylogeny alone. The phylogenetic correlations between the interacting plant and AMF were modified by the competitive intransitivity (Laird and Schamp, 2006) and AMF species competition within a plant host (Roger et al., 2013). Therefore, future studies should involve factors, such as plant and AMF functional traits, species competition, climates, and soil nutrients, which can well explain the AMF community dynamics.

The network structure of 23 common plants and AMF was characterized by high connectance, high nestedness, anti-modularity, and anti-specialization, which was in line with the characteristics of the woody plant-AMF network in a subtropical forest in China (Chen et al., 2017). Generally, with the increase of connectance, the nestedness increased and the modularity decreased (Põlme et al., 2018), while the nestedness decreased, the modularity and the specialization increased (van der Heijden et al., 2015), as found in our network. High network connectance and nestedness and low network modularity indicated less segregation or sparse connections within subnetworks and dense connections between subnetworks for the plant-AMF network. These network properties enhanced the stability of the communities in the mutually beneficial network, which was considered to be an important property to promote the coexistence of species in the mutual system (Thebault and Fontaine, 2010). Theoretical studies suggested that the common nestedness patterns in the species network can determine the feasibility, resilience, durability, and structural stability of ecological communities (Toju et al., 2014), and the higher the nestedness of the interaction network, the better it can adapt to the effect of environmental disturbance.

In the analysis of plant-AMF phylogenetic signals based on the association frequency matrix, the results showed that the phylogenetic signals of plants and AMF had significant effects on the structure of the plant-AMF network. The phylogenetic signal from plants was stronger than that from AMF (**Table 1**). Close relatives of plants often interacted with AMF OTU species in the same group, but the interaction between AMF and plant species had a low correlation with AMF phylogeny, which was consistent with the study by Chen et al. (2017). In contrast, findings by Montesinos-Navarro et al. (2012a,b) showed that AMF phylogenetic diversity might also explain that there were different plant-AMF network structures in different ecosystems. In the AMF community with a more diverse phylogeny, there were more opportunities for specific AMF to coexist with common host plants, thus forming a highly nested symbiotic network structure (Chen et al., 2017). The phylogeny of plants and AMF played an important role in the non-random pattern of the AMF network in subtropical forest sites (Chen et al., 2017). In addition, the plant root traits in subtropical forests also showed strong interspecific phylogenetic signals (Kong et al., 2014). The modularity and nestedness in the plant-AMF network were caused by a variety of ecological processes, such as habitat heterogeneity (Olesen et al., 2007), specific selection of plant and AMF combination, relative species abundance and phylogenetic diversity, or AMF competition within the root (Verdu and Valiente-Banuet, 2011). The complex symbiotic interaction between plants and AMF has a potential effect on community assembly. Our study found that the characteristics of the plant-AMF network with high connectance and nestedness promote the stable symbiosis and interdependence between plants and AMF in Tibetan alpine meadows. Plants established network relationships with underground AMF through selection, which may affect the nutrient cycle of symbionts and even the succession of grassland community, so as to improve the adaptation to alpine ecological environment and stress. Therefore, further studies are required to elucidate the reciprocal symbiotic selection strategy, the coexistence pattern, community construction mechanism, and community dynamic rules of plant and AMF species. Furthermore, to enhance our understanding of the influence factors in the coevolution of plant-AMF is of great significance to study community structure, species evolution, and biodiversity.

CONCLUSION

This study assesses the relationship between the common plant phylogeny and AMF and the characteristics of the plant-AMF symbiotic network in a Tibetan alpine meadow. There was a significant positive correlation between the phylogenetic distance of the 23 herbs and their AMF community dissimilarity, indicating the selectivity of plant species on their AMF community. The network structure of the plant and AMF was characterized by high connectance, high nestedness, anti-modularity, and anti-specialization, which potentially promoted the stable symbiosis and interdependence between plants and AMF in Tibetan alpine meadows. The plant-AMF network was affected by the plant-AMF phylogenies, and the phylogenetic signal from plants was stronger than that from AMF. This study emphasizes that plant phylogeny and plant-AMF network play an important role in the complex plant-AMF community mechanism and enhance our understanding of the interaction between aboveground and belowground communities.

DATA AVAILABILITY STATEMENT

The datasets presented in this study can be found in online repositories. The names of the repository/repositories and accession number(s) can be found below: https://www.ncbi.nlm.nih.gov/, PRJNA748864.

AUTHOR CONTRIBUTIONS

QD, BJ, and YL designed the experiments, which were then carried out by QD, KC, and SR. QD, XG, and YL collected the data and conducted the statistical analyses. QD wrote the first draft of the manuscript. QD, MM, JZ, YL, and BJ reviewed and edited

the manuscript before submission. All authors made substantial contributions to the discussion of the content.

FUNDING

This study was supported by the Strategic Priority Research Program of the Chinese Academy of Sciences (XDA2005010402), the Second Tibetan Plateau Scientific Expedition and Research (2019QZKK0302), the National Natural Science Foundation of China (31800380 and 41871067), and the National Key Research and Development Program of China (2016YFC0501802).

ACKNOWLEDGMENTS

We thank Ping Wang for his help in providing data analysis methods and Congcong Li, Yinhang Luo, and Zhen Fang for their help in field sampling and lab analysis.

SUPPLEMENTARY MATERIAL

The Supplementary Material for this article can be found online at: https://www.frontiersin.org/articles/10.3389/fpls.2021.804861/full#supplementary-material

REFERENCES

Bai-ping, Z., Xiao-dong, C., Bao-lin, L., and Yong-hui, Y. (2002). Biodiversity and conservation in the Tibetan Plateau. *J. Geogr. Sci.* 12, 135–143. doi: 10.1007/BF02837467

Barberan, A., Bates, S. T., Casamayor, E. O., and Fierer, N. (2012). Using network analysis to explore co-occurrence patterns in soil microbial communities. *ISME J.* 6, 343–351. doi: 10.1038/ismej.2011.119

Bauer, J. T., Blumenthal, N., Miller, A. J., Ferguson, J. K., Reynolds, H. L., and Brudvig, L. (2017). Effects of between-site variation in soil microbial communities and plant-soil feedbacks on the productivity and composition of plant communities. *J. Appl. Ecol.* 54, 1028–1039. doi: 10.1111/1365-2664.12937

Bever, J. D. (2002). Negative feedback within a mutualism: host-specific growth of mycorrhizal fungi reduces plant benefit. *Proc. Biol. Sci.* 269, 2595–2601. doi: 10.1098/rspb.2002.2162

Bever, J. D., Richardson, S. C., Lawrence, B. M., Holmes, J., and Watson, M. (2009). Preferential allocation to beneficial symbiont with spatial structure maintains mycorrhizal mutualism. *Ecol. Lett.* 12, 13–21. doi: 10.1111/j.1461-0248.2008.01254.x

Blackwell, M. (2000). Terrestrial life-fungal from the start? *Science* 289, 1884–1885. doi: 10.1126/science.289.5486.1884

Bonfante, P., and Genre, A. (2008). Plants and arbuscular mycorrhizal fungi: an evolutionary-developmental perspective. *Trends Plant Sci.* 13, 492–498. doi: 10.1016/j.tplants.2008.07.001

Caporaso, J. G., Kuczynski, J., Stombaugh, J., Bittinger, K., Bushman, F. D., Costello, E. K., et al. (2010). QIIME allows analysis of high-throughput community sequencing data. *Nat. Methods* 7, 335–336. doi: 10.1038/nmeth.f.303

Chagnon, P. L., Bradley, R. L., and Klironomos, J. N. (2012). Using ecological network theory to evaluate the causes and consequences of arbuscular mycorrhizal community structure. *New Phytol.* 194, 307–312. doi: 10.1111/j.1469-8137.2011.04044.x

Chagnon, P.-L., Bradley, R. L., and Klironomos, J. N. (2015). Trait-based partner selection drives mycorrhizal network assembly. *Oikos* 124, 1609–1616. doi: 10.1111/oik.01987

Chen, C., Chen, H., Zhang, Y., Thomas, H. R., Frank, M. H., He, Y., et al. (2020). TBtools: an integrative toolkit developed for interactive analyses of big biological data. *Mol. Plant* 13, 1194–1202. doi: 10.1016/j.molp.2020.06.009

Chen, E. C. H., Morin, E., Beaudet, D., Noel, J., Yildirir, G., Ndikumana, S., et al. (2018). High intraspecific genome diversity in the model arbuscular mycorrhizal symbiont *Rhizophagus irregularis*. *New Phytol.* 220, 1161–1171. doi: 10.1111/nph.14989

Chen, L., Zheng, Y., Gao, C., Mi, X. C., Ma, K. P., Wubet, T., et al. (2017). Phylogenetic relatedness explains highly interconnected and nested symbiotic networks of woody plants and arbuscular mycorrhizal fungi in a Chinese subtropical forest. *Mol. Ecol.* 26, 2563–2575. doi: 10.1111/mec.14061

Cui, S., Meng, F., Suonan, J., Wang, Q., Li, B., Liu, P., et al. (2017). Responses of phenology and seed production of annual *Koenigia islandica* to warming in a desertified alpine meadow. *Agric. Meteorol.* 247, 376–384. doi: 10.1016/j.agrformet.2017.08.034

Deepika, S., and Kothamasi, D. (2015). Soil moisture–a regulator of arbuscular mycorrhizal fungal community assembly and symbiotic phosphorus uptake. *Mycorrhiza* 25, 67–75. doi: 10.1007/s00572-014-0596-1

Dormann, C. F., Fründ, J., Blüthgen, N., and Gruber, B. (2013). Open access indices, graphs and null models: analyzing bipartite ecological networks. *Open Ecol. J.* 2, 7–24. doi: 10.2174/1874213000902010007

Duan, A. M., Wu, G. X., Zhang, Q., and Liu, Y. M. (2006). New proofs of the recent climate warming over the Tibetan Plateau as a result of the increasing greenhouse gases emissions. *Chin. Sci. Bull.* 51, 1396–1400. doi: 10.1007/s11434-006-1396-6

Edgar, R. C. (2013). UPARSE: highly accurate OTU sequences from microbial amplicon reads. *Nat. Methods* 10, 996–998. doi: 10.1038/nmeth.2604

Gai, J. P., Christie, P., Cai, X. B., Fan, J. Q., Zhang, J. L., Feng, G., et al. (2009). Occurrence and distribution of arbuscular mycorrhizal fungal species in three types of grassland community of the Tibetan Plateau. *Ecol. Res.* 24, 1345–1350. doi: 10.1007/s11284-009-0618-1

Gai, J. P., Tian, H., Yang, F. Y., Christie, P., Li, X. L., and Klironomos, J. N. (2012). Arbuscular mycorrhizal fungal diversity along a Tibetan elevation gradient. *Pedobiologia* 55, 145–151. doi: 10.1016/j.pedobi.2011.12.004

Gao, C., Montoya, L., Xu, L., Madera, M., Hollingsworth, J., Purdom, E., et al. (2019). Strong succession in arbuscular mycorrhizal fungal communities. *ISME J.* 13, 214–226. doi: 10.1038/s41396-018-0264-0

Gao, Q.-M., and Guo, L.-D. (2010). A comparative study of arbuscular mycorrhizal fungi in forest, grassland and cropland in the Tibetan Plateau, China. *Mycology* 1, 163–170. doi: 10.1080/21501203.2010.510123

Genre, A., Lanfranco, L., Perotto, S., and Bonfante, P. (2020). Unique and common traits in mycorrhizal symbioses. *Nat. Rev. Microbiol.* 18, 649–660. doi: 10.1038/s41579-020-0402-3

Goberna, M., Montesinos-Navarro, A., Valiente-Banuet, A., Colin, Y., Gomez-Fernandez, A., Donat, S., et al. (2019). Incorporating phylogenetic metrics to microbial co-occurrence networks based on amplicon sequences to discern community assembly processes. *Mol. Ecol. Resour.* 19, 1552–1564. doi: 10.1111/1755-0998.13079

Gomez, J. M., Verdu, M., and Perfectti, F. (2010). Ecological interactions are evolutionarily conserved across the entire tree of life. *Nature* 465, 918–U916. doi: 10.1038/nature09113

Horn, S., Caruso, T., Verbruggen, E., Rillig, M. C., and Hempel, S. (2014). Arbuscular mycorrhizal fungal communities are phylogenetically clustered at small scales. *ISME J.* 8, 2231–2242. doi: 10.1038/ismej.2014.72

Ives, A. R., and Godfray, H. C. J. (2006). Phylogenetic analysis of trophic associations. *Am. Nat.* 168, E1–E14. doi: 10.1086/505157

Ji, B. M., and Bever, J. D. (2016). Plant preferential allocation and fungal reward decline with soil phosphorus: implications for mycorrhizal mutualism. *Ecosphere* 7:e01256. doi: 10.1002/ecs2.1256

Kembel, S. W., Cowan, P. D., Helmus, M. R., Cornwell, W. K., Morlon, H., Ackerly, D. D., et al. (2010). Picante: R tools for integrating phylogenies and ecology. *Bioinformatics* 26, 1463–1464. doi: 10.1093/bioinformatics/btq166

Kiers, E. T., Duhamel, M., Beesetty, Y., Mensah, J. A., Franken, O., Verbruggen, E., et al. (2011). Reciprocal rewards stabilize cooperation in the mycorrhizal symbiosis. *Science* 333, 880–882. doi: 10.1126/science.1208473

Kong, D., Ma, C., Zhang, Q., Li, L., Chen, X., Zeng, H., et al. (2014). Leading dimensions in absorptive root trait variation across 96 subtropical forest species. *New Phytol.* 203, 863–872. doi: 10.1111/nph.12842

Laird, R. A., and Schamp, B. S. (2006). Competitive intransitivity promotes species coexistence. *Am. Nat.* 168, 182–193. doi: 10.1086/506259

Li, X., Gai, J., Cai, X., Li, X., Christie, P., Zhang, F., et al. (2014). Molecular diversity of arbuscular mycorrhizal fungi associated with two co-occurring perennial plant species on a Tibetan altitudinal gradient. *Mycorrhiza* 24, 95–107. doi: 10.1007/s00572-013-0518-7

Li, X., Zhang, J., Gai, J., Cai, X., Christie, P., and Li, X. (2015). Contribution of arbuscular mycorrhizal fungi of sedges to soil aggregation along an altitudinal alpine grassland gradient on the Tibetan Plateau. *Environ. Microbiol.* 17, 2841–2857. doi: 10.1111/1462-2920.12792

Liu, Y., He, J., Shi, G., An, L., Opik, M., and Feng, H. (2011). Diverse communities of arbuscular mycorrhizal fungi inhabit sites with very high altitude in Tibet Plateau. *FEMS Microbiol. Ecol.* 78, 355–365. doi: 10.1111/j.1574-6941.2011.01163.x

Lumini, E., Orgiazzi, A., Borriello, R., Bonfante, P., and Bianciotto, V. (2010). Disclosing arbuscular mycorrhizal fungal biodiversity in soil through a land-use gradient using a pyrosequencing approach. *Environ. Microbiol.* 12, 2165–2179. doi: 10.1111/j.1462-2920.2009.02099.x

McGonigle, T. P., Miller, M. H., Evans, D. G., Fairchild, G. L., and Swan, J. A. (1990). A new method which gives an objective measure of colonization of roots by vesicular-arbuscular mycorrhizal fungi. *New Phytol.* 115, 495–501. doi: 10.1111/j.1469-8137.1990.tb00476.x

Miehe, G., Mlehe, S., Kaiser, K., Liu, J. Q., and Zhao, X. Q. (2008). Status and dynamics of *Kobresia pygmaea* ecosystem on the Tibetan plateau. *Ambio* 37, 272–279. doi: 10.1579/0044-7447(2008)37[272:sadotk]2.0.co;2

Montesinos-Navarro, A., Segarra-Moragues, J. G., Valiente-Banuet, A., and Verdu, M. (2012a). The network structure of plant-arbuscular mycorrhizal fungi. *New Phytol.* 194, 536–547. doi: 10.1111/j.1469-8137.2011.04045.x

Montesinos-Navarro, A., Segarra-Moragues, J. G., Valiente-Banuet, A., and Verdu, M. (2012b). Plant facilitation occurs between species differing in their associated arbuscular mycorrhizal fungi. *New Phytol.* 196, 835–844. doi: 10.1111/j.1469-8137.2012.04290.x

Olesen, J. M., Bascompte, J., Dupont, Y. L., and Jordano, P. (2007). The modularity of pollination networks. *Proc. Natl. Acad. Sci. U.S.A.* 104, 19891–19896. doi: 10.1073/pnas.0706375104

Põlme, S., Bahram, M., Jacquemyn, H., Kennedy, P., Kohout, P., Moora, M., et al. (2018). Host preference and network properties in biotrophic plant-fungal associations. *New Phytol.* 217, 1230–1239. doi: 10.1111/nph.14895

Qiu, J. (2008). The third pole. *Nature* 454, 393–396. doi: 10.1038/454393a

Reinhart, K. O., and Anacker, B. L. (2014). More closely related plants have more distinct mycorrhizal communities. *AoB Plants* 6:lu051. doi: 10.1093/aobpla/plu051

Roger, A., Colard, A., Angelard, C., and Sanders, I. R. (2013). Relatedness among arbuscular mycorrhizal fungi drives plant growth and intraspecific fungal coexistence. *ISME J.* 7, 2137–2146. doi: 10.1038/ismej.2013.112

Sargent, R. D., Kembel, S. W., Emery, N. C., Forrestel, E. J., and Ackerly, D. D. (2011). Effect of local community phylogenetic structure on pollen limitation in an obligately insect-pollinated plant. *Am. J. Bot.* 98, 283–289. doi: 10.3732/ajb.1000329

Smith, S. E., and Read, D. J. (2008). *Mycorrhizal Symbiosis*. London: Academic Press. doi: 10.1016/B978-0-12-370526-6.X5001-6

Tedersoo, L., Bahram, M., and Zobel, M. (2020). How mycorrhizal associations drive plant population and community biology. *Science* 367:eaba1223. doi: 10.1126/science.aba1223

Thebault, E., and Fontaine, C. (2010). Stability of ecological communities and the architecture of mutualistic and trophic networks. *Science* 329, 853–856. doi: 10.1126/science.1188321

Thompson, J. N. (2005). Coevolution: the geographic mosaic of coevolutionary arms races. *Curr. Biol.* 15, R992–R994. doi: 10.1016/j.cub.2005.11.046

Toju, H., Guimaraes, P. R., Olesen, J. M., and Thompson, J. N. (2014). Assembly of complex plant-fungus networks. *Nat. Commun.* 5:5273. doi: 10.1038/ncomms6273

Toju, H., Tanabe, A. S., and Ishii, H. S. (2016). Ericaceous plant-fungus network in a harsh alpine-subalpine environment. *Mol. Plant* 25, 3242–3257. doi: 10.1111/mec.13680

Ulrich, W., and Gotelli, N. J. (2007). Null model analysis of species nestedness patterns. *Ecology* 88, 1824–1831. doi: 10.1890/06-1208.1

van der Heijden, M. G. A., Martin, F. M., Selosse, M.-A., and Sanders, I. R. (2015). Mycorrhizal ecology and evolution: the past, the present, and the future. *New Phytol.* 205, 1406–1423. doi: 10.1111/nph.13288

Van Geel, M., Busschaert, P., Honnay, O., and Lievens, B. (2014). Evaluation of six primer pairs targeting the nuclear rRNA operon for characterization of arbuscular mycorrhizal fungal (AMF) communities using 454 pyrosequencing. *J. Microbiol. Methods* 106, 93–100. doi: 10.1016/j.mimet.2014.08.006

Vandenkoornhuyse, P., Ridgway, K. P., Watson, I. J., Fitter, A. H., and Young, J. P. W. (2003). Co-existing grass species have distinctive arbuscular mycorrhizal communities. *Mol. Plant* 12, 3085–3095. doi: 10.1046/j.1365-294X.2003.01967.x

Verdu, M., and Valiente-Banuet, A. (2011). The relative contribution of abundance and phylogeny to the structure of plant facilitation networks. *Oikos* 120, 1351–1356. doi: 10.1111/j.1600-0706.2011.19477.x

Veresoglou, S. D., and Rillig, M. C. (2014). Do closely related plants host similar arbuscular mycorrhizal fungal communities? A meta-analysis. *Plant Soil* 377, 395–406. doi: 10.1007/s11104-013-2008-2

Walder, F., and van der Heijden, M. G. (2015). Regulation of resource exchange in the arbuscular mycorrhizal symbiosis. *Nat. Plants* 1:15159. doi: 10.1038/nplants.2015.159

Wang, B., and Qiu, Y. L. (2006). Phylogenetic distribution and evolution of mycorrhizas in land plants. *Mycorrhiza* 16, 299–363. doi: 10.1007/s00572-005-0033-6

Wang, Z. Q., Zhang, Y. Z., Yang, Y., Zhou, W., Gang, C. C., Zhang, Y., et al. (2016). Quantitative assess the driving forces on the grassland degradation in the Qinghai-Tibet Plateau, in China. *Ecol. Inform.* 33, 32–44. doi: 10.1016/j.ecoinf.2016.03.006

Werner, G. D. A., and Kiers, E. T. (2015). Partner selection in the mycorrhizal mutualism. *New Phytol.* 205, 1437–1442. doi: 10.1111/nph.13113

Wipf, D., Krajinski, F., van Tuinen, D., Recorbet, G., and Courty, P. E. (2019). Trading on the arbuscular mycorrhiza market: from arbuscules to common mycorrhizal networks. *New Phytol.* 223, 1127–1142. doi: 10.1111/nph.15775

Xu, M., Li, X., Cai, X., Li, X., Christie, P., and Zhang, J. (2017). Land use alters arbuscular mycorrhizal fungal communities and their potential role in carbon sequestration on the Tibetan Plateau. *Sci. Rep.* 7:3067. doi: 10.1038/s41598-017-03248-0

Zanne, A. E., Tank, D. C., Cornwell, W. K., Eastman, J. M., Smith, S. A., FitzJohn, R. G., et al. (2014). Three keys to the radiation of angiosperms into freezing environments. *Nature* 506, 89–92. doi: 10.1038/nature12872

Zhang, J., Wang, F., Che, R. X., Wang, P., Liu, H. K., Ji, B. M., et al. (2016). Precipitation shapes communities of arbuscular mycorrhizal fungi in Tibetan alpine steppe. *Sci. Rep.* 6:23488. doi: 10.1038/srep23488

Zhang, L., Zhou, J., George, T. S., Limpens, E., and Feng, G. (2021). Arbuscular mycorrhizal fungi conducting the hyphosphere bacterial orchestra. *Trends Plant Sci.* doi: 10.1016/j.tplants.2021.10.008 [Epub ahead of print].

Conflict of Interest: The authors declare that the research was conducted in the absence of any commercial or financial relationships that could be construed as a potential conflict of interest.

Publisher's Note: All claims expressed in this article are solely those of the authors and do not necessarily represent those of their affiliated organizations, or those of the publisher, the editors and the reviewers. Any product that may be evaluated in this article, or claim that may be made by its manufacturer, is not guaranteed or endorsed by the publisher.

Copyright © 2021 Dong, Guo, Chen, Ren, Muneer, Zhang, Li and Ji. This is an open-access article distributed under the terms of the Creative Commons Attribution License (CC BY). The use, distribution or reproduction in other forums is permitted, provided the original author(s) and the copyright owner(s) are credited and that the original publication in this journal is cited, in accordance with accepted academic practice. No use, distribution or reproduction is permitted which does not comply with these terms.

frontiers in Plant Science

ORIGINAL RESEARCH
published: 20 December 2021
doi: 10.3389/fpls.2021.792123

Differential Responses of Plant Primary Productivity to Nutrient Addition in Natural and Restored Alpine Grasslands in the Qinghai Lake Basin

*Chunli Li[1], Yonghui Li[1], Xinwei Li[1], Li Ma[2], Yuanming Xiao[3] and Chunhui Zhang[1]**

[1] State Key Laboratory of Plateau Ecology and Agriculture, Qinghai University, Xining, China, [2] Key Laboratory of Cold Regions Restoration Ecology, Northwest Institute of Plateau Biology, Chinese Academy of Science, Xining, China, [3] Key Laboratory of Tibetan Medicine Research, Northwest Institute of Plateau Biology, Chinese Academy of Science, Xining, China

OPEN ACCESS

Edited by:
Jian Sun,
Institute of Tibetan Plateau Research (CAS), China

Reviewed by:
Gang Fu,
Institute of Geographic Sciences and Natural Resources Research, Chinese Academy of Sciences (CAS), China
Jianshuang Wu,
Institute of Environment and Sustainable Development in Agriculture, Chinese Academy of Agricultural Sciences (CAAS), China

***Correspondence:**
Chunhui Zhang
zhangcqhu@163.com

Specialty section:
This article was submitted to Functional Plant Ecology, a section of the journal Frontiers in Plant Science

Received: *09 October 2021*
Accepted: *22 November 2021*
Published: *20 December 2021*

Citation:
Li C, Li Y, Li X, Ma L, Xiao Y and Zhang C (2021) Differential Responses of Plant Primary Productivity to Nutrient Addition in Natural and Restored Alpine Grasslands in the Qinghai Lake Basin. Front. Plant Sci. 12:792123. doi: 10.3389/fpls.2021.792123

Climate, land-use changes, and nitrogen (N) deposition strongly impact plant primary productivity, particularly in alpine grassland ecosystems. In this study, the differential responses of plant community primary productivity to N and phosphorus (P) nutrient application were investigated in the natural (NG) and "Grain for Green" restored (RG) alpine grasslands by a continuous 3-year experiment in the Qinghai Lake Basin. N addition only significantly promoted plant aboveground biomass (AGB) by 42% and had no significant effect on belowground biomass (BGB) and total biomass (TB) in NG. In comparison with NG, N addition elevated AGB and BGB concurrently in RG by 138% and 24%, respectively, which further significantly increased TB by 41% in RG. Meanwhile, N addition significantly decreased BGB and the AGB ratio (R/S) both in NG and RG. Compared with N addition, P addition did not perform an evident effect on plant biomass parameters. Additionally, AGB was merely negatively influenced by growing season temperatures (GST) under the N addition treatment in NG. AGB was negatively associated with GST but positively related to growing season precipitation (GSP) in RG. By contrast, changes in the R/S ratio in RG were positively correlated with GST and negatively related to GSP. In sum, the results revealed that plant community biomass exhibited convergent (AGB and R/S) and divergent (BGB and TB) responses to N addition between NG and RG. In addition, the outcomes suggested that climate warming would enhance plant biomass allocation to belowground under ongoing N deposition, and indicated the significance of precipitation for plant growth and AGB accumulation in this restored alpine grassland ecosystem.

Keywords: alpine grassland, plant primary productivity, nitrogen and phosphorus additions, restored grassland, climate change

INTRODUCTION

As a representation of primary productivity and carbon (C) uptake by plants, biomass is a foundational measure that can be used to infer aspects of nutrient cycling and energy flow in terrestrial ecosystems (Borer et al., 2014; Fay et al., 2015; Grace et al., 2016; Kohli et al., 2019). Accounting for approximately one-third of the Earth's terrestrial net primary production, the plant community biomass is central to understanding the structure and functioning of grasslands, and is vital for the C storage and biogeochemical cycling of ecosystems (Hoekstra et al., 2005; Luyssaert et al., 2008; Borer et al., 2014; Erb et al., 2018; Zhang and Xi, 2021). Humans have heavily impacted grasslands, and more than two-thirds of their biomass has been converted to human-dominated uses (primarily agriculture; Borer et al., 2014; Fay et al., 2015).

Plant growth and biomass allocation are susceptible to climatic change and are limited by complex and multiple resource availabilities, such as soil nutrients, water, and light (Hoekstra et al., 2005; Elser et al., 2007; LeBauer and Treseder, 2008; Poorter et al., 2012; Borer et al., 2014). Plant community productivity and soil C sequestration of grassland ecosystems are widely accepted to be nutrient limited, largely depending on the bioavailability of nitrogen (N) and phosphorus (P) (Elser et al., 2007; Ågren et al., 2012; Fay et al., 2015; Wieder et al., 2015). The availability of N has been deemed an essential determinant of the aboveground net primary productivity (ANPP) across terrestrial ecosystems, and N fertilization could promote plant N uptake and ultimately improve plant biomass production (Elser et al., 2007; LeBauer and Treseder, 2008; Borer et al., 2014; Fay et al., 2015; Wang et al., 2020). However, nutrient co-limitation of grassland productivity is common and more widely recognized (Ågren et al., 2012; Borer et al., 2014; Fay et al., 2015; Wang et al., 2020).

Land-use transitions, as the most intensive anthropogenic interference, alter plant coverage, composition, and productivity directly (Lal, 2002; Sartori et al., 2007; Jelinski and Kucharik, 2009; Li et al., 2016a,b). Generally, cultivation results in massive losses of C and N from the soil; with plant restoration on cropped land, soil nutrient content can be recovered to some extent (Jelinski and Kucharik, 2009; Li et al., 2016a, 2019). Associated with human activities, such as the heavy use of inorganic fertilizers in the process of farming, human-induced N and P deposition has continued to increase during the past several decades worldwide (Galloway et al., 2008; Phoenix et al., 2012). This phenomenon has caused a substantial increase in N and P bioavailability. These element depositions supply an important potential nutrient source for maintaining grassland primary productivity, which would be beneficial to the growth of plant community (Fay et al., 2015; Stevens et al., 2015; Zhu et al., 2016; Wang et al., 2020); however, the additional nutrient input might have adverse effects on plant community composition, structure, and alter ecosystem functionality (Phoenix et al., 2012; Penuelas et al., 2013; Zhu et al., 2016). In addition, the ongoing but imbalanced element depositions potentially induce limitation by other resources (Penuelas et al., 2013; Grace et al., 2016). Numerous studies have shown that N deposition could promote grassland ANPP, and highlighted the importance of N and P synergistic co-limitation in grasslands (Borer et al., 2014; Fay et al., 2015; Grace et al., 2016; Zhao et al., 2019; Wang et al., 2020). N and P fertilizers have received considerable attention in grassland restoration (Fay et al., 2015; Cerasoli et al., 2018; Wang et al., 2018, 2020). However, to date, previous researches have focused primarily on natural grasslands (Borer et al., 2014; Fay et al., 2015; Grace et al., 2016; Zhao et al., 2019). The consequences and effects of anthropogenic nutrient inputs (N and P) vary according to land use, and this remains poorly understood on restored grasslands. It is crucial for potential C sequestration in terrestrial ecosystems and is challenging to predict.

Owing to its ecological uniqueness in Eurasia, the alpine grassland of the Qinghai-Tibetan Plateau (QTP) is critical to global C sequestration and the development of regional husbandry (Shen et al., 2014; Wei et al., 2019; Dong et al., 2020). Plant growth and productivity are ordinarily limited by soil available N and P, resulting from the low temperatures and high altitude in the QTP (Jiang et al., 2013; Fu et al., 2015; Fu and Shen, 2016a,b). As the main alpine grassland area of Qinghai province, the Qinghai Lake Basin (QLB) is a distinctive geographical unit within the QTP. The ecosystem's internal fragility, coupled with external environmental and land-use changes, makes the alpine grasslands in QLB highly sensitive to human activities and ongoing climate change (Cui and Li, 2015; Tao et al., 2021). Therefore, studying the relationships among the environment, ecology, and agriculture/pasture development embedded within climate change scenarios is essential. Because of agriculture and the "Grain for Green" project, native alpine grasslands in the QLB were extensively cultivated to obtain farmland in the mid-1950s; following severe degradation of soil quality, cropped land was returned to grassland in the early 2000s. Previous studies have validated the significant effects of land-use changes on soil C stock patterns and revealed that N and P additions could improve soil quality (Li et al., 2016a, 2019). To date, however, few studies have explored the interaction effects of land use, element depositions, and changes in meteorological factors on the community productivity of the "Grain for Green" grassland (i.e., restored grassland). It is urgent to obtain detailed information about the multiple impacts of land use and nutrient addition on vegetation community primary productivity and biomass allocation between above- and belowground. The results will permit a better understanding of their profound influences on ecosystem productivity and soil C sequestration under a background of global change and accordingly altered climatic and edaphic conditions.

Here, a consecutive 3-year field experiment *in situ* was manipulated in two types of grassland around the QLB, including the natural alpine grassland (NG) and the "Grain for Green" (restored) alpine grassland (RG). The study aimed (1) to determine the presence and magnitude of N and P addition effects on plant community biomass; (2) to investigate the convergent and divergent responses of plant community biomass to nutrient application in the natural and restored grasslands; (3) to explore the influence of interannual meteorological factors on primary productivity and biomass allocation. The findings will provide more detailed information and explanations

for nutrient limitations, resulting from land use and climate change scenarios.

MATERIALS AND METHODS

Study Site

The field experiment was carried out in Gangcha County, located on the northern margin of Qinghai Lake and within the northeast part of the QTP. The mean annual temperature in this region is around −0.6°C, and the mean annual precipitation is ∼370.5 mm (<400 mm), which occurs almost exclusively in the plant-growing season (from June to August). The soil type of the study site belongs to Dark Chestnut [QPARPO (Qinghai province agricultural resource planning office), 1995]. The two grasslands, NG and RG (37°21′N, 100°04′E, and 3,313 m a.s.l.), both experienced minimal disturbance from human activity and animal grazing in recent years, following the exclusion of livestock grazing by fencing. The NG was dominated by *Stipa purpurea*, *Kobresia humilis*, *Elymus nutans*, *Leymus secalinus*, and *Melissilus ruthenicus*. The RG was used as cropland until the early 2000s but has undergone no grass harvesting, grazing, fertilization, or irrigation since 2002. The constructive grass species of RG was *Elymus nutans*, and other principal plant species included *Elymus nutans*, *Leymus secalinus*, and *Potentilla anserine* at the present restoration stage.

Experiment Design

The manipulative experiments were established with a randomized block design in June 2012. Four treatments were included: (1) CK (control, without N or P addition); (2) N, nitrogen addition; (3) P, phosphorus addition; and (4) N × P, a combination of nitrogen and phosphorus addition. N was added in the form of NH_4NO_3 at the rate of 10 g N·m^{-2} year^{-1}, and P was added in the form of $Ca(H_2PO_4)_2{\cdot}H_2O$ at the rate of 5 g P·m^{-2} year^{-1}. The addition rates were applied based on the typical amounts frequently used in the QTP alpine grassland (Jing et al., 2016). Six blocks (replicated plots) were established for each treatment. Each plot had 3 × 3-m quadrat areas, and 24 plots were included in each grassland, with a 1-m buffer belt between plots. Nutrient addition was conducted in late June or early July, coinciding with the vigorous growth period of the vegetation. N and P were added one time per year in 2012, 2013, and 2014.

Field Sampling

Plant materials were collected in middle-late August annually, coinciding with the period of greatest aboveground biomass. One 50 × 50-cm quadrat was randomly placed within each plot. Briefly, all the standing green shoots were cut at the soil surface and oven-dried at 65°C to constant weights to obtain plant community aboveground biomass (AGB). After the aboveground plant and surface litter were removed, the belowground roots were obtained with stainless steel root auger (8 cm diameter) from three random points in the topsoil (0–10 cm, more than 70% root distributed in this soil layer, Li et al., 2016a) of each quadrat. The three subsamples were then mixed as one sample and sealed in a polyethylene bag. After transport to the laboratory, visible root materials were carefully picked out through a 2.-mm sieve, washed, then oven-dried at 65°C to constant mass. This material was used to estimate plant community belowground biomass (BGB). The total plant community biomass (TB) was equal to the sum of AGB and BGB. The ratio of root and shoot (R/S, BGB: AGB) was used to represent the biomass allocation pattern. In brief, plant community biomass parameters include AGB, BGB, TB, and R/S in this study.

Statistical Analysis

All statistical analyses were analyzed using SPSS 21.0 software (SPSS, Chicago, USA). General linear models and ANOVAs were applied to test the main and interaction effects of nutrient addition and sampling year on AGB, BGB, TB, R/S; a *t*-test was employed to test significant differences of plant community biomass parameters between the two grasslands. Multiple comparisons proceeded using the least standard difference method. For improving normality, data were log-transformed as necessary. Ordinary regression models were built to estimate the effects of climatic factors on plant community biomass parameters using the most powerful explanatory models. Pearson correlation was used to analyze the relationships between biomass parameters. We obtained the plant-growing season (from June to August) temperatures (GST) and precipitation (GSP) data from the China meteorological data sharing service system. All figures were completed using Excel and CorelDraw software.

RESULTS

Effects of Nutrient Addition on Plant Community Biomass

The plant community biomass of the alpine grassland was affected by N addition (**Table 1**). By contrast, no detectable effect of P addition and the interaction of N and P additions were found for all the plant biomass parameters ($p > 0.05$, **Table 1**). Therefore, the effects of nutrient addition on plant community biomass only referred to N addition hereafter.

Nitrogen N addition significantly increased plant AGB of NG and RG by 42 and 138%, respectively ($p < 0.001$, **Table 1**; **Figure 1A**). N addition significantly increased BGB and TB in RG by 24 and 41% ($p < 0.01$, **Table 1**; **Figures 1B,C**), respectively; it showed no evident effects on BGB and TB in NG ($p > 0.05$, **Table 1**; **Figures 1B,C**). N addition significantly decreased the R/S ratio of NG and RG by 28 and 45%, respectively ($p < 0.001$, **Table 1**; **Figure 1D**).

Comparisons of Plant Community Biomass Between NG and RG

Plant AGB of NG was significantly higher than that of RG across different sampling years in treatments without N addition ($p < 0.001$, **Figure 2A**). In treatments with N addition, AGB of RG was significantly lower than that of NG in the first 2 years of the experiment ($p < 0.05$), whereas significantly higher than that of NG in the 3rd sampling year ($p < 0.05$, **Figure 2B**). On average, AGB of NG was substantially higher than that of RG

TABLE 1 | Effects of nitrogen addition (N), phosphorus addition (P), and sampling year (Y) and their interaction effects on plant community AGB, BGB, TB, and R/S in the natural (NG) and restored (RG) grasslands.

		N		P		Y		N×P		N×Y		P×Y		N×P×Y	
		F	*p*	*F*	*p*	*F*	*p*	*F*	*p*	*F*	*p*	*F*	*p*	*F*	*p*
AGB	NG	**59.762**	**<0.001**	2.751	0.102	**6.389**	**0.003**	3.322	0.073	0.083	0.920	1.332	0.272	0.411	0.655
	RG	**323.95**	**<0.001**	0.985	0.325	**92.213**	**<0.001**	0.024	0.878	**6.643**	**0.002**	0.142	0.868	0.368	0.693
BGB	NG	0.133	0.716	0.005	0.944	2.464	0.094	0.958	0.332	1.417	0.250	0.760	0.472	0.524	0.595
	RG	**12.949**	**<0.001**	3.427	0.069	0.655	0.523	0.026	0.873	1.227	0.300	0.718	0.492	0.599	0.553
TB	NG	0.367	0.547	0.293	0.590	2.214	0.118	1.387	0.244	1.790	0.176	0.977	0.382	0.369	0.693
	RG	**56.444**	**<0.001**	2.890	0.094	**7.675**	**0.001**	0.002	0.965	0.589	0.558	0.654	0.524	0.546	0.582
R/S	NG	**11.549**	**0.001**	0.095	0.759	0.101	0.904	0.145	0.705	1.344	0.268	0.075	0.928	0.678	0.512
	RG	**60.896**	**<0.001**	3.881	0.053	**27.428**	**<0.001**	0.003	0.956	**4.619**	**0.014**	0.358	0.700	0.368	0.694

AGB, aboveground biomass; BGB, belowground biomass; TB, total biomass; R/S, the ratio of root and shoot. Significant results ($p < 0.05$) were bolded.

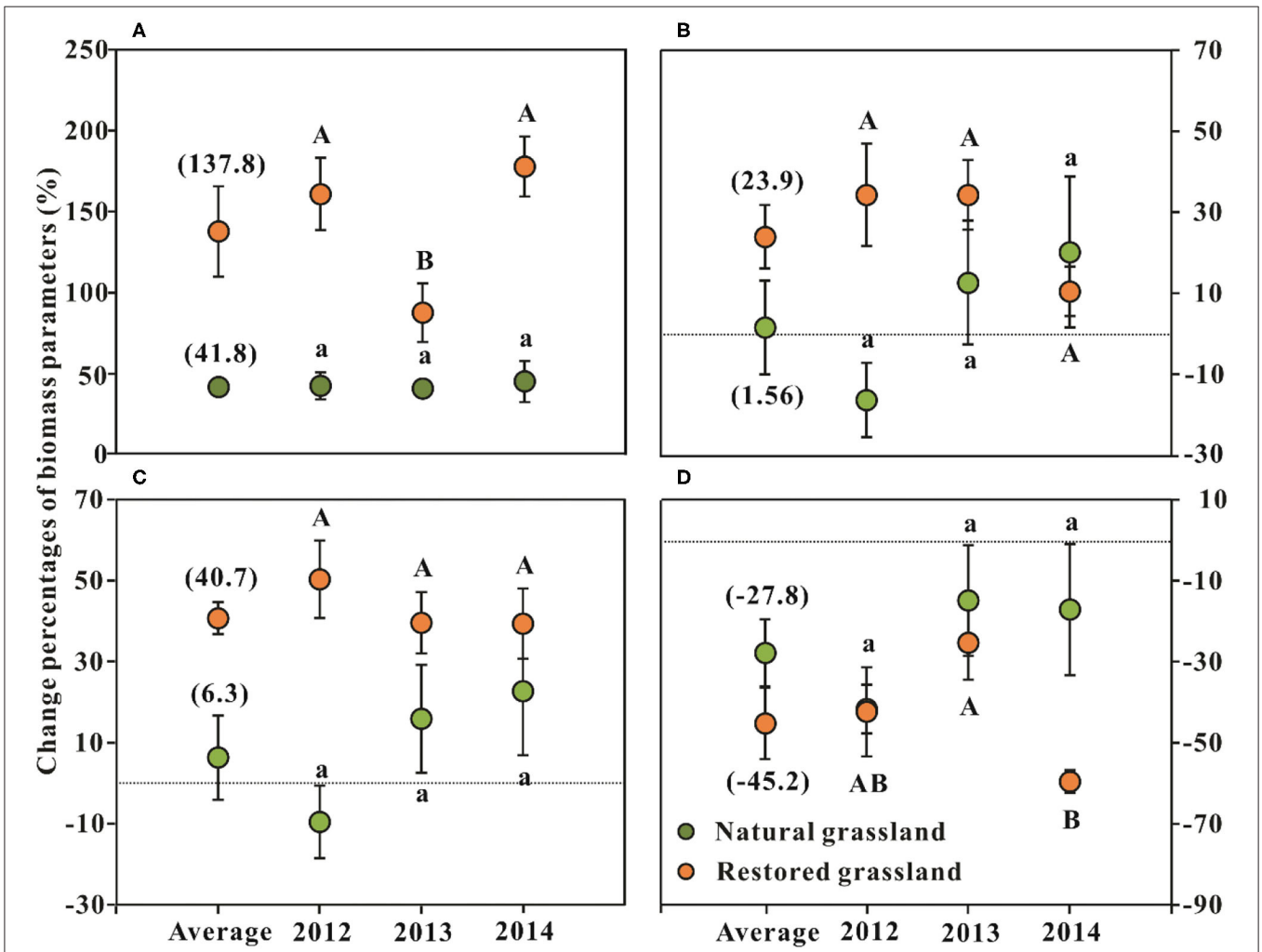

FIGURE 1 | Effects of nitrogen addition on the changes in plant community biomass parameters (mean ± SE, $n = 6$) in the alpine grasslands around Qinghai Lake Basin. **(A)** Aboveground biomass; **(B)** belowground biomass; **(C)** total biomass; **(D)** R/S ratio. R/S = The ratio of root (below-) and shoot (aboveground) biomass; Average represents the average effect across the three sampling years (mean ± SE, $n = 18$). Different lowercase letters indicate significant differences among sampling years in the natural grassland at $p < 0.05$, and uppercase letters indicate significant differences between sampling years in the restored grassland at $p < 0.05$.

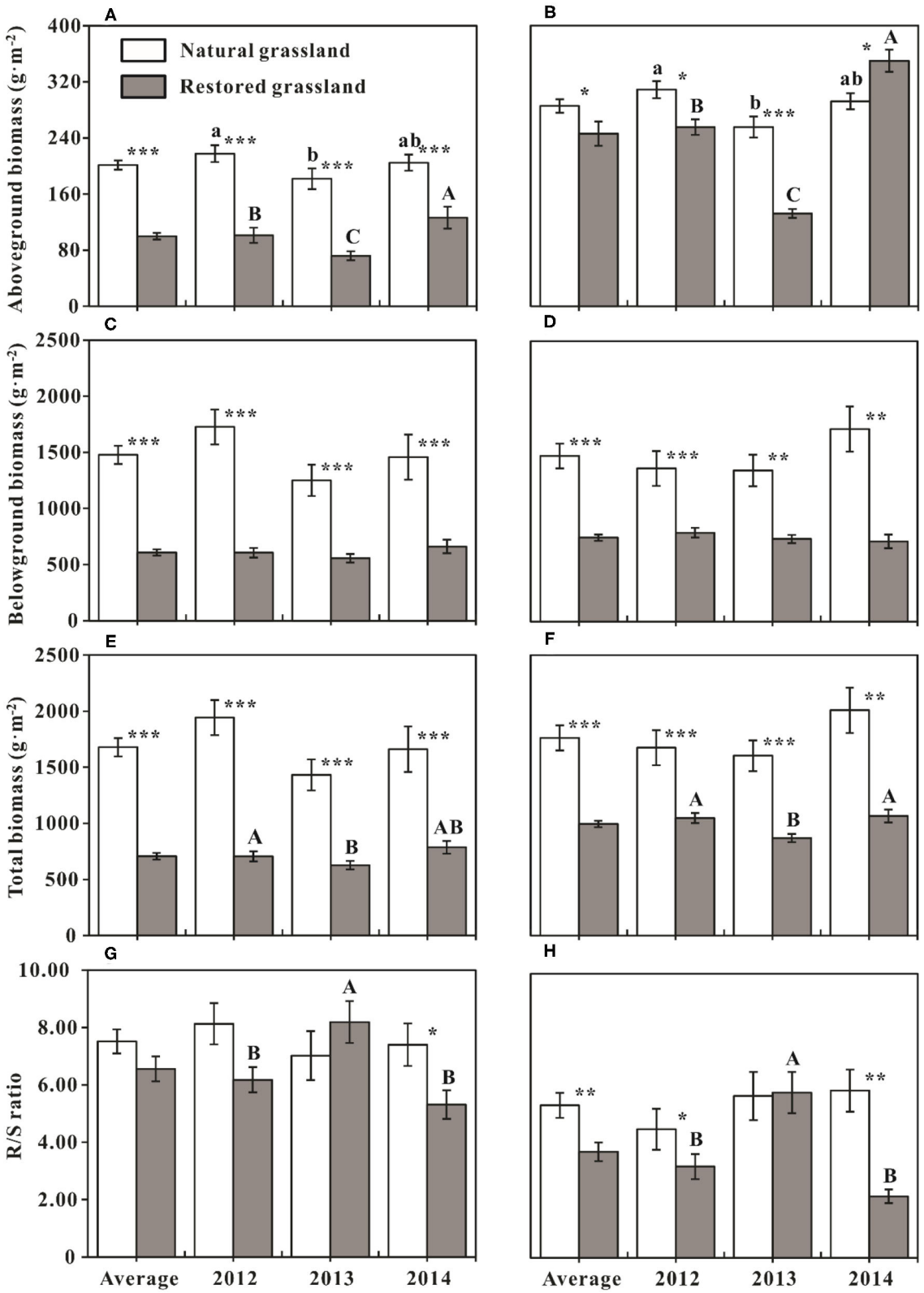

FIGURE 2 | Comparisons of biomass parameters (mean ± SE, $n = 12$) among sampling years in the same grassland and between the natural and restored grasslands in the same years. **(A,C,E,G)** Comparisons of aboveground, belowground, plant community total biomass, and the ratio of root and shoot biomass in treatments without nitrogen addition, respectively. **(B,D,F,H)** Comparisons of aboveground, belowground, plant community total biomass, and the ratio of root and

(Continued)

FIGURE 2 | shoot biomass in treatments with nitrogen addition, respectively. Average represents the average effect across the three sampling years (mean ± SE, n = 36). Different lowercase letters indicate significant differences of biomass parameters among sampling years in the natural grassland at $p < 0.05$, and uppercase letters indicate significant differences of biomass parameters among sampling years in the restored grassland at $p < 0.05$. *$p < 0.05$; **$p < 0.01$; ***$p < 0.001$, indicate the differences of biomass parameters between the natural and restored grasslands in the same sampling year and same treatment.

in the ambient environment (without N addition, $p < 0.001$, **Figure 2A**); N addition weakened the difference of AGB between NG and RG ($p = 0.05$, **Figure 2B**). BGB and TB of NG were significantly higher than that of RG ($p < 0.01$, **Figures 2C–F**), which was consistent across the 3 experimental years regardless of N addition. Although there was no significant difference in R/S between the two grasslands in the first 2 years of the experiment in treatments without N addition ($p > 0.05$), the R/S of NG was significantly higher than that of RG in 2014 ($p < 0.05$, **Figure 2G**). In the N addition treatments, R/S of RG was significantly lower than that of NG in 2012 and 2014 ($p < 0.05$, **Figure 2H**), but no difference was found in 2013 ($p > 0.05$, **Figure 2H**).

Interannual Dynamics of Plant Community Biomass and the Influences of Climate Factors

AGB of NG and RG, TB, and the R/S ratio of RG displayed apparent interannual variation ($p < 0.01$, **Table 1**). Therefore, only the plant biomass parameters with evident year-to-year changes were analyzed.

AGB was lowest in 2013, both in the treatments with and without N addition, and this pattern was consistent between the two grasslands ($p < 0.05$, **Figures 2A,B**). Compared with NG, the interannual dynamic of AGB in RG was more evident during the whole experiment period, regardless of N addition or not ($p < 0.05$, **Figures 2A,B**). AGB of RG was highest in 2014, significantly higher than that of the other 2 years; AGB of RG in 2012 was significantly higher than that of 2013 ($p < 0.05$, **Figures 2A,B**). TB of RG in 2013 was significantly lower than that of the other 2 years ($p < 0.05$, **Figures 2E,F**), and R/S of RG in 2013 was significantly higher than that of the other 2 years ($p < 0.05$, **Figures 2G,H**).

The regression analysis indicated the interannual dynamic of AGB in NG was negatively related to GST with N addition ($p < 0.05$, **Figure 3A**). Interannual dynamics of AGB in RG was significantly negatively related to GST and was significantly positively associated with GSP, regardless of N addition or not ($p < 0.001$, **Figures 3A,B**). TB of RG was negatively correlated with GST, but no evident relationship with GSP between the sampling years (**Figures 3C,D**). The annual fluctuations of the R/S ratio in RG were positively related to GST and negatively associated with GSP (**Figures 3E,F**).

Interaction of N Addition With Sampling Year on AGB and R/S in RG

The interaction of N addition with the sampling year was found for the AGB and R/S in RG ($p < 0.05$, **Table 1**). The AGB increment in 2013 was significantly lower than that of the other 2 years ($p < 0.05$, **Figure 1A**). The changes in AGB were significantly negatively related to GST ($p < 0.05$) but had no relationship with GSP ($p > 0.05$, **Figures 4A,B**). The decrement of R/S in 2014 was higher than that of the first 2 years ($p < 0.05$, **Figure 1D**). The reductions of R/S were significantly positively correlated with GST ($p < 0.05$) while showing a weak relation with GSP ($p = 0.054$, **Figures 4C,D**).

Correlations Between TB and AGB, TB and BGB, R/S and AGB, and R/S and BGB

No significant correlation was observed between AGB and TB in NG ($p > 0.05$, **Table 2**). There was a highly positive correlation between BGB and TB ($r > 0.99$, $p < 0.01$, **Table 3**). For RG, AGB, and BGB both showed positive correlations with TB ($p < 0.01$, **Tables 2**, **3**). However, the Pearson correlations between BGB and TB ($r = 0.890$) were stronger than those between AGB and TB ($r = 0.630$; **Tables 2**, **3**). When all data during the study were pooled, BGB played a vital role in the composition of TB for the alpine grassland ($r = 0.990$, $p < 0.001$), although AGB also played an important role in the form of TB ($r = 0.450$, $p < 0.001$).

The variations of R/S in NG were correlated with AGB and BGB ($p < 0.05$, **Tables 4**, **5**); but the correlation between BGB and R/S was higher than that of ABG and R/S (**Tables 4**, **5**). The variation of R/S in RG was mainly affected by AGB changes ($p < 0.001$, **Table 4**), and had no significant relation with BGB ($p < 0.05$, **Table 5**).

DISCUSSION

Effects of Nutrient Additions on Plant Community Biomass in the Alpine Grassland Around QLB

Commonly, nutrient availability limits the primary productivity of grasslands, and fertilization can increase soil quality and nutrient bioavailability, effectively alleviating nutrient restriction and consequently yielding positive effects on plant community productivity of grassland ecosystems (Bracken et al., 2015; Fay et al., 2015; Fu and Shen, 2016a, 2017; Wang et al., 2020). In general, compared with the aggregate responses to N and P addition individually, the responses of grassland primary productivity to N and P addition simultaneously are greater (Harpole et al., 2011; Fay et al., 2015; Cerasoli et al., 2018; Wang et al., 2020). Such previous findings indicate the synergistic co-limitation of N and P on grassland productivity and highlight the critical role of P for primary production. However, the presence and magnitude of nutrient effects depend on site-specific factors, soil development stage, soil fertility, and climate factors (Walker and Syers, 1976; Laliberte et al., 2012).

In this study, N addition promoted AGB considerably, both for NG and RG (**Table 1**; **Figure 1A**). The result was consistent with numerous previous studies in grassland ecosystems on a

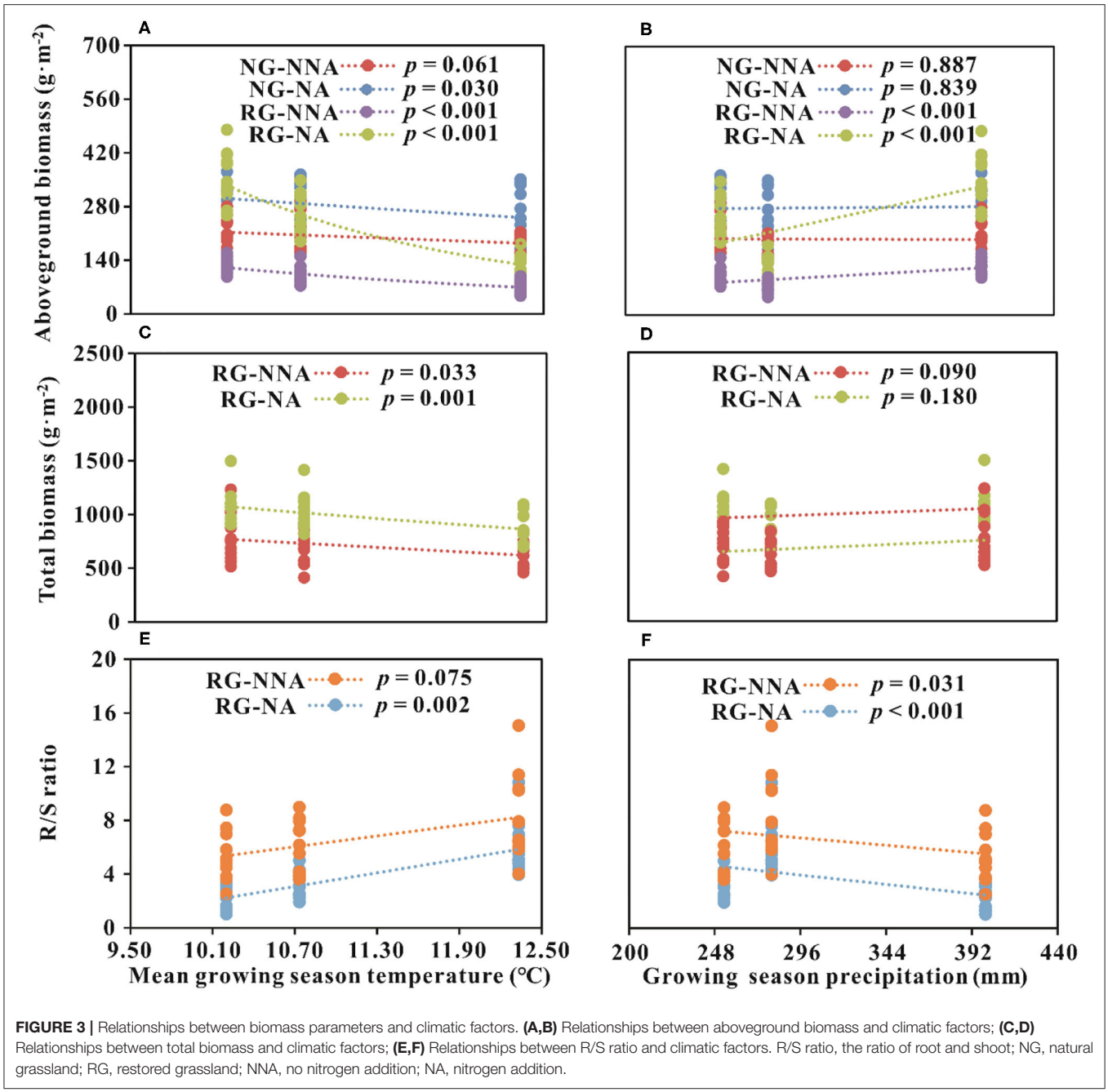

FIGURE 3 | Relationships between biomass parameters and climatic factors. **(A,B)** Relationships between aboveground biomass and climatic factors; **(C,D)** Relationships between total biomass and climatic factors; **(E,F)** Relationships between R/S ratio and climatic factors. R/S ratio, the ratio of root and shoot; NG, natural grassland; RG, restored grassland; NNA, no nitrogen addition; NA, nitrogen addition.

global scale and in the QTB (Borer et al., 2014; Fay et al., 2015; Wang et al., 2015, 2020; Fu and Shen, 2016a; Zhao et al., 2019). BGB in RG increased significantly with N addition (**Table 1**; **Figure 1B**). However, P addition did not present significant effects on any plant biomass parameter, and an interaction effect of N and P was also not evident (**Table 1**). The results implied that N was still the predominant limiting nutrient, and P was less limited for plant growth in the alpine grassland around QLB. This observation was consistent with the conclusion that N limitation generally peaked in cool sites (Fay et al., 2015). Meanwhile, another study also reported that P addition alone did not affect AGB and BGB in a continuous 4-year fertilization experiment in an alpine grassland on the QTP (Luo et al., 2019). However, the results of previous studies and our study were inconsistent with numerous research findings that grassland primary productivity was co-limited by N and P (Grace et al., 2016; Cerasoli et al., 2018; Wang et al., 2020). The following potential reasons might be responsible for the observations.

The properties of N and P determine their degree of limitation on primary productivity. N is regularly bound with the organic substrate by the strongly integrated covalent C–N chemical bond, which requires considerable energy to break apart (McGill and Cole, 1981). Moreover, the primary way for N to enter a terrestrial ecosystem is by fixation of N_2 by diazotrophs,

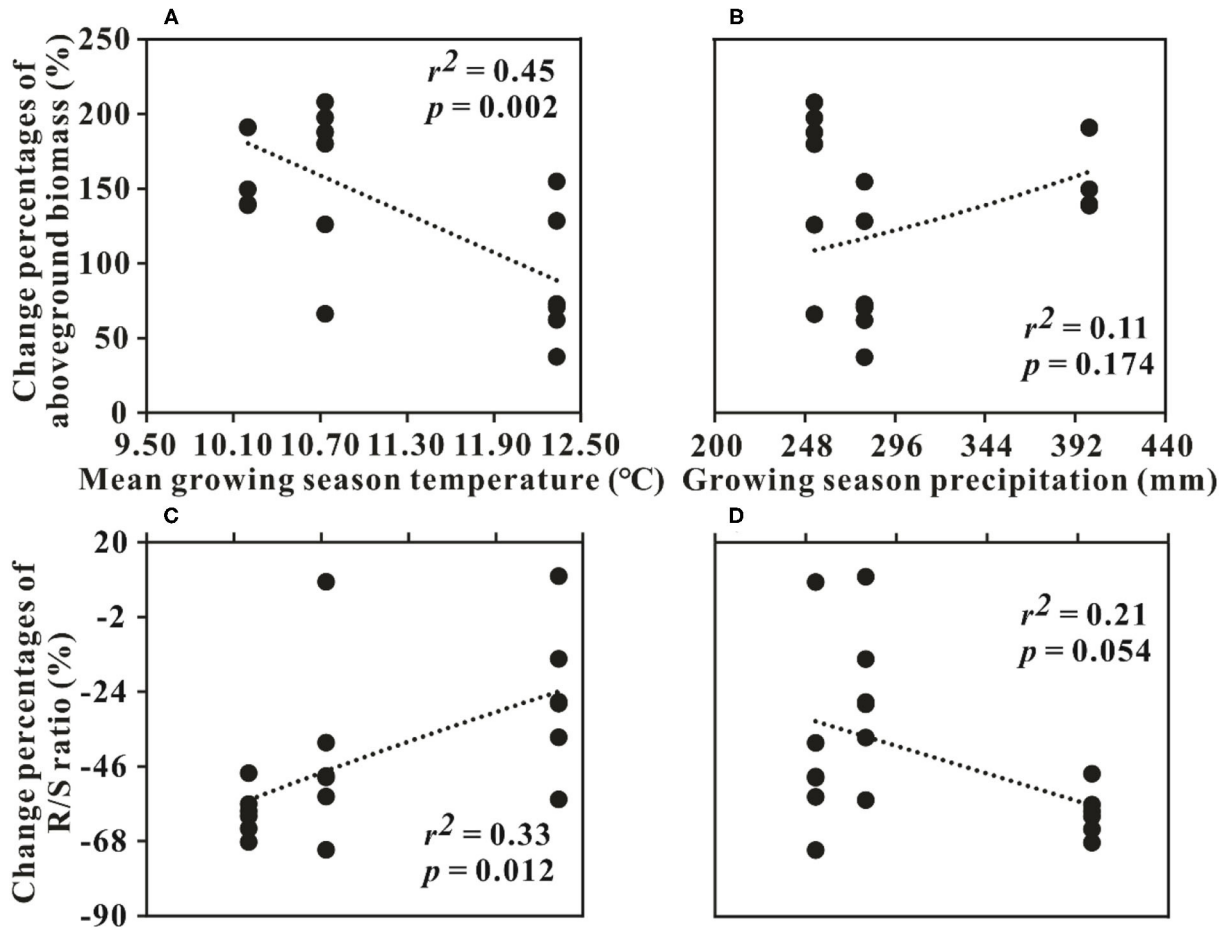

FIGURE 4 | Relationships between the changes in aboveground biomass, **(A,B)** R/S ratio; **(C,D)** and climatic factors in the restored grassland around Qinghai Lake Basin. R/S ratio, the ratio of root and shoot.

resulting in a slower biological process for N cycling in natural ecosystems. Soil N mineralization is sensitive to temperature (McGill and Cole, 1981; Booth et al., 2005; van Heerwaarden et al., 2010). By contrast, P is a sedimentary element and enters the terrestrial ecosystem primarily *via* weathering of soil native minerals (Walker and Syers, 1976; van Heerwaarden et al., 2010). Therefore, temperate and cooler ecosystems, such as the QLB with relatively short soil development periods and low temperatures, are more likely to have relatively abundant P and to be limited by N (Yuan and Chen, 2009; Vitousek et al., 2010; Fay et al., 2015). Furthermore, compared with N, P has low mobility and only a tiny part of its surface application to soil could reach the root system (Guo et al., 2016). Generally, soil moisture is positively associated with GSP (Fu et al., 2018). Precipitation around QLB, a semiarid region, is low (∼370 mm), which results in lower soil moisture, further lowering the absorption and utilization of P. Thus, additional P could not be sufficiently utilized. This was indicated by the positive correlation between soil P content and moisture in this region (Li et al., 2019). Additionally, P mineralization is closely related to soil pH, and high pH could fix P in the soil and reduce its utilization efficiency (Devau et al., 2009; Li et al., 2019). Therefore, the high pH in this alpine grassland ecosystem might reduce the P availability and the effects of P addition on plant production (Li et al., 2019).

Nevertheless, P addition elevated plant AGB of NG significantly in 2014 (Li et al., 2016b). The following two factors may cause this effect. First, soil available P is significantly positively related to GSP in NG (Li et al., 2019). GSP (399.5 mm) in 2014 was higher than that of the other 2 years (253.2 mm for 2012 and 279.8 mm for 2013). The relatively higher precipitation increased P mobility in soil, allowing plant roots to absorb P. Besides, soil total N (STN) content was likewise positively associated with GSP and significantly increased with N addition in this region (Li et al., 2019). Considering that the soil N background status is the crucial factor affecting soil available N (SAN) in the alpine grassland ecosystem around the QLB, the increasing STN could further mitigate the N limitation in the alpine grassland ecosystems (Fu and Shen, 2017). According to Liebig's Law of the Minimum, plant growth is limited by the most restrictive resource in the ecosystem. Therefore, the responses of vegetation to N and P additions depended on whether limitations from other ecological factors existed after

TABLE 2 | Correlations between plant community total and aboveground biomass in the natural (NG) and restored (RG) alpine grasslands around Qinghai Lake Basin.

Data analysis		Pearson correlation (*r*)	*p*
Annual data (*n* = 24)			
NG	2012	−0.128	0.551
	2013	0.085	0.692
	2014	0.348	0.096
RG	2012	**0.702**	**<0.001**
	2013	**0.599**	**0.002**
	2014	**0.525**	**0.008**
Grassland type (*n* = 72)			
NG		0.181	0.129
RG		**0.630**	**<0.001**
All data pool (*n* = 144)		**0.450**	**<0.001**

Significant results ($p < 0.05$) were bolded.

TABLE 3 | Correlations between plant community total and belowground biomass in the natural (NG) and restored (RG) alpine grasslands around Qinghai Lake Basin.

Data analysis		Pearson correlation (*r*)	*p*
Annual data (*n* = 24)			
NG	2012	**0.993**	**<0.001**
	2013	**0.992**	**0.007**
	2014	**0.996**	**<0.001**
RG	2012	**0.941**	**<0.001**
	2013	**0.982**	**<0.001**
	2014	**0.847**	**<0.001**
Grassland type (n = 72)			
NG		**0.994**	**<0.001**
RG		**0.890**	**<0.001**
All data pool (*n* = 144)		**0.990**	**<0.001**

Significant results ($p < 0.05$) were bolded.

TABLE 4 | Correlations between the ratio of root and shoot and aboveground biomass in the natural (NG) and restored (RG) alpine grasslands around Qinghai Lake basin.

Data analysis		Pearson correlation	*p*
Annual data (*n* = 24)			
NG	2012	**−0.662**	**<0.001**
	2013	**−0.532**	**0.007**
	2014	**−0.421**	**0.041**
RG	2012	**−0.793**	**<0.001**
	2013	**−0.693**	**<0.001**
	2014	**−0.813**	**<0.001**
Grassland type (*n* = 72)			
NG		**−0.518**	**<0.001**
RG		**−0.760**	**<0.001**
All data pool (*n* = 144)		**−0.494**	**<0.001**

Significant results ($p < 0.05$) were bolded.

TABLE 5 | Correlations between the ratio of root and belowground biomass in the natural (NG) and restored (RG) alpine grasslands around Qinghai Lake basin.

Data analysis		Pearson correlation (*r*)	*p*
Annual data (*n* = 24)			
NG	2012	**0.868**	**<0.001**
	2013	**0.846**	**<0.001**
	2014	**0.736**	**<0.001**
RG	2012	0.085	0.694
	2013	0.266	0.209
	2014	**0.446**	**0.029**
Grassland type (*n* = 72)			
NG		**0.781**	**<0.001**
RG		0.167	0.162
All data pool (*n* = 144)		**0.563**	**<0.001**

Significant results ($p < 0.05$) were bolded.

alleviation or elimination of N limitation. STN of NG in 2014 was significantly higher than in the other 2 years (Li et al., 2019). Hence, as N limitation was alleviated with STN elevated significantly, the limiting effect of P was more evident in 2014. Meanwhile, N addition might reduce the soil pH (Fu and Shen, 2017) and accordingly increase the P availability. In terms of the results mentioned above, we predicted that N is the primary limiting element, and the ecosystem responds more rapidly to N addition in the alpine grassland around QLB. Even so, P would become a limiting factor in plant productivity, especially with a warmer and wetter climate change background.

This prediction is consistent with the results of soil of N and P content changes with nutrient addition and temperature and precipitation fluctuations (Li et al., 2019), as well as the finding that plant biomass varied with P addition between wet and dry years (Wang et al., 2018). The conclusion was supported by the result that N addition had a robust promotion effect, but P addition almost had no significant effect on plant community biomass parameters in RG (**Table 1**). This may be because RG had lower BGB, soil background N values, and moisture, but higher soil P content and pH (Li et al., 2019). However, this prediction needs to be verified over extended periods and in different areas of the QLB.

Convergent and Divergent Responses of Plant Community Biomass to N Addition and Interannual Dynamics Between NG and RG

In this 3-year nutrient addition experiment, the response of AGB to N addition in RG was higher than that in the NG (**Figure 1A**). BGB in RG was also improved significantly by 24% with N addition (**Table 1**; **Figure 1B**). Meanwhile, plant community total biomass (TB) of RG concurrently increased by 41% on account of the promotion of AGB and BGB with N application (**Table 1**; **Figure 1C**). BGB and TB of NG showed no apparent response to N addition (**Table 1**). This pattern was in line with the results reported by N addition experiments in Inner Mongolia

grasslands (Gao et al., 2011). They found the eliminating limiting resource increased the ANPP of intermediately grazed grassland, but the increase was lower than that of heavily grazed grassland (Gao et al., 2011). Additionally, soil N contents (including soil available and total N) in RG were remarkably lower than that of NG at the existing plant community succession stage (Li et al., 2019). Thus, according to the discussion above, we concluded that N was extremely deficient and was the most crucial factor limiting vegetation growth in RG. Therefore, the plant community biomass of RG had a more intense response to N addition. The results indicated that exogenous N input (ongoing and future N deposition) would be conducive to restoring vegetation growth and primary productivity in the degraded alpine grassland around QLB. This prediction could be illustrated by the result that N addition weakened the difference of AGB between NG and RG on average, and AGB of RG was significantly higher than that of NG in 2014 (**Figure 2B**).

Besides the convergent and divergent responses to nutrient addition, the interannual dynamics of plant community biomass in NG and RG were likewise diverse. Year-to-year variation of AGB was significantly evident in this study, both for the NG and RG (**Table 1**). Generally, temperature and precipitation are found to regulate plant biomass and affect the response of plant biomass to N addition in alpine grassland ecosystems (Fu and Shen, 2016a; Wang et al., 2020). AGB of 2013 was significantly lower than that of the other two sampling years in the two grassland types (**Figures 2A,B**). Our results showed that GST had a negative effect, while GSP showed a positive impact on the year-to-year fluctuations of AGB (**Figures 3A,B**). For NG, the interannual dynamics of AGB were mainly influenced by GST, especially under treatments with N addition (**Figure 3A**). While, for RG, the interannual dynamics of AGB were significantly impacted both by GST and GSP in the two treatments (**Figures 3A,B**). As a crucial limiting environmental factor, lower temperature constrains the mineralization of soil N, and it is not advantageous to plant growth and ANPP accumulation in alpine regions (Fu et al., 2015; Fu and Shen, 2016a, 2017; Xu et al., 2016; Chen et al., 2017). Theoretically, warming would promote AGB in the alpine grasslands of the QTP (Fu et al., 2015; Fu and Shen, 2016a; Xu et al., 2016; Chen et al., 2017). However, the intensity and direction of plant response to temperature depend on soil moisture to a certain degree (Chen et al., 2017; De Boeck et al., 2018; Fu et al., 2018, 2019; Li et al., 2018; Xu et al., 2018). Warming could decrease biomass by reducing soil moisture and inhibiting plant growth (Fu et al., 2015, 2019; Zhang et al., 2021), and could increase biomass by promoting organic matter accumulation by enhancing plant uptake of mineral nutrients (Xu et al., 2015a,b; De Boeck et al., 2018; Li et al., 2018). Therefore, there is much uncertainty about the effect of temperature on plant biomass, and the warming effect is partly regulated by soil moisture in the QTP (Fu and Shen, 2016b; Fu et al., 2019; Zhang et al., 2021).

Generally, climate warming would promote plant growth under humid conditions, whereas inhibiting ecosystem C absorption under drought condition (Fu and Shen, 2016b; Li et al., 2018; Quan et al., 2019). In this semiarid ecosystem around QLB, water availability might be another limiting factor restricting plant growth, which resulted in the negative feedback of AGB to GST (**Figure 3A**). Vegetation coverage in RG (40%) was lower than that of NG (80%; Li et al., 2016b), which would lead to comparatively intense soil evaporation, and climatic warming would subsequently affect soil moisture in RG. Soil moisture of NG changed little between the experimental years and was relatively higher than that of RG (Li et al., 2019). Therefore, the AGB of NG was relatively stable (**Figure 2A**), and its interannual dynamics were not evidently influenced by GST and GSP in the natural state (**Figures 3A,B**). In the treatments with exogenous N addition, the rapid growth of plants requires a large amount of water, leading to a significant negative correlation between the annual change in AGB and GST (**Figure 3A**). A previous meta-analysis in the QTP showed N addition tended to cause warming and drying soil conditions (Fu and Shen, 2016a). This might be the other reason that GST had a negative effect on the AGB. For RG, lower plant coverage resulted in soil moisture of RG in 2013 was significantly lower than in the other 2 years (Li et al., 2019). Consequently, the fluctuation of AGB was notable (**Figures 2A,B**), and impacted greatly by GST and GSP (**Figures 3A,B**). The results implied the importance of precipitation to the restoration of degraded alpine grasslands and was supported by the other studies on the QTP (Sun et al., 2019; Wei et al., 2019). In sum, our study could provide profound insight into exploring the responses of alpine grasslands to the ongoing and future climate change with land use on the QTP.

Compared with AGB, BGB was comparatively stable, with minor changes year to year (**Table 1**; **Figures 2C,D**). Plant community TB was predominantly driven by BGB (**Table 3**) and was unaffected by AGB in NG (**Table 2**). This further resulted in stable intra-annual changes of TB in NG among sampling years (**Table 1**). For RG, AGB and BGB both significantly contributed to TB (**Tables 2**, **3**). Therefore, TB of RG showed significant intra-annual variation among sampling years (**Table 1**) and was significantly affected by GST (**Figure 3C**). A weak relationship between TB and GSP in RG likely resulted from BGB accounting for more TB. Besides, interannual variations in meteorological factors likely changed the effects of N on AGB among sampling years. In RG, AGB was negatively related to GST while positively related to precipitation, suggesting the effects of climate change on plant primary production are a trade-off between warming and precipitation change. This trade-off is likely to be regulated by soil moisture (Fu and Shen, 2016a; Fu et al., 2018; Wang et al., 2020). Based on the preceding results, we concluded that climate warming would reduce soil moisture, and our study showed a sequentially indirect negative effect on plant community AGB and TB. Moisturizing (including precipitation and soil water content increasing) would be beneficial to enhance ANPP during the restoration of grasslands.

Plant Community Biomass Allocation Patterns in NG and RG

As the major component of plant biomass and the C pool, BGB is central to the functioning of terrestrial ecosystems, related to ecosystem nutrient, water, and C cycling (Bardgett et al., 2014; Ottaviani et al., 2020). On a global scale, belowground biomass

accounts for ∼67% of grassland ecosystems (Ma et al., 2021). In our study, the proportion of root biomass approached 85% in the surface soil layer in the natural state (without N addition), resulting in a relatively high R/S (around 7), both for the NG and RG. This value was higher than the global level but in line with the conclusion that more biomass will be allocated to the underground roots. This represents a trade-off in resource allocation in cold and dry ecosystems because nutrient supply and water availability are lower in these regions (Reich et al., 2014; Ledo et al., 2018; Qi et al., 2019; Ma et al., 2021).

With nutrient enrichment, the R/S ratio usually decreased (Peng and Yang, 2016). The R/S variation reflected the functional balance between the distribution of resources that exist above and below (water, nutrients) the soil surface (Chen and Reynolds, 1997; Franklin et al., 2012). In this study, N addition reduced the R/S ratio significantly by 28 and 35% for the NG and RG, respectively (**Figure 1D**). This was consistent with previous studies (Peng and Yang, 2016). R/S ratio variations of NG were associated with AGB and BGB, and more correlated with BGB (**Tables 4**, **5**). This result might explain the stability of R/S among sampling years (**Table 1**).

The R/S ratio changes of RG were only dependent on AGB (**Table 4**), and had little correlation with BGB (**Table 5**). This pattern could generate significant inter-annual dynamics of the R/S ratio in RG (**Table 1**). Additionally, interannual variations in meteorological factors likely changed the effects of N on the differences of the R/S ratio among years. The R/S ratio and the decrement of R/S ratio were positively associated with GST and negatively with precipitation, suggesting that climate warming may exacerbate water limitation and would cause more plant biomass to be allocated to underground roots for absorbing more nutrients and water. Increasing precipitation could be conducive to the growth of plant aboveground part. It was totally in line with the previous outcomes (Ma et al., 2021). Combined with the preceding analyses, our results indicated that climate change (warming and precipitation increasing) could affect plant community biomass accumulation and allocation mainly by regulating soil moisture in the alpine grasslands around QLB.

However, interestingly, the R/S in the two grasslands did not show a significant difference in the natural state (**Figure 2G**), although soil nutrient and moisture were most pronounced in NG (Li et al., 2019). That is, the allocation of plant biomass between above- and belowground was similar in the NG and RG. The results indicated that the RG was also in a relatively stable state after a 10-year restoration. Given the above results, higher AGB might signify a higher BGB for maintaining a stable R/S ratio and balancing above- and belowground biomass.

CONCLUSIONS

This study determined the various responses of plant community biomass to N and P additions in NG and RG by a 3-year *in situ* manipulation experiment around the QLB. Our results suggested that the ongoing N deposition would benefit plant growth and primary productivity for the alpine grassland around QLB under future climate warming and precipitation scenarios, especially by implementing the "Grain for Green" project.

DATA AVAILABILITY STATEMENT

The raw data supporting the conclusions of this article will be made available by the authors, without undue reservation.

AUTHOR CONTRIBUTIONS

CL collected and analyzed the data and wrote the original draft. CZ analyzed the data, reviewed, and reorganized the manuscript. YL, XL, LM, and YX participated in discussions. All authors contributed to the article and approved the submitted version.

FUNDING

This study was supported by the Fundamental Research Project of Qinghai Province (2019-ZJ-935Q), the Open Project of State Key Laboratory of Plateau Ecology and Agriculture, Qinghai University (2018-ZZ-02, 2020-ZZ-07), the Joint Research Project of Three-River- Resource National Park funded by Chinese Academy of Sciences and Qinghai Provincial People's Government (LHZX-2020-08). CZ was supported by the 1,000 Talent program of Qinghai Province.

ACKNOWLEDGMENTS

The authors are grateful to Dr. Zhenhua Zhang and Dr. Xiang Liu for helpful and constructive comments in the preparation of this manuscript. The authors are grateful to the editor and reviewers for their helpful comments on this manuscript.

REFERENCES

Ågren, G. I., Wetterstedt, J. Å., and Billberger, M. F. K. (2012). Nutrient limitation on terrestrial plant growth-modeling the interaction between nitrogen and phosphorus. *New Phytol.* 194, 953–960. doi: 10.1111/j.1469-8137.2012.04116.x

Bardgett, R. D., Mommer, L., and De Vries, F. T. (2014). Going underground: root traits as drivers of ecosystem processes. *Trends Ecol. Evol.* 29, 692–699. doi: 10.1016/j.tree.2014.10.006

Booth, M. S., Rastetter, E., and Stark, J. (2005). Controls on nitrogen cycling in terrestrial ecosystems: a synthetic analysis of literature data. *Ecol. Monogr.* 75, 139–157. doi: 10.1890/04-0988

Borer, E. T., Seabloom, E. W., Gruner, D. S., Harpole, W. S., Hillebrand, H., Lind, E. M., et al. (2014). Herbivores and nutrients control grassland plant diversity via light limitation. *Nature* 508, 517–520. doi: 10.1038/nature13144

Bracken, M. E. S., Hillebrand, H., Borer, E. T., Seabloom, E. W., Cebrian, J., Cleland, E. E., et al. (2015). Signatures of nutrient limitation and co-limitation: responses of autotroph internal nutrient concentrations to nitrogen and phosphorus additions. *Oikos* 124, 113–121. doi: 10.1111/oik.01215

Cerasoli, S., Campagnolo, M., Faria, J., Nogueira, C., and Caldeira, M. D. C. (2018). On estimating the gross primary productivity of Mediterranean grasslands under different fertilisation regimes using vegetation indices and hyperspectral reflectance. *Biogeosciences* 15, 5455–5471. doi: 10.5194/bg-15-5455-2018

Chen, J., Luo, Y. Q., Xia, J. Y., Wilcox, K. R., Cao, J. J., and Zhou, X. H., et al. (2017). Warming effects on ecosystem carbon fluxes are modulated by plant functional types. *Ecosystems* 20, 515–526. doi: 10.1007/s10021-016-0035-6

Chen, J. L., and Reynolds, J. F. (1997). A coordination model of whole-plant carbon allocation in relation to water stress. *Ann. Bot.* 80, 45–55. doi: 10.1006/anbo.1997.0406

Cui, B. L., and Li, X. Y. (2015). Runoff processes in the Qinghai Lake Basin, Northeast Qinghai-Tibet Plateau, China: insights from stable isotope and hydrochemistry. *Quat. Int.* 380, 123–132. doi: 10.1016/j.quaint.2015.02.030

De Boeck, H. J., Hiltbrunner, E., Verlinden, M., Bassin, S., and Zeiter, M. (2018). Legacy effects of climate extremes in alpine grassland. *Front. Plant Sci.* 9:1586. doi: 10.3389/fpls.2018.01586

Devau, N., Cadre, E. L., Hinsinger, P., Jaillard, B., and Gérard, F. (2009). Soil pH controls the environmental availability of phosphorus: experimental and mechanistic modelling approaches. *Appl. Geochem.* 24, 2163–2174. doi: 10.1016/j.apgeochem.2009.09.020

Dong, S. K., Shang, Z. H., Gao, J. X., and Boone, R. B. (2020). Enhancing sustainability of grassland ecosystems through ecological restoration and grazing management in an era of climate change on Qinghai-Tibetan Plateau. *Agric. Ecosyst. Environ.* 287:106684. doi: 10.1016/j.agee.2019.106684

Elser, J. J., Bracken, M. E. S., Cleland, E. E., Gruner, D. S., and Harpole, W. S., Hillebrand, H., et al. (2007). Global analysis of nitrogen and phosphorus limitation of primary producers in freshwater, marine and terrestrial ecosystems. *Ecol. Lett.*10, 1135–1142. doi: 10.1111/j.1461-0248.2007.01113.x

Erb, K. H., Kastner, T., Plutzar, C., Bais, A. L. S., Carvalhais, N., Fetzel, T., et al. (2018). Unexpectedly large impact of forest management and grazing on global vegetation biomass. *Nature* 553, 73–76. doi: 10.1038/nature25138

Fay, P. A., Prober, S. M., Harpole, W. S., Knops, J. M. H., Bakker, J. D., Borer, E. T., et al. (2015). Grassland productivity limited by multiple nutrients. *Nat. Plants* 1:15080. doi: 10.1038/nplants.2015.80

Franklin, O., Johansson, J., Dewar, R. C., Dieckmann, U., McMurtrie, R. E., Brännström, A., et al. (2012). Modeling carbon allocation in trees: a search for principles. *Tree Physiol.* 32, 648–666. doi: 10.1093/treephys/tpr138

Fu, G., Shen, Z., X., Sun, W., Zhong, Z., M., et al. (2015). A meta-analysis of the effects of experimental warming on plant physiology and growth on the Tibetan Plateau. *J. Plant Growth Regul.* 34, 57–65. doi: 10.1007/s00344-014-9442-0

Fu, G., and Shen, Z. X. (2016a). Response of alpine plants to nitrogen addition on the Tibetan Plateau: a meta-analysis. *J. Plant Growth Regul.* 35, 974–979. doi: 10.1007/s00344-016-9595-0

Fu, G., and Shen, Z. X. (2016b). Environmental humidity regulates effects of experimental warming on vegetation index and biomass production in an alpine meadow of the Northern Tibet. *PloS ONE* 11:e0165643. doi: 10.1371/journal.pone.0165643

Fu, G., and Shen, Z. X. (2017). Response of alpine soils to nitrogen addition on the Tibetan Plateau: a meta-analysis. *Appl. Soil Ecol.* 114, 99–104. doi: 10.1016/j.apsoil.2017.03.008

Fu, G., Shen, Z. X., and Zhang, X. Z. (2018). Increased precipitation has stronger effects on plant production of an alpine meadow than does experimental warming in the Northern Tibetan Plateau. *Agr. For. Meteorol.* 249, 11–21. doi: 10.1016/j.agrformet.2017.11.017

Fu, G., Zhang, H. R., and Sun, W. (2019). Response of plant production to growing/non-growing season asymmetric warming in an alpine meadow of the Northern Tibetan Plateau. *Sci. Total Environ.* 650, 2666–2673. doi: 10.1016/j.scitotenv.2018.09.384

Galloway, J. N., Townsend, A. R., Erisman, J. W., Bekunda, M., Cai, Z., Freney, J. R., et al. (2008). Transformation of the nitrogen cycle: recent trends, questions, and potential solutions. *Science* 320, 889–892. doi: 10.1126/science.1136674

Gao, Y. Z., Chen, Q., Lin, S., Giese, M., and Brueck, H. (2011). Resource manipulation effects on net primary production, biomass allocation and rain-use efficiency of two semiarid grassland sites in Inner Mongolia, China. *Oecologia* 165, 855–864. doi: 10.1007/s00442-010-1890-z

Grace, J. B., Anderson, T. M., Seabloom, E. W., Borer, E. T., Adler, P. B., Harpole, W. S., et al. (2016). Integrative modelling reveals mechanisms linking productivity and plant species richness. *Nature* 529, 390–393. doi: 10.1038/nature16524

Guo, Y. J., Du, Q. F., Li, G. D., Ni, Y., Zhang, Z., Ren, W. B., et al. (2016). Soil phosphorus fractions and arbuscular mycorrhizal fungi diversity following long-term grazing exclusion on semi-arid steppes in Inner Mongolia. *Geoderma* 269, 79–90. doi: 10.1016/j.geoderma.2016.01.039

Harpole, W. S., Ngai, J. T., Cleland, E. E., Seabloom, E. W., Borer, E. T., Bracken, M. E. S., et al. (2011). Nutrient co-limitation of primary producer communities. *Ecol. Lett.* 14, 852–862. doi: 10.1111/j.1461-0248.2011.01651.x

Hoekstra, J. M., Boucher, T. M., Ricketts, T. H., and Roberts, C. (2005). Confronting a biome crisis: global disparities of habitat loss and protection. *Ecol. Lett.* 8, 23–29. doi: 10.1111/j.1461-0248.2004.00686.x

Jelinski, N. A., and Kucharik, C. J. (2009). Land-use effects on soil carbon and nitrogen on a U.S. Midwestern floodplain. *Soil Sci. Soc. Am. J.* 73, 217–225. doi: 10.2136/sssaj2007.0424

Jiang, J., Zong, N., Song, M. H., Shi, P. L., Ma, W. L., Fu, G., et al. (2013). Responses of ecosystem respiration and its components to fertilization in an alpine meadow on the Tibetan Plateau. *Eur. J. Soil Biol.* 56, 101–106. doi: 10.1016/j.ejsobi.2013.03.001

Jing, X., Yang, X. X., Ren, F., Zhou, H. K., Zhu, B., and He, J. S. (2016). Neutral effect of nitrogen addition and negative effect of phosphorus addition on topsoil extracellular enzymatic activities in an alpine grassland ecosystem. *Appl. Soil Ecol.* 107, 205–213. doi: 10.1016/j.apsoil.2016.06.004

Kohli, M., Borer, E. T., Kinkel, L., and Seabloom, E. W. (2019). Stability of grassland production is robust to changes in the consumer food web. *Ecol. Lett.* 22, 707–716. doi: 10.1111/ele.13232

Lal, R. (2002). Soil carbon sequestration in China through agricultural intensification, restoration of degraded and decertified ecosystems. *Land Degrad. Dev.*13, 469–478. doi: 10.1002/ldr.531

Laliberte, E., Turner, B. L., Costes, T., Pearse, S. J., and Wyrwoll, K. H., Zemunik, G., et al. (2012). Experimental assessment of nutrient limitation along a 2-million-year dune chronosequence in the south-western Australia biodiversity hotspot. *J. Ecol.* 100, 631–642. doi: 10.1111/j.1365-2745.2012.01962.x

LeBauer, D. S., and Treseder, K. K. (2008). Nitrogen limitation of net primary productivity in terrestrial ecosystems is globally distributed. *Ecology* 89, 371–379. doi: 10.1890/06-2057.1

Ledo, A., Paul, K. I., Burslem, D. F. R. P., Ewel, J. J., Barton, C., Battaglia, M., et al. (2018). Tree size and climatic water deficit control root to shoot ratio in individual trees globally. *New Phytol.* 217, 8–11. doi: 10.1111/nph.14863

Li, C., Peng, F., Xue, X., You, Q., Lai, C., Zhang, W., et al. (2018). Productivity and quality of alpine grassland vary with soil water availability under experimental warming. *Front. Plant Sci.* 9:1790. doi: 10.3389/fpls.2018.01790

Li, C. L., Li, Q., Zhao, L., Ge, S. D., Chen, D. D., Dong, Q. M., et al. (2016a). Land-use effects on organic and inorganic carbon patterns in the topsoil around Qinghai Lake basin, Qinghai-Tibetan Plateau. *Catena* 147, 345–355. doi: 10.1016/j.catena.2016.07.040

Li, C. L., Li, Q., Zhao, L., and Zhao, X. Q. (2016b). Responses of plant community biomass to nitrogen and phosphorus additions in natural and restored grasslands around Qinghai Lake Basin. China. *J. Plant Ecol.* 40:1015. doi: 10.17521/cjpe.2016.0048

Li, C. L., Luo, S. H., Ge, S. D., Zhao, L., Dong, Q. M., Li, Q., et al. (2019). Convergent and divergent responses of topsoil nitrogen and phosphorus content to nutrient addition in natural and restored alpine grasslands around the Qinghai Lake Basin. *Agric. Ecosyst. Environ.* 282, 1–12. doi: 10.1016/j.agee.2019.05.010

Luo, R. Y., Fan, J. L., Wang, W. J., Luo, J. F., Kuzyakov, Y., He, J. S., et al. (2019). Nitrogen and phosphorus enrichment accelerates soil organic carbon loss in alpine grassland on the Qinghai-Tibetan Plateau. *Sci. Total Environ.* 650, 303–312. doi: 10.1016/j.scitotenv.2018.09.038

Luyssaert, S., Schulze, E. D., Borner, A., Knohl, A., Hessenmoller, D., Law, B. E., et al. (2008). Old-growth forests as global carbon sinks. *Nature* 455, 213–215. doi: 10.1038/nature07276

Ma, H. Z., Mo, L. D., Crowther, T. W., Maynard, D. S., van den Hoogen, J., Stocker, B. D., et al. (2021). The global distribution and environmental drivers of aboveground vs. belowground plant biomass. *Nat. Ecol. Evol.* 5, 1110–1122. doi: 10.1038/s41559-021-01485-1

McGill, W. B., and Cole, C. V. (1981). Comparative aspects of cycling of organic C, N, S and P through soil organic matter. *Geoderma* 26, 267–286. doi: 10.1016/0016-7061(81)90024-0

Ottaviani, G., Molina-Venegas, R., Charles-Dominique, T., Chelli, S., Campetella, G., Canullo, R., et al. (2020). The neglected belowground dimension of plant dominance. *Trends Ecol. Evol.* 35, 763–766. doi: 10.1016/j.tree.2020.06.006

Peng, Y. F., and Yang, Y. H. (2016). Allometric biomass partitioning under nitrogen enrichment: evidence from manipulative experiments around the world. *Sci. Rep*. 6:28918. doi: 10.1038/srep28918

Penuelas, J., Poulter, B., Sardans, J., Ciais, P., van der Velde, M., Bopp, L., et al. (2013). Human-induced nitrogen-phosphorus imbalances alter natural and managed ecosystems across the globe. *Nat. Commun*. 4, 94–105. doi: 10.1038/ncomms3934

Phoenix, G. K., Emmett, B. A., Britton, A. J., Caporn, S., Dise, N. B., Helliwell, R. C., et al. (2012). Impacts of atmospheric nitrogen deposition: responses of multiple plant and soil parameters across contrasting ecosystems in long-term field experiments. *Glob. Chang. Biol.* 18, 1197–1215. doi: 10.1111/j.1365-2486.2011.02590.x

Poorter, H., Niklas, K. J., Reich, P. B., Oleksyn, J., Poot, P., and Mommer, L. (2012). Biomass allocation to leaves, stems and roots: meta-analyses of interspecific variation and environmental control. *New Phytol.* 193, 30–50. doi: 10.1111/j.1469-8137.2011.03952.x

Qi, Y. L., Wei, W., Chen, C. G., and Chen, L. D. (2019). Plant root-shoot biomass allocation over diverse biomes: a global synthesis. *Glob. Ecol. Conserv*. 18:e00606. doi: 10.1016/j.gecco.2019.e00606

QPARPO (Qinghai province agricultural resource planning office) (1995). Qinghai Soil Records. Beijing: China Agriculture Press, (In Chinese).

Quan, Q., Tian, D. S., Luo, Y. Q., Zhang, F. Y., Crowther, T. W., Zhu, K., et al. (2019). Water scaling of ecosystem carbon cycle feedback to climatic warming. *Sci. Adv*. 5:eaav1131. doi: 10.1126/sciadv.aav1131

Reich, P. B., Luo, Y. J., Bradford, J. B., Poorter, H., Perry, C. H., and Oleksyn, J. (2014). Temperature drives global patterns in forest biomass distribution in leaves, stems, and roots. *Proc. Natl. Acad. Sci. U. S. A*.111, 13721–13726. doi: 10.1073/pnas.1216053111

Sartori, F., Lal, R., Ebinger, M. H., and Eaton, J. A. (2007). Changes in soil carbon and nutrient pools along a chronosequence of poplar plantations in the Columbia Plateau, Oregon, USA. *Agric. Ecosyst. Environ.* 122, 325–339. doi: 10.1016/j.agee.2007.01.026

Shen, M. G., Zhang, G. X., Cong, N., Wang, S. P., Kong, W. D., and Piao, S. L. (2014). Increasing altitudinal gradient of spring vegetation phenology during the last decade on the Qinghai-Tibetan Plateau. *Agric. For. Meteorol.* 189, 71–80. doi: 10.1016/j.agrformet.2014.01.003

Stevens, C. J., Lind, E. M., Hautier, Y., Harpole, W. S., Borer, E. T., Hobbie, S., et al. (2015). Anthropogenic nitrogen deposition predicts local grassland primary production worldwide. *Ecology* 96, 1459–1465. doi: 10.1890/14-1902.1

Sun, J., Hou, G., Liu, M., Fu, G., Zhan, T. Y., Zhou, H. K., et al. (2019). Effects of climatic and grazing changes on desertification of alpinegrasslands, Northern Tibet. *Ecol. Indi.* 107:105647. doi: 10.1016/j.ecolind.2019.105647

Tao, H., Hao, L., Li, S., Wu, T., Qin, Z., and Qiu, J. (2021). Geochemistry and petrography of the sediments from the marginal areas of Qinghai Lake, Northern Tibet Plateau, China: implications for weathering and provenance. *Front. Earth Sci.* 9:725553. doi: 10.3389/feart.2021.725553

van Heerwaarden, L. M., Toet, S., and Aerts, R. (2010). Nitrogen and phosphorus resorption efficiency and proficiency in six sub-arctic bog species after 4 years of nitrogen fertilization. *J. Ecol.* 91, 1060–1070. doi: 10.1046/j.1365-2745.2003.00828.x

Vitousek, P. M., Porder, S., Houlton, B. Z., and Chadwick, O. A. (2010). Terrestrial phosphorus limitation: Mechanisms, implications, and nitrogen-phosphorus interactions. *Ecol. Appl.* 20, 5–15. doi: 10.1890/08-0127.1

Walker, T. W., and Syers, J. K. (1976). The fate of phosphorus during pedogenesis. *Geoderma* 15, 1–19. doi: 10.1016/0016-7061(76)90066-5

Wang, D. J., He, Z. B., Zhang, Z., Du, Q. F., Zhang, Y., Hou, X. Y., et al. (2018). Responses of herbage yield and soil phosphorus fractions to phosphorus fertilisation on a degraded arid steppe. *Crop Pasture Sci.* 69, 846–858. doi: 10.1071/CP18217

Wang, D. J., Zhou, H. K., Yao, B. Q., Wang, W. Y., Dong, S. K., Shang, Z. H., et al. (2020). Effects of nutrient addition on degraded alpine grasslands of the Qinghai-Tibetan Plateau: a meta-analysis. *Agric. Ecosyst. Environ.* 301, 106970. doi: 10.1016/j.agee.2020.106970

Wang, J. S., Wang, Z. K., Zhang, X. Z., Zhang, Y. J., Ran, C. Q., Zhang, J. L., et al. (2015). Response of *Kobresia pygmaea* and *Stipa purpurea* grassland communities in northern Tibet to nitrogen and phosphate addition. *Mt. Res. Dev.* 35, 78–86. doi: 10.1659/MRD-JOURNAL-D-11-00104.1

Wei, H. X., Zhao, J. X., and Luo, T. X. (2019). The effect of pika grazing on *Stipa purpurea* is amplified by warming but alleviated by increased precipitation in an alpine grassland. *Plant Ecol.* 220, 371–381. doi: 10.1007/s11258-019-00920-5

Wieder, W. R., Cleveland, C. C., Smith, W. K., and Todd-Brown, K. (2015). Future productivity and carbon storage limited by terrestrial nutrient availability. *Nat. Geosci.* 8, 441–444. doi: 10.1038/ngeo2413

Xu, M. H., Liu, M., Xue, X., and Zhai, D. T. (2016). Warming effects on plant biomass allocation and correlations with the soil environment in an alpine meadow, China. *J. Arid Land* 8, 773–786. doi: 10.1007/s40333-016-0013-z

Xu, M. H., Peng, F., You, Q. G., Guo, J., Tian, X. F., Liu, M., et al. (2015b). Effects of warming and clipping on plant and soil properties of an alpine meadow in the Qinghai-Tibetan Plateau, China. *J. Arid Land* 7, 189–204. doi: 10.1007/s40333-014-0010-z

Xu, M. H., Peng, F., You, Q. G., Guo, J., Tian, X. F., Xue, X., et al. (2015a). Year-round warming and autumnal clipping lead to downward transport of root biomass, carbon and total nitrogen in soil of an alpine meadow. *Environ. Exp. Bot.*109, 54–62. doi: 10.1016/j.envexpbot.2014.07.012

Xu, W., Zhu, M. Y., Zang, Z. H., Ma, Z. Y., Liu, H. Y., Chen, L. T., et al. (2018). Experimentally simulating warmer and wetter climate additively improves rangeland quality on the Tibetan Plateau. *J. Appl. Ecol.* 55, 1486–1497. doi: 10.1111/1365-2664.13066

Yuan, Z. Y., and Chen, H. Y. H. (2009). Global-scale patterns of nutrient resorption associated with latitude, temperature and precipitation. *Global Ecol. Biogeogr.* 18, 11–18. doi: 10.1111/j.1466-8238.2008.00425.x

Zhang, C., and Xi, N. (2021). Precipitation changes regulate plant and soil microbial biomass via plasticity in plant biomass allocation in grasslands: a meta-analysis. *Front. Plant Sci*. 12:614968. doi: 10.3389/fpls.2021.614968

Zhang, G. Y., Shen, Z. X., and Fu, G. (2021). Function diversity of soil fungal community has little exclusive effects on the response of aboveground plant production to experimental warming in alpine grasslands. *Appl. Soil Ecol.* 168, 104153. doi: 10.1016/j.apsoil.2021.104153

Zhao, Y. N., Yang, B., Li, M. X., Xiao, R. Q., Rao, K. Y., Wang, J. Q., et al. (2019). Community composition, structure and productivity in response to nitrogen and phosphorus additions in a temperate meadow. *Sci. Total Environ* 654, 863–871. doi: 10.1016/j.scitotenv.2018.11.155

Zhu, J., Wang, Q., He, N., Melinda, S. D., Elser, J. J., Du, J., et al. (2016). Imbalanced atmospheric nitrogen and phosphorus depositions in China: implications for nutrient limitation. *J. Geophys. Res-Biogeo.* 121, 1605–1616. doi: 10.1002/2016JG003393

Conflict of Interest: The authors declare that the research was conducted in the absence of any commercial or financial relationships that could be construed as a potential conflict of interest.

Publisher's Note: All claims expressed in this article are solely those of the authors and do not necessarily represent those of their affiliated organizations, or those of the publisher, the editors and the reviewers. Any product that may be evaluated in this article, or claim that may be made by its manufacturer, is not guaranteed or endorsed by the publisher.

Copyright © 2021 Li, Li, Li, Ma, Xiao and Zhang. This is an open-access article distributed under the terms of the Creative Commons Attribution License (CC BY). The use, distribution or reproduction in other forums is permitted, provided the original author(s) and the copyright owner(s) are credited and that the original publication in this journal is cited, in accordance with accepted academic practice. No use, distribution or reproduction is permitted which does not comply with these terms.

frontiers in Plant Science

ORIGINAL RESEARCH
published: 04 January 2022
doi: 10.3389/fpls.2021.798633

The Change in Environmental Variables Linked to Climate Change Has a Stronger Effect on Aboveground Net Primary Productivity Than Does Phenological Change in Alpine Grasslands

Jiangwei Wang[1,2†], Meng Li[3†], Chengqun Yu[1] and Gang Fu[1]*

[1] Lhasa Plateau Ecosystem Research Station, Key Laboratory of Ecosystem Network Observation and Modeling, Institute of Geographic Sciences and Natural Resources Research, Chinese Academy of Sciences, Beijing, China, [2] University of Chinese Academy of Sciences, Beijing, China, [3] School of Geographic Sciences, Nantong University, Nantong, China

OPEN ACCESS

Edited by:
Gao-Lin Wu,
Northwest A&F University, China

Reviewed by:
Miaogen Shen,
Beijing Normal University, China
Luca Vitale,
Institute for Agricultural and Forestry Systems in the Mediterranean, National Research Council of Italy (CNR), Italy

***Correspondence:**
Gang Fu
fugang@igsnrr.ac.cn;
fugang09@126.com

[†] These authors have contributed equally to this work

Specialty section:
This article was submitted to Functional Plant Ecology, a section of the journal Frontiers in Plant Science

Received: 20 October 2021
Accepted: 25 November 2021
Published: 04 January 2022

Citation:
Wang J, Li M, Yu C and Fu G (2022) The Change in Environmental Variables Linked to Climate Change Has a Stronger Effect on Aboveground Net Primary Productivity Than Does Phenological Change in Alpine Grasslands. Front. Plant Sci. 12:798633. doi: 10.3389/fpls.2021.798633

More and more studies have focused on responses of ecosystem carbon cycling to climate change and phenological change, and aboveground net primary productivity (ANPP) is a primary component of global carbon cycling. However, it remains unclear whether the climate change or the phenological change has stronger effects on ANPP. In this study, we compared the effects of phenological change and climate change on ANPP during 2000–2013 across 36 alpine grassland sites on the Tibetan Plateau. Our results indicated that ANPP showed a positive relationship with plant phenology such as prolonged length of growing season and advanced start of growing season, and environmental variables such as growing season precipitation (GSP), actual vapor pressure (E_a), relative humidity (RH), and the ratio of GSP to ≥5°C accumulated temperature (GSP/AccT), respectively. The linear change trend of ANPP increased with that of GSP, E_a, RH, and GSP/AccT rather than phenology variables. Interestingly, GSP had the closer correlation with ANPP and meanwhile the linear slope of GSP had the closer correlation with that of ANPP among all the concerned variables. Therefore, climate change, mainly attributed to precipitation change, had a stronger effect on ANPP than did phenological change in alpine grasslands on the Tibetan Plateau.

Keywords: green-up date, growing season length, warming, precipitation, alpine ecosystem, Tibetan Plateau

INTRODUCTION

Aboveground net primary productivity (ANPP) is a primary component of global carbon cycling in terrestrial ecosystems and understanding its drivers has long been a goal of ecology (Wu et al., 2011; Robinson et al., 2013). Climate change, especially warming and precipitation change, is a vital abiotic variable in driving ANPP variations (Rustad et al., 2001; Wu et al., 2011). More and more studies have analyzed responses of ANPP to warming and precipitation variations

(Klein et al., 2007; Wu et al., 2011; Wang et al., 2012; Fu Z. et al., 2015). Warming and water availability not only directly affect plant physiology related to plant photosynthesis and in turn plant photosynthesis (Fu G. et al., 2015) but also indirectly affect plant growth by altering nitrogen availability, species composition, and plant phenology (Wan et al., 2005; Wang et al., 2012). The net effect of climate change on ANPP is dependent on the relative strength of climate change-induced direct effect and indirect effect on ANPP. Many studies have indicated that the effect of precipitation change on ANPP is stronger than that of warming (Wu et al., 2011; Shen et al., 2014), while some other studies have found quite the contrary results (Wang et al., 2012). Therefore, it remains unclear on the relative effects of warming and precipitation change on ANPP.

Plant phenology (e.g., start of growing season, SGS; end of growing season, EGS; and length of growing season, LGS), as a critical aspect of biological systems (Dorji et al., 2013), is an important biotic variable in affecting ANPP (Berdanier and Klein, 2011). A growing number of studies have focused on the correlations between plant phenology and plant productivity (Parmentier et al., 2011; Miller and Smith, 2012; Kross et al., 2014), while there are no consistent findings, with positive (Wu et al., 2012), negative (Jia et al., 2010), or no effects (Parmentier et al., 2011; Zhu et al., 2017) of prolonged LGS on plant productivity. Plant phenology itself is sensitive to climate change, and both warming and water availability can alter plant phenology (Prieto et al., 2009; Chen et al., 2011; Shen et al., 2011; Westergaard-Nielsen et al., 2017). These diverse findings imply that the effects of plant phenology on plant productivity can be regulated by climate changes (Wu et al., 2012; Wang et al., 2017). Moreover, these previous studies have mainly focused on gross primary production, net primary production, and net ecosystem production (Piao et al., 2007; Zhao and Liu, 2012; Takagi et al., 2015) rather than ANPP (Baptist et al., 2010; Berdanier and Klein, 2011). Therefore, the effects of plant phenology on ANPP remains unclear.

The Tibetan Plateau is one of the most sensitive regions to climate change and is mainly covered by alpine grasslands. A large number of studies have examined plant phenological changes and their driving mechanisms related to climate change in alpine grasslands on the Tibetan Plateau (Piao et al., 2011; Shen, 2011; Cong et al., 2012; Dorji et al., 2013; Ding et al., 2016; Ganjurjav et al., 2016b). However, only a few studies have compared the effects of climate change and phenological change on productivity (i.e., gross primary productivity, net primary productivity, and net ecosystem productivity) in alpine grasslands on the Tibetan Plateau (Yang et al., 2015; Wang et al., 2017; Zhu et al., 2017), and no studies have investigated the responses of ANPP to climate change and phenological change. Alpine grasslands are main pasture, and the ANPP in alpine grasslands plays vital roles in sustainable development of pastoral livestock industry on the Tibetan Plateau. Therefore, in this study, we analyzed the correlations of ANPP with phenological variables (i.e., SGS, EGS, and LGS) and climate variables (e.g., precipitation and temperature). The main objective of this study was to better predict future changes in ANPP under global change by comparing the relative effects of climate and phenological variables on ANPP in alpine grasslands on the Tibetan Plateau.

MATERIALS AND METHODS

Aboveground Biomass Sampling and Aboveground Net Primary Productivity Estimation

Articles published in 2000–2015 were searched using the Web of Science and the China National Knowledge Infrastructure to obtain aboveground biomass (AGB) in alpine grasslands on the Tibetan Plateau. There were 195 AGB data (2.99–759.19 g m^{-2}), which were sampled during July–August of 2000–2013. There were 123 sampling sites (**Supplementary Figure 1**). Moderate Resolution Imaging Spectroradiometer (MODIS) NDVI data (MOD13A3, Collection 6) during June–September of 2000–2013 were downloaded. The relationship between AGB and NDVI was developed (**Supplementary Figure 2**). Then, the AGB were obtained during June–September of 2000–2013 in alpine grasslands on the whole Tibetan Plateau using the models mentioned above. Many previous studies, which were conducted in alpine grasslands on the Tibetan Plateau, have indicated that the maximum AGB during the growing season could be treated as aboveground net primary production (ANPP; Klein et al., 2007; Wang et al., 2012). Therefore, the maximum AGB during June–September was treated as ANPP in this study.

MOD13A2 and Phenological Metrics

NDVI data were obtained from MODIS vegetation indices product (MOD13A2, Collection 6). The spatial and temporal resolutions of MOD13A2 NDVI are 1 km × 1 km and 16 days, respectively. Images collected during 2000–2013 were used for this study. The Timesat-SG method was used to estimate SGS, EGS, and LGS (Cong et al., 2012). In this study, 20 and 50% was used as the two dynamic thresholds to determine SGS and EGS, respectively (Cong et al., 2012; Wang et al., 2017).

Climate Data

Climate data were obtained from 36 meteorological stations (**Figure 1**) of the China Meteorological Data Sharing Service System (Deng et al., 2013; Zhang et al., 2013). The climate data included growing-season precipitation (GSP), actual vapor pressure (E_a), relative humidity (RH), minimum relative humidity (RH_{min}), vapor pressure deficit (VPD), air temperature (T_a), minimum air temperature (T_{amin}), maximum air temperature (T_{amax}), ≥5°C accumulated temperature (AccT), and the ratio of GSP to AccT (GSP/AccT). The GSP/AccT ratio is a synthesized factor of temperature and precipitation, which has been used in several previous studies (Wang et al., 2013; Wu et al., 2014; Fu et al., 2018). The GSP, E_a, RH, RH_{min}, and VPD could be used as variables related to water availability, and T_a, T_{amin}, T_{amax}, and AccT could be used as variables related to temperature.

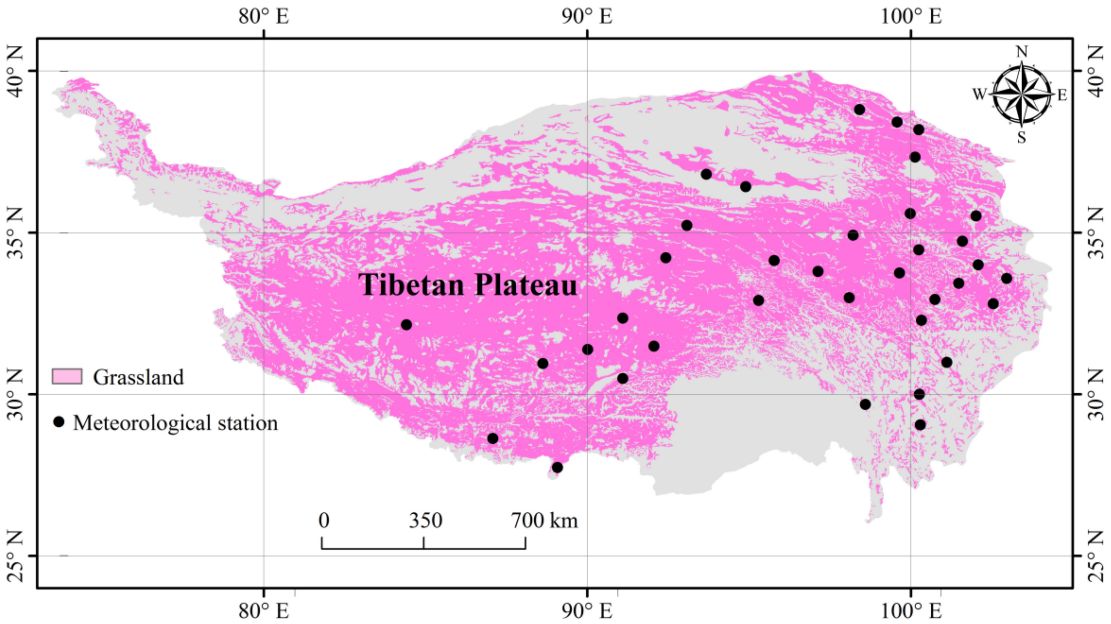

FIGURE 1 | Location of 36 meteorological stations on the Tibetan Plateau.

Statistical Analysis

Although spatial interpolation is a general approach to obtain climate data at regional scale (Attorre et al., 2007; Hashimoto et al., 2008), there remains some errors in the interpolated climate data, especially for precipitation (Hashimoto et al., 2008; Fu et al., 2017). Therefore, we only analyzed the effects of climate change on aboveground productivity at the 36 meteorological stations in this study. Simple linear regressions of ANPP with SGS, EGS, LGS, GSP, E_a, RH, RH_{min}, VPD, T_a, T_{amin}, T_{amax}, AccT, and GSP/AccT were performed using all the data, respectively. Correlation coefficients of ANPP with SGS, EGS, LGS, GSP, Ea, RH, RH_{min}, VPD, T_a, T_{amin}, T_{amax}, AccT, and GSP/AccT were conducted for each site, respectively. The largest absolute value of correlation coefficients of ANPP with these concerned variables was treated as the dominated factor. The variation of ANPP was partitioned using climate variables (i.e., GSP, Ea, RH, RH_{min}, VPD, T_a, T_{amin}, T_{amax}, AccT, and GSP/AccT) and phenological variables (i.e., SGS, EGS, and LGS) was partitioned using varpart function. Linear regression coefficients (i.e., slope) between ANPP, SGS, EGS, LGS, GSP, Ea, RH, RH_{min}, VPD, T_a, T_{amin}, T_{amax}, AccT, GSP/AccT, and time series (i.e., from 2000 to 2013) were conducted to obtain the temporal changes of these concerned parameters during 2000–2013 for each one of the 36 sites. The linear changes of ANPP, SGS, EGS, LGS, GSP, Ea, RH, RH_{min}, VPD, T_a, T_{amin}, T_{amax}, AccT, and GSP/AccT were labeled as slope_ANPP, slope_SGS, slope_EGS, slope_LGS, slope_GSP, slope_Ea, slope_RH, slope_RH_{min}, slope_VPD, slope_T_a, slope_T_{amin}, slope_T_{amax}, slope_AccT, and slope_GSP/AccT, respectively. Simple linear regressions of slope_ANPP with slope_SGS, slope_EGS, slope_LGS, slope_GSP, slope_Ea, slope_RH, slope_RH_{min}, slope_VPD, slope_T_a, slope_T_{amin}, slope_T_{amax}, slope_AccT, and slope_GSP/AccT were performed, respectively. The variation of slope_ANPP was partitioned using climate change (i.e., slope_GSP, slope_Ea, slope_RH, slope_RH_{min}, slope_VPD, slope_T_a, slope_T_{amin}, slope_T_{amax}, slope_AccT, and slope_GSP/AccT) and phenological change (i.e., slope_SGS, slope_EGS, and slope_LGS) was partitioned using varpart function.

RESULTS

Climate Change

The change trends of climate variables are listed in **Supplementary Table 1**. The GSP in seven sites showed decreasing trends by −15.23 to −0.14 mm a^{-1}, while that in the other 29 sites showed increasing trends by 0.90–13.27 mm a^{-1}. The E_a in 20 sites showed decreasing trends by −0.02 to −0.12 kPa a^{-1}, while that in the other 16 sites showed increasing trends by 0.001–0.04 kPa a^{-1}. The RH in 35 sites showed decreasing trends by −1.00 to −0.02% a^{-1}, while that in the other one site showed an increasing trend by 0.07% a^{-1}. The RH_{min} in all the 36 sites showed decreasing trends by −1.98 to −0.12% a^{-1}. The VPD in only two sites showed decreasing trends by −0.04 to −0.002 kPa a^{-1}, while that in the other 34 sites showed increasing trends by 0.002–0.13 kPa a^{-1}. The T_a in seven sites showed decreasing trends by −0.07 to −0.01°C a^{-1}, while that in the other 29 sites showed increasing trends by 0.02–0.11°C a^{-1}. The T_{amax} in seven sites showed decreasing trends by −0.09 to −0.01°C a^{-1}, while that in the other 29 sites showed increasing trends by 0.00–0.18°C a^{-1}. The T_{amin} in seven sites showed decreasing trends by −0.08 to −0.01°C a^{-1}, while that in the other 29 sites showed increasing trends by 0.00–0.15°C a^{-1}. The AccT in only two sites showed decreasing trends by

−5.60 to −5.28°C a^{-1}, while that in the other 34 sites showed increasing trends by 2.02–45.48°C a^{-1}. The GSP/AccT ratio in 14 sites showed decreasing trends by −0.01 to −0.0002 mm $°C^{-1}$ a^{-1}, while that in the other 22 sites showed increasing trends by 0.0001–0.02 mm $°C^{-1}$ a^{-1}.

Phenological Change and Aboveground Net Primary Productivity Change

The change trends of phenology variables and ANPP are listed in **Supplementary Table 1**. The SGS in 25 sites showed decreasing trends by −2.53 to −0.05 day a^{-1}, while that in the other 11 sites showed increasing trends by 0.10–1.54 day a^{-1}. The EGS in 16 sites showed decreasing trends by −1.83 to −0.07 day a^{-1}, while that in the other 20 sites showed increasing trends by 0.03–1.62 day a^{-1}. The LGS in 12 sites showed decreasing trends by −2.23 to −0.06 day a^{-1}, while that in the other 24 sites showed increasing trends by 0.002–3.89 day a^{-1}. The decreases in SGS and, meanwhile, the increases in EGS resulted in the increases in LGS in 13 sites. The decreased magnitudes of SGS were greater than those of EGS, which caused the increases in LGS in the other eight sites. The increased magnitudes of EGS were greater than those of SGS, which resulted in the increases in LGS in the other three sites. The increases in SGS and, meanwhile, the decreases in EGS caused the decreases in LGS in four sites. The increased magnitudes of SGS were greater than those of EGS, which resulted in the decreases in LGS in the other four sites. The decreased magnitudes of EGS were greater than those of SGS, which caused the decreases in LGS in the other four sites.

The ANPP in 14 sites showed decreasing trends by −10.48 to −0.03 g m^{-2} a^{-1}, while that in the other 22 sites showed increasing trends by 0.01–8.62 g m^{-2} a^{-1}.

Effects of Climate Change and Phenological Change on Aboveground Net Primary Productivity

The ANPP increased exponentially with E_a, RH, RH_{min}, GSP, GSP/AccT and LGS, but decreased exponentially with VPD and SGS (**Figures 2**, **3**). The ANPP showed a significant quadratic correlation with T_a, T_{amax}, and T_{amin} (**Figure 2**). The E_a, RH, RH_{min}, GSP, VPD, GSP/AccT, T_a, T_{amax}, T_{amin}, SGS, and LGS explained significantly 21, 37, 30, 39, 23, 10, 13, 12, 9, 20, and 9% variation of ANPP, respectively (**Figures 2**, **3**). Moreover, the correlation coefficients of ANPP with AccT ($p = 0.181$) and EGS ($p = 0.068$) were not significant. The varpart analysis showed that climate variables and phenological variables exclusivity explained 37 and 3% variation of ANPP, respectively, and they together explained 15% variation of ANPP (**Figure 4A**); i.e., the variations of ANPP were more explained by climate variables rather than phenology variables.

The changes of ANPP were dominated by SGS at three sites, by LGS at three sites, by water availability at 17 sites, by temperature variables at 11 sites, and by GSP/AccT ratio at two sites (**Figure 5**); i.e., phenology changes predominated ANPP changes at only six sites, while climate changes predominated ANPP changes at 30 sites. The slope_ANPP increased significantly with increasing slope_E_a, slope_RH, slope_RH_{min}, slope_GSP, slope_GSP/AccT, and slope_T_{amin} (**Figure 6**). However, slope_ANPP was not linearly correlated with slope_VPD ($p = 0.141$), slope_T_a ($p = 0.262$), slope_AccT ($p = 0.709$), slope_SGS ($p = 0.213$), slope_EGS ($p = 0.106$), slope_LGS ($p = 0.940$), and slope_T_{amax} ($p = 0.622$). Climate change exclusively explained about 0.4% variation of slope_ANPP, but phenology change did not exclusively explain the variation of slope_ANPP (**Figure 4B**).

DISCUSSION

Effects of Climate Change on Aboveground Net Primary Productivity

There was the most likely optimum temperature for ANPP in alpine grasslands (**Figure 2**), which was in line with several previous studies (Wang et al., 2013). This finding implied that climate warming may not always increase ANPP in alpine regions. In fact, there were diverse responses of ANPP to climate warming in alpine regions, with increases (Wang et al., 2012; Ganjurjav et al., 2015), decreases (Klein et al., 2007; Ganjurjav et al., 2016a), or no change (Natali et al., 2012). These diverse effects of climate warming on ANPP were attributed to the following mechanisms. First, ANPP was more sensitive to warming in the colder environment in alpine regions (Rustad et al., 2001). Second, Shi et al. (2014) ascribed the relatively low effect of warming on ANPP to the that alpine plants had a low optimal temperature, high-temperature adaptation, and strong resilience to short-term temperature fluctuations. Third, warming generally resulted in soil drying (Lu et al., 2013), and the lower limit of soil moisture was 11.8% for alpine grassland growth (Ma et al., 2004). Warming-induced soil drying can dampen the effect of increased temperature on ANPP by reducing leaf area and inducing stomatal closure (Broeckx et al., 2014). Fourth, warming-induced decreases in species richness and diversity can influence warming effects on ANPP because ANPP had some relations with species diversity (Ma et al., 2010; Wang et al., 2013; Wu et al., 2014). Fifth, warming can accelerate plant maturity and actually shorten LGS (Li et al., 2004). The diverse correlations between plant productivity and LGS in this study could result in inconsistent responses of ANPP to warming.

Precipitation has increased by 0.67 mm a^{-1} during 1961–2010 on the Tibetan Plateau (Li X. Y. et al., 2016) and will continue to increase in the 21st century (Ji and Kang, 2013). Increased precipitation will most likely increase ANPP in alpine grasslands on the Tibetan Plateau (**Figure 2**). Likewise, ANPP increased significantly with increasing GSP in alpine grasslands on the Northern Tibetan Plateau (Wu et al., 2014). ANPP increased with increasing GSP across the widely distributed temperate and alpine grasslands of China (Ma et al., 2010). A previous meta-analysis found that increased precipitation increased ANPP, while decreased precipitation reduced ANPP at a global scale (Wu et al., 2011).

Water availability had stronger effects on ANPP than did temperature (**Figures 2**, **6**), which was consistent with several previous studies (Wu et al., 2011; Fu and Shen, 2016a; Xu et al., 2016). For example, rainfall fluctuation had a more profound effect on the ANPP dynamics than temperature variation in

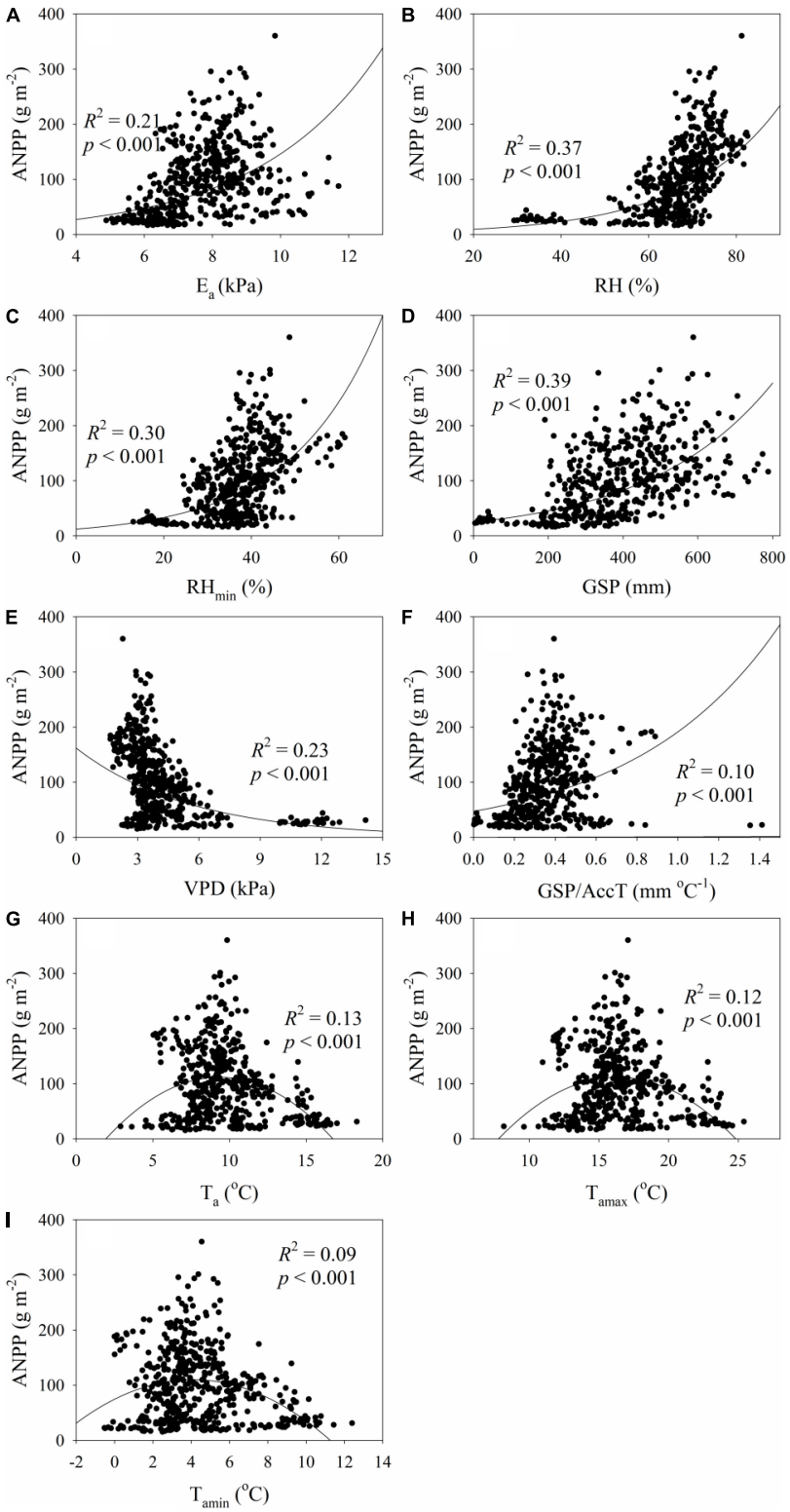

FIGURE 2 | Relationships **(A)** between aboveground net primary production (ANPP) and growing season average actual vapor pressure (E_a), **(B)** between ANPP and growing season average relative humidity (RH), **(C)** between ANPP and growing season minimum RH (RH_{min}), **(D)** between ANPP and growing season total precipitation (GSP), **(E)** between ANPP and growing season average vapor pressure deficit (VPD), **(F)** between ANPP and the ratio of GSP to accumulated temperature (GSP/AccT), **(G)** between ANPP and growing season average air temperature (T_a), **(H)** between ANPP and maximum air temperature (T_{amax}), and **(I)** between ANPP and minimum air temperature (T_{amin}).

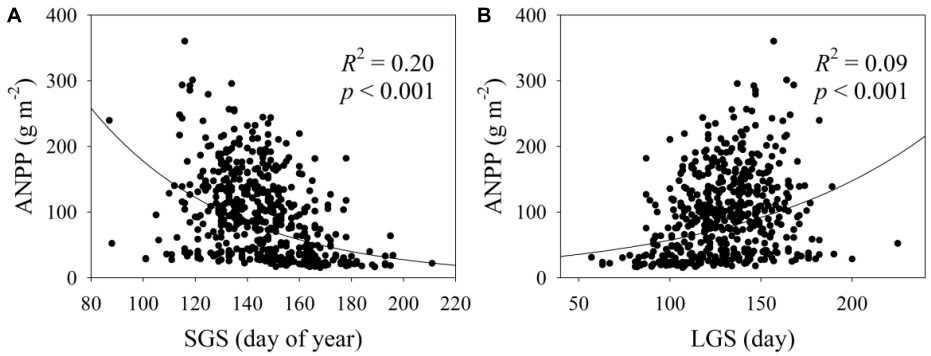

FIGURE 3 | Relationships **(A)** between ANPP and start of growing season (SGS) and **(B)** between ANPP and length of growing season (LGS).

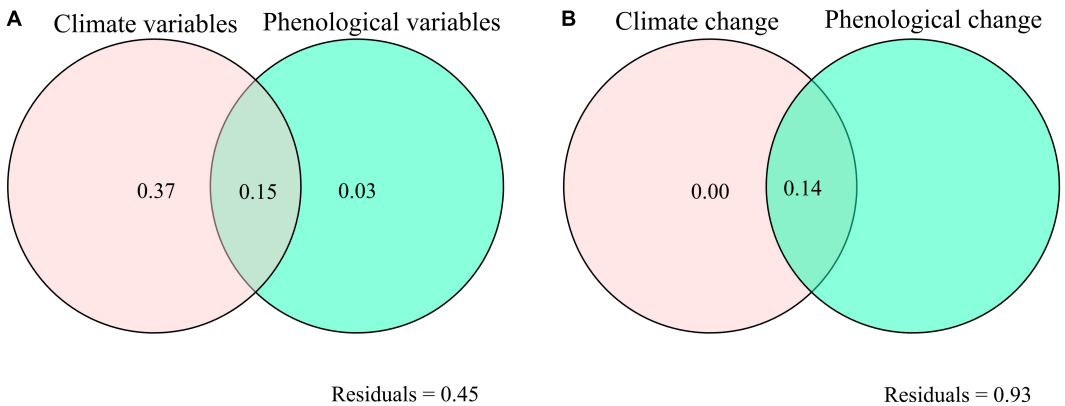

FIGURE 4 | Varpart analysis, showing **(A)** the exclusive and shared effects of climate variables [growing season precipitation (GSP), E_a, RH, minimum RH, vapor pressure deficit, air temperature, minimum air temperature, maximum air temperature, accumulated ≥5°C air temperature, ratio of GSP to accumulated ≥5 air temperature], and phenological variables [LGS, SGS, and end of growing season (EGS)] on ANPP, **(B)** the exclusive and shared effects of climate change (linear slopes of GSP, E_a, RH, minimum RH, vapor pressure deficit, air temperature, minimum air temperature, maximum air temperature, accumulated ≥5°C air temperature, ratio of GSP to accumulated ≥5°C air temperature), and phenological change (linear slopes of LGS, SGS, and EGS) on the changes in ANPP.

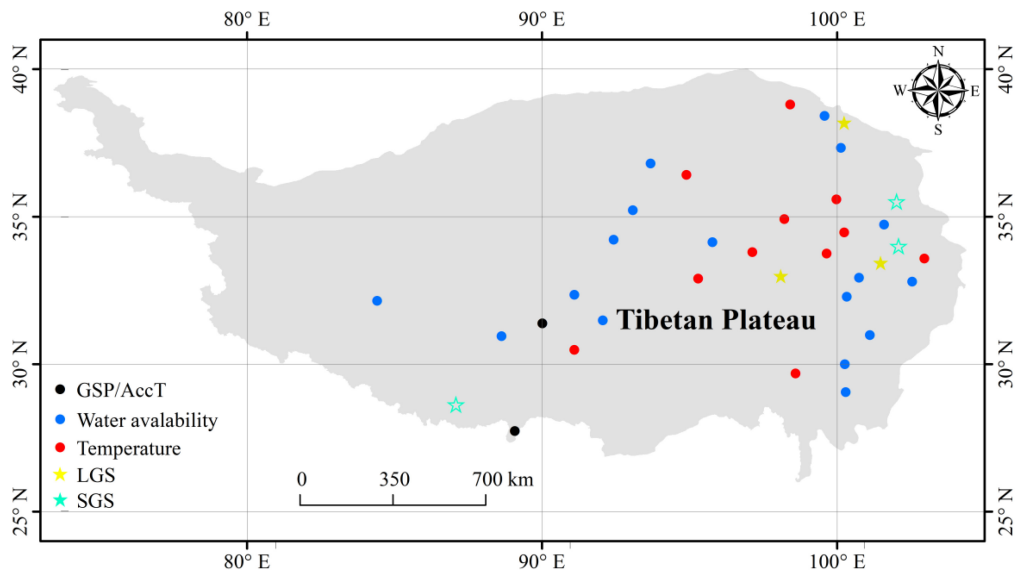

FIGURE 5 | The spatial distribution of the dominant variables of ANPP.

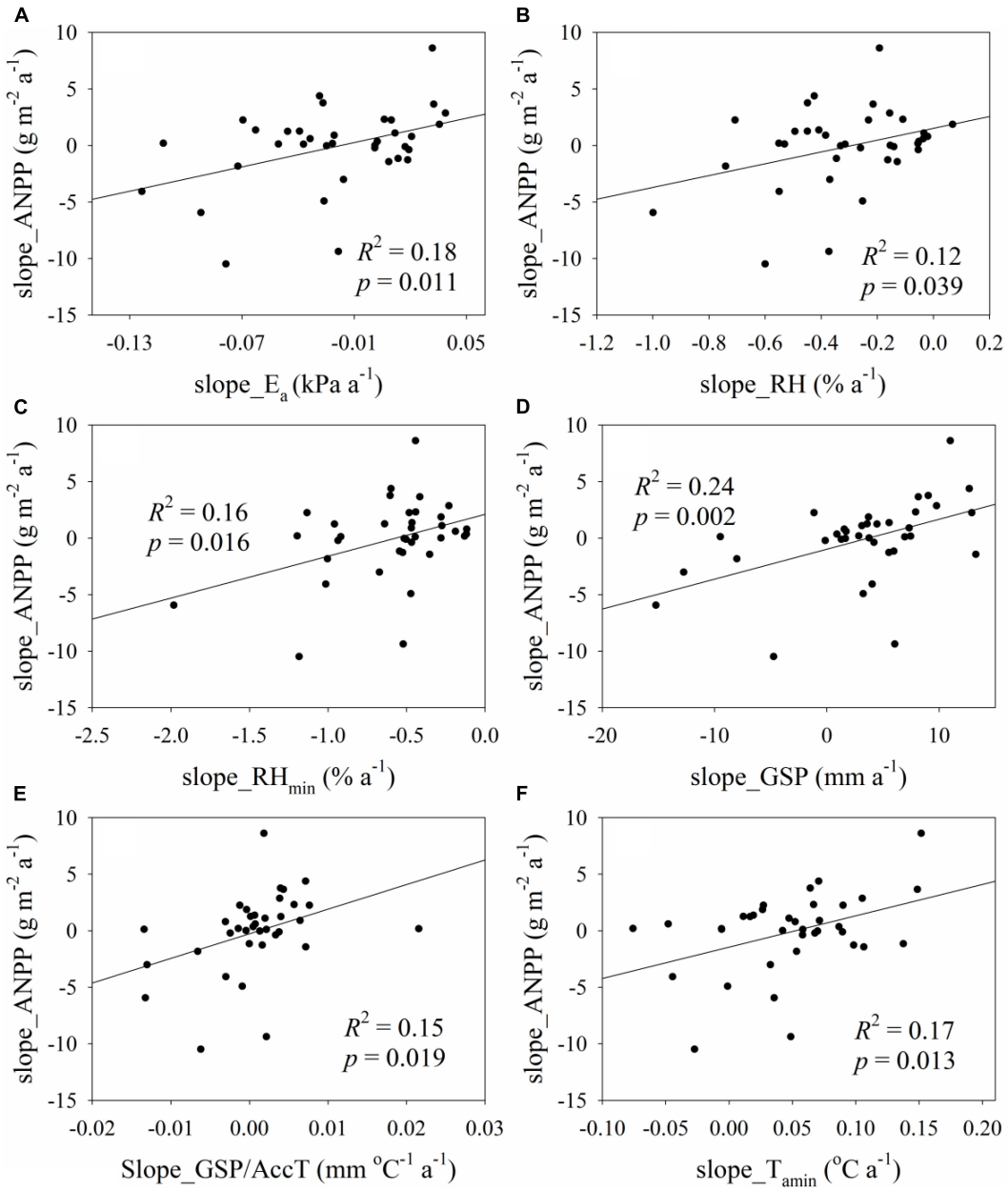

FIGURE 6 | Relationships **(A)** between linear slope of ANPP (slope_ANPP) and that of growing season average E_a (slope_E_a), **(B)** between slope_ANPP and that of growing season average RH (slope_RH), **(C)** between slope_ANPP and that of growing season minimum RH (slope_RH_{min}), **(D)** between slope_ANPP and that of growing season average precipitation (slope_GSP), **(E)** between slope_ANPP and that of the ratio of GSP to accumulated temperature (slope_GSP/AccT), and **(F)** between slope_ANPP and that of minimum air temperature (slope_T_{amin}).

the Tibetan alpine grasslands (Shi et al., 2014). Growing-season maximum normalized difference vegetation index had a closer correlation with water availability than temperature across the Tibetan Plateau during 2000–2012 (Shen et al., 2014).

Effects of Phenological Changes on Aboveground Net Primary Productivity

The effect of SGS on ANPP was stronger than that of EGS and LGS across all the years and sites (**Figure 3**). Likewise, the effect of SGS on annual net ecosystem production was stronger than that of LGS in alpine shrubland on the Qinghai-Tibetan Plateau (Li H. Q. et al., 2016). SGS had a higher correlation with net primary production than did EGS in alpine ecosystems on the Tibetan Plateau (Yang et al., 2015; Wang et al., 2017). SGS had a greater correlation with gross primary production than did EGS in temperate deciduous broadleaved forests in North America (Zhao and Liu, 2012).

Across all the years and sites, ANPP increased with prolonged SGS and LGS (**Figure 3**). Likewise, ANPP increased with LGS across a suite of high elevation meadows in the United States and Asia (Berdanier and Klein, 2011). Both advanced SGS and prolonged LGS showed a positive effect on gross primary production across eight larch forests in East Asia (Takagi et al., 2015). In the Northern Hemisphere, LGS was strongly correlated with gross primary production and net primary production (Piao et al., 2007). However, there were spatial variations in SGS, EGS, and LGS changes during the past 14 years, which could also be observed by several previous studies (Piao et al., 2007; Shen et al., 2011; Song et al., 2011). The spatial variations in phenological changes, in turn, may partially result in diverse relationships between ANPP and these three phenological variables among all the 36 sites. Previous studies also found that responses of plant productivity to LGS were dependent on sites (Berdanier and Klein, 2011). For example, a prolonged LGS increased aboveground biomass under warming conditions in a tallgrass prairie, United States (Wan et al., 2005). There was no increase in alpine snowbed ANPP in response to experimental prolonged LGS (Baptist et al., 2010). Although experimental warming extended LGS, there was no increase in gross primary production and species-level coverage in response to experimental warming in a semiarid grassland (Xia and Wan, 2012). In addition, both extended LGS and advanced SGS resulted in less net ecosystem productivity in a subalpine forest in the Colorado Rocky Mountains (Jia et al., 2010).

These diverse responses of plant productivity to plant phenological change could be contributed to the following mechanisms. First, prolonged LGS, advanced SGS, and delayed EGS may lead to a greater temporal species overlap, reduce phenological complementarity, and increase water and nutrient competition among species (Xia and Wan, 2012; Dorji et al., 2013). This may cause species loss, which, in turn, increased complexity on the relationships between plant productivity and plant phenology, considering the diverse correlations between plant productivity and species diversity in alpine regions (Wang et al., 2012, 2013; Wu et al., 2014). Second, plant intrinsic developmental capacities (e.g., periodic species and aperiodic species) varied among species (Baptist et al., 2010). Third, advanced SGS may lead to potential detrimental effects of early frosts, which, in turn, result in a reduction in plant productivity (Baptist et al., 2010). Fourth, plant photosynthetic CO_2 uptake depended on snowmelt (Jia et al., 2010). Advanced SGS may result in earlier snowmelt, which, in turn, affected plant productivity (Jia et al., 2010). Fifth, SGS showed a negative correlation with GSP and E_a, and LGS showed a positive correlation with GSP and E_a in this study. This indicated that advanced SGS and prolonged LGS can increase water availability during the growing season. Accumulated precipitation within phenological duration was positively related to plant productivity (Xia and Wan, 2012). Sixth, plant growth in alpine regions is generally nitrogen-limited (Fu and Shen, 2016b). A delayed SGS and shortened LGS had a greater positive effect on ANPP by increasing soil fertility than did an advanced SGS and prolonged LGS (Baptist et al., 2010).

Stronger Effect of Climate Change on Aboveground Net Primary Productivity Than That of Phenological Change

Our findings implied that climate variables (especially GSP) rather than phenological variables (i.e., LGS and SGS) predominated ANPP changes across all the alpine grassland sites on the Tibetan Plateau. These results were in line with previous studies on the response of plant productivity to climate and phenological changes. For example, shortened growing seasons did not affect both gross primary production and net primary production under experimental warming, which was attributed to the seasonal variation of precipitation in an alpine meadow on the Tibetan Plateau (Zhu et al., 2017). The changes in gross primary production and species-level coverage were positively correlated to the accumulated precipitation within phenological duration but not the length of phenological duration in a semiarid grassland (Xia and Wan, 2012). Gross primary production did not increase with longer LGS, but increased with growing-season temperature sum in the northeastern Siberian tundra (Parmentier et al., 2011).

CONCLUSION

In this study, we compared the effect of phenological variables and climate variables on aboveground net primary production in alpine grasslands on the Tibetan Plateau. LGS and SGS explained 9 and 20% variation of ANPP, while GSP, RH, E_a, VPD, and GSP/AccT explained 39, 37, 21, 23, and 10% variation of ANPP, respectively. Moreover, the linear slope of ANPP showed a positive relationship with that of GSP ($R^2 = 0.24$), RH ($R^2 = 0.12$), E_a ($R^2 = 0.18$), and GSP/AccT ($R^2 = 0.15$) but did not correlate to that of LGS and SGS. Therefore, precipitation change predominated the variation of ANPP and responses of ANPP to climate change were greater than those of phenological change.

DATA AVAILABILITY STATEMENT

The datasets presented in this article are not readily available because the datasets generated for this study are available on request to the corresponding author. Requests to access the datasets should be directed to GF.

AUTHOR CONTRIBUTIONS

JW wrote the first manuscript, which revised by GF and CY. ML collected the data. All authors contributed to the article and approved the submitted version.

FUNDING

This research was supported by the Youth Innovation Promotion Association of the Chinese Academy of Sciences [2020054], the National Key Research Projects of China [2017YFA0604801], the National Natural Science Foundation of China [31600432], the

Bingwei Outstanding Young Talents Program of the Institute of Geographic Sciences and Natural Resources Research, Chinese Academy of Sciences [2018RC202], and the Tibet Science and Technology Major Projects of the Pratacultural Industry [XZ202101ZD0003N].

SUPPLEMENTARY MATERIAL

The Supplementary Material for this article can be found online at: https://www.frontiersin.org/articles/10.3389/fpls.2021.798633/full#supplementary-material

REFERENCES

Attorre, F., Alfo, M., De Sanctis, M., Francesconi, F., and Bruno, F. (2007). Comparison of interpolation methods for mapping climatic and bioclimatic variables at regional scale. *Int. J. Climatol.* 27, 1825–1843. doi: 10.1002/joc.1495

Baptist, F., Flahaut, C., Streb, P., and Choler, P. (2010). No increase in alpine snowbed productivity in response to experimental lengthening of the growing season. *Plant Biol.* 12, 755–764. doi: 10.1111/j.1438-8677.2009.00286.x

Berdanier, A. B., and Klein, J. A. (2011). Growing season length and soil moisture interactively constrain high elevation aboveground net primary production. *Ecosystems* 14, 963–974. doi: 10.1007/s10021-011-9459-1

Broeckx, L. S., Verlinden, M. S., Berhongaray, G., Zona, D., Fichot, R., and Ceulemans, R. (2014). The effect of a dry spring on seasonal carbon allocation and vegetation dynamics in a poplar bioenergy plantation. *Glob. Change Biol. Bioenergy* 6, 473–487. doi: 10.1111/gcbb.12087

Chen, H., Zhu, Q. A., Wu, N., Wang, Y. F., and Peng, C. H. (2011). Delayed spring phenology on the Tibetan Plateau may also be attributable to other factors than winter and spring warming. *Proc. Natl. Acad. Sci. U.S.A.* 108, E93–E93. doi: 10.1073/pnas.1100091108

Cong, N., Piao, S., Chen, A., Wang, X., Lin, X., Chen, S., et al. (2012). Spring vegetation green-up date in China inferred from SPOT NDVI data: a multiple model analysis. *Agric. For. Meteorol.* 165, 104–113. doi: 10.1016/j.agrformet.2012.06.009

Deng, S. F., Yang, T. B., Zeng, B., Zhu, X. F., and Xu, H. J. (2013). Vegetation cover variation in the Qilian Mountains and its response to climate change in 2000-2011. *J. Mt. Sci.* 10, 1050–1062. doi: 10.1007/s11629-013-2558-z

Ding, M. J., Chen, Q., Li, L. H., Zhang, Y. L., Wang, Z. F., Liu, L. S., et al. (2016). Temperature dependence of variations in the end of the growing season from 1982 to 2012 on the Qinghai-Tibetan Plateau. *GISci. Remote Sens.* 53, 147–163. doi: 10.1080/15481603.2015.1120371

Dorji, T., Totland, O., Moe, S. R., Hopping, K. A., Pan, J. B., and Klein, J. A. (2013). Plant functional traits mediate reproductive phenology and success in response to experimental warming and snow addition in Tibet. *Glob. Change Biol.* 19, 459–472. doi: 10.1111/gcb.12059

Fu, G., and Shen, Z. X. (2016a). Environmental humidity regulates effects of experimental warming on vegetation index and biomass production in an alpine meadow of the Northern Tibet. *PLoS One* 11:e0165643. doi: 10.1371/journal.pone.0165643

Fu, G., and Shen, Z. X. (2016b). Response of alpine plants to nitrogen addition on the Tibetan Plateau: a meta-analysis. *J. Plant Growth Regul.* 35, 974–979. doi: 10.1007/s00344-016-9595-0

Fu, G., Shen, Z. X., Sun, W., Zhong, Z. M., Zhang, X. Z., and Zhou, Y. T. (2015). A meta-analysis of the effects of experimental warming on plant physiology and growth on the Tibetan Plateau. *J. Plant Growth Regul.* 34, 57–65. doi: 10.1007/s00344-014-9442-0

Fu, G., Shen, Z. X., and Zhang, X. Z. (2018). Increased precipitation has stronger effects on plant production of an alpine meadow than does experimental warming in the Northern Tibetan Plateau. *Agric. For. Meteorol.* 249, 11–21. doi: 10.1016/j.agrformet.2017.11.017

Fu, G., Sun, W., Li, S. W., Zhang, J., Yu, C. Q., and Shen, Z. (2017). Modeling aboveground biomass using MODIS images and climatic data in grasslands on the Tibetan Plateau. *J. Resour. Ecol.* 8, 42–49. doi: 10.5814/j.issn.1674-764x.2017.01.006

Fu, Z., Niu, S. L., and Dukes, J. S. (2015). What have we learned from global change manipulative experiments in China? A meta-analysis. *Sci. Rep.* 5:12344. doi: 10.1038/srep12344

Ganjurjav, H., Gao, Q. Z., Schwartz, M. W., Zhu, W. Q., Liang, Y., Li, Y., et al. (2016b). Complex responses of spring vegetation growth to climate in a moisture-limited alpine meadow. *Sci. Rep.* 6:23356. doi: 10.1038/srep23356

Ganjurjav, H., Gao, Q. Z., Gornish, E. S., Schwartz, M. W., Liang, Y., Cao, X. J., et al. (2016a). Differential response of alpine steppe and alpine meadow to climate warming in the central Qinghai-Tibetan Plateau. *Agric. For. Meteorol.* 223, 233–240. doi: 10.1016/j.agrformet.2016.03.017

Ganjurjav, H., Gao, Q. Z., Zhang, W. N., Liang, Y., Li, Y. W., Cao, X. J., et al. (2015). Effects of warming on CO2 Fluxes in an alpine meadow ecosystem on the central Qinghai-Tibetan Plateau. *PLoS One* 10:e0132044. doi: 10.1371/journal.pone.0132044

Hashimoto, H., Dungan, J. L., White, M. A., Yang, F., Michaelis, A. R., Running, S. W., et al. (2008). Satellite-based estimation of surface vapor pressure deficits using MODIS land surface temperature data. *Remote Sens. Environ.* 112, 142–155. doi: 10.1016/j.rse.2007.04.016

Ji, Z. M., and Kang, S. C. (2013). Double-nested dynamical downscaling experiments over the Tibetan Plateau and their projection of climate change under two RCP Scenarios. *J. Atmos. Sci.* 70, 1278–1290. doi: 10.1175/JAS-D-12-0155.1

Jia, H. U., Moore, D. J. P., Burns, S. P., and Monson, R. K. (2010). Longer growing seasons lead to less carbon sequestration by a subalpine forest. *Glob. Change Biol.* 16, 771–783. doi: 10.1111/j.1365-2486.2009.01967.x

Klein, J. A., Harte, J., and Zhao, X. Q. (2007). Experimental warming, not grazing, decreases rangeland quality on the Tibetan Plateau. *Ecol. Appl.* 17, 541–557. doi: 10.1890/05-0685

Kross, A. S. E., Roulet, N. T., Moore, T. R., Lafleur, P. M., Humphreys, E. R., Seaquist, J. W., et al. (2014). Phenology and its role in carbon dioxide exchange processes in northern peatlands. *J. Geophys. Res. Biogeosci.* 119, 1370–1384. doi: 10.1002/2014JG002666

Li, H. Q., Zhang, F. W., Li, Y. N., Wang, J. B., Zhang, L. M., Zhao, L., et al. (2016). Seasonal and inter-annual variations in CO2 fluxes over 10 years in an alpine shrubland on the Qinghai-Tibetan Plateau, China. *Agric. For. Meteorol.* 228, 95–103. doi: 10.1016/j.agrformet.2016.06.020

Li, X. Y., Yao, Z. Y., Xiao, J. H., and Wang, H. W. (2016). Analysis of the spatial-temporal variation characteristics of precipitation over the Tibetan Plateau from 1961 through 2010. *J. Glaciol. Geocryol.* 38:1233.

Li, Y. N., Zhao, L., Zhao, X. Q., and Zhou, H. K. (2004). Effects of a 5-years mimic temperature increase to the structure and productivity of Kobresia Humilis meadow. *Acta Agrestia Sin.* 12, 236–239.

Lu, M., Zhou, X. H., Yang, Q., Li, H., Luo, Y. Q., Fang, C. M., et al. (2013). Responses of ecosystem carbon cycle to experimental warming: a meta-analysis. *Ecology* 94, 726–738. doi: 10.1890/12-0279.1

Ma, K. M., Fu, B. J., Liu, S. L., Guan, W. B., Liu, G. H., Lu, Y. H., et al. (2004). Multiple-scale soil moisture distribution and its implications for ecosystem restoration in an arid river valley, China. *Land Degrad. Dev.* 15, 75–85. doi: 10.1002/ldr.584

Ma, W. H., He, J. S., Yang, Y. H., Wang, X. P., Liang, C. Z., Anwar, M., et al. (2010). Environmental factors covary with plant diversity-productivity relationships among Chinese grassland sites. *Glob. Ecol. Biogeogr.* 19, 233–243. doi: 10.1111/j.1466-8238.2009.00508.x

Miller, P. A., and Smith, B. (2012). Modelling tundra vegetation response to recent Arctic warming. *Ambio* 41, 281–291. doi: 10.1007/s13280-012-0306-1

Natali, S. M., Schuur, E. A. G., and Rubin, R. L. (2012). Increased plant productivity in Alaskan tundra as a result of experimental warming of soil and permafrost. *J. Ecol.* 100, 488–498. doi: 10.1111/j.1365-2745.2011.01925.x

Parmentier, F. J. W., van der Molen, M. K., van Huissteden, J., Karsanaev, S. A., Kononov, A. V., Suzdalov, D. A., et al. (2011). Longer growing seasons do not increase net carbon uptake in the northeastern Siberian tundra. *J. Geophys. Res. Biogeosci.* 116:G04013. doi: 10.1029/2011JG001653

Piao, S., Cui, M., Chen, A., Wang, X., Ciais, P., Liu, J., et al. (2011). Altitude and temperature dependence of change in the spring vegetation green-up date from 1982 to 2006 in the Qinghai-Xizang Plateau. *Agric. For. Meteorol.* 151, 1599–1608. doi: 10.1016/j.agrformet.2011.06.016

Piao, S., Friedlingstein, P., Ciais, P., Viovy, N., and Demarty, J. (2007). Growing season extension and its impact on terrestrial carbon cycle in the Northern Hemisphere over the past 2 decades. *Glob. Biogeochem. Cycles* 21, 1148–1154. doi: 10.1029/2006GB002888

Prieto, P., Penuelas, J., Niinemets, U., Ogaya, R., Schmidt, I. K., Beier, C., et al. (2009). Changes in the onset of spring growth in shrubland species in response to experimental warming along a north-south gradient in Europe. *Glob. Ecol. Biogeogr.* 18, 473–484. doi: 10.1111/j.1466-8238.2009.00460.x

Robinson, T. M. P., La Pierre, K. J., Vadeboncoeur, M. A., Byrne, K. M., Thomey, M. L., and Colby, S. E. (2013). Seasonal, not annual precipitation drives community productivity across ecosystems. *Oikos* 122, 727–738. doi: 10.1111/j.1600-0706.2012.20655.x

Rustad, L. E., Campbell, J. L., Marion, G. M., Norby, R. J., Mitchell, M. J., Hartley, A. E., et al. (2001). A meta-analysis of the response of soil respiration, net nitrogen mineralization, and aboveground plant growth to experimental ecosystem warming. *Oecologia* 126, 543–562. doi: 10.1007/s004420000544

Shen, M. G. (2011). Spring phenology was not consistently related to winter warming on the Tibetan Plateau. *Proc. Natl. Acad. Sci. U.S.A.* 108, E91–E92. doi: 10.1073/pnas.1018390108

Shen, M. G., Tang, Y. H., Chen, J., Zhu, X. L., and Zheng, Y. H. (2011). Influences of temperature and precipitation before the growing season on spring phenology in grasslands of the central and eastern Qinghai-Tibetan Plateau. *Agric. For. Meteorol.* 151, 1711–1722. doi: 10.1016/j.agrformet.2011.07.003

Shen, Z. X., Fu, G., Yu, C. Q., Sun, W., and Zhang, X. Z. (2014). Relationship between the growing season maximum enhanced vegetation index and climatic factors on the Tibetan Plateau. *Remote Sens.* 6, 6765–6789. doi: 10.3390/rs6086765

Shi, Y., Wang, Y., Ma, Y., Ma, W., Liang, C., Flynn, D. F. B., et al. (2014). Field-based observations of regional-scale, temporal variation in net primary production in Tibetan alpine grasslands. *Biogeosci.* 11, 2003–2016. doi: 10.5194/bg-11-2003-2014

Song, C. Q., You, S. C., Ke, L. H., Liu, G. H., and Zhong, X. K. (2011). Spatio-temporal variation of vegetation phenology in the Northern Tibetan Plateau as detected by MODIS remote sensing. *Chin. J. Plant Ecol.* 35, 853–863. doi: 10.3724/SP.J.1258.2011.00853

Takagi, K., Hirata, R., Ide, R., Ueyama, M., Ichii, K., Saigusa, N., et al. (2015). Spatial and seasonal variations of CO2 flux and photosynthetic and respiratory parameters of larch forests in East Asia. *Soil Sci. Plant Nutr.* 61, 61–75. doi: 10.1080/00380768.2014.990349

Wan, S. Q., Hui, D. F., Wallace, L., and Luo, Y. Q. (2005). Direct and indirect effects of experimental warming on ecosystem carbon processes in a tallgrass prairie. *Glob. Biogeochem. Cycles* 19:GB2014. doi: 10.1029/2004GB002315

Wang, S., Zhang, B., Yang, Q., Chen, G., Yang, B., Lu, L., et al. (2017). Responses of net primary productivity to phenological dynamics in the Tibetan Plateau, China. *Agric. For. Meteorol.* 232, 235–246. doi: 10.1016/j.agrformet.2016.08.020

Wang, S. P., Duan, J. C., Xu, G. P., Wang, Y. F., Zhang, Z. H., Rui, Y. C., et al. (2012). Effects of warming and grazing on soil N availability, species composition, and ANPP in an alpine meadow. *Ecology* 93, 2365–2376. doi: 10.1890/11-1408.1

Wang, Z., Luo, T. X., Li, R. C., Tang, Y. H., and Du, M. Y. (2013). Causes for the unimodal pattern of biomass and productivity in alpine grasslands along a large altitudinal gradient in semi-arid regions. *J. Veg. Sci.* 24, 189–201. doi: 10.1111/j.1654-1103.2012.01442.x

Westergaard-Nielsen, A., Lund, M., Pedersen, S. H., Schmidt, N. M., Klosterman, S., Abermann, J., et al. (2017). Transitions in high-Arctic vegetation growth patterns and ecosystem productivity tracked with automated cameras from 2000 to 2013. *Ambio* 46, S39–S52. doi: 10.1007/s13280-016-0864-8

Wu, C. Y., Gonsamo, A., Chen, J. M., Kurz, W. A., Price, D. T., Lafleur, P. M., et al. (2012). Interannual and spatial impacts of phenological transitions, growing season length, and spring and autumn temperatures on carbon sequestration: a North America flux data synthesis. *Glob. Planet. Change* 92-93, 179–190. doi: 10.1016/j.gloplacha.2012.05.021

Wu, J., Shen, Z., and Zhang, X. (2014). Precipitation and species composition primarily determine the diversity-productivity relationship of alpine grasslands on the Northern Tibetan Plateau. *Alpine Bot.* 124, 13–25. doi: 10.1007/s00035-014-0125-z

Wu, Z. T., Dijkstra, P., Koch, G. W., Penuelas, J., and Hungate, B. A. (2011). Responses of terrestrial ecosystems to temperature and precipitation change: a meta-analysis of experimental manipulation. *Glob. Change Biol.* 17, 927–942. doi: 10.1111/j.1365-2486.2010.02302.x

Xia, J. Y., and Wan, S. Q. (2012). The effects of warming-shifted plant phenology on ecosystem carbon exchange are regulated by precipitation in a semi-arid grassland. *PLoS One* 7:e0032088. doi: 10.1371/journal.pone.0032088

Xu, Z. Z., Hou, Y. H., Zhang, L. H., Liu, T., and Zhou, G. S. (2016). Ecosystem responses to warming and watering in typical and desert steppes. *Sci. Rep.* 6:34801. doi: 10.1038/srep34801

Yang, B. J., Wang, S. Y., Chang, Q., Sun, Y. X., Yin, H., and Wang, X. Y. (2015). Response of NPP to phenology changes in the Tibet Plateau. *Geogr. Geoinf. Sci.* 31, 115–120.

Zhang, L., Guo, H. D., Ji, L., Lei, L. P., Wang, C. Z., Yan, D. M., et al. (2013). Vegetation greenness trend (2000 to 2009) and the climate controls in the Qinghai-Tibetan Plateau. *J. Appl. Remote. Sens.* 7:073572. doi: 10.1117/1.JRS.7.073572

Zhao, J. J., and Liu, L. Y. (2012). Effects of phenological change on ecosystem productivity of temperate deciduous broadleaved forests in North America. *Chin. J. Plant Ecol.* 36, 363–371. doi: 10.3724/SP.J.1258.2012.00363

Zhu, J. T., Zhang, Y. J., and Jiang, L. (2017). Experimental warming drives a seasonal shift of ecosystem carbon exchange in Tibetan alpine meadow. *Agric. For. Meteorol.* 233, 242–249. doi: 10.1016/j.agrformet.2016.12.005

Conflict of Interest: The authors declare that the research was conducted in the absence of any commercial or financial relationships that could be construed as a potential conflict of interest.

Publisher's Note: All claims expressed in this article are solely those of the authors and do not necessarily represent those of their affiliated organizations, or those of the publisher, the editors and the reviewers. Any product that may be evaluated in this article, or claim that may be made by its manufacturer, is not guaranteed or endorsed by the publisher.

Copyright © 2022 Wang, Li, Yu and Fu. This is an open-access article distributed under the terms of the Creative Commons Attribution License (CC BY). The use, distribution or reproduction in other forums is permitted, provided the original author(s) and the copyright owner(s) are credited and that the original publication in this journal is cited, in accordance with accepted academic practice. No use, distribution or reproduction is permitted which does not comply with these terms.

frontiers in Plant Science

ORIGINAL RESEARCH
published: 05 January 2022
doi: 10.3389/fpls.2021.791343

Environmental Controls on Multi-Scale Dynamics of Net Carbon Dioxide Exchange From an Alpine Peatland on the Eastern Qinghai-Tibet Plateau

Hu Yao[1,2,3], Haijun Peng[1,2,4], Bing Hong[1,2,4]*, Qian Guo[1,2,3], Hanwei Ding[1,2,3], Yetang Hong[1], Yongxuan Zhu[1], Cheng Cai[5] and Jinshu Chi[6]*

[1] State Key Laboratory of Environmental Geochemistry, Institute of Geochemistry, Chinese Academy of Sciences, Guiyang, China, [2] Bayinbuluk Alpine Wetland Carbon Flux Research Station, Chinese Flux Observation and Research Network, Beijing, China, [3] University of Chinese Academy of Sciences, Beijing, China, [4] CAS Center for Excellence in Quaternary Science and Global Change, Xi'an, China, [5] School of Chemical Engineering, Guizhou Institute of Technology, Guiyang, China, [6] Department of Forest Ecology and Management, Swedish University of Agricultural Sciences, Umeå, Sweden

OPEN ACCESS

Edited by:
Gao-Lin Wu,
Northwest A&F University, China

Reviewed by:
Luca Vitale,
Institute for Agricultural and Forestry Systems in the Mediterranean, National Research Council of Italy (CNR), Italy
Huai Chen,
Chengdu Institute of Biology, Chinese Academy of Sciences (CAS), China

***Correspondence:**
Haijun Peng
penghaijun@mail.gyig.ac.cn
Bing Hong
hongbing@mail.gyig.ac.cn

Specialty section:
This article was submitted to Functional Plant Ecology, a section of the journal Frontiers in Plant Science

Received: 08 October 2021
Accepted: 10 December 2021
Published: 05 January 2022

Citation:
Yao H, Peng H, Hong B, Guo Q, Ding H, Hong Y, Zhu Y, Cai C and Chi J (2022) Environmental Controls on Multi-Scale Dynamics of Net Carbon Dioxide Exchange From an Alpine Peatland on the Eastern Qinghai-Tibet Plateau. Front. Plant Sci. 12:791343. doi: 10.3389/fpls.2021.791343

Peatlands are characterized by their large carbon storage capacity and play an essential role in the global carbon cycle. However, the future of the carbon stored in peatland ecosystems under a changing climate remains unclear. In this study, based on the eddy covariance technique, we investigated the net ecosystem CO_2 exchange (NEE) and its controlling factors of the Hongyuan peatland, which is a part of the Ruoergai peatland on the eastern Qinghai-Tibet Plateau (QTP). Our results show that the Hongyuan alpine peatland was a CO_2 sink with an annual NEE of −226.61 and −185.35 g C m^{-2} in 2014 and 2015, respectively. While, the non-growing season NEE was 53.35 and 75.08 g C m^{-2} in 2014 and 2015, suggesting that non-growing seasons carbon emissions should not be neglected. Clear diurnal variation in NEE was observed during the observation period, with the maximum CO_2 uptake appearing at 12:30 (Beijing time, UTC+8). The Q_{10} value of the non-growing season in 2014 and 2015 was significantly higher than that in the growing season, which suggested that the CO_2 flux in the non-growing season was more sensitive to warming than that in the growing season. We investigated the multi-scale temporal variations in NEE during the growing season using wavelet analysis. On daily timescales, photosynthetically active radiation was the primary driver of NEE. Seasonal variation in NEE was mainly driven by soil temperature. The amount of precipitation was more responsible for annual variation of NEE. The increasing number of precipitation event was associated with increasing annual carbon uptake. This study highlights the need for continuous eddy covariance measurements and time series analysis approaches to deepen our understanding of the temporal variability in NEE and multi-scale correlation between NEE and environmental factors.

Keywords: NEE, eddy covariance, alpine peatland, wavelet analysis, Qinghai-Tibetan Plateau

INTRODUCTION

Peatlands worldwide have been shown to be an important player in the global carbon cycle in the recent past (Page and Baird, 2016; Helbig et al., 2019; D'Angelo et al., 2021). Even though they cover only approximately 3% of the global land area, the carbon stored in their soils has been estimated to be more than 600 Pg (1 Pg = 10^{15} g) worldwide since the Last Glacial Maximum (Yu et al., 2010). The carbon storage in peatlands accounts for about one third of the total global soil carbon pool (Wilson et al., 2016). It is generally thought that the intensity of carbon sinks in peatlands is higher than that in other terrestrial ecosystems due to primary production exceeding decomposition and other losses (León and Oliván, 2014). However, the carbon sink function of peatlands can be substantially altered due to climate warming, land-use change, and other human disturbances (Ward et al., 2012; Lupascu et al., 2014). Thus, a profound understanding on spatiotemporal variation characteristics of the carbon flux in peatlands and how the flux responds to its controlling factors is vital for the global carbon cycle research.

The Qinghai-Tibet Plateau (QTP), known as "the third pole", occupies approximately 2.5 × 10^6 km^2 with an average elevation of over 4,000 m (Zhang et al., 2014). The eastern part of QTP is more vulnerable to climate change due to the superimposed influence of the Indian summer monsoon, Eastern Asian summer monsoon, and westerly circulation (Kang et al., 2010). In recent years, several studies into the alpine wetland CO_2 exchange and its environmental factors have been conducted on the QTP (Peng et al., 2015; Wang et al., 2016; Kang et al., 2018). However, the magnitude of the carbon budgets, exchange, and direction (net sink/absorption or net source/emission) varies with temporal dynamics. Some studies suggested that the alpine wetland on the QTP was a huge organic carbon sink that was highly sensitive to global climate change (Hao et al., 2011; Cao et al., 2017; Niu et al., 2017). But other studies identified the alpine wetland on the QTP as a carbon source (Zhang et al., 2008; Zhao et al., 2010; Zhu et al., 2020). In addition, the main environmental factors that affect the carbon source/sink functions of the alpine wetland on the QTP have not been clearly understood. Many studies (e.g., Aslan-Sungur et al., 2016; Kang et al., 2018; D'Angelo et al., 2021) showed that wetland CO_2 fluxes are affected by a variety of ecological factors, such as temperature, soil water content, and solar radiation. Furthermore, some studies (Ali et al., 2008; Wu et al., 2020) suggested that whether alpine wetland acted as a CO_2 sink or a CO_2 source depended on the length of the growing season. Overall, there is no consensus as to the carbon source or sink of wetland ecosystems on the QTP due to different environmental factors in different wetland ecosystems. Besides, previous studies mainly focused on the growing season, making it difficult to fully explain the dynamics of wetland ecosystem carbon exchange and its impact mechanism. Therefore, a long-term and continuous field observation is needed to better understand the dynamic changes of carbon exchange of alpine wetland ecosystems (Griffis et al., 2000; Song et al., 2011).

Most studies on carbon exchange on the QTP were carried out by the traditional static chamber method (Wang et al., 2007; Pei et al., 2009; Wei et al., 2012). But Koskinen et al. (2014) pointed out that the installation of gas chambers may change the micrometeorological environment of the measured area and the gas diffusion gradient in the soil profile. The eddy covariance (EC) method provides reliable flux measurements (Zhao et al., 2010) and has been widely used to measure CO_2 fluxes in terrestrial ecosystem (Aubinet et al., 2000; Yamamoto et al., 2001). It could not only offer a direct signal of CO_2 fluxes but also record continuous NEE, which is ideally suited for time series analysis. Wavelet analysis has been demonstrated to be a powerful data analysis method to reveal the temporal variability in NEE and its dependencies on environmental control factors (e.g., Stoy et al., 2005; Furon et al., 2008; Jia et al., 2018). In this study, the EC method was used to measure the NEE between an alpine peatland ecosystem and the atmosphere in 2014 and 2015. Based on the quasi-continuous half-hour CO_2 fluxes, the temporal dynamics of alpine peatland CO_2 exchange and its environmental controls on time-scales ranging from hourly to annually were investigated.

The main objectives of this paper are to (1) investigate the CO_2 sequestration potential of alpine peatland ecosystem on the QTP; (2) assess the diurnal and seasonal variations in NEE, and (3) explore the effects of environmental factors on NEE at different timescales. Based on preliminary research, we hypothesize that (1) Hongyuan peatland is a CO_2 sink and has a greater potential for CO_2 sequestration capacity compared with other alpine meadow and alpine steppe ecosystems at similar elevation and latitude on the QTP, (2) NEE exhibited clear diurnal and seasonal variations, and (3) photosynthetically active radiation, soil temperature, and precipitation are the main environmental factors that affect NEE variations on the daily, seasonal, and interannual timescales, respectively.

MATERIALS AND METHODS

Site Description

The study was carried out at the Hongyuan Peatland Carbon Flux Monitoring and Research Station (32°46′ N, 102°30′ E; 3,510 m above sea level), which was established by the Institute of Geochemistry, Chinese Academy of Sciences. The Hongyuan peatland is a part of the Ruoergai peatland located on the eastern QTP (**Figure 1A**), and is characterized by wet and humid summers with cool and dry winters. The mean annual precipitation and air temperature in this area is 746 mm and 1.8°C, respectively, according to the meteorological data (1981 ∼ 2010) from the Nation Benchmark Climate Station in Hongyuan[1]. More than 75% of annual precipitation occurs during May and September. The dominant vegetation species are *Carex mulieensis* and *Kobresia tibetica* with an average height of about 40 cm during the growing season. Before the installation of the research station, the spatial distribution of the peatland was investigated using a MALÅ ProEx ground penetrating radar (MALÅ Geosciences, Sweden) and a Russian Peat Corer. The results showed that the depth of Hongyuan peatland ranges from 0.5 and 6.5 m. The total area of the Hongyuan peatland was measured to be 1.1 km^2. The EC tower was installed in the center

[1]http://data.cma.cn/

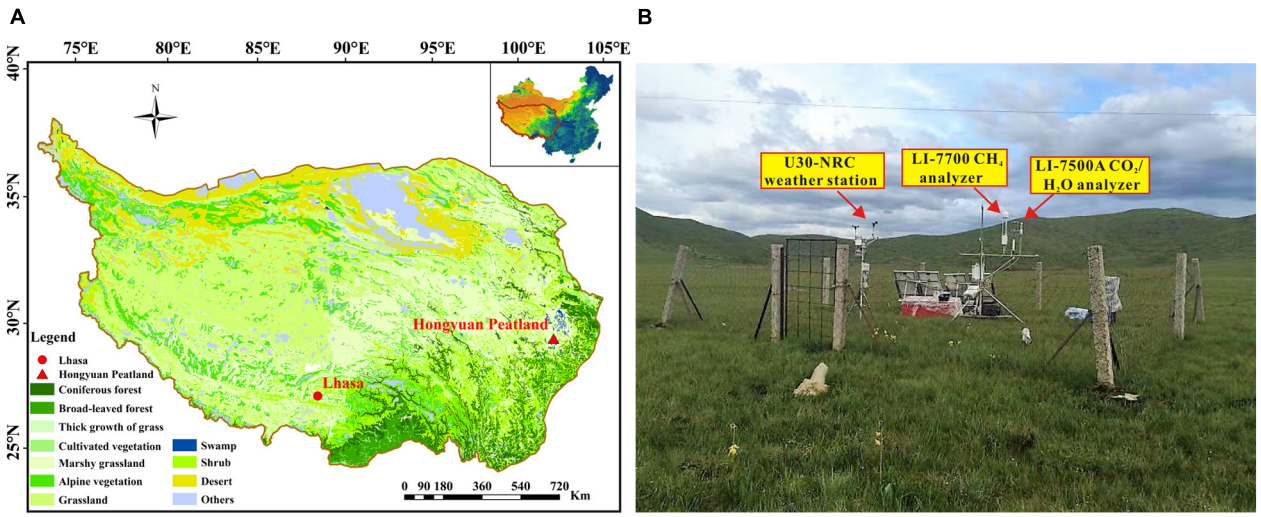

FIGURE 1 | (A) Vegetation types on the QTP. The red triangle represents the location of the site. The data was retrieved from the Data Center for Resources and Environmental Sciences of Chinese Academy of Sciences (http://www.csdb.cn); **(B)** Landscape and instruments at the Hongyuan Peatland Carbon Flux Monitoring and Research Station.

of the Hongyuan peatland, where the terrain is flat and serves as an ideal place for micrometeorological flux measurements. The flux footprint analysis indicated that 90% of the CO_2 flux originated from an area within 200 m of the EC tower, demonstrating that the measured fluxes are representative of the Hongyuan peatland area.

Flux Measurements

The eddy covariance system consists of a Gill WindMaster (Pro) three-dimensional (3-D) ultrasonic anemometer (Gill Instruments Ltd., Lymington, Hampshire, United Kingdom), which measures 3-D wind velocities and virtual air temperatures, and an open path infrared CO_2/H_2O gas analyzer (LI-7500A, LI-COR, United States), which measures concentrations of CO_2 and water vapor. The EC system was installed on a tripod tower 2.5 m above canopy (**Figure 1B**). The height of the EC system above ground was determined by the maximum height of vegetation during the growing season. To avoid water accumulation on the lens, the LI-7500A sensor was tilted 10° in the main wind direction. The raw data were recorded at a frequency of 10 Hz and stored as separate files by a data logger (LI-COR Inc., United States).

Environmental Factors

Meteorological variables, including air temperature (Ta), soil temperature (Ts), soil water content (SWC), global radiation (Rg), relative humidity (RH) and precipitation (PPT), were monitored on every half-hour basis using a HOBO U30-NRC (Onset Computer Corporation, United States) weather station installed near the EC tower (**Figure 1**). Ts was measured at depths of 10 cm, 25 cm, and 40 cm below the ground. Ta was measured at a height of 2 m above the ground, with a 12-Bit Temp Smart Sensor (S-TMB-M006, Onset Computer Corporation, United States). Vapor pressure deficit (VPD) was calculated using the Ta and RH measurements. SWC was measured at a depth of 10 cm below the ground using a 10 HS Soil Moisture Smart Sensor (S-SMD-M005, Onset Computer Corporation, United States). Wind direction and speed were measured using smart sensors (S-WSA-M003, Onset Computer Corporation, United States; S-WDA-M003, Onset Computer Corporation, United States). Solar radiation was measured using a silicon pyranometer sensor (S-LIB-M003, Onset Computer Corporation, United States). PPT was measured using a rainfall smart sensor (S-RGB-M002, Onset Computer Corporation, United States). Water table level was observed using a ZKGD3000-M digital water level gauge (Beijing Zhongke Guangda Automation Technology, China) in a 2-m deep hydrological well near the EC tower.

Data Processing

The EddyPro software version 6.2.0 (LI-COR, Inc., United States) was used to process raw data to obtain 30-min fluxes for analysis and recording. The main calculation procedures include cross wind correction of the sonic temperature (Liu et al., 2001), double coordinate rotation (Wilczak et al., 2001), Webb-Pearman-Leuning (WPL) correction (Webb et al., 1980), time lag compensation, statistical testing (Vickers and Mahrt, 1997), spectral correction (Moncrieff et al., 1997) and a footprint analysis (Kljun et al., 2004).

After the data-processing in EddyPro, the following steps were used to filter out the abnormal flux data based on sensor malfunctions and stable atmospheric conditions. First, poor quality fluxes with flag 2 (bad quality) were discarded (Foken et al., 2004). Second, in order to avoid the underestimation of nighttime NEE under calm climate conditions, the friction velocity (u^*) threshold was determined by the BGC-jean online gap-filling tool (BGC16, Sect. 3) (Wutzler et al., 2018). In this study, all CO_2 fluxes were excluded from analysis when $u^* < 0.091$ m s^{-1}. Finally, an outlier detection method was used

to filter out occasional spikes based on the method reported in Papale et al. (2006). In this method, each 30 min CO_2 flux NEE_i corresponds to a value d_i, which is calculated as:

$$d_i = (NEE_i - NEE_{i-1}) - (NEE_{i+1} - NEE_i) \quad (1)$$

Accordingly, NEE_i is flagged as spike if:

$$d_i < Md - (z \cdot MAD/0.6745) \quad (2)$$

or

$$d_i = Md + (z \cdot MAD/0.6745) \quad (3)$$

where

$$\text{MAD} = \text{median}\left(\left|d_i - Md\right|\right) \quad (4)$$

Md is the median of the differences; z is a threshold value, which equals to 5.5 in this study. Following the micrometeorology convention, negative NEE values indicate a net uptake of CO_2 by the peatland while positive NEE values represent a net release to the atmosphere.

After applying the QA/QC criteria, ∼60% of the original measurements remained in the dataset. To obtain the NEE of a continuous time series, the REddyProcWeb online tool[2] was used to fill gaps and to partition NEE into gross primary production (GPP) and ecosystem respiration (R_{eco}) (**Figure 5**; Wutzler et al., 2018).

The Q_{10} value is used to describe the magnitude of the respiratory rate variation with a temperature change of 10°C. The Q_{10} based equation is as follows (Reichstein et al., 2002):

$$Q_{10} = e^{10b} \quad (5)$$

Where b is obtained from the model $R_{eco} = ae^{bT}$ (Xu and Baldocchi, 2004). T is the daily average soil temperature (at a depth of 10 cm below the ground) during the nighttime; R_{eco} is the daily averaged ecosystem respiration.

The Normalized Difference Vegetation Index (NDVI) has a good correlation with vegetation leaf area index (LAI) and biomass (Deng et al., 2006; Zhang et al., 2010); therefore, the NDVI can be used as an indicator of green area in Landsat imagery. NDVI was obtained from Landsat surface reflectance product [Landsat 7 ETM+ (30 m) and Landsat 8 OLI (30 m)], downloaded from the United States Geological Survey (USGS) EarthExplorer[3]. The Landsat imagery has been preprocessed with atmospheric correction and topographic correction before the analysis (Hwang et al., 2011). The effect of clouds and cirrus on reflectance was excluded (Zhou et al., 2016).

The Division of Seasons

In order to explore the seasonal variation of CO_2 flux, the seasons were divided into four time periods according to different biophysical conditions, including (1) the growing season, which starts from the first day of seven consecutive days when the daily average Ta is higher than 5°C and ends on the first day of seven consecutive days when the daily average Ta is lower than 5°C (Lund et al., 2010), (2) soil freezing, from the last day of the growing season to a day when the daily average Ts of two consecutive days is lower than 0°C, (3) soil thawing, between the growing season and winter (Lund et al., 2010), and (4) winter, from the last day of the soil freezing period to the day when the Ts is above 0°C. Non-growing season comprises soil thawing, soil freezing, and winter periods (**Table 1**).

Wavelet Analysis

Continuous wavelet transform (CWT) with the Morlet wavelet was used to investigate the spectral characteristics of NEE and environmental variables. The Morlet wavelet is composed of a real part and an imaginary part, which makes it easy to analyze amplitude and phase, respectively (Grinsted et al., 2004). Wavelet spectral analysis is a more powerful tool for analyzing time series with non-stationary (including trace-gas flux data measured by eddy covariance), compared to the Fourier analysis (Vargas et al., 2010; Hatala et al., 2012). The wavelet coherence spectrum is expressed as the local correlation between two variables in frequency-time space, and its high coherence indicates a phase-locked behavior between two time series (Grinsted et al., 2004). For time periods with significant wavelet coherence, we used the phase angle to judge the time lag between the correlation oscillations of the two sequences (Hatala et al., 2012). To avoid spurious correlations between NEE and environmental variables, missing values were filled with median values before and after the gap. All wavelet analyses were performed in MATLAB (R2016a, MathWorks Inc., United States).

RESULTS

Environmental Conditions

During the observation period, the Hongyuan peatland was characterized by strong variations in temperature (Ta and Ts), SWC, PPT, VPD, and photosynthetically active radiation (PAR) (**Figure 2**). Most of precipitation in this area occurred during the growing season when the sunshine was abundant and temperature was high (**Figures 2B,C**). Such climate conditions are conducive to plant growth and residue accumulation, which is beneficial for the development of peatlands. The daily mean Ta ranged from −15.6 to 15.8°C in 2014 and −18.1 to 16.4°C in 2015 (**Figure 2A**). The mean annual Ta was 2.8 and 2.7°C in 2014 and 2015, respectively. Ts at different depths showed similar seasonal patterns during the observation period, with its maximum values (at a depth of 10 cm) appearing around late June and early June in 2014 and 2015, respectively (**Figure 2B**). The daily mean PAR in the growing season was 420 μmol photons m^{-2} s^{-1} in 2014 and 443 μmol photons m^{-2} s^{-1} in 2015, which was higher than that in the non-growing season (338 μmol photons m^{-2} s^{-1} in 2014 and 358 μmol photons m^{-2} s^{-1} in 2015) (**Figure 2E**). The maximum monthly PAR of the growing season in both years occurred in July. Annual precipitation was 794.8 and 586.8 mm in 2014 and 2015, with most of the precipitation occurring during the growing season (**Figure 2C**). There also existed significant differences of monthly precipitation sums during the growing season in these 2 years. The maximum rainfall

[2]https://www.bgc-jena.mpg.de/bgi/index.php/Services/REddyProcWeb
[3]http://earthexplorer.usgs.gov/

TABLE 1 | Cumulative NEE, GPP, and R_{eco} and daily mean of NEE, GPP, and R_{eco} (g C m^{-2}) in 2014 and 2015.

Period	Year	Total NEE	Total GPP	Total R_{eco}	Daily mean NEE	Daily mean GPP	Daily mean R_{eco}	Number of days
Growing season	2014	−279.96	783.55	503.59	−1.64	4.58	2.95	171
	2015	−260.43	649.66	389.23	−1.68	4.19	2.51	155
Soil freezing	2014	23.56	57.09	80.65	0.38	0.92	1.30	62
	2015	35.53	64.32	99.85	0.50	0.90	1.40	71
Winter	2014	22.16	23.46	45.62	0.24	0.25	0.48	94
	2015	21.82	42.16	63.98	0.25	0.48	0.73	87
Soil thawing	2014	7.63	33.88	41.51	0.20	0.89	1.09	38
	2015	17.73	20.70	38.43	0.34	0.40	0.88	52

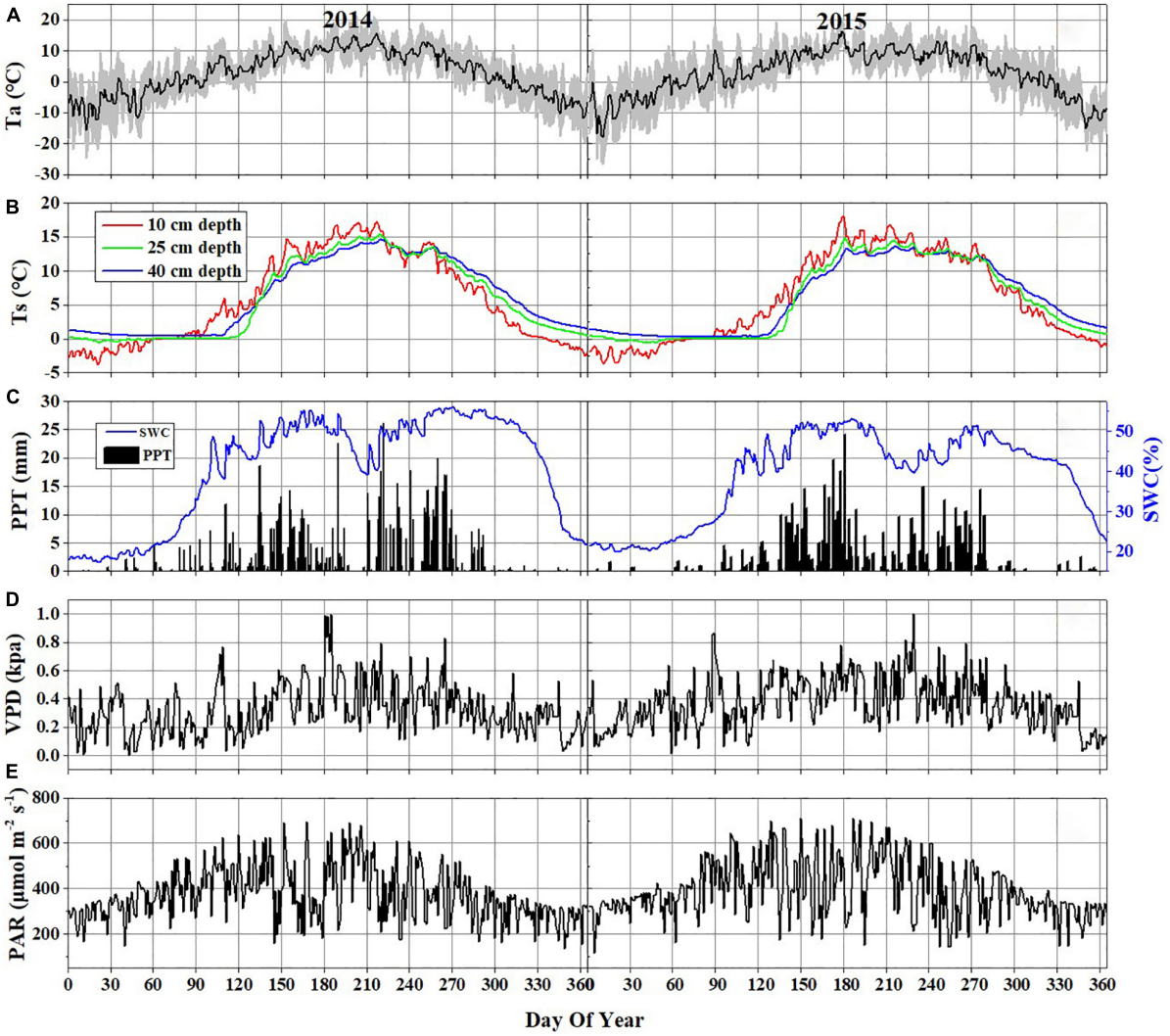

FIGURE 2 | Daily variations of major environmental variables in 2014 and 2015: **(A)** air temperature (Ta) at 2 m above the ground (the black line represents daily means and the shaded area denotes standard deviation for each half-hour interval); **(B)** soil temperature (Ts) at 10 cm (blue line), 25 cm (green line), and 40 cm (red line) below the ground; **(C)** daily precipitation (PPT) and daily mean soil water content (SWC) at 10 cm depth below the ground; **(D)** daily mean VPD; **(E)** daily mean PAR.

occurred in September of 2014 (191.4 mm) and in June of 2015 (174.8 mm). The variations in precipitation and temperature in these 2 years had obvious effects on SWC (**Figures 2A,C**). The seasonal pattern of SWC in 2014 was similar to that in 2015 (**Figure 2C**). However, a higher SWC value in 2014 was observed due to more precipitation than in 2015. The SWC remained

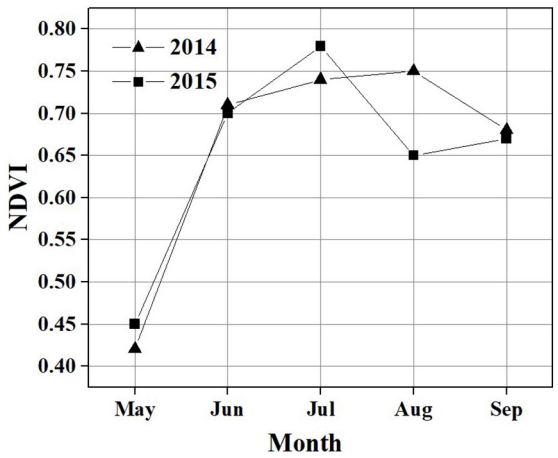

FIGURE 3 | Monthly variation in NDVI during the growing season in 2014 and 2015.

below 20% before the rainy season began in late April in each year. Due to a sudden drop in rainfall in July 2014, the SWC decreased to ≤ 45%. The daily mean VPD exhibited similar seasonal patterns in both years, with high values (0.41 kPa in 2014 and 0.47 kPa in 2015) during the growing season and low values (0.24 kPa in 2014 and 0.29 kPa in 2015) during the non-growing season (**Figure 2D**). Overall, the VPD values in 2015 were higher than those in 2014. The maximum NDVI was 0.75 in August 2014 and 0.78 in July 2015. The NDVI from June to August in 2014 was significantly higher than that in 2015 (**Figure 3**). The mean NDVI was 0.658 and 0.65 during the growing season of 2014 and 2015, respectively.

Diurnal Variations in Net Ecosystem CO_2 Exchange

The NEE showed a clear diurnal pattern during the non-growing season in 2014 and 2015, with a negative value occurring between 10:00–16:00 (**Supplementary Figure 1A**). The CO_2 flux in this period varied from -0.64 ± 0.19 (mean ± standard error) to 0.84 ± 0.13 μmol m^{-2} s^{-1} in 2014 and from -0.65 ± 0.21 to 1.28 ± 0.17 μmol m^{-2} s^{-1} in 2015. This may be attributed to that weak photosynthesis still existed in the early stage of soil freezing. However, due to the short duration and small absolute value of NEE, the Hongyuan peatland acted as a weak carbon source during this period. In the growing seasons, the NEE showed a significant diurnal variation pattern, with a negative value occurring between 7:00–19:00 (**Figure 4A**), during which the CO_2 uptake rate started to increase at around 7:00, reached a peak value of -8.1 ± 0.34 μmol m^{-2} s^{-1} at 12:30, and then decreased to -0.75 ± 0.11 μmol m^{-2} s^{-1} at 19:00. After 19:00, the Hongyaun peatland started to release CO_2 into the atmosphere, with a peak value of 2.8 ± 0.07 μmol m^{-2} s^{-1} occurring at 21:00. Clear diurnal variation patterns were also observed in PAR (**Figure 4B**), SWC (**Figure 4C**), VPD (**Figure 4D**), Ta (**Figure 4E**), and Ts-10 (**Figure 4F**) in these 2 years. But there are no strong diurnal patterns in Ts-25 (**Supplementary Figure 1B**) and Ts-40 (**Supplementary Figure 1C**). The peak NEE value appeared earlier than VPD, Ta and Ts, later than SWC, but coincides with PAR. Nonetheless, these diurnal variation patterns are calculated based on the average and standard error of the seasonal time scale, and thus cannot represent their real-time fluctuations. Therefore, wavelet analysis is used to reveal short-time scale changes in NEE and environmental variables.

Seasonal Variations in Net Ecosystem CO_2 Exchange

The seasonal variations in NEE showed similar patterns in 2014 and 2015 (**Figure 5**), with the maximum CO_2 uptake (-4.92 and -4.96 g C m^{-2} d^{-1} in 2014 and 2015, respectively) in late July, and the minimum CO_2 uptake (0.001 and 0.003 g C m^{-2} d^{-1} in 2014 and 2015, respectively) in early January, which are consistent with the variations in Ta and Ts-10 (**Figures 2A,B**). During the growing seasons, the daily NEE became slightly negative since late May, reached minimum value in late July, and then increased through August and September. However, there were more days (171 days) during the growing season in 2014 than those in 2015 (155 days) (**Table 1**). Thus, the total NEE during the growing season in 2014 (-279.96 g C m^{-2}) was higher than that in 2015 (-260.43 g C m^{-2}) (**Table 1**). No significant fluctuation in CO_2 flux was observed during soil freezing, winter and soil thawing (**Figure 5**). At the beginning of rainy season in 2014 and 2015, both GPP and R_{eco} started to increase significantly. Daily R_{eco} displayed relatively smooth seasonal pattern with the range of 1.09–5.11 and 0.94–4.7 g C m^{-2} d^{-1} during the growing seasons in 2014 and 2015, respectively. GPP showed a similar seasonal variation pattern to NEE. The maximum daily GPP occurred in July, with the values of 7.2 g C m^{-2} d^{-1} in 2014 and 9.2 g C m^{-2} d^{-1} in 2015.

During the soil freezing period, the cumulative NEE was 23.56 g C m^{-2} in 2014 and 35.53 g C m^{-2} in 2015. In the winter, the NEE remained at a constantly low level, with mean values of 0.24 and 0.25 g C m^{-2} d^{-1} in 2014 and 2015, respectively. And the cumulative NEE was 22.16 g C m^{-2} in 2014 and 21.82 g C m^{-2} in 2015. In the soil thawing period, the daily mean NEE was 0.20 and 0.34 g C m^{-2} d^{-1} in 2014 and 2015, respectively. The cumulative NEE, R_{eco}, and GPP over the 2 years were -226.61, 671.37, and 897.98 g C m^{-2} in 2014, and -185.35, 591.49, and 776.84 g C m^{-2} in 2015 (**Supplementary Figure 2**).

Variations in Net Ecosystem CO_2 Exchange and Environmental Factors in the Time-Frequency Domain

The global wavelet power spectral of NEE, Ts-10, VPD, PAR and Ta all showed strong peaks at 1-day period (**Figure 6**). But a weak spectral energy peak was observed for SWC. The PAR also displayed a clear peak at the 0.5-day (i.e., diurnal) period, but the spectral energy peak was much lower than that at the 1-day period. Meanwhile, the PAR had relatively higher spectral energy peaks than other variables on the daily scale.

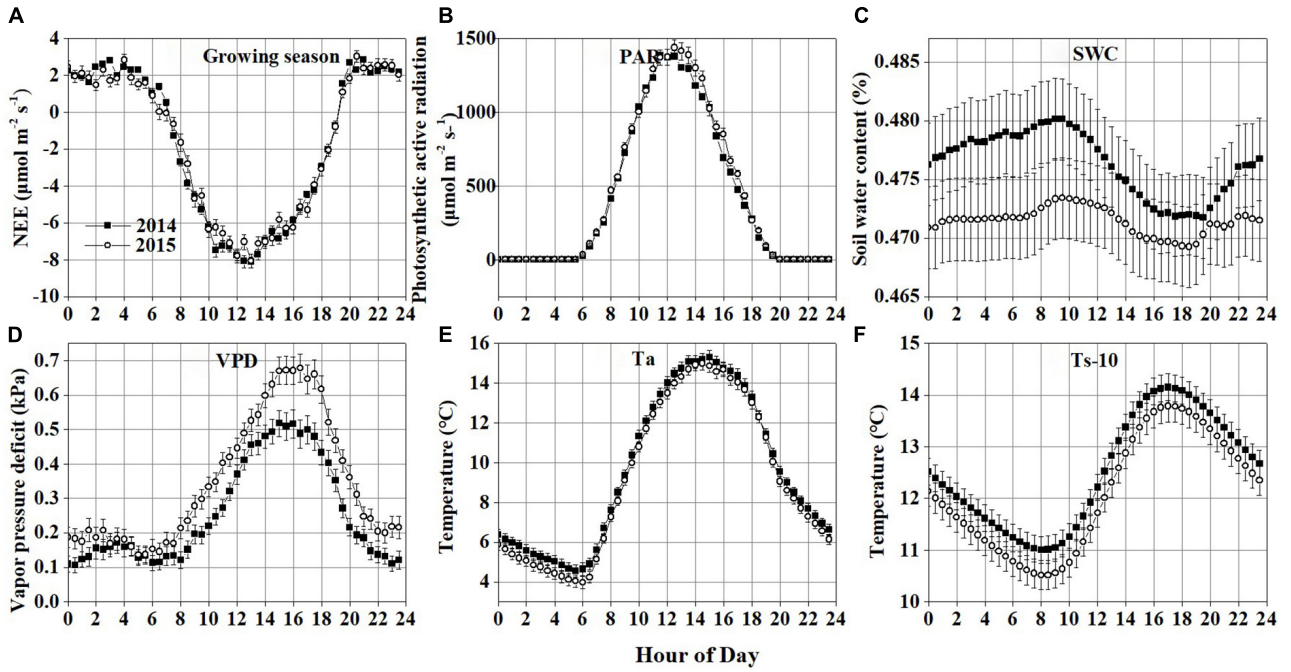

FIGURE 4 | Average diurnal variations during the growing season in 2014 and 2015: **(A)** net ecosystem CO_2 exchange (NEE) during the growing season; **(B)** photosynthetically active radiation (PAR); **(C)** soil water content (SWC); **(D)** vapor pressure deficit (VPD); **(E)** air temperature (Ta); **(F)** soil temperature at 10 cm depth below the ground (Ts-10). Error bars in all plots denote the standard errors. The time axes in the graph record Beijing time (UTC+8).

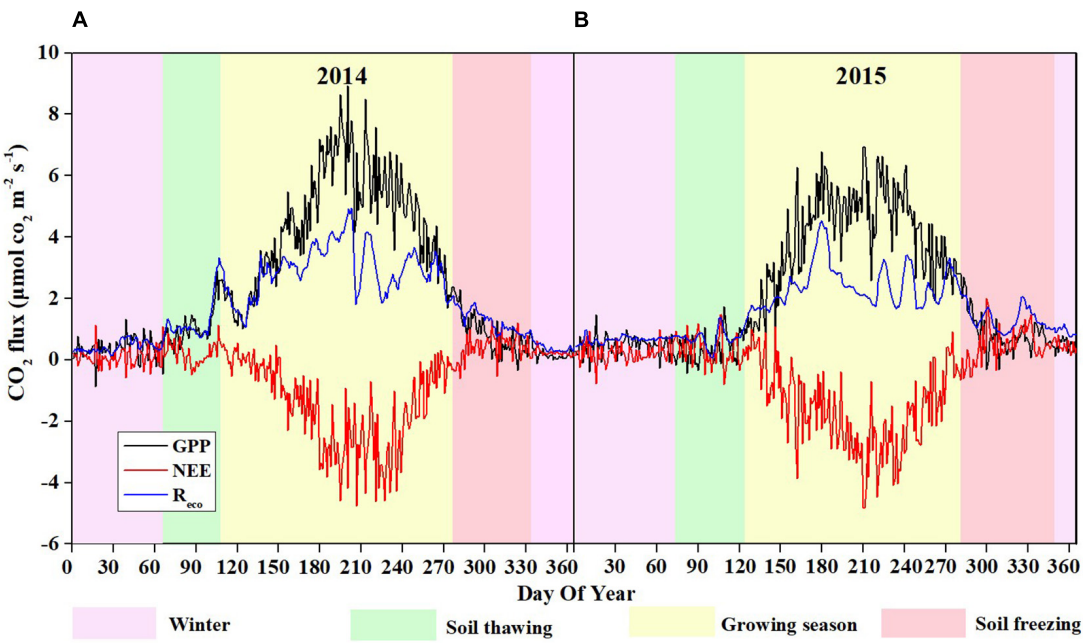

FIGURE 5 | Seasonal patterns of daily NEE, GPP, and R_{eco} in 2014 **(A)** and 2015 **(B)**.

Continuous wavelet transformation has revealed the local characteristics of NEE and environmental variables in the time-frequency domain (**Figure 7**). The diurnal variation of NEE was inconsistent throughout the growing season. The NEE oscillated strongly at 1-day period from early June to late September, while it oscillated weakly in May (**Figure 7A**). The areas of the significant wavelet power for PAR, VPD, SWC, Ta, and Ts (**Figures 7B–F**) corresponded to their spectral peaks in **Figure 6**.

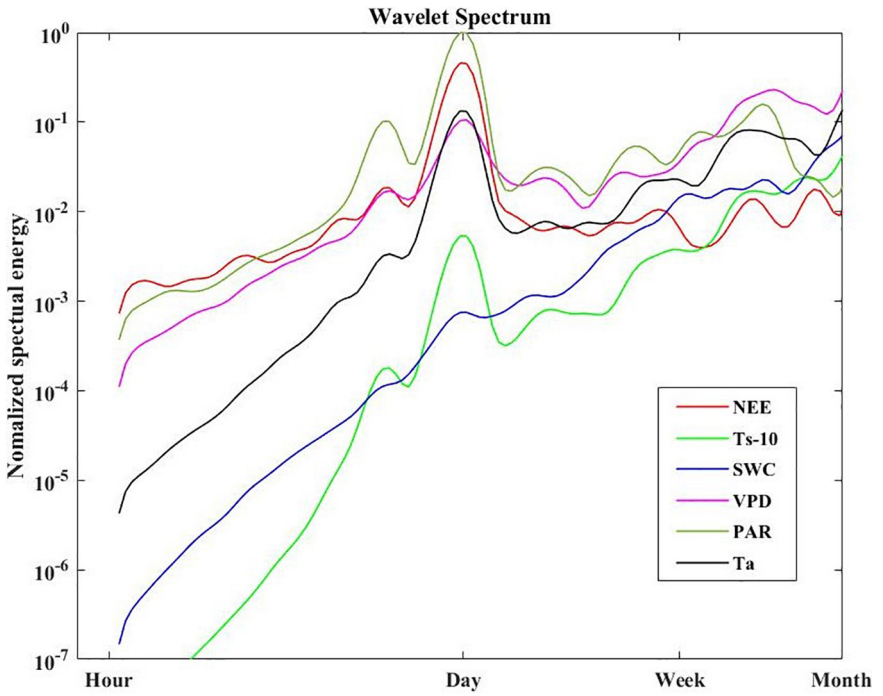

FIGURE 6 | Normalized global wavelet energy spectra for NEE, Ts-10, SWC, VPD, PAR, Ta.

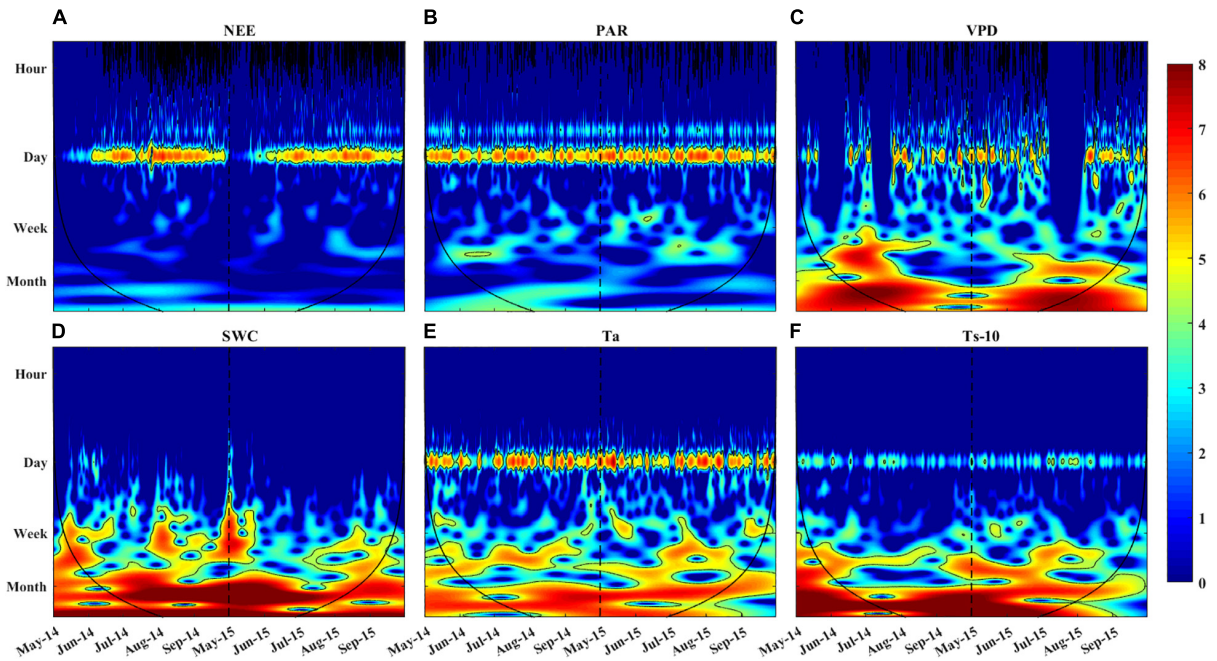

FIGURE 7 | Wavelet power spectrum for **(A)** NEE, **(B)** PAR, **(C)** VPD, **(D)** SWC, **(E)** Ta, and **(F)** Ts-10 during the growing season in 2014 and 2015. The black line represents the cone of influence, beyond which edge effects are abundant and thus the results should be interpreted with caution. The color codes for power values are from dark blue (low values) to dark red (high values). The dotted line is used to distinguish the growing season of 2014 and 2015.

We noted that the SWC, Ta, and Ts oscillated strongly at periods between weekly to monthly as indicated in the time-frequency domain.

The relationship between NEE and single environmental variable in the time-frequency domain could be described using the wavelet coherence (**Figure 8**). The patterns of correlation

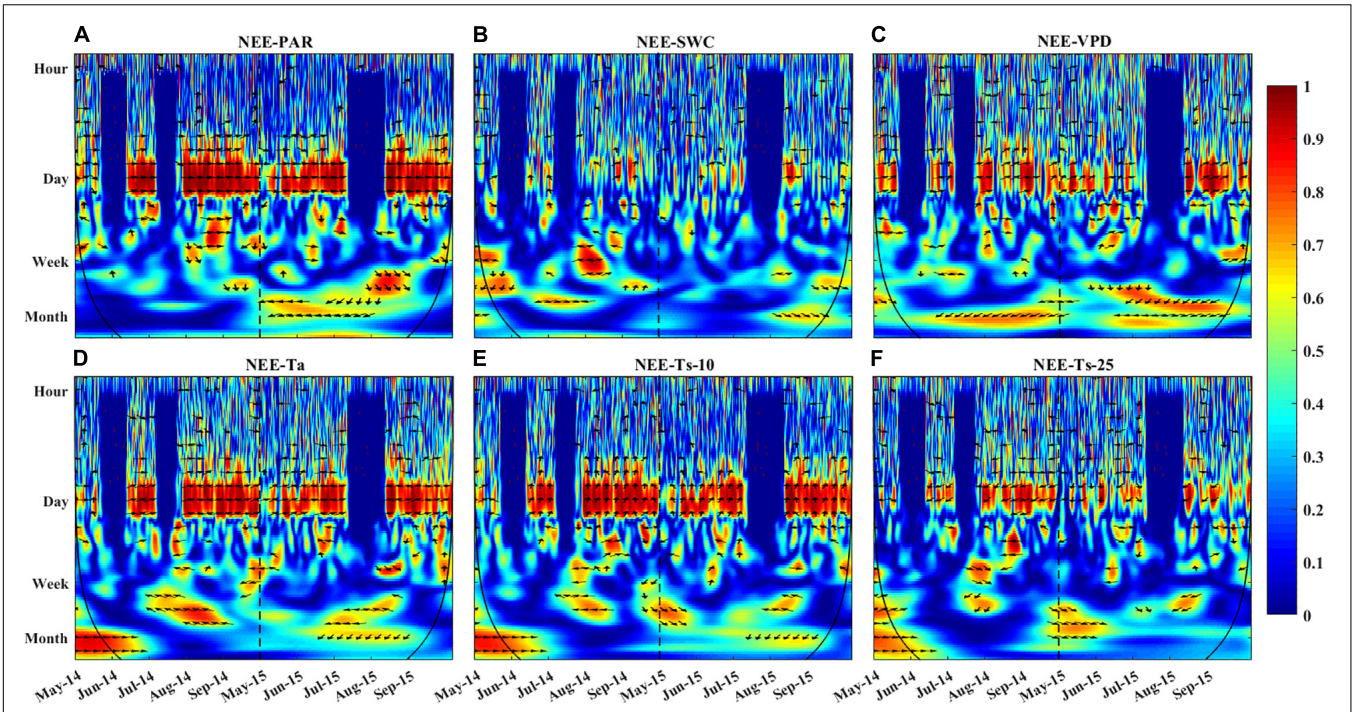

FIGURE 8 | Wavelet coherence between NEE and **(A)** PAR, **(B)** SWC, **(C)** VPD, **(D)** Ta, **(E)** Ts-10, and **(F)** Ts-25. Red color indicates a high correlation between NEE and variables on the given time scale. The direction of arrows represents phase shift between NEE and associated variables (right: NEE and variables are in phase, which means the series are perfectly correlated; up: NEE leads variable by $\pi/2$; left: NEE and variables are out of phase; down: NEE lags variable by $\pi/2$). The black line represents the cone of influence, beyond which edge effects are abundant and results should be interpreted with caution. The dotted line is used to distinguish the growing season of 2014 and 2015.

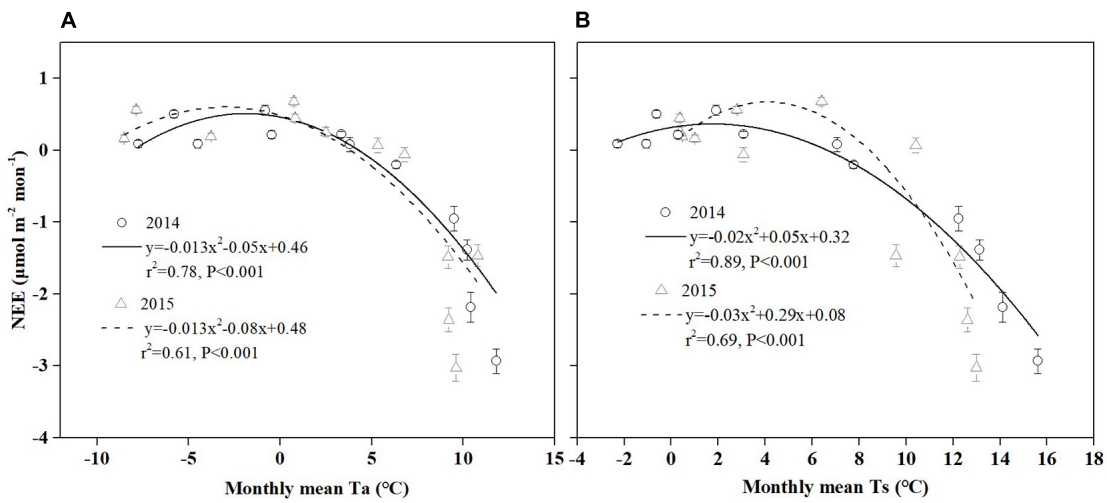

FIGURE 9 | The monthly relationship between NEE and temperature [**(A)** Ta, **(B)** Ts] during 2014 and 2015 in the Hongyuan peatland ecosystem. Error bars in all plots denote the standard errors.

between NEE and diverse variables (PAR, VPD, Ta, and Ts) were similar. However, the phase shift between the NEE flux and these variables was different, especially on shorter timescales. For example, all environmental variables showed obvious correlations with NEE on daily time scale, but only the fluctuations of PAR and NEE were synchronized (**Figure 8A**). Besides, the VPD, Ta, SWC, and Ts (**Figures 8B–F**) were all correlated with NEE from daily to seasonal timescales. But

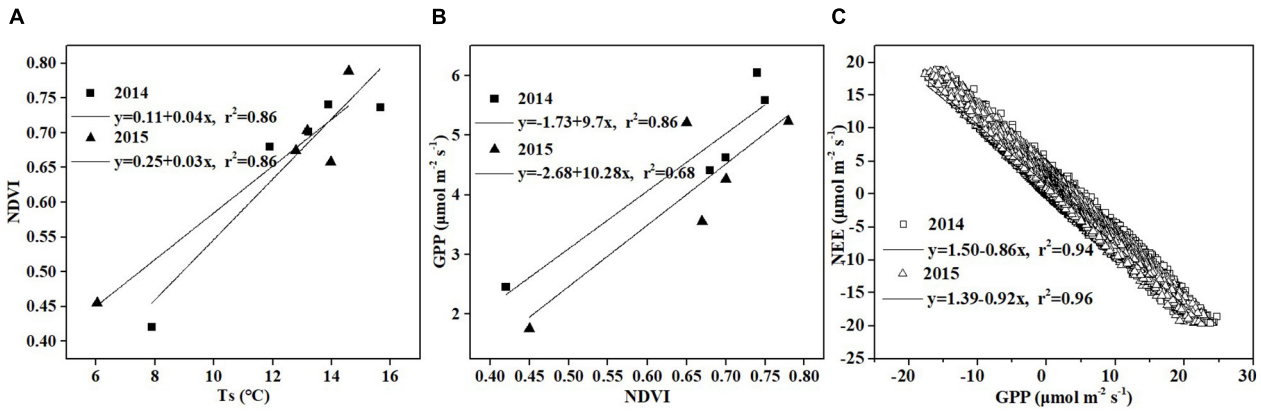

FIGURE 10 | Relationship between **(A)** Ts and NDVI, **(B)** NDVI and GPP, and **(C)** GPP and NEE.

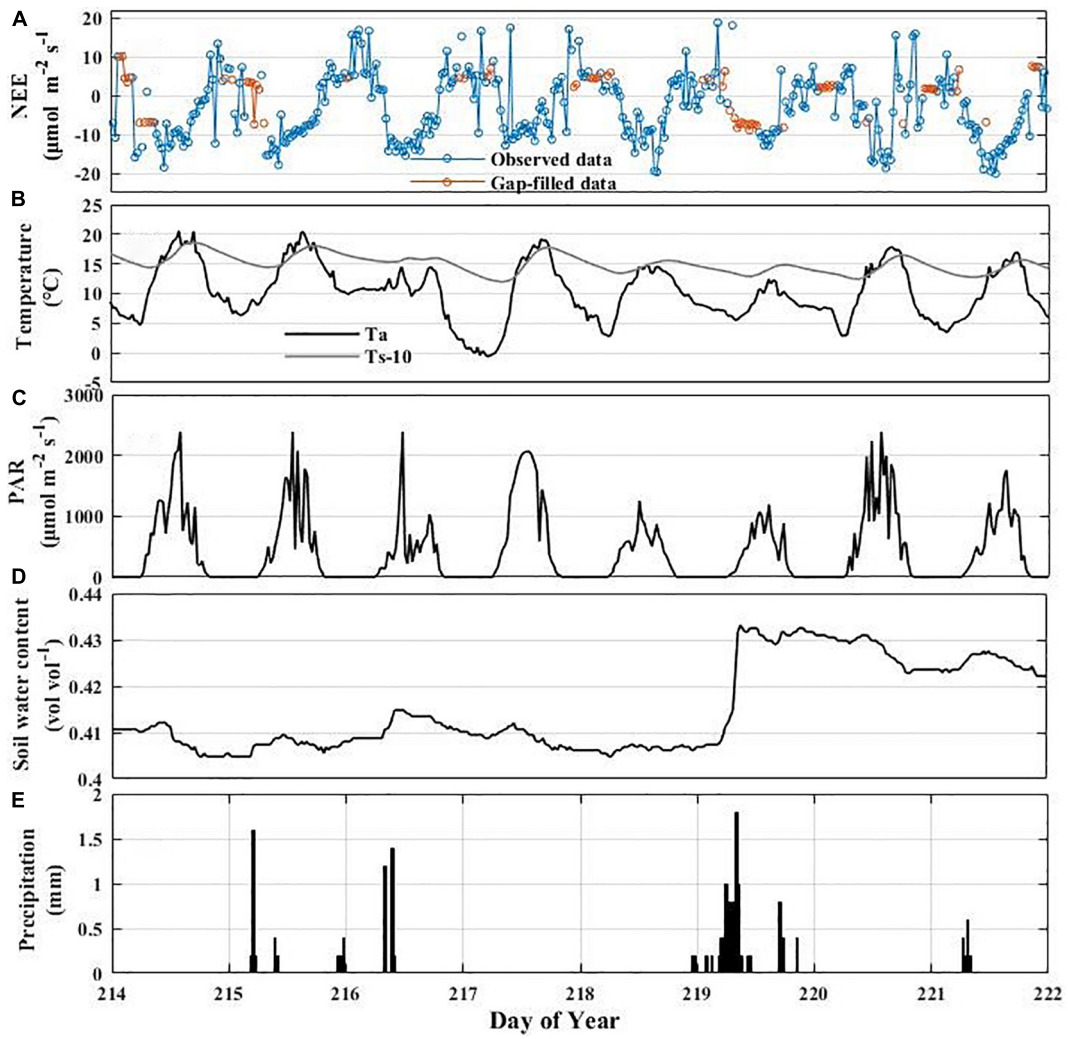

FIGURE 11 | Variation in NEE and environmental variables associated with rainfall events: synoptic variations of half-hourly NEE **(A)**, air temperature and soil temperature at 10 cm depth **(B)**, PAR **(C)**, soil water content (SWC) **(D)**, and precipitation (PPT) **(E)**.

strong coherencies occurred at the daily timescales, which were maintained for the duration of the growing season.

DISCUSSION

Diurnal Variation in Net Ecosystem CO_2 Exchange

The diurnal variation of NEE generally shows different patterns and magnitudes due to the diversity of vegetation types, climate conditions and underlying surface conditions (Vitale et al., 2007; Han et al., 2020; Zhu et al., 2020; D'Angelo et al., 2021). For example, a significant bimodal diurnal variation was observed in the coastal zone, where nearshore water served as an atmospheric CO_2 sink throughout the day (Chien et al., 2018). Previous studies have found that the pattern and magnitude of NEE were strongly regulated by Rg, VPD, and water use efficiency, which are important drivers of plant photosynthesis (Chapin et al., 2002; Vitale et al., 2007). In this study, a clear unimodal diurnal variation pattern occurred in the Hongyuan peatland during the observation period. This diurnal variation pattern is related to the variations in total solar radiation and PAR induced by the solar cycle throughout the day (Stoy et al., 2005; Zhao et al., 2006; Ouyang et al., 2014). Specially, the change of the solar altitude angle will shorten or extend the length of daylight. When the solar altitude angle is high and the PAR is strong (such as June and July) (**Figure 2E**), the duration of positive value will be short, while the duration of negative value will be long. On the other hand, during the early and late periods of the growing season (such as May or September) when the solar altitude angle is relatively low and the PAR is weak, the duration of the positive values will be longer, and the duration of the negative values will be shorter (Ouyang et al., 2014).

Wavelet coherence analysis showed that NEE was more tightly correlated with PAR than other environmental factors at the daily time scale (**Figure 8A**). PAR has more oscillating power than other environmental variables at the daily scale (**Figure 6**), which may transmit more variation to ecosystem function (e.g., NEE). Besides, the daily course of NEE precedes that of VPD, Ta, Ts-10 (**Figures 8C–E**), but lags that of Ts-25 (**Figure 8F**). Thus, PAR was considered to be the primary driver for NEE during the growing season at the diurnal time scale. Previous studies have also demonstrated that carbon absorption is largely affected by PAR (Yang et al., 2011; Jia et al., 2014), whereas carbon release is mainly controlled by temperature (Sha et al., 2021).

In addition, the maximum CO_2 uptake in the Hongyuan peatland was compared with that observed in other sites located at similar latitudes (**Supplementary Table 1**). We found that the maximum CO_2 uptake of the Hongyuan peatland (-12.3 and -12.2 μmol m^{-2} s^{-1} in 2014 and 2015, respectively) was similar to that measured in an alpine wetland in Southwest China (-12.3 μmol m^{-2} s^{-1}, Hao et al., 2011), but was higher than those in alpine steppe ecosystems (-3.44 μmol m^{-2} s^{-1}, Zhu et al., 2015; -3.4 μmol m^{-2} s^{-1}, Wang et al., 2018) and in alpine meadow ecosystems on the QTP (-3.74 μmol m^{-2} s^{-1}, Zhao et al., 2010; -8.3 μmol m^{-2} s^{-1}, Shi et al., 2006). This indicates that the alpine peatland has a higher potential of CO_2 uptake than the alpine meadow and alpine steppe ecosystems at similar elevation and latitude, which may be linked to aboveground biomass. The average aboveground biomass for the Ruoergai alpine peatland was 340 g m^{-2} (Ma et al., 2017), which was higher than that in alpine meadow ($\leq$151 g m^{-2}, Shi et al., 2006) and alpine steppe ($\leq$108 g m^{-2}, Zhu et al., 2015) ecosystems on the QTP. Han et al. (2013) also found that aboveground biomass showed significant negative relationship with NEE over a reed wetland. This probably occurred because the direct and indirect effects of biomass on plant physiological metabolism process through the photosynthesis and respiration. Firstly, to some extent, aboveground biomass was associated with photosynthetic capacity of plant (Han et al., 2013), therefore NEE was regulated by the amount of plant biomass (Larmola et al., 2003). Secondly, biomass is a good proxy for accounting for variation in both autotrophic and heterotrophic capacity for respiration (Tong et al., 2017) and therefore the variation in aboveground biomass regulated the variability in ecosystem respiration (Wohlfahrt et al., 2008). Lastly, aboveground biomass was related to the leaf area index (Wickland et al., 2001), which could affect NEE by controlling ecosystem light absorption capacity (Lund et al., 2010).

Seasonal and Interannual Variation in Net Ecosystem CO_2 Exchange

Due to the limitations of climate conditions and observation instruments, less attention has been paid to the CO_2 exchange during the non-growing season (Zhu et al., 2015; Shang et al., 2016; Xu et al., 2020). In this study, the annual NEE during the growing season in 2014 and 2015 was 1.2 times and 1.4 times of the annual total, respectively, indicating that the net carbon emission (53.35 g C m^{-2} in 2014 and 75.08 g C m^{-2} in 2015) during the non-growing seasons could not be ignored (**Table 1**). Considering that the total area of the undisturbed peatland in the Ruoergai region is 3,179 km^2 (Chen et al., 2014), the estimated total CO_2-C emission from the Ruoergai peatland during the non-growing season is about 0.17 Tg C, implying that the CO_2 flux in the non-growing season could not be ignored. The Q_{10} value during the non-growing season was estimated to be 3.32 in both 2014 and 2015, which was higher than that during the growing season (2.58 and 2.22 in 2014 and 2015, respectively). This suggests that CO_2 exchange during the non-growing season is more sensitive to warming than that in the growing season.

The length of the growing season had an important effect on CO_2 sequestration (Churkina et al., 2005; Loisel et al., 2012). Some studies found that a longer growing season resulted in a greater CO_2 uptake (Baldocchi et al., 2001; Euskirchen et al., 2006). However, others showed that a longer growing season lead to the net carbon loss of ecosystem (Hu et al., 2010; Piao et al., 2011; Wu et al., 2013). Our data revealed that the longer the growing season was, the greater the magnitude of CO_2 uptake became. In the Hongyuan peatland, the CO_2 uptake of the ecosystem would increase by 1.2 g C m^{-2} for each

additional day in the growing season. Similar phenomenon was also observed by Wu et al. (2020) over an alpine meadow in the northeastern edge of the QTP, China. Various biophysical factors (such as Ts, Ta, phenology) can influence the length of the growing season, and the factors are different in different kinds of ecosystems (Lund et al., 2010; Garrity et al., 2011). In the Hongyuan peatland, we thought that the Ts was the dominant factor. The average diurnal Ts in 2014 was about 0.42°C higher than that in 2015, resulting in the growing season in 2014 to arrive 2 weeks earlier than in 2015. This may be primarily due to earlier thaw of soil driven by higher temperature, which accelerated the vegetation activity (Euskirchen et al., 2006).

The inter-annual variation of NEE in wetland ecosystems could be affected by many factors, which vary with climate conditions or vegetation styles (Lafleur et al., 2003; Hao et al., 2011; Cao et al., 2017). In the Hongyuan peatland, the annual PPT was likely to be the main factor controlling the inter-annual variation of NEE. The annual PPT in 2014 was 35% more than that in 2015, and the ecosystem in 2014 fixed 22% more carbon than in 2015. This may be caused by the wet conditions that could increase the photosynthesis of vegetation and thus promoted the carbon sequestration capacity in an ecosystem (Trudeau et al., 2014). Other studies have also proposed that the carbon cycle in wetland ecosystems was dominated by PPT (Griffis and Rouse, 2001; Aslan-Sungur et al., 2016; Drollinger et al., 2019). A significant negative correlation of NEE with PPT in an arid desert wetland ecosystem has been established by Gou et al. (2017). And higher CO_2 uptake has been measured in a sedge fen during wet years, which was attributed to the higher photosynthetic capacity of the vegetation in wet years (Aurela et al., 2007). Sonnentag et al. (2010) suggested that the inter-annual variability of CO_2 fluxes in a minerotrophic fen was mainly controlled by soil water content and water table level.

Effect of Temperature on Net Ecosystem CO_2 Exchange

Temperature has a strong effect on photosynthesis and carbon sequestration of vegetation in alpine peatland ecosystem (Hao et al., 2011; Kang et al., 2018). Temperature has been thought to be one of the key environmental factors controlling the photosynthesis rate as the temperature has an important impact on plant dormancy, leaf phenology and late growth (Ueyama et al., 2013). In addition, temperature can influence soil microbial activity, enzyme activity and organic matter decomposition (Zhu et al., 2020). Our results showed that a significant correlation was observed between temperature (Ts and Ta) and NEE in Hongyuan alpine peatland, and higher temperature increased CO_2 uptake (**Figure 9**). The Ta and Ts could explain 70 and 79% of the variations in NEE, respectively, indicating that Ts has a stronger effect on CO_2 exchange in the Hongyaun peatland. Although previous studies of the CO_2 exchange in alpine wetlands have mentioned the importance of temperature (Cao et al., 2017; Zhu et al., 2020), such a clear correlation between NEE and Ts has not been described. The high dependence of NEE on Ts could be related to two factors. First, the belowground biomass accounts for a larger proportion relative to the aboveground biomass. In Ruoergai peatland, the belowground biomass (3,262.93 g m^{-2}) was about 10 times the aboveground biomass (341.01 g m^{-2}) (Ma et al., 2017). The fact that a large proportion of belowground biomass may lead to a high correlation between Ts and NEE (Ma et al., 2017). Second, the increase in Ts could cause the elevation of NDVI (**Figure 10A**), which in turn leads to high GPP (**Figure 10B**). Similar pattern was also observed over the northern high latitudes (Myneni et al., 1997) and the QTP (Shen et al., 2011). Our observation showed that NEE has a negative relationship with GPP, indicating that the ecosystem with higher GPP possibly has greater net CO_2 uptake (**Figure 10C**). This could be explained by the fact that high Ts can promote vegetation growth, thereby improving the photosynthesis and carbon sequestration capacity of vegetation.

Effects of Rain Pulses on Net Ecosystem CO_2 Exchange

The impact of rain pulses on NEE has also been well documented in many ecosystems (Aires et al., 2008; Hao et al., 2011). For example, Chou et al. (2008) suggested that the rain pulse had a crucial effect on regulating the CO_2 balance in grassland ecosystem. In this study, we found that rainfall events triggered the pulse dynamics of NEE in the Hongyuan peatland ecosystem (**Figure 11**). NEE started to increase significantly and even reached a positive value once the heavy rain occurred on DOY 219 (10 mm) (**Figures 11A,E**). Our result is consistent with experimental data in an alpine wetland on the QTP of Zhu et al. (2020) that found the increase of precipitation could accelerate the carbon loss. This may be caused by that rainwater penetration can quickly make the physical environment favorable to microbes and that the soil water produced by the rain pulse may displace the CO_2 stored in the soil pores. Another reason may be the decomposition, mineralization and release of inorganic carbon when the soil dries out due to lack of rain in summer and then is rewetted by precipitation (Jarvis et al., 2007).

The CO_2 uptake reached its maximum value 1–2 days after the rainfall events on DOY 219 and DOY 215–216 (**Figures 11A,E**). This may be linked to the environmental conditions that are optimum for carbon assimilation after rainfall events (**Figures 11B–D**). This finding agrees with the observations in other ecosystems. Jia et al. (2014) observed that the NEE peak lagged behind the rain pulse by 1–2 days in a semiarid shrubland. Similarly, it took 4–5 days to reach the maximum value after the rainfall events in a saline desert ecosystem (Liu et al., 2012). Furthermore, Aires et al. (2008) observed that heavy rainfall events could lead to the growth of C_4 grasses and the subsequent CO_2 sequestration in the Mediterranean grassland. Jarvis et al. (2007) has also confirmed that the enhancement of the ecosystem respiration and the hysteresis of the maximum NEE during rainfall events may be caused by the rapid response of soil organic matter and microorganisms. It is noteworthy that not all rain pulses have the same impacts on NEE (**Figure 11A**).

For example, NEE was relatively insensitive to a smaller rainfall event on DOY 221 (1.4 mm). This may be ascribed to other biophysical factors that confound the NEE response to sudden increases in water availability (Chen et al., 2009). Compared with the rainfall events on DOY 219, the rainfall events on DOY 221 have less effect on Ta, Ts, SWC, and PAR, which could explain the result that the DOY 221 rainfall events did not cause a large fluctuation in NEE.

CONCLUSION

This paper investigated the CO_2 fluxes observed during a 2-year period using the open-path eddy covariance method over an alpine peatland on the eastern Qinghai-Tibetan Plateau. Our results show that the Hongyuan alpine peatland was a CO_2 sink with an annual NEE of −226.61 and −185.35 g C m^{-2} in 2014 and 2015, respectively. The non-growing season NEE was 53.35 and 75.08 g C m^{-2} in 2014 and 2015, suggesting that non-growing seasons carbon emissions should not be neglected. Diurnal variation in NEE was observed during the growing season, with peak flux being recorded at 12:30 daily. In addition, we analyzed multi-scale dynamics and environmental controls on NEE in Hongyuan peatland. The spectral analysis showed how multiple environmental factors interact on different timescales and how their relative importance shifts during the growing season. PAR was the primary controlling factor of NEE on daily timescales. Seasonal variation in NEE was mainly driven by Ts. PPT was likely to be the main factor regulating the inter-annual variation in NEE. Our results provide important data for quantifying and modeling regional and global CO_2 budget from alpine peatlands.

DATA AVAILABILITY STATEMENT

The original contributions presented in the study are included in the article/**Supplementary Material**, further inquiries can be directed to the corresponding author/s.

AUTHOR CONTRIBUTIONS

HY performed conceptualization and writing – original draft. HP and BH performed conceptualization and writing – review and editing. YH and YZ performed conceptualization and resources. QG performed methodology. HD performed data curation. CC performed software. JC performed writing – review and editing. All authors contributed to the article and approved the submitted version.

FUNDING

This research was funded by the Strategic Priority Research Program of Chinese Academy of Sciences (Grant No. XDB40010300), the National Natural Science Foundation of China (Grant Nos. 41673119, 41773140, and 41907288), and the Science and Technology Foundation of Guizhou Province (Grant Nos. [2019]1317 and [2020]1Y193). HP would like to thank the Chinese Academy of Sciences' "Light of West China" Program and the CAS Scholarship for their financial support.

SUPPLEMENTARY MATERIAL

The Supplementary Material for this article can be found online at: https://www.frontiersin.org/articles/10.3389/fpls.2021.791343/full#supplementary-material

REFERENCES

Aires, L. M. I., Pio, C. A., and Pereira, J. S. (2008). Carbon dioxide exchange above a Mediterranean C3/C4 grassland during two climatologically contrasting years. *Glob. Change Biol.* 14, 539–555. doi: 10.1111/j.1365-2486.2007.01507.x

Ali, A. A., Ghaleb, B., Garneau, M., Asnong, H., and Loisel, J. (2008). Recent peat accumulation rates in minerotrophic peatlands of the Bay James region, Eastern Canada, inferred by Pb-210 and Cs-137 radiometric techniques. *Appl. Radiat. Isot.* 66, 1350–1358. doi: 10.1016/j.apradiso.2008.02.091

Aslan-Sungur, G., Lee, X. H., Evrendilek, F., and Karakaya, N. (2016). Large interannual variability in net ecosystem carbon dioxide exchange of a disturbed temperate peatland. *Sci. Total Environ.* 554-555, 192–202. doi: 10.1016/j.scitotenv.2016.02.153

Aubinet, M., Grelle, A., Ibrom, A., Rannik, Ü, Moncrieff, J., Foken, T., et al. (2000). Estimates of the annual net carbon and water vapor exchange of forests: the EUROFLUX methodology. *Adv. Ecol. Res.* 30, 113–175. doi: 10.1016/S0065-2504(08)60018-5

Aurela, M., Riutta, T., Laurila, T., Tuovinen, J. P., Vesala, T., Tuittila, E. S., et al. (2007). CO2 exchange of a sedge fen in southern Finland—the impact of a drought period. *Tellus* 59B, 826–837. doi: 10.1111/j.1600-0889.2007.00309.x

Baldocchi, D., Falge, E., Gu, L. H., Olson, R., Hollinger, D., Running, S., et al. (2001). FLUXNET: a new tool to study the temporal and spatial variability of ecosystem-scale carbon dioxide, water vapor, and energy flux densities. *Bull. Am. Meteorol. Soc.* 82, 2415–2434.

Cao, S. K., Cao, G. C., Feng, Q., Han, G. Z., Lin, Y. Y., Yuan, J., et al. (2017). Alpine wetland ecosystem carbon sink and its controls at the qinghai lake. *Environ. Earth Sci.* 76, 210. doi: 10.1007/s12665-017-6529-5

Chapin, F. S. III, Matson, P. A., and Mooney, H. A. (2002). "Carbon input to terrestrial ecosystems," in *Principles of Terrestrial Ecosystem Ecology*, eds P. A. Matson, F. S. Chapin III, and H. A. Mooney (New York, NY: Springer).

Chen, H., Yang, G., Peng, C. H., Zhang, Y., Zhu, D., Zhu, Q. A., et al. (2014). The carbon stock of alpine peatlands on the qinghai-tibetan plateau during the holocene and their future fate. *Q. Sci. Rev.* 95, 151–158. doi: 10.1016/j.quascirev.2014.05.003

Chen, J., Shen, M. G., and Kato, T. (2009). Diurnal and seasonal variations in light-use efficiency in an alpine meadow ecosystem: causes and implications for remote sensing. *J. Plant Ecol.* 2, 173–185. doi: 10.1093/jpe/rtp020

Chien, H., Zhong, Y. Z., Yang, K. H., and Cheng, H. Y. (2018). Diurnal variability of CO2 flux at coastal zone of Taiwan based on eddy covariance observation. *Cont. Shelf Res.* 162, 27–38. doi: 10.1016/j.csr.2018.04.006

Chou, W. W., Silver, W., Jackson, R. D., Thompson, A. W., and Allen-Diaz, B. (2008). The sensitivity of annual grassland carbon cycling to the quantity and timing of rainfall. *Glob. Change Biol.* 14, 1382–1394. doi: 10.1111/j.1365-2486.2008.01572.x

Churkina, G., Schimel, D., Braswell, B. H., and Xiao, X. M. (2005). Spatial analysis of growing season length control over net ecosystem exchange. *Glob. Change Biol.* 11, 1777–1787. doi: 10.1111/j.1365-2486.2005.001012.x

D'Angelo, B., Leroy, F., Guimbaud, C., Jacotot, A., Zocatelli, R., Gogo, S., et al. (2021). Carbon balance and spatial variability of CO2 and CH4 fluxes in a sphagnum-dominated peatland in a temperate climate. *Wetlands* 41:5. doi: 10.1007/s13157-021-01411-y

Deng, F., Chen, J. M., Plummer, S., Chen, M., and Pisek, J. (2006). Algorithm for global leaf area index retrieval using satellite imagery. *Int. J. Remote Sens.* 44, 2219–2229. doi: 10.1109/TGRS.2006.872100

Drollinger, S., Maier, A., and Glatzel, S. (2019). Interannual and seasonal variability in carbon dioxide and methane fluxes of a pine peat bog in the Eastern Alps, Austria. *Agric. For. Meteorol.* 275, 69–78. doi: 10.1016/j.agrformet.2019.05.015

Euskirchen, E. S., Mcguire, A. D., Kicklighter, D. W., Zhuang, Q., Clein, J. S., Dargville, R. J., et al. (2006). Importance of recent shifts in soil thermal dynamics on growing season length, productivity, and carbon sequestration in terrestrial high-latitude ecosystems. *Glob. Change Biol.* 12, 731–750. doi: 10.1111/j.1365-2486.2006.01113.x

Foken, T., Göckede, M., Mauder, M., Mahrt, L., Amiro, B., and Munger, W. (2004). "Post-field data quality control," in *Handbook of Micrometeorology*, eds B. Law, W. Massman, and X. Lee (Dordrecht: Springer), 181–208. doi: 10.1007/s11606-010-1529-0

Furon, A. C., Wagner-Riddle, C., Smith, C. R., and Warland, J. S. (2008). Wavelet analysis of wintertime and spring thaw CO2 and N2O fluxes from agricultural fields. *Agric. For. Meteorol.* 148, 1305–1317. doi: 10.1016/j.agrformet.2008.03.006

Garrity, S. R., Bohrer, G., Maurer, K. D., Mueller, K. L., Vogel, C. S., and Curtis, P. S. (2011). A comparison of multiple phenology data sources for estimating seasonal transitions in deciduous forest carbon exchange. *Agric. For. Meteorol.* 151, 1741–1752. doi: 10.1016/j.agrformet.2011.07.008

Gou, Q. Q., Wang, G. H., and Qu, J. J. (2017). Variation in NEE and its response to environmental factors in an extremely arid desert wetland ecosystem. *Contemp. Problems Ecol.* 10, 575–582. doi: 10.1134/S1995425517050043

Griffis, T. J., and Rouse, W. R. (2001). Modelling the interannual variability of net ecosystem CO2 exchange at a subarctic sedge fen. *Glob. Change Biol.* 7, 511–530. doi: 10.1046/j.1354-1013.2001.00403.x

Griffis, T. J., Rouse, W. R., and Waddington, J. M. (2000). Scaling net ecosystem CO2 exchange from the community to landscape-level at a subarctic fen. *Glob. Change Biol.* 6, 459–473. doi: 10.1046/j.1365-2486.2000.00330.x

Grinsted, A., Moore, J. C., and Jevrejeva, S. (2004). Application of the cross wavelet transform and wavelet coherence to geophysical time series. *Nonlinear Process. Geophys.* 11, 561–566. doi: 10.5194/npg-11-561-2004

Han, G. X., Yang, L. Q., Yu, J. B., Wang, G. M., Mao, P. L., and Gao, Y. J. (2013). Environmental controls on net ecosystem CO2 Exchange over a reed (*Phragmites australis*) wetland in the yellow river delta, China. *Estuar. Coasts* 36, 401–413. doi: 10.1007/s12237-012-9572-1

Han, L., Wang, Q. F., Chen, Z., Yu, G. R., Zhou, G. S., Chen, S. P., et al. (2020). Spatial patterns and climate controls of seasonal variations in carbon fluxes in China's terrestrial ecosystems. *Glob. Planet. Change* 189:103175. doi: 10.1016/j.gloplacha.2020.103175

Hao, Y. B., Cui, X. Y., Wang, Y. F., Mei, X. R., Kang, X. M., Wu, N., et al. (2011). Predominance of precipitation and temperature controls on ecosystem CO2 exchange in zoige alpine wetlands of southwest China. *Wetlands* 31, 413–422. doi: 10.1007/s13157-011-0151-1

Hatala, J. A., Detto, M., and Baldocchi, D. D. (2012). Gross ecosystem photosynthesis causes a diurnal pattern in methane emission from rice. *Geophys. Res. Lett.* 39:L06409. doi: 10.1029/2012GL051303

Helbig, M., Humphreys, E. R., and Todd, A. (2019). Constasting temperature sensitivity of CO2 exchange in peatlands of the husdson bay lowlands, Canada. *Biogeosciences* 124, 2126–2143. doi: 10.1029/2019JG005090

Hu, J., Moore, D. J. P., Burns, S. P., and Monson, R. K. (2010). Longer growing seasons lead to less carbon sequestration by a subalpine forest. *Glob. Change Biol.* 16, 771–783. doi: 10.1111/j.13652486.2009.01967.x

Hwang, T., Song, C., Bolstad, P. V., and Band, L. E. (2011). Downscaling real-time vegetation dynamics by fusing multi-temporal MODIS and Landsat NDVI in topographically complex terrain. *Remote Sens. Environ.* 115, 2499–2512. doi: 10.1016/j.rse.2011.05.010

Jarvis, P., Rey, A., Petsikos, C., Wingate, L., Rayment, M., Pereira, J., et al. (2007). Drying and wetting of Mediterranean soils stimulates decomposition and carbon dioxide emission: the "Birch effect". *Tree Physiol.* 27, 929–940. doi: 10.1093/treephys/27.7.929

Jia, X., Zha, T. S., Gong, J. N., Zhang, Y. Q., Wu, B., and Qin, S. G. (2018). Multi-scale dynamics and environmental controls on net ecosystem CO2 exchange over a temperate semiarid shrubland. *Agric. For. Meteorol.* 259, 250–259. doi: 10.1016/j.agrformet.2018.05.009

Jia, X., Zha, T. S., Wu, B., Zhang, Y. Q., Gong, J. N., Qin, S. G., et al. (2014). Biophysical controls on net ecosystem CO2 exchange over a semiarid shrubland in northwest China. *Biogeosciences* 11, 4679–4693. doi: 10.5194/bg-11-4679-2014

Kang, S. M., Yan, L., Cui, L. J., Zhang, X. D., Hao, Y. B., Wu, H. D., et al. (2018). Reduced carbon dioxide sink and methane source under extreme drought condition in an alpine peatland. *Sustainability* 10:4285. doi: 10.3390/su10114285

Kang, S., Xu, Y., You, Q., Flügel, W. A., Pepin, N., and Yao, T. (2010). Review of climate and cryospheric change in the Tibetan Plateau. *Environ. Res. Lett.* 5:015101. doi: 10.1088/1748-9326/5/1/015101

Kljun, N., Calanca, P., Rotach, M. W., and Schmid, H. P. (2004). A simple parameterisation for flux footprint predictions. *Boundlay Meteorol.* 112, 503–523. doi: 10.1023/B:BOUN.0000030653.71031.96

Koskinen, M., Minkkinen, K., Ojanen, P., Kamarainen, M., Laurila, T., and Lohila, A. (2014). Measurements of CO2 exchange with an automated chamber system throughout the year: challenges in measuring night-time respiration on porous peat soil. *Biogeosciences* 10, 14195–14238. doi: 10.5194/bgd-10-14195-2013

Lafleur, P., Roulet, N. T., Bubier, J. L., Frolking, S., and Moore, T. (2003). Interannual variability in the peatland- atmosphere carbon dioxide exchange at an ombrotrophic bog. *Glob. Biogeochem. Cycles* 2:1036. doi: 10.1029/2002GB001983

Larmola, T., Alm, J., Juutinen, S., Martikainen, P. J., and Silvola, J. (2003). Ecosystem CO2 exchange and plant biomass in the littoral zone of a boreal eutrophic lake. *Freshw. Biol.* 48, 1295–1310. doi: 10.1046/j.1365-2427.2003.01079.x

León, C. A., and Oliván, G. (2014). Recent rates of carbon and nitrogen accumulation in peatlands of Isla Grande de Chiloé-Chile. *Rev. Chil. Hist. Nat.* 87:26. doi: 10.1186/s40693-014-0026-y

Liu, H., Peters, G., and Foken, T. (2001). New equations for sonic temperature variance and buoyancy heat flux with an omnidirectional sonic anemometer. *Boundary Layer Meteorol.* 100, 459–468. doi: 10.1023/A:1019207031397

Liu, R., Li, Y., and Wang, Q. X. (2012). Variations in water and CO2 fluxes over a saline desert in western China. *Hydrol. Precess.* 26, 513–522. doi: 10.1002/hyp.8147

Loisel, J., Gallego-Sala, A. V., and Yu, Z. (2012). Global-scale pattern of peatland Sphagnum growth driven by photosynthetically active radiation and growing season length. *Biogeosciences* 9, 2737–2746. doi: 10.5194/bg-9-2737-2012

Lund, M., Lafleur, P. M., Roulet, N. T., Lindroth, A., Christensen, T. R., Aurela, M., et al. (2010). Variability in exchange of CO2 across 12 northern peatland and tundra sites. *Glob. Change Biol.* 16, 2436–2448. doi: 10.1111/j.1365-2486.2009.02104.x

Lupascu, M., Welker, J. M., Seibt, U., Xu, X., Velicogna, I., Lindsey, D. S., et al. (2014). The amount and timing of precipitation control the magnitude, seasonality and sources (14C) of ecosystem respiration in a polar semi-desert, NW Greenland. *Biogeosciences* 11, 2457–2496. doi: 10.5194/bgd-11-2457-2014

Ma, Q. F., Cui, L. J., Song, H. T., Gao, C. J., Hao, Y. Q., Luan, J. W., et al. (2017). Aboveground and belowground biomass relationships in the zoige peatland, eastern qinghai–tibetan plateau. *Wetlands* 37, 461–469. doi: 10.1007/s13157-017-0882-8

Moncrieff, J. B., Massheder, J. M., deBruin, H., Elbers, J., Friborg, T., Heusinkveld, B., et al. (1997). A system to measure surface fluxes of momentum, sensible heat, water vapour and carbon dioxide. *J. Hydrol.* 189, 589–611. doi: 10.1016/S0022-1694(96)03194-0

Myneni, R. B., Keeling, C. D., Tucker, C. J., Asrar, G., and Nemani, R. R. (1997). Increased plant growth in the northern high latitudes from 1981 to 1991. *Nature* 386, 698–702. doi: 10.1038/386698a0

Niu, S., Fu, Z., Luo, Y., Stoy, P. C., Keenan, T. F., Poulter, B., et al. (2017). Interannual variability of ecosystem carbon exchange: from observation to prediction. *Glob. Ecol. Biogeogr.* 26, 1225–1237. doi: 10.1111/geb.12633

Ouyang, Z. T., Chen, J. Q., Becker, R., Chu, H. S., Xie, J., Shao, C. L., et al. (2014). Disentangling the confounding effects of PAR and air temperature on net ecosystem exchange at multiple time scales. *Ecol. Complex.* 19, 46–58. doi: 10.1016/j.ecocom.2014.04.005

Page, S. E., and Baird, A. J. (2016). Peatlands and global change: response and resilience. *Annu. Rev. Environ. Resour.* 41, 35–57. doi: 10.1146/annurev-environ-110615-085520

Papale, D., Reichstein, M., Aubinet, M., Canfora, E., Bernhofer, C., Kutsch, W., et al. (2006). Towards a standardized processing of Net ecosystem exchange measured with eddy covariance technique: algorithms and uncertainty estimation. *Biogeosciences* 3, 571–583. doi: 10.5194/bg-3-571-2006

Pei, Z. Y., Ouyang, H., Zhou, C. P., and Xu, X. L. (2009). Carbon balance in an alpine steppe in the qinghai-tibet plateau. *J. Integr. Plant Biol.* 51, 521–526. doi: 10.1111/j.1744-7909.2009.00813.x

Peng, H. J., Hong, B., Hong, Y. T., Zhu, Y. X., Cai, C., Yuan, L. G., et al. (2015). Annual ecosystem respiration variability of alpine peatland on the eastern qinghai–tibet plateau and its controlling factors. *Environ. Monit. Assess.* 187, 1–9. doi: 10.1007/s10661-015-4733-x

Piao, S., Ciais, P., Lomas, M., Beer, C., Liu, H., Fang, J., et al. (2011). Contribution of climate change and rising CO2 toterrestrial carbon balance in East Asia: a multi-model analysis. *Glob. Planet. Change* 75, 133–142. doi: 10.1016/j.gloplacha.2010.10.014

Reichstein, M., Tenhunen, J. D., Roupsard, O., Ourcival, J. M., Rambal, S., Dore, S., et al. (2002). Ecosystem respiration in two mediterranean evergreen holm oak forests: drought effects and decomposition dynamics. *Funct. Ecol.* 16, 27–39. doi: 10.2307/826627

Sha, L. Q., Teramoto, M., Noh, N. J., Hashimoto, S. J., Yang, M., Sanwangsri, M., et al. (2021). Soil carbon flux research in the Asian region: review and future perspectives. *J. Agric. Meteorol.* 77, 24–51. doi: 10.2480/agrmet.D-20-00013

Shang, L. Y., Zhang, Y., Lyu, S. H., and Wang, S. Y. (2016). Seasonal and inter-annual variations in carbon dioxide exchange over an alpine grassland in the eastern qinghai-tibetan plateau. *PLoS One* 11:e0166837. doi: 10.1371/journal.pone.0166837

Shen, M., Tang, Y., Chen, J., Zhu, X., and Zheng, Y. (2011). Influences of temperature and precipitation before the growing season on spring phenology in grasslands of the central and eastern qinghai-tibetan plateau. *Agric. For. Meteorol.* 151, 1711–1722. doi: 10.1016/j.agrformet.2011.07.003

Shi, P. L., Sun, X. M., Xu, L. L., Zhang, X. Z., He, Y. T., Zhang, D. Q., et al. (2006). Net ecosystem CO2 exchange and controlling factors in a steppe- kobresia meadow on the tibetan plateau. *Sci. China Ser. D* 49, 207–218. doi: 10.1007/s11430-006-8207-4

Song, C. C., Sun, L., Huang, Y., Wang, Y. S., and Wan, Z. M. (2011). Carbon exchange in a freshwater marsh in the Sanjiang Plain, northeastern China. *Agric. For. Meteorol.* 151, 1131–1138. doi: 10.1016/j.agrformet.2011.04.001

Sonnentag, O., Kamp, G. V. D., Barr, A. G., and Chen, J. M. (2010). On the relationship between water table depth and water vapor and carbon dioxide fluxes in a minerotrophic fen. *Glob. Change Biol.* 16, 1762–1776. doi: 10.1111/j.1365-2486.2009.02032.x

Stoy, P. C., katul, G. G., Siqueira, M. B., Juang, J. Y., McCarthy, H. R., Kim, H. S., et al. (2005). Variability in net ecosystem exchange from hourly to inter-annual time scales at adjacent pine and hardwood forests: a wavelet analysis. *Tree Physiol.* 25, 887–902. doi: 10.1093/treephys/25.7.887

Tong, X., Li, J., Nolan, R. H., and Yu, Q. (2017). Biophysical controls of soil respiration in a wheat-maize rotation system in the North China Plain. *Agric. For. Meteorol.* 246, 231–240. doi: 10.1016/j.agrformet.2017.07.005

Trudeau, N. C., Garneau, M., and Pelletier, L. (2014). Interannual variability in the CO2 balance of a boreal patterned fen, James Bay, Canada. *Biogeochemistry* 118, 371–387. doi: 10.1007/s10533-013-9939-9

Ueyama, M., Iwata, H., Harazono, Y., Euskirchen, E. S., Oechel, W. C., and Zona, D. (2013). Growing season and spatial variations of carbon fluxes of Arctic and boreal ecosystems in Alaska (USA). *Ecol. Appl.* 23, 1798–1816. doi: 10.1890/11-0875.1

Vargas, R., Detto, M., Baldocchi, D. D., and Allen, M. F. (2010). Multiscale analysis of temporal variability of soil CO2 production as influenced by weather and vegetation. *Glob. Change Biol.* 16, 1589–1605. doi: 10.1111/j.1365-2486.2009.02111.x

Vickers, D., and Mahrt, L. (1997). Quality control and flux sampling problems for tower and aircraft data. *J. Atmos. Ocean. Technol.* 14, 512–526. doi: 10.1175/1520-0426(1997)014<0512:qcafsp>2.0.co;2

Vitale, L., Tommasi, P. D., Arena, C., Fierro, A., Santo, A. V. D., and Magliulo, V. (2007). Effects of water stress on gas exchange of field grown *Zea mays* L. in Southern Italy: an analysis at canopy and leaf level. *Acta Physiol. Plant.* 29, 317–326. doi: 10.1007/s11738-007-0041-6

Wang, J. F., Wang, G. X., Wang, Y. B., and Li, Y. S. (2007). Influence of the degradation of swamp and alpine meadows on CO2 emission during growing season on the qinghai-tibet plateau. *Chinese Sci. Bull.* 52, 2565–2574. doi: 10.1007/s11434-007-0343-5

Wang, L., Liu, H. Z., Shao, Y. P., Liu, Y., and Sun, J. H. (2018). Water and CO2 fluxes over semiarid alpine steppe and humid alpine meadow ecosystems on the tibetan plateau. *Theor. Appl. Climatol.* 131, 547–556. doi: 10.1007/s00704-016-1997-1

Wang, S. Y., Zhang, Y., Lü, S. H., and Shang, L. Y. (2016). Biophysical regulation of carbon fluxes over an alpine meadow ecosystem in the eastern tibetan plateau. *Geophys. Res. Abstr.* 60, 801–812. doi: 10.1007/s00484-015-1074-y

Ward, S., Ostle, N., Oakley, S., Quirk, H., Stott, A., Henrys, P. A., et al. (2012). Fire accelerates assimilation and transfer of photosynthetic carbon from plants to soil microbes in a northern peatland. *Ecosystems* 15, 1245–1257. doi: 10.1007/s10021-012-9581-8

Webb, E. K., Pearman, G. I., and Leuning, R. (1980). Correction of flux measurements for density effects due to heat and water vapour transfer. *Q. J. R. Meteorol. Soc.* 106, 85–100. doi: 10.1002/qj.49710644707

Wei, D., Ri, X., Wang, Y. H., Wang, Y. S., Liu, Y. W., and Yao, T. D. (2012). Responses of CO2, CH4 and N2O fluxes to livestock exclosure in an alpine steppe on the tibetan plateau, China. *Plant Soil* 359, 45–55.

Wickland, K. P., Striegl, R. G., Mast, M. A., and Clow, D. W. (2001). Carbon gas exchange at a southern Rocky Mountain wetland, 1996–1998. *Glob. Biogeochem. Cycles* 15, 321–335. doi: 10.1029/2000GB001325

Wilczak, J. M., Oncley, S. P., and Stage, S. A. (2001). Sonic anemometer tilt correction algorithms. *Boundary Layer Meteorol.* 99, 127–150. doi: 10.1023/A:1018966204465

Wilson, R. M., Hopple, A. M., Tfaily, M. M., Sebestyen, S. D., Schadt, C. W., Pfeifer-Meister, L., et al. (2016). Stability of peatland carbon to rising temperatures. *Nat. Commun.* 7:13723. doi: 10.1038/ncomms13723

Wohlfahrt, G., Anderson-Dunn, M., Bahn, M., Balzarolo, M., Berninger, F., Campbell, C., et al. (2008). Biotic, abiotic, and management controls on the net ecosystem CO2 exchange of European mountain grassland ecosystems. *Ecosystems* 11, 1338–1351. doi: 10.1007/s10021-008-9196-2

Wu, C., Chen, J. M., Black, T. A., Price, D. T., Kurz, W. A., Desai, A., et al. (2013). Interannual variability of net ecosystem productivity in forests is explained by carbon flux phenology in autumn. *Glob. Ecol. Biogeogr.* 22, 994–1006. doi: 10.1111/geb.12044

Wu, J. K., Wu, H., Ding, Y. J., Qin, J., Li, H. Y., and Liu, S. W. (2020). Interannual and seasonal variations in carbon exchanges over an alpine meadow in the northeastern edge of the qinghai-tibet plateau, China. *PLoS One* 15:e0228470. doi: 10.1371/journal.pone.0228470

Wutzler, T., Lucas-Moffat, A., Migliavacca, M., Knauer, J., Sickel, K., Šigut, L., et al. (2018). Basic and extensible post-processing of eddy covariance flux data with REddyProc. *Biogeosciences* 15, 5015–5030. doi: 10.5194/bg-15-5015-2018

Xu, L., and Baldocchi, D. D. (2004). Seasonal variation in carbon dioxide exchange over a Mediterranean annual grassland in California. *Agric. For. Meteorol.* 123, 79–96. doi: 10.1016/j.agrformet.2003.10.004

Xu, X. Y., Song, C. C., Sun, L., Wang, X. W., and Tan, W. W. (2020). Towards an improved utilization of eddy covariance data: growing season CO2 exchange from a permafrost peatland in the Great Hing'an Mountains, Northeast China. *Ecol. Indic.* 115:106427. doi: 10.1016/j.ecolind.2020.106427

Yamamoto, S., Saigusa, N., Ohtani, Y., Inoue, G., Hirano, T., and Fukushima, Y. (2001). "Present status of AsiaFlux network and a view toward the future," in *Proceedings of the AGU Fall Meeting Abstracts*, (Washington, DC: AGU), 404–407. doi: 10.1080/07303084.1989.10606343

Yang, F. L., Zhou, G. S., Hunt, J. E., and Zhang, F. (2011). Biophysical regulation of net ecosystem carbon dioxide exchange over a temperate desert steppe in inner mongolia, China. *Agric. Ecosyst. Environ.* 142, 318–328. doi: 10.1016/j.agee.2011.05.032

Yu, Z. C., Loisel, J., Brosseau, D. P., Beilman, D. W., and Hunt, S. J. (2010). Global peatland dynamics since the Last glacial maximum. *Geophys. Res. Lett.* 37, 69–73. doi: 10.1029/2010GL043584

Zhang, F. W., Liu, A. H., Li, Y. N., Li, I., Zhao, L., Wang, Q., et al. (2008). CO2 flux in alpine wetland ecosystem on the qinghai-tibetan plateau, China. *Acta Ecol. Sin.* 28, 453–462. doi: 10.1016/S1872-2032(08)60024-4

Zhang, W., Liu, C. Y., Zheng, X. H., Fu, Y. F., Hu, X. X., Cao, G. M., et al. (2014). The increasing distribution area of zokor mounds weaken greenhouse gas uptakes by alpine meadows in the qinghai-tibetan plateau. *Soil Biol. Biochem.* 71, 105–112. doi: 10.1016/j.soilbio.2014.01.005

Zhang, Z. J., Liu, Z. H., Guo, Y. F., and Zhai, J. (2010). Biomass modeling of different grassland types based on NDVI in Tibet. *Plateau Mountain Meteorol. Res.* 30, 43–47.

Zhao, L., Li, J., Xu, S., Zhou, H., Li, Y., Gu, S., et al. (2010). Seasonal variations in carbon dioxide exchange in an alpine wetland meadow on the qinghai-tibetan plateau. *Biogeosciences* 7, 1207–1221. doi: 10.5194/bg-7-1207-2010

Zhao, L., Li, Y. N., Xu, S. X., Zhou, H. K., Gu, S., Yu, G. R., et al. (2006). Diurnal, seasonal and annual variation in net ecosystem CO2 exchange of an alpine shrubland on qinghai-tibetan plateau. *Glob. Change Biol.* 12, 1940–1953. doi: 10.1111/j.1365-2486.2006.01197.x

Zhou, Y., Xiao, X., Qin, Y., Dong, J., Zhang, G., Kou, W., et al. (2016). Mapping paddy rice planting area in rice-wetland coexistent areas through analysis of Landsat 8 OLI and MODIS images. *Int. J. Appl. Earth Obs. Geoinf.* 46, 1–12. doi: 10.1016/j.jag.2015.11.001

Zhu, J. B., Zhang, F. W., Li, H. Q., He, H. D., Li, Y. N., Yang, Y. S., et al. (2020). Seasonal and interannual variations of CO2 fluxes over 10 years in an alpine wetland on the qinghai-tibetan plateau. *Biogeosciences* 125:e2020JG006011. doi: 10.1029/2020JG006011

Zhu, Z. K., Ma, Y. M., Li, M. S., Hu, Z. Y., Xu, C., Zhang, L., et al. (2015). Carbon dioxide exchange between an alpine steppe ecosystem and the atmosphere on the nam coarea of the tibetan plateau. *Agric. For. Meteorol.* 203, 169–179. doi: 10.1016/j.agrformet.2014.12.013

Conflict of Interest: The authors declare that the research was conducted in the absence of any commercial or financial relationships that could be construed as a potential conflict of interest.

Publisher's Note: All claims expressed in this article are solely those of the authors and do not necessarily represent those of their affiliated organizations, or those of the publisher, the editors and the reviewers. Any product that may be evaluated in this article, or claim that may be made by its manufacturer, is not guaranteed or endorsed by the publisher.

Copyright © 2022 Yao, Peng, Hong, Guo, Ding, Hong, Zhu, Cai and Chi. This is an open-access article distributed under the terms of the Creative Commons Attribution License (CC BY). The use, distribution or reproduction in other forums is permitted, provided the original author(s) and the copyright owner(s) are credited and that the original publication in this journal is cited, in accordance with accepted academic practice. No use, distribution or reproduction is permitted which does not comply with these terms.

frontiers in Plant Science

ORIGINAL RESEARCH
published: 07 January 2022
doi: 10.3389/fpls.2021.775015

Spatiotemporal Dynamics of the Carbon Budget and the Response to Grazing in Qinghai Grasslands

*Xiaotao Huang[1,2,3], Chunbo Chen[3,4], Buqing Yao[1,2,3], Zhen Ma[1,2,3] and Huakun Zhou[1,2,3]**

[1] Key Laboratory of Restoration Ecology for Cold Regions Laboratory in Qinghai, Northwest Institute of Plateau Biology, Chinese Academy of Sciences, Xining, China, [2] Key Laboratory of Adaptation and Evolution of Plateau Biota, Chinese Academy of Sciences, Xining, China, [3] University of the Chinese Academy of Sciences, Beijing, China, [4] State Key Laboratory of Desert and Oasis Ecology, Xinjiang Institute of Ecology and Geography, Chinese Academy of Sciences, Urumqi, China

Estimating the grassland carbon budget is critically important for ensuring that grassland resources are used sustainably. However, the spatiotemporal dynamics of the carbon budget and the response to grazing have not yet been characterized in Qinghai grasslands. Here, we estimated the gross primary productivity (GPP) and net ecosystem exchange (NEE) in Qinghai grasslands using the improved Biome-BGCMuSo model to characterize the spatiotemporal dynamics of the carbon budget and the response to grazing in this region from 1979 to 2018. The GPP of Qinghai grasslands fluctuated during the study period, with an average annual value of 118.78 gC/m^2. The NEE of Qinghai grasslands fluctuated from 1979 to 2018, with an average value of −5.16 gC/m^2. After 2,000, GPP increased, and NEE decreased in a fluctuating manner. There were clear regional differences in GPP and NEE. GPP was low in most areas of Qinghai, and GPP was high in eastern and southern Qinghai. The southern, southeastern, and northeastern parts of Qinghai were mainly carbon sinks, and the northwestern part of Qinghai and the region between the southeastern and northeastern parts of Qinghai were mainly carbon sources. Grazing generally decreased GPP and increased NEE in Qinghai grasslands from 1979 to 2018. There was spatial heterogeneity in the effect of grazing on GPP and NEE. Under grazing, GPP and NEE were significantly decreased mainly in eastern Qinghai, and GPP and NEE were significantly increased mainly in southern and eastern Qinghai. NEE was most affected by grazing in eastern Qinghai. The results of this study aid our understanding of the mechanism driving variation in the grassland carbon budget and provide new data that could be used to support local grassland management.

Keywords: spatiotemporal dynamics, gross primary productivity, net ecosystem exchange, grazing, model

OPEN ACCESS

Edited by:
Boris Rewald,
University of Natural Resources and Life Sciences Vienna, Austria

Reviewed by:
Dima Chen,
China Three Gorges University, China
Liming Ye,
Ghent University, Belgium

***Correspondence:**
Huakun Zhou
hkzhou@nwipb.cas.cn

Specialty section:
This article was submitted to Functional Plant Ecology, a section of the journal Frontiers in Plant Science

Received: *13 September 2021*
Accepted: *14 December 2021*
Published: *07 January 2022*

Citation:
Huang X, Chen C, Yao B, Ma Z and Zhou H (2022) Spatiotemporal Dynamics of the Carbon Budget and the Response to Grazing in Qinghai Grasslands. Front. Plant Sci. 12:775015. doi: 10.3389/fpls.2021.775015

INTRODUCTION

Quantitative assessment of the carbon budget of terrestrial ecosystems is essential for regional carbon sink management and the implementation of action plans for climate change mitigation (Webb et al., 2019; Giltrap et al., 2020; Li et al., 2020). Assessment of the spatiotemporal dynamics of the terrestrial ecosystem carbon budget is not only an important goal of research on ecosystems

and global change but is also key for achieving objectives set by the United Nations Framework Convention on climate change and global greenhouse gas management (Ford et al., 2016; Bakhtiari, 2018; Qiu et al., 2021). Gross primary productivity (GPP) is the amount of CO_2 that is taken up by plants from the atmosphere through photosynthesis (Chai et al., 2017), and it directly reflects the photosynthetic capacity of plants (Zhu et al., 2016; Liu et al., 2021). The net ecosystem exchange (NEE) is the difference between GPP and the efflux of CO_2 released back to the atmosphere through ecosystem respiration processes (Hao et al., 2020; Nascimento Alves et al., 2021). It directly reflects the carbon sink capacity of ecosystems (Yang et al., 2019). They are both key indicators of the terrestrial carbon budget. Accurate estimation of GPP and NEE is important for determining the global carbon budget. Grassland ecosystems are an important part of terrestrial ecosystems. In addition to providing high-quality forage and livestock products, conserving water and soil, and maintaining biodiversity, they also absorb CO_2 from the atmosphere through photosynthesis and play a key role in the carbon cycle. The grassland carbon budget depends on climate change and management. Several studies have examined the carbon budget of grassland ecosystems at different scales (Chai et al., 2017; Wang et al., 2019; Li et al., 2020; Song et al., 2020). These previous studies have shown that estimates of the carbon budget can vary greatly among regions and depend on the methods used and the grassland types analyzed (Gilmanov et al., 2007; Moinet et al., 2017; Rong et al., 2017; Zhao et al., 2019; Song et al., 2020; You et al., 2020).

Qinghai is located in the northeastern part of the Qinghai-Tibet Plateau, which is known as "the roof of the world." It is the site of origin of the Yellow River, Yangtze River, and Lancang River, and it has high ecological significance (Schaller et al., 1988; Gao et al., 2017; Dong Y. et al., 2020). Grassland is the most widely distributed ecosystem in this region. It greatly affects the carbon balance of the regional ecosystem and is the largest carbon pool among the terrestrial ecosystems of Qinghai (Liu et al., 2018; Song et al., 2020). Because of the harsh climate and environment in this region, the ecosystem is extremely fragile and highly sensitive to climate change and human activities (Dong et al., 2015; Sun et al., 2019). Grazing is the most important form of land use of the grasslands in this region, and grassland degradation is widespread because of excessive grazing. Grazing directly affects the grassland carbon budget and thus the sustainable utilization of local grassland resources (Dong et al., 2015; Abdalla et al., 2018; Dong S. K. et al., 2020). Studying the effects of climate change and grazing on the carbon budget in Qinghai grasslands is important for characterizing the pathways and mechanisms driving the grassland carbon cycle. Several studies have examined the carbon budget in Qinghai grasslands (Peng et al., 2017; Sun et al., 2019; Xu et al., 2019; Song et al., 2020). However, previous studies have been conducted at single sites. Consequently, our understanding of the spatiotemporal dynamics of the grassland carbon budget and the response to grazing in Qinghai is poor in light of heterogeneity in terrain, climate, and grazing, and this impedes the sustainable utilization of local grassland resources.

The effect of grazing on the carbon budget of grassland ecosystems has mainly been evaluated through experimental observations, remote sensing, and model simulation (Lin et al., 2017; Jia et al., 2018; Ford et al., 2021; Li et al., 2021). Experimental observations are often too time-consuming and labor-intensive to be conducted over large areas, especially when there is high spatial heterogeneity in climate, terrain, and management regimes. In addition, humans are barred from setting foot in large areas of the grasslands in Qinghai. Thus, a robust understanding of the spatiotemporal dynamics of the grassland carbon budget cannot be feasibly achieved *via* experimental observations. Although remote sensing can be used over large areas, the response of grassland ecosystems to grazing cannot be determined because remote sensing images only provide insight into real scenarios. Model simulation combined with observational data is considered the most effective method for studying the spatiotemporal dynamics of the grassland carbon budget and the response to grazing over large areas because it allows different scenarios (e.g., grazed and ungrazed scenarios) to be evaluated in the same region *via* model estimation (Anh Nguyet and Kawasaki, 2017; Sanchez-Ruiz et al., 2018; Tian et al., 2020). Observational data can then be used to validate the reliability of model outputs. The Biome-BGC model, which is a process-based model, has been used to study the carbon cycle in many regions such as the Qinghai-Tibet Plateau (Bond-Lamberty et al., 2007; Hidy et al., 2012; Mao et al., 2017; You et al., 2019). Hidy et al. (2016) developed the Biome-BGCMuSo model, which is based on the Biome-BGC model. This new model can better simulate the carbon budget of grassland ecosystems than the Biome-BGC model, especially in areas under energy and water stress. In Qinghai, plant growth is mainly limited by energy because of the alpine environment (Shi et al., 2018; Sun et al., 2019). Arid and semi-arid grasslands are widely distributed in this region (Shi et al., 2018; Niu et al., 2021). Thus, the Biome-BGCMuSo model is more applicable to Qinghai than the Biome-BGC model. In addition, the effect of the grazing process is also included in the Biome-BGCMuSo model. The disadvantage of the Biome-BGCMuSo model is that it can only be used for site simulation, which limits its application over large areas (Hidy et al., 2016).

The aim of this study was to examine the spatiotemporal dynamics of the carbon budget and the response to grazing in Qinghai. Therefore, we developed a spatially explicit Biome-BGCMuSo model and used the improved Biome-BGCMuSo model combined with field data from Qinghai grasslands to (1) simulate and analyze the spatial and temporal dynamics of GPP and NEE under climate change and (2) quantify the effect of grazing on GPP and NEE in Qinghai grasslands from 1979 to 2018.

MATERIALS AND METHODS

Study Area

Qinghai is located in northwestern China and the northeastern part of the Qinghai-Tibet Plateau (31°39′–39°19′N, 89°35′–103°04′E). Mountains are numerous, and the terrain is diverse. The average altitude is over 3,000 m. The region features a plateau continental climate. The summers are short, and the

annual average temperature ranges from −6 to 9°C. The average annual precipitation is between 250 and 550 mm. Qinghai has the largest range in precipitation among all provinces in China. Qinghai is one of the main pastoral areas in China. The natural grassland area (4.19×10^7 hm^2) accounts for 10.72% of the total grassland area in China, and the available grassland area is approximately 3.87×10^7 hm^2. The grasslands are mainly distributed in the Qilian Mountains, Qingnan Plateau, and Qaidam Basin. The ecological environment in this region is sensitive to climate change and human activities. Grassland degradation was previously widespread in Qinghai because of unrestricted grazing activities (**Figure 1**; Gao et al., 2017; Zhao et al., 2020).

Methods

In the Biome-BGCMuSo model, GPP was estimated using Farquhar's photosynthesis routine (Farquhar et al., 1980) and the enzyme kinetics model (Woodrow and Berry, 1988). NEE was calculated as follows:

$$NEE = GPP - mr - gr - hr - dr \quad (1)$$

where, mr is maintenance respiration, gr is growth respiration, hr is heterotrophic respiration, and dr is the defoliation rate.

The parameters used in this study were based on default values for C_3 grass (Hidy et al., 2016; You et al., 2019). Some parameters were corrected based on data collected from local investigations. The simulation process was divided into two stages. The first stage was the spinup simulation, which estimates the initial values of the carbon and nitrogen pools. The second stage is the normal simulation, which uses the results of the spinup simulation as initial values for the state variable and generates estimates of GPP and NEE in the Qinghai grassland ecosystem.

The R package RBBGCMuso[1] supports the application of the Biome-BGCMuSo model in the R environment. This means that we can run the Biome-BGCMuSo model using RBBGCMuso. To apply the Biome-BGCMuSo model over a large area, a loop program was designed to iteratively run the RBBGCMuso model; the Biome-BGCMuSo model can be run at different sites when running the loop program. To obtain GPP and NEE over large areas, we divided the study area into grids with a 10 × 10 km resolution, and a loop program was designed to run the Biome-BGCMuSo model in different pixels of Qinghai grasslands. To analyze the effect of grazing on the carbon budget, two scenarios were designed in this study: climate change and climate change combined with grazing. The effect of grazing on the carbon budget was determined by taking the difference between the two scenarios.

Data

Meteorological Data

Data from 1979 to 2018 for precipitation, temperature, saturated vapor pressure difference, day length, and solar radiation were input into the model in daily steps. These data were extracted from the China meteorological forcing dataset by programming. This dataset was based on existing international Princeton reanalysis data, GLDAS data, GEWEX-SRB radiation data, and TRMM Precipitation Data as the background field and integrated with conventional meteorological observation data of the China Meteorological Administration. The spatial resolution was 10 km × 10 km. Comparison of this dataset with the observed data (including station observations in Qinghai) by the producer revealed that the dataset was accurate and superior to the existing reanalysis data (He et al., 2020; Yao et al., 2021).

Grazing Data

The grazing intensity data for the year 2010 were derived from global livestock information system data, which were generated by the Food and Agriculture Organization of the United Nations (FAO) by interpolation according to the global livestock number at sampling points and environmental data. The gridded livestock data were presented at a spatial resolution of 0.083333 decimal degrees (approximately 10 km at the equator) in the raw data.[2] We resampled these data to 10 km × 10 km so that they matched the spatial resolution of meteorological data from the China meteorological forcing dataset. To produce time series grazing data and ensure high precision, we corrected the data using livestock numbers for the year 2010 for different regions and then conducted linear interpolation using livestock statistics from 1979 to 2018 for different regions. The livestock statistics were obtained from the local government. The grazing calendar was set according to a local survey. In this study, we used sheep units to integrate data from different types of livestock. One yak equals 4.5 sheep, one cow equals 6.0 sheep, one goat equals 0.9 sheep, one horse equals 6.0 sheep, and one camel equals 8.0 sheep. These conversion coefficients were determined by the Ministry of Agriculture of the People's Republic of China[3] and a survey of local herdsmen.

Observational Data

Observational data included GPP and NEE. These data were point-based and collected from previous studies to validate the outputs of the Biome-BGCMuSo model. GPP data were obtained from Maqin County for the year 2006, Tongde County for the years 2012–2016, Golmud for the years 2015–2016 and 2019, Menyuan County for the years 2002–2016, and Qilian County for the years 2002–2003, 2006–2009, 2013, and 2015–2016. Three sites were grazed grasslands, and six sites were ungrazed grasslands (Wu et al., 2010; Sun et al., 2019; Xu et al., 2019; Song et al., 2020; Wang et al., 2020). NEE data were obtained from Maqin County for the years 2006 and 2008, Qilian County for the years 2013, 2015, and 2016, Tongde County for the years 2012–2016, Gonghe County for the year 2015, Golmud for the years 2015–2016 and 2019, Gangcha County for the years 2014–2015, Haiyan County for the years 2010–2011, and Menyuan County for the years 2002–2016. Eight sites were grazed grasslands, and seven sites were ungrazed grasslands (Wu et al., 2010, 2018; Zhang et al., 2012; Peng et al., 2017; Wang et al., 2017, 2020; Chai et al., 2018; He et al., 2019; Li et al., 2019;

[1] https://github.com/hollorol/RBBGCMuso

[2] http://www.fao.org/AG/againfo/resources/en/glw/home.html

[3] http://down.foodmate.net/standard/yulan.php?itemid=82804

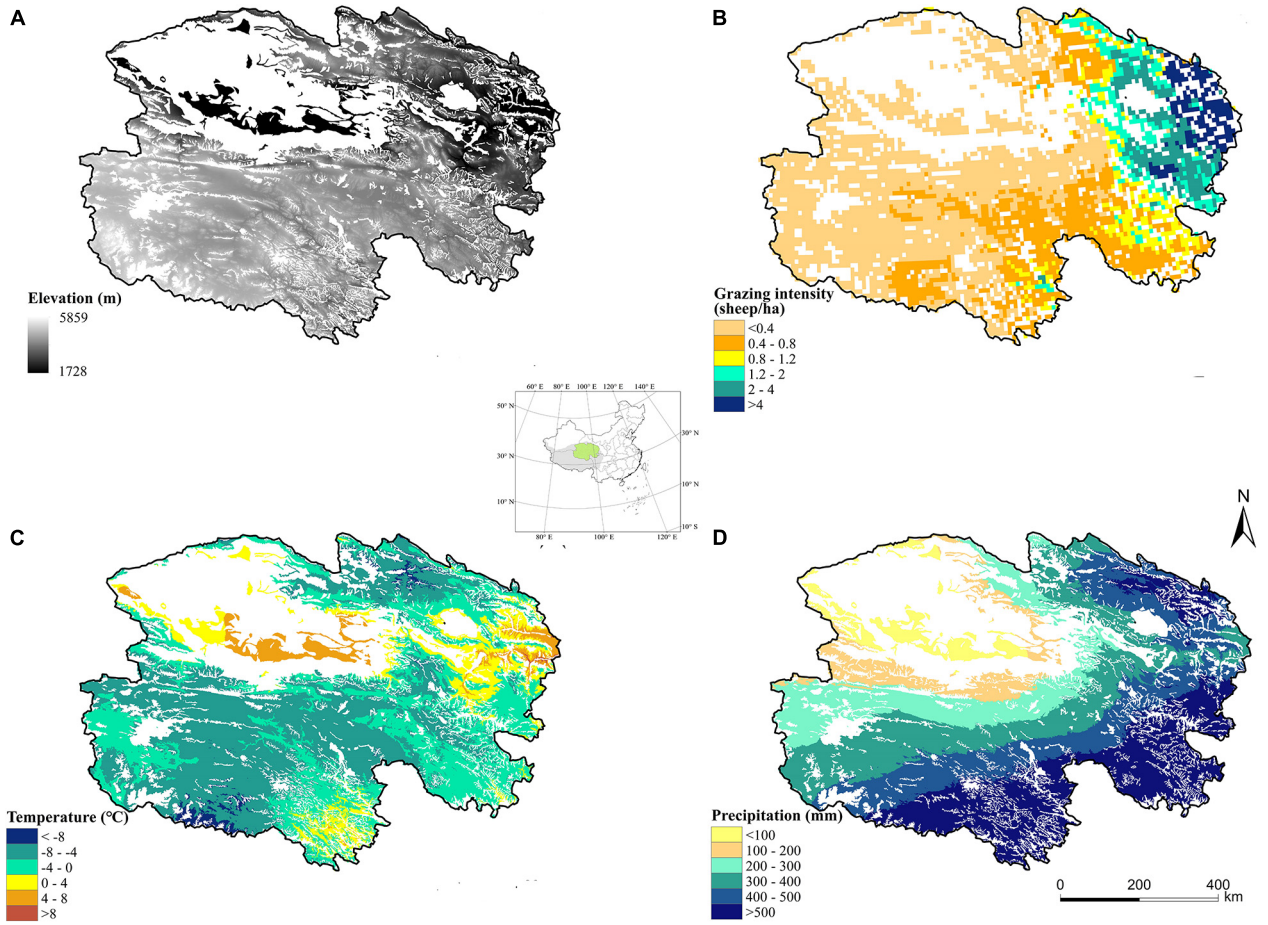

FIGURE 1 | Elevation **(A)**, average annual grazing intensity **(B)**, average annual temperature **(C)**, and average annual precipitation **(D)** in Qinghai grasslands from 1979 to 2018.

Sun et al., 2019; Song et al., 2020; Zhu et al., 2021). Observed NEE data in Menyuan County for the years 2014 to 2015 were collected under both the grazed and ungrazed scenarios at the same site (Li et al., 2019).

Other Auxiliary Data

Other auxiliary data included elevation data and soil data. Elevation data were obtained from the Geographic Data Sharing Infrastructure, College of Urban and Environmental Science, Peking University.[4] Soil data, including texture and pH, were obtained from the Harmonized World Soil Database (HWSD)[5].

RESULTS

Model Validation

In this study, the reliability of the model outputs was validated by comparing simulated results with observed data. **Figures 2A,B** shows that the Biome-BGCMuSo model performed well in predicting GPP under both the grazed (R^2 = 0.90′) and ungrazed grasslands (R^2 = 0.94). **Figures 2C,D** shows that the Biome-BGCMuSo model performed well in predicting NEE under both the grazed (R^2 = 0.91) and ungrazed grasslands (R^2 = 0.91).

Temporal and Spatial Dynamics of Gross Primary Productivity and Net Ecosystem Exchange

The GPP of Qinghai grasslands fluctuated from 1979 to 2018. The annual value fluctuated between 86.33 and 186.00 gC/m^2, with an average annual value of 118.78 gC/m^2. After 2,000, GPP increased, and the average annual rate of increase was 4.74 gC/m^2, indicating that photosynthesis was enhanced during this period (**Figure 3A**). There were obvious regional differences in GPP and its standard deviation. GPP values in most areas of Qinghai were low, and the high values were mainly distributed in eastern and southern Qinghai (**Figure 3B**). The spatial distribution of the standard deviation of GPP was generally similar to that of the annual average GPP (absolute values), which indicated that the regions with large interannual change in GPP were mainly concentrated in the regions with high absolute values

[4]http://geodata.pku.eud.cn

[5]http://www.fao.org/soils-portal/soil-survey/soil-properties/zh/

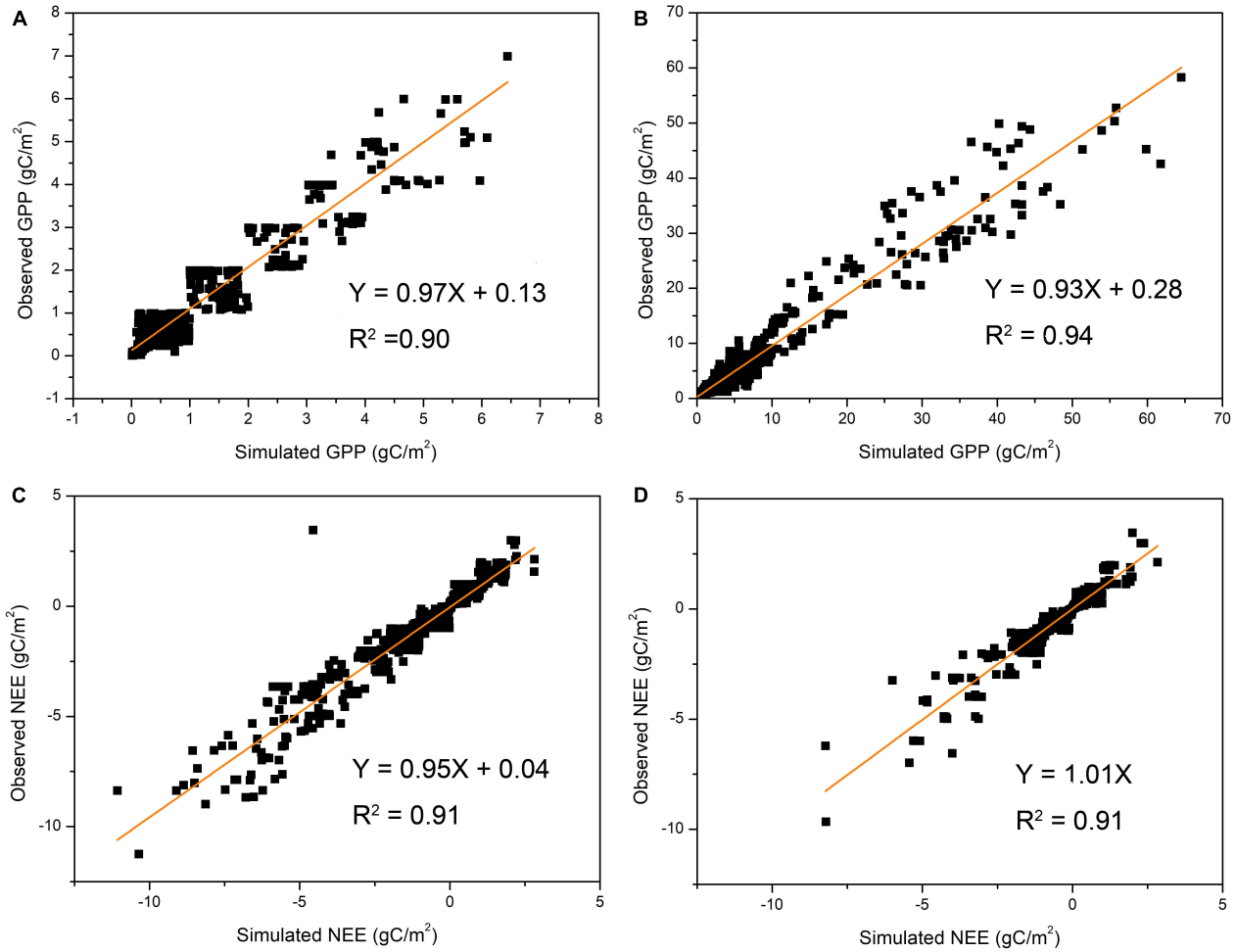

FIGURE 2 | Comparison of GPP values based on simulated and observational data under grazed **(A)** and ungrazed **(B)** conditions and NEE values under grazed **(C)** and ungrazed **(D)** conditions (GPP, gross primary productivity, NEE, net ecosystem exchange).

of the annual averages. On the contrary, the regions with small interannual change in GPP were mainly distributed in the regions with low absolute values of the annual averages (**Figure 3C**).

The NEE of Qinghai grasslands fluctuated from 1979 to 2018, with an average value of −5.16 gC/m^2; in most years, NEE values were negative, indicating that this region was a carbon sink. After 2,000, the NEE of Qinghai grasslands decreased in a fluctuating manner, with an average annual rate of decrease of 1.16 gC/m^2 (**Figure 4A**). There were pronounced regional differences in NEE and its standard deviation, indicating that the carbon source/sink status varied among areas. The southern, southeastern, and northeastern parts of Qinghai were mainly carbon sinks. The northwestern region and the region between the southeastern and northeastern parts of Qinghai were mainly carbon sources (**Figure 4B**). The spatial distribution of the standard deviation of NEE was generally similar to that of the annual average NEE (absolute values), which indicated that the regions with large interannual change in NEE were mainly concentrated in the regions with high absolute values of the annual averages. On the contrary, the regions with small interannual change in NEE were mainly distributed in the regions with low absolute values of the annual averages (**Figure 4C**).

Effect of Grazing on Gross Primary Productivity and Net Ecosystem Exchange

Interannual variation in GPP under the grazed scenario was similar to that under the ungrazed scenario in Qinghai grasslands from 1979 to 2018. In general, the GPP under the grazed scenario (average annual value of 115.56 gC/m^2) was slightly lower than that under the ungrazed scenario, indicating that grazing weakened the photosynthetic capacity of grassland. The difference between the grazed and ungrazed scenarios tended to increase slowly over the study period (**Figure 5A**). Under the grazed scenario, the GPP values decreased in most areas, and significant decreases in GPP were mainly observed in eastern Qinghai. Under the grazed scenario, significant increases in GPP were mainly observed in southern and eastern Qinghai (**Figure 5B**). The spatial distribution of the standard deviation of

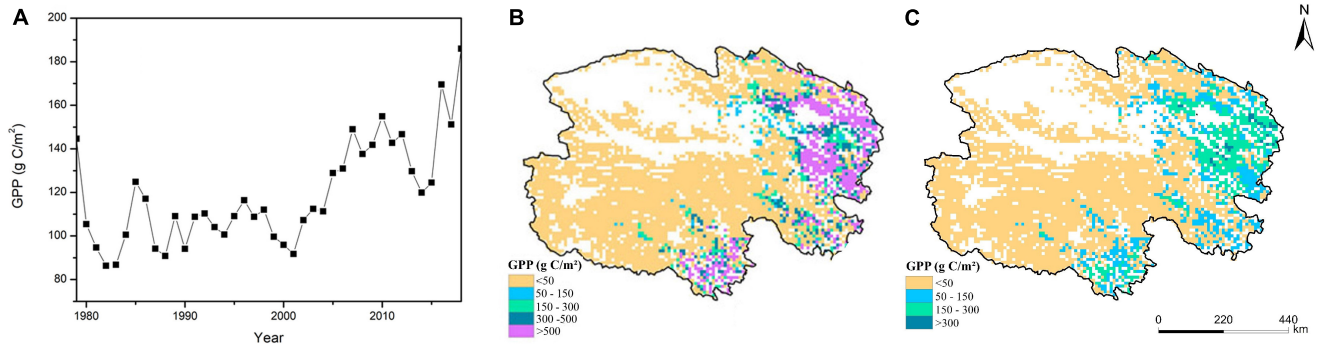

FIGURE 3 | Temporal **(A)** and spatial **(B)** dynamics of GPP and the map of its standard deviation **(C)** in Qinghai grasslands from 1979 to 2018.

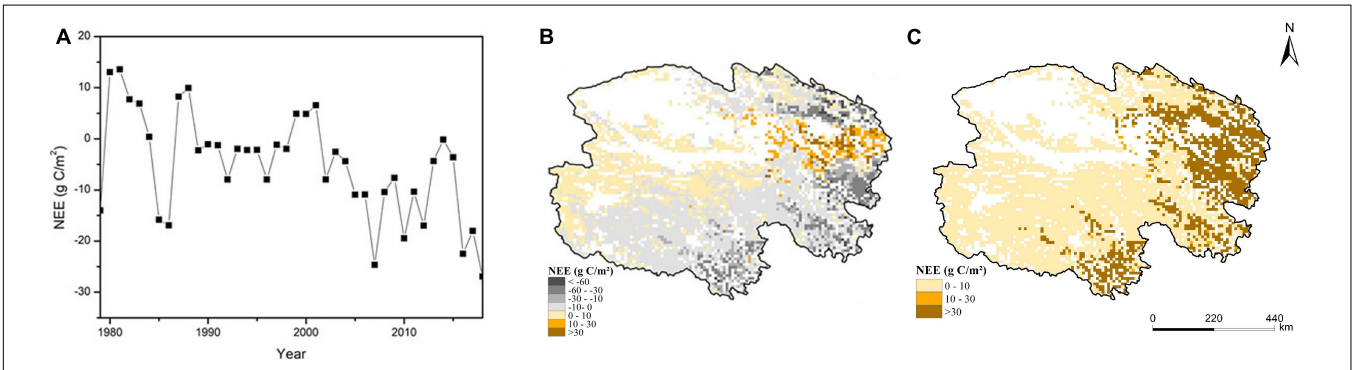

FIGURE 4 | Temporal **(A)** and spatial **(B)** dynamics of NEE and the map of its standard deviation **(C)** in Qinghai grasslands from 1979 to 2018.

GPP difference between the grazed and ungrazed scenarios was generally similar to that of the annual average GPP difference (absolute values), which indicated that the regions with large interannual change in standard deviation of GPP difference were mainly concentrated in the regions with high absolute values of the annual averages. On the contrary, the regions with small interannual change in standard deviation of GPP difference were mainly distributed in the regions with low absolute values of the annual averages (**Figure 5C**).

From 1979 to 2018, interannual variation in NEE under the grazed scenario was similar to that under the ungrazed scenario. In general, NEE under the grazed scenario fluctuated around the average annual value of -4.64 gC/m^2, which was slightly higher than that under the ungrazed scenario (-5.05 gC/m^2), indicating that grazing weakened the carbon sink function of Qinghai grasslands. Under the grazed scenario, the average annual carbon sequestration was 2.14 Tg C in Qinghai grasslands from 1979 to 2018. Under the ungrazed scenario, the average annual fixed carbon was 2.33 Tg C from 1979 to 2018. Grazing decreased carbon fixation by 7.6 Tg C in Qinghai grasslands from 1979 to 2018 (**Figure 6A**). There were regional differences in the effect of grazing on NEE in Qinghai grasslands. NEE was most strongly affected by grazing in eastern Qinghai (**Figure 6B**). The spatial distribution of the standard deviation of NEE difference between the grazed and ungrazed scenarios was generally similar to that of the annual average NEE difference (absolute values), which indicated that the regions with large interannual change in standard deviation of NEE difference were mainly concentrated in the regions with high absolute values of the annual averages. On the contrary, the regions with small interannual change in standard deviation of NEE difference were mainly distributed in the regions with low absolute values of the annual averages (**Figure 6C**).

DISCUSSION

Temporal and Spatial Dynamics of Gross Primary Productivity and Net Ecosystem Exchange and the Responses to Grazing

Our study indicated that GPP and NEE fluctuated in Qinghai grasslands from 1979 to 2018 in response to changes in climate. The GPP of grasslands increased and NEE decreased in Qinghai from 2001 to 2018, indicating that the carbon sink capacity was enhanced under the climate change scenario. This was consistent with the results of previous studies (Sun et al., 2016; Lin et al., 2017; You et al., 2019). Our results showed that grasslands in Qinghai generally acted as carbon sinks from 1979 to 2018, which may be associated with the low temperature in most areas of Qinghai grasslands (**Figure 1C**). Due to the high altitude in Qinghai, the temperature is relatively low, and this decreases the rate of decomposition of organic matter, which

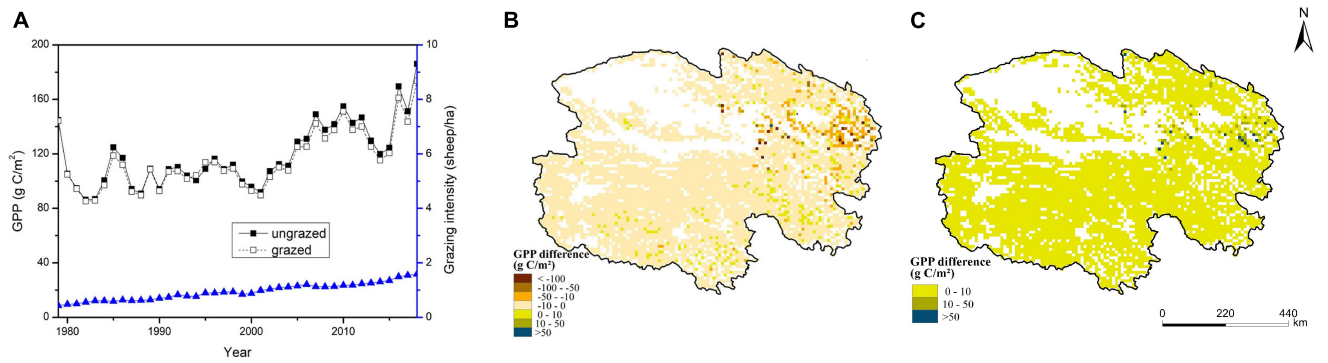

FIGURE 5 | Effect of grazing on the temporal **(A)** and spatial **(B)** dynamics of GPP and the map of the standard deviation of GPP difference **(C)** in Qinghai grasslands from 1979 to 2018 (GPP difference indicates the average annual difference between the grazed and ungrazed scenarios from 1979 to 2018).

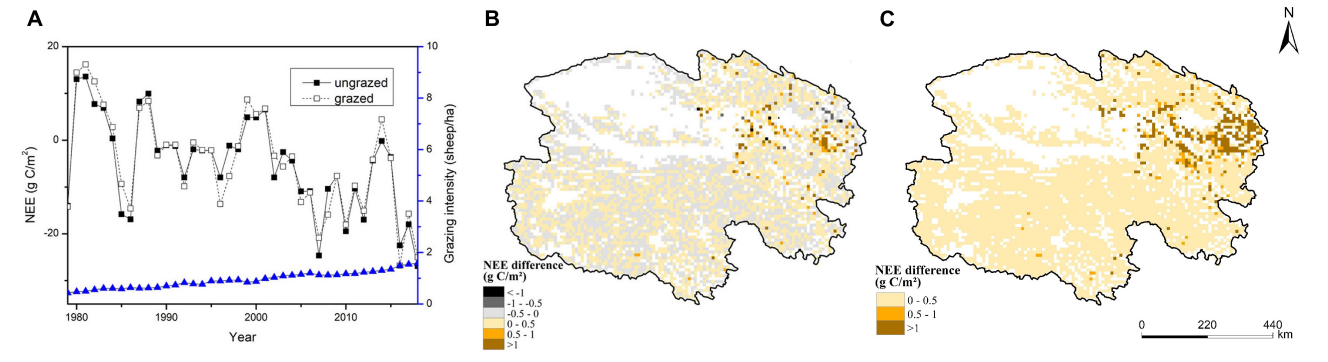

FIGURE 6 | Effect of grazing on the temporal **(A)** and spatial **(B)** dynamics of NEE and the map of the standard deviation of NEE difference **(C)** in Qinghai grasslands from 1979 to 2018 (NEE difference indicates the average annual difference between the grazed and ungrazed scenarios from 1979 to 2018).

promotes carbon accumulation (Lin et al., 2017; Song et al., 2020). Spatial heterogeneity in GPP and NEE was driven by spatial differences in climatic conditions (**Figures 1C,D**). In general, the hydrothermal conditions were favorable in eastern and southern Qinghai; thus, the photosynthetic capacity and carbon sink capacity were strong for most of the grasslands in this area (Huang et al., 2018; Wang et al., 2019). The opposite pattern was observed in other areas. The low temperature in the southwestern portion of Qinghai weakened the photosynthetic capacity and carbon sink capacity (**Figure 1C**). Low precipitation in northwestern Qinghai weakened the photosynthetic capacity and carbon sink capacity (**Figure 1D**; Zhu et al., 2016; Xu et al., 2019). The carbon sink capacity in the southwestern portion of Qinghai was slightly stronger than that in the northwestern portion of Qinghai, which mainly stemmed from differences in temperature. The temperature in the southwestern portion of Qinghai was lower than that in the northwestern portion of Qinghai; this caused the rate of organic matter decomposition to be lower in the southwestern portion of Qinghai, which was more conducive to carbon accumulation (**Figure 1C**; Lagomarsino et al., 2008; Gomez-Casanovas et al., 2012). GPP was high in the area between the southeastern and northeastern parts of Qinghai. However, the grassland ecosystem in this area is a strong carbon source. This observation might be related to the high level of respiration associated with the high temperature in this area (Dubbert et al., 2014; Peng et al., 2017).

Grazing is the most important use of grasslands in Qinghai, and it has an important impact on the local carbon budget. In this study, the effects of grazing on the grassland ecosystem carbon budget were analyzed by comparing simulation results between grazed and ungrazed scenarios in Qinghai from 1979 to 2018 using the improved Biome-BGCMuSo model. Grazing generally weakened the photosynthetic capacity and carbon sink function of Qinghai grasslands from 1979 to 2018. This was consistent with the widespread unrestricted grazing activities in Qinghai that took place during these years (Dong et al., 2015; Abdalla et al., 2018; Dong S. K. et al., 2020). In general, the GPP under the grazed scenario was slightly lower than that under the ungrazed scenario, and the difference in GPP between these two scenarios tended to increase slowly over the study period, indicating that the extent of excessive grazing was increasing, which is inconsistent with the suggestions of previous studies (Sun et al., 2016; Xu et al., 2016; Wei et al., 2019). These previous studies have shown that ecological restoration driven by the local government coupled with the implementation of effective management measures has greatly improved the ecological environment of Qinghai grasslands. However, in our study, we found that GPP under the grazed and ungrazed

scenarios both increased in volatility, and NEE under the grazed and ungrazed scenarios both decreased in a fluctuating manner from 2001 to 2018. Thus, we can infer that climate change, not management, was the main driver of the improvement of the ecological environment of Qinghai grasslands in recent years. In some years (including 1979, 1987–1989, 1992, 1996–1997, 2003, 2005–2006, 2008, and 2015–2016), NEE was lower under the grazed scenario than under the ungrazed scenario, which indicated that grazing generally enhanced the carbon sink function of grasslands in these years. The difference between the NEE values under the grazed and ungrazed scenarios varied depending on the interaction between grass and livestock. Grass growth is closely related to climatic conditions (Zhang et al., 2015; Huang et al., 2018). Thus, the effect of grazing on the carbon sink function depends not only on grazing management but also on climate conditions.

There was pronounced spatial heterogeneity in the effect of grazing on the carbon budget in Qinghai grasslands because of spatial heterogeneity in grazing management and climate conditions. In general, GPP and NEE values were more strongly affected by grazing in eastern Qinghai, which was consistent with the high grass yield (stemming from the favorable hydrothermal conditions) and high grazing intensity in this area (**Figure 1B**; Huang et al., 2018; Wang et al., 2019). In central and western Qinghai, unfavorable hydrothermal conditions led to low grass yield and low grazing intensity, which was consistent with the small changes in GPP and NEE values observed under the grazed scenario relative to the ungrazed scenario (**Figures 5B**, **6B**). In some areas, grazing enhanced the photosynthetic capacity and carbon sink function, which helped achieve a grass–livestock balance. This pattern may be closely related to the significant overcompensation of the growth of grass under moderate grazing (Huang et al., 2018; Mipam et al., 2019). The opposite pattern was observed in most other areas.

The carbon budget is closely related to variation in climate and grazing management regime in Qinghai grasslands. Appropriate levels of grazing can enhance the photosynthetic capacity and carbon sink function of grasslands. To achieve a balance between grass and livestock, suitable grazing management measures should be implemented depending on the local conditions because of dynamic temporal and spatial variation in climate.

Comparison With Other Studies

Previous studies of the grassland carbon budget have been conducted in Qinghai grasslands. For example, Zhang et al. (2012) found that the alpine meadow grassland ecosystem acted as a carbon sink on the northern shore of Qinghai Lake using the eddy covariance method. Wu et al. (2018) found that the alpine wet meadow ecosystem around Qinghai Lake behaved as a carbon source using the eddy covariance method. Sun et al. (2019) found that the alpine meadow ecosystem in Arou, Yakou, and Dashalong was a carbon sink using the eddy covariance method. He et al. (2019) found that *Elymus nutans* grassland was a weak carbon sink in a pasture in Tongde County using the eddy covariance method. Song et al. (2020) found that NEE varied seasonally in a grassland ecosystem at Fenghuoshan catchment using data from an eddy covariance tower and chamber-based measurements. Wang et al. (2020) found that an alpine meadow ecosystem was a strong and consistent carbon sink based on a continuous eddy covariance dataset from the Arou super-station. Zhu et al. (2021) found that the alpine meadow at Haibei station was a carbon sink during the growing season using the eddy covariance technique. Most previous studies have shown that the Qinghai grasslands are a carbon sink. This was consistent with the results of our study. However, previous studies have been conducted using data from single sites. Although these previous studies contribute to an in-depth understanding of the carbon budget at the site scale, such studies based on sparse sites do not provide insight into the spatiotemporal dynamics of the grassland carbon budget and the response to grazing because of the high degree of spatial heterogeneity in climate change, terrain, and grazing in Qinghai. In our study, a loop program was used to run the Biome-BGCMuSo model in different pixels of Qinghai grasslands to determine GPP and NEE over large areas. The effect of grazing on the carbon budget was also analyzed by comparing the difference between grazed and ungrazed scenarios.

Uncertainties in Estimates

In this study, GPP and NEE were estimated in Qinghai grasslands from 1979 to 2018 using the Biome-BGCMuSo model. The reliability of the model outputs was validated by comparison with a large set of observational data under both the grazed and ungrazed scenarios. However, some degree of uncertainty is inevitable.

First, all the models are simplifications of reality. Like many other models, the Biome-BGCMuSo model can introduce uncertainty in the outputs of simulated GPP and NEE because it does not consider the full complexity of the grassland carbon cycle. For example, previous studies have shown that the freezing-thawing cycle substantially affects plant carbon fixation. However, few studies have examined this topic. Thus, the underlying interaction between the freezing-thawing cycle and alpine grasslands could not be fully accounted for in the model, which inevitably introduces uncertainty in the results. In the Biome-BGCMuSo model, the study area was assumed to be composed of a single vegetation type, which means that mixed-species scenarios are not considered. However, overgrazing can lead to the invasion of other grass types, including noxious grasses, that can also fix carbon. This may lead to an underestimation of carbon fixation when the Biome-BGCMuSo model is run under an overgrazing scenario. The trampling of livestock also has an effect on topsoil compaction and plant growth. However, the trampling effect was not considered in the model because it has not been quantified in the previous studies, and this inevitably introduces uncertainty in the results (Hidy et al., 2012, 2016).

Second, model inputs are also a source of uncertainty in the results. In this study, the main inputs of the model were meteorological data and grazing data. Although the accuracy of the meteorological input data in our study is higher compared with the existing reanalysis data, their accuracy is still lower than actual observational data, which inevitably results in uncertainty in model outputs (He et al., 2020). Data on the grazing intensity were produced through spatial interpolation by FAO

(see text footnote 2), which inevitably introduces some error. Although we corrected the grazing intensity data according to livestock statistics from the local government to ensure their high precision, a robust correction of these data is difficult given the macroscopic nature of the statistical data from the government.

The spatial heterogeneity in the standard deviations of the model predictions indicated that there were obviously regional differences in the accuracy level of the model predictions. Higher standard deviation is associated with lower reliability of mean value. And in this study the spatial distributions of the standard deviations of the model predictions were generally similar to those of their respective annual means(absolute values). Thus, in Qinghai grasslands the regions with relatively low reliability of the model predictions were mainly concentrated in the regions with high absolute values of the annual average predictions. On the contrary, the regions with relatively high reliability of the model predictions were mainly distributed in the regions with low absolute values of the annual average predictions (**Figures 3B,C**, **4B,C**, **5B,C**, **6B,C**).

CONCLUSION

In this study, the spatiotemporal dynamics of the carbon budget and the response to grazing in Qinghai grasslands from 1979 to 2018 were analyzed using the improved Biome-BGCMuSo model. In general, Qinghai grasslands were carbon sinks. After 2,000, GPP increased and NEE decreased in a fluctuating manner in Qinghai grasslands because of climate change. There was spatial heterogeneity in GPP and NEE under the ungrazed scenario because of differences in climate conditions. In general, high GPP and low NEE occurred in areas with favorable hydrothermal conditions, whereas low GPP and high NEE occurred in areas with unfavorable hydrothermal conditions. Grazing generally weakened the photosynthetic capacity and carbon sink capacity in Qinghai grasslands. There was spatial heterogeneity in the effect of grazing on GPP and NEE because of differences in climate conditions and grazing management measures. In general, GPP and NEE values were more strongly affected by grazing in eastern Qinghai, which was consistent with the high grass yield (stemming from the favorable hydrothermal conditions) and high grazing intensity in this area. The results of this study aid our understanding of the mechanism driving variation in the grassland carbon budget and provide data that could be used to aid local grassland management.

DATA AVAILABILITY STATEMENT

The raw data supporting the conclusions of this article will be made available by the authors, without undue reservation.

AUTHOR CONTRIBUTIONS

XH and HZ conceived, performed, and designed the experiments. XH and CC analyzed the data and performed the computational analysis. XH, BY, ZM, and HZ wrote the manuscript. All authors have approved the final version of the manuscript.

FUNDING

This research was funded by the Chinese Academy of Sciences (CAS) "Light of West China" Program (2018), "The effect of grazing on grassland productivity in the basin of Qinghai Lake," State Key Laboratory of Plateau Ecology and Agriculture (2021-KF-08), and the Second Tibetan Plateau Scientific Expedition and Research program (2019QZKK0302).

ACKNOWLEDGMENTS

We are grateful to Hongfei Zhao for excellent technical support.

SUPPLEMENTARY MATERIAL

The Supplementary Material for this article can be found online at: https://www.frontiersin.org/articles/10.3389/fpls.2021.775015/full#supplementary-material

REFERENCES

Abdalla, K., Mutema, M., Chivenge, P., Everson, C., and Chaplot, V. (2018). Grassland degradation significantly enhances soil CO_2 emission. *Catena* 167, 284–292. doi: 10.1016/j.catena.2018.05.010

Anh Nguyet, D., and Kawasaki, A. (2017). Integrating biophysical and socio-economic factors for land-use and land-cover change projection in agricultural economic regions. *Ecol. Modell.* 344, 29–37. doi: 10.1016/j.ecolmodel.2016.11.004

Bakhtiari, F. (2018). International cooperative initiatives and the United Nations framework convention on climate change. *Clim. Policy* 18, 655–663.

Bond-Lamberty, B., Gower, S. T., and Ahl, D. E. (2007). Improved simulation of poorly drained forests using Biome-BGC. *Tree Physiol.* 27, 703–715. doi: 10.1093/treephys/27.5.703

Chai, X., Li, Y., Duan, C., Zhang, T., Zong, N., Shi, P., et al. (2018). CO_2 flux dynamics and its limiting factors in the alpine shrub-meadow and steppe-meadow on the Qinghai-Xizang Plateau. *Chin. J. Plant Ecol.* 42, 6–19.

Chai, X., Shi, P. L., Zong, N., He, Y. T., Zhang, X. Z., Xu, M. J., et al. (2017). A growing season climatic index to simulate gross primary productivity and carbon budget in a Tibetan alpine meadow. *Ecol. Indic.* 81, 285–294. doi: 10.1016/j.ecolind.2017.05.064

Dong, Q. M., Zhao, X. Q., Wu, G. L., and Chang, X. F. (2015). Optimization yak grazing stocking rate in an alpine grassland of Qinghai-Tibetan Plateau, China. *Environ. Earth Sci.* 73, 2497–2503. doi: 10.1007/s12665-014-3597-7

Dong, S. K., Shang, Z. H., Gao, J. X., and Boone, R. B. (2020). Enhancing sustainability of grassland ecosystems through ecological restoration and grazing management in an era of climate change on Qinghai-Tibetan Plateau. *Agric. Ecosyst. Environ.* 287:106684. doi: 10.1016/j.agee.2019.106684

Dong, Y., Zhai, J., Zhao, Y., Li, H., Wang, Q., Jiang, S., et al. (2020). Teleconnection patterns of precipitation in the Three-River Headwaters region, China. *Environ. Res. Lett.* 15:104050. doi: 10.1088/1748-9326/aba8c0

Dubbert, M., Piayda, A., Cuntz, M., Correia, A. C., Costa E Silva, F., Pereira, J. S., et al. (2014). Stable oxygen isotope and flux partitioning demonstrates

understory of an oak savanna contributes up to half of ecosystem carbon and water exchange. *Front. Plant Sci.* 5:530. doi: 10.3389/fpls.2014.00530

Farquhar, G. D., Caemmerer, S. V., and Berry, J. A. (1980). A biochemical-model of photosynthetic CO_2 assimilation in leaves of C-3 species. *Planta* 149, 78–90. doi: 10.1007/bf00386231

Ford, H., Healey, J. R., Webb, B., Pagella, T. F., and Smith, A. R. (2021). Hedgerow effects on CO_2 emissions are regulated by soil type and season: implications for carbon flux dynamics in livestock-grazed pasture. *Geoderma* 382:114697. doi: 10.1016/j.geoderma.2020.114697

Ford, J., Maillet, M., Pouliot, V., Meredith, T., Cavanaugh, A., and Team, I. R. (2016). Adaptation and indigenous peoples in the United Nations framework convention on climate change. *Clim. Change* 139, 429–443. doi: 10.1007/s10584-016-1820-0

Gao, J. L., Huang, X. D., Ma, X. F., Feng, Q. S., Liang, T. G., and Xie, H. J. (2017). Snow disaster early warning in pastoral areas of Qinghai Province, China. *Rem. Sens.* 9:475. doi: 10.3390/rs9050475

Gilmanov, T. G., Soussana, J. E., Aires, L., Allard, V., Ammann, C., Balzarolo, M., et al. (2007). Partitioning European grassland net ecosystem CO_2 exchange into gross primary productivity and ecosystem respiration using light response function analysis. *Agric. Ecosyst. Environ.* 121, 93–120. doi: 10.1016/j.agee.2006.12.008

Giltrap, D. L., Kirschbaum, M. U. F., Laubach, J., and Hunt, J. E. (2020). The effects of irrigation on carbon balance in an irrigated grazed pasture system in New Zealand. *Agric. Syst.* 182:102851. doi: 10.1016/j.agsy.2020.102851

Gomez-Casanovas, N., Matamala, R., Cook, D. R., and Gonzalez-Meler, M. A. (2012). Net ecosystem exchange modifies the relationship between the autotrophic and heterotrophic components of soil respiration with abiotic factors in prairie grasslands. *Glob. Change Biol.* 18, 2532–2545. doi: 10.1111/j.1365-2486.2012.02721.x

Hao, G. C., Hu, Z. M., Di, K., and Li, S. G. (2020). Rainfall pulse response of carbon exchange to the timing of natural intra-annual rainfall in a temperate grass ecosystem. *Ecol. Indic.* 118:106730. doi: 10.1016/j.ecolind.2020.106730

He, F., Li, Q., Chen, D., Zhao, X., Luo, C., Xu, Q., et al. (2019). Variation characteristics of CO_2 fluxes of elymus nutans artificial grassland for a planting cycle in agro-pastoral transition area of Sanjiangyuan. *Ecol. Environ. Sci.* 28, 918–929.

He, J., Yang, K., Tang, W., Lu, H., Qin, J., Chen, Y., et al. (2020). The first high-resolution meteorological forcing dataset for land process studies over China. *Sci. Data* 7:25. doi: 10.1038/s41597-020-0369-y

Hidy, D., Barcza, Z., Haszpra, L., Churkina, G., Pinter, K., and Nagy, Z. (2012). Development of the Biome-BGC model for simulation of managed herbaceous ecosystems. *Ecol. Modell.* 226, 99–119. doi: 10.1016/j.ecolmodel.2011.11.008

Hidy, D., Barcza, Z., Marjanovic, H., Sever, M. Z. O., Dobor, L., Gelybo, G., et al. (2016). Terrestrial ecosystem process model Biome-BGCMuSo v4.0: summary of improvements and new modeling possibilities. *Geosci. Model Dev.* 9, 4405–4437. doi: 10.5194/gmd-9-4405-2016

Huang, X., Luo, G., and Han, Q. (2018). Temporospatial patterns of human appropriation of net primary production in Central Asia grasslands. *Ecol. Indic.* 91, 555–561. doi: 10.1016/j.ecolind.2018.04.045

Jia, W. X., Liu, M., Wang, D. D., He, H. L., Shi, P. L., Li, Y. N., et al. (2018). Uncertainty in simulating regional gross primary productivity from satellite based models over northern China grassland. *Ecol. Indic.* 88, 134–143. doi: 10.1016/j.ecolind.2018.01.028

Lagomarsino, A., De Angelis, P., Moscatelli, M. C., and Grego, S. (2008). The influence of temperature and labile C substrates on heterotrophic respiration in response to elevated CO_2 and nitrogen fertilization. *Plant Soil* 317, 223–234. doi: 10.1007/s11104-008-9804-0

Li, H., Zhang, F., Mao, S., Zhu, J., He, H., Wei, Y., et al. (2019). Effects of Grazing Density on Ecosystem CO_2 Exchange of Haibei Alpine Kobresia humilßs Meadow in Qinghai. *Chin. J. Grassland* 41, 16–21.

Li, X., Xiao, J. F., Fisher, J. B., and Baldocchi, D. D. (2021). ECOSTRESS estimates gross primary production with fine spatial resolution for different times of day from the International Space Station. *Rem. Sens. Environ.* 258:112360. doi: 10.1016/j.rse.2021.112360

Li, Z., Chen, Y., Zhang, Q., and Li, Y. (2020). Spatial patterns of vegetation carbon sinks and sources under water constraint in Central Asia. *J. Hydrol.* 590:125355. doi: 10.1016/j.jhydrol.2020.125355

Lin, X., Han, P., Zhang, W., and Wang, G. (2017). Sensitivity of alpine grassland carbon balance to interannual variability in climate and atmospheric CO_2 on the Tibetan Plateau during the last century. *Glob. Planet. Change* 154, 23–32. doi: 10.1016/J.gloplacha.2017.05.008

Liu, D., Li, Y., Wang, T., Peylin, P., MacBean, N., Ciais, P., et al. (2018). Contrasting responses of grassland water and carbon exchanges to climate change between Tibetan Plateau and Inner Mongolia. *Agric. For. Meteorol.* 249, 163–175. doi: 10.1016/j.agrformet.2017.11.034

Liu, W., Mo, X., Liu, S., Lin, Z., and Lv, C. (2021). Attributing the changes of grass growth, water consumed and water use efficiency over the Tibetan Plateau. *J. Hydrol.* 598:126464. doi: 10.1016/j.jhydrol.2021.126464

Mao, F., Zhou, G., Li, P., Du, H., Xu, X., Shi, Y., et al. (2017). Optimizing selective cutting strategies for maximum carbon stocks and yield of Moso bamboo forest using BIOME-BGC model. *J. Environ. Manag.* 191, 126–135. doi: 10.1016/j.jenvman.2017.01.016

Mipam, T.-D., Zhong, L.-L., Liu, J.-Q., Miehe, G., and Tian, L.-M. (2019). Productive Overcompensation of Alpine Meadows in Response to Yak Grazing in the Eastern Qinghai-Tibet Plateau. *Front. Plant Sci.* 10:925. doi: 10.3389/fpls.2019.00925

Moinet, G. Y. K., Cieraad, E., Turnbull, M. H., and Whitehead, D. (2017). Effects of irrigation and addition of nitrogen fertiliser on net ecosystem carbon balance for a grassland. *Sci. Total Environ.* 579, 1715–1725. doi: 10.1016/j.scitotenv.2016.11.199

Nascimento Alves, J. D., Ribeiro, A., Rody, Y. P., Loos, R. A., and Hall, K. B. (2021). Carbon uptake and water vapor exchange in a pasture site in the Brazilian Cerrado. *J. Hydrol.* 594:125943. doi: 10.1016/j.jhydrol.2020.125943

Niu, W. L., Chen, H., and Wu, J. S. (2021). Soil moisture and soluble salt content dominate changes in Foliar δ^{13} C and δ^{15} N of desert communities in the Qaidam Basin, Qinghai-Tibetan Plateau. *Front. Plant Sci.* 12:675817. doi: 10.3389/fpls.2021.675817

Peng, Y., Li, F., Zhou, G., Fang, K., Zhang, D., Li, C., et al. (2017). Linkages of plant stoichiometry to ecosystem production and carbon fluxes with increasing nitrogen inputs in an alpine steppe. *Glob. Change Biol.* 23, 5249–5259. doi: 10.1111/gcb.13789

Qiu, L. J., Wu, Y. P., Yu, M. Z., Shi, Z. Y., Yin, X. W., Song, Y. N., et al. (2021). Contributions of vegetation restoration and climate change to spatiotemporal variation in the energy budget in the loess plateau of china. *Ecol. Indic.* 127:107780. doi: 10.1016/j.ecolind.2021.107780

Rong, Y., Johnson, D. A., Wang, Z., and Zhua, L. (2017). Grazing effects on ecosystem CO_2 fluxes regulated by interannual climate fluctuation in a temperate grassland steppe in northern China. *Agric. Ecosyst. Environ.* 237, 194–202. doi: 10.1016/j.agee.2016.12.036

Sanchez-Ruiz, S., Chiesi, M., Fibbi, L., Carrara, A., Maselli, F., and Amparo Gilabert, M. (2018). Optimized application of biome-BGC for modeling the daily GPP of natural vegetation over peninsular Spain. *J. Geophys. Res.-Biogeosci.* 123, 531–546. doi: 10.1002/2017jg004360

Schaller, G. B., Ren, J. R., and Qiu, M. J. (1988). Status of the snow leopard panther-uncia in Qinghai-province and Gansu-province, China. *Biol. Conserv.* 45, 179–194. doi: 10.1016/0006-3207(88)90138-3

Shi, J. B., Li, X. W., Dong, S. K., Zhuge, H. J., and Mu, Y. L. (2018). Trans-boundary conservation of Chiru by identifying its potential movement corridors in the alpine desert of Qinghai-Tibetan Plateau. *Glob. Ecol. Conserv.* 16:e00491. doi: 10.1016/j.gecco.2018.e00491

Song, C., Wang, G., Hu, Z., Zhang, T., Huang, K., Chen, X., et al. (2020). Net ecosystem carbon budget of a grassland ecosystem in central Qinghai-Tibet Plateau: integrating terrestrial and aquatic carbon fluxes at catchment scale. *Agric. For. Meteorol.* 290:108021. doi: 10.1016/j.agrformet.2020.108021

Sun, Q., Li, B., Xu, L., Zhang, T., Ge, J., and Li, F. (2016). Analysis of NDVI change trend and its impact factors in the three-River Headwater Region from 2000 to 2013. *J. Geo-Inform. Sci.* 18, 1707–1716.

Sun, S., Che, T., Li, H., Wang, T., Ma, C., Liu, B., et al. (2019). Water and carbon dioxide exchange of an alpine meadow ecosystem in the northeastern Tibetan Plateau is energy-limited. *Agric. For. Meteorol.* 275, 283–295. doi: 10.1016/j.agrformet.2019.06.003

Tian, H., Xu, R., Canadell, J. G., Thompson, R. L., Winiwarter, W., Suntharalingam, P., et al. (2020). A comprehensive quantification of global nitrous oxide sources and sinks. *Nature* 586, 248–256. doi: 10.1038/s41586-020-2780-0

Wang, B., Jin, H., Li, Q., Chen, D., Zhao, L., Tang, Y., et al. (2017). Diurnal and seasonal variations in the net ecosystem CO_2 exchange of a pasture in the Three-River Source Region of the Qinghai-Tibetan Plateau. *PLoS One* 12:e0170963. doi: 10.1371/journal.pone.0170963

Wang, N., Quesada, B., Xia, L., Butterbach-Bahl, K., Goodale, C. L., and Kiese, R. (2019). Effects of climate warming on carbon fluxes in grasslands- A global meta-analysis. *Glob. Change Biol.* 25, 1839–1851. doi: 10.1111/gcb.14603

Wang, Y., Ma, Y., Li, H., and Yuan, L. (2020). Carbon and water fluxes and their coupling in an alpine meadow ecosystem on the northeastern Tibetan Plateau. *Theor. Appl. Climatol.* 142, 1–18. doi: 10.1007/s00704-020-03303-3

Webb, J. R., Santos, I. R., Maher, D. T., and Finlay, K. (2019). The importance of aquatic carbon fluxes in net ecosystem carbon budgets: a catchment-scale review. *Ecosystems* 22, 508–527. doi: 10.1007/s10021-018-0284-7

Wei, X., Yan, C., and Wei, W. (2019). Grassland dynamics and the driving factors based on net primary productivity in Qinghai Province, China. *ISPRS Int. J. Geo-Inform.* 8:73. doi: 10.3390/ijgi8020073

Woodrow, I. E., and Berry, J. A. (1988). Enzymatic regulation of photosynthetic CO_2 fixation in C-3 plants. *Annu. Rev. Plant Physiol. Plant Mol. Biol.* 39, 533–594. doi: 10.1146/annurev.arplant.39.1.533

Wu, F., Cao, S., Cao, G., Han, G., Lin, Y., and Cheng, S. (2018). Variation of CO_2 Flux of Alpine Wetland Ecosystem of Kobresia tibetica Wet Meadow in Lake Qinghai. *J. Ecol. Rural Environ.* 34, 124–131.

Wu, L., Gu, S., Zhao, L., Xu, S., Zhou, H., Feng, C., et al. (2010). Variation in net CO_2 exchange,gross primary production and its affecting factors in the planted pasture ecosystem in Sanjiangyuan Region of the Qinghai-Tibetan Plateau of China. *Acta Phytoecol. Sin.* 34, 770–780.

Xu, H.-J., Wang, X.-P., and Zhang, X.-X. (2016). Alpine grasslands response to climatic factors and anthropogenic activities on the Tibetan Plateau from 2000 to 2012. *Ecol. Eng.* 92, 251–259. doi: 10.1016/j.ecoleng.2016.04.005

Xu, H.-J., Zhao, C.-Y., and Wang, X.-P. (2019). Spatiotemporal differentiation of the terrestrial gross primary production response to climate constraints in a dryland mountain ecosystem of northwestern China. *Agric. For. Meteorol.* 276:107628. doi: 10.1016/j.agrformet.2019.107628

Yang, F., Zhang, Q., Zhou, J., Yue, P., Wang, R., and Wang, S. (2019). East Asian summer monsoon substantially affects the inter-annual variation of carbon dioxide exchange in semi-arid grassland ecosystem in Loess Plateau. *Agric. Ecosyst. Environ.* 272, 218–229. doi: 10.1016/j.agee.2018.11.016

Yao, T., Lu, H., Yu, Q., Feng, W., and Xue, Y. (2021). Change and attribution of pan evaporation throughout the Qinghai-Tibet Plateau during 1979-2017 using China meteorological forcing dataset. *Int. J. Climatol.* 1–15. doi: 10.1002/joc.7312

You, Y., Wang, S., Ma, Y., Wang, X., and Liu, W. (2019). Improved modeling of gross primary productivity of Alpine Grasslands on the Tibetan Plateau using the biome-BGC model. *Rem. Sens.* 11:1287. doi: 10.3390/rs11111287

You, Y., Wang, S., Pan, N., Ma, Y., and Liu, W. (2020). Growth stage-dependent responses of carbon fixation process of alpine grasslands to climate change over the Tibetan Plateau, China. *Agric. For. Meteorol.* 291:108085. doi: 10.1016/j.agrformet.2020.108085

Zhang, F., Li, Y., Cao, G., Li, F., Ye, G., Liu, J., et al. (2012). CO_2 fluxes and their driving factors over alpine meadow grassland ecosystems in the northern shore of Qinghai Lake,China. *Acta Phytoecol. Sin.* 36, 187–198.

Zhang, T., Zhang, Y., Xu, M., Zhu, J., Wimberly, M. C., Yu, G., et al. (2015). Light-intensity grazing improves alpine meadow productivity and adaption to climate change on the Tibetan Plateau. *Sci. Rep.* 5:15949. doi: 10.1038/srep15949

Zhao, H., Jia, G., Wang, H., Zhang, A., and Xu, X. (2019). Seasonal and interannual variations in carbon fluxes in East Asia semi-arid grasslands. *Sci. Total Environ.* 668, 1128–1138. doi: 10.1016/j.scitotenv.2019.02.378

Zhao, H., Li, X., Zhang, D., and Xiao, R. (2020). Aboveground biomass in grasslands in Qinghai Province estimated from MODIS data and its influencing factors. *Acta Pratacult. Sin.* 29, 5–16.

Zhu, J., Zhang, F., Li, H., Yang, Y., Wang, C., Zhang, G., et al. (2021). The response of CO_2 fluxes to the amplitude of diurnal temperature in alpine meadow during growing season from 2002 to 2016 at the southern foot of Qilian Mountains. *Chin. Sci. Bull.* 66, 85–95.

Zhu, X. J., Yu, G. R., Wang, Q. F., Gao, Y. N., He, H. L., Zheng, H., et al. (2016). Approaches of climate factors affecting the spatial variation of annual gross primary productivity among terrestrial ecosystems in China. *Ecol. Indic.* 62, 174–181. doi: 10.1016/j.ecolind.2015.11.028

Conflict of Interest: The authors declare that the research was conducted in the absence of any commercial or financial relationships that could be construed as a potential conflict of interest.

Publisher's Note: All claims expressed in this article are solely those of the authors and do not necessarily represent those of their affiliated organizations, or those of the publisher, the editors and the reviewers. Any product that may be evaluated in this article, or claim that may be made by its manufacturer, is not guaranteed or endorsed by the publisher.

Copyright © 2022 Huang, Chen, Yao, Ma and Zhou. This is an open-access article distributed under the terms of the Creative Commons Attribution License (CC BY). The use, distribution or reproduction in other forums is permitted, provided the original author(s) and the copyright owner(s) are credited and that the original publication in this journal is cited, in accordance with accepted academic practice. No use, distribution or reproduction is permitted which does not comply with these terms.

frontiers in Plant Science

ORIGINAL RESEARCH
published: 07 January 2022
doi: 10.3389/fpls.2021.821954

A Meta-Analysis on Degraded Alpine Grassland Mediated by Climate Factors: Enlightenment for Ecological Restoration

Jiale Yu[1,2†], Lingfan Wan[1,2†], Guohua Liu[1,2], Keming Ma[1,2], Hao Cheng[1,2], Yu Shen[1,2], Yuqing Liu[1,2] and Xukun Su[1,2*]*

[1] State Key Laboratory of Urban and Regional Ecology, Research Center for Eco-environmental Sciences, Chinese Academy of Sciences, Beijing, China, [2] College of Resources and Environment, University of Chinese Academy of Sciences, Beijing, China

Alpine grassland is the main ecosystem on the Qinghai-Tibet Plateau (QTP). Degradation and restoration of alpine grassland are related to ecosystem function and production, livelihood, and wellbeing of local people. Although a large number of studies research degraded alpine grassland, there are debates about degradation patterns of alpine grassland in different areas and widely applicable ecological restoration schemes due to the huge area of the QTP. In this study, we used the meta-analysis method to synthesize 80 individual published studies which were conducted to examine aboveground and underground characteristics in non-degradation (ND), light degradation (LD), moderate degradation (MD), heavy degradation (HD), and extreme degradation (ED) of alpine grassland on the QTP. Results showed that aboveground biomass (AGB), belowground biomass (BGB), Shannon-Wiener index (H′), soil moisture (SM), soil organic carbon (SOC), soil total nitrogen (TN), and available nitrogen (AN) gradually decreased along the degradation gradient, whereas soil bulk density (BD) and soil *pH* gradually increased. In spite of a tendency to soil desertification, losses of other soil nutrients and reduction of enzymes, there was no linear relationship between the variations with degradation gradient. Moreover, the decreasing extent of TN was smaller in areas with higher precipitation and temperature, and the decreasing extent of AGB, SOC, and TN was larger in areas with a higher extent of corresponding variables in the stage of ND during alpine grassland degradation. These findings suggest that in areas with higher precipitation and temperature, reseeding and sward cleavage can be used for restoration on degraded alpine grassland. Fencing and fertilization can be used for alpine grassland restoration in areas with lower precipitation and temperature. Microbial enzymes should not be used to restore degraded alpine grassland on a large scale on the QTP without detailed investigation and analysis. Future studies should pay more attention to the effects of climate factors on degradation processes and specific ecological restoration strategies in different regions of the QTP.

Keywords: meta-analysis, climate factors, ecological restoration, Qinghai-Tibet Plateau (QTP), alpine grassland, degradation

OPEN ACCESS

Edited by:
Shiliang Liu,
Beijing Normal University, China

Reviewed by:
Shikui Dong,
Beijing Forestry University, China
Hui Fan,
Yunnan University, China

***Correspondence:**
Xukun Su
xksu@rcees.ac.cn
Keming Ma
mkm@rcees.ac.cn

† These authors have contributed equally to this work

Specialty section:
This article was submitted to Functional Plant Ecology, a section of the journal Frontiers in Plant Science

Received: *25 November 2021*
Accepted: *07 December 2021*
Published: *07 January 2022*

Citation:
Yu J, Wan L, Liu G, Ma K, Cheng H, Shen Y, Liu Y and Su X (2022) A Meta-Analysis on Degraded Alpine Grassland Mediated by Climate Factors: Enlightenment for Ecological Restoration. Front. Plant Sci. 12:821954. doi: 10.3389/fpls.2021.821954

INTRODUCTION

The Qinghai-Tibet Plateau (QTP) is not only the highest plateau in the world (Qiu, 2008) but also an important husbandry production basement (Zhou et al., 2016) and ecological security shelter (Duan et al., 2021) in China and even Asia. Alpine grassland ecosystem covers approximately 60% of the total area of the QTP, which is approximately 2.5 million km[1] (Dong and Sherman, 2015). It provides not only critical ecosystem services in water regulation, soil conservation, biodiversity maintenance, sand fixation, climate change mitigation, carbon sequestration, and others (Dong and Sherman, 2015; Ding et al., 2016; Ren et al., 2016; Liu et al., 2018; Cao et al., 2020) but also a large number of husbandry products and plant resources required by a human for maintaining social and economic development at local, regional, and global scales (Zhang et al., 2015; Zhuang et al., 2019; Xu et al., 2020). In recent years, due to the impact of global warming and intensified human activities, coupled with unreasonable utilization and management of alpine grassland, nearly half of the alpine grassland is facing degradation (Mao et al., 2008; Dong et al., 2010; Pan et al., 2017b). Alpine grassland degradation will inevitably lead to the further decline of its ecosystem services, which will lead the QTP into a vicious circle of "ecological deterioration and economic poverty," and ultimately result in great loss of the ecological security shelter and even "ecological disaster" (Zhang, 2006; Liu et al., 2012). The livelihoods of more than 12 million herders living on the QTP will be directly affected by alpine grassland degradation, and the health and well-being of hundreds of millions of people living downstream will also be indirectly affected (Harris, 2010; Dong and Sherman, 2015). Given the seriousness of this situation, our study aims to reveal the processes and driving factors of alpine grassland degradation, providing theoretical support and restoration strategies for preventing alpine grassland degradation and promoting sustainable utilization of alpine grassland ecosystems of QTP.

Due to the aggravation of alpine grassland degradation, not only degradation and restoration of alpine grassland have become a research hotspot but also the demand for ecological restoration engineering with universality, practicability, and operability is becoming more and more urgent (Zhang Q. et al., 2019; Bai et al., 2020; He et al., 2020a,b). In the process of degradation, huge changes have taken place in the vegetation coverage, biomass and biodiversity (Peng et al., 2012; Tang et al., 2015), soil physical and chemical properties (Ma X. et al., 2020; Wen et al., 2020), soil microbial biomass, and enzymes of alpine grassland (Zhang et al., 2017; Zhou et al., 2019). Understanding the processes and stages of alpine grassland degradation and the effects of climate factors and soil properties is the premise of adopting correct restoration strategies (Gao and Li, 2016; Feng et al., 2019; Li et al., 2019). At present, there are numerous studies on alpine grassland degradation, which are mainly divided into two classes, namely, regional research by remote sensing and GIS (Feng et al., 2017; Yu et al., 2017; Chen et al., 2021) and local research by single-site case studies such as field observation and experimental measurement (Li et al., 2014b, 2020; Jing et al., 2015). Regional research is difficult to describe the mechanisms of degradation due to the lack of field experiments. Local research is difficult to ensure deducing a prevailing reaction type of plant and soil and their interaction due to the huge area of QTP. It is very important to comprehensively analyze the alpine grassland degradation on the QTP by meta-analysis. However, the existing studies using meta-analysis ignore the changes of microbial enzymes in the degradation process and do not consider the effects of climate factors and soil properties (Yan et al., 2020; Zhang W. et al., 2019; Chen et al., 2020; Teng et al., 2020; Liu et al., 2021). Some studies suggest that increasing alpine grassland degradation is significantly affected by climate changes (Huang et al., 2016; Pan et al., 2017b; Ran et al., 2019). It is necessary to conduct a comprehensive analysis to understand the effects of climate factors on degradation processes. There are gaps and doubts on the relationship between soil conditions and alpine grassland degradation on the QTP. The relationships among vegetation, soil, and microbial characteristics with different climate and soil properties in the degradation process of alpine grassland are also not well understood.

Therefore, using the meta-analysis method to study the linkage of vegetation, soil, and microbial characters with different precipitation and temperature in the degradation process of alpine grassland can supplement the shortcomings of the above. We tried to determine the differences of vegetation, soil, and microbial characteristics in the four degradation stages [i.e., light degradation (LD), moderate degradation (MD), heavy degradation (HD), and extreme degradation (ED)] of alpine grassland and the association of climate factors and soil properties of non-degradation (ND) on them. We synthesized to address the following: (1) changes of vegetation, soil, and microbial characteristics in degradation gradients of alpine grassland; (2) effects of climate factors and soil properties on alpine grassland degradation; and (3) implications of ecological restoration strategies to achieve sustainable development of alpine grassland on the QTP.

MATERIALS AND METHODS

Data Collection

Peer-reviewed papers published were searched from the Web of Science and China National Knowledge Infrastructure[2] using the combined keywords "soil," "degradation or degeneration or degraded," "alpine grassland or alpine meadow or alpine steppe," and "Qinghai-Tibetan Plateau or Tibetan Plateau or Tibet" until April 28, 2021. Only studies meeting the following criteria were included in this meta-analysis: (a) degradation stages were clearly stated and consistent with the classification of alpine grassland degradation on the QTP (**Supplementary Table 1**; Ma et al., 2002); (b) data from paired ND and degraded alpine grassland were reported, and the initial climate conditions, species compositions, and soil properties were similar in the degraded and ND alpine grassland; (c) the study contained at

[1]http://www.worldclim.org/

[2]http://www.cnki.net

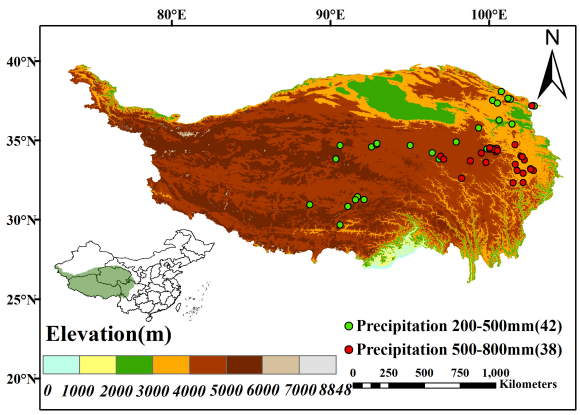

FIGURE 1 | Distribution map of the study site for publications on the Qinghai-Tibet Plateau (QTP) of China. Green points represent sites with 200–500 mm mean annual precipitation (MAP) (42 sites), and red points represent sites with 500–800 mm MAP (38 sites).

least one of the soil property and microbial variables (**Figure 2**); (d) the mean, SD, and sample size (n) for each variable could be obtained.

A total of 209 paired observations from 80 publications were calculated in our meta-analysis (**Figure 1** and **Supplementary Appendix**). We extracted four plant variables, 15 soil property variables, and 12 microbial variables from the papers. Except for microbial biomass carbon (MBC), we also recorded 11 types of enzymes related to soil C, N, and P cycling. They included oxidative C-cycling enzymes: (1) phenol oxidase and (2) peroxidase; hydrolytic C-cycling enzymes: (3) α-1,4-glucosidase, (4) β-1,4-glucosidase, (5) cellobiohydrolase, (6) β-1,4-xylosidase, and (7) invertase; *N*-cycling enzymes: (8) *N*-acetyl-β-glucosaminidase, (9) L-leucine aminopeptidase, and (10) urease; and P-cycling enzymes: (11) phosphatase. These enzymes are good proxies of soil biogeochemical cycling (Kandeler et al., 1999; German et al., 2011) and are widely used to estimate the ecosystem functionality of microbial communities (Delgado-Baquerizo et al., 2016; Zhou et al., 2020). We used the digitizing software WebPlotDigitizer to extract results presented in figures (Burda et al., 2017). The location, mean annual temperature (MAT), and mean annual precipitation (MAP) were also gathered and recorded. If climate factors were absent from the source papers, we extracted MAT and MAP from the relevant latitude and longitude of the global climate layers of WorldClim (1 km^2 spatial resolution[2]). The Map of China was provided by the "National Tibetan Plateau Data Center."[3] The digital elevation model (DEM) data were downloaded from the United States Geological Survey (USGS) at 30-m spatial resolution.[4]

Data Analysis

In this meta-analysis, the effects of alpine grassland degradation were calculated using the natural log of the response ratio (RR) (Hedges et al., 1999). The *RR* and its corresponding pooled variance (v) were calculated as follows:

$$\mathrm{RR} = \ln\left(\frac{X_\mathrm{d}}{X_\mathrm{nd}}\right) \quad (1)$$

$$v = \frac{\mathrm{SD}_\mathrm{nd}^2}{n_\mathrm{nd}X_\mathrm{nd}^2} + \frac{\mathrm{SD}_\mathrm{d}^2}{n_\mathrm{d}X_\mathrm{d}^2} \quad (2)$$

where X_nd and X_d are the mean values of a specific variable in the ND and degraded alpine grassland, respectively; n_nd and n_d are the sample sizes for the ND and degraded groups, respectively; and SD_nd and SD_d are the SDs for the ND and degraded groups, respectively. In the studies that neither SD nor SE was reported, we assigned the SD as 1/10 of the mean (Zhou et al., 2017). For ease of understanding, we synthesized 11 enzymes into 4 categories (i.e., oxidative C-cycling enzymes, hydrolytic C-cycling enzymes, N-cycling enzymes, and P-cycling enzymes). In addition, the random-effect model was used to calculate RRs of oxidative C-cycling enzymes, hydrolytic C-cycling enzymes, and N-cycling enzymes for each observation (Zhou et al., 2020). The mixed-effect model was used to calculate the weighted *RR* (RR_{++}) and corresponding 95% CIs of target variables with a moderator of degradation stages. We performed the omnibus test (Q_M) to test whether the responses differed among different degradation stages. When the Q_M values were significant ($P < 0.05$), the responses among stages were different. For ease of understanding, the weighted *RR* and its corresponding 95% CI were transformed to the percentage change calculated by the following formula: $(e^{\mathrm{RR}}{}_{++} - 1) \times 100\%$. The groups with the small sample size (<5) were removed in these analyses. Moreover, publication bias within each variable was assessed using a regression test for funnel plot asymmetry (Egger et al., 1997). Our results showed that most variables had no publication bias (**Supplementary Table 2**). The possible publication bias within several variables would not affect our results because Rosenberg's fail-safe number indicated that these results were robust (Rosenberg, 2005).

We used single meta-regression models to quantify how effects of degradation varied depending on climate factors (i.e., MAT and MAP) and corresponding variables of non-degradation grassland [i.e., aboveground biomass (AGB), belowground biomass (BGB), soil organic carbon (SOC), soil total nitrogen (TN), and microbial biomass carbon (MBC)]. Finally, we conducted a Pearson correlation analysis to investigate the relationships among RRs of all variables. All statistical analyses were conducted using R software version 4.0.0 (R Development Core Team, 2020).

RESULTS

Changes of Vegetation, Soil, and Microbial Variables Along the Degradation Gradient

For four plant variables, the losses escalated with the degradation of alpine grasslands and differed significantly ($P < 0.001$) between

[3]https://data.tpdc.ac.cn/zh-hans/

[4]http://earthexplorer.usgs.gov/

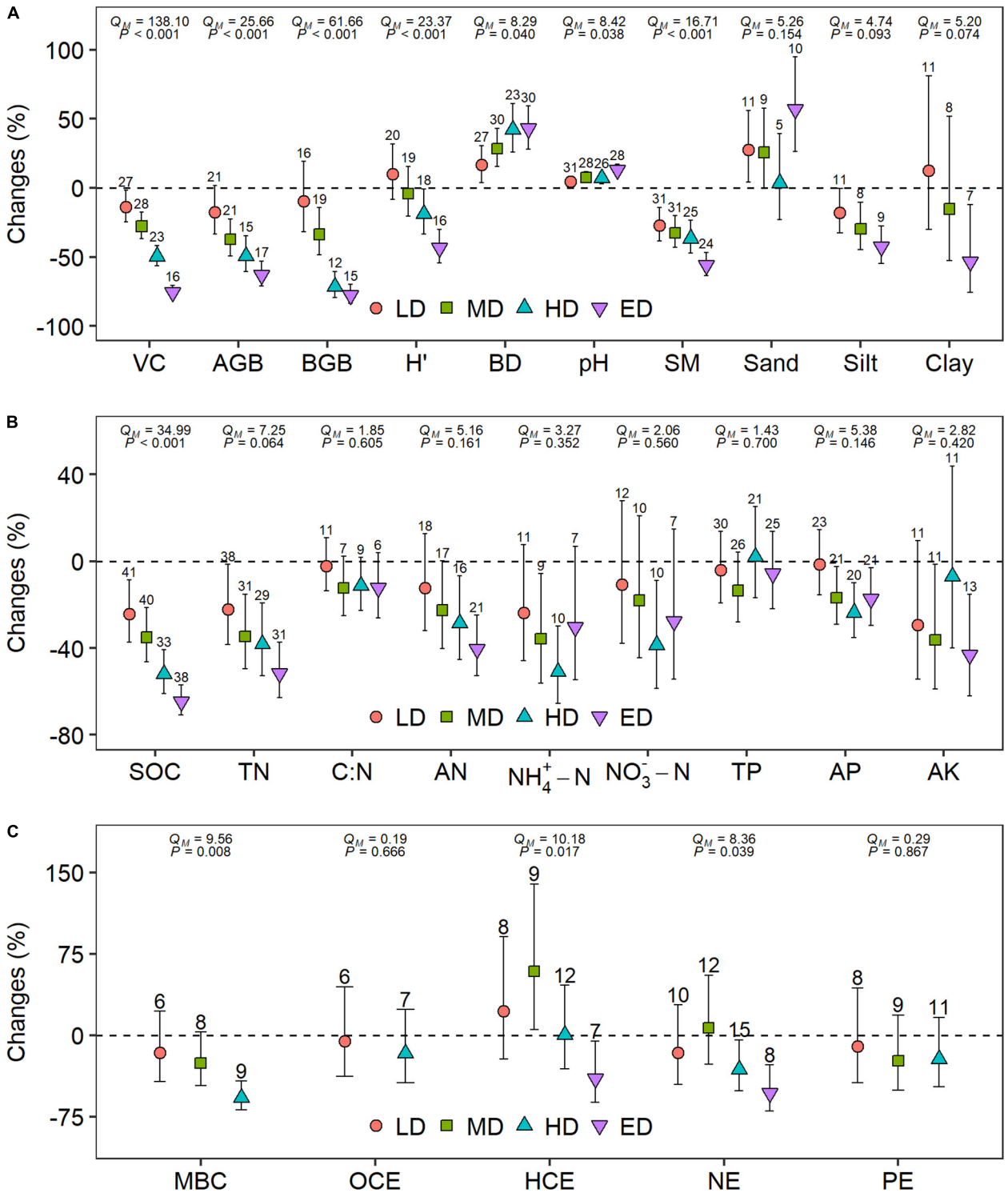

FIGURE 2 | Percent changes of **(A)** plant and six soil property variables, **(B)** soil nutrient variables, and **(C)** microbial variables after grassland degradation across different degradation stages. Weighted means and their 95% CIs of percent changes are given. The numbers at the top of the CIs represent the sample sizes. The significances of degradation stages are tested by the omnibus test (QM). LD, light degradation; MD, moderate degradation; HD, heavy degradation; ED, extreme degradation; VC, vegetation cover; AGB, aboveground biomass; BGB, belowground biomass; H', Shannon-Wiener index; BD, soil bulk density; SM, soil moisture; SOC, soil organic carbon (C); TN, total nitrogen (N); AN, available N; NH_4-N, ammonium N; NO_3^--N, nitrate N; TP, total phosphorus (P); AP, available P; AK, available potassium; MBC, microbial biomass C; OCE, oxidative C-cycling enzymes; HCE, hydrolytic C-cycling enzymes; NE, N-cycling enzymes; PE, P-cycling enzymes. Source data are provided as a Source Data file.

the different degradation stages (**Figure 2A**). However, only vegetation cover significantly decreased at all four degradation stages. The reduction in AGB and BGB was not significant at the stage of LD, and the Shannon-Wiener index only showed a significant reduction at the stages of HD and ED.

Soil bulk density (BD) and soil *pH* significantly increased at all four degradation stages with significantly ($P < 0.05$) higher at the stage of ED than that at the stage of LD (**Figure 2B**). SM significantly decreased at all four degradation stages with significantly ($P < 0.001$) lower at the stage of ED than that at the stage of LD (**Figure 2A**). Changes in soil texture showed no significant difference ($P > 0.05$) between the different degradation stages (**Figure 2A**). Sand content showed a significant increase at the stages of LD and ED. Silt content showed a significant decrease at the stages of HD and ED. In addition, clay content showed a significant decrease at the stage of ED. SOC and TN significantly decreased at all four degradation stages and the reduction both gradually increased along the degradation gradient (**Figure 2B**). The losses of SOC were significantly higher at the stage of HD and ED compared to those at the stage of LD ($P < 0.001$). The difference in TN losses was not significant ($P > 0.05$) between the different degradation stages. Soil C:N ratio and TP showed no significant changes in all degradation stages ($P > 0.05$). Other nutrients also had a trend to decline, but the variations were rarely consistent at different degradation stages.

For microbial variables, MBC significantly decreased at the stage of HD (**Figure 2C**). Hydrolytic C-cycling enzymes significantly increased at the stage of MD and significantly decreased at the stage of ED. N-cycling enzymes significantly decreased at the stages of HD and ED. In other degradation stages, the microbial variables did not show significant changes.

Driving Factors of Alpine Grassland Degradation

The meta-regression results showed that the reduction of TN was smaller in areas with higher MAT and MAP (**Figure 3**). The increase of soil *pH* was larger in areas with higher MAT and MAP (**Supplementary Figures 1a,b**). Moreover, the decreasing extent in SM was larger in areas with higher MAP (**Supplementary Figure 1c**). The losses of AGB, SOC, and TN were larger in areas with a higher extent of corresponding variables in the stage of ND (**Figure 4**). Correlation analysis showed that most RRs of variables were significantly positively related to each other (**Figure 5**). Especially, the RRs of vegetation cover, BGB, and Shannon-Wiener index were negatively related to the *RR* of soil *pH*.

DISCUSSION

Processes and Mechanisms in Vegetation and Soil Degradation

With more variables included in our study, our results reveal more comprehensive plant, soil, and microbial changes during degradation processes than previous meta-analyses (Zhang W. et al., 2019; Teng et al., 2020; Liu et al., 2021). At the stage of LD, the insignificant changes of AGB and BGB were probably due to the increasing biomass of forbs, which could cancel out the decline in the biomass of graminoids and sedges (Wang et al., 2009; Zhang W. et al., 2019). The Shannon-Wiener index only significantly decreased in the stages of HD and ED, which implied that the light and moderate environmental disturbance might have a neutral effect on vegetation communities (Wang et al., 2009). With the proportion of poisonous plants and the disturbance intensity increasing, plant community structure gradually deteriorates, leading to the reduction of plant diversity (Li et al., 2014a). As shown in correlation analysis, the deterioration of soil properties was closely associated with alpine grassland degradation. Following the loss of vegetation cover, the soil surface losses its protection and undergoes erosion from wind and water, resulting in the increase of sand content and decline in silt and clay content (Xu et al., 2019). Moreover, as topsoil was eroded, subsoil with higher *pH* values would be exposed and form new topsoil (Ma X. et al., 2020), so that the *pH* values also escalated with degradation stages. In fact, accompanied by vegetation degradation, changes in soil properties would further influence other properties. For instance, the shift of plant composition might enlarge the plant transpiration as the big leaves of forbs might exacerbate water loss (Peng et al., 2018). The increase in sand content and decline in SOC also have negative effects on soil water retention, resulting in the reduction of SM with degradation (Pan et al., 2017a; Dai et al., 2021). In addition, the increase of soil BD is also the combined effect of the compaction from livestock trampling, and the loss of SOC as SOM is loose and porous (Ruehlmann and Koerschens, 2009).

Previous studies have proposed some mechanisms to explain the SOC loss with alpine grassland degradation, which mainly focuses on two aspects: (1) the biological and ecological processes and (2) the physical processes. First, the significant decrease of AGB and BGB will directly reduce the input of C to the soil. The previous study has proved that forbs can lead to higher fine root decomposition and enhance the SOC mineralization compared with grass (Fornara et al., 2009). Therefore, changes in the plant community during degradation may lead to a higher rate of SOC mineralization. Our results also showed that the C-cycling enzyme activities would not decrease except the stage of ED, indicating that microbial metabolism related to SOC mineralization would not be hampered when the degradation intensity was not severe. Second, wind and water erosion directly remove SOM. In addition, the physical protection of SOM can be broken by external disturbances such as livestock trampling, which stimulates decomposition (Dong et al., 2020b). Our results showed that the soil C:N ratio did not have significant changes in all degeneration stages, indicating that the N (nitrogen) mostly came from organic sources and was closely related to SOC. Therefore, mechanisms for the loss of SOC could be considered to interpret the loss of soil TN with degradation. Nevertheless, available nitrogen (AN) did not significantly decrease in the stage of LD and MD, possibly resulting from the decline of graminoids which are N-extravagant plants (Turner et al., 2007).

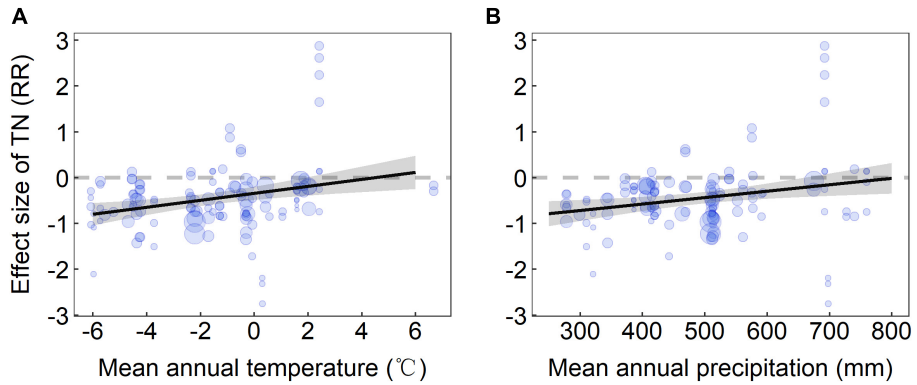

FIGURE 3 | Change in soil total nitrogen with **(A)** mean annual temperature and **(B)** MAP. RR, response ratio. *RR* = 0, dashed gray line; predicted mean effect size (with 95% CI in gray), black lines. The size of data points (in blue) is proportional to the sampling variance. Results were obtained with single meta-regressions.

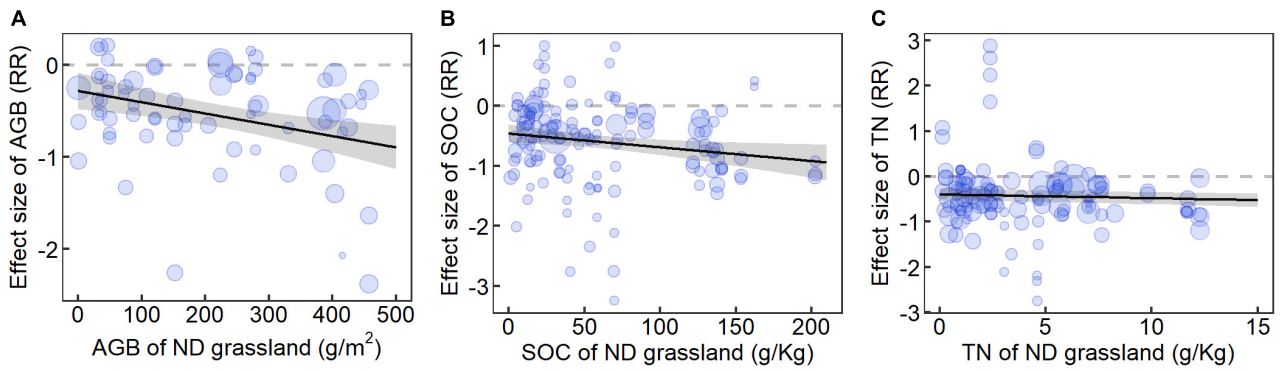

FIGURE 4 | Changes in **(A)** aboveground biomass, **(B)** soil organic carbon, and **(C)** soil total nitrogen with corresponding variables of non-degradation grassland. *RR*, response ratio. *RR* = 0, dashed gray line; predicted mean effect size (with 95% CI in gray), black lines. The size of data points (in blue) is proportional to the sampling variance. Results were obtained with single meta-regressions.

Other nutrients mostly had no significant changes at different degradation stages, implying that the influence of degradation on them might be slight and negligible. For microbial variables, our results showed that enzyme activities only significantly decreased in the stage of HD or ED, indicating that HD or ED might be the turning point for enzymes during alpine grassland degradation as the biological or abiotic factors (such as microbial biomass and *pH*) change (Ma W. et al., 2020; Wu et al., 2020).

The Effect of Climate Factors and Soil Properties on Degradation Processes

Due to the importance of climate factors and soil properties on degradation, we analyzed the relationship between climate factors and soil properties of ND and degraded alpine grassland to improve our understanding of alpine grassland degradation and restoration on the QTP. We found that climatic factors played an important role in alpine grassland degradation, especially for TN, which was consistent with previous studies (Pan et al., 2017b). We also found that AGB, SOC, and TN of ND had significant effects on AGB, SOC, and TN at different degradation stages (Huang et al., 2021). Through these analyses, we can understand the effects of environmental factors during degradation and provide a scientific theory for grassland restoration and sustainable management.

Our results showed that in areas with higher precipitation and temperature, the loss of TN decreased in the alpine grassland degradation process. If that will be the case, there is a "hydrothermal-hole effect" (Shang et al., 2006) in the process of alpine grassland degradation on the QTP. Theoretically, the alpine grassland degradation of QTP is often accompanied by vegetation reduction and soil property changes, and alpine grassland is bare if degradation continues. A large amount of water and heat is lost through the bare land, which makes the "vegetation-soil-microorganism" system of alpine grassland unstable. It accelerates the area of grassland degradation, the invasion of poisonous weeds, and the loss of soil nutrients, thus aggravating the degree of degradation (Dong et al., 2020a). These effects are caused by water and heat entering the atmosphere due to bare soil, which in turn lead to increased degradation, air exchanges of water, and heat decrease with precipitation and temperature increasing. With precipitation and temperature increasing, the effects of the "hydrothermal-hole effect" on degraded alpine grassland can be slowed down, and the loss of TN is also reduced. The more AGB, SOC, and TN are lost in areas with the more AGB, SOC, and TN of ND alpine grassland

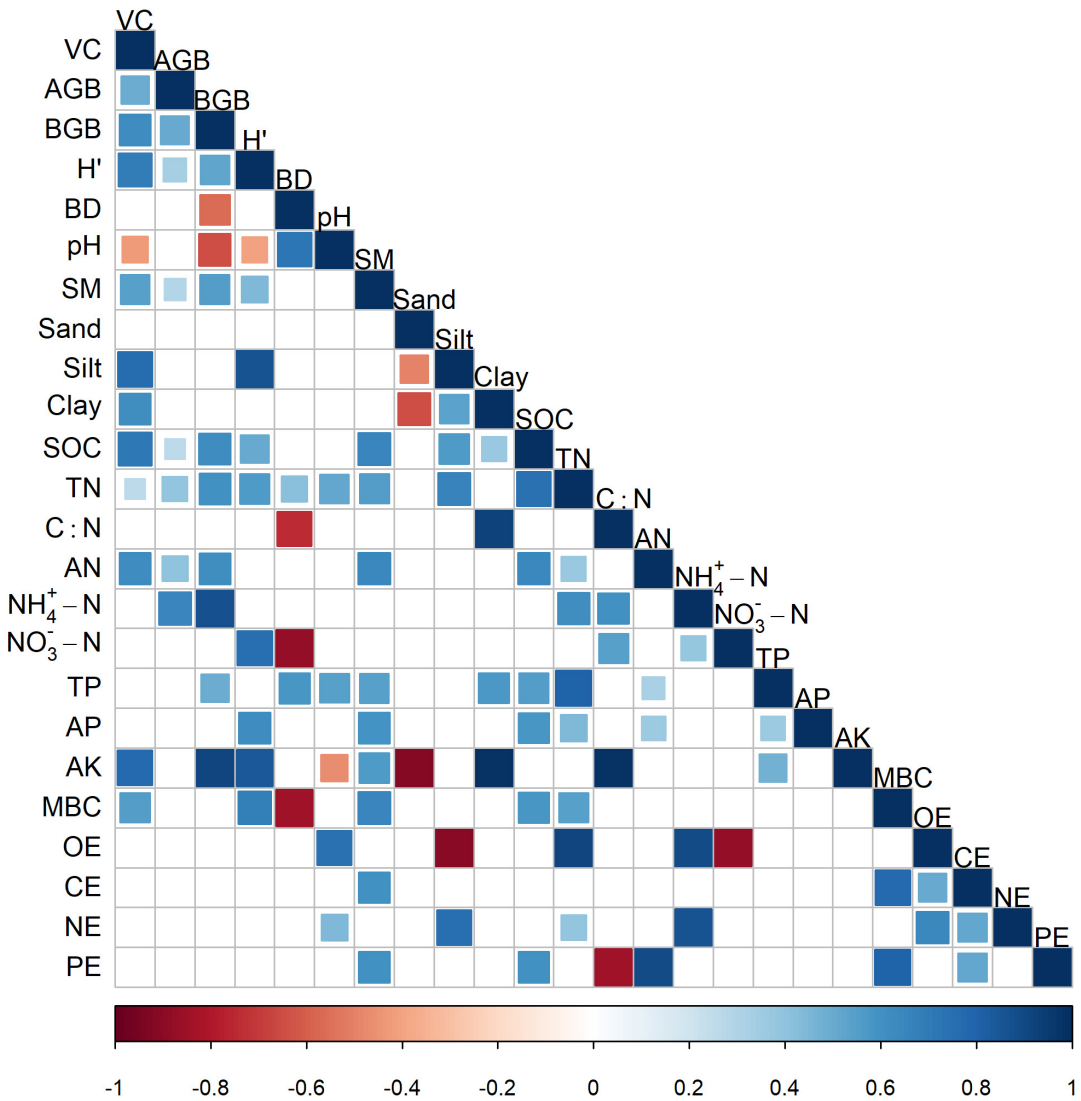

FIGURE 5 | Relationships of the effect sizes of each variable with others. Square size and colors represent Pearson correlations. Only significant results with a sufficient sample size ($n > 4$) were displayed.

during alpine grassland degradation. Studies have shown that the alpine steppe and alpine meadow ecosystems on the QTP have the strongest resistance stability, the weakest resilience stability, and the longest recovery time (Huang et al., 2021). The species-poor systems are more resistant to perturbation than the species-rich systems and show a larger initial resilience following a perturbation (Pfisterer and Schmid, 2002). Our results showed that it was a positive correlation between effect sizes of species richness and SOC, TN, AP, NO_3^--N, and AK. Previous research results showed that there was a positive correlation between most soil properties and species richness in high-altitude natural grassland (Wang et al., 2014). Therefore, the alpine grassland with better soil conditions degenerates more seriously in degradation processes, which is more vulnerable to grassland degradation and needs more recovery time. For example, most of the extreme degradation of "black soil land" occurs in the Sanjiangyuan National Park with better soil properties of ND, but it rarely appears in the alpine grassland in the Northern Tibetan region of China with poor soil properties of ND. We speculate that grassland degradation may be more serious where the resistance stability is better. In areas with better soil properties, the lower the resilience stability of the grassland ecosystem leads to AGB, SOC, and TN loss increasing during alpine grassland degradation.

Restoration Strategies of Degraded Alpine Grassland

The degradation process is different at various degraded alpine grassland ecosystems, and climate and soil properties play a significant role in the degradation process. According to the comprehensive analysis, our research points out the main ecological restoration directions in different areas on

the QTP. In view of the severe degradation of the alpine grassland ecosystem caused by environmental changes and human activities, restoration efforts have been paid more and more attention. In terms of degradation gradient, different restoration measures should be adopted for different degradation areas. "Black soil land" (ED alpine grassland) is difficult to recover without human intervention because it has lost its ability to self-recover (Shang et al., 2006). Artificial planting should be used for restoration in the ED alpine grasslands. In the LD alpine grassland, the soil nutrients and excellent pasture species have not been lost a lot so fencing enclosure for a short time is adopted for restoration. Some scholars believe that 3–4 years is a suitable time for alpine grassland fencing on the QTP (Zhu et al., 2016). In terms of climate factors, fencing and fertilization can be used for alpine grassland restoration in lower precipitation and temperature areas (Dong et al., 2010). Reseeding and sward cleavage can be used for restoration on degraded alpine grassland in higher precipitation and temperature areas (He et al., 2020b). In terms of soil conditions, not only the fragile alpine grassland needs to be protected but also the alpine grassland with the strongest resistance and stability needs more protection due to the longest recovery time (Andrade et al., 2015). If alpine grassland degradation occurs, the alpine meadow is more difficult to recover than the alpine steppe. Microbial enzymes should not be used to restore degraded alpine grassland in large areas on the QTP due to the huge area and diversity of the QTP. If ecological restoration is carried out from the perspective of microbial enzymes, detailed investigation and research must be carried out (Zhang et al., 2021). Grazing management is the first priority for the restoration of degraded alpine grassland (Jiang et al., 2020). According to the degradation degree of alpine grassland, fencing with different lengths of time should be used. In artificial cultivation, species based on different functional traits and different functional groups are selected to make better use of resources (Weisser et al., 2017).

CONCLUSION

Our meta-analysis quantitatively assessed the effects of alpine grassland degradation on vegetation, soil, and microbial variables on the QTP. We presented more plentiful data for soil properties and much more information on microbial variables, providing a crucial reference for future studies on alpine grassland degradation. Results showed that the loss of TN tended to alleviate in areas with higher precipitation and temperature during alpine grassland degradation, but the losses of AGB, SOC, and TN tended to aggravate in areas with more contents of ND alpine grassland. These findings improve our understanding of how climate variables and AGB, SOC, and TN of ND alpine grassland regulate degradation stages at a large scale. Ecological restoration of degraded alpine grassland can be carried out by means of fence and fertilization in regions with lower precipitation and temperature. Severe degraded alpine grassland can be restored by reseeding and mowing. Grazing management and artificial cultivation are the most widely used and most effective methods. Implementing different restoration methods in alpine grassland with different degradation gradients and different environmental conditions is necessary to achieve targets of ecological restoration on the QTP.

DATA AVAILABILITY STATEMENT

The datasets presented in this study can be found in online repositories. The names of the repository/repositories and accession number(s) can be found in the article/ **Supplementary Material**.

AUTHOR CONTRIBUTIONS

JY and LW conceived the idea, assembled the data, and wrote the first draft of the manuscript. JY did the statistical analyses. GL, KM, and XS advised in the process of manuscript writing. All authors contributed substantially to the interpretation of the results and revision of the manuscript.

FUNDING

This study was supported by the Second Tibetan Plateau Scientific Expedition and Research Program (STEP), grant no. 2019QZKK0402, and the Strategic Priority Research Program of Chinese Academy of Sciences, grant no. XDA20020402.

ACKNOWLEDGMENTS

The authors thank all people for helping us to complete data collection and the reviewers who helped us to improve the manuscript.

SUPPLEMENTARY MATERIAL

The Supplementary Material for this article can be found online at: https://www.frontiersin.org/articles/10.3389/fpls.2021.821954/full#supplementary-material

REFERENCES

Andrade, B. O., Koch, C., Boldrini, I. I., Velez-Martin, E., Hasenack, H., Hermann, J. M., et al. (2015). Grassland degradation and restoration: a conceptual framework of stages and thresholds illustrated by southern Brazilian grasslands. *Nat. Conserv.* 13, 95–104. doi: 10.1016/j.ncon.2015.08.002

Bai, Y. F., Ma, L. N., Degen, A. A., Rafiq, M. K., Kuzyakov, Y., Zhao, J. X., et al. (2020). Long-term active restoration of extremely degraded alpine grassland accelerated turnover and increased stability of soil carbon. *Glob. Change Biol.* 26, 7217–7228. doi: 10.1111/gcb.15361

Burda, B. U., O'Connor, E. A., Webber, E. M., Redmond, N., and Perdue, L. A. (2017). Estimating data from figures with a web-based program: considerations for a systematic review. *Res. Synth. Methods* 8, 258–262. doi: 10.1002/jrsm.1232

Cao, W., Wu, D., Huang, L., and Liu, L. L. (2020). Spatial and temporal variations and significance identification of ecosystem services in the Sanjiangyuan National Park, China. *Sci. Rep.* 10:13. doi: 10.1038/s41598-020-63137-x

Chen, L. T., Jiang, L., Jing, X., Wang, J. L., Shi, Y., Chu, H. Y., et al. (2021). Above- and belowground biodiversity jointly drive ecosystem stability in natural alpine grasslands on the Tibetan Plateau. *Glob. Ecol. Biogeogr.* 30, 1418–1429. doi: 10.1111/geb.13307

Chen, Y., Feng, J. G., Yuan, X., and Zhu, B. (2020). Effects of warming on carbon and nitrogen cycling in alpine grassland ecosystems on the Tibetan Plateau: a meta-analysis. *Geoderma* 370:10. doi: 10.1016/j.geoderma.2020.114363

Dai, L., Guo, X., Ke, X., Du, Y., Mang, F., and Cao, G. (2021). The variation in soil water retention of alpine shrub meadow under different degrees of degradation on northeastern Qinghai-Tibetan plateau. *Plant Soil* 458, 231–244. doi: 10.1007/s11104-020-04522-3

Delgado-Baquerizo, M., Maestre, F. T., Reich, P. B., Jeffries, T. C., Gaitan, J. J., Encinar, D., et al. (2016). Microbial diversity drives multifunctionality in terrestrial ecosystems. *Nat. Commun.* 7:10541. doi: 10.1038/ncomms10541

Ding, J. Z., Li, F., Yang, G. B., Chen, L. Y., Zhang, B. B., Liu, L., et al. (2016). The permafrost carbon inventory on the Tibetan Plateau: a new evaluation using deep sediment cores. *Glob. Change Biol.* 22, 2688–2701. doi: 10.1111/gcb.13257

Dong, S. K., and Sherman, R. (2015). Enhancing the resilience of coupled human and natural systems of alpine rangelands on the Qinghai-Tibetan Plateau. *Rangel. J.* 37, 1–3. doi: 10.1071/rj14117

Dong, S. K., Wen, L., Zhu, L., and Li, X. Y. (2010). Implication of coupled natural and human systems in sustainable rangeland ecosystem management in HKH region. *Front. Earth Sci.* 4:42–50. doi: 10.1007/s11707-010-0010-z

Dong, S., Shang, Z., Gao, J., and Boone, R. B. (2020a). Enhancing sustainability of grassland ecosystems through ecological restoration and grazing management in an era of climate change on Qinghai-Tibetan Plateau. *Agric. Ecosyst. Environ.* 287:106684. doi: 10.1016/j.agee.2019.106684

Dong, S., Zhang, J., Li, Y., Liu, S., Dong, Q., Zhou, H., et al. (2020b). Effect of grassland degradation on aggregate-associated soil organic carbon of alpine grassland ecosystems in the Qinghai-Tibetan Plateau. *Eur. J. Soil Sci.* 71, 69–79. doi: 10.1111/ejss.12835

Duan, H. C., Xue, X., Wang, T., Kang, W. P., Liao, J., and Liu, S. L. (2021). Spatial and temporal differences in alpine meadow, alpine steppe and all vegetation of the Qinghai-Tibetan Plateau and their responses to climate change. *Remote Sens.* 13:669. doi: 10.3390/rs13040669

Egger, M., Smith, G. D., Schneider, M., and Minder, C. (1997). Bias in meta-analysis detected by a simple, graphical test. *Br. Med. J.* 315, 629–634. doi: 10.1136/bmj.315.7109.629

Feng, X., Qu, J. J., Fan, Q. B., Tan, L. H., and An, Z. S. (2019). Characteristics of desertification and short-term effectiveness of differing treatments on shifting sand dune stabilization in an Alpine Rangeland. *Int. J. Environ. Res. Public Health* 16:4968. doi: 10.3390/ijerph16244968

Feng, Y. F., Wu, J. S., Zhang, J., Zhang, X. Z., and Song, C. Q. (2017). Identifying the relative contributions of climate and grazing to both direction and magnitude of alpine grassland productivity dynamics from 1993 to 2011 on the Northern Tibetan Plateau. *Remote Sens.* 9:136. doi: 10.3390/rs9020136

Fornara, D. A., Tilman, D., and Hobbie, S. E. (2009). Linkages between plant functional composition, fine root processes and potential soil N mineralization rates. *J. Ecol.* 97, 48–56. doi: 10.1111/j.1365-2745.2008.01453.x

Gao, J., and Li, X. L. (2016). Degradation of frigid swampy meadows on the Qinghai-Tibet Plateau: current status and future directions of research. *Progr. Phys. Geogr.Earth Environ.* 40, 794–810. doi: 10.1177/0309133316659283

German, D. P., Weintraub, M. N., Grandy, A. S., Lauber, C. L., Rinkes, Z. L., and Allison, S. D. (2011). Optimization of hydrolytic and oxidative enzyme methods for ecosystem studies. *Soil Biol. Biochem.* 43, 1387–1397. doi: 10.1016/j.soilbio.2011.03.017

Harris, R. B. (2010). Rangeland degradation on the Qinghai-Tibetan plateau: a review of the evidence of its magnitude and causes. *J. Arid Environ.* 74, 1–12. doi: 10.1016/j.jaridenv.2009.06.014

He, J., Bu, H., Hu, X., Feng, Y., Li, S., Zhu, J., et al. (2020a). Close-to-nature restoration of degraded alpine grasslands: theoretical basis and technical approach. *Chin. Sci. Bull.* 65, 3898–3908.

He, J., Liu, Z., Yao, T., Sun, S., Lu, Z., Hu, X., et al. (2020b). Analysis of the main constraints and restoration techniques of degraded grassland on the Tibetan Plateau. *Sci. Technol. Rev.* 38, 66–80.

Hedges, L. V., Gurevitch, J., and Curtis, P. S. (1999). The meta-analysis of response ratios in experimental ecology. *Ecology* 80, 1150–1156.

Huang, K., Zhang, Y. J., Zhu, J. T., Liu, Y. J., Zu, J. X., and Zhang, J. (2016). The influences of climate change and human activities on vegetation dynamics in the Qinghai-Tibet Plateau. *Remote Sens.* 8:876. doi: 10.3390/rs8100876

Huang, W. J., Wang, W., Cao, M., Fu, G., Xia, J. Y., Wang, Z. X., et al. (2021). Local climate and biodiversity affect the stability of China's grasslands response to drought. *Sci. Total Environ.* 768:145482. doi: 10.1016/j.scitotenv.2021.145482

Jiang, S., Feng, T., Liu, G., and He, J. (2020). A bibliometric analysis of the application of grassland ecological restoration technology. *Pratacultural Sci.* 37, 685–702.

Jing, X., Sanders, N. J., Shi, Y., Chu, H. Y., Classen, A. T., Zhao, K., et al. (2015). The links between ecosystem multifunctionality and above- and belowground biodiversity are mediated by climate. *Nat. Commun.* 6:8. doi: 10.1038/ncomms9159

Kandeler, E., Luxhoi, J., Tscherko, D., and Magid, J. (1999). Xylanase, invertase and protease at the soil-litter interface of a loamy sand. *Soil Biol. Biochem.* 31, 1171–1179. doi: 10.1016/s0038-0717(99)00035-8

Li, J.-H., Yang, G.-J., and Wang, S.-P. (2020). Vegetation and soil characteristics of degraded alpine meadows on the Qinghai-Tibet Plateau, China: a review. *Yingyong Shengtai Xuebao* 31, 2109–2118. doi: 10.13287/j.1001-9332.202006.002

Li, X. L., Gao, J., Zhang, J., Wang, R., Jin, L. Q., and Zhou, H. K. (2019). Adaptive strategies to overcome challenges in vegetation restoration to coalmine wasteland in a frigid alpine setting. *Catena* 182:104142. doi: 10.1016/j.catena.2019.104142

Li, Y.-Y., Dong, S.-K., Liu, S., Wang, X., Wen, L., and Wu, Y. (2014a). The interaction between poisonous plants and soil quality in response to grassland degradation in the alpine region of the Qinghai-Tibetan Plateau. *Plant Ecol.* 215, 809–819. doi: 10.1007/s11258-014-0333-z

Li, Y. Y., Dong, S. K., Wen, L., Wang, X. X., and Wu, Y. (2014b). Soil carbon and nitrogen pools and their relationship to plant and soil dynamics of degraded and artificially restored grasslands of the Qinghai-Tibetan Plateau. *Geoderma* 213, 178–184. doi: 10.1016/j.geoderma.2013.08.022

Liu, J., Milne, R. I., Cadotte, M. W., Wu, Z. Y., Provan, J., Zhu, G. F., et al. (2018). Protect third pole's fragile ecosystem. *Science* 362, 1368–1368. doi: 10.1126/science.aaw0443

Liu, X., Long, R., and Shang, Z. (2012). Interactive mechanism of service function of alpine rangeland ecosystems in Qinghai-Tibetan Plateau. *Acta Ecol. Sin.* 32, 7688–7697.

Liu, X., Wang, Z., Zheng, K., Han, C., Li, L., Sheng, H., et al. (2021). Changes in soil carbon and nitrogen stocks following degradation of alpine grasslands on the Qinghai-Tibetan Plateau: a meta-analysis. *Land Degrad. Dev.* 32, 1262–1273. doi: 10.1002/ldr.3796

Ma, W., Li, G., Wu, J., Xu, G., and Wu, J. (2020). Response of soil labile organic carbon fractions and carbon-cycle enzyme activities to vegetation degradation in a wet meadow on the Qinghai-Tibet Plateau. *Geoderma* 377:114565. doi: 10.1016/j.geoderma.2020.114565

Ma, X., Asano, M., Tamura, K., Zhao, R., Nakatsuka, H., Wuyunna, et al. (2020). Physicochemical properties and micromorphology of degraded alpine meadow soils in the Eastern Qinghai-Tibet Plateau. *Catena* 194:104649. doi: 10.1016/j.catena.2020.104649

Ma, Y., Lang, B., Li, Q., Shi, J., and Dong, Q. (2002). Study on rehabilitating and rebuilding technologies for degenerated alpine meadow in the Changjiang and Yellow river source region. *Pratacultural Sci.* 19, 1–5.

Mao, F., Zhang, Y.-H., Hou, Y.-Y., Tang, S.-H., Lu, Z.-G., and Zhang, J.-H. (2008). Dynamic assessment of grassland degradation in Naqu of northern Tibet. *J. Appl. Ecol.* 19, 278–284.

Pan, T., Hou, S., Wu, S., Liu, Y., Liu, Y., Zou, X., et al. (2017a). Variation of soil hydraulic properties with alpine grassland degradation in the eastern Tibetan Plateau. *Hydrol. Earth Syst. Sci.* 21, 2249–2261. doi: 10.5194/hess-21-2249-2017

Pan, T., Zou, X. T., Liu, Y. J., Wu, S. H., and He, G. M. (2017b). Contributions of climatic and non-climatic drivers to grassland variations on the Tibetan Plateau. *Ecol. Eng.* 108, 307–317. doi: 10.1016/j.ecoleng.2017.07.039

Peng, F., Xue, X., You, Q., Huang, C., Dong, S., Liao, J., et al. (2018). Changes of soil properties regulate the soil organic carbon loss with grassland degradation

on the Qinghai-Tibet Plateau. *Ecol. Indic.* 93, 572–580. doi: 10.1016/j.ecolind.2018.05.047

Peng, J., Liu, Z. H., Liu, Y. H., Wu, J. S., and Han, Y. A. (2012). Trend analysis of vegetation dynamics in Qinghai-Tibet Plateau using hurst exponent. *Ecol. Indic.* 14, 28–39. doi: 10.1016/j.ecolind.2011.08.011

Pfisterer, A. B., and Schmid, B. (2002). Diversity-dependent production can decrease the stability of ecosystem functioning. *Nature* 416, 84–86. doi: 10.1038/416084a

Qiu, J. (2008). The third pole. *Nature* 454, 393–396. doi: 10.1038/454393a

R Development Core Team (2020). *R: A Language and Environment for Statistical Computing*. Vienna: The R Foundation for Statistical Computing.

Ran, Q. W., Hao, Y. B., Xia, A. Q., Liu, W. J., Hu, R. H., Cui, X. Y., et al. (2019). Quantitative assessment of the impact of physical and anthropogenic factors on vegetation spatial-temporal variation in Northern Tibet. *Remote Sens.* 11:1183. doi: 10.3390/rs11101183

Ren, Y. J., Lu, Y. H., and Fu, B. J. (2016). Quantifying the impacts of grassland restoration on biodiversity and ecosystem services in China: a meta-analysis. *Ecol. Eng.* 95, 542–550. doi: 10.1016/j.ecoleng.2016.06.082

Rosenberg, M. S. (2005). The file-drawer problem revisited: a general weighted method for calculating fail-safe numbers in meta-analysis. *Evolution* 59, 464–468. doi: 10.1554/04-602

Ruehlmann, J., and Koerschens, M. (2009). Calculating the effect of soil organic matter concentration on soil bulk density. *Soil Sci. Soc. Am. J.* 73, 876–885. doi: 10.2136/sssaj2007.0149

Shang, Z., Long, R., and Ma, Y. (2006). Discussion on Restoration and rebuilding of blackion soil patch' degraded meadow in the headwater area of yangtze and yellow rivers. *Chin. J. Grassl.* 28, 69–74.

Tang, L., Dong, S. K., Sherman, R., Liu, S. L., Liu, Q. R., Wang, X. X., et al. (2015). Changes in vegetation composition and plant diversity with rangeland degradation in the alpine region of Qinghai-Tibet Plateau. *Rangel. J.* 37, 107–115. doi: 10.1071/rj14077

Teng, Y., Zhan, J., Agyemang, F. B., and Sun, Y. (2020). The effects of degradation on alpine grassland resilience: a study based on meta-analysis data. *Glob. Ecol. Conserv.* 24:e01336. doi: 10.1016/j.gecco.2020.e01336

Turner, M. G., Smithwick, E. A. H., Metzger, K. L., Tinker, D. B., and Romme, W. H. (2007). Inorganic nitrogen availability after severe stand-replacing fire in the greater yellowstone ecosystem. *Proc. Natl. Acad. Sci. U.S.A.* 104, 4782–4789. doi: 10.1073/pnas.0700180104

Wang, C. T., Long, R. J., Wang, Q. L., Jing, Z. C., and Shi, J. J. (2009). Changes in plant diversity, biomass and soil C, in alpine meadows at different degradation stages in the headwater region of three rivers, China. *Land Degrad. Dev.* 20, 187–198. doi: 10.1002/ldr.879

Wang, D., Wu, G. L., Chang, X. F., Shi, Z. H., Sun, L., and Wei, X. H. (2014). Higher species diversity occurs in more fertile habitats without fertilizer disturbance in an alpine natural grassland community. *J. Mt. Sci.* 11, 755–761. doi: 10.1007/s11629-013-2703-8

Weisser, W. W., Roscher, C., Meyer, S. T., Ebeling, A., Luo, G. J., Allan, E., et al. (2017). Biodiversity effects on ecosystem functioning in a 15-year grassland experiment: patterns, mechanisms, and open questions. *Basic Appl. Ecol.* 23, 1–73. doi: 10.1016/j.baae.2017.06.002

Wen, J., Qin, R. M., Zhang, S. X., Yang, X. Y., and Xu, M. H. (2020). Effects of long-term warming on the aboveground biomass and species diversity in an alpine meadow on the Qinghai-Tibetan Plateau of China. *J. Arid Land* 12, 252–266. doi: 10.1007/s40333-020-0064-z

Wu, J., Wang, H., Li, G., Ma, W., Wu, J., Gong, Y., et al. (2020). Vegetation degradation impacts soil nutrients and enzyme activities in wet meadow on the Qinghai-Tibet Plateau. *Sci. Rep.* 10:21271. doi: 10.1038/s41598-020-78182-9

Xu, H. P., Zhang, J., Pang, X. P., Wang, Q., Zhang, W. N., Wang, J., et al. (2019). Responses of plant productivity and soil nutrient concentrations to different alpine grassland degradation levels. *Environ. Monit. Assess.* 19:678. doi: 10.1007/s10661-019-7877-2

Xu, T., Zhao, X., Zhang, X., Wang, X., Geng, Y., Hu, L., et al. (2020). Sustainable development of ecological grass-based livestock husbandry in Qinghai- Tibet Plateau alpine area:principle,technology and practice. *Acta Ecol. Sin.* 40, 6324–6337.

Yan, L., Li, Y., Wang, L., Zhang, X. D., Wang, J. Z., Wu, H. D., et al. (2020). Grazing significantly increases root shoot ratio but decreases soil organic carbon in Qinghai-Tibetan Plateau grasslands: a hierarchical meta-analysis. *Land Degrad. Dev.* 31, 2369–2378. doi: 10.1002/ldr.3606

Yu, K. F., Lehmkuhl, F., and Falk, D. (2017). Quantifying land degradation in the Zoige Basin, NE Tibetan Plateau using satellite remote sensing data. *J. Mt. Sci.* 14, 77–93. doi: 10.1007/s11629-016-3929-z

Zhang, L. (2006). Exploration of ecological pitfalls embeded in the human-land interaction. *Acta Ecol. Sin.* 26, 2167–2173.

Zhang, Q., Liu, K. S., Shao, X. Q., Li, H., He, Y. X., Sirimuji, et al. (2021). Microbes require a relatively long time to recover in natural succession restoration of degraded grassland ecosystems. *Ecol. Indic.* 129:107881. doi: 10.1016/j.ecolind.2021.107881

Zhang, Q., Ma, L., Zhang, Z., Xu, W., Zhou, B., Song, M., et al. (2019). Ecological restoration of degraded grassland in Qinghai-Tibet alpine region: degradation status,restoration measures, effects and prospects. *Acta Ecol. Sin.* 39, 7441–7451.

Zhang, R., Wang, X., Pu, X., Xu, C., and Yu, Y. (2015). Analysis of rangeland and livestock production systems in alpine pastoral area of Qinghai-Tibet Plateau. *J. Yunnan Agric. Univ.* 30, 755–759.

Zhang, W., Xue, X., Peng, F., You, Q., and Hao, A. (2019). Meta-analysis of the effects of grassland degradation on plant and soil properties in the alpine meadows of the Qinghai-Tibetan Plateau. *Glob. Ecol. Conserv.* 20:e00774. doi: 10.1016/j.gecco.2019.e00774

Zhang, Y., Dong, S. K., Gao, Q. Z., Liu, S. L., Ganjurjav, H., Wang, X. X., et al. (2017). Soil bacterial and fungal diversity differently correlated with soil biochemistry in alpine grassland ecosystems in response to environmental changes. *Sci. Rep.* 7:43077 . doi: 10.1038/srep43077

Zhou, H., Zhang, D. G., Jiang, Z. H., Sun, P., Xiao, H. L., Wu, Y. X., et al. (2019). Changes in the soil microbial communities of alpine steppe at Qinghai-Tibetan Plateau under different degradation levels. *Sci. Total Environ.* 651, 2281–2291. doi: 10.1016/j.scitotenv.2018.09.336

Zhou, Q., Chen, S., and Guo, Z. (2016). The principles and practice of standardized demonstration ranches construction. *Chin. Sci. Bull.* 61, 231–238.

Zhou, Z., Wang, C., and Luo, Y. (2020). Meta-analysis of the impacts of global change factors on soil microbial diversity and functionality. *Nat. Commun.* 11:3072. doi: 10.1038/s41467-020-16881-7

Zhou, Z., Wang, C., Zheng, M., Jiang, L., and Luo, Y. (2017). Patterns and mechanisms of responses by soil microbial communities to nitrogen addition. *Soil Biol. Biochem.* 115, 433–441. doi: 10.1016/j.soilbio.2017.09.015

Zhu, J. T., Zhang, Y. J., and Liu, Y. J. (2016). Effects of short-term grazing exclusion on plant phenology and reproductive succession in a Tibetan alpine meadow. *Sci. Rep.* 6:27781. doi: 10.1038/srep27781

Zhuang, M. H., Gongbuzeren, Zhang, J., and Li, W. J. (2019). Community-based seasonal movement grazing maintains lower greenhouse gas emission intensity on Qinghai-Tibet Plateau of China. *Land Use Policy* 85, 155–160.

Conflict of Interest: The authors declare that the research was conducted in the absence of any commercial or financial relationships that could be construed as a potential conflict of interest.

Publisher's Note: All claims expressed in this article are solely those of the authors and do not necessarily represent those of their affiliated organizations, or those of the publisher, the editors and the reviewers. Any product that may be evaluated in this article, or claim that may be made by its manufacturer, is not guaranteed or endorsed by the publisher.

Copyright © 2022 Yu, Wan, Liu, Ma, Cheng, Shen, Liu and Su. This is an open-access article distributed under the terms of the Creative Commons Attribution License (CC BY). The use, distribution or reproduction in other forums is permitted, provided the original author(s) and the copyright owner(s) are credited and that the original publication in this journal is cited, in accordance with accepted academic practice. No use, distribution or reproduction is permitted which does not comply with these terms.

frontiers in Plant Science

ORIGINAL RESEARCH
published: 13 January 2022
doi: 10.3389/fpls.2021.830119

Assessing the Impact of Climate Change on Potential Distribution of *Meconopsis punicea* and Its Influence on Ecosystem Services Supply in the Southeastern Margin of Qinghai-Tibet Plateau

Ning Shi[1,2†], Niyati Naudiyal[1†], Jinniu Wang[1,3], Narayan Prasad Gaire[4,5], Yan Wu[1], Yanqiang Wei[6], Jiali He[1] and Chunya Wang[1]*

[1] Chengdu Institute of Biology, Chinese Academy of Sciences, Chengdu, China, [2] College of Life Sciences, University of Chinese Academy of Sciences, Beijing, China, [3] Mangkang Ecological Station, Tibet Ecological Safety Monitor Network, Chengdu, China, [4] Key Lab of Tropical Forest Ecology, Xishuangbanna Tropical Botanical Garden (XTBG), Chinese Academy of Sciences, Mengla, China, [5] Department of Environmental Science, Patan Multiple Campus, Tribhuvan University, Lalitpur, Nepal, [6] Northwest Institute of Eco-Environment and Resources, Chinese Academy of Sciences, Lanzhou, China

OPEN ACCESS

Edited by:
Jian Sun,
Institute of Tibetan Plateau Research, Chinese Academy of Sciences (CAS), China

Reviewed by:
Yafeng Wang,
Nanjing Forestry University, China
Su Xu,
Qinghai Normal University, China

***Correspondence:**
Jinniu Wang
wangjn@cib.ac.cn

† These authors have contributed equally to this work and share first authorship

Specialty section:
This article was submitted to Functional Plant Ecology, a section of the journal Frontiers in Plant Science

Received: *06 December 2021*
Accepted: *22 December 2021*
Published: *13 January 2022*

Citation:
Shi N, Naudiyal N, Wang J, Gaire NP, Wu Y, Wei Y, He J and Wang C (2022) Assessing the Impact of Climate Change on Potential Distribution of Meconopsis punicea and Its Influence on Ecosystem Services Supply in the Southeastern Margin of Qinghai-Tibet Plateau. Front. Plant Sci. 12:830119. doi: 10.3389/fpls.2021.830119

Meconopsis punicea is an iconic ornamental and medicinal plant whose natural habitat has degraded under global climate change, posing a serious threat to the future survival of the species. Therefore, it is critical to analyze the influence of climate change on possible distribution of *M. punicea* for conservation and sustainable utilization of this species. In this study, we used MaxEnt ecological niche modeling to predict the potential distribution of *M. punicea* under current and future climate scenarios in the southeastern margin region of Qinghai-Tibet Plateau. Model projections under current climate show that 16.8% of the study area is suitable habitat for *Meconopsis*. However, future projections indicate a sharp decline in potential habitat for 2050 and 2070 climate change scenarios. Soil type was the most important environmental variable in determining the habitat suitability of *M. punicea*, with 27.75% contribution to model output. Temperature seasonality (16.41%), precipitation of warmest quarter (14.01%), and precipitation of wettest month (13.02%), precipitation seasonality (9.41%) and annual temperature range (9.24%) also made significant contributions to model output. The mean elevation of suitable habitat for distribution of *M. punicea* is also likely to shift upward in most future climate change scenarios. This study provides vital information for the protection and sustainable use of medicinal species like *M. punicea* in the context of global environmental change. Our findings can aid in developing rational, broad-scale adaptation strategies for conservation and management for ecosystem services, in light of future climate changes.

Keywords: *Meconopsis punicea*, MaxEnt modeling, habitat suitability, ecosystem service, climate change, Qinghai-Tibet Plateau

INTRODUCTION

Climate not only plays a significant role in the growth and reproduction of plants, but also governs factors concerning the survival, development, and distribution of species (Kozak et al., 2008; Wu et al., 2011; Ford and HilleRisLambers, 2019; Criado et al., 2020; Dolezal et al., 2020; Wang et al., 2021). Detrimental influences of rapid climatic warming on global biodiversity include the changing the life history of species, community composition, vegetation pattern, and ecosystem function (Williams, 2000; Thomas C. D. et al., 2004; Thomas J. A. et al., 2004; McKenney et al., 2007; Thuiller, 2007; Bellard et al., 2012; Alberto et al., 2013; Al-Qaddi et al., 2017; Xu et al., 2018). Among them, the variation of species distribution range, which is a direct visible response of species toward climate change, is a key issue that has garnered international attention (Mantyka-pringle et al., 2012; Anderson, 2013; Pacifici et al., 2015). The effects of climate change are more pronounced at high altitudes than at low altitudes (Wilmking and Juday, 2005; Gou et al., 2007; Peng et al., 2011). Higher elevations are warming faster than the average (Diaz and Bradley, 1997; Diaz and Eischeid, 2007; Wang Q. et al., 2014), and this has been confirmed and verified by many researchers across different mountainous ecosystems around the world (Wang Q. et al., 2014), including the Rocky Mountain (Minder et al., 2018), the European Alps (Pauli et al., 2007), the mountains of the western United States (Oyler et al., 2015), and the Greater Alpine Region (Palazzi et al., 2019). Similarly, the Qinghai-Tibet Plateau, also known as the world's third pole, has a much higher warming rate than the global average (Liu and Chen, 2000; Niu et al., 2004; Pauli et al., 2007). The intensity as well as the frequency of heat waves and droughts in alpine regions have increased in the last decades (Easterling et al., 2000; Orsenigo et al., 2014; Corona-Lozada et al., 2019; Francon et al., 2020). Continued warming without any corresponding increase in rainfall suggests that the future climate would be hotter and drier (Zhang et al., 2020). Additionally, the frequency of extreme climate events has also increased significantly in the past few decades, which could trigger a multitude of biophysical and economic impacts on the functioning of alpine ecosystems and their associated services (Wester et al., 2019). The most alarming direct evidence of climate change observed on the Qinghai-Tibet Plateau over the past 35 years is the rapid early growth of alpine grassland vegetation, shortened optimal growth times, increased vegetation biomass in spring, and decreased vegetation biomass in autumn (Wang et al., 2020). Changes in grassland vegetation growth patterns directly affect the survival of millions of cattle and sheep, as well as a large number of ungulates, and thus the livelihoods of local pastoralists on the Qinghai-Tibet Plateau.

Climate change will lead to fragmentation of suitable habitats for species, which may result in the decline of habitat quality (Li et al., 2015). The composition of plant communities is also expected to change, with a dominance of species adapted to warmer climates, which in turn would lead to a decline in the abundance of species suited for colder regional climates, particularly in alpine and arctic regions (Bertrand et al., 2011; Gottfried et al., 2012). Additionally, distributional shifts of plant species and communities, to higher latitudes and/or altitudes are expected under potential climate change scenarios (Bugmann, 2001; Hörsch, 2003; Wang et al., 2011). As a result, species richness and diversity can potentially decrease in the lower altitudes and latitudes, while endangered species present at higher altitudes and latitudes face exacerbated risks of extinction due to increased competition among species (Lotstein, 2013; Wang et al., 2016). Alpine ecosystems are more sensitive and vulnerable to climate change than vegetation in other regions due to lack of plasticity, migration constraints, and insufficient genetic variation to respond to novel selection pressures (KrÄuchi and Kienast, 1993; Bugmann, 2001; Hörsch, 2003; Chauchard et al., 2007; Wang et al., 2011, 2016). The Qinghai-Tibet Plateau region has already witnessed the adverse impacts of climate change on its diverse and unique flora and fauna with evidences of change in growth and phenology of species and shifts in their natural distribution range (Zhang et al., 2011; Zhao et al., 2011; Schickhoff et al., 2016; Song et al., 2018; Singh et al., 2019; Dorji et al., 2020). Many alpine species have high ornamental, economic and medicinal value, and contribute to the livelihood of local and ethnic communities. Even though this valuable flora is under imminent threat from rapid climate change in the region, there has been no systematic study that addresses the bioclimatic factors controlling species growth and distribution, in the region.

Species Distribution Models (SDMs) typically construct a mathematical relationship between known species occurrence records and the corresponding environmental variables and predicts the environmental conditions within which a species' population can be maintained, thereby estimating the suitable spatial distribution for that species across the study area (Pearson et al., 2007). Among the many SDMs available, MaxEnt has shown greater accuracy than other models, especially with limited species occurrences data (Merow and Silander, 2014; Radosavljevic and Anderson, 2014). It can visually provide the size of the distribution area of species in different periods, and through comparison, the response model of the same species to different climate changes can be obtained. In this study, we selected *Meconopsis* as a representative genus/species to study the impact of climate and climate change on the distribution of ecologically and socio-economically valuable sub-alpine and alpine plants in the fragile and sensitive area in Qinghai-Tibet Plateau.

Meconopsis, commonly known as blue poppy, belongs to the Papaveraceae family with 79 species worldwide, about 80% of which are in China, mainly distributed in the Himalayan-Hengduan Mountain region (Grey-Wilson, 2014). *Meconopsis punicea* Maxim (*M. punicea*) is a perennial herb with high ornamental value that grows in alpine scrubs and meadows at elevation of 3,000–4,800 m (Shang et al., 2015). As a Chinese traditional Tibetan medicine, flowers of *M. punicea* have been used for thousands of years by the local people to treat pain, fever, cough, inflammation, liver and lung inflammation in humans and animals (Shang et al., 2015). Meanwhile, the beautiful flowers are also used as ornamental plants across the Tibetan region. However, degradation of its natural habitat and overexploitation are increasingly threatening the survival of wild *M. punicea*, and it has been listed as an endangered species on the China Species Red List in 1999 (Qu and Qu, 2012).

Once a species is extinct, it cannot be regenerated, let alone used by other organisms in the ecosystem or for human well-being as an ecosystem service. Changes in temperature and precipitation patterns caused by climate change affect individual species and the way they interact with their habitats, resulting in changes in the structure and function of ecosystems and, ultimately, in biodiversity and ecosystem services (Nogués-Bravo et al., 2007; Locatelli et al., 2008; Shaw et al., 2011; Díaz et al., 2019). Moreover, the disappearance of one species can have a cascading effect, leading to the threat or extinction of another 10–30 species (Lv, 2009). Diverse biomes and well-functioning ecosystems are essential for maintaining ecosystem services that support human well-being (Díaz et al., 2019). Therefore, to avoid further habitat fragmentation and loss of species diversity, it is critical to develop adequate conservation strategies and measures. However, the development of strategies requires a comprehensive understanding of the relationship between the geographical distribution of species and climate change, as well as a reasonable understanding of the distribution range of species under future climatic conditions. Hence, analyzing the relationship between the distribution of species and climate factors to reasonably predict the impact of climate change on the species distribution and proposing conservation countermeasures, has a very important theoretical and practical significance for future biodiversity conservation. A widely used research tool in this context is MaxEnt model that enables us to identify land cover change changes under future climate change scenarios (Faleiro et al., 2013) which can be used to predict biodiversity loss (Bertrand et al., 2012), assess the risk of biological invasion (Gallagher et al., 2010), cultivate rare medicinal materials (Lu et al., 2012; Guo et al., 2016), and manage and protect endangered species (Li et al., 2013). It is also one of the most effective and extensively used approach for studying the impact of climate change on the suitability of species habitats (Araújo et al., 2019).

In this study, we use MaxEnt modeling to explore the influence of climate change on potential distribution of wild *M. punicea* by (1) identifying the most significant environmental factors influencing the potential distribution of *M. punicea* in the study area; (2) evaluating the potential changes in its distribution; and (3) assessing the implications for its critical ecosystem services The results of the present study could aid in conservation and management of *M. punicea* in headwater region of Min River and other habitats in China.

MATERIALS AND METHODS

Study Area

The study was conducted in the headwater region of Min River, situated at the southeast edge of the Qinghai-Tibet Plateau in Songpan County of Sichuan Province in China. The distribution of specimen data recorded in the Chinese Virtual Herbarium (CVH[1]) indicates that this region is one of the hotspots for the distribution of *M. punicea* (**Figure 1**). Most parts of this region is above 3,400 m in elevation. The region experiences a typical alpine climate with large variability in temperature day and night time, with an annual average temperature of 2.8°C. The average monthly temperature ranges from −7.6°C in January to 9.7°C in July. The annual precipitation of 700–800 mm is mainly concentrated in the months of May and August (Guan et al., 2002; Wang J. et al., 2014; Naudiyal et al., 2021), and the region experiences an average of 1,827.5 h of sunshine per year (Chen, 2004; Wang J. et al., 2014). The soil is approximately 60 cm deep and classified as mountain brown meadow soil.

The vegetation in headwater region of Min River has distinct altitudinal zonation and horizontal distribution with strong floristic transition and abundant plant species. Due to the complex undulating terrain solar incident radiation does not illuminate the entire region uniformly creating comparatively shaded and sun-facing aspects, which act like ecological islands creating habitats that support a wide variety of species with different ecological requirements. The sunny slopes are mostly covered by *Sabina chinensis* with *Spirea*, *Sibiraea*, and *Berberis* patched bushes, while the vegetation on shaded slopes mainly comprises of *Picea* and *Abies* forests with an understory of *Rhododendron*, *Salix*, and *Lonicera* shrubs (Chen, 2004). Most of the *M. punicea* population grows in shaded and semi-shaded mountain slopes with shrub or grassland (Shang et al., 2015; Wang et al., 2016). Above the treeline, mosaics of *Rhododendron*, *Salix*, *Spiraea*, *Sibiraea*, and *Dasiphora* form shrub belt for nearly 200 m vertical distance followed upslope by alpine meadows, dominated by species from genus Compositae, Cyperaceae, and Gentianaceae.

Species Characteristics and Occurrence Records

Meconopsis punicea is a monocarpic perennial, with a fibrous root system, usually growing 30–75 cm tall. All leaves are basal and form a rosette, the leaf shape is oblanceolate or narrowly obovate, and both surfaces have dense setae. Its remarkable carmine flowers, of high ornamental value, usually have four petals arranged in an elliptic formation. The species is naturally distributed in the southwestern Gansu, southeastern Qinghai, northwestern Sichuan and northeastern Tibet (Zhang and Christopher, 2008).

The occurrence data for *M. punicea* was collated from primary and secondary sources which included field surveys, Global Biodiversity Information Facility[2] database and the CVH. Primary data collection was done between July and September in 2019. All presence data points were carefully evaluated to remove duplicate data points and secondary data points that lacked detailed location information. Presence locations collected from secondary sources were carefully validated with Google Earth to eliminate possible errors. We ensured that the selected presence points of *M. punicea* were spatially isolated and evenly distributed throughout the study area to avoid sampling bias (Veloz, 2009) while ensuring the inclusion of occurrence data across the area where the species is known to occur in the available literature. Based on this selection and elimination criteria, resulting in 100

[1]https://www.cvh.ac.cn/

[2]https://www.gbif.org

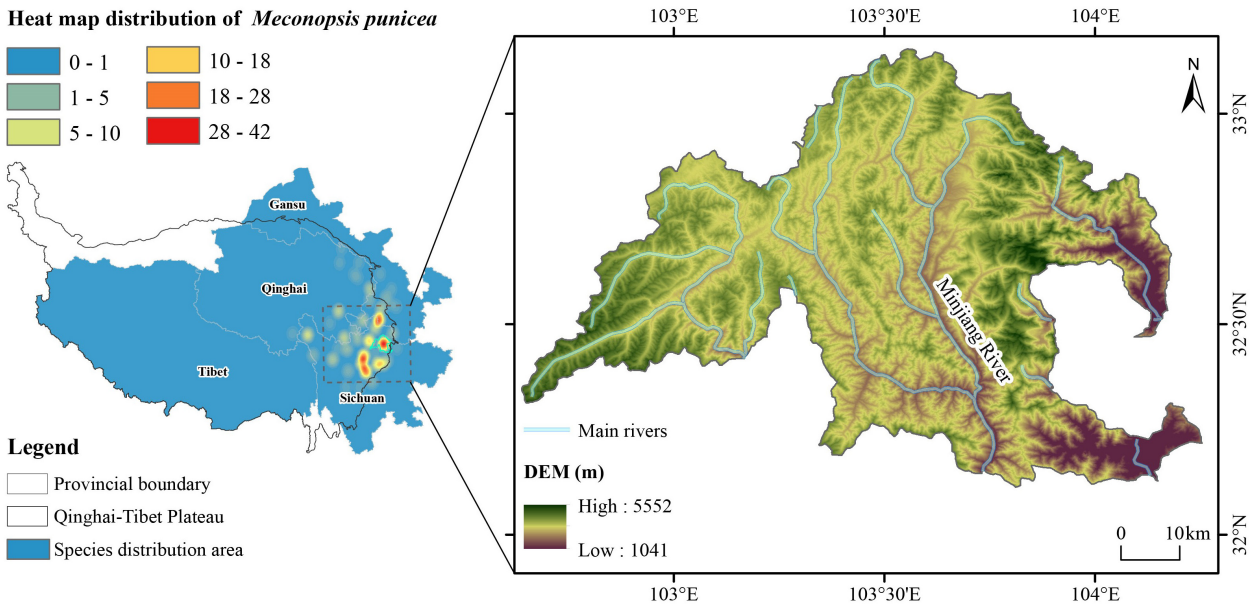

FIGURE 1 | Distribution map of herbarium sampling and map of the study region.

spatially separated presence records were retained to simulate habitat suitability.

Environmental Variables

Environmental variables included bioclimatic, topographic and soil variables. Bioclimatic variables were obtained with 1 km spatial resolution from WorldClim dataset (Hijmans et al., 2005),[3] which generated using monthly temperature and rainfall records from 1950 to 2000. The dataset is commonly used in species distribution modeling studies around the world because it provides biologically meaningful information on climate trends and seasonality (Kumar, 2012). Our projections included current and two future periods (2050s and 2070s) under current and four Representative Concentration Pathways (R) scenarios from most optimistic to most pessimistic, these include: RCP 2.6 (most optimistic scenario), RCP 4.5 (intermediate scenario), RCP 6.0 (pessimistic scenario) and RCP 8.5 (highly pessimistic scenario). RCP represents a representative pathway for greenhouse gas emissions and atmospheric concentrations, air pollutant emissions and land use in the 21st century (Vuuren et al., 2011). Two general circulation models [BCC-CSM1.1 (Beijing Climate Center, China Meteorological Administration, China) and HadGEM2-ES (Met Office Hadley Centre, United Kingdom)], which are commonly used for species distribution modeling in the Hindu-Kush Himalaya and Qinghai-Tibet Plateau regions (Kumar, 2012; He et al., 2019; Zhang et al., 2019), were used in this study.

Among topographic information variables, elevation data as was downloaded from digital elevation model (DEM) datasets with a spatial resolution of 30 m, slope and aspect data were extracted from the elevation data using ARC-GIS ver. 10.1. The soil data were derived from Soil and Terrain Database of China (SOTER China), which provides detailed spatial information on topographic attributes and basic soil characteristics (e.g., organic carbon content and pH) of an area that has been widely used for agroecological assessments and climate studies.

All environmental variables (climatic, topographic, and soil) were resampled and brought to the same spatial resolution (30 arc-seconds) using ArcGIS for before further analysis.

MaxEnt Modeling Procedures

We used a presence only niche model, MaxEnt (Maximum Entropy) to predict the potential distribution of *M. punicea* under current and future climate scenarios. MaxEnt is a robust species distribution model that has been extensively used for species distribution modeling across the globe (He et al., 2019; Xu et al., 2019; Zhang et al., 2019) and works well with small sample sizes as compared to other modeling methods (Khanum et al., 2013).

Selection of Predictor Variables

Since bioclimatic variables are often highly correlated to each other (Feilhauer et al., 2012; Dormann et al., 2013), all environmental variables used in in this study were tested for multicollinearity using Pearson product-moment correlation (Yang et al., 2013). ENM tools, a Perl script based graphical user interface that provides a table of cross-correlation values (−1 to 1) between input variables was used to compute the correlations between ASCII raster grid layers of input variables. Based on the results of this analysis, from each set of highly correlated variables ($r = 0.7$ or $r \leq -0.7$) only one was included in the final model, reducing the total number of variables used for modeling to 12 (**Table 1**), that included eight bioclimatic variables, one soil variable, and three topographic variables.

[3]www.worldclim.org

TABLE 1 | Environmental variables used in the study and their percent contribution to the model output for *Meconopsis punicea*.

Abbreviation	Description	Unit	% contribution	Cumulative contributions
Soil	Soil type	–	27.75	27.75
Bio 4	Temperature seasonality	–	16.41	44.16
Bio 18	Precipitation of warmest quarter	mm	14.01	58.17
Bio 13	Precipitation of wettest month	mm	13.02	71.19
Bio 15	Precipitation seasonality	–	9.41	80.6
Bio 7	Annual temperature range	°C	9.24	89.84
Slo	Slope	°	5.12	94.96
Asp	Aspect	°	3.43	98.39
Bio 8	Mean temperature of wettest quarter	°C	0.83	99.22
Bio 2	Mean diurnal range [mean of monthly (max temp/min temp)]	°C	0.78	100
Bio 3	Isothermality (Bio2/Bio7) (×100)	–	0	100
Ele	Elevation	m	0	100

Model Implementation and Accuracy Assessment

Processing parameters were kept consistent for all model runs with the regularization multiplier set at "2" to reduce overfitting. A maximum of 1,000 iterations were allowed for each model run to ensure sufficient time for model convergence. The model estimates a probability distribution of species based on its current presence points and associated environmental variables and provides a spatial representation of habitat suitability varying from 0 (lowest suitability) to 1 (highest suitability). The model thus trained using current climate data was projected on future climate change bioclimatic datasets for all RCP scenarios to identify potential species habitat of species in 2050s and 2070s.

The Jackknife test was used to assess the relative importance of environmental variables in determining the potential distribution of species (Kumar, 2012; Yang et al., 2013; Kumar et al., 2014). Species response curves were created to investigate the relationship between habitat suitability and environmental factors. Model accuracy was evaluated through area under receiver operating characteristics (ROC) curve. The AUC (Area Under Curve) is capable of evaluating the ability of a model to discriminate presence from absence (Elith et al., 2006; Fourcade et al., 2014), with values range from 0 to 1, where 0 represents least perfect and 1 represents most perfect discrimination between sites (Phillips et al., 2006). Models with mean AUC scores between 0.7 and 0.8 are considered "fair," between 0.8 and 0.9 are "good," and greater than 0.9 are "excellent" (Swets, 1988). In general, we consider that all models with AUC values greater than 0.75 are acceptable (Elith et al., 2006).

Analysis of Model Predictions

Model outputs were exported to ArcGIS platform for post processing and analysis of model predictions. Species distribution prediction was reclassified into three arbitrary habitat suitability categories: low (25–50% probability of occurrence), medium (50–75% probability of occurrence) and high (75% probability of occurrence) with values below 25% omitted as unsuitable habitat based on logical thresholds (Chakraborty et al., 2016). Area under each habitat suitability category was calculated to assess potential area changes from distribution under current climate to future climate change scenarios.

The influence of climate change on elevational shifts in *M. punicea* distribution was assessed through 100 random points generated in regions with medium and high suitability for occurrence. The elevation of each randomly chosen point was obtained from the digital elevation model of the region, based on which the minimum, maximum, and mean elevations at which the species is expected to exist was calculated for each RCP. Mean elevations of potential species occurrence under future climate conditions were compared with mean elevation of species distribution under current climate to estimate the net elevational shift of species.

RESULTS

Model Evaluation and Contribution of Environmental Variables

The model for current and future climate change scenarios performed well with AUC values > 0.9. The mean AUC value for model performance under current climatic condition was 0.92 over 10 replicates with a standard deviation of 0.045, indicating that the predicted distribution model is better than the random model, with robust stability between each repetition. Therefore, the model performance for this study can be considered good-excellent (Swets, 1988).

Percentage contribution values of each predictor variable are average values established over 10 replicate runs (**Table 1**). Results reveal that soil type (14 different types of soils, including mollic leptosols, and haplic luvisols, etc.) has the most significant contribution (27.75%) to model output under current climate. In addition to soil, climate variables also play a key role in determining the distribution of *M. punicea*. The major contributing climate variables were temperature seasonality (Bio 4, 16.41%), precipitation of warmest quarter (Bio 18, 14.01%), and precipitation of wettest month (Bio 13, 13.02%), precipitation seasonality (Bio 15, 9.41%), annual temperature range (Bio 7, 9.24%), accounting for 62.09% of variation in total. Since the cumulative contribution rate of these six environmental variables is 89.84%, it is reasonable to say that they contain the most significant and useful information for predicting species

distribution as compared to another environmental variables included in this study. Besides, soil type, temperature seasonality and precipitation of warmest quarter were observed to have a crucial role in estimating the potential distribution pattern of *M. punicea*. However, isothermality and elevation have little influence on model output.

According to the response curves of the dominant environmental variables (**Figure 2**), it can be observed that the soil types most suitable for the survival of *M. punicea* are mollic leptosols and eutric leptosols. Meanwhile the most conducive annual temperature for species growth is close to 34°C, accompanied by approximately 130 mm of precipitation in the wettest month. However, with increase of temperature seasonality and precipitation of warmest quarter, the range suitable for species distribution is not obvious from the curve, which indicates these response curves of two variables cannot be referred to assess the most suitable range of *M. punicea*.

Potential Distribution of *Meconopsis punicea* Under Multiple Climate Change Scenarios

Based on the known distribution data and environmental variables, the potential geographic distribution map of *M. punicea* was constructed and its survival area was predicted in the headwater region for Minjiang River. The potential distribution of *M. punicea* for two GCMs (BCC and HADGEM2-ES) in near (2050s) and distant (2070s) future climate change scenarios is represented in **Figure 3**. The suitable habitats of *M. punicea* are relatively fragmented, with high suitable habitats mainly limited to the northern part of the study area under current climate. Based on model outputs the regions which have high, medium, and low suitability of *M. punicea* occupy an area of 269.7, 428, and 733 km^2, respectively. In total, suitable habitat occupies 16.8% of the study area.

Compared with the area of total suitable habitat under current climate scenarios, the predicted future ranges of habitat showed a sharp decline for both 2050 and 2070 (**Figures 3**, **4**). However, the magnitude of impact is different for each general circulation model (GCM) and RCPs within those GCMs. The area of suitable habitat of *M. punicea* under the RCP 2.6, RCP 4.5, RCP 6.0, and RCP 8.5 scenarios for 2050 decreased by 35.60, 36.60, 74.00, and 50.90% in BCC model, and decreased 64.80, 73.60, 72.20, and 61.60% in HAD model predicted, respectively. By the 2070, the area of suitable habitat of *M. punicea* is likely to decline by 64, 65.3, 60.9, and 92.2% (BCC data), and 60.6, 67.3, 70.6, and 77.7% (HADGEM2-ES data), for RCP 2.6, RCP 4.5, RCP 6.0, and RCP 8.5, respectively. For the 2050 climate scenario, the suitable habitats declined the most under the RCP 6.0 (BCC data). However, for the 2070 climate scenario, the suitable habitats have the greatest reduction under the RCP 8.5 (BCC data). In most of future climate scenarios, habitat loss of *M. punicea* exceeds 60% in comparison to its current potential distribution.

Model outputs reveal that changes in species distribution vary amongst all habitat suitability classes. The changes in distribution areas of regions with low, medium, and high habitat suitability is represented in **Figure 4**. The results highlight those regions with high habitat suitability were most severely influenced by climate change, regardless of the time and emission scenario. However, areas of with medium probability of species occurrence decreased more than those with low probability, except for RCP 2.6 scenario in BCC model (2050) and RCP 6.0 and RCP 8.5 scenarios in HAD model (2050). The distribution of *M. punicea* in the short-term (2050) has been less affected by climate change in comparison with that in the long-term (2070).

Climate Change Induced Changes in Elevational Range of *Meconopsis punicea*

In most future climate change scenarios, the mean elevation of suitable habitat for distribution of *M. punicea* is likely to shift upward (**Table 2**). Upward movement of *M. punicea* distribution is likely to be accompanied with a reduction in its overall elevational range. In most of the future climate scenarios analyzed in this study, we find that *M. punicea* is likely to inhabit a narrower elevational range as compared to its distribution under current climate scenario (**Table 2**). The reduction in range implies that there would be a net loss in area conducive for *M. punicea* occurrence. These results show that in future we can expect a potential decrease in the climatic niches of *M. punicea*, the extent of which would depend on the GHG emission scenario. Given that other environmental factors and human interference in this region have not been taken into account in the modeling exercise, the potential impact is expected to be much higher than current model predictions.

DISCUSSION

Factors Controlling the Distribution of *Meconopsis punicea*

Habitat suitability of a species is influenced by environmental factors that play a key role in driving biological processes of the species growth, which is a critical aspect in modeling (Beaumont et al., 2005; Gavilán, 2005). Our study found that the distribution of *M. punicea* was mainly controlled by three precipitation-related bioclimatic variables (Bio 18: precipitation of warmest quarter; Bio 13: precipitation of wettest month; Bio 15: precipitation seasonality), two temperature-related bioclimatic variables (Bio 4: temperature seasonality; Bio 7: annual temperature range), and soil type. Changes in precipitation patterns due to climate change can affect plant physiological and ecological processes at different scales (Barker et al., 2006; Tognetti et al., 2007), including plasticity response of vegetative growth (Heisler-white et al., 2009) and reproductive growth (Molina-Montenegro et al., 2010; Pol et al., 2010) characteristics of plants. In addition, precipitation can affect soil moisture and nutrient availability, thus regulating plant growth and development (Brant and Chen, 2015). For instance, the influence of increasing temperature and precipitation on the greening and average flowering of *Kobresia pygmaea* has been observed in the Qinghai-Tibet Plateau (Ganjurjav et al., 2020).

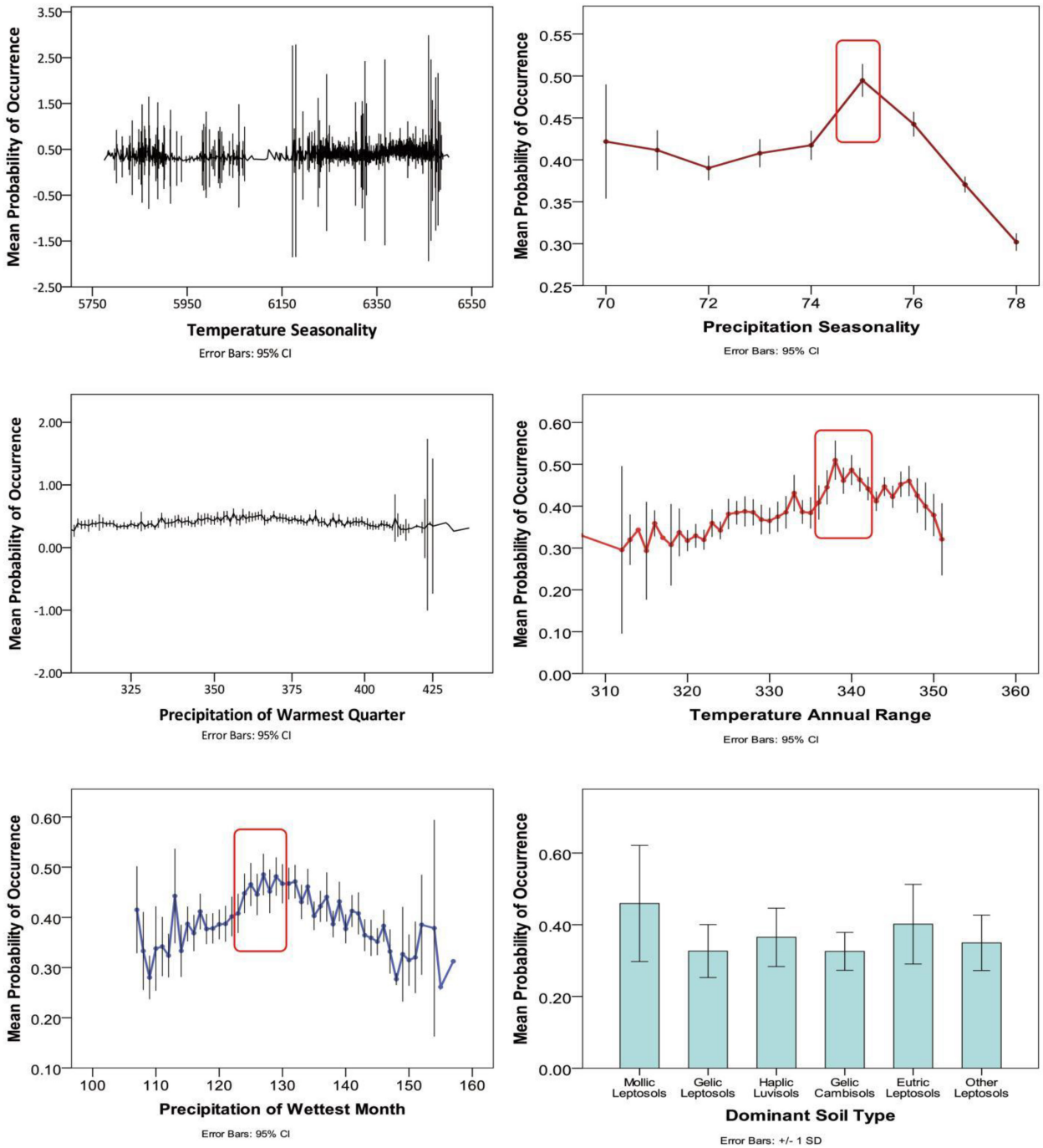

FIGURE 2 | Response curves for dominant environmental predictors in the species distribution model for *Meconopsis punicea*.

In addition to precipitation, temperature is another key environment variable that directly influences plant growth and distribution by maintaining plant physiological and biochemical activities such as photosynthesis, respiration, and material transfer (Henry and Molau, 1997; Arft et al., 1999; Klanderud and Totland, 2005; Walther et al., 2005). Experimental study has shown that temperature changes can directly influence the photosynthetic capacity and growth rate of plants (Jarvis et al., 2004), while indirectly affecting the soil moisture content and plant nutrient uptake and utilization (Shah and Paulsen, 2003). Our findings are in concordance with previous research on *Meconopsis* distribution, emphasizing precipitation and temperature as key climatic factors influencing species distribution (He et al., 2019; Li et al., 2020).

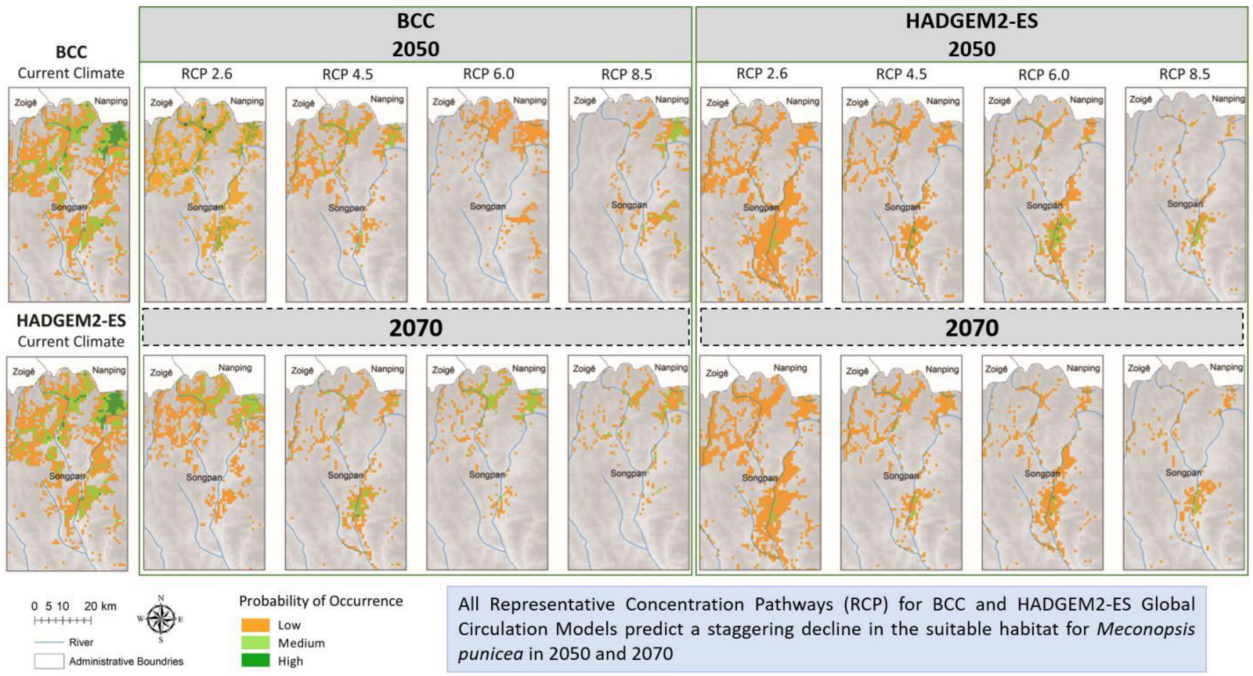

FIGURE 3 | Distribution of varying habitat suitability for *M. punicea* under different climate change scenarios.

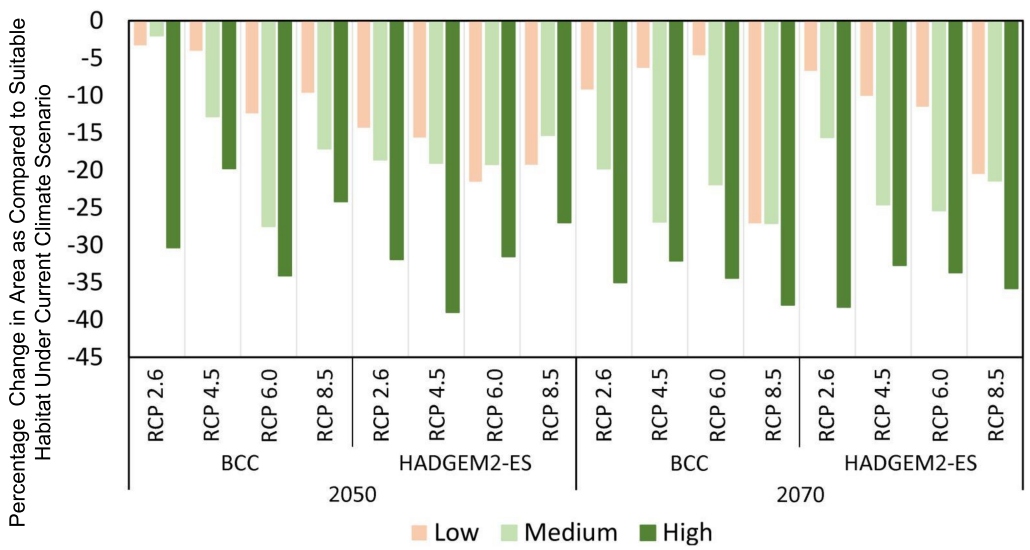

FIGURE 4 | Changes of distribution areas for *M. punicea* under different climate change scenarios.

Soil type is another crucial variable to determine the distribution of *M. punicea* in our study area. Soil is the product of a combination of soil forming parent material, climate, biology, topography and time, among which climate and biology are more active factors (Huang and Xu, 2010). Each species undergoes its own specific biogeochemical cycle, resulting in soil properties that are most favorable for its growth and establishment (Naudiyal et al., 2021). Due to the interaction between environmental variables and organisms, changes in temperature and precipitation may cause changes in soil biogeochemical cycles (Huang and Xu, 2010; Naudiyal et al., 2021), thus changing soil types. Studies have shown that plants are quite sensitive to changes in soil properties driven by temperature changes (Sullivan, 2016; Ma and Chang, 2019). Similarly, this trend is likely to exist in our study area, which undoubtedly

TABLE 2 | The four scenarios of BCC-CSM1-1 (BC) and HadGEM2-ES (HAD) models projections for distribution in elevation (m ± standard deviation) between the current time period, the year 2050 and 2070 for *M. punicea* (Based on randomly chosen sampling points in regions with medium to high probability of species occurrence in each climate change scenario).

			Minimum		Maximum	Mean		Std. deviation
Current climate			2,627		4,170	3,451		467
2050	BCC-CSM1-1	RCP 2.6	2,658	⟷	4,095	3,559	↑	311
		RCP 4.5	2,373	⟷	4,151	3,483		314
		RCP 6.0	2,551		4,151	3,556	↑	331
		RCP 8.5	2,331		4,159	3,539	↑	328
	HadGEM2-ES	RCP 2.6	2,551		4,152	3,482	↑	319
		RCP 4.5	2,609		4,211	3,482	↑	298
		RCP 6.0	2,920	⟷	4,203	3,502	↑	298
		RCP 8.5	2,647	⟷	4,126	3,538	↑	299
2070	BCC-CSM1-1	RCP 2.6	2,581	⟷	4,045	3,469	↑	665
		RCP 4.5	2,857	⟷	4,151	3,458		431
		RCP 6.0	2,678	⟷	4,212	3,525	↑	316
		RCP 8.5	2,373		4,170	3,538	↑	294
	HadGEM2-ES	RCP 2.6	2,418		4,203	3,467		343
		RCP 4.5	2,618	⟷	4,055	3,478	↑	300
		RCP 6.0	2,618	⟷	4,199	3,488	↑	290
		RCP 8.5	2,803	⟷	4,131	3,512	↑	459

⟷ *Narrower range as compared with current range.*
↑ *Increase in elevation compared with current mean elevation.*

further increases the vulnerability of *M. punicea* to persistent climate change.

This modeling provided strong statistical validation and robust maps of the potential distribution of *M. punicea* based on existing data. However, accurate spatial data on variables such as biotic interactions, anthropogenic disturbance, and land use/land cover change were not included in this study due to a lack of accurate data on these variables. If spatial information on these variables were available, it would help to build a more robust model for better prediction of species distribution. Limitations in spatial data (Rocchini et al., 2011) and the assumption that species can migrate to climate-friendly areas under climate change (Engler et al., 2009) have led to uncertainty in species distribution projections. The actual movement of species in a changing climate may be fraught with numerous challenges such as competition, predation, physical barriers, and lack of dispersal vectors among others. Despite the predictions made by species distribution models have certain limitations, they remain an important data source for future suitability predictions to assess scientific adaptation strategies at the community and ecosystem levels to offset the effects of future warming on biota (Wiens et al., 2009; Ackerly et al., 2010).

Impacts of Climate Change on *Meconopsis punicea*

Model projections suggest that climate change will reduce suitable habitat for *M. punicea* (**Figure 3**), which is consistent with the findings of He et al. (2019) and Li et al. (2020). The effects of climate change on the distribution of alpine species does not follow a fixed pattern, with impacts varying with the species' life history and resource requirements. While several studies predict a dramatic decline in suitable habitat of alpine floral species with climate change (Frishkoff et al., 2016; Fragnière et al., 2020), there are some species that also benefit from it and may cover larger area in the future (Wang et al., 2019). For instance, the distribution of alpine herb specie *Pedicularis kansuensis* is expected to expand with climate change, under RCP scenarios RCP 2.6 and RCP 8.5, with a northward shift in distribution (Wang et al., 2019). Meanwhile suitable area for the alpine plant *Papaver occidentaleis* would decrease considerably in the coming decades (Fragnière et al., 2020). Climate warming is expected to promote seedling emergence phenology in other alpine herbs such as *Primula alpicola*, *Pedicularis fletcheri*, *Meconopsis integrifolia* and *M. racemose* (Wang et al., 2018), while species such as *Canacomyrica monticola* and *Fritillaria cirrhosa* face threats of rapid habitat loss and extinction (Davies et al., 2009; Kumar and Stohlgren, 2009; Barnosky et al., 2011; Wang J. J. et al., 2014).

With varied responses of species to climate change it is hard to discern one specific pattern. In such situations, geographical distribution of a species can be an indicator of its ecological resilience to an extent. We find that *M. punicea* covers a small geographical range and has limited distribution in the study area under current climate, which is expected to decline further with climate change. Species with smaller geographical ranges, such as *Meconopsis*, can be regarded as more vulnerable to extinction (Davies et al., 2009) since their limited distribution is typically considered an indicator for low ecological tolerance and high sensitivity to environmental changes (Murray et al., 2011). Such species are therefore vulnerable and are more likely to face local extinction due to habitat loss under climate change scenarios (Staude et al., 2020). Generally, small ranged species also tend to have smaller local populations (Brown, 1984;

Gaston et al., 2000), with the decrease of population size, the anti-interference ability to the environment is weakened (Schoener and Spiller, 1987). Moreover, species with small populations are often characterized by increased inbreeding, decreased population fitness and decreased genetic diversity due to a bottleneck effect, and therefore face a higher risk of extinction than other species (Hoffmann et al., 2010; Nayak and Davidar, 2010; Delmas et al., 2014; Theodorou and Couvet, 2015). With global climate warming, it has been estimated that species with narrow ecological ranges occupying cold climate niches are likely to be extinct, while other species that occupy warm climate niches could benefit (Frishkoff et al., 2016). While global warming promotes the growth of vegetation (Cao et al., 2004; Xu et al., 2015) the continuous increase in temperature has had an adverse impact on alpine plants (Xu and Xuan, 2013). Over the past two decades, soil water content in inland areas of East Asia has shown a significant drying trend as temperatures have risen (Zhang et al., 2020). Field warming experiments of alpine meadow ecosystems on the Qinghai-Tibet Plateau show that there is a threshold of soil water content (SWC) that promotes net carbon uptake by terrestrial ecosystems (Quan et al., 2019). Since temperature is one critical factor in determining the distribution of *M. punicea*, an increase in temperature might trigger a habitat shift from a lower elevation to a higher elevation. According to the trend of precipitation, the climate of Qinghai-Tibet Plateau will become warmer and drier in future (Wei et al., 2021), which may intensify the vulnerability of *M. punicea* to the new climate regime.

Climate warming affects not only the distribution of alpine herbs but also other aspects. Studies have proven that temperature stress affects the secondary metabolites of plants, which are usually the basis of their medicinal activity (Schär et al., 2004). Metabolic components vary with habitat quality and are directly or indirectly influenced by factors such as growing environment, climate and soil conditions. This implies that the efficacy of traditional medicines may be affected by climate change. The influence of abiotic factors on phyto-chemistry have been documented by some researchers. Zhang (2009) found that altitude significantly influenced the amount of luteolin in *Meconopsis quintuplinervia*. Similarly, a study by Liu et al. (2014) showed that total alkaloids content of *Coptis chinensis* was significantly affected by topographic factors such as slope, slope direction and altitude. Previous studies found that the concentrations of berberine and palmatine in the rhizomes of *Coptis chinensis* increased with elevation over a range of elevations (Zhang et al., 2008), which was also observed in a similar experimental study by Li et al. (2020). Therefore, as the distribution area of *M. punicea* changes under global climate change, we expect that the medicinal properties of this species will also change.

This study conducted with two GCMs and all four RCP scenarios will help to better understand of the vulnerability and sensitivity of *M. punicea* to climate change. Moreover, since this study focused on a relatively smaller geographical region, we expect to have more accurate results as compared to other maximum entropy modeling case for predicting the distribution of *M. punicea*. Thus, for a more comprehensive assessment of future changes, not only a wider range of GCMs and RCP scenarios need to be considered, but additional regional or local climate change model also be incorporated to make a reliable prediction.

Influence on Climate Change on Ecosystem Services From *Meconopsis punicea*

Ecosystem services are the environmental basis for human survival (Boyd and Banzhaf, 2007), through products and services obtained directly or indirectly from ecosystems (Costanza et al., 1997). Millennium Ecosystem Assessment (2005) divides ecosystem services into provisioning, regulation, cultural and supporting services. Provisioning services refer to material goods provided by ecosystem like food. Regulating services refer to indirect benefits such as climate regulation. Cultural services refer to immaterial services such as tourism and esthetic value of an ecosystem. Meanwhile supporting services maintain overall ecosystem functioning for providing all aforementioned services (Tian et al., 2015). As an organism in the ecosystem, *M. punicea* can provide diversified ecosystem services (**Figure 5**).

Over the past three decades, the global loss of species diversity due to climate warming has had a serious direct impact on ecosystem functions (Dib et al., 2020), which could cause significant damage to the ecosystem products and services on which human survival depends on (Cardinale et al., 2012; Hooper et al., 2012; Isbell et al., 2013). Human-driven habitat loss and fragmentation has been occurring for thousands of years, leading to biodiversity loss and extinction in many areas, which has accelerated significantly in recent decades (Dawson et al., 2011). Biodiversity is linked to many ecosystem services that are critical for human well-being and its change can affect ecological stability and the sustainability of ecosystem functions and services (Pennekamp et al., 2018). It is known that species loss in ecosystems may alter overall ecosystem structure and function by influencing the physical formation of habitats, biogeochemical cycles, and ecosystem productivity (Jones et al., 1996; Power et al., 1996). As a higher plant, *M. punicea* plays a unique role in maintaining biodiversity and participating in primary production and primary productivity is critical to all ecosystem services and products (Srivastava and Vellend, 2005; Duffy et al., 2017).

As an ornamental plant unique to alpine habitat, *M. punicea* has captured the attention of several European explorers and horticulturalists. Most notable amongst them was E. H. Wilson, a British plant collector and explore, who wrote extensively about the beauty of *Meconopsis* and is credited with introducing this plant to the western world (Xu, 2016). Based on his works several beautiful hybrids of the species have been created at the Scottish Rock Garden, including *Meconopsis* × *Cookei* "Old Rose," a hybrid of *M. punicea* and *M. quintuplinervia* (Christie, 2007). In Tibetan Buddhism, the prototype of the ubala flower held by the Green Tara is *Meconopsis*. The flowers can also be seen in various frescoes and thangkas, and are believed to relieve suffering. In addition to its cultural and supporting services, *M. punicea* is also essential as a resource for direct utilization by the local Tibetan population. It is a traditional Tibetan medicinal plant,

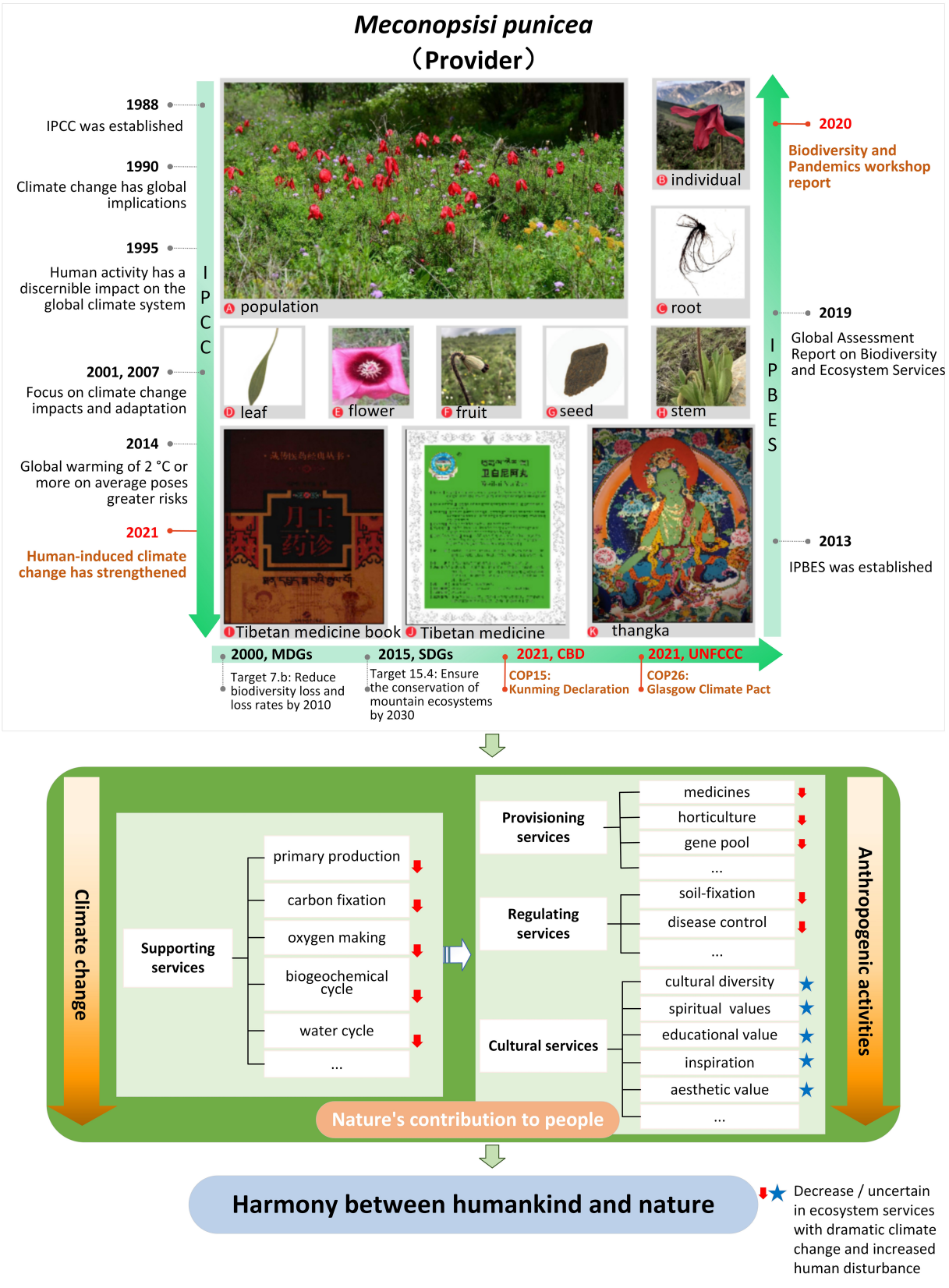

FIGURE 5 | Synthetical assessing ecosystem services of *M. punicea* under frameworks of international importance.

whose efficiency has been well documented in classic Tibetan medicine works such as Yueangyaozhen and Jingzhubencao (Liu et al., 2019). Local populations living on the Qinghai-Tibet Plateau thousands of years ago mastered its usage for health benefits (Shang et al., 2015). *Meconopsis punicea* has been used by local people to treat pain, fever, cough, inflammation, liver fever and lung fever in humans and animals for millennia, and there are five medicinal preparations containing *M. punicea* that have been listed in Drug Standard of the Ministry of Public Health, People's Republic of China (Tibetan medicine volume) (Shang et al., 2015).

With climate change and ever-increasing human disturbance, the ecosystem services provided by *M. punicea* are also changing. In particular, there is a decline in supporting and regulating services due to habitat loss. The changes in cultural services are difficult to quantify since they are largely subjective and based on individual associations to nature (**Figure 5**). This study indicates a sharp decline in the area of suitable habitat of *M. punicea* in the future climate change scenarios, coupled with the disturbance of human activities, the population of *M. punicea* will experience the crisis of shrinking, which will affect the primary production, carbon sequestration, hydrological functions, biogeochemical cycles and other supporting services provided by *M. punicea*. A decline in supporting services, which are the basis of other ecosystem services, will inevitably lead to a decline of diverse services provided, such as medical supplies, the provision of horticultural materials, and gene banks to store germplasm resources; regulating services like soil and water conservation, controlling human disease will be affected consequently. Meanwhile, even though the influence on cultural services, such as spiritual and religious value, medicinal use, and esthetic value, if often not explicitly noticeable, it is a critical ecosystem service and should also be acknowledged (**Figure 5**).

Today, society recognizes the need for an objective and scientific assessment of climate change impacts on the ecosystem (Siebenhüner, 2002). Ecosystem assessments provide useful knowledge for stakeholder decision-making, strategy formulation, and ecosystem management. Assessment reports by the Intergovernmental Panel on Climate Change (IPCC) and Intergovernmental Science-Policy Platform on Biodiversity and Ecosystem Services (IPBES) have time and again highlighted the risks of climate change and need for timely action toward conservation and mitigation. The latest IPCC report (Climate Change 2021: the Physical Science Basis) shows that human-induced extreme climate change has intensified since the Fifth Assessment Report. The Glasgow Climate Pact was adopted at the 26th Conference (COP26) of the Parties to the United Nations Framework Convention on Climate Change (UNFCCC) in 2021, aims to limit global warming to 1.5°C and thus preserve the chance of saving the world from catastrophic climate change. Millenium Development Goals and Sustainable Development Goals put forward by the United Nations also explicitly address the need to reduce biodiversity loss and protect mountain ecosystems. The Kunming Declaration adopted at the 15th Conference of the Parties (COP15) to the United Nations Convention on Biological Diversity (CBD) in 2021 calls for action to halt biodiversity loss, enhance human well-being and achieve sustainable development. IPBES links Biodiversity and Ecosystem Services in its assessment report (Díaz et al., 2019), which noted that species distribution, population size and migration time in the Asia-pacific region will be affected under the influence of climate change and extreme events. Since the novel Coronavirus pandemic in 2019, serious damage has been done. In response to the link between biodiversity and pandemics, the report of IPBES workshop on biodiversity and pandemics was published, which states that the emergence of COVID-19 is entirely driven by human activities driving climate change and biodiversity loss. The risk of pandemics can be significantly reduced by reducing human activities that contribute to biodiversity loss, enhancing protected areas, and taking measures to reduce unsustainable exploitation of high biodiversity areas. A series of changes caused by climate change could have serious implications for biodiversity and the goods and services derived from ecosystems (Chettri and Sharma, 2016). Climate change caused by human activities threaten the survival and development of the wild population of *M. punicea*, which calls for immediate measures to protect and conserve the species in its natural habitat.

Conservation Priorities and Outlook

Meconopsis punicea is an endangered indigenous plant species (Qu and Qu, 2012) with multiple functions, values, and services. Detailed knowledge of its distribution is a prerequisite for the recovery and sustainable use of this species. Our model projections indicate that *M. punicea* will be at high-risk of habitat loss in response to climate change. Without timely conservation measures, the stability and sustainability of the habitat of *M. punicea* habitat may decline rapidly due to habitat specificity. This decline is likely to be accelerated further by anthropogenic disturbances (Ghimire et al., 2008). The headwater region of Min River is located right on the famous Jiuzhai-Huanglong tourist circuit and is inhabited by different ethnic groups including Tibetans, Qiang, Hui, and Han Chinese. Human disturbances in *M. punicea* habitat comes not only from local community, but also from high tourism flows at high environmental costs. These chronic anthropogenic disturbances, combined with climate change, can lead to severe habitat destruction of endemic mountain plant species (Naudiyal et al., 2021). Thus, it is important to protect habitats of this species for the benefit to the local communities whose diverse cultures and traditional knowledge are rooted in the principles of environmental protection and harmony between humans and nature.

One of the key aspects for handling this impending climatic crisis is monitoring through long-term observational data, which is currently lacking. Localized long-term hydrometeorological monitoring need to be improved for robust climate change analysis and adaptation. Even though elevation-dependent warming has been verified by many studies (Pepin et al., 2015; Minder et al., 2018), at a local level there are multiple feedback mechanisms underlying climate change such as snow-albedo interactions, which can also affect local climates. Policies and planning should focus on improved disaster warning

systems, management and mitigation measures to address hydrometeorological extremes (Wester et al., 2019). Creating nature reserves is another effective *in situ* strategy for the protection of biodiversity and ecosystem services. We suggest that future adaptation management strategies should consider the impacts of climate change on the distribution of *M. punicea* in particular and other alpine flora in general and ecosystem-based solutions for its ecological conservation. An integrated habitat conservation plan for *M. Punicea* should be developed and implemented with grassroots assistance in these fragile environmental areas, applying the principles of "preparing for the worst" in the decision-making process (Wright et al., 2015). Since, rainfall is one of the main factors influencing the distribution of *M. punicea*, implementing integrated programs aimed at soil and water conservation will increase *M. punicea* habitat suitability, which may not just support *M. punicea* but several other important endemic species playing critical role in maintaining the ecosystem functioning of the study area. Appropriate conservation strategies based on a socio-ecological framework for landscape planning are the need of the hour (Virapongse et al., 2016).

In this study we attempted to highlight the possible influence of climate change on *M. punicea* distribution. However, like other modeling studies, our inferences are subject to some limitations. Therefore, further research is required to improve the data availability and modeling precision by integrating other important factors except bioclimatic variables into the models or developing an integration model across multi-scales.

CONCLUSION

The models presented here predict the potential impacts of current and future climate on the distribution of *M. punicea*. The results suggest that the potential suitable distribution areas of *M. punicea* would decrease and shift toward higher elevation. To protect the ecological niche, this study suggests incorporating future climate scenarios into current restoration and conservation policies to protect ecologically sensitive species in current habitats. Furthermore, the findings of this study are helpful to better understand the influence of environmental factors on the current distribution of *M. punicea*. At the same time, based on the geographical range of *M. punicea*, further detailed study is needed to evaluate the conservation status and provide reference for the future protection and management of *M. punicea* in headwater region of Min River.

This study not only provides solid baseline information on the impact of climate change on *M. punicea* in ecotone of sub-alpine forests and alpine grassland on the southeastern margin of Qinghai-Tibet Plateau, but may also help in developing rational broad-scale adaptation strategies for forest conservation and management for ecosystem services, in the face of future climate changes.

DATA AVAILABILITY STATEMENT

The raw data supporting the conclusions of this article will be made available by the authors, without undue reservation.

AUTHOR CONTRIBUTIONS

NS: investigation, data curation, formal analysis, and writing – original draft. NN: conceptualization, methodology, software, and writing – review and editing. JW: funding acquisition, investigation, project administration, resources, supervision, and writing – review and editing. NG and YWe: validation and writing – review and editing. YWu: resources, supervision, validation, and writing – review and editing. JH: investigation and data curation. CW: graphing. All authors contributed to the article and approved the submitted version.

FUNDING

This research was funded by National Natural Science Foundation of China (31971436 and 41661144045), Talented Young Scientist Program (Indian-18-008) by China Science and Technology Exchange Centre, Ministry of Science and Technology, and State Key Laboratory of Cryospheric Science, Northwest Institute of Eco-Environment and Resources, Chinese Academy Sciences (SKLCS-OP-2018-07).

ACKNOWLEDGMENTS

Special thanks to Ji Suonan from Qinghai Normal University for providing us with the photos.

REFERENCES

Ackerly, D. D., Loarie, S. R., Cornwell, W. K., Weiss, S. B., Hamilton, H., Branciforte, R., et al. (2010). The geography of climate change: implications for conservation biogeography. *Divers. Distrib.* 16, 476–487. doi: 10.1111/j.1472-4642.2010.00654.x

Alberto, F. J., Aitken, S. N., Alía, R., González-Martínez, S. C., Hänninen, H., Kremer, A., et al. (2013). Potential for evolutionary responses to climate change-evidence from tree populations. *Glob. Change Biol.* 19, 1645–1661. doi: 10.1111/gcb.12181

Al-Qaddi, N., Vessella, F., Stephan, J., Al-Eisawi, D., and Schirone, B. (2017). Current and future suitability areas of kermes oak (*Quercus coccifera* L.) in the Levant under climate change. *Region. Environ. Change* 17, 143–156. doi: 10.1007/s10113-016-0987-2

Anderson, R. P. (2013). A framework for using niche models to estimate impacts of climate change on species distributions. *Ann. N.Y. Acad. Sci.* 1297, 8–28. doi: 10.1111/nyas.12264

Araújo, M. B., Anderson, R. P., Márcia Barbosa, A., Beale, C. M., Dormann, C. F., Early, R., et al. (2019). Standards for distribution models in biodiversity assessments. *Sci. Adv.* 5, 1–10. doi: 10.1126/sciadv.aat4858

Arft, A. M., Walker, M. D., Gurevitch, J., Alatalo, J. M., Bret-Harte, M. S., Dale, M., et al. (1999). Responses of tundra plants to experimental warming: meta-analysis of the international tundra experiment. *Ecol. Monogr.* 69, 491–511. doi: 10.1007/s004420000544

Barker, D. H., Vanier, C., Naumburg, E., Charlet, T. N., Nielsen, K. M., Newingham, B. A., et al. (2006). Enhanced monsoon precipitation and nitrogen deposition affect leaf traits and photosynthesis differently in spring and summer in the desert shrub *Larrea tridentata*. *New Phytol.* 169, 799–808. doi: 10.1111/j.1469-8137.2006.01628.x

Barnosky, A. D., Matzke, N., Tomiya, S., Wogan, G. O. U., Swartz, B., Quental, T. B., et al. (2011). Has the Earth's sixth mass extinction already arrived? *Nature* 471, 51–57. doi: 10.1038/nature09678

Beaumont, L. J., Hughes, L., and Poulsen, M. (2005). Predicting species distributions: use of climatic parameters in BIOCLIM and its impact on predictions of species' current and future distributions. *Ecol. Model.* 186, 251–270. doi: 10.1016/j.ecolmodel.2005.01.030

Bellard, C., Bertelsmeier, C., Leadley, P., Thuiller, W., and Courchamp, F. (2012). Impacts of climate change on the future of biodiversity. *Ecol. Lett.* 15, 365–377. doi: 10.1111/j.1461-0248.2011.01736.x

Bertrand, R., Lenoir, J., Piedallu, C., Riofrío-Dillon, G., de Ruffray, P., Vidal, C., et al. (2011). Changes in plant community composition lag behind climate warming in lowland forests. *Nature* 479, 517–520. doi: 10.1038/nature10548

Bertrand, R., Perez, V., and Gégout, J. C. (2012). Disregarding the edaphic dimension in species distribution models leads to the omission of crucial spatial information under climate change: the case of *Quercus pubescens* in France. *Glob. Change Biol.* 18, 2648–2660. doi: 10.1111/j.1365-2486.2012.02679.x

Boyd, J., and Banzhaf, S. (2007). What are ecosystem services? The need for standardized environmental accounting units. *Ecol. Econ.* 63, 616–626. doi: 10.1016/j.ecolecon.2007.01.002

Brant, A. N., and Chen, H. Y. H. (2015). Patterns and mechanisms of nutrient resorption in plants. *Crit. Rev. Plant Sci.* 34, 471–486. doi: 10.1080/07352689.2015.1078611

Brown, J. H. (1984). On the relationship between abundance and distribution of species. *Am. Nat.* 124, 255–279.

Bugmann, H. (2001). A review of forest gap models. *Clim. Change* 51, 259–305. doi: 10.1023/A:1012525626267

Cao, M., Prince, S. D., Small, J., and Goetz, S. J. (2004). Remotely sensed interannual variations and trends in terrestrial net primary productivity 1981-2000. *Ecosystems* 7, 233–242. doi: 10.1007/s10021-003-0189-x

Cardinale, B. J., Duffy, J. E., Gonzalez, A., Hooper, D. U., Perrings, C., Venail, P., et al. (2012). Biodiversity loss and its impact on humanity. *Nature* 486, 59–67. doi: 10.1038/nature11148

Chakraborty, A., Joshi, P. K., and Sachdeva, K. (2016). Predicting distribution of major forest tree species to potential impacts of climate change in the central Himalayan region. *Ecol. Eng.* 97, 593–609. doi: 10.1016/j.ecoleng.2016.10.006

Chauchard, S., Carcaillet, C., and Guibal, F. (2007). Patterns of land-use abandonment control tree-recruitment and forest dynamics in Mediterranean mountains. *Ecosystems* 10, 936–948. doi: 10.1007/s10021-007-9065-4

Chen, W. (2004). A comparison of species diversity between the shady-slopes and the sunny slopes in the sources of the Minjiang river. *J. Neijiang Norm. Univ.* 19, 31–34.

Chettri, N., and Sharma, E. (2016). Reconciling mountain biodiversity conservation and human wellbeing: drivers of biodiversity loss and new approaches in the Hindu-Kush Himalayas. *Proc. Indian Natl. Sci. Acad.* 82, 53–73. doi: 10.16943/ptinsa/2016/v82i1/48378

Christie, I. (2007). *Meconopsis x cookei 'Old Rose.'*. Scotland: Scottish Rock Garden Club, 64–69.

Corona-Lozada, M. C., Morin, S., and Choler, P. (2019). Drought offsets the positive effect of summer heat waves on the canopy greenness of mountain grasslands. *Agric. For. Meteorol.* 276-277:107617. doi: 10.1016/j.agrformet.2019.107617

Costanza, R., d'Arge, R., de Groot, R., Farber, S., Grasso, M., Hannon, B., et al. (1997). The value of the world's ecosystem services and natural capital. *Nature* 387, 253–260. doi: 10.1038/387253a0

Criado, M. G., Myers-Smith, I. H., Bjorkman, A. D., Lehmann, C. E. R., and Stevens, N. (2020). Woody plant encroachment intensifies under climate change across tundra and savanna biomes. *Glob. Ecol. Biogeogr.* 29, 925–943. doi: 10.1111/geb.13072

Davies, T. J., Purvis, A., and Gittleman, J. L. (2009). Quaternary climate change and the geographic ranges of mammals. *Am. Nat.* 174, 297–307. doi: 10.1086/603614

Dawson, T. P., Jackson, S. T., House, J. I., Prentice, I. C., and Mace, G. M. (2011). Beyond predictions: biodiversity conservation in a changing climate. *Science* 332, 53–58. doi: 10.1126/science.1200303

Delmas, C. E. L., Cheptou, P. O., Escaravage, N., and Pornon, A. (2014). High lifetime inbreeding depression counteracts the reproductive assurance benefit of selfing in a mass-flowering shrub. *BMC Evol. Biol.* 14:7. doi: 10.1186/s12862-014-0243-7

Diaz, H. F., and Bradley, R. S. (1997). Temperature variations during the last century at high elevation sites. *Clim. Change* 36, 253–279. doi: 10.1023/A:1005335731187

Diaz, H. F., and Eischeid, J. K. (2007). Disappearing "alpine tundra" Köppen climatic type in the western United States. *Geophys. Res. Lett.* 34:L18707. doi: 10.1029/2007GL031253

Díaz, S., Settele, J., Brondizio, E. S., Ngo, H. T., Guèze, M., and Agard, J. (2019). *IPBES: Summary for Policymakers of the Global Assessment Report on Biodiversity and Ecosystem Services*. Bonn: Intergovernmental Science-Policy Platform on Biodiversity and Ecosystem Services.

Dib, V., Pires, A. P. F., Casa Nova, C., Bozelli, R. L., and Farjalla, V. F. (2020). Biodiversity-mediated effects on ecosystem functioning depend on the type and intensity of environmental disturbances. *Oikos* 129, 433–443. doi: 10.1111/oik.06768

Dolezal, J., Kurnotova, M., Stastna, P., and Klimesova, J. (2020). Alpine plant growth and reproduction dynamics in a warmer world. *New Phytol.* 228, 1295–1305. doi: 10.1111/nph.16790

Dorji, T., Hopping, K. A., Meng, F., Wang, S., Jiang, L., and Klein, J. A. (2020). Impacts of climate change on flowering phenology and production in alpine plants: the importance of end of flowering. *Agric. Ecosyst. Environ.* 291:106795. doi: 10.1016/j.agee.2019.106795

Dormann, C. F., Elith, J., Bacher, S., Buchmann, C., Carl, G., Carré, G., et al. (2013). Collinearity: a review of methods to deal with it and a simulation study evaluating their performance. *Ecography* 36, 1–20. doi: 10.1111/j.1600-0587.2012.07348.x

Duffy, J. E., Godwin, C. M., and Cardinale, B. J. (2017). Biodiversity effects in the wild are common and as strong as key drivers of productivity. *Nature* 549, 261–264. doi: 10.1038/nature23886

Easterling, D. R., Meehl, G. A., Parmesan, C., Changnon, S. A., Karl, T. R., and Mearns, L. O. (2000). Climate extremes: observations, modeling, and impacts. *Science* 289, 2068–2074. doi: 10.1126/science.289.5487.2068

Elith, J., Graham, C., Anderson, R., Dudík, M., Ferrier, S., Guisan, A., et al. (2006). Novel methods improve prediction of species' distributions from occurrence data. *Ecography* 29, 129–151. doi: 10.1111/j.2006.0906-7590.04596.x

Engler, R., Randin, C. F., Vittoz, P., Czáka, T., Beniston, M., Zimmermann, N. E., et al. (2009). Predicting future distributions of mountain plants under climate change: does dispersal capacity matter? *Ecography* 32, 34–45. doi: 10.1111/j.1600-0587.2009.05789.x

Faleiro, F. V., Machado, R. B., and Loyola, R. D. (2013). Defining spatial conservation priorities in the face of land-use and climate change. *Biol. Conserv.* 158, 248–257. doi: 10.1016/j.biocon.2012.09.020

Feilhauer, H., He, K. S., and Rocchini, D. (2012). Modeling species distribution using niche-based proxies derived from composite bioclimatic variables and MODIS NDVI. *Remote Sens.* 4, 2057–2075. doi: 10.3390/rs4072057

Ford, K. R., and HilleRisLambers, J. (2019). Soil alters seedling establishment responses to climate. *Ecol. Lett.* 23, 140–148. doi: 10.1111/ele.13416

Fourcade, Y., Engler, J. O., Rödder, D., and Secondi, J. (2014). Mapping species distributions with MaxEnt using a geographically biased sample of presence data: a performance assessment of methods for correcting sampling bias. *PLoS One* 9:e97122. doi: 10.1371/journal.pone.0097122

Fragnière, Y., Pittet, L., Clément, B., Sébastien, B., Gerber, E., Ronikier, M., et al. (2020). Climate change and alpine screes: no future for glacial relict *Papaver occidentale* (Papaveraceae) in Western Prealps. *Diversity* 2020:346. doi: 10.3390/d12090346

Francon, L., Corona, C., Till-Bottraud, I., Carlson, B. Z., and Stoffel, M. (2020). Some (do not) like it hot: shrub growth is hampered by heat and drought at the alpine treeline in recent decades. *Am. J. Bot.* 107, 607–617. doi: 10.1002/ajb2.1459

Frishkoff, L. O., Karp, D. S., Flanders, J. R., Zook, J., Hadly, E. A., and Daily, G. C. (2016). Climate change and habitat conversion favour the same species. *Ecol. Lett.* 19, 1081–1090. doi: 10.1111/ele.12645

Gallagher, R. V., Hughes, L., Leishman, M. R., and Wilson, P. D. (2010). Predicted impact of exotic vines on an endangered ecological community under future climate change. *Biol. Invas.* 12, 4049–4063. doi: 10.1007/s10530-010-9814-8

Ganjurjav, H., Gornish, E. S., Hu, G., Schwartz, M. W., Wan, Y., and Li, Y. (2020). Warming and precipitation addition interact to affect plant spring phenology in alpine meadows on the central Qinghai-Tibetan Plateau. *Agric. For. Meteorol.* 287:107943. doi: 10.1016/j.agrformet.2020.107943

Gaston, K. J., Blackburn, T. M., Greenwood, J. J. D., Gregory, R. D., Quinn, R. M., and Lawton, J. H. (2000). Abundance-occupancy relationships. *J. Appl. Ecol.* 37, 39–59. doi: 10.1046/j.1365-2664.2000.00485.x

Gavilán, R. G. (2005). The use of climatic parameters and indices in vegetation distribution. A case study in the Spanish Sistema Central. *Int. J. Biometeorol.* 50, 111–120. doi: 10.1007/s00484-005-0271-5

Ghimire, S. K., Sapkota, I. B., and Oli, B. R. (2008). *Non-Timber Forest Products of Nepal Himalaya: Database of Some Important Species Found in the Mountain Protected Areas, and Surrounding Regions*. Kathmandu: WWF Nepal, 1–4.

Gottfried, M., Pauli, H., Futschik, A., Akhalkatsi, M., Barančok, P., Benito Alonso, J. L., et al. (2012). Continent-wide response of mountain vegetation to climate change. *Nat. Clim. Change* 2, 111–115. doi: 10.1038/nclimate1329

Gou, X., Chen, F., Jacoby, G., Cook, E., Yang, M., and Peng, J. (2007). Rapid tree growth with respect to the last 400 years in response to climate warming, northeastern Tibetan Plateau. *Int. J. Climatol.* 27, 1497–1503. doi: 10.1002/joc.1480

Grey-Wilson, C. (2014). *The Genus Meconopsis: Blue Poppies, and Their Relatives*. Kew: Kew Publishing, 1–5.

Guan, W., Wu, J., Liang, G., Wang, B., Ma, K., and Liu, G. (2002). "Vegetation classification and the main types in the headwater area of the Minjiang river. Biodiversity conservation and research in China," in *Proceedings of the 5th National Conference on Biodiversity Conservation and Sustainable Utilization*, (Beijing: China Meteorological Press), 296–308.

Guo, Y., Wei, H., Lu, C., Gao, B., and Gu, W. (2016). Predictions of potential geographical distribution and quality of Schisandra sphenanthera under climate change. *PeerJ* 4:e2554. doi: 10.7717/peerj.2554

He, X., Burgess, K. S., Yang, X. F., Ahrends, A., Gao, L. M., and Li, D. Z. (2019). Upward elevation and northwest range shifts for alpine *Meconopsis* species in the Himalaya-Hengduan Mountains region. *Ecol. Evol.* 9, 4055–4064. doi: 10.1002/ece3.5034

Heisler-white, J. L., Blair, J. M., Kelly, E. F., Harmoney, K., and Knapp, A. K. (2009). Contingent productivity responses to more extreme rainfall regimes across a grassland biome. *Glob. Change Biol.* 15, 2894–2904. doi: 10.1111/j.1365-2486.2009.01961.x

Henry, G. H. R., and Molau, U. (1997). Tundra plants and climate change: the International Tundra Experiment (ITEX). *Glob. Change Biol.* 3, 1–9. doi: 10.1111/j.1365-2486.1997.gcb132.x

Hijmans, R. J., Cameron, S. E., Parra, J. L., Jones, P. G., and Jarvis, A. (2005). Very high resolution interpolated climate surfaces for global land areas. *Int. J. Climatol.* 25, 1965–1978. doi: 10.1002/joc.1276

Hoffmann, M., Hilton-Taylor, C., Angulo, A., Böhm, M., Brooks, T., Butchart, S., et al. (2010). The impact of conservation on the status of the world's vertebrates. *Science* 330, 1503–1509. doi: 10.1126/science.1194442

Hooper, D. U., Adair, E. C., Cardinale, B. J., Byrnes, J. E. K., Hungate, B. A., Matulich, K. L., et al. (2012). A global synthesis reveals biodiversity loss as a major driver of ecosystem change. *Nature* 486, 105–108. doi: 10.1038/nature11118

Hörsch, B. (2003). Modelling the spatial distribution of montane and subalpine forests in the central Alps using digital elevation models. *Ecol. Model.* 168, 267–282. doi: 10.1016/S0304-3800(03)00141-8

Huang, C. Y., and Xu, J. M. (2010). *Soil Science*. Beijing: China Agriculture Press, 80–88.

Isbell, F., Reich, P. B., Tilman, D., Hobbie, S. E., Polasky, S., and Binder, S. (2013). Nutrient enrichment, biodiversity loss, and consequent declines in ecosystem productivity. *PNAS* 110, 11911–11916. doi: 10.1073/pnas.1310880110

Jarvis, A. J., Stauch, V. J., Schulz, K., and Young, P. C. (2004). The seasonal temperature dependency of photosynthesis and respiration in two deciduous forests. *Glob. Change Biol.* 10, 939–950. doi: 10.1111/j.1529-8817.2003.00743.x

Jones, C. G., Lawton, J. H., and Shachak, M. (1996). "Organisms as ecosystem engineers," in *Ecosystem Management*, eds F. B. Samson and F. L. Knopf (New York, NY: Springer), 130–147. doi: 10.1353/pbm.2003.0003

Khanum, R., Mumtaz, A. S., and Kumar, S. (2013). Predicting impacts of climate change on medicinal asclepiads of Pakistan using Maxent modeling. *Acta Oecol.* 49, 23–31. doi: 10.1016/j.actao.2013.02.007

Klanderud, K., and Totland, Ø (2005). Simulated climate change altered dominance hierarchies and diversity of an alpine biodiversity hotspot. *Ecology* 86, 2047–2054. doi: 10.1890/04-1563

Kozak, K. H., Graham, C. H., and Wiens, J. J. (2008). Integrating GIS-based environmental data into evolutionary biology. *Trends Ecol. Evol.* 23, 141–148. doi: 10.1016/j.tree.2008.02.001

KrÄuchi, N., and Kienast, F. (1993). Modelling subalpine forest dynamics as influenced by a changing environment. *Water Air Soil Pollut.* 68, 185–197. doi: 10.1007/BF00479402

Kumar, P. (2012). Assessment of impact of climate change on Rhododendrons in Sikkim Himalayas using Maxent modelling: limitations and challenges. *Biodivers. Conserv.* 21, 1251–1266. doi: 10.1007/s10531-012-0279-1

Kumar, S., Graham, J., West, A. M., and Evangelista, P. H. (2014). Using district-level occurrences in MaxEnt for predicting the invasion potential of an exotic insect pest in India. *Comput. Electron. Agric.* 103, 55–62. doi: 10.1016/j.compag.2014.02.007

Kumar, S., and Stohlgren, T. (2009). Maxent modeling for predicting suitable habitat for threatened and endangered tree Canacomyrica monticola in New Caledonia. *J. Ecol. Nat. Environ.* 1, 94–98.

Li, J., Fan, G., and He, Y. (2020). Predicting the current and future distribution of three Coptis herbs in China under climate change conditions, using the MaxEnt model and chemical analysis. *Sci. Tot. Environ.* 698:134141. doi: 10.1016/j.scitotenv.2019.134141

Li, R., Xu, M., Wong, M. H. G., Qiu, S., Li, X., Ehrenfeld, D., et al. (2015). Climate change threatens giant panda protection in the 21st century. *Biol. Conserv.* 182, 93–101. doi: 10.1016/j.biocon.2014.11.037

Li, X., Tian, H., Wang, Y., Li, R., Song, Z., Zhang, F., et al. (2013). Vulnerability of 208 endemic or endangered species in China to the effects of climate change. *Region. Environ. Change* 13, 843–852. doi: 10.1007/s10113-012-0344-z

Liu, M., Li, Q., Ji, D., and Lu, Y. (2019). Determination of total flavonoids in *Meconopsis punicea* Maxim and optimization of extraction technology. *J. Seed Ind. Guide* 09, 8–11.

Liu, X., Huang, H., Yang, Y., and Wu, H. (2014). Analysis of effect of topographical conditions on content of total alkaloid in Coptidis Rhizoma in Chongqin,China. *China J. Chinese Mater. Med.* 39, 4748–4753. doi: 10.4268/cjcmm20142410

Liu, X. D., and Chen, B. D. (2000). Climatic warming in the Tibetan Plateau during recent decades. *Int. J. Climatol.* 20, 1729–1742. doi: 10.1002/1097-0088(20001130)20:14<1729::aid-joc556>3.0.co;2-y

Locatelli, B., Kanninen, M., Brockhaus, M., Colfer, C. J. P., Murdiyarso, D., and Santoso, H. (2008). Facing an uncertain future: how forest and people can adapt to climate change. *Center Int. For. Res.* 28:2600. doi: 10.17528/cifor/002600

Lotstein, E. L. (2013). Global climate change impacts in the United States: a state of knowledge report from the U.S. global climate change research program. *J. Geogr.* 40:178. doi: 10.1080/00221341.2013.770905

Lu, C. Y., Gu, W., Dai, A. H., and Wei, H. Y. (2012). Assessing habitat suitability based on geographic information system (GIS) and fuzzy: a case study of *Schisandra sphenanthera* Rehd. et Wils. in Qinling Mountains, China. *Ecol. Model.* 242, 105–115. doi: 10.1016/j.ecolmodel.2012.06.002

Lv, Z. H. (2009). *The Impacts of Climate Change on the Distribution of Rare or Endangered Species in China and Adaptations Strategies*. Beijing: Chinese Research Academy of Environmental Sciences.

Ma, M., and Chang, R. (2019). Temperature drive the altitudinal change in soil carbon and nitrogen of montane forests: implication for global warming. *Catena* 182:104126. doi: 10.1016/j.catena.2019.104126

Mantyka-pringle, C. S., Martin, T. G., and Rhodes, J. R. (2012). Interactions between climate and habitat loss effects on biodiversity: a systematic review and meta-analysis. *Glob. Change Biol.* 18, 1239–1252. doi: 10.1111/j.1365-2486.2011.02593.x

McKenney, D. W., Pedlar, J. H., Lawrence, K., Campbell, K., and Hutchinson, M. F. (2007). Potential impacts of climate change on the distribution of North American trees. *Bioscience* 57, 939–948. doi: 10.1641/B571106

Merow, C., and Silander, J. A. Jr. (2014). A comparison of Maxlike and MaxEnt for modelling species distributions. *Methods Ecol. Evol.* 5, 215–225. doi: 10.1111/2041-210X.12152

Millennium Ecosystem Assessment (2005). *Ecosystems and Human Well-Being: Synthesis*. Washington, DC: Island Press, 39–40.

Minder, J. R., Letcher, T. W., and Liu, C. (2018). The character and causes of elevation-dependent warming in high-resolution simulations of Rocky Mountain climate change. *J. Clim.* 31, 2093–2113. doi: 10.1175/JCLI-D-17-0321.1

Molina-Montenegro, M. A., Atala, C., and Gianoli, E. (2010). Phenotypic plasticity and performance of *Taraxacum officinale* (dandelion) in habitats of contrasting environmental heterogeneity. *Biol. Invas.* 12, 2277–2284. doi: 10.1007/s10530-009-9638-6

Murray, K. A., Rosauer, D., McCallum, H., and Skerratt, L. F. (2011). Integrating species traits with extrinsic threats: closing the gap between predicting and preventing species declines. *Proc. R. Soc. B Biol. Sci.* 278, 1515–1523. doi: 10.1098/rspb.2010.1872

Naudiyal, N., Wang, J. N., Wu, N., Gaire, N. P., Shi, P. L., Wei, Y. Q., et al. (2021). Potential distribution of Abies, Picea, and *Juniperus* species in the sub-alpine forest of Minjiang headwater region under current and future climate scenarios and its implications on ecosystem services supply. *Ecol. Indic.* 121:107131. doi: 10.1016/j.ecolind.2020.107131

Nayak, K. G., and Davidar, P. (2010). Pollinator limitation and the effect of breeding systems on plant reproduction in forest fragments. *Acta Oecol.* 36, 191–196. doi: 10.1016/j.actao.2009.12.004

Niu, T., Chen, L., and Zhou, Z. (2004). The characteristics of climate change over the Tibetan Plateau in the last 40 years and the detection of climatic jumps. *Adv. Atmos. Sci.* 21, 193–203. doi: 10.1007/BF02915705

Nogués-Bravo, D., Araújo, M. B., Errea, M. P., and Martínez-Rica, J. P. (2007). Exposure of global mountain systems to climate warming during the 21st century. *Glob. Environ. Change* 17, 420–428. doi: 10.1016/j.gloenvcha.2006.11.007

Orsenigo, S., Mondoni, A., Rossi, G., and Abeli, T. (2014). Some like it hot and some like it cold, but not too much: plant responses to climate extremes. *Plant Ecol.* 215, 677–688. doi: 10.1007/s11258-014-0363-6

Oyler, J. W., Dobrowski, S. Z., Ballantyne, A. P., Klene, A. E., and Running, S. W. (2015). Artificial amplification of warming trends across the mountains of the western United States. *Geophys. Res. Lett.* 42, 153–161. doi: 10.1002/2014GL062803

Pacifici, M., Foden, W. B., Visconti, P., Watson, J. E. M., Butchart, S. H. M., Kovacs, K. M., et al. (2015). Assessing species vulnerability to climate change. *Nat. Clim. Change* 5, 215–224. doi: 10.1038/nclimate2448

Palazzi, E., Mortarini, L., Terzago, S., and von Hardenberg, J. (2019). Elevation-dependent warming in global climate model simulations at high spatial resolution. *Clim. Dyn.* 52, 2685–2702. doi: 10.1007/s00382-018-4287-z

Pauli, H., Gottfried, M., Reiter, K., Klettner, C., and Grabherr, G. (2007). Signals of range expansions and contractions of vascular plants in the high Alps: observations (1994-2004) at the GLORIA* master site Schrankogel, Tyrol, Austria. *Glob. Change Biol.* 13, 147–156. doi: 10.1111/j.1365-2486.2006.01282.x

Pearson, R. G., Raxworthy, C. J., Nakamura, M., and Townsend Peterson, A. (2007). Predicting species distributions from small numbers of occurrence records: a test case using cryptic geckos in Madagascar. *J. Biogeogr.* 34, 102–117. doi: 10.1111/j.1365-2699.2006.01594.x

Peng, C., Ma, Z., Lei, X., Zhu, Q., Chen, H., Wang, W., et al. (2011). A drought-induced pervasive increase in tree mortality across Canada's boreal forests. *Nat. Clim. Change* 1, 467–471. doi: 10.1038/nclimate1293

Pennekamp, F., Pontarp, M., Tabi, A., Altermatt, F., Alther, R., Choffat, Y., et al. (2018). Biodiversity increases and decreases ecosystem stability. *Nature* 563, 109–112. doi: 10.1038/s41586-018-0627-8

Pepin, N., Bradley, R. S., Diaz, H. F., Baraer, M., Caceres, E. B., Forsythe, N., et al. (2015). Elevation-dependent warming in mountain regions of the world. *Nat. Clim. Change* 5, 424–430. doi: 10.1038/nclimate2563

Phillips, S. J., Anderson, R. P., and Schapire, R. E. (2006). Maximum entropy modeling of species geographic distributions. *Ecol. Model.* 190, 231–259. doi: 10.1016/j.ecolmodel.2005.03.026

Pol, R. G., Pirk, G. I., and Marone, L. (2010). Grass seed production in the central Monte desert during successive wet and dry years. *Plant Ecol.* 208, 65–75. doi: 10.1007/s11258-009-9688-y

Power, M., Tilman, D., Estes, J., Menge, B., Bond, W., Mills, L., et al. (1996). Challenges in the quest for keystones: identifying keystone species is difficult-but essential to understanding how loss of species will affect ecosystems. *Bioscience* 46, 609–620. doi: 10.2307/1312990

Qu, Y., and Qu, Z. (2012). The research advancement on the genus Meconpsis. *Northern Hortic.* 02, 191–194.

Quan, Q., Tian, D., Luo, Y., Zhang, F., Crowther, T. W., Zhu, K., et al. (2019). Water scaling of ecosystem carbon cycle feedback to climate warming. *Sci. Adv.* 5:eaav1131. doi: 10.1126/sciadv.aav1131

Radosavljevic, A., and Anderson, R. P. (2014). Making better MaxEnt models of species distributions: complexity, overfitting and evaluation. *J. Biogeogr.* 41, 629–643. doi: 10.1111/jbi.12227

Rocchini, D., Hortal, J., Lengyel, S., Lobo, J. M., Jiménez-Valverde, A., Ricotta, C., et al. (2011). Accounting for uncertainty when mapping species distributions: the need for maps of ignorance. *Prog. Phys. Geogr. Earth Environ.* 35, 211–226. doi: 10.1177/0309133311399491

Schär, C., Vidale, P. L., Lüthi, D., Frei, C., Häberli, C., Liniger, M. A., et al. (2004). The role of increasing temperature variability in European summer heatwaves. *Nature* 427, 332–336. doi: 10.1038/nature02300

Schickhoff, U., Bobrowski, M., Böhner, J., Bürzle, B., Chaudhary, R. P., Gerlitz, L., et al. (2016). "Climate change and treeline dynamics in the Himalaya," in *Climate Change, Glacier Response, and Vegetation Dynamics in the Himalaya*, eds R. B. Singh, U. Schickhoff, and S. Mal (Switzerland: Springer International Publishing), 271–306.

Schoener, T. W., and Spiller, D. A. (1987). High population persistence in a system with high turnover. *Nature* 330, 474–477. doi: 10.1038/330474a0

Shah, N. H., and Paulsen, G. M. (2003). Interaction of drought and high temperature on photosynthesis and grain-filling of wheat. *Plant Soil* 257, 219–226. doi: 10.1023/A:1026237816578

Shang, X., Wang, D., Miao, X., Wang, Y., Zhang, J., Wang, X., et al. (2015). Antinociceptive and anti-tussive activities of the ethanol extract of the flowers of *Meconopsis punicea* Maxim. *BMC Complement. Altern. Med.* 15:154. doi: 10.1186/s12906-015-0671-y

Shaw, M. R., Pendleton, L., Cameron, D. R., Morris, B., Bachelet, D., Klausmeyer, K., et al. (2011). The impact of climate change on California's ecosystem services. *Clim Change* 109, 465–484. doi: 10.1007/s10584-011-0313-4

Siebenhüner, B. (2002). How do scientific assessments learn?: Part 1. Conceptual framework and case study of the IPCC. *Environ. Sci. Policy* 5, 411–420. doi: 10.1016/S1462-9011(02)00050-3

Singh, S. P., Sharma, S., and Dhyani, P. P. (2019). Himalayan arc and treeline: distribution, climate change responses and ecosystem properties. *Biodivers. Conserv.* 28, 1997–2016. doi: 10.1007/s10531-019-01777-w

Song, Y., Jin, L., and Wang, H. (2018). Vegetation changes along the qinghai-tibet plateau engineering corridor since 2000 induced by climate change and human activities. *Remote Sens.* 10:95. doi: 10.3390/rs10010095

Srivastava, D. S., and Vellend, M. (2005). Biodiversity-ecosystem function research: is it relevant to conservation? *Annu. Rev. Ecol. Evol. Syst.* 36, 267–294. doi: 10.1146/annurev.ecolsys.36.102003.152636

Staude, I. R., Navarro, L. M., and Pereira, H. M. (2020). Range size predicts the risk of local extinction from habitat loss. *Glob. Ecol. Biogeogr.* 29, 16–25. doi: 10.1111/geb.13003

Sullivan, P. F. (2016). Evidence of soil nutrient availability as the proximate constraint on growth of treeline trees in northwest Alaska: reply. *Ecology* 97, 803–808. doi: 10.1890/15-1734.1

Swets, J. A. (1988). Measuring the accuracy of diagnostic systems. *Science* 240, 1285–1293. doi: 10.1126/science.3287615

Theodorou, K., and Couvet, D. (2015). The efficiency of close inbreeding to reduce genetic adaptation to captivity. *Heredity* 114, 38–47. doi: 10.1038/hdy.2014.63

Thomas, C. D., Cameron, A., Green, R. E., Bakkenes, M., Beaumont, L. J., Collingham, Y. C., et al. (2004). Extinction risk from climate change. *Nature* 427, 145–148. doi: 10.1038/nature02121

Thomas, J. A., Telfer, M. G., Roy, D. B., Preston, C. D., Greenwood, J. J. D., Asher, J., et al. (2004). Comparative losses of british butterflies, birds, and plants and the global extinction crisis. *Science* 303, 1879–1881. doi: 10.1126/science.1095046

Thuiller, W. (2007). Climate change and the ecologist. *Nature* 448, 550–552. doi: 10.1038/448550a

Tian, N., Poudyal, N. C., Hodges, D. G., Young, T. M., and Hoyt, K. P. (2015). Understanding the factors influencing nonindustrial private forest landowner interest in supplying ecosystem services in Cumberland Plateau, Tennessee. *Forests* 6, 3985–4000. doi: 10.3390/f6113985

Tognetti, R., Cherubini, P., Marchi, S., and Raschi, A. (2007). Leaf traits and tree rings suggest different water-use and carbon assimilation strategies by two co-occurring *Quercus* species in a Mediterranean mixed-forest stand in Tuscany, Italy. *Tree Physiol.* 27, 1741–1751. doi: 10.1093/treephys/27.12.1741

Veloz, S. D. (2009). Spatially auto-correlated sampling falsely inflates measures of accuracy for presence-only niche models. *J. Biogeogr.* 36, 2290–2299. doi: 10.1111/j.1365-2699.2009.02174.x

Virapongse, A., Brooks, S., Metcalf, E. C., Zedalis, M., Gosz, J., Kliskey, A., et al. (2016). A social-ecological systems approach for environmental management. *J. Environ. Manage.* 178, 83–91. doi: 10.1016/j.jenvman.2016.02.028

Vuuren, D. P., Van Edmonds, J., Kainuma, M., Riahi, K., Nakicenovic, N., Smith, S. J., et al. (2011). The representative concentration pathways: an overview. *Clim. Change* 109, 5–31. doi: 10.1007/s10584-011-0148-z

Walther, G. R., Beißner, S., and Burga, C. A. (2005). Trends in the upward shift of alpine plants. *J. Veg. Sci.* 16, 541–548. doi: 10.1111/j.1654-1103.2005.tb02394.x

Wang, B., Chen, T., Xu, G., Liu, X., Wang, W., Wu, G., et al. (2016). Alpine timberline population dynamics under climate change: a comparison between Qilian juniper and Qinghai spruce tree species in the middle Qilian Mountains of northeast Tibetan Plateau. *Boreas* 45, 411–422. doi: 10.1111/bor.12161

Wang, D., Cui, B., Duan, S., Chen, J., Fan, H., Lu, B., et al. (2019). Moving north in China: the habitat of *Pedicularis kansuensis* in the context of climate change. *Sci. Total Environ.* 697:133979. doi: 10.1016/j.scitotenv.2019.133979

Wang, G., Baskin, C. C., Baskin, J. M., Yang, X., Liu, G., Ye, X., et al. (2018). Effects of climate warming and prolonged snow cover on phenology of the early life history stages of four alpine herbs on the southeastern Tibetan Plateau. *Am. J. Bot.* 105, 1–10. doi: 10.1002/ajb2.1104

Wang, J., Shi, F., Xu, B., Wang, Q., Wu, Y., and Wu, N. (2014). Uptake and recovery of soil nitrogen by bryophytes and vascular plants in an alpine meadow. *J. Mountain Sci.* 11, 475–484. doi: 10.1007/s11629-013-2707-4

Wang, J. J., Cao, B., Bai, C. K., Zhang, L. L., and Che, L. (2014). Potential distribution prediction and suitability evaluation of *Fritillaria cirrhosa* D.don based on MaxEnt modeling and GIS. *Bull. Bot. Res.* 34, 642–649. doi: 10.7525/j.issn.1673-5102.2014.05.010

Wang, Q., Fan, X., and Wang, M. (2014). Recent warming amplification over high elevation regions across the globe. *Clim. Dyn.* 43, 87–101. doi: 10.1007/s00382-013-1889-3

Wang, S., Zhang, Y., Ju, W., Jing, M. C., Ciais, P., Cescatti, A., et al. (2020). Recent global decline of CO2 fertilization effects on vegetation photosynthesis. *Science* 370, 1295–1300. doi: 10.1126/science.abb7772

Wang, X., Cheng, G., and Zhong, X. (2011). Assessing potential impacts of climatic change on subalpine forests on the eastern Tibetan Plateau. *Clim. Change* 108, 225–241. doi: 10.1007/s10584-010-0008-2

Wang, Y., Liang, E., Lu, X., Camarero, J. J., Babst, F., Shen, M., et al. (2021). Warming-induced shrubline advance stalled by moisture limitation on the Tibetan Plateau. *Ecography* 44, 1631–1641. doi: 10.1111/ecog.05845

Wei, Y., Zhang, L., Wang, J., Wang, W., Niyati, N., and Guo, Y. (2021). Chinese caterpillar fungus (*Ophiocordyceps sinensis*) in China: current distribution, trading, and futures under climate change and overexploitation. *Sci. Total Environ.* 755:142548. doi: 10.1016/j.scitotenv.2020.142548

Wester, P., Mishra, A., Mukherji, A., and Shrestha, A. B. (2019). *The Hindu Kush Himalaya Assessment*. Kathmandu: Springer, 144–151.

Wiens, J. A., Stralberg, D., Jongsomjit, D., Howell, C. A., and Snyder, M. A. (2009). Niches, models, and climate change: assessing the assumptions and uncertainties. *PNAS* 106, 19729–19736. doi: 10.1073/pnas.0901639106

Williams, J. E. (2000). The biodiversity crisis and adaptation to climate change: a case study from Australia's forests. *Environ. Monit. Assess* 61, 65–74. doi: 10.1023/A:1006361917359

Wilmking, M., and Juday, G. P. (2005). Longitudinal variation of radial growth at Alaska's northern treeline-recent changes and possible scenarios for the 21st century. *Glob. Planet. Change* 47, 282–300. doi: 10.1016/j.gloplacha.2004.10.017

Wright, A. N., Hijmans, R. J., Schwartz, M. W., and Shaffer, H. B. (2015). Multiple sources of uncertainty affect metrics for ranking conservation risk under climate change. *Divers. Distrib.* 21, 111–122. doi: 10.1111/ddi.12257

Wu, J., Xu, H. G., and Chen, L. (2011). A review of impacts of climate change on species. *J. Ecol. Rural Environ.* 27, 1–6.

Xu, B. (2016). Meconopsis, the legend of the Himalayas. *Hum. Kind* 4, 14–29.

Xu, D., Zhuo, Z., Wang, R., Ye, M., and Pu, B. (2019). Modeling the distribution of *Zanthoxylum armatum* in China with MaxEnt modeling. *Glob. Ecol. Conserv.* 19:e00691. doi: 10.1016/j.gecco.2019.e00691

Xu, H., Wang, X., Zhao, C., and Yang, X. (2018). Diverse responses of vegetation growth to meteorological drought across climate zones and land biomes in northern China from 1981 to 2014. *Agric. For. Meteorol.* 262, 1–13. doi: 10.1016/j.agrformet.2018.06.027

Xu, M., Peng, F., You, Q., Guo, J., Tian, X., Xue, X., et al. (2015). Year-round warming and autumnal clipping lead to downward transport of root biomass, carbon and total nitrogen in soil of an alpine meadow. *Environ. Exp. Bot.* 109, 54–62. doi: 10.1016/j.envexpbot.2014.07.012

Xu, M., and Xuan, X. (2013). Analysis on the effects of climate warming on growth and phenology of alpine plants. *J. Arid Land Resour. Environ.* 27, 137–141. doi: 10.13448/j.cnki.jalre.2013.03.026

Yang, X. Q., Kushwaha, S. P. S., Saran, S., Xu, J., and Roy, P. S. (2013). MaxEnt modeling for predicting the potential distribution of medicinal plant, Justicia adhatoda L. in lesser Himalayan foothills. *Ecol. Eng.* 51, 83–87. doi: 10.1016/j.ecoleng.2012.12.004

Zhang, C. (2009). *Studies on Chemical Constituents of Alkaloids and Flavonoids of Meconopsis Quintuplinervia Regel*. Xining: Northwest Institute of Plateau Biology.

Zhang, J., Cai, C. T., Cai, Z. Q., Liu, G. Z., Luo, Y., and Yang, Z. X. (2008). Variation patterns of Coptis teeta biomass and its major active compounds along an altitude gradient. *Chinese J. Appl. Ecol.* 7, 1465–1461.

Zhang, K., Zhang, Y., Zhou, C., Meng, J., Sun, J., Zhou, T., et al. (2019). Impact of climate factors on future distributions of *Paeonia ostii* across China estimated by MaxEnt. *Ecol. Inform.* 50, 62–67. doi: 10.1016/j.ecoinf.2019.01.004

Zhang, M. L., and Christopher, G. W. (2008). *Flora of China*. Beijing: Science Press.

Zhang, P., Jeong, J. H., Yoon, J. H., Kim, H., Wang, S. Y. S., Linderholm, H. W., et al. (2020). Abrupt shift to hotter and drier climate over inner East Asia beyond the tipping point. *Science* 370, 1095–1099. doi: 10.1126/science.abb3368

Zhang, Y., Shao, X., and Wilmking, M. (2011). Dynamic relationships between *Picea crassifolia* growth and climate at upper treeline in the Qilian Mts., Northeast Tibetan Plateau, China. *Dendrochronologia* 29, 185–199. doi: 10.1016/j.dendro.2010.11.001

Zhao, D., Wu, S., Yin, Y., and Yin, Z. Y. (2011). Vegetation distribution on Tibetan Plateau under climate change scenario. *Region. Environ. Change* 11, 905–915. doi: 10.1007/s10113-011-0228-7

Conflict of Interest: The authors declare that the research was conducted in the absence of any commercial or financial relationships that could be construed as a potential conflict of interest.

Publisher's Note: All claims expressed in this article are solely those of the authors and do not necessarily represent those of their affiliated organizations, or those of the publisher, the editors and the reviewers. Any product that may be evaluated in this article, or claim that may be made by its manufacturer, is not guaranteed or endorsed by the publisher.

Copyright © 2022 Shi, Naudiyal, Wang, Gaire, Wu, Wei, He and Wang. This is an open-access article distributed under the terms of the Creative Commons Attribution License (CC BY). The use, distribution or reproduction in other forums is permitted, provided the original author(s) and the copyright owner(s) are credited and that the original publication in this journal is cited, in accordance with accepted academic practice. No use, distribution or reproduction is permitted which does not comply with these terms.

frontiers in Plant Science

ORIGINAL RESEARCH
published: 14 January 2022
doi: 10.3389/fpls.2021.792002

Comparative Microbial Nitrogen Functional Gene Abundances in the Topsoil vs. Subsoil of Three Grassland Habitats in Northern China

Yuqing Liu[1,2,3], Qiaodong Chi[3], Hui Cheng[3], Huanxin Ding[7], Teng Wen[3], Jun Zhao[3,5,6]*, Xiaojuan Feng[4], Jinbo Zhang[3,5,6], Zucong Cai[3,6,8] and Guohua Liu[1]*

[1] State Key Laboratory of Urban and Regional Ecology, Research Center for Eco-Environmental Sciences, Chinese Academy of Sciences (CAS), Beijing, China, [2] College of Resources and Environment, University of Chinese Academy of Sciences (CAS), Beijing, China, [3] School of Geography, Nanjing Normal University, Nanjing, China, [4] State Key Laboratory of Vegetation and Environmental Change, Institute of Botany, Chinese Academy of Sciences (CAS), Beijing, China, [5] Jiangsu Center for Collaborative Innovation in Geographical Information Resource Development and Application, Nanjing, China, [6] Zhongke Clean Soil (Guangzhou) Technology Service Co., Ltd., Guangzhou, China, [7] Suzhou Station of Farmland Quality Protection, Suzhou, China, [8] Key Laboratory of Virtual Geographical Environment, Ministry of Education, Nanjing Normal University, Nanjing, China

OPEN ACCESS

Edited by:
Shiliang Liu, Beijing Normal University, China

Reviewed by:
Roberta Pastorelli, Council for Agricultural and Economics Research (CREA), Italy
Dima Chen, China Three Gorges University, China
Jiapeng Wu, Guangzhou University, China

***Correspondence:**
Teng Wen
wenteng@njnu.edu.cn
Jun Zhao
junzhao37@njnu.edu.cn

Specialty section:
This article was submitted to Functional Plant Ecology, a section of the journal Frontiers in Plant Science

Received: *09 October 2021*
Accepted: *09 December 2021*
Published: *14 January 2022*

Citation:
Liu Y, Chi Q, Cheng H, Ding H, Wen T, Zhao J, Feng X, Zhang J, Cai Z and Liu G (2022) Comparative Microbial Nitrogen Functional Gene Abundances in the Topsoil vs. Subsoil of Three Grassland Habitats in Northern China. Front. Plant Sci. 12:792002. doi: 10.3389/fpls.2021.792002

The microbial groups of nitrogen fixers, ammonia oxidizers, and denitrifiers play vital roles in driving the nitrogen cycle in grassland ecosystems. However, the understanding of the abundance and distribution of these functional microorganisms as well as their driving factors were limited mainly to topsoil. In this study, the abundances of nitrogen functional genes (NFGs) involved in nitrogen fixation (*nifH*), ammonia oxidation (*amoA*), and denitrification (*nirK*, *nirS*, and *nosZ*) were investigated in both topsoil (0–10 cm, soil layer with concentrated root) and subsoil (30–40 cm, soil layer with spare root) of three grassland habitats in northern China. The abundance of NFGs decreased with soil depth except for the archaeal *amoA* gene and the distribution of *nifH*, archaeal *amoA*, *nirK*, and *nirS* gene was significantly impacted by grassland habitats. Moreover, the distribution of NFGs was more responsive to the vertical difference than horizontal spatial heterogeneity. Redundancy analysis revealed that the distribution pattern of overall NFGs was regulated by grassland habitats, and these regulations were more obvious in the subsoil than in the topsoil. Variance partitioning analysis further indicated that soil resource supply (e.g., organic matter) may control the vertical distribution of NFGs. Taken together, the findings in this study could fundamentally improve our understanding of the distribution of N cycling-associated microorganisms across a vertical scale, which would be useful for predicting the soil N availability and guiding the soil N management in grassland ecosystems.

Keywords: grassland ecosystem, nitrogen functional gene, soil depth, real-time PCR, abundance

INTRODUCTION

Nitrogen (N) cycling is considered a vital biogeochemical cycle on Earth as it controls the availability of nitrogenous nutrients and biological productivity in natural ecosystems (Vitousek and Howarth, 1991; Nelson et al., 2016). The underlying microbe-mediated functions are associated with the availability of nitrogenous nutrient supply and, thus, influence plant-based primary

production ecosystems (Wang H. et al., 2017; Song et al., 2020; Wang et al., 2021; Zhou et al., 2021). A better understanding of the distribution of N functional microbes remains constrained.

Soil N cycle serves as an important component of the global N cycle, and the transformation among various N forms is largely accomplished by the enzymes encoded by several N functional genes (NFGs) harbored in diverse soil microbes (Robertson and Groffman, 2007; Hu et al., 2015). For instance, the nitrogen fixation (*nifH*) gene encodes the nitrogenase and catalyzes the conversion of N_2 to NH_4^+, which, thereby, provides a primary source of N to natural ecosystems (Levy-Booth et al., 2014). Nitrification is a two-step process linking the reduced and oxidized forms of N, in which ammonia oxidation (*amoA*) is thought to be a rate-limiting step and mediated by the ammonia-oxidizing archaea (AOA) and ammonia-oxidizing bacteria (AOB) with the monooxygenase encoded by the gene *amoA* (Prosser and Nicol, 2008; Levy-Booth et al., 2014). Increasing evidence suggested that the NFGs abundances were correlated with the rate of the N cycling processes to some extent, and some of their ratios were considered as a useful indicator for the potential of N turnover capacity (Prosser and Nicol, 2012; Carey et al., 2016). Based on path analysis, AOA/AOB and nirK/S and nosZ gene abundances were the most important variables to predict nitrification and denitrification potential rates across terrestrial ecosystems (Xiong et al., 2012). Regional-scale experiments offered direct evidence of the relationship between N cycling process rate and N functional gene abundance (Chen et al., 2018). Moreover, the relative abundance of NFGs, such as AOA/AOB and (AOA + AOB)/(*nirK* + *nirS*) quantified as N turnover potential capacity, represented dominance in ammonia oxidization and NO_3-N leaching, respectively (Tang et al., 2016, 2018). Therefore, better understanding the abundance and distribution of NFGs will offer an insight to know the soil N availability for a given natural ecosystem and thus to guide for predicting plant primary productivity.

Over the past few decades, spatial patterns and drivers of soil microbial communities have attracted extensive interest at various spatial scales (Fierer et al., 2010; Serna-Chavez et al., 2013; Fierer, 2017). These studies demonstrated that microbial taxa inhabiting varied surface soil habitats exhibit biogeographic patterns across broad geographical space (Chu et al., 2010; Brockett et al., 2012). It is believed that environmental factors, such as altitude, longitude, and latitude, usually covary with the changes in the geographical distance (Fierer and Jackson, 2006; Griffiths et al., 2011; Jia et al., 2017). Such horizontal differences are often characterized by heterogeneity of soil type, climate, vegetation, etc., and, of course, pronouncedly shape the distribution of microorganisms (Zhang et al., 2006; Hu et al., 2014; Chen et al., 2018). Moreover, the geographical distribution of microbial populations was also driven by geographical isolation even with similar characteristics and common ancestry (O'Malley, 2008). A previous study found that there is habitat specificity for microbial diversity and is no considerable dispersal limitation in bacteria distribution at a large scale in China (Wang X. B. et al., 2017). Although these findings have drastically improved our understanding of the pattern of microbes, we are still not sure if there is a horizontal difference in N-cycling microbes over hundreds of kilometers. Such knowledge is needed to improve our understanding of the N transformation processes in the grassland ecosystem especially under the ground of global climate change.

It is well recognized that both the biotic and abiotic factors could impact the abundance and distribution of N-cycling microbial communities (Hayden et al., 2010; Stone et al., 2015; Chen et al., 2018). For instance, Wei et al. (2017) and Cheng et al. (2019) exhibited that plant traits such as plant type, species richness, and biomass were important predictors of abundance and activity of ammonia-oxidizing and denitrifying communities in the grassland ecosystem. In contrast, numerous studies indicated that abiotic factors such as precipitation, soil pH, and organic carbon were pivotal to the proliferation of N-cycling microorganisms (Chen et al., 2015; Barrett et al., 2016; Zhou et al., 2021). Moreover, abiotic factors, especially precipitation, could indirectly affect the soil N-cycling microbes by impacting the accumulation of grassland biomass (Prober et al., 2015; Wang X. B. et al., 2017). However, these reports are restricted to the N-cycling microbes residing in near-surface soil while there was still less knowledge about their counterpart microbes inhabiting in deeper soil depths. Especially, Wakelin et al. (2008) provided evidence where soil C is strongly linked to diazotrophic ecology, pointing out that the quality and quantity of soil C influence the N-fixing bacteria. In addition, Chen et al. (2018) exhibited that abiotic and plant factors greatly predict the abundance and activity of ammonia-oxidizing and denitrifying communities across the Qinghai-Tibetan plateau.

Soil depth is regarded as an important factor in determining the distribution of microbial communities because of the environmental gradients along with the soil vertical profiles (Bai et al., 2017). Particularly, the oxygen level, moisture, nutrient availability, etc., sharply decrease with soil depth, and the soil layer of >30 cm is commonly characterized as the oligotrophic environment (Whitman et al., 1998; Eilers et al., 2012). Especially, more than 80% of roots distribute in the top 30 cm of soil in the grassland ecosystem (Yang et al., 2010). In fact, root vertical distribution could impact the microbial populations between soil depths mainly by providing different quantity and type of organic carbons and nutrients within a soil profile via root exudates and/or root litter decomposition (Peng et al., 2017; Shi et al., 2018). Therefore, the microbial biomass and activity considerably declined with the increasing depths as a consequence, which might lead to a reduction in population size as well as changes in the composition and diversity of microbial communities (Babujia et al., 2010; Bai et al., 2015). For example, researchers observed that both AOA and AOB rapidly decreased between 0 and 30 cm depth and then tended to mildly reduce below 30 cm soil depth (Banning et al., 2015; Tang et al., 2018). It has been widely accepted that AOA is preferred to adaptation in poor nutrient conditions and low soil pH environments (Prosser and Nicol, 2012), making the AOA less responsive to soil depth (Wang et al., 2014). In addition, different taxa might respond dissimilarly to the changes in abiotic factors along with soil profile (Tang et al., 2018). Until present, we still lack a comprehensive understanding of the N-turnover functional gene in the grassland ecosystem, which

impedes our ability to predict the key services provided by the grassland ecosystem.

Grasslands are the dominant landscapes in China, which cover 41.7% of the national territory and are mainly distributed in the northern temperate zone, ranging from temperate grasslands to alpine grasslands (Kang et al., 2007). To control the precipitation variable, sampling sites were designed along the 400 mm isohyet in the grasslands of northern China to evaluate the distribution difference and N-transformation potential in the grasslands of Northern China (Wang et al., 2018). In this study, we use quantitative polymerase chain reaction of samples taken at two soil depths, namely, topsoil at 0–10 cm depth and subsoil at 30–40 cm depth from the representative steppe, and compare the difference between soil depths over hundreds of kilometers. In this study, we use the ratio of *nifH*/*nosZ* and (AOA + AOB)/(*nirK* + *nirS*) as the proxy of potential microbial N storage and NO_3^--N leaching. We hypothesized that the abundance of NFGs varied with geographical distance and soil depth. It is expected that vertical difference and horizontal geographical differences in environmental factors would shape the distinct N-cycling microbial community. We also hypothesized that the major driving factors shifted from topsoil to subsoil, and we expected that soil resources prevailed over soil edaphic parameters in driving the variation of N-cycling microbes residing in the subsoil.

MATERIALS AND METHODS

Site Description and Soil Sample Collection

Four study sites with three representative grassland habitat types were located in the transition zone along 400 mm isohyet from the meadow steppe, typical steppe to the alpine meadow (**Figure 1**). Two sites were located on the Inner Mongolian Plateau, with meadow steppe dominated by *Leymus chinensis* in Eerguna [called EEGN at 520 m average sea level (a.s.l.)] and the other was typical steppe dominated by *Stipa grandis* in Xilinhot (called XLHT at 1250 m a.s.l.). The other two sites, namely Menyuan (MY, 3200 m a.s.l.) and Naqu (NQ, 4611 m a.s.l.), were located on the Qinghai-Tibet Plateau with the alpine meadow dominated by *Kobresia humilis* and *Potentilla nivea*. The aboveground biomass in the EEGN, XLHT, MY, and NQ sites was 112, 103, 350, and 116 g m^{-2}, respectively; belowground biomass was 711, 2512, 3000, and 1509 g m^{-2}, respectively (**Table 1**). According to the root distribution characteristics of plants, we collected soil samples from a depth of 0–10 cm (topsoil) and 30–40 cm (subsoil) at each study site in the plant growing season in September 2016. At each study site, five 1 m × 1 m subplots were established, one at each corner and one in the center of a 10 m × 10 m plot. The soil samples collected from the same layer at each plot were mixed into single composite samples, which were passed through 2 mm sieves and removed root materials. In total, 24 sieved soils (4 study sites × 3 replicates × 2 soil depths) were processed and stored as appropriate for physicochemical, biological, and molecular analyses.

Soil Physicochemical Analyses

Soil pH was measured using a glass electrode meter (S200 K, Mettler-Toledo International Inc., Shanghai, China) with a soil/water ratio of 1:2.5. Soil organic matter (OM) content was determined by H_2SO_4-$K_2Cr_2O_7$ oxidation, while the total N (TN) content was analyzed by semimicro Kjeldahl digestion. Dissolved organic carbon (DOC) was measured in a 4:1 water/soil extract using an Analyzer Multi N/C (Analytic Jena, Jena, Germany). Soil NH_4^+-N and NO_3^--N were extracted using 2 M KCl with a soil/solution ratio of 1:5 and measured using a continuous-flow analyzer (Skalar, Breda, Netherlands). The moisture content was determined gravimetrically by oven drying at 105°C to constant mass.

DNA Extraction and Real-Time PCR Assay

Soil genomic DNA was extracted, quality-controlled, and quantified as described previously by Zhao et al. (2018). After extraction, the DNA samples were stored at −20°C for subsequent molecular analysis. Real-time PCR was performed on a CFX-96 thermocycler (Bio-Rad Laboratories Inc., CA, United States) to enumerate the abundances of microbial NFGs that involved in nitrogen fixation (*nifH*), ammonia oxidation (archaeal *amoA* and bacterial *amoA*), and denitrification (*nirK*, *nirS*, and *nosZ*) using the primer pairs listed in **Table 2**. The reaction mixture contained 10 μl of *Premix Ex* Taq^{TM} (Takara Bio Inc., Kyoto, Japan), 2 μl of DNA extract (20 ng μl^{-1}), 1 μl of each primer (10 μM), and 6 μl of sterile distilled water. The PCR procedure consisted of 2 min at 95°C, followed by 39 cycles of 10 s at 95°C, 20 s at 58°C, and 30 s at 72°C. Standard curves were plotted using 10-fold serial dilutions of the plasmid DNA inserted with the fragment of interest, following a previously established procedure (Zhao et al., 2016), and the amplification efficiencies ranged from 88.3 to 97.0% for different genes. The melting curve analysis was performed to ensure the amplification specificity, and the copy numbers were $\log_{10}$-transformed to normalize the values prior to statistical analysis.

Statistical Analyses

The PASW Statistics 18 (SPSS Inc., Chicago, United States) and R (version 3.3.1) (R Core Team, 2012) were used to perform statistical analysis, and P-value of <0.05 was considered statistically significant. Data were tested for normality (Shapiro–Wilk normality test) and homogeneity of variance and were logarithm transformed when necessary to meet the criteria for a normal distribution. Multiple analysis of variance (MANOVA) was used to determine the effects of geographical location and soil depth on soil properties and NFGs abundance. For a given soil depth, the significant difference among sampling sites was tested using one-way ANOVA followed by LSD *post hoc* test. For a given site, two-tailed unpaired *t*-tests were used to compare each measurement between soil depths. The abundance of overall NFGs and soil properties was visualized with redundancy analysis (RDA). The Monte

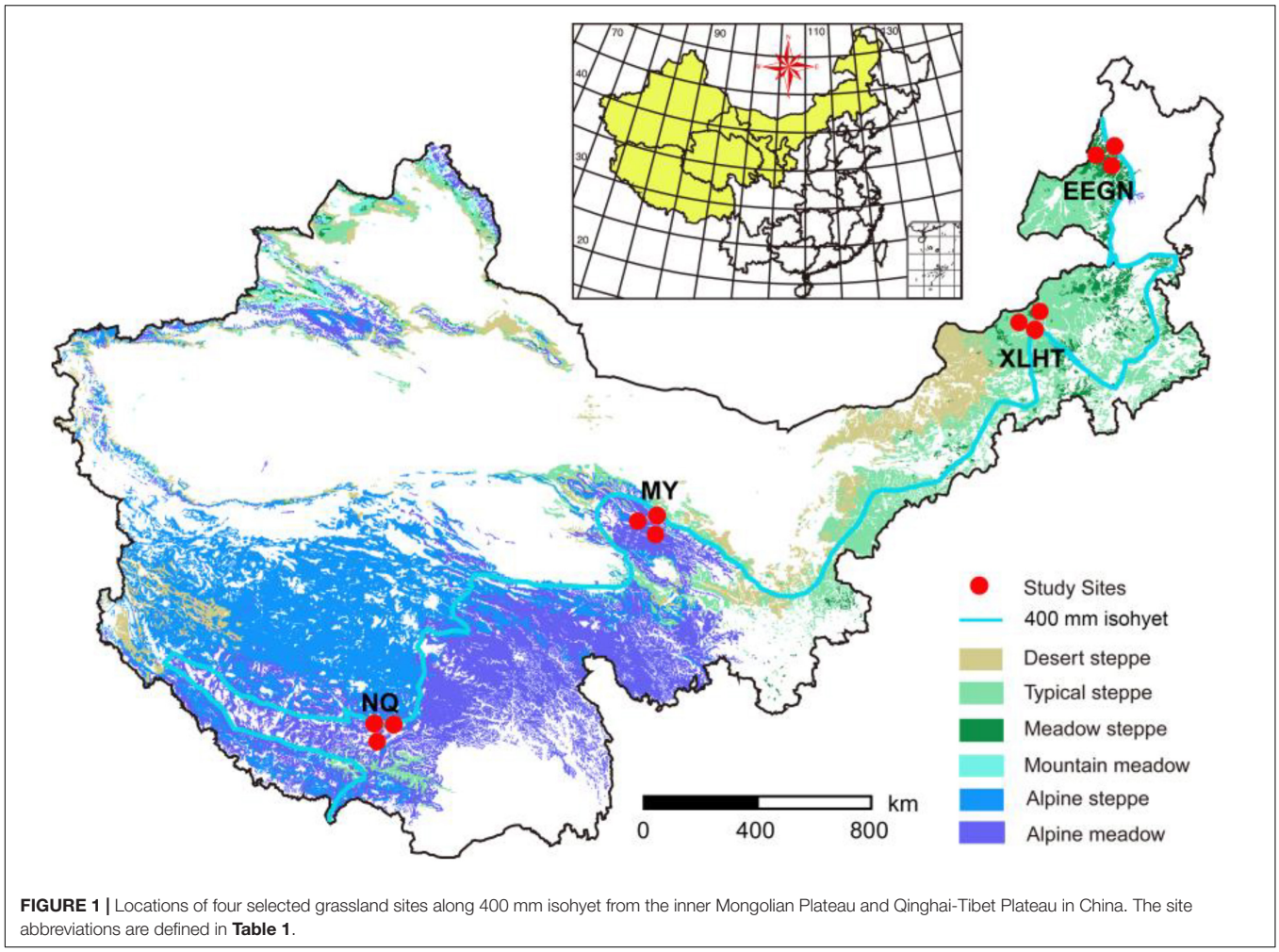

FIGURE 1 | Locations of four selected grassland sites along 400 mm isohyet from the inner Mongolian Plateau and Qinghai-Tibet Plateau in China. The site abbreviations are defined in **Table 1**.

TABLE 1 | Characterization information of the natural grassland sites selected in this study.

Site[§]	Latitude	Longitude	Altitude (m)	MAP[a] (mm)	MAT[b] (°C)	Habitat type	Dominant plant species	Biomass (g m^{-2})*		Soil type
								Aboveground	Belowground	
EEGN	50°12′N	119°30′E	520	370	−2.14	Meadow steppe	*Leymus chinensis*	112	711	Chernozem
XLHT	43°38′N	116°42′E	1250	342	1.68	Typical steppe	*Stipa grandis*	103	2512	Calcicorthic aridisol
MY	37°37′N	101°19′E	3200	458	−0.78	Alpine meadow	*Kobresia humilis*, *Potentilla nivea*	350	3000	Alpine meadow soil
NQ	31°39′N	92°01′E	4611	405	−1.41	Alpine meadow	*Kobresia humilis*, *Potentilla nivea*	116	1509	Mollic-cryic cambisol

[a] *MAP, mean annual precipitation.*
[b] *MAT, mean annual temperature; data from https://www.worldclim.org/.*
**Estimated from its corresponding aboveground biomass according to Yang et al. (2010).*
[§] *Sites: EEGN, Eerguna; XLHT, Xilinot; MY, Menyuan; NQ, Naqu.*

Carlo test (999 permutations) was further used to assess the effects of edaphic factors on the distribution of NFGs. Variance partitioning analysis was also performed to determine the relative contributions of soil edaphic parameters (soil pH and moisture) and soil sources (OM, DOC, TN, and NH_4^+-N content) on the variation in NFGs distribution in both soil depths.

RESULTS

Soil Physicochemical Properties

Overall, physicochemical properties of the topsoil or subsoil differed significantly ($P < 0.05$) among the selected grassland sites except for the soil NO_3^--N content in the subsoil. However, the different physicochemical properties varied among these

TABLE 2 | Summary of the genes investigated, the enzymes they encoded, and their functions in the nitrogen cycle.

Target gene	Primer set	Primer sequence (5′–3′)	Enzyme	Process	References
nifH	PolF	TGCGA**Y**CC**S**AA**R**GC**B**GACTC	Nitrogenase	Nitrogen fixation (N_2-NH_4^+)	Poly et al., 2001
	PolR	AT**S**GCCATCAT**Y**TC**R**CCGGA			
Archaeal *amoA*	Arch-amoAF	**S**TAATGGTCTGGCTTAGACG	α subunit of ammonia monooxygenase	Ammonia oxidation (NH_4^+-NO_2^-)	Francis et al., 2005
	Arch-amoAR	GCGGCCATCCATCTGTATGT			
Bacterial *amoA*	AmoA1F*	GGGG**H**TT**Y**TACTGGTGGT	α subunit of ammonia monooxygenase	Ammonia oxidation (NH_4^+-NO_2^-)	Stephen et al., 1998
	AmoA2R	CCCCTC**K**G**S**AAAGCCTTCTTC			
nirS	Cd3aF	GT**S**AACGT**S**AAGGA**R**AC**S**GG	Nitrite reductase	Denitrification (NO_2^--NO)	Throbäck et al., 2004
	R3cd	GA**S**TTCGG**R**TG**S**GTCTTGA			
nirK	nirK1F	GG**M**ATGGT**K**CC**S**TGGCA	Nitrite reductase	Denitrification (NO_2^--NO)	Braker et al., 1998
	nirK5R	GCCTCGATCAG**R**TT**R**TGG			
nosZ	nosZFb	AACGCCTA**Y**AC**S**AC**S**CTGTTC	Nitrous oxide reductase	Denitrification (N_2O-N_2)	Rosch and Bothe, 2005
	nosZRb	TCCATGTGCAG**N**GC**R**TGGCAGAA			

**Boldface letters denote degenerate positions. M = A/C; R = A/G; S = G/C; Y = C/T; K = G/T; B = G/C/T; H = A/C/T; N = A/G/C/T.*

four sampling sites at both topsoil and subsoil (**Table 3**). For instance, soil OM, TN, and NH_4^+-N contents were highest in the topsoil of the MY site, followed by the NQ, EEGN, and XLHT sites, while the highest NO_3^--N content was observed in the EEGN site, followed by the NQ, XLHT, and MY sites. In the subsoil, soil OM and TN content were highest in the MY site, followed by the EEGN, XLHT, and NQ sites, whereas the highest NH_4^+-N and NO_3^--N contents were observed in the EEGN site, with the lowest value being in the XLHT and MY sites, respectively (**Table 3**). Moreover, most tested soil physicochemical properties showed a decreasing trend from topsoil to the subsoil, whereas soil pH increased ($P < 0.05$) with the soil depth, except for the EEGN site (**Table 3**). The results of MANOVA showed that all soil edaphic properties were affected ($P < 0.05$) by geographical location, soil depth, and the geographical location × soil depth interaction term except for the soil DOC content (**Table 4**).

Abundance of Nitrogen Fixers and Ammonia Oxidizers

The abundance of nitrogen fixers decreased with the increase in soil depth at all the grassland sites except for the MY site, ranging from 1.29×10^7 to 3.01×10^8 copies·g^{-1} dry soil, and significant differences between topsoil and subsoil were observed in the EEGN and NQ sites (**Figure 2A**). Moreover, the population of nitrogen fixers differed significantly among the sampling sites in the topsoil, being higher at the EEGN and XLHT sites as compared with the MY site, while no significant difference was observed in the subsoil. The distribution of nitrogen fixers was affected ($P < 0.05$) by the sampling site and soil depth (**Figure 2A**).

Unlike the results of nitrogen fixers, the population size of AOA increased with the increasing soil depth in all sampling sites except for the EEGN site, ranging from 6.16×10^8 to 6.27×10^9 copies·g^{-1} dry soil, although there was no significant difference between soil depth for a given site (**Figure 2B**). Furthermore, significant differences were observed among sampling sites in both topsoil and subsoil. For instance, the abundance of AOA was higher in the EEGN and XLHT sites than that in the MY and NQ sites in the topsoil. In contrast, the abundance of AOB showed a declining trend from topsoil to subsoil at all the grassland sites, ranging from 2.52×10^5 to 6.29×10^6 copies·g^{-1} dry soil (**Figure 2C**). A significant difference between soil depth was observed only in the XLHT site. The abundance of AOB changed considerably ($P < 0.05$) among the sampling sites in the topsoil, whereas there was no significant difference in the subsoil. In addition, MANOVA results revealed that the distribution of AOA was affected by the sampling site while the distribution of AOB was impacted by soil depth (**Figures 2B,C**).

Abundance of Nitrite Reductase (*nirS* and *nirK*) and Nitrous Oxide Reductase (*nosZ*) Genes

The abundance of *nirK*- and *nirS*-type nitrite reductase gene shifted from 3.49×10^6 to 3.85×10^7 and from 1.01×10^6 to 2.45×10^7 copies·g^{-1} dry soil, respectively, in all soil samples. They consistently decreased from topsoil to subsoil in all the sampling sites except for *nirS*-type nitrite reductase gene at the MY site. These declines were significant ($P < 0.05$) in the EEGN and MY sites for *nirK*-type nitrite reductase gene and the EEGN and NQ sites for *nirS*-type nitrite reductase gene, respectively (**Figures 2D,E**). Significant differences in abundance were observed in the subsoil of *nirK*-type nitrite reductase gene and the topsoil of *nirS*-type nitrite reductase gene among the sampling sites. Both sampling sites and soil depth significantly affected the distributions of *nirK*- and *nirS*-type nitrite reductase gene (**Figures 2D,E**). The abundance of nitrous oxide reductase (*nosZ*) gene ranged from 1.81×10^7 to 2.03×10^8 copies g^{-1} dry soil in all soil samples and accounted for the largest proportion (43.9–88.4%) of denitrifies. It declined considerably ($P < 0.05$) with the increasing soil depth in all the grassland sites, whereas there were no significant differences among the sites for both soil layers (**Figure 2F**). Thus, only soil depth was the significant ($P < 0.001$) factor influencing the distribution of nitrous oxide reductase (*nosZ*) gene.

TABLE 3 | Physicochemical characteristics of soils from different natural grassland sites and soil depths.

Physicochemical measurements	Sampling site[§] and soil depth							
	Topsoil				Subsoil			
	EEGN	XLHT	MY	NQ	EEGN	XLHT	MY	NQ
pH	6.70 ± 0.07 b(a)	7.41 ± 0.18 a(b)	7.63 ± 0.15 a(b)	6.66 ± 0.09 b(b)	6.78 ± 0.17 b(a)	8.23 ± 0.02 a(a)	8.11 ± 0.05 a(a)	7.22 ± 0.02 b(a)
Moisture (%)	21.0 ± 0.7 b(a)	13.0 ± 0.5 d(a)	29.8 ± 2.8 a(a)	17.6 ± 0.5 c(a)	13.6 ± 2.6 b(b)	6.2 ± 1.0 c(b)	24.2 ± 0.4 a(a)	6.9 ± 0.3 c(b)
OM (g kg^{-1})	70.1 ± 3.7 c(a)	49.1 ± 10.5 d(a)	151.7 ± 15.2 a(a)	114.9 ± 3.4 b(a)	40.7 ± 0.8 b(b)	28.2 ± 2.8 c(b)	47.3 ± 5.8 a(b)	13.1 ± 0.0 d(b)
DOC (mg kg^{-1})	477.3 ± 26.7 b(a)	602.9 ± 196.8 ab(a)	968.7 ± 291.5 a(a)	590.7 ± 167.2 b(a)	121.6 ± 8.5 d(b)	344.6 ± 38.4 b(a)	455.8 ± 31.9 a(b)	193.5 ± 14.7 c(b)
Total N (g kg^{-1})	3.00 ± 0.11 c(a)	2.69 ± 0.47 c(a)	7.07 ± 0.86 a(a)	4.81 ± 0.37 b(a)	1.62 ± 0.12 b(b)	1.52 ± 0.11 b(b)	2.65 ± 0.34 a(b)	0.77 ± 0.00 c(b)
C/N	13.6 ± 0.4 a(a)	10.5 ± 0.4 b(a)	12.5 ± 1.6 a(a)	13.9 ± 0.9 a(a)	14.6 ± 0.7 a(a)	10.8 ± 0.3 b(a)	10.3 ± 0.1 bc(a)	9.9 ± 0.0 c(b)
NH_4^+-N (mg kg^{-1})	2.05 ± 0.14 c(a)	1.84 ± 0.26 c(a)	3.17 ± 0.12 a(a)	2.61 ± 0.42 b(a)	1.98 ± 0.06 a(a)	1.67 ± 0.14 b(a)	1.87 ± 0.12 ab(b)	1.77 ± 0.22 ab(b)
NO_3^--N (mg kg^{-1})	45.0 ± 3.2 a(a)	20.2 ± 6.1 c(a)	5.6 ± 0.4 d(a)	36.6 ± 2.3 b(a)	14.4 ± 9.2 a(b)	9.0 ± 1.9 a(b)	5.5 ± 0.1 a(a)	6.6 ± 2.5 a(b)

OM, organic matter; DOC, dissolved organic carbon.
Values are means ± SD (n = 3).
Different letters outside brackets represent significant differences within the same soil layer of the four sites at $P < 0.05$ according to LSD post hoc test, and different letters within brackets represent significant differences between two layers in the same site at $P < 0.05$ according to Student's t-test.
*[§] The site abbreviations are defined in **Table 1**.*

TABLE 4 | Overall effects of the sampling site and soil depth on the soil physicochemical characteristics analyzed by two-way ANOVA.

	Sites (*df* = 3)		Soil depth (*df* = 1)		Sites × depth (*df* = 3)	
	MS	*F*	MS	*F*	MS	*F*
pH (H_2O)	2.1	165.9***	1.4	113.2***	0.1	11.7***
Moisture	0.03	168.0***	0.04	169.3***	0.001	3.5*
OM	39.5	77.5***	246.3	483.3***	30.6	60.0***
DOC	187,677.5	9.7***	871,110.8	44.9***	16,673.0	0.9
Total N	9.6	61.6***	45.3	291.9***	4.4	28.3***
C/N	12.9	28.6***	9.0	19.9***	8.0	17.8***
NH_4^+-N	0.6	13.8***	2.1	46.5***	0.5	11.2***
NO_3^--N	634.2	34.3***	1946.9	105.3***	335.0	18.1***

df, degrees of freedom; MS, mean square; F, variance ratio.
**Means $P < 0.05$; ***means $P < 0.001$.*

Potential Nitrogen-Cycling Capacity

The topsoil N-storage potential at the EEGN and XLHT sites was significantly ($P < 0.05$) higher than that at the MY and NQ sites. The N-storage potential increased with the increase in soil depth at all the grassland sites, and the significant differences between topsoil and subsoil were observed at the MY and NQ sites (**Figure 3A**). The NO_3^--N leaching potential in the EEGN and XLHT topsoil was almost two times higher than that at the MY and NQ sites, and the NO_3^--N leaching potential significantly ($P < 0.05$) decreased with soil depth at all the sites except for MY (**Figure 3B**).

Relationships Between Overall Nitrogen Functional Genes and Soil Edaphic Factors

The Monte Carlo permutation test showed a significant ($F = 2.71$, $P = 0.004$) and positive correlation between the ordination of overall NFGs and soil edaphic properties. The RDA biplot revealed that the ordination of the overall NFGs was separated from the soil layers in the first axis, and the pattern of ordination in the topsoil was considerably distinct from that in the subsoil (**Figure 4** and **Supplementary Figure 1**). In topsoil, the ordinations of overall NFGs at the MY and NQ sites were similar, with clear separation from that at the EEGN sites and a small overlap in the XLHT site (**Figure 4A**). The differences in the ordination of overall NFGs were enlarged in the subsoil. Especially, the ordinations of NFGs at the MY and NQ sites were grouped together, and they were distinctly separated from that at the EEGN and XLHT sites, with the EEGN and XLHT sites being separated from each other (**Figure 4B**). The effect of individual soil factors on the ordination of NFGs is shown by the direction and the length of the vectors. Soil moisture, OM, DOC, TN, and NH_4^+-N contents were closely ($P < 0.05$) correlated with the ordination of the overall NFGs in topsoil, whereas no significant correlations were observed between the NFGs ordination and individual soil property in the subsoil (**Figure 4** and **Supplementary Figure 1**). Variance partitioning analysis

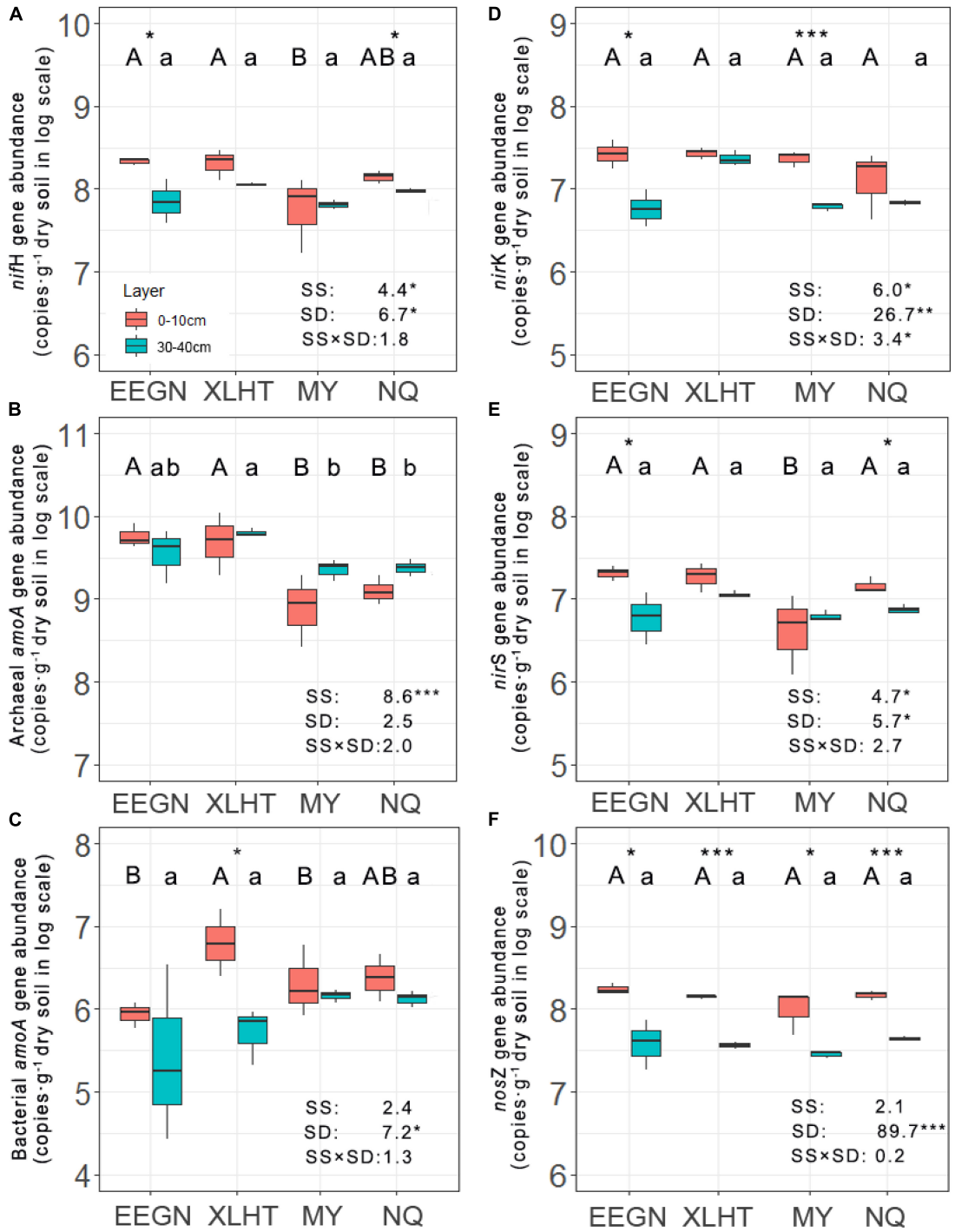

FIGURE 2 | Abundances of *nifH* **(A)**, archaeal *amoA* **(B)**, bacterial *amoA* **(C)**, *nirK* **(D)**, *nirS* **(E)**, and *nosZ* **(F)** genes at soil depths of 0–10 and 30–40 cm at four grassland sites. Different uppercase and lowercase letters above the boxes indicate significant differences at $P < 0.05$ between sites according to LSD *post hoc* test in the topsoil and subsoil, respectively. An asterisk above the boxes indicates a significantly different level at $P < 0.05$ according to the student *t*-test for a given site. An asterisk next to the number indicates a significantly different level at $P < 0.05$ according to multiple analyses of variance. SS, sampling site; SD, soil depth; SS × SD, sampling site × soil depth. *$P < 0.05$; **$P < 0.01$; ***$P < 0.001$. The site abbreviations are defined in **Table 1**.

showed the relative contributions of soil physical parameters and soil resource supply on NFGs distribution (**Figure 4**). The soil edaphic parameters and soil resource variables explained 23.9 and 34.1% of the observed variation in NFGs distribution in the topsoil, while these variables explained 9.7 and 26.2% of the observed variation, respectively (**Figure 5**).

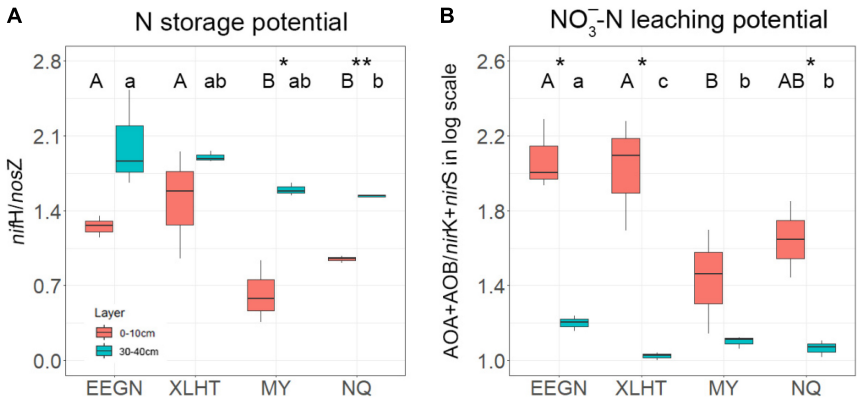

FIGURE 3 | Microbial N storage potential **(A)** and nitrate leaching potential **(B)** at soil depths of 0–10 and 30–40 cm at four grassland sites. Values (means ± SD, $n = 3$) within the same soil depth followed by different letters are significantly different at $P < 0.05$ according to LSD *post hoc* test. An asterisk above the bars indicates a significantly different level at $P < 0.05$ according to the student *t*-test for a given sampling site. $^{*}P < 0.05$; $^{**}P < 0.01$. The site abbreviations are defined in **Table 1**.

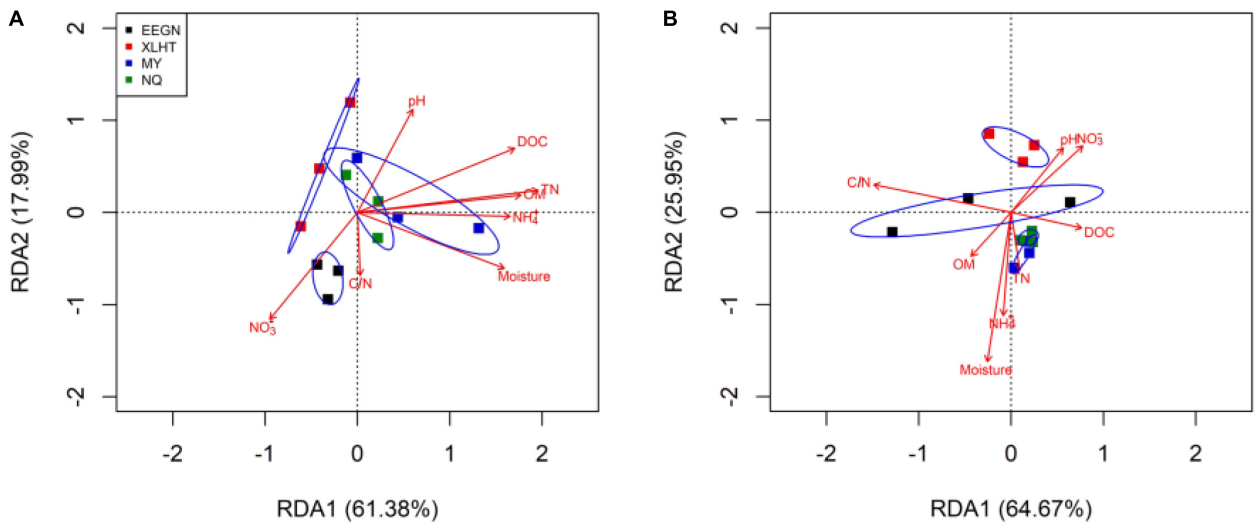

FIGURE 4 | Redundancy analysis of overall nitrogen functional genes and soil characteristics for individual samples at a soil depth of 0–10 cm **(A)** and 30–40 cm **(B)**, respectively. The site abbreviations are defined in **Table 1**.

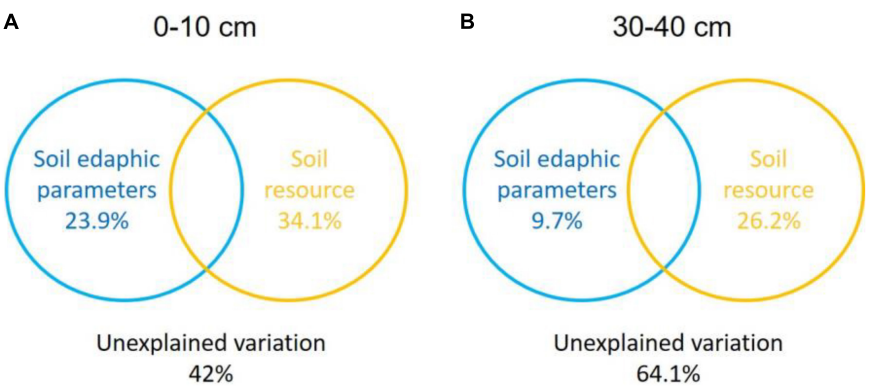

FIGURE 5 | Variance partitioning analysis (VPA) of the effects of soil physical parameter and soil resource supply on the variation in the NFGs distribution at a soil depth of 0–10 cm **(A)** and 30–40 cm **(B)**. Circles on the edges of the triangle show the percentage of variation explained by each variable.

DISCUSSION

Changes in the Distribution of Nitrogen-Cycling Microbes Across Three Grassland Habitats

We assumed that the effect of the geographical distance on N-cycling microorganisms was embodied in the effects of temperature and/or precipitation (Griffiths et al., 2011; Brockett et al., 2012; Yang et al., 2014). As a result, our experiment was designed along with 400 mm isohyet and thus eliminated differences in the environmental factors relating to geographical location (Jia et al., 2017). In this study, geographical location considerably impacted the distribution of N-fixer, AOA, *nirK*-type, and *nirS*-type denitrifiers, suggesting that a geographical distance over hundreds of kilometers might influence the distribution pattern of N-cycling microorganisms (De Vries et al., 2012; Chu et al., 2016). This result might be attributed to heterogeneous climate, vegetation, and soil type caused by geographical distances between every pair of sites ranging from 762 to 3069 km (**Supplementary Table 1**). As per the principle of microbial biogeography, everything is everywhere, but the environment selects (de Wit and Bouvier, 2006), distribution of free-living microbial taxa exhibited dissimilarity with increasing geographical distance (Chu et al., 2016; Azziz et al., 2017; Escalas et al., 2021). The AOA gene abundance was significantly influenced by the geomorphic zones at the landscape scale (Hayden et al., 2010; Song et al., 2020; Zhou et al., 2021), which was consistent with this study. Previous studies also found that soil type exerted an effect on the abundance of the *nirK*-type and *nirS*-type denitrifies from two geographical zones (Azziz et al., 2017). Notably, the abundance of AOB and *nosZ* genes was less responsive to geographical location (**Figure 2**), suggesting that dispersal limitation might slightly influence the distribution of AOB and *nosZ*-type denitrifier in the study area (Chu et al., 2016; Wang X. B. et al., 2017). The ratio of *nifH*/*nosZ* and (AOA + AOB)/(*nirK* + *nirS*) in the EEGN and XLHT topsoil is significantly higher than that in the MY and NQ topsoil, suggesting that the temperate meadow might have a higher potential N fixation and NO_3^--N leaching than alpine meadow (Tang et al., 2018). This result might be explained by the fact that microbes related energy-consume N process habitat preference and, thus, microbes in an alpine meadow with lower temperature may limit N fixation and NO_3^--N leaching capacity than that in temperature meadow (Chen et al., 2018; Frindte et al., 2019).

Shifts in the Abundance of Nitrogen Functional Genes Between Soil Depths

In general, subsoil differed in a range of edaphic factors from topsoils (Fierer et al., 2003; Rumpel and Kögel-Knabner, 2011; Schnecker et al., 2015), such as soil pH, moisture, oxygen level, and nutrient availability and consequently led to a shift in the abundance of soil microorganisms (Eilers et al., 2012; Wang et al., 2014; Ying et al., 2017). Alternatively, the distribution of AOA was not affected by the soil depth, thus indicating that AOA preferred to adaptation in lower soil depth with poor nutrient condition (Prosser and Nicol, 2012; Sun et al., 2019; Wang et al., 2019). It is also likely that the root system of vegetation cannot reach a certain depth of soil, supporting a depth-related root disturbance on the soil microbial community (Haichar et al., 2008; Shi et al., 2018). The relatively low N-cycling gene in the alpine meadow might be attributed to the fact that alpine grasslands have a relatively much shallower root distribution than temperate grassland (Yang et al., 2010). These observations together indicate that the N processes and soil functionality decline along with soil profiles, which is consistent with the results of previous studies (Bai et al., 2017; Jones et al., 2018; Tang et al., 2018), demonstrating that the soil functionality was greatly affected by soil depths (Yao et al., 2018; Xu et al., 2020). Researchers have found that *nirK* and *nirS*-type denitrifiers preferred to reside in surface soil with high organic C (Bru et al., 2011; Petersen et al., 2012; Prosser and Nicol, 2012). Soil C source and C/N ratio decreased from topsoil with dense root to subsoil with spare root, resulting in the reduction of *nirK* and *nirS*-type denitrifiers, and thus decrease in NO_3^--N leaching potential between soil depths (Fierer et al., 2003; Tang et al., 2018). However, an increase in N-storage potential with increasing soil depths was observed in the MY and NQ sites, which might be attributed to permafrost-affected deeper alpine meadow soil (Chen et al., 2018).

Soil Resource Supply Drives the Distribution of Nitrogen Functional Genes

As shown by RDA, the abundances in NFGs at the NQ and MY sites were grouped together, and they were distinctly separated from the EEGN and MY sites, respectively, in the subsoil, suggesting their distinct N-cycling microbial pattern in the subsoil from kilometers apart. These results are supported by previous findings that the abundance and distribution of dominant taxonomic groups varied across habitats in the Chinese northern dryland (Wang X. B. et al., 2017). These findings together indicate that the distribution of N-cycling microbes is structured by habitat-associated vegetation type in the subsoil. In this study, the overall distribution of NFGs depicted a habitat-specific pattern, reflecting their ecological characteristics such as physiological capabilities or habitat preferences (Fierer et al., 2007; Pointing et al., 2009). We found that variation in the distribution of NFGs in the subsoil was primarily related to soil resource supply, but not to the soil edaphic parameters. The clear and broad consensus is that soil microbes are limited by soil resources including C and N availability (Fierer et al., 2003; Hu et al., 2014; Chen et al., 2016). Recently, Chen et al. (2018) examined the geographical pattern of the functional N gene using intensive soil sampling across the Tibetan alpine grassland and exhibited that soil resource was the main predictor of N-cycling microbial community, while plant traits affected them *via* altering the SOC availability (Li et al., 2017). Likewise, we observed that soil resource was an important predictor in the topsoil. Moreover, the soil resource explained more variation in N-cycling microbial community in deeper soil depth, indicating that the distribution of N-cycling microbes residing in the deeper soil depths was associated with soil resource supply (Yang et al., 2013; Liu et al., 2020). This result was supported by the finding that the vertical distribution

of N-cycling microorganisms was largely attributed to the decline in soil C availability. Barrett et al. (2016) reported that the C amendment resulted in the increase of denitrifies abundance and this impact changed with soil depth due to the decline in C availability. In addition, the interaction of plant and edaphic factors in temperate grasslands affects the microbial community distribution and the effect depends on the soil depth (Yao et al., 2018). Hou et al. (2018) also presented direct evidence that root exudates can act as inducible C sources for heterotrophic denitrifying bacteria. Thus, the plant–soil interaction (i.e., rhizosphere effect and litter decomposition) involved in the distribution of NFGs should be further studied to reveal how the plant traits regulate the abundance of NFGs.

CONCLUSION

In general, the abundance of NFGs gradually decreased with soil depth in the three grassland habitats. We also found that the distribution of free N-cycling microbial taxa exhibited dissimilarity at the landscape scale. In addition, NFGs distribution was more responsive to the vertical difference than horizontal spatial heterogeneity except for the archaeal *amoA* gene. The variation in N-transformation potential among the three grassland habitats may be connected with the energy-consuming N-cycling microorganism habitat preference. The distribution of overall NFGs exerted a habitat-specific pattern and the driving factors of NFGs shifted from the topsoil to the subsoil. Moreover, soil resource supply controlled the vertical distribution of NFGs rather than soil edaphic parameters.

Uncertainties and Perspectives

The first uncertainty was the sampling rule along 400 mm isohyet, which neglects various environmental factors across the large geographical distance. It is also difficult to completely disentangle the vertical N-cycling ecological processes by only determining the NFGs abundance in limited sampling sites. Intensive sampling would be helpful to improve the understanding of active functional groups within the surface and subsoils and determine how these functional groups change with the soil profile. Second, we assume the copy number of a gene provides information about the potential N store and N release capacity of soil microorganisms in grassland, which may overestimate the nitrogen turnover potential. Besides, our research takes no account of other N-cycling processes, such as the mineralization of fungi. We do not provide a complete insight into measuring the capacity of microbial N turnover. Molecular analyses can be integrated with gene expression and rhizosphere isotopic tracing techniques to measure actual N storage and turnover potentials in future research.

DATA AVAILABILITY STATEMENT

The raw data supporting the conclusions of this article will be made available by the authors, without undue reservation.

AUTHOR CONTRIBUTIONS

JBZ, XF, JZ, and TW devised the study. YL carried out the experiments, analyzed the data, and wrote the first draft of the manuscript. QC, HC, and HD assisted with the experiments. All authors contributed to the preparation of the manuscript.

FUNDING

This work was financially supported by the National Natural Science Foundation of China (41977084 and 41977032), the Key-Area Research and Development Program of Guangdong Province (2020B0202010006), and the Opening Project of Zhejiang Key Laboratory of Urban Environmental Processes and Pollution Control (NUEORS202002).

SUPPLEMENTARY MATERIAL

The Supplementary Material for this article can be found online at: https://www.frontiersin.org/articles/10.3389/fpls.2021.792002/full#supplementary-material

REFERENCES

Azziz, G., Monza, J., Etchebehere, C., and Irisarri, P. (2017). nirS- and nirK-type denitrifier communities are differentially affected by soil type, rice cultivar and water management. *Eur. J. Soil Biol.* 78, 20–28. doi: 10.1016/j.ejsobi.2016.11.003

Babujia, L. C., Hungria, M., Franchini, J. C., and Brookes, P. C. (2010). Microbial biomass and activity at various soil depths in a *Brazilian oxisol* after two decades of no-tillage and conventional tillage. *Soil Biol. Biochem.* 42, 2174–2181.

Bai, R., Wang, J.-T., Deng, Y., He, J.-Z., Feng, K., and Zhang, L.-M. (2017). Microbial community and functional structure significantly varied among distinct types of paddy soils but responded differently along gradients of soil depth layers. *Front. Microbiol.* 8:945. doi: 10.3389/fmicb.2017.00945

Bai, R., Xi, D., He, J.-Z., Hu, H.-W., Fang, Y.-T., and Zhang, L.-M. (2015). Activity, abundance and community structure of anammox bacteria along depth profiles in three different paddy soils. *Soil Biol. Biochem.* 91, 212–221. doi: 10.1016/j.soilbio.2015.08.040

Banning, N. C., Maccarone, L. D., Fisk, L. M., and Murphy, D. V. (2015). Ammonia-oxidising bacteria not archaea dominate nitrification activity in semi-arid agricultural soil. *Sci. Rep.* 5:11146. doi: 10.1038/srep11146

Barrett, M., Khalil, M. I., Jahangir, M. M. R., Lee, C., Cardenas, L. M., Collins, G., et al. (2016). Carbon amendment and soil depth affect the distribution and abundance of denitrifiers in agricultural soils. *Environ. Sci. Pollut. Res.* 23, 7899–7910. doi: 10.1007/s11356-015-6030-1

Braker, G., Fesefeldt, A., and Witzel, K. P. (1998). Development of PCR primer systems for amplification of nitrite reductase genes (nirK and nirS) to detect denitrifying bacteria in environmental samples. *Appl. Environ. Microbiol.* 64, 3769–3775.

Brockett, B. F. T., Prescott, C. E., and Grayston, S. J. (2012). Soil moisture is the major factor influencing microbial community structure and enzyme activities across seven biogeoclimatic zones in western Canada. *Soil Biol. Biochem.* 44, 9–20. doi: 10.1016/j.soilbio.2011.09.003

Bru, D., Ramette, A., Saby, N. P., Dequiedt, S., Ranjard, L., Jolivet, C., et al. (2011). Determinants of the distribution of nitrogen-cycling microbial communities at the landscape scale. *ISME J.* 5, 532–542. doi: 10.1038/ismej.2010.130

Carey, C. J., Dove, N. C., Beman, J. M., Hart, S. C., and Aronson, E. L. (2016). Meta-analysis reveals ammonia-oxidizing bacteria respond more strongly to nitrogen addition than ammonia-oxidizing archaea. *Soil Biol. Biochem.* 99, 158–166. doi: 10.1016/j.soilbio.2016.05.014

Chen, D., Cheng, J., Chu, P., Hu, S., Xie, Y., Tuvshintogtokh, I., et al. (2015). Regional-scale patterns of soil microbes and nematodes across grasslands on the Mongolian plateau: relationships with climate, soil, and plants. *Ecography* 38, 622–631. doi: 10.1111/ecog.01226

Chen, Y., Kou, D., Li, F., Ding, J., Yang, G., Fang, K., et al. (2018). Linkage of plant and abiotic properties to the abundance and activity of N-cycling microbial communities in Tibetan permafrost-affected regions. *Plant Soil* 434, 453–466. doi: 10.1007/s11104-018-3845-9

Chen, Y. L., Ding, J. Z., Peng, Y. F., Li, F., Yang, G. B., Liu, L., et al. (2016). Patterns and drivers of soil microbial communities in Tibetan alpine and global terrestrial ecosystems. *J. Biogeogr.* 43, 2027–2039.

Cheng, Y., Wang, J., Chang, S. X., Cai, Z., Müller, C., and Zhang, J. (2019). Nitrogen deposition affects both net and gross soil nitrogen transformations in forest ecosystems: a review. *Environ. Pollut.* 244, 608–616. doi: 10.1016/j.envpol.2018.10.054

Chu, H., Fierer, N., Lauber, C. L., Caporaso, J. G., Knight, R., and Grogan, P. (2010). Soil bacterial diversity in the Arctic is not fundamentally different from that found in other biomes. *Environ. Microbiol.* 12, 2998–3006. doi: 10.1111/j.1462-2920.2010.02277.x

Chu, H., Sun, H., Tripathi, B. M., Adams, J. M., Huang, R., Zhang, Y., et al. (2016). Bacterial community dissimilarity between the surface and subsurface soils equals horizontal differences over several kilometers in the western Tibetan Plateau. *Environ. Microbiol.* 18, 1523–1533. doi: 10.1111/1462-2920.13236

De Vries, F. T., Manning, P., Tallowin, J. R. B., Mortimer, S. R., Pilgrim, E. S., Harrison, K. A., et al. (2012). Abiotic drivers and plant traits explain landscape-scale patterns in soil microbial communities. *Ecol. Lett.* 15, 1230–1239.

de Wit, R., and Bouvier, T. (2006). 'Everything is everywhere, but, the environment selects'; what did Baas Becking and Beijerinck really say? *Environ. Microbiol.* 8, 755–758. doi: 10.1111/j.1462-2920.2006.01017.x

Eilers, K. G., Debenport, S., Anderson, S., and Fierer, N. (2012). Digging deeper to find unique microbial communities: the strong effect of depth on the structure of bacterial and archaeal communities in soil. *Soil Biol. Biochem.* 50, 58–65. doi: 10.1016/j.soilbio.2012.03.011

Escalas, A., Paula, F. S., Guilhaumon, F., Yuan, M., Yang, Y., Wu, L., et al. (2021). Macroecological distributions of gene variants highlight the functional organization of soil microbial systems. *ISME J.* doi: 10.1038/s41396-021-01120-8

Fierer, N. (2017). Embracing the unknown: disentangling the complexities of the soil microbiome. *Nat. Rev. Microbiol.* 15, 579–590. doi: 10.1038/nrmicro.2017.87

Fierer, N., Bradford, M. A., and Jackson, R. B. (2007). Toward an ecological classification of soil bacteria. *Ecology* 88, 1354–1364. doi: 10.1890/05-1839

Fierer, N., and Jackson, R. B. (2006). The diversity and biogeography of soil bacterial communities. *Proc. Natl. Acad. Sci. U.S.A.* 103:626. doi: 10.1073/pnas.0507535103

Fierer, N., Schimel, J. P., and Holden, P. A. (2003). Variations in microbial community composition through two soil depth profiles. *Soil Biol. Biochem.* 35, 167–176.

Fierer, N., Strickland, M. S., Liptzin, D., Bradford, M. A., and Cleveland, C. C. (2010). Global patterns in belowground communities. *Ecol. Lett.* 12, 1238–1249. doi: 10.1111/j.1461-0248.2009.01360.x

Francis, C. A., Roberts, K. J., Beman, J. M., Santoro, A. E., and Oakley, B. B. (2005). Ubiquity and diversity of ammonia-oxidizing archaea in water columns and sediments of the ocean. *Proc. Natl. Acad. Sci. U.S.A.* 102:14683. doi: 10.1073/pnas.0506625102

Frindte, K., Pape, R., Werner, K., Loffler, J., and Knief, C. (2019). Temperature and soil moisture control microbial community composition in an arctic-alpine ecosystem along elevational and micro-topographic gradients. *ISME J.* 13, 2031–2043. doi: 10.1038/s41396-019-0409-9

Griffiths, R. I., Thomson, B. C., James, P., Bell, T., Bailey, M. J., and Whiteley, A. S. (2011). The bacterial biogeography of British soils. *Environ. Microbiol.* 13, 1642–1654.

Haichar, F. Z., Marol, C., Berge, O., Rangel-Castro, J. I., Prosser, J. I., Balesdent, J., et al. (2008). Plant host habitat and root exudates shape soil bacterial community structure. *ISME J.* 2, 1221–1230. doi: 10.1038/ismej.2008.80

Hayden, H. L., Drake, J., Imhof, M., Oxley, A. P. A., Norng, S., and Mele, P. M. (2010). The abundance of nitrogen cycle genes amoA and nifH depends on land-uses and soil types in South-Eastern Australia. *Soil Biol. Biochem.* 42, 1774–1783. doi: 10.1016/j.soilbio.2010.06.015

Hou, S., Ai, C., Zhou, W., Liang, G., and He, P. (2018). Structure and assembly cues for rhizospheric nirK- and nirS-type denitrifier communities in long-term fertilized soils. *Soil Biol. Biochem.* 119, 32–40. doi: 10.1016/j.soilbio.2018.01.007

Hu, H. W., Chen, D., and He, J. Z. (2015). Microbial regulation of terrestrial nitrous oxide formation: understanding the biological pathways for prediction of emission rates. *FEMS Microbiol. Rev.* 39, 729–749. doi: 10.1093/femsre/fuv021

Hu, Y., Xiang, D., Veresoglou, S. D., Chen, F., Chen, Y., Hao, Z., et al. (2014). Soil organic carbon and soil structure are driving microbial abundance and community composition across the arid and semi-arid grasslands in northern China. *Soil Biol. Biochem.* 77, 51–57. doi: 10.1016/j.soilbio.2014.06.014

Jia, J., Feng, X., He, J.-S., He, H., Lin, L., and Liu, Z. (2017). Comparing microbial carbon sequestration and priming in the subsoil versus topsoil of a Qinghai-Tibetan alpine grassland. *Soil Biol. Biochem.* 104, 141–151. doi: 10.1016/j.soilbio.2016.10.018

Jones, D. L., Magthab, E. A., Gleeson, D. B., Hill, P. W., Sánchez-Rodríguez, A. R., Roberts, P., et al. (2018). Microbial competition for nitrogen and carbon is as intense in the subsoil as in the topsoil. *Soil Biol. Biochem.* 117, 72–82. doi: 10.1016/j.soilbio.2017.10.024

Kang, L., Han, X., Zhang, Z., and Sun, O. J. (2007). Grassland ecosystems in China: review of current knowledge and research advancement. *Philos. Trans. R. Soc. B Biol. Sci.* 362, 997–1008. doi: 10.1098/rstb.2007.2029

Levy-Booth, D. J., Prescott, C. E., and Grayston, S. J. (2014). Microbial functional genes involved in nitrogen fixation, nitrification and denitrification in forest ecosystems. *Soil Biol. Biochem.* 75, 11–25. doi: 10.1016/j.soilbio.2014.03.021

Li, H., Yang, S., Xu, Z., Yan, Q., Li, X., van Nostrand, J. D., et al. (2017). Responses of soil microbial functional genes to global changes are indirectly influenced by aboveground plant biomass variation. *Soil Biol. Biochem.* 104, 18–29. doi: 10.1016/j.soilbio.2016.10.009

Liu, Y., Ma, W., Kou, D., Niu, X., Wang, T., Chen, Y., et al. (2020). A comparison of patterns of microbial C:N:P stoichiometry between topsoil and subsoil along an aridity gradient. *Biogeosciences* 17, 2009–2019. doi: 10.5194/bg-17-2009-2020

Nelson, M. B., Martiny, A. C., and Martiny, J. B. H. (2016). Global biogeography of microbial nitrogen-cycling traits in soil. *Proc. Natl. Acad. Sci. U.S.A.* 113, 8033–8040. doi: 10.1073/pnas.1601070113

O'Malley, M. A. (2008). 'Everything is everywhere: but the environment selects': ubiquitous distribution and ecological determinism in microbial biogeography. *Stud. Hist. Philos. Biol. Biomed. Sci.* 39, 314–325. doi: 10.1016/j.shpsc.2008.06.005

Peng, Y., Guo, D., and Yang, Y. (2017). Global patterns of root dynamics under nitrogen enrichment. *Glob. Ecol. Biogeogr.* 26, 102–114. doi: 10.1111/geb.12508

Petersen, D. G., Blazewicz, S. J., Firestone, M., Herman, D. J., Turetsky, M., and Waldrop, M. (2012). Abundance of microbial genes associated with nitrogen cycling as indices of biogeochemical process rates across a vegetation gradient in Alaska. *Environ. Microbiol.* 14, 993–1008. doi: 10.1111/j.1462-2920.2011.02679.x

Pointing, S. B., Chan, Y., Lacap, D. C., Lau, M. C., Jurgens, J. A., and Farrell, R. L. (2009). Highly specialized microbial diversity in hyper-arid polar desert. *Proc. Natl. Acad. Sci. U.S.A.* 106, 19964–19969. doi: 10.1073/pnas.0908274106

Poly, F., Ranjard, L., Nazaret, S., Gourbiere, F., and Monrozier, L. J. (2001). Comparison of nifH gene pools in soils and soil microenvironments with contrasting properties. *Appl. Environ. Microbiol.* 67, 2255–2262. doi: 10.1128/AEM.67.5.2255-2262.2001

Prober, S. M., Leff, J. W., Bates, S. T., Borer, E. T., Firn, J., Harpole, W. S., et al. (2015). Plant diversity predicts beta but not alpha diversity of soil microbes across grasslands worldwide. *Ecol. Lett.* 18, 85–95. doi: 10.1111/ele.12381

Prosser, J. I., and Nicol, G. W. (2008). Relative contributions of archaea and bacteria to aerobic ammonia oxidation in the environment. *Environ. Microbiol.* 10, 2931–2941. doi: 10.1111/j.1462-2920.2008.01775.x

Prosser, J. I., and Nicol, G. W. (2012). Archaeal and bacterial ammonia-oxidisers in soil: the quest for niche specialisation and differentiation. *Trends Microbiol.* 20, 523–531. doi: 10.1016/j.tim.2012.08.001

R Core Team (2012). *R: A Language and Environment for Statistical Computing*. Vienna: R Foundation for Statistical Computing.

Robertson, G. P., and Groffman, P. M. (2007). "13 - Nitrogen transformations," in *Soil Microbiology, Ecology and Biochemistry*, Third Edn, ed. E. A. Paul (San Diego: Academic Press), 341–364.

Rosch, C., and Bothe, H. (2005). Improved assessment of denitrifying, N2-fixing, and total-community bacteria by terminal restriction fragment length polymorphism analysis using multiple restriction enzymes. *Appl. Environ. Microbiol.* 71, 2026–2035. doi: 10.1128/AEM.71.4.2026-2035.2005

Rumpel, C., and Kögel-Knabner, I. (2011). Deep soil organic matter—a key but poorly understood component of terrestrial C cycle. *Plant Soil* 338, 143–158. doi: 10.1007/s11104-010-0391-5

Schnecker, J., Wild, B., Takriti, M., Eloy Alves, R. J., Gentsch, N., Gittel, A., et al. (2015). Microbial community composition shapes enzyme patterns in topsoil and subsoil horizons along a latitudinal transect in Western Siberia. *Soil Biol. Biochem.* 83, 106–115. doi: 10.1016/j.soilbio.2015.01.016

Serna-Chavez, H. M., Fierer, N., and van Bodegom, P. M. (2013). Global drivers and patterns of microbial abundance in soil. *Global Ecol. Biogeogr.* 22, 1162–1172. doi: 10.1111/geb.12070

Shi, S., Herman, D. J., He, Z., Pett-Ridge, J., Wu, L., Zhou, J., et al. (2018). Plant roots alter microbial functional genes supporting root litter decomposition. *Soil Biol. Biochem.* 127, 90–99. doi: 10.1016/j.soilbio.2018.09.013

Song, Y., Liu, C., Wang, X., Ma, X., Jiang, L., Zhu, J., et al. (2020). Microbial abundance as an indicator of soil carbon and nitrogen nutrient in permafrost peatlands. *Ecol. Indic.* 115:106362. doi: 10.1016/j.ecolind.2020.106362

Stephen, J. R., Kowalchuk, G. A., Bruns, M.-A. V., McCaig, A. E., Phillips, C. J., Embley, T. M., et al. (1998). Analysis of β-subgroup proteobacterial ammonia oxidizer populations in soil by denaturing gradient gel electrophoresis analysis and hierarchical phylogenetic probing. *Appl. Environ. Microbiol.* 64, 2958–2965. doi: 10.1128/AEM.64.8.2958-2965.1998

Stone, M. M., Kan, J., and Plante, A. F. (2015). Parent material and vegetation influence bacterial community structure and nitrogen functional genes along deep tropical soil profiles at the Luquillo Critical Zone Observatory. *Soil Biol. Biochem.* 80, 273–282. doi: 10.1016/j.soilbio.2014.10.019

Sun, R., Myrold, D. D., Wang, D., Guo, X., and Chu, H. (2019). AOA and AOB communities respond differently to changes of soil pH under long-term fertilization. *Soil Ecol. Lett.* 1, 126–135. doi: 10.1007/s42832-019-0016-8

Tang, Y., Yu, G., Zhang, X., Wang, Q., Ge, J., and Liu, S. (2018). Changes in nitrogen-cycling microbial communities with depth in temperate and subtropical forest soils. *Appl. Soil Ecol.* 124, 218–228. doi: 10.1016/j.apsoil.2017.10.029

Tang, Y., Zhang, X., Li, D., Wang, H., Chen, F., Fu, X., et al. (2016). Impacts of nitrogen and phosphorus additions on the abundance and community structure of ammonia oxidizers and denitrifying bacteria in Chinese fir plantations. *Soil Biol. Biochem.* 103, 284–293. doi: 10.1016/j.soilbio.2016.09.001

Throbäck, I. N., Enwall, K., Jarvis, Å, and Hallin, S. (2004). Reassessing PCR primers targeting nirS, nirK and nosZ genes for community surveys of denitrifying bacteria with DGGE. *FEMS Microbiol. Ecol.* 49, 401–417. doi: 10.1016/j.femsec.2004.04.011

Vitousek, P. M., and Howarth, R. W. (1991). Nitrogen limitation on land and in the sea: how can it occur? *Biogeochemistry* 13, 87–115. doi: 10.1007/BF00002772

Wakelin, S. A., Macdonald, L. M., Rogers, S. L., Gregg, A. L., Bolger, T. P., and Baldock, J. A. (2008). Habitat selective factors influencing the structural composition and functional capacity of microbial communities in agricultural soils. *Soil Biol. Biochem.* 40, 803–813. doi: 10.1016/j.soilbio.2007.10.015

Wang, D., Rui, Y., Ding, K., Cui, X., Hao, Y., Tang, L., et al. (2018). Precipitation drives the biogeographic distribution of soil fungal community in Inner Mongolian temperate grasslands. *J. Soils Sediments* 18, 222–228. doi: 10.1007/s11368-017-1727-z

Wang, H., Bu, L., Song, F., Tian, J., and Wei, G. (2021). Soil available nitrogen and phosphorus affected by functional bacterial community composition and diversity as ecological restoration progressed. *Land Degrad. Dev.* 32, 183–198. doi: 10.1002/ldr.3707

Wang, H., Li, X., Li, X., Li, X., Wang, J., and Zhang, H. (2017). Changes of microbial population and N-cycling function genes with depth in three Chinese paddy soils. *PLoS One* 12:e0189506. doi: 10.1371/journal.pone.0189506

Wang, J., Zhang, L., Lu, Q., Raza, W., Huang, Q., and Shen, Q. (2014). Ammonia oxidizer abundance in paddy soil profile with different fertilizer regimes. *Appl. Soil Ecol.* 84, 38–44. doi: 10.1016/j.apsoil.2014.06.009

Wang, X. B., Lu, X. T., Yao, J., Wang, Z. W., Deng, Y., Cheng, W. X., et al. (2017). Habitat-specific patterns and drivers of bacterial beta-diversity in China's drylands. *ISME J.* 11, 1345–1358. doi: 10.1038/ismej.2017.11

Wang, Z., Cao, Y., Wright, A. L., Shi, X., and Jiang, X. (2019). Different ammonia oxidizers are responsible for nitrification in two neutral paddy soils. *Soil Tillage Res.* 195:104433. doi: 10.1016/j.still.2019.104433

Wei, X., Reich, P. B., Hobbie, S. E., and Kazanski, C. E. (2017). Disentangling species and functional group richness effects on soil N cycling in a grassland ecosystem. *Glob. Change Biol.* 23, 4717–4727. doi: 10.1111/gcb.13757

Whitman, W. B., Coleman, D. C., and Wiebe, W. J. (1998). Prokaryotes: the unseen majority. *Proc. Natl. Acad. Sci. U.S.A.* 95, 6578–6583. doi: 10.1073/pnas.95.12.6578

Xiong, J., Liu, Y., Lin, X., Zhang, H., Zeng, J., Hou, J., et al. (2012). Geographic distance and pH drive bacterial distribution in alkaline lake sediments across Tibetan plateau. *Environ. Microbiol.* 14, 2457–2466. doi: 10.1111/j.1462-2920.2012.02799.x

Xu, T., Chen, X., Hou, Y., and Zhu, B. (2020). Changes in microbial biomass, community composition and diversity, and functioning with soil depth in two alpine ecosystems on the Tibetan plateau. *Plant Soil* 459, 137–153. doi: 10.1007/s11104-020-04712-z

Yang, Y., Fang, J., Ma, W., Guo, D., and Mohammat, A. (2010). Large-scale pattern of biomass partitioning across China's grasslands. *Glob. Ecol. Biogeogr.* 19, 268–277. doi: 10.1111/j.1466-8238.2009.00502.x

Yang, Y., Gao, Y., Wang, S., Xu, D., Yu, H., Wu, L., et al. (2014). The microbial gene diversity along an elevation gradient of the Tibetan grassland. *ISME J.* 8, 430–440. doi: 10.1038/ismej.2013.146

Yang, Y., Wu, L., Lin, Q., Yuan, M., Xu, D., Yu, H., et al. (2013). Responses of the functional structure of soil microbial community to livestock grazing in the Tibetan alpine grassland. *Glob. Change Biol.* 19, 637–648. doi: 10.1111/gcb.12065

Yao, X., Zhang, N., Zeng, H., and Wang, W. (2018). Effects of soil depth and plant–soil interaction on microbial community in temperate grasslands of northern China. *Sci. Total Environ.* 630, 96–102. doi: 10.1016/j.scitotenv.2018.02.155

Ying, J., Li, X., Wang, N., Lan, Z., He, J., and Bai, Y. (2017). Contrasting effects of nitrogen forms and soil pH on ammonia oxidizing microorganisms and their responses to long-term nitrogen fertilization in a typical steppe ecosystem. *Soil Biol. Biochem.* 107, 10–18. doi: 10.1016/j.soilbio.2016.12.023

Zhang, Y., Li, D., Wang, H., Xiao, Q., and Liu, X. (2006). Molecular diversity of nitrogen-fixing bacteria from the Tibetan Plateau, China. *FEMS Microbiol. Lett.* 260, 134–142. doi: 10.1111/j.1574-6968.2006.00317.x

Zhao, J., Ni, T., Li, J., Lu, Q., Fang, Z., Huang, Q., et al. (2016). Effects of organic–inorganic compound fertilizer with reduced chemical fertilizer application on crop yields, soil biological activity and bacterial community structure in a rice–wheat cropping system. *Appl. Soil Ecol.* 99, 1–12. doi: 10.1016/j.apsoil.2015.11.006

Zhao, J., Zhou, X., Jiang, A., Fan, J., Lan, T., Zhang, J., et al. (2018). Distinct impacts of reductive soil disinfestation and chemical soil disinfestation on soil fungal communities and memberships. *Appl. Microbiol. Biotechnol.* 102, 7623–7634. doi: 10.1007/s00253-018-9107-1

Zhou, S., Xue, K., Zhang, B., Tang, L., Pang, Z., Wang, F., et al. (2021). Spatial patterns of microbial nitrogen-cycling gene abundances along a precipitation gradient in various temperate grasslands at a regional scale. *Geoderma* 404:115236. doi: 10.1016/j.geoderma.2021.115236

Conflict of Interest: JZ, JBZ, and ZC were employed by the company Zhongke Clean Soil (Guangzhou) Technology Service Co., Ltd.

The remaining authors declare that the research was conducted in the absence of any commercial or financial relationships that could be construed as a potential conflict of interest.

Publisher's Note: All claims expressed in this article are solely those of the authors and do not necessarily represent those of their affiliated organizations, or those of the publisher, the editors and the reviewers. Any product that may be evaluated in this article, or claim that may be made by its manufacturer, is not guaranteed or endorsed by the publisher.

Copyright © 2022 Liu, Chi, Cheng, Ding, Wen, Zhao, Feng, Zhang, Cai and Liu. This is an open-access article distributed under the terms of the Creative Commons Attribution License (CC BY). The use, distribution or reproduction in other forums is permitted, provided the original author(s) and the copyright owner(s) are credited and that the original publication in this journal is cited, in accordance with accepted academic practice. No use, distribution or reproduction is permitted which does not comply with these terms.

frontiers in Plant Science

ORIGINAL RESEARCH
published: 17 January 2022
doi: 10.3389/fpls.2021.827618

Feedback and Trigger of Household Decision-Making to Ecological Protection Policies in Sanjiangyuan National Park

Xukun Su[1,2], Yu Shen[1,2], Shikui Dong[3], Yuqing Liu[1,2], Hao Cheng[1,2], Lingfan Wan[1,2] and Guohua Liu[1,2]**

[1] State Key Laboratory of Urban and Regional Ecology, Research Center for Eco-Environmental Sciences, Chinese Academy of Sciences, Beijing, China, [2] College of Resources and Environment, University of Chinese Academy of Sciences, Beijing, China, [3] College of Grassland Science, Beijing Forestry University, Beijing, China

OPEN ACCESS

Edited by:
Shiliang Liu,
Beijing Normal University, China

Reviewed by:
Yuanyuan Li,
Policy Research Center for Environment and Economy, Ministry of Ecology and Environment, China
Zhanhuan Shang,
Lanzhou University, China
Ruiying Chang,
Institute of Mountain Hazards and Environment, Chinese Academy of Sciences (CAS), China

***Correspondence:**
Shikui Dong
dongshikui@bjfu.edu.cn
Guohua Liu
ghliu@rcees.ac.cn

Specialty section:
This article was submitted to Functional Plant Ecology, a section of the journal Frontiers in Plant Science

Received: *02 December 2021*
Accepted: *17 December 2021*
Published: *17 January 2022*

Citation:
Su X, Shen Y, Dong S, Liu Y, Cheng H, Wan L and Liu G (2022) Feedback and Trigger of Household Decision-Making to Ecological Protection Policies in Sanjiangyuan National Park. Front. Plant Sci. 12:827618. doi: 10.3389/fpls.2021.827618

Ignoring the responses of local households to ecological protection policies can not only seriously limit sustainable development of the alpine grassland ecosystem, but also not improve livelihood on the Qinghai-Tibetan Plateau (QTP). It is of vital importance to clearly understand coupling feedback and trigger between household decision-making of local herdsmen with the implementation of ecological protection policies. We selected Sanjiangyuan National Park (SNP) as the study area which was in the hinterland of the QTP and the first national park in China. We used the global rangeland (G-Range) model to simulate alpine grassland changes and DEcisions under Conditions of Uncertainty by Modeled Agents (DECUMA) model to identify household decision-making of local herdsmen. Results showed that: (1) distribution of livestock density was basically consistent with the distribution of habitat suitability of local households in the SNP; (2) more than half of the uneducated households (52 and 70%) opposed the eco-compensation and eco-migration policies; (3) most of the households (53.7%) never traded livestock for maintaining their livelihood; and (4) When local households owed 65,000 yuan (≈10,000 dollars) in debts, as the critical value (trigger), they traded livestock to support their livelihood. We suggest that feedback and trigger of household decision-making should be fully considered by managers of national park and policymakers of local governments in planning ecological protection policies to maintain sustainable development of alpine grassland, which is of practical significance to long-term conservation and sustainable utilization of natural resources in the SNP.

Keywords: alpine grassland, G-Range model, DECUMA model, household decision-making, local herdsmen, Sanjiangyuan National Park

HIGHLIGHTS

- Spatial distributions of livestock density and habitat suitability of local households were basically consistent in the Sanjiangyuan National Park.
- Most of the local households (nearly 70%) opposed eco-migration policy.
- When local households owed 65,000 yuan (≈10,000 dollars) in debts as the trigger, they traded livestock to support their livelihood.

INTRODUCTION

The Intergovernmental Platform on Biodiversity and Ecosystem Services (IPBES) aims to establish links between scientific research and policymaking to enhance the conservation and utilization of biodiversity and to ensure long-term human wellbeing and the sustainable development of societies (Wan et al., 2021). Recently, a series of assessments from the IPBES show that sustainable goals may be likely to be achieved with an improved understanding of the feedback relationship between society and ecosystems, in global, while improved effectiveness of governance systems also matters (Mastrangelo et al., 2019; Ma et al., 2020). For obtaining more wellbeing from ecosystems, humans alter natural ecosystems, either directly or indirectly (Thiault et al., 2018). Due to the high intensity of human activities, the authenticity of natural ecosystems has deviated over the past few decades (Díaz et al., 2019; Zhao et al., 2020). Humans depend on and mainly drive both changes of ecosystems and their services. People obtain various benefits from ecosystems by harvesting food, earning income, gaining protection, or deriving social and cultural meaning, which underpin human wellbeing (Thiault et al., 2018). Dealing with social and ecological problems has puzzled many researchers for a long time (Liu et al., 2016). It is the overarching challenge that relationships between human wellbeing and ecosystem conservation are difficult to integrate into tools to effectively guide decision-making (Thiault et al., 2018). Maintaining sustainable development and improving human wellbeing have been highly considered by policymakers in China. The long-term social and ecological protection policies and plans have significantly contributed to maintain local ecological stability (Ma et al., 2020).

Natural reserves are the cornerstone of biodiversity conservation. Enhancement of human wellbeing and protection of natural ecosystems in natural reserves have been of international concerns on sustainable development (Fang, 2013; Mastrangelo et al., 2019; Zheng et al., 2020). Of all the effort, natural reserves have been the most prevalent approach shared by governments in over 150 countries (Ma et al., 2020). The report of the 19th National Congress of the Communist Party of China has explicitly proposed to "construction of protected areas system with national parks as the main body" which is a major measure of ecological civilization of China (Du et al., 2020; Gu et al., 2020; Zhao, 2021). Its targets are to protect the authenticity and integrity of the ecosystems and to achieve the harmonious development between humans and nature (Zhao et al., 2020; Zhao, 2021). Construction of national parks in China is still in the experimental stage, requiring further progress and following a top-down management model (Ma et al., 2020). As the primary type of protected area, national park has been playing an important role in biodiversity conservation (Ma et al., 2020). As the first national park in China, the establishment of Sanjiangyuan National Park (SNP) on the Qinghai-Tibetan Plateau (QTP) brings a sustainability focus and is vital for wildlife protection with respect to both phylogenetic resources and conservation efforts (Lin and Zhang, 2020; Xi et al., 2020; Su et al., 2021). Alpine grassland, which is the main ecosystem in the SNP, can provide multiple ecosystem services which contain provision services (e.g., food provision to wildlife and livestock), regulatory services (e.g., flood and disease control), cultural services (e.g., spiritual, recreational, and cultural benefits), and support services (e.g., ecosystem nutrient cycling) (Wang et al., 2016). The SNP is also the main habitat of endemic wildlife and livestock, and the local people depend on these special animals for survival and development (Shen and Tan, 2012; Han et al., 2018; Dai et al., 2019; Wang et al., 2020). A total of 22 ecological restoration strategies have been implemented for more than 20 years (Wang et al., 2016; Sheng et al., 2019). Aiming to reduce ecosystem degradation, alleviating rural poverty with central government supports, and promoting local sustainable development of economy, these plans bring enormous social and ecological benefits to the SNP (Ma et al., 2020). Local households obtain almost all their living necessities from grazing their livestock, such as yaks, Tibetan sheep, and horses in the SNP (Wang et al., 2016). Historically, they migrated in long distances from summer pastures to winter pastures to graze more livestock and to avoid loss from frequent natural disasters, especially snowstorms (Wang et al., 2016). It can be understood as an integrated socio-ecological system that local households, their livestock, and alpine grassland ecosystem develop interaction between feedbacks after thousands of years of adaptation (Wang et al., 2016; Yeh et al., 2017). The traditional lifestyle of local households is the result of a long period of adaptation to the harsh climatic and geographical characteristics of the QTP (Wang et al., 2016). Local households are the dominant and direct beneficiaries of the alpine grassland ecosystem, and their feedbacks and decision-making determine whether the alpine grassland ecosystem can be sustainable development in the future (Yang et al., 2020). Meanwhile, grassland ecosystem also affects the feedback and decision-making of local households, such as the quality of herbage and water supply (Daily and Matson, 2008; Zheng et al., 2020). Current research on ecological protection behaviors of residents commonly adopts the socioeconomic approach at the individual level, which might ignore the impacts of potential psychological factors on resident behaviors, such as willingness and perception of farmers to conservation (Ma et al., 2020). Eco-compensation and eco-migration are two main grassland protection policies on the QTP. Eco-compensation is an institutional arrangement of rules, which aims to protect and sustainably use alpine grassland, adjusts the interests of local households mainly by economic means, promotes compensation activities, and arouses the enthusiasm of ecological protection (Zhao, 2021). Eco-migration policy, also known as environmental migration, refers to people who move out of their original residence in protected areas, areas severely damaged by ecological environment, ecologically fragile areas, and areas with poor natural environment and no living conditions for human beings, and who settle and rebuild their homes in other places (Zhai et al., 2020; Zhao, 2021).

Ignoring the responses and decision-making of local households to protection policies will seriously affect and directly determine the development direction of the local ecosystems in the future. It eventually leads to that efficiency of protection policies is not significant to maintain biodiversity and cannot fundamentally alleviate alpine grassland degradation in the SNP

(Guo et al., 2021). It also cannot improve the livelihood and wellbeing of local households and ultimately cannot realize the sustainable utilization of alpine grassland ecosystem in the SNP (Wu et al., 2020). Household decision-making of local herdsmen should be an important part of the management and utilization of ecological environment in the SNP (Wan et al., 2021). It should be fully considered in planning sustainable development management policies which are of practical significance to the long-term protection and sustainable utilization of natural resources in the SNP. Therefore, there is an urgent need to use new methods to research on response of household decision-making to protection policies, coupling natural ecological and social-economic systems.

Aiming to clearly understand coupling relationships and feedback mechanisms of household decision-making to ecological protection policies, through using global rangeland (G-Range) model to simulate alpine grassland changes and DEcisions under Conditions of Uncertainty by Modeled Agents (DECUMA) model to identify household decision-making of local herdsmen, we documented: (1) habitat suitability changes of local households and spatial distributions of livestock density from 2000 to 2015, (2) feedback and trigger of household decision-making to ecological protection policies, and (3) management framework of a newly established national park.

MATERIALS AND METHODS

Study Area

The SNP locates in the hinterland of the QTP (**Figure 1**). Due to the birthplace of the Yangtze River, the Yellow River, and the Lancang River, it is a critical area for water resource conservation, and its ecosystem is very sensitive and fragile (Zhai et al., 2020). It covers a 3.6×10^5 km^2 area, with an average altitude of 4,000 m (the altitude range is 2,582–6,815 m a.s.l.) (Ma et al., 2020). As the main parts of the SNP, Yangtze River Source Park, Yellow River Source Park, and Lancang River Source Park have their own position and orientation. The Yangtze River Source Park is positioned to protect alpine marshes, alpine meadows, and desert ecosystems; the Yellow River Source Park is positioned to protect the alpine wetland ecosystem; and the Lancang River Source Park is positioned to protect alpine valley landforms and the most abundant ecosystem types, including alpine meadow, alpine grassland, alpine shrub, and natural arbor forest (Xi et al., 2020). As the main ecosystem type, alpine grassland includes alpine meadow and alpine steppe, which account for approximately 76 and 23% of the total grassland area, which provides multiple ecological services for the upstream and downstream areas, such as food production, water conservation, and habitat support (Yu et al., 2021). Its annual precipitation is 262–773 mm and occurs mostly from June to September each year (Fang, 2013). The grass growth period is less than 3 months when there is no absolute frost-free period in the study area.

Data Sources

Spatial Data Collection

Land use and cover change (LUCC) data in 2000, 2005, 2010, and 2015, distribution data of settlements (locations of cities, counties, and villages) and roads (national highways, provincial highways, county roads, and village roads), and river data (vector) were provided by the "National Tibetan Plateau Data

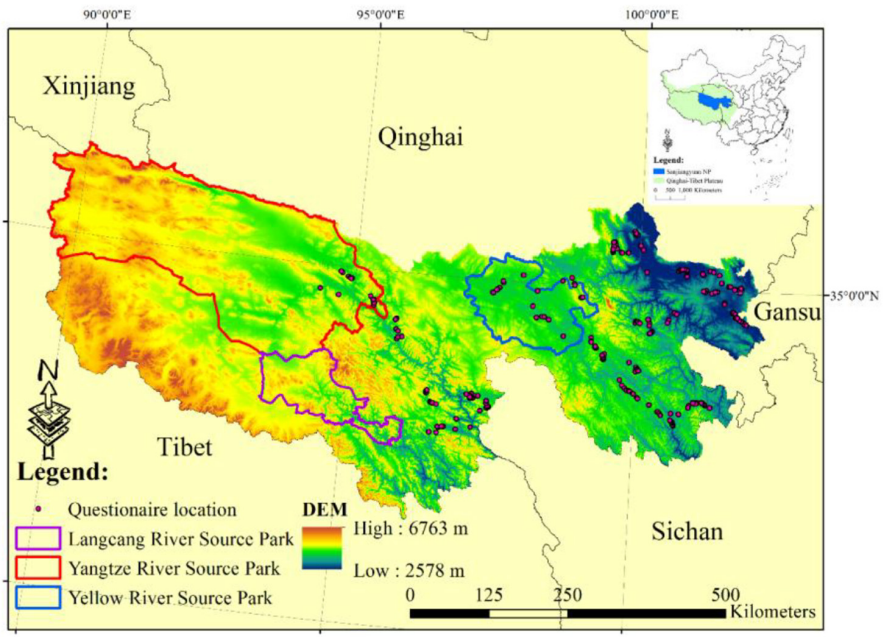

FIGURE 1 | Location of the study area.

Center."[1] All LUCC data were raster with a resolution of 30 m × 30 m. The Digital Elevation Model (DEM) data with a 30-m spatial resolution were downloaded from the United States Geological Survey (USGS).[2] Historical weather data from the Climatic Research Unit (CRU) database (CRU, 2008) at 1° and 0.5° resolution for the years 2000–2015 were currently included with model files available for download from the G-Range model website (NREL, 2013; Sircely et al., 2019). All spatial data need to be transferred to ASCII data with a 0.25° × 0.25° resolution.

Questionnaire Investigation

We conducted a field survey to obtain 503 questionnaires with the pastoral interview of households from 2013 to 2015 in the SNP. According to the grazing intensity, alpine grassland type, and administration, 13 counties of four Tibetan autonomous prefectures were selected as the main interview areas, such as Yushu County, Zaduo County, and Qumalai County of Yushu Tibetan Autonomous Prefecture; Maqin County, Maduo County, Dari County, Banma County, Jiuzhi County, and Gande County of Guoluo Tibetan Autonomous Prefecture; Xinghai County and Tongde County of Huangnan Tibetan Autonomous Prefecture; and Zeku County and Henan Mongolian Autonomous County of Hainan Tibetan Autonomous Prefecture. The main contents of the questionnaire were divided into the following five parts: family information (including member, education, and location), livestock (including the total number of yaks, Tibetan sheep, and horses), household incomes (i.e., salary, livestock trade, *Cordyceps sinensis* trade, etc.), expenditure (i.e., food, clothes, medical costs, etc.), and others (mainly including awareness of eco-compensation and eco-migration) (**Table 1**).

[1]http://data.tpdc.ac.cn

[2]http://earthexplorer.usgs.gov/

TABLE 1 | Household variables represented in the DECUMA model.

Attribute	Class	Unit	Notes
Family	Member	Person	Classify by age and gender
	Education		Uneducated, primary education, middle school, high school
	Location	Degree	Longitude and latitude
Livestock	Tibetan sheep	/	By sex
	Yak		
	Horse		
Income	Livestock trade	RMB (Yuan/a)	/
	Livestock products		/
	Cordyceps sinensis trade		/
	Other incomes		Salary
Expenditure	Food		/
	Clothes		
	Medical cost for people		
	Medical cost for livestock		
	Transportation cost		Transportation costs between summer and winter pastures
	Education cost		/
	Cultural cost		Praying or blessing costs in temples
	Other costs		/
Others	Perception of relevant protection policies		
	Whether snow disasters cause livestock death		
	Triggers to trade livestock		

Data Analysis

G-Range Model

The G-Range model coupled biogeochemical submodels from the soil organic matter model (CENTURY model) with submodels of dynamic populations for herbs, shrubs, and trees to support spatial simulation and forecasting in the rangeland ecosystems (Sircely et al., 2019). The G-Range model could capture interannual and intra-annual variation and directional shifts in essential ecosystem processes, as well as differences in ecosystem process rates and competition among major rangeland plant growth forms (Sircely et al., 2019). The G-Range model was performed on a monthly time step and was a spatially explicit model at grid-cell scale, with model inputs from spatial layers driving ecosystem processes and vegetation dynamics according to the location and rangeland type (biome) of the grid/cell (Sircely et al., 2019). Based on the total area of the study area, we selected 0.25° as the basic resolution to run the G-Range model which currently supported grid/cell resolutions of 1°, 0.5°, 0.25°, 0.167°, 0.1°, and 0.083°.

DEcisions Under Conditions of Uncertainty by Modeled Agents Model

As a spatially explicit household model, the DECUMA model was used to simulate decision-making and behaviors by pastoral households as they relate to ecosystem services (Boone et al., 2006). This model described the decision-making of local households to maintain their own survival and development in the process of uncertain future environmental changes. Measures reflecting livelihood of local households, such as livestock dynamics and holdings, energy flows where caloric gains from foods eaten were tallied and compared to energy needs, and cash flows, which included regularly scheduled income and expenses, as well as short term sales or purchases, were tracked (**Figure 2**; Boone et al., 2011). The DECUMA model linked to the G-Range model that could quantify ecosystem changes (e.g., forage availability) and could simulate the effects of livestock grazing on ecosystem (Thornton et al., 2003; Boone et al., 2011). With no fixed requirement for spatial scale, we simulated the effects of livestock grazing on ecosystem and feedbacks of ecosystem to livestock grazing coupling with G-Range model. The simulation process of DECUMA model mainly focused on the following two aspects: livestock distribution and dynamics and decision-making changes of local households. Among them, distribution and dynamics of livestock mainly included the following aspects: (1) simulated distribution of livestock (i.e., yak, Tibetan sheep, and horse) was determined based on the amount of edible forage provided by G-Range model and (2) total energy requirement was determined based on the available forage that livestock obtained, i.e., energy consumption (body

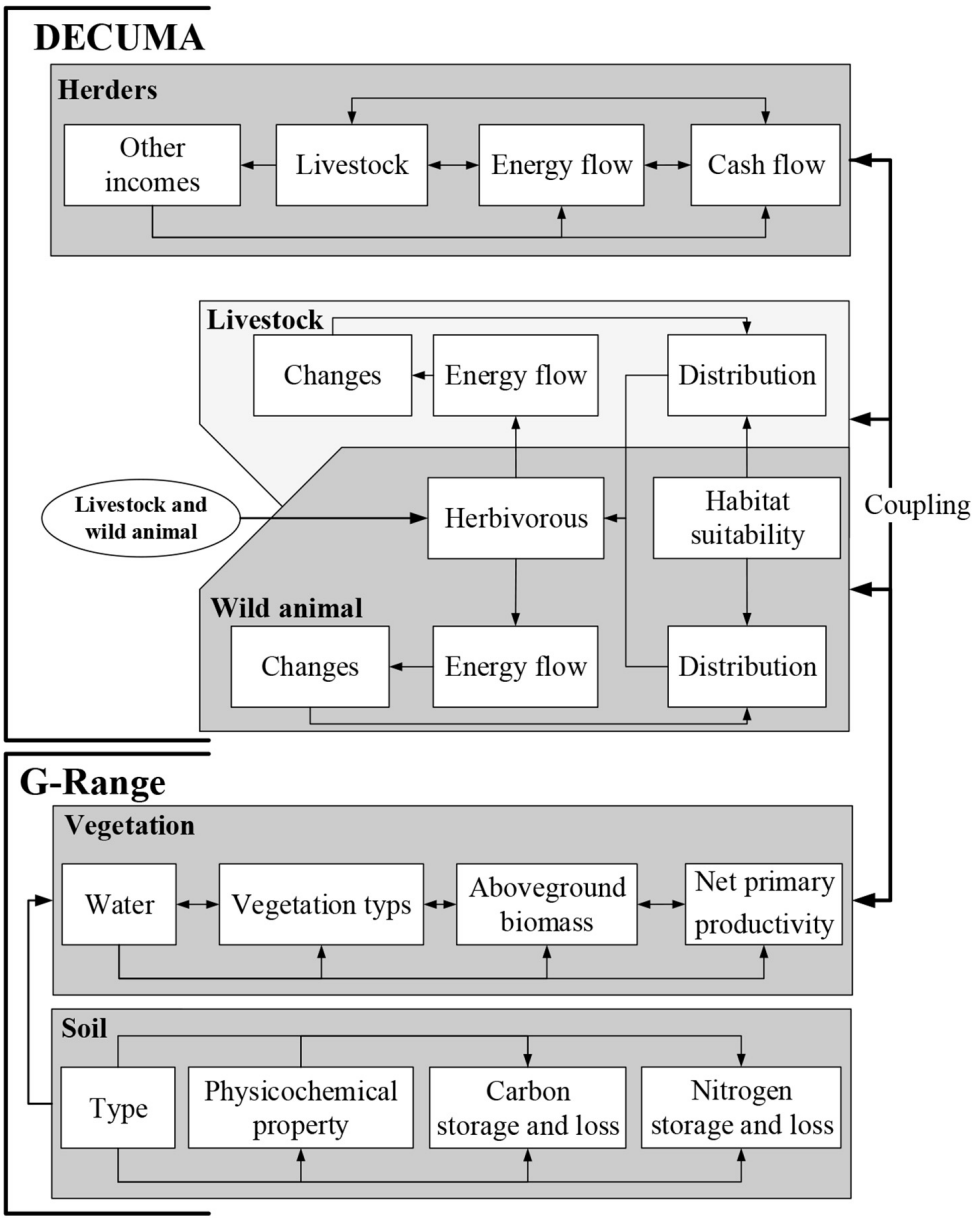

FIGURE 2 | Detailed information flows linking G-Range model and DECUMA model.

weight changes of livestock). Population changes of livestock were closely related to birth and death rates of livestock, mainly by comparing the current number of livestock with the expected number of livestock in the future. Changes in the decision-making of local household were mainly based on the following aspects: (1) energy flow was the relative ratio of calories obtained from food and potential energy demands in each household; (2) cash flow mainly included economic income and expenditure of households; (3) livestock trade; and (4) cash needs were estimated for the next 3 months, which was related to the decision of the pastoralist to trade livestock (purchase, sale, or transfer of livestock) (Thornton et al., 2003; Boone et al., 2011).

RESULTS

Changes in Habitat Suitability

During the study period, unsuitable areas were mainly located at the western SNP where Yangtze River Source Park was located (**Figure 3**). Areas with high habitat suitability index (HSI) were mainly located in Chenduo County, Yushu County, and Maqin County in the middle and eastern SNP from 2000 to 2010 (**Figures 3A–C**). Areas with low HSI value appeared in the southeast SNP from 2000 to 2010 which transferred to areas with high and moderate HSI values in 2015. All unsuitable areas were located at Zhiduo County and Qumalai County in

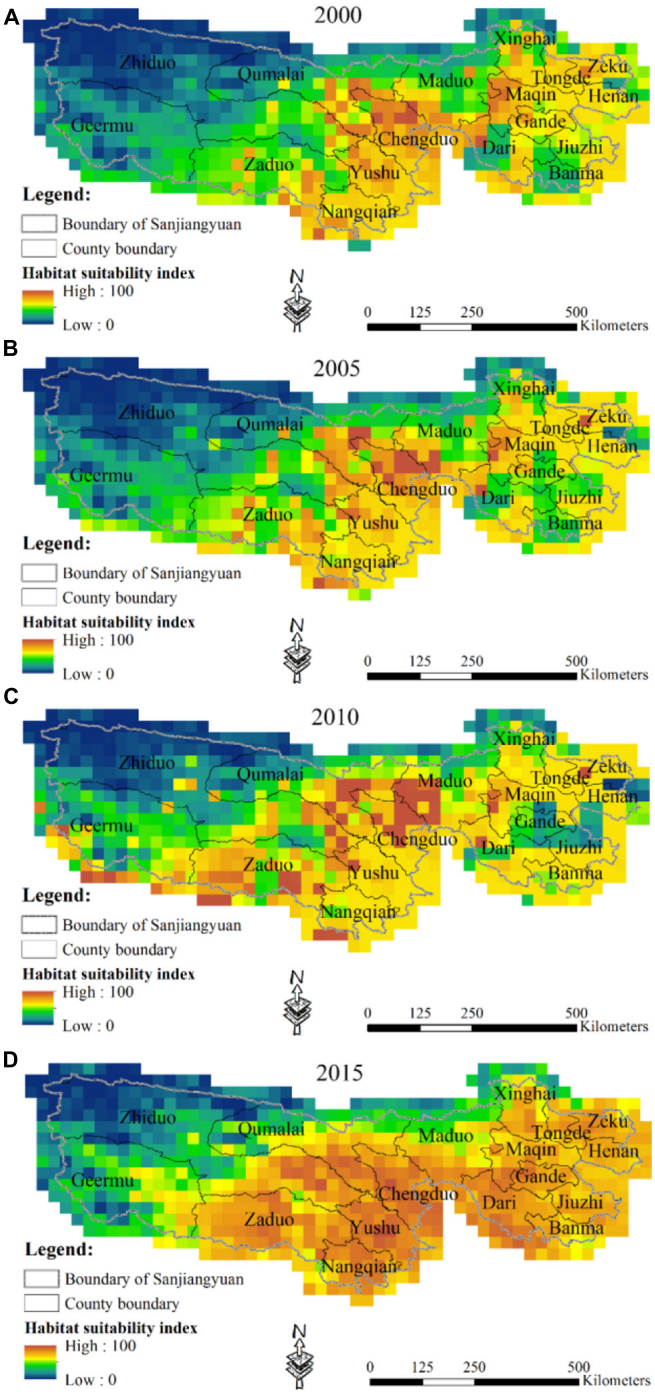

FIGURE 3 | Habitat suitability index (HSI) changes in 1990 **(A)**, 2005 **(B)**, 2010 **(C)**, and 2015 **(D)**.

the northwestern SNP in 2015 (**Figure 3D**). With an area of approximately 2.4 × 10^5 km^2, about two-third of the SNP with high and moderate HSI value was in the central and eastern SNP in 2015. Compared with 2000, the HSI value of the eastern SNP showed an overall upward trend in 2015, while the change was not obvious in the central and western SNP. In 2000, unsuitable areas reached its maximum in the SNP. During the study period, areas with high and moderate HSI values gradually expanded westward in the SNP.

Livestock Density Changes

On the whole, the average number of Tibetan sheep, yaks, and horses in a household decreased from 80, 60, and 15 in 2000 to 39, 52, and 2 in 2015 in the SNP (**Figure 4**). Especially in 2011,

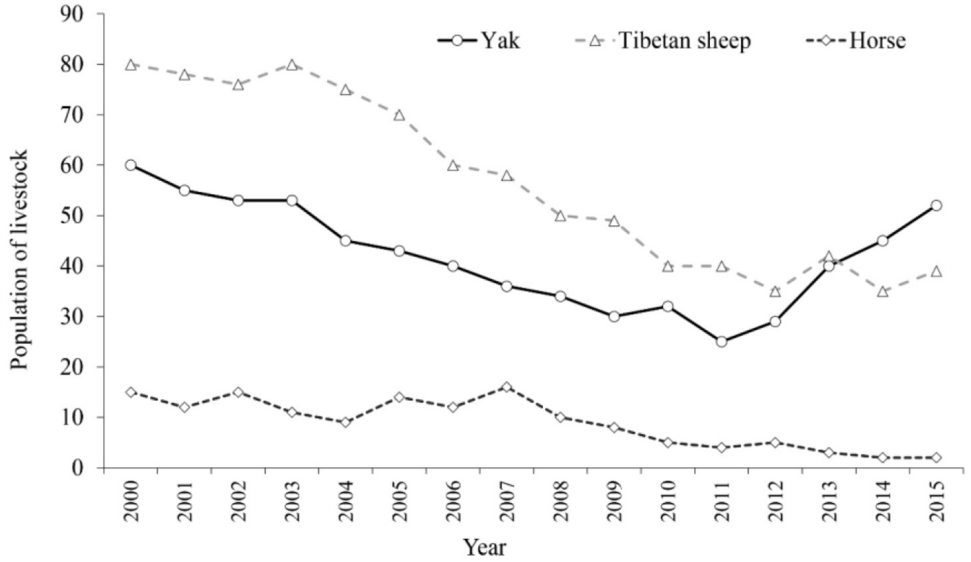

FIGURE 4 | Annual changes of the average number of livestock (i.e., yaks, Tibetan sheep, and horses) from 2000 to 2015.

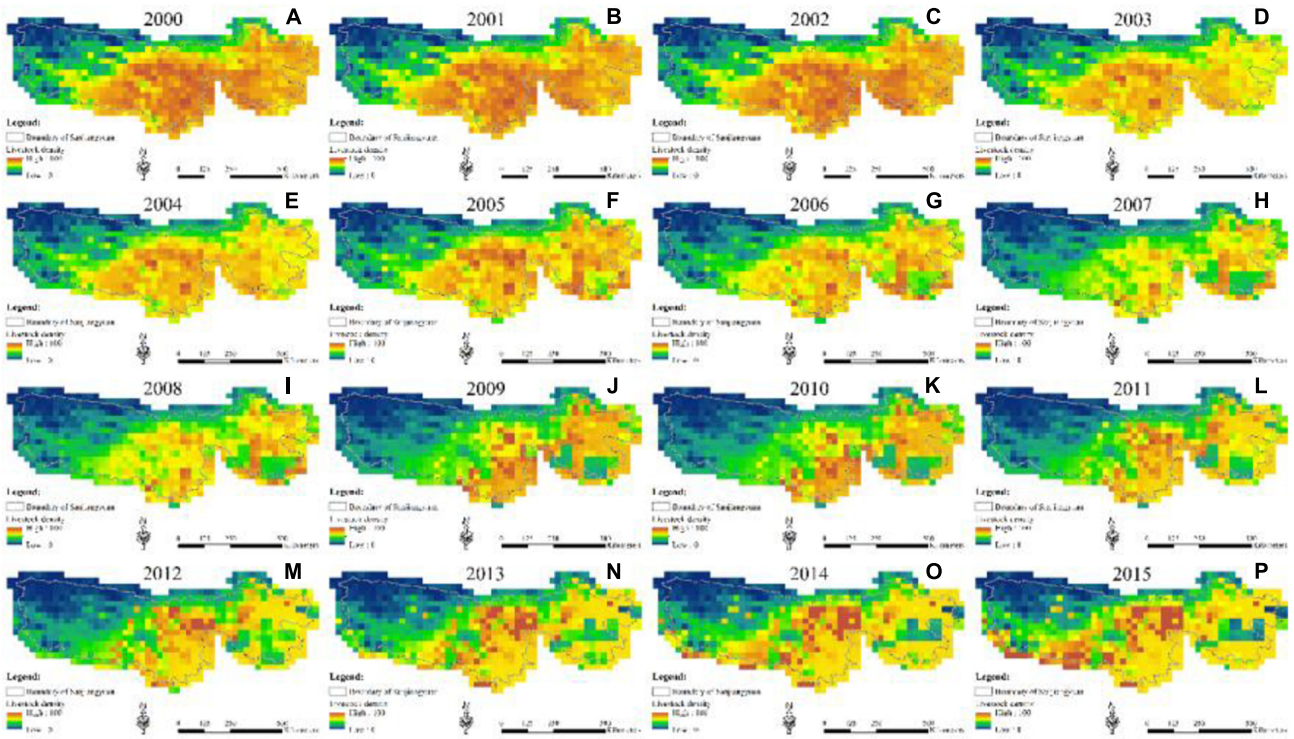

FIGURE 5 | Livestock density changes in 2000 **(A)**, 2001 **(B)**, 2002 **(C)**, 2003 **(D)**, 2004 **(E)**, 2005 **(F)**, 2006 **(G)**, 2007 **(H)**, 2008 **(I)**, 2009 **(J)**, 2010 **(K)**, 2011 **(L)**, 2012 **(M)**, 2013 **(N)**, 2014 **(O)**, and 2015 **(P)**.

the average number of yaks and Tibetan sheep had fallen by half to 25 and 40. The average number of Tibetan sheep and horses showed a significant decrease trend from 2000 to 2011, except for the average number of yaks, which recovered from 25 in 2011 to 52 in 2015. The average number of yaks held by local households was more than the average number of Tibetan sheep in 2015.

Spatial distribution of livestock density was basically consistent with distribution of habitat suitability of households in the SNP (**Figure 5**). The central and eastern SNP were the main distribution areas of livestock from 2000 to 2015. Since 2000, livestock density in the SNP showed a significant decrease trend. Areas with high livestock density gradually

decreased during the study period. Especially in 2010, livestock density decreased most obviously in the study area. From 2010 to 2015, livestock density still maintained decrease trend in the whole nation park. However, the livestock density showed increase trend in the central part of the SNP (e.g., Maduo County, Chenduo County, Yushu County, and Nangqian County). Particularly, in 2015, the livestock density in Maduo County (Yellow River Source Park) showed a sharp increase trend (**Figure 5P**). Since 2007, the livestock density decreased significantly, mainly in Maqin County, Gande County, and Jiuzhi County of Guoluo Tibetan Autonomous Prefecture which were mainly in the eastern SNP (**Figures 5H–P**).

Feedbacks to Ecological Protection Policies

Local households with different education levels had different cognitions to ecological protection policies (**Figure 6**). A total of 52% uneducated households opposed eco-compensation policy to reduce the number of livestock, and 16% of uneducated households supported to adopt eco-compensation policy and accepted livestock reduction to protect alpine grassland (**Figure 6A**). There were 6% of local households with primary education level who opposed the implementation of eco-compensation policy, while only 2% of local households supported. However, households with a high school education level and above (including college education or university education) also opposed the eco-compensation policy.

Notably, 70% of uneducated households strongly opposed the implementation of eco-migration policy and thus to change their tradition and nomadic lifestyle, while only 7% of the uneducated households supported the eco-migration policy in the SNP (**Figure 6B**). Of note, 8% of households with primary school education level and 1% of households with middle school education level opposed this policy. Only 1% of households with high school education level and above (including college education or university education) did not oppose eco-migration policy.

More than a half (55.2%) of local households did not adopt any protection measures to protect their pastures and 37.8% of those adopted livestock reduction in 2015 (**Table 2**). Only 4% of local households selected grazing prohibition to protect alpine grassland.

Triggers of Household Decision-Making

The average annual income of local households was 11,374 yuan, and the average annual expenditure was 4,441 yuan, and thus the net income of local households was 6,933 yuan (≈1,000 dollars). Income of *Cordyceps sinensis* trade accounted for 83% (9,398 yuan) of the total income of household, income of livestock trade accounted for 11% (1,249 yuan), and other income accounted for 6% (727 yuan) in 2015 (**Figure 7A**). Food cost accounted for the largest proportion of 27% (1,188 yuan), followed by clothes cost and medical cost, both accounted for 15% (**Figure 7B**). Transportation, education, and culture costs (including praying and blessing costs in temples) accounted for 13 (560 yuan), 8, and 6%, respectively. More than half (53.7%) of households never chose to trade livestock for maintaining their livelihood. When local households owed 65,000 yuan (≈10,000 dollars) in debts (critical value of livestock trade), they chose to sell livestock to support their livelihood.

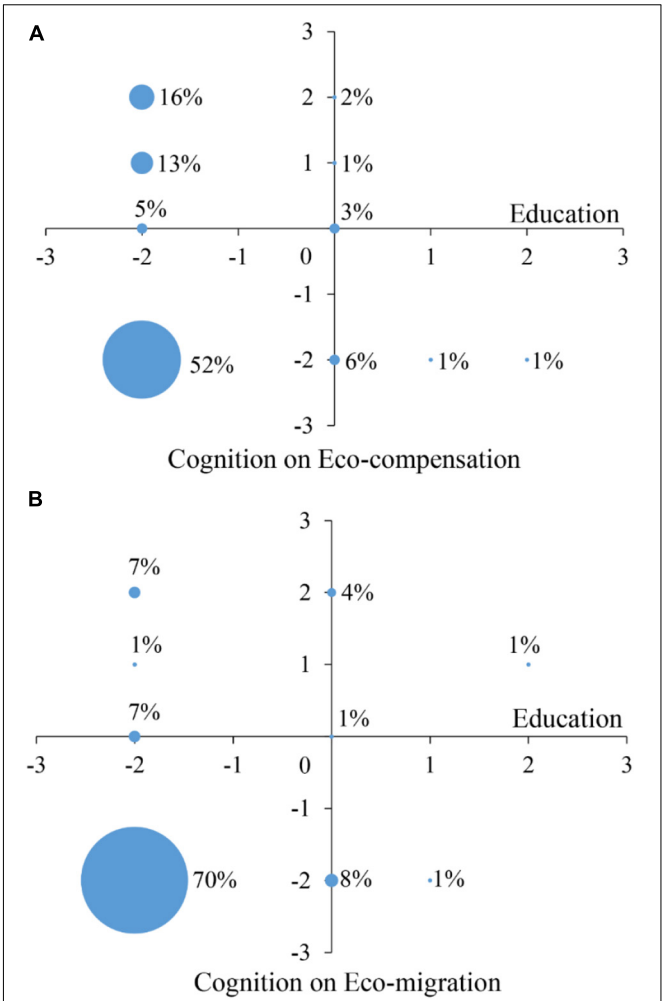

FIGURE 6 | Cognition on eco-compensation **(A)** and eco-migration **(B)** of households with different education levels in the SNP. Education level: -2 stands for uneducated; -1 stands for temple education; 0 (zero) stands for primary school; 1 stands for middle school; and 2 stands for high school or above. The cognition on eco-compensation and eco-migration policies: -2 stands for against; -1 stands for mixed; 0 (zero) stands for no idea; 1 stands for medium; and 2 stands for support.

TABLE 2 | Obligation of local households on protecting alpine grassland linked to protection policies.

Grassland protection measures	Number of households	Percentage (%)
No actions	278	55.2
Livestock reduction	190	37.8
Grazing prohibition	20	4.0
Others	15	3.0
Total	200	100%

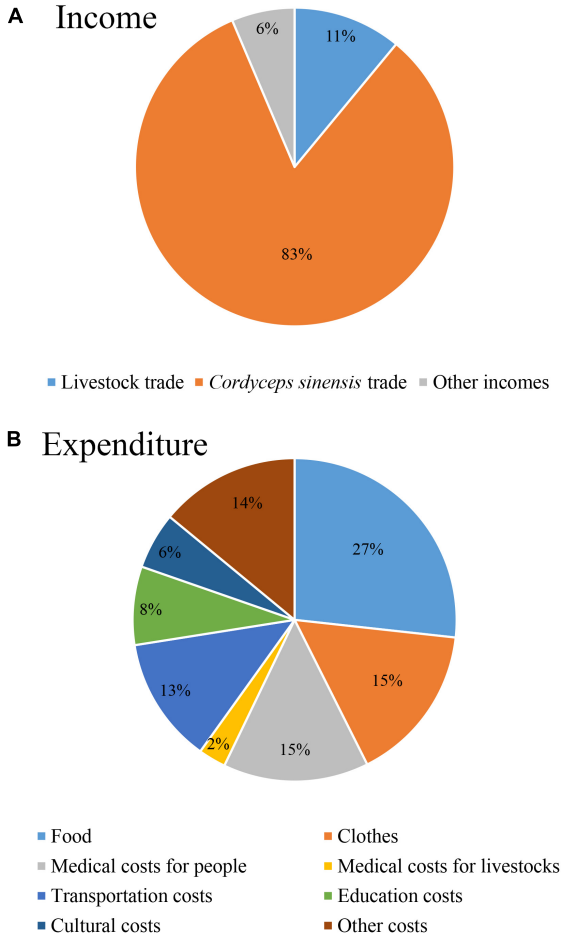

FIGURE 7 | Income **(A)** and expenditure **(B)** of local households in the SNP.

DISCUSSION

Effects of Ecological Protection Policies

Our results indicated that livestock density distribution was basically consistent with the distribution of habitat suitability of local households in the SNP. Habitat deterioration was not improved at the beginning of Sanjiangyuan National Nature Reserve establishment in 2000, but habitat suitability was greatly improved after the implementation of alpine grassland protection policies in 2015. Most of the Yangtze River Source Park was an unsuitable area for local households, which was mainly located at Kekexili National Nature Reserve and listed as a representative of no man's land in China. Most areas with high and moderate HSI values were located at Yellow River Source Park and Lancang River Source Park, which gradually expanded westward in the SNP from 2000 to 2015. Despite the strict implementation of eco-migration policy in the Yellow River Source Park, livestock density was still more concentrated and not in decline, especially in Maduo County. Although local households have moved out of this reserve and settled down, they returned back to their pasture for livestock grazing in the summer. This indicates that the implementation of eco-migration policy has not achieved the effect of alleviating the grazing pressure and protecting the alpine grassland ecosystem.

The average number of horses decreased sharply during the study period, which was not the main livestock held by local households, with the development of transportation infrastructure in the SNP. The average number of yaks held by local households was more than the number of Tibetan sheep in 2015. With the implementation of alpine grassland protection policies, local households will selectively reduce livestock, especially decreasing the number of Tibetan sheep, while the number of yaks (especially the number of female yaks) remains stable, because yaks can provide more dairy products (shortening, yogurt, etc.) and other husbandry products to maintain a livelihood. It indicates that implementation of eco-compensation only changes livestock structure and has no good effects on reducing the livestock population in the SNP.

Feedback and Trigger

Cognition of local households toward alpine grassland protection policies (i.e., eco-compensation and eco-migration) changed during the study period. Local households differ in their education levels and do have significant feedbacks to ecological protection policies, practical schedules in livestock grazing, and managing their pastures (Yang et al., 2020). The proportion of local households who supported the eco-compensation policy increased from 54% (42% fully supported the policy and 12% moderately supported) in 2013 to 70% (50% fully supported the policy and 20% moderately supported) in 2015. The percentage of local households who opposed the implementation of eco-compensation policy decreased from 41% in 2013 to 26% in 2015. It indicates that local households in the national park gradually begin to accept eco-compensation policy. In 2013, only 18% of local households supported the eco-migration policy (16% fully supported it and 2% moderately supported it), and 76% opposed it. In 2015, the number of households who supported the eco-migration policy increased to 34% (20% of households fully supported the policy and 14% of herdsmen moderately supported it), while the number of households who opposed eco-migration policy decreased to 60%. Therefore, local households gradually begin to accept the eco-migration policy. Although more and more households are beginning to support eco-migration policy, most of the households still have against the implementation of eco-migration during the study period. With synchronous implementation of eco-compensation and eco-migration, cognition and acceptance of local households of eco-compensation policy are significantly higher than that of eco-migration policy.

Income of local households primarily derives from *Cordyceps sinensis* collection, traditional livestock husbandry, policy allowance, and sporadic side jobs in the SNP (Guo et al., 2021). Incidents of wildlife injuring people and livestock occur, which poses a risk to the life, property, and safety of local households, without any reasonable compensation standards or safeguard measures in place (Guo et al., 2021). Local households attribute alpine grassland conditions and observe their own management practices to their pastures, rotation grazing in winter and

summer pastures, livestock reduction, and grazing prohibition (Yeh et al., 2017). Medical costs of livestock accounted for only 2% of total expenditure. Due to the implementation of eco-compensation, local governments provide more free veterinary medicines and veterinary services to local households who can reduce living costs. Livestock grazing is the basic condition for local households to survive and develop. To trade livestock and reduce its population are not only related to the survival and development of local households but also affect the formulation of alpine grassland protection policies. Therefore, analyzing the critical points of livestock trade is particularly important to balance human wellbeing and ecosystem protection. In this research, owing 65,000 yuan (≈10,000 dollars) in debts is the critical point (trigger) to trade livestock for supporting their livelihood by local households. In practice, this trigger should be considered in designing and planning eco-compensation policy by national park managers and local government policymakers.

Effective Management Framework

The QTP is an integral ecological functional area in China and plays an important role in national ecological security shelter of China (Fan and Fang, 2020). The establishment of national parks is an important component of the ecological identity of China and an essential measure to achieving ecological civilization through natural-ecological protection and socioeconomic development (Guo et al., 2021). The provincial government of Qinghai established Sanjiangyuan provincial nature reserve in 2000 and officially approved it as a national nature reserve in 2003. Accompanied by the ecological civilization system reform, the SNP was one of the national park pilots in China in 2015 and was established as the first national park of China in 2021 (Xi et al., 2020; Guo et al., 2021). It is also of particularly important to end a national park pilot program and to establish an official national park, which has aimed to protect the local ecosystem for improving ecosystem services of alpine grassland, restoring biodiversity, and achieving breakthroughs in the management system on the QTP (Guo et al., 2021; Ma et al., 2021; Su et al., 2021). More importantly, effective management and law enforcement system of a newly established national park are key urgent problems that demand a prompt solution (Su et al., 2021). Based on more technical supports from scientific research, adaptive management on the carrying capacity of alpine grassland and its utilization strategy should be strengthened by managers and policymakers who wish to achieve policy outcomes

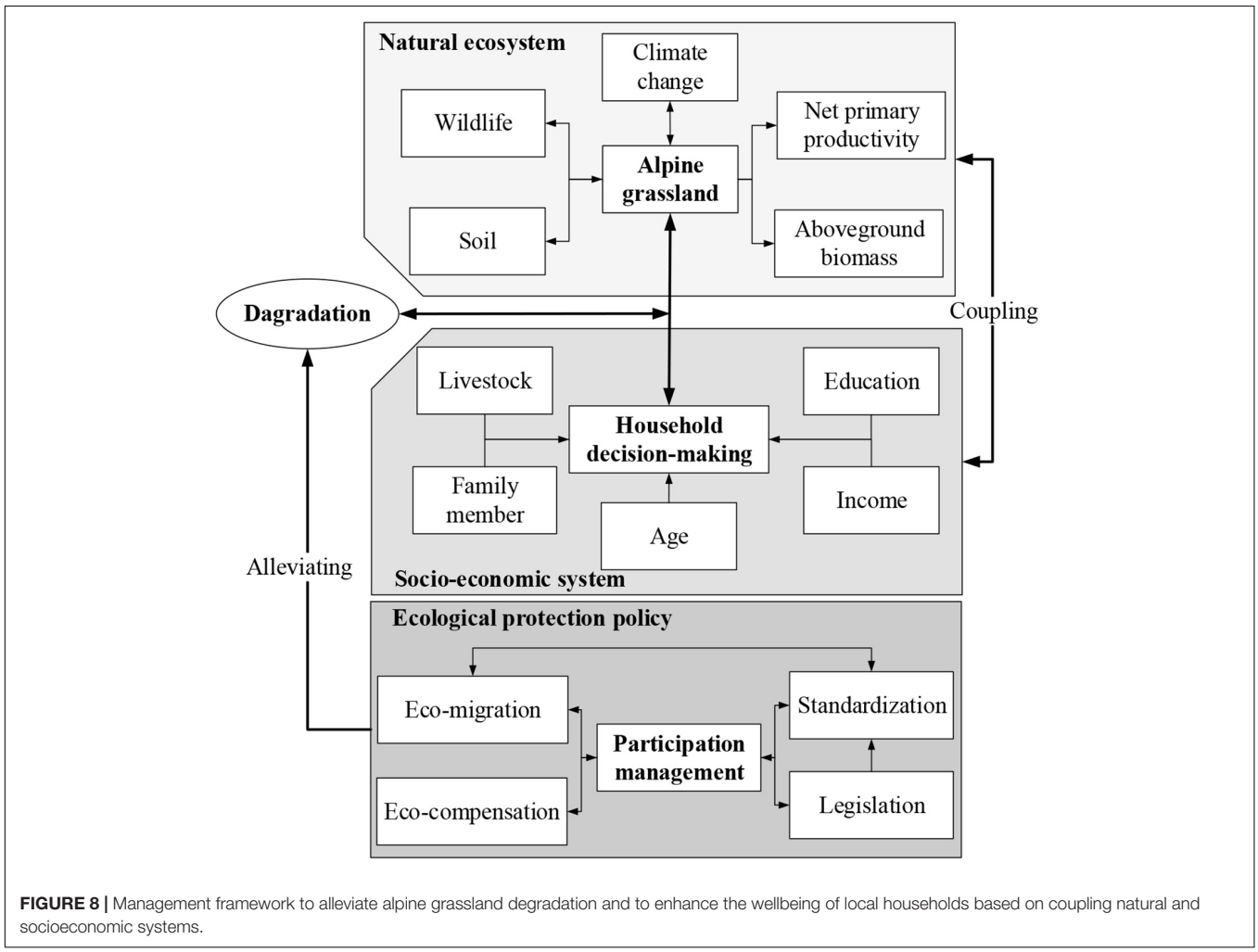

FIGURE 8 | Management framework to alleviate alpine grassland degradation and to enhance the wellbeing of local households based on coupling natural and socioeconomic systems.

that benefit both local households and alpine grassland may do well to fully consider household decision-making with existing knowledge, education levels, cultural context, and management practices of local herdsmen (Yang et al., 2020). Specifically, managers and policymakers need to understand that limiting livestock grazing to a sustainable level is a more reasonable approach if overgrazing exists based on carrying capacity of alpine grassland (Zhao et al., 2020).

Differences in stakeholder values are at the heart of protection policies, with dissimilarities in objectives fueling the challenges of managing complex, dynamic systems (Mason et al., 2018; St John et al., 2021). In this research, we propose a new management framework of the SNP coupling natural ecosystem with socioeconomic system, which needs to fully consider the decision-making of households and their feedback and trigger to ecological protection policies (**Figure 8**). Managers and policymakers should carry out household-based participation management which needs to be adjusted in real time according to different feedback and trigger of household decision-making to face future challenges. Conventionally, this management framework needs to focus on reducing pressures that affect alpine grassland, such as conflicts between biodiversity conservation and natural resources utilization. Meanwhile, it should also have the ability to balance short-term needs with long-term requirements for the future sustainability of alpine grassland and to integrate the dynamic and complex relationships between local herdsmen and alpine grassland (Thiault et al., 2018). In total, it should be a more complex and integrative approach coupling humans with nature rather than a normal method in biodiversity conservation and natural resource management.

CONCLUSION

This research indicates that livestock density distribution is basically consistent with the distribution of habitat suitability of households in the SNP. The implementation of alpine grassland protection policies can decline habitat deterioration and greatly enhance habitat suitability of local households. Local households have different cognitions to eco-compensation and eco-migration policies due to their different education levels. Moreover, there is a trigger that local households make decisions to trade livestock to support their livelihood. Our results suggest that it is necessary to design a new framework to effectively manage the newly established national park. This framework should fully consider feedback and trigger of household decision-making which can guide policymakers to plan ecological protection policies for maintaining sustainable development of alpine grassland.

DATA AVAILABILITY STATEMENT

The original contributions presented in the study are included in the article/supplementary material, further inquiries can be directed to the corresponding author/s.

AUTHOR CONTRIBUTIONS

XS, SD, and GL designed the research. YL, YS, and HC performed the analysis. XS drafted this article. All authors contributed to the interpretation of this article, approved the submitted version, and collected data in the field.

FUNDING

This research was supported by the Second Tibetan Plateau Scientific Expedition and Research Program (STEP) (grant nos. 2019QZKK0402 and 2019QZKK0307) and the Strategic Priority Research Program of Chinese Academy of Sciences (grant no. XDA20020402).

ACKNOWLEDGMENTS

We thank all people for helping us to complete field surveys and appreciate the valuable suggestions and comments provided by editor and reviewers.

REFERENCES

Boone, R. B., Galvin, K. A., BurnSilver, S. B., Thornton, P. K., Ojima, D. S., and Jawson, J. R. (2011). Using coupled simulation models to link pastoral decision making and ecosystem services. *Ecol. Soc.* 16:6.

Boone, R. B., Galvin, K. A., Thornton, P. K., Swift, D. M., and Coughenour, M. B. (2006). Cultivation and conservation in ngorongoro conservation area,tanzania. *Hum. Ecol.* 34, 809–828. doi: 10.1007/s10745-006-9031-3

CRU (2008). *CRU Time Series (TS) 3.0 high resolution gridded datasets*. Norwich Research Park: CRU.

Dai, Y. C., Hacker, C. E., Zhang, Y. G., Li, W. W., Zhang, Y., Liu, H. D., et al. (2019). Identifying climate refugia and its potential impact on Tibetan brown bear (*Ursus arctos* pruinosus) in Sanjiangyuan National Park. China. *Ecol. Evol.* 9, 13278–13293. doi: 10.1002/ece3.5780

Daily, G. C., and Matson, P. A. (2008). Ecosystem services: from theory to implementation. *Proc. Natl. Acad. Sci. USA* 105, 9455–9456. doi: 10.1073/pnas.0804960105

Díaz, S., Settele, J., Brondizio, E. S., Ngo, H. T., Agard, J., Arneth, A., et al. (2019). Pervasive human-driven decline of life on Earth points to the need for transformative change. *Science* 366:eaax3100. doi: 10.1126/science.aax3100

Du, A., Cui, T., Song, T. Y., and Ouyang, Z. Y. (2020). International experiences of national park selection criteria and the inspirations to China. *Acta Ecol. Sinica* 40, 7231–7237. doi: 10.5846/stxb201911112380

Fan, Y. P., and Fang, C. L. (2020). Evolution process and obstacle factors of ecological security in western China, a case study of Qinghai province. *Ecol. Indic.* 117:106659. doi: 10.1016/j.ecolind.2020.106659

Fang, Y. P. (2013). Managing the three-rivers headwater region, china: from ecological engineering to social engineering. *Ambio* 42, 566–576. doi: 10.1007/s13280-012-0366-2

Gu, Y. Y., Zhang, F. L., Liang, X. Y., Liu, C., Xing, S. H., and Ingchun, C. (2020). Integration of natural reserves based on potential habitat protection of the Amur tiger Chinese. *J. Ecol.* 39, 1590–1599.

Guo, J., Zhao, X. Q., Wei, Z., Chen, Z., and Zhou, H. K. (2021). Progress, problems, and key directions for establishing the first national park demonstration

province in Qinghai. China. *Int. J. Geoherit. Parks* 2021:10. doi: 10.1016/j.ijgeop.2021.11.010

Han, Z., Song, W., Deng, X. Z., and Xu, X. L. (2018). Grassland ecosystem responses to climate change and human activities within the Three-River Headwaters region of China. *Sci. Rep.* 8:9079. doi: 10.1038/s41598-018-27150-5

Lin, H. L., and Zhang, F. L. (2020). Fragmentation and percolation thresholds in the degradation process of alpine meadow in the Three-River Headwaters region of Qinghai-Tibetan Plateau. China. *Rangeland. J.* 42, 171–177. doi: 10.1071/rj20005

Liu, H. L., Willems, P., Bao, A. M., Wang, L., and Chen, X. (2016). Effect of climate change on the vulnerability of a socio-ecological system in an arid area. *Glob. Plan. Chan.* 137, 1–9. doi: 10.1016/j.gloplacha.2015.12.014

Ma, T., Min, Q. W., Xu, K., and Sang, W. G. (2021). Resident willingness to pay for ecotourism resources and associated factors in sanjiangyuan national park. China. *J. Res. Ecol.* 12, 693–706.

Ma, T., Xu, K., Xing, Y. M., Shu, H., and Sang, W. G. (2020). Tendencies of residents in sanjiangyuan national park to the optimization of livelihoods and conservation of the natural reserves. *Sustainability* 12:5173. doi: 10.3390/su12125173

Mason, T. H. E., Pollard, C. R. J., Chimalakonda, D., Guerrero, A. M., Kerr-Smith, C., Milheiras, S. A. G., et al. (2018). Wicked conflict: using wicked problem thinking for holistic management of conservation conflict. *Conserv. Lett.* 11:e12460. doi: 10.1111/conl.12460

Mastrangelo, M. E., Perez-Harguindeguy, N., Enrico, L., Bennett, E., Lavorel, S., Cumming, G. S., et al. (2019). Key knowledge gaps to achieve global sustainability goals. *Nat. Sustain.* 2, 1115–1121. doi: 10.1038/s41893-019-0412-1

NREL (2013). *G-Range homepage. Natural Resources Ecology Laboratory*. Colorado: StateUniversity.

Shen, X. L., and Tan, J. X. (2012). Ecological conservation, cultural preservation, and a bridge between: the journey of shanshui conservation center in the sanjiangyuan region, qinghai-tibetan plateau, china. *Ecol. Soc.* 17:38. doi: 10.5751/es-05345-170438

Sheng, W. P., Zhen, L., Xiao, Y., and Hu, Y. F. (2019). Ecological and socioeconomic effects of ecological restoration in Chins's three rivers source region. *Sci. Total. Environ.* 650, 2307–2313. doi: 10.1016/j.scitotenv.2018.09.265

Sircely, J., Conant, R. T., and Boone, R. B. (2019). Simulating rangeland ecosystems with G-Range: model description and evaluation at global and site scales. *Rangeland Ecol. Manag.* 72, 846–857. doi: 10.1016/j.rama.2019.03.002

St John, F. A. V., Mason, T. H. E., and Bunnefeld, N. (2021). The role of risk perception and affect in predicting support for conservation policy under rapid ecosystem change. *Conserv. Sci. Pract.* 3:e316. doi: 10.1111/csp2.316

Su, H. Q., Wang, N., and Su, Y. (2021). The experience and its reference study of law enforcement system of Sanjiangyuan National Park pilot. *Biodiver. Sci.* 29, 304–306.

Thiault, L., Marshall, P., Gelcich, S., Collin, A., Chlous, F., and Claudet, J. (2018). Mapping social-ecological vulnerability to inform local decision making. *Conserv. Biol.* 32, 447–456. doi: 10.1111/cobi.12989

Thornton, P. K., Galvin, K. A., and Boone, R. B. (2003). An agro-pastoral household model for the rangelands of East Africa. *Agr. Syst.* 76, 601–622. doi: 10.1016/S0308-521X(01)00094-4

Wan, H. W., Li, H. X., Wu, J. H., and Liu, Y. P. (2021). Spatial distribution pattern in mammal and bird richness and their relationship with ecosystem services in Sanjiangyuan National Park. China. *J. Mt. Sci.* 18, 1662–1677. doi: 10.1007/s11629-020-6515-3

Wang, B. L., An, R., Jiang, T., Xing, F., and Ju, F. (2020). Image spectral resolution enhancement for mapping native plant species in a typical area of the three-river headwaters region, china. *Remote Sens.* 12:3146. doi: 10.3390/rs12193146

Wang, P., Wolf, S. A., Lassoie, J. P., Poe, G. L., Morreale, S. J., Su, X. K., et al. (2016). Promise and reality of market-based environmental policy in China: Empirical analyses of the ecological restoration program on the Qinghai-Tibetan Plateau. *Glob. Environ. Chang.* 39, 35–44. doi: 10.1016/j.gloenvcha.2016.04.004

Wu, J. Y., Wu, G. F., Zheng, T. L., Zhang, X. B., and Zhou, K. (2020). Value capturecapture mechanisms, transaction costs, and heritage conservation: a case study of Sanjiangyuan National Park. China. *Land Use Policy* 90, 4246–4246.

Xi, C. B., Chi, Y., Qian, T. L., Zhang, W. H., and Wang, J. C. (2020). Simulation of human activity intensity and its influence on mammal diversity in sanjiangyuan National Park. China. *Sustainability* 12:4601. doi: 10.3390/su12114601

Yang, M. Y., Dong, S. K., Dong, Q. M., Wang, P., Liu, W. T., and Zhao, X. Y. (2020). Cooperative grassland management practices promoted by land tenure system transformation benefit social-ecological systems of pastoralism on the Qinghai-Tibetan plateau. China. *J. Environ. Manage.* 261:110215. doi: 10.1016/j.jenvman.2020.110215

Yeh, E. T., Samberg, L. H., Gaerrang, H., Volkmar, E., and Harris, R. B. (2017). Pastoralist decision-making on the tibetan plateau. *Hum. Ecol.* 45, 333–343. doi: 10.1007/s10745-017-9891-8

Yu, R. Y., Yao, Y. J., Wang, Q., Wan, H., Xie, Z. J., Tang, W. J., et al. (2021). Satellite-derived estimation of grassland aboveground biomass in the three-river headwaters region of china during 1982-2018. *Remote Sens.* 13:2993. doi: 10.3390/rs13152993

Zhai, X. H., Liang, X. L., Yan, C. Z., Xing, X. G., Jia, H. W., Wei, X. X., et al. (2020). Vegetation dynamic changes and their response to ecological engineering in the sanjiangyuan region of china. *Remote Sens.* 12:4035. doi: 10.3390/rs12244035

Zhao, X. Q. (2021). The five integrative management strategies of Sanjiangyuan National Park. *Biodiver. Sci.* 29, 301–303.

Zhao, X. Q., Xu, T. W., Ellis, J., He, F. Q., Hu, L. Y., and Li, Q. (2020). Rewilding the wildlife in Sangjiangyuan National Park, Qinghai-Tibetan Plateau. *Ecosyst. Health Sust.* 6, 1–3. doi: 10.1080/20964129.2020.1776643

Zheng, D. F., Wang, Y. H., Hao, S., Xu, W. J., Lv, L. T., and Yu, S. (2020). Spatial -temporal variation and tradeoffs/synergies analysis on multiple ecosystem services: A case study in the Three-River Headwaters region of China. *Ecol. Indic.* 116:106494. doi: 10.1016/j.ecolind.2020.106494

Conflict of Interest: The authors declare that the research was conducted in the absence of any commercial or financial relationships that could be construed as a potential conflict of interest.

Publisher's Note: All claims expressed in this article are solely those of the authors and do not necessarily represent those of their affiliated organizations, or those of the publisher, the editors and the reviewers. Any product that may be evaluated in this article, or claim that may be made by its manufacturer, is not guaranteed or endorsed by the publisher.

Copyright © 2022 Su, Shen, Dong, Liu, Cheng, Wan and Liu. This is an open-access article distributed under the terms of the Creative Commons Attribution License (CC BY). The use, distribution or reproduction in other forums is permitted, provided the original author(s) and the copyright owner(s) are credited and that the original publication in this journal is cited, in accordance with accepted academic practice. No use, distribution or reproduction is permitted which does not comply with these terms.

frontiers in Plant Science

ORIGINAL RESEARCH
published: 17 January 2022
doi: 10.3389/fpls.2021.760551

Dynamic Disturbance Analysis of Grasslands Using Neural Networks and Spatiotemporal Indices Fusion on the Qinghai-Tibet Plateau

Fengli Zou[1], Qingwu Hu[1]*, Haidong Li[2], Jie Lin[3], Yichuan Liu[1] and Fulin Sun[4]*

[1] School of Remote Sensing and Information Engineering, Wuhan University, Wuhan, China, [2] Nanjing Institute of Environmental Sciences, Ministry of Ecology and Environment, Nanjing, China, [3] Collaborative Innovation Center of Sustainable Forestry in Southern China of Jiangsu Province, Nanjing Forestry University, Nanjing, China, [4] GeoScene Information Technology Co., Ltd., Beijing, China

OPEN ACCESS

Edited by:
Jian Sun,
Institute of Tibetan Plateau Research, Chinese Academy of Sciences (CAS), China

Reviewed by:
Xuyang Lu,
Institute of Mountain Hazards and Environment (IMHE), Chinese Academy of Sciences (CAS), China
Yuke Zhou,
Institute of Geographic Sciences and Natural Resources Research, Chinese Academy of Sciences (CAS), China

***Correspondence:**
Fengli Zou
zoufengli@whu.edu.cn
Qingwu Hu
huqw@whu.edu.cn

Specialty section:
This article was submitted to Functional Plant Ecology, a section of the journal Frontiers in Plant Science

Received: *18 August 2021*
Accepted: *29 November 2021*
Published: *17 January 2022*

Citation:
Zou F, Hu Q, Li H, Lin J, Liu Y and Sun F (2022) Dynamic Disturbance Analysis of Grasslands Using Neural Networks and Spatiotemporal Indices Fusion on the Qinghai-Tibet Plateau. Front. Plant Sci. 12:760551. doi: 10.3389/fpls.2021.760551

Grassland is the vegetation type with the widest coverage on the Qinghai-Tibet Plateau. Under the influence of multiple factors, such as global climate change and human activities, grassland is undergoing temporal and spatially different disturbances and changes, and they have a significant impact on the grassland ecosystem of the Qinghai-Tibet Plateau. Therefore, timely and dynamic monitoring of grassland disturbances and distinguishing the reasons for the changes are essential for ecological understanding and management. The purpose of this research is to propose a knowledge-based strategy to realize grassland dynamic distribution mapping and analysis of grassland disturbance changes in the region that are suitable for the Qinghai-Tibet Plateau. The purpose of this study is to propose an analysis algorithm that uses first annual mapping and then establishes temporal disturbance rules, which is applicable to the integrated exploration of disturbance changes in highland-type grasslands. The characteristic indexes of greenness and disturbance indices in the growing period were constructed and integrated with deep neural network learning to dynamically map the grassland for many years. The overall accuracy of grassland mapping was 94.11% and that of Kappa was 0.845. The results show that the area of grassland increased by 11.18% from 2001 to 2017. Then, the grassland disturbance change analysis method is proposed in monitoring the grassland distribution range, and it is found that the area of grassland with significant disturbance change accounts for 10.86% of the total area of the Qinghai-Tibet Plateau, and the disturbance changes are specifically divided into seven types. Among them, the type of degradation after disturbance mainly occurs in Tibet, whereas the main types of vegetation greenness increase in Qinghai and Gansu. At the same time, the study finds that climate change, altitude, and human grazing activities are the main factors affecting grassland disturbance changes in the Qinghai-Tibet Plateau, and there are spatial differences.

Keywords: Qinghai-Tibetan Plateau, grassland, temporal-deep neural network classification, disturbance, change analysis

INTRODUCTION

The dynamic change of vegetation cover is the main driving force of global environmental change (Avissar et al., 2002). Dynamic understanding and monitoring of the distribution of surface vegetation coverage is an important factor for environmental research (Schipper et al., 2014). The grassland ecosystem is one of the most widely distributed types of terrestrial ecosystems, covering about 37% of the earth's terrestrial area (Piao et al., 2004; O'Mara, 2012) and playing an important role in the global ecosystem balance with ecosystem services, such as climate regulation, soil and water conservation, sand fixation, soil improvement, and biodiversity maintenance, especially in ecologically fragile plateau areas (Xie et al., 2008; Fan et al., 2012; Yue-Jun et al., 2012; Bernacchi and Vanloocke, 2015). Grassland is the most important vegetation type on the Qinghai-Tibet Plateau, accounting for 70% of the total vegetation area (Wang et al., 2013). Because of its excellent pasture quality, it is also one of the important grassland animal husbandry bases in China (Kemp et al., 2013). However, in recent years, under the dual effects of climate change and human activities, large-scale degradation of grassland on the Qinghai-Tibet Plateau has directly affected its ecological service functions. This situation restricts the sustainable development of alpine grassland animal husbandry, but the temporal and spatial dynamics of grassland degradation are not comprehensive and timely for environmental managers (David et al., 2008). Therefore, timely and accurate access to dynamic information on natural grassland is essential to realize the ecological sustainable development of the Qinghai-Tibet Plateau (Zavaleta et al., 2003).

In recent years, remote sensing has been widely used in regional and global vegetation cover monitoring. For the Qinghai-Tibet Plateau, where ground monitoring data is difficult to obtain, environmental monitoring combined with remote sensing image mapping has become more important (Xiao et al., 2009; Cornelius et al., 2013; Hansen et al., 2013). As a result, a large number of global land cover data sets exist, such as Global Land Cover 2000 (GLC2000) (Bartholome and Belward, 2005), MODIS's Land Cover Collections (MAD12C5) (Friedl et al., 2010), and MERIS's Global Cover (Arino et al., 2008), with resolution ranging from 300 m to 1 km. However, some studies also highlight the inconsistencies and uncertainties between these global land cover maps (Fritz et al., 2010; Tchuenté et al., 2011). The main problems are low accuracy and low levels of agreement between each other (Xiang et al., 2013). This makes it very inaccurate to obtain regional, high-precision, long-term dynamic grassland mapping based on global land cover data sets. We can improve land cover mapping based on remote sensing by using smarter algorithms, more suitable image acquisition time, and improved classification categories to make it more suitable for land cover research in characteristic areas (Tchuenté et al., 2011).

Research shows that a remote sensing index based on the time series of the year is an important method to effectively obtain vegetation phenological characteristics and can be used for land cover mapping and change monitoring (Cohen et al., 2010; Jamali et al., 2015; Ahmed et al., 2017; Hirschmugl et al., 2017). Methods of land use mapping and vegetation change detection based on remote sensing images are generally divided into two categories: machine learning algorithms and methods based on specific knowledge (Xie et al., 2008; Yin et al., 2020). With the development of remote sensing multisource big data, various machine learning algorithms are used more and more widely (Zhang et al., 2016; Qiu et al., 2017). However, in some areas where it is difficult to obtain sufficient training data and there is heterogeneity between different years of surface coverage, the superiority of machine learning algorithms is somewhat limited (Waldner et al., 2015; Shih et al., 2017). The method based on specific knowledge focuses on feature mining and geographic understanding, which can reduce dependence on a large amount of training data and overcome the drawbacks of machine learning algorithms to a certain extent. Knowledge-based methods mainly improve the detection and classification of remote sensing changes by constructing variables and proposing rules and hypotheses and are increasingly used for surface vegetation mapping and monitoring; however, these methods are limited by a fixed threshold of characteristic indicators (Mahyou et al., 2016; Qi et al., 2017). Therefore, the combination of prior knowledge, such as vegetation phenology, and machine learning models is one of the effective ways to improve land cover type mapping and change analysis based on remote sensing (Feng et al., 2021; Wang et al., 2021). However, long-term dynamic mapping and change analysis based on remote sensing images are a challenge for a large number of multisource data processing calculations (Mutanga and Kumar, 2019). Currently, free cloud platforms provide new methods for geospatial analysis. Google Earth Engine (GEE) avoids the preprocessing of large amounts of data, provides JavaScript and Python coding environment, facilitates data calculation, and improves the efficiency of application research based on remote sensing data (Liu et al., 2020).

So far, a large number of studies analyzes the grassland changes in the Qinghai-Tibet Plateau. Among them, the research based on remote sensing data is mainly based on the interannual trend changes of vegetation indicators, such as single NDVI and NPP, and the methods mainly include the NDVI trend threshold determination, trend residual, and vegetation net primary productivity evaluation methods (Genxu et al., 2004; Liang et al., 2007; Bian et al., 2008; Huilan and Yingjun, 2016; Chong-Yang et al., 2019). The study finds that climate change has a significant impact on the productivity of the entire Qinghai-Tibet Plateau (Zhang et al., 2007; Peng et al., 2012). In arid and semiarid regions, NDVI is related to rainfall and temperature and has strong spatial heterogeneity (Sun et al., 2016). In the source region of the Yangtze River, overgrazing causes serious grassland degradation, but at the same time (Li et al., 2013), some studies show that light intensity grazing has a positive effect on the productivity of alpine meadows (Zhang et al., 2015). These seemingly contradictory results indicate that the growth of grassland has a certain anti-disturbance ability to adapt to the environment, making the process of grassland change relatively complex and not a simple positive–negative trend change (Huang et al., 2016). Therefore, it is necessary to realize a more timely and comprehensive analysis of the grassland disturbance change process, especially in ecologically fragile plateau regions.

Based on the mapping of grassland dynamic distribution, this study comprehensively applies greenness and disturbance change indicators and further explores the analysis of the grassland disturbance change process in the Qinghai-Tibet Plateau without setting a subjective evaluation threshold. We aim to propose a comprehensive analysis algorithm that is applicable to the alpine cold region, which is first Annual Mapping and then establishes Temporal Disturbance Rules. Specifically (AMTDR). This study mainly includes three tasks: (1) to develop a novel grassland mapping algorithm by exploring the integration of the greening abundance index and disturbance index time-series characteristic deep neural network method that can be applied to the Qinghai-Tibet Plateau; (2) on the basis of dynamic mapping changes of grassland, to obtain multiyear grassland distribution maps and propose analysis rules for grassland disturbance changes in the Qinghai-Tibet Plateau from 2001 to 2017 with combining the trend changes of the greening abundance and disturbance indices; and (3) to explore the factors affecting the grassland disturbance changes in the Qinghai-Tibet Plateau from multiple perspectives, such as nature and humans.

MATERIALS AND METHODS

Study Area

The Qinghai-Tibet Plateau (26°50′–39°19′N, 78°25′–103°04′E) includes the Tibet Autonomous Region; Qinghai Province; and parts of Sichuan Province, Gansu Province, Xinjiang Uygur Autonomous Region, and Yunnan Province. With an average altitude above 4,000 m, it is known as the "roof of the world" and is the highest plateau with the highest average altitude in the world (**Figure 1**). In the unique alpine climate, from southeast to northwest, there are vegetation types, such as alpine meadow, alpine grassland, alpine semidesert, and alpine desert. Grassland resources are extremely rich, accounting for one third of the total grassland area in the country. It has been one of the important pastoral areas in China since ancient times. Among them, the eastern alpine meadow is not only the essence of grassland animal husbandry, but also the birthplace of rivers such as the Yellow and Yangtze Rivers. As a unique, ecologically sensitive, and fragile area in the world, the Qinghai-Tibet Plateau has a significant impact on global climate change and is also an important ecological barrier for China.

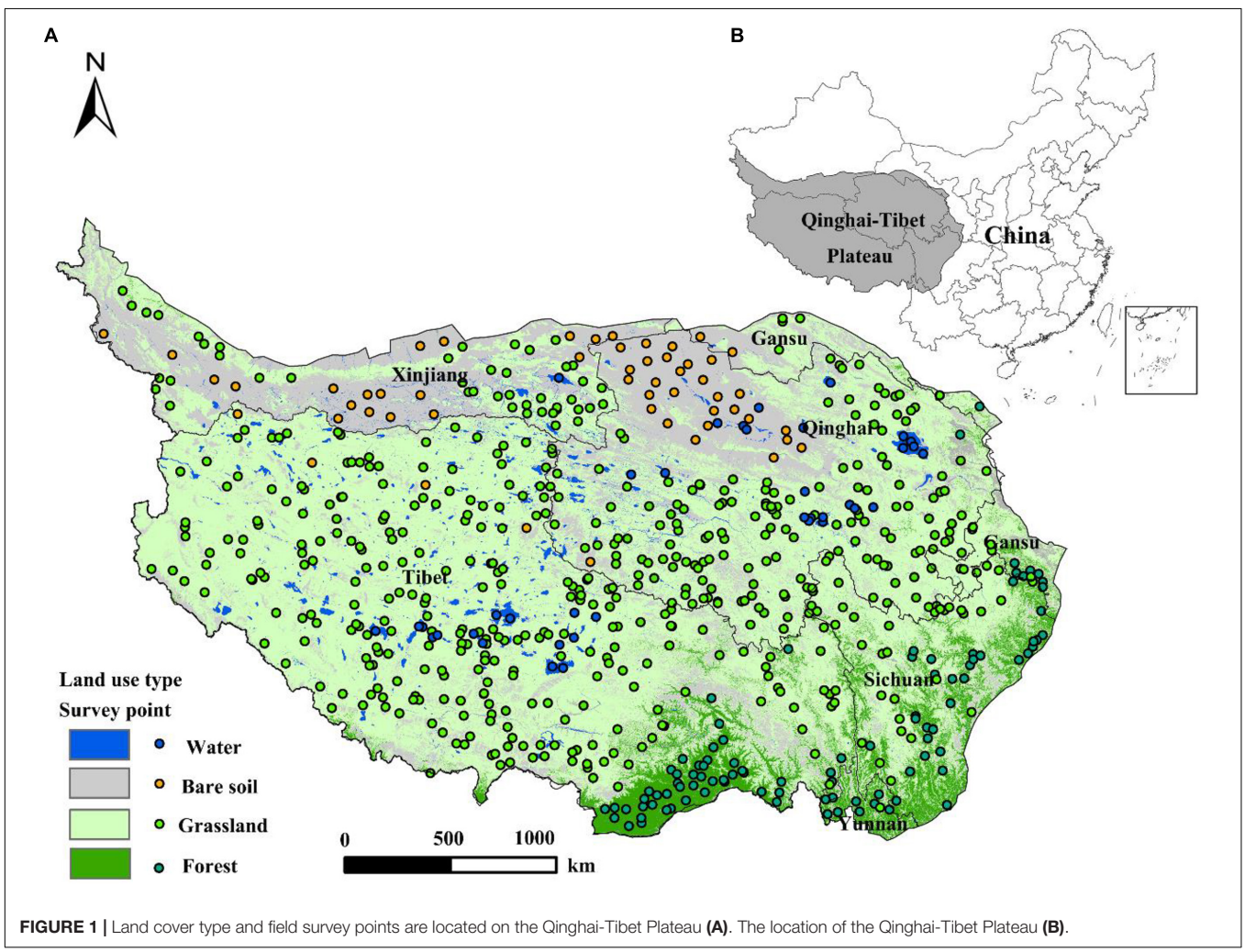

FIGURE 1 | Land cover type and field survey points are located on the Qinghai-Tibet Plateau **(A)**. The location of the Qinghai-Tibet Plateau **(B)**.

Data Sources and Preparation

The MOD09A1 collection 6 data of the Qinghai-Tibet Plateau region from 2001 to 2017, synthesized for 8 days and with a spatial resolution of 500 m was used. The images use a quality layer (QA band) to exclude any 8-day composite images contaminated by clouds and perform geometric correction by pixel. The geo-reference datum is Mercator (UTM) projection and WGS 84 datum. In this paper, the linear interpolation method is used to encrypt the data and produce the daily data of 365 days a year.

Multiple spectral indices are calculated using MODIS time series data sets. Near infrared reflectance of terrestrial vegetation (NIRv) is the product of total scene NIR reflectance (NIR_T) and the normalized difference vegetation index (NDVI). It can deal with the challenges of mixed pixels and the complexity of determining the photosynthetic capacity of vegetation (Badgley et al., 2017). Brightness, greenness, and wetness were derived based on the first, second, and third tasseled cap transformation (TC1 TC2 TC3) (Zhang et al., 2002).

Meteorological data were derived from the "grid data of temperature and precipitation over the QTP and surrounding areas from 2001 to 2017" released by the National Qinghai-Tibet Plateau Scientific Data Center[1].

Reference points for the main land cover types of the Qinghai-Tibet Plateau are based on field surveys from July 2012 to September 2017 and visual interpretation of Google Earth's high-resolution subimages: The total reference point is 696, of which grassland is 523, water is 24, bare soil is 53, and forest is 96, used for verifying the overall accuracy of grassland mapping (see locations in **Figure 1**).

Other data sets include stock census data and land cover data. Livestock census data is downloaded from the National Bureau of Statistics of China (NSBC)[2], and they were collected through sampling statistics. The land use data used in this thesis include 2001, 2005, and 2010 data from the 30-m resolution GlobaLand30 product[3] with an overall accuracy of 80.3% (Chen et al., 2015). Copernicus Global Land Cover CGLS-LC100 series 3 products 2015, 2017 data[4] with overall accuracy at the continental level is around 80% with the highest accuracy of 83.7% for Asia (Buchhorn et al., 2020). GlobaLand30 and CGLS-LC100 series 3 land use data are better than the MODIS-MCD12Q1 land use product. In this paper, the land use data of 2001, 2005, 2010, 2015, and 2017 are resampled by 500. In the study area, 3,000 stable points without land use type change during 2001–2017 were randomly selected as the training data of the neural network deep learning model. Due to the particularity of the natural environment of the Qinghai-Tibet Plateau, the area suitable for crops only accounts for 0.9% of the area. Therefore, we aggregated the land cover map of 1:1 million land use survey results in 2001 into 500 m, which was used as the mask data to obtain the basic data containing only natural vegetation types. It is a natural land cover area and is further used for grassland identification and disturbance analysis.

[1]http://www.tpdc.ac.cn/zh-hans/data/c954daad-6086-4edd-a6c5-f69c581e5c31/

[2]http://www.stats.gov.cn/english/

[3]http://www.globallandcover.com/

[4]https://developers.google.com/earth-engine/datasets/catalog/COPERNICUS_Landcover_100m_Proba-V-C3_Global?hl=en

Methodology

In this study, a comprehensive analysis algorithm is proposed for alpine regions by first AMTDR (**Figure 2**). Based on the fusion of knowledge-based time-series phenological features and neural network methods to achieve annual dynamic monitoring and mapping of grassland, the process of long time series grassland disturbance change is quantified and mined. It includes the following procedures: data preprocessing, construction of feature metrics, classification algorithms and validation, perturbation change rules, and influence factor analysis. The whole process is implemented based on Matlab, GEE[5], and Python.

Developing Indices of Greening Abundance and Disturbance

Due to the geographical characteristics of the alpine plateau in the Qinghai-Tibet Plateau, the annual phenology of all vegetation types in this area is one season, the main growth period is May to September (Zou et al., 2020), and the green coverage of different vegetation types during the growth period is relatively large (**Figure 3**). Therefore, this study obtains the greening abundance (GA) indicator by calculating the average value of the time profile between the maximum and minimum values of the NIRv indicator in the time series of the year from May to September.

Disturbance index (DI) is based on the linear combination of the three components of the tasseled cap transformation (Healey et al., 2005). It was originally used to detect forest disturbances, and then the algorithm was further adapted by looking for decadal changes in DI (Healey et al., 2005; Masek et al., 2008). In this study, we started with the original method (Healey et al., 2005) and calculated DI based on the standardized values (brightness, greenness, and wetness) of the tassel cap indicators,

[5]https://earthengine.google.com

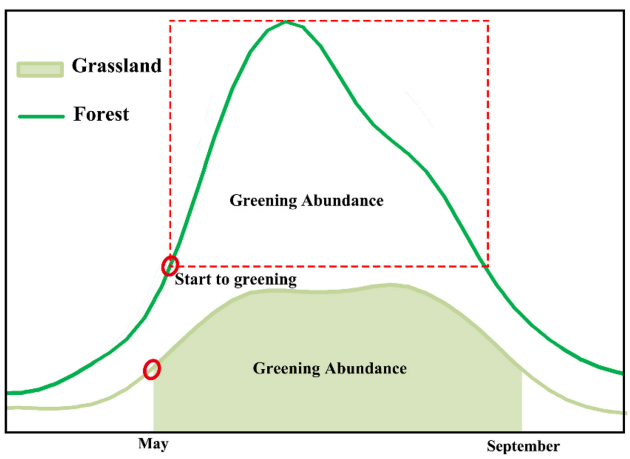

FIGURE 3 | Time profile of annual growth knowledge-based features of NIRv grassland and forest in the Qinghai-Tibet Plateau region.

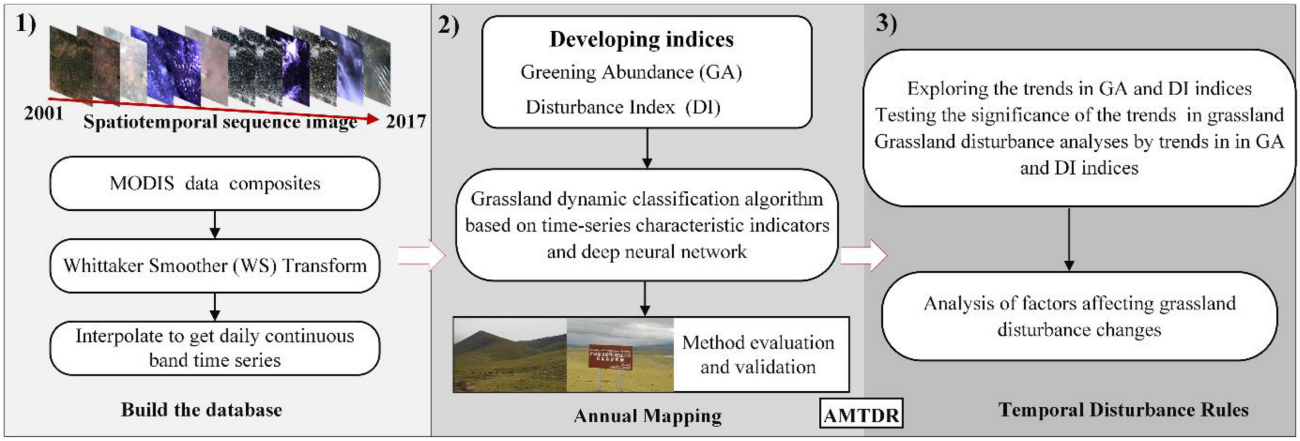

FIGURE 2 | Methodological overview.

where the average and standard deviation of these indicators are based on a standardized data set adapted to the vegetation of the Qinghai-Tibet Plateau. The standard normalization formulas are as follows:

$$B_r = (B - B_u)/B_\sigma$$
$$G_r = (G - G_u)/G_\sigma$$
$$W_r = (W - W_u)/W_\sigma$$

Among them, B_r, G_r, and W_r are the standardized tasseled cap brightness, greenness, and wetness components. Therefore, the calculation formula of DI is:

$$DI = B_r - (G_r + W_r).$$

When the grass is disturbed, reducing the humidity and greenness and increasing the brightness make the DI value higher. For example, the grassland in the grazing area has a higher greenness and humidity at the beginning, and the surface is less exposed. When the grazing intensity increases rapidly, the humidity and greenness decrease, and the brightness increases significantly. If the grazing is controlled for a period of time thereafter, the greenness degree and humidity are restored to a certain extent. If the degree of grazing continues to increase, the greenness and humidity are further reduced.

The main vegetation types on the Qinghai-Tibet Plateau are natural grassland and forest, of which grassland accounts for about 70% of the area of the Qinghai-Tibet Plateau, and other land covers are desert-type bare soil and water (Tian et al., 2014). In this study, we obtained 174 site locations for the four main types of land cover types, including grassland, forest, bare soil, and water, in the Qinghai-Tibet Plateau from field investigation and visual interpretation by Google Earth and obtained the time series of characteristics land types within the year that are stable on GA and DI indicators (**Figure 4**). When the vegetation is disturbed, increasing the brightness and reducing the greenness and wetness result in a higher DI value (Healey et al., 2005). Based on the GA calculated during the growing season, the greening abundance characteristics of different land cover types are further prominent.

Grassland Classification

Deep Neural Network Model

Deep neural networks (DNN) are the foundation of deep learning. Neural networks are based on extensions of perceptrons, and DNN can be understood as neural networks with many hidden layers. DNN is also referred to as multilayer perceptron (MLP). According to the position of different layers of DNN, the neural network layer inside DNN can be divided into three types: input, hidden, and output layers. The layers are fully connected; that is, any neuron in layer 1 must be connected to any neuron in layer i +1. Although DNN looks very complex, for small local models, it is the same as a perceptron, that is, a linear relationship $z = \sum wixi + b$ plus an activation function $\delta(z)$. Because there are many layers of DNN, our linear relationship coefficient W and the number of bias B also contain a lot. The neural network learns to represent the present state by some indicator. Then, take this index as the benchmark to find the optimal weight parameters. The neural network takes an index as a clue to find the optimal weight parameters. The index used in the learning of neural networks is called the loss function. This loss function can be represented by any function, and cross-entropy error is chosen in this paper. Cross-entropy error is also often used as a loss function. The loss can be described as

$$\text{loss}(x, \text{class}) = -\log(\exp(x[\text{class}])/\sum j\exp(x[j])$$
$$= -x[\text{class}]\log(\sum \exp(x[j])).$$

The process of the DNN model trained in this paper is as **Figure 5**. In this paper, a total of 3,000 sample data points were used for DNN model training, 80% of which were selected for model training and 20% for model accuracy verification.

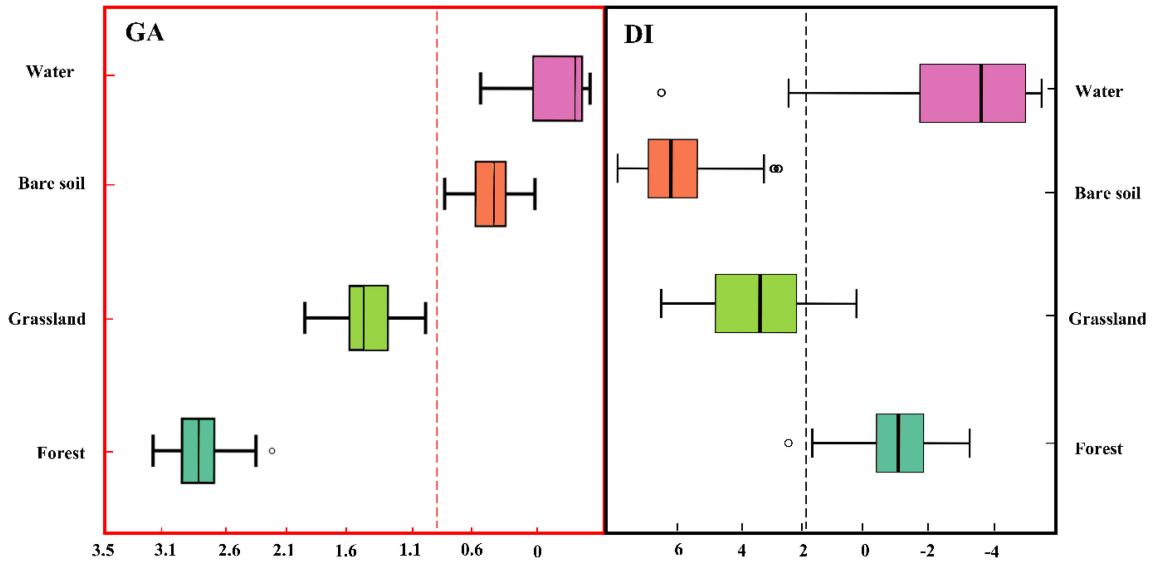

FIGURE 4 | Different characteristics of natural land cover types on the Qinghai-Tibet Plateau in GA and DI indicators.

The accuracy of the model was 90.74%. Sample data for model training can be shared as accessible data through GEE.

Deep Neural Network Model Classification

The dynamic grassland mapping algorithm was developed by combining the characteristic indices representing the regional vegetation cover types on the Qinghai-Tibet Plateau with the deep network (**Figure 6**). The implementation process and part of pseudocode are as follows:

1. # Name the output training and test set
2. trainFilePrefix = 'Training_data'
3. testFilePrefix = 'Testing_demo'
4. # Training and testing data attributes (CLASS; Grassland, others (water body, forest land, bare soil), and contents of bands are 5*3 latitude attribute indexes
5. featureNames = list(bands)
6. featureNames.append(label)
7. trainingTask = image.select(bands).sampleRegions({
9. collection = training,
10. description = ' Training set ',

Training DNN model in Pytorch

11. def DNN (trainDataset_dict, label)
12. DNNModel (trainDataset)
13. # Test the DNN model
14. model.evaluate(testDataset)

Classification Algorithm Accuracy Verification

Accuracy assessment is based on reference sites. The sources of reference data are field surveys and high-resolution images of Google Earth. A random stratified sample design was used to evaluate the results of grassland recognition. A total of 696 reference points were collected, including one for grassland and one for other land cover types. The overall verification accuracy was 94.11%. Kappa was 0.845. And More specific verification information reference (**Table 1**).

Grassland Disturbance Analysis Method

When the grassland has a disturbance change, the DI value changes accordingly, so when the grassland has a disturbance change on an interannual basis, the DI shows an interannual trend change. When the grassland is disturbed to different degrees, its greening abundance shows different changes, corresponding to the trend of GA. To be able to analyze the interannual disturbance change form of grassland more accurately, we combined analysis of the possible change trend of DI and GA. The trend change range of the DI and GA indices is calculated according to the non-parametric Sen method. If the slope of Sen is obviously not equal to zero, there is a trend in the time series. At the same time, the MK test is used to quantify the degree of change in DI and GA index trends. When the DI trend is significant, it is quantified as a disturbance change. At the same time, when the corresponding GA trend is significant, it is quantified as a significant change in greenness after disturbance. When the trend of the GA indicator is not significant, it is quantified as the potential change of greenness after disturbance. The specific analysis rules are shown in **Figure 7**.

Because the growth of grassland has strong anti-interference, when the intensity of the disturbance of the grassland is within its anti-interference degree, although the green coverage changes in a trend, it does not change significantly. Define this potential change after disturbance: According to the positive and negative trends of green coverage, the types of potential changes can be divided into potential recovery after disturbance, potential degradation after disturbance, and potential greenness increase. When the intensity of the disturbance change in the grassland causes a significant trend change in the green coverage, this situation is judged as the type of postdisturbance

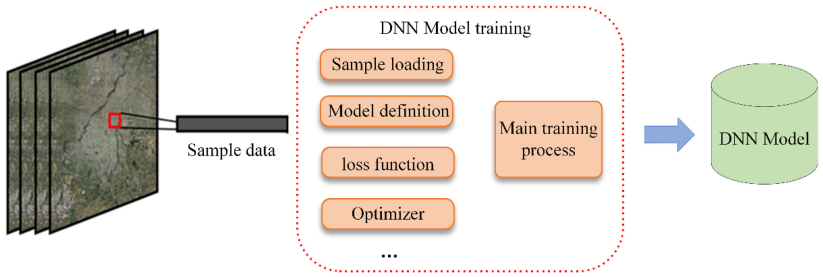

FIGURE 5 | DNN model training process.

change. According to the positive or negative trend of the green coverage, the significant change type can be divided into recovery after disturbance, degradation, and greenness increase after disturbance.

RESULTS

The Temporal and Spatial Distribution Map of Grassland

The grassland mapping algorithm based on GA and DI time series characteristic indices and deep network learning was applied to the multiyear grassland mapping, and the continuous dynamic distribution of grassland on the Qinghai-Tibet Plateau was obtained from 2001 to 2017 (**Figure 8**). The total area of the Qinghai-Tibet Plateau in the selected study area is 272.49 × 10^4 km^2. The grassland on the Qinghai-Tibet Plateau monitored by the DNN algorithm is mainly distributed in most areas of Qinghai and Tibet. The total area has increased from 165.25 × 104 km^2 in 2001 to 174.34 × 104 km^2 in 2007, 176.61 × 104 km^2 in 2012, and 183.72 × 104 km^2 in 2017; its spatial distribution is shown in **Figures 8A–D**; the overall area increases year by year and also fluctuates to a certain extent.

From 2001 to 2017, the grassland area of the Qinghai-Tibet Plateau was greater than 60% of the entire region. From 60.65% in 2001 to 67.42% in 2017, the area increased by 11.18% in 17 years. Although the overall area is increasing, there are large fluctuations in each year, indicating that the grassland area is expanding, and there are also certain disturbances (**Figure 9**).

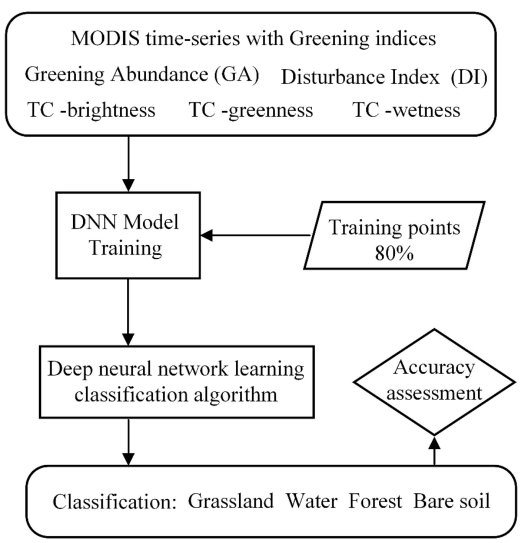

FIGURE 6 | Flow chart of grassland classification.

TABLE 1 | Accuracy assessment using ground reference sites.

	Total	Grassland	Other land cover types	Product accuracy (%)
Grassland	523	498	25	95.22
Other land cover types	173	16	157	90.75
User accuracy (%)		96.89	86.26	
Overall accuracy (%)	94.11			
Kappa	0.845			

Spatiotemporal Analysis of Grassland Disturbance Changes From 2001 to 2017

According to the above disturbance analysis method, the distribution map of grassland disturbance changes in the Qinghai-Tibet Plateau region from 2001 to 2017 is obtained (**Figure 10**). It can be found that there are obvious spatial differences in the perturbation changes of grassland in 17 years. The regions with disturbance changes are mainly distributed in Tibet in the southwest of the Qinghai-Tibet Plateau, Qinghai in the northeast region and Gansu in the north. Among them, the types of degradation after the disturbance mainly occur in the Tibet region. In particular, the grasslands in central and southern Tibet are not only degraded in a large area, but also with a high degree of degradation. On the contrary, in Qinghai and Gansu, the main types of vegetation greenness increase are the main types. The vegetation coverage in this area is relatively sparse, and there are many desertification areas, but the grassland disturbance change type is a trend toward increasing greenness, indicating that, in this area, the ecological environment has improved to some extent in recent years. From 2001 to 2017, the grassland area in the study area with significant disturbance changes was 29.59 × 10^4 km^2, accounting for 10.86% of the

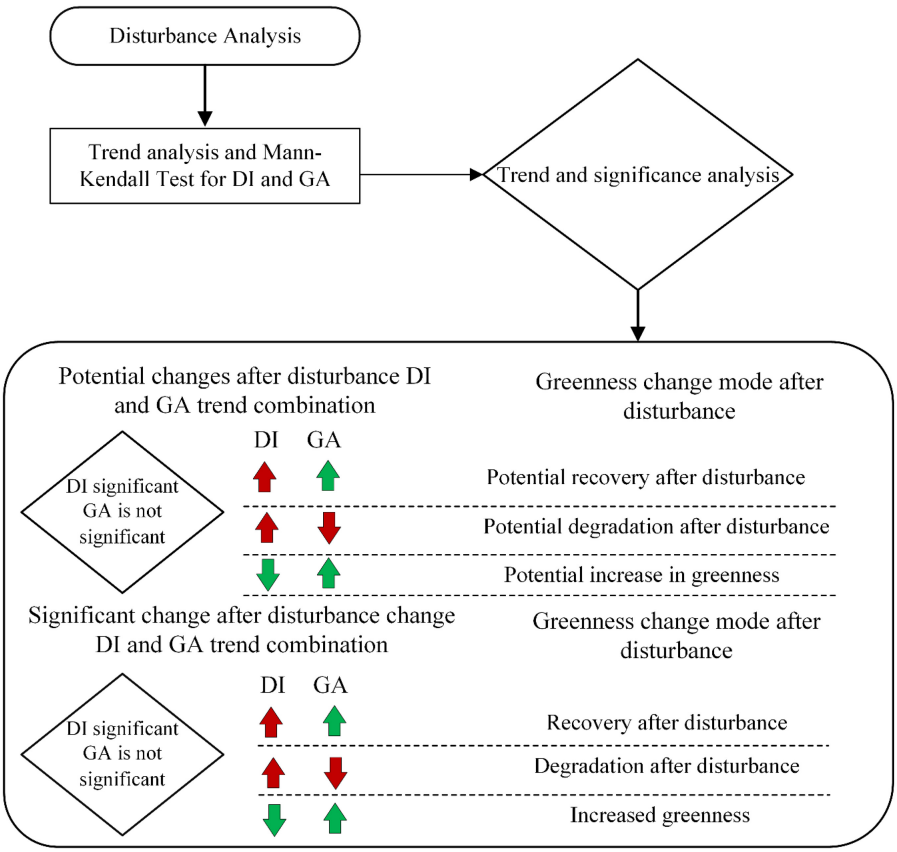

FIGURE 7 | Establish analysis rules for grassland disturbance changes and corresponding change types in DI and GA indices.

total area of the Qinghai-Tibet Plateau. In the areas where there were disturbance changes, the recovery after disturbance accounted for 10.4%, mainly in the northern part of Tibet; the potential recovery after disturbance accounted for 31.7%, which is the largest change type, indicating that grassland has a certain potential for recovery from disturbance, mainly in the northern and central northern parts of Tibet. Degradation after disturbance accounted for 4.7%, mainly distributed in the southwestern part of the Qinghai-Tibet Plateau and central and northwestern parts of Tibet. Grassland in this area is significantly degraded and needs timely and effective attention and improvement; the potential degradation after disturbance accounts for 27.1%, which is also a large proportion. It is distributed in the southwestern part of the Qinghai-Tibet Plateau and most of Tibet. If these areas are effectively improved, there is still a certain possibility of recovery; the increased in greenness and the potential increase in greenness accounted for 11.8 and 6.7% respectively, mainly distributed in areas with relatively low vegetation coverage in the northern Qinghai-Tibet Plateau, such as Xinjiang, Qinghai, and Gansu. The area that turned into water accounted for 7.5%, mainly distributed on the edge of the lake distribution area in the middle of the Qinghai-Tibet Plateau, indicating that some lakes on the Qinghai-Tibet Plateau have a tendency to expand.

Analysis of Influence Factors of Grassland Disturbance

The Impact of Climate on Grassland Disturbance

Due to the special geographical environment of the Qinghai-Tibet Plateau, the climate in the region has strong spatial heterogeneity. According to the above analysis (**Figure 9**), it can be found that the areas of grassland disturbance change in the Qinghai-Tibet Plateau are mainly distributed in Tibet and Qinghai provinces. Therefore, we take the main regions of Qinghai and Tibet as examples to calculate the changes in climate trends from 2001 to 2017 (**Figure 11**) and do a correlation analysis with the DI change trend of the corresponding grassland. In terms of precipitation, the precipitation in Tibet is in the range of 294.88∼494.23 mm with an average of 382.95 mm; the precipitation in Qinghai Province is in the range of 273.11∼471.6 mm with an average of 336.35 mm. In terms of temperature, the temperature in Tibet is in the range of −0.36∼1.79°C with an average of 0.47°C. The temperature in Qinghai Province is in the range of −1.71∼−0.47 with an average of −1.21°C. From 2001 to 2017, the temperature and precipitation in Tibet and Qinghai show an overall upward trend. The correlation coefficient between precipitation trend and grassland disturbance change trend in Tibet is 0.33, and the correlation coefficient between

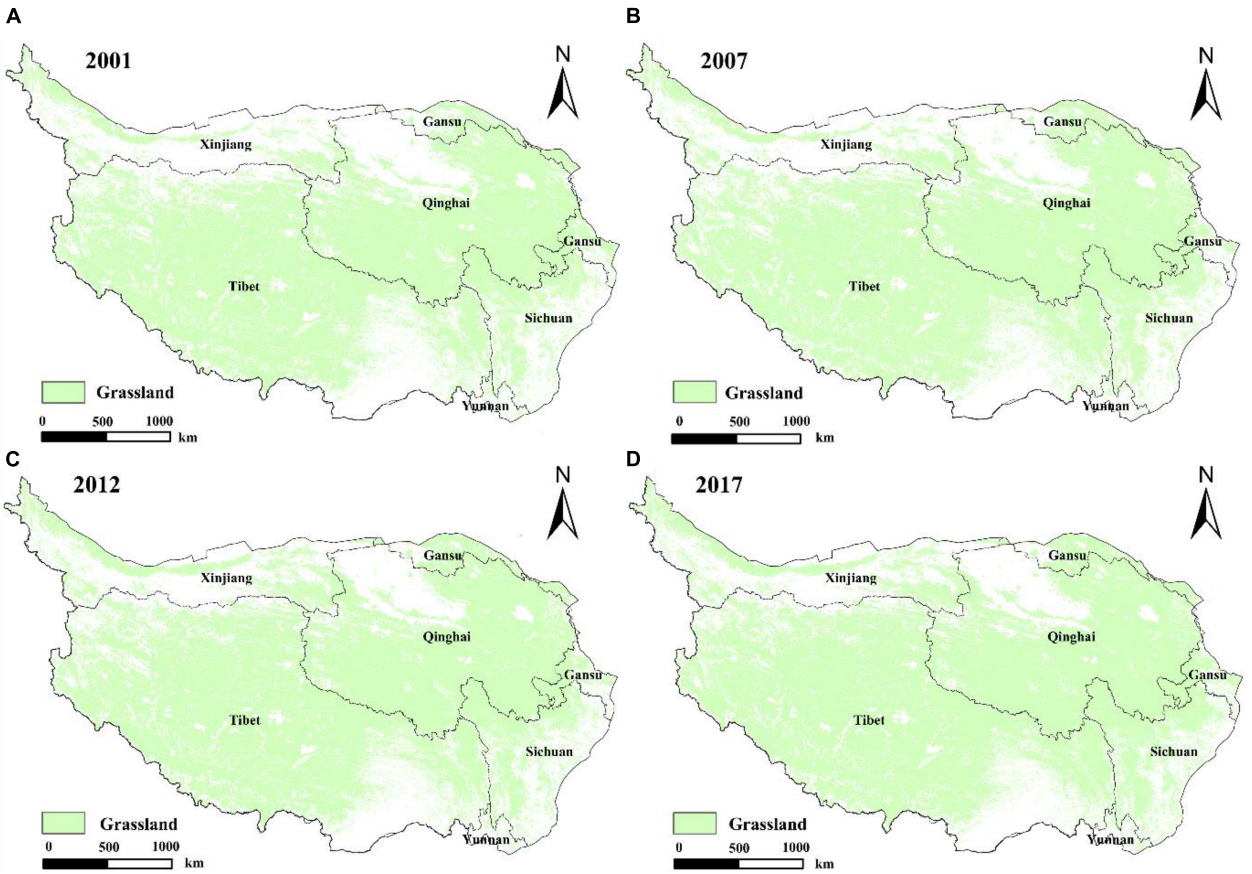

FIGURE 8 | Grassland spatial distribution map from 2001 to 2017.

precipitation trend and grassland disturbance change trend in Qinghai is 0.122; the correlation is less than 0.5, indicating that the precipitation and grassland disturbance change have a certain correlation but the impact is small. The correlation between temperature and the grassland disturbance change trend in Tibet is 0.66, and the change trend of temperature and grassland disturbance in Qinghai Province is 0.23. The correlation between temperature in Tibet and Qinghai on grassland disturbance is higher than precipitation, especially in Tibet, which is located in the southern Qinghai-Tibet Plateau. All in all, in the main areas of the Qinghai-Tibet Plateau, climate is one of the factors affecting grassland disturbance changes, and there is spatial heterogeneity. In the southern part of the Qinghai-Tibet Plateau, temperature has a greater impact on the disturbance of grassland, whereas precipitation has a small impact on the disturbance of grassland. In the northern part of the Qinghai-Tibet Plateau, both temperature and precipitation have a small impact on the disturbance and change of grassland, but the same is the greater impact of temperature. Therefore, temperature is the main factor affecting grassland disturbance changes among climate factors, and it has a greater impact on the southern part of the Qinghai-Tibet Plateau. The rising trend of temperature and precipitation in the northern Qinghai-Tibet Plateau is one of the main reasons for the increase in grassland greenness. However, the types of grassland changes in the southern Qinghai-Tibet Plateau after disturbance are complex. Climate factors are not the only factors affecting grassland disturbance changes, and further exploration and analysis are needed.

Influence of Elevation on Grassland Disturbance

As the altitude changes, the vertical spatial distribution and distributed clustering of the grassland DI index in the Qinghai-Tibet Plateau is shown in **Figures 12A,B**. Combining **A** and **B** in **Figure 12**, we can find that the DI value of grassland increases with different heights of sea waves, and the altitude varies from < 1,000 to > 6,000, showing different trends. When the altitude is less than 1,000 m, the trend of grassland disturbance index decreases with the increase of altitude, and the value of each year fluctuates slightly. When the altitude is between 1,000 and 2,500 m, the trend of grassland disturbance index increases with the increase in altitude, and the fluctuation of each year begins to increase. When the altitude is greater than 3,000 m, the change trend of the disturbance change index of the grassland presents an unstable fluctuating change that first decreases, then rises, and then decreases, and when the altitude is higher than 4,500 m, the DI value fluctuates in different years at the same altitude and is also larger. It

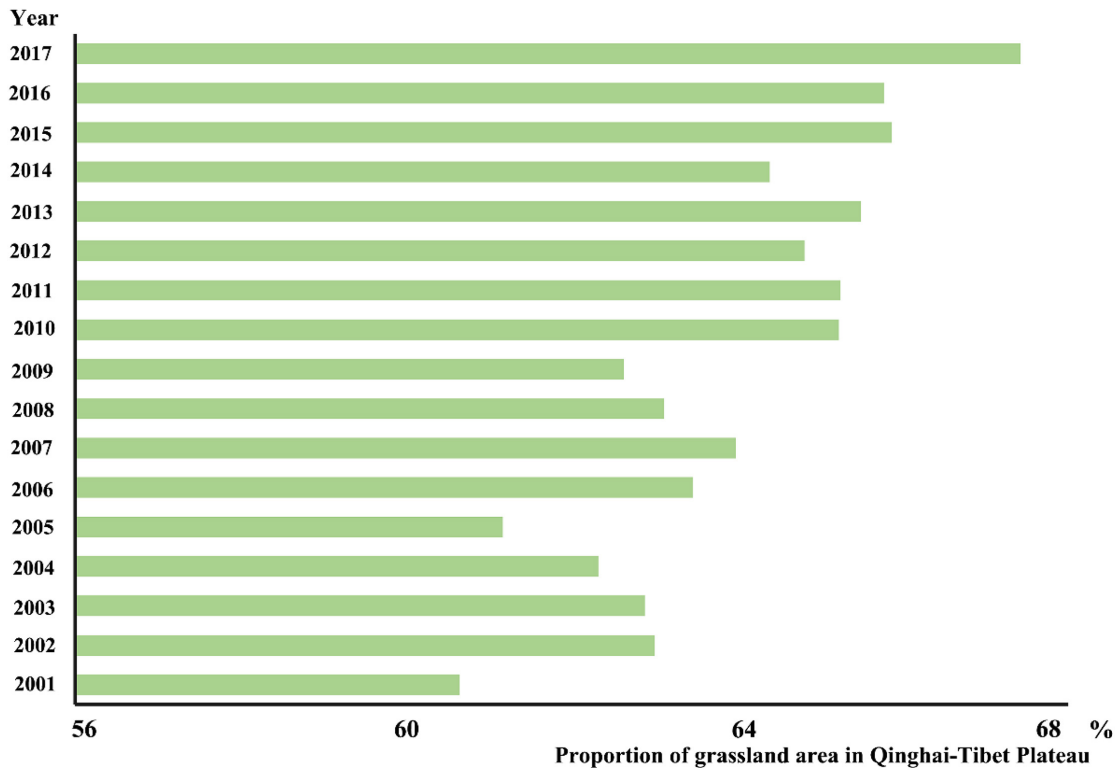

FIGURE 9 | The percentage of grassland area in the Qinghai-Tibet Plateau area from 2001 to 2017.

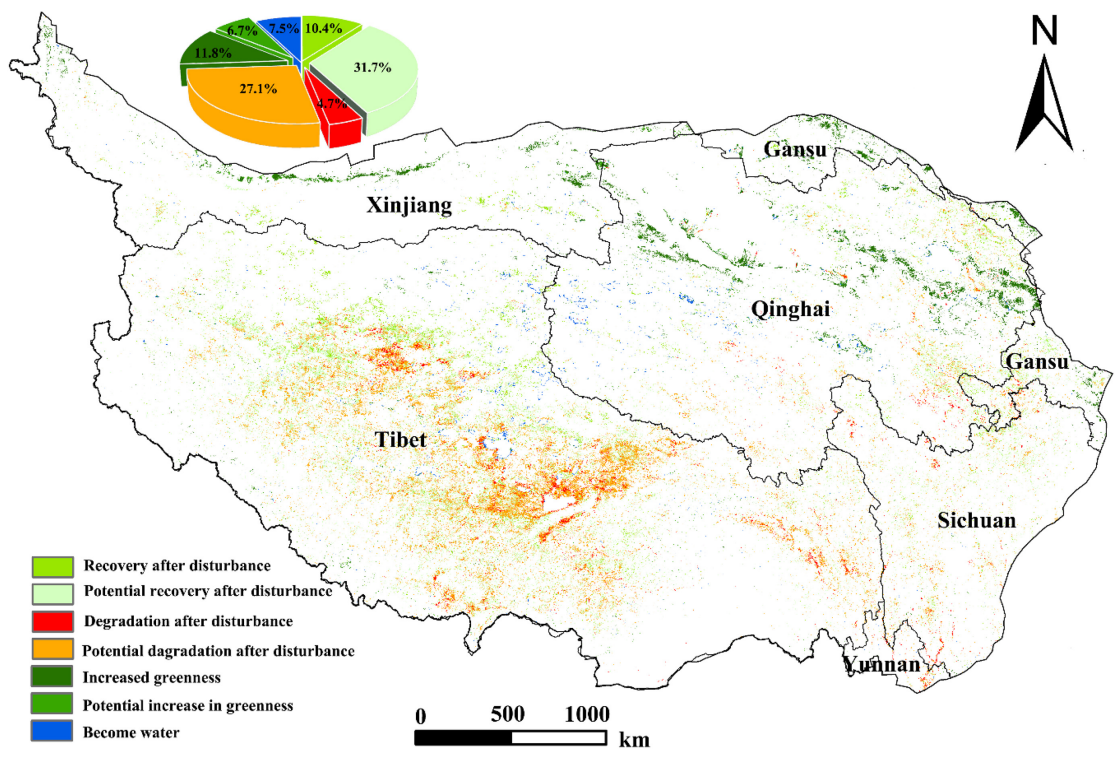

FIGURE 10 | Distribution map of grassland disturbance change in the Qinghai-Tibet Plateau from 2001 to 2017.

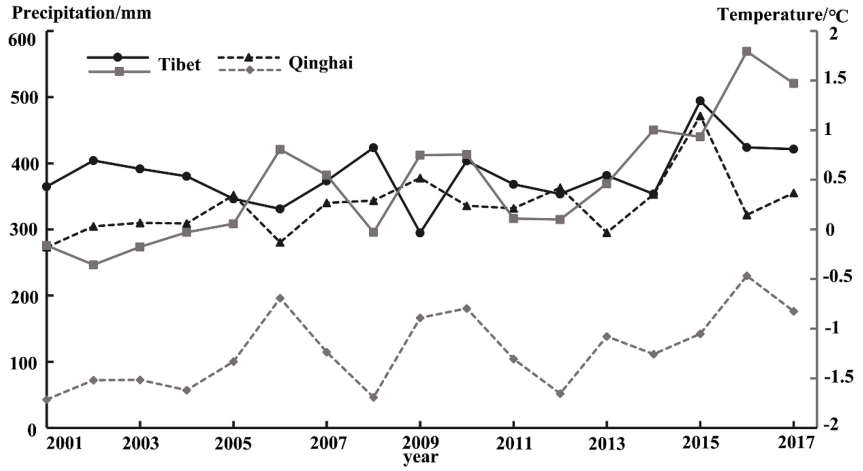

FIGURE 11 | Changes in temperature and precipitation in Qinghai and Tibetan from 2001 to 2017.

can be found that the change trend of grassland disturbance on the Qinghai-Tibet Plateau is dependent on altitude, but it is not a simple linear relationship. Among different altitudes, the correlation between grassland disturbance changes and low altitude is greater than that of high altitude. In the same altitude, the higher the altitude, the greater the fluctuation trend of grassland disturbance changes in each year. The study also found that in 2005–2010, 2010–2015, and 2015–2017, the degree of grassland disturbance gradually increased when the altitude was in the range of 3,000–6,000 m, and the relationship between grassland disturbance and altitude was small when the altitude was below 3,000 m.

Influence of Human Grazing on Grassland Disturbance

Grazing is one of the most important uses of grassland ecosystems in the Qinghai-Tibet Plateau. Overgrazing may be an important reason for grassland degradation (Hong-Qin et al., 2018). From the above analysis of grassland disturbance changes, it can be seen that the main area of greenness degradation after grassland disturbance is central and southern Tibet, and the main geographical areas of its specific distribution are Damxung, Nagqu, Nierong, and Bangor Counties. In this area, the interannual trend changes of the grassland DI index from 2001 to 2017 and the correlation analysis with the interannual change trend of the annual livestock production statistics in the corresponding area are shown in **Figure 13**. It can be found that, in the corresponding areas in which the greenness of the grassland is significantly degraded after the disturbance, the DI index in 2001–2017 showed a significant upward trend. It can be found that, in the corresponding areas where the greenness of the grassland is significantly degraded after the disturbance, the DI index in 2001–2017 showed a significant upward trend, and the correlation coefficients with the corresponding interannual variation trend of livestock production were all greater than 0.5, of which Damxung County in the regions of Nagqu and Nierong Counties, the correlation coefficients were 0.78, 0.84, and 0.91, respectively, with $p < 0.01$, showing a very significant positive correlation. The correlation coefficient in the Bangor County area is 0.58, $P < 0.05$, which is a significant positive correlation. It can be proved that, in areas where the greenness of the grassland is degraded after disturbance, the upward trend of livestock production is the same as the change trend of grassland disturbance, and the correlation is high. Therefore, grazing is one of the main causes of disturbance degradation in the greenness degraded area of the Qinghai-Tibet Plateau grassland after disturbance. In addition, from the characteristic values found in the graph, the eigenvalues (mean, STD, Max, min, percentile_value) of the DI multiyear changes in different areas and the change of multiyear livestock production in the area of characteristic value was no regular distribution because of the different quality of grass growth in different regions. More data support and more in-depth research are needed to obtain the boundary carrying value of livestock quantity that does not affect grassland growth change. Reasonable grazing planning in areas degraded by grassland disturbances is worthy of attention to regional ecological management.

DISCUSSION

As a unique natural area on the earth, the Qinghai-Tibet Plateau is a sensitive area and ecologically fragile zone of global climate change, and grassland is the most important ecological security barrier in the region (Yuan-He and Shi-Long, 2006). How to dynamically monitor the spatiotemporal changes of grassland and realize the exploration and excavation of its long-term change process mechanism has become an urgent need. In the evaluation study of grassland degradation grades based on vegetation coverage and empirical thresholds, as of 2013, the grassland degradation area of the Qinghai-Tibet Plateau accounted for about 30% with slight degradation as the main component (Xu-juan et al., 2019). Based on the algorithm

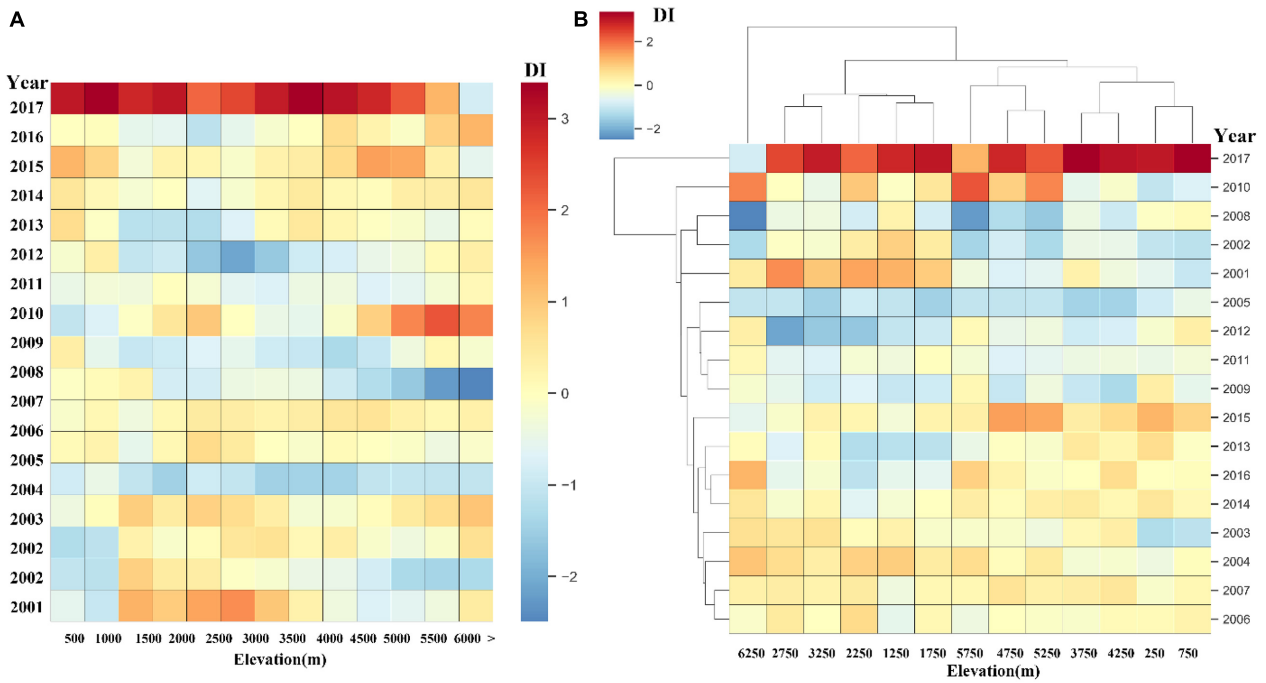

FIGURE 12 | The annual average DI values of grassland with elevation in different altitudinal zones from 2001 to 2017.

of AMTDR, this study uses mathematical statistics to obtain 10.86% of the total area of the Qinghai-Tibet Plateau that has undergone significant disturbance changes as of 2017. The main type of change is recovery after disturbance. This comparison shows that the restoration effect of degraded grassland in the Qinghai-Tibet Plateau has been significant in recent years, which is similar to the results of some related policies and research findings in the region. For example, the national and local governments have successively carried out grassland ecological protection projects in the Three River Sources of Qinghai and Qiangtang in Tibet, which have obvious effects on the restoration of grassland degradation (Xu et al., 2017). In the Three River Source area of Qinghai, nature reserves and national parks have been established successively, and a series of measures have been implemented, such as retiring people, reducing livestock, and returning grazing to grassland, and the ecological environment has been significantly improved (Shao et al., 2016). Based on remote sensing data, the more specific disturbance changes of grassland can be obtained comprehensively and objectively under the introduction of non-parameters. To a certain extent, this overcomes the existing problems of grassland degradation research in the Qinghai-Tibet Plateau region: In the case of difficulty in obtaining field monitoring data, there is a lack of a deeper dynamic quantitative monitoring of the grassland disturbance change process in the region.

Grassland disturbance changes are the result of the combined effects of many factors. Climate change and human activities have an important impact on the grassland growth process, but the impact trend is not necessary (Cui and Graf, 2009; Cai et al., 2014). Regionally, Qinghai and Tibet have different water vapor sources and heating systems (Yang et al., 2014). The altitude of Tibet is relatively higher than Qinghai, which makes Tibet's temperature warming trend faster, and the relatively higher vegetation coverage in the Qinghai area can change the surface sensible heat flux through stronger evapotranspiration to slow the surface warming effect (Jeong et al., 2009). This is consistent with the results of the study in this study that the temperature in southern Qinghai-Tibet Plateau, which is dominated by Tibet, has a higher impact on grassland disturbance changes than that in Qinghai, which is dominated by the northern Qinghai-Tibet Plateau. The spatial pattern of precipitation is more complicated than temperature changes (Zhang et al., 2013). In this study, the linear correlation of the influence of precipitation on grassland disturbance changes in the southern and northern Qinghai-Tibet Plateau is not significant.

Because Tibet in the southern part of the Qinghai-Tibet Plateau is more unfavorable to economic development than Qinghai in the northern part of the Qinghai-Tibet Plateau, the environmental factors are more unfavorable, and the economic structure of Tibet is relatively single, which makes Tibet more dependent on the development of animal husbandry (Huang et al., 2016). In recent decades, the rapid development of Tibet's increased efforts in animal husbandry has made Tibet's total livestock grazing increase faster than Qinghai. In this study, in the areas of grassland disturbance change, the areas where grassland degradation occurred were mainly concentrated in southern Tibet in the southern part of the Qinghai-Tibet Plateau, and the main reason for the degradation was overgrazing.

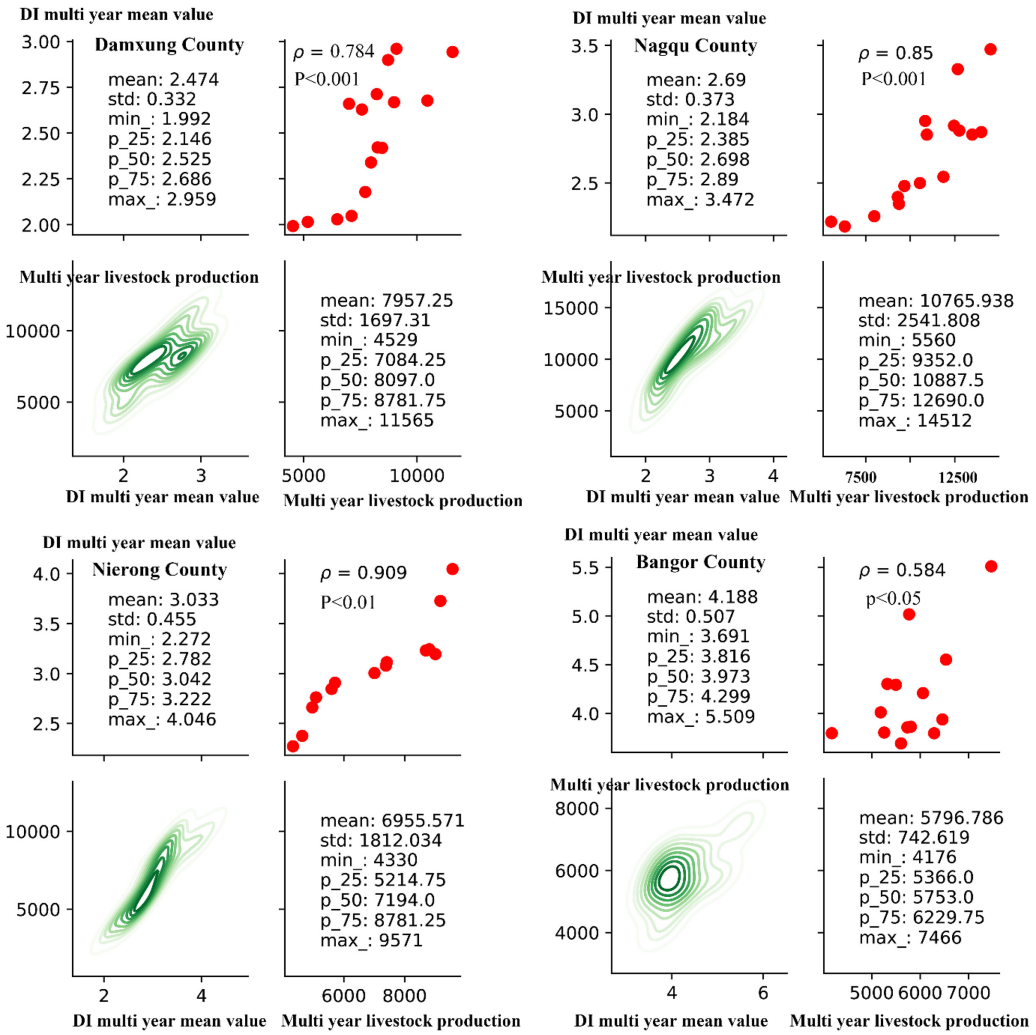

FIGURE 13 | Correlation between the annual average value of grassland DI in the main distribution areas of grassland disturbance degradation types on the Qinghai-Tibet Plateau and the corresponding annual livestock production.

The accuracy of this research is affected by some facts. Although the process of grassland disturbance change can be further dynamically quantified and monitored, it cannot directly indicate the cause and effect of the change. In this paper, due to the limitation of the spatially explicit data of the regional grazing intensity, the analysis of the quantified process of the disturbance change and the reasons for the disturbance change are not in-depth enough. In addition, the inconsistency of the hysteresis effects of climate change and overgrazing requires the use of comprehensive models supported by more relevant factors to further explore the driving mechanism.

CONCLUSION

As the main distribution region of alpine grassland in the world, the Qinghai-Tibet Plateau is sensitive to climate change, so it is very important to grasp the spatiotemporal pattern of the grassland ecosystem in time to predict the ecological environment change safely. This research relies on a large number of remote sensing application data sets, and the GEE platform is combined to solve the problems of data acquisition, processing, and storage. We propose a kind of suitable for comprehensive analysis algorithm in high latitude area, the first AMTDR. In this method, based on the combination of knowledge-based, time-series phenology characteristics and DNN method to achieve the multiyear dynamic monitoring mapping of grassland, the multiyear time-series characteristics of feature indexes were further explored, and the rule algorithm for analyzing the changes of temporal disturbances of grassland was proposed, which is independent of the index threshold division. Therefore, it has realized the comprehensive continuous dynamic monitoring of multiyear disturbance change mode by monitoring the spatiotemporal mapping of alpine grassland year by year

in a large area and long time series and further explored the application of remote sensing image in the monitoring of alpine grassland ecosystem change.

Based on the long-term monitoring of grassland disturbance changes, the relationship between climate change, altitude and human grazing activities and grassland disturbance changes in the Qinghai-Tibet Plateau is also briefly quantified. In this study, in the main areas of the Qinghai-Tibet Plateau, climate is one of the factors affecting grassland disturbance changes, and there are differences in spatial distribution. The influence on the southern part of the Qinghai-Tibet Plateau is greater than the northern part, but in the northern part of the Qinghai-Tibet Plateau, temperature is one of the main reasons for the increase in grassland greenness. The temperature in the southern part of the Qinghai-Tibet Plateau is just one of the reasons for the various disturbances in the grassland. The grassland disturbance change trend of the Qinghai-Tibet Plateau has a relationship with altitude. Among different altitudes, the correlation between grassland disturbance changes and low altitude is greater than that of high altitude. At the same altitude, the higher the altitude, the greater the annual fluctuation trend of grassland disturbance. In areas where grassland greenness is degraded after disturbance, the increasing trend of livestock production is the same as that of grassland disturbance, and the correlation is high. Therefore, grazing is one of the main causes of disturbance degradation in the green degradation area of Qinghai-Tibet Plateau grassland after disturbance.

DATA AVAILABILITY STATEMENT

The raw data supporting the conclusions of this article will be made available by the authors, without undue reservation.

AUTHOR CONTRIBUTIONS

FZ: conceptualization, methodology, software, data curation, and writing—original draft preparation. HL and JL: visualization. QH, YL, and FS: investigation and data curation.

FUNDING

The research was supported by the Innovative team project of Nanjing Institute of Environmental Sciences, Ministry of Ecology and Environment (GYZX210101), the National Key R&D Program of China (2018YFD1100104), and for the Central Level Scientific Research Institutes, Nanjing Institute of Environmental Sciences, Ministry of Ecology and Environment R&D A Basic Special Business Fund for (GYZX190101).

SUPPLEMENTARY MATERIAL

The Supplementary Material for this article can be found online at: https://www.frontiersin.org/articles/10.3389/fpls.2021.760551/full#supplementary-material

REFERENCES

Ahmed, O. S., Wulder, M. A., White, J. C., Hermosilla, T., Coops, N. C., and Franklin, S. E. (2017). Classification of annual non-stand replacing boreal forest change in Canada using Landsat time series: a case study in northern Ontario. *Remote Sens. Lett.* 8, 29–37.

Arino, O., Gross, D., Ranera, F., Bourg, L., and Weber, J. L. (2008). "GlobCover: ESA service for global land cover from MERIS," in *Proceedings of the 2007 IEEE International Geoscience & Remote Sensing Symposium*, (Barcelona).

Avissar, R., Dias, P. L. S., Dias, M. A. F., and Nobre, C. (2002). The large-scale biosphere-atmosphere experiment in amazonia (LBA): insights and future research needs. *J. Geophys. Res.* 107:8086.

Badgley, G., Field, C. B., and Berry, J. A. (2017). Canopy near-infrared reflectance and terrestrial photosynthesis. *Sci. Adv.* 3:e1602244. doi: 10.1126/sciadv.1602244

Bartholome, E., and Belward, A. S. (2005). GLC2000: a new approach to global land cover mapping from Earth observation data. *Int. J. Remote Sens.* 26, 1959–1977.

Bernacchi, C. J., and Vanloocke, A. (2015). Terrestrial ecosystems in a changing environment: a dominant role for water. *Annu. Rev. Plant Biol.* 66:599. doi: 10.1146/annurev-arplant-043014-114834

Bian, D., Chun, L. I., Yang, X. H., Bian, B. C., and Lin, L. I. (2008). Analysis of the situation of grassland degradation and it's mechanism of the alpine pastoral area in northwestern Tibet. *J. Nat. Resour.* 23, 254–262.

Buchhorn, M., Bertels, L., Smets, B., De Roo, B., Lesiv, M., Tsendbazar, N.-E., et al. (2020). *Copernicus Global Land Service: Land Cover 100m: Version 3 Globe 2015-2019: Algorithm Theoretical Basis Document*. Geneve: Zenodo.

Cai, D., Fraedrich, K., Sielmann, F., Guan, Y., Guo, S., Zhang, L., et al. (2014). Climate and vegetation: an ERA-interim and GIMMS NDVI analysis. *J. Clim.* 27, 5111–5118.

Chen, J., Chen, J., Liao, A., Cao, X., Chen, L., Chen, X., et al. (2015). Global land cover mapping at 30 m resolution: a POK-based operational approach. *ISPRS J. Photogramm. Remote Sens.* 103, 7–27. doi: 10.1371/journal.pone.0069679

Chong-Yang, L. I., Wen-Tao, F., Guo-Mei, L. I., Jing, G., Zeng, T., and Ren-De, S. (2019). Driving force analysis of changes in grassland coverage on the Qinghai-Tibet Plateau based on NDVI in 2000-2016. *Acta Pratacult. Sin.* 28, 25–32.

Cohen, W. B., Yang, Z., and Kennedy, R. (2010). Detecting trends in forest disturbance and recovery using yearly Landsat time series: 2. TimeSync — tools for calibration and validation. *Remote Sens. Environ.* 114, 2911–2924.

Cornelius, S., Dirk, P., Sebastian, V. D. L., and Patrick, H. (2013). Mapping rubber plantations and natural forests in Xishuangbanna (Southwest China) using multi-spectral phenological metrics from MODIS time series. *Remote Sens.* 5, 2795–2795.

Cui, X., and Graf, H.-F. (2009). Recent land cover changes on the Tibetan Plateau: a review. *Clim. Chang.* 94, 47–61.

David, L., Oyama, M. D., Nobre, C. A., and Sampaio, G. (2008). A new world natural vegetation map for global change studies. *Anais Acad. Bras. Cienc.* 80, 397–408. doi: 10.1590/s0001-37652008000200017

Fan, Y., Hou, X., Shi, H., and Shi, S. (2012). Effect of carbon cycling in grassland ecosystems on climate warming. *Acta Pratacult. Sin.* 21, 294–302.

Feng, L., Wang, Y., Zhang, Z., and Du, Q. (2021). Geographically and temporally weighted neural network for winter wheat yield prediction. *Remote Sens. Environ.* 262:112514.

Friedl, M. A., Sulla-Menashe, D., Tan, B., Schneider, A., Ramankutty, N., Sibley, A., et al. (2010). MODIS Collection 5 global land cover: algorithm refinements and characterization of new datasets. *Remote Sens. Environ.* 114, 168–182.

Fritz, S., See, L., and Rembold, F. (2010). Comparison of global and regional land cover maps with statistical information for the agricultural domain in Africa. *Int. J. Remote Sens.* 31, 2237–2256.

Genxu, W., Yongjian, D., Jian, W., and Shiyin, L. (2004). Land ecological changes and evolutional patterns in the source regions of the yangtze and yellow rivers in recent 15 years. *Acta Geogr. Sin.* 59, 163–173. doi: 10.1007/s10661-006-7232-2

Hansen, M. C., Potapov, P. V., Moore, R., Hancher, M., and Turubanova, S. A. (2013). High-resolution global maps of 21st-century forest cover change. *Science* 324, 850–853.

Healey, S. P., Cohen, W. B., Zhiqiang, Y., and Krankina, O. N. (2005). Comparison of Tasseled Cap-based Landsat data structures for use in forest disturbance detection. *Remote Sens. Environ.* 101, 301–310.

Hirschmugl, M., Gallaun, H., Dees, M., Datta, P., Deutscher, J., Koutsias, N., et al. (2017). Methods for mapping forest disturbance and degradation from optical earth observation data: a review. *Curr. For. Rep.* 3, 32–45.

Hong-Qin, L. I., Ya-Xi, W., Hui-Dan, H. E., Yong-Sheng, Y., and Ying-Nian, L. I. (2018). Effects of grazing density on nitrous oxide effluxes in alpine *Kobresia humilis* meadow on the Qinghai-Tibetan Plateau. *Chin. J. Agrometeorol.* 39:27.

Huang, K., Zhang, Y., Zhu, J., Liu, Y., Zu, J., and Zhang, J. (2016). The influences of climate change and human activities on vegetation dynamics in the Qinghai-Tibet Plateau. *Remote Sens.* 8:876. doi: 10.1007/s10661-020-08606-6

Huilan, W., and Yingjun, Q. (2016). Analysis of grassland degradation of the Tibet Plateau and human driving forces based on remote sensing. *Pratacult. Sci.*

Jamali, S., Jönsson, P., Eklundh, L., Ardö, J., and Seaquist, J. (2015). Detecting changes in vegetation trends using time series segmentation. *Remote Sens. Environ.* 156, 182–195.

Jeong, S. J., Ho, C. H., Kim, K. Y., and Jeong, J. H. (2009). Reduction of spring warming over East Asia associated with vegetation feedback. *Geophys. Res. Lett.* 36:L18705.

Kemp, D. R., Guodong, H., Xiangyang, H., Michalk, D. L., Fujiang, H., Jianping, W., et al. (2013). Innovative grassland management systems for environmental and livelihood benefits. *Proc. Natl. Acad. Sci. U.S.A.* 110, 8369–8374. doi: 10.1073/pnas.1208063110

Li, X. L., Gao, J., Brierley, G., Qiao, Y. M., Zhang, J., and Yang, Y. W. (2013). Rangeland degradation on the Qinghai-Tibet plateau: implications for rehabilitation. *Land Degrad. Dev.* 24, 72–80.

Liang, S., Chen, J., Jin, X., Wan, L., and Gong, B. (2007). Regularity of vegetation coverage changes in the Tibetan Plateau over the last 21 years. *Adv. Earth Sci.* 22, 33–40.

Liu, C., Li, W., Zhu, G., Zhou, H., Yan, H., and Xue, P. (2020). Land use/land cover changes and their driving factors in the northeastern Tibetan Plateau based on geographical detectors and google earth engine: a case study in Gannan prefecture. *Remote Sens.* 12:3139.

Mahyou, H., Louhaichi, M., Mimouni, J., Tychon, B., and Balaghi, R. (2016). A knowledge-based approach for mapping land degradation in the Arid Rangelands of North Africa. *Land Degrad. Dev.* 27, 1574–1585.

Masek, J. G., Huang, C., Wolfe, R., Cohen, W., Hall, F., Kutler, J., et al. (2008). North American forest disturbance mapped from a decadal Landsat record. *Remote Sens. Environ.* 112, 2914–2926.

Mutanga, O., and Kumar, L. (2019). *Google Earth Engine Applications*. Basel: Multidisciplinary Digital Publishing Institute.

O'Mara, F. P. (2012). The role of grasslands in food security and climate change. *Ann. Bot.* 110, 1263–1270. doi: 10.1093/aob/mcs209

Peng, J., Liu, Z., Liu, Y., Wu, J., and Han, Y. (2012). Trend analysis of vegetation dynamics in Qinghai–Tibet Plateau using Hurst Exponent. *Ecol. Indic.* 14, 28–39. doi: 10.1038/s41598-017-04038-4

Piao, S. L., Fang, J. Y., He, J. S., and Xiao, Y. (2004). Spatial distribution of grassland biomass in China. *Acta Phytoecol. Sin.* 28, 491–498.

Qi, Z., Yeh, G. O., and Li, X. (2017). A crop phenology knowledge-based approach for monthly monitoring of construction land expansion using polarimetric synthetic aperture radar imagery. *ISPRS J. Photogramm. Remote Sens.* 133, 1–17.

Qiu, B., Lu, D., Tang, Z., Chen, C., and Zou, F. (2017). Automatic and adaptive paddy rice mapping using Landsat images: case study in Songnen Plain in Northeast China. *Sci. Total Environ.* 598, 581–592. doi: 10.1016/j.scitotenv.2017.03.221

Schipper, L. A., Parfitt, R. L., Fraser, S., Littler, R. A., Baisden, W. T., and Ross, C. (2014). Soil order and grazing management effects on changes in soil C and N in New Zealand pastures. *Agric. Ecosyst. Environ.* 184, 67–75.

Shao, Q., Fan, J., Liu, J., Huang, L., Cao, W., Xu, X., et al. (2016). Assessment on the effects of the first-stage ecological conservation and restoration project in Sanjiangyuan region. *Acta Geogr. Sin.* 71, 3–20.

Shih, H. C., Stow, D. A., Weeks, J. R., and Coulter, L. L. (2017). Determining the type and starting time of land cover and land use change in Southern Ghana based on discrete analysis of dense landsat image time series. *IEEE J. Sel. Top. Appl. Earth Observ. Remote Sens.* 9, 2064–2073.

Sun, J., Qin, X., and Yang, J. (2016). The response of vegetation dynamics of the different alpine grassland types to temperature and precipitation on the Tibetan Plateau. *Environ. Monit. Assess.* 188, 1–11. doi: 10.1007/s10661-015-5014-4

Tchuenté, A. T. K., Roujean, J. L., and Jong, S. M. D. (2011). Comparison and relative quality assessment of the GLC2000, GLOBCOVER, MODIS and ECOCLIMAP land cover data sets at the African continental scale. *Int. J. Appl. Earth Observ. Geoinf.* 13, 207–219.

Tian, L., Zhang, Y., and Zhu, J. (2014). Decreased surface albedo driven by denser vegetation on the Tibetan Plateau. *Environ. Res. Lett.* 9:104001.

Waldner, F. O., Canto, G. S., and Defourny, P. (2015). Automated annual cropland mapping using knowledge-based temporal features. *ISPRS J. Photogramm. Remote Sens.* 110, 1–13.

Wang, C. S., Meng, F. D., Li, X. E., Jiang, L. L., and Wang, S. P. (2013). Responses of alpine grassland ecosystem on Tibetan Plateau to climate change: a mini review. *Chin. J. Ecol.* 32, 1587–1595.

Wang, Y., Zhang, Z., Feng, L., Ma, Y., and Du, Q. (2021). A new attention-based CNN approach for crop mapping using time series Sentinel-2 images. *Comput. Electron. Agric.* 184:106090.

Xiang, Z., Peipei, X., Tao, Z., Qing, L., and Donghai, W. (2013). Distribution and variation of forests in China from 2001 to 2011: a study based on remotely sensed data. *Forests* 4, 632–649.

Xiao, X., Biradar, C., Czarnecki, C., Alabi, T., and Keller, M. (2009). A simple algorithm for large-scale mapping of evergreen forests in Tropical America, Africa and Asia. *Remote Sens.* 1, 355–374.

Xie, Y., Sha, Z., and Yu, M. (2008). Remote sensing imagery in vegetation mapping: a review. *J. Plant Ecol.* 1, 9–23.

Xu, X., Wang, L., Li, J., and Cai, H. (2017). Analysis of the grassland restoration trend and degradation situation in the "Three-River headwaters" region since the implementation of the ecological project. *J. Geo Inf. Sci.* 19, 50–58.

Xu-juan, C., Ganjurjav, H., Guo-zheng, H., and Qing-zhu, G. (2019). Characteristics of grassland degradation in the Qinghai Tibetan Plateau, based on NDVI3g data. *Chin. J. Agrometeorol.* 40:86.

Yang, K., Wu, H., Qin, J., Lin, C., Tang, W., and Chen, Y. (2014). Recent climate changes over the Tibetan Plateau and their impacts on energy and water cycle: a review. *Glob. Planet. Change* 112, 79–91.

Yin, H., Brando, A., Buchner, J., Helmers, D., and Radeloff, V. C. (2020). Monitoring cropland abandonment with Landsat time series. *Remote Sens. Environ.* 246:111873.

Yuan-He, Y., and Shi-Long, P. (2006). Variations in grassland vegetation cover in relation to climatic factors on the Tibetan Plateau. *J. Plant Ecol.* 30, 1–8.

Yue-Jun, F., Xiang-Yang, H., Hong-Xiao, S., and Shang-Li, S. (2012). Effect of carbon cycling in grassland ecosystems on climate warming. *Acta Pratacult. Sin.* 21, 294–302.

Zavaleta, E. S., Shaw, M. R., Chariello, N. R., Thomas, B. D., Cleland, E. E., Field, C. B., et al. (2003). Grassland and responses to three years of elevated temperature, CO[sub 2], precipitation, and N deposition. *Ecol. Monogr.* 73, 585–604.

Zhang, D., Huang, J., Guan, X., Chen, B., and Zhang, L. (2013). Long-term trends of precipitable water and precipitation over the Tibetan Plateau derived from satellite and surface measurements. *J. Quant. Spectrosc. Radiat. Transf.* 122, 64–71.

Zhang, J., Yao, F., Zheng, L., and Yang, L. (2007). Evaluation of grassland dynamics in the Northern-Tibet Plateau of China using remote sensing and climate data. *Sensors* 7, 3312–3328. doi: 10.3390/s7123312

Zhang, P., Gong, M., Su, L., Liu, J., and Li, Z. (2016). Change detection based on deep feature representation and mapping transformation for

multi-spatial-resolution remote sensing images. *ISPRS J. Photogramm. Remote Sens.* 116, 24–41.

Zhang, T., Zhang, Y., Xu, M., Zhu, J., Wimberly, M. C., Yu, G., et al. (2015). Light-intensity grazing improves alpine meadow productivity and adaption to climate change on the Tibetan Plateau. *Sci. Rep.* 5:15949. doi: 10.1038/srep15949

Zhang, X., Schaaf, C. B., Friedl, M. A., Strahler, A. H., and Hodges, J. C. F. (2002). "MODIS tasseled cap transformation and its utility," in *Proceedings of the Geoscience and Remote Sensing Symposium, 2002. IGARSS '02. 2002 IEEE International*, (Torondo, ON).

Zou, F., Li, H., and Hu, Q. (2020). Responses of vegetation greening and land surface temperature variations to global warming on the Qinghai-Tibetan Plateau, 2001–2016. *Ecol. Indic.* 119:106867.

Conflict of Interest: FS was employed by the company GeoScene Information Technology Co., Ltd.

The remaining authors declare that the research was conducted in the absence of any commercial or financial relationships that could be construed as a potential conflict of interest.

Publisher's Note: All claims expressed in this article are solely those of the authors and do not necessarily represent those of their affiliated organizations, or those of the publisher, the editors and the reviewers. Any product that may be evaluated in this article, or claim that may be made by its manufacturer, is not guaranteed or endorsed by the publisher.

Copyright © 2022 Zou, Hu, Li, Lin, Liu and Sun. This is an open-access article distributed under the terms of the Creative Commons Attribution License (CC BY). The use, distribution or reproduction in other forums is permitted, provided the original author(s) and the copyright owner(s) are credited and that the original publication in this journal is cited, in accordance with accepted academic practice. No use, distribution or reproduction is permitted which does not comply with these terms.

frontiers in Plant Science

ORIGINAL RESEARCH
published: 20 January 2022
doi: 10.3389/fpls.2021.771424

Community Composition and Structure Affect Ecosystem and Canopy Water Use Efficiency Across Three Typical Alpine Ecosystems

Yuzhe Li[1], Xinyuan Zhang[1,2], Quanqin Shao[1]*, Jiangwen Fan[1], Zhi Chen[3], Jinwei Dong[1], Zhongmin Hu[4] and Yue Zhan[5]*

[1] Key Laboratory of Land Surface Pattern and Simulation, Institute of Geographical Sciences and Natural Resources Research, Chinese Academy of Sciences, Beijing, China, [2] School of Earth Sciences and Resources, China University of Geosciences, Beijing, China, [3] Key Laboratory of Ecosystem Network Observation and Modeling, Synthesis Research Center of Chinese Ecosystem Research Network, Institute of Geographic Sciences and Natural Resources Research, Chinese Academy of Sciences, Beijing, China, [4] School of Geography, South China Normal University, Guangzhou, China, [5] College of Forestry, Nanjing Forestry University, Nanjing, China

Unique ecosystems distributed in alpine areas of the Qinghai–Tibetan Plateau play important roles in climate change mitigation, local food supply, and conservation of species diversity. To understand the water use efficiency (WUE) of this fragile and sensitive region, this study combined observed data from the eddy covariance system and the Shuttleworth–Wallace (S-W) model to measure the continuous mass exchange, including gross primary productivity (GPP), evapotranspiration (ET), and canopy transpiration (T) throughout 2 or 3 years (2016–2018) in three common alpine ecosystems (i.e., alpine steppe, alpine meadow, and alpine swamp). These ecosystems represent a water availability gradient and thus provide the opportunity to quantify environmental and biological controls on WUE at various spatiotemporal scales. We analyzed the ecosystem WUE (WUEe; defined as the ratio of GPP to ET) and canopy WUE (WUEc; defined as the ratio of GPP and canopy T). It was found that the yearly WUEe was 1.40, 1.63, and 2.16 g C kg^{-1} H_2O, and the yearly WUEc was 8.93, 2.46, and 5.19 g C kg^{-1} H_2O in the three typical ecosystems, respectively. The controlling factors of yearly WUE diverged between WUEe and WUEc. We found that plant functional group proportion (e.g., gramineous and Cyperaceae) highly explained the yearly WUEe variation across sites, and a good correlation was observed between community species diversity and WUEc. These findings suggest that community composition and trait change are critical in regulating WUEe and WUEc across different alpine ecosystems and that the regulation mechanisms may differ fundamentally between WUEe and WUEc.

Keywords: evapotranspiration partition, ecosystem water use efficiency, canopy water use efficiency, Qinghai–Tibetan Plateau, alpine ecosystem, community characteristics

OPEN ACCESS

Edited by:
Huakun Zhou, Key Laboratory of Restoration Ecology in Cold Regions, Northwest Institute of Plateau Biology (CAS), China

Reviewed by:
Quangang You, Northwest Institute of Eco-Environment and Resources, Chinese Academy of Sciences , Chinese Academy of Sciences (CAS), China
Xiaoying Gong, Fujian Normal University, China

****Correspondence:***
Yuzhe Li
liyuzhe@igsnrr.ac.cn
Quanqin Shao
Shaoqq@igsnrr.ac.cn

Specialty section:
This article was submitted to Functional Plant Ecology, a section of the journal Frontiers in Plant Science

Received: *06 September 2021*
Accepted: *21 December 2021*
Published: *20 January 2022*

Citation:
Li Y, Zhang X, Shao Q, Fan J, Chen Z, Dong J, Hu Z and Zhan Y (2022) Community Composition and Structure Affect Ecosystem and Canopy Water Use Efficiency Across Three Typical Alpine Ecosystems. Front. Plant Sci. 12:771424. doi: 10.3389/fpls.2021.771424

INTRODUCTION

The Qinghai–Tibetan Plateau has received international attention because of its contribution to the global carbon budget and the sensitivity and fragility of the alpine ecosystems. This region is considered one of the world's most sensitive areas to climate change (Liu D. et al., 2018; Liu S. et al., 2018). The Three Rivers Headwaters Region, located in the central of Qinghai–Tibetan Plateau, is the most critical area for reserving water resources and maintaining alpine biodiversity (Liu et al., 2008; Wang et al., 2019), and is also an important pasture for the local free-grazing livestock production (Zhang L.X. et al., 2014; Zhang et al., 2019). This area has already experienced a considerable climate change, including air temperature increase (0.16°C decade^{-1}) and precipitation change (Wang et al., 2008). These changes may profoundly affect local carbon and water cycles, thus influencing the sustainable use of regional limited water, forage resources, and the welfare of the local people.

Water use efficiency (WUE), the ratio of water loss to carbon gain, links water and carbon cycling together (Hu et al., 2008; Keenan et al., 2013; Ali et al., 2017) and is an important and inherent ecosystem characteristic related to ecosystem productivity and water budget (Ponton et al., 2006; Zhou et al., 2018). WUE change may greatly impact on both forage productivity and regional water balance. Thus, a more accurate and deeper understanding of the dynamics of WUE at various observation scales is conducive to the verification and improvement of the accuracy of assessment of regional resource use (Hu et al., 2008; Niu et al., 2008) and the prediction of the climate effect on the limited forage supply and water resource change.

Ecosystem-scale WUE (WUEe) is commonly defined as the ratio between gross primary productivity (GPP) and evapotranspiration (ET) (Law et al., 2008), whereas canopy-scale WUE (WUEc) is defined as the ratio between GPP and canopy transpiration (T) (Niu et al., 2008, 2011). Owing to various analysis scales and data collection techniques, there are differences in the calculation of "productivity" and "water loss" in previous research on WUE and its controlling factors (Zhou et al., 2018; Liu R. et al., 2021). Previous studies have indicated that the variation and composition of ecosystem vapor losses play an important role in shaping WUE and regional environmental conditions of ecologically fragile areas (Bremer et al., 2001; Hu et al., 2009, 2010). However, water resource management based on ET measurements may overestimate the actual water losses of communities, resulting in low WUE (Li et al., 2016). Accordingly, it is necessary to separate the composition of ET accurately and reliably when investigating WUEe, WUEc, and their controlling mechanisms. Measurements, such as manipulative measurement with portable infrared analyzer (Ens et al., 2015; Li et al., 2016), stable isotopes (Williams et al., 2004; Hu et al., 2014), lysimeter (Gebler et al., 2015), and eddy covariance techniques (Li et al., 2019b), are used to estimate ET and its components. Eddy covariance systems are feasible methods of continuous observation of ET (Ponton et al., 2006; Li et al., 2016), but are weak in partitioning ET components. The Shuttleworth–Wallace (S-W) model (Shuttleworth and Wallace, 2010), characterized by its strength in partitioning ecosystem ET components, has been widely used for extracting T from ET since its publication (Hu et al., 2008; Li et al., 2015). Using the data obtained for the eddy covariance system as input, the measured ET can be divided into T and E at a half-hourly resolution, which might resolve the difficulty of continuous ET observation with partitioning.

Understanding the mechanisms underlying variation in WUE response at different scales is necessary to provide data for the validation of any upscaling method (Wu et al., 2015; Liu D. et al., 2018), but there are still biases and conflicts of understanding in WUE controlling mechanisms. In previous studies, WUEe was commonly predicted to decrease under climate warming (Bell et al., 2015), and decrease (Huxman et al., 2004; Scanlon and Albertson, 2010) or no change (Lauenroth et al., 2000) with increasing precipitation. Leaf area index (LAI) and carbon assimilation are positively related to WUEe (Farquhar et al., 1989; Hu et al., 2008). In canopy scale, WUEc suspected depends on the responses of both plant physiology and community structure (Niu et al., 2011). The plant community is usually constituted with many coexisting species that differ in water use strategies that adapt the various ecological niches and the changing environment (Ens et al., 2015; Li et al., 2019a), thereby promoting stability of community and ecosystem productivity. Correspondingly, it can be inferred that changes in community traits, especially species composition, may fundamentally affect WUE (De Boeck et al., 2006). Nevertheless, few attempts (Niu et al., 2011; Li et al., 2016) have been made to compare WUE response, especially WUEc to community structure and composition change. In the Qinghai–Tibetan Plateau, the mountain upheaval has caused a distinct elevation gradient and blocking effect, producing a drastic variation in species composition and a varied community structure. To the best of our knowledge, no attempt has been made to analyze the relationships between community traits and different scales of WUE in this region. Reducing this uncertainty would help local pasture and water resources management in accurate predictions and adaptation to climate change.

The overall objective of this study was to quantify the seasonal and site-to-site variations in the WUEe and WUEc in three typical Qinghai–Tibetan Plateau ecosystems (i.e., alpine steppe, alpine meadow, and alpine swamp). In particular, we were interested in the underlying regulation mechanism of the less-reported WUEc and the relationship between alpine community traits variation and WUE. The specific objectives of our study were as follows: (1) to compare the carbon assimilation and ET components, and WUEe and WUEc among the three alpine ecosystems; (2) to improve the current understanding of driving factors on seasonal variation of WUEe and WUEc in alpine ecosystems; and (3) to test our hypothesis that the community composition plays a special role in regulating WUE across alpine ecosystems.

MATERIALS AND METHODS

Study Sites

Observation and field survey were conducted at three alpine sites located in the Qinghai–Tibetan Plateau. The community of these sites represents the most prevalent vegetation types of the Qinghai–Tibetan Plateau and exhibits a clear water availability gradient (**Figure 1**). They include an alpine steppe located in Maduo County, dominated by *Stipa purpurea*, the soil of this community is frigid calcic soil; an alpine meadow located in Batang, Yushu County, dominated by *Kobresia humilis*, the soil of this community is felty soil; and an alpine swamp located in Longbao Nature Reserve, Yushu County, dominated by *Kobresia littledalei*, the soil of this community is bog soil. The land use of the three sites was free grazing and all the sites are located in Plateau mountain climate areas. The three sites were fully instrumented to enable the state-of-the-art measurements of vapor and CO_2 fluxes. The geographical location, elevation, dominant species, and soil physicochemical properties of the three sites are listed in **Table 1**.

Observation of Fluxes, Meteorological Parameters, and Leaf Area Index

The device configuration was kept consistent across the three sites; each observation site had a 4-m high micrometeorological observation tower, with the open eddy covariance system (OPEC) installed at 2.5 m height. The OPEC system is mainly used for observation of turbulent flux and includes a three-dimensional ultrasonic anemometer (CSAT3; Campbell, CA, United States) and infrared gas analyzer (EC150; Campbell, CA, United States) to determine the three-dimensional wind speed and the density of CO_2 and H_2O in the atmosphere. The data collector (CR3000; Campbell, CA, United States) had a sampling frequency of 10 Hz and was responsible for the collection and calculation of the average flux of 30 min for storage. Observation equipment of the aboveground micrometeorological elements includes NR01 four-component net radiation sensor, HMP155a temperature and humidity sensor, and NR-LITE net radiation sensor. The soil water content (SWC) was recorded using an underground CS616 soil moisture sensor, and the soil temperature was recorded using a 109SS soil temperature sensor.

ChinaFLUX has developed a series of methods for processing flux data including flux calculation, gap-filling, partitioning, and quality assurance methods (Yu et al., 2006; Han et al., 2020). In this study, the flux data were filtered and corrected using the standard ChinaFLUX process, which involves coordinate rotation, Webb–Pearman–Leuning correction (Webb et al., 2010), outlier filtering, nighttime CO_2 flux correction using site-specific thresholds of friction velocity (u^*), and gap-filling (Reichstein et al., 2005). The net ecosystem productivity (NEP) values were obtained based on the fully interpolated 30-min data. NEP was partitioned into respiration (Re) and GPP using the functional relationship between nighttime fluxes and soil temperature. The computations were performed using MATLAB software (Math Works Inc., Natick, MA, United States).

At each site, although LAI was measured by harvesting the aboveground biomass at the peak of the growing season (August), these data were not continuous. To configure the integrated LAI dataset with relatively fine-time resolution, normalized difference vegetation index (NDVI) data (8-day average at 1-km resolution[1]) were adopted for the estimation of LAI.

[1]https://ladsweb.modaps.eosdis.nasa.gov/

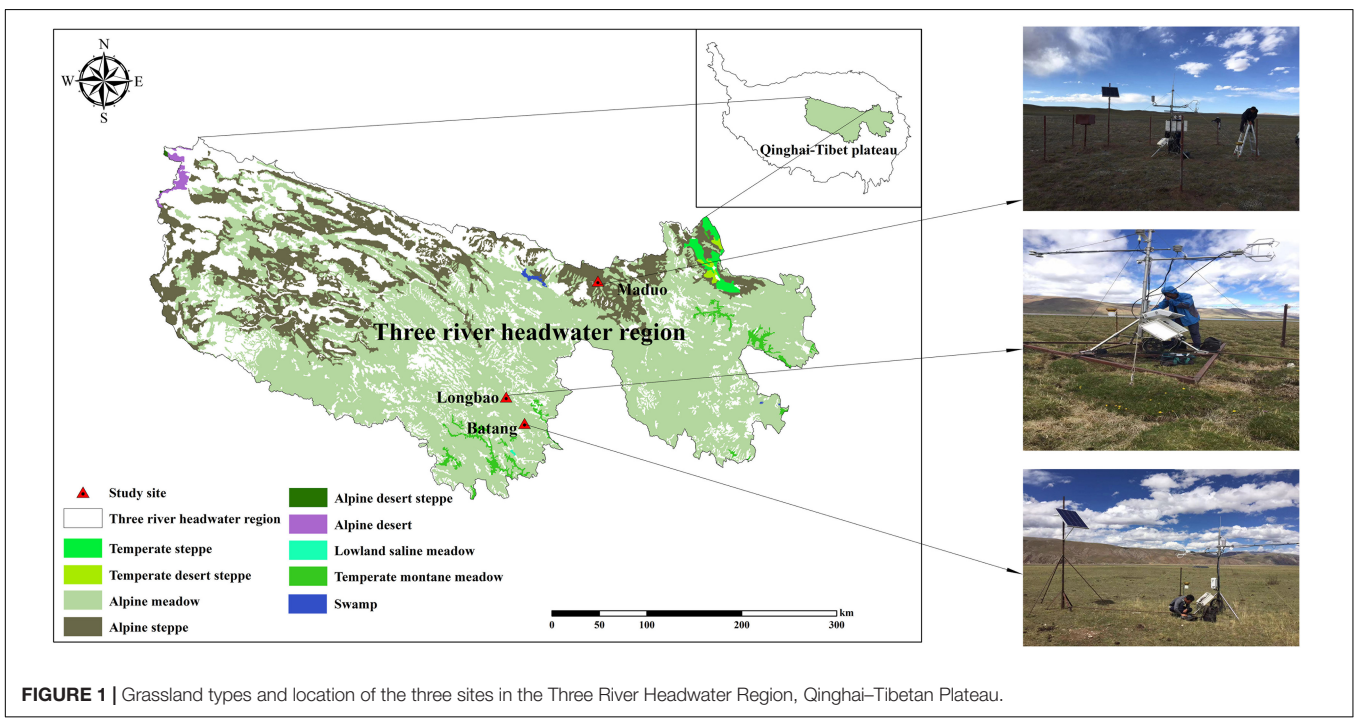

FIGURE 1 | Grassland types and location of the three sites in the Three River Headwater Region, Qinghai–Tibetan Plateau.

TABLE 1 | Site information and community characteristics of the three grassland ecosystems on the Qinghai–Tibetan Plateau.

Site	Alpine steppe	Alpine meadow	Alpine swamp
Location	35°6′12″N, 97°58′40″E	32°50′49″N, 96°57′3″E	33°12′14″N, 96°33′7″E
Elevation (m)	4316	3980	4220
Mean precipitation (mm)	392.99	578.78	573.73
Mean temperature(°C)	−3.36	2.12	0.74
Soil type	Frigid calcic soils	Felty soils	Bog soils
Dominant species	*Stipa purpurea*	*Kobresia humilis*	*Kobresia littledalei*
Cover (%)	66.67 ± 3.33a	99.33 ± 0.67b	100.00 ± 0.00b
Height (cm)	20.3 ± 0.57a	46.00 ± 12.17b	21.67 ± 1.67a
Maximum LAI (m^2 m^{-2})	0.6	2.8	2.5
Aboveground biomass (g m^{-2})	66.29 ± 11.22a	275.92 ± 25.36b	313.28 ± 25.41b
Total biomass (kg m^{-2})	2.00 ± 0.23a	3.75 ± 0.30b	19.88 ± 4.12c
Gramineous biomass proportion (%)	62.41 ± 12.50a	42.08 ± 12.32b	0.00 ± 0.00c
Cyperaceae biomass proportion (%)	20.55 ± 9.96a	17.96 ± 9.65a	83.00 ± 6.74b
Specie richness	5.33 ± 0.67a	15.33 ± 0.88b	10.67 ± 0.67c
Shannon–Wiener index	1.31 ± 0.11a	2.52 ± 0.06b	2.02 ± 0.18c

Mean ± SD; different letters in the same row indicate significant difference at $p < 0.05$.

TABLE 2 | Sum of daily GPP, ET, T, and LAI during each growing season and annual WUE at the three Qinghai–Tibetan Plateau ecosystems.

Site	Year	Precipitation (mm)	LAI sum	GPP (gC m^{-2})	ET (kg H_2O m^{-2})	T (kg H_2O m^{-2})	WUEe (gC kg^{-1} H_2O)	WUEc (gC kg^{-1} H_2O)
Alpine steppe	2016	388.73	67.13	320.54	233.60	38.35	1.37	8.36
	2017	383.62	74.85	379.57	254.75	37.35	1.49	10.16
	2018	530.17	83.04	369.83	275.35	44.68	1.34	8.28
Alpine meadow	2017	627.97	294.79	812.94	549.55	337.48	1.48	2.41
	2018	629.19	287.94	866.13	481.12	345.01	1.80	2.51
Alpine swamp	2017	596.12	239.30	1289.71	596.21	248.48	2.16	5.19
	2018	614.60	234.31	1240.47	574.28	239.44	2.16	5.18

Evapotranspiration Partitioning and the Shuttleworth–Wallace Model

The S-W model, developed based on the Penman–Monteith model, is widely used in the study of ET in ecosystems, such as farmland, grassland, and forest. This model considers that the latent heat flux from E and the T are two independent sources. In this model, methods for estimating soil surface resistance (R_{SS}) and canopy resistance (R_C) are usually study specific. In this study, R_{SS} was calculated with an empirical function of surface SWC (Mahfouf and Noilhan, 2015) as follows:

$$R_{SS} = b_1\left(\frac{\theta_S}{\theta}\right)^{b_2} + b_3 \quad (1)$$

where θ is the average volumetric soil moisture content between 0 and 10 cm, θ_S is the saturated water content in the surface soil, and b_1, b_2, and b_3 are empirical constants. R_C was calculated with the modified Ball–Berry model (Ball et al., 1987) as follows:

$$R_C = \frac{1}{g_0 + a_1\left(\frac{\theta-\theta_w}{\theta_f-\theta_w}\right)P_n h_s/C_s} \quad (2)$$

where g_0 and a_1 are empirical parameters; θ_f and θ_w are ground soil capacity and wilting points, respectively; P_n is the photosynthetic rate; h_s is the leaf surface relative humidity; and C_s is the leaf surface CO_2 concentration.

In Equations 1, 2, five parameters, namely, b_1, b_2, b_3, g_0, and a_1, are estimated using the Monte Carlo method (Hu et al., 2009), and the estimation method of other resistances (i.e., air resistance from blade surface to canopy, air resistance from soil surface to canopy, and air resistance from canopy to reference height) is consistent with Shuttleworth and Wallace (2010).

Survey of Community Characteristics

Every year, at the peak of the growing season (August), a randomized quadrat method with a total of 15 survey quadrats (1 m × 1 m) was applied in each site. At each site, we randomly installed 5 replicate biomass harvest quadrats and 10 species survey quadrats. The percentage cover of each species and the entire vegetation cover were visually estimated in the biomass harvest quadrats. In addition, the harvest quadrats were used for destructive sampling to determine the community characteristics, including aboveground and belowground biomass, and soil properties. The aboveground biomass of each species in each destructive sampling plot was clipped to ground level and the living fraction was separated. The 0- to 30-cm belowground biomass was sampled using the root drill method, as described by Fan et al. (2008). All the aboveground biomass and belowground

biomass were oven-dried at 70°C for 48 h and then weighed. In each species survey quadrat, the species composition, percentage cover, and average height of each species were recorded.

The following species diversity indices were calculated as follows:

(1) Species richness, *S*, was calculated as the total number of species appeared in observation site; and
(2) The Shannon–Wiener index (H') (Shannon, 1948) was calculated as follows:

$$H' = -\sum Pi \ln Pi \quad (3)$$

where *Pi* is the importance value (*IV*) of species *i*; and *IV* (Li et al., 2019a) was calculated as follows:

$$IV = (\text{relative height} + \text{relative coverage} + \text{relative frequency})/3 \quad (4)$$

Ecosystem and Canopy Water Use Efficiency Calculation

In this study, the WUEe was defined as the ratio between GPP and ET (Li et al., 2016) as follows:

$$\text{WUE}_e = \frac{GPP}{ET} \quad (5)$$

The WUEc was defined as the ratio of GPP to T (Niu et al., 2011) as follows:

$$\text{WUE}_e = \frac{GPP}{T} \quad (6)$$

where ET is obtained by the eddy covariance system, *T* is obtained by the S-W model, and GPP is obtained as follows (Li et al., 2019b):

$$\text{GPP} = -\text{NEP} + \text{Re} \quad (7)$$

The NEP can be obtained from the eddy covariance system as nighttime ecosystem Re was observed by the eddy covariance system and daytime Re was calculated using the functional relationship between nighttime fluxes and soil temperature (Reichstein et al., 2005).

Statistical Analysis

One-way ANOVA with Tukey's honestly significant difference (HSD) test was used to analyze the differences in the community characteristics of the three alpine sites. The paired *t*-test was used to compare the seasonal dynamics of ecosystem H_2O and CO_2 exchange as well as WUEc and WUEe of the three sites. Linear regression analysis and root mean squard error (RMSE) were applied to examine the consistency between ET measured by the eddy covariance system and that modeled by the S-W model. Linear regression analysis was used to evaluate the relationships between T/ET, LAI, GPP, ET, T, ecosystem microclimate factors, and WUEe or WUEc. Exponential regression analysis was applied to evaluate the relationships between T/ET, LAI, and WUEc. All statistical analyses were performed using SPSS version 12.0 (IBM, Armonk, NY, United States).

RESULTS

Microclimate and Community Characteristics at the Three Sites

Seasonal air temperature at the three ecosystems showed a similar one-peak pattern. Both the maximum and minimum air temperatures occurred at the alpine steppe site that is located at a higher altitude (**Figure 2**). The SWC at the alpine swamp site remained relatively high throughout the growing seasons, whereas SWC at the alpine steppe site was more variable. The rainfall at the alpine steppe site was much lower than that at the other two sites. The maximum LAI commonly occurred in July (**Figure 2D**).

The community structure and species composition were clearly different between sites. The dominant species is *S. purpurea* at the alpine steppe site, and its gramineous biomass portion (about 62.41%) was consistently significantly higher than that of alpine meadow and alpine swamp sites ($p < 0.05$), for which the dominant species were the Cyperaceae family (*K. humilis* and *K. littledalei*, respectively). The species diversity was highest in the alpine meadow with H' reaching 2.52. Similar to H', the species richness was low in the alpine steppe (**Table 1**).

Seasonal Variations in Gross Primary Productivity and the Components of Evapotranspiration at the Three Sites

Seasonal variations in net ecosystem exchange (NEE), Re, GPP, and ET at the three sites are shown in **Figure 3**. NEE refers to the change in ecosystem carbon storage, which mainly reflects the carbon budget of the ecosystem from the perspective of flux observation and has the same physical significance as NEP under certain assumptions. The difference between NEP and NEE is that positive NEP indicates a carbon absorption ecosystem, while when NEE is negative, it indicates the presence of a carbon absorption process. In this study, the NEE showed an apparent U-shaped curve, low in the active periods and high in the early and the late growing season (**Figure 3A**). However, NEE varied with two or more peaks during each growing season at alpine steppe, and is likely to be caused by summer drought, which is supported by rain and SWC records. The Re typically showed a one-peak seasonal pattern, with the peak occurring in July (**Figure 3C**). The GPP showed a one-peak pattern similar to Re at the three alpine sites, except for the alpine steppe in 2016 (**Figure 3C**). The ET showed similar patterns to GPP at the three ecosystems (**Figure 3D**), suggesting a coupling between carbon and vapor flux.

Seasonal Variations in Canopy Transpiration/Evapotranspiration and Canopy Transpiration Simulated With the Shuttleworth–Wallace Model at the Three Sites

As shown in **Figure 4A**, the S-W model could successfully estimate vapor losses for the alpine ecosystems (all $R^2 = 0.80$, RMSE = 0.66), and the RMSE was slightly lower in the alpine

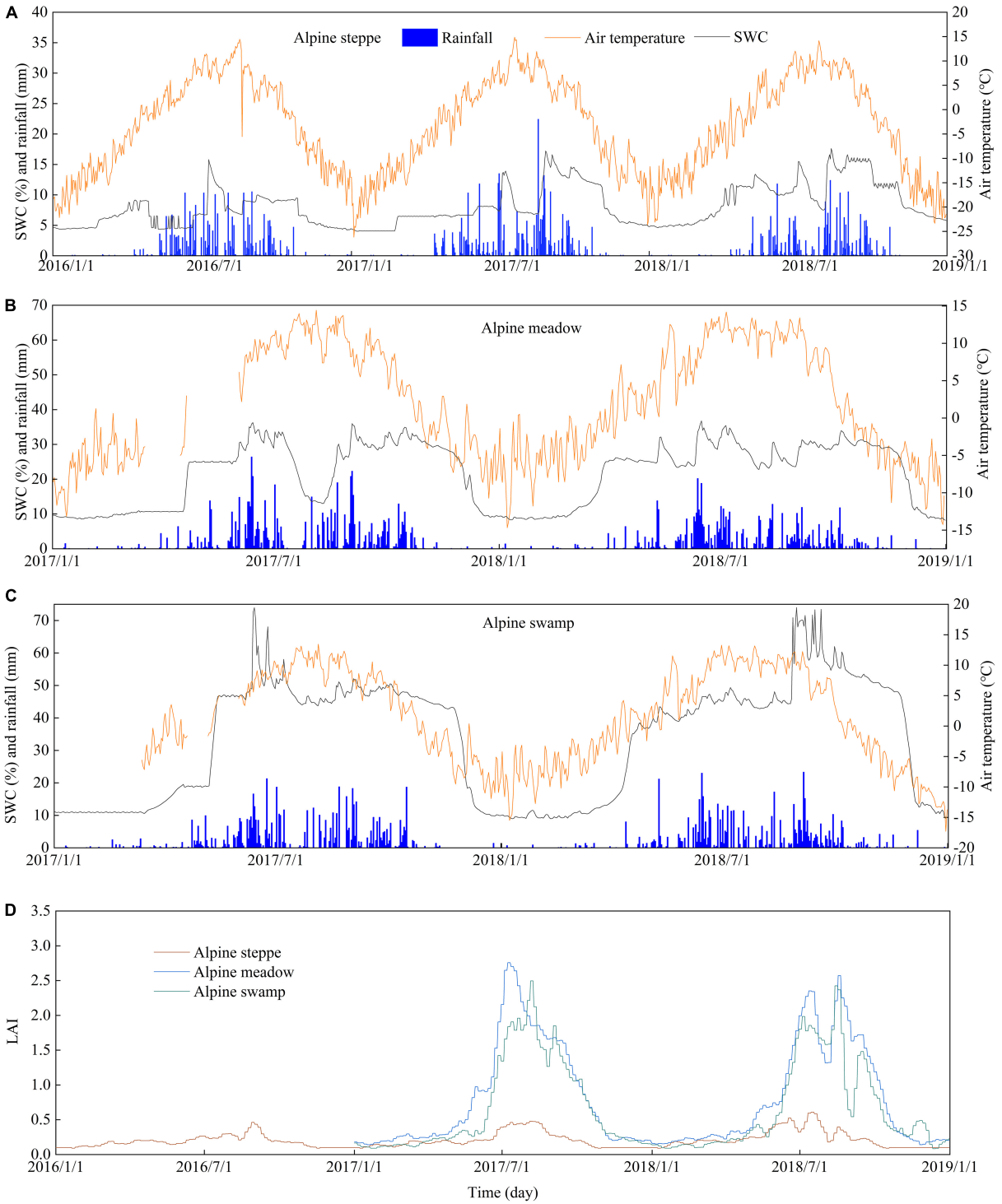

FIGURE 2 | Daily time series of air temperature, rainfall, and soil water content at 20-cm depth at the **(A)** alpine steppe, **(B)** alpine meadow, and **(C)** alpine swamp sites, and **(D)** leaf area index (LAI) at the alpine steppe, alpine meadow, and alpine swamp sites. Note that the *y*-axis scales vary among panels for better presentation.

meadow. This suggests that the model performs best in mild ecosystems and acceptably in dry steppe and humid swamps. The modeled and measured ET was simulated at the three sites, and the fitting curves were mostly distributed near the 1:1 straight line (**Figure 4A**). Although the R^2 values varied among the sites, when taking the three sites as a whole, the change

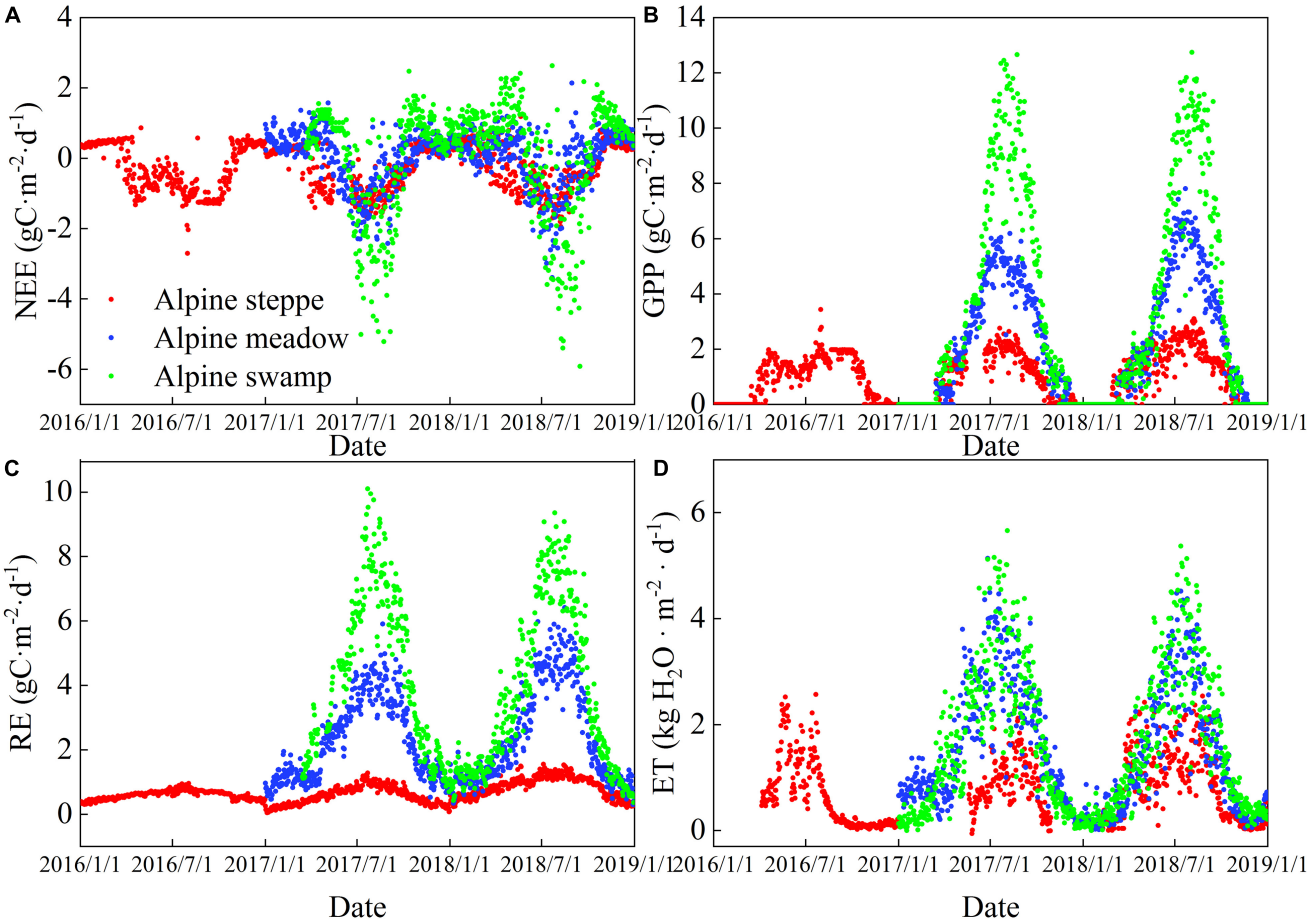

FIGURE 3 | Daily time series of **(A)** net ecosystem exchange, **(B)** gross primary productivity, **(C)** respiration, and **(D)** evapotranspiration (ET) at the alpine steppe, alpine meadow, and alpine swamp sites.

of measured ET explained 80% of the modeled ET, suggesting that the S-W model can be successfully applied in most of the alpine ecosystems.

The seasonal dynamics of T/ET and the comparison of daily T/ET are shown in **Figures 4B,C**, respectively. Seasonal variation of T/ET was one-peak pattern at the three alpine sites. The multiyear average daily T/ET values were 0.13, 0.49, and 0.32 in alpine steppe, alpine meadow, and alpine swamp, respectively (**Figure 4C**). The T showed one-peak pattern at the three alpine sites (**Figure 4D**).

Comparison of Ecosystem Water Use Efficiency and Canopy Water Use Efficiency at the Three Sites

For all ecosystems, WUEc was lower in the peak growing periods and higher in the early and late growing season (**Figure 5B**), which is almost opposite to the WUEe trends (**Figure 5A**). However, the trends of alpine steppe were much less consistent than those of the other two ecosystems, which may be attributed to the harsh and arid environmental conditions that frequently cause drought and frost damage to the vegetation.

The mean daily WUEc and WUEe variation values between years were relatively low at a single site ($p > 0.05$; **Figures 5C,D**); however, the WUEc values were significantly different between the different sites ($p < 0.05$), while the WUEe values were not ($p < 0.05$). The mean daily WUEc values were 7.28, 2.76, and 5.75 g C kg^{-1} H_2O in alpine steppe, alpine meadow, and alpine swamp, respectively. The mean daily WUEe values were 1.65, 1.61, and 2.24 g C kg^{-1} H_2O in these three ecosystems, respectively.

Daily Variations in Water Use Efficiency and Its Driving Factors

The T/ET and LAI values were often significantly correlated with the WUEe and WUEc values (**Figure 6**); WUEe exhibited positive linear relations with T/ET or LAI in each of the three ecosystems and all three together, whereas WUEc exhibited exponential relations with T/ET or LAI in alpine meadow, alpine swamp, and all three ecosystems together. However, the alpine steppe was a unique case that showed lower R^2, which might be attributed to the frequent meteorological disturbance

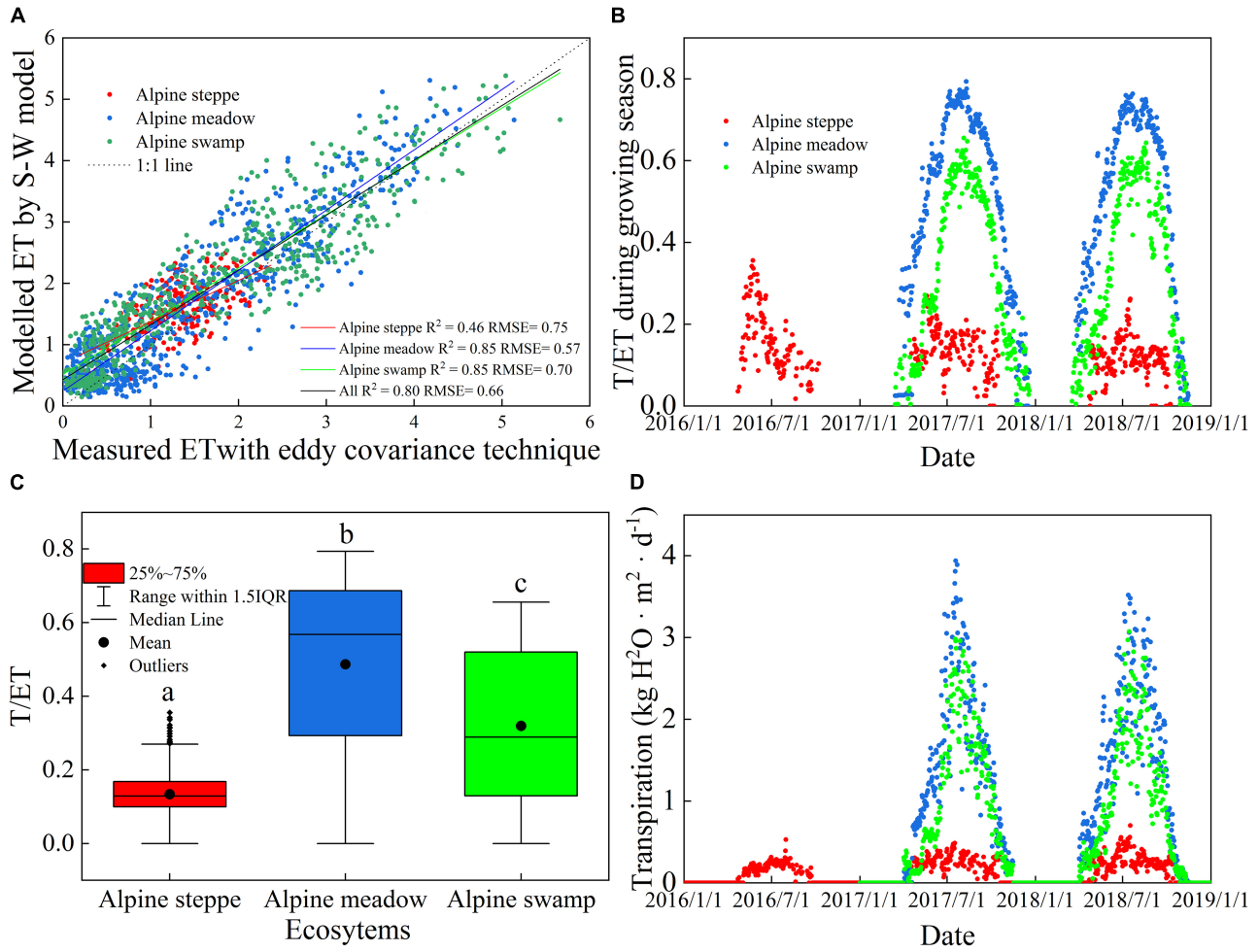

FIGURE 4 | Comparison of **(A)** measured and modeled daily ET, **(B)** daily time series of modeled ratio of transpiration to ET (transpiration [T]/ET), **(C)** the range of daily T/ET, and **(D)** T at the three sites. Different small letters indicate significant differences ($P < 0.05$).

that restricted the growth of local vegetation in the alpine steppe area.

Inter-Annual and Inter-Ecosystem Variations in Water Use Efficiency and Its Driving Factors

Our results showed that gramineous biomass proportion variation across the three alpine ecosystems explained 99% of the WUEe change (**Figure 7B**, $p < 0.001$). Besides, Cyperaceae biomass proportion changes showed a significant positive relationship with WUEe across the three alpine ecosystems. Unlike WUEe, no significant relationships were detected between community biomass characteristics and WUEc. However, community species diversity exhibited strong correlations with WUEc, the species richness change among the alpine ecosystems was negatively related to WUEc (**Figure 7C**, $p < 0.01$), and the H' change explained 99% of the WUEc variation (**Figure 7D**, $p < 0.001$).

DISCUSSION

Comparison of the Ecosystem Water Use Efficiency and Canopy Water Use Efficiency in the Three Alpine Ecosystems

Water use efficiency has been intensively analyzed at the leaf scale through the chamber and isotopic methods and at regional scales through modeling within remotely sensed data (Béziat et al., 2013; Kool et al., 2014; Liu W. et al., 2021). In this study, the overall mean observed that WUEe varied relatively lesser among the three alpine ecosystems and between years (**Figure 4C**; **Table 2**). The mean daily WUEe in alpine steppe and alpine meadow is slightly higher than the results obtained in a dry alpine steppe (0.31–1.38 g C kg^{-1} H_2O) by Hu et al. (2008), when compared with the growing season monthly WUEe (0.03–1.64 g C kg^{-1} H_2O) of FLUXNET sites (Law et al., 2008). The yearly WUEe of the alpine swamp was compared with the WUEe in peak growing season of various land use of temperate steppe of Inner Mongolia

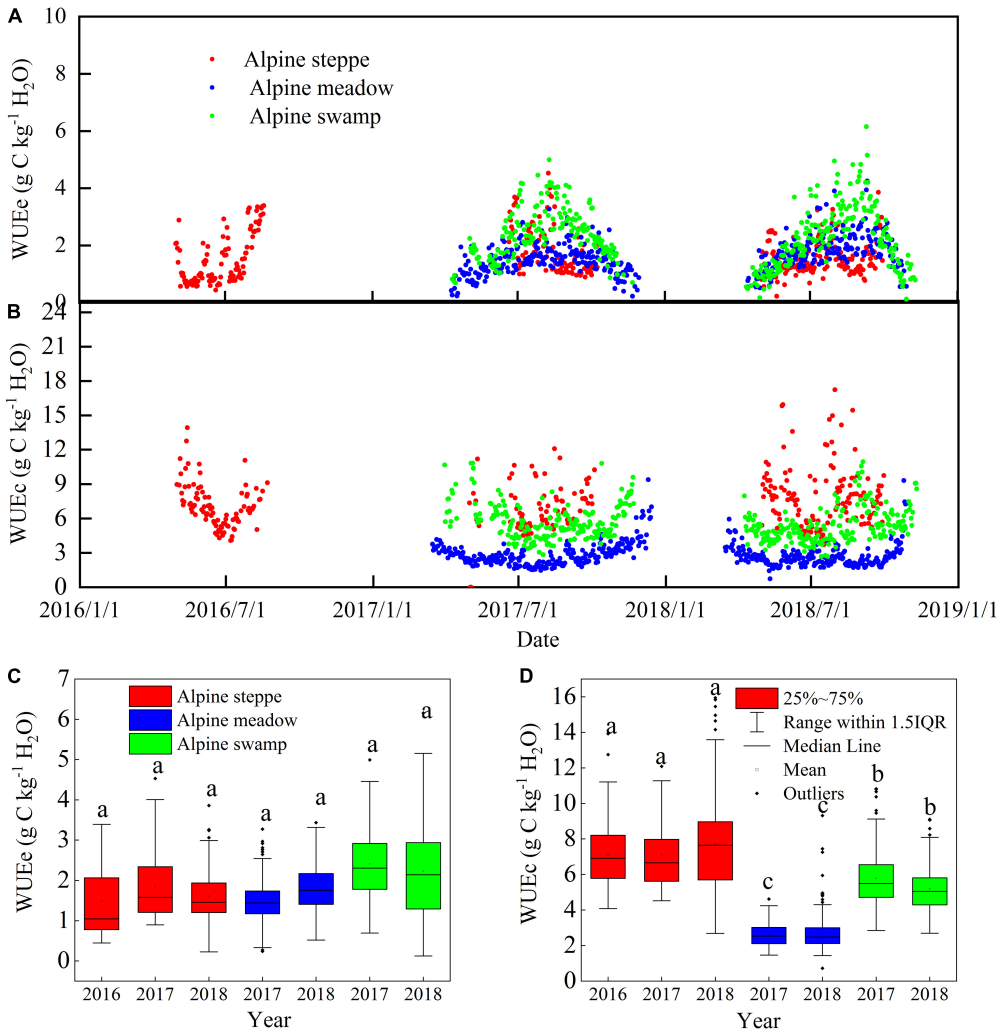

FIGURE 5 | Comparison of seasonal dynamics of **(A)** WUEc and **(B)** WUEe, and the range of daily **(C)** WUEc and **(D)** WUEe in alpine steppe, alpine meadow, and alpine swamp during the study period. Different small letters indicate significant differences ($P < 0.05$).

(more than 2 g C kg^{-1} H$_2$O) (Niu et al., 2011; Li et al., 2016), which indicates that alpine swamp had a higher ecosystem WUE, perhaps implying that increased water availability may improve the WUEe in alpine ecosystems. This could be attributed to the GPP increase response to water availability being more sensitive than the response to ET, which was also concluded in a temperate grassland manipulative experiment (Niu et al., 2011).

The variation range of overall mean daily WUEc of the three alpine ecosystems was larger than that of WUEe (**Figure 4D**) and, unlike WUEe, the WUEc values of the three sites were significantly different from each other. However, the lower site of alpine meadow (**Figure 4C**) was compared with that of temperate steppe (2.1–4.6 g C kg^{-1} H$_2$O) (Niu et al., 2011); WUEc of alpine steppe (**Figure 4D**) was nearly two times higher than other reported temperate ecosystems and was even higher than the monthly results of peak growing season (4.9 g C kg^{-1} H$_2$O) (Li et al., 2016). Besides, the moisture limits, which commonly occurred in the arid or semi-arid steppe area, accordingly caused ET suppression (Cienciala et al., 1994; Zhu et al., 2016). This may also be attributed to the high elevation of these two ecosystems (both higher than 4,000 m; **Table 1**), which are accompanied by strong photosynthetically active radiation at a low temperature (**Figure 1**). Correspondingly, the improved GPP and suppressed T jointly promoted WUEc.

Comparison of the Regulation Mechanism Between Seasonal Variation of Ecosystem Water Use Efficiency and Canopy Water Use Efficiency

Few studies have examined the alpine ecosystem WUE response to changing environmental factors, especially for WUEc. It is generally understood that control of WUE varies with the scale of analysis (Hu et al., 2008; Niu et al., 2011). Thereby, limited understanding of the mechanisms controlling WUEc makes it

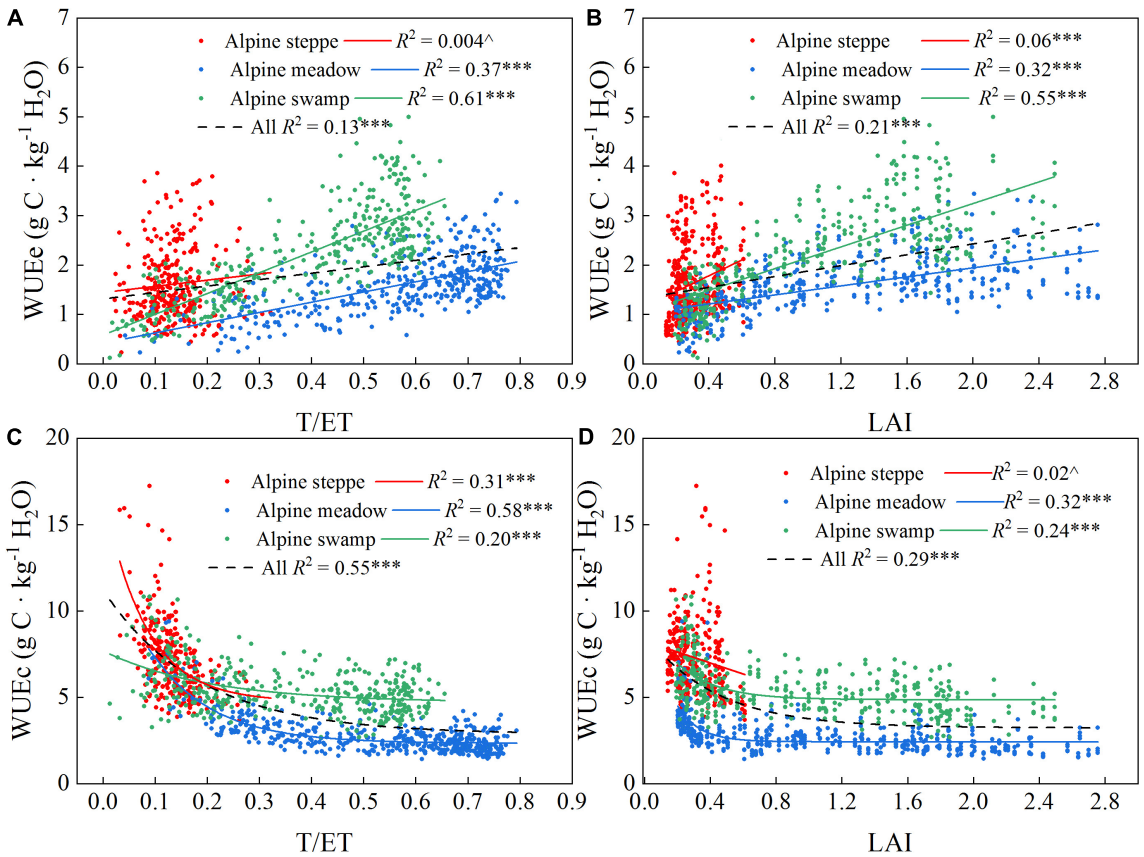

FIGURE 6 | Correlations between T/ET, LAI to WUEe **(A,B)** and T/ET, and LAI to WUEc **(C,D)** of the three alpine ecosystems. R^2 and probabilities of regressions are shown for each correlation. ^$p > 0.05$; ***$p < 0.001$.

more difficult to help Tibetan people to mitigate and adapt to the rapid regional change. As the data and analysis showed in this research, the LAI increases were significantly positively related to WUEe at all three sites (**Figure 6D**, $p < 0.001$), which is consistent with a temperate case study (Hu et al., 2008). However, the T/ET, which is commonly positively related to LAI change, was assumed to have a similar relationship with WUEe. This is the case for alpine meadow and swamp (**Figure 6A**, $p < 0.001$), but the positive relationship was not significant in the alpine steppe, which may be caused by T/ET coupling variation and the metrological and climatological disasters that frequently occur in the alpine steppe area, resulting in severe disturbance to WUE. The T/ET and LAI consistently showed exponential relationships with WUEc (**Figures 6C,D**), which suggests that the higher WUEc occurred when the plant began to grow. At this early growth stage, the photosynthetic conditions show younger leaf tissue with more active enzymes (Nath et al., 2013; Panda and Sarkar, 2013), and the leaves generally do not shade each other. As the plants gradually grew toward the maximum leaf coverage limitation for each community, the light competition and shading effect increased in the community, and consequently, the GPP growth would not catch up with the T growth and the rapidly decreased WUEc of early spring showed a gentler decrease (**Figure 6C**). This would then present as a WUEc decrease to a stable lower level when LAI had sufficiently increased (**Figure 6D**).

Effect of Community Traits on the Inter-Annual and Inter-Ecosystem Variation in Ecosystem Water Use Efficiency and Canopy Water Use Efficiency

Leaf area index, T/ET, and the components of ET are common and critical regulation factors of WUEe (Hu et al., 2008; Li et al., 2016). The community characteristics, including species composition and diversity, have been reported to be closely related to LAI or carbon and vapor exchange (Dong et al., 2015; Li et al., 2015; Wei et al., 2015). The plant community is usually constituted with many coexisting species that may differ in water use strategy (Niu et al., 2011; Ens et al., 2015), thus appearing as considerable differences in WUE in leaf scale of species (Cernusak et al., 2010). The water use characteristics of various species that grow in the Qinghai–Tibetan Plateau were especially diversiform (Wang et al., 2004) because of their great habitat diversity. Proper plant functional group dividing methods would unexpectedly explain WUE variation across ecosystems (**Figures 7A, B**). The results shown in **Figure 7B** support this hypothesis as

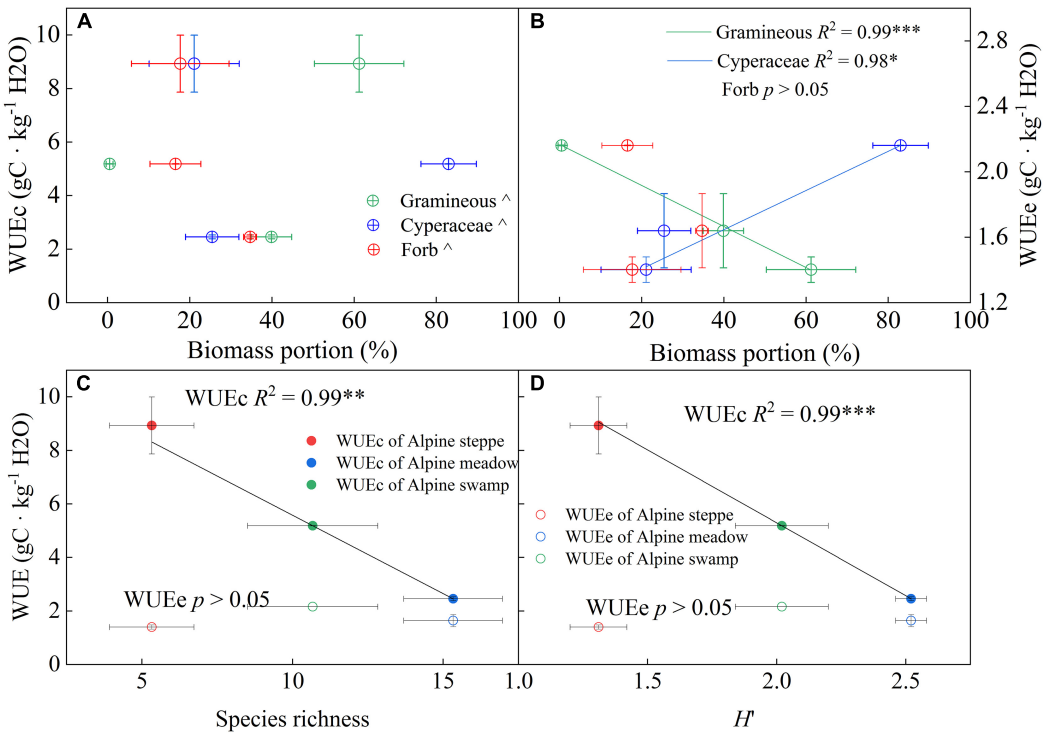

FIGURE 7 | Relationships between yearly WUEe and WUEc and **(A)** total biomass, **(B)** gramineous biomass proportion, and species diversity indices **(C)** species richness and **(D)** Shannon–Wiener diversity index (*H'*) across the three alpine ecosystems. R^2 and probabilities of the regressions are shown. ^$p > 0.05$; *$p < 0.05$; **$p < 0.01$; ***$p < 0.001$. Error bars show the standard deviation.

the gramineous biomass proportion was significantly negatively related to WUEe ($p < 0.001$). This may be attributed to the stronger drought-endurance of gramineous species (Panda and Sarkar, 2013; Hamilton et al., 2015; Zhang et al., 2017). A higher gramineous biomass proportion may, therefore, suggest a dry environment, which implied a lower WUEe and T/ET.

The species diversity indices were commonly negatively correlated with WUEc across alpine ecosystems (**Figures 7C,D**). We supposed that, in the community with complex synusia, the species with higher synusia occupy the best light conditions (Zhang L. et al., 2014), and usually obtained the higher WUE at the leaf scale, thus the species in lower synusia could only use the residue light resources. In a non-water limited situation, because abundant resources compensate for a lack of resources (Lassaletta et al., 2014), the GPP of lower synusia would decrease more than T, thereby the lower WUEc of these supplementary species in low synusia would suppress the WUE of the entire canopy. In contrast, in dry or other extreme environments, the community could only maintain simple synusia and few dominant species, and the vegetation cover would be too low to cause light competition between species, which may explain the high WUEc in barren ecosystems such as alpine steppe.

Limitation and Outlook

There were three observation sites of typical ecosystems in this unique high-altitude region involved in this research, which limited the accurate understanding and creditable analysis across varied ecosystems within large spatial differences. For instance, the positive correlation trends observed between WUEe and LAI (**Figure 6B**) might be subject to amendment, if more different ecosystems had been included in the analysis, since LAI of more humid ecosystems might largely exceed the present maxim LAI recorded in the alpine meadow. Since the linear positive relationship probably has a threshold value, it could bend the trend. Besides, there is still uncertainty in obtaining the accurate daytime Re (Tcherkez et al., 2017), and the approach applied in our research has been argued to overestimate GPP in temperate forests (Wehr et al., 2016), which might hamper the accurate calculation of WUE.

Our findings were concentrated on revealing the regulation between community composition and structure with WUE in ecosystem and canopy scale, which could promote the understanding and accurate access to WUE modified by human activities and climate-driven community change. However, they lack an insightful understanding of the physiological mechanisms that drive the variation in WUEc across these varied alpine ecosystems. In addition, it should be stressed out that our observed phenomenon (e.g., **Figure 7B**) might only be applied to assess WUE in a limited area (alpine grasslands of Tibetan Plateau) or other grasslands dominated by gramineous and Cyperaceae plants, where the ecosystems commonly consist of two clearly divided function groups that largely diverge in water use strategy.

In our mind, a crucial direction for future progress will be used to determine the accurate regulation trends between community composition and structure and WUE, which covers more humid and arid ecosystems and observation sites distributed on the Qinghai–Tibetan plateau. With a deeper understanding of the suitable applied spatial range to these trends, the question of how to obtain a more accurate WUE variation trend and its suitable applied spatial range should be rephrased as follows: Does the composition and structure change across spatial distance or time series present a consistent regulation? Can the obtained trends be successfully applied to a more extreme environment and be mechanically explained by physiological factors? Once the mechanistic scaling of the community composition and structure effects on WUE response to human activities and climate change is successfully established, such a model would inform dynamic Earth-system models to calculate the effects of changing community on ecosystem atmosphere carbon and water exchange, which in turn promotes the accurate prediction on future water and carbon balance of the Qinghai–Tibetan Plateau.

CONCLUSION

Combining the continuously observed eddy covariance system data with the ET partitioning ability of the S-W model, this study was divided into specific components of ecohydrological processes in the three typical alpine ecosystems. Our results showed that the mean yearly GPP was 356.65, 839.54, and 1265.09 g C m^{-2} in the alpine steppe, alpine meadow, and alpine swamp ecosystems, respectively; the mean yearly ET was 254.57, 515.34, and 585.25 kg H_2O m^{-2} in the three typical ecosystems, respectively; the yearly WUEe was 1.40, 1.63, and 2.16 g C kg^{-1} H_2O, in the three typical ecosystems, respectively, and the yearly WUEc was 8.93, 2.46, and 5.19 g C kg^{-1} H_2O in the three typical ecosystems, respectively. A nonlinear effect in WUEc was regulated by LAI and T/ET in alpine ecosystems. Our results also imply that changes in community composition and structure across alpine ecosystems may have a primary impact on WUEc. Our findings indicate that there is a fundamental divergence in driving factors and regulation mechanisms between WUEe and WUEc in the alpine ecosystems.

DATA AVAILABILITY STATEMENT

The original contributions presented in the study are included in the article/supplementary material, further inquiries can be directed to the corresponding authors.

AUTHOR CONTRIBUTIONS

YL and ZH provided the idea for this research and prepared the manuscript. YL and QS contributed to the experimental design. YL and XZ collected the data in the study site. ZC and XZ contributed to the data analysis and figure-making. JD and YZ contributed to the revision of this manuscript. All authors contributed to the article and approved the submitted version.

FUNDING

This research was jointly funded by the National Key Research and Development Program of China (2017YFA0604801 and 2017YFC0506500), the National Natural Science Foundation of China (41971276), and the Second Tibetan Plateau Scientific Expedition and Research Program (2019QZKK0608).

ACKNOWLEDGMENTS

The authors thank Jiyuan Liu and Renhua Zhang for designing the systematic distribution of observation sites.

REFERENCES

Ali, S., Xu, Y., Ma, X., Ahmad, I., Kamran, M., Dong, Z., et al. (2017). Planting patterns and deficit irrigation strategies to improve wheat production and water use efficiency under simulated rainfall conditions. *Front. Plant Sci.* 8:1408. doi: 10.3389/fpls.2017.01408

Ball, J. T., Woodrow, I. E., and Berry, J. A. (1987). "A model predicting stomatal conductance and its contribution to the control of photosynthesis under different environmental conditions," in *Progress in Photosynthesis Research*, ed. I. Biggens (Dordrecht: Springer Netherlands), 221–224. doi: 10.1016/j.envpol.2006.04.007

Bell, J. E., Weng, E., and Luo, Y. (2015). Ecohydrological responses to multifactor global change in a tallgrass prairie: a modeling analysis. *J. Geophy. Res. Biogeosci.* 115, 701–719. doi: 10.1029/2009JG001120

Béziat, P., Rivalland, V., Tallec, T., Jarosz, N., Boulet, G., Gentine, P., et al. (2013). Evaluation of a simple approach for crop evapotranspiration partitioning and analysis of the water budget distribution for several crop species. *Agric. For. Meteorol.* 177, 46–56.

Bremer, D. J., Auen, L. M., Ham, J. M., and Owensby, C. E. (2001). Evapotranspiration in a prairie ecosystem. *Agron. J.* 93, 338–348. doi: 10.2134/agronj2001.932338x

Cernusak, L. A., Aranda, J., Marshall, J. D., and Winter, K. (2010). Large variation in whole-plant water-use efficiency among tropical tree species. *New Phytol.* 173, 294–305. doi: 10.1111/j.1469-8137.2006.01913.x

Cienciala, E., Lindroth, A., Cermak, J., and Haellgren, J. E. (1994). The effects of water availability on transpiration, water potential and growth of Picea abies during a growing season. *J. Hydrol.* 155, 753–764. doi: 10.1093/treephys/19.9.551

De Boeck, H. J., Lemmens, C. M. H. M., Bossuyt, H., Malchair, S., Carnol, M., Merckx, R., et al. (2006). How do climate warming and plant species richness affect water use in experimental grasslands? *Plant Soil* 288, 249–261. doi: 10.1007/s11104-006-9112-5

Dong, J. W., Xiao, X. M., Wagle, P., Zhang, G. L., Zhou, Y. T., Jin, C., et al. (2015). Comparison of four EVI-based models for estimating gross primary production of maize and soybean croplands and tallgrass prairie under severe drought. *Remote Sensing Environ.* 162, 154–168. doi: 10.1016/j.rse.2015.02.022

Ens, E., Hutley, L. B., Rossiter-Rachor, N. A., Douglas, M. M., and Setterfield, S. A. (2015). Resource-use efficiency explains grassy weed invasion in a low-resource savanna in north Australia. *Front. Plant Sci.* 6:560. doi: 10.3389/fpls.2015.00560

Fan, J., Zhong, H., Harris, W., Yu, G., Wang, S., Hu, Z., et al. (2008). Carbon storage in the grasslands of China based on field measurements of above-and below-ground biomass. *Climatic Change* 86, 375–396.

Farquhar, G. D., Hubick, K. T., Condon, A. G., and Richards, R. A. (1989). Carbon isotope fractionation and plant water-use efficiency. *Stable Isotopes Ecol. Res.* 68, 21–40. doi: 10.1007/978-1-4612-3498-2_2

Gebler, S., Franssen, H., Pütz, T., Post, H., Schmidt, M., and Vereecken, H. (2015). Actual evapotranspiration and precipitation measured by lysimeters: a comparison with eddy covariance and tipping bucket. *Hydrol. Earth Syst. Sci.* 19, 2145–2161. doi: 10.5194/hess-19-2145-2015

Hamilton, S. K., Hussain, M. Z., Bhardwaj, A. K., Basso, B., and Robertson, G. P. (2015). Comparative water use by maize, perennial crops, restored prairie, and poplar trees in the US Midwest. *Environ. Res. Lett.* 10: 064015.

Han, L., Wang, Q. F., Chen, Z., Yu, G. R., and Guo, J. X. (2020). Spatial patterns and climate controls of seasonal variations in carbon fluxes in China's terrestrial ecosystems. *Glob. Planet. Change.* 189:103175.

Hu, Z. M., Wen, X. F., Sun, X. M., Li, L. H., Yu, G. R., Lee, X. H., et al. (2014). Partitioning of evapotranspiration through oxygen isotopic measurements of water pools and fluxes in a temperate grassland. *J. Geophy. Res. Biogeosci.* 119, 358–372. doi: 10.1002/2013jg002367

Hu, Z. M., Yu, G. R., Fan, J. W., Zhong, H. P., Wang, S. Q., Li, S. G., et al. (2010). Precipitation-use efficiency along a 4500-km grassland transect. *Glob. Ecol. Biogeogr.* 19, 842–851.

Hu, Z. M., Yu, G. R., Fu, Y. L., Sun, X. M., Li, Y. N., Shi, P. L., et al. (2008). Effects of vegetation control on ecosystem water use efficiency within and among four grassland ecosystems in China. *Glob. Chang Biol.* 14, 1609–1619. doi: 10.1111/j.1365-2486.2008.01582.x

Hu, Z. M., Yu, G. R., Zhou, Y. L., Sun, X. M., Li, Y. N., Shi, P. L., et al. (2009). Partitioning of evapotranspiration and its controls in four grassland ecosystems: application of a two-source model. *Agric. For. Meteorol.* 149, 1410–1420. doi: 10.1016/j.agrformet.2009.03.014

Huxman, T. E., Smith, M. D., Fay, P. A., Knapp, A. K., Shaw, M. R., Loik, M. E., et al. (2004). Convergence across biomes to a common rain-use efficiency. *Nature* 429, 651–654. doi: 10.1038/nature02561

Keenan, T. F., Hollinger, D. Y., Bohrer, G., Dragoni, D., Munger, J. W., Schmid, H. P., et al. (2013). Increase in forest water-use efficiency as atmospheric carbon dioxide concentrations rise. *Nature* 499:324. doi: 10.1038/nature12291

Lassaletta, L., Billen, G., Grizzetti, B., Juliette, A., and Josette, G. (2014). 50 year trends in nitrogen use efficiency of world cropping systems: the relationship between yield and nitrogen input to cropland. *Environ. Res. Lett.* 9:105011. doi: 10.1088/1748-9326/9/10/105011

Lauenroth, W. K., Burke, I. C., and Paruelo, J. M. (2000). Patterns of production and precipitation-use efficiency of winter wheat and native grasslands in the central great plains of the United States. *Ecosystems* 3, 344–351. doi: 10.1007/s100210000031

Law, B., Williams, M., Anthoni, P., Baldocchi, D., and Unsworth, M. (2008). Measuring and modelling seasonal variation of carbon dioxide and water vapour exchange of a *Pinus ponderosa* forest subject to soil water deficit. *Glob. Change Biol.* 6, 613–630. doi: 10.1046/j.1365-2486.2000.00339.x

Li, Y., Fan, J., and Yu, H. (2019a). Grazing exclusion, a choice between biomass growth and species diversity maintenance in beijing—tianjin sand source control project. *Sustainability* 11:1941. doi: 10.3390/su11071941

Li, Y., Fan, J., Hu, Z., Shao, Q., and Harris, W. (2016). Comparison of evapotranspiration components and water-use efficiency among different land use patterns of temperate steppe in the Northern China pastoral-farming ecotone. *Int. J. Biometeorol.* 60, 827–841. doi: 10.1007/s00484-015-1076-9

Li, Y., Fan, J., Hu, Z., Shao, Q., Zhang, L., Yu, H., et al. (2015). Influence of land use patterns on evapotranspiration and its components in a temperate grassland ecosystem. *Adv. Meteorol.* 2015, 1–12. doi: 10.1155/2015/452603

Li, Y., Shao, Q., Fan, J., Chen, Y., Chen, Z., Guan, H., et al. (2019b). Effects of grassland cultivation on ecosystem water use efficiency in a grazed temperate grassland area. *Acta Pratacult. Sin.* 28, 1–12.

Liu, D., Li, Y., Wang, T., Peylin, P., MacBean, N., Ciais, P., et al. (2018). Contrasting responses of grassland water and carbon exchanges to climate change between Tibetan Plateau and Inner Mongolia. *Agric. For. Meteorol.* 249, 163–175.

Liu, J., Xu, X., and Shao, Q. Q. (2008). The spatil and temporal characteristics of grassland degradation in the three-river headwaters region in Qinghai Province. *J. Geograph. Sci.* 63, 364–376.

Liu, R., Zhu, P. F., Wang, Y. S., Chen, Z., Zhu, J. R., Shu, L. Z., et al. (2021). Alternate partial root-zone drip nitrogen fertigation reduces residual nitrate loss while improving the water use but not nitrogen use efficiency. *Front. Plant Sci.* 12:2237. doi: 10.3389/fpls.2021.722459

Liu, S., Zamanian, K., Schleuss, P.-M., Zarebanadkouki, M., and Kuzyakov, Y. (2018). Degradation of Tibetan grasslands: consequences for carbon and nutrient cycles. *Agric. Ecosyst. Environ.* 252, 93–104.

Liu, W., Mo, X., Liu, S., Lin, Z., and Lv, C. (2021). Attributing the changes of grass growth, water consumed and water use efficiency over the Tibetan Plateau. *J. Hydrol.* 598:126464. doi: 10.1016/j.jhydrol.2021.126464

Mahfouf, J., Noihan, J., (1991). Comparative study of various formulations of evaporation from bare soil using *in situ* data. *J. Appl. Meteorol.* 30, 1354–1365.

Nath, K., Phee, B., Jeong, S., Lee, S., Tateno, Y., Allakhverdiev, S., et al. (2013). Age-dependent changes in the functions and compositions of photosynthetic complexes in the thylakoid membranes of *Arabidopsis thaliana*. *Photosynth. Res.* 117, 547–556. doi: 10.1007/s11120-013-9906-2

Niu, S. L., Wu, M. Y., Han, Y., Xia, J. Y., Li, L. H., and Wan, S. Q. (2008). Water-mediated responses of ecosystem carbon fluxes to climatic change in a temperate steppe. *New Phytol.* 177, 209–219. doi: 10.1111/j.1469-8137.2007.02237.x

Niu, S. L., Xing, X. R., Zhang, Z., Xia, J. Y., Zhou, X. H., Song, B., et al. (2011). Water-use efficiency in response to climate change: from leaf to ecosystem in a temperate steppe. *Glob. Change. Biol.* 17, 1073–1082. doi: 10.1111/j.1365-2486.2010.02280.x

Panda, D., and Sarkar, R. K. (2013). Natural leaf senescence: probed by chlorophyll fluorescence, CO2 photosynthetic rate and antioxidant enzyme activities during grain filling in different rice cultivars. *Physiol. Mol. Biol. Plants* 19, 43–51. doi: 10.1007/s12298-012-0142-6

Ponton, S., Flanagan, L. B., Alstad, K. P., Johnson, B. G., Morgenstern, K., Kljun, N., et al. (2006). Comparison of ecosystem water use efficiency among Douglas-fir forest, aspen forest and grassland using eddy covariance and carbon isotope techniques. *Glob. Change Biol.* 12, 294–310. doi: 10.1111/j.1365-2486.2005.01103.x

Reichstein, M., Falge, E., Baldocchi, D., Papale, D., Aubinet, M., Berbigier, P., et al. (2005). On the separation of net ecosystem exchange into assimilation and ecosystem respiration: review and improved algorithm. *Glob. Change. Biol.* 11, 1424–1439. doi: 10.1111/j.1365-2486.2005.001002.x

Scanlon, T. M., and Albertson, J. D. (2010). Canopy scale measurements of CO2 and water vapor exchange along a precipitation gradient in southern Africa. *Glob. Change Biol.* 10, 329–341. doi: 10.1046/j.1365-2486.2003.00700.x

Shannon, E. C. (1948). A mathematical theory of communication. *Bell Syst. Tech. J.* 27, 379–423.

Shuttleworth, W. J., and Wallace, J. S. (2010). Evaporation from sparse crops-an energy combination theory. *Q. J. R. Meteorol. Soc.* 111, 839–855. doi: 10.1002/qj.49711146910

Tcherkez, G., Gauthier, P., Buckley, T. N., Busch, F. A., Barbour, M. M., Bruhn, D., et al. (2017). Leaf day respiration: low co2 flux but high significance for metabolism and carbon balance. *New. Phytol.* 216, 986–1001. doi: 10.1111/nph.14816

Wang, B., Bao, Q., Hoskins, B., Wu, G., and Liu, Y. (2008). Tibetan Plateau warming and precipitation changes in East Asia. *Geophys. Res. Lett.* 35:L14702. doi: 10.1029/2008GL034330

Wang, L., Houyuan, L. U., and Naiqin, W. U. (2004). Discovery of C4 species at high altitude in Qinghai-Tibetan Plateau. *Chinese Sci. Bull.* 49, 1392–1396.

Wang, S., Fan, J., Li, Y., and Huang, L. (2019). Effects of grazing exclusion on biomass growth and species diversity among various grassland types of the tibetan plateau. *Sustainability* 11:1705. doi: 10.3390/su11061705

Webb, E. K., Pearman, G. I., and Leuning, R. (2010). Correction of flux measurements for density effects due to heat and water vapour transfer. *Q. J. R. Meteorol. Soc.* 106, 85–100. doi: 10.1002/qj.49710644707

Wehr, R., Munger, J. W., Mcmanus, J. B., Nelson, D. D., Zahniser, M. S., Davidson, E. A., et al. (2016). Seasonality of temperate forest photosynthesis and daytime respiration. *Nature* 534, 680–683. doi: 10.1038/nature17966

Wei, Y., Hu, Z. M., Zhao, Y. P., Zhang, X. Z., Fan, Y. Z., Shi, P. L., et al. (2015). Modeling net ecosystem carbon exchange of alpine grasslands with a satellite-driven model. *PLoS one* 10:e0122486. doi: 10.1371/journal.pone.0122486

Williams, D. G., Cable, W., Hultine, K., Hoedjes, J. C., Yepez, E. A., Simonneaux, V., et al. (2004). Evapotranspiration components determined by stable isotope, sap flow and eddy covariance techniques. *Agric. For. Meteorol.* 125, 241–258. doi: 10.1016/j.agrformet.2004.04.008

Wu, G., Liu, X., Chen, T., Xu, G., Wang, W., Zeng, X., et al. (2015). Elevation-dependent variations of tree growth and intrinsic water-use efficiency in Schrenk spruce (*Picea schrenkiana*) in the western Tianshan Mountains, China. *Front. Plant Sci.* 6:309. doi: 10.3389/fpls.2015.00309

Yu, G. R., Wen, X. F., Sun, X. M., Tanner, B. D., Lee, X. H., and Chen, J. Y. (2006). Overview of ChinaFLUX and evaluation of its eddy covariance measurement. *Agric. For. Meteorol.* 137, 125–137. doi: 10.1016/j.agrformet.2006.02.011

Zhang, L. X., Fan, J. W., Shao, Q. Q., Tang, F. P., Zhang, H. Y., and Li, Y. Z. (2014). Changes in grassland yield and grazing pressure in the Three Rivers headwater region before and after the implementation of the eco-restoration project. *Acta Pratacult. Sin.* 23, 116–123.

Zhang, L., Zhongmin, H. U., Fan, J., Zhou, D., and Tang, F. (2014). A meta-analysis of the canopy light extinction coefficient in terrestrial ecosystems. *Front. Earth Sci.* 8:599–609. doi: 10.1093/aob/mcw099

Zhang, P., Wei, T., Cai, T., Ali, S., Han, Q., Ren, X., et al. (2017). Plastic-film mulching for enhanced water-use efficiency and economic returns from maize fields in semiarid China. *Front. Plant Sci.* 8:512. doi: 10.3389/fpls.2017.00512

Zhang, T., Xu, M. J., Zhang, X. Z., Zhao, T. H., An, T. T., Li, Y. G., et al. (2019). Grazing-induced increases in soil moisture maintain higher productivity during droughts in alpine meadows on the Tibetan Plateau. *Agric. For. Meteorol.* 269, 249–256.

Zhou, S., Yu, B., Zhang, Y., Huang, Y., and Wang, G. (2018). Water use efficiency and evapotranspiration partitioning for three typical ecosystems in the Heihe River Basin, northwestern China. *Agric. For. Meteorol.* 253–254, 261–273. doi: 10.1016/j.agrformet.2018.02.002

Zhu, X., Shao, M., Zeng, C., Jia, X., Huang, L., Zhang, Y., et al. (2016). Application of cosmic-ray neutron sensing to monitor soil water content in an alpine meadow ecosystem on the northern Tibetan Plateau. *J. Hydrol.* 536, 247–254. doi: 10.1016/j.jhydrol.2016.02.038

Conflict of Interest: The authors declare that the research was conducted in the absence of any commercial or financial relationships that could be construed as a potential conflict of interest.

Publisher's Note: All claims expressed in this article are solely those of the authors and do not necessarily represent those of their affiliated organizations, or those of the publisher, the editors and the reviewers. Any product that may be evaluated in this article, or claim that may be made by its manufacturer, is not guaranteed or endorsed by the publisher.

Copyright © 2022 Li, Zhang, Shao, Fan, Chen, Dong, Hu and Zhan. This is an open-access article distributed under the terms of the Creative Commons Attribution License (CC BY). The use, distribution or reproduction in other forums is permitted, provided the original author(s) and the copyright owner(s) are credited and that the original publication in this journal is cited, in accordance with accepted academic practice. No use, distribution or reproduction is permitted which does not comply with these terms.

frontiers in Plant Science

ORIGINAL RESEARCH
published: 27 January 2022
doi: 10.3389/fpls.2021.772503

The Complex Biodiversity-Ecosystem Function Relationships for the Qinghai-Tibetan Grassland Community

Wei Qi[1†], Xiaomei Kang[1†], Johannes M. H. Knops[2], Jiachang Jiang[3], A. Abuman[3] and Guozhen Du[1]*

[1] State Key Laboratory of Grassland Agro-ecosystems, School of Life Sciences, Lanzhou University, Lanzhou, China, [2] Department of Health and Environmental Sciences, Xi'an Jiaotong Liverpool University, Suzhou, China, [3] Gansu Provincial Extension Station of Grassland Techniques, Lanzhou, China

Despite the long history of the study of the biodiversity-ecosystem function relationship, uncertainty remains about the relationship of natural grassland ecosystems under stressful conditions. Recently, trait- and phylogenetic-based tests provide a powerful way to detect the relationship in different spaces but have seldom been applied to stressful zones on a large spatial scale. We selected Qinghai-Tibetan as the study area and collected a grassland community database involving 581 communities. We calculated biomass and species', functional, and phylogenetic diversity of each community and examined their relationships by using linear and non-linear regression models. Results showed an overall positive biodiversity-productivity relationship in species', functional and phylogenetic space. The relationship, however, was non-linear, in which biodiversity explained better the variation in community biomass when species diversity was more than a threshold, showing a weak effect of biodiversity on ecosystem function in low species diversity communities. We also found a filled triangle for the limit of the relationship between species and functional diversity, implying that functional diversity differs significantly among communities when their species diversity is low but finally converges to be a constant with increasing communities' species diversity. Our study suggests that multiple niche processes may structure the grassland communities, and their forces tend to balance in high-biodiversity communities.

Keywords: biodiversity, community assembly, ecosystem function, functional diversity, phylogenetic diversity, specific leaf area, seed mass, Tibetan grassland

OPEN ACCESS

Edited by:
Junran Jimmy Li,
University of Tulsa, United States

Reviewed by:
Nuria Pistón,
Federal University of Rio de Janeiro, Brazil
Xiaodong Wu,
Chinese Academy of Sciences (CAS), China

****Correspondence:***
Wei Qi
qiw@lzu.edu.cn

† These authors have contributed equally to this work

Specialty section:
This article was submitted to Functional Plant Ecology, a section of the journal Frontiers in Plant Science

Received: *08 September 2021*
Accepted: *10 December 2021*
Published: *27 January 2022*

Citation:
Qi W, Kang X, Knops JMH, Jiang J, Abuman A and Du G (2022) The Complex Biodiversity-Ecosystem Function Relationships for the Qinghai-Tibetan Grassland Community. Front. Plant Sci. 12:772503. doi: 10.3389/fpls.2021.772503

INTRODUCTION

The worldwide biodiversity decline has led to an increasing scientific interest in examining how biodiversity changes affect ecosystem functioning (Hooper et al., 2005; Cadotte et al., 2009). A well-supported hypothesis is that plant species differ in traits that generate different abilities to exploit resources, such as light, water, nutrients, pollinators, etc. Thus, because of different traits, with higher species richness a plant community is able to use more resources, increase productivity, and thereby ecosystem functioning (Liu et al., 2015; Duffy et al., 2017).

However, species richness may be a poor proxy for biodiversity, because the number of plant species often cannot capture the diversity in species traits that determines total resource use (Chalcraft et al., 2009). Therefore, the current research focus has shifted to other aspects of diversity. Functional diversity may quantify trait differences that define species interactions better

(Reiss et al., 2009; Rosenfield and Müller, 2020), and therefore capture how the diversity within a community influences both resource acquisition (Violle et al., 2007) and community productivity (Chollet et al., 2014). However, questions remain about which traits need to be considered, and how to translate trait differences into ecological differences (Cadotte et al., 2009; Cadotte, 2017). Another alternative approach is to use the phylogenetic distances among co-occurred species to calculate a phylogenetic relatedness index. Functional trait dissimilarity is correlated with species evolutionary divergence time (Cadotte et al., 2009; Cadotte, 2017), thus a community phylogenetic relatedness index may be a good way to capture the functional, evolutionary, and ecological dissimilarity among species (Kraft et al., 2007; Cadotte et al., 2009; Lemoine et al., 2015). However, the explanatory power of phylogenetic diversity is largely dependent on the species pool and is often questioned because inter-specific functional or niche differences are rarely caused by their evolutionary divergence (Chollet et al., 2014; Lososová et al., 2016). Therefore, recent research focus has shifted to integrating aspects of species richness, functional and phylogenetic diversity and such integrated methods are more effective in capturing variation along environmental gradients in ecosystem productivity, and community structure (Cadotte et al., 2009; Bu et al., 2014; Liu et al., 2015; Rolo et al., 2016; Lyu et al., 2017; de la Riva et al., 2018).

The relationship between species richness and either functional or phylogenetic diversity can also provide insight into the mechanism driving ecosystem functioning and community assembly (Micheli and Halpern, 2005). A positive linear relationship indicates that each species has unique traits or is phylogenetic distinct. Such a positive relationship implies that functional or phylogenetic diversity is complementary among species and that each species contributes equally to ecosystem functioning. In contrast, the absence of a relationship implies functional redundancy, reflecting that species share similar traits or are closely related (Micheli and Halpern, 2005; Mensah et al., 2018). Non-linear relationships imply that the relationship between species richness and either functional or phylogenetic diversity varies depending on species richness (Guerrero et al., 2014). For example, a logarithmic relationship between species richness and functional diversity implies that functional diversity is strongly positively correlated with species richness at low species richness levels, and much less at higher species richness levels (Micheli and Halpern, 2005; Bu et al., 2014). Furthermore, the pattern of this relationship may depend on which functional traits are selected. For instance, Lososová et al. (2016) found a positive correlation of species richness and functional diversity in dispersal traits (dispersal type, seed mass, and seed bank type) and competitiveness traits (plant height, SLA, and LDMC). However, in contrast, there was no relationship for species richness in relation to niche trait preferences for light, temperature, soil moisture, and nutrients. Therefore, different kinds of traits, reflecting different aspects of plants' function, have to be combined to gain a better understanding of the overall relationship (de la Riva et al., 2018).

The species, functional and phylogenetic aspects of diversity have been examined in many plant communities where environmental stress is non-significant (Hooper et al., 2005; Chalcraft et al., 2009; Jaillard et al., 2014; Zhu et al., 2016; Duffy et al., 2017). In these communities, competition for resources dominates species interactions and functional redundancy among species is common because a small number of dominant species with similar optimal traits structure the communities (thus functional clustering; Micheli and Halpern, 2005; Kang et al., 2015; Mensah et al., 2018; Rosenfield and Müller, 2020; but seen in Mayfield and Levine, 2010, they have assumed in theory that competition for resources may drive functional/phylogenetic over-dispersion or clustering because species have traits contributing to both competitive ability and niche differences). However, in some stressful ecosystems, facilitation, i.e., positive interactions between plant species, have been documented (Callaway et al., 2002; Michalet et al., 2014; Fichtner et al., 2017). Functional dissimilarity is essential for positive species interactions (Maestre et al., 2009; Lyu et al., 2017), thus functional complementation among species should be expected. However, even in communities where facilitation occurs, competition is also frequently documented. Thus, examining the relationships between species richness and functional or phylogenetic diversity in a stressful ecosystem, e.g., Qinghai-Tibetan Plateau (QTP), where both competitive and facilitative plant interactions, as well as meantime significant environmental filtering, operate (Choler et al., 2001; Anthelme et al., 2014; He and Bertness, 2014), may provide new insights into species coexistence and ecosystem functioning.

Alpine/subalpine grasslands are common on the eastern and central QTP covering ∼1.282 million km^2, or ∼13.4% of China's total area. These high-altitude grasslands are exposed to extreme weather conditions and vary dramatically in plant richness, abundance, productivity, species composition, and plant traits along environmental gradients (Wu and Chen, 2004; Yang et al., 2009; Qi et al., 2021). This large variability may give rise to the significant differences in species' interactions among communities with different structure traits or under different environmental conditions (Choler et al., 2001; Callaway et al., 2002; Schöb et al., 2013; Michalet et al., 2014; Lyu et al., 2017), resulting in a possibly significant shift in the relationships among species richness, productivity, and plant functional traits. Recently, in QTP grasslands the relationship between productivity and different aspect of diversity have been observed in a few small-scale observational studies (Zhu et al., 2015; Zhang et al., 2018) and a dozen manipulative studies, such as fertilization (Niu et al., 2014; Li et al., 2015), mowing or grazing management (Niu et al., 2016), and planting or removing individuals (Liu et al., 2015; Lyu et al., 2017). The often conflicting findings about how the diversity affects community productivity (e.g., positive species diversity effect on productivity in Lyu et al., 2017; Zhang et al., 2018, but negative effect in Niu et al., 2014) as well as which aspects of biodiversity and which kinds of traits or trait combination (e.g., plant height in Li et al., 2015; Liu et al., 2015, but specific leaf area and leaf dry matter content in Zhu et al., 2016) are more important in explaining community productivity, however, call for a large-scale study involving different aspects of relationships to reveal universal patterns of the natural ecosystem.

Here, we collected a large dataset encompassing 40% of the QTP area to examine relationships between different aspects of diversity and community productivity as well as between species richness and plant functional or phylogenetic diversity. We hypothesize that (1) species are largely complementary in stressful QTP environments, thus we predict a positive linear relationship between species richness and productivity; (2) species' functional dissimilarity is hypothesized to be essential for facilitation, and therefore, we hypothesize that functional diversity will be more effective than species richness in explaining grassland productivity of QTP where facilitative interactions are significant (Choler et al., 2001; Anthelme et al., 2014); (3) the relationship between species richness and either functional or phylogenetic diversity may be complicated because facilitative interactions call for functional or phylogenetic complementary among species, resulting in a positive relationship, or strong environmental filtering enhancing functional or phylogenetic similarity among species, resulting in a non-linear relationship. In addition, we examined the relationship between species richness or community productivity and functional diversity of different dimensions (i.e., stem, leaf, seed, and their combinations) to assess whether the relationship is independent of selected traits.

MATERIALS AND METHODS

Study Area

This study was conducted along seven transects (four west-east and three north-south transects) is mainly alpine and subalpine grasslands located across the eastern and central part of the Qinghai-Tibetan Plateau. Due to the restrictions of terrain and available roads, the transects' shape appears to be irregular and non-linear. The study area is 1,220 km long and 1,070 km wide, covering a geographic area within the latitude of 29.14–38.84° N and longitude of 88.15–101.51° E.

Field Sampling and Trait Measurement

Field surveys were conducted during late July to early September in 2014 and 2017 and 118 sites were finally surveyed along the seven transects according to the criterion of every 50–60 km interval unless there were no grassland vegetations (e.g., forest, shrub, salt marsh, barren and stony land, lake, farmland, or residential area) (**Figure 1** and **Supplementary Appendix 1**). Field time is the peak aboveground biomass and cover time for most species in the vegetation (Zhu et al., 2015, 2016). All sampling sites were used as yak and sheep winter grazing pasture (from late autumn to early spring) and no obvious summer grazing by livestock or rodents was observed. In total, 118 sites were selected which were as follows: 17 desert steppes, 19 steppes, 26 steppes meadow, 37 meadows, 12 wet meadows, and 7 cushion vegetation (altogether six grassland types). Moreover, seven plots were in the subglacial belt, 35 in the subalpine (including cold temperate), and 76 in the alpine belt. These sites represent an elevational range from 2,792 to 5,217 m, with the climatic range covering a gradient in mean annual temperature (MAT) of -9.04 to 6.07°C and mean annual precipitation (MAP) of 44–716 mm. For selected sites, the number proportion of each grassland vegetation or climate belt is roughly equal to its area proportion in the studied zone (Wu, 1980). In total, we recorded 719 angiosperm species which included almost all dominant species and more than 65% common species in the study region (Wu and Chen, 2004) and we used 719 as the regional species pool number.

For each site, we recorded the geographical coordinates, elevation, slope gradient, and aspect. Five 1 m × 1 m quadrats were laid at a distance of 30–40 m from each other within each 100 m × 100 m site and all vascular plant species were recorded. In the meadow, wet meadow and cushion vegetation individual plants have a very high abundance (up to 2,200/m^2), thus, for aboveground biomass and abundance, we sampled a smaller0.5 m × 0.5 m quadrat located within the 1 m^2 quadrats and calculated each species 1 m^2 abundance and biomass. In total, we sampled 581 quadrats due to the loss of plant material or recording problems in 9 quadrats of 6 sites.

For the vegetation measurements, in each quadrat we recorded the canopy cover, species number, individual plant number, height, and the percent cover and aboveground biomass of each species. Each species aboveground biomass was clipped to the soil level and then weighed after removing any dead parts (standing dead and litter) and dried at 75°C for 48 h to a constant weight.

We selected four traits tightly associated with plant life strategy and functional tradeoff: specific leaf area (SLA), leaf size, plant height, and seed mass. SLA is correlated with other plant traits such as leaf nitrogen content, leaf lifespan, relative growth rate, representing, thus, a trade-off between the leaf carbon acquisition rate and the longevity of plant tissues (Schöb et al., 2013; Qi et al., 2014; Lemoine et al., 2015; Rolo et al., 2016). Plant height and leaf size indicate a trade-off between the competitive or interception ability for light and support structure (e.g., stem, twig, and petiole biomass construction) cost; while seed mass signifies the trade-off between dispersal probability and a seedling establishment's ability (Cadotte et al., 2009; Niu et al., 2014; Qi et al., 2015; Wagg et al., 2017). Thus, community-level distribution patterns (e.g., clustering or divergence) for these traits can disentangle the importance of these trade-offs during community assembly and help predict how assembly processes respond to environmental changes (Lemoine et al., 2015; Qi et al., 2015; Schmitz et al., 2015; Rolo et al., 2016; Wagg et al., 2017). There were 7,905 species records (samplings) in 581 quadrats (average 13.61 species per quadrat). For each sampling, 3–5 mature individuals and 5–20 fully developed but not senescing leaves were randomly chosen to measure plant height and leaf traits, respectively. The seed mass of most species was from a large database based on our previous studies. The methods of trait measurement referred to Qi et al. (2014, 2015), and their details are described in **Supplementary Appendix 2**.

Species Diversity, Phylogenetic Diversity, and Functional Diversity

For each quarter, we first calculated each species' important value index (IVI) as the average of its relative biomass, relative cover, and relative density. We used IVI instead of the frequently used

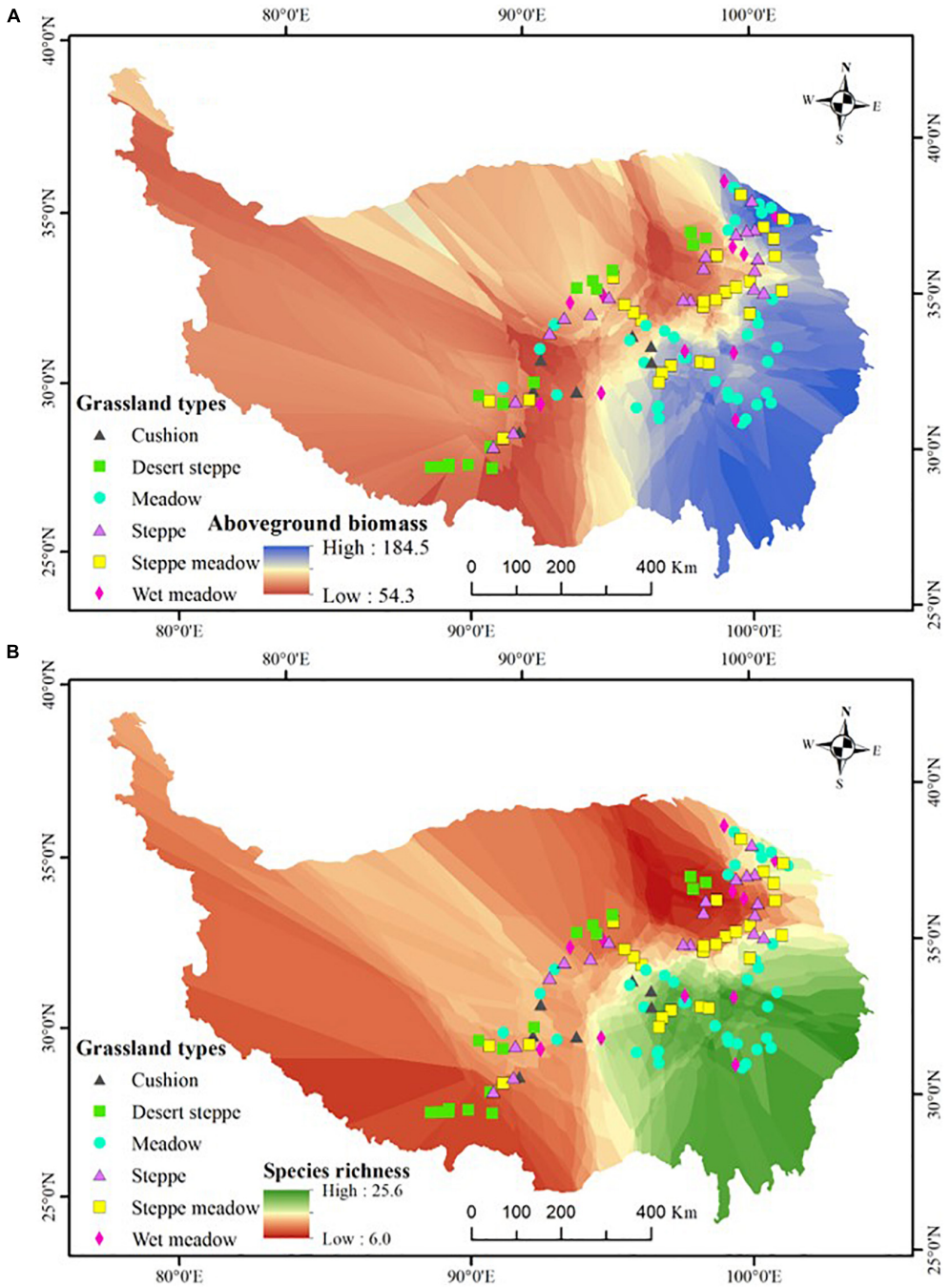

FIGURE 1 | The geographic variation in aboveground biomass **(A)** and species richness **(B)**, and the distribution of the 118 study sites. The map showed the outline of the Qinghai-Tibetan Plateau, which was edited and generated with ArcGIS 10.2 software, http://www.esri.com/. Coordinate system: E, east longitude; N, north latitude.

relative density because the former (1) represents more clearly the status and performance of species in a community, and (2) standardizes the data and makes the variance independent of the mean, which is better for this study with obvious differences in species composition and community structure among sites. Species diversity in each quarter was estimated with both species' richness and the Shannon–Wiener index [$H = -\Sigma\ (p_i \times \ln p_i)$, where p_i is the IVI of species i].

Rao's quadratic index (FD_Q) was used to estimate the community functional diversity. FD_Q is the sum of the pairwise trait distances between species weighted by their IVI. FD_Q for single and multiple traits was calculated by using R and

FDiversity (Casanoves et al., 2011). We used Rao's quadratic index (FD_Q) for two reasons. First, Carboni et al. (2013) has advocated that this measure is more comprehensive for describing the community trait diversity. Secondly, FD_Q can be used to examine both single and multiple trait space, therefore better to predict variations in ecosystem functions (Butterfield and Suding, 2013).

We calculated the plant community phylogenetic diversity, which was assessed on the basis of a published angiosperm supertree (Phylomatic tree R20120829)[1]. Branch lengths were assigned using the BLADJ algorithm in Phylocom 4.2 software (Webb et al., 2008). To quantify community phylogenetic diversity, we calculated the mean pairwise phylogenetic distance (MPD) using the "construct" function in Phylocom 4.2 software (Webb et al., 2008). The calculation of MPD is mathematically similar to FD_Q, and thus, the combination of MPD and FD_Q can provide a uniform and effective assessment of functional and phylogenetic community patterns. Based on the phylogenetic tree, we also calculated the phylogenetic signal of each plant trait, and the methods and results of the calculation were referred to in **Supplementary Appendix 3**.

Species number and abundance varied dramatically among sampled quadrats in our data. To remove any effect of sample size, we calculated the standardized effect size (SES) of MPD and FD_Q against a null model by generating 10,000 random assemblages for each community, while preserving the species IVI and shuffling the taxon names. For MPD, we calculated SES_M as: $SES_M = (MPD_{OBS} - MPD_{RANDOM})/sd(MPD_{RANDOM})$, where $sd(MPD_{RANDOM})$ is the standard deviation of the random MPD values. For FD_Q, we calculated SES_{FD} as: $SES_{FD} = (FD_{OBS} - FD_{RANDOM})/sd(FD_{RANDOM})$. A positive/negative SES_{FD} or SES_M indicates that traits or phylogeny are dispersed/clustered within a community. The difference in species, functional, and phylogenetic diversity among six grassland types is shown in **Supplementary Appendix 4**, in which meadow had highest species richness, aboveground biomass, SES_M and SES_{FD} of leaf size, SLA, and multiple traits, steppe had highest SES_{FD} of plant height and seed mass, desert steppe had lowest aboveground biomass, species richness and SES_{FD} of SLA, the wet meadow had lowest SES_M and SES_{FD} of seed mass, and cushion vegetation had lowest SES_{FD} of leaf size, plant height, and multiple traits.

Statistical Analyses

Data on functional traits, aboveground biomass, and species richness were log-transformed to improve normality. We used regression analyses to test for the relationship among aboveground biomass, species diversity (species richness and H), and various functional and phylogenetic diversity indexes. For all regressions, we examined the fit of linear, quadratic, and piecewise models using stat and segmented packages from Software R 4.2.1, and identified the best fit model based on the explained variance (higher R^2) and parameter significance (lower *P*-values). We constrained the maximum number of breakpoints to one per model to avoid overfitting. In piecewise models, the significance of the difference in regression slope between either side of breakpoint was evaluated by using Davies' test. In addition, we used the difference in AIC (Akaike information criterion) value (ΔAIC) to compare among models. If ΔAIC was < 5 between linear and non-linear (quadratic and piecewise) models, models were considered not different (Segura et al., 2015), and the simple linear model was selected as the best model.

Communities' phylogenetic or functional diversity may be structured by multiple niche processes (see the "Introduction"), resulting in a potential high variance among communities even with similar species diversity. Thus, there may be more than a single slope (i.e., rate of change) describing the relationship between species and phylogenetic (or functional) diversity (de Carvalho and Tejerina-Garro, 2015). Accordingly, we then used quantile regression analysis with phylogenetic or each functional diversity index as the response variable. The analysis can identify the limits, boundaries, and shifting within our bivariate distributions by estimating slopes not only through the median but also through each quantile (or percentile) of the relationship. We examined the nature of this upper (lower) bound with quantile regressions with data points in the 0.95 (0.05) quantile using Quantreg package (Koenker, 2018) for R. The significance of the slopes of quantile regressions was assessed with bootstrapped standard errors (with 999 permutations; Silva et al., 2016).

RESULTS

Structure traits varied dramatically among communities, with species richness ranging from 3 to 37 species, aboveground biomass from 12.4 to 327.64 g, and individual density (abundance) from 4 to 2,252 in a 1 m^2 quarter (**Supplementary Appendix 1**). Similar trends were found in various diversity indexes, in which H ranged from 0.58 to 3.13, SES_M from −4.54 to 1.84, and SES_{FD} of leaf size, SLA, plant height, seed mass, and multi-traits from −3.43, −3.00, −2.86, −3.22, and −2.39, to 3.21, 2.18, 3.31, 2.76, and 2.32, respectively. Moreover, based on 95% confidence intervals (CI), the mean SES_M (95% CI: −0.541 to −0.385, same below) was significantly lower, while the mean SES_{FD} of leaf size (0.108–0.278), plant height (0.189–0.407) and multi-traits (0.051–0.184) were significantly but slightly higher than zero, indicating an overall phylogenetic clustering and a functional overdispersion within a community. SES_{FD} of SLA (−0.032 to −0.115) and seed mass (−0.120 to −0.034), however, were non-significantly different from zero (**Supplementary Figure 1**).

Overall, communities' aboveground biomass significantly increased with species diversity (species richness and H), and the best fit model for both relationships was the piecewise regression model, in which the breakpoint was found at about 11.2 species/m^2 (log-scale species richness = 1.05; 95% CI: 0.94–1.15) and H = 1.74 (1.51–1.97), with the ABP varying non-significantly before the breakpoint and increasing dramatically with species richness or H after the breakpoint (**Table 1** and **Figure 2**). Besides, the fit model for the relationship between ABP and SES_{FD} of most of plant traits except for seed mass was also

[1]https://github.com/camwebb/phylomatic-awk

piecewise regression, in which ABP firstly decreased slowly but significantly with SES_{FD} of leaf traits and then increased rapidly from the breakpoint at SES_{FD} of leaf size and SLA equal to −1.21 and −1.00, respectively, but ABP firstly increased rapidly with SES_{FD} of plant height and then varying non-significantly after the breakpoint (**Table 1** and **Figure 3**). Finally, the fit model for the relationship between ABP and SES_M and SES_{FD} of multi-traits were similar, they both showed non-significant relationship before the breakpoint and significantly positive relationship after the breakpoint (**Table 1** and **Figure 3**).

There was no consistent relationship between species richness and functional and phylogenetic community diversity. For example, the best model fitting the relationship related to SES_M and SES_{FD} of leaf size, SLA, and multi-traits was also the piecewise model (**Table 2**) with estimated species diversity thresholds (about 9–11 species/m^2 for different traits, details were seen in **Table 2**) slightly lower than those estimated to aboveground biomass. Moreover, the piecewise model was still the optimal model suitable for the relationship between species richness and SES_{FD} of plant height, with SES_{FD} value firstly decreasing significantly but slowly and then increasing rapidly when species richness was more than the breakpoint (about 12 species/m^2). On the contrary, the species richness-SES_{FD} of seed mass relationship was obscure, and not suitable for any regression model (**Table 2**).

Quantile regression showed a significant shift in linear regression coefficient (sign and slope) among the upper (95th), median (50th), and lower (5th) quantiles for the relationship between species diversity and functional and phylogenetic diversity (**Supplementary Table 1**). For example, the relationships of species richness (**Figure 4**) or H (**Supplementary Figure 2**) were significantly and strongly positive to SES_M and SES_{FD} of all traits at the lower (5th) quantile, significantly and strongly or weakly positive to SES_M and SES_{FD} of leaf size, SLA, plant height and multi-traits but non-significantly positive to SES_{FD} of seed mass at the median (50th) quantile, and significantly but weakly positive to SES_{FD} of leaf traits and SES_M, significantly negative to SES_{FD} of plant height and seed mass, but non-significantly positive to SES_M and SES_{FD} of multi-traits at the upper (95th) quantile.

DISCUSSION

Instead of considering species richness as the only facet of diversity, phylogenetic and functional diversity can be widely considered a proxy for ecological differentiation, influencing the structure and composition of communities and thus ecosystem process and function. Consistent with the general pattern, we found an overall positive biodiversity-productivity relationship in species', functional and phylogenetic metrics (Jaillard et al., 2014; Rolo et al., 2016; Duffy et al., 2017). Our study also demonstrated that species diversity explained better the variation in aboveground biomass only when it was more than a diversity threshold, thereby implying that low species diversity cannot drive the variation of community function. The boundaries of the bivariate distribution of the relationship between species richness or Shannon–Wiener index (H) and SES_M and single- and multi-trait SES_{FD} formed a filled triangle, showing convergence in the limit of the community's functional and phylogenetic divergence with increasing species diversity. Combined, these results indicate that different assembly processes, such as niche-based deterministic processes like environmental filtering and biotic interactions, and spatial-based neutral processes like dispersal limitation, may structure these communities.

Overall Patterns in Functional and Phylogenetic Community Diversity

Our analysis evidenced an overall pattern of strongly phylogenetic clustering, but weakly functional overdispersion in the individual and multivariate trait space. The strongly phylogenetic clustering appears to be a result of a stochastic process, such as dispersal limitation. Tibetan Plateau is characteristic of high elevation and a series of huge mountains, which restricts the spread of alpine plants, resulting in the coexistence of closely related plant species with similar evolutionary history. However, to maintain the coexistence and avoid inter-specific resource competition because of similar ecological adaptation, these related species may undergo trait shifts ("character displacement"; Schluter, 2000), thereby reducing niche overlap. Some studies have evidenced that, in many cases, closely related species coexist in close proximity, but are well-separated ecologically and functionally (Lemoine et al., 2015; Qi et al., 2015; Lyu et al., 2017). Moreover, a degree of random functional trait distribution within the phylogeny may also contribute to the inconsistency between functional and phylogenetic community patterns to some extend (Kraft et al., 2007). For instance, the diversity (i.e., mean SES_{FD} value) of leaf size and plant height, the traits whose variation are restricted less by phylogeny (based on traits' phylogenetic signal, seen in **Supplementary Appendix 3**), have more significant differences to phylogenetic diversity (i.e., mean SES_M value) in this study.

The Relationship Between Biodiversity and Grassland Productivity

Our study supports hypothesis 1, i.e., an overall positive relationship between aboveground biomass and species', functional and phylogenetic diversity, indicating the important role of biodiversity at different aspects in maintaining ecosystem functioning for the QTP grasslands. But surprisingly, the optimum species diversity-productivity relationship shows a two-stage pattern, in which, with increasing species diversity, communities' productivity increases non-significantly at low diversity levels but significantly at middle and high levels. The pattern is opposite to general relationships (e.g., positively linear, logarithmic, unimodal, or neutral), and thus it cannot be explained by common hypotheses such as rivet, compensatory/keystone species, redundant species, or null hypothesis (O'Connor and Crowe, 2005; Kang et al., 2015), but rather a unique mechanism potentially adapted to plant communities along environmental pressure gradients. The mechanism emphasizes a species diversity threshold, and below it, extreme environmental conditions (e.g., extreme

TABLE 1 | A comparison of linear, quadratic, and piecewise regression models for the relationship between various (species, functional and phylogenetic) diversity indexes (x-axis) and aboveground biomass production (ABP, y-axis) of the Tibetan grassland communities.

Diversity indexes (x-axis)	Linear				Quadratic				Piecewise			
	Shape	R^2	Sig.	ΔAIC	Shape	R^2	Sig.	ΔAIC	Shape (Breakpoint)	R^2	Sig.	ΔAIC
Species richness	Increase	0.246	<0.001	47.87	U-type	0.296	<0.001	9.97	**Unchange + Increase (1.05)**	**0.310**	**<0.001**	**0**
Shannon–Wiener (H)	Increase	0.166	<0.001	29.83	U-type	0.201	<0.001	7.18	**Unchange + Increase (1.74)**	**0.214**	**<0.001**	**0**
SES_{FD} of leaf size	**Increase**	**0.130**	**<0.001**	**27.75**	U-type*	0.140	<0.001	22.99	Decrease + Inchange* (−1.21)	0.177	<0.001	0
SES_{FD} of SLA	**Increase**	**0.160**	**<0.001**	**36.52**	U-type*	0.193	<0.001	15.16	Decrease + Inchange* (–1.00)	0.217	<0.001	0
SES_{FD} of plant height	Increase	0.089	<0.001	28.66	Unimodal	0.112	<0.001	15.73	**Increase + Unchange (1.11)**	**0.139**	**<0.001**	**0**
SES_{FD} of seed mass	Unchange	< 0.001	0.768	0	Unimodal	0.001	0.659	1.25	–	–	–	–
SES_{FD} of multi-traits	**Increase**	**0.119**	**<0.001**	**22.05**	U-type*	0.127	<0.001	18.55	Unchange + Increase* (–0.79)	0.157	<0.001	0
SES_M (SES of MPD)	**Increase**	**0.057**	**<0.001**	**13.63**	U-type*	0.067	<0.001	9.36	Unchange + Increase* (–1.32)	0.085	<0.001	0

"Shape" column showed the overall shape of the binary regression line, while "R^2" and "Sig." columns represented the explanatory power and its significance of regression models, respectively. The shape of the regression line before and after breakpoint (x value; it was a log value of species/m^2 for species richness, but a dimensionless quantity for other diversity indexes) in piecewise models was arranged on both sides of the plus sign (+). For every binary relationship, a model with the lowest AIC (Akaike information criterion) value was assigned as ΔAIC = 0. "Unchange" meant that the slope of the (segmented) regression line was non-significantly different from zero, while "-" indicated no piecewise regression model suitable for the relationship. In the piecewise regression, it slope for species richness, Shannon–Wiener index, SES_{FD} of leaf size, SLA, plant height, multi-traits and SES_M were 0.04 (95% CI: −0.17, 0.25; same below), −0.07 (−0.20, 0.06), −0.16 (−0.28, −0.04), −0.16 (−0.27, −0.04), 0.12 (0.09, 0.15), −0.13 (−0.26, 0.01) and −0.07 (−0.15, 0.02) before the breakpoint, but 1.16 (0.94, 1.38), 0.37 (0.30, 0.45), 0.13 (0.11, 0.16), 0.19 (0.16, 0.22), −0.07 (−0.14, 0.01), 0.17 (0.14, 0.21) and 0.12 (0.08, 0.15) after the breakpoint, respectively. The best fit model was shown in bold.

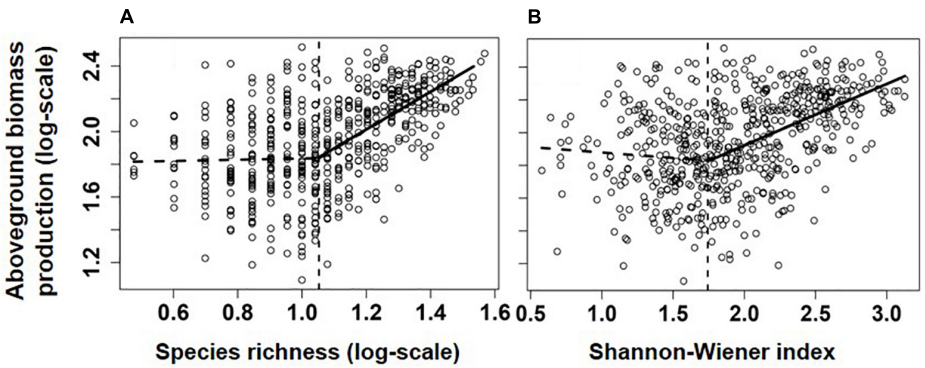

FIGURE 2 | Relationships between aboveground biomass production (log-scale, y-axis, g/m^2) and species richness (**A**, species/m^2) and Shannon-Weaver index **(B)**. Lines showed the best models fitting the relationship, and their significance and explanatory power were shown in **Table 1**.

low temperatures and intense radiation in some alpine zones, and low soil nutrients and drought stress in desert steppe zones) filter out most species, resulting in the coexistence of few species. The life history strategy of surviving species is to adapt to these environments, resulting in the lack of strong interaction and significant niche complementarity among them. Thus, the biomass production of these communities may be largely determined by restrictive resources or environmental factors, rather than by species composition and diversity. In other communities, no resources are significantly limited, which allows the coexistence of multiple species with different ways of resource utilization. Increasing species diversity will enhance plant use efficiency of different resources, and ultimately increase community productivity (Liu et al., 2015; Duffy et al., 2017). These results, meantime, suggest the common finding that facilitative plant interactions drive high-altitude plant diversity and every species contributes to community functioning, especially when species diversity is high (Maestre et al., 2009; Michalet et al., 2014). On the contrary, the best model for explaining the functional diversity-productivity relationship for most traits is positively linear, confirming the general prediction that functional differences among coexisting species are the basis of niche complementarity, and a great inter-specific functional difference will enhance community-level resource utilization efficiency (Wagg et al., 2017; Mensah et al., 2018).

Contrary to our predictions (hypothesis 2) and most previous studies (Cadotte et al., 2009; Chalcraft et al., 2009; Lemoine et al., 2015; Liu et al., 2015; Rolo et al., 2016; Zhu et al., 2016; Rosenfield and Müller, 2020), phylogenetic and functional diversity explain less biomass variation of the QTP grassland communities than species richness. Strong environmental filtering effect on functional traits may have caused this inconsistency (Kraft et al., 2007; Rolo et al., 2016). In general, only fewer evolutionarily related species with similar morphological features can survive under stressful environments. In this case, species' functional traits may better predict their response to environmental stress but not their community status and relationships to other species (Schöb et al., 2013; He and Bertness, 2014). For most QTP

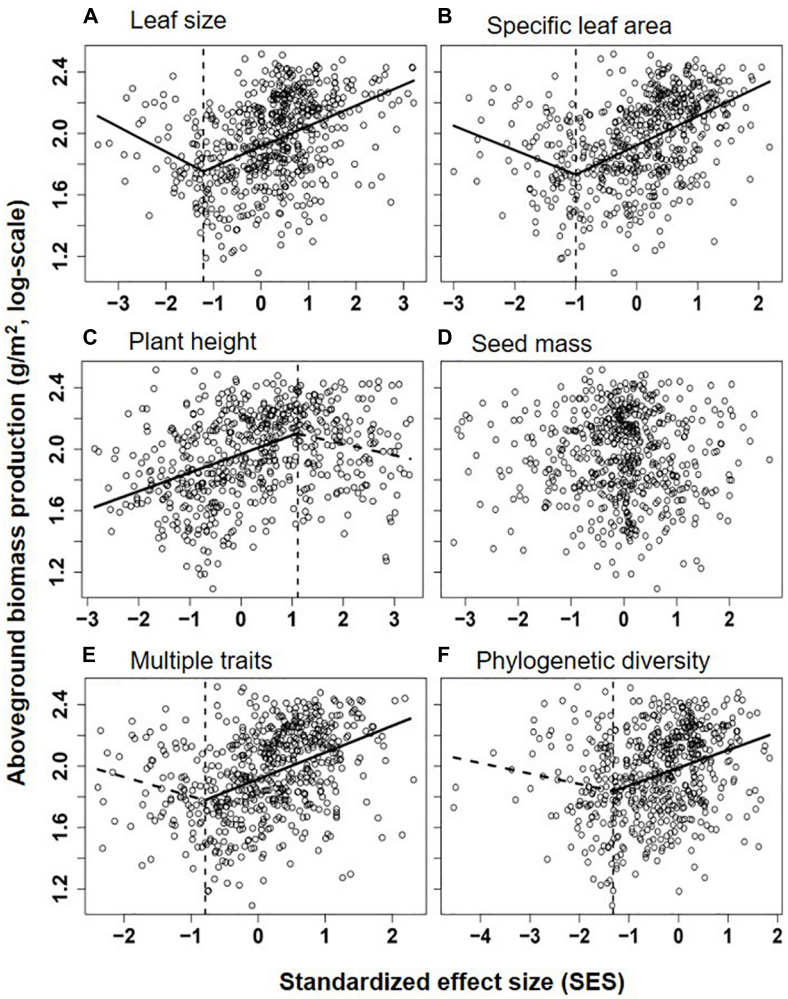

FIGURE 3 | Relationships between aboveground biomass production (log-scale, y-axis) and the standardized effect size (SES) of Rao's quadratic diversity (FD_Q) for leaf size **(A)**, specific leaf area (SLA, **B)**, plant height **(C)**, seed mass **(D)**, multiple traits **(E)**, and phylogenetic diversity (MPD, **F)**. Lines showed the best models fitting the relationship (the segmented line in piecewise regression was shown as dotted lines when its slope was non-significantly different from zero), and their significance and explanatory power were shown in **Table 1**.

TABLE 2 | A comparison of linear, quadratic, and piecewise regression models for the relationship between species richness (x-axis) and six functional and phylogenetic community diversity indexes (y-axis).

Diversity indexes (y-axis)	Linear				Quadratic				Piecewise			
	Shape	R^2	Sig.	ΔAIC	Shape	R^2	Sig.	ΔAIC	Shape (Breakpoint)	R^2	Sig.	ΔAIC
SES_{FD} of leaf size	Increase	0.188	<0.001	17.56	U-type	0.214	<0.001	1.12	**Unchange + Increase (0.98)**	**0.218**	**<0.001**	**0**
SES_{FD} of SLA	Increase	0.284	<0.001	18.59	U-type	0.306	<0.001	2.70	**Unchange + Increase (0.95)**	**0.311**	**<0.001**	**0**
SES_{FD} of plant height	Increase	0.007	0.038	16.70	U-type	0.035	0.001	2.27	**Decrease + Increase (1.08)**	**0.042**	**<0.001**	**0**
SES_{FD} of seed mass	Unchange	0.006	0.070	0	U-type	0.008	0.084	0.33	–	–	–	–
SES_{FD} of multi-traits	Increase	0.108	<0.001	23.38	U-type	0.143	<0.001	1.90	**Unchange + Increase (0.96)**	**0.149**	**<0.001**	**0**
SES_M (SES of MPD)	Increase	0.197	<0.001	17.04	U-type	0.215	<0.001	5.80	**Unchange + Increase (0.98)**	**0.225**	**<0.001**	**0**

*'Shape' column showed the overall shape of the binary regression line, "unchange" meant that the slope of the (segmented) regression line was non-significantly different from zero, while symbols (i.e., +, –) and abbreviations (i.e., AIC, ΔAIC, Sig., R^2) were as specified in **Table 1**. Species richness breakpoint in piecewise regression models was a log value of species/m^2 (i.e., 0.95 ≈ 9 species/m^2). The slope of the piecewise regression for the relationships between species richness and SES_{FD} of leaf size, SLA, plant height, multi-traits, and SES_M were −0.08 (95% CI: −1.25, 1.08; same below), 0.40 (−0.69, 1.49), −1.32 (−2.34, −0.29), −0.69 (−1.24, 0.26) and 0.20 (−0.86, 1.25) before the breakpoint, but 3.03 (2.38, 3.69), 2.94 (2.47, 3.41), 2.56 (1.14, 3.98), 2.14 (1.61, 2.67) and 2.88 (2.29, 3.48) after the breakpoint, respectively. The best fit model was shown in bold.*

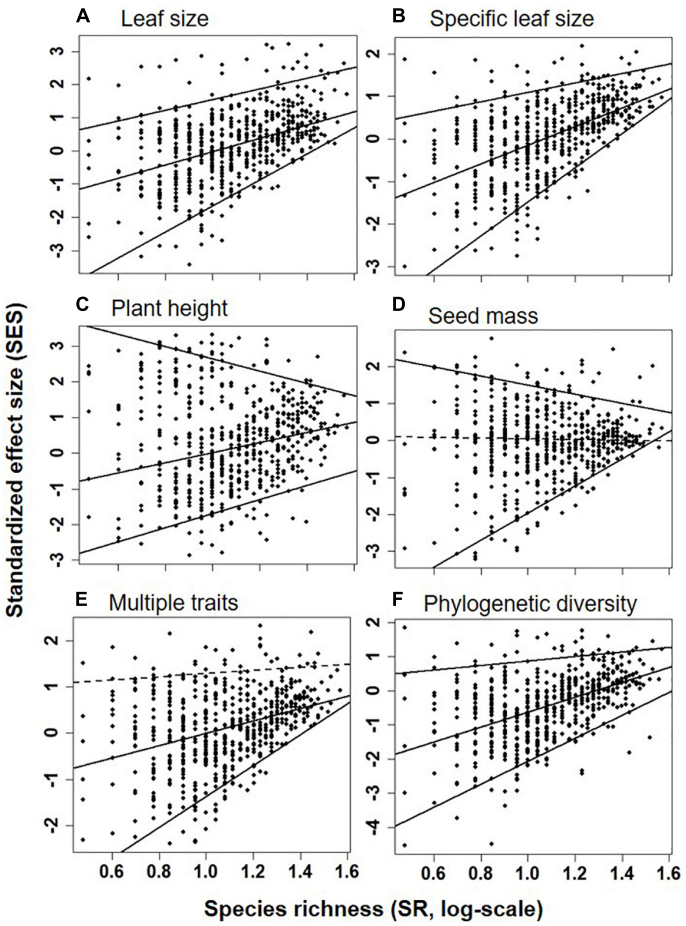

FIGURE 4 | SES of FD_Q for leaf size **(A)**, specific leaf area **(B)**, plant height **(C)**, seed mass **(D)**, multiple traits **(E)**, and phylogenetic diversity **(F)** in relation to the species richness (SR, log-scale, species/m^2, x-axis) at the upper (95th), median (50th), and lower (5th) quantile levels. Positive (or negative) SES value indicated greater (or lower) functional and phylogenetic diversity than null. Significant and non-significant linear relationships (at $\alpha = 0.05$) were shown as solid and dashed lines, respectively.

grassland communities, plants live under rich soil nutrition and light resources but harsh climate conditions. As a result, species' adaption to climate, rather than interspecific competition for resources, may be the primary force structuring these communities, resulting in the decoupling of species traits and community function to a certain extent (Schmitz et al., 2015; Cadotte, 2017). Meantime, our result implies the importance of species diversity in maintaining the function of some special ecosystems even though coexisting species show similar morphological traits.

The Relationship Among Different Diversity Metrics

Consistent with hypothesis 3, our best model for explaining the species' and functional or phylogenetic diversity relationship for the QTP grasslands is non-linear, in which functional or phylogenetic diversity (SES_{FD} of muli-traits and SES_M) increases significantly with species richness after it exceeds a threshold. The result demonstrates that high functional and phylogenetic divergence, representing significant species' niche differentiation or interspecific difference (dissimilarity) in resource acquisition or other life-history strategies (Violle et al., 2007; Bu et al., 2014; Rolo et al., 2016; Lyu et al., 2017), is important to maintain species coexistence in high species diversity communities. In low species diversity communities, however, interspecific competition for resource and (or) interspecific life history differences are not strong determinants of species coexistence, and as a result, species' niche differentiation may be determined mainly by stochastic processes, leading to less dependence of average trait divergence (dissimilarity) to species diversity.

It has been frequently reported that two opposite niche processes, species interaction and habitat filtering, may not be mutually exclusive but instead operate simultaneously across grassland communities (Anthelme et al., 2014; Michalet et al., 2014; Zhu et al., 2016). Quantile regression for the functional species diversity relationship may help to disentangle their effects in structuring community, in which the upper (or lower) bound should represent the maximum competitive effect (or filtering effect) due to the higher (or lower) functional divergence

among species. Our result, however, shows that the relationship changed across quantiles, shifting from a significantly and steeply positive slope in the lower quantile to a slightly positive or negative slope for a single trait and even a near-zero for multi-traits or phylogeny in the upper quantile. This suggests a filled triangle for the limit of the bivariate distribution, implying that functional diversity differs significantly among communities when their species diversity is low but finally converges to be a constant with increasing communities' species diversity. The reason for big functional diversity differences for low-species diversity communities may be that they are dominated by strong species competition, which excludes low-competitive species and increases inter-specific trait dissimilarity, or alternatively, by strong habitat filtering, which excludes low-adaptive species and increases inter-specific trait similarity. By decreasing the effect of species competition or habitat filtering, more species can coexist, and these opposite niche processes may operate simultaneously and tend to balance each other (He and Bertness, 2014; Fichtner et al., 2017). Accordingly, a constant interspecific trait divergence (similar to limiting similarity theory; Kembel and Hubbell, 2006), representing the result of species' response to the combined effect of opposite niche processes, enables the community to adapt to the fluctuations of environment, to sufficiently use local resources, and to keep community productivity at a high level.

The Diversity-Functionality Relationship of Different Traits

According to the best model, we show significantly different patterns in the relationship between functional diversity of plant height, leaf and seed traits and community productivity and (or) species diversity, suggesting the different roles of these traits in structuring the QTP grasslands. Leaf traits (leaf size and SLA) significantly contribute to achieving a predictive framework for community species diversity and ecosystem functioning. Leaf traits are tightly related to light resource acquisition and plant growth strategy and identified as a key functional predictor of the plant capacity of adaptation to changeful and stressful environments. The result is in accordance with previous studies suggesting that the diversity pattern of leaf traits, especially SLA, can be used to predict communities' productivity, carbon storage and assembly rule (Long et al., 2011; Lemoine et al., 2015). By contrast, the relationships between diversity patterns of plant height and seed mass and community species diversity and productivity are generally weak or non-significant, implying that plant's light interception capability and seedling establishment's ability may be less important in structuring QTP grassland communities with a rich light resource for under plants. Moreover, most Tibetan grassland species are typically rosette (or semi-rosette) plants or primarily reproduce asexually (Nagy and Grabherr, 2009; Qi et al., 2014; Chen et al., 2017). These unique plants' architectural and reproductive traits would weaken the effects of plant height and seed mass on supporting leaf light interception and enhancing seedling establishment and survival, respectively, and thus diminish their roles in driving community assembly. In addition, the piecewise model shows that communities with lowest functional diversity of leaf traits usually have no lowest productivity (**Table 1** and **Figure 3**), implying that, in some special zones (e.g., desert steppe) where light competition is not severe, similar leaf traits may be more helpful for coexisting species to adapt to the environment and use various resources.

CONCLUSION

Across the QTP grassland communities, we showed an overall positive biodiversity-productivity relationship in species', functional and phylogenetic space. The relationship, however, was non-linear, in which increasing species diversity, communities' productivity increased significantly at middle and high diversity levels but not at the low level, suggesting a weak effect of biodiversity on ecosystem function in low species diversity communities. In the meantime, phylogenetic and functional diversity explained less biomass variation of the grassland communities than species richness, highlighting species diversity in maintaining grassland community stability and ecosystem functions. We also found a filled triangle for the limit of the relationship between species and functional diversity, implying that functional diversity differs significantly among communities when their species diversity is low but finally converges to be a constant with increasing communities' species diversity. The above findings suggest that multiple niche processes may structure the grassland communities, and their forces tend to balance in high-biodiversity communities.

DATA AVAILABILITY STATEMENT

The original contributions presented in the study are included in the article/**Supplementary Material**, further inquiries can be directed to the corresponding author/s.

AUTHOR CONTRIBUTIONS

XK, WQ, GD, and JK conceived the ideas. All authors but XK and JK collected the data. XK and WQ analyzed the data. XK, WQ, and JK contributed to the writing of the manuscript. All authors contributed to the article and approved the submitted version.

FUNDING

The study was supported by the Project of the National Natural Science Foundation of China (31770448, 32171518, 31870435, and 41171214) and the Science and Technology Support Project of Department of Agriculture and Rural Affairs of Gansu Province (HT-GSZYTC-ZCJC-18027/02) and the Science and Technology Support Project of Ecological Grassland Restoration and Management in Gansu Province granted to WQ (Letter of the Forestry and Grassland Bureau of Gansu Province: [2020]72). The study was also supported by the Gannan Grassland Ecosystem National Observation and Research Station.

ACKNOWLEDGMENTS

We thank Peng Jia, Shuangwei Luo, Han Chen, Miaojun Ma, and Guixin Li for their help with field work.

SUPPLEMENTARY MATERIAL

The Supplementary Material for this article can be found online at: https://www.frontiersin.org/articles/10.3389/fpls.2021.772503/full#supplementary-material

Supplementary Figure 1 | Mean (± 95% CI) standardized effect size (SES) of functional diversity (FD_Q) for single- and multi-traits and of phylogenetic diversity in the Tibetan grassland communities. Symbols in black indicate values significantly different from zero.

Supplementary Figure 2 | SES of FD_Q for leaf size **(A)**, specific leaf area (SLA, **B**), plant height **(C)**, seed mass **(D)**, multiple traits **(E)**, and phylogenetic diversity (MPD, **F**) in relation to the Shannon–Wiener index (H, x-axis) at the upper (95th), median (50th), and lower (5th) quantile levels. Significant and non-significant linear relationships (at $\alpha = 0.05$) were shown as solid and dashed lines, respectively.

Supplementary Appendix 1 | A comparison of location, climate attributes, and community characters of the 118 study sites. "Richness" and "Abundance" represent species number and total individual number in a 1 m^2 quarter.

REFERENCES

Anthelme, F., Cavieres, L. A., and Dangles, O. (2014). Facilitation among plants in alpine environments in the face of climate change. *Front. Plant Sci.* 5:387. doi: 10.3389/fpls.2014.00387

Bu, W., Zang, R., and Ding, Y. (2014). Functional diversity increases with species diversity along successional gradient in a secondary tropical lowland rainforest. *Trop. Ecol.* 55, 393–401.

Butterfield, B. J., and Suding, K. N. (2013). Single-trait functional indices outperform multi-trait indices in linking environmental gradients and ecosystem services in a complex landscape. *J. Ecol.* 101, 9–17. doi: 10.1111/1365-2745.12013

Cadotte, M. W. (2017). Functional traits explain ecosystem function through opposing mechanisms. *Ecol. Lett.* 20, 989–996. doi: 10.1111/ele.12796

Cadotte, M. W., Cavender-Bares, J., Tilman, D., and Oakley, T. H. (2009). Using phylogenetic, functional and trait diversity to understand patterns of plant community productivity. *PLoS One* 4:e5695. doi: 10.1371/journal.pone.0005695

Callaway, R. M., Brooker, R. W., Choler, P., Kikvidze, Z., Lortie, C. J., Michalet, R., et al. (2002). Positive interactions among alpine plants increase with stress. *Nature* 417, 844–848.

Carboni, M., Acosta, A. T., and Ricotta, C. (2013). Are differences in functional diversity among plant communities on Mediterranean coastal dunes driven by their phylogenetic history? *J. Veg. Sci.* 24, 932–941. doi: 10.1111/jvs.12095

Casanoves, F., Pla, L., Di Rienzo, J. A., and Díaz, S. (2011). FDiversity: a software package for the integrated analysis of functional diversity. *Methods Ecol. Evol.* 2, 233–237. doi: 10.1111/j.2041-210X.2010.00082.x

Chalcraft, D. R., Wilsey, B. J., Bowles, C., and Willig, M. R. (2009). The relationship between productivity and multiple aspects of biodiversity in six grassland communities. *Biodivers. Conserv.* 18, 91–104. doi: 10.1007/s10531-008-9457-6

Chen, J., Li, Y., Yang, Y., and Sun, H. (2017). How cushion communities are maintained in alpine ecosystems: a review and case study on alpine cushion plant reproduction. *Plant Divers.* 39, 221–228. doi: 10.1016/j.pld.2017.07.002

Choler, P., Michalet, R., and Callaway, R. M. (2001). Competition and facilitation on gradients in alpine communities. *Ecology* 82, 3295–3308. doi: 10.2307/2680153

Chollet, S., Rambal, S., Fayolle, A., Hubert, D., Foulquié, D., and Garnier, E. (2014). Combined effects of climate, resource availability, and plant traits on biomass produced in a Mediterranean rangeland. *Ecology* 95, 737–748. doi: 10.1890/13-0751.1

de Carvalho, R. A., and Tejerina-Garro, F. L. (2015). Relationships between taxonomic and functional components of diversity: implications for conservation of tropical freshwater fishes. *Freshw. Biol.* 60, 1854–1862. doi: 10.1111/fwb.12616

de la Riva, E. G., Violle, C., Pérez-Ramos, I. M., Marañón, T., Navarro-Fernández, C. M., Olmo, M., et al. (2018). A multidimensional functional trait approach reveals the imprint of environmental stress in mediterranean woody communities. *Ecosystems* 21, 248–262. doi: 10.1007/s10021-017-0147-7

Duffy, J. E., Godwin, C. M., and Cardinale, B. J. (2017). Biodiversity effects in the wild are common and as strong as key drivers of productivity. *Nature* 549:261. doi: 10.1038/nature23886

Fichtner, A., Härdtle, W., Li, Y., Bruelheide, H., Kunz, M., and von Oheimb, G. (2017). From competition to facilitation: how tree species respond to neighbourhood diversity. *Ecol. Lett.* 20, 892–900. doi: 10.1111/ele.12786

Guerrero, I., Carmona, C. P., Morales, M. B., Oñate, J. J., and Peco, B. (2014). Non-linear responses of functional diversity and redundancy to agricultural intensification at the field scale in Mediterranean arable plant communities. *Agr. Ecosyst. Environ.* 195, 36–43. doi: 10.1016/j.agee.2014.05.021

He, Q., and Bertness, M. D. (2014). Extreme stresses, niches, and positive species interactions along stress gradients. *Ecology* 95, 1437–1443. doi: 10.1890/13-2226.1

Hooper, D. U., Chapin, F. S., Ewel, J. J., Hector, A., Inchausti, P., Lavorel, S., et al. (2005). Effects of biodiversity on ecosystem functioning: a consensus of current knowledge. *Ecol. Monogr.* 75, 3–35. doi: 10.1890/04-0922

Jaillard, B., Rapaport, A., Harmand, J., Brauman, A., and Nunan, N. (2014). Community assembly effects shape the biodiversity-ecosystem functioning relationships. *Funct. Ecol.* 28, 1523–1533. doi: 10.1111/1365-2435.12267

Kang, S., Ma, W., Li, F. Y., Zhang, Q., Niu, J., Ding, Y., et al. (2015). Functional redundancy instead of species redundancy determines community stability in a typical steppe of Inner Mongolia. *PLoS One* 10:e0145605. doi: 10.1371/journal.pone.0145605

Kembel, S. W., and Hubbell, S. P. (2006). The phylogenetic structure of a neotropical forest tree community. *Ecology* 87, S86–S99.

Koenker, R. (2018). *Quantreg: Quantile Regression. R Package Version 5.36*. Available online at: https://CRAN.R-project.org/package=quantreg (accessed June 06, 2021).

Kraft, N. J. B., Cornwell, W. K., Webb, C. O., and Ackerly, D. D. (2007). Trait evolution, community assembly, and the phylogenetic structure of ecological communities. *Am. Nat* 170, 271–283. doi: 10.1086/519400

Lemoine, N. P., Shue, J., Verrico, B., Erickson, D., Kress, W. J., and Parker, J. D. (2015). Phylogenetic relatedness and leaf functional traits, not introduced status, influence community assembly. *Ecology* 96, 2605–2612. doi: 10.1890/14-1883.1

Li, W., Cheng, J., Yu, K., Epstein, H. E., Guo, L., Jing, G., et al. (2015). Plant functional diversity can be independent of species diversity: observations based on the impact of 4-yrs of nitrogen and phosphorus additions in an alpine meadow. *PLoS One* 10:e0136040. doi: 10.1371/journal.pone.0136040

Liu, J., Zhang, X., Song, F., Zhou, S., Cadotte, M. W., and Bradshaw, C. J. (2015). Explaining maximum variation in productivity requires phylogenetic diversity and single functional traits. *Ecology* 96, 176–183. doi: 10.1890/14-1034.1

Long, W., Zang, R., Schamp, B. S., and Ding, Y. (2011). Within- and among-species variation in specific leaf area drive community assembly in a tropical cloud forest. *Oecologia* 167, 1103–1113. doi: 10.1007/s00442-011-2050-9

Lososová, Z., Čeplová, N., Chytrý, M., Tichý, L., Danihelka, J., Fajmon, K., et al. (2016). Is phylogenetic diversity a good proxy for functional diversity of plant communities? A case study from urban habitats. *J. Veg. Sci.* 27, 1036–1046. doi: 10.1111/jvs.12414

Lyu, S., Liu, X., Venail, P., and Zhou, S. (2017). Functional dissimilarity, not phylogenetic relatedness, determines interspecific interactions among plants in the Tibetan alpine meadows. *Oikos* 126, 381–388. doi: 10.1111/oik.03378

Maestre, F. T., Callaway, R. M., Valladares, F., and Lortie, C. J. (2009). Refining the stress-gradient hypothesis for competition and facilitation in plant communities. *J. Ecol.* 97, 199–205. doi: 10.1111/j.1365-2745.2008.01476.x

Mayfield, M. M., and Levine, J. M. (2010). Opposing effects of competitive exclusion on the phylogenetic structure of communities. *Ecol. Lett.* 13, 1085–1093. doi: 10.1111/j.1461-0248.2010.01509.x

Mensah, S., du Toit, B., and Seifert, T. (2018). Diversity-biomass relationship across forest layers: implications for niche complementarity and selection effects. *Oecologia* 187, 783–795. doi: 10.1007/s00442-018-4144-0

Michalet, R., Le Bagousse-Pinguet, Y., Maalouf, J. P., and Lortie, C. J. (2014). Two alternatives to the stress-gradient hypothesis at the edge of life: the collapse of facilitation and the switch from facilitation to competition. *J. Veg. Sci.* 25, 609–613. doi: 10.1111/jvs.12123

Micheli, F., and Halpern, B. S. (2005). Low functional redundancy in coastal marine assemblages. *Ecol. Lett.* 8, 391–400.

Nagy, L., and Grabherr, G. (2009). *The Biology of Alpine Habitats*. Oxford: Oxford University Press on Demand.

Niu, K., Choler, P., de Bello, F., Mirotchnick, N., Du, G., and Sun, S. (2014). Fertilization decreases species diversity but increases functional diversity: a three-year experiment in a Tibetan alpine meadow. *Agr. Ecosyst. Environ.* 182, 106–112. doi: 10.1016/j.agee.2013.07.015

Niu, K., He, J., Zhang, S., and Lechowicz, M. J. (2016). Grazing increases functional richness but not functional divergence in tibetan alpine meadow plant communities. *Biodivers. Conserv.* 25, 2441–2452.

O'Connor, N. E., and Crowe, T. P. (2005). Biodiversity loss and ecosystem functioning: distinguishing between number and identity of species. *Ecology* 86, 1783–1796. doi: 10.1890/04-1172

Qi, W., Bu, H., Liu, K., Li, W., Knops, J. M. H., Wang, J., et al. (2014). Biological traits are correlated with elevational distribution range of eastern Tibetan herbaceous species. *Plant Ecol.* 215, 1187–1198. doi: 10.1007/s11258-014-0377-0

Qi, W., Jia, P., Luo, S., Kang, X., and Du, G. (2021). Disentangling the effects of environmental and communities' factors on species'biomass inequality in Qinghai-Tibetan grassland systems. *Ecol. Indic.* 122:107309. doi: 10.1016/j.ecolind.2020.107309

Qi, W., Zhou, X., Ma, M., Knops, J. M. H., Li, W., and Du, G. (2015). Elevation, moisture and shade drive the functional and phylogenetic meadow communities' assembly in the northeastern Tibetan Plateau. *Commun. Ecol.* 16, 66–75. doi: 10.1556/168.2015.16.1.8

Reiss, J., Bridle, J. R., Montoya, J. M., and Woodward, G. (2009). Emerging horizons in biodiversity and ecosystem functioning research. *Trends Ecol. Evol.* 24, 505–514. doi: 10.1016/j.tree.2009.03.018

Rolo, V., Rivest, D., Lorente, M., Kattge, J., and Moreno, G. (2016). Taxonomic and functional diversity in Mediterranean pastures: insights on the biodiversity-productivity trade-off. *J. Appl. Ecol.* 53, 1575–1584. doi: 10.1111/1365-2664.12685

Rosenfield, M. F., and Müller, S. C. (2020). Plant traits rather than species richness explain ecological processes in subtropical forests. *Ecosystems* 23, 52–66. doi: 10.1007/s10021-019-00386-6

Schluter, D. (2000). Ecological character displacement in adaptive radiation. *Am. Nat.* 156, S4–S16. doi: 10.2307/3079223

Schmitz, O. J., Buchkowski, R. W., Burghardt, K. T., and Donihue, C. M. (2015). Functional traits and trait-mediated interactions: connecting community- level interactions with ecosystem functioning. *Adv. Ecol. Res.* 52, 319–343. doi: 10.1016/bs.aecr.2015.01.003

Schöb, C., Armas, C., Guler, M., Prieto, I., and Pugnaire, F. I. (2013). Variability in functional traits mediates plant interactions along stress gradients. *J. Ecol.* 101, 753–762. doi: 10.1111/1365-2745.12062

Segura, A. M., Calliari, D., Kruk, C., Fort, H., Izaguirre, I., Saad, J. F., et al. (2015). Metabolic dependence of phytoplankton species richness. *Glob. Ecol. Biogeogr.* 24, 472–482. doi: 10.1111/geb.12258

Silva, I. A., Sfair, J. C., van Melis, J., Weiser, V. L., and Martins, F. R. (2016). Does phylogeny have a role in the liana-phorophyte interaction in tropical forests? *Perspect. Plant Ecol.* 21, 14–22. doi: 10.1016/j.ppees.2016.04.002

Violle, C., Navas, M. L., Vile, D., Kazakou, E., Fortunel, C., Hummel, I., et al. (2007). Let the concept of trait be functional! *Oikos* 116, 882–892. doi: 10.2307/40235131

Wagg, C., Ebeling, A., Roscher, C., Ravenek, J., Bachmann, D., Eisenhauer, N., et al. (2017). Functional trait dissimilarity drives both species complementarity and competitive disparity. *Funct. Ecol.* 31, 2320–2329. doi: 10.1111/1365-2435.12945

Webb, C. O., Ackerly, D. D., and Kembel, S. W. (2008). Phylocom: software for the analysis of phylogenetic community structure and trait evolution. *Bioinformatics* 18, 2098–2100. doi: 10.1093/bioinformatics/btn358

Wu, C., and Chen, S. (2004). *Flora Reipublicae Popularis Sinicae Tomus 1*. Beijing: Science Press. (in Chinese).

Wu, Z. (1980). *The Vegetation of China*. Beijing: Science Press.

Yang, Y., Fang, J., Pan, Y., and Ji, C. (2009). Aboveground biomass in Tibetan grasslands. *J. Arid. Environ.* 73, 91–95. doi: 10.1016/j.jaridenv.2008.09.027

Zhang, H., Qi, W., and Liu, K. (2018). Functional traits associated with plant colonizing and competitive ability influence species abundance during secondary succession: evidence from subalpine meadows of the Qinghai-Tibetan Plateau. *Ecol. Evol.* 8, 6529–6536. doi: 10.1002/ece3.4110

Zhu, J., Jiang, L., and Zhang, Y. (2016). Relationships between functional diversity and aboveground biomass production in the Northern Tibetan alpine grasslands. *Sci. Rep.* 6:34105. doi: 10.1038/srep34105

Zhu, Z., Ma, Y., Li, M., Hu, Z., Xu, C., Zhang, L., et al. (2015). Carbon dioxide exchange between an alpine steppe ecosystem and the atmosphere on the Nam Co area of the Tibetan Plateau. *Agr. For. Meteorol.* 203, 169–179. doi: 10.1016/j.agrformet.2014.12.013

Conflict of Interest: The authors declare that the research was conducted in the absence of any commercial or financial relationships that could be construed as a potential conflict of interest.

Publisher's Note: All claims expressed in this article are solely those of the authors and do not necessarily represent those of their affiliated organizations, or those of the publisher, the editors and the reviewers. Any product that may be evaluated in this article, or claim that may be made by its manufacturer, is not guaranteed or endorsed by the publisher.

Copyright © 2022 Qi, Kang, Knops, Jiang, Abuman and Du. This is an open-access article distributed under the terms of the Creative Commons Attribution License (CC BY). The use, distribution or reproduction in other forums is permitted, provided the original author(s) and the copyright owner(s) are credited and that the original publication in this journal is cited, in accordance with accepted academic practice. No use, distribution or reproduction is permitted which does not comply with these terms.

frontiers in Plant Science

ORIGINAL RESEARCH
published: 28 January 2022
doi: 10.3389/fpls.2021.785971

Specific Rhizobacteria Responsible in the Rhizosheath System of *Kengyilia hirsuta*

Youjun Chen[1,2], Chen Chen[1,2], Qingping Zhou[1,2], Jian Hu[1,2], Yingxia Lei[2] and Wenhui Liu[3]*

[1] Sichuan Zoige Alpine Wetland Ecosystem National Observation and Research Station, Chengdu, China, [2] Institute of the Qinghai-Tibetan Plateau, Southwest Minzu University, Chengdu, China, [3] Qinghai Academy of Animal Science and Veterinary Medicine Qinghai University, Xining, China

The rhizosheath is a critical interface supporting the exchange of resources between plants and their associated environment of soil. Favorable microenvironment of rhizosphere soil provides the rhizosheath formed and then promotes desert plant survival. However, it remains unclear how rhizosheath benefits the colonization of pioneer plants in alpine desert under changing environment. In this study, we investigated the effect of different soil moisture and sterilization treatments (three moisture levels and unsterilized or sterilized soil) on rhizosheath forming process of *Kengyilia hirsuta* (*K. hirsuta*), a sand-inhabiting and drought-resistant pioneer plant of the Tibetan Plateau desert. The results showed that in both unsterilized and sterilized soil, increasing soil moisture first increased and then decreased rhizosheath weight, with the highest value is 25%. During rhizosheath formation, developing rhizosheaths were selectively enriched in the bacterial genera *Massilia* and *Arthrobacter*. These suggest the existence of a highly specialized signal recognition system during rhizosheath formation that involves the accumulation of bacteria. These bacterial species exhibited different roles in the process of rhizosheath formation and is an advantageous strategy for *K. hirsuta*.

Keywords: ***Kengyilia hirsuta*, rhizobacteria, rhizosheath, formation, aggregation**

OPEN ACCESS

Edited by:
Gao-Lin Wu,
Northwest A&F University, China

Reviewed by:
Gang Fu,
Institute of Geographic Sciences and Natural Resources Research, Chinese Academy of Sciences (CAS), China
Mushtak Faraj Kisko,
University of Montpellier, France

***Correspondence:**
Chen Chen
chenchen@swun.edu.cn

Specialty section:
This article was submitted to Functional Plant Ecology, a section of the journal Frontiers in Plant Science

Received: *29 September 2021*
Accepted: *06 December 2021*
Published: *28 January 2022*

Citation:
Chen Y, Chen C, Zhou Q, Hu J, Lei Y and Liu W (2022) Specific Rhizobacteria Responsible in the Rhizosheath System of Kengyilia hirsuta. Front. Plant Sci. 12:785971. doi: 10.3389/fpls.2021.785971

INTRODUCTION

The genus *Kengyilia* (Triticeae) comprises a group of pioneer plant species predominantly distributed on sandy grasslands of the Tibetan Plateau (TP) and adjacent northern areas in China. The phylogenetically most advanced species, *Kengyilia hirsuta* (*K. hirsuta*), is found at the highest elevations of the TP region (Baum et al., 1995). The composition of the sandy grassland plant community in sand grassland is driven by sandy desertification and is related to plant functional traits in the presence of environmental changes (Yue, 2017). As a pioneer species of the sandy desert plant community and a well-adapted forage grass, *K. hirsuta* is able to accommodate different environmental stresses.

The rhizosheath is defined as the portion of soil that physically adheres to the root system and encases the entire root system of certain plants (Baum et al., 1995; Pang et al., 2017). Plant root hairs, soil moisture (Pang et al., 2017), fungal hyphae of soil microbes, and microbial- and plant-derived mucilage are responsible for the aggregation of sand particles in the rhizosheath

system (Marasco et al., 2018). The beneficial effect of the rhizosheath has been demonstrated by the observation of a positive correlation between rhizosheath mass and plant growth under stress conditions (Ashraf et al., 2006). In grasslands undergoing desertification, the rhizosheath has been shown to provide mechanical protection to roots, thereby promoting water conservation and uptake under drought conditions (Young, 2006; Brown et al., 2017). In addition, the rhizosheath can serve as a resource for microorganisms, which can feed on organic substances and live in relatively stable environmental conditions compared with barren sandy land. Meanwhile, the rhizosheath structure provides an ecological niche with available microclimatic conditions for microbial growth and development (Danin, 1996). A rhizosheath-root system is formed around the roots of grasses in families Poaceae and Haemodoraceae (Young, 2006; Brown et al., 2017); coincidentally, we observed the rhizosheath in *K. hirsuta* root. The ability of *K. hirsuta* to inhabit arid environments may primarily be related to the presence of a rhizosheath. As it is well known, moisture and bacteria are limited factors for desert plant survival and growth.

According to a report, a comparison of rhizosheaths in different soil layers revealed that rhizosheaths in the dry layer were five times the volume of the subtending root, whereas rhizosheath volumes were only 1.5 times larger than those of the root in the wet layer in field (Brown et al., 2017). In the dry layer, the mucilage of roots and microorganisms enhanced their adhesiveness for the stabilization of the rhizosheath; as a consequence, the rhizosheath was more easily removed from roots growing in wet soil than dry soil (Watt et al., 1994). In the process of rhizosheath formation, the microbial community plays an important role (Pointing and Belnap, 2012). Soil microbes stimulate plant roots to produce more mucilage, which promotes rhizosheath formation; besides, soil microbes decompose and use soil organic matter for rhizosheath formation (Marasco et al., 2018). As we known that a few microbial cultivation-based studies have been conducted on the root system of desert grasses (Othman et al., 2004; Hanna et al., 2013), for example, two phyla (Glomeromycota and Zygomycota) and two trophic modes (Symbiotroph and Pathotroph-Saprotroph) were the differentially ecological functions in monitoring desertification conditions, they can be used to indicate desertification gradient (Zong and Fu, 2021).

Soil sterilization may alter the root growth and community structure of newly developed bacterial populations (Wertz et al., 2007; Marasco et al., 2012) and, thus, also influence rhizosheath development.

Taken together, soil moisture and the specific microorganisms that strongly influence plant rhizosheaths (Watt et al., 1994; Danin, 1996), but the information on the development of rhizosheaths has been lacking. Given these issues, we studied *K. hirsuta* rhizosheath weight in unsterilized and sterilized desert soil at three different moisture levels. Next, high-throughput sequencing technology was used to explore whether specific rhizobacteria are responsible for the aggregation of sand particles in the rhizosheath system of *K. hirsuta*. Finally, experiments were conducted to examine their possible role in altering the root growth and the weight of rhizosheaths. The key point of this study was to discuss the special rhizobacteria that could help *K. hirsuta* to better developing rhizosheaths in different moisture and environment of soil.

MATERIALS AND METHODS

Sampling Approach

Seed Collection

In September 2017, seeds of healthy, same-sized seedlings of *K. hirsuta* growing in northwest of Sichuan, China (elevation, 3,450 m; longitude, N 33°18′, latitude, E 102°62′) were selected for cultivation.

Soil Samples

The soil used in laboratory experiments was collected from an experimental field at the Institute of the TP, Southwest Minzu University, Hongyuan, China. The field, which had been enclosed for the past 10 years, contained plots harboring mainly shrub and grass species such as *Hippophae rhamnoides*, *Orobanche coerulescens*, *Leymus secalinus*, *Artemisia desertorum*, *Potentilla anserine*, and *Kobresia pygmaea*.

Soil sterilization may alter the root growth and community structure of the bacterial diversity and abundance (Marschner and Bredow, 2002; Wertz et al., 2007), So, we choose the autoclaving method that may also influence the development of rhizosheaths. Autoclaving is known to alter physicochemical characteristics of soil (Mcnamara et al., 2003; Berns et al., 2010; Traoré et al., 2010). Autoclaving is known to increase the soil pH (Jörn et al., 1993), to decrease the cation exchange capacity (CEC), and increasing the electrical conductivity (EC) of soil and N (NH_4^+ and NO_3^-) is not an significant change (Sandler et al., 1988). After collection, the sampled soil was divided into two portions, one of which was sterilized by autoclaving at 121°C for 1 h. Soil physicochemical characteristics are given in **Table 1**.

Plant Growth Experiments

Experiments were conducted in plastic flower plots (5.5 cm inner diameter × 7 cm depth) filled with 750 g of sterilized or unsterilized soil. Nine seeds of *K. hirsuta* were sown per pot. The final soil moisture content of each pot was adjusted to 10, 25, or 40% of field water capacity and maintained throughout the experiment as indicated by daily weighing. All the experiments

TABLE 1 | Physicochemical properties of sandy soil used in this study.

Parameter	Treatment of soil	
	Sterilization	Unsterilization
Field capacity(%)	21.31 ± 2.01a	20.58 ± 1.34a
pH (1:1,soil:water)	7.68 ± 0.02a	7.23 ± 0.01b
Electrical conductivity ($\mu \cdot S \cdot m^{-1}$)	531.10 ± 7.45a	349.75 ± 3.12b
NH4 + N ($mg \cdot kg^{-1}$)	9.82 ± 1.11a	9.44 ± 1.28a
NO3−N ($mg \cdot kg^{-1}$)	4.61 ± 0.73a	3.80 ± 0.52a

Different lowercase letters in the same row indicate significant differences ($p < 0.05$).

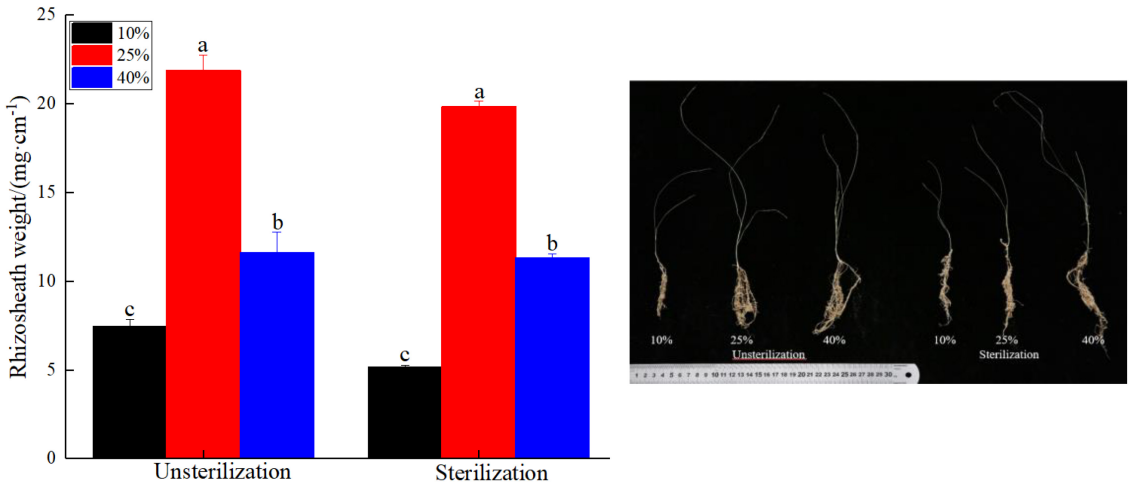

FIGURE 1 | The differences in rhizosheath weight due to different soil and moisture treatment. Different lowercase letters in the figure indicate significant differences ($p < 0.05$).

were repeated four times per treatment in an artificial climate incubator in October. Experimental conditions were as follows: 14-h/10-h light-dark photoperiod, 25°C, 55% relative humidity, and 1,000–1,200 μmol m^{-2} s^{-1} photon flux density. To study the effects of moisture and soil treatments on plant growth, we investigated the rhizosheath soil of seedlings at the three-leaf stage. In the first experiment, we analyzed the weight of rhizosheath soil for insoluble saccharides (Delhaize et al., 2012). Differences between treatments of rhizosheath weight were tested with the two-way ANOVA. In the second experiment, we examined the microbial diversity of the rhizosheath soil.

Deoxyribonucleic Acid Extraction and Sequencing

Total DNA was extracted from 0.5 ± 0.05 g samples of sandy rhizosheath soil subjected to different moisture and sterilization treatments using the DNA Isolation Kit (BioTeke Corporation, Beijing, China). The bacterial 16S ribosomal RNA (16S rRNA) gene was PCR amplified in triplicate from the extracted DNA using primers 27 F and 1,492 R (Bolger et al., 2014). For high-throughput sequencing, each rhizosphere soil sample was extracted using the Power Soil DNA Isolation Kit. DNA quality was monitored by 0.8% agarose gel electrophoresis and the extracted DNA was diluted to a concentration of 1 ng/μl and stored at –20°C until further processing. The diluted DNA was used as a template for PCR amplification of bacterial 16S rRNA genes with bar-coded primers and the HiFi HotStart ReadyMix (Kapa).

For the bacterial diversity analysis, V3-V4 variable regions of 16S rRNA genes were amplified with universal primers 343 F and 798 R (Tanja and Salzberg, 2011). Amplicon quality was checked by gel electrophoresis. The amplified DNA was purified with AMPure XP beads (Agencourt Bioscience Corporation, Shanghai, China) and subjected to another PCR amplification round. After repurification with AMPure XP beads, the final product was quantified using the Qubit dsDNA Assay Kit. Equal amounts of purified DNA were pooled for subsequent sequencing at Shanghai OE Biotechnology Corporation (Shanghai, China) using the MiSeq platform.

Processing of High-Throughput Sequencing Data

High-throughput sequencing yielded raw sequencing data in FASTQ format. The paired-end reads were preprocessed using Trimmomatic software version 0.36 (Caporaso et al., 2010) to detect and remove ambiguous ("N") bases. We then removed low-quality sequences with an average quality score below 20 using a sliding window trimming approach. After trimming, we used fast length adjustment of short read (FLASH) software version 1.2.11 to assemble paired-end reads (Edgar et al., 2011). Parameters of the assembly were 10-bp minimal overlap, 200-bp maximum overlap, and 20% maximum mismatch rate. To remove additional noise from the data, reads with ambiguous, homologous sequences and those containing fewer than 200 bp were eliminated, while reads with 75% of bases above Q20 were retained. Finally, chimeric reads were detected and removed. These two steps were achieved using quantitative insights into microbial ecology (QIIME) software version 1.8.0 (Rognes et al., 2016). Clean reads were subjected to primer sequence removal and clustered to generate operational taxonomic units (OTUs) using UPARSE software with a 97% similarity cutoff (Amann et al., 1990). Representative reads for each OTU were selected using QIIME software. All the representative reads were annotated and blasted against the Silva database (version 123) using ribosomal database project (RDP) classifier with a confidence threshold of 70% (Subbureddiar et al., 2007).

Analysis of High-Throughput Sequencing Data

Alpha diversity was calculated using the R version 3.4.3 "vegan" package and plotted using Origin 2017. The Mann–Whitney *U* test was used to test differences in alpha diversity between

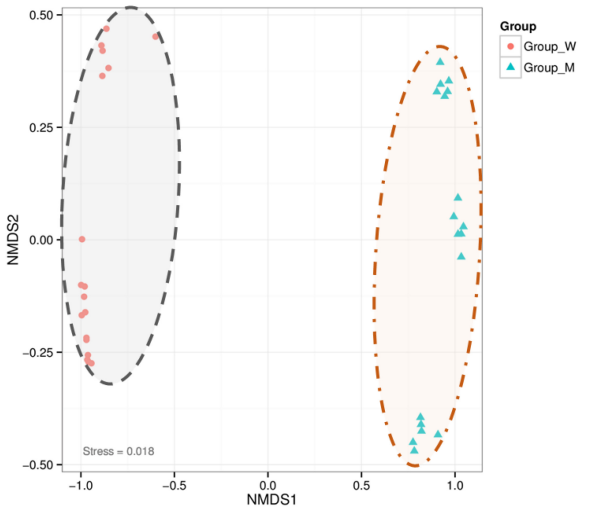

FIGURE 2 | Non-metric multidimensional scaling (NMDS) comparison of bacterial communities in the different treatment groups. The group W represents unsterilized treatment sample in graph and the group M represents sterilized treatment sample in graph.

groups. A heatmap of the top 30 genera was generated with the R "pheatmap" package. Non-metric multidimensional scaling (NMDS) based on Morisita–Horn and Jaccard dissimilarities was performed using the R "vegan" package to investigate differences among rhizosheath bacterial communities in the different treatment samples. Permutational multivariate ANOVA was used to test for statistically significant differences among moisture degree or soil sterilization treatment on the basis of bacterial OTU richness or bacterial phylogenetic diversity (0/1 matrix) and was performed using the "vegan" R package. Venn diagrams were generated using the R "VennDiagram" package. All other graphs were generated in Origin 2017.

Growth-Promoting Activity of Bacterial Operational Taxonomic Units for *Kengyilia hirsuta*

Three bacterial strains were chosen for soil inoculation experiments: OTU16 (*Arthrobacter* strain A6; GenBank accession number NC_011886), OTU6 (*Sphingomonas* strain S-130; NZ_BBWU01000045), and OTU10 (*Massilia* strain CP177-4; KY945685). Plump seeds of *K. hirsuta* collected from northwestern Sichuan in China were selected for experiment. The seeds were surface disinfected in 75% ethanol for 3 min followed by 0.5% NaClO for 3 min, rinsed in sterile water, and placed in a sterile plastic cup (7 cm diameter × 7.5 cm height) with 650 g of sterilized soil. The bacteria were incubated in tryptic soy broth for 24 h and then diluted to an OD_{600} of 0.5–0.6 using a spectrophotometer (Thermo Fisher Scientific, Chengdu, China). Bacterial suspensions (3 ml) were added to the soil of 7-day-old seedlings, with sterilized bacterial suspension used as a control. Each plant–bacterial OTU combination included four replicates. The plants were grown for 60 days (25°C, 55% humidity, 14-h/10-h day/night photoperiod, 1,000–1,200 μmol m^{-2} s^{-1} illumination intensity) until harvested to measure root and rhizosheath weights. Sterilized water was used to maintain moisture as needed. Root and rhizosheath weights were plotted using Origin 2019 and differences between treatments and controls were tested with the two-way ANOVA, the Mann–Whitney *U* test, and the Kruskal–Wallis test using the SPSS software version 22 (Chengdu, China).

RESULTS

Kengyilia hirsuta Rhizosheath Under Different Water and Soil Sterilization Treatment Conditions

Rhizosheaths were found in all the plant samples. Under different soil moisture treatments, rhizosheath weights varied from 7.46 to 21.90 mg cm^{-1} in unsterilized soil and from 5.16 to 19.88 mg cm^{-1} in sterilized soil (**Figure 1**). The interaction between soil treatment and water difference in rhizosheath weight was not significant (**Supplementary Figure 1**, $p > 0.05$). Rhizosheath weights observed at the 25% moisture level in unsterilized and sterilized soil conditions 21.90 and 19.88 mg cm^{-1}, respectively, were significantly higher ($p < 0.05$) than the corresponding weights obtained at the two other moisture levels.

Profile of Bacteria Based on High-Throughput Sequencing

Sequencing of 18 sterilized and 18 unsterilized rhizosphere soils generated 1,312,862 valid raw reads. A total of 20,783 to 44,698 sequencing reads, of which 80.21 to 86.51% were valid, were generated per sample (**Supplementary Table 1**). After filtering out OTUs associated with mitochondria and chloroplasts, an OTU table was generated for further analysis. The rarefaction curve reached saturation at approximately 12,000 sequences and the number of species was higher in unsterilized than sterilized soil (**Supplementary Figure 2**).

Bacterial Diversity Based on Alpha and Beta Indexes

To investigate the bacterial component and diversity in informed processing of *K. hirsuta* rhizosheath, we compared the bacterial diversity of the treatment groups using different alpha indexes. According to the Chao index, the abundance of rhizosphere soils in the sterilized and unsterilized treatment groups was significantly different (Mann–Whitney *U* test, $p < 0.05$). Identically, a comparison revealed significant differences among moisture levels (**Supplementary Table 2**). Bacterial diversity was also measured using the Shannon and Simpson indexes (**Supplementary Figure 3**). According to Simpson index, rhizosheaths in unsterilized soil were more diverse than those in sterilized soil ($p < 0.05$) and similar were found among moisture levels in both the unsterilized and sterilized soil treatment groups ($p > 0.05$).

A total of 27 phyla and 16 classes were identified by high-throughput sequencing (**Supplementary Table 3**). Proteobacteria

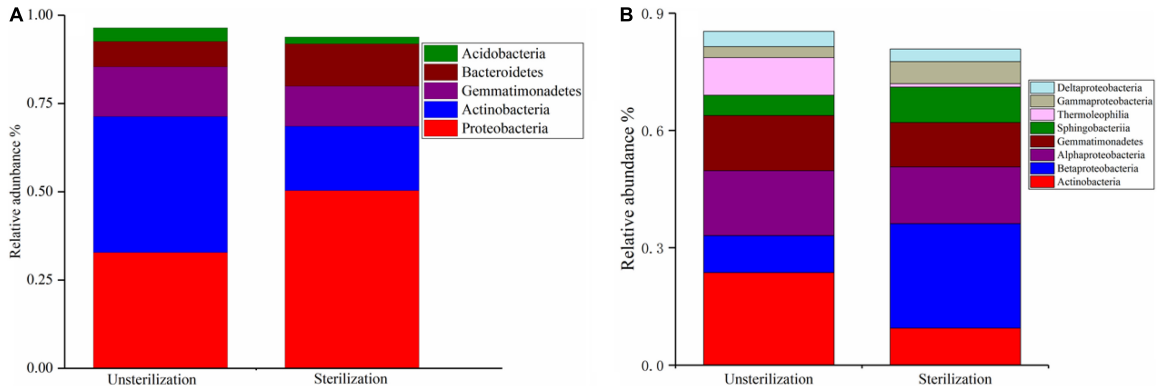

FIGURE 3 | Relative abundance of bacterial phyla under different soil sterilization treatments **(A)**. Relative abundance of bacterial classes under different soil sterilization treatments **(B)**.

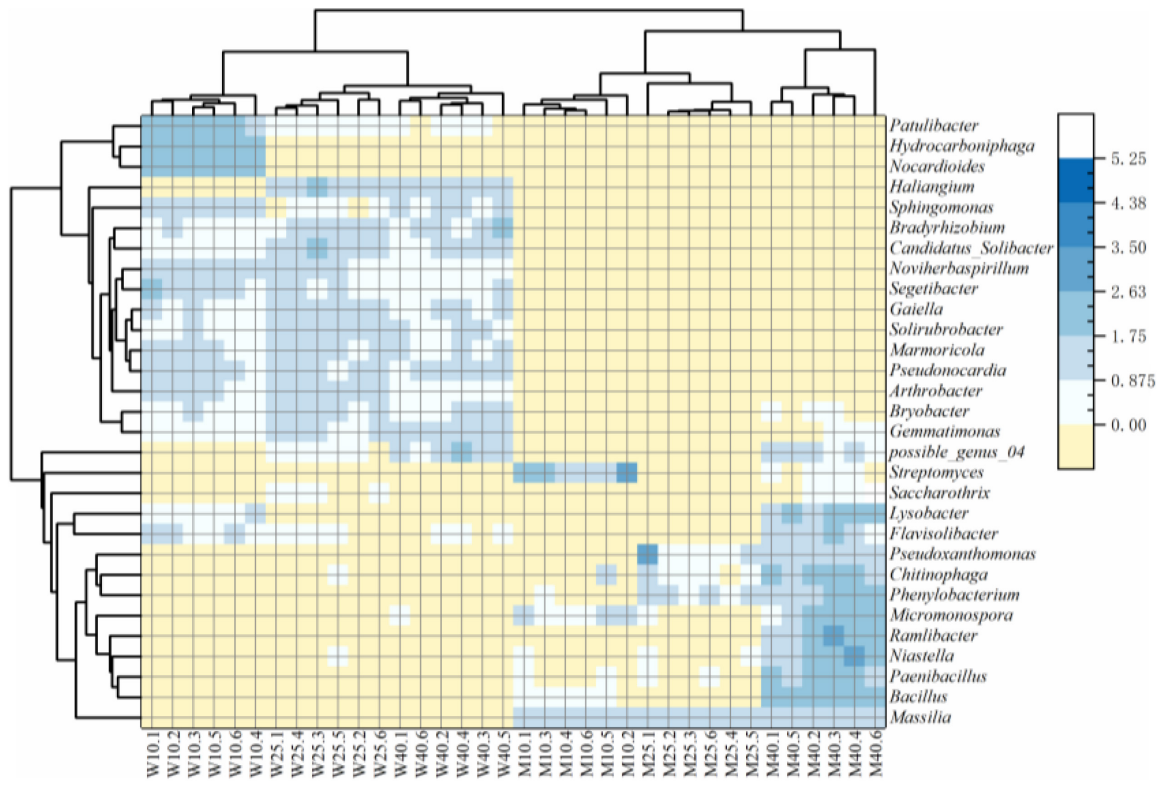

FIGURE 4 | Heatmap of relative abundances of the top 30 genera from the different treatment.

(41.12%), Actinobacteria (28.87%), Gemmatimonadetes (12.87%), and Bacteroidetes (9.44%) were the dominant phyla. The most abundant classes were Actinobacteria (20.28%), Betaproteobacteria (17.70%), Alphaproteobacteria (15.64%), Gemmatimonadetes (12.87%), Sphingobacteriia (6.98%), Thermoleophilia (5.43%), Gammaproteobacteria (4.09%), Deltaproteobacteria (3.56%), Acidobacteria (2.46%), Acidimicrobiia (2.38%), Cytophagia (2.34%), and Bacilli (2.21%). The following genera and generic categories accounted for 65.75% of total reads: other (24.46%), uncultured (12.31%), *Gemmatimonas* (5.97%), *Sphingomonas* (5.30%), *Arthrobacter* (5.14%), *Pseudonocardia* (4.00%), uncultured bacterium (3.65%), *Patulibacter* (2.75%), and ambiguous taxa (2.17%).

Enrichment of Specific Soil Bacteria in the *Kengyilia hirsuta* Rhizosheath Under Sterilization and Water Treatments

Because our experiments indicated that rhizosheaths formed under all the tested conditions and that rhizosheath weights

varied among soil sterilization and moisture level treatments, the specific bacteria were enriched in developing *K. hirsuta* rhizosheaths in response to particular treatment conditions. The NMDS analysis clearly divided the bacterial community into two groups on the basis of treatment in abscissa (**Figure 2**), namely, soil treatment (unsterilized and sterilized soil groups) and water treatment (10, 25, and 40%) (Jaccard dissimilarity index, $p = 0.001$). According to these results, the amount of variation due to differences in moisture levels was smaller than that arising from the soil sterilization treatment. Significant differences were observed in the bacterial community between the soil treatment groups (sterilized and unsterilized soil) and among moisture levels (10, 25, and 40%). According to the NMDS analysis, the soil sterilization treatment was responsible for the largest percentage of explained variation in beta diversity.

We first compared the bacterial community in soil sterilization treatment groups (unsterilized vs. sterilized) at different phylogenetic levels. At the phylum level, the relative abundance of Actinobacteria was significantly higher ($p < 0.01$) in rhizosheaths in unsterilized soil (38.49%) than in sterilized soil (18.22%). Proteobacteria and Bacteroidetes were significantly less represented ($p < 0.01$) in the unsterilized soil group (32.81 and 7.21%, respectively) than in the sterilized soil group (50.32 and 12.01%, respectively). Gemmatimonadetes was common in both the unsterilized (14.10%) and sterilized (11.37%) groups (**Figure 3A**).

At the class level, Actinobacteria dominated in the unsterilized soil group, representing 23.67% of OTUs in unsterilized conditions compared with 16.37% in rhizosheaths in sterilized soil ($p < 0.01$). The relative abundance of Betaproteobacteria was significantly higher ($p < 0.01$) in the sterilized group (26.74%) than in the unsterilized group (9.44%). Members of Alphaproteobacteria were more abundant in rhizosheaths in unsterilized soil (16.60%) than in sterilized soil (14.50%); a similar result was observed for Gemmatimonadetes: 14.10% in unsterilized soil vs. 11.37% in sterilized soil (**Figure 3B**).

As shown in the heatmap (**Figure 4**), bacterial communities were divided at the genus level into two major groups on the basis of soil sterilization and moisture treatment. *Sphingomonas*, *Arthrobacter*, *Pseudonocardia*, *Patulibacter*, *Haliangium*, *Solirubrobacter*, *Noviherbaspirillum*, *Marmoricola*, *Candidatus-Solibacter*, *Gaiella*, and *Bradyrhizobium* were significantly more abundant in the unsterilized than sterilized groups ($p < 0.05$, Mann–Whitney *U* test). In contrast, the abundances of *Massilia*, *Flavisolibacter*, *Lysobacter*, *Bacillus*, *Niastella*, *Phenylobacterium*, *Ramlibacter*, *Micromonospora*, *Streptomyces*, *Saccharothrix*, *Chitinophaga*, *Pseudoxanthomonas*, and *Paenibacillus* were significantly higher in the sterilized group than the unsterilized group ($p < 0.05$, Mann–Whitney *U* test). Other genera, such as *Gemmatimonas*, *Nocardioides*, *Bryobacter*, *Segetibacter*, *possible_genus_04*, and *Hydrocarboniphaga* were equally represent in rhizosheaths developed in unsterilized and sterilized soils.

In total, 3,632 OTUs were present in both the unsterilized and sterilized soil groups, whereas 1,983 OTUs were present only in rhizosheaths from unsterilized soil and 607 OTUs were unique to sterilized soil conditions (**Figure 5C**). More than 86% of OTUs in the sterilized soil group were also found in the unsterilized group, thus indicating a high overlap between the two bacterial communities. Next, we compared the distribution of the top 30 bacterial OTUs between the sterilized and unsterilized soil treatment groups (**Figures 5A,B**). We found that OTU16, OTU9, OTU10, and OTU6 were abundant in rhizosheaths from both types of soil.

Among the top 30 OTUs, OTU16 (18.56%) and OTU6 (11.72%) were the most dominant OTUs in the unsterilized soil group. In contrast, OTU10 was predominant in the sterilized soil treatment group. Bacteria in the rhizosheath were, thus, most likely selectively recruited from soil. The five most abundant OTUs in the rhizosheath that were common to both soil types were OTU16 (*Arthrobacter*), OTU6 (*Sphingomonas*), OTU126 (*Gemmatimonas*), OTU10 (*Massilia*), and OTU12 (*Sphingomonas*). Most OTUs belonged to genera *Massilia* and *Arthrobacter* accounted for over 60% of reads. The bacteria in developing rhizosheath in the two soil treatment groups were, thus, different.

Plant Growth Promotion of Bacteria Isolated From *K. hirsuta* Rhizosheath

Three bacterial strains, OTU16, OTU6, and OTU10, were used in this experiment. Weights of *K. hirsuta* roots grown in sterilized soil inoculated with OTU6, OTU10, or OTU16 were not significantly different ($p > 0.05$) from those of the control, but root weights were significantly increased ($p < 0.05$) by inoculation of soil with a mixture of three strains (**Figure 6A**). Although inoculation of sterilized soil with OTU6 had no significant effect on the rhizosheath weight of *K. hirsuta* ($p > 0.05$), rhizosheath weights were significantly increased ($p < 0.05$) by inoculation with OTU16, OTU10, and a mixture of three strains (**Figure 6B**).

DISCUSSION

Rhizosheath Weight Changes in Soil Moisture and Sterilization

Kengyilia hirsuta has an advanced rhizosheath structure that aids the successful establishment of this species in sand (Oláh, 2004). The rhizosheath structure comprises soil particle and water from soil, the root architecture, root exudates, and soil microorganisms (Young, 2006). Both treatments of unsterilized and sterilized soils, we observed the effect of soil moisture level (10, 25, and 40%) on rhizosheath weight and *K. hirsuta* plants with their robust rhizosheaths were more successfully established in both unsterilized and sterilized soil at the 25% moisture level. Similar results have produced in some earlier studies; the rhizosheath volume in the dry soil layer was five times that of the subtending root, but only 1.5 times the volume of the root in the wet layer. Rhizosheaths are thicker and held to the root with greater tenacity when formed in the drier soils of midsummer and they are less substantial and more easily removed from roots growing in the wetter soils of early spring; when the root is growing under relatively dry conditions, the mucilage is a crucial element for soil adhesion (Watt et al., 1994). Therefore, rhizosheaths easily formed in relatively drier soil.

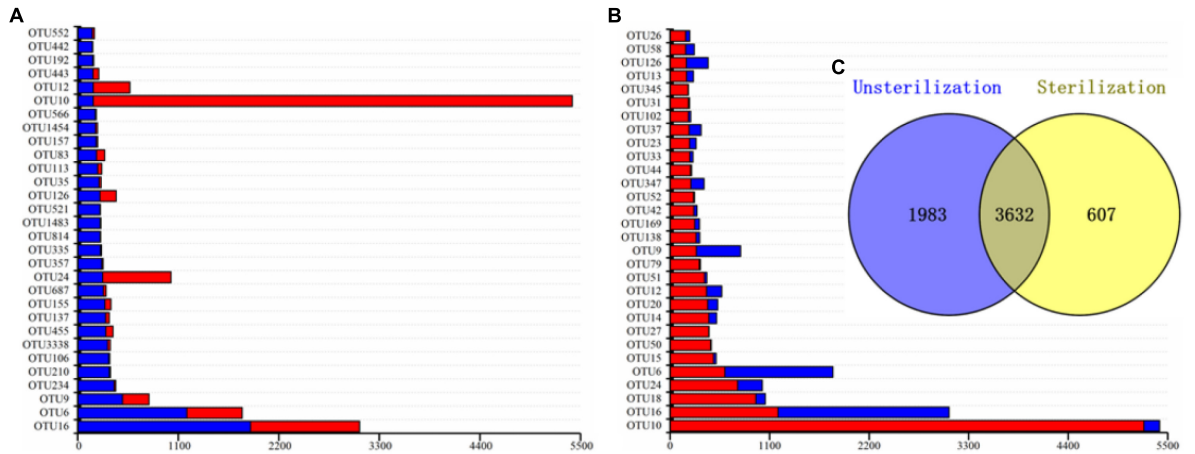

FIGURE 5 | Asymmetrical distribution of operational taxonomic units (OTUs) in the unsterilization soils and sterilization soils. Cumulative histogram of the top 30 bacterial OTUs isolated from *Kengyilia hirsuta* rhizosheaths in unsterilized soil **(A)**. Cumulative histogram of the top 30 bacterial OTUs isolated from *Kengyilia hirsuta* rhizosheaths in sterilized soil **(B)**. Number of OTUs present under different soil sterilization treatment conditions **(C)**. The relative abundance of each OTU, depicted in red (from sterilized soil) or blue (from sterilized soil), is expressed as the log2(x + 1)-transformed number of sequencing reads from a given isolation source.

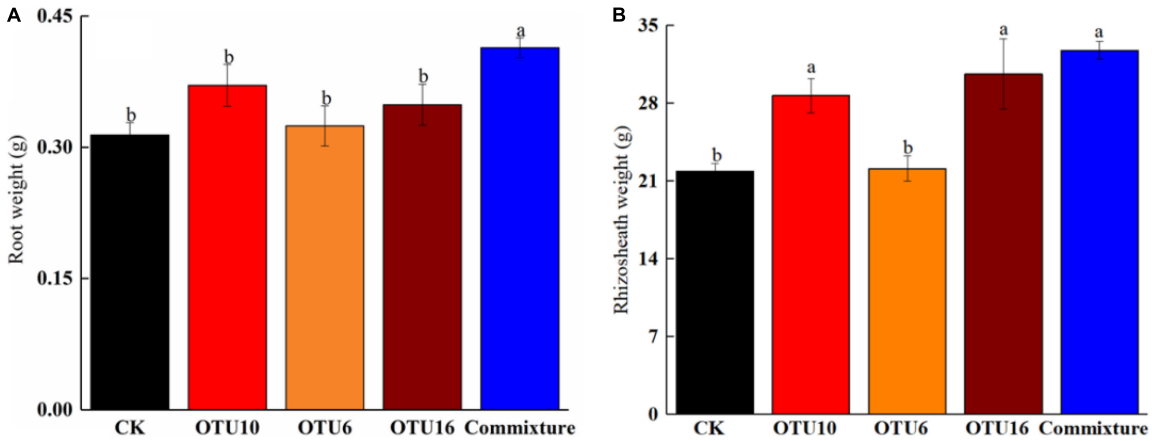

FIGURE 6 | Root-weight-promoting effects of bacterial strains isolated from *K. hirsuta* rhizosheaths **(A)**. Rhizosheath weight-promoting effects of bacterial strains isolated from *K. hirsuta* rhizosheaths **(B)**. The black column represent no infection (CK), the red column represent with OTU10 infected, the yellow column represent with OTU6 infected, the brown column represent with OTU16 infected, the blue column represent with commixture infected (OTU10, OTU6, and OTU16).

Our data indicated that soil sterilization reduced the EC and pH of soil, but the rhizosheath weight was not affected; such changes was observed in this study too (Lynch, 1982). This is because in sterilized soil, it probably favored the growth of efficient exopolysaccharide (EPS)-producing bacteria, thus causing increased soil aggregation around roots and the root exudate, e.g., phytohormones, plays a central role in the recruitment of bacteria in rhizosheath informed processes (Mahmood et al., 2014). In this study, the result showed that special bacteria can be recruited in rhizosheath formed processes.

Bolting the Special Bacteria in Rhizosheath Formed Processes

The structure of the rhizosheath generates a favorable bacteria for the establishment of complex diverse bacterial populations in sandy soils of different factors such as moisture, bacteria, and so on (Othman et al., 2004; Moreno et al., 2007; Hanna et al., 2013). We found that specific bacteria were selectively enriched in developing *K. hirsuta* rhizosheath, which led to a significant switch in bacterial composition at different moisture and sterilization of soil. The data indicate that the choice of soil sterilization treatment (unsterilized soil vs. sterilized soil) rather than moisture level played a very critical role in the variation of the bacterial community.

Bacterial communities during rhizosheath formation in unsterilized soil varied more significantly than those in sterilized soil, a result that was mainly due to the enrichment of genera *Arthrobacter* and *Massilia* in unsterilization, as reflected by the high abundance of OTU16 (*Arthrobacter*) and OTU10 (*Massilia*). The genera *Massilia* mainly enrichment in sterilization, as reflected by the high abundance of OTU10 (*Massilia*). Several pieces of evidence indicate that the process of rhizosheath

formation is responsible for the accumulation of specific bacteria from the rhizosphere. First, the physicochemical nature of soil can be altered and shaped by the specific rhizosphere community (Long et al., 2009). Second, specific bacterial communities are strongly influenced by soil moisture (Pereira et al., 2016). In this study, we observed a large variation in the bacterial composition of the rhizosheath under different conditions, which suggests that the specific bacterial community plays a key role in the establishment of rhizosheath formation.

Arthrobacter and *Massilia* are common bacteria in soil; in a previous study, species of *Arthrobacter* were isolated from the tomato rhizosphere and strains with high phosphate-solubilizing ability were then tested against a wide range of temperature, pH, and environmental stresses (Banerjee et al., 2010). Those strains also exhibited various plant growth-promoting and biocontrol activities, including indole acetic acid production, and have the potential to be used as plant growth-promoting rhizobacteria (Faure et al., 2013). In another study, a strain of *Massilia* significantly increased the growth of potato nodal explants in tissue culture (Turnbull et al., 2012); these reports indicate the existence of a molecular signal recognition system for the accumulation of specific groups of bacteria in the rhizosphere by plants.

Recruitment of microaggregates by the rhizosheath structure may also drive greater microbial diversity (Bach et al., 2018). In this study, *K. hirsuta* with a strong rhizosheath was more successfully established in unsterilized or sterilized soil. This result explains why rhizosheath weight is influenced by different moisture levels and why rhizosheath formation can be optimized to a particular moisture level.

Growth-Promoting Activity of Special Microbial Underlying Rhizosheath Formation

Rhizosheath structure is a topic of interest in regard to the promotion of microbial diversity to enhance plant growth (e.g., nitrogen fixation) and protection under stress conditions (e.g., exopolysaccharide production) (Othman et al., 2004; Ashraf et al., 2006). The rhizosheath bacterial community is considered to be a potentially effective tool for plant growth (Sessitsch et al., 2012).

The abundance of *Arthrobacter*, *Massilia*, *Sphingomonas*, and *Cytophagaceae* was significantly increased in condition of unsterilization and sterilization, which have been successfully cultured and have been reported to promote the growth of several plant species (Zhang et al., 2019). In this study, a mixture of three strains of bacteria isolated from the *K. hirsuta* rhizosheath (OTU16, OTU6, and OTU10) significantly increased root weight. We also found that OTU16, OTU10, and a co-mixture significantly positively influenced the rhizosheath weight of *K. hirsuta.* OTU16 was found to play an important recruitment role in rhizosheath formation in unsterilized soil, while OTU10 exhibited a similar key role in sterilized soil. A mixture of strains, rather than a single strain, may have a stronger contribution to variation of the bacterial community to influence root and rhizosheath weights. Other studies have provided evidence that the composition of special microbe resources, namely, root exudates such as endogenous hormones, plays a critical role in the recruitment of specific bacteria from rhizosphere soil and the process of rhizosheath formation (Bais et al., 2006; Long et al., 2009). These results suggest that different strains have specific functions in *K. hirsuta* root growth and rhizosheath formation. Because our inoculation experiment used seedlings from only a single set of *K. hirsuta* plants, however, this hypothesis remains to be confirmed. In future studies, we accordingly plan to explore whether uniform effects are observed across various growth periods in additional plants including those from the same geographical source.

CONCLUSION

Our data verified that rhizosheaths of *K. hirsuta* easily formed in relatively drier soil. Sterilized soil rather than moisture level played a very critical role in the variation of the bacterial community. *Arthrobacter* and *Massilia* play an important recruitment role in rhizosheath formation in unsterilized soil; *Massilia* mainly provides enrichment in sterilization, suggesting that the recognition mechanism may be conserved special bacteria in the *K. hirsuta* root growth and rhizosheath formation. The underlying physiological and molecular mechanisms need further elucidation. Taken together, our results provide a novel understanding of the physiological and molecular changes during the *K. hirsuta* rhizosheaths formation and environmental adaptation of sandy plants on the TP.

DATA AVAILABILITY STATEMENT

The data presented in the study are deposited in the NCBI (http://www.ncbi.nlm.nih.gov/bioproject/790485) repository, accession number PRJNA790485.

AUTHOR CONTRIBUTIONS

CC and YC contributed to the study design. CC, YC, QZ, JH, YL, and WL were involved in drafting the manuscript and agreed to be accountable for the work. All authors read and approved the final version of the manuscript.

FUNDING

This study was funded by the National Natural Science Foundation of China (Grant No. 31802123), the Survey of Forage Resources in Southern China (2017FY100602), "the Fundamental Research Funds for the Central Universities." Southwest Minzu University (2021PTJS30), System of MOF and MARA(CAS34), and Laboratory of Superior Forage Germplasm in the Qinghai-Tibetan Plateau (2020-ZJ-Y03).

SUPPLEMENTARY MATERIAL

The Supplementary Material for this article can be found online at: https://www.frontiersin.org/articles/10.3389/fpls.2021.785971/full#supplementary-material

REFERENCES

Amann, R. I., Binder, B. J., Olson, R. J., and Chisholm, S. W. (1990). Combination of 16S rRNA-targeted oligonucleotide probes with flow cytometry for analyzing mixed microbial populations. *Appl. Environ. Microbiol.* 56, 1919–1925. doi: 10.1128/aem.56.6.1919-1925.1990

Ashraf, M., Hasnain, S., and Berge, O. J. (2006). Effect of exo-polysaccharides producing bacterial inoculation on growth of roots of wheat (*Triticum aestivum* L.) plants grown in a salt-affected soil. *Int. J. Environ. Sci. Technol.* 3, 43–51.

Bach, E. M., Williams, R. J., Hargreaves, S. K., Yang, F., and Hofmockel, K. B. (2018). Greatest soil microbial diversity found in micro-habitats. *Biochemistry* 118, 217–226.

Bais, H. P., Weir, L., Perry, L. G., Gilroy, S., and Vivanco, J. M. (2006). The role of root exudates in rhizosphere interactions with plants and other organisms. *Plant Biol.* 57, 233–266. doi: 10.1146/annurev.arplant.57.032905.105159

Banerjee, S. R., Palit, C. S., and Standing, D. J. (2010). Stress induced phosphate solubilization by *Arthrobacter* sp. and *Bacillus* sp. isola ted from tomato rhizosphere. *Aust. J. Crop Sci.* 4, 378–383.

Baum, B. R., Yang, J. L., and Yen, C. J. (1995). Taxonomic separation of *Kengyilia*(Poaceae: Triticeae) in relation to nearest related *Roegneria Elymus* and *Agropyron* based on some morphological characters. *Evolution* 194, 123–132.

Berns, A. E., Philipp, H. D., Narres, P., Burauel, H., and Vereecken, S. (2010). Effect of gamma-sterilization and autoclaving on soil organic matter structure as studied by solid state NMR, UV and fluorescence spectroscopy. *Eur. J. Soil Sci.* 59, 540–550. doi: 10.1111/j.1365-2389.2008.01016.x

Bolger, A. M., Marc, L., and Bjoern, U. (2014). Trimmomatic: a flexible trimmer for Illumina sequence data. *Bioinformatics* 30, 2114–2120. doi: 10.1093/bioinformatics/btu170

Brown, L. K., George, T. S., Neugebauer, K., and White, P. J. (2017). The rhizosheath-a potential trait for future agricultural sustainability occurs in orders throughout the angiosperms. *Plant Soil* 418, 115–128. doi: 10.1007/s11104-017-3220-2

Caporaso, J. G., Kuczynski, J., Stombaugh, J., Bittinger, K., Bushman, F. D., Costello, E. K., et al. (2010). QIIME allows analysis of high-throughput community sequencing data. *Nat. Methods* 7, 335–336. doi: 10.1038/nmeth.f.303

Danin, A. (1996). "Plant adaptations to environmental stresses in desert dunes," in *Plant of Desert Dunes*, ed. A. Danin (Berlin: Springer), 133–134.

Delhaize, E., James, R. A., and Ryan, P. P. (2012). Aluminium tolerance of root hairs underlies genotypic differences in rhizosheath size of wheat (*Triticum aestivum*) grown on acid soil. *New Phytol.* 195, 609–619. doi: 10.1111/j.1469-8137.2012.04183.x

Edgar, R. C., Haas, B. J., Clemente, J. C., Quince, C., and Knight, R. B. (2011). Ucheime improves sensitivity and speed of chimera detection. *Bioinformatics* 27:2194. doi: 10.1093/bioinformatics/btr381

Faure, D., Cirou, A., and Dessaux, Y. (2013). *Chemicals Promoting the Growth of N-Acylhomoserine Lactone-Degrading Bacteria, U.S. Patent No. US8354265B2.*

Hanna, A. L., Youssef, H. H., Amer, W. M., Monib, M., Fayez, M., and Hegazi, N. R. (2013). Diversity of bacteria nesting the plant cover of north Sinai deserts, Egypt. *J. Adv. Res.* 4, 13–26. doi: 10.1016/j.jare.2011.11.003

Jörn, A., Stefan, S., and Geoderma, J. (1993). Effects of biocidal treatments on biological and nutritional properties of a mull-structured woodland soil. *Geoderma* 56, 435–448. doi: 10.1016/b978-0-444-81490-6.50035-2

Long, H. H., Sonntag, D. G., Schmidt, D. D., and Baldwin, I. P. (2009). The structure of the culturable root bacterial endophyte community of Nicotiana attenuata is organized by soil composition and host plant ethylene production and perception. *New Phytol.* 185, 554–567. doi: 10.1111/j.1469-8137.2009.03079.x

Lynch, M. J. (1982). Limits to microbial growth in soil. *Microbiology* 128, 405–410. doi: 10.1099/00221287-128-2-405

Mahmood, T., Mehnaz, F., Fleischmann, R. A., Hashmi, P., and Iqbal, P. (2014). Soil sterilization effects on root growth and formation of rhizosheaths in wheat seedlings. *Pedobiologia* 57, 123–130. doi: 10.1016/j.pedobi.2013.12.005

Marasco, R., Mosqueira, M. J., Fusi, M., Ramond, J. B., Merlino, G., Booth, J. M., et al. (2018). Rhizosheath microbial community assembly of sympatric desert speargrasses is independent of the plant host. *Microbiome* 6:215. doi: 10.1186/s40168-018-0597-y

Marasco, R., Rolli, E., Ettoumi, B., Vigani, G., Mapelli, F., Borin, S., et al. (2012). A drought resistance-promoting microbiome is selected by root system under desert farming. *PLoS One* 7:48479. doi: 10.1371/journal.pone.0048479

Marschner, B., and Bredow, A. (2002). Temperature effects on release and ecologically relevant properties of dissolved organic carbon in sterilised and biologically active soil samples. *Soil Biol. Biochem.* 34, 459–466. doi: 10.1016/s0038-0717(01)00203-6

Mcnamara, N. P., Black, N. A., Beresford, N., and Parekh, E. (2003). Effect of acute gamma irradiation on chemical, physical and biological properties of soils. *Appl. Soil Ecol.* 24, 117–132. doi: 10.1016/s0929-1393(03)00073-8

Moreno, I. P., Rivera, B. F., Ferrara, G. M., and Leon, G. F. (2007). Role of root-hairs and hyphae in adhesion of sand particles. *Soil Biol. Biochem.* 39, 2520–2526.

Oláh, K. S. (2004). The modern management of hirsutism. *Rev. Gynaecol. Pract.* 4, 211–220. doi: 10.1016/j.rigp.2004.05.001

Othman, A. A., Amer, W. M., Fayez, M., and Hegazi, N. A. (2004). Rhizosheath of sinai desert plants is a potential repository for associative diazotrophs. *Microbiol. Res.* 159, 285–293. doi: 10.1016/j.micres.2004.05.004

Pang, J., Ryan, M. H., Siddique, K. H., and Simpson, R. (2017). Unwrapping the rhizosheath. *Plant Soil* 418, 129–139. doi: 10.1007/s11104-017-3358-y

Pereira, S. N., Eusébio, F. A., Almeida, O. W., Silva, C., and Leila, A. (2016). Rock biofertilizer and earthworm compost on sugarcane performance and soil attributes in two consecutive years. *Sci. Agric.* 73, 29–33. doi: 10.1590/0103-9016-2015-0005

Pointing, S. B., and Belnap, J. M. (2012). Microbial colonization and controls in dryland systems. *Nat. Rev. Microbiol.* 10, 551–562. doi: 10.1038/nrmicro2831

Rognes, T., Flouri, T., Nichols, B., Quince, C., and Mahé, F. P. (2016). *Vseaech*: a versatile open source tool for metagenomics. *PeerJ* 4:e2584. doi: 10.7717/peerj.2584

Sandler, H. A., Carroll, R. B., and Sparks, D. J. (1988). Effect of biocidal treatments on cation exchange capacity and fusarium blight of soybean in delaware soils. *Agron. J.* 80, 8–12. doi: 10.2134/agronj1988.00021962008000010003x

Sessitsch, A., Hardoim, P., Doring, J., Weilharter, A., Krause, A., Woyke, T., et al. (2012). Functional characteristics of an endophyte community colonizing rice roots as revealed by metagenomic analysis. *Mol. Plant Microbe Interact.* 25, 28–36. doi: 10.1094/MPMI-08-11-0204

Subbureddiar, R., Mukkamala, S., Shankarpani, M., and Andrew, S. H. (2007). Mining audit data for intrusion detection systems using support vector machines and neural networks. *Int. J. Inf. Sci. Comput.* 1, 7410–7419.

Tanja, M., and Salzberg, S. B. (2011). Flash: fast length adjustment of short reads to improve genome assemblies. *Bioinformatics* 27, 2957–2963. doi: 10.1093/bioinformatics/btr507

Traoré, O., Groleau, R., Plantureux, S., Tubeileh, A., and Boeuf, T. (2010). Effect of root mucilage and modelled root exudates on soil structure. *Agron. J.* 51, 575–581. doi: 10.1111/j.1365-2389.2000.00348.x

Turnbull, A. L., Liu, Y., and Lazarovits, G. (2012). Isolation of bacteria from the rhizosphere and rhizoplane of potato (*Solanum tuberosum*) grown in two distinct soils using semi selective media and characterization of their biological properties. *Am. J. Potato Res.* 89, 294–305. doi: 10.1007/s12230-012-9253-4

Watt, M., Mccully, M. E., and Canny, M. P. (1994). Formation and stabilization of rhizosheaths of *Zea mays* L.(effect of soil water content). *Plant Physiol.* 106, 179–186. doi: 10.1104/pp.106.1.179

Wertz, S., Czarnes, S., Bartoli, F., Renault, P., Commeaux, C., and Guillaumaud, N. (2007). Early-stage bacterial colonization between a sterilized remoulded

soil clod and natural soil aggregates of the same soil. *Soil Biol. Biochem.* 39, 3127–3137. doi: 10.1016/j.soilbio.2007.07.005

Young, I. M. (2006). Variation in moisture contents between bulk soil and the rhizosheath of wheat (*Triticum aestivum* L. cv. Wembley). *New Phytol.* 130, 135–139. doi: 10.1111/j.1469-8137.1995.tb01823.x

Yue, M. (2017). Using phylogeny and functional traits for assessing community assembly along environmental gradients: a deterministic process driven by elevation. *Ecol. Evol.* 7, 5056–5069. doi: 10.1002/ece3.3068

Zhang, S. W., Chen, Q. D., Zhong, X. L., and Zhuang, Z. H. (2019). Microbial community analyses associated with nine varieties of wine grape carposphere based on high-throughput sequencing. *Microorganisms* 7:668. doi: 10.3390/microorganisms7120668

Zong, N., and Fu, G. (2021). Variations in species and function diversity of soil fungal community along a desertification gradient in an alpine steppe. *Ecol. Indic.* 131:108197. doi: 10.1016/j.ecolind.2021.108197

Conflict of Interest: The authors declare that the research was conducted in the absence of any commercial or financial relationships that could be construed as a potential conflict of interest.

Publisher's Note: All claims expressed in this article are solely those of the authors and do not necessarily represent those of their affiliated organizations, or those of the publisher, the editors and the reviewers. Any product that may be evaluated in this article, or claim that may be made by its manufacturer, is not guaranteed or endorsed by the publisher.

Copyright © 2022 Chen, Chen, Zhou, Hu, Lei and Liu. This is an open-access article distributed under the terms of the Creative Commons Attribution License (CC BY). The use, distribution or reproduction in other forums is permitted, provided the original author(s) and the copyright owner(s) are credited and that the original publication in this journal is cited, in accordance with accepted academic practice. No use, distribution or reproduction is permitted which does not comply with these terms.

frontiers in Plant Science

ORIGINAL RESEARCH
published: 03 February 2022
doi: 10.3389/fpls.2022.822594

Land Degradation Changes the Role of Above- and Belowground Competition in Regulating Plant Biomass Allocation in an Alpine Meadow

Yong Zhang[1,2], Qiuzhu Zheng[1,2], Xiaoxia Gao[3], Yandan Ma[1,2], Kemin Liang[1,2], Haitao Yue[1,2], Xiaoxia Huang[4], Kaiting Wu[1,2] and Xiaorong Wang[1,2]*

[1] Yunnan Key Laboratory of Plateau Wetland Conservation, Restoration and Ecological Services, College of Wetlands, Southwest Forestry University, Kunming, China, [2] National Plateau Wetlands Research Center, Southwest Forestry University, Kunming, China, [3] State Key Laboratory of Vegetation and Environmental Change, Institute of Botany, Chinese Academy of Sciences, Beijing, China, [4] School of Earth Sciences, Yunnan University, Kunming, China

OPEN ACCESS

Edited by:
Shiliang Liu,
Beijing Normal University, China

Reviewed by:
Shikui Dong,
Beijing Forestry University, China
Hao Shen,
Beijing Normal University, China

***Correspondence:**
Yong Zhang
zhy1902@126.com

Specialty section:
This article was submitted to Functional Plant Ecology, a section of the journal Frontiers in Plant Science

Received: *26 November 2021*
Accepted: *05 January 2022*
Published: *03 February 2022*

Citation:
Zhang Y, Zheng Q, Gao X, Ma Y, Liang K, Yue H, Huang X, Wu K and Wang X (2022) Land Degradation Changes the Role of Above- and Belowground Competition in Regulating Plant Biomass Allocation in an Alpine Meadow. Front. Plant Sci. 13:822594. doi: 10.3389/fpls.2022.822594

The allocation pattern of plant biomass presents the strategy of the plant community to adopt environmental changes, while the driver of biomass allocation is still unclear in degraded alpine grassland ecosystems. To explore the issue, this study investigated the shoot-to-root (R/S) ratio, plant aboveground traits, and root competition of three functional groups (i.e., grasses, sedges, and forbs) at three degradation levels (i.e., no obvious degradation, ND; moderate degradation, MD; and severe degradation, SD) in an alpine meadow in the eastern Qinghai-Tibetan Plateau. The relationships among plant aboveground traits, root competition, and R/S ratio were tested using the structural equation model (SEM). The results showed that the shoot and root biomass tended to decrease, but the R/S ratio of the plant community did not change along the degradation gradient. Plant height, lateral spread, and leaf length of most plant functional groups reduced, while leaf width and leaf area of most plant functional groups did not change along the degradation gradients. The root competition ability (presented as the fraction of root biomass in total biomass) of sedges in MD was the lowest, while that of grasses was the highest. The effects of aboveground competition on the R/S ratio were non-linear because of the different roles of plant height, lateral spread, and leaf area in regulating the R/S ratio along the degradation gradient. In contrast, the effects of belowground competition on the R/S ratio were linear because belowground competition promoted the R/S ratio, and the strength of this effect reduced along the degradation gradient. These results indicate that plant competition might be a critical factor to maintain the high R/S ratio in degraded alpine meadows.

Keywords: land degradation, aboveground traits, root competition, R/S ratio, alpine meadow, eastern Qinghai-Tibetan Plateau

INTRODUCTION

According to the Food and Agriculture Organization of the United Nations, the grasslands and woodland ecosystems cover nearly 35% of the terrestrial area around the world (Dubois, 2011). The grassland ecosystem has a crucial role in global carbon exchange because of its high carbon storage (Scurlock and Hall, 2002). Especially, the biomass allocation of plants [i.e., the shoot-to-root (R/S) ratio] is an important factor for carbon modeling in terrestrial ecosystems (Poeplau, 2016). The R/S ratio of plant community in the grassland ecosystem is widely discussed (Donald, 1958; Wilson, 1988; Yang et al., 2018). Generally, the root biomass is higher than the shoot biomass in grassland ecosystems (Dai et al., 2020). The increase in the R/S ratio could promote the stability of the grassland ecosystem (Tilman et al., 2006) and indicate the response of the plant community to environmental stresses (Agathokleous et al., 2018). Usually, environmental stress (e.g., intense herbivory and drought) could lead to an increase in the R/S ratio (McNaughton et al., 1998; López–Mársico et al., 2015; Wilson et al., 2018; Alon et al., 2019; Hao and He, 2019). The availability of nutrients and water (Wang et al., 2018) or a restoration process (Gao et al., 2021), however, could reduce the R/S ratio of the plant community. Therefore, the increase in the R/S ratio might indicate that the habitat of the plant community gets worse. Habitat deterioration could change the species richness of the plant community. The change in species richness will inevitably shift the competition pattern among plant species (Herben et al., 2003).

The competition, which could be described as the disequilibrium of biomass among species, is a primary perspective to explain the construction of the plant community (Wilson, 1988; Tilman, 2020). Both the aboveground competition and belowground competition are always positively correlated but they play different roles in shaping the R/S ratio because the aboveground competition of plants focuses on the snatch of light resources, while the belowground competition of plants focuses on the uptake of nutrients and water (Donald, 1958). Obviously, larger shoot biomass will lead to a lower R/S ratio, and larger root biomass will lead to a higher R/S ratio (Pugnaire and Luque, 2001). But the effects of plant competition on plant biomass remain unclear. The controlled experiment suggested that the plant biomass is positively correlated (Bonser and Reader, 1995) or did not correlate (Schofield et al., 2019) with plant competition intensity. However, some field investigations suggested a negative correlation between them (Nötzold et al., 1997).

The Qinghai-Tibetan Plateau (QTP), which is also called the third pole of the world, is the largest alpine region around the world and is mostly occupied by alpine meadows (Dong et al., 2020). In recent decades, these alpine meadows are suffering serious degradation due to climate changes and inappropriate anthropic disturbance (Cao et al., 2019). Land degradation increased the R/S ratio of alpine meadows in the QTP due to a significant decrease in aboveground biomass and a weak change in belowground biomass (Zhang et al., 2019). Moreover, the negative effects of land degradation on plant species richness, plant composition, and plant competition have been widely studied in the QTP (Wang et al., 2014; Tang et al., 2015; Luo et al., 2020; Peng et al., 2020). However, it is still unclear whether the land degradation would change the role of above- and belowground competition in regulating the R/S ratio. To explore this issue, we conducted a field survey in an alpine meadow with different degradation gradients in the eastern QTP. We hypothesized the following: (1) The aboveground competition would reduce, while the belowground competition would promote the R/S ratio, and (2) the effects of above- and belowground competition on the R/S ratio would decrease along the degradation gradient.

MATERIALS AND METHODS

Study Site

This study was conducted on an alpine meadow in Shangri-La (27°47.992′ N, 99°39.094′ E, 3,200∼3,350 m a.s.l.), Yunnan Province, China (**Figure 1**). Shangri-La, located in the eastern QTP, distributes nearly 1,400 km^2 alpine meadows. These meadows maintain the development of local communities by supporting tourism and livestock husbandry. The annual precipitation is 619.5 mm, and the annual temperature is 6.9°C (2,000∼2,016) in Shangri-La. Tourist trampling and significant warming trend have been leading to alpine meadow degrading in this region (Huang et al., 2015; Lehnert et al., 2016).

Three degradation levels (i.e., ND, MD, and SD) were identified according to the width of tourism trails and plant coverage, plant height, soil bulk density, and water content of surface soil aside from the road (10 cm aside the edge of the trial) (**Table 1**). The primary species of grasses were *Elymus burchan-buddae*, *Eragrostis nigra*, and *Poa annua*. The primary species of sedges were *Kobresia duthiei*, *Kobresia pygmaea,* and *Carex enervis*. For forbs, the primary species were *Saussurea romuleifolia*, *Stellera chamaejasme*, *Iris ruthenica var. nana,* and *Potentilla*. The grasses, sedges, and forbs varied among these three degradation levels (**Supplementary Figure 1**).

Field Sampling and Sample Handling

Collecting Data on Plant Aboveground Morphological Traits

Along the degradation gradients, 27 1 m × 1 m investigation quadrats (three degradation levels × three repetitions at each level × three parallels at each repetition) were conducted in July 2018. In each quadrat, the aboveground portion of the dominated plant individuals was collected at each sampling quadrat to measure the height, lateral spread, leaf length, leaf width, and leaf area of meadow plants. In total, 627 individuals (including 183 individuals of grasses, 147 individuals of sedges, and 297 individuals of forbs) were measured (**Table 2**). The plant height reflected the vertical competition potential of plants, while the lateral spread and leaf area reflected the horizontal competition potential of plants.

Collecting Data on the Shoot and Root Biomass

According to a pre-survey in this study area, we found that the distribution depth of most plant roots is less than 20 cm in the soil. Alongside each 1 m × 1 m investigation quadrat, a soil cube

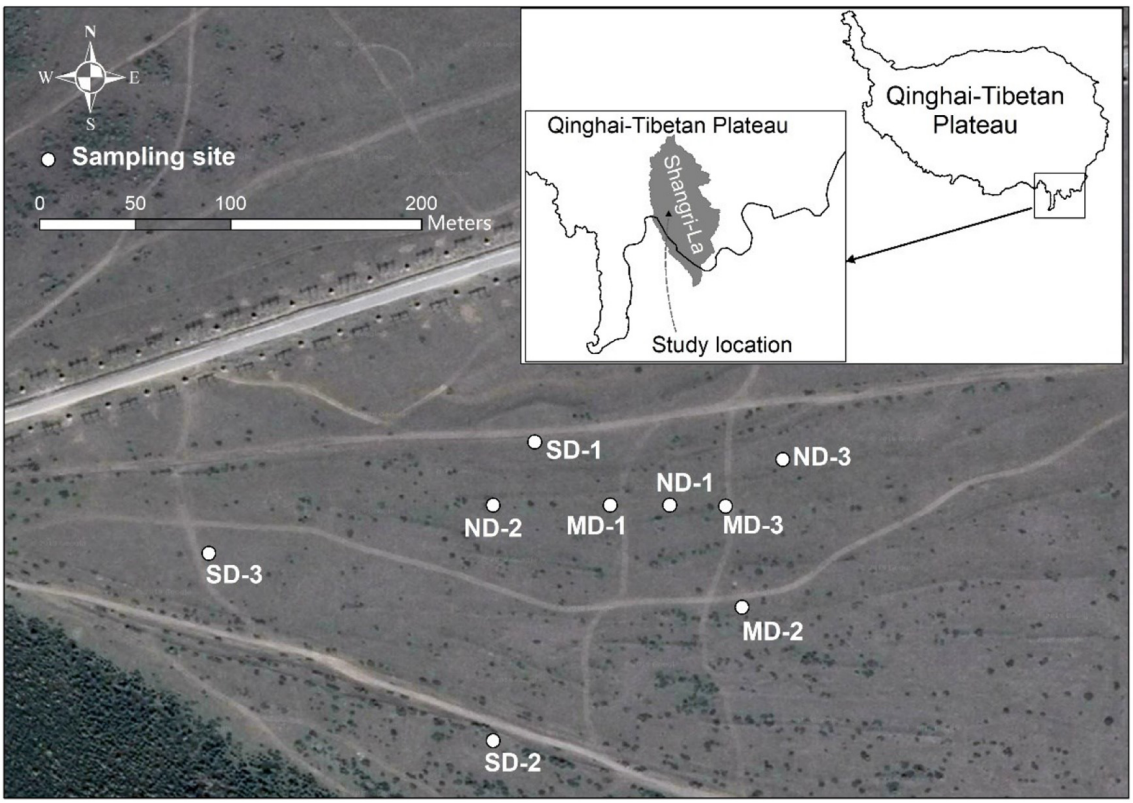

FIGURE 1 | The location of the study area and the distribution of sampling sites.

TABLE 1 | The width of tourism trails (WTT), plant coverage (PC), plant height (PHt), soil bulk density (SBD), and water content of surface soil (WCSS) in no obvious degradation (ND), moderate degradation (MD), and severe degradation (SD) plots in this study (n = 27, α = 0.05).

Degradation level	WTT (m)	PC (%)	PHt (cm)	SBD (g/cm^3)	WCSS (%)
ND	No trail	89.72 ± 0.68a	11.55 ± 0.53a	0.68 ± 0.04b	54.27 ± 3.09a
MD	1.8∼1.9	77.89 ± 1.33b	8.44 ± 0.27b	0.70 ± 0.05b	47.56 ± 3.16a
SD	2.5∼3	63.00 ± 2.06c	5.81 ± 0.25c	0.97 ± 0.05a	31.41 ± 1.84b

Different lowercase letters mean significant differences among degradation gradients.

TABLE 2 | The species and number of plant individuals that were collected in no obvious degradation (ND), moderate degradation (MD), and severe degradation (SD) plots.

	Grasses	Sedges	Forbs
ND	*Elymus burchan-buddae* (21) *Eragrostis nigra* (22)	*Kobresia duthiei* (22) *Kobresia pygmaea* (14)	*Saussurea romuleifolia* (22) *Stellera chamaejasme* (5) *Potentilla* spp. (21) *Iris ruthenica var. nana* (24)
MD	*E. burchan-buddae* (35) *E. nigra* (30) *Poa annua* (5)	*Carex enervis* (5) *K. duthiei* (34)	*Potentilla* spp. (45) *S. romuleifolia* (5) *Leontopodium franchetii* (25) *S. chamaejasme* (5) *Lomatogonium carinthiacum* (5) *I. ruthenica var. nana* (30)
SD	*E. burchan-buddae* (25) *E. nigra* (45)	*C. enervis* (18) *K. duthiei* (45) *K. pygmaea* (9)	*Plantago major* (5) *Potentilla* spp. (53) *S. romuleifolia* (2) *L. franchetii* (15) *I. ruthenica var. nana* (35)
	183	147	297

with a size of 20 cm × 20 cm × 20 cm carrying aboveground biomass was collected to obtain shoot and root biomass. The collected soil cubes were washed four times to remove all soil and dead roots. The cleaned individuals were separated into different functional groups (i.e., grasses, sedges, and forbs). Each individual was split into aboveground and belowground sections (**Figure 2**). These aboveground and belowground materials were dried and weighted to obtain the shoot and root biomass, respectively. Then, the R/S ratio was calculated according to the root and shoot biomass at the functional group level. The root competition was defined as the proportion of root biomass among different functional groups, i.e., for a functional group, a higher proportion of root biomass means a stronger root competition potential.

Statistical Analysis

One-way ANOVA was conducted to test the variance of R/S ratio, root biomass, and morphological traits (including height, lateral spread, leaf length, leaf width, and leaf area) among degradation levels. Tukey's *post hoc* test was conducted at the level of $\alpha = 0.05$. Linear regression was conducted to reveal the relationship between aboveground biomass, belowground biomass, and the R/S ratio. The relationship between height and lateral spread was tested using regression analysis. The one-way ANOVA and regression analysis were conducted in R3.5.1.

The structural equation model (SEM) was used to test the direct and indirect effects of plant aboveground morphological traits (i.e., plant height, lateral spread, and leaf area) on the R/S ratio. We hypothesized that the vertical advantages (i.e., the height) and horizontal advantages (i.e., the lateral spread and leaf area) could directly affect the R/S ratio; meanwhile, they could indirectly affect the R/S ratio by changing root competition. According to this hypothesis, we constructed an *a priori* model that contained all potential paths (**Supplementary Figure 2**). The exogenous variables were plant height, lateral spread, and leaf area. The endogenous variables were root competition and R/S ratio. The model was optimized by stepwise removal of non-significant paths in ND, MD, and SD (**Supplementary Tables 1–3**). The qualified model was symbolized by a non-significant chi-square test ($p > 0.05$), low root mean square error of approximation (RMSEA < 0.05), high comparative fit index (CFI > 0.95), high Tucker-Lewis index (TLI > 0.95), low Akaike information criterion (AIC) value, and high squared multiple correlations (SMC) of endogenous variables. The SEM was conducted in IBM SPSS AMOS 24.

RESULTS

Effects of Land Degradation on Plant Biomass Allocation

Land degradation reduced the shoot biomass but did not affect the root biomass of the plant community. At the functional group level, land degradation did not change the shoot biomass and root biomass of grasses, sedges, and forbs (**Figures 3A,B**).

The biomass distribution among functional groups varied among different degradation levels. The shoot biomass of grasses and forbs was higher than that of sedges in ND and MD, while the shoot biomass did not vary among these three functional groups in SD (**Figure 3A**). The root biomass did not vary among different functional groups in ND and SD. The order of root biomass was forbs > grasses > sedges in MD (**Figure 3B**).

The R/S ratio was >2 in all degradation conditions (**Figure 3C**). The R/S ratio of the plant community, grasses, and forbs did not differ among ND, MD, and SD (**Figure 3C**). For sedges, the R/S ratio was the lowest at MD, and it was the highest at SD (**Figure 3C**). The R/S ratio of different functional groups varied at each degradation gradient. In ND and SD, the R/S ratio of sedges was the highest. In MD, the R/S ratio of forbs was the highest (**Figure 3C**).

The shoot biomass positively correlated with the root biomass at both the community and functional group levels (**Figure 3D**),

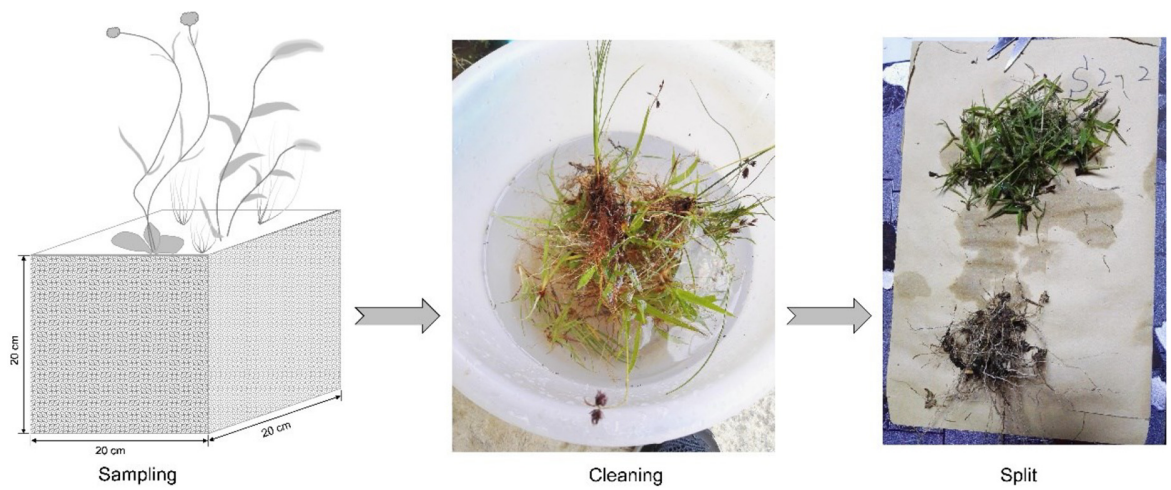

FIGURE 2 | Collection of root and shoot biomass.

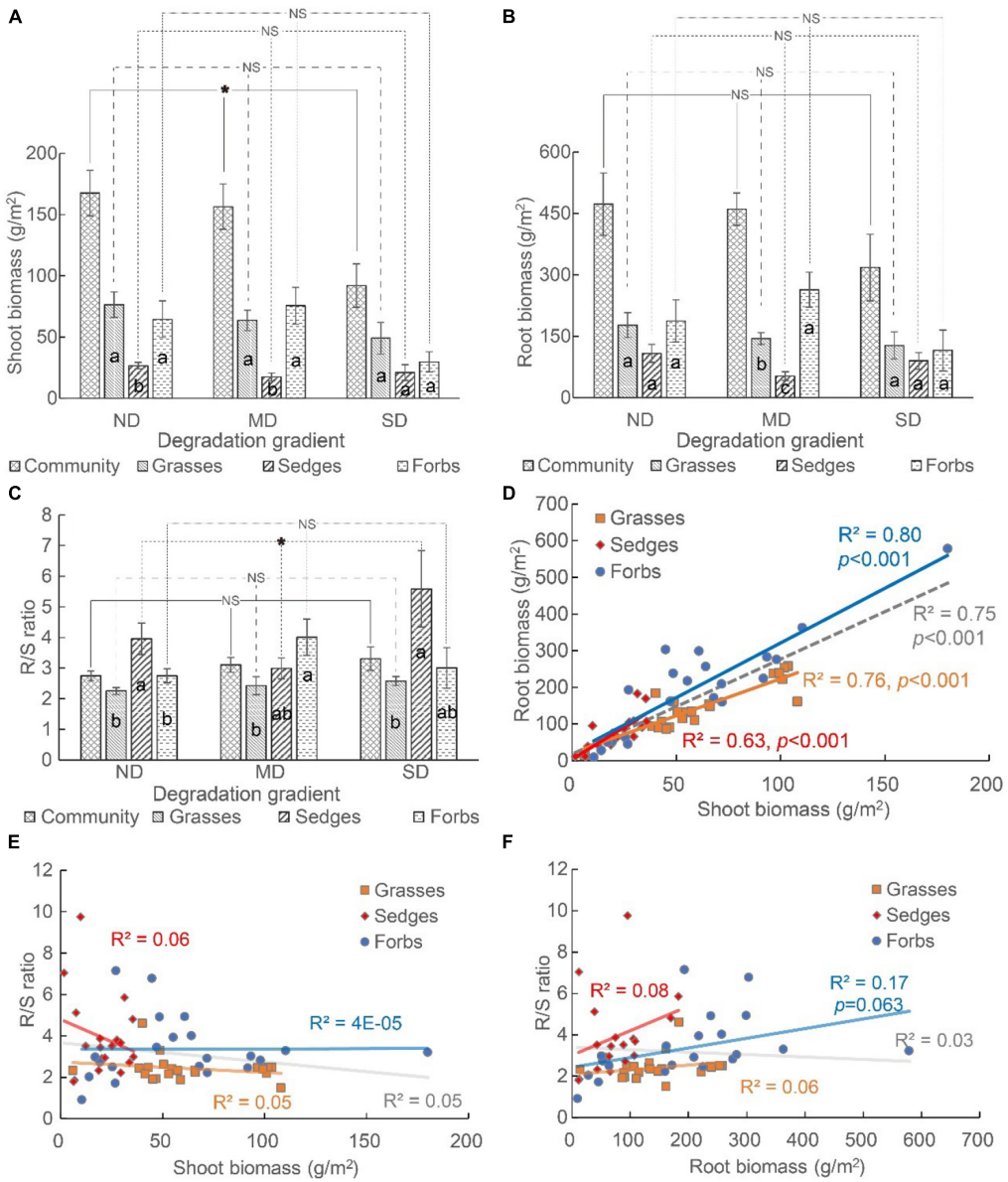

FIGURE 3 | The **(A)** shoot biomass, **(B)** root biomass, and **(C)** root-to-shoot ratio (i.e., R/S ratio) of plant community and different functional groups (i.e., grasses, sedges, and forbs), and **(D–F)** the relationship among shoot biomass, root biomass, and R/S ratio. The "*" means the significant difference among functional groups along the degradation gradient. NS means no differences were detected. The different lowercase letters mean significant differences among functional groups in each degradation gradient.

while the relationship between the R/S ratio and the shoot biomass or root biomass was non-significant (**Figures 3E,F**).

Effects of Land Degradation on Plant Aboveground Traits and Root Competition

For the whole community, the average height, lateral spread, leaf length, and leaf area decreased, but the leaf width did not change along the degradation gradient (**Figures 4A–E**). For grasses, the lateral spread and leaf length decreased, but the height, leaf width, and leaf area did not change along the degradation gradient. For sedges, the height and leaf length decreased, while the lateral spread, leaf width, and leaf area did not change along the degradation gradient. For forbs, all traits except leaf width decreased along the degradation gradient (**Figures 4A–E**).

Most aboveground traits of grasses, sedges, and forbs were different at each degradation level. The height and leaf length of these three functional groups showed the same pattern, i.e., height and leaf length of sedges and forbs were higher than that of grasses in ND; the height and leaf length of sedges were higher (or larger) than that of grasses and forbs in MD and SD (**Figures 4A,C**). The lateral spread of forbs was higher than that of sedges but did not vary with that of grasses in ND.

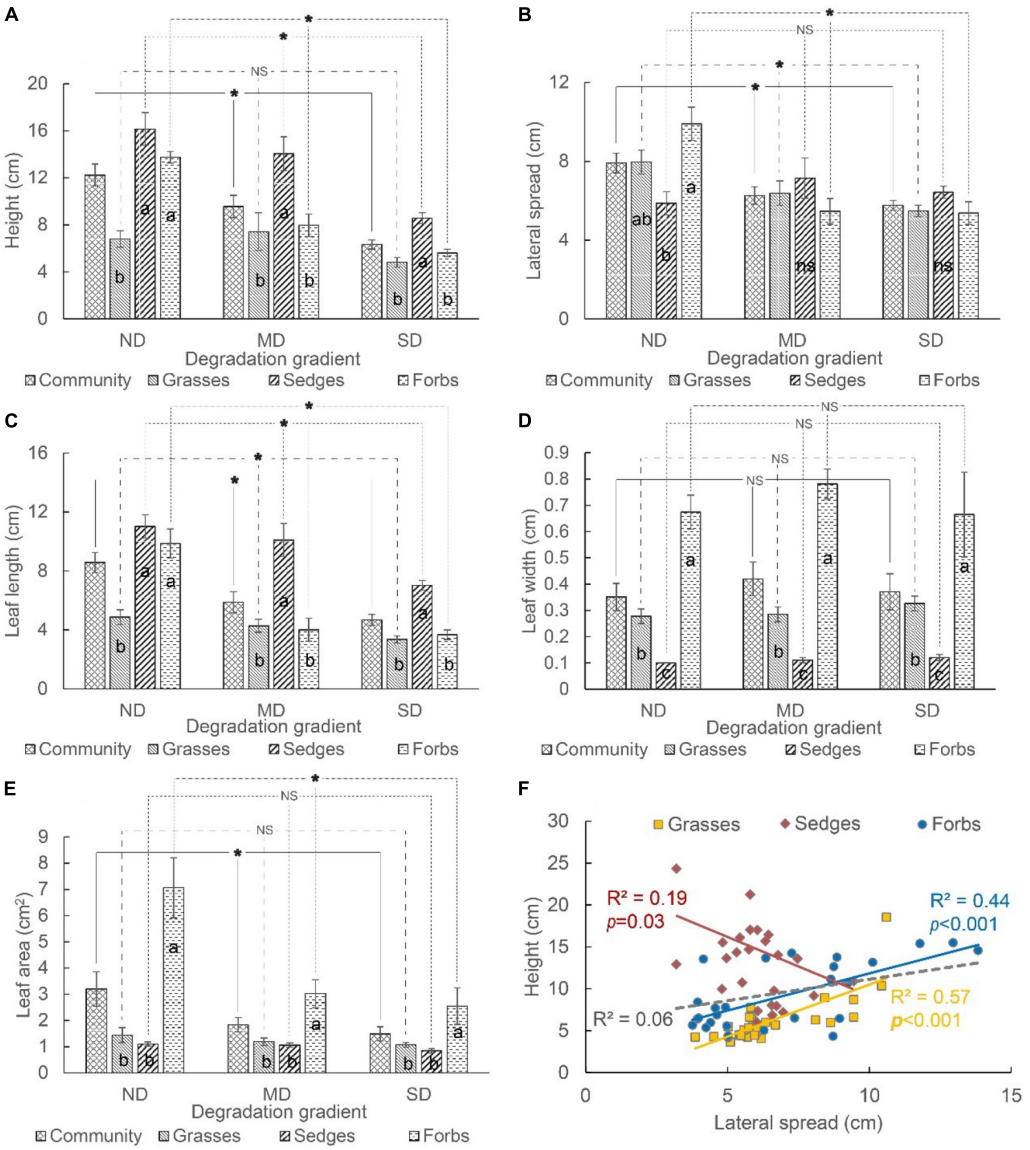

FIGURE 4 | The **(A)** height, **(B)** lateral spread, **(C)** leaf length, **(D)** leaf width, and **(E)** leaf area of different functional groups (i.e., grasses, sedges, and forbs) in different degradation gradients. The relationship between plant height and lateral spread varied among different functional groups **(F)**. The "*" means a significant difference between functional groups among degradation gradients. The different lowercase letters mean significant differences between functional groups in each degradation gradient. "NS" and "ns" mean no differences.

The lateral spread did not differ among grasses, sedges, and forbs in MD and SD (**Figure 4B**). The order of leaf width was forbs > grasses > sedges in ND, MD, and SD (**Figure 4D**). The leaf area of forbs was higher than that of grasses and sedges. The leaf area of grasses and sedges did not vary significantly in each degradation level (**Figure 4E**).

A non-significant correlation between the lateral spread and height was tested at the community level. It was a positive correlation between these two indicators for grasses and forbs, while it was a negative correlation for sedges (**Figure 4F**).

The root competition (i.e., the percentage of root biomass in the gross root biomass of a functional group) of grasses, sedges, and forbs was similar in ND and SD. In MD, the root competition was ordered as forbs > grasses > sedges (**Figure 5**). The root competition of grasses did not vary among degradation levels, while the root competition of sedges was the lowest and the root competition of forbs was the highest in MD (**Figure 5**).

Linkages Among Aboveground Traits, Root Competition, and Biomass Allocation

The effects of aboveground traits and root competition on the R/S ratio varied among different degradation levels. In ND plots, plant height and root competition positively affected the R/S ratio, while the lateral spread negatively affected the R/S ratio in

a direct path. The leaf area weakly affected the R/S ratio through the lateral spread and root competition (**Figure 6A** and **Table 3**). In MD plots, the R/S ratio was positively affected by the lateral spread, leaf area, and root completion in a direct path. The plant height affected the R/S ratio through the lateral spread (**Figure 6B** and **Table 3**). In SD plots, the R/S ratio was positively affected by plant height in a direct path. The direct effects of lateral spread, leaf area, and root competition on the R/S ratio were weak (**Figure 6C** and **Table 3**).

DISCUSSION

Generally, a considerable fraction of plant biomass distributes in belowground in grassland ecosystems (Jackson et al., 1997; Peng et al., 2020). It is always a positive relationship between the root and shoot biomass (Mokany et al., 2006; Chen et al., 2019). We got the same result at both the community and functional group levels in this study.

The R/S ratio is strongly affected by the root and shoot biomass. The plant root is the fundamental structure for plants to uptake water and nutrients and plays an important role in carbon sink in grassland ecosystems (Jackson et al., 1997; Pausch and Kuzyakov, 2018). However, the root biomass is hard to be evaluated accurately (Ma et al., 2021). The quadrat-scale sampling (usually 1 m × 1 m) for shoot biomass and the soil core-scale sampling (usually with a diameter of 5–10 cm) for root biomass were always used in field surveys to investigate the shoot and root biomass in grassland ecosystems (Yang et al., 2010). This asynchronous sampling, i.e., the different locations of the shoot biomass and root biomass, might cause significant effects on the R/S ratio calculation. Meanwhile, it is inaccurate to select the live root from soil cores according to its properties (such as color and attached fine roots), which might misestimate the R/S ratio as well. In this study, the integrated shoot and root sampling method was used, which could improve the accuracy of the estimation of the R/S ratio. Based on these matched biomass data, we found that it was hard to directly predict the R/S ratio according to the shoot biomass or root biomass.

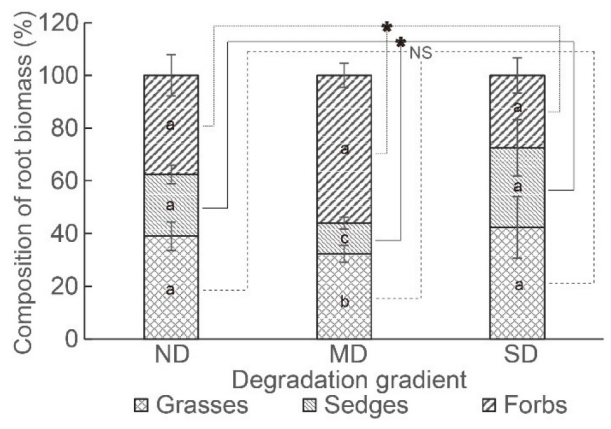

FIGURE 5 | The root competition in different degradation gradients. The "*" means a significant difference among degradation gradients. Different lowercase letters mean significant differences between functional groups in each degradation gradient.

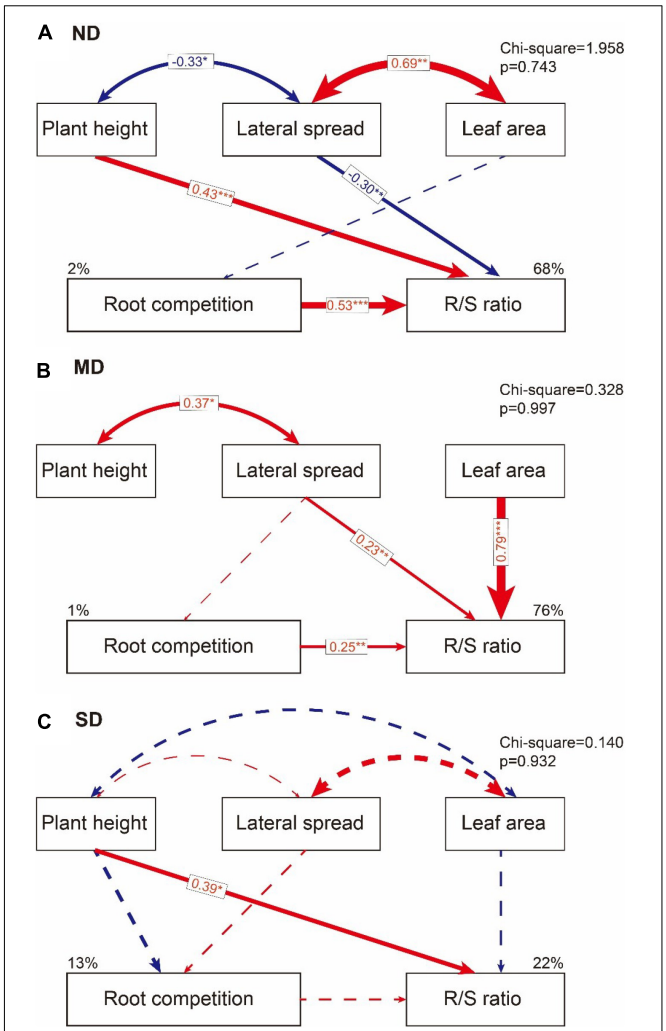

FIGURE 6 | The direct and indirect effects of plant height, lateral spread, and leaf area on root competition and R/S ratio in **(A)** no obvious degradation (ND) plots, **(B)** moderate degradation (MD) plots, and **(C)** severe degradation (SD) plots. The blue line means negative effects and the red line means positive effects. The solid line means significant path (*$p < 0.1$; **$p < 0.05$; ***$p < 0.01$). The dashed line means a non-significant path that helped to improve model quality.

Plants should invest more energy to uptake nutrients and water from the soil to adapt to harsh habitats (Dai et al., 2020). Consequently, the R/S ratio tends to be high (always >1) in some biomes (e.g., tundra and grassland) distributed in cold and dry habitats (Jackson et al., 1996; Poorter et al., 2012). In this study, we found that the R/S ratio of all meadow plants is >2 at both community level and functional group level under the land degradation conditions. Furthermore, the R/S ratio of plant community did not vary among degradation gradients because the shoot biomass decreased but the root biomass did not change along the

TABLE 3 | Standardized total effects of plant height, lateral spread, leaf area, and root competition on R/S ratio in different degradation gradients in an alpine meadow in the eastern Qinghai-Tibetan Plateau.

Treatment		Height	Lateral spread	Leaf area	Root competition
ND	Root competition	/	0.44	−0.14	/
	R/S ratio	0.43	−0.30	−0.08	0.53
MD	Root competition	/	0.11	/	/
	R/S ratio	/	0.26	0.79	0.25
SD	Root competition	−0.33	0.18	/	/
	R/S ratio	0.33	0.03	−0.21	0.19

degradation gradient. This phenomenon was consistent with findings obtained by other studies (Zhang et al., 2019). Root competition would decrease if soil nutrient levels increased (Casper and Jackson, 1997). Contrarily, grassland degradation, which always decreases soil nutrients (Liu et al., 2020), would improve soil nutrient limitation and might increase root competition. Therefore, the little change of root biomass in the present study might be obligated to the intensification of root competition.

At the functional group level, we found that the root biomass of grasses, sedges, and forbs did not vary in ND and SD, but it was ordered as forbs > grasses > sedges in MD. This phenomenon could be explained by the moderate interference theory. The R/S ratio of grasses and forbs did not change; however, the R/S ratio of sedges increased along the degradation gradients. This result revealed that the change in the R/S ratio caused by land degradation might be considered more at the functional group level rather than the community level in alpine meadow ecosystems.

The factors that affect the R/S ratio are widely discussed (Yang et al., 2018). Some evidence suggests that root interactions could affect the allocation pattern of plant biomass (Poorter et al., 2012). Especially, from the competition view, it suggests that root competition is always more important than shoot competition in affecting the performance of plant survival (Donald, 1958; Wilson, 1988). In this study, we found that the effects of root competition on the R/S ratio were always positive and linearly decreased along the degradation gradients. The total effects of shoot competition (including vertical and horizontal competition) on the R/S ratio were positive but showed a non-linear decrease along the degradation gradients because the vertical competition (presented by the plant height) and horizontal competition (presented by lateral spread and leaf area) played different roles in regulating the R/S ratio at different degradation conditions. When the meadow was healthy (e.g., ND in this study) or severely degraded (e.g., SD in this study), the vertical and horizontal competition played opposite roles, i.e., the vertical competition promoted the R/S ratio, while the horizontal competition reduced it. However, when it was a moderate degradation (e.g., MD in this study), the horizontal competition promoted the R/S ratio, but the vertical competition did not affect it. These results suggested that the first hypothesis of this study was denied, while the second hypothesis was confirmed.

In addition to biotic factors, climatic conditions could strongly affect the R/S ratio of plants, e.g., the cold and dry conditions tended to a high R/S ratio (Reich et al., 2014; Ma et al., 2021). But the R/S ratio is hard to be estimated by climatic indicators (e.g., temperature and precipitation) (Yang et al., 2010). Therefore, the indirect-observed R/S ratio inferred according to climatic indicators, which may occur in large-scale studies, should be cautiously used.

CONCLUSION

The root competition promoted the R/S ratio, and this process linearly decreased with land degradation gradients. The shoot competition promoted the R/S ratio as well, but the effects of shoot competition on the R/S ratio showed a non-linear decrease along the degradation gradients because the vertical and horizontal competition always played opposite roles in affecting the R/S ratio. These results indicate that plant competition might be a critical factor to explain why degraded alpine ecosystem has a high R/S ratio.

DATA AVAILABILITY STATEMENT

The original contributions presented in the study are included in the article/**Supplementary Material**, further inquiries can be directed to the corresponding author.

AUTHOR CONTRIBUTIONS

YZ designed the experiment. QZ, YM, KL, HY, KW, and XW conducted the field survey and laboratorial works. YZ, XG, and XH wrote the manuscript, the other co-authors discussed and improved the manuscript. All authors contributed to the article and approved the submitted version.

FUNDING

This research was supported by grants from the Second Tibetan Plateau Scientific Expedition and Research (2019QZKK0307), National Natural Science Foundation of China (31901394), and Biodiversity Survey, Monitoring and Assessment (2019HB2096001006).

ACKNOWLEDGMENTS

The authors thank the reviewers and editor for their time and effort.

SUPPLEMENTARY MATERIAL

The Supplementary Material for this article can be found online at: https://www.frontiersin.org/articles/10.3389/fpls.2022.822594/full#supplementary-material

REFERENCES

Agathokleous, E., Belz, R. G., Kitao, M., Koike, T., and Calabrese, E. J. (2018). Does the root to shoot ratio show a hormetic response to stress? An ecological and environmental perspective. *J. Forestry Res.* 30, 1569–1580.

Alon, M., Sternberg, M., and Overbeck, G. (2019). Effects of extreme drought on primary production, species composition and species diversity of a Mediterranean annual plant community. *J. Veg. Sci.* 30, 1045–1061. doi: 10.1111/jvs.12807

Bonser, S. P., and Reader, R. J. (1995). Plant competition and herbivory in relation to vegetation biomass. *Ecology* 76, 2176–2183. doi: 10.2307/1941691

Cao, J. J., Adamowski, J. F., Deo, R. C., Xu, X. Y., Gong, Y. F., and Feng, Q. (2019). Grassland degradation on the Qinghai–Tibetan Plateau: reevaluation of causative factors. *Rangeland Ecol. Manag.* 72, 988–995. doi: 10.1016/j.rama.2019.06.001

Casper, B. B., and Jackson, R. B. (1997). Plant competition underground. *Annu. Rev. Ecol. Syst.* 28, 545–570. doi: 10.1146/annurev.ecolsys.28.1.545

Chen, F., Xia, H., and Qin, X. J. (2019). Effect of mixture sowing on biomass allocation in the artificially–planted pastures, Southeastern Tibetan. *J. Mt. Sci.* 16, 54–63. doi: 10.1007/s11629-018-5062-7

Dai, L. C., Guo, X. W., Ke, X., Lan, Y. T., Zhang, F. W., Li, Y. K., et al. (2020). Biomass allocation and productivity–richness relationship across four grassland types at the Qinghai Plateau. *Ecol. Evol.* 10, 506–516. doi: 10.1002/ece3.5920

Donald, C. M. (1958). The interaction of competition for light and for nutrients. *Aust. J. Agric. Res.* 9, 421–435. doi: 10.1071/ar9580421

Dong, S. K., Shang, Z. H., Gao, J. X., and Boone, R. B. (2020). Enhancing sustainability of grassland ecosystems through ecological restoration and grazing management in an era of climate change on Qinghai–Tibetan Plateau. *Agric. Ecosyst. Environ.* 287:106684. doi: 10.1016/j.agee.2019.106684

Dubois, O. (2011). *The State of the World's Land and Water Resources for Food and Agriculture: Managing Systems at Risk*. London: Earthscan.

Gao, X. X., Dong, S. K., Xu, Y. D., Fry, E. L., Li, Y., Li, S., et al. (2021). Plant biomass allocation and driving factors of grassland revegetation in a Qinghai-Tibetan Plateau chronosequence. *Land Degrad. Dev.* 32, 1732–1741. doi: 10.1002/ldr.3819

Hao, Y. Q., and He, Z. W. (2019). Effects of grazing patterns on grassland biomass and soil environments in China: a meta–analysis. *PLoS One* 14:e0215223. doi: 10.1371/journal.pone.0215223

Herben, T., Krahulec, F., Hadincova, V., Pechackova, S., and Wildova, R. (2003). Year–to–year variation in plant competition in a mountain grassland. *J. Ecol.* 91, 103–113. doi: 10.2307/3599541

Huang, X. X., Sheng, Z. L., Zhang, Y., Ding, J., and He, K. J. (2015). Impacts of trails on plants, soil and their interactions in the subalpine meadows of Mount Jade Dragon, Northwestern Yunnan of China. *Grassl. Sci.* 61, 204–216. doi: 10.1111/grs.12100

Jackson, R. B., Canadell, J., Ehleringer, J. R., Mooney, H. A., Sala, O. E., and Schulze, E. D. (1996). A global analysis of root distribution for terrestrial biomes. *Oecologia* 108, 389–411. doi: 10.1007/BF00333714

Jackson, R. B., Mooney, H. A., and Schulze, E. D. (1997). A global budget for fine root biomass, surface area, and nutrient contents. *Proc. Natl. Acad. Sci. U.S.A.* 94, 7362–7366. doi: 10.1073/pnas.94.14.7362

Lehnert, L. W., Wesche, K., Trachte, K., Reudenbach, C., and Bendix, J. (2016). Climate variability rather than overstocking causes recent large scale cover changes of Tibetan pastures. *Sci. Rep.* 6:24367. doi: 10.1038/srep24367

Liu, X., Wang, Z. Q., Zheng, K., Han, C. L., Li, L. H., Sheng, H. Y., et al. (2020). Changes in soil carbon and nitrogen stocks following degradation of alpine grasslands on the Qinghai–Tibetan Plateau: a meta–analysis. *Land Degrad. Dev.* 32, 1262–1273. doi: 10.1002/ldr.3796

López–Mársico, L., Altesor, A., Oyarzabal, M., Baldassini, P., and Paruelo, J. M. (2015). Grazing increases below–ground biomass and net primary production in a temperate grassland. *Plant Soil* 392, 155–162. doi: 10.1007/s11104-015-2452-2

Luo, J. F., Ma, L., Li, G. J., Deng, D. Z., Chen, D. C., Zhang, L., et al. (2020). The effects of land degradation on plant community assembly: implications for the restoration of the Tibetan Plateau. *Land Degrad. Dev.* 31, 2819–2829. doi: 10.1002/ldr.3613

Ma, H. Z., Mo, L. D., Crowther, T. W., Maynard, D. S., van den Hoogen, J., Stocker, B. D., et al. (2021). The global distribution and environmental drivers of aboveground versus belowground plant biomass. *Nat. Ecol. Evol.* 5, 1110–1122. doi: 10.1038/s41559-021-01485-1

McNaughton, S. J., Banyikwa, F. F., and McNaughton, M. M. (1998). Root biomass and productivity in a grazing ecosystem: the Serengeti. *Ecology* 79, 587–592. doi: 10.1890/0012-9658(1998)079[0587:rbapia]2.0.co;2

Mokany, K., Raison, R. J., and Prokushkin, A. S. (2006). Critical analysis of root: shoot ratios in terrestrial biomes. *Glob. Change Biol.* 12, 84–96. doi: 10.1890/04-1724

Nötzold, R., Blossey, B., and Newton, E. (1997). The influence of below ground herbivory and plant competition on growth and biomass allocation of purple loosestrife. *Oecologia* 113, 82–93. doi: 10.1007/s004420050356

Pausch, J., and Kuzyakov, Y. (2018). Carbon input by roots into the soil: quantification of rhizodeposition from root to ecosystem scale. *Glob. Change Biol.* 24, 1–12. doi: 10.1111/gcb.13850

Peng, F., Xue, X., You, Q. G., Sun, J., Zhou, J., Wang, T., et al. (2020). Change in the trade-off between aboveground and belowground biomass of alpine grassland: implications for the land degradation process. *Land Degrad. Dev.* 31, 105–117. doi: 10.1002/ldr.3432

Poeplau, C. (2016). Estimating root: shoot ratio and soil carbon inputs in temperate grasslands with the RothC model. *Plant Soil* 407, 293–305. doi: 10.1007/s11104-016-3017-8

Poorter, H., Niklas, K. J., Reich, P. B., Oleksyn, J., Poot, P., and Mommer, L. (2012). Biomass allocation to leaves, stems and roots: meta–analyses of interspecific variation and environmental control. *New Phytol.* 193, 30–50. doi: 10.1111/j.1469-8137.2011.03952.x

Pugnaire, F. I., and Luque, M. T. (2001). Changes in plant interactions along a gradient of environmental stress. *OIKOS* 93, 42–49. doi: 10.1034/j.1600-0706.2001.930104.x

Reich, P. B., Luo, Y., Bradford, J. B., Poorter, H., Perry, C. H., and Oleksyn, J. (2014). Temperature drives global patterns in forest biomass distribution in leaves, stems, and roots. *Proc. Natl. Acad. Sci. U.S.A.* 111, 13721–13726. doi: 10.1073/pnas.1216053111

Schofield, E. J., Rowntree, J. K., Paterson, E., Brewer, M. J., Price, E. A. C., Brearley, F. Q., et al. (2019). Cultivar differences and impact of plant–plant competition on temporal patterns of nitrogen and biomass accumulation. *Front. Plant Sci.* 10:215. doi: 10.3389/fpls.2019.00215

Scurlock, J. M. O., and Hall, D. O. (2002). The global carbon sink: a grassland perspective. *Glob. Change Biol.* 4, 229–233. doi: 10.1046/j.1365-2486.1998.00151.x

Tang, L., Dong, S. K., Sherman, R., Liu, S. L., Liu, Q. R., Wang, X. X., et al. (2015). Changes in vegetation composition and plant diversity with rangeland degradation in the alpine region of Qinghai–Tibet Plateau. *Rangeland J.* 37, 107–115. doi: 10.1071/RJ14077

Tilman, D. (2020). *Resource Competition and Community Structure. (MPB-17)*, Vol. 17. Princeton, NJ: Princeton University Press, doi: 10.1515/9780691209654

Tilman, D., Reich, P. B., and Knops, J. M. (2006). Biodiversity and ecosystem stability in a decade–long grassland experiment. *Nature* 441, 629–632. doi: 10.1038/nature04742

Wang, X. X., Dong, S. K., Yang, B., Li, Y. Y., and Su, X. K. (2014). The effects of grassland degradation on plant diversity, primary productivity, and soil fertility in the alpine region of Asia's headwaters. *Environ. Monit. Assess.* 186, 6903–6917. doi: 10.1007/s10661-014-3898-z

Wang, Y. B., Meng, B., Zhong, S. Z., Wang, D. L., Ma, J. Y., and Sun, W. (2018). Aboveground biomass and root/shoot ratio regulated drought susceptibility of ecosystem carbon exchange in a meadow steppe. *Plant Soil* 432, 259–272. doi: 10.1007/s11104-018-3790-7

Wilson, C. H., Strickland, M. S., Hutchings, J. A., Bianchi, T. S., and Flory, S. L. (2018). Grazing enhances belowground carbon allocation, microbial biomass, and soil carbon in a subtropical

grassland. *Glob. Change Biol.* 24, 2997–3009. doi: 10.1111/gcb.14070

Wilson, J. B. (1988). Shoot competition and root competition. *J. Appl. Ecol.* 25, 279–296. doi: 10.2307/2403626

Yang, Y. H., Fang, J. Y., Ma, W. H., Guo, D. L., and Mohammat, A. (2010). Large–scale pattern of biomass partitioning across China's grasslands. *Glob. Ecol. Biogeogr.* 19, 268–277. doi: 10.1111/j.1466-8238.2009.00502.x

Yang, Y., Dou, Y. X., An, S. S., and Zhu, Z. L. (2018). Abiotic and biotic factors modulate plant biomass and root/shoot (R/S) ratio in grassland on the Loess Plateau, China. *Sci. Total Environ.* 636, 621–631. doi: 10.1016/j.scitotenv.2018.04.260

Zhang, W. J., Xue, X., Peng, F., You, Q. G., and Hao, A. H. (2019). Meta–analysis of the effects of grassland degradation on plant and soil properties in the alpine meadows of the Qinghai–Tibetan Plateau. *Glob. Ecol. Conserv.* 20:e00774. doi: 10.1016/j.gecco.2019.e00774

Conflict of Interest: The authors declare that the research was conducted in the absence of any commercial or financial relationships that could be construed as a potential conflict of interest.

Publisher's Note: All claims expressed in this article are solely those of the authors and do not necessarily represent those of their affiliated organizations, or those of the publisher, the editors and the reviewers. Any product that may be evaluated in this article, or claim that may be made by its manufacturer, is not guaranteed or endorsed by the publisher.

Copyright © 2022 Zhang, Zheng, Gao, Ma, Liang, Yue, Huang, Wu and Wang. This is an open-access article distributed under the terms of the Creative Commons Attribution License (CC BY). The use, distribution or reproduction in other forums is permitted, provided the original author(s) and the copyright owner(s) are credited and that the original publication in this journal is cited, in accordance with accepted academic practice. No use, distribution or reproduction is permitted which does not comply with these terms.

frontiers in Plant Science

ORIGINAL RESEARCH
published: 04 February 2022
doi: 10.3389/fpls.2022.822268

Effects of Soil Physico-Chemical Properties on Plant Species Diversity Along an Elevation Gradient Over Alpine Grassland on the Qinghai-Tibetan Plateau, China

*Wangya Han[1,2], Li Chen[2,3], Xukun Su[2,4], Dan Liu[5], Tiantian Jin[6], Songlin Shi[7], Tao Li[2,4] and Guohua Liu[2,4]**

[1] Jiangsu Key Laboratory of Agricultural Meteorology, Institute of Ecology, School of Applied Meteorology, Nanjing University of Information Science and Technology, Nanjing, China, [2] State Key Laboratory of Urban and Regional Ecology, Research Center for Eco-Environmental Sciences, Chinese Academy of Sciences, Beijing, China, [3] Torch High Technology Industry Development Center, Ministry of Science and Technology, Beijing, China, [4] College of Resources and Environment, University of Chinese Academy of Sciences, Beijing, China, [5] Institute of Qinghai-Tibetan Plateau, Southwest Minzu University, Chengdu, China, [6] China Institute of Water Resources and Hydropower Research, Beijing, China, [7] College of Tourism and Urban-Rural Planning, Chengdu University of Technology, Chengdu, China

OPEN ACCESS

Edited by:
Jian Sun,
Institute of Tibetan Plateau Research, Chinese Academy of Sciences (CAS), China

Reviewed by:
Xiaotao Huang,
Northwest Institute of Plateau Biology, Chinese Academy of Sciences (CAS), China
Jingxue Zhao,
Lanzhou University, China
Xu Manhou,
Taiyuan Normal University, China

***Correspondence:**
Guohua Liu
ghliu@rcees.ac.cn

Specialty section:
This article was submitted to Functional Plant Ecology, a section of the journal Frontiers in Plant Science

Received: 25 November 2021
Accepted: 04 January 2022
Published: 04 February 2022

Citation:
Han W, Chen L, Su X, Liu D, Jin T, Shi S, Li T and Liu G (2022) Effects of Soil Physico-Chemical Properties on Plant Species Diversity Along an Elevation Gradient Over Alpine Grassland on the Qinghai-Tibetan Plateau, China. Front. Plant Sci. 13:822268. doi: 10.3389/fpls.2022.822268

Elevation gradient can reflect the effects of soil physico-chemical properties on plant species diversity. Alpine grassland on the QTP has suffered from a serious decline in plant species diversity. In this study, we investigated 112 sites recording plant community characteristics and collecting soil samples along an elevation gradient (3,500–5,200 m asl) in alpine meadow on the QTP. We analyzed the effects of soil physico-chemical properties on plant species composition and diversity by canonical ordination and spatial regression along an elevation gradient. The results showed that species richness of the overall plant communities decreased with the increasing elevation, and the Simpson dissimilarity index (β_{sim}) had a maximum at low elevation (3,500–4,000 m) with the value of 0.37. Soil available nitrogen content was the primary soil parameter affecting plant species composition and diversity in alpine grassland. The effect of soil available nitrogen content on plant species richness varied at different elevations. For Gramineae plants (G), plant species richness declined with the increase in soil available nitrogen content at low elevation (3,500–4,000 m), but rose at middle elevation (4,000–4,500 m). Soil available nitrogen content had a more significant limiting effect on species richness at high elevation (>4,500 m). These findings increase our understanding about the drivers of plant species diversity changes in alpine grassland on the QTP, and will provide insights into grassland restoration and sustainable management.

Keywords: alpine grassland, plant community, species diversity, soil physico-chemical properties, elevation gradient

INTRODUCTION

Plant species diversity is the crucial factor that has important impact on plant community structure and types, focusing on species coexistence in alpine grassland ecosystem (Xu et al., 2011; Dong et al., 2019). The study of plant species diversity is the basis for evaluating ecosystem functions (Wang et al., 2012). There has been a strong relationship between plant species diversity and key ecosystem functions including plant production and soil organic matters (Hooper et al., 2012; Zhu et al., 2020). It has been reported that soil physico-chemical properties lead to changes in plant species diversity. The relationship between plant diversity and soil physico-chemical properties is vulnerable to ecological contexts (Grace et al., 2016; Zhu et al., 2020), therefore, it is imperative to evaluate the effect of soil physico-chemical properties on plant species diversity along environmental gradients.

Some studies have documented that plant species diversity is affected by environmental parameters, such as temperature, humidity, solar radiation, and soil nutrients (Dong et al., 2019). Most studies address temperature as the dominant factor of species diversity (Barbarossa et al., 2021; Lai et al., 2021). A series of studies have analyzed the relationship between plant species diversity and environmental parameters. The relationships between plant species diversity and soil physico-chemical properties have been analyzed in terms of topographic parameters (Li X. et al., 2018), such as geological structure and lithology (Do Carmo and Jacobi, 2016; Hanaka et al., 2019). Natural gradient studies have been conducted to explore the mechanisms of species diversity changes, and elevation gradient is one of the important research contents because elevation affects the distribution of moisture and energy (Li X. et al., 2018). In addition, the elevation gradient plays an important role in exploring how species diversity affected by environmental parameters (Supriya et al., 2019; Lai et al., 2021). Although a variety of elevational species diversity patterns have been detected, few studies have considered the responses of species diversity to environmental variation among different plant community types, analyzing the community dissimilarity along the elevation gradient. The community dissimilarity can be quantified by β-diversity (Haider et al., 2018), so the diversity variation should be carried out combining both α-diversity and β-diversity of plant communities.

The QTP has complex topographic features with contiguous mountains and hills. As the highest and most extensive highland in the world, QTP has extensive species diversification and alpine endemic species (Yu et al., 2019). Moreover, the warming rate on the QTP has been almost twice that of general global warming over recent decades (Kuang and Jiao, 2016; Guo et al., 2018). Due to spatially complex topography configurations and climate changes, the QTP has suffered from serious decline of species diversity (Li et al., 2019). Alpine meadow is the main ecosystem on the QTP (Liu et al., 2018), accounting for approximately 35% of the total plateau area (Xu et al., 2011). It has important ecological and socio-economic roles, such as storing carbon, altering biodiversity by evolving grass species that shape environments (Gieselman et al., 2013; Dong et al., 2019). The species diversity of alpine meadow on the QTP has attracted the attention of numerous researchers (Ebersbach et al., 2017; Yu et al., 2019). However, the responses of species diversity to soil physico-chemical properties distinguishing between different community types along an elevation gradient were rarely conducted.

In this study, we focused on the relationship between plant species diversity and soil physico-chemical properties. We explored the effect of soil physico-chemical properties on α and β diversity of plant species along an elevation gradient, providing information for restoration and sustainable development of alpine meadow. The specific objectives were to (1) identify changes of plant species diversity and soil physico-chemical properties along the elevation gradient; (2) clarify which soil physico-chemical properties affect plant species composition and diversity, and (3) elucidate the effects of key soil parameters on species diversity at different elevations.

MATERIALS AND METHODS

Study Area

The study area is located in the mid-eastern part of the QTP (89°30′∼104° 20′ E, 28° 35′∼36° 24′ N) (**Figure 1**), and includes Naqu, Jiali, Changdu, Basu, and Baqing Counties in the Tibetan autonomous prefecture, Qumalai, Zhiduo, Zaduo, and Nangqian Counties in Qinghai Province, and Ruoergai, Aba, Ganzi, and Hongyuan Counties in Sichuan Province. It covers an area of 5.3×10^5 km^2 and accounts for nearly 25% of the QTP. The elevation ranges from 3,500 to 5,200 m above sea level, with geographical characteristics of mountains and valley plains. The study area is in the temperate semi-arid monsoon climate zone. In the past 35 years (1980–2015), the mean annual temperature ranges from −9.5°C to 11.4°C, and the multi-year average precipitation is from 152 to 1,218 mm. The vegetation type is mainly alpine meadow. The soil types are mainly felt soil, meadow soil, and frigid calcic soil, followed by dark felt soil, permafrost soil, and dark brown soil (Chinese Soil Taxonomy Research Group, 1995).

Sampling Design

The plant community was sampled during the growing season between July and August, 2017 and 2018. We selected 112 field sites [low elevation (3,500–4,000 m): 45, middle elevation (4,000–4,500 m): 38, high elevation (>4,500 m): 29] with representative alpine meadow in space-for-time substitution (Niu et al., 2019), ranging from 3,500 to 5,200 m. These sites were under similar site condition, with the middle slope position and slope degree ranging from 12° to 18°. The grazing intensity is moderate grazing, according to the classification of grazing intensity from Sun et al. (2019). They contained natural vegetation and were homogeneous sites within the study area (**Figure 1**). Each site covered an area of 900 m^2 (30 m × 30 m). We established five 1 m × 1 m quadrats, which were placed at the four corners and at the center of the site. Within each quadrat, we measured the cover, height, and density of every vascular plant species, and we recorded latitude, longitude, elevation, and topographic slope

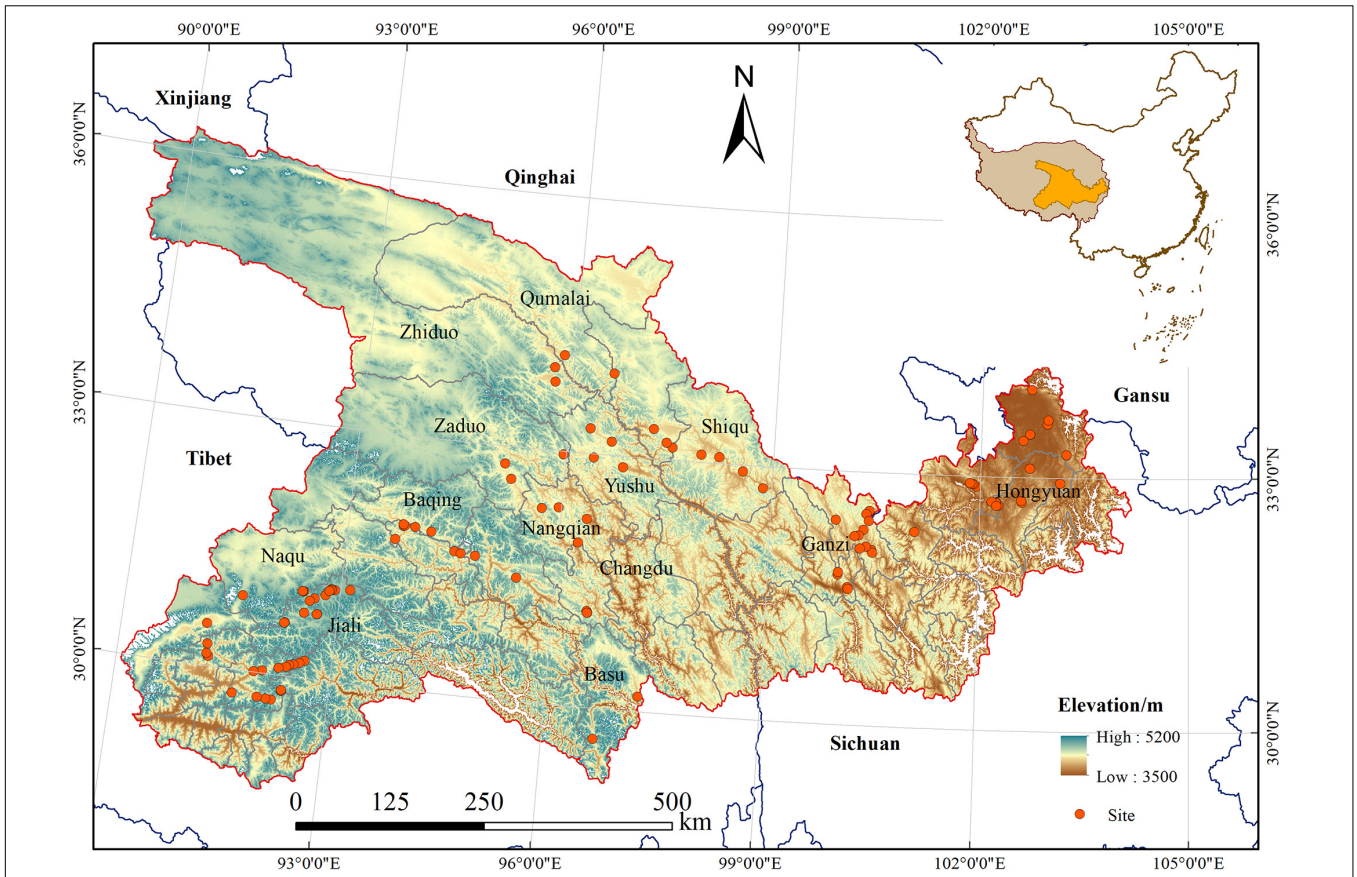

FIGURE 1 | Location of the study area.

using a handheld global positioning system (GPS) device. Five soil samples were collected at a depth of 0–20 cm in each quadrat.

Data Collection and *Analysis*

Vegetation Data Collection

We recorded the coverage of all plants as the fractional vegetation cover, and the species names and abundance of each vascular plant species. The height of each species was evaluated by randomly measuring five individual plants (Han W. Y. et al., 2019). We also recorded the coverage and frequency of each species in each quadrat. The nomenclature follows Flora of China[1]. The importance values (IVs) of the species were calculated as follows (Li C. et al., 2018):

$$P_i = \left(\frac{C_i}{\sum_i^S C_i} + \frac{H_i}{\sum_i^S H_i} + \frac{F_i}{\sum_i^S F_i} \right) \Big/ 3 \times 100$$

where P_i is the importance value (IVs) of species i; C_i is the coverage of species i; H_i is the height of species i; and F_i is the frequency of species i.

We used α diversity and β diversity to describe species diversity. The α diversity indices used were the species richness index (R), the Shannon-Wiener index (H'), and Pielou's evenness index (J). For β diversity, the Sørenson's dissimilarity index (β_{sor}) was used to measure the overall diversity based on presence-absence species data and represented diversity among communities, and β_{sor} was partitioned into the Simpson dissimilarity index (β_{sim}) and the nestedness resultant dissimilarity index (β_{sne}). The diversity indices were calculated as follows (Wu and Ding, 2020; Lai et al., 2021):

$$R = S$$

$$H' = -\sum_{i=1}^{s} (P_i lnP_i)$$

$$J = -\sum_{i=1}^{s} (P_i lnP_i) / lnS$$

$$\beta_{sor} = \frac{a+b}{2t+a+b}$$

$$\beta_{sim} = \frac{min(a,b)}{a+min(a,b)}$$

$$\beta_{nes} = \beta_{sor} - \beta_{sim}$$

[1] foc.iplant.cn

where S is the number of species in the plot; t is the number of species shared by two communities or plots; a and b represent the total number of species in two communities or plots, respectively.

Soil Physico-Chemistry Analysis

Soil samples were collected at a depth of 0–20 cm from the surface in each field quadrat. A total of five soil samples were collected from each quadrat and the soil parameters were the average of the five samples. The soil samples were air-dried and sieved, and the soil moisture content and soil bulk density were determined by the oven drying method according to Thomasson (2010). Soil pH was measured using a pH meter and a 1:1 water/soil suspension, and soil total carbon content and soil total nitrogen content were measured using the flash dynamic combustion method and a gas chromatographic separation and thermal conductivity detection system (vario EL cube Elementar, Germany), respectively (Feng et al., 2017). Soil organic carbon content was determined by the dichromate oxidation method and soil available nitrogen content was measured by the alkali-hydrolysis reduction diffusion method (Bao, 2000). Soil available phosphorus content was extracted using the ammonium bicarbonate method and soil available potassium content was extracted using the acetamide extraction method (Zhang et al., 2018).

Climate and Topography Data

The climate parameters were interpolated into climate surface data using thin plate smoothing splines method by the ANUSPLIN software package (version 4.4) (Hutchinson and Xu, 2013; Xu and Hutchinson, 2013). The output statistics are interpreted with the partial spline model for N ($N = 135$) observed data values z_i given by,

$$z_i = f(x_i) + b^T y_i + e_i \quad (i = 1, ..., N)$$

where each x_i (temperature and precipitation data) is a d-dimensional vector of spline independent variables, f is an unknown smooth function of the x_i, each y_i is a p-dimensional vector of coefficients of the y_i (elevation data) and each e_i is an independent (Hutchinson and Xu, 2013). The temperature and precipitation data were derived from the national weather stations data for 1982–2015 (freely available at the website: http://data.cma.cn/site). The elevation data was derived from digital elevation models at a 1 km resolution and were obtained by resampling the data from CGIAR-CSI (freely available at the website: http://srtm.csi.cgiar.org).

Statistical Analysis

We used the *vegan*, *betapart*, and *cluster* packages in R version 3.5.0 to analyze species composition and diversity in the different communities. The plant communities were classified by hierarchical clustering using Ward's method and the Bray-Curtis distance. We used non-metric multidimensional scaling (NMDS) analysis to show the species cluster characteristics of the different plant communities.

Statistical analyses of soil parameters were performed using SPSS Statistics software (version 20). One-way analysis of variance (ANOVA) was used to compare significant differences among the soil physico-chemical properties of the different plant communities. A paired significance analysis was undertaken using the Scheffé test when the variation was significant ($p < 0.05$). The correlations between species diversity (species richness, Shannon-Wiener index, and evenness) and soil physico-chemical properties were calculated using Pearson's correlation coefficient by the function cor and psych package in R version 3.5.0. Stepwise multiple linear regression was used to screen the variables affecting species richness. The vegan package in R version 3.5.0 was used to perform a canonical correspondence analysis (CCA) to further confirm the relationships between species data and soil parameters in the different plant communities. A Mantel test (999 permutations) was used to test the significance of the relationships and the linear model (LM) was used to explore the significant relationship between species richness and its primary factor. The partial correlation analysis was used to eliminate the interference of other soil parameters to soil available nitrogen content.

RESULTS

Changes in Plant Species Composition and Diversity Along the Elevation Gradient

There were 369 herbaceous plant species belonging to 174 genera and 49 families. Families with larger IVs (>1) included Cyperaceae, Gramineae, Rosaceae, Compositae, Ranunculaceae, Polygonaceae, Leguminosae, Gentianaceae, Scrophulariaceae, Euphorbiaceae, Labiaceae, Primulaceae, and Umbelliferae in descending order. The plant communities were classified into six clusters by the cluster analysis, which was based on Bray-Curtis distance matrices (**Supplementary Figure 1**). After combining the cluster results with ecological background information and other related studies (Antony et al., 2016; Zhang et al., 2018), the classifications were as follows: *Kobresia pygmaea* (Kp), *Kobresia pygmaea* + miscellaneous plants (KpM); *Kobresia setchwanensis* (Ks), *Carex moorcroftii* (Cm), miscellaneous plants (M); and Gramineae plants (G). The dominant species in the different plant communities were characterized by their IVs (**Table 1**).

The relative proportions of the families in six plant communities were distinct (**Figure 2**). Kp, KpM, Cm, and M were dominated by the Cyperaceae; the Cyperaceae and Compositae proportions were similar for Ks; and Gramineae (22.66%) was predominant in G. The NMDS plot (**Figure 2**) shows the species composition characteristics of the different plant communities along coordinate 1 and coordinate 2 of an elevation gradient (I, low elevation; II, middle elevation; III, high elevation). The species composition profile of Kp at high elevation was different from the other elevation classes. The species composition profiles at low and middle elevations for all community types except Ks tended to group together (**Figure 2**). The Cyperaceae proportions rose in all the community types other than Ks and G with increasing elevation gradient. For Kp and KpM, the Compositae proportions decreased as elevation increased, but the Compositae proportion in Cm obviously increased with an average growth rate of 30.44%. For M, the Gramineae proportion decreased as

TABLE 1 | The dominance of species selected by IVs across six plant community types.

Plant community types	Species names	Family	IV
Kp	*Kobresia pygmaea*	Cyperaceae	9.472
	Carex moorcroftii	Cyperaceae	3.750
	Potentilla saundersiana	Rosaceae	2.984
	Leontopodium leontopodioides	Compositae	1.823
	Stipa capillata	Gramineae	1.150
	Astragalus propinquus	Leguminosae	1.062
	Kobresia tibetica	Cyperaceae	0.833
	Kobresia setschwanensis	Cyperaceae	0.817
	Poa crymophila	Gramineae	0.780
	Taraxacum mongolicum	Compositae	0.738
	Anaphalis sinica	Compositae	0.728
	Oxytropis alpina	Leguminosae	0.702
	Polygonum macrophyllum	Polygonaceae	0.656
	Potentilla anserina	Rosaceae	0.584
	Aster himalaicus	Compositae	0.544
KpM	*Kobresia pygmaea*	Cyperaceae	3.090
	Potentilla saundersiana	Rosaceae	1.524
	Carex moorcroftii	Cyperaceae	1.022
	Leontopodium leontopodioides	Compositae	0.936
	Salix cupularis	Salicaceae	0.638
	Polygonum viviparum	Polygonaceae	0.522
Ks	*Kobresia setschwanensis*	Cyperaceae	1.607
	Potentilla saundersiana	Rosaceae	0.817
	Kobresia pygmaea	Cyperaceae	0.676
	Carex moorcroftii	Cyperaceae	0.572
	Elymus nutans	Gramineae	0.503
Cm	*Carex moorcroftii*	Cyperaceae	2.292
	Kobresia pygmaea	Cyperaceae	1.302
	Potentilla saundersiana	Rosaceae	0.780
	Polygonum viviparum	Polygonaceae	0.686
	Kobresia setschwanensis	Cyperaceae	0.660
	Leontopodium leontopodioides	Compositae	0.570
	Potentilla anserina	Rosaceae	0.542
M	*Kobresia pygmaea*	Cyperaceae	1.813
	Carex moorcroftii	Cyperaceae	1.624
	Kobresia setschwanensis	Cyperaceae	1.589
	Potentilla saundersiana	Rosaceae	1.299
	Leontopodium leontopodioides	Compositae	0.768
	Polygonum viviparum	Polygonaceae	0.670
	Kobresia tibetica	Cyperaceae	0.657
G	*Elymus nutans*	Gramineae	0.762
	Poa crymophila	Gramineae	0.530

Kp, Kobresia pygmaea; KpM, Kobresia pygmaea + Miscellaneous plants; Ks, Kobresia setchwanensis; Cm, Carex moorcroftii; M, Miscellaneous plants; G, Gramineae plants.

elevation increased and reached a minimum of 6.78% at high elevation (**Figure 2**).

The α-diversity characteristics of plant species (species richness, Shannon-Wiener index, and Pielou's evenness index) showed a certain regularity along the elevation gradient (**Table 2**). The species richness of the overall plant communities showed an obviously decreasing trend as the elevation rose, and followed the order of low elevation (35.24) > middle elevation (29.45) > high elevation (22.24) (**Figure 3A**). At low elevation, species richness in Ks was significantly higher than in Kp, KpM, Cm, M, and G. The species richness for Kp and KpM dropped gradually as the elevation increased, and species richness for Cm and M rose at first and then decreased as the elevation increased (**Figure 3B**). The Shannon-Wiener index for the overall communities showed a downward trend as elevation increased and the Pielou's evenness index reached a maximum at middle elevation. There was a difference in β-diversity of the overall plant communities along the elevation gradient, but the differences among elevation classes were not significant (**Table 3**). Simpson dissimilarity index (β_{sim}) at low elevation was 0.37, as the largest one among elevation classes. Nestedness resultant dissimilarity index (β_{sne}) continued to increase with the rise of elevation. For different community types, the highest Sørenson's dissimilarity index (β_{sor}) was between KpM and Ks with a value of 0.68, followed by the index between KpM and G (0.63) (**Supplementary Table 1**).

Variation in Soil Physical and Chemical Properties Along the Elevation Gradient

Elevation had a significant impact ($p < 0.05$) on soil physico-chemical properties, such as soil moisture content, soil pH, and soil available nitrogen content, in all the plant communities (**Table 4**). However, the soil physico-chemical properties were not significantly influenced ($p < 0.05$) by plant community type at the same elevation class. Soil moisture content for Kp was significantly greater by 1.8 times at high elevation compared to the low and middle elevations. Soil pH significantly varied ($p < 0.05$) along the elevation gradient for Kp in the order high elevation (5.53) < low elevation (5.89) < middle elevation (6.67). Soil available nitrogen content increased significantly ($p < 0.05$) from middle elevation to high elevation for KpM and Cm, and was 8.5 and 2.6 times greater at high elevation than at middle elevation for KpM and Cm, respectively. A significant ($p < 0.05$) increase in soil available nitrogen content for Kp was observed at high elevation, with an average of 246.45 mg kg^{-1} at high elevation, 56.98 mg kg^{-1} at low elevation, and 43.67 mg kg^{-1} at middle elevation. Soil available nitrogen content was significantly greater ($p < 0.05$) by six times at high elevation compared to low elevation for M (**Supplementary Figure 2**).

Soil Physico-Chemical Properties Effects on Plant Diversity

Figure 4 shows the Pearson's correlations between species diversity and soil physico-chemical properties. Species richness was significantly negatively correlated with soil available nitrogen content ($r = -0.41$, $p < 0.01$), soil bulk density ($r = -0.29$, $p < 0.01$), and soil moisture content ($r = -0.19$, $p < 0.05$). Species richness was significantly positive correlated with the Shannon-Wiener index ($r = 0.96$, $p < 0.01$), and with species evenness ($r = 0.58$, $p < 0.01$). Therefore, species richness was chosen as the species variable. A stepwise multiple linear regression was used to determine the effect of plant species

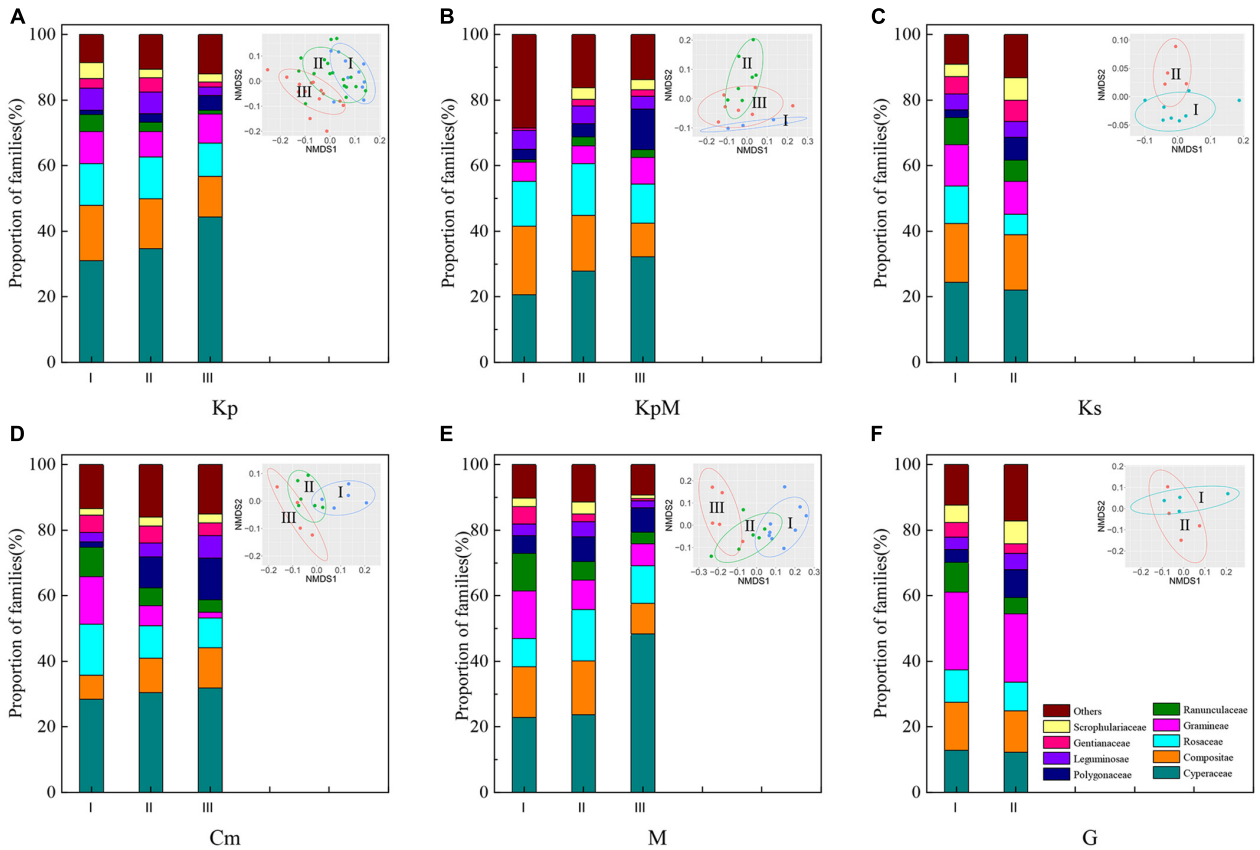

FIGURE 2 | Composition of the plant communities at the family level and non-metric multidimensional scaling analysis (NMDS) of plant composition based on the Bray-Curtis distance. **(A)** Kp, *Kobresia pygmaea*; **(B)** KpM, *Kobresia pygmaea*+ Miscellaneous plants; **(C)** Ks, *Kobresia setchwanensis*; **(D)** Cm, *Carex moorcroftii*; **(E)** M, Miscellaneous plants; **(F)** G, Gramineae plants.

TABLE 2 | Characteristics of species α-diversity at different elevation classes.

Diversity characteristics	Plant community type	Low elevation	Middle elevation	High elevation
Richness index	Kp	28.56 ± 4.83	25.50 ± 3.85	20.93 ± 3.32
	KpM	29.25 ± 5.56	26.00 ± 4.43	25.29 ± 10.72
	Ks	45.25 ± 8.20	34.25 ± 2.50	–
	Cm	32.20 ± 5.45	34.50 ± 4.65	24.50 ± 2.38
	M	35.78 ± 5.73	35.83 ± 5.22	20.80 ± 5.26
	G	40.50 ± 9.61	38.50 ± 9.95	–
Shannon-Wiener index	Kp	2.87 ± 0.34	2.71 ± 0.38	2.52 ± 0.21
	KpM	2.72 ± 0.16	2.74 ± 0.19	2.69 ± 0.36
	Ks	3.34 ± 0.31	3.09 ± 0.13	–
	Cm	2.97 ± 0.35	3.03 ± 0.31	2.75 ± 0.15
	M	3.03 ± 0.39	3.04 ± 0.57	2.53 ± 0.35
	G	3.24 ± 0.36	3.24 ± 0.27	–
Pielou's evenness index	Kp	0.87 ± 0.03	0.85 ± 0.04	0.83 ± 0.04
	KpM	0.81 ± 0.03	0.85 ± 0.03	0.85 ± 0.03
	Ks	0.88 ± 0.04	0.88 ± 0.02	–
	Cm	0.86 ± 0.02	0.86 ± 0.02	0.86 ± 0.03
	M	0.85 ± 0.04	0.87 ± 0.03	0.84 ± 0.05
	G	0.88 ± 0.04	0.89 ± 0.02	–

Kp, Kobresia pygmaea; KpM, Kobresia pygmaea + Miscellaneous plants; Ks, Kobresia setchwanensis; Cm, Carex moorcroftii; M, Miscellaneous plants; G, Gramineae plants.

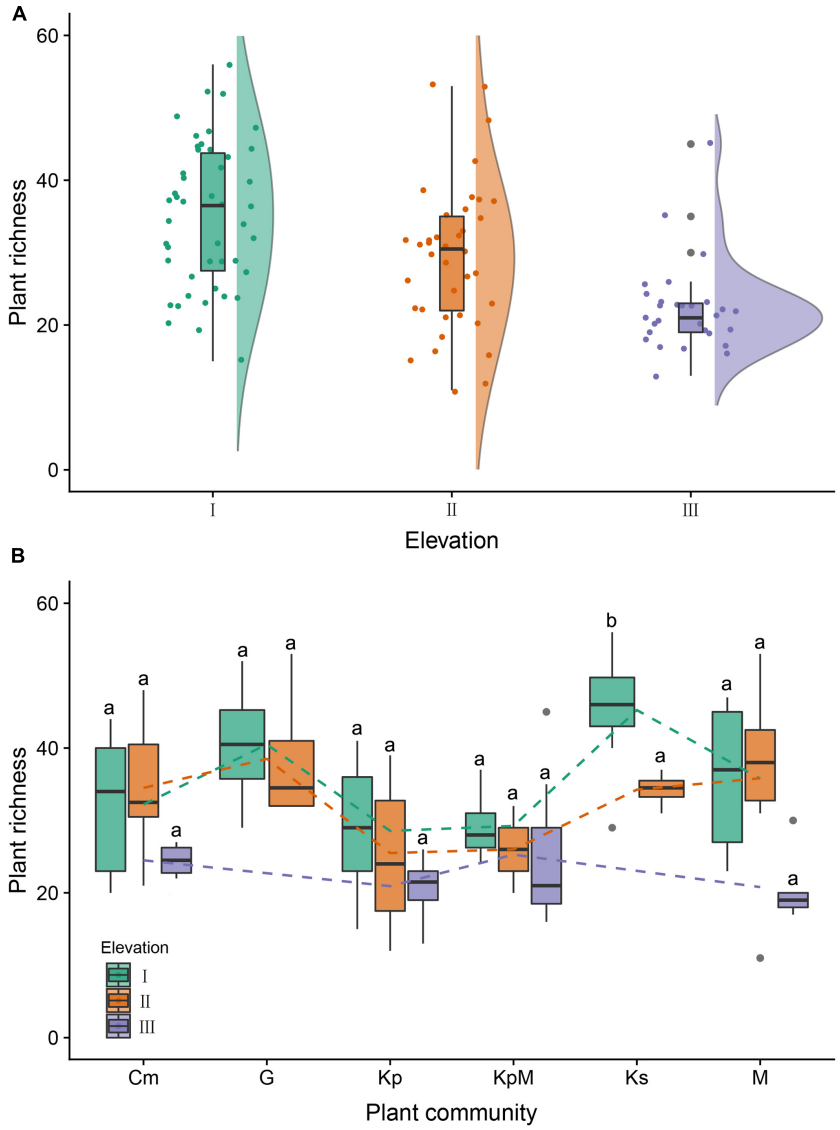

FIGURE 3 | Box and raincloud plots of plant richness along the elevation gradient. **(A)** Plant species richness as influenced by elevation. I: low elevation (3,500–4,000 m), II: middle elevation (4,000–4,500 m), III: high elevation (>4,500 m). **(B)** Plant species richness as influenced by elevation under different plant communities. Kp, *Kobresia pygmaea*; KpM, *Kobresia pygmaea*+ Miscellaneous plants; Ks, *Kobresia setchwanensis*; Cm, *Carex moorcroftii*; M, Miscellaneous plants; G, Gramineae plants. Bars with the same letter within the same elevation class denote means that are not significantly different at $p \leq 0.05$. Error bars depict standard error of the means.

richness on the explanatory variables, such as soil physico-chemical properties and community types (Type 1: Kp, *Kobresia pygmaea*; Type 2: Cm, *Carex moorcroftii*; Type 3: Ks, *Kobresia setchwanensis*; Type 4: KpM, *Kobresia pygmaea* + Miscellaneous plants; Type 5: M, Miscellaneous plants) (**Table 5**). The ANOVA analysis indicated that soil available nitrogen content, Type 2, and soil pH had significant impacts ($p < 0.01$) on species richness. Soil available nitrogen content contributed the most (46.1%) to the variance in species richness explained by the regression model ($R^2 = 0.35$), followed by Type 2 (23.5%), soil pH (14.1%), community type 5 (9.9%), and soil bulk density (6.3%).

The CCA results indicated that soil available nitrogen content and soil moisture content were the most influential factors among the soil parameters because they drove changes in the composition and diversity of plant species. Plant species composition and diversity followed the first two axes of the ordination with soil parameters (**Figure 5**). The overall Mantel significance test was significant ($F = 2.411$, $p < 0.001$), and the significance test was also significant for the first axis ($F = 7.107$, $p < 0.001$) and the second axis ($F = 2.555$, $p < 0.001$). The first axis accounted for 42.11% of the total variation with an eigenvalue of 0.4261 and the second axis accounted for 15.14% with an eigenvalue of 0.1532. Soil available nitrogen content was

TABLE 3 | The ANOVA result of β-diversity along the elevation gradient.

Elevation	β_{sor}	β_{sim}	β_{sne}	β_{ratio}
Low elevation	0.46 ± 0.17^{ns}	0.37 ± 0.14^{ns}	0.08 ± 0.05^{ns}	0.82 ± 0.10^{ns}
Middle elevation	0.45 ± 0.09^{ns}	0.35 ± 0.10^{ns}	0.10 ± 0.07^{ns}	0.77 ± 0.14^{ns}
High elevation	0.47 ± 0.06^{ns}	0.34 ± 0.11^{ns}	0.13 ± 0.07^{ns}	0.72 ± 0.20^{ns}

β_{sor}, Sørenson's dissimilarity index; β_{sim}, Simpson dissimilarity index; β_{sne}, nestedness resultant dissimilarity index; β_{ratio}, the ratio of β_{sim} to β_{sor}. ns, no significant differences ($P > 0.05$).

TABLE 4 | Soil physico-chemical properties as influenced significantly by elevation for different plant communities.

Plant community type	Soil physico-chemical property	Low elevation	Middle elevation	High elevation
Kp	SMC	24.79 ± 7.95a	22.38 ± 7.15a	62.41 ± 15.71b
	SpH	5.89 ± 0.53a	6.67 ± 0.64b	5.53 ± 0.26a
	SAN	56.98 ± 15.95a	43.57 ± 16.06a	246.45 ± 56.21b
KpM	SAN	43.11 ± 12.36a	45.44 ± 12.36a	384.65 ± 62.15b
Cm	SAN	57.87 ± 4.49a	61.82 ± 12.50a	161.59 ± 43.27b
M	SAN	59.11 ± 28.69a	47.74 ± 15.55a	313.59 ± 47.86b

Analyses of variance (*p*-values)

Variable	Elevation class	Community type	Elevation × Community
SMC	$p < 0.01$	0.196	$p < 0.05$
SpH	$p < 0.05$	0.27	0.059
SAN	$p < 0.001$	0.788	0.469

Kp, Kobresia pygmaea; KpM, Kobresia pygmaea + Miscellaneous plants; Cm, Carex moorcroftii; M, Miscellaneous plants; SMC, soil moisture content; SpH, soil pH; SAN, soil available nitrogen content. Letters indicate significant differences among elevation classes ($p < 0.05$).

strongly negatively correlated (−0.94) and soil bulk density was negatively correlated (−0.39) with the first axis. Soil moisture content had a strong negative correlation with the second axis (–0.76) and soil pH was positively correlated with the second axis (0.60).

Figure 6 shows the partial correlation coefficients between species diversity and soil available nitrogen content along an elevation gradient, regardless of soil moisture content. At low elevation, species diversity decreased insignificantly with the increase of soil available nitrogen content. At middle elevation, species diversity had a significant negative relationship with soil available nitrogen content [species richness ($R^2_{partial} = 0.70$, $p_{partial} < 0.001$), Shannon-Wiener index ($R^2_{partial} = 0.68$, $p_{partial} < 0.001$), evenness ($R^2_{partial} = 0.24$, $p_{partial} < 0.01$)]. At high elevation, species richness decreased significantly with increasing soil available nitrogen content ($R^2_{partial} = 0.38$, $p_{partial} < 0.01$), and Shannon-Wiener index had a significant negative relationship with soil available nitrogen content ($R^2_{partial} = 0.27$, $p_{partial} < 0.05$).

DISCUSSION

Effects of Soil Available Nitrogen Content on Species Composition and Diversity Along the Elevation Gradient

Elevation is a decisive factor influencing the distribution pattern of plant species because it leads to variations in hydrothermal conditions (Antony et al., 2016; Tesfaye et al., 2016). Our study showed that the species richness of all plant communities declined as elevation increased (**Figure 3A**). The species richness of Ks was significantly higher than other communities at low elevation, because Cyperaceae and Compositae had the similar proportions in Ks, with larger niche dimension (Xu et al., 2011). The Sørensen dissimilarity index (β_{sor}) of the overall plant communities based on the species richness was smallest at middle elevation, with no obvious trend as the increasing elevation. Simpson's dissimilarity index (β_{sim}) as a component of β-diversity is not considered the influence of the richness gradient, and the nestedness resultant dissimilarity index (β_{sne}) is based on subsets with lowest species richness (Baselga, 2010). β_{sim} of the overall plant communities decreased and β_{sne} increased gradually with the increasing elevation (**Table 3**). β_{sor} between KpM and Ks was the largest at low elevation and middle elevation. It may be considered with physiologic limitation as *Kobresia setchwanensis* is hard to survive due to the low temperature at high elevation (Xie et al., 2014).

The conversion of soil available nitrogen is impeded due to the extreme climate conditions in alpine regions (Xu et al., 2011). Elevation is a restrictive factor for soil available nitrogen content. It influences the soil available nitrogen conversion because the hydrothermal conditions vary at different elevations. Plant growth in an alpine meadow ecosystem is strongly limited by available nitrogen (Jiang et al., 2017; Han Y.H. et al., 2019). The partial correlation coefficient between plant species richness and soil available nitrogen content was insignificant on the overall elevation, and there was a decrease in species richness of

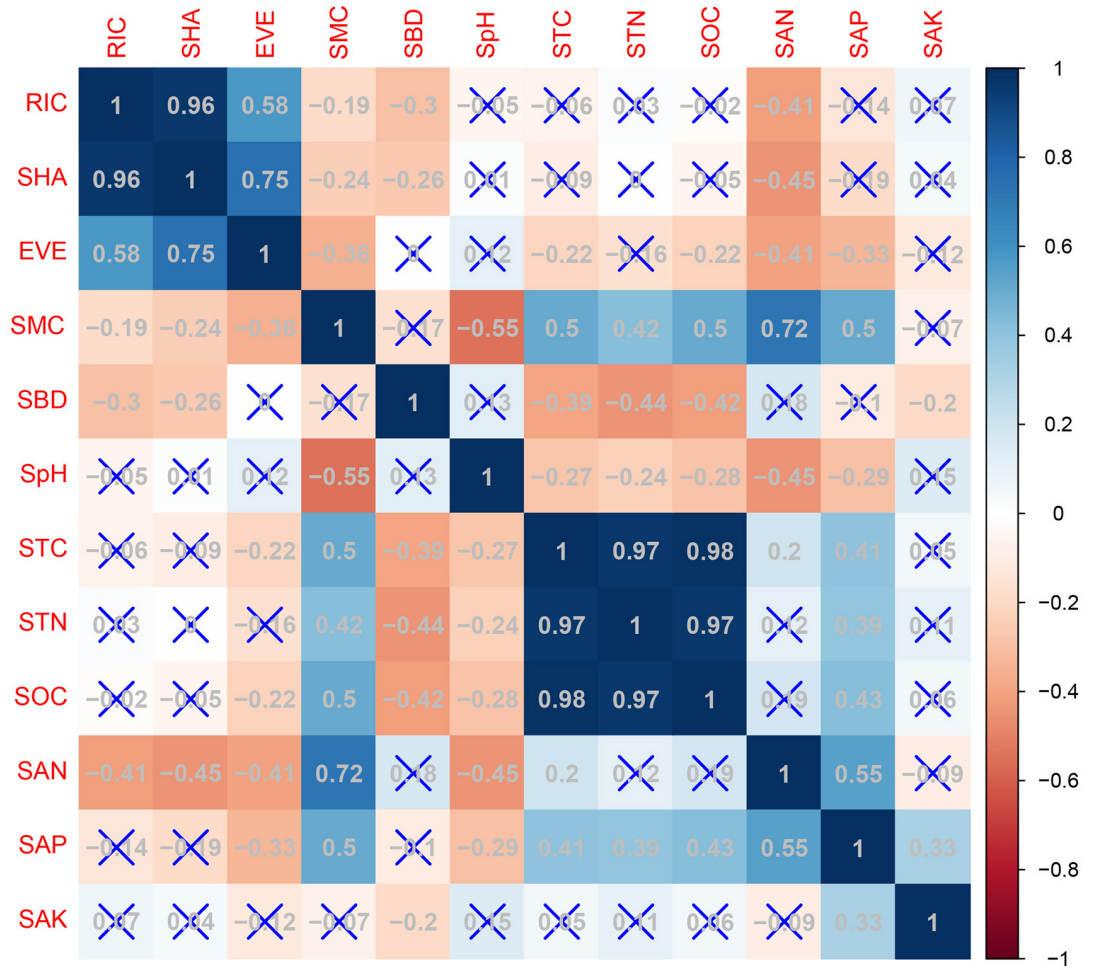

FIGURE 4 | Pearson's correlations between species diversity and soil parameters (RIC, species richness; SHA, Shannon-Wiener index; EVE, species evenness; SMC, soil moisture content; SBD, soil bulk density; SpH, soil pH; STC, soil total carbon content; STN, soil total nitrogen content; SOC, soil organic carbon content; SAN, soil available nitrogen content; SAP, soil available phosphorus content; SAK, soil available potassium content).

0.916 with every 100 mg kg^{-1} increase in soil available nitrogen content. For different elevations, the relationships between species richness and soil available nitrogen content shown by the partial correlation regression tended to decrease insignificantly (**Supplementary Figure 3**).

TABLE 5 | Results of a stepwise multiple linear regression of species richness against explanatory variables.

Variable	Estimate (standard error)	ANOVA		Relative importance
		F-value	Pr(>F)	
SAN	0.65	22.32	***	46.1%
Type 2	0.17	18.81	***	23.5%
SpH	−0.40	16.25	***	14.0%
Type 5	−0.36	14.47	***	10.0%
SBD	−0.49	12.10	***	6.3%

*SAN, soil available nitrogen content; Type, plant community type (Type 1: Kp, Kobresia pygmaea; Type 2: Cm, Carex moorcroftii; Type 3: Ks, Kobresia setchwanensis; Type 4: KpM, Kobresia pygmaea+ Miscellaneous plants; Type 5: M, Miscellaneous plants); SpH, soil pH; SBD, soil bulk density. *** Shows the significant correlation at 0.001 levels.*

Species richness was affected by soil available nitrogen content to different extents at the different elevations (**Figure 6**). Our study eliminated the redundancy effects of each factor by using stepwise multiple linear regression. The results showed that soil available nitrogen content explained the most variance (46.1%) in the regression model for species richness against the explanatory variables. The LM analysis, which controlled the elevation variable (**Figure 6**), showed that Cm species richness significantly increased [1.14 ± 0.73 (mg kg^{-1})$^{-1}$] and the species richness of Ks significantly decreased [−0.47 ± 0.23 (mg kg^{-1})$^{-1}$] with increasing soil available nitrogen content at low elevation. The species richness value for G had the highest intercept [2.13 ± 1.57 (mg kg^{-1})$^{-1}$] at middle elevation. Furthermore, species richness decreased for all plant communities (Kp, KpM, Cm, and M) appearing at high elevation, but this was not obvious (**Table 6**).

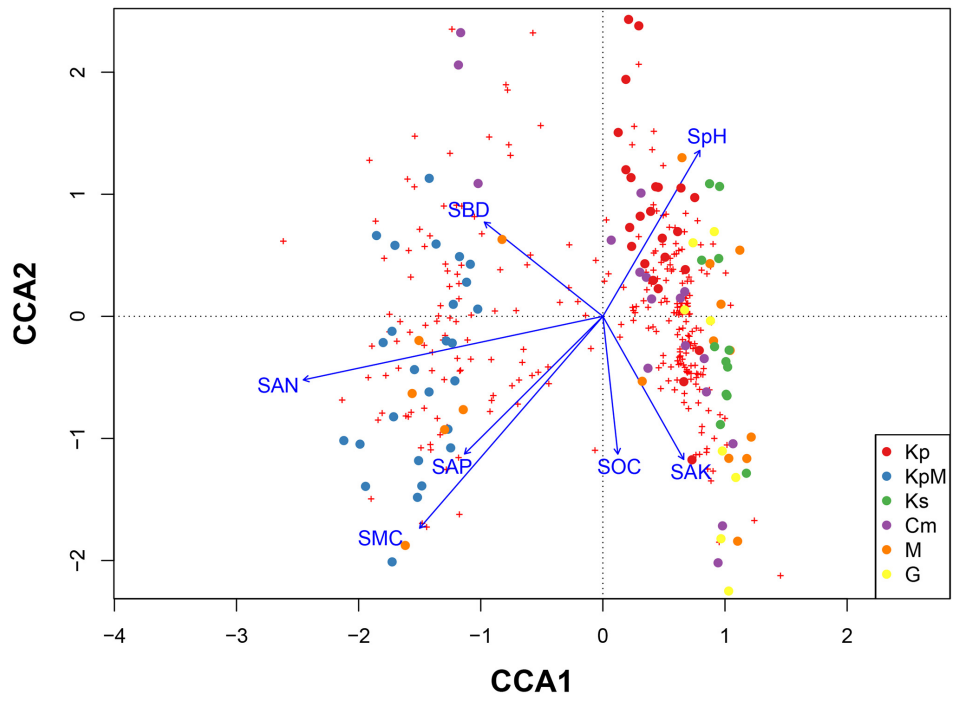

FIGURE 5 | Canonical correspondence analysis showing the relationships between species and soil parameters across different plant communities. Kp, *Kobresia pygmaea*; KpM, *Kobresia pygmaea*+ Miscellaneous plants; Ks, *Kobresia setchwanensis*; Cm, *Carex moorcroftii*; M, Miscellaneous plants; G, Gramineae plants; SMC, soil moisture content; SBD, soil bulk density; SpH, soil pH; STC, soil total carbon content; STN, soil total nitrogen content; SOC, soil organic carbon content; SAN, soil available nitrogen content; SAP, soil available phosphorus content; SAK, soil available potassium content.

Effects of Climate Factors on Species Richness and Soil Available Nitrogen

In addition to the changes of hydrothermal conditions caused by elevation, the climatic background had impacts on species richness and soil available nitrogen content. The climate of the study area located in the southeast of the QTP is clearly warming and the rates of the temperature rise have been found to increase with increasing elevation (Song et al., 2014; Kuang and Jiao, 2016). The precipitation on the QTP is generally increasing, but annual precipitation in the study area shows an insignificant downward trend. The variation in precipitation does not have a uniform spatial distribution and the changes in precipitation are not as pronounced as the changes in temperature (Kuang and Jiao, 2016). It is widely acknowledged that climate factors are the main drivers of species richness patterns because they influence the effects of temperature on rates of species evolution or interactions between organisms (Kubota et al., 2015). Some studies have found that climate warming enhances the mineralization of soil organic matter, which contains most of the soil nitrogen (Kahmen et al., 2006; Manning et al., 2008). This mineralization leads to soil nutrient enrichment and the available nitrogen in soil increases (Klein et al., 2004). The multiple regression analysis of soil available nitrogen content against its influential factors indicated that temperature ranked next to elevation among the environmental factors at 8.4% (**Supplementary Table 2**). The increase in temperature will accelerate the decomposition of nitrogen in soil organic matter, which will affect soil available nitrogen content.

Implications for Alpine Grassland Management

Analyzing the effects of soil physico-chemical properties on plant species composition and diversity within different plant communities along an elevation gradient helps explain species distribution patterns and the formation of communities. The resource utilization modes used by different plant species vary among community types. They depend on the characteristic differences among the niches utilized by the dominant species (Thakur and Wright, 2017). Nitrogen is the main limiting element on plant growth in alpine grassland ecosystems (Gao et al., 2013; Jiang et al., 2017), especially for Cyperaceae plants. Soil available nitrogen content increased along axis 1 from right to left, and KpM was mainly distributed across a spatial area with a high soil available nitrogen content (**Figure 6**). Climate warming causes plants to migrate from lower to higher altitudes, and it can also directly reduce plant diversity by replacing dominant and native species that have been disappeared due to habitat loss (Steinbauer et al., 2018; Niu et al., 2019). The result that nitrogen enrichment caused by soil warming reduces the loss of plant species diversity provides a theoretical foundation for scientific fertilization (Xu et al., 2011). The results can be used to provide guidance to the grassland management of different community types, improving grassland

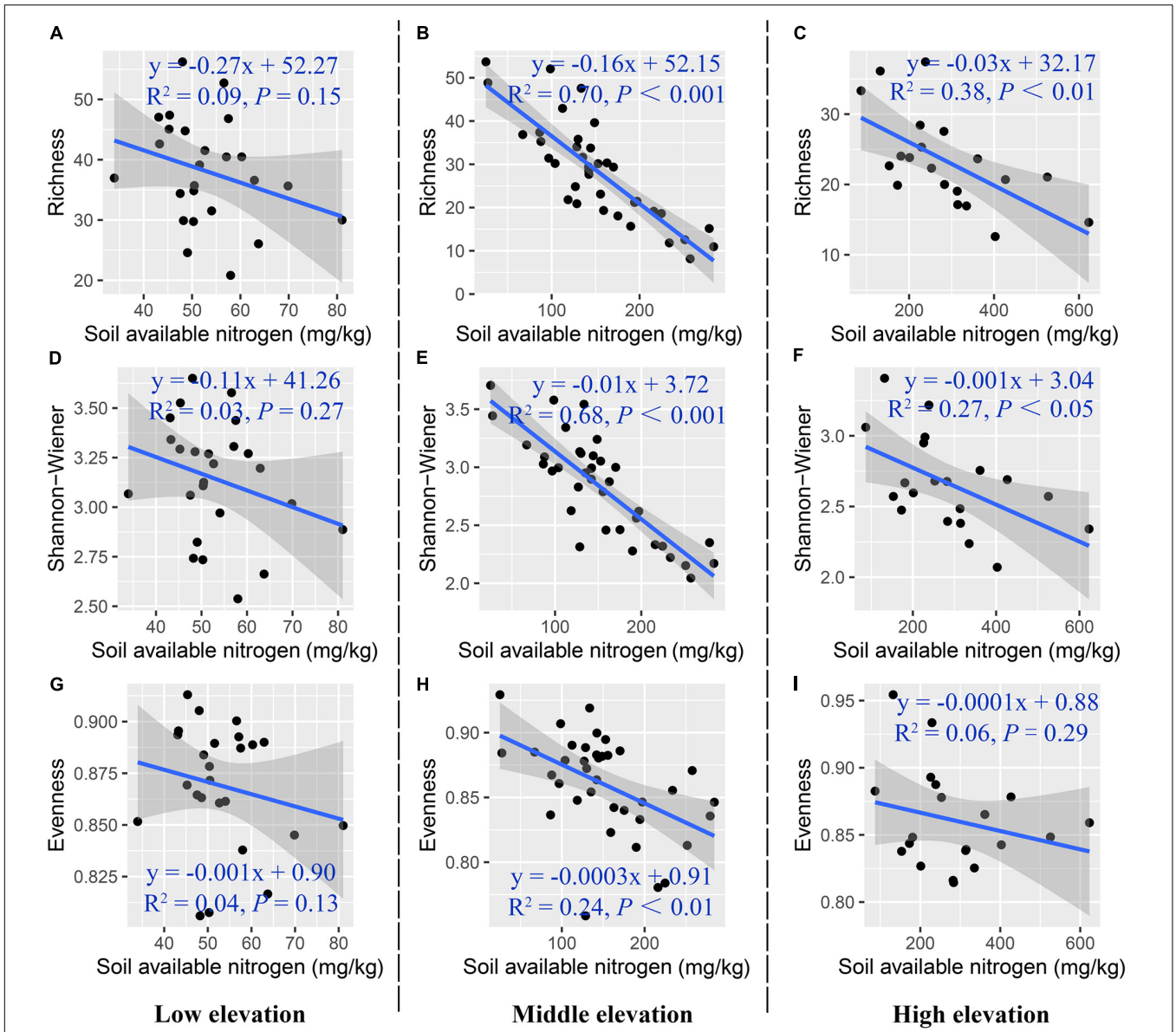

FIGURE 6 | Partial correlation between plant species diversity and soil available nitrogen content along the elevation gradient. **(A–C)** Species richness, **(D–F)** Shannon-Wiener index, **(G–I)** species evenness.

TABLE 6 | Intercepts for species richness response to soil available nitrogen content by the different plant communities along the elevation gradient.

Plant community type	Low elevation		Middle elevation		High elevation	
	Intercept	Standard error	Intercept	Standard error	Intercept	Standard error
Kp	0.260	0.153	0.280	0.126	−0.001	0.007
KpM	0.021	0.018	0.065	0.026	−0.030	0.015
Cm	1.142	0.732	0.461	0.310	−0.008	0.009
M	−0.145	0.044	−0.065	0.019	−0.005	0.009
Ks	−0.467	0.232	−0.367	0.281		
G	−0.311	0.270	2.131	1.579		

Kp, Kobresia pygmaea; KpM, Kobresia pygmaea + Miscellaneous plants; Ks, Kobresia setchwanensis; Cm, Carex moorcroftii; M, Miscellaneous plants; G, Gramineae plants.

restoration programs and the construction of alpine grassland (Li X. et al., 2018).

CONCLUSION

In this study, we divided plant communities into six types based on species importance values and analyzed how plant species composition/diversity was influenced by soil parameters along an elevation gradient. The results showed that species richness decreased as elevation increased for all plant communities, but the trend was not significant among community types. β-diversity of the overall plant communities varied insignificantly among different elevation classes. For different community types, the Sørenson's dissimilarity index (β_{sor}) between KpM and Ks was the largest (0.68). Soil available nitrogen content was the most important factor driving the changes in plant species composition and diversity among the soil parameters. Our results further indicated that the effect of soil available nitrogen content on plant species richness was influenced by elevation, and that the limiting effect of soil available nitrogen content was more obvious at high elevation. Furthermore, climate warming accelerated the decomposition of soil organic nitrogen and temperature was the most important environmental factor after elevation. Therefore, nitrogen mineralization caused by climate warming exacerbated the decline in species richness at high elevation. Our study explores the responses of plant species diversity to physico-chemical properties by distinguishing different community types along an elevation, and might provide detective meaning for sustainable management of alpine grassland.

DATA AVAILABILITY STATEMENT

The original contributions presented in the study are included in the article/ **Supplementary Material**, further inquiries can be directed to the corresponding author/s.

AUTHOR CONTRIBUTIONS

WH and GL designed the study. LC and DL conducted the experiments and organized and analyzed the data. XS, TL, TJ, and SS participated in the field works. WH and LC led the writing of the manuscript. GL and XS modified manuscript structure. All authors contributed to the article and approved the submitted version.

FUNDING

This work was supported by the Second Tibetan Plateau Scientific Expedition and Research Program (STEP) (grant no. 2019QZKK0402), National Key Research and Development Program of China (grant no. 2016YFC0502102), and Startup Foundation for Introducing Talent of Nanjing University of Information Science and Technology (grant No. 2021r098).

ACKNOWLEDGMENTS

We thank all the students from Chengdu University of Technology who helped us to survey alpine grassland in the field.

SUPPLEMENTARY MATERIAL

The Supplementary Material for this article can be found online at: https://www.frontiersin.org/articles/10.3389/fpls.2022.822268/full#supplementary-material

REFERENCES

Antony, V., Erskine, P., Mulligan, D., Repin, R., and Karim, R. (2016). Vegetation on ultramafic edaphic 'islands' in kinabalu park (sabah, malaysia) in relation to soil chemistry and elevation. *Plant Soil* 403, 77–101. doi: 10.1007/s11104-016-2831-3

Bao, S. (2000). *Soil and Agricultural Chemistry Analysis*. Beijing: China Agriculture Press.

Barbarossa, V., Bosmans, J., Wanders, N., King, H., Bierkens, M. F. P., Huijbregts, M. A. J., et al. (2021). Threats of global warming to the world's freshwater fishes. *Nat. Commun.* 12:1701. doi: 10.1038/s41467-021-21655-w

Baselga, A. (2010). Partitioning the turnover and nestedness components of beta diversity. *Global Ecol. Biogeogr.* 19, 134–143. doi: 10.1111/j.1466-8238.2009.00490.x

Chinese Soil Taxonomy Research Group (1995). *Chinese Soil Taxonomy*. Beijing: Science Press, 58–147.

Do Carmo, F. F., and Jacobi, C. M. (2016). Diversity and plant trait-soil relationships among rock outcrops in the Brazilian Atlantic rainforest. *Plant Soil* 403, 7–20. doi: 10.1007/s11104-015-2735-7

Dong, S. K., Sha, W., Su, X. K., Zhang, Y., Li, S., Gao, X. X., et al. (2019). The impacts of geographic, soil and climatic factors on plant diversity, biomass and their relationships of the alpine dry ecosystems: cases from the aerjin mountain nature reserve, china. *Ecol. Eng.* 127, 170–177. doi: 10.1016/j.ecoleng.2018.10.027

Ebersbach, J., Muellner-Riehl, A. N., Michalak, I., Tkach, N., Hoffmann, M. H., Röser, M., et al. (2017). In and out of the qinghai-tibet plateau: divergence time estimation and historical biogeography of the large arctic-alpine genus *Saxifraga* L. *J. Biogeogr.* 44, 900–910. doi: 10.1111/jbi.12899

Feng, C., Yan, M., Fu, S., and Chen, H. (2017). Soil carbon and nutrient dynamics following cessation of anthropogenic disturbances in degraded subtropical forests. *Land Degrad. Dev.* 28, 2457–2467. doi: 10.1002/ldr.2781

Gao, Y., Zhou, X., Wang, Q., Wang, C., Zhan, Z., Chen, L., et al. (2013). Vegetation net primary productivity and its response to climate change during 2001–2008 in the tibetan plateau. *Sci. Total Environ.* 444, 356–362. doi: 10.1016/j.scitotenv.2012.12.014

Gieselman, T. M., Hodges, K. E., and Vellend, M. (2013). Human-induced edges alter grassland community composition. *Biol. Conserv.* 158, 384–392. doi: 10.1016/j.biocon.2012.08.019

Grace, J. B., Anderson, T. M., Seabloom, E. W., Borer, E. T., Adler, P. B., Harpole, W. S., et al. (2016). Integrative modelling reveals mechanisms linking productivity and plant species richness. *Nature* 529, 390–393. doi: 10.1038/nature16524

Guo, L., Chen, J., Luedeling, E., He, J. S., Cheng, J., Wen, Z., et al. (2018). Early-spring soil warming partially offsets the enhancement of alpine grassland aboveground productivity induced by warmer growing seasons on the

qinghai-tibetan plateau. *Plant Soil* 425, 177–188. doi: 10.1007/s11104-018-3582-0

Haider, S., Kueffer, C., Bruelheide, H., Seipel, T., Alexander, J. M., Rew, L. J., et al. (2018). Mountain roads and non-native species modify elevational patterns of plant diversity. *Global Ecol. Biogeogr.* 27, 667–678. doi: 10.1111/geb.12727

Han, W. Y., Lu, H. T., Liu, G. H., Wang, J. S., and Su, X. K. (2019). Quantifying degradation classifications on alpine grassland in the lhasa river basin, qinghai-tibetan plateau. *Sustainability* 11:7067. doi: 10.3390/su11247067

Han, Y. H., Dong, S. K., Zhao, Z. Z., Sha, W., Li, S., Shen, H., et al. (2019). Response of soil nutrients and stoichiometry to elevated nitrogen deposition in alpine grassland on the qinghai-tibetan plateau. *Geoderma* 343, 263–268. doi: 10.1016/j.geoderma.2018.12.050

Hanaka, A., Plak, A., Zagórski, P., Ozimek, E., Rysiak, A., Majewska, M., et al. (2019). Relationships between the properties of spitsbergen soil, number and biodiversity of rhizosphere microorganisms, and heavy metal concentration in selected plant species. *Plant Soil* 436, 49–69. doi: 10.1007/s11104-018-3871-7

Hooper, D. U., Adair, E. C., Cardinale, B. J., Byrnes, J., Hungate, B. A., Matulich, K. L., et al. (2012). A global synthesis reveals biodiversity loss as a major driver of ecosystem change. *Nature* 486, 105–108. doi: 10.1038/nature11118

Hutchinson, M. F., and Xu, T. (2013). *Anusplin Version 4.4 User Guide*. Canberra, ACT: The Australian National University.

Jiang, L., Wang, S., Zhe, P., Wang, C., Kardol, P., Zhong, L., et al. (2017). Effects of grazing on the acquisition of nitrogen by plants and microorganisms in an alpine grassland on the tibetan plateau. *Plant Soil* 416, 1–12. doi: 10.1007/s11104-017-3205-1

Kahmen, A., Renker, C., Unsicker, S. B., and Buchmann, N. (2006). Niche complementarity for nitrogen: an explanation for the biodiversity and ecosystem functioning relationship? *Ecology* 87, 1244–1255. doi: 10.1890/0012-9658(2006)87[1244:ncfnae]2.0.co;2

Klein, J. A., Harte, J., and Zhao, X. Q. (2004). Experimental warming causes large and rapid species loss, dampened by simulated grazing, on the tibetan plateau. *Ecol. Lett.* 7, 1170–1179. doi: 10.1111/j.1461-0248.2004.00677.x

Kuang, X., and Jiao, J. J. (2016). Review on climate change on the tibetan plateau during the last half century. *J. Geophys. Res. Atmospheres* 121, 3979–4007. doi: 10.1002/2015JD024728

Kubota, Y., Shiono, T., and Kusumoto, B. (2015). Role of climate and geohistorical factors in driving plant richness patterns and endemicity on the east asian continental islands. *Ecography* 38, 639–648. doi: 10.1111/ecog.00981

Lai, Y., Liu, Y. H., and Liu, X. Y. (2021). Elevational diversity patterns of green lacewings (neuroptera: chrysopidae) uncovered with DNA barcoding in a biodiversity hotspot of southwest China. *Front. Ecol. Evol.* 9:778686. doi: 10.3389/fevo.2021.778686

Li, C., Peng, F., Xue, X., You, Q. G., Lai, C. M., Zhang, W. J., et al. (2018). Productivity and quality of alpine grassland vary with soil water availability under experimental warming. *Front. Plant Sci.* 9:1790. doi: 10.3389/fpls.2018.01790

Li, X., Gao, J., and Zhang, J. (2018). A topographic perspective on the distribution of degraded meadows and their changes on the qinghai-tibet plateau, west china. *Land Degrad. Dev.* 29, 1574–1582. doi: 10.1002/ldr.2952

Li, Y., Dong, S., Liu, S., Su, X., Wang, X., Zhang, Y., et al. (2019). Relationships between plant diversity and biomass production of alpine grasslands are dependent on the spatial scale and the dimension of biodiversity. *Ecol. Eng.* 127, 375–382. doi: 10.1016/j.ecoleng.2018.12.015

Liu, S., Zamanian, K., Schleuss, P. M., Zarebanadkouki, M., and Kuzyakov, Y. (2018). Degradation of tibetan grasslands: consequences for carbon and nutrient cycles. *Agric. Ecosyst. Environ.* 252, 93–104. doi: 10.1016/j.agee.2017.10.011

Manning, P., Morrison, S. A., Bonkowski, M., and Bardgett, R. D. (2008). Nitrogen enrichment modifies plant community structure via changes to plant-soil feedback. *Oecologia* 157, 661–673. doi: 10.1007/s00442-008-1104-0

Niu, Y., Yang, S., Zhou, J., Chu, B., Ma, S., Zhu, H., et al. (2019). Vegetation distribution along mountain environmental gradient predicts shifts in plant community response to climate change in alpine meadow on the tibetan plateau. *Sci. Total Environ.* 650, 505–514. doi: 10.1016/j.scitotenv.2018.08.390

Song, C., Pei, T., and Zhou, C. (2014). The role of changing multiscale temperature variability in extreme temperature events on the eastern and central tibetan plateau during 1960–2008. *Int. J. Climatol.* 34, 3683–3701. doi: 10.1002/joc.3935

Steinbauer, M. J., Grytnes, J. A., Jurasinski, G., Kulonen, A., Lenoir, J., Pauli, H., et al. (2018). Accelerated increase in plant species richness on mountain summits is linked to warming. *Nature* 556:231. doi: 10.1038/s41586-018-0005-6

Sun, J., Zhan, T., Liu, M., Zhang, Z., Wang, Y., Liu, S., et al. (2019). Verification of the biomass transfer hypothesis under moderate grazing across the tibetan plateau: a meta-analysis. *Plant Soil* 458, 139–150.

Supriya, K., Moreau, C. S., Sam, K., and Price, T. D. (2019). Analysis of tropical and temperate elevational gradients in arthropod abundance. *Front. Biogeogr.* 11:e43104. doi: 10.21425/F5FBG43104

Tesfaye, M. A., Bravo, F., Ruiz-Peinado, R., Pando, V., and Bravo-Oviedo, A. (2016). Impact of changes in land use, species and elevation on soil organic carbon and total nitrogen in ethiopian central highlands. *Geoderma* 261, 70–79.

Thakur, M. P., and Wright, A. J. (2017). Environmental filtering, niche construction, and trait variability: the missing discussion. *Trends Ecol. Evol.* 32, 884–886. doi: 10.1016/j.tree.2017.09.014

Thomasson, A. J. (2010). Towards an objective classification of soil structure. *Eur. J. Soil Sci.* 29, 38–46. doi: 10.1111/j.1365-2389.1978.tb02029.x

Wang, L., Xu, D. M., and Zhang, J. J. (2012). Effects of enclosure on composition of plant community and species diversity of desert steppe. *Pratacul. Sci.* 29, 1512–1516. doi: 10.1002/ece3.4611

Wu, H., and Ding, J. (2020). Abiotic and biotic determinants of plant diversity in aquatic communities invaded by water hyacinth [eichhornia crassipes (mart.) solms]. *Front. Plant Sci.* 11:1306. doi: 10.3389/fpls.2020.01306

Xie, X. L., Zhou, R., Xie, H. S., Shen, Z. X., and Deng, Z. F. (2014). The clonal phenotypic variation and reproductive strategies of kobresia setchwanensis along altitude in northern tibet. *Pratacul. Sci.* 31, 2270–2276.

Xu, T., and Hutchinson, M. F. (2013). New developments and applications in the anuclim spatial climatic andbioclimatic modelling package. *Environ. Mod. Softw.* 40, 267–279. doi: 10.1016/j.envsoft.2012.10.003

Xu, X., Ouyang, H., Cao, G., Richter, A., Wanek, W., and Kuzyakov, Y. (2011). Dominant plant species shift their nitrogen uptake patterns in response to nutrient enrichment caused by a fungal fairy in an alpine meadow. *Plant Soil* 341, 495–504.

Yu, H., Favre, A., Sui, X., Chen, Z., Qi, W., and Xie, G. (2019). Mapping the genetic patterns of plants in the region of the qinghai–tibet plateau: implications for conservation strategies. *Div. Distri.* 25, 310–324.

Zhang, R., Wang, Z., Han, G., Schellenberg, M. P., Qian, W., and Chen, G. (2018). Grazing induced changes in plant diversity is a critical factor controlling grassland productivity in the desert steppe, northern china. *Agric. Ecosyst. Environ.* 265, 73–83. doi: 10.1016/j.agee.2018.05.014

Zhu, Y., Delgado-Baquerizo, M., Shan, D., Yang, X. H., Liu, Y. S., and Eldridge, D. (2020). Diversity-productivity relationships vary in response to increasing land-use intensity. *Plant Soil* 450, 511–520. doi: 10.1007/s11104-020-04516-1

Conflict of Interest: The handling editor declared a shared affiliation, though no other collaboration, with several of the authors WH, LC, XS, TL, and GL at the time of the review.

The remaining authors declare that the research was conducted in the absence of any commercial or financial relationships that could be construed as a potential conflict of interest.

Publisher's Note: All claims expressed in this article are solely those of the authors and do not necessarily represent those of their affiliated organizations, or those of the publisher, the editors and the reviewers. Any product that may be evaluated in this article, or claim that may be made by its manufacturer, is not guaranteed or endorsed by the publisher.

Copyright © 2022 Han, Chen, Su, Liu, Jin, Shi, Li and Liu. This is an open-access article distributed under the terms of the Creative Commons Attribution License (CC BY). The use, distribution or reproduction in other forums is permitted, provided the original author(s) and the copyright owner(s) are credited and that the original publication in this journal is cited, in accordance with accepted academic practice. No use, distribution or reproduction is permitted which does not comply with these terms.

frontiers in Plant Science

ORIGINAL RESEARCH
published: 09 February 2022
doi: 10.3389/fpls.2022.827035

Synchronous Responses of Plant Functional Traits to Nitrogen Deposition From Dominant Species to Functional Groups and Whole Communities in Alpine Grasslands on the Qinghai-Tibetan Plateau

Shuai Li[1†], Zhenzhen Zhao[2†], Shikui Dong[3], Hao Shen[3], Yudan Xu[4], Jiannan Xiao[5], Xiaoxia Gao[5], Shengnan Wu[3] and Paul Stufkens[6]*

[1] College of Resource and Environment, Shanxi Agricultural University, Jinzhong, China, [2] School of Environmental and Chemical Engineering, Shanghai University, Shanghai, China, [3] School of Grassland Science, Beijing Forestry University, Beijing, China, [4] College of Grassland Science, Shanxi Agricultural University, Jinzhong, China, [5] School of Environment, Beijing Normal University, Beijing, China, [6] English Department, Zamorano University, Tegucigalpa, Honduras

Nitrogen deposition is recognized as one of the major threats to the ecosystem function of alpine grasslands on the Qinghai-Tibetan Plateau (QTP). However, few studies have documented the gradient responses of plant species, functional groups, and communities in alpine grassland ecosystems to various levels of N deposition on the QTP. We applied eight linear mixed-effect models combing acidification, eutrophication, and phosphorus availability to explore if the responses of functional traits (particularly plant height and specific leaf area) of plants from dominant species to functional groups and whole communities in different types of grassland to nitrogen deposition were consistent with the same or different models. We found that the specific leaf area of *Stipa capillata*, non-forb, and community-weighted mean value in the alpine steppe were synchronous and related to acidification with nitrogen addition; the height of *Stipa capillata*, non-forb, and community-weighted mean value in the alpine steppe was synchronous and related to acidification, eutrophication, and phosphorus availability with nitrogen addition; the height and specific leaf area of *Elymus breviaristatus* to functional groups and community-weighted mean value in cultivated grasslands (CGs) were synchronous and related to acidification, eutrophication, and phosphorus availability with nitrogen addition. Most of the responses of functional traits of plants to acidification, eutrophication, and phosphorus availability associated with nitrogen deposition in the alpine steppe and the CG were synchronous, while only the response of the specific leaf area of forb functional groups to eutrophication associated with N deposition in the alpine steppe was asynchronous.

Keywords: plant functional traits, nitrogen deposition, alpine steppe, cultivated grassland, Qinghai-Tibet Plateau

OPEN ACCESS

Edited by:
Junran Jimmy Li,
University of Tulsa, United States

Reviewed by:
Xukun Su,
Research Center for Eco-Environmental Sciences, Chinese Academy of Sciences (CAS), China
Tao Zhang,
Northeast Normal University, China

***Correspondence:**
Shikui Dong
dongshikui@bjfu.edu.cn;
dongshikui@sina.com

† These authors have contributed equally to this work

Specialty section:
This article was submitted to Functional Plant Ecology, a section of the journal Frontiers in Plant Science

Received: *01 December 2021*
Accepted: *11 January 2022*
Published: *09 February 2022*

Citation:
Li S, Zhao Z, Dong S, Shen H, Xu Y, Xiao J, Gao X, Wu S and Stufkens P (2022) Synchronous Responses of Plant Functional Traits to Nitrogen Deposition From Dominant Species to Functional Groups and Whole Communities in Alpine Grasslands on the Qinghai-Tibetan Plateau. Front. Plant Sci. 13:827035. doi: 10.3389/fpls.2022.827035

HIGHLIGHTS

- Dominant specie, non-forb, and community were related to acidification with N addition in AS.
- Responses of height were more sensitive to N addition than SLA in both AS and CG.
- Responses of SLA and height in CG were more sensitive to N addition than AS.
- Responses of SLA of dominant specie, non-forb, and community were synchronous with N addition.
- Only response of SLA of forb was asynchronous compared to others with N addition in AS.

INTRODUCTION

Nitrogen (N) deposition is recognized as one of the major threats to global biodiversity (Phoenix et al., 2010; Payne et al., 2017), which has increased sixfold since the 1860s (Field et al., 2014) and is expected to continue to increase in the future on a global scale (Bobbink et al., 2010). In China, the average N deposition rate was 13.2 kg N/ha/year in the 1980s and became 21.1 kg N/ha/year in the 2000s (Liu et al., 2013). On the Qinghai-Tibetan Plateau (QTP), known as "the Third Pole of the Earth," a significant increase in the N deposition rate has been found since the 1980s (Chen et al., 2013; Liu et al., 2013), and the current rate ranges from 8.7 to 13.8 kg N/ha/year in the 2000s (Liu et al., 2013). Alpine grasslands, including mainly alpine meadow, alpine steppe (AS), and alpine desert steppe, occupy more than half the area of the QTP territory (Dong et al., 2010; Zhao et al., 2017), with a low-atmospheric N-input environment historically (Zhang et al., 2014), and are very sensitive to N deposition (Piao et al., 2011; Shen et al., 2014; Ma et al., 2019). However, few studies have documented the gradient responses of plant species, functional groups, and communities in alpine grassland ecosystems to various levels of N deposition on the QTP.

It is widely reported that there are mainly three pathways in which N deposition can affect a plant community, namely, acidification, eutrophication, and phosphorus (P) limit (Phoenix et al., 2010, 2012; Stevens et al., 2010). Soil acidity derived directly or indirectly from N deposition (Liu et al., 2012; Greaver et al., 2016) can lead to migration of metals, a loss of basic cations, an imbalance among N-containing compounds, and the ultimate alteration of THE composition of a plant community (Stevens et al., 2010; Laliberté et al., 2014). N is generally known to be the limiting factor in most terrestrial ecosystems (Jing et al., 2016; Wang et al., 2018). Some scholars believe that an increasing N deposition rate may lead to the transition from N limitation to N saturation in ecosystems (Lu et al., 2010), which may benefit the coexistence of species by excluding non-nitrophilous plants (Bobbink et al., 2010). In contrast, some other scholars think that the immobilization of NO_3-N was reduced and NH_4-N was increased in the process of transition from N limitation to N saturation (Phoenix et al., 2012), which may limit the coexistence of species due to differences in plant preferences and tolerances of NH_4-N or NO_3-N (van den Berg et al., 2016). Some studies have shown that other nutrient limitations (such as P) become more important in the context of an increased rate of N deposition, although N is still the prime limiting factor in most ecosystems (Lu et al., 2010; Stevens et al., 2010; Phoenix et al., 2012), since the main driver for activating P in the soil is weathering (Cleland and Harpole, 2010). Particularly, in a low-temperature environment, such as alpine grassland areas of the QTP, the uptake of P by plants will be limited (Laliberté et al., 2014). However, these three pathways are not necessarily independent, as the absorption of N and P by plants is synergistic (Stevens et al., 2010; Phoenix et al., 2012), and the pH also has an effect on the absorption of N and P in plants (Laliberté et al., 2014).

The response of plant communities to N deposition is mostly focused on plant richness in the field of academic studies (Zavaleta et al., 2003; Clark and Tilman, 2008; Zhang et al., 2014; van den Berg et al., 2016). However, there is limited literature documenting the effects of N deposition on functional traits, except for a few scholars who highlighted the application of trait-based approaches to exploring the response of plants to N deposition (De Deyn et al., 2008; Lavorel et al., 2013). Functional-based hypotheses insisted that plant interactions will shift from soil N competition to light competition (Suding et al., 2005; Stevens et al., 2006; Hautier et al., 2009; Bobbink et al., 2010; Cleland and Harpole, 2010; Borer et al., 2014; Humbert et al., 2016; Ma et al., 2019) with the increase in the N deposition rate, potentially affecting the functional traits of plants related to light acquisition or N availability, such as height or specific leaf area (SLA) (Reich et al., 1998; Diekmann and Falkengren-Grerup, 2002). N deposition can positively affect the functional groups of grass by promoting their growth and negatively impacting other functional groups, such as forbs by limiting their growth (Johansson et al., 2012; Borer et al., 2014; Humbert et al., 2016; Zhang et al., 2020). Until present, the limited studies from temperate and tropical forests have shown inconsistent results about the responses of the functional traits of plants to N deposition, i.e., some scholars stated that functional traits were the conductors of the N deposition on communities (Wang et al., 2018), whereas some other scholars reported that plant traits were not related to N deposition (Moreau et al., 2015). In addition, it is even less clear about the responses of functional traits of plants from dominant species to functional groups, and whole communities in different types of grassland to N deposition were consistent with the same or different.

As for alpine grassland ecosystems on the QTP, few researchers other than Wang et al. (2018) have explored the effects of N addition on the functional traits of plants of the alpine meadow. AS is one of the most important ecosystems on the QTP, and cultivated grassland (CG) is the key intervention to prevent severe grassland degradation driven mainly by climatic change and livestock overgrazing (Zhao et al., 2017; Zhang et al., 2020); both of them are critically important for sustainable development of both upstream and downstream regions. On the one hand, according to the mass ratio hypothesis, the ecosystems are largely controlled by the characteristics of dominant species or the dominant functional group (Grime, 1998); in contrast, the complementary effect may be important for the responses to N deposition, as the responses may be eliminated or weakened by complex species interactions (Cleland et al., 2006). Therefore,

studies are needed to clarify the impacts of acidification, eutrophication, and P limitation associated with N deposition on the functional traits of plants from dominant species to functional groups and communities in AS and CG ecosystems. Within this context, we conducted the manipulated experiments with N addition at different gradients in both AS and CG on the QTP to test three hypotheses, namely, (1) eutrophication, acidification, and P availability associated with N deposition impact the functional traits of plants of alpine grasslands; (2) there are cascading effects of N deposition on the functional traits of plants from dominant species to functional groups and whole communities of the alpine grasslands; and (3) the responses of alpine plant functional traits to N deposition vary with grassland types.

MATERIALS AND METHODS

Study Site

This study was conducted in Tiebujia town, Gonghe County (99°35′N, 37°02′E, 3,270 m ASL), which is located at the west side of Qinghai Lake (**Figure 1**) in Qinghai Province, China. In this town, the mean annual temperature is approximately −0.4 to 1.2°C, the mean annual precipitation is approximately 360–430 mm, and the annual evaporation capacity is around 1,550 mm. The typical vegetation is AS, dominated by *Stipa capillata*. The CG next to the AS was plowed before and planted with *Elymus brevaristatus* in 2012. In both grasslands, the soil is predominantly sandy loam.

Experimental Design

In May 2015, 18 plots (i.e., replicates) of 2 m × 5 m were, respectively, placed in uniform sites (with similar topography, vegetation, and soil) of AS and CG. The plots were randomly treated by six levels of N addition with granular ammonium nitrate (NH_4NO_3) mixed with soil in three replicates for each N treatment, 0 N (CK), 8 kg N/ha/year (NI), which equals to the annual N deposition on the QTP reported by Lu and Tian in 2007 (Lu and Tian, 2007), 24 kg N/ha/year (NII), 40 kg N/ha/year (NIII), 56 kg N/ha/year (NIV), and 72 kg N/ha/year (NV) (**Figure 1**), and we applied N monthly basis in the growing season. We recorded the species composition of 72 sampling plots (6 treatments × 3 replicates × 2 grassland types × 2 years) at the peak growth rate in late July to early August of 2015 and 2016.

Soil Sampling

We sampled three cores of the surface soil (0–20 cm and 3.5 cm in diameter) from each sampling plot and mixed them well in the mid-August of 2015 and 2016. The soil samples were sealed in polyethylene bags and transported to the lab for extraction after being air-dried, ground, and sieved (18 mesh sieves were used for pH measurement, and 100 mesh sieves were used for soil nutrient measurement). We used a glass electrode to measure the soil pH in the supernatant by homogeneously mixing 5 g of soil and 25 ml of water. Total nitrogen (TN) was measured using an element analyzer (EA 3000, Italy). NH_4-N and NO_3-N were measured using a flow injection autoanalyzer (AACE, Germany). The concentrations of total phosphorus (TP) and available phosphorus (AP) were measured using inductively coupled plasma spectrometers (ICP; SPECTRO ARCOS EOP, Germany). The measurement of soil nutrients is performed following the approach of Han et al. (2019).

Plant Sampling

We randomly placed one 1 m × 1 m quadrat for sampling plant species composition of 72 sampling plots (6 treatments × 3 replicates × 2 grassland types × 2 years) at the peak growth rate in late July to early August of 2015 and 2016; the survey included species name, abundances for each species, plant height, and plant coverage (visual estimation of % cover of each species). We recorded 28 species in AS, including 9 species of non-forb and 19 species of forb, and 25 species in CG, including 9 species of non-forb and 16 species of forb. We randomly selected more than five individuals of each species in each plot for measuring the plant height (CI-202, America); plant height was the basic and easily measurable functional trait, and it significantly and positively correlated with N deposition (Diekmann and Falkengren-Grerup, 2002). In addition, we also calculated the SLA (i.e., a measure of projected leaf area per unit dry mass) by measuring leaf area (CI-202, America) and leaf weight (i.e., balance); the SLA was related to the changing pattern of the photosynthesis-N relationship based on mass and area (Reich et al., 1998). At the species level, we chose the dominant species (i.e., *Stipa capillata* in AS and *Elymus breviaristatus* in CG), since both coverages of *Stipa capillata* (about 15%) and *Elymus breviaristatus* (about 35%) in each plot were the largest in all species; at the functional group level, we divided different species into forb and non-forb, since there were few species for sedge and legume; at the community level, we calculated the community-weighted mean value (CWM) (Lavorel et al., 2008) by combining species relative abundances with population-based plant height and plant SLA from each plot.

Statistical Analysis

We modeled plant height, SLA, CWM height, and CWM-SLA of AS and CG as dependent variables, and pH, TN, NH4-N, NO3-N, AP, and TP as independent variables using the linear mixed-effects model (LMM). In the models, replicates were included as a random effect to account for spatial autocorrelation, and years were included as a random effect to annual variations in functional traits at the species level and CWMs within the same grassland type and treatment; replicates, years, and species (i.e., variations among different species of the same functional group) were included as a random effect for the functional group level within the same grassland type and treatment.

To assess the relative influence of N addition gradients, acidification, eutrophication, and P limitation on functional traits and CWMs of different grassland types, we tested eight candidate models, namely, (1) a null model with only $\log_{10}$ N addition gradients (Zhang et al., 2016), i.e., considering background value reported by Lu and Tian in 2007 (Lu and Tian, 2007), of 8 kg N/ha/year of N deposition in the Qinghai-Tibet Plateau, 8 kg N/ha/year for CK, 16 kg N/ha/year for NI, 30 kg N/ha/year for NII, 48 kg N/ha/year for NIII, 64 kg N/ha/year for NIV,

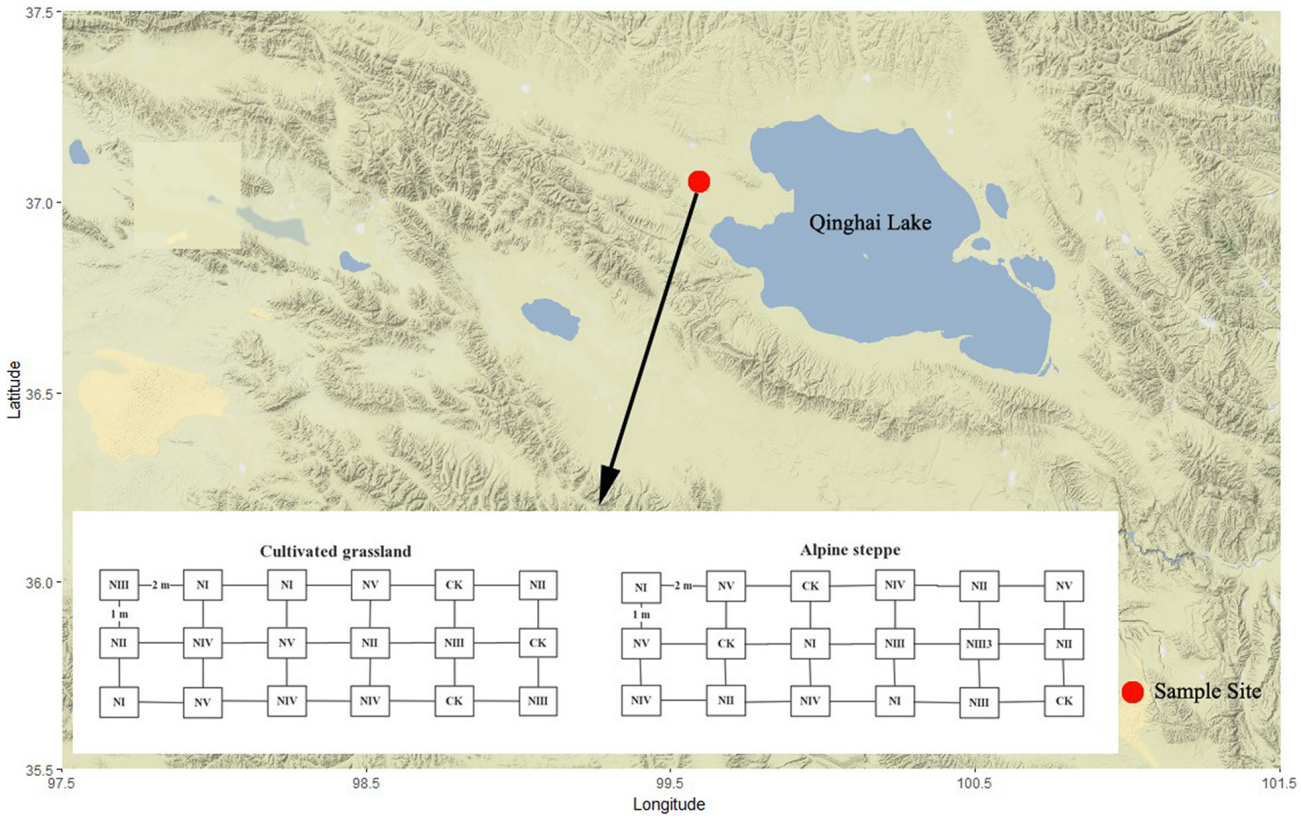

FIGURE 1 | Geographical location of the study site on the terrain-background map. CK, no N addition, NI, addition at 8 kg N/ha/year, NII, addition at 24 kg N/ha/year, NIII, addition at 40 kg N/ha/year, NIV, addition at 56 kg N/ha/year, and NV, addition at 72 kg N/ha/year.

80 kg N/ha/year for NV, and random effects for both AS and CG; (2) a eutrophication model in which TN and NH_4-N were added to the null model for AS, and TN, NH_4-N, and NO_3-N were added to the null model for CG; (3) an acidification model in which pH was added to the null model for both AS and CG; (4) a P availability model in which AP and TP were added to the null model for AS, and TP was added to the null model for CG; (5) a eutrophication and acidification model in which TN, NH_4-N, and pH were added to the null model for AS, and TN, NH_4-N, NO_3-N, and pH were for CG; (6) a eutrophication and P availability model in which TN, NH_4-N, AP, and TP were added to the null model for AS, and TN, NH_4-N, NO_3-N, and TP for CG; (7) an acidification and P availability model in which pH, AP, and TP were added to the null model for AS, and pH and TP for CG; (8) a full model including all variables (i.e., $\log_{10}$ N addition gradients, TN, NH_4-N, pH, AP, and TP) for AS, and $\log_{10}$ N addition gradients, TN, NH_4-N, pH, and TP for CG. There was collinearity between NO_3-N and NH_4-N (Pearson correlation coefficient = −0.86), and NH_4-N and TP (Pearson correlation coefficient = 0.70) in AS (**Supplementary Figure 1**); AP and TP (Pearson correlation coefficient = 0.76), and NH_4-N and AP (Pearson correlation coefficient = −0.77) in CG (**Supplementary Figure 2**). The best model was chosen by the lowest Akaike Information Criterion (AIC) models (Burnham and Anderson, 2002), within 2 units are generally considered to have equal weight (Lin et al., 2014), and the predictor variables of the best model were evaluated with the largest statistically significant parameter values (based on standardized data), judged as having the greatest relative impact on functional traits and CWMs of different grassland types, and marginal R^2 represents the variance explained by fixed factors, and conditional R^2 is interpreted as variance explained by both fixed and random factors (Johnson, 2014).

We used the "FD" packages to calculate CWM; "lme4" and "lmerTest" packages to perform LMM, and "MuMIn" packages to perform the goodness of fit (pseudo-R^2) of the LMM (Zurr et al., 2009) in the R version 3.5.1 (R Development Core Team).

RESULTS

Responses of Plant Functional Traits at the Species Level

The model with all factors at the species level provided the best fit for the height of *Stipa capillata* and *Elymus breviaristatus*, the SLA of *Elymus breviaristatus* with the lowest AIC values (**Tables 1**, **2**), indicating that N addition gradients, acidification, eutrophication, and P availability showed significant effects on *Stipa capillata* height (**Figure 2A**), *Elymus breviaristatus* height, and *Elymus breviaristatus* SLA. Soil pH was the most important

TABLE 1 | ΔAIC values of the linear mixed models of plant height and community weighted mean value of height in alpine steppe and cultivated grassland.

	Alpine steppe				Cultivated grassland			
	Species	**Non-forb**	**Forb**	**Community**	**Species**	**Non-forb**	**Forb**	**Community**
(1)	16.35	4.01	8.46	11.93	16.63	18.75	12.56	24.87
(2)	9.60	2.55	10.22	9.08	11.32	7.96	6.42	12.75
(3)	9.80	3.21	3.12	7.70	11.43	15.54	8.45	18.22
(4)	14.02	5.09	4.67	8.82	16.98	17.75	13.89	19.42
(5)	3.21	**0**	6.12	4.95	2.46	3.95	**0**	6.75
(6)	6.72	3.01	8.89	3.59	7.95	6.45	7.12	5.42
(7)	6.82	2.71	**0**	5.32	10.31	13.54	9.75	5.35
(8)	**0**	**0.58**	3.98	**0**	**0**	**0**	**1.45**	**0**

AIC values of the best models are shown in bold. (1) represents only log_{10} N addition gradients; (2) represents N addition gradients and eutrophication; (3) represents N addition gradients and acidification; (4) represents N addition gradients and P limit; (5) represents N addition gradients, eutrophication, and acidification; (6) represents N addition gradients, eutrophication, and P limit; (7) represents N addition gradients, acidification, and P limit; and (8) represents N addition gradients, acidification, eutrophication, and P limit.

TABLE 2 | ΔAIC values of the linear mixed models of SLA and community weighted mean value of SLA of alpine steppe and cultivated grassland.

	Alpine steppe				Cultivated grassland			
	Species	**Non-forb**	**Forb**	**Community**	**Species**	**Non-forb**	**Forb**	**Community**
(1)	3.04	**0.52**	3.31	**1.89**	8.88	4.14	8.46	7.67
(2)	2.52	2.61	**0**	2.23	3.06	**1.24**	**1.02**	2.25
(3)	**0**	**0**	3.45	**0**	5.42	2.54	7.43	5.29
(4)	6.39	6.60	9.42	7.43	16.07	4.85	10.32	15.80
(5)	**0.86**	2.01	**0.30**	**1.65**	7.84	**0.15**	**0**	8.27
(6)	4.02	6.23	5.48	4.61	10.79	**1.02**	2.54	10.54
(7)	4.02	5.96	9.75	7.26	12.97	3.43	9.33	13.38
(8)	**1.59**	5.62	6.21	4.33	**0**	**0**	**1.50**	**0**

AIC values of the best models are shown in bold. (1) represents only log_{10} N addition gradients; (2) represents N addition gradients and eutrophication; (3) represents N addition gradients and acidification; (4) represents N addition gradients and P limit; (5) represents N addition gradients, eutrophication, and acidification; (6) represents N addition gradients, eutrophication, and P limit; (7) represents N addition gradients, acidification, and P limit; and (8) represents N addition gradients, acidification, eutrophication, and P limit.

predictor of *Elymus breviaristatus* height, and the effect was positive (**Figure 2E**), but for *Elymus breviaristatus*, SLA and TP were the most important predictors (**Figure 3E**).

The model with log_{10} N addition gradients and pH provided the best fit for *Stipa capillata* SLA (**Table 2**), indicating that N addition gradients and acidification presented significant effects on *Stipa capillata* SLA (**Figure 3A**). However, low values of R^2 (0.09) of fixed factors suggested that much of the variation in *Stipa capillata* SLA remained unexplained (**Table 3**).

Responses of Plant Functional Traits at the Functional Group Level

The model with all factors for the functional groups of non-forbs and forbs in the CG provided the best fit for both height and SLA with the lowest AIC values (**Tables 1**, **2**), indicating that both N addition gradients, acidification, eutrophication, and P availability showed significant effects on the height and SLA of non-forbs and forbs in the CG. However, low values of R^2 (0.05) of fixed factors for non-forb SLA (**Figure 3F**) in the CG suggested that much of the variation in non-forb SLA remained unexplained (**Table 4**). NH_4-N was the most important predictor with negative impacts for the height of non-forb (**Figure 2B**) and forb functional groups in the CG (**Figures 2F,G**). In addition, log_{10} N and pH were the most important predictors with positive impacts for the height of forb functional groups in the CG (**Figure 2G**). NO_3-N was the most important predictor with a positive impact for the SLA of the forb group (**Figure 3G**).

The best model with the lowest AIC values for the height and SLA of non-forbs and forbs in the AS was inconsistent, e.g., N addition gradients and acidification were found as the key impact factors for the height of the non-forb functional group in the AS (**Table 1**), while the N addition gradients, acidification, and P availability were found as the key impact factors for the height of the forb functional group in the AS (**Table 1**). N addition gradients and acidification were identified as the key impact factors for the SLA of the non-forb functional group (**Figure 3B**) in the AS (**Table 2**), whereas N addition gradients and eutrophication were identified as the key impact factors for the SLA of the forb functional group in the AS (**Table 2**). However, values of R^2 of fixed factors were low (< 0.10) for non-forb height in the AS, non-forb SLA in the AS, and forb SLA in the AS (**Tables 3**, **4**). AP, TP, and pH were the most important predictors with positive effects for the height of the

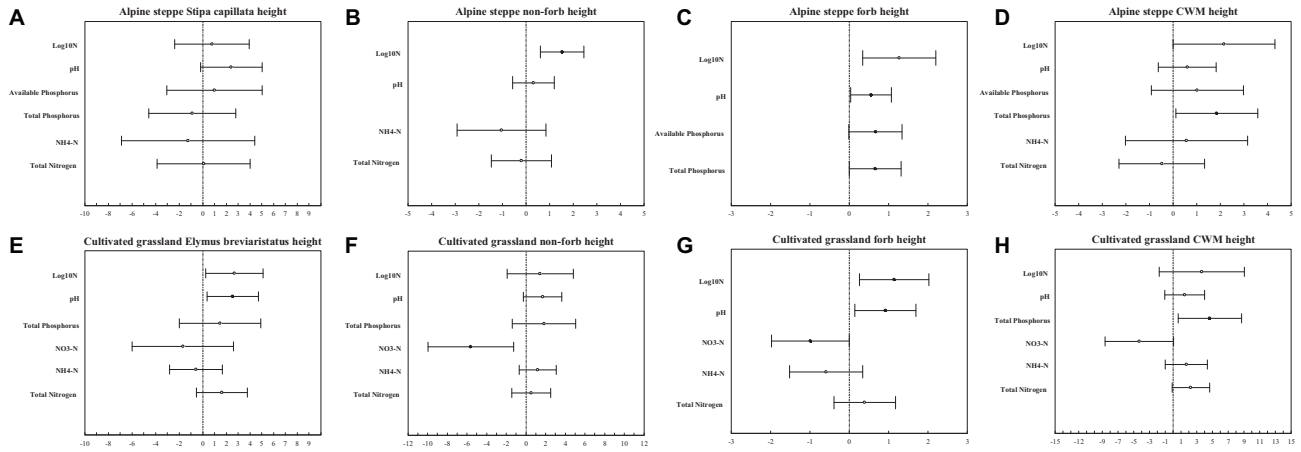

FIGURE 2 | Standardized parameter estimates (±2 SE) of $\log_{10}$ nitrogen addition gradients, pH, available phosphorus, total phosphorus NH_4-N, NO_3-N, and total nitrogen for *Stipa capillata* height **(A)**, non-forb height of alpine steppe **(B)**, forb height of alpine steppe **(C)**, community weighted mean value of height of alpine steppe **(D)**, *Elymus breviaristatus* height **(E)**, non-forb height of cultivated grassland **(F)**, forb height of cultivated grassland **(G)**, and community-weighted mean value of height of cultivated grassland **(H)**. Filled circles indicate significant effects ($p < 0.05$).

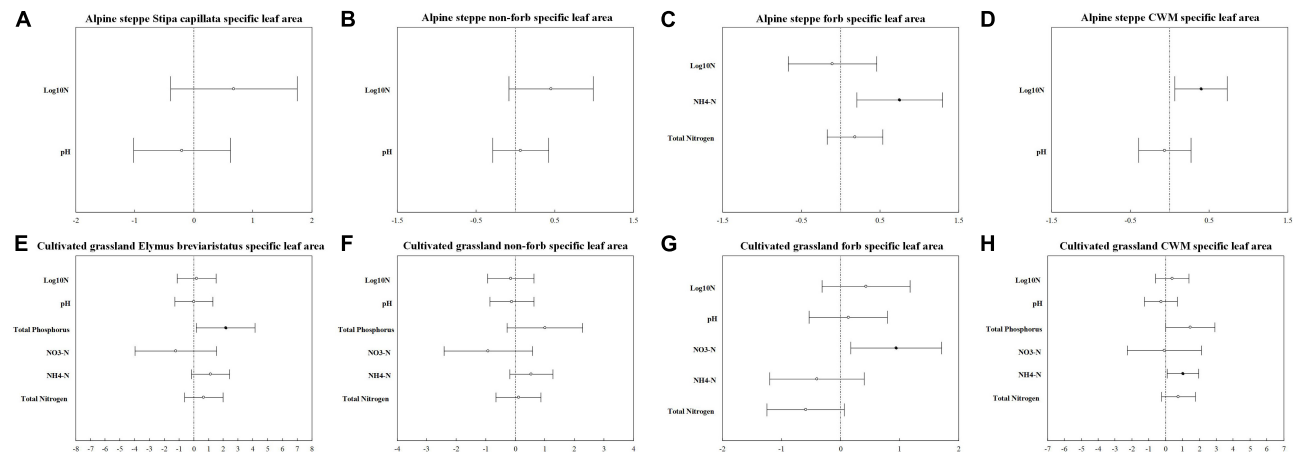

FIGURE 3 | Standardized parameter estimates (±2 SE) of $\log_{10}$ nitrogen addition gradients, pH, available phosphorus, total phosphorus NH_4-N, NO_3-N, and total nitrogen for *Stipa capillata* SLA **(A)**, non-forb SLA of alpine steppe **(B)**, forb SLA of alpine steppe **(C)**, community-weighted mean value of SLA of alpine steppe **(D)**, *Elymus breviaristatus* SLA **(E)**, non-forb SLA of cultivated grassland **(F)**, forb SLA of cultivated grassland **(G)**, and community-weighted mean value of SLA of cultivated grassland **(H)**. Filled circles indicate significant effects ($p < 0.05$).

forb functional group in the AS (**Figure 2C**). Ammoniacal N was the most important predictor with positive effects for the SLA of the forb functional group in the AS (**Figure 3C**).

Responses of Plant Functional Traits at the Community Level

The model with all factors at CWM height in AS and CG, CWM SLA in CG, provided the best fit with the lowest AIC values (**Tables 1**, **2**), indicating that N addition gradients, acidification, eutrophication, and P availability showed significant effects on the CWM height of plant communities in the AS and CG and on the CWM SLA in the CG (**Figures 3D,H**). TP was the most important predictor with positive effects for CWM height of plant communities in AS and CG (**Figures 2D,H**).

The model with $\log_{10}$ N addition gradients and pH at CWM SLA in AS provided the best fit with the lowest AIC values (**Table 2**), indicating that N addition gradients and acidification showed significant effects on CWM SLA of plant communities in the AS. The N addition gradient was the most important predictor with positive effects for CWM SLA of plant communities in the AS (**Figure 3D**).

DISCUSSION

At the species level, the responses of the height of *Stipa capillata* and the height and SLA of *Elymus breviaristatus* to N deposition can support our first hypothesis, i.e., eutrophication, acidification, and P availability associated with N deposition

TABLE 3 | The pseudo-R^2 of the linear mixed models of plant height and community weighted mean value of height in alpine steppe and cultivated grassland.

Rm^2/Rc^2	Alpine steppe				Cultivated grassland			
	Species	**Non-forb**	**Forb**	**Community**	**Species**	**Non-forb**	**Forb**	**Community**
(1)	0.01/0.09	0.02/0.61	0.05/0.67	0.23/0.46	0.18/0.21	0.02/0.78	0.03/0.66	0.14/0.44
(2)	0.14/0.14	0.04/0.65	0.05/0.70	0.23/0.81	0.22/0.24	0.05/0.81	0.09/0.66	0.21/0.54
(3)	0.07/0.24	0.02/0.61	0.06/0.69	0.25/0.49	0.26/0.35	0.03/0.78	0.04/0.66	0.19/0.45
(4)	0.03/0.12	0.02/0.62	0.09/0.68	0.32/0.53	0.21/0.22	0.03/0.79	0.04/0.65	0.21/0.51
(5)	0.22/0.22	**0.04/0.64**	0.06/0.70	0.22/0.78	0.28/0.64	0.07/0.83	**0.11/0.68**	0.26/0.54
(6)	0.14/0.14	0.03/0.62	0.09/0.68	0.37/0.51	0.25/0.27	0.10/0.86	0.10/0.67	0.30/0.62
(7)	0.09/0.28	0.02/0.62	**0.10/0.70**	0.33/0.56	0.28/0.28	0.04/0.80	0.09/0.66	0.23/0.50
(8)	**0.22/0.22**	**0.03/0.62**	0.10/0.70	**0.37/0.53**	**0.27/0.52**	**0.15/0.90**	**0.11/0.68**	**0.31/0.63**

Rm^2 represents the variance explained by fixed factors; Rc^2 is interpreted as variance explained by both fixed and random factors. (1) represents only log_{10} N addition gradients; (2) represents N addition gradients and eutrophication; (3) represents N addition gradients and acidification; (4) represents N addition gradients and P limit; (5) represents N addition gradients, eutrophication, and acidification; (6) represents N addition gradients, eutrophication and P limit; (7) represents N addition gradients, acidification, and P limit; and (8) represents N addition gradients, acidification, eutrophication, and P limit. AIC values of the best models are shown in bold.

TABLE 4 | The pseudo-R^2 of the linear mixed models of specific leaf area (SLA) and community weighted mean value of SLA of alpine steppe and cultivated grassland.

Rm^2/Rc^2	Alpine steppe				Cultivated grassland			
	Species	**Non-forb**	**Forb**	**Community**	**Species**	**Non-forb**	**Forb**	**Community**
(1)	0.08/0.24	0.03/0.21	>0.01/0.37	**0.16/0.16**	>0.01/0.02	>0.01/0.33	0.03/0.66	>0.01/0.16
(2)	0.10/0.26	0.04/0.30	**0.04/0.41**	0.34/0.83	0.10/0.10	0.07/0.32	**0.09/0.66**	0.09/0.26
(3)	**0.09/0.22**	**0.03/0.21**	>0.01/0.37	**0.16/0.16**	0.03/0.03	>0.01/0.32	0.04/0.66	0.01/0.13
(4)	0.09/0.24	0.04/0.26	0.01/0.36	0.19/0.19	0.16/0.60	0.05/0.53	0.04/0.65	0.14/0.69
(5)	0.11/0.23	0.04/0.29	0.04/0.41	**0.34/0.84**	0.11/0.11	**0.07/0.32**	**0.11/0.68**	0.12/0.21
(6)	0.13/0.25	0.11/0.51	0.04/0.41	0.34/0.93	0.19/0.66	0.05/0.43	0.10/0.67	0.20/0.84
(7)	0.09/0.24	0.04/0.26	>0.01/0.36	0.19/0.19	0.15/0.57	0.06/0.55	0.09/0.66	0.14/0.71
(8)	0.14/0.23	0.11/0.50	0.04/0.41	0.34/0.93	**0.18/0.67**	**0.05/0.49**	**0.11/0.68**	**0.21/0.87**

Rm^2 represents the variance explained by fixed factors; Rc^2 is interpreted as variance explained by both fixed and random factors. (1) represents only log_{10} N addition gradients; (2) represents N addition gradients and eutrophication; (3) represents N addition gradients and acidification; (4) represents N addition gradients and P limit; (5) represents N addition gradients, eutrophication, and acidification; (6) represents N addition gradients, eutrophication, and P limit; (7) represents N addition gradients, acidification, and P limit; and (8) represents N addition gradients, acidification, eutrophication, and P limit. AIC values of the best models are shown in bold.

interdependently impact the functional traits of plants of alpine grasslands. This is consistent with viewpoints of previous researchers that N, P, and pH were strongly interdependent with plant metabolism (Stevens et al., 2010; Phoenix et al., 2012; Laliberté et al., 2014). However, we observed that the SLA of *Stipa capillata* did not support this hypothesis, i.e., only acidification associated with N addition gradients was related to the SLA of *Stipa capillata*. In this study, we found that the SLA of *Stipa capillata* was not significantly correlated with any soil factors. We speculated that this may be related to the leaf configuration and leaf structure of *Stipa* spp., whose leaf blade is naturally curled and needle-shaped, unlike *Elymus breviaristatus*. Besides, the result from this study was inconsistent with the previous finding that plant height was significantly positively correlated with N deposition (Diekmann and Falkengren-Grerup, 2002). This could be buffer feedback for the alpine grassland ecosystem in coping with N deposition.

At the functional group level, non-forb functional groups were higher and larger than the forb functional groups due to stronger light competition under N deposition (Suding et al., 2005; Stevens et al., 2006; Cleland and Harpole, 2010; Borer et al., 2014), meaning that acidification, eutrophication, and P availability associated with N deposition were more conducive to non-forb functional group species. We observed that in log_{10} N addition gradients, NO_3-N was significantly positively related to plant height of non-forb functional groups in the AS; pH, AP, and TP were also significantly related to the plant height of forb functional groups in the AS. In contrast, we found that NO_3-N was significantly negatively related to the plant height of both forb and non-forb functional groups in the CG. This can support our third hypothesis, i.e., the responses of alpine plant functional traits to N deposition vary with grassland types/land-use types. The different responses between non-forb functional groups and forb functional groups in the same type of alpine grasslands to N application may be related to competitive interaction (Kardol et al., 2010); the subdominant species (e.g., forb species in either AS or CG) may respond to the changed competitive interaction with the dominant species (e.g., non-forb species in either AS or CG). In addition, we found that the SLA of forb functional groups was more sensitive to soil factors than the SLA of non-forb functional groups in both AS and CG. We speculated that the responses of the non-forb functional group may be light-driven,

shifting from soil N competition to light competition (Stevens et al., 2006; Cleland and Harpole, 2010; Borer et al., 2014; Zhang et al., 2020), while the responses of the forb functional groups may be nutrient-driven, competing for nutrients especially in the context of N deposition. Further studies are needed to test this assumption.

At the community level, we confirmed our first hypothesis by finding that the eutrophication, acidification, and P availability associated with N deposition inter- impacted the CWM height of plant communities in both AS and CG and the CWM SLA of the plant community in the CG. Since the abundance of each species was considered in the analysis, CWMs of plant communities would significantly increase due to the niche complementarity or over-yielding in the context of N addition (Wang et al., 2018), mainly due to increased dominance of grasses and the decreased dominance of forbs (Zavaleta et al., 2003; Clark and Tilman, 2008; Zhang et al., 2014, 2020; van den Berg et al., 2016). However, we only observed a similar phenomenon on the SLA of plant communities in the AS. We assumed the P availability associated with N deposition may play determining roles for this, as we found that TP and AP were significantly related to the CWM height of plant communities in the AS and the CGs and CWM SLA of the plant community in the CG. Although our previous studies indicated that lower than 14 of soil N:P ratio in both AS and CG along low-high N addition gradients (Han et al., 2019) implied these alpine grasslands were ecosystems with N limitation rather than P limitation (Stevens et al., 2006), the results derived from the responses of the functional traits of plants in this study suggest that it might be biased to conclude the ecosystems are N limited or P limited solely based on the soil N:P ratio.

The responses of the functional traits of alpine plants to N depositions showed the cascading effects from dominant species to functional groups and plant communities. This supports our second hypothesis. We assumed that the synchronous or asynchronous reactions of alpine plant traits of dominant species to functional groups and plant communities to N depositions were dependent mainly on two effects, namely, the mass effect and complementary effect. The mass effect hypothesis (Grime, 1998) emphasized that the ecosystems are largely controlled by the characteristics of dominant species or functional groups. The complementary effect may be important for the responses to N deposition, as the responses may be eliminated or weakened by complex species interactions (Cleland et al., 2006). We believed that the cascading responses from dominant grass species to non-forb functional groups were mainly controlled by mass effects, and the cascading responses from functional groups and plant communities were mainly regulated by the complementary effect, since the different reactions between non-forb plants and forb plants to N deposition may modify the overall biotic responses at the community level. The different cascading reactions of plant functional traits from dominant species to functional groups and plant communities to N deposition imply that the alpine grassland ecosystem is sensitive to N deposition. This is inconsistent with the finding of Wang et al. (2018) from the alpine meadow, which stressed that plant community-level traits can mediate effects of N addition. We think it is necessary to deduce the cascading responses of alpine plants to N deposition by combining the results from different alpine ecosystems.

Although we found that most of the cascading effects were synchronous in both the AS and the CG, we did catch a signal of the "insurance effect" in the SLA of forbs in the AS but not in the CG. As species diversity affected the stability of resistance of ecosystem functions to environmental disturbances according to the "insurance hypothesis" (Kahmen et al., 2005), we did see more resistance of plant functional traits, such as the heights and SLA in the AS with higher species diversity than the CG with lower species diversity in response to increasing N deposition. This can further support our third hypothesis that grassland types/land-use types can alter the responses of alpine plant functional traits to N deposition.

In summary, we applied eight linear mixed-effect models to explore the synchronous or asynchronous responses of cascading effects of plant functional traits (particularly, plant height and SLA) from dominant species to functional groups and whole communities in different types of grassland to N deposition. In conclusion, most of the responses of plant functional traits to acidification, eutrophication, and P availability associated with N deposition in the AS and the CG were synchronous, while only the response of the SLA of forb functional groups to eutrophication associated with N deposition in the AS was asynchronous. These findings may provide new insights for facilitating sound adaption strategies for sustainable grassland management to cope with N deposition in the alpine regions of the QTP or worldwide.

DATA AVAILABILITY STATEMENT

The raw data supporting the conclusions of this article will be made available by the authors, without undue reservation.

AUTHOR CONTRIBUTIONS

SL: investigation, data curation, formal analysis, and writing the original draft. ZZ: conceptualization and review. SD: funding acquisition, investigation, project administration, resources, supervision, and writing review and editing. HS, YX, JX, XG, SW, and PS: investigation and data curation. All authors contributed to the article and approved the submitted version.

FUNDING

This research was financially supported by grants from the National Science Foundation of China (Contract No. U20A2007-01), Second Tibetan Plateau Scientific Expedition and Research Program (2019QZKK0307), Grant from Key Project of Science and Technology of National Forestry and Grassland Administration, China (No. LCZD202007), Doctoral Research Startup Foundation of Shanxi Agricultural University (2021BQ34 and 2021BQ61), and Scientific research projects with reward funds for doctoral graduates and postdoctoral researchers working in Shanxi Province (SXBYKY2021067).

ACKNOWLEDGMENTS

We thank the reviewers for their helpful comments; the endeavor of editors and reviewers was also appreciated.

SUPPLEMENTARY MATERIAL

The Supplementary Material for this article can be found online at: https://www.frontiersin.org/articles/10.3389/fpls.2022.827035/full#supplementary-material

REFERENCES

Bobbink, R., Hicks, K., Galloway, J., Spranger, T., Alkemade, R., Ashmore, M., et al. (2010). Global assessment of nitrogen deposition effects on terrestrial plant diversity: a synthesis. *Ecol. Appl.* 20, 30–59. doi: 10.2307/27797787

Borer, E. T., Seabloom, E. W., Gruner, D. S., Harpole, W. S., Hillebrand, H., Lind, E. M., et al. (2014). Herbivores and nutrients control grassland plant diversity via light limitation. *Nature* 508:517. doi: 10.1038/nature13144

Burnham, K. P., and Anderson, D. R. (2002). *Models Selection and Multimodel Inference: a Practical Information-Theoretic Approach*, 2nd Edn. New York: Springer. doi: 10.1198/tech.2003.s146

Chen, H., Zhu, Q., Peng, C., Wu, N., Wang, Y., Fang, X., et al. (2013). The impacts of climate change and human activities on biogeochemical cycles on the Qinghai Tibetan Plateau. *Global Change Biol.* 19, 2940–2955. doi: 10.1111/gcb.12277

Clark, C. M., and Tilman, D. (2008). Loss of plant species after chronic low-level nitrogen deposition to prairie grasslands. *Nature* 451:712. doi: 10.1038/nature06503

Cleland, E. E., Chiariello, N. R., Loarie, S. R., Mooney, H. A., and Field, C. B. (2006). Diverse responses of phenology to global changes in a grassland ecosystem. *Proc. Natl. Acad. Sci. U. S. A.* 103, 13740–13744. doi: 10.1111/10.1073/pnas.0600815103

Cleland, E. E., and Harpole, W. S. (2010). Nitrogen enrichment and plant communities. *Ann. N. Y. Acad. Sci.* 1195, 46–61. doi: 10.1111/j.1749-6632.2010.05458.x

De Deyn, G. B., Cornelissen, J. H., and Bardgett, R. D. (2008). Plant functional traits and soil carbon sequestration in contrasting biomes. *Ecol. Lett.* 11, 516–531. doi: 10.1111/j.1461-0248.2008.01164.x

Diekmann, M., and Falkengren-Grerup, U. (2002). Prediction of species response to atmospheric nitrogen deposition by means of ecological measures and life history traits. *J. Ecol.* 90, 108–120. doi: 10.1046/j.0022-0477.2001.00639.x

Dong, S., Wen, L., Zhu, L., and Li, X. (2010). Implication of coupled natural and human systems in sustainable rangeland ecosystem management in HKH region. *Front. Earth Sci. Prc.* 4, 42–50. doi: 10.1007/s11707-010-0010-z

Field, C. D., Dise, N. B., Payne, R. J., Britton, A. J., Emmett, B. A., Helliwell, R. C., et al. (2014). The role of nitrogen deposition in widespread plant community change across semi-natural habitats. *Ecosystems* 17, 864–877. doi: 10.1007/s10021-014-9765-5

Greaver, T. L., Clark, C. M., Compton, J. E., Vallano, D., Talhelm, A. F., Weaver, C. P., et al. (2016). Key ecological responses to nitrogen are altered by climate change. *Nat. Clim. Change* 6:836. doi: 10.1038/nclimate3088

Grime, J. P. (1998). Benefits of plant diversity to ecosystems: immediate, filter and founder effects. *J. Ecol.* 86, 902–910. doi: 10.1046/j.1365-2745.1998.00306.x

Han, Y., Dong, S., Zhao, Z., Sha, W., Li, S., Shen, H., et al. (2019). Response of soil nutrients and stoichiometry to elevated nitrogen deposition in alpine grassland on the Qinghai-Tibetan Plateau. *Geoderma* 343, 263–268. doi: 10.1016/j.geoderma.2018.12.050

Hautier, Y., Niklaus, P. A., and Hector, A. (2009). Competition for light causes plant biodiversity loss after eutrophication. *Science* 324, 636–638. doi: 10.1126/science.1169640

Humbert, J. Y., Dwyer, J. M., Andrey, A., and Arlettaz, R. (2016). Impacts of nitrogen addition on plant biodiversity in mountain grasslands depend on dose, application duration and climate: a systematic review. *Global Change Biol.* 22, 110–120. doi: 10.1111/gcb.12986

Jing, X., Yang, X., Ren, F., Zhou, H., Zhu, B., and He, J. S. (2016). Neutral effect of nitrogen addition and negative effect of phosphorus addition on topsoil extracellular enzymatic activities in an alpine grassland ecosystem. *Appl. Soil. Ecol.* 107, 205–213. doi: 10.1016/j.apsoil.2016.06.004

Johansson, O., Palmqvist, K., and Olofsson, J. (2012). Nitrogen deposition drives lichen community changes through differential species responses. *Global Change Biol.* 18, 2626–2635. doi: 10.1111/j.1365-2486.2012.02723.x

Johnson, P. C. (2014). Extension of Nakagawa & Schielzeth's R2GLMM to random slopes models. *Methods Ecol. Evol.* 5, 944–946. doi: 10.1111/2041-210X.12225

Kahmen, A., Perner, J., and Buchmann, N. (2005). Diversity dependent productivity in semi-natural grasslands following climate perturbations. *Funct. Ecol.* 19, 594–601. doi: 10.1111/j.1365-2435.2005.01001.x

Kardol, P., Campany, C. E., Souza, L., Norby, R. J., Weltzin, J. F., and Classen, A. T. (2010). Climate change effects on plant biomass alter dominance patterns and community evenness in an experimental old field ecosystem. *Global Change Biol.* 16, 2676–2687. doi: 10.1111/j.1365-2486.2010.02162.x

Laliberté, E., Zemunik, G., and Turner, B. L. (2014). Environmental filtering explains variation in plant diversity along resource gradients. *Science* 345, 1602–1605. doi: 10.1126/science.1256330

Lavorel, S., Grigulis, K., McIntyre, S., Williams, N. S., Garden, D., Dorrough, J., et al. (2008). Assessing functional diversity in the field–methodology matters! *Funct. Ecol.* 22, 134–147. doi: 10.1111/j.1365-2435.2007.01339.x

Lavorel, S., Storkey, J., Bardgett, R. D., de Bello, F., Berg, M. P., Le Roux, X., et al. (2013). Linking functional diversity of plants and other trophic levels for the quantification of ecosystem services. *J. Veg. Sci.* 24, 942–948. doi: 10.1111/jvs.12083

Lin, F., Comita, L. S., Wang, X., Bai, X., Yuan, Z., Xing, D., et al. (2014). The contribution of understory light availability and biotic neighborhood to seedling survival in secondary versus old-growth temperate forest. *Plant Ecol.* 215, 795–807. doi: 10.1007/s11258-014-0332-0

Liu, X., Zhang, Y., Han, W., Tang, A., Shen, J., Cui, Z., et al. (2013). Enhanced nitrogen deposition over China. *Nature* 494:459. doi: 10.1038/nature11917

Liu, Y., Shi, G., Mao, L., Cheng, G., Jiang, S., Ma, X., et al. (2012). Direct and indirect influences of 8 yr of nitrogen and phosphorus fertilization on Glomeromycota in an alpine meadow ecosystem. *New Phytol.* 194, 523–535. doi: 10.1111/j.1469-8137.2012.04050.x

Lu, C. Q., and Tian, H. Q. (2007). Spatial and temporal patterns of nitrogen deposition in China: synthesis of observational data. *J. Geophys. Res. Atmos.* 112:10.

Lu, X., Mo, J., Gilliam, F. S., Zhou, G., and Fang, Y. (2010). Effects of experimental nitrogen additions on plant diversity in an old growth tropical forest. *Global Change Biol.* 16, 2688–2700. doi: 10.1111/j.1365-2486.2010.02174.x

Ma, B., Zhou, X., Zhang, Q., Qin, M., Hu, L., Yang, K., et al. (2019). How do soil micro-organisms respond to N, P and NP additions? Application of the ecological framework of (co-) limitation by multiple resources. *J. Ecol.* 107, 2329–2345. doi: 10.1111/1365-2745.13179

Moreau, D., Pivato, B., Bru, D., Busset, H., Deau, F., Faivre, C., et al. (2015). Plant traits related to nitrogen uptake influence plant- microbe competition. *Ecology* 96, 2300–2310. doi: 10.1890/14-1761.1

Payne, R. J., Dise, N. B., Field, C. D., Dore, A. J., Caporn, S. J., and Stevens, C. J. (2017). Nitrogen deposition and plant biodiversity: past, present, and future. *Front. Ecol. Environ.* 15, 431–436. doi: 10.1002/fee.1528

Phoenix, G. K., Emmett, B. A., Britton, A. J., Caporn, S. J., Dise, N. B., Helliwell, R., et al. (2012). Impacts of atmospheric nitrogen deposition: responses of multiple plant and soil parameters across contrasting ecosystems in long-term field experiments. *Global Change Biol.* 18, 1197–1215. doi: 10.1111/j.1365-2486.2011.02590.x

Phoenix, G. K., Hicks, W., and Cinderby, S. (2010). Opinion: atmospheric nitrogen deposition in world biodiversity hotspots: the need for a greater global perspective in assessing n deposition impacts. *Global Change Biol.* 12, 470–476. doi: 10.1111/j.1365-2486.2006.01104.x

Piao, S., Wang, X., Ciais, P., Zhu, B., Wang, T., and Liu, J. (2011). Changes in satellite derived vegetation growth trend in temperate and boreal Eurasia from

1982 to 2006. *Global Change Biol.* 17, 3228–3239. doi: 10.1111/j.1365-2486.2011.02419.x

Reich, P. B., Ellsworth, D. S., and Walters, M. B. (1998). Leaf structure (specific leaf area) modulates photosynthesis–nitrogen relations: evidence from within and across species and functional groups. *Funct. Ecol.* 12, 948–958. doi: 10.2307/2390490

Shen, M., Zhang, G., Cong, N., Wang, S., Kong, W., and Piao, S. (2014). Increasing altitudinal gradient of spring vegetation phenology during the last decade on the Qinghai–Tibetan Plateau. *Agr. For. Meteorol.* 189, 71–80. doi: 10.1016/j.agrformet.2014.01.003

Stevens, C. J., Dise, N. B., Gowing, D. J., and Mountford, J. O. (2006). Loss of forb diversity in relation to nitrogen deposition in the UK: regional trends and potential controls. *Global Change Biol.* 12, 1823–1833. doi: 10.1111/j.1365-2486.2006.01217.x

Stevens, C. J., Thompson, K., Grime, J. P., Long, C. J., and Gowing, D. J. (2010). Contribution of acidification and eutrophication to declines in species richness of calcifuge grasslands along a gradient of atmospheric nitrogen deposition. *Funct. Ecol.* 24, 478–484. doi: 10.1111/j.1365-2435.2009.01663.x

Suding, K. N., Collins, S. L., Gough, L., Clark, C., Cleland, E. E., Gross, K. L., et al. (2005). Functional- and abundance-based mechanisms explain diversity loss due to n fertilization. *Proc. Natl. Acad. Sci. U. S. A.* 102:4387. doi: 10.1073/pnas.0408648102

van den Berg, L. J., Jones, L., Sheppard, L. J., Smart, S. M., Bobbink, R., Dise, N. B., et al. (2016). Evidence for differential effects of reduced and oxidised nitrogen deposition on vegetation independent of nitrogen load. *Environ. Pollut.* 208, 890–897. doi: 10.1016/j.envpol.2015.09.017

Wang, F., Shi, G., Nicholas, O., Yao, B., Ji, M., Wang, W., et al. (2018). Ecosystem nitrogen retention is regulated by plant community trait interactions with nutrient status in an alpine meadow. *J. Ecol.* 106, 1570–1581. doi: 10.1111/1365-2745.12924

Zavaleta, E. S., Shaw, M. R., Chiariello, N. R., Mooney, H. A., and Field, C. B. (2003). Additive effects of simulated climate changes, elevated CO2, and nitrogen deposition on grassland diversity. *Proc. Natl. Acad. Sci. U. S. A.* 100, 7650–7654. doi: 10.1073/pnas.0932734100

Zhang, L., Zhu, T., Liu, X., Nie, M., Xu, X., and Zhou, S. (2020). Limited inorganic N niche partitioning by nine alpine plant species after long-term nitrogen addition. *Sci. Total Environ.* 718:137270. doi: 10.1016/j.scitotenv.2020.137270

Zhang, Y., Loreau, M., Lü, X., He, N., Zhang, G., and Han, X. (2016). Nitrogen enrichment weakens ecosystem stability through decreased species asynchrony and population stability in a temperate grassland. *Global Change Biol.* 22, 1445–1455. doi: 10.1111/gcb.13140

Zhang, Y., Lü, X., Isbell, F., Stevens, C., Han, X., He, N., et al. (2014). Rapid plant species loss at high rates and at low frequency of N addition in temperate steppe. *Global Change Biol.* 20, 3520–3529. doi: 10.1111/gcb.12611

Zhao, Z., Dong, S., Jiang, X., Liu, S., Ji, H., Li, Y., et al. (2017). Effects of warming and nitrogen deposition on CH4, CO2 and N2O emissions in alpine grassland ecosystems of the Qinghai-Tibetan Plateau. *Sci. Total Environ.* 592, 565–572. doi: 10.1016/j.scitotenv.2017.03.082

Zurr, A. F., Ieno, E. N., Walker, N. J., Saveliev, A. A., and Smith, G. M. (2009). *Mixed Effects Models and Extensions in Ecology With R*. New York: Springer. doi: 10.1111/j.1467-985X.2010.00663_9.x

Conflict of Interest: The authors declare that the research was conducted in the absence of any commercial or financial relationships that could be construed as a potential conflict of interest.

Publisher's Note: All claims expressed in this article are solely those of the authors and do not necessarily represent those of their affiliated organizations, or those of the publisher, the editors and the reviewers. Any product that may be evaluated in this article, or claim that may be made by its manufacturer, is not guaranteed or endorsed by the publisher.

Copyright © 2022 Li, Zhao, Dong, Shen, Xu, Xiao, Gao, Wu and Stufkens. This is an open-access article distributed under the terms of the Creative Commons Attribution License (CC BY). The use, distribution or reproduction in other forums is permitted, provided the original author(s) and the copyright owner(s) are credited and that the original publication in this journal is cited, in accordance with accepted academic practice. No use, distribution or reproduction is permitted which does not comply with these terms.

frontiers in Plant Science

ORIGINAL RESEARCH
published: 09 February 2022
doi: 10.3389/fpls.2021.824296

Precipitation Alters the Effects of Temperature on the Ecosystem Multifunctionality in Alpine Meadows

Yunhe Ma[1,2], *Lihua Tian*[3], *Guangpeng Qu*[2], *Ruicheng Li*[4], *Weiwei Wang*[5] and *Jingxue Zhao*[1,2]*

[1] State Key Laboratory of Grassland Agro-Ecosystems, Institute of Innovation Ecology and College of Life Sciences, Lanzhou University, Lanzhou, China, [2] State Key Laboratory of Hulless Barley and Yak Germplasm Resources and Genetic Improvement, Grassland Science Institute, Tibet Academy of Agricultural and Animal Husbandry Sciences, Lhasa, China, [3] Institute of Qinghai-Tibetan Plateau, Southwest Minzu University, Chengdu, China, [4] Key Laboratory for Earth Surface Processes of the Ministry of Education, Department of Ecology, College of Urban and Environmental Sciences, Peking University, Beijing, China, [5] Key Laboratory of Plateau Mountain Animal Genetics, Breeding and Reproduction, Ministry of Education, College of Animal Science, Guizhou University, Guiyang, China

Precipitation and temperature are major controls on multiple ecosystem functions in alpine grasslands. There is scant evidence for the interactive effects of temperature and precipitation changes on the ecosystem multifunctionality (EMF) in alpine meadows. To explore the interactive effects of temperature and precipitation changes on the EMF in alpine meadows, we transplanted meadow blocks reciprocally among three altitudes (4,650, 4,950, and 5,200 m) on the central Tibetan Plateau. Compared with the home sites (control), the EMF has a trend to increase when meadow blocks were downward transplanted (experimental warming) to the high-precipitation sites but decrease as meadow blocks were downward transplanted to the low-precipitation sites. However, the experimental cooling (upward transplantation) consistently reduced the EMF regardless of the precipitation change. The increase of EMF under the experimental warming was closely related to the variation of both plant and soil functions, whereas the reduction of EMF under the cooling was highly correlated with the decrease of plant function. Our results highlight that climate warming effects on the EMF are greatly associated with precipitation changes in the semi-arid alpine ecosystems.

Keywords: alpine meadow, ecosystem multifunctionality, climate change, reciprocal transplantation, Tibetan Plateau

OPEN ACCESS

Edited by:
Jian Sun,
Institute of Tibetan Plateau Research (CAS), China

Reviewed by:
Gang Fu,
Institute of Geographic Sciences and Natural Resources Research, Chinese Academy of Sciences (CAS), China
Xiaofeng Chang,
Northwest A&F University, China

***Correspondence:**
Jingxue Zhao
zjx@lzu.edu.cn

Specialty section:
This article was submitted to Functional Plant Ecology, a section of the journal Frontiers in Plant Science

Received: *29 November 2021*
Accepted: *27 December 2021*
Published: *09 February 2022*

Citation:
Ma Y, Tian L, Qu G, Li R, Wang W and Zhao J (2022) Precipitation Alters the Effects of Temperature on the Ecosystem Multifunctionality in Alpine Meadows. Front. Plant Sci. 12:824296. doi: 10.3389/fpls.2021.824296

HIGHLIGHTS

- Cooling consistently reduces EMF regardless of the precipitation change.
- Warming effects on EMF are highly associated with precipitation changes.

INTRODUCTION

Ecosystem functioning and services are being increasingly threated by climate change (Hooper et al., 2005, 2012; Balvanera et al., 2006). Ecosystem multifunctionality (EMF), which simultaneously represents the provision of multiple ecosystem functions, has been proposed as a reliable indicator to reflect the effects of climate change on ecosystem services and functioning

(Hector and Bagchi, 2007; Isbell et al., 2011; Manning et al., 2018). Plant and soil microorganisms are major producers and decomposers of terrestrial ecosystems, and have been considered as key drivers in regulating the EMF (Wardle et al., 2004; Bardgett and van der Putten, 2014). Evidence is mounting that global climate change are altering above and belowground biodiversity and which might directly and indirectly influence the EMF (Maestre et al., 2012; Jing et al., 2015; Hu et al., 2021). Understanding how climate change affect the EMF, is important for predicting future ecosystem functions and their provision of services such as productivity, nutrient and carbon cycling.

Plant and soil microbial diversity have been shown to enhance the EMF in grasslands (Maestre et al., 2012; Berdugo et al., 2020; Hu et al., 2021). However, it is noticed that the relationships between biodiversity and EMF depend greatly on the environmental gradient (Isbell et al., 2011; Perkins et al., 2015; Yang et al., 2017). Precipitation is considered as major control on the EMF in grasslands (Maestre et al., 2012; Hu et al., 2021). Higher precipitation generally associated with higher soil water conditions and nutrient availability, which could facilitate resource use by plant and soil microorganisms, and ultimately may attribute to higher EMF (Wu et al., 2012; Jing et al., 2015; Wang et al., 2021a). Several studies have shown that climate warming can directly and indirectly influence plant community, vegetation productivity and soil microbe (Xu et al., 2013; Wang et al., 2021b; Wu et al., 2021), which may attribute to the EMF by altering resources cycling, carbon cycling and other processes involved in the EMF (Zhao et al., 2019; Wang et al., 2021b). However, in grasslands, temperature elevation is often accompanied with precipitation change (Flanagan and Johnson, 2005; Hu et al., 2016). It is likely that warming effects on the EMF may be strongly dependent on precipitation in grassland ecosystems (Jing et al., 2015; Zhao et al., 2019; Hu et al., 2021).

The Tibetan Plateau has become warmer and wetter in recent decades, with the magnitude of climate warming dramatically larger than surrounding areas (Yang et al., 2014; Kuang and Jiao, 2016). The Plateau contains the highest and largest alpine grasslands in the world (Lehnert et al., 2016; Li et al., 2020), which has been regarded sensitive and vulnerable to climate change (Sun et al., 2020). The climate warming with concomitant changes in precipitation is expected to have remarkable effects on the EMF of alpine grasslands by altering ecosystem functions such as vegetation growth, biological diversity and biogeochemical processes (Li et al., 2016b; Ma et al., 2017; Yu et al., 2019; Wang et al., 2020a). Considerable studies have highlighted the responses of EMF to nitrogen addition (Cui et al., 2020; Liu et al., 2021), livestock grazing (Wang et al., 2020b) and environmental changes (Jing et al., 2015; Wang et al., 2021a) in alpine grasslands. Although previous studies have explored the linkages between biodiversity and EMF and further demonstrated the possible consequences of climate change on the EMF in the alpine grasslands (Jing et al., 2015; Pan et al., 2017; Wang et al., 2021b), little attention has been paid to clarify the interactive effects of temperature and precipitation changes on the EMF in the Tibetan alpine meadows.

To examine the effects of climate change on the EMF in alpine meadows, we performed a reciprocal transplantation experiment along an altitudinal gradient of the Nyaiqentanglha Mountains on the central Tibetan Plateau. We simulated warming treatment expected under future climate change and cooling treatment usually occurred over temperature anomalies events through transplanting meadow blocks to lower and higher altitudes (Zhao et al., 2018; Wang et al., 2019a,b). Previous studies have provided basic ecological information along the altitudinal gradient of the Nyaiqentanglha Mountains including plant phenology (Li et al., 2016a, 2020), species distribution (Li et al., 2013; Wang et al., 2013) and carbon dynamics (Zhao et al., 2016, 2018). In this study, we evaluated how the EMF of alpine meadows would response to temperature and precipitation changes across altitudes. Our study aimed to address the following issues: (1) the different response patterns of the EMF to warming and cooling and (2) the underlying mechanisms of precipitation mediate the EMF responses to temperature changes.

MATERIALS AND METHODS

Study Sites

The experiment was conducted at a slope of the Nyaiqentanglha Mountains (30°30′-30°32′N, 91°03′E; 4,650, 4,950, and 5,200 m) on the central Tibetan Plateau (**Figure 1**; **Supplementary Figure S1**). This region has a semi-arid climate, characterized by Indian monsoon in summer and the westerlies in winter. Annual precipitation was 479 mm and annual mean air temperature was 1.8°C (Wang et al., 2013). Along the south slope of the Nyaiqentanglha Mountains, annual precipitation increased with increasing altitude, but annual mean air temperature and soil temperature decreased with increasing altitude (**Supplementary Figure S2**). Alpine meadows dominated by *Kobresia pygmaea* distributed at altitudes between 4,650 m (lower limit) and 5,200 m (upper limit), with a distribution center at 4,950 m. Other coexisting species mainly included *Kobresia humilis*, *Kobresia humilis*, *Androsace tapete*, *Polygonum macrophyllum*, *Thalictrum alpinum* etc. (Zhao et al., 2016). The vegetation cover at the studies sites is about 50–90% and the alpine meadows generally turn green in May and the plant biomass reach its peak in August. The soils were poorly developed characterized by low clay content within surface soil horizons and the soil types changed from alpine steppe soil to alpine meadow soil along the altitudinal gradient. HOBO weather stations (Onset Inc., Bourne, MA, USA) were set up along the altitudinal gradient from 4,400 to 5,200 m. Air temperature and precipitation (1.5 m aboveground) were recorded by the HOBO data logger to characterize altitudinal environments along the slope.

Experimental Design

Intact meadow blocks (70 cm × 70 cm wide × 40 cm depth) with attached vegetation were cut off for reciprocal transplantation from the plots at 4,650, 4,950, and 5,200 m in September of 2011 (**Figure 1**). There were six replicate intact meadow blocks from each altitude, which were randomly transferred throughout the study site. For each of the 3 altitudes, 6 of the 18 intact meadow blocks were reinstated at the same

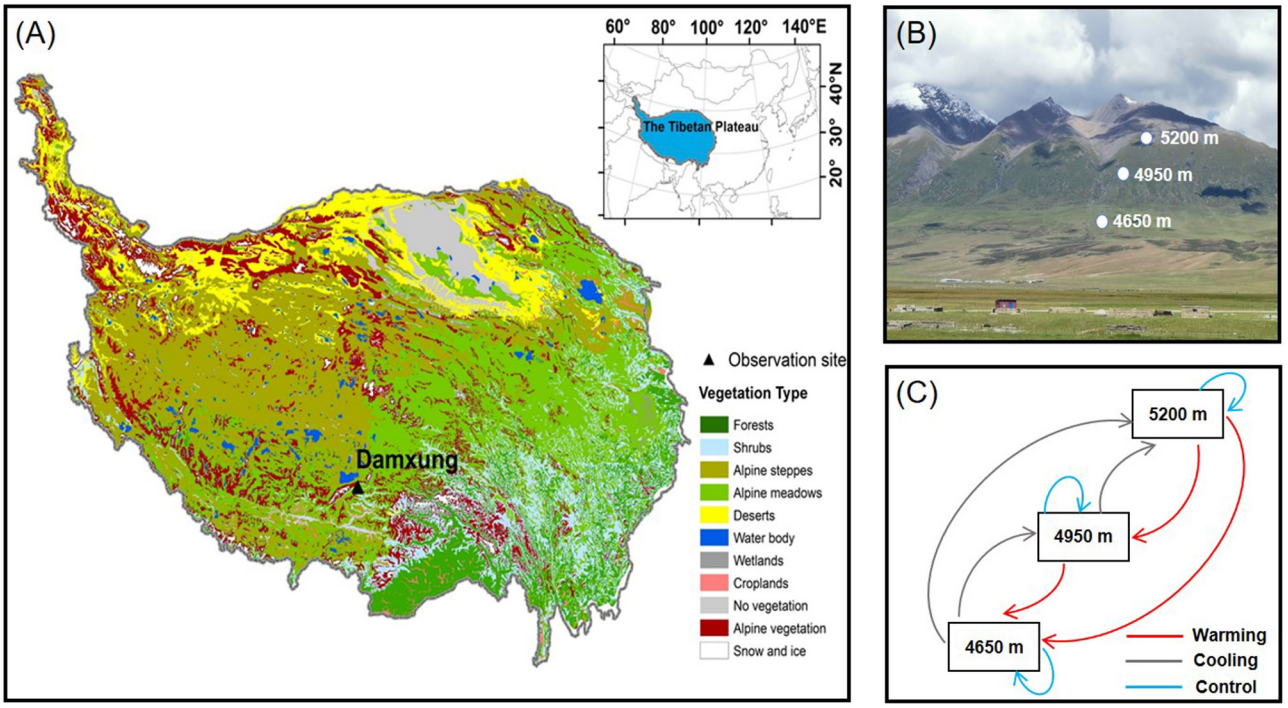

FIGURE 1 | (A) Vegetation map of the Tibetan Plateau and the location of study site. **(B)** Diagram of the landscape and experimental sites along the slope of Nyaiqentanglha Mountains. **(C)** Reciprocal transplants experiment along an altitudinal gradient in the Tibetan alpine meadows.

altitude as control (home sites), and the other 12 intact meadow blocks were transferred equally between the other 2 altitudes (translocated plots). Thus, 54 intact meadow blocks (18 soil blocks per altitude × 3 altitudes) were used in the experiment. Compared with the home sites, the meadow blocks transferred from higher altitudes to lower altitudes (translocated sites) can expose to warmer conditions (warming) and transferred from lower altitudes to higher altitudes expose to cooler conditions (cooling). The experimental design was described elsewhere in detail (Zhao et al., 2018).

Vegetation Measurement

In Mid-August of 2014, we sampled a 50 × 50 cm quadrat within each meadow block and measured the vegetation cover (VC) and community height (CH) at each quadrat. The species richness (SR) was defined according to the number of plant species. Aboveground plant biomass (AGB) was estimated using a non-destructive sampling method, and the detailed information was described elsewhere (Wang et al., 2013; Zhao et al., 2018). The belowground plant biomass (BGB) was estimated through collecting five soil cores (diameter 3.0 cm; depth 10 cm) and washing off the soil by a 2-mm sieve. The BGB samples were dried by an oven at 65°C for 48 h and weighed. The Shannon-Wiener index was calculated to quantify species diversity (SD) of alpine meadow using the following function: $SD = \sum_{i=1}^{S}(PiLnPi)$, where S is the total number of alpine meadow community and *Pi* is the relative importance value (IV) of the *i*th species calculated as: IV = (relative height + relative cover + relative biomass)/3 (Wu et al., 2009).

Ecosystem Respiration and Physiochemical Data Measurements

On sunny days during the growing season (June–September), diurnal variation (08:00–18:00, local time) of ecosystem respiration (Re) at 2 h intervals were measured twice a month in 2014 using the opaque chamber of Li-8100 103 automatic soil CO_2 flux system (LI-COR Biosciences, Lincoln, NE, USA). Soil temperature (ST) and soil moisture (SM) at each collar were measured simultaneously with Re by a Time Domain Reflectometer. Top soil samples (0–10 cm in depth) were collected with a soil auger (diameter: 3.0 cm) within each quadrat. Soil samples for measuring soil organic carbon (SOC) and soil total nitrogen (STN) were air-dried at room temperature and sieved (2–mm mesh). Soil samples for measuring soil microbial biomass carbon (MBC) and soil microbial biomass nitrogen (MBN), ammonium nitrogen (NH_4^+-N) and nitrate nitrogen (NO_3^--N) analysis were immediately stored in the lab at −20°C until processing. The SOC was measured by the Walkley and Black dichromate oxidation method (Walkley and Black, 1934). The determination of STN was based on the Kjeldahl method (Gallaher et al., 1976). Soil inorganic nitrogen Soil ammonium nitrogen (NH_4^+-N) and nitrate nitrogen (NO_3^--N) were measured with an auto-analyser (Bran Luebbe, Germany) in 0.05 M K_2SO_4 extracts. The MBC and MBN were

measured using the chloroform fumigation-extraction method (Vance et al., 1987).

Ecosystem Multifunctionality

To determine the average multifunctionality, we calculated Z-scores of the 15 ecosystem functions (VC, CH, SR, PD, AGB, BGB, SOC, STN, MBC, MBN, NH_4^+-N, NO_3^--N, ST, SM, Re) evaluated before the analysis, and considered the EMF index as the average Z-score of all the 15 ecosystem functions measured within the plot (Maestre et al., 2012): $EMF = \sum_i^N (Zij/N)$, where *Zij* represents Z-score of the *i*th ecosystem function in the *j*th plot and N is the total number of ecosystem functions evaluated (Wang et al., 2021b).

Statistical Analysis

One-way analysis of variance (ANOVA) and the Tukey-HSD test was applied to assess the differences in the VC, CH, SR, PD, AGB, ST, SM, SOC, STN, MBC, MBN, NH_4^+-N, NO_3^--N, Re, and the EMF at home sites among the three altitudes (4,650, 4,950, and 5,200 m). Independent sample *t*-test was used to test the differences in these plant and soil functions as well as the EMF between control and transplanted plots. The relative changes (Δ) in the ecosystem functions and the EMF between the control and transplanted plots was calculated as: Relative change (Δ) = Transplanted – Control. Pearson correlation and a simple linear model (y = a + bx) was used to determine correlations of the relative changes in the ecosystem functions with that of the EMF. All statistical analyses were performed using SPSS 20.0 (SPSS Inc., Chicago, Illinois, USA), and graphics were drawn using the OriginPro 2019 software (OriginLab Corporation, Northampton, MA, USA).

RESULTS

Vegetation Characteristics

The CH at the home sites generally decreased with increasing altitude from 4,650 to 5,200 m, and there were no significant differences in the SR and PD at home sites among three altitudes (**Supplementary Figure S3**). However, we found that VC, AGB, and BGB home site were greatly higher at 4,950 m than

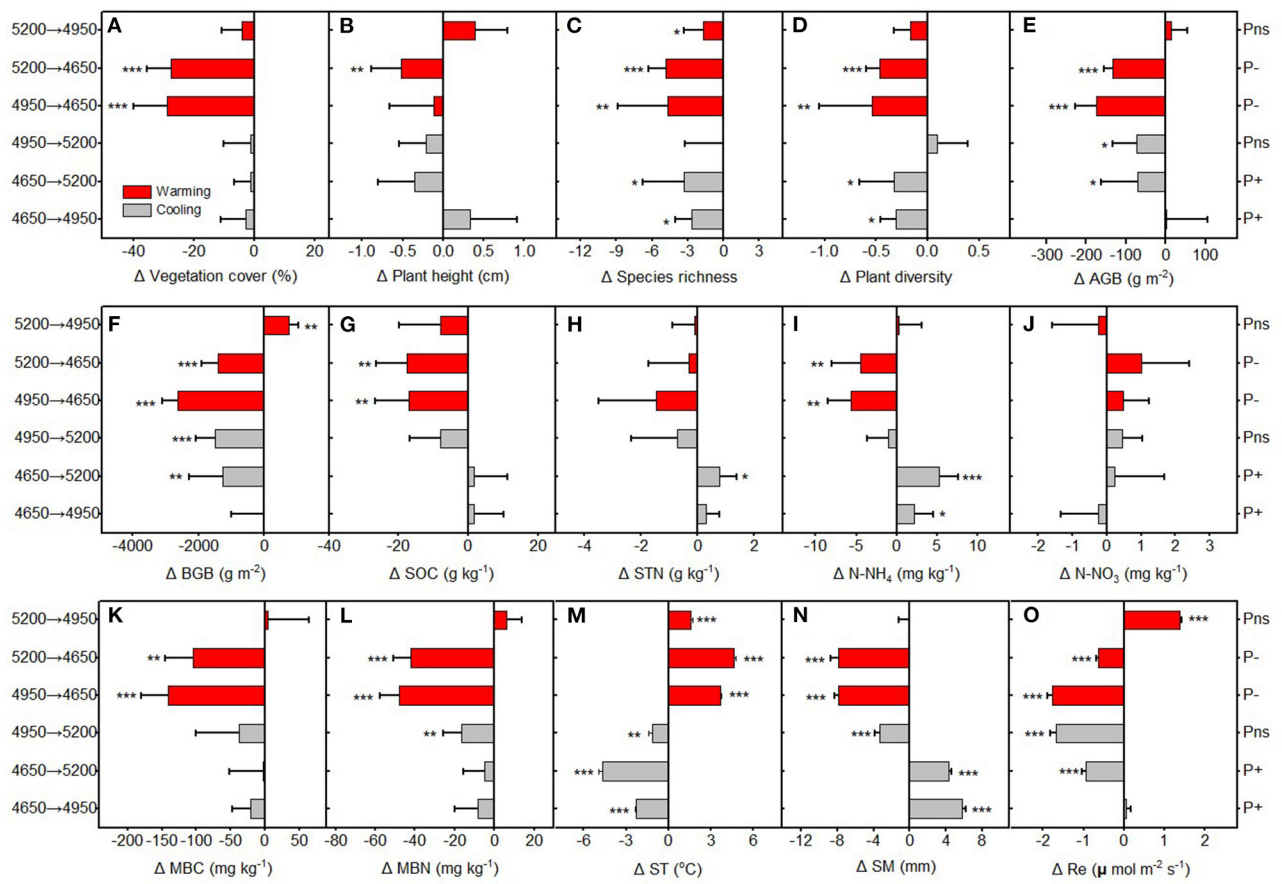

FIGURE 2 | The relative changes in **(A)** vegetation cover (VC), **(B)** community height (CH), **(C)** species richness (SR), **(D)** plant diversity (PD), **(E)** above ground biomass (AGB), **(F)** belowground ground biomass (BGB), **(G)** soil organic carbon (SOC), **(H)** soil total nitrogen (STN), **(I)** ammonium nitrogen (NH_4^+–N), **(J)** nitrate nitrogen (NO_3^- –N), **(K)** soil microbial biomass carbon (MBC) and **(L)** soil microbialbiomass nitrogen (MBN), **(M)** soil temperature (ST), **(N)** soil moisture (SM) and **(O)** ecosystem respiration (Re) between translocated sites and control sites (home-sites) along the altitudinal gradient. P+, precipitation increased; P−, precipitation decreased; Pns, precipitation unchanged. Asterisks are significant at different levels between translocated sites and control sites. *$p < 0.05$; **$p < 0.01$; ***$p < 0.001$. Mean±SD is shown in errorbars.

that at 4,650 and 5,200 m (**Supplementary Figure S3**). Both the upward transplantation (cooling) and downward transplantation (warming) resulted in a decrease of the VC, CH, and SR, as compared with the home sites (**Figures 2A,C,D**). Cooling resulted in a decrease of the AGB and BGB regardless of the precipitation change (**Figures 2E,F**). However, warming significantly decreased AGB and BGB at the drier destination sites (transplanted from 5,200 and 4,950 m to 4,650 m), but increased BGB at the wetter destination site (transplanted from 5,200 to 4,950 m) (**Figures 2E,F**).

Soil Properties and Ecosystem Respiration

The SOC, STN, MBC, and MBN at the home sites were significant higher at 4,950 m compared with that at 4,650 and 5,200 m (**Supplementary Figure S3**). The NO_3^--N at the home sites generally decreased with increasing altitude (**Supplementary Figure S3**). However, NH_4^+-N were significantly lower at 4,650 m than that at 4,950 and 5,200 m (**Supplementary Figure S3**). Compared with the home sites, cooling had no significant effects on SOC, MBC, and MBN, whereas experimental warming significantly decreased SOC, MBC, and MBN as downward transplanted to the drier destination sites (transplanted from 5,200 and 4,950 m to 4,650 m) (**Figures 2G,K,L**). Warming tended to decrease NH_4^+-N at drier destination sites, but cooling has a trend to increase NH_4^+-N at wetter destination sites (**Figure 2I**). Both the upward transplantation (cooling) and downward transplantation (warming) have no significant effects on STN and NO_3^--N, as compared with the relative home sites (**Figures 2H,J**). The ST significantly decreased with increasing altitudes (**Supplementary Figure S3**). However, SM were significant lower at 4,650 m than that at 4,950 and 5,200 m (**Supplementary Figure S3**). The growing season Re at the home sites was the highest at 4,950 m (**Supplementary Figure S3**). Cooling generally decreased Re as compared with the relative home sites (**Figure 2O**). Warming significantly decreased the Re as downward transplanted to the relative drier destination sites, but increased the Re as downward transplanted to the relative wetter destination site (**Figure 2O**).

Ecosystem Multifunctionality

The EMF index at the home sites varies greatly along altitudinal gradient, with the highest value at the 4,950 m and the lowest value at 4,650 m (**Figure 3A**). The responses of EMF index to warming and cooling also differed remarkable with altitudes. Regardless of the precipitation change, experimental cooling generally resulted in a decrease of the EMF (**Figure 3B**). However, experimental warming tended to decrease the EMF as downward transplanted to the drier sites but increase the EMF when downward transplanted to the wetter site (**Figure 3B**). We fitted a linear model to evaluate the relationships between multiple biotic and abiotic factors and the EMF (**Figure 4**). We found that VC, SR, PD, vegetation productivity (AGB and BGB), SOC, STN, NH_4^+-N, MBC, MBN, SM, and Re were positively related with the EMF, whereas NO_3^--N was negatively associated with the EMF across altitudes (**Figure 4**). We found that transplant-induced changes in most of the plant and soil functions were greatly attributed to that of the EMF (**Supplementary Figure S4A**), but only the transplant-induced changes in CH, AGB, BGB, STN, and SM were significantly associated with that of the EMF (**Supplementary Figure S4B**). The annual air temperature and ST showed a weakly association with the EMF, but warming-induced changes in ST was significantly and negatively correlated with that of the EMF (**Figures 4M**, **5A,C**). Additionally, the annual precipitation and SM showed a positively association with the EMF, and warming-induced relatively changes in SM was significantly and positively correlated with that of EMF (**Supplementary Figure S4**; **Figures 5B,D**).

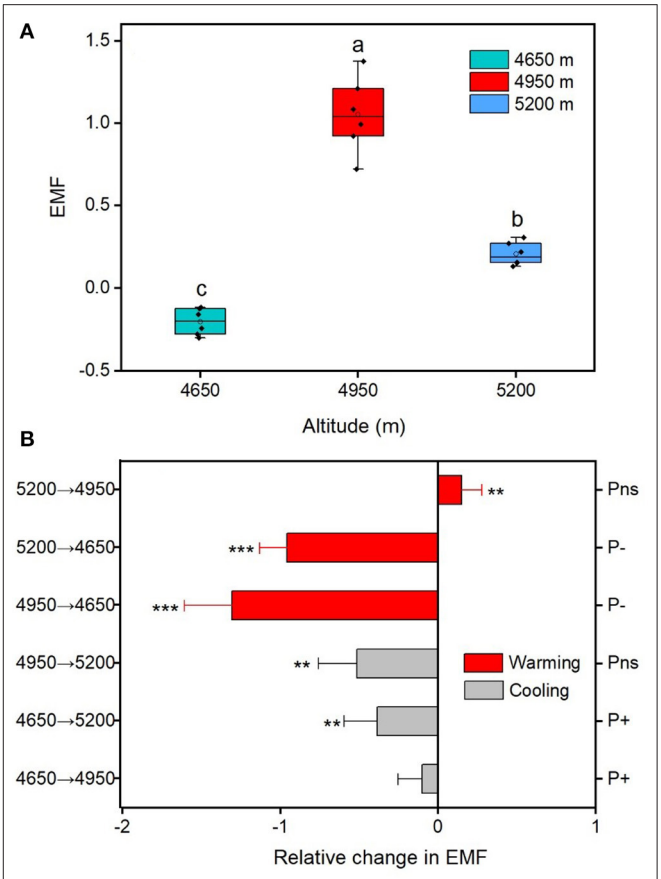

FIGURE 3 | Characteristics of ecosystem multifunctionality (EMF) in alpine meadows. **(A)** Difference of EMF for the home sites across the three altitudes. **(B)** The relative changes in EMF between translocated sites and control sites (home-sites). Asterisks are significant at different levels between translocated sites and control sites. $^{**}p < 0.01$; $^{***}p < 0.001$. Different letters between altitudes indicate the significant difference at 0.05 level. Values in parentheses indicate SD of mean.

DISCUSSIONS

In alpine grasslands, numerous studies have explored the relationships among plant or soil microbial diversity and the EMF in alpine grasslands and further demonstrated that

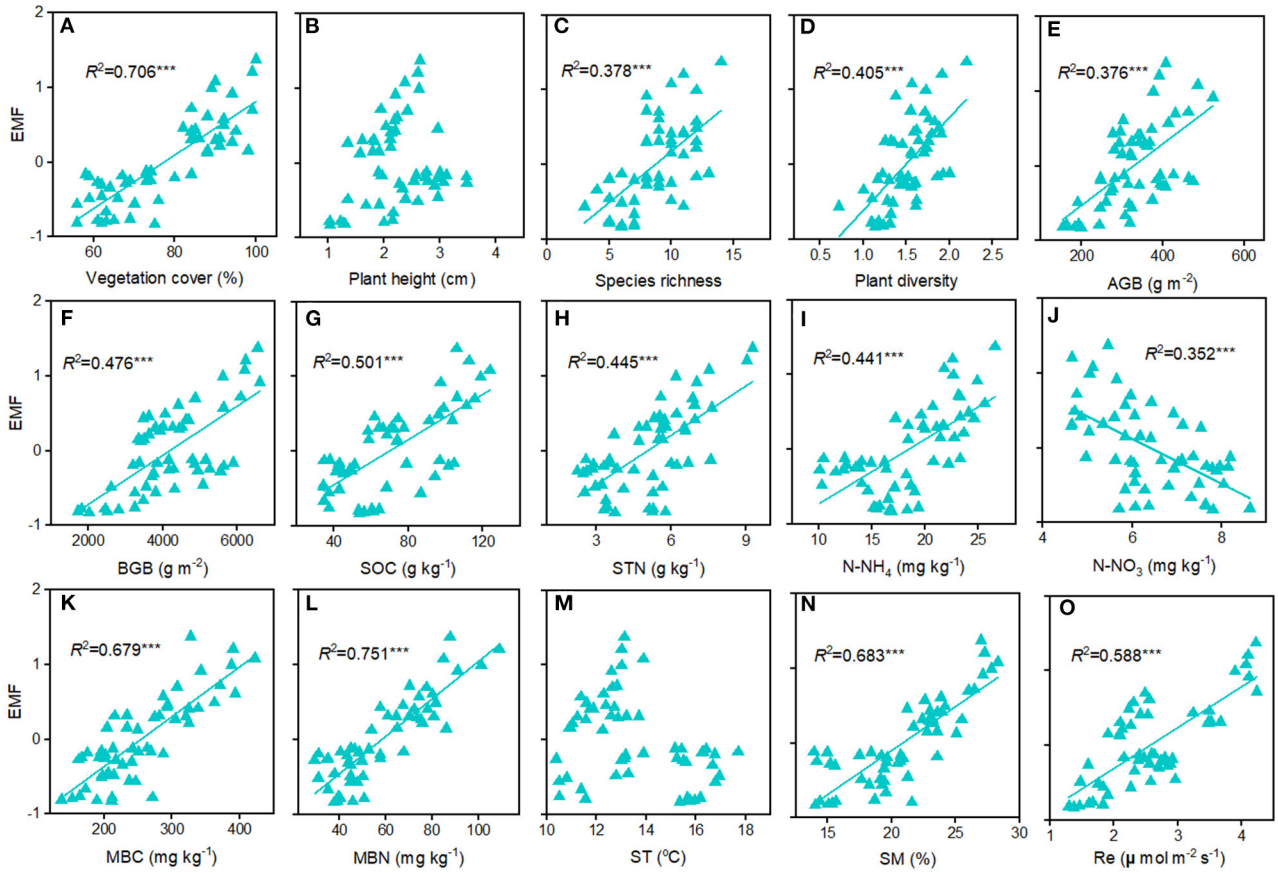

FIGURE 4 | Relationships among ecosystem multifunctionality and factors in the Tibetan alpine meadows. **(A)** VC, vegetation cover; **(B)** CH, community height; **(C)** PD, plant diversity; **(D)** SR, species richness; **(E)** AGB, above ground biomass; **(F)** BGB, belowground ground biomass; **(G)** SOC, soil organic carbon; **(H)** STN, soil total nitrogen; **(I)** NH_4^+–N, ammonium nitrogen; **(J)** NO_3^-–N, nitrate nitrogen; **(K)** MBC, soil microbial biomass carbon; **(L)** MBN, soil microbial biomass nitrogen; **(M)** ST, soil temperature; **(N)** SM, soil moisture; **(O)** Re, ecosystem respiration. ***$p < 0.001$.

aboveground or belowground biodiversity generally positively related to the EMF (Jing et al., 2015; Wang et al., 2021a). Our study, along an altitudinal gradient on the central Tibetan Plateau, also found that vegetation productivity and plant diversity were positively correlated with the EMF in alpine meadows (**Figures 4C–F**). In grasslands, MBC and MBN were strongly linked to soil microbial activity and usually were treated as indicators of nutrient availability for soil microorganisms (Bastida et al., 2016). Likewise, in the present study, the best-fitting relationships were found between the EMF and MBC and MBN (**Figures 4K,L**), suggesting that belowground biodiversity may be positively correlated with the EMF. However, we also found that transplant-induced changes in the SM rather than ST could well explain that of the EMF (**Figure 4N**; **Supplementary Figure S4B**), which indicate that the positive relationships between biodiversity and the EMF in alpine meadows could be particularly modified by precipitation changes.

Climatic changes on the EMF are particularly important in alpine meadows because their biological activity is mainly driven by temperature and precipitation (Zhao et al., 2019), which can affect the EMF through influencing plants and soil microorganisms (Zhao et al., 2019; Wang et al., 2021b). Previous study suggested that the annual mean temperature and total precipitation on the Tibetan Plateau are predicted to increase by 2.8–4.9°C and by 15–21%, respectively, by the end of the twenty-first century (Gao et al., 2014). Ongoing climate warming is likely to reduce aboveground and belowground biodiversity, which will negatively affect the EMF in semi-arid alpine grasslands (Fu et al., 2012; Hu et al., 2020). Our results suggested that experimental warming tended to decrease plant species, vegetation production, MBC and MBN as well as the EMF at the low-precipitation sites but increase those factors at the high-precipitation site (**Figure 2**). It is possible that plant growth and soil microbial activity might be limited by soil water and nutrient conditions under low precipitation, while under high precipitation, plant and soil microorganisms might play positive roles on the EMF, as observed under the experimental warming (**Figure 4**; **Supplementary Figure S4**). In the present study, we found that species richness, plant diversity, vegetation productivity, MBC and MBN were positively correlated with the EMF (**Figures 4C,D**), the increased EMF under warming can

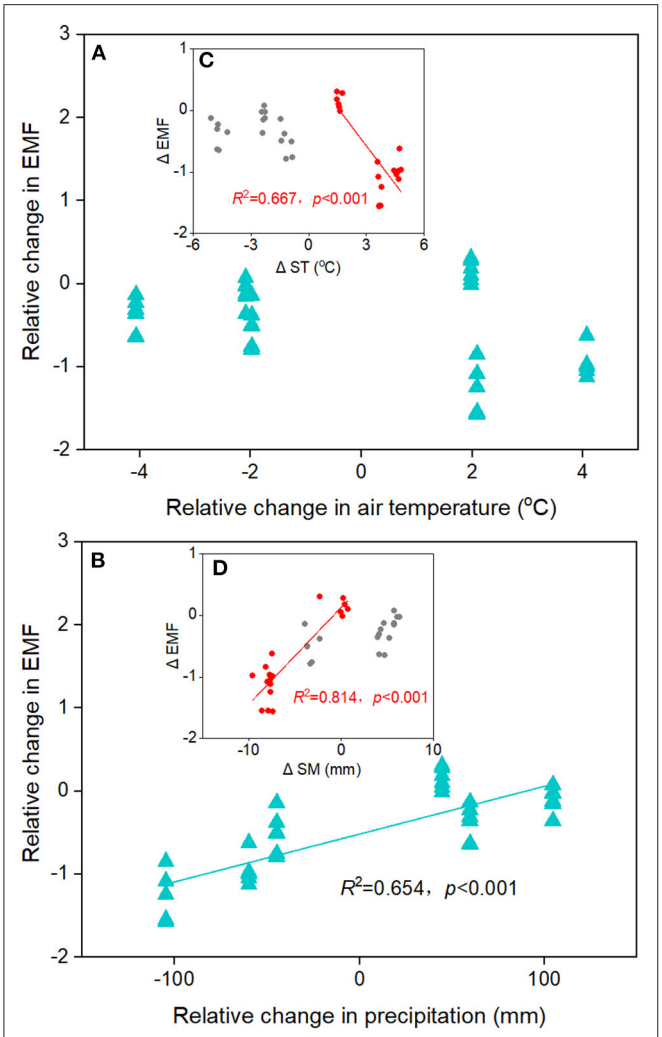

FIGURE 5 | The relationships between transplant-induced changes in **(A)** air temperature and **(B)** precipitation with ecosystem multifunctionality (EMF) in alpine meadows. Insert: the relationships between transplant-induced changes in **(C)** soil temperature (ST) and **(D)** soil moisture (SM) with EMF.

be partly attributed to the increase of soil microbe induced by the higher water conditions and nutrient availability after the transplantation. As reported by the previous studies (Wang et al., 2013; Zhu et al., 2017), the Tibetan alpine vegetation usually suffered from water deficiency due to high evapotranspiration, which might be further aggravated in the semi-arid regions. Reflecting this, the decline of species richness, plant diversity and EMF under downward transplantation (experimental warming) was probably due to the warming-induced drought stress. On the other hand, experimental cooling generally tended to decrease the EMF in alpine meadows (**Figure 3B**). In high-altitude grasslands, especially for the upper limit of alpine meadows above 5,200 m, low temperature often limits water or nutrients availability and restrains plant growth and soil microbial activity (Wang et al., 2013; Li et al., 2013), that may further attribute to a decrease of the EMF (**Figure 3B**). This result suggests that temperature rather than precipitation might be the major factor for the decreased EMF of high-altitude (above 4,500 m) alpine meadows under the experimental cooling.

Precipitation and soil moisture are important drivers of the EMF in alpine grasslands (Jing et al., 2015; Pan et al., 2017). Previous studies have showed that changes in precipitation can directly influence plant and soil microbial diversity as well as the EMF, especially in water-limited ecosystems (Liu et al., 2009; Hu et al., 2021). We found that precipitation was significantly associated with the EMF, and warming effects on the EMF were highly dependent on precipitation (**Figures 3B**, **5B**). Such positive relationship between precipitation and the EMF found in the present study is consistent with observed results in alpine grasslands (Jing et al., 2015). The inconsistent effects of experimental warming on the EMF under lower or higher precipitation conditions highlight the importance of precipitation changes on the EMF, especially in the water-limited ecosystems. In grassland ecosystems, higher precipitation and are generally associated with higher soil water conditions and nutrient availability, which could facilitate plant growth and soil microbial activity (Hu et al., 2021; Wang et al., 2021a). The increased precipitation could ameliorate water deficiency and minimize biodiversity losses in semi-arid alpine ecosystems and potentially resulted in increase of the EMF. We also found that precipitation reduction generally resulted in a decrease of the EMF (**Figure 3B**), which is possibly due to the limitation of microbial activities or the decrease of plant species caused by drought stress. However, the effects of precipitation change on the EMF also largely depended on the temperature environments. In the high-altitude grasslands, where low temperature becomes a limiting factor for plant growth and soil microbial activity, we found that the changes of precipitation would have little influence on the EMF. However, in future, studies are still needed to assess the critical point at which temperature and precipitation both limit the EMF and how the threshold point varies with climate change.

CONCLUSION

Our work showed that experimental warming by the downward transplantation tended to increase the EMF when meadow blocks were transplanted to the high-precipitation sites but decrease the EMF as meadow blocks were transplanted to the low-precipitation sites. However, the experimental cooling by the upward transplantation consistently reduced the EMF regardless of the precipitation change. Further analysis showed that the increase of the EMF under experimental warming was closely related to the increase of plant species and biomass, whereas the reduction of EMF under cooling was highly correlated with the decrease of soil temperature. The increase of EMF under the experimental warming was closely related to the variation of both plant and soil functions, whereas the reduction of EMF under the cooling was highly correlated with the decrease of plant function. Our study provides insight into how the EMF of alpine meadows will response to warming expected under future climate change and to cooling that usually occurred over temperature anomalies events.

DATA AVAILABILITY STATEMENT

The original contributions presented in the study are included in the article/**Supplementary Material**, further inquiries can be directed to the corresponding author.

AUTHOR CONTRIBUTIONS

YM, GQ, and JZ: investigation and writing. GQ and LT: conceptualization and methodology. WW and JZ: analyzed the data. LT and JZ: review and editing. All authors contributed to the article and approved the submitted version.

FUNDING

This work was funded by the Second Tibetan Plateau Scientific Expedition and Research Program (2019QZKK0106), the National Natural Science Foundation of China (42071058, 91837312, and 41701276), and a grant from Grassland Science Institute, Tibet Academy of Agricultural and Animal Husbandry Sciences (CYS-TC-2021-001).

SUPPLEMENTARY MATERIAL

The Supplementary Material for this article can be found online at: https://www.frontiersin.org/articles/10.3389/fpls.2021.824296/full#supplementary-material

REFERENCES

Balvanera, P., Pfisterer, A., Buchmann, N., He, J.-S., Nakashizuka, T., Raffaelli, D., et al. (2006). Quantifying the evidence for biodiversity effects on ecosystem functioning and services. *Ecol. Lett.* 9, 1146–1156. doi: 10.1111/j.1461-0248.2006.00963.x

Bardgett, R., and van der Putten, W. (2014). Below ground biodiversity and ecosystem functioning. *Nature* 515, 505–511. doi: 10.1038/nature13855

Bastida, F., Torres, I., Moreno, J., Baldrian, P., Ondono, S., Ruiznavarro, A., et al. (2016). The active microbial diversity drives ecosystem multifunctionality and is physiologically related to carbon availability in Mediterranean semi-arid soils. *Mol. Ecol.* 25, 4660–4673. doi: 10.1111/mec.13783

Berdugo, M., Delgado-Baquerizo, M., Soliveres, S., Hernández-Clemente, R., Zhao, Y., Gaitán, J., et al. (2020). Global ecosystem thresholds driven by aridity. *Science* 367, 787–790. doi: 10.1126/science.aay5958

Cui, H., Sun, W., Delgado-Baquerizo, M., Song, W., Ma, J.-Y., Wang, K., et al. (2020). Contrasting effects of N fertilization and mowing on ecosystem multifunctionality in a meadow steppe. *Soil Ecol. Lett.* 2, 268–280. doi: 10.1007/s42832-020-0046-2

Flanagan, L., and Johnson, B. (2005). Interacting effects of temperature, soil moisture and plant biomass production on ecosystem respiration in a northern temperate grassland, *Agric. For. Meteorol.* 130, 237–253. doi: 10.1016/j.agrformet.2005.04.002

Fu, G., Shen, Z., Zhang, X., and Zhou, Y. (2012). Response of soil microbial biomass to short-term experimental warming in alpine meadow on the Tibetan Plateau. *Appl. Soil Ecol.* 61, 158–160. doi: 10.1016/j.apsoil.2012.05.002

Gallaher, R., Weldon, C., and Boswell, F. (1976). A semiautomated procedure for total nitrogen in plant and soil samples. *Soil Sci. Soc. Am. J.* 40, 887–889. doi: 10.2136/sssaj1976.03615995004000060026x

Gao, Q., Li, Y., Xu, H., Wan, Y., and Jiangcun, W. (2014). Adaptation strategies of climate variability impacts on alpine grassland ecosystems in Tibetan Plateau. *Mitig. Adapt. Strateg. Glob. Change.* 19, 199–209. doi: 10.1007/s11027-012-9434-y

Hector, A., and Bagchi, R. (2007). Biodiversity and ecosystem multifunctionality. *Nature* 448, 188–190. doi: 10.1038/nature05947

Hooper, D., Adair, E., Cardinale, B., Byrnes, J., Hungate, B., Matulich, K., et al. (2012). A global synthesis reveals biodiversity loss as a major driver of ecosystem change. *Nature* 486, 105–108. doi: 10.1038/nature11118

Hooper, D., Chapin, F., Ewel, J., Hector, A., Inchausti, P., Lavorel, S., et al. (2005). Effects of biodiversity on ecosystem functioning: a consensus of current knowledge. *Ecol. Monogr.* 75, 3–35. doi: 10.1890/04-0922

Hu, W., Ran, J., Dong, L., Du, Q., Ji, M., Yao, S., et al. (2021). Aridity-driven shift in biodiversity–soil multifunctionality relationships. *Nat. Commun.* 12:5350. doi: 10.1038/s41467-021-25641-0

Hu, Y., Jiang, L., Wang, S., Zhang, Z., Luo, C., Bao, X., et al. (2016). The temperature sensitivity of ecosystem respiration to climate change in an alpine meadow on the Tibet plateau: a reciprocal translocation experiment. *Agric. For. Meteorol.* 216, 93–104. doi: 10.1016/j.agrformet.2015.10.002

Hu, Y., Wang, S., Niu, B., Chen, Q., Wang, J., Zhao, J., et al. (2020). Effect of increasing precipitation and warming on microbial community in Tibetan alpine steppe. *Environ. Res.* 189:109917. doi: 10.1016/j.envres.2020.109917

Isbell, F., Calcagno, V., Hector, A., Connolly, J., Stanley Harpole, W., Reich, P., et al. (2011). High plant diversity is needed to maintain ecosystem services. *Nature* 477, 199–202. doi: 10.1038/nature10282

Jing, X., Sanders, N. J., Shi, Y., Chu, H., Classen, A. T., Zhao, K., et al. (2015). The links between ecosystem multifunctionality and above- and belowground biodiversity are mediated by climate. *Nat. Commun.* 6:8159. doi: 10.1038/ncomms9159

Kuang, X., and Jiao, J. J. (2016). Review on climate change on the Tibetan Plateau during the last half century. *J. Geophys. Res. Atmos.* 121, 3979–4007. doi: 10.1002/2015JD024728

Lehnert, L., Wesche, K., Trachte, K., Reudenbach, C., and Bendix, J. (2016). Climate variability rather than overstocking causes recent large scale cover changes of Tibetan pastures. *Sci. Rep.* 6:24367. doi: 10.1038/srep24367

Li, R., Luo, T., Mölg, T., Zhao, J., Li, X., Cui, X., et al. (2016a). Leaf unfolding of Tibetan alpine meadows captures the arrival of monsoon rainfall. *Sci. Rep.* 6:20985. doi: 10.1038/srep20985

Li, R., Luo, T., Tang, Y., Du, M., and Zhang, X. (2013). The altitudinal distribution center of a widespread cushion species is related to an optimum combination of temperature and precipitation in the central Tibetan Plateau. *J. Arid Environ.* 88, 70–77. doi: 10.1016/j.jaridenv.2012.07.018

Li, X., Jiang, L., Meng, F., Wang, S., Niu, H., Iler, A., et al. (2016b). Responses of sequential and hierarchical phenological events to warming and cooling in alpine meadows. *Nat. Commun.* 7:12489. doi: 10.1038/ncomms12489

Li, X., Zhang, L., and Luo, T. (2020). Rainy season onset mainly drives the spatiotemporal variability of spring vegetation green-up across alpine dry ecosystems on the Tibetan Plateau. *Sci. Rep.* 10:18797. doi: 10.1038/s41598-020-75991-w

Liu, W., Zhang, Z., and Wan, S. (2009). Predominant role of water in regulating soil and microbial respiration and their responses to climate change in a semiarid grassland. *Glob Change Biol.* 15, 184–195. doi: 10.1111/j.1365-2486.2008.01728.x

Liu, X., Shi, X., and Zhang, S. (2021). Soil abiotic properties and plant functional diversity co-regulate the impacts of nitrogen addition on ecosystem multifunctionality in an alpine meadow. *Sci. Total Environ.* 780:146476. doi: 10.1016/j.scitotenv.2021.146476

Ma, Z., Liu, H., Mi, Z., Zhang, Z., Wang, Y., Xu, W., et al. (2017). Climate warming reduces the temporal stability of plant community biomass production. *Nat.Commun.* 8:15378. doi: 10.1038/ncomms15378

Maestre, F., Quero, J., Gotelli, N., Escudero, A., Ochoa, V., Delgado-Baquerizo, M., et al. (2012). Plant species richness and ecosystem multifunctionality in global drylands. *Science* 335, 214–218. doi: 10.1126/science.1215442

Manning, P., van der Plas, F., Soliveres, S., Allan, E., Maestre, F. T., Mace, G., et al. (2018). Redefining ecosystem multifunctionality. *Nat. Ecol. Evol.* 2, 427–436. doi: 10.1038/s41559-017-0461-7

Pan, Y., Wu, J., Luo, L., Tu, Y., Yu, C., Zhang, X., et al. (2017). Climatic and geographic factors affect ecosystem multifunctionality through biodiversity in the Tibetan alpine grasslands. *J. Mt. Sci.* 14, 1604–1614. doi: 10.1007/s11629-016-4242-6

Perkins, D., Bailey, R., Dossena, M., Gamfeldt, L., Reiss, J., Mark, T., et al. (2015). Higher biodiversity is required to sustain multiple ecosystem processes across temperature regimes. *Glob Change Biol.* 21, 396–406. doi: 10.1111/gcb.12688

Sun, J., Zhou, T., Liu, M., Chen, Y., Liu, G., Xu, M., et al. (2020). Water and heat availability are drivers of the aboveground plant carbon accumulation rate in alpine grasslands on the Tibetan Plateau. *Glob. Ecol. Biogeogr.* 29, 50–64. doi: 10.1111/geb.13006

Vance, E., Brookes, P., and Jenkinson, D. (1987). An extraction method for measuring soil microbial biomass C. *Soil Biol. Biochem.* 19, 703–707. doi: 10.1016/0038-0717(87)90052-6

Walkley, A., and Black, I. (1934). An examination of the Degtjareff method for determining soil organic matter, and a proposed modification of the chromic acid titration method. *Soil Sci.* 37, 29–38. doi: 10.1097/00010694-193401000-00003

Wang, H., Liu, H., Cao, G., Ma, Z., Li, Y., Zhang, F., et al. (2020a). Alpine grassland plants grow earlier and faster but biomass remains unchanged over 35 years of climate change. *Ecol. Lett.* 23, 701–710. doi: 10.1111/ele.13474

Wang, L., Delgado-Baquerizo, M., Wang, D., Isbell, F., Liu, J., Feng, C., et al. (2019a). Diversifying livestock promotes multidiversity and multifunctionality in managed grasslands. *Proc. Natl. Acad. Sci. U. S. A.* 116, 6187–6192. doi: 10.1073/pnas.1807354116

Wang, Q., Zhang, Z., Du, R., Wang, S., Duan, J., Marie IIer, A., et al. (2019b). Richness of plant communities plays a larger role than climate in determining responses of species richness to climate change. *J. Ecol.* 107, 1944–1955. doi: 10.1111/1365-2745.13148

Wang, X., Li, F., Wang, Y., Liu, X., Cheng, J., Zhang, J., et al. (2020b). High ecosystem multifunctionality under moderate grazing is associated with high plant but low bacterial diversity in a semi-arid steppe grassland. *Plant Soil* 448, 265–276. doi: 10.1007/s11104-020-04430-6

Wang, Y., Liu, M., Chen, Y., Zeng, T., Lu, X., Yang, B., et al. (2021b). Plants and microbes mediate the shift in ecosystem multifunctionality from low to high patterns across alpine grasslands on the Tibetan plateau. *Front. Plant Sci.* 12:760599. doi: 10.3389/fpls.2021.760599

Wang, Y., Sun, J., Ye, C., and Zeng, T. (2021a). Climatic factors drive the aboveground ecosystem functions of alpine grassland via soil microbial biomass nitrogen on Qingzang Plateau. *Chin. J. Plant Ecol.* 45, 434–443. doi: 10.17521/cjpe.2020.0204

Wang, Z., Luo, T., Li, R., Tang, Y., and Du, M. (2013). Causes for the unimodal pattern of biomass and productivity in alpine grasslands along a large altitudinal gradient in semi-arid regions. *J. Veg. Sci.* 24, 189–201. doi: 10.1111/j.1654-1103.2012.01442.x

Wardle, D., Bardgett, R., Klironomos, J., Setälä, H., van der Putten, W and Wall, D. (2004). Ecological linkages between aboveground and belowground biota. *Science* 304, 1629–1633. doi: 10.1126/science.1094875

Wu, G.-L., Cheng, Z., Alatalo, J., Zhao, J., and Liu, Y. (2021). Climate warming consistently reduces grassland ecosystem productivity. *Earth's Future.* 9:e2020EF001837. doi: 10.1029/2020EF001837

Wu, G.-L., Du, G., Liu, Z. H., and Thirgood, S. (2009). Effect of fencing and grazing on a Kobresia-dominated meadow in the Qinghai-Tibetan Plateau. *Plant Soil.* 319, 115–126. doi: 10.1007/s11104-008-9854-3

Wu, Z., Dijkstra, P., Koch, G., and Hungate, B. (2012). Biogeochemical and ecological feedbacks in grassland responses to warming. *Nat. Clim. Change* 2, 458–461 doi: 10.1038/nclimate1486

Xu, X., Thornton, P., and Post, W. (2013). A global analysis of soil microbial biomass carbon, nitrogen and phosphorus in terrestrial ecosystems. *Glob. Ecol. Biogeogr.* 22, 737–749. doi: 10.1111/geb.12029

Yang, K., Wu, H., Qin, J., Lin, C., Tang, W., and Chen, Y. (2014). Recent climate changes over the Tibetan Plateau and their impacts on energy and water cycle: a review. *Glob. Planet Change* 112, 79–91. doi: 10.1016/j.gloplacha.2013.12.001

Yang, T., Adams, J., Shi, Y., He, J.-S., Jing, X., Chen, L., et al. (2017). Soil fungal diversity in natural grasslands of the Tibetan Plateau: Associations with plant diversity and productivity. *New Phytol.* 215, 756–765. doi: 10.1111/nph.14606

Yu, C., Han, F., and Fu, G. (2019). Effects of 7 years experimental warming on soil bacterial and fungal community structure in the Northern Tibet alpine meadow at three elevations. *Sci. Total Environ.* 655, 814–822. doi: 10.1016/j.scitotenv.2018.11.309

Zhao, J., Luo, T., Li, R., Li, X., and Tian, L. (2016). Grazing effect on growing season ecosystem respiration and its temperature sensitivity in alpine grasslands along a large altitudinal gradient on the central Tibetan Plateau. *Agric. For. Meteorol.* 218–219, 114–121. doi: 10.1016/j.agrformet.2015.12.005

Zhao, J., Luo, T., Li, R., Wei, H., Li, X., Du, M., et al. (2018). Precipitation alters temperature effects on ecosystem respiration in Tibetan alpine meadows. *Agric. For. Meteorol.* 252, 121–129. doi: 10.1016/j.agrformet.2018.01.014

Zhao, J., Luo, T., Wei, H., Deng, Z., Li, X., Li, R., et al. (2019). Increased precipitation offsets the negative effect of warming on plant biomass and ecosystem respiration in a Tibetan alpine steppe. *Agric. For. Meteorol.* 279:107761. doi: 10.1016/j.agrformet.2019.107761

Zhu, J., Zhang, Y., and Jiang, L. (2017). Experimental warming drives a seasonal shift of ecosystem carbon exchange in Tibetan alpine meadow. *Agric. For. Meteorol.* 233, 242–249. doi: 10.1016/j.agrformet.2016.12.005

Conflict of Interest: The authors declare that the research was conducted in the absence of any commercial or financial relationships that could be construed as a potential conflict of interest.

Publisher's Note: All claims expressed in this article are solely those of the authors and do not necessarily represent those of their affiliated organizations, or those of the publisher, the editors and the reviewers. Any product that may be evaluated in this article, or claim that may be made by its manufacturer, is not guaranteed or endorsed by the publisher.

Copyright © 2022 Ma, Tian, Qu, Li, Wang and Zhao. This is an open-access article distributed under the terms of the Creative Commons Attribution License (CC BY). The use, distribution or reproduction in other forums is permitted, provided the original author(s) and the copyright owner(s) are credited and that the original publication in this journal is cited, in accordance with accepted academic practice. No use, distribution or reproduction is permitted which does not comply with these terms.

frontiers in Plant Science

ORIGINAL RESEARCH
published: 24 February 2022
doi: 10.3389/fpls.2022.814059

Leaf Stoichiometry of *Potentilla fruticosa* Across Elevations in China's Qilian Mountains

Yanyan Qin[1,2,3], Wei Liu[2,3], Xiaofang Zhang[2], Jan F. Adamowski[4] and Asim Biswas[5]*

[1] Key Laboratory of Land Surface Process and Climate Change in Cold and Arid Regions, Northwest Institute of Eco-Environment and Resources, Chinese Academy of Sciences, Lanzhou, China, [2] Key Laboratory of Ecohydrology of Inland River Basin, Northwest Institution of Eco-Environment and Resources, Chinese Academy of Sciences, Lanzhou, China, [3] Qilian Mountains Eco-environment Research Center in Gansu Province, Lanzhou, China, [4] Department of Bioresource Engineering, Faculty of Agricultural and Environmental Sciences, McGill University, Sainte-Anne-de-Bellevue, QC, Canada, [5] School of Environmental Sciences, University of Guelph, Guelph, ON, Canada

OPEN ACCESS

Edited by:
Shiliang Liu,
Beijing Normal University, China

Reviewed by:
Hao Shen,
Beijing Normal University, China
Vladimir Onipchenko,
Lomonosov Moscow State University, Russia
Zhen Ma,
Northwest Institute of Plateau Biology (CAS), China
Gang Fu,
Institute of Geographic Sciences and Natural Resources Research (CAS), China

***Correspondence:**
Wei Liu
weiliu@lzb.ac.cn

Specialty section:
This article was submitted to Functional Plant Ecology, a section of the journal Frontiers in Plant Science

Received: 19 November 2021
Accepted: 10 January 2022
Published: 24 February 2022

Citation:
Qin Y, Liu W, Zhang X, Adamowski JF and Biswas A (2022) Leaf Stoichiometry of Potentilla fruticosa Across Elevations in China's Qilian Mountains. Front. Plant Sci. 13:814059. doi: 10.3389/fpls.2022.814059

As an individual plant species can develop its own leaf stoichiometry to adapt to environmental changes, this stoichiometry can provide critical information about a plant species' growth and its potential management in the ecosystem housing it. However, leaf stoichiometry is largely undocumented in regions with large environmental changes arising from differences in elevation. The leaf stoichiometry of *Potentilla fruticosa* L., a major alpine shrub playing an important role in supporting ecosystem functions and services in China's Qilian Mountains (Northeast Qinghai–Tibetan Plateau), was investigated at different elevations (2,400, 2,600, 2,800, 3,000, 3,200, 3,500, and 3,800 m). At each elevation, leaf elemental (C, N, and P) concentrations were measured in *P. fruticosa* leaves sampled from three plots (10 × 10 m), and edaphic properties were assessed in nine quadrats (1 × 1 m, three quadrats per plot). Temperature and precipitation were calculated using an empirical formula. Maximum and minimum leaf carbon (C) concentrations ($[C]_{leaf}$) of 524 ± 5.88 and 403 ± 3.01 g kg^{-1} were measured at 2,600 and 3,500 m, respectively. Leaf nitrogen (N) concentration ($[N]_{leaf}$) showed a generally increasing trend with elevation and peaked at 3,500 m (27.33 ± 0.26 g kg^{-1}). Leaf phosphorus (P) concentration ($[P]_{leaf}$) varied slightly from 2,400 to 3,200 m and then dropped to a minimum (0.60 ± 0.10 g kg^{-1}) at 3800 m. The $[C]_{leaf}$:$[N]_{leaf}$, $[C]_{leaf}$:$[P]_{leaf}$, and $[N]_{leaf}$:$[P]_{leaf}$ varied little from 2,400 to 3,000 m but fluctuated somewhat at higher elevations. The main factors affecting *P. fruticosa* leaf stoichiometry were soil organic C, pH, and soil total P, and the main limiting element for the growth of *P. fruticosa* in the study area was P. In conclusion, changes in elevation affected leaf stoichiometry of *P. fruticosa* mainly due to altered soil properties, and addressing phosphorus limitation, especially at higher elevations mainly due to losses caused by high precipitation and sparse vegetation, is a key measure to promote *P. fruticosa* growth in this region.

Keywords: Mountainous regions, plant growth, plant adaptation, plant traits, *Potentilla*

INTRODUCTION

A vigorous, floriferous, deciduous shrub of high genetic diversity, the widely distributed rosaceous shrub *Potentilla fruticosa* L. (a.k.a. shrubby *Potentilla* or shrubby cinquefoil), supports many ecosystem functions in the world's colder habitats, which makes it particularly sensitive to global warming (Elkington, 1969; Miliauskas et al., 2010; Shimono et al., 2010; Yuichiro et al., 2010). Its chemical composition (Ganenko et al., 1988; Zeng et al., 2019), edibility and cosmetic properties (Nkiliza, 1999; Liu et al., 2016), antioxidant content (Miliauskas et al., 2010; Luo et al., 2016), and effects on the expression of key enzymes and hormones of glucose and lipid metabolism in rats (Yan et al., 2019) have been documented. *P. fruticosa's* nutritive value has been shown to be influenced by grazing (Yao et al., 2019). Its leaf morphology, physiological and biochemical characteristics have been found to be altered by atmospheric pollution and soil salinity (NaCl and Na_2SO_4) (Liu et al., 2013; Lugovskaya et al., 2018).

However, the leaf stoichiometry of *P. fruticosa* at high elevations on the Qinghai–Tibetan Plateau (QTP) remains relatively undocumented. Leaf stoichiometry can reflect the balance and limitations in the uptake of plant macronutrients (C, N, P) that influence plants' growth rate and life history strategies (Baxter and Dilkes, 2012; Zhu et al., 2020) and global C, N, P biogeochemical cycles (Moe et al., 2005; Liu et al., 2018). Leaf stoichiometry information is critical developing an understanding of nutrient cycling processes, in developing biogeochemical models, and in predicting plant responses to global climate change (Zhao et al., 2014, 2018). Previous studies have shown that besides disturbances such as increased CO_2, N, and P availability (Esmeijer-Liu et al., 2009; Scott et al., 2013) and grazing (Bai et al., 2012), topographic factors such as slope, aspect, and elevation (e.g., Qin et al., 2019; Cao et al., 2020) can also affect leaf stoichiometry. This occurs through their influence on soil formation (Jenny, 1941), water distribution, and microclimate. However, topographic factors are rarely considered in leaf stoichiometry, especially for individual species.

This study's overall objective was to examine the effects of elevation (from 2,400 to 3,800 m) on leaf stoichiometry of *P. fruticosa*, a major alpine shrub. The study was conducted in the Qilian Mountains of the Qinghai–Tibetan Plateau (QTP), the world's highest elevation plateau. Since mean annual precipitation (MAP), mean annual temperature (MAT), and soil properties vary with elevation (**Table 1**), our hypothesis was that leaf stoichiometry of *P. fruticosa* would vary with elevation, and, based on Cao et al. (2020), that P would be a limiting nutrient for *P. fruticosa* growth.

MATERIALS AND METHODS

Study Area

With a mean elevation of 4,000 m (closer to 3,000 m in the northeast), mean annual precipitation (MAP) of 400 mm, and mean annual temperature (MAT) below −4°C, the Qinghai–Tibetan Plateau covers 2.5×10^6 km^2. Ranging in elevation from 2,200 to 5,500 m, and located in the northeastern portion of the QTP, the Qilian Mountains present two main slope aspects: south-facing and north-facing. On the south-facing slope aspects, grasslands growing on sandy-textured Kastanozem are the dominant vegetation type, whereas on the north-facing slope aspects, Qinghai spruce (*Picea crassifolia* Kom.), growing on silty-sand-textured Podzol, is the dominant species (Qin et al., 2016).

Field Sampling

In August and September 2018, when most plant species were at the late flowering or fruiting stages, leaves from top and middle of *P. fruticosa* plants were sampled from three random 10 × 10 m plots situated at each of seven elevations: 2,400, 2,600, 2,800, 3,000, 3,200, 3,500, and 3,800 m (**Figure 1**). In each plot, multiple soil samples were collected from three quadrats (1 × 1 m) along the diagonal transect. A 70-mm diameter soil drill was used to sample from 3 depth profiles (0–10, 10–20, and 20–40 cm).

Laboratory Analyses

The leaves were dried and ground to determine leaf carbon (C) concentration ($[C]_{leaf}$), leaf nitrogen (N) concentration ($[N]_{leaf}$), and leaf phosphorus (P) concentration ($[P]_{leaf}$). Soil samples were air-dried and ground to pass through a 100-mesh sieve prior to the analysis of soil properties. A volumetric potassium dichromate method was used to determine $[C]_{leaf}$ and soil organic carbon (SOC) (Nelson and Sommers, 1982), and a SmartChen 200 (AMS Rome, Italy) element analyzer was used to measure $[N]_{leaf}$, $[P]_{leaf}$, soil total nitrogen (STN), and soil total phosphorus (STP). A standard pH meter was used to determine soil pH in a slurry of 2.5:1 water to air-dried soil ratio (Cao et al., 2018).

Data Analysis

The MAT and MAP (**Table 1**) were based on Zhao et al. (2005, 2006). For the Qilian Mountain region, these were calculated as:

$$MAT = 20.96 - 5.49 \times 10^{-3}\ ELEV - 0.17\ LAT + 8.9 \times 10^{-3}\ LONG \quad R^2 = 0.98 \tag{1}$$

$$MAP = 1.68 \times 10^3 + 0.12\ ELEV + 12.41\ LAT - 75.26\ LONG \quad R^2 = 0.92 \tag{2}$$

where MAT = mean annual temperature (°C), MAP = mean annual precipitation (mm), ELEV = elevation (m), LAT = latitude (°), and LONG = longitude (°). R^2 indicates the coefficient of determination.

All data were expressed as mean and standard error (SE). The fixed effect (elevation) and random effect (plot) on soil properties and leaf ecological stoichiometry of *P. fruticosa* were tested by fitting generalized linear mixed models (GLMMs). The *t*-test was used to check the significant difference ($p < 0.05$) of each measured parameter between different elevations. Redundancy analysis (RDA) was performed to find the dominant environmental variables influencing leaf stoichiometry of *P. fruticosa* (Maccherini et al., 2011; Yang et al., 2018a). The significance of the eigenvalues of the canonical axes was tested by a reduced Monte Carlo model with 270 unrestricted

TABLE 1 | Effects of elevation on soil properties and leaf stoichiometry of *P. fruticose* (n = 9).

Parameters	Elevation (fixed effect)			R^2 [Fixed effect and random effect (plot)]	*df*
	F	*P*	R^2		
SOC	109.77	**<0.001**	0.94	0.95	6
STN	102.62	**<0.001**	0.94	0.96	6
STP	4.15	**0.013**	0.33	0.39	6
SOC:STN	5.20	**0.005**	0.44	0.60	6
SOC:STP	10.73	**<0.001**	0.51	0.51	6
STN:STP	10.70	**<0.001**	0.51	0.51	6
pH	328.46	**<0.001**	0.98	0.99	6
$[C]_{leaf}$	39.33	**<0.001**	0.79	0.79	6
$[N]_{leaf}$	358.35	**<0.001**	0.98	0.99	6
$[P]_{leaf}$	1.94	0.143	0.16	0.16	6
$[C]_{leaf}$:$[N]_{leaf}$	110.969	**<0.001**	0.92	0.93	6
$[C]_{leaf}$:$[P]_{leaf}$	1.13	0.396	0.10	0.10	6
$[N]_{leaf}$:$[P]_{leaf}$	2.11	0.118	0.17	0.17	6

SOC, soil organic carbon; STN, soil total nitrogen; STP, soil total phosphorus; $[C]_{leaf}$, leaf carbon (C) concentration; $[N]_{leaf}$, leaf nitrogen (N) concentration; $[P]_{leaf}$, leaf phosphorus (P) concentration.
Significant p values ($p < 0.05$) are in bold.

permutations (Sun et al., 2017; Yuan, 2017). The Pearson's correlation coefficient was used to determine the correlation between leaf stoichiometry and abiotic factors. SPSS 22.0 for Windows (SPSS, Inc., Chicago, IL, United States) was used to determine the Pearson's correlation coefficient. Other analyses were performed in R4.1.1 (*vegan* and *nlme* packages). The figures were prepared using Origin 2021 (OriginLab Corp, Roundhouse Plaza, Northampton, MA, United States) and R4.1.1 (*ggplot2* and *ggrepel* packages).

RESULTS

Effects of Elevation on Soil Properties and Leaf Stoichiometry of *Potentilla fruticosa*

The results from GLMMs showed that except $[P]_{leaf}$, $[C]_{leaf}$:$[P]_{leaf}$, and $[N]_{leaf}$:$[P]_{leaf}$, soil properties and other elemental stoichiometries of *P. fruticosa* were significantly affected by elevation (**Table 1**). Compared to elevations below 3,000 m, SOC and STN significantly increased (3- to 4-fold) at elevations of 3,200 m and above. However, STP did not show this trend, as it peaked at 2,600 m (0.58 ± 0.02 g kg^{-1}). Variation in SOC:STN across elevations was minimal, with the largest value (11.22 ± 0.10) occurring at 3,500 m and the smallest (8.96 ± 0.46) at 2,600 m. For SOC:STP and STN:STP, the largest and the smallest values were at 3,500 m (487 ± 133 and 42.74 ± 11.46, respectively) and 2,600 m (20.90 ± 0.67 and 2.43 ± 0.12, respectively), respectively. Soil pH values shifted from 6.12 ± 0.03 at 3,500 m to 8.54 ± 0.02 at 2,600 m. The MAT showed a decreasing trend from 2,400 to 3,800 m, whereas MAP showed a converse trend (**Table 2**).

At 3,500 m, $[C]_{leaf}$ (403 ± 3.01g kg^{-1}) was significantly lower than that at any other elevation, whereas at 2,600 m $[C]_{leaf}$ (524 ± 5.88 g kg^{-1}) was significantly greater than at any other elevations except 3,000 m (**Figure 2A**). The $[N]_{leaf}$ showed an increasing trend with increasing elevation. At 3,500 m, $[N]_{leaf}$ (27.33 ± 0.26 g kg^{-1}) was significantly greater than at other elevations, whereas $[N]_{leaf}$ at 2,800 m (18.15 ± 0.10 g kg^{-1}) was significantly lower than that at any other elevations (**Figure 2B**). The $[P]_{leaf}$ changed slightly at elevations between 2,400 and 3,200 m and had a decreasing trend at elevations from 3,500 to 3,800 m, with the lowest value (0.60 ± 0.10 g kg^{-1}) recorded at 3,800 m, which was significantly lower than that at 2,600, 3,200, or 3,500 m (**Figure 2C**). From 2,400 to 3,000 m, $[C]_{leaf}$:$[N]_{leaf}$ varied little, but increased significantly at or above 3,200 m. However, from 3,200 to 3,800 m, $[C]_{leaf}$:$[N]_{leaf}$ showed a decreasing and then an increasing trend, with the value at 3,500 m (14.74 ± 0.19) being significantly lower than that at other elevations (**Figure 2D**). Changes in $[C]_{leaf}$:$[P]_{leaf}$ and $[N]_{leaf}$:$[P]_{leaf}$ along the elevation gradients were similar. Both of them varied slightly between 2,400 and 3,000 m; however, from 3,000 to 3,800 m, their values first decreased and then increased and reached minimums and maximums at 3,200 (392 ± 35.28 and 19.43 ± 1.50, respectively) and 3,800 m (1097 ± 349 and 62.79 ± 19.81, respectively), respectively (**Figures 2E,F**).

Dominant Factors Influencing Leaf Stoichiometry of *Potentilla fruticosa* at Different Elevations

The RDA results showed that the eigenvalues of the first and second axes were 0.27 and 0.02, respectively (**Figure 3**), indicating that the two axes could explain about 29.00% of the total variation in leaf stoichiometry of *P. fruticosa* across elevations. Based on the RDA result, SOC, STP, and pH had significant effects on this variation, and they could explain 7.10, 6.80, and 6.00% of it, respectively (**Table 3**).

TABLE 2 | Changes of temperature, precipitation, and soil properties at different elevations (mean ± standard error, $n = 9$).

Parameter	Elevation						
	2,400 m	**2,600 m**	**2,800 m**	**3,000 m**	**3,200 m**	**3,500 m**	**3,800 m**
SOC (g kg^{-1})	13.12 ± 0.73 e	12.05 ± 0.52 e	15.08 ± 0.63 d	12.28 ± 0.61 e	35.60 ± 3.19 c	58.64 ± 1.65 a	50.14 ± 1.65 b
STN (g kg^{-1})	1.46 ± 0.08 de	1.41 ± 0.08 de	1.62 ± 0.09 d	1.35 ± 0.10 e	3.48 ± 0.23 c	5.24 ± 0.13 a	4.72 ± 0.13 b
STP (g kg^{-1})	0.53 ± 0.02 a	0.58 ± 0.02 a	0.44 ± 0.02 ab	0.32 ± 0.03 b	0.53 ± 0.03 a	0.27 ± 0.05 b	0.54 ± 0.12 a
SOC:STN	9.01 ± 0.19 c	8.96 ± 0.46 c	9.40 ± 0.27 bc	9.24 ± 0.35 c	10.09 ± 0.32 ab	11.22 ± 0.10 a	10.61 ± 0.23 a
SOC:STP	26.03 ± 2.27 d	20.90 ± 0.67 d	35.48 ± 1.50 c	41.29 ± 4.03 c	67.50 ± 3.43 b	487 ± 133.00 a	183 ± 32.61 b
STN:STP	2.89 ± 0.24 d	2.43 ± 0.12 d	3.77 ± 0.14c	4.46 ± 0.36 c	6.69 ± 0.26 b	42.74 ± 11.46 a	17.32 ± 3.18 b
pH	8.43 ± 0.04 b	8.54 ± 0.02 a	8.36 ± 0.04 b	8.51 ± 0.03 a	8.08 ± 0.04 c	6.44 ± 0.05 d	6.12 ± 0.03 e
LONG	100°21′55″	100°17′3″	100°14′28″	100°14′26″	100°22′35″	101°21′0″	101°22′12″
LAT	38°37′5″	38°33′17″	38°33′9″	38°33′22″	38°38′15″	37°40′48″	37°41′24″
MAT (°C)	2.26	1.17	0.08	−1.02	−2.13	−3.61	−5.26
MAP (mm)	304.71	331.32	355.7	379.22	398.58	518.42	553.62

SOC, soil organic carbon; STN, soil total nitrogen; STP, soil total phosphorus; LONG, longitude; LAT, latitude; MAT, mean annual temperature; MAP, mean annual precipitation.

Row-wise non-matching letters indicate a significant difference among elevations ($p < 0.05$).

Soil pH was positively related to $[C]_{leaf}$ and $[C]_{leaf}$:$[N]_{leaf}$ and negatively with $[N]_{leaf}$, $[C]_{leaf}$:$[P]_{leaf}$, and $[N]_{leaf}$:$[P]_{leaf}$ (**Table 4**). In contrast, the relationship between SOC and leaf stoichiometry was the opposite of those of soil pH, except that there was no significant relationship between SOC and $[C]_{leaf}$:$[P]_{leaf}$. The STP was not related to any index of leaf stoichiometry.

DISCUSSION

Reasons for Variation in Soil Properties and Leaf Stoichiometry of *Potentilla fruticosa* With Elevation

By mainly influencing solar radiation and condensation of water vapor (Sevruk, 1997; Ohmura, 2012), elevation regulates temperature and precipitation (Lozano-García et al., 2016; Zhu et al., 2019), which in turn exerts effects on the distribution of vegetation. For example, in the Qilian Mountains, temperature decreases and precipitation increases with increasing elevation (Chang et al., 2014), resulting in shifting vegetation types: <2,400 m, steppe desert; 2,400–3,300 m, forest steppe; 3,300–3,600 m, subalpine scrub and grassland; 3,600–3,900 m, alpine scrubs and meadow; >3,900 m, ice and snow (Zhu et al., 2019). Likewise, different elevations differ in vegetation types, biomass, quantity and quality of litter, roots, and soil microbial communities (Bargali et al., 2018; Yang et al., 2018b), which in turn affect soil physical and chemical properties (**Tables 1**, **2**; Zhou et al., 2013; Qin et al., 2019). In addition, microlandforms such as slope aspect, slope position, and slope gradient can also influence soil properties by reshaping hydrothermal conditions and patterns in the movement of the material and energy (Måren et al., 2015; Nabiollahi et al., 2018; Zhang et al., 2020) as found in this study (data unpublished).

With changes of biotic and abiotic environments with elevation, leaf stoichiometry of *P. fruticosa* also varied with elevation (**Figure 2**), concurring with other studies (e.g., Badano et al., 2005; Zhang et al., 2019). However, only $[C]_{leaf}$, $[N]_{leaf}$, and $[C]_{leaf}$:$[N]_{leaf}$ of *P. fruticosa* were significantly affected by elevation (**Table 1**), partly supporting our hypothesis that the leaf stoichiometry of *P. fruticosa* would vary with elevation. In contrast, Cao et al. (2020) found that except for $[N]_{leaf}$:$[P]_{leaf}$, leaf stoichiometries of *Oxytropis ochrocephala* Bunge in the Qilian Mountains were significantly affected by elevation. This suggests that each species may have its unique strategies to adapt to local environmental changes.

From 2,400 to 3,800 m, $[C]_{leaf}$ of *P. fruticosa* showed a decreasing trend (**Figure 2A**), which was in contrast to Zhao et al. (2014) and Rong et al. (2016), who found that $[C]_{leaf}$ increased with decreasing temperature to balance the osmotic pressure of cells and resist freezing. This result may reflect the fact that low temperatures inhibit photosynthesis in *P. fruticosa*. In contrast, $[N]_{leaf}$ of *P. fruticosa* showed an increasing trend with a decrease in temperature (**Figure 2B**), as reported by others (e.g., Oleksyn and Przybyl, 1987; Cao et al., 2020). This may be because $[N]_{leaf}$ can enhance metabolic activity and the growth rate of tissues in cold habitats and short growing seasons (Ågren, 2008; Zhang et al., 2017). With a $[C]_{leaf}$ decrease and $[N]_{leaf}$ increase, *P. fruticosa* $[C]_{leaf}$:$[N]_{leaf}$ decreased with rising elevation (**Figure 2D**). Similar observations were reported by Sun et al. (2017). Generally, $[C]_{leaf}$:$[N]_{leaf}$ reflects a plant's ability to simultaneously absorb C and N, and a low value can benefit plant growth (He et al., 2008; Yan et al., 2015).

The Dominant Environmental Factors Influencing Leaf Stoichiometry of *Potentilla fruticosa*

Based on RDA (**Figure 3** and **Table 3**), it is clear that SOC, STP, and pH had a greater effect on leaf stoichiometry of *P. fruticosa* than temperature or precipitation in the Qilian Mountains. This is in slight contradiction with other studies (Sardans et al., 2011; Zhang et al., 2012a; Cao et al., 2020). For example, Cao et al. (2020) found that, across various elevations in the Qilian

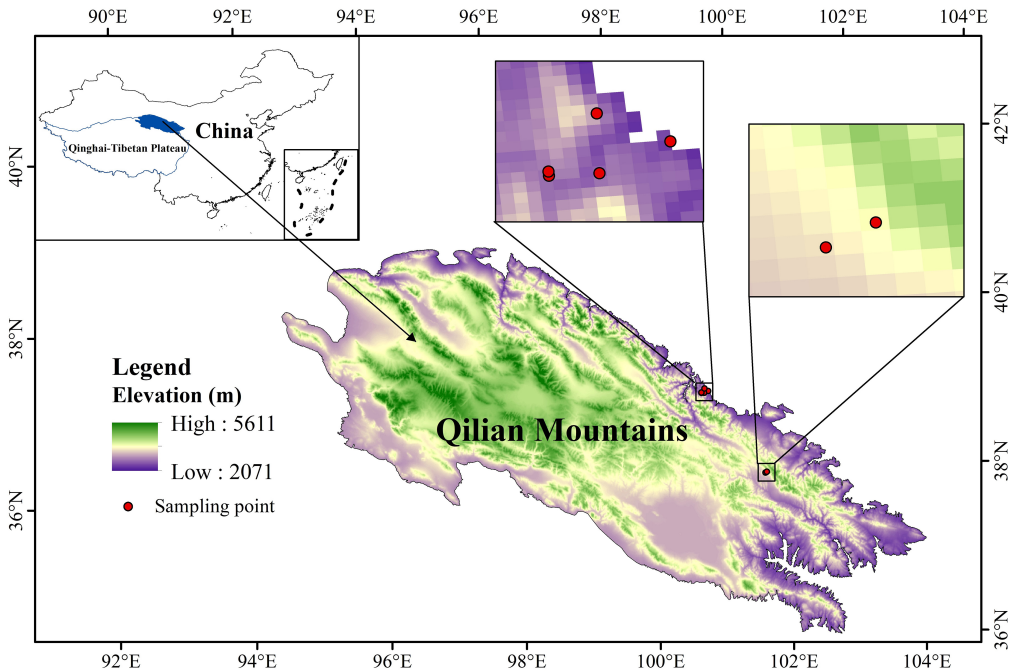

FIGURE 1 | Sampling sites at different elevations (2,400, 2,600, 2,800, 3,000, and 3,200, 3,500, and 3,800 m) in the study area.

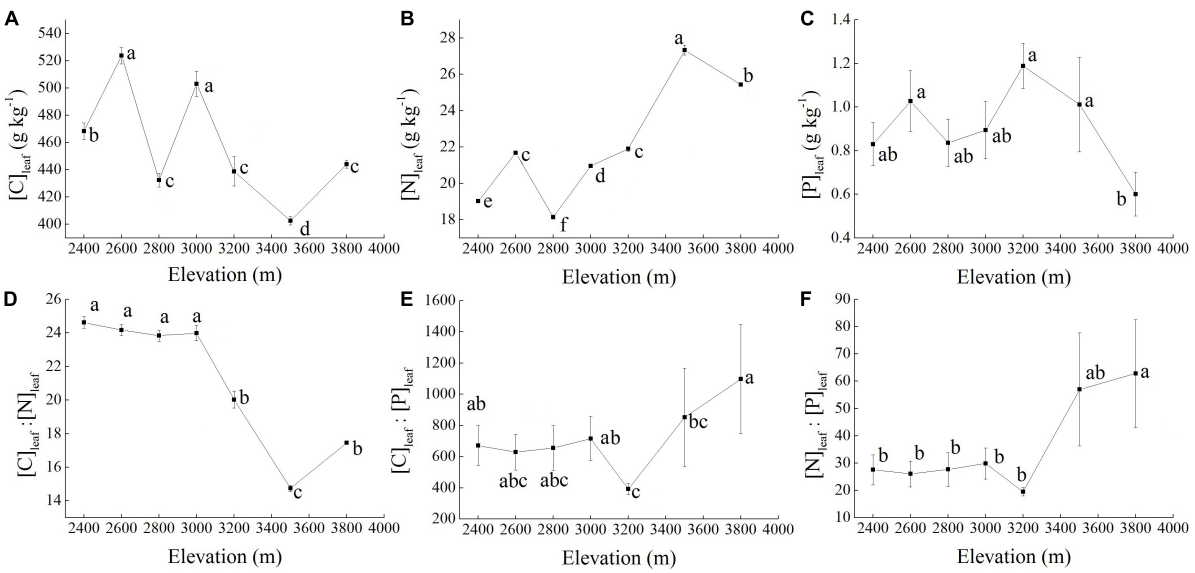

FIGURE 2 | *Potentilla fruticosa* $[C]_{leaf}$ **(A)**, $[N]_{leaf}$ **(B)**, and $[P]_{leaf}$ **(C)** and $[C]_{leaf}$:$[N]_{leaf}$ **(D)**, $[C]_{leaf}$:$[P]_{leaf}$ **(E)**, and $[N]_{leaf}$:$[P]_{leaf}$ **(F)** ratios from 2,400 to 3,800 m (n = 9). $[C]_{leaf}$, leaf carbon (C) concentration; $[N]_{leaf}$, leaf nitrogen (N) concentration; $[P]_{leaf}$, leaf phosphorus (P) concentration. Data are described by their mean and standard error (SE). Different lowercase letters indicate a significant difference among elevations at $p < 0.05$.

Mountains, temperature significantly affected leaf stoichiometry of *O. ochrocephala*, as it could dictate or control nutrient availability in soils, root absorption, and the plant nutrient budget (Reich and Oleksyn, 2004; Isles et al., 2017; Liu et al., 2019). Likewise, Zhang et al. (2012a) found that temperature and precipitation directly affected the spatial patterns of leaf elemental stoichiometry across China, as precipitation regulates the mobilization of soil nutrients (Müller et al., 2017).

Although SOC, STP, and pH were the main contributors to differences in leaf stoichiometry of *P. fruticosa*, STP was not related to any index of leaf stoichiometry (**Table 4**), suggesting that it had a synthetic effect on leaf stoichiometry of *P. fruticosa*

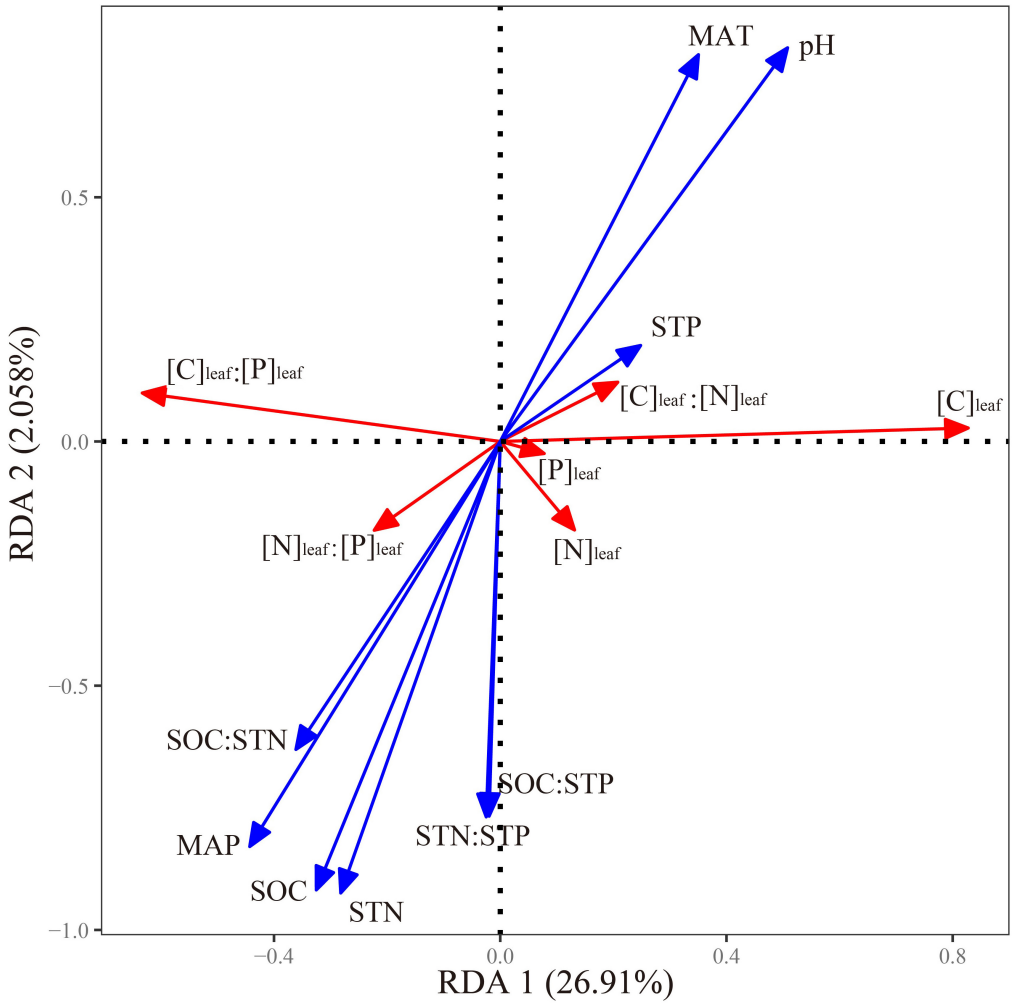

FIGURE 3 | Redundancy analysis (RDA) ordination for the leaf stoichiometric indices of *P. fruticosa* and environmental characteristics. SOC, soil organic carbon; STN, soil total nitrogen; STP, soil total phosphorus; $[C]_{leaf}$, leaf carbon (C) concentration; $[N]_{leaf}$, leaf nitrogen (N) concentration; $[P]_{leaf}$, leaf phosphorus (P) concentration; MAT, mean annual temperature; MAP, mean annual precipitation.

TABLE 3 | Relationships between environmental factors and the two RDA axes, and also environmental factors that are significant contributors to leaf stoichiometry of *P. fruticosa* across elevations.

Environmental factors	RDA1	RDA2	R^2	*P**	Explains (%)	*F*	*P***
SOC	−0.362	−0.932	0.85	**0.001**	6.00	4.20	**0.034**
STN	−0.350	−0.937	0.84	**0.001**	3.30	2.20	0.130
STP	0.514	0.858	0.07	0.097	6.80	5.40	**0.018**
SOC:STN	−0.408	−0.913	0.47	**0.001**	2.60	1.80	0.176
SOC:STP	−0.275	−0.962	0.48	**0.001**	3.30	2.40	0.100
STN:STP	−0.277	−0.961	0.49	**0.001**	<0.10	<0.10	0.800
pH	0.419	0.908	0.80	**0.001**	7.10	4.60	**0.024**
MAT (°C)	0.382	0.924	0.68	**0.001**	0.50	0.40	0.532
MAP (mm)	−0.401	−0.916	0.79	**0.001**	0.50	0.40	0.506

SOC, soil organic carbon; STN, soil total nitrogen; STP, soil total phosphorus; $[C]_{leaf}$, leaf carbon (C) concentration; $[N]_{leaf}$, leaf nitrogen (N) concentration; $[P]_{leaf}$, leaf phosphorus (P) concentration; MAT, mean annual temperature; MAP, mean annual precipitation.
Significant p-values ($p < 0.05$) are in bold.
"" indicates the environmental factor was significantly related to the two axes from the RDA.*
*"**" indicates the variance of each environmental factor significantly contributed to the total variance.*

TABLE 4 | Relationships between leaf stoichiometry of *P. fruticosa* and the dominant factors from the RDA.

Leaf stoichiometry	SOC	STP	pH
$[C]_{leaf}$	−.639**	0.175	.562**
$[N]_{leaf}$	.869**	−0.216	−.867**
$[P]_{leaf}$	−0.055	0.045	0.167
$[C]_{leaf}$:$[N]_{leaf}$	−.929**	0.206	.882**
$[C]_{leaf}$:$[P]_{leaf}$	0.199	−0.192	−.263*
$[N]_{leaf}$:$[P]_{leaf}$	.367**	−0.216	−.416**

SOC, soil organic carbon; STN, soil total nitrogen; STP, soil total phosphorus; $[C]_{leaf}$, leaf carbon (C) concentration; $[N]_{leaf}$, leaf nitrogen (N) concentration; $[P]_{leaf}$, leaf phosphorus (P) concentration.
"" $p < 0.05$, and "**"$p < 0.01$.*

in the Qilian Mountains, but this needs further study. Except $[P]_{leaf}$, leaf nutrient concentrations and their ratios were all significantly related to SOC or pH or both (**Table 4**). The SOC was negatively related to $[C]_{leaf}$, which was not consistent with Niu et al. (2016) who found that these were positively correlated because the C in leaves can enter the soil through litter. In this study, elevations ≥3,200 m had greater SOC but lower temperatures (**Table 1**), which limited photosynthesis and thus resulted in lower $[C]_{leaf}$ (**Figure 2A**). This suggests that the relationship between $[C]_{leaf}$ of *P. fruticosa* and SOC in the Qilian Mountains may not represent a true causality. This may also suggest that the C in soil is the structural basis for plants (Schade et al., 2003; Liu et al., 2011) as less C is captured from the atmosphere by leaves subjected to low temperatures. The SOC was positively related to $[N]_{leaf}$ of *P. fruticosa*, because SOC from amino acid metabolism contains N and it can be transferred from soil to plants by the process of nutrient cycling (Delgado-Baquerizo et al., 2015; Zhang et al., 2019). Given the positive relationship between SOC and $[N]_{leaf}$, there exists a negative or positive relationship with $[C]_{leaf}$:$[N]_{leaf}$, or $[N]_{leaf}$:$[P]_{leaf}$ (**Table 4**). Generally, SOC and pH are negatively correlated, as acidic soil is beneficial to the adsorption of organic C (Zhang et al., 2012b; Hobara et al., 2016). Therefore, the relationships between pH and leaf stoichiometry of *P. fruticosa* were converse to relationships between SOC and leaf stoichiometry (**Table 4**).

In this study, the measured parameters can only explain about 30.00% of the total variation of leaf stoichiometry of *P. fruticosa* (**Figure 3**), indicating that other factors, such as plant community composition (Wang and Moore, 2014; Zhang et al., 2019), may also control the variations. As the plant community in the study area changed with elevation, effects of intra- and interspecies competitions on leaf stoichiometry of *P. fruticosa* should also be considered to achieve a comprehensive understanding.

Limiting Nutrients for *Potentilla fruticosa* Across Elevations

It is well known that $[N]_{leaf}$:$[P]_{leaf}$ rather than $[N]_{leaf}$ or $[P]_{leaf}$ individually can provide a better assessment of a plant's nutrient limitations (Li et al., 2018) although this assessment is still debated. According to Soudzilovskaia et al. (2005), the growth of alpine vascular plants is limited first by N, then by P, with a mean foliar N:P mass ratio of 29 in their study area. In this study, the $[N]_{leaf}$:$[P]_{leaf}$ of *P. fruticosa* at 3,000, 3,500, and 3,800 m were all >29 (**Figure 2F**). Following the criteria provided by Soudzilovskaia et al. (2005), our results suggest that P limited the growth of *P. fruticosa* at higher elevations. Soil P deficiency is common across China (Han et al., 2005; Zhao et al., 2016), including across the entire QTP (Niu et al., 2016) and the Qilian Mountains (Xu et al., 2018, 2019; Zhang et al., 2019; Cao et al., 2020). Furthermore, at elevations ≥3,500 m, the $[N]_{leaf}$:$[P]_{leaf}$ was >50 (**Figure 2F**), suggesting that *P. fruticosa* growth was greatly restricted by available P. It is well known that in the Qilian Mountains, soil surface coverage by vegetation decreases as elevation increases. In combination with P leaching through the soil profile (Chardon and Schoumans, 2007), the lack of vegetative cover at high elevations can easily increase P losses through erosion and surface run-off (Nest et al., 2014) and can make P scarcer. However, Reich and Oleksyn (2004) concluded that plant growth in high elevations was more limited by N. This suggests that limitation of nutrient elements for plants is dependent on region.

CONCLUSION

In the Qilian Mountains of the northeast QTP, soil properties were more sensitive to elevations (ranging from 2,400 to 3,800 m) than leaf stoichiometry of *P. fruticosa*. From low to high elevation, $[C]_{leaf}$ and $[P]_{leaf}$ decreased, whereas $[N]_{leaf}$ of *P. fruticosa* increased, as an adaptation for maintaining metabolic activity in cold habitats.

Elevation only affected *P. fruticosa* $[C]_{leaf}$, $[N]_{leaf}$, and $[C]_{leaf}$:$[N]_{leaf}$, mainly through its effects on SOC, STP, and pH. Although $[N]_{leaf}$:$[P]_{leaf}$ of *P. fruticosa* was not influenced by elevation, its value across all elevations was relatively large. This suggests that in the study area, *P. fruticosa* growth was commonly limited by soil P, especially regarding its growth at higher elevations. As *P. fruticosa* is a major alpine shrub, reducing P losses and improving its growth conditions will play an important role in maintaining the ecologically integrated functions and services of the whole QTP.

DATA AVAILABILITY STATEMENT

The raw data supporting the conclusions of this article will be made available by the authors.

AUTHOR CONTRIBUTIONS

YQ: conception and design of the research. XZ and YQ: acquisition of data. WL: analysis and interpretation of data. XZ: statistical analysis. WL, XZ, and YQ: drafting the manuscript. JA and AB: revision of manuscript drafting and revision of manuscript. All authors read and approved the final manuscript.

FUNDING

This study was supported by the Second Tibetan Plateau Scientific Expedition and Research Program (2019QZKK0103), the Strategic Priority Research Program of the Chinese Academy of Sciences (XDA2006010101), the National Natural Science Fund of China (41771252), Forestry and Grassland Science and Technology Innovation Program of Gansu Province [GYCX(2020)01], and the Natural Science of Gansu Province (21JR7RA045).

REFERENCES

Ågren, G. I. (2008). Stoichiometry and nutrition of plant growth in natural communities. *Annu. Rev. Ecol. Evol. Syst.* 39, 153–170. doi: 10.1146/annurev.ecolsys.39.110707.173515

Badano, E. I., Cavieres, L. A., Molina-Montenegro, M. A., and Quiroz, C. L. (2005). Slope aspect influences plant association patterns in the mediterranean matorral of central Chile. *J. Arid. Environ.* 62, 93–108. doi: 10.1016/j.jaridenv.2004.10.012

Bai, Y., Wu, J., Clark, C. M., Pan, Q., Zhang, L., Chen, S., et al. (2012). Grazing alters ecosystem functioning and C: N: P stoichiometry of grasslands along a regional precipitation gradient. *J. Appl. Ecol.* 49, 1204–1215. doi: 10.1111/j.1365-2664.2012.02205.x

Bargali, K., Manral, V., Padalia, K., Bargali, S. S., and Upadhyay, P. U. (2018). Effect of vegetation type and season on microbial biomass carbon in Central Himalayan forest soils, India. *Catena* 171, 125–135. doi: 10.1016/j.catena.2018.07.001

Baxter, I., and Dilkes, B. P. (2012). Elemental profiles reflect plant adaptations to the environment. *Science* 336, 1661–1663. doi: 10.1126/science.1219992

Cao, J., Wang, X., Adamowski, J. F., Biswas, A., Liu, C., Chang, Z., et al. (2020). Response of leaf stoichiometry of *Oxytropis ochrocephala* to elevation and slope aspect. *Catena* 194:104772. doi: 10.1016/j.catena.2020.104772

Cao, J., Xu, X., Deo, R. C., Holden, N. M., Adamowski, J. F., Gong, Y., et al. (2018). Multi-household grazing management pattern maintains better soil fertility. *Agron. Sustain. Dev.* 38:6. doi: 10.1007/s13593-017-0482-2

Chang, X. F., Zhu, X. X., Wang, S. P., Cui, S. J., Luo, C. Y., Zhang, Z. H., et al. (2014). Impacts of management practices on soil organic carbon in degraded alpine meadows on the Tibetan Plateau. *Biogeosciences* 11, 3495–3503. doi: 10.5194/bg-11-3495-2014

Chardon, W. J., and Schoumans, O. F. (2007). Soil texture effects on the transport of phosphorus from agricultural land in river deltas of Northern Belgium, The Netherlands and North-West Germany. *Soil Use Manage.* 23, 16–24. doi: 10.1111/j.1475-2743.2007.00108.x

Delgado-Baquerizo, M., García-Palacios, P., Milla, R., Gallardo, A., and Maestre, F. T. (2015). Soil characteristics determine soil carbon and nitrogen availability during leaf litter decomposition regardless of litter quality. *Soil Biol. Biochem.* 81, 134–142. doi: 10.1016/j.soilbio.2014.11.009

Elkington, T. T. (1969). Cytonaxonomic variation in *Potentilla fruticosal*. *New Phytol.* 68, 151–160. doi: 10.1111/j.1469-8137.1969.tb06428.x

Esmeijer-Liu, A. J., Aerts, R., Kürschner, W. M., Bobbink, R., Lotter, A. F., and Verhoeven, J. T. A. (2009). Nitrogen enrichment lowers *Betula pendula* green and yellow leaf stoichiometry irrespective of effects of elevated carbon dioxide. *Plant Soil* 316, 311–322. doi: 10.1007/s11104-008-9783-1

Ganenko, T. V., Lutskii, B. I., Larin, M. F., Vereshchagin, A. L., and Semenov, A. A. (1988). Chemical composition of *Potentilla fruticosa. I. Flavonoids*. *Chem. Nat. Comp.* 3, 387–388. doi: 10.1007/BF00598597

Han, W., Fang, J., Guo, D., and Zhang, Y. (2005). Leaf nitrogen and phosphorus stoichiometry across 753 terrestrial plant species in China. *New Phytol.* 168, 377–385. doi: 10.1111/j.1469-8137.2005.01530.x

He, J., Wang, L., Flynn, D. F. B., Wang, X., Ma, W., and Fang, J. (2008). Leaf nitrogen: phosphorus stoichiometry across Chinese grassland biomes. *Oecologia* 155, 301–310. doi: 10.1007/s00442-007-0912-y

Hobara, S., Kushida, K., Kim, Y., Koba, K., Lee, B. Y., and Ae, N. (2016). Relationships among pH, minerals, and carbon in soils from tundra to boreal forest across Alaska. *Ecosystems* 19, 1092–1103. doi: 10.1007/s10021-016-9989-7

Isles, P. D. F., Xu, Y., Stockwell, J. D., and Schroth, A. W. (2017). Climate-driven changes in energy and mass inputs systematically alter nutrient concentration and stoichiometry in deep and shallow regions of Lake Champlain. *Biogeochemistry* 133, 201–217. doi: 10.1007/s10533-017-0327-8

Jenny, H. (1941). Factors of soil formation: a system of quantitative pedology. *Soil Sci.* 5, 415–426. doi: 10.1134/S1064229309120138

Li, F., Hu, J., Xie, Y., Yang, G., Hu, C., Chen, X., et al. (2018). Foliar stoichiometry of carbon, nitrogen, and phosphorus in wetland sedge *Carex brevicuspis* along a small-scale elevation gradient. *Ecol. Indic.* 92, 322–329. doi: 10.1016/j.ecolind.2017.04.059

Liu, G., Ye, X., Huang, Z., and Cornelissen, J. H. C. (2019). Leaf and root nutrient concentrations and stoichiometry along aridity and soil fertility gradients. *J. Veg. Sci.* 2, 291–300. doi: 10.1111/jvs.12717

Liu, R. T., Zhao, H. L., Zhao, X. Y., and Drake, S. (2011). Facilitative effects of shrubs in shifting sand on soil macro-faunal community in Horqin Sand Land of Inner Mongolia, Northern China. *Eur. J. Soil Biol.* 47, 316–321. doi: 10.1016/j.ejsobi.2011.07.006

Liu, X., Zhang, Y., Han, W., Tang, A., Shen, J., Cui, Z., et al. (2013). Enhanced nitrogen deposition over China. *Nature* 494, 459–462. doi: 10.1038/nature11917

Liu, Y., Liu, Q., Wang, T., and Fang, S. (2018). Leaf nitrogen and phosphorus stoichiometry of *Cyclocarya paliurus* across China. *Forests* 9:771. doi: 10.3390/f9120771

Liu, Z., Luo, Z., Jia, C., Wang, D., and Li, D. (2016). Synergistic effects of *Potentilla fruticosa* L. leaves combined with green tea polyphenols in a variety of oxidation systems. *J. Food. Sci.* 81, C1091–C1101. doi: 10.1111/1750-3841.13292

Lozano-García, B., Parras-Alcántara, L., and Brevik, E. C. (2016). Impact of topographic aspect and vegetation (native and reforested areas) on soil organic carbon and nitrogen budgets in Mediterranean natural areas. *Sci. Total Environ.* 544, 963–970. doi: 10.1016/j.scitotenv.2015.12.022

Lugovskaya, A. Y., Khramova, E., and Chankina, O. V. (2018). Effect of transport and industrial pollution on morphometric parameters and element composition of *Potentilla fruticosa*. *Contemp. Probl. Ecol.* 1, 89–98. doi: 10.1134/S1995425518010092

Luo, Z., Wang, S., and Wang, D. (2016). Phenolic profiles and antioxidant capacities of crude extracts and subsequent fractions from *Potentilla fruticosa* L. leaves. *Nat. Prod. Res.* 30, 1890–1895. doi: 10.1080/14786419.2015.1084303

Maccherini, S., Marignani, M., Gioria, M., Renzi, M., Rocchini, D., Santi, E., et al. (2011). Determinants of plant community composition of remnant biancane badlands: a hierarchical approach to quantify species-environment relationships. *Appl. Veg. Sci.* 14, 378–387. doi: 10.1111/j.1654-109x.2011.01131.x

Måren, I. E., Karki, S., Prajapati, C., Yadav, R. K., and Shrestha, B. B. (2015). Facing north or south: does slope aspect impact forest stand characteristics and soil properties in a semiarid trans-Himalayan valley? *J. Arid Environ.* 121, 112–123. doi: 10.1016/j.jaridenv.2015.06.004

Miliauskas, G., Beek, T. A. V., Venskutonis, P. R., Linssen, J. P. H., Waard, P., and Sudhölter, E. J. R. (2010). Antioxidant activity of *Potentilla fruticosa*. *J. Sci. Food Agric.* 84, 1997–2009. doi: 10.1002/jsfa.1914

Moe, S. J., Stelzer, R. S., Forman, M. R., Harpole, W. S., Daufresne, T., and Yoshida, T. (2005). Recent advances in ecological stoichiometry: insights for population and community ecology. *Oikos* 109, 29–39. doi: 10.1111/j.0030-1299.2005.14056.x

Müller, M., Oelmann, Y., Schickhof, U., Böhner, J., and Scholten, T. (2017). Himalayan treeline soil and foliar C: N: P stoichiometry indicate nutrient shortage with elevation. *Geoderma* 291, 21–32. doi: 10.1016/j.geoderma.2016.12.015

Nabiollahi, K., Golmohamadi, F., Taghizadeh-Mehrjardi, R., Kerry, R., and Davari, M. (2018). Assessing the effects of slope gradient and land use change on soil quality degradation through digital mapping of soil quality indices and soil loss rate. *Geoderma* 318, 16–28. doi: 10.1016/j.geoderma.2017.12.024

Nelson, D. W., and Sommers, L. E. (1982). "Total carbon, organic carbon, and organic matter," in *Methods Of Soil Analysis Part 2. Chemical And Microbiological Properties*, ed. A. L. Page (Madison, WI: American Society of Agronomy), 539–579.

Nest, T. V., Vandecasteele, B., Ruysschaert, G., Cougnon, M., Merckx, R., and Reheul, D. (2014). Effect of organic and mineral fertilizers on soil P and C levels, crop yield and P leaching in a long term trial on a silt loam soil. *Agric. Ecosyst. Environ*. 197, 309–317. doi: 10.1016/j.agee.2014.07.019

Niu, R., Gao, X., Xu, F., Wang, W., Wang, L., Sun, P., et al. (2016). Carbon, nitrogen, and phosphorus stoichiometric characteristics of soil and leaves from young and middle aged *Larix principis-rupprechtii* growing in a Qinling Mountain plantation. *Acta Ecol. Sin.* 36, 7384–7392. doi: 10.5846/stxb201601080057

Nkiliza, J. (1999). *Process for Extracting Catechin Polyphenols From Potentillas, Extract Obtained and Its Use*. United States Berkem (Gardonne, FR) 5928646. Available online at: https://www.freepatentsonline.com/5928646.html (accessed July 27, 1999).

Ohmura, A. (2012). Enhanced temperature variability in high-altitude climate change. *Theor. Appl. Climatol*. 110, 499–508. doi: 10.1007/s00704-012-0687-x

Oleksyn, J., and Przybyl, K. (1987). Oak decline in the Soviet Union-scale and hypotheses. *Eur. J. For. Pathol*. 6, 321–336. doi: 10.1111/1439-0329.ep8118658

Qin, Y., Adamowski, J. F., Deo, R. C., Hu, Z., Cao, J., Zhu, M., et al. (2019). Controlling factors of plant community composition with respect to the slope aspect gradient in the Qilian Mountains. *Ecosphere* 10:e02851. doi: 10.1002/ecs2.2851

Qin, Y., Feng, Q., Holden, N. M., and Cao, J. (2016). Variation in soil organic carbon by slope aspect in the middle of the Qilian Mountains in the upper Heihe River Basin, China. *Catena* 147, 308–314. doi: 10.1016/j.catena.2016.07.025

Reich, P. B., and Oleksyn, J. (2004). Global patterns of plant leaf N and P in relation to temperature and latitude. *Proc. Natl. Acad. Sci. U.S.A.* 101, 11001–11006. doi: 10.1073/pnas.0403588101

Rong, Q., Liu, J., Cai, Y., Lu, Z., Zhao, Z., Yue, W., et al. (2016). "Fertile island" effects of *Tamarix chinensis Lour*. on soil N and P stoichiometry in the coastal wetland of Laizhou Bay, China. *J. Soil Sediment*. 16, 864–877. doi: 10.1007/s11368-015-1296-y

Sardans, J., Rivas-Ubach, A., and Peñuelas, J. (2011). Factors affecting nutrient concentration and stoichiometry of forest trees in Catalonia (NE Spain). *For. Ecol. Manag*. 262, 2024–2034. doi: 10.1016/j.foreco.2011.08.019

Schade, J. D., Kyle, M., Hobbie, S. E., Fagan, W. F., and Elser, J. J. (2003). Stoichiometric tracking of soil nutrients by a desert insect herbivore. *Ecol. Lett*. 6, 96–101. doi: 10.1046/j.1461-0248.2003.00409.x

Scott, E. E., Prater, C., Norman, E., Baker, B. C., Evans-White, M., and Scott, J. T. (2013). Leaf-litter stoichiometry is affected by streamwater phosphorus concentrations and litter type. *Freshw. Sci*. 32, 753–761. doi: 10.1899/12-215.1

Sevruk, B. (1997). Regional dependency of precipitation-altitude relationship in the swiss alps. *Clim. Change High Elevation Sites* 36, 355–369. doi: 10.1007/978-94-015-8905-5_7

Shimono, A., Ueno, S., Gu, S., Zhao, X., Tsumura, Y., and Tang, Y. (2010). Range shifts of *Potentilla fruticosa* on the Qinghai-Tibetan Plateau during glacial and interglacial periods revealed by chloroplast DNA sequence variation. *Heredity* 104:534. doi: 10.1038/hdy.2009.158

Soudzilovskaia, N. A., Onipchenko1, V. G., Cornelissen, J. H. C., and Aerts, R. (2005). Biomass production, N: P ratio and nutrient limitation in a Caucasian alpine tundra plant community. *J Veg. Sci*. 16, 399–406. doi: 10.1111/j.1654-1103.2005.tb02379.x

Sun, L., Zhang, B., Wang, B., Zhang, G., Zhang, W., Zhang, B., et al. (2017). Leaf elemental stoichiometry of *Tamarix Lour*. species in relation to geographic, climatic, soil, and genetic components in China. *Ecol. Eng*. 106, 448–457. doi: 10.1016/j.ecoleng.2017.06.018

Wang, M., and Moore, T. R. (2014). Carbon, nitrogen, phosphorus, and potassium stoichiometry in an ombrotrophic peatland reflects plant functional type. *Ecosystems* 17, 673–684. doi: 10.1007/s10021-014-9752-x

Xu, X., Qin, Y., and Cao, J. (2019). Variation characteristics of potentilla bifurca leaf stoichiometry along the elevation gradient on the northeastern Qinghai-Tibetan Plateau. *Acta Ecol. Sin.* 39, 9044–9051. doi: 10.5846/stxb201805231128

Xu, X., Qin, Y., Cao, J., Li, M., Gong, Y., and Zhang, X. (2018). Elevational variations of leaf stoichiometry in *Leontopodium leontopodioides* on the Qinghai-Tibetan Plateau, China. *Ying Yong Sheng Tai Xue Bao* 29, 3934–3940. doi: 10.13287/j.1001-9332.201812.021

Yan, P., Liu, L., Zeng, Y., Chen, H., Li, M., and Li, J. (2019). Effects of *Fruticosa potentilla* L. on expression of glucose and lipid metabolism key enzymes and hormones in T2DM rats. *Chinese Pharmacol. Bull.* 35, 293–294. doi: 10.3969/j.issn.1001-1978.2019.02.029

Yan, Z., Kim, N., Han, W., Guo, Y., Han, T., and Du, E. (2015). Effects of nitrogen and phosphorus supply on growth rate, leaf stoichiometry, and nutrient resorption of *Arabidopsis thaliana*. *Plant Soil* 2, 147–155. doi: 10.1007/s11104-014-2316-1

Yang, F., Niu, K., Collins, C. G., Yan, X., Ji, Y., Ling, N., et al. (2018a). Grazing practices affect the soil microbial community composition in a Tibetan alpine meadow. *Land Deg. Dev*. 30, 49–59. doi: 10.1002/ldr.3189

Yang, F., Wu, J., Zhang, D., Chen, Q., Zhang, Q., and Cheng, X. (2018b). Soil bacterial community composition and diversity in relation to edaphic properties and plant traits in grasslands of southern China. *Appl. Soil Ecol*. 128, 43–53. doi: 10.1016/j.apsoil.2018.04.001

Yao, X., Wu, J., and Gong, X. (2019). Precipitation and seasonality affect grazing impacts on herbage nutritive values in alpine meadows on the Qinghai-Tibet Plateau. *J. Plant Ecol.* 6, 993–1008. doi: 10.1093/jpe/rtz027

Yuan, Z. (2017). Factors affecting lucerne-rich vegetation under revegetation in a semi-arid environment. *Ecol. Eng.* 108, 249–254. doi: 10.1016/j.ecoleng.2017.08.030

Yuichiro, Y., Yoko, S., Mitsuru, H., Ayako, S., and Toshiyuki, O. (2010). The role of shrub (*Potentilla fruticosa*) on ecosystem CO_2 fluxes in an alpine shrub meadow. *J. Plant Ecol*. 2, 89–97. doi: 10.1093/jpe/rtq011

Zeng, Y., Sun, Y., Meng, X., Yu, T., and Zhang, Y. (2019). A new methylene bisflavan-3-ol from the branches and leaves of *Potentilla fruticosa*. *Nat. Prod. Res*. 34, 1–8. doi: 10.1080/14786419.2018.1557169

Zhang, J., Zhao, N., Liu, C., Yang, H., Li, M., Yu, G., et al. (2017). C: N: P stoichiometry in China's forests: from organs to ecosystems. *Funct. Ecol*. 32, 50–60. doi: 10.1111/1365-2435.12979

Zhang, S., Zhang, J., Slik, J., and Cao, K. (2012a). Leaf element concentrations of terrestrial plants across China are influenced by taxonomy and the environment. *Glob. Ecol. Biogeogr*. 8, 809–818. doi: 10.1111/j.1466-8238.2011.00729.x

Zhang, S., Chen, D., Sun, D., Wang, X., Smith, J., and Du, G. (2012b). Impacts of altitude and position on the rates of soil nitrogen mineralization and nitrification in alpine meadows on the eastern Qinghai-Tibetan Plateau, China. *Biol. Fertil. Soils*. 4, 393–400. doi: 10.1007/s00374-011-0634-5

Zhang, X., Adamowski, J. F., Liu, C., Zhou, J., Zhu, G., Dong, X., et al. (2020). Which slope aspect and gradient provides the best afforestation-driven soil carbon sequestration on the China's Loess Plateau? *Ecol. Eng*. 147:105782. doi: 10.1016/j.ecoleng.2020.105782

Zhang, X., Liu, X., Jing, W., and Cao, J. (2019). Variation characteristics of *Leontopodium leontopodioides* leaf stoichiometry with altitude and their relationship with soil nutrients in Qilian Mountains, Northwest China. *Chinese J. Appl. Ecol.* 30, 4012–4020. doi: 10.13287/j.1001-9332.201912.009

Zhao, C., Nan, Z., and Cheng, G. (2005). Methods for modelling of temporal and spatial distribution of air temperature at landscape scale in the southern Qilian mountains, China. *Ecol. Model*. 189, 209–220. 016 doi: 10.1016/j.ecolmodel.2005.03

Zhao, C., Nan, Z., Cheng, G., Zhang, J., and Feng, Z. (2006). GIS-assisted modelling of the spatial distribution of Qinghai spruce (*Picea crassifolia*) in the Qilian Mountains, northwestern China based on biophysical parameters. *Ecol. Model*. 191, 487–550. doi: 10.1016/j.ecolmodel.2005.05.018

Zhao, N., He, N., Wang, Q., Zhang, X., Wang, R., Xu, Z., et al. (2014). The altitudinal patterns of leaf C: N: P stoichiometry are regulated by plant growth form, climate and soil on Changbai Mountain. China. *PLoS One* 9:e95196. doi: 10.1371/journal.pone.0095196

Zhao, W. Q., Reich, P. B., Yu, Q., Zhao, N., Yin, C., Zhao, C., et al. (2018). Shrub type dominates the vertical distribution of leaf C : N : P stoichiometry across an extensive altitudinal gradient. *Biogeosciences* 15, 2033–2053.

Zhao, W., Liu, X., Jin, M., Zhang, X., Che, Z., Jing, W., et al. (2016). Ecological stoichiometric characteristics of carbon, nitrogen and phosphorus in leaf-litter-soil system of *Picea crassifolia* forest in the Qilian Mountains. *Acta Pedol. Sin.* 53, 477–489. doi: 10.11766/trxb201501080511

Zhou, Z., Guo, C., and Meng, H. (2013). Temperature sensitivity and basal rate of soil respiration and their determinants in temperate forests of North China. *PLoS One* 8:e81793. doi: 10.1371/journal.pone.0081793

Zhu, D., Hui, D., Wang, M., Yang, Q., and Yu, S. (2020). Light and competition alter leaf stoichiometry of introduced species and native mangrove species. *Sci. Total Environ.* 738:140301. doi: 10.1016/j.scitotenv.2020.140301

Zhu, M., Feng, Q., Zhang, M., Liu, W., Deo, R. C., Zhang, C., et al. (2019). Soil organic carbon in semiarid alpine regions: the spatial distribution, stock estimation, and environmental controls. *J. Soil. Sediment* 19, 3427–3441. doi: 10.1007/s11368-019-02295-6

Conflict of Interest: The authors declare that the research was conducted in the absence of any commercial or financial relationships that could be construed as a potential conflict of interest.

Publisher's Note: All claims expressed in this article are solely those of the authors and do not necessarily represent those of their affiliated organizations, or those of the publisher, the editors and the reviewers. Any product that may be evaluated in this article, or claim that may be made by its manufacturer, is not guaranteed or endorsed by the publisher.

Copyright © 2022 Qin, Liu, Zhang, Adamowski and Biswas. This is an open-access article distributed under the terms of the Creative Commons Attribution License (CC BY). The use, distribution or reproduction in other forums is permitted, provided the original author(s) and the copyright owner(s) are credited and that the original publication in this journal is cited, in accordance with accepted academic practice. No use, distribution or reproduction is permitted which does not comply with these terms.

frontiers in Plant Science

ORIGINAL RESEARCH
published: 02 March 2022
doi: 10.3389/fpls.2022.829381

Differentiate Responses of Soil Microbial Community and Enzyme Activities to Nitrogen and Phosphorus Addition Rates in an Alpine Meadow

*Hongbiao Zi[1], Lei Hu[2] and Changting Wang[2]**

[1] State Key Laboratory of Grassland Agro-Ecosystems, and College of Pastoral Agriculture Science and Technology, Lanzhou University, Lanzhou, China, [2] Institute of Qinghai-Tibetan Plateau Research, Southwest Minzu University, Chengdu, China

Nitrogen (N) and phosphorus (P) are the dominant limiting nutrients in alpine meadows, but it is relatively unclear how they affect the soil microbial community and whether their effects are rate dependent. Here, N and P addition rates (0, 10, 20, and 30 g m^{-2} $year^{-1}$) were evaluated in an alpine meadow and variables related to plants and soils were measured to determine the processes affecting soil microbial community and enzyme activities. Our results showed that soil microbial biomass, including bacteria, fungi, gramme-negative bacteria, and actinomycetes, decreased along with N addition rates, but they first decreased at low P addition rates (10 g m^{-2} $year^{-1}$) and then significantly increased at high P addition rates (30 g m^{-2} $year^{-1}$). Both the N and P addition stimulated soil invertase activity, while urease and phosphatase activities were inhibited at low N addition rate and then increased at high N addition rate. P addition generally inhibited peroxidase and urease activities, but increased phosphatase activity. N addition decreased soil pH and, thus, inhibited soil microbial microorganisms, while P addition effects were unimodal with addition rates, achieved through altering sedge, and available P in the soil. In conclusion, our studies indicated that soil microbial communities and enzyme activities are sensitive to short-term N and P addition and are also significantly influenced by their addition rates.

Keywords: N and P addition, phospholipid fatty acid, soil enzyme activities, rate dependent, alpine meadow

OPEN ACCESS

Edited by:
Jian Sun,
Institute of Tibetan Plateau Research (CAS), China

Reviewed by:
Yan Yang,
Institute of Mountain Hazards and Environment (CAS), China
Jingxue Zhao,
Lanzhou University, China

****Correspondence:***
Changting Wang
wangct6@163.com

Specialty section:
This article was submitted to Functional Plant Ecology, a section of the journal Frontiers in Plant Science

Received: *05 December 2021*
Accepted: *13 January 2022*
Published: *02 March 2022*

Citation:
Zi H, Hu L and Wang C (2022) Differentiate Responses of Soil Microbial Community and Enzyme Activities to Nitrogen and Phosphorus Addition Rates in an Alpine Meadow. Front. Plant Sci. 13:829381. doi: 10.3389/fpls.2022.829381

INTRODUCTION

Nitrogen (N) and phosphorus (P) addition, either individually or in combination, have been shown to influence the above- and belowground ecosystem performance in many terrestrial ecosystems (Humbert et al., 2016; Li et al., 2016). N and P fertiliser addition increased plant biomass relative to unfertilised plants by 81 and 22%, respectively (Craine and Jackson, 2009), but reduced plant community richness and diversity (Chen et al., 2013; Isbell et al., 2013). In addition, a marked difference showed that N addition favoured grasses (Clark and Tilman, 2008), while P addition favoured legume growth (Zhao et al., 2019) due to N fixing (Marleau et al., 2011).

As an important component of the belowground ecosystems, soil microorganisms usually interact with the plants through roots and, thus, form cooperative or competitive relationships (Zhou et al., 2021). In most ecosystems, plants would supply labile carbon and receive nutrients from microorganisms in return (Brundrett, 2009). In some cases, soil microorganisms are strong competitors for N or P, at least in the short term, because they temporarily incorporate limiting nutrients in their biomass, making them unavailable to nutrient-limited plants (Kuzyakov and Xu, 2013; Wild et al., 2018). In general, plant diversity and density are directly correlated with soil microbial diversity and function (Porazinska et al., 2018; Navratilova et al., 2019) and soil microbial biomass also directly depends on plant species richness (Geisseler and Scow, 2014). These plant effects on soil microorganisms indicated that changes in plants would surely affect soil microbial community, while these effects remain elusive when N or P fertilisers are applied.

Except for plant effects, fertiliser addition directly alters soil microbial community, especially depending on addition rate. A meta-analysis showed that N addition could inhibit soil microbial diversity and 15% of soil microbial biomass on average (Wang et al., 2018) for significant changes in soil pH (Lucas et al., 2011; Wang et al., 2017), but a more copiotrophic microbial phyla or fungal biomass would increase (Cusack et al., 2011; Fierer et al., 2012). However, other studies demonstrated that N addition had neutral or slightly negative effects on soil microbial abundance and activity (Treseder, 2004; Camenzind et al., 2018). The soil microbial responses to N addition also varied between ecosystem types. In a semi-arid temperate steppe, soil microbial biomass slightly increased at low N addition rate, but decreased at high N addition rate (Zhang et al., 2008). In an alpine meadow, soil microorganisms, such as the arbuscular mycorrhizal fungal community, were influenced by N addition and the high N rate decreased the arbuscular mycorrhizal fungal spore (Zheng et al., 2014). In a subtropical agricultural ecosystem, organic fertilisers would also improve soil microbial activity, but microbial growth would not increase with fertiliser application (Dong et al., 2014). However, in a lowland tropical rain forest, the response of soil microbial biomass to a decade of N addition was not significant (Turner and Joseph, 2013). N-rich tropical forests even have an increase in fungal biomass with N addition (Cusack et al., 2011). The different soil microorganism responses showed us that the effect of N addition might depend on the interaction between the studied ecosystem types and the N addition rate (Geisseler and Scow, 2014; Yao et al., 2014; Zhou et al., 2016).

Unlike N addition effects, P addition effects on soil microorganisms are relatively unknown (Treseder, 2008), especially in alpine meadows. Soil pH, the key factor influencing soil microorganisms, was not significantly changed by P addition (Mao et al., 2017) and it did not even increase, as shown by a meta-analysis (Xiao et al., 2018). However, P addition directly alters the plant community productivity, especially the legume biomass (Zhao et al., 2019), and it indirectly significantly affects the surrounding microorganisms (Hartmann et al., 2008; Berendsen et al., 2012) through rhizodeposition (Zak et al., 2003; Eisenhauer et al., 2010) or symbiotic N fixation (Augusto et al., 2013; Diáková et al., 2018) and the increasing mycorrhizal colonisation of plant roots (Lagrange et al., 2013). Thus, the effects of P addition on soil microorganisms might be correlated with plant factors, but not with soil factors.

Otherwise, the effects of N and P addition interact and directly change the soil nutrient ratio in many ecosystems. With increasing N addition, the limiting effect of P on the aboveground net primary production would increase severely (Li et al., 2016). P addition would also augment the effects of N addition on grassland such as soil respiration (Liu et al., 2020). The alpine meadow, the dominant grassland type of the Qinghai-Tibet Plateau, has been also demonstrated to be N and P colimited (Xu et al., 2015; He et al., 2016). Most studies conducted in alpine meadows were only focussed the effects of N addition on plant or soil microbial community characteristics (Ren et al., 2016; Guo et al., 2017; Wang et al., 2017, 2019). Some studies have demonstrated a neutral effect of N addition, but a negative effect of P addition on extracellular enzymatic activities (Jing et al., 2016), where P was the key limiting factor for soil microorganisms in alpine meadows (Dong et al., 2020). Overall, few studies simultaneously have showed how N and P affect the soil microbial community and whether their effects are rate dependent.

Here, N and P addition was conducted in alpine meadows and the plant community, soil microbial community, as well as soil physicochemical properties were measured. We first aimed to differentiate the effects of N and P addition on soil microbial community and then we focussed on the extent of their effect by evaluating N and P addition rates in an alpine meadow in the Qinghai-Tibet Plateau. We aimed to: (1) determine that the responses of soil microbial communities and enzyme activities to N and P addition rates and (2) explore the main abiotic and biotic factors structuring soil microbial community. Based on the previous studies, we hypothesised that: (1) the effect of N and P addition on the soil microbial community would be rate dependent, especially in the different soil microbial groups and (2) different soil and plant factors drive soil microorganisms under N and P addition.

MATERIALS AND METHODS

Study Site

This experiment was conducted in an alpine meadow, located at Hongyuan County (N: 32°50′–33°22′, E: 102°01′–103°23′) of the Qinghai-Tibet Plateau. With an average altitude of 3,500 m, the Hongyuan alpine meadow has a mean annual temperature of 0.9°C ranging from −10.3 at January to 10.9°C at July and mean annual precipitation of 657–730 mm, characterised by the high altitude and low temperature all the year round. Based on the field survey, the natural plant community was dominated by Cyperaceae plants such as *Kobresia humilis* and *Blysmus sinocom*, Gramineae plants such as *Elymus nutans* and *Agrostis clavata*, accompanying by Compositae plants such as *Saussurea nigrescens* and *Anaphalis lacteal* and Ranunculaceae plants such as *Anemone trullifolia* and *Anemone rivularis*. The soil at this site was Mollisols, with low pH (4.6–6.0) and soil organic matter (SOM) ranging from 80 to 120 $g{\cdot}kg^{-1}$ (Hu et al., 2017).

Experimental Design

The two factors, N addition (four addition rates: CK, 0; N10, 10 g m^{-2} $year^{-1}$, N20, 20 g m^{-2} $year^{-1}$, and N30, 30 g m^{-2} $year^{-1}$) and P addition (four addition rates: CK, 0; P10, 10 g m^{-2} $year^{-1}$, P20, 20 g m^{-2} $year^{-1}$, and P30, 30 g m^{-2} $year^{-1}$), in a completely randomised block design, formed 7 treatments with 6 replications. There were 42 subplots (3 m × 3 m) separated by 2-m buffer zones to avoid the marginal effect located in the 300 m × 300 m alpine meadow site fenced with wire netting to prevent disturbance from grazing or other animals. The N fertiliser of urea [$CO(NH_2)_2$] and P fertiliser of calcium superphosphate [$Ca(H_2PO_4)\cdot H_2O$] were uniformly added once a year in a cloudy day of early growing seasons in the alpine meadow since late April 2012.

Field Sampling

On three randomly selected subplots from the six ones, all the plants within a 50 cm × 50 cm quadrat were harvested and separated into four functional groups (grasses, sedges, legumes, and forbs) in the late August 2013. For each subplot, the height, abundance, and coverage of each species recorded.

After removal of aboveground plants, soil samples in 0–10 cm were randomly collected by a soil auger (5 cm in diameter) in a V-shaped pattern for 5 times from the selected subplots. Soil samples were uniformity mixed and then transported in cooled boxes to the laboratory and sieved (0.25 mm). One part was stored at 4°C for measuring soil microbes and soil enzyme activities and the others were dried for soil pH and soil nutrients. Fine roots were sampled in five soil cores (5 cm in diameter) at 0–10 cm and then isolated by sieving 2 mm mesh. The total roots and the mowed aboveground plants were dried at 60°C for 48 h and then weighed.

Soil Physicochemical Properties

The air-dried soil samples were sieved through a 2-mm mesh to measure their physicochemical properties. Soil pH was determined with a glass electrode by using a soil to water ratio of 1:1 (Chu et al., 2007). SOM concentration was determined by a modification of the chromic acid titration method—Degtjareff method (Walkley and Black, 1934). Soil total N (TN) was determined by the Kjeldahl method (Bremner, 1960). Soil total P (TP) was determined by after digestion in HF-$HClO_4$ (Jackson, 1974). The available N (AN) was measured by using an automated procedure (Skalar SANplus Segmented Flow Analyser, Skaler Incorporation, Breda, Netherlands) and the available P (AP) was assayed by molybdenum blue colorimetry and flame photometry and measured with a spectrophotometer (Hach DR 2700, Hach Company, Loveland, Colorado, United States).

Soil Microbial Community and Enzyme Activities

Soil microbial communities were assessed by using phospholipid fatty acid (PLFA) analysis described by Frostegård et al. (1993). Based on the previous results and the method of PLFA biomarkers, the appraised carbon chain length of measured PLFA was C13–C18 for abundant species, including saturated, unsaturated, and cyclic PLFAs, of which there were 24 types in total. The Gramme-positive bacteria (G^+) were estimated as the sum of i15:0, i16:0, i17:0, i18:0, a15:0, a17:0, and a18:0 and the Gramme-negative bacteria (G^-) were estimated as the sum of cy15:0, cy17:0, 16:1ω7c, 16:1ω9c, 18:1ω7t, and 18:1ω7c (Frostegård et al., 1993; Frostegård and Bååth, 1996; McKinley et al., 2005; Ramsey et al., 2006). Actinomycetes (Ac) were estimated as the sum of 2Me 18:0, 10Me 17:0, and 10Me 18:0 (McKinley et al., 2005) and fungi were estimated as the sum of 18:1ω9c and 18:2ω69c (Frostegård and Bååth, 1996; Frostegård et al., 2011). The left PLFAs were indicative of general bacteria (GB) (Frostegård et al., 1993; Frostegård and Bååth, 1996).

The substrate status of soil microorganisms could be inferred from measurements of soil enzyme activities because investment in enzyme synthesis was assumed to reflect biological nutrient demand (Turner and Joseph, 2013). Soil enzymes involved in the acquisition of N and P, such as the β-glucosaminidase phosphatase, could be used to infer microbial nutrient demand for N and P (Marklein and Houlton, 2012). Therefore, fertilisers-induced microbial response should be also assessed by soil enzyme activities (Hu et al., 2014; Rosinger et al., 2019). Thus, we measured the activities of soil urease, invertase, peroxidase, and acid phosphatase by using colorimetric method for three times, respectively (Guan, 1983).

Data Analysis

All the response variables, including soil pH and nutrients, plant community characteristics, soil enzyme activities, and soil microbial indexes, along N and P addition rates, were analysed by the one-way ANOVA followed by Duncan's multiple range test by using SPSS 19.0 software package (SPSS Incorporation, Chicago, Illinois, United States), respectively. The data of response variables were transformed with the natural logarithm to improve normality.

We used multiple regressions on distance matrices (MRM) in the *ecodist* package to estimate the importance of plant and soil factors on soil microbial PLFAs and enzyme activities. The respective soil microbial PLFAs were indicated by soil microbial PLFA biomass, PLFA richness, and the PLFA biomass of GB, the G^+, the G^-, Ac, and fungi. The plant factors included plant biomass, plant richness, root biomass, and the biomass of forbs, grasses, legumes, and sedges. The soil factors included soil pH, AN, AP, TN, TP, and SOM. The Euclidean distance matrices for the plant, soil factors, and microbial variables standardised with decostand function (standardise method) of the vegan package were used in MRM models. Then, the Spearman's rank correlation test was to check the relationships between soil microbial variables and factors of the plant and soil.

Structural equation modeling (SEM) was used to analyse the hypothetical pathways of N and P addition effects on soil enzyme activities and soil microbial communities by using Amos version 23.0 (Amos Development, Spring House, Armonk, United States). Before the SEM analysis, the dominant factors affecting soil microbial variables according to the Spearman's rank correlation test were selected. Soil microbial PLFAs were presented by the first principal components (PLFA PC1) and the second principal components (PLFA PC2). Soil enzyme activities

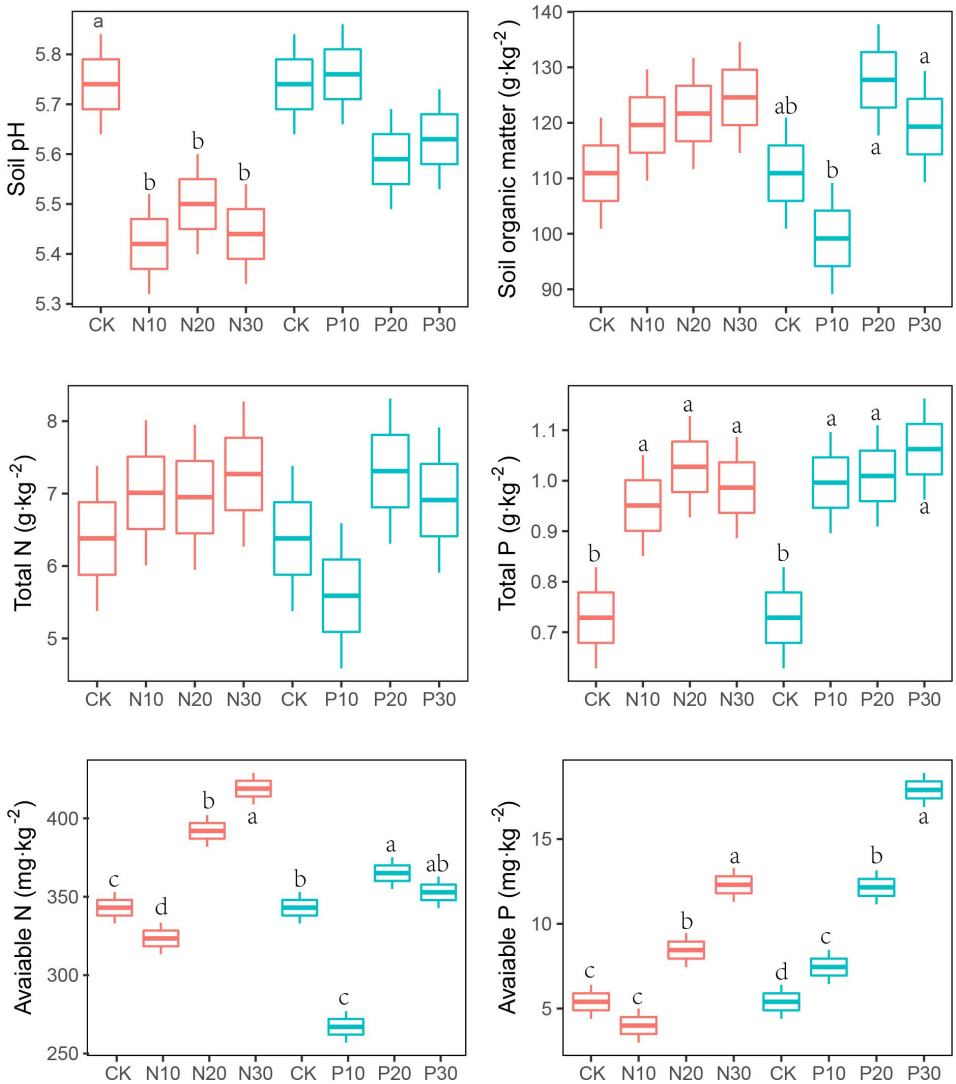

FIGURE 1 | Effects of nitrogen (N) and phosphorus (P) addition on soil physicochemical. Values are means ± SE (n = 3). Different lowercase letters indicate significant difference among the levels of N or P addition in the same below.

were presented by the first principal components (enzyme PC1) and the second principal components (enzyme PC2) in the following SEM analysis. Maximum likelihood estimation method was applied in the process of SEM and the goodness-of-fit of the models was determined by the chi-squared tests, the Akaike information criterion (AIC), and the root mean square error of approximation (RMSEA).

RESULTS

Soil Physicochemical Properties

The N addition significantly decreased soil pH, but not altered the contents of SOM and TN. Soil pH and TN were not significantly changed along P addition rates. Compared with unfertilised soils, the AN was lower in the low N and P addition rate (N10 and P10), but higher in the moderate and high addition rate (N20, P20, N30, and P30). The soil AP showed a significant increase with P addition rate (**Figure 1** and **Table 1**).

Plant Community

The N addition did not significantly alter plant community biomass, which was significantly increased in P addition treatment, especially in moderate and high addition rate. Both the N and P addition decreased the plant richness (**Figure 2** and **Table 1**).

Although the plant community biomass was not significantly induced by N addition, the response of four plant functional groups was significantly different. Low N addition rate (N10) increased forb and legume biomass, but inhibited grass and sedge biomass, which was opposite to the response of their biomass to N20 and N30 addition. The forb and grass biomass decreased

TABLE 1 | ANOVA for the four groups (soil physicochemical properties, plant community, soil enzyme activities, and soil microbial community) in nitrogen (N) and phosphorus (P) addition.

		N addition		P addition	
		F	*P*	F	*P*
Soil physicochemical properties	Soil pH	6.51	0.015	2.06	0.184
	Soil organic matter	1.03	0.426	4.47	0.040
	Total nitrogen	0.42	0.742	1.66	0.252
	Total phosphorus	5.39	0.025	6.66	0.014
	Available nitrogen	57.79	< 0.001	58.64	< 0.001
	Available phosphorus	40.59	< 0.001	92.59	< 0.001
Plant communities	Plant biomass	3.01	0.059	8.11	0.001
	Plant richness	5.33	0.009	2.51	0.093
	Grass biomass	102.85	< 0.001	1.35	0.291
	Sedge biomass	6.24	0.005	3.47	0.039
	Legume biomass	9.14	0.001	10.79	< 0.001
	Forbs biomass	4.24	0.021	4.28	0.020
	Root biomass	15.01	< 0.001	13.89	< 0.001
Soil enzyme activities	Urease	26.27	< 0.001	9.79	0.001
	Invertase	11.28	< 0.001	7.32	0.003
	Peroxidase	16.29	< 0.001	17.09	< 0.001
	Phosphatase	16.67	< 0.001	13.42	< 0.001
Soil microbial community	PLFA biomass	311.67	< 0.001	141.97	< 0.001
	PLFA richness	2.15	0.172	18.04	0.001
	General bacteria	805.76	< 0.001	35.52	< 0.001
	Fungi	4.85	0.033	45.30	< 0.001
	Gramme-positive bacteria	84.80	< 0.001	23.55	< 0.001
	Gramme-negative bacteria	2.15	0.172	5.00	0.031
	Actinomycetes	4.06	0.050	3.99	0.052

in P10, but increased in P20 and P30, respectively. The legume biomass significantly increased with the P addition rate. The sedge biomass was not altered in P10 and P20, but significantly decreased in P30. Plant root biomass was increased following N and P addition rate, but its response was more sensitive in P addition than that in N addition, of which only N20 significantly increased root biomass (**Figure 2** and **Table 1**).

Soil Enzyme Activities

Invertase activities uniformly increased in response to the N and P addition and reached the maximum in N20 and P20 (**Figure 3**). The peroxidase, urease, and phosphatase activities significantly declined in N10 and N20, but were significantly increased in N30 (**Figure 3**). The response of these three soil enzyme activities varied in response to P addition. Peroxidase activity was significantly inhibited (**Figure 3**), while phosphatase activity increased with P addition (**Figure 3**). Urease activity was significantly decreased in P10 and P30, but slightly increased in P20 (**Figure 3**).

Soil Microbial Composition

Principal component analysis of the soil microbial PLFA composition along N and P addition rate is shown in **Figure 4**. The PC1 explained 68.9% and the PC2 explained 13.4% of the variance for the N addition, respectively (**Figure 4A**). The locations of the three N addition rates and CK were distinct, which indicated that the dominant PLFA was different from each other. All the G^+ indicated by PLFA a15:0, i18:0, a18:0, i17:0, a 17:0, and i16:0 were on the left of the PC2, while the GB indicated by PLFA C13:0, C14:0, C15:0, and C16:0 were on the right of the PC2. This demonstrated that along N addition rate, the G^+ were increasing, especially in the high N addition rate, while fewer GB were found. Otherwise, the G^- indicated by PLFA cy 15:0, 16:1ω7c, 18:1ω7c, 18:1ω7t, and 16:1ω9c, Ac indicated by PLFA 2Me 18:0, 10Me 18:0, and 10Me 17:0, and fungal PLFA indicated by 18:1ω9c and 18:2ω6,9c were found along the PC1 axis from −1.0 to 1.0, which demonstrated that these soil PLFAs were not different between N addition and the CK.

The PC1 and PC2 explained the 45.6 and 30.8% of the variance for the P addition (**Figure 4B**). Although P addition differentiated the soil PLFAs from the CK, the PLFAs in low (P10) and moderate P addition rate (P20) were similar, in which both the G^+ and the G^- PLFAs were found. It was distinct that the fungal PLFAs and Ac PLFAs were located near the high P addition rate (P30), while the whole GB PLFAs were found near the CK. These results demonstrated that soil microbial PLFAs were sensitive to P addition, especially at the P30 addition rate.

Although the N addition dominated the soil G^+, while P addition affected soil fungi and Ac; some soil microorganisms at the individual PLFA level showed similar responses to N and P addition. These PLFAs, such as the saturated fatty acid C13:0, C14:0, and C15:0, as well as some monochain fatty acids 16:1ω9c and 18:1ω9c, were always located near the CK and not affected by the N or P addition. On the contrary, some PLFAs, such as a15:0 and 16:1ω7c, were found near the N30 and P30, and the PLFAs 18:1ω7c was found near the N20 and P20 (**Figure 4**).

Soil Microbial Biomass

Soil PLFA biomass (**Figure 5A**), including GB (**Figure 5C**), fungal (**Figure 5D**), and Ac biomass (**Figure 5G**), was significantly decreased along N addition rates, while the G^+ were significantly increased (**Figure 5E**). Soil PLFA richness (**Figure 5B**) and the G^- (**Figure 5F**) were not statistically significant, while they showed an increasing and decreasing trend along N addition rates, respectively.

Along the P addition rates, the biomass of soil microorganisms, GB, fungi, and the G^- was first decreased and then increased at the high P addition rate (P30), which was significantly higher than that in the unfertilised treatment (CK). Soil PLFA richness and the G^+ were significantly increased along the P addition rates (**Figure 5**).

Importance of Plant and Soil Factors on Soil Microbial Variables

Multiple regressions on distance matrices was used to estimate the importance of ecological factors (plant and soil factors) on soil microbial variables. Collectively, 74 and 67% of the total variations occur in soil microbial PLFAs of the N and P addition, respectively (**Figures 6A,C**). However, 8% of the total variations was alone explained by plant factors in the N addition, which was significantly lower than that (30%) in the P addition.

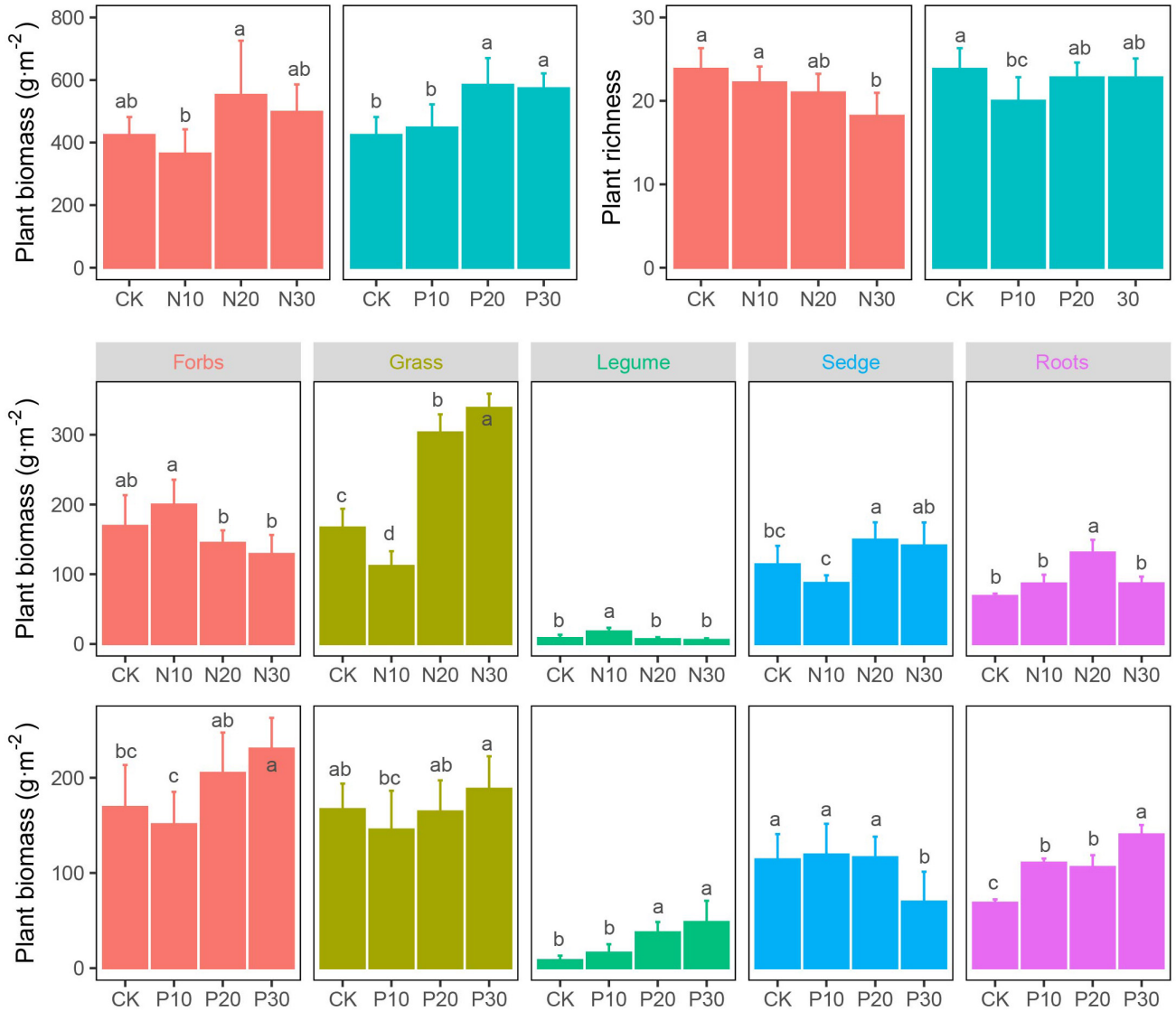

FIGURE 2 | Effects of N and P addition on plant community characteristics.

On the contrary, the soil factors alone explained 33% in the N addition and 5% of the total variations in the P addition. This suggested that soil factors dominated soil microbial PLFAs in the N addition, but plant factors did not dominated soil microbial PLFAs in the P addition. Further investigation also showed that two most important variables were soil pH and plant richness in the addition, but the sedge biomass and soil AP in the P addition.

When the soil microbial PLFAs were taken into account to explain soil enzyme activities, the overall 80 and 50% of the total variations occur in the N and P addition, respectively (**Figures 6B,D**). Plants, soils, and PLFAs alone explained 6, 7, and 31% in the N addition, but 14, 6, and 10% of the total variations in the P addition. The biomass of total PLFAs and the G^+ was the two most important variables explaining soil enzyme activities, but the biomass of total plants and legumes was the two important variables, followed by the GB PLFAs.

Pathways Determining Soil Microbial Phospholipid Fatty Acids and Enzyme Activities

Based on the most important factors explaining soil microbial variables, we conducted an optimal SEM analysis to explore the pathways determining soil microbial variables. The results showed that the pathways of N and P addition determining soil microbial PLFAs and enzyme activities were significantly different.

The width of lines from N addition to the plant and soil factors showed that N addition would drive soil microbial variables mainly via decreasing plant richness (−0.75), increasing

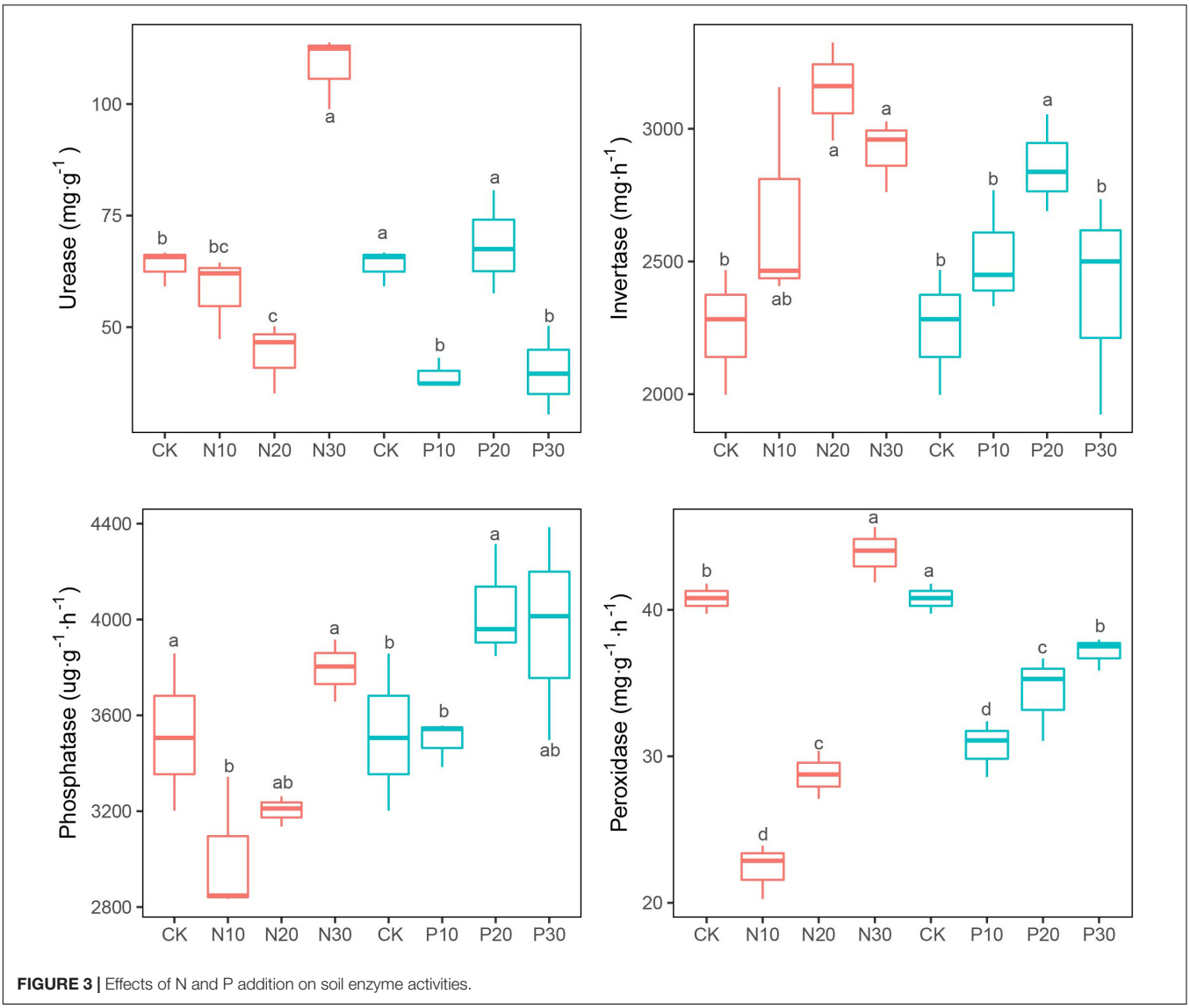

FIGURE 3 | Effects of N and P addition on soil enzyme activities.

sedge biomass (0.74), followed by decreasing soil pH (−0.64) (**Figure 7**). The total effects of N addition on the soil microbial PLFA PC2 was 0.008 (**Supplementary Figure 1A**), but it reached 0.808 on soil microbial PLFA PC2 (**Supplementary Figure 1C**). Similarly, the total effects of N addition on soil enzyme PC2 were 0.690 (**Supplementary Figure 1D**), which were bigger than that (0.145) on soil enzyme PC1 (**Supplementary Figure 1B**).

The P addition would significantly affect soil microbial variables mainly via increasing AP (0.76) determined, followed by decreasing sedge biomass (−0.44) and plant richness (−0.34) (**Figure 7**). In addition, the total effects of P addition on soil microbial PLFA PC1 and enzyme PC1 were more than the corresponding PC2, respectively (**Supplementary Figure 1**).

According to the PCA analysis (**Supplementary Figure 2A**), soil PLFA PC1 was mainly indicated by soil PLFA biomass, the biomass of fungi, and Ac. Soil PLFA PC2 was mainly positively correlated with the G^+ and PLFA richness and negatively correlated with GB. They indicated that N addition would dominant the structure of the G^+ and GB, while P addition would determine soil PLFA biomass, the biomass of fungi, and Ac. Similarly, P addition was more important to soil phosphatase and peroxidase activity, while N addition was more important to soil invertase activity (**Supplementary Figure 2B**).

DISCUSSION

The alpine meadows in the Qinghai-Tibetan Plateau are strongly limited in terms of available N and P levels (Xu et al., 2015; He et al., 2016). Soil microorganisms are an important decomposer in alpine meadows and they are sensitive to changes in nutrient supply such as N or P addition. This study examined soil microbial PLFAs, including the biomass of soil GB, fungi, G^-, and Ac, which were all rate dependently inhibited by N addition. Although they decreased at low and moderate P addition rate

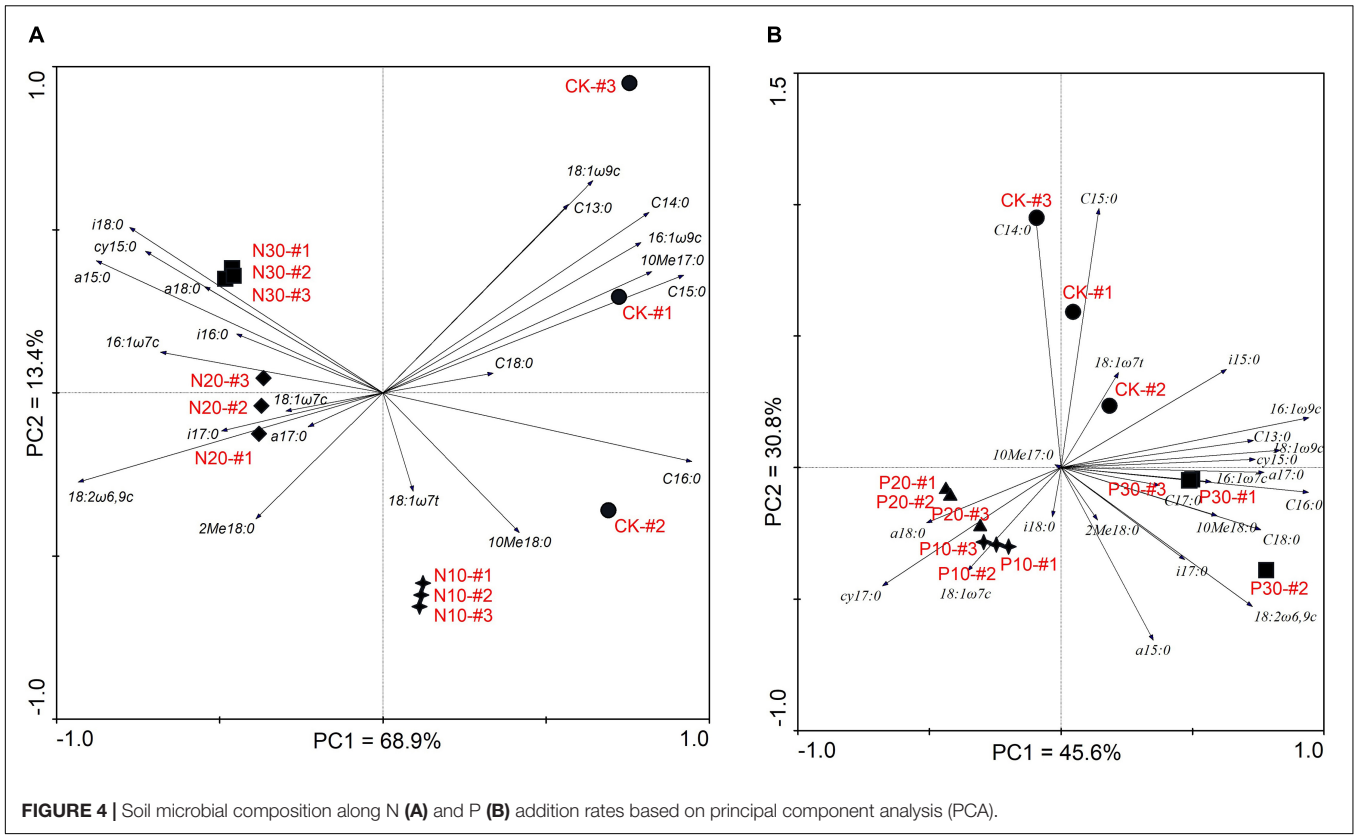

FIGURE 4 | Soil microbial composition along N **(A)** and P **(B)** addition rates based on principal component analysis (PCA).

(<20 g m^{-2} $year^{-1}$), soil microbial PLFAs significantly increased at high P addition rate (30 g m^{-2} $year^{-1}$) and showed the unimodal changes responding to P addition. Both the N and P effects were rate dependent, which support our first hypothesis.

Effects of Nitrogen and Phosphorus Addition on Soil Physicochemical Properties

The urea containing ammonium N released more hydrogen (H^+) into the soils through bacterial nitrification, thus reducing soil pH. High N addition rate saturating the soil with N was also suggested to be an important reason for N-induced soil acidification (Lu et al., 2014), consistent with global observations (Tian and Niu, 2015). In contrast to the response of soil pH to N addition, soil pH was not significantly altered by P addition. This might be for that N uptakes were enhanced by P addition, resulting in less excess N in the soils, potentially delaying soil acidification (Mori et al., 2010; Chen et al., 2015; Li et al., 2016).

Nitrogen and P addition would enhance plant carbon assimilation and stimulated more litters into soils and, thus, increased SOM. Meanwhile, N and P addition would also stimulate N and P absorbed by plants and it resulted in less carbon into soils through roots. The trade-off in the contribution of litter carbon and root carbon into SOM was usually found in the low N and P addition rate and, thus, led to decrease in SOM. When high N and P addition rates were applied, litter carbon into soils surpassed root carbon inputs leading to increased SOM (Van der Heijden et al., 2008).

Soil N and P were mainly formed from deposition and fertiliser supply. The N and P addition directly increased the soil TN and TP contents (Cao et al., 2015; Du, 2017), especially the N addition significantly increased soil TP content for the N-limited plants that would not uptake soil P and resulted in the P accumulation (Song et al., 2019; Li et al., 2022). However, the soil AN was significantly decreased at low N and P addition rate, but it increased at medium and high N and P addition rate. This was for that low N addition rate. The AN from low N addition rate would stimulate N-limited plants absorbing the more AN from soils, which resulted in lower soil available content (Zhang et al., 2005). The P addition has been demonstrated to be significantly correlated with soil nitrogen cycle (Shi et al., 2021) and it would significantly promote the *nifH* gene expression and the biological nitrogen fixation rate (Chu et al., 2008).

Effects of Nitrogen and Phosphorus Addition on the Plant Functional Groups

Previous studies found that lack of N and P availability can be limiting factors to plant growth and productivity in grasslands (Craine and Jackson, 2009; Fay et al., 2015), but in this study, the biomass of the four plant functional groups was differently responding to N and P addition. High N addition rate favoured grasses over the other functional groups, while P addition favoured the growth of legumes in the alpine meadow. The

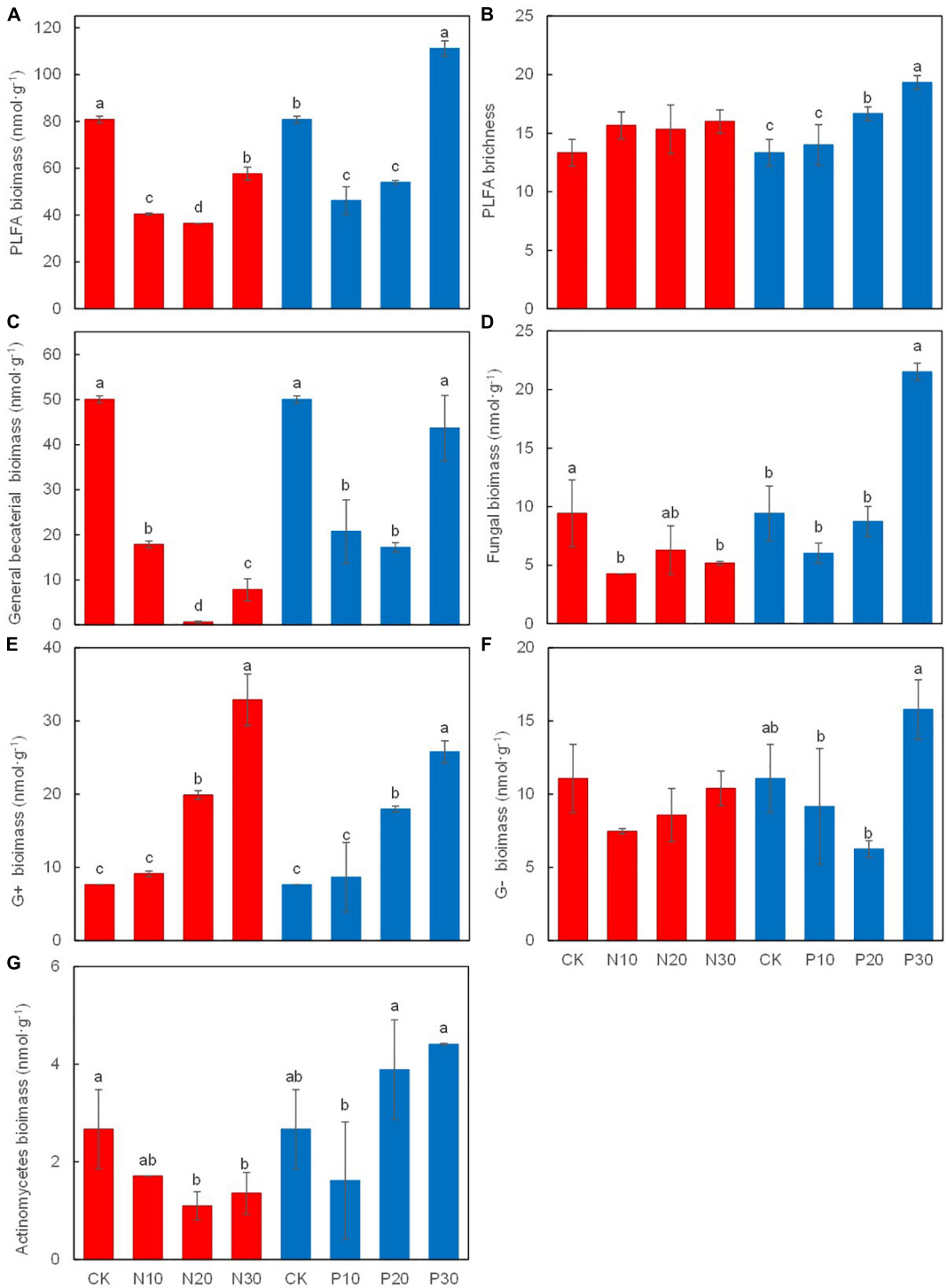

FIGURE 5 | Effects of N and P addition on soil microbial biomass **(A)**, PLFA richness **(B)**, the biomass of grenral bacteria **(C)**, fungi **(D)**, gram-positive bacteria **(E)**, gram-negative bacteria **(F)**, and actinomycetes **(G)**.

N-induced increase in grasses was consistent with most studies hypothesising that the plant community would be dominated by grasses in grassland ecosystems with N addition (Clark and Tilman, 2008; You et al., 2017; Zheng et al., 2019) due to their greater ability to take-up nutrients (Guo et al., 2017). The P-induced increase in legumes (Zhao et al., 2019) demonstrated that although the plant community was limited by N and P, the legumes were mostly limited by P due to their N-fixing ability

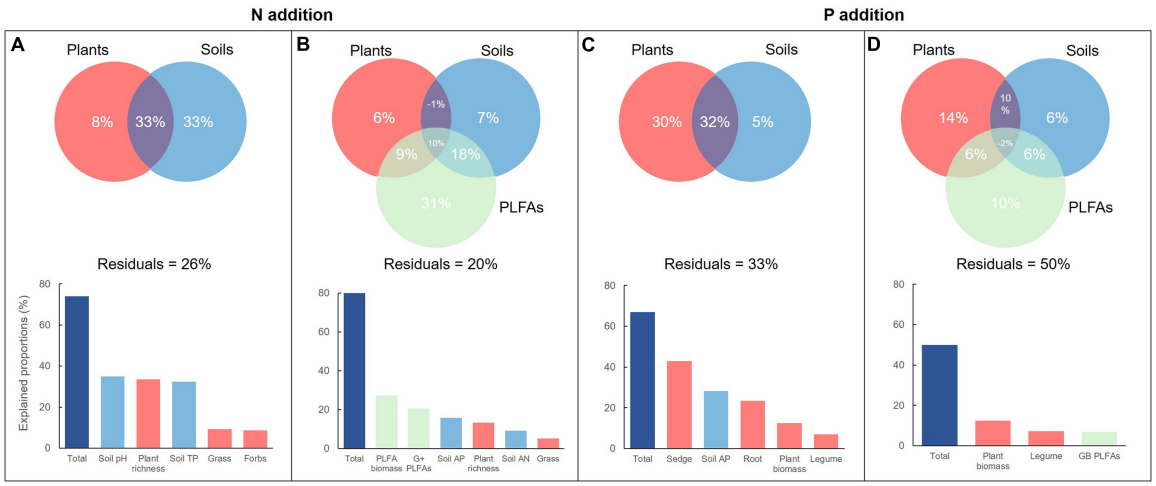

FIGURE 6 | The relative contributions of plants and soils to the variations in soil PLFAs **(A,C)** and enzyme activities **(B,D)** along N and P addition rates.

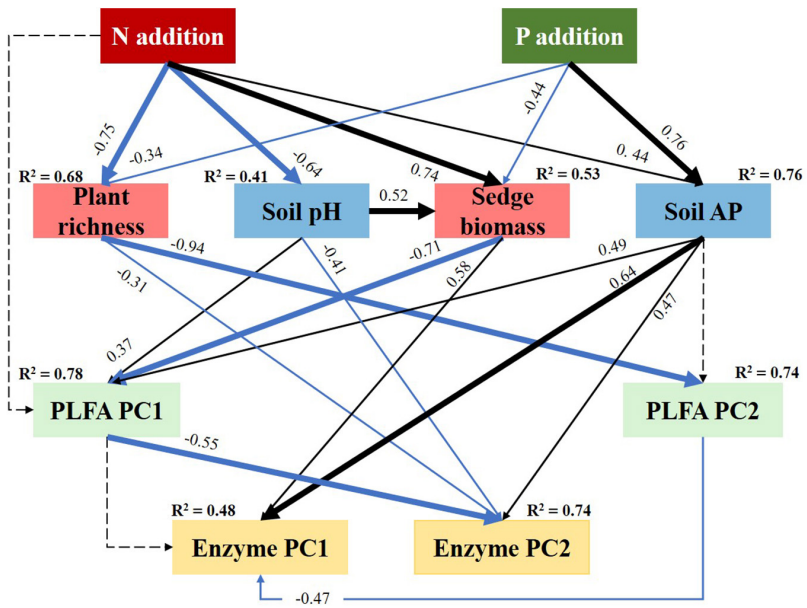

FIGURE 7 | Structural equation modeling (SEM) analysis evaluating the effects of N and P addition on soil microbial PLFAs and enzyme activities via pathways of plants and soils. Result of model fitting: chi-squared test = 23.56, df = 21, and $P = 0.315$. Here, high P-values with the chi-squared tests indicate good model fit to data. Black and blue solid arrows indicate significantly positive and negative effects ($P < 0.05$), respectively. Dashed arrows indicate the effects are not significant ($P > 0.05$). Values associated with arrows represent standardised path coefficients. R^2 associated with response variables indicates the proportion of variation explained by relationships with other variables.

(Marleau et al., 2011). Therefore, in an alpine meadow, N or P addition would drive the differentiation of plant community composition and structure (Tischer et al., 2015; Xu et al., 2015).

Effects of Nitrogen and Phosphorus Addition on Soil Enzyme Activities

Soil enzymes are mainly produced by soil microorganisms to decompose organic matter into available nutrients for its assimilation and soil enzymes activities could be an indicator of soil microbial nutrient demand (Fan et al., 2018). N addition significantly increased the invertase activity (**Figure 3**), as found in other studies (Xiao et al., 2021). This result supports the resource allocation theory, which states that N addition stimulates the activities of C- and P-cycling enzymes, but inhibits N-cycling enzyme activities (Allison and Vitousek, 2005). However, we found that peroxidase activity indicative of C-cycling, urease activity indicative of N-cycling, and phosphatase activity indicative of P-cycling were first decreased at low N rates and then increased at high N rates, which were

partially consistent with these results (Zhou et al., 2012; Han et al., 2018). The non-linear changes in soil enzyme activities are affected by a series of abiotic and biotic factors such as soil nutrient contents, soil microbial communities, soil respiration intensity, and plant community characteristics (Hu et al., 2014), especially in terms of soil microbial biomass (Acosta-Martínez et al., 2008). In this study, soil enzyme activities corresponding to N addition rates were mainly consistent with changes in soil PLFA biomass.

Our results showed that P addition generally suppressed peroxidase and urease activities, but increased invertase activities. Phosphatase activity only increased significantly at medium and high P addition rates, but showed no significant changes at low rate (**Figure 3**). These results contrasted with other studies (Jing et al., 2016; Rosinger et al., 2019; Xiao et al., 2021) showing negative effects of P addition on soil enzymes, especially soil phosphatase activity, where soil microorganisms would reduce the production cost of N-rich phosphatase enzymes when the available P was enough. In this study, although soil TP (1.01–1.06 $g{\cdot}kg^{-1}$) and AP (12.15–17.90 $mg{\cdot}kg^{-1}$) increased along with P addition rates, they were far less than the TP (2.30 $g{\cdot}kg^{-1}$) in the alpine meadows soils in the Qinghai-Tibet Plateau (Wang et al., 2013). When soil P supply is not enough, the negative effects of P addition on phosphatase activity are not triggered and are, thus, delayed (Olander and Vitousek, 2000; Weintraub and Schimel, 2005). Insufficient P supply, in turn, stimulates plant roots secretion of phosphatase (Tadano and Sakai, 1991), which was also found in this study, where root biomass significantly increased with P addition rates (**Figure 2**). Additionally, phosphatase activity upon P addition might be derived from stabilised extracellular enzymes, which are not sensitive to P addition, rather than actively synthesised enzymes (Turner and Joseph, 2013).

Effects of Nitrogen and Phosphorus Addition on Soil Microbial Phospholipid Fatty Acids

N and P addition altered the ratio of N and P supply for plants and soil microorganisms and, thus, affected their relationships, growth, and biomass. Čapek et al. (2018) demonstrated that when the soil N-P ratio was between 6.3 and 42.4, plants were N limited and soil microorganisms were P limited. In this study, the soil N:P ratio at the three N and P addition rates was < 9.0 (**Supplementary Figure 3**), which further demonstrated that soil microorganisms in the grasslands were mainly limited by P (Rosinger et al., 2019). The negative relationship between N addition and soil microbial biomass (Leff et al., 2015) was also found in this study. In the short term, soil microorganisms compete for available N in the soil better than plants (Kuzyakov and Xu, 2013; Wild et al., 2018), which further leads to a lower soil C:N ratio and less tested fungi (Soares and Rousk, 2019). As a whole, N addition stimulated the P-limited effect in soil microorganisms (Li et al., 2016) and inhibited the soil microbial process in the alpine meadows, which was consistent with other studies (Zhou et al., 2017; Wang et al., 2018).

In contrast with expectations, a low P rate did not alleviate the limiting effect of P on soil microorganisms in this study. It has been reported that soil microorganisms in low-P soil are involved in efficient P cycling (Beauregard et al., 2010) and most of the available P was used to increase plant root biomass in legume plants through N_2 fixation (Augusto et al., 2013), which was also demonstrated (**Figure 2**). Additionally, high P addition rate might limit N for microbial activity (Vitousek et al., 2010) including soil GB, fungi, the G^-, the G^+, and Ac (**Figure 5**).

Importance of Plants and Soils for Soil Microorganisms

The growth strategies and environmental tolerance of soil microbial taxa are diverse (Schimel et al., 2007; Dong et al., 2020) and the response of soil microbial taxa to changes in plants and soils induced by N and P addition should be usually different.

The sustained decline in soil microbial biomass with N addition rate, expected for the soil G^+, was mainly seen in the decreasing soil pH, followed by plant richness and soil TP. Soil bacteria are sensitive to decreased soil pH (Bååth and Anderson, 2003), which would lead to limited available calcium and magnesium (Lucas et al., 2011) as well as aluminium toxicity (Bowman et al., 2008), inhibiting soil bacterial community. In general, soil bacteria taxa have relatively narrow growth tolerances of soil pH (Rousk et al., 2010) and deviations of 1.5 pH units from the *in situ* pH of bacterial communities consistently reduce their activity by 50% (Fernandez-Calvino and Baath, 2010). However, soil fungi generally exhibit wider soil pH ranges for optimal growth than bacteria (Beales, 2004; Rousk et al., 2010). Therefore, soil bacteria decreased significantly, but the extent of soil fungi change was smaller.

Nitrogen addition also altered soil microbial PLFAs through plant richness, which was almost equal to the effect of soil pH in this study (**Figure 6A**). Plant effects, such as biomass (Reich et al., 2012), diversity, and composition (Lange et al., 2014), could also determine soil microbial growth and composition. More plant species supply more food resources and more host species supply more soil microorganisms by increasing the diversity of available nutrients pools (Klironomos et al., 2011). In some cases, plant richness determines soil microbial biomass (Zeng et al., 2016). N addition would change the C allocation of the aboveground plants and belowground roots and further lead to the priming effects of C deficiency on soil microorganisms (Silva-Sánchez et al., 2019). In this study, the biomass of grasses and forbs also accounted for 9.35 and 8.76% of the variation in soil microbial PLFAs, respectively. The priming effects of grass and forbs might account for the specific soil microbial taxa. However, the soil G^+ significantly increased with decreasing soil pH induced by N addition rates. This was consistent with previous studies (Aciego Pietri and Brookes, 2009; Zhou et al., 2017), which have demonstrated that the soil G^+ possessed specific mechanisms to survive in acidic environments (Cotter and Hill, 2003). Simonin et al. (2017) also considered the soil G^+ as the K-strategist indicating soil microbial community resistance.

Compared with N addition, P addition effects on soil microorganisms were obviously unimodal. Except for the soil G^+, the other microbial groups significantly decreased at P10 and P20 rates and increased at P30 rate. This soil microbial pattern along P addition rates mainly derived from plants (Yang et al., 2012; Rui et al., 2015; Wang et al., 2018), which accounted for 30% of the total variation, compared with the 5% derived from soils (**Figure 6**). The low P addition rate would not significantly change plant biomass and even decreased the biomass of forbs and grass, which led to less C substrate to soil microorganisms. Meanwhile, increased root biomass at high P addition rate directly enhanced the rate of C cycles to soil microorganisms (Jing et al., 2017).

The overall increase in soil nutrients affected specific PLFAs in both the N and P addition. In this study, 16:1ω7c and 18:1ω7c PLFAs were significantly increased by N and P addition rate and their correlation with soil TP, AP, and AN content has been already demonstrated (Dong et al., 2014; Chen et al., 2019; Hu et al., 2019). Conversely, some PLFAs, such as C13:0, C14:0, C15:0, 16:1ω9c, and 18:1ω9c, were not significantly changed by N and P addition. This difference might be due to the different microorganism growth strategies and the varying communication between them (Schimel et al., 2007). For instance, fungal PLFA 18:1ω9c was more resistant to changing microenvironments compared with bacteria (Wardle et al., 2003), but soil bacteria were more inhibited by N addition (Zhang et al., 2016). Furthermore, soil microorganisms produce more *cis*-structured PLFAs, such as 16:1ω7c and 18:1ω7c, with abundant available nutrients (Ludvigsen et al., 1999). These changes in individual PLFA affected by N and P addition would together help to structure the soil microbial taxa.

In this study, soil microbial community and enzyme activities are sensitive and significantly affected by the N and P addition rates. The N addition has negative effects on soil microbial community and enzyme activities along the addition rates. However, the effects of P addition are negative at low addition rates, but positive at high addition rates. Specifically, the soil microbial PLFA, bacteria, fungi, G^-, and Ac are significantly inhibited along N addition rates and at low P addition rates. However, these PLFA groups are increased at high P addition rate. It is similar that both the N and P additions stimulate soil microbial richness and significantly increase the G^+. Soil enzyme activities involved in C cycling are increased, but that involved in P cycling are inhibited at low addition rates and increased in high addition rates. The responses of urease activities are significantly different to N and P addition rates. These changes in soil microbial community are significantly correlated with soil pH with N addition rates, but with soil available P and sedge biomass with P addition rates. In the alpine meadow, both the N and P are the key limiting factors structuring soil microorganisms and 30 $g \cdot m^{-2}$ are better P addition rate for soil microbial community. Our studies indicated that soil microbial communities and enzyme activities are sensitive to short-term N and P addition and are also significantly influenced by their addition rates.

DATA AVAILABILITY STATEMENT

The raw data supporting the conclusions of this article will be made available by the authors, without undue reservation.

AUTHOR CONTRIBUTIONS

LH and CW contributed to the design of the study. LH organised the database. HZ performed the statistical analysis. LH and HZ wrote the first draft of the manuscript. All authors contributed to manuscript revision, read, and approved the submitted version.

FUNDING

This study was supported by the National Natural Science Foundation of China (U20A2008 and 31870407), the Second Tibetan Plateau Scientific Expedition and Research (STEP) Programme (2019QZKK0302), and the Fundamental Research Funds for the Central Universities (lzujbky-2019-it01).

SUPPLEMENTARY MATERIAL

The Supplementary Material for this article can be found online at: https://www.frontiersin.org/articles/10.3389/fpls.2022.829381/full#supplementary-material

REFERENCES

Aciego Pietri, J. C., and BR00ookes, P. C. (2009). Substrate inputs and pH as factors controlling microbial biomass, activity and community structure in an arable soil. *Soil Biol. Biochem.* 41, 1396–1405. doi: 10.1016/j.soilbio.2009.03.017

Acosta-Martínez, V., Acosta-Mercado, D., Sotomayor-Ramírez, D., and Cruz-Rodríguez, L. (2008). Erratum to "Microbial communities and enzymatic activities under different management in semiarid soils. *Appl. Soil Ecol.* 39, 358–358. doi: 10.1016/j.apsoil.2008.01.004

Allison, S. D., and Vitousek, P. M. (2005). Responses of extracellular enzymes to simple and complex nutrient inputs. *Soil Biol. Biochem.* 37, 937–944. doi: 10.1016/j.soilbio.2004.09.014

Augusto, L., Delerue, F., Gallet-Budynek, A., and Achat, D. L. (2013). Global assessment of limitation to symbiotic nitrogen fixation by phosphorus availability in terrestrial ecosystems using a meta-analysis approach. *Glob. Biogeochem. Cycles* 27, 804–815. doi: 10.1002/gbc.20069

Bååth, E., and Anderson, T. H. (2003). Comparison of soil fungal/bacterial ratios in a pH gradient using physiological and PLFA-based techniques. *Soil Biol. Biochem.* 35, 955–963. doi: 10.1016/s0038-0717(03)00154-8

Beales, N. (2004). Adaptation of microorganisms to cold temperatures, weak acid preservatives, low pH, and osmotic stress: a review. *Compr. Rev. Food Sci. Food Saf.* 3, 1–20. doi: 10.1111/j.1541-4337.2004.tb00057.x

Beauregard, M. S., Hamel, C., Atul, N., and St-Arnaud, M. (2010). Long-term phosphorus fertilization impacts soil fungal and bacterial diversity but not AM fungal community in alfalfa. *Microb. Ecol.* 59, 379–389. doi: 10.1007/s00248-009-9583-z

Berendsen, R. L., Pieterse, C. M., and Bakker, P. A. (2012). The rhizosphere microbiome and plant health. *Trends Plant Sci.* 17, 478–486. doi: 10.1016/j.tplants.2012.04.001

Bowman, W. D., Cleveland, C. C., Halada, Å, Hreško, J., and Baron, J. S. (2008). Negative impact of nitrogen deposition on soil buffering capacity. *Nat. Geosci.* 1, 767–770. doi: 10.1038/ngeo339

Bremner, J. M. (1960). Determination of nitrogen in soil by the Kjeldahl method. *J. Agr. Sci.* 55, 11–33. doi: 10.1017/s0021859600021572

Brundrett, M. C. (2009). Mycorrhizal associations and other means of nutrition of vascular plants: understanding the global diversity of host plants by resolving conflicting information and developing reliable means of diagnosis. *Plant Soil* 320, 37–77. doi: 10.1007/s11104-008-9877-9

Camenzind, T., Hättenschwiler, S., Treseder, K. K., Lehmann, A., and Rillig, M. C. (2018). Nutrient limitation of soil microbial processes in tropical forests. *Ecol. Monogr.* 88, 4–21. doi: 10.1002/ecm.1279

Cao, W. X., Li, W., Li, X. L., Xu, C. L., Shi, S. L., and Han, T. H. (2015). Effects of nitrogen fertilization on plant community structure and soil nutrient in alpine meadow steppe. *J. Desert Res.* 35, 658–666. doi: 10.7522/j.issn.1000-694X.2015.00043

Čapek, P., Manzoni, S., Kastovska, E., Wild, B., Diakova, K., Barta, J., et al. (2018). A plant-microbe interaction framework explaining nutrient effects on primary production. *Nat. Ecol. Evol.* 2, 1588–1596. doi: 10.1038/s41559-018-0662-8

Chen, D. M., Lan, Z. C., Bai, X., Grace, J. B., and Bai, Y. F. (2013). Evidence that acidification-induced declines in plant diversity and productivity are mediated by changes in below-ground communities and soil properties in a semi-arid steppe. *J. Ecol.* 101, 1322–1334. doi: 10.1111/1365-2745.12119

Chen, F., Tan, M., Yang, Y., Ma, J., Zhang, S., and Li, G. (2015). The diversity changes of soil microbial communities stimulated by climate, soil type and vegetation type analyzed via a functional gene array. *World J. Microbiol. Biotechnol.* 31, 1755–1763. doi: 10.1007/s11274-015-1926-y

Chen, X., Hao, B., Jing, X., He, J.-S., Ma, W., and Zhu, B. (2019). Minor responses of soil microbial biomass, community structure and enzyme activities to nitrogen and phosphorus addition in three grassland ecosystems. *Plant Soil* 444, 21–37. doi: 10.1007/s11104-019-04250-3

Chu, H., Fujii, T., Morimoto, S., Lin, X., and Yagi, K. (2008). Population size and specific nitrification potential of soil ammonia-oxidizing bacteria under long-term fertilizer management. *Soil Biol. Biochem.* 40, 1960–1963. doi: 10.1016/j.soilbio.2008.01.006

Chu, H., Lin, X., Fujii, T., Morimoto, S., Yagi, K., Hu, J., et al. (2007). Soil microbial biomass, dehydrogenase activity, bacterial community structure in response to long-term fertilizer management. *Soil Biol. Biochem.* 39, 2971–2976. doi: 10.1016/j.soilbio.2007.05.031

Clark, C. M., and Tilman, D. (2008). Loss of plant species after chronic low-level nitrogen deposition to prairie grasslands. *Nature* 451, 712–715. doi: 10.1038/nature06503

Cotter, P. D., and Hill, C. (2003). Surviving the acid test: responses of gram-positive bacteria to low pH. *Microbiol. Mol. Biol. Rev.* 67, 429–453. doi: 10.1128/MMBR.67.3.429-453.2003

Craine, J. M., and Jackson, R. D. (2009). Plant nitrogen and phosphorus limitation in 98 North American grassland soils. *Plant Soil.* 334, 73–84. doi: 10.1007/s11104-009-0237-1

Cusack, D. F., Silver, W. L., Torn, M. S., Burton, S. D., and Firestone, M. K. (2011). Changes in microbial community characteristics and soil organic matter with nitrogen additions in two tropical forests. *Ecology* 92, 621–632. doi: 10.1890/10-0459.1

Dong, J., Wang, S., Niu, H., Cui, X., Li, L., Pang, Z., et al. (2020). Responses of soil microbes and their interactions with plant community after nitrogen and phosphorus addition in a Tibetan alpine steppe. *J. Soils Sediments* 20, 2236–2247. doi: 10.1007/s11368-020-02586-3

Diáková, K., Biasi, C., Èapek, P., Martikainen, P. J., Marushchak, M. E., Patova, E. N., et al. (2018). Variation in N2 fixation in subarctic tundra in relation to landscape position and nitrogen pools and fluxes. *Arct. Antarct. Alp. Res.* 48, 111–125. doi: 10.1657/aaar0014-064

Dong, W. Y., Zhang, X. Y., Dai, X. Q., Fu, X. L., Yang, F. T., Liu, X. Y., et al. (2014). Changes in soil microbial community composition in response to fertilization of paddy soils in subtropical China. *Appl. Soil Ecol.* 84, 140–147. doi: 10.1016/j.apsoil.2014.06.007

Du, Q. F. (2017). *The Responses of Degraded Typical Steppe Vegetation and Soil to Nitrogen and Phosphorus Fertilizations in Inner Mongolia*. Ph.D thesis, Pune: Southwest University.

Eisenhauer, N., Bessler, H., Engels, C., Gleixner, G., Habekost, M., Milcu, A., et al. (2010). Plant diversity effects on soil microorganisms support the singular hypothesis. *Ecology* 91, 485–496. doi: 10.1890/08-2338.1

Fan, Z., Wang, X., Wang, C., and Bai, E. (2018). Effect of nitrogen and phosphorus addition on soil enzyme activities: a meta-analysis. *Chinese J. Appl. Ecol.* 29, 1266–1272. doi: 10.13287/j.1001-9332.201804.024

Fay, P. A., Prober, S. M., Harpole, W. S., Knops, J. M., Bakker, J. D., Borer, E. T., et al. (2015). Grassland productivity limited by multiple nutrients. *Nat. Plants* 1:15080. doi: 10.1038/nplants.2015.80

Fernandez-Calvino, D., and Baath, E. (2010). Growth response of the bacterial community to pH in soils differing in pH. *FEMS Microbiol. Ecol.* 73, 149–156. doi: 10.1111/j.1574-6941.2010.00873.x

Fierer, N., Lauber, C. L., Ramirez, K. S., Zaneveld, J., Bradford, M. A., and Knight, R. (2012). Comparative metagenomic, phylogenetic and physiological analyses of soil microbial communities across nitrogen gradients. *ISME J.* 6, 1007–1017. doi: 10.1038/ismej.2011.159

Frostegård, Å, Bååth, E., and Tunlio, A. J. (1993). Shifts in the structure of soil microbial communities in limed forests as revealed by phospholipid fatty acid analysis. *Soil Biol. Biochem.* 25, 723–730. doi: 10.1016/0038-0717(93)90113-p

Frostegård, Å, and Bååth, E. J. B. (1996). The use of phospholipid fatty acid analysis to estimate bacterial and fungal biomass in soil. *Biol. Fertil. Soils* 22, 59–65. doi: 10.1007/bf00384433

Frostegård, Å, Tunlid, A., and Bååth, E. (2011). Use and misuse of PLFA measurements in soils. *Soil Biol. Biochem.* 43, 1621–1625. doi: 10.1016/j.soilbio.2010.11.021

Geisseler, D., and Scow, K. M. (2014). Long-term effects of mineral fertilizers on soil microorganisms - A review. *Soil Biol. Biochem.* 75, 54–63. doi: 10.1016/j.soilbio.2014.03.023

Guan, S. (1983). *Research Methods on Soil Enzymes*. Beijing: China Agricultural Press.

Guo, H., Ye, C., Zhang, H., Pan, S., Ji, Y., Li, Z., et al. (2017). Long-term nitrogen & phosphorus additions reduce soil microbial respiration but increase its temperature sensitivity in a Tibetan alpine meadow. *Soil Biol. Biochem.* 113, 26–34. doi: 10.1016/j.soilbio.2017.05.024

Han, Y., Liu, Y., Ye, Y., Da, B., Gao, Y., Zhao, Y., et al. (2018). The Effect of nitrogen deposition on soil enzyme activity in the forest-grassland landscape boundary of Tibet. *J. Land Res.* 10, 93-98.

Hartmann, A., Schmid, M., Tuinen, D., and Berg, G. (2008). Plant-driven selection of microbes. *Plant Soil* 321, 235–257. doi: 10.1007/s11104-008-9814-y

He, D., Xiang, X. J., He, J. S., Wang, C., Cao, G. M., Adams, J., et al. (2016). Composition of the soil fungal community is more sensitive to phosphorus than nitrogen addition in the alpine meadow on the Qinghai-Tibetan Plateau. *Biol. Fertil. Soils* 52, 1059–1072. doi: 10.1007/s00374-016-1142-4

Hu, K., Tao, J., He, D., Huang, K., and Wang, W. (2019). Effects of root growth on dynamic of microbes and enzyme activities during litter decomposition. *Chinese J. Appl. Ecol.* 30, 1993–2001. doi: 10.13287/j.1001-9332.201906.022

Hu, L., Wang, C., Wang, G., Ma, L., Liu, W., and Xiang, Z. (2014). Changes in the activities of soil enzymes and microbial community structure at different degradation successional stages of alpine meadow in the headwater region of Three Rivers. *China. Acta Prataculturae Sin.* 23, 8–19. doi: 10.11686/cyxb20140302

Hu, L., Zi, H., Ade, L., Lerdau, M., and Wang, C. (2017). Effects of zokors (*Myospalax baileyi*) on plant, on abiotic and biotic soil characteristic of an alpine meadow. *Ecol. Eng.* 103, 95–105. doi: 10.1016/j.ecoleng.2017.03.010

Humbert, J. Y., Dwyer, J. M., Andrey, A., and Arlettaz, R. (2016). Impacts of nitrogen addition on plant biodiversity in mountain grasslands depend on dose, application duration and climate: a systematic review. *Glob. Chang. Biol.* 22, 110–120. doi: 10.1111/gcb.12986

Isbell, F., Reich, P. B., Tilman, D., Hobbie, S. E., Polasky, S., and Binder, S. (2013). Nutrient enrichment, biodiversity loss, and consequent declines in ecosystem productivity. *Proc. Nat. Acad. Sci.* 110, 11911–11916. doi: 10.1073/pnas.1310880110

Jackson, M. (1974). *Soil Chemical Analysis – An Advanced Course*. Madison, WI: Department of Soil Science, University of Wisconsin.

Jing, D. W., Liu, F. C., Wang, M. Y., Ma, H. L., Du, Z. Y., Ma, B. Y., et al. (2017). Effects of root pruning on the physicochemical properties and microbial activities of poplar rhizosphere soil. *PLoS One* 12:e0187685. doi: 10.1371/journal.pone.0187685

Jing, X., Yang, X., Ren, F., Zhou, H., Zhu, B., and He, J. S. (2016). Neutral effect of nitrogen addition and negative effect of phosphorus addition on topsoil

extracellular enzymatic activities in an alpine grassland ecosystem. *Appl. Soil Ecol.* 107, 205–213. doi: 10.1016/j.apsoil.2016.06.004

Klironomos, J., Zobel, M., Tibbett, M., Stock, W. D., Rillig, M. C., Parrent, J. L., et al. (2011). Forces that structure plant communities: quantifying the importance of the mycorrhizal symbiosis. *New Phytol.* 189, 366–370. doi: 10.1111/j.1469-8137.2010.03550.x

Kuzyakov, Y., and Xu, X. (2013). Competition between roots and microorganisms for nitrogen: mechanisms and ecological relevance. *New Phytol.* 198, 656–669. doi: 10.1111/nph.12235

Lagrange, A., L'Huillier, L., and Amir, H. (2013). Mycorrhizal status of Cyperaceae from New Caledonian ultramafic soils: effects of phosphorus availability on arbuscular mycorrhizal colonization of *Costularia comosa* under field conditions. *Mycorrhiza* 23, 655–661. doi: 10.1007/s00572-013-0503-1

Lange, M., Habekost, M., Eisenhauer, N., Roscher, C., Bessler, H., Engels, C., et al. (2014). Biotic and Abiotic properties mediating plant diversity effects on soil microbial communities in an experimental grassland. *PLoS One* 9:e96182. doi: 10.1371/journal.pone.0096182

Leff, J. W., Jones, S. E., Prober, S. M., Barberan, A., Borer, E. T., Firn, J. L., et al. (2015). Consistent responses of soil microbial communities to elevated nutrient inputs in grasslands across the globe. *Proc. Natl. Acad. Sci. U.S.A.* 112, 10967–10972. doi: 10.1073/pnas.1508382112

Li, C. Y., Miao, Y., Xue, Y. L., Zhang, B. B., Wang, Y., Dang, Y. H., et al. (2022). Ecological stoichiometric characteristics of soil-microorganism-plant system in the Loess upland under long-term fertilization. *Acta Ecol. Sinica* 42, 1–9. doi: 10.5864/stxb202003050411

Li, Y., Niu, S., and Yu, G. (2016). Aggravated phosphorus limitation on biomass production under increasing nitrogen loading: a meta-analysis. *Glob. Chang. Biol.* 22, 934–943. doi: 10.1111/gcb.13125

Liu, Y. Z., Zhao, C. C., Guo, J. W., Zhang, L. N., Juan, X., Chen, A. Q., et al. (2020). Short-term phosphorus addition augments the effects of nitrogen addition on soil respiration in a typical steppe. *Sci. Total Environ.* 761:143211. doi: 10.1016/j.scitotenv.2020.143211

Lu, X., Mao, Q., Gilliam, F. S., Luo, Y., and Mo, J. (2014). Nitrogen deposition contributes to soil acidification in tropical ecosystems. *Glob. Chang. Biol.* 20, 3790–3801. doi: 10.1111/gcb.12665

Lucas, R. W., Klaminder, J., Futter, M. N., Bishop, K. H., Egnell, G., Laudon, H., et al. (2011). A meta-analysis of the effects of nitrogen additions on base cations: implications for plants, soils, and streams. *For. Ecol. Manage.* 262, 95–104. doi: 10.1016/j.foreco.2011.03.018

Ludvigsen, L., Albrechtsen, H., Ringelberg, D. B., Ekelund, F., and Christensen, T. H. (1999). Distribution and composition of microbial populations in a landfill leachate contaminated aquifer (Grindsted, Denmark). *Microb. Ecol.* 37, 197–207. doi: 10.1007/s002489900143

Mao, Q., Lu, X., Zhou, K., Chen, H., Zhu, X., and Mori, T. (2017). Effects of long-term nitrogen and phosphorus additions on soil acidification in an N-rich tropical forest. *Geoderma* 285, 57–63. doi: 10.1016/j.geoderma.2016.09.017

Marklein, A. R., and Houlton, B. Z. (2012). Nitrogen inputs accelerate phosphorus cycling rates across a wide variety of terrestrial ecosystems. *New Phytol.* 193, 696–704. doi: 10.1111/j.1469-8137.2011.03967.x

Marleau, J. N., Jin, Y., Bishop, J. G., Fagan, W. F., and Lewis, M. A. (2011). A stoichiometric model of early plant primary succession. *Am. Nat.* 177, 233–245. doi: 10.1086/658066

McKinley, V. L., Peacock, A. D., and White, D. C. (2005). Microbial community PLFA and PHB responses to ecosystem restoration in tallgrass prairie soils. *Soil Biol. Biochem.* 37, 1946–1958. doi: 10.1016/j.soilbio.2005.02.033

Mori, T., Ohta, S., Ishizuka, S., Konda, R., Wicaksono, A., Heriyanto, J., et al. (2010). Effects of phosphorus addition on N2O and NO emissions from soils of anAcacia mangiumplantation. *Soil Sci. Plant Nutr.* 56, 782–788. doi: 10.1111/j.1747-0765.2010.00501.x

Navratilova, D., Tlaskalova, P., Kohout, P., Drevojan, P., Fajmon, K., Chytry, M., et al. (2019). Diversity of fungi and bacteria in species-rich grasslands increases with plant diversity in shoots but not in roots and soil. *FEMS Microbiol. Ecol.* 95:fiy208. doi: 10.1093/femsec/fiy208

Olander, L. P., and Vitousek, P. M. (2000). Regulation of soil phosphatase and chitinase activity by N and P availability. *Biogeochemistry* 49, 175–191. doi: 10.1023/a:1006316117817

Porazinska, D. L., Farrer, E. C., Spasojevic, M. J., Bueno de Mesquita, C. P., Sartwell, S. A., Smith, J. G., et al. (2018). Plant diversity and density predict belowground diversity and function in an early successional alpine ecosystem. *Ecology* 99, 1942–1952. doi: 10.1002/ecy.2420

Ramsey, P. W., Rillig, M. C., Feris, K. P., Holben, W. E., and Gannon, J. E. (2006). Choice of methods for soil microbial community analysis: PLFA maximizes power compared to CLPP and PCR-based approaches. *Pedobiologia* 50, 275–280. doi: 10.1016/j.pedobi.2006.03.003

Reich, P. B., Tilman, D., Isbell, F., Mueller, K., Hobbie, S. E., Flynn, D. F., et al. (2012). Impacts of biodiversity loss escalate through time as redundancy fades. *Science* 336, 589–592. doi: 10.1126/science.1217909

Ren, F., Song, W., Chen, L., Mi, Z., Zhang, Z., Zhu, W., et al. (2016). Phosphorus does not alleviate the negative effect of nitrogen enrichment on legume performance in an alpine grassland. *J. Plant Ecol.* 10, 822–830. doi: 10.1093/jpe/rtw089

Rosinger, C., Rousk, J., and Sanden, H. (2019). Can enzymatic stoichiometry be used to determine growth-limiting nutrients for microorganisms? A critical assessment in two subtropical soils. *Soil Biol. Biochem.* 128, 115–126. doi: 10.1016/j.soilbio.2018.10.011

Rui, J., Li, J., Wang, S., An, J., Liu, W. T., Lin, Q., et al. (2015). Responses of bacterial communities to simulated climate changes in alpine meadow soil of the Qinghai-Tibet Plateau. *Appl. Environ. Microbiol.* 81, 6070–6077. doi: 10.1128/AEM.00557-15

Rousk, J., Baath, E., BR00ookes, P. C., Lauber, C. L., Lozupone, C., Caporaso, J. G., et al. (2010). Soil bacterial and fungal communities across a pH gradient in an arable soil. *ISME J.* 4, 1340–1351. doi: 10.1038/ismej.2010.58

Schimel, J., Balser, T., and Wallenstein, M. (2007). Microbial stress-response physiology and its implications for ecosystem function. *Ecology* 88, 1386–1394. doi: 10.1890/06-0219

Shi, W., Zhang, L. M., Wang, J. S., Li, C. P., Gu, Z. L., and Zhao, H. Y. (2021). The subsequent effects of phosphorus fertilization in upland red soils and the underlying mechanisms. *Acta Pedologica Sin.* 1–14.

Silva-Sánchez, A., Soares, M., and Rousk, J. (2019). Testing the dependence of microbial growth and carbon use efficiency on nitrogen availability, pH, and organic matter quality. *Soil Biol. Biochem.* 134, 25–35. doi: 10.1016/j.soilbio.2019.03.008

Simonin, M., Nunan, N., Bloor, J. M. G., Pouteau, V., and Niboyet, A. (2017). Short-term responses and resistance of soil microbial community structure to elevated CO_2 and N addition in grassland mesocosms. *FEMS Microbiol. Lett.* 364:fnx077. doi: 10.1093/femsle/fnx077

Soares, M., and Rousk, J. (2019). Microbial growth and carbon use efficiency in soil: links to fungal-bacterial dominance, SOC-quality and stoichiometry. *Soil Biol. Biochem.* 131, 195–205. doi: 10.1016/j.soilbio.2019.01.010

Song, Y. H., Ai, Z. M., Qiao, L. L., Zhai, J. Y., Li, Y. Z., and Li, Y. Y. (2019). Effects of fertilization on ecological stoichiometric ratio soil carbon, nitrogen, and phosphorus in farmland of the Loess Plateau. *Res. Soil Water Conser.* 26, 38–45. doi: 10.13869/j.cnki.rswc.2019.06.006

Tadano, T., and Sakai, H. (1991). Secretion of acid phosphatase by the roots of several crop species under phosphorus-deficient conditions. *Soil Sci. Plant Nutr.* 37, 129–140. doi: 10.1080/00380768.1991.10415018

Tian, D., and Niu, S. (2015). A global analysis of soil acidification caused by nitrogen addition. *Environ. Res. Lett.* 10:024019. doi: 10.1088/1748-9326/10/2/024019

Tischer, A., Werisch, M., Dobbelin, F., Camenzind, T., Rillig, M. C., Potthast, K., et al. (2015). Above- and belowground linkages of a nitrogen and phosphorus co-limited tropicalmountain pasture system-responses to nutrient enrichment. *Plant Soil* 391, 333–352. doi: 10.1007/s11104-015-2431-7

Treseder, K. K. (2004). A meta-analysis of mycorrhizal responses to nitrogen, phosphorus, and atmospheric CO_2 in field studies. *New Phytol.* 164, 347–355. doi: 10.1111/j.1469-8137.2004.01159.x

Treseder, K. K. (2008). Nitrogen additions and microbial biomass: a meta-analysis of ecosystem studies. *Ecol. Lett.* 11, 1111–1120. doi: 10.1111/j.1461-0248.2008.01230.x

Turner, B. L., and Joseph, W. S. (2013). The response of microbial biomass and hydrolytic enzymes to a decade of nitrogen, phosphorus, and potassium addition in a lowland tropical rain forest. *Biogeochemistry* 117, 115–130. doi: 10.1007/s10533-013-9848-y

Van der Heijden, M. G., Bardgett, R. D., and van Straalen, N. M. (2008). The unseen majority: soil microbes as drivers of plant diversity and productivity in

terrestrial ecosystems. *Ecol. Lett*. 11, 296–310. doi: 10.1111/j.1461-0248.2007.01139.x

Vitousek, P. M., Porder, S., Houlton, B. Z., and Chadwick, O. A. (2010). Terrestrial phosphorus limitation: mechanisms, implications, and nitrogen-phosphorus interactions. *Ecol. Appl.* 20, 5–15. doi: 10.1890/08-0127.1

Walkley, A., and Black, I. A. (1934). An examination of the Degtjareff method for determining soil organic matter, and a proposed modification of the chromic acid Titration method. *Soil Sci.* 37, 29–38. doi: 10.1097/00010694-193401000-00003

Wang, C., Cao, Z., Wang, L., and Liu, X. (2013). Ecological effects of leguminous plants on microorganism community in rhizosphere soils. *Ecol. Environ. Sci.* 22, 85–89. doi: 10.16258/j.cnki.1674-5906.2013.01.019

Wang, C., Liu, D., and Bai, E. (2018). Decreasing soil microbial diversity is associated with decreasing microbial biomass under nitrogen addition. *Soil Biol. Biochem.* 120, 126–133. doi: 10.1016/j.soilbio.2018.02.003

Wang, J., Song, B., Ma, F., Tian, D., Li, Y., Yan, T., et al. (2019). Nitrogen addition reduces soil respiration but increases the relative contribution of heterotrophic component in an alpine meadow. *Funct. Ecol.* 33, 2239–2253. doi: 10.1111/1365-2435.13433

Wang, Y., Li, C., Kou, Y., Wang, J., Bo, T., Li, H., et al. (2017). Soil pH is a major driver of soil diazotrophic community assembly in Qinghai-Tibet alpine meadows. *Soil Biol. Biochem.* 115, 547–555. doi: 10.1016/j.soilbio.2017.09.024

Wardle, D. A., Nilsson, M.-C., Zackrisson, O., and Gallet, C. (2003). Determinants of litter mixing effects in a Swedish boreal forest. *Soil Biol. Biochem.* 35, 827–835. doi: 10.1016/s0038-0717(03)00118-4

Weintraub, M. N., and Schimel, J. P. (2005). The seasonal dynamics of amino acids and other nutrients in Alaskan Arctic tundra soils. *Biogeochemistry* 73, 359–380. doi: 10.1007/s10533-004-0363-z

Wild, B., Alves, R. J. E., Bárta, J., Èapek, P., Gentsch, N., Guggenberger, G., et al. (2018). Amino acid production exceeds plant nitrogen demand in Siberian tundra. *Environ. Res. Lett.* 13:034002. doi: 10.1088/1748-9326/aaa4fa

Xiao, H., Yang, H., Zhao, M., Monaco, T. A., Rong, Y., Huang, D., et al. (2021). Soil extracellular enzyme activities and the abundance of nitrogen-cycling functional genes responded more to N addition than P addition in an Inner Mongolian meadow steppe. *Sci. Total. Environ.* 759:143541. doi: 10.1016/j.scitotenv.2020.143541

Xiao, W., Chen, X., Jing, X., and Zhu, B. (2018). A meta-analysis of soil extracellular enzyme activities in response to global change. *Soil Biol. Biochem*. 123, 21–32. doi: 10.1016/j.soilbio.2018.05.001

Xu, D. H., Fang, X. W., Zhang, R. Y., Gao, T. P., Bu, H. Y., and Du, G. Z. (2015). Influences of nitrogen, phosphorus and silicon addition on plant productivity and species richness in an alpine meadow. *AoB Plants* 7:plv125. doi: 10.1093/aobpla/plv125

Yang, H., Jiang, L., Li, L., Li, A., Wu, M., and Wan, S. (2012). Diversity-dependent stability under mowing and nutrient addition: evidence from a 7-year grassland experiment. *Ecol. Lett.* 15, 619–626. doi: 10.1111/j.1461-0248.2012.01778.x

Yao, M., Rui, J., Li, J., Dai, Y., Bai, Y., Hedìnec, P., et al. (2014). Rate-specific responses of prokaryotic diversity and structure to nitrogen deposition in the Leymus chinensis steppe. *Soil Biol. Biochem*. 79, 81–90. doi: 10.1016/j.soilbio.2014.09.009

You, C. M., Wu, F. Z., Gan, Y. M., Yang, W. Q., Hu, Z. M., Xu, Z. F., et al. (2017). Grass and forbs respond differently to nitrogen addition: a meta-analysis of global grassland ecosystems. *Sci. Rep.* 7:1563. doi: 10.1038/s41598-017-01728-x

Zak, D. R., Holmes, W. E., White, D. C., Peacock, A. D., and Tilman, D. (2003). Plant diversity, soil microbial communities, and ecosystem function: are there any links? *Ecology* 84, 2042–2050. doi: 10.1890/02-0433

Zeng, J., Liu, X., Song, L., Lin, X., and Chu, H. (2016). Nitrogen fertilization directly affects soil bacterial diversity and indirectly affects bacterial community composition. *Soil Biol. Biochem.* 92, 41–49. doi: 10.1016/j.soilbio.2015.09.018

Zhang, N., Wan, S., Li, L., Bi, J., Zhao, M., and Ma, K. (2008). Impacts of urea N addition on soil microbial community in a semi-arid temperate steppe in northern China. *Plant Soil* 311, 19–28. doi: 10.1007/s11104-008-9650-0

Zhang, Q., Xie, J., Lyu, M., Xiong, D., Wang, J., Chen, Y., et al. (2016). Short-term effects of soil warming and nitrogen addition on the N:P stoichiometry of *Cunninghamia lanceolata* in subtropical regions. *Plant Soil* 411, 395–407. doi: 10.1007/s11104-016-3037-4

Zhang, Y. D., Sun, Z. H., and Shen, Y. X. (2005). Effect of fertilization on soil microorganism of deteriorated grassland in dry-hot valley region of Jinsha River. *J. Soil Water Conser*. 19, 88–91. doi: 10.13870/j.cnki.stbcxb.2005.02.03

Zhao, Y., Yang, B., Li, M., Xiao, R., Rao, K., Wang, J., et al. (2019). Community composition, structure and productivity in response to nitrogen and phosphorus additions in a temperate meadow. *Sci. Total Environ.* 654, 863–871. doi: 10.1016/j.scitotenv.2018.11.155

Zheng, Y., Kim, Y. C., Tian, X. F., Chen, L., Yang, W., Gao, C., et al. (2014). Differential responses of arbuscular mycorrhizal fungi to nitrogen addition in a near pristine Tibetan alpine meadow. *FEMS Microbiol. Ecol.* 89, 594–605. doi: 10.1111/1574-6941.12361

Zheng, Z., Bai, W., and Zhang, W. (2019). Root trait-mediated belowground competition and community composition of a temperate steppe under nitrogen enrichment. *Plant Soil* 437, 341–354. doi: 10.1007/s11104-019-03989-z

Zhou, J., Jiang, X., Zhou, B., Zhao, B., Ma, M., Guan, D., et al. (2016). Thirty four years of nitrogen fertilization decreases fungal diversity and alters fungal community composition in black soil in northeast China. *Soil Biol. Biochem.* 95, 135–143. doi: 10.1016/j.soilbio.2015.12.012

Zhou, T. C., Sun, J., and Shi, P. L. (2021). Plant-microbe interactions regulate the aboveground community nitrogen accumulation rate in different environmental conditions on the Tibetan Plateau. *Catena* 204:105407. doi: 10.1016/j.catena.2021.105407

Zhou, X., Zhang, Y., and Downing, A. (2012). Non-linear response of microbial activity across a gradient of nitrogen addition to a soil from the Gurbantunggut Desert, northwestern China. *Soil Biol. Biochem.* 47, 67–77. doi: 10.1016/j.soilbio.2011.05.012

Zhou, Z., Wang, C., Zheng, M., Jiang, L., and Luo, Y. (2017). Patterns and mechanisms of responses by soil microbial communities to nitrogen addition. *Soil Biol. Biochem.* 115, 433–441. doi: 10.1016/j.soilbio.2017.09.015

Conflict of Interest: The authors declare that the research was conducted in the absence of any commercial or financial relationships that could be construed as a potential conflict of interest.

Publisher's Note: All claims expressed in this article are solely those of the authors and do not necessarily represent those of their affiliated organizations, or those of the publisher, the editors and the reviewers. Any product that may be evaluated in this article, or claim that may be made by its manufacturer, is not guaranteed or endorsed by the publisher.

Copyright © 2022 Zi, Hu and Wang. This is an open-access article distributed under the terms of the Creative Commons Attribution License (CC BY). The use, distribution or reproduction in other forums is permitted, provided the original author(s) and the copyright owner(s) are credited and that the original publication in this journal is cited, in accordance with accepted academic practice. No use, distribution or reproduction is permitted which does not comply with these terms.

frontiers in Plant Science

ORIGINAL RESEARCH
published: 04 March 2022
doi: 10.3389/fpls.2022.839920

Ecosystem Coupling and Ecosystem Multifunctionality May Evaluate the Plant Succession Induced by Grazing in Alpine Meadow

Yingxin Wang[1,2,3], *Zhe Wu*[1,2], *Zhaofeng Wang*[1,2], *Shenghua Chang*[1,2], *Yongqiang Qian*[3], *Jianmin Chu*[4], *Zhiqing Jia*[4], *Qingping Zhou*[5] *and Fujiang Hou*[1,2*]

[1] State Key Laboratory of Grassland Agro-Ecosystems, College of Pastoral Agriculture Science and Technology, Lanzhou University, Lanzhou, China, [2] Key Laboratory of Grassland Livestock Industry Innovation, Ministry of Agriculture and Rural Affairs, College of Pastoral Agriculture Science and Technology, Lanzhou University, Lanzhou, China, [3] Grassland Research Center of National Forestry and Grassland Administration, Research Institute of Ecological Protection and Restoration, Chinese Academy of Forestry, Beijing, China, [4] Research Institute of Forestry, Chinese Academy of Forestry, Beijing, China, [5] College of Qinghai Tibet Plateau Research, Southwest Minzu University, Chengdu, China

Most alpine meadow on the Tibetan Plateau are at different stages of community succession induced by grazing practices. Quantifying the succession sequence and assessing the dynamics of plant composition, ecosystem coupling, and multifunctionality across successional stages are essential for reasonable restoration of degraded alpine meadow. Here, we selected areas with different grazing disturbance histories and used them as a space series (i.e., space-for-time substitution) to study the community succession. Our work quantified the plant succession sequence of alpine meadow induced by grazing with plant functional group approach. The plant succession sequence is from the tall sedge community with erect growth to the short undesirable toxic forbs community with prostrate growth. Ecosystem coupling, ecosystem multifunctionality and their relationships were all the lowest in Stage 4. Compared to Stage 4, the ecosystem multifunctionality index increased in Stages 1, 2, and 3 by 102.6, 89.8, and 207.6%, respectively; the extent of ecosystem coupling increased by 20.0, 16.8, and 21.2%, respectively. Our results indicated that the driving factors of ecosystem coupling and ecosystem multifunctionality were soil factor individual in early successional stage to plant-soil simultaneously in late successional stage. Our results also highlighted the importance of toxic weeds during the late stage of degraded succession and suggest that the expansion of toxic plants is a consequence of their greater suitability from a successional perspective. The findings of this study would provide valuable guidance for optimizing the management and restoration practice of alpine meadow.

Keywords: plant succession, ecosystem coupling, ecosystem multifunctionality, grazing, alpine meadow

OPEN ACCESS

Edited by:
Jian Sun,
Institute of Tibetan Plateau Research (CAS), China

Reviewed by:
Zhenchao Zhang,
Northwest A&F University, China
Wei Wanrong,
China West Normal University, China

***Correspondence:**
Fujiang Hou
cyhoufj@lzu.edu.cn

Specialty section:
This article was submitted to Functional Plant Ecology, a section of the journal Frontiers in Plant Science

Received: *20 December 2021*
Accepted: *17 January 2022*
Published: *04 March 2022*

Citation:
Wang Y, Wu Z, Wang Z, Chang S, Qian Y, Chu J, Jia Z, Zhou Q and Hou F (2022) Ecosystem Coupling and Ecosystem Multifunctionality May Evaluate the Plant Succession Induced by Grazing in Alpine Meadow. Front. Plant Sci. 13:839920. doi: 10.3389/fpls.2022.839920

INTRODUCTION

Plant community succession is the process of species replacement (Lavorel and Garnier, 2010; Milchunas and Vandever, 2013) or the change in plant functional traits over time (Kahmen and Poschlod, 2004; He et al., 2019). Facilitation, inhibition, and tolerance are the three main different turnovers between species in the succession pathways (Maggi et al., 2011; Zhang and Tielbrger, 2019). Biological mechanisms that underlie succession events include competition colonization

trade-off, successional niche mechanisms, facilitation, interactions with enemies, and the resource-ratio hypothesis (Rodríguez et al., 2007; Muscarella et al., 2016; Prugh and Sivy, 2020). Furthermore, three successional processes were dissected which included site availability, differential species availability, and differential species manifestation (Baeten et al., 2010). Specifically, the mechanisms within each process are driven by biotic and abiotic factors and their interactions, which are further regulated through such factors as climate change, fire, and livestock grazing (Nicolai, 2019; Leizeaga et al., 2020).

The effect of livestock grazing on the differential performance of plants is important in successional process (Milchunas and Vandever, 2013; Howard et al., 2020). In addition to directly foraging and ingesting the shoot of plants and changing the competitive balance among plant species (Duhamel et al., 2019), livestock grazing can also influence successional rates and successional trajectories by impacting seed dispersal and colonization patterns (Wang et al., 2018; Ma et al., 2020). Grazing can cause "arrested successional development" that results from preferential feeding on late successional species (Kemp and King, 2001). Selective feeding of livestock on early successional species can promote the emergence and growth of late successional species, thereby accelerating succession (Devaney et al., 2020). Meanwhile, diversified livestock assemblage has additive or complementary effects on successional trends (Wang et al., 2019). For example, cold-season grazing could encourage alpine grassland succession from a sedge/forb community to a grass/forb community because yak and Tibetan sheep prefer to consume sedge plants (Shi et al., 2019; Sun et al., 2020). Also, seedling herbivory and defense play a fundamental role in regulating the successional trajectories by livestock grazing (Hanley and Lamont, 2001). At this period, particularly, plants are easily vulnerable to organs loss in their life cycle (Hanley and Lamont, 2001). Hence, herbivory can decrease seedling vigor, further to affect the competitive ability and opportunity of long-term survival, even lead to mortality (Bestelmeyer et al., 2010; Barton and Hanley, 2013). A 6-fold reduction in plant seedling survivorship resulted from feeding by large herbivores in Panamanian forests (Asquith et al., 1997). The mechanism behind them is likely to the interspecific difference in seedling tastiness, size, and morphology, also from differences in species richness, pattern of spatial distribution, and seedling emergence occasion (Lusk and Kelly, 2003). Further, seedling establishment can be favored from microsite availability promotion via physical disturbances of livestock, and from creating more chances for seedling recruitment by reducing litter loads and increasing availability of light (Marcora et al., 2013; Ameztegui and Lluí, 2015). Additionally, change in plant species composition influencing energy and nutrient flow and ecosystem succession by altering litter decomposition (Song et al., 2017; Barnes et al., 2018).

Evaluation of dynamics of plant and soil properties can offer more details on ecosystem stability and sustainability, thereby contribute to predict the successional trajectory induced by grazing practices (Tang et al., 2010; Paterno et al., 2016; Shi et al., 2018).

In China, researches related to the classification of the degradation succession of grazed grasslands (e.g., a typical steppe (Zhao et al., 2017), desert steppe (Hu et al., 2016) have long been recognized, but relatively little is known about the degradation succession of alpine meadow. Increased grazing pressure and climate change accelerated grassland degradation, leading to dysfunction of the alpine meadow ecosystem. Overgrazing may also decrease sward height, vegetation cover, and biomass and may increase undesirable and unpalatable grass species and even the occurrence of species that are toxic to animals (Wu et al., 2015). Besides, a reduction litter decomposition to the soil, which results from the degradation of vegetation, can lead to a substantial decrease in amination, nitrification, and nitrogen fixation, resulting in a rapid decrease in soil fertility (Dong et al., 2015; Howard et al., 2020). These effects, in turn, reduce the flow of energy and substance circulation in the ecosystem, finally resulting in discordance between the two dominant components (i.e., soil and plant), as well as in the disruption of ecosystem multifunctionality (Wang et al., 2020a; Zhang R. Y. et al., 2021).

More tightly coupled ecosystems can in favor of more extensive ecosystem functions, which are likely to be associated with a higher efficiency in resources utilization and material cycle (Risch et al., 2018). However, a dearth of information on this topic on effects of succession stages induced by grazing on ecosystem coupling and multiple ecosystem functions. Additionally, we have little knowledge about how these bidirectional interactions and relationships may vary throughout the successional process, and their underlying mechanisms. To address these knowledge issues, we used plant functional groups instead of plant species to identify and quantify the stages of succession. We also have addressed the following questions: (1) Are there substantial differences in plant composition, ecosystem coupling, ecosystem multifunctionality, and the relationships among these functions during the different successional stages? If yes, (2) What the main driving mechanism in difference of ecosystem coupling and ecosystem multifunctionality affected by plant succession? We assumed that (1) plant composition, ecosystem coupling, ecosystem multifunctionality and their relationships would change in different successional stages? (2) the environmental factors and driving mechanism associated with ecosystem coupling, ecosystem multifunctionality would differ among successional stages induced by grazing. The results of this study provide valuable guidance for optimizing the management and restoration practice of alpine meadow.

MATERIALS AND METHODS

Study Site

The experiment was carried on at the Institute of Tibetan Plateau at Southwest Minzu University (32°48'N, 102°33'E, 3,500 m above mean sea level), located about 4 km north of Hongyuan County, Sichuan, China. The mean annual temperature and precipitation is 1.1°C and 700 mm, respectively (Liu et al., 2020). The coldest month is January (∼9.7°C) and the warmest month is July (11.1°C). The majority of rainfall is concentrated

in warm season (June to September). The soil type is alpine meadow soil (Chinese Soil Taxonomy Research Group, 1995). The type of vegetation is classified as alpine meadow and comprises sedges (most frequently *Kobresia cristata*, *Scirpus pumilus*), grasses (most frequently *Elymus nutans*, *Poa pratensis*, and *Agrostis* species), and forbs (dominated by *Saussurea* species and *Anemone* species). The study site has been used for trial plots under different land use patterns caused by different grazing practices since 2007.

Field Methods

There are various vegetation structure and composition in the experimental areas that have different grazing disturbance histories. The common approach referred to as space-for-time substitution (Pickett, 1989) was used to infer successional patterns of alpine meadow. The advantage of this approach is that plant community variation can be investigated well without long-term observations of a single plot, which need take decades to finish (Li et al., 2015). The belt transect method was used to measure vegetation in the experimental area in August, 2018. We randomly set 10 belt transects with a length of 200 m each. Three quadrats (0.5 × 0.5 m) were randomly selected in every 10 m of each sample strip. In total, there were ∼600 quadrats (samples).

Data Collection

Sampling of Plant Properties

To investigate the community structure and species composition of each quadrat, the height of the tallest stem of each plant species was recorded. Total number of plant species of each quadrat represent plant species richness (SR). All on-ground plants were removed and bagged to bring back to the lab. Then, we separated them for each species and weighed to obtain aboveground biomass (AGB) after oven-dried at 65°C for 48 h.

Sampling of Soil Properties

The surface layer's (a depth of 10 cm) soil temperature (ST) and soil water content (SM) of each quadrat were measured using Field-Scout TDR-100 (Spectrum Technologies, Plainfield, IL, USA). Cutting ring method was used to measure Soil bulk density (SBD). The soil was sampled in the middle of each 0.5 × 0.5 m quadrat using a soil auger, and then placed them in mesh bags (2-mm mesh). After being air-dried about a month outdoors, the soil samples were separated root and soil sub-samples. The root sub-sample was washed free of soil and weighed to acquire belowground biomass (BGB) in the following being oven-dried at 115°C for 48 h.

The soil sub-samples were further to air-dried in laboratory at room temperature and were sieved through a 0.2-mm mesh. An Element Analyzer was used to determine soil total carbon (STC), soil total nitrogen (STN), and soil total sulfur (STS). Soil total phosphorus (STP) was measured using the molybdate colorimetric test after perchloric acid digestion.

Ecosystem Characteristic Calculations

Plant Species Evenness Index

The Camargo evenness index (EV) is calculated independently of SR (Camargo, 1993), and is defined as formula 1:

$$E = 1 - \sum_{i}^{s} \sum_{j=i+1}^{s} \left(\left| P_i - P_j \right| / S \right) \quad (1)$$

where E is the Camargo evenness index, P_i is the biomass proportion of plant species i in the sample, P_j is the biomass proportion of plant species j in the sample, and S is the total number of plant species of the quadrat.

Ecosystem Coupling Between Soil and Plant

The indicator of coupling coordination degree between plant and soil subsystems can be used for evaluating the ecosystem coupling between soil and plant (EC_SP). To eliminate the influence of dimension and magnitude, we first standardized the raw data using two formulas (Tang, 2015; Wang et al., 2020a).

For the positive index, we used formula 2:

$$X'_i = \frac{X_i - minX_i}{\max X_i - minX_i} \quad (2)$$

For a negative index, we used formula 3:

$$X'_i = \frac{\max X_i - X_i}{\max X_i - minX_i} \quad (3)$$

where, X_i represent the original value of index i, X'_i represent the standardized value of index i, and $maxX_i$ and $minX_i$indicate the maximum and minimum value of the index i.

To evaluate the soil and plant subsystem, we supposed X_1, X_2, …, X_i to stand for soil subsystem indexes (X_s), and Y_1, Y_2, …, Y_j to stand for plant subsystem indexes (Y_p). Then calculated by formula 4 and 5:

$$S(X) = \sum_{s=1}^{i} W_s X'_s \quad (4)$$

$$P(Y) = \sum_{p=1}^{j} W_p Y'_p \quad (5)$$

where $S(X)$ and $P(Y)$ are the integral value of the soil and plant subsystem, respectively; X'_s and Y'_p are the standardized values of X_s and Y_p, respectively, and W_s and W_p are the weight of $S(X)$ and $P(Y)$, respectively, which can be calculated by principal component analysis (PCA).

The degree of coupling coordination was calculated as formula 6:

$$D_{sp} = \sqrt{\left(\frac{[S(X) \times P(Y)]^{\frac{1}{2}}}{\frac{[S(X)+P(Y)]}{2}} \right) \times [\alpha \times S(X) + \beta \times P(Y)]} \quad (6)$$

where D_{sp} stand for the coupling coordination degree and α and β stand for the contribution from the soil and plants, respectively.

Ecosystem Functions

To quantify the quantity and value of ecosystem functions, we chose 12 plant and soil variables including AGB, BGB, SR, plant density (PD), plant height (PH), ST, SM, SBD, STC, STN, STP, and STS in the current study. Based on the selected indicators, the plant growth index (PGI), soil carbon accumulation index (SCI), soil nutrient cycling index (SNI), and ecosystem multifunctional index (EMF) was calculated via an average method as formula 7:

$$EMF = \frac{1}{N}\sum_{i=1}^{N} f(xi) \quad (7)$$

where N is the number of measured functions and equal to 12 in this study, x_i represents the measured value of function i, $f(xi)$ is the standardization of x_i via Z-score standardization.

Statistical Analysis

Clustering detection (Ward method) was performed to reveal the trend and direction of plant community succession of alpine meadow (**Supplementary Figure S1**). The data for the vegetation and soil properties of the 30 quadrats associated with each stage of succession were used for data statistical analyses.

All data analyses were performed in R version 4.1.2 (R Core Team, 2021). Data distributions and normality was examined through Shapiro-Wilk goodness-of-fit test. First, general linear model from the "ASREML" package (Gilmour et al., 2015) to test the effects of succession stage on the SR, EV, AGB, BGB, PD, PH, SBD, SM, ST, STC, STN, STP, PGI, SCI, SNI, EC_SP, EMF, and the biomass proportion of toxic plants. Thereafter, Tukey's HSD test in the "AGRICOLAE" package (de Mendiburu, 2014) was conducted to assess the differences among means. Second, correlation analysis was performed using the "GGCOR" package (Huang, 2019) to acquire the relationships among SR, EV, PGI, SCI, SNI, and EMF, along with their relationships to EC_SP (Mantel test). Third, simple regression analysis was used to compute the relationships between EC_SP and EMF at different successional stages, along with their relationships to the biomass proportion of toxic plants. Fourth, gradient regression analysis in "GBM" package was used to analysis the relative importance of biotic and abiotic factors to EC_SP and EMF. In the nonlinear model, Friedman's H-statistic was calculated to evaluate the relative strength of the interaction effect (Li et al., 2021). Finally, heatmap analysis from the "PHEATMAP" to realize correlations between SR, EC, ecosystem function indexes (PGI, SCI, SNI, and EMF) and plant, soil properties. All figures were drawn using Origin 2021b and the "GGPLOT2" package.

RESULTS

Quantification of Plant Succession

Biomass ratios of plant functional groups was used to quantify the stages of succession (**Figure 1**). The succession series is as follows: Stage 1 (sedges, 46%; desirable forbs, 28%; grasses, 15%), Stage 2 (desirable forbs, 36%; grasses, 25%; sedges, 24%), Stage 3 (desirable forbs, 38%; undesirable toxic plants, 29%; sedges, 23%), and Stage 4 (undesirable toxic plants, 44%; desirable forbs, 37%; grasses, 11%). From the tall *Kobresia* community with erect growth to the short undesirable toxic forbs community (e.g., *Gentianaceae*, *Ranunculaceae*) with prostrate growth; the vertical, perennial desirable forbs community represented the transition between these two stages (**Figure 1**).

Changes in Characteristics of Plant and Soil Factors Across the Successional Stages

The SR, EV, AGB, PD, PH, and STN of Stage 4 was significantly ($P < 0.05$) lower than that of the other three stages (**Figures 2**, **3**). In contrast, SBD and ST in Stage 4 was significantly ($P < 0.05$) higher than that of the other three stages (**Figure 3**). The gamma diversity of each stage (from Stage 1, 2, 3, and 4) was 61, 55, 47, and 49 species, respectively (**Figure 2C**). There was no significant difference ($P > 0.05$) in SM among four stages (**Figure 3**).

Ecosystem Functions and Ecosystem Coupling and Their Relationships Across the Successional Stages

The SCI and SNI of Stage 3 were both significantly ($P < 0.05$) higher than that for the other three stages (**Figures 4B,C**). The EMF and extent of EC_SP were both at their lowest levels in Stage 4 (**Figures 4D,E**). Compared with the EMF in Stage 4, this index increased by 102.6, 89.8, and 207.6% in Stage 1, 2, and 3, respectively (**Figure 4D**). Compared with the extent of EC_SP in Stage 4, there was a 20.0, 16.8, and 21.2% increase in coupling in Stage 1, 2, and 3, respectively (**Figure 4E**). Biomass proportion of toxic plants in Stage 3 and Stage 4 was significantly ($P < 0.05$) higher than that in Stage 1 and Stage 2 (**Figure 4F**).

In general, there was a significant positive relationship ($R^2 = 0.57$, $P < 0.05$) between the extent of EC_SP and EMF (**Figure 5B**). Relationships between EC_SP and EMF were at variance in different stages (**Figure 5A**). Coefficients of correlation between EC_SP and EMF in Stage 1 and Stage 2 were higher than those in Stage 3 and Stage 4 (**Figure 5A**). EC_SP and EMF were both significantly ($P < 0.05$) and positively related to SCI and SNI in Stage 1 and 2 and to the soil nutrient index in Stage 4 (**Figure 5A**). In Stage 3 and Stage 4, EC_SP and EMF both had significant relationships with PGI and SR (**Figure 5A**).

DISCUSSION

Plant Succession Sequence Based on Plant Function Group

Quantification of sequence of community succession is central for raveling out the function and structure of alpine meadow (Bagchi et al., 2013; Avolio et al., 2015). The best way to characterize and identify the process of succession is by analyzing the changes in vegetation composition over the course of a long-term, single-site experiment (Kahmen and Poschlod, 2004; Abbas et al., 2019). However, long-term records of trajectories of community change do not exist, either empirically or experimentally, probably because, at least for plants, the process of succession from pioneer to climax species may take 25–150

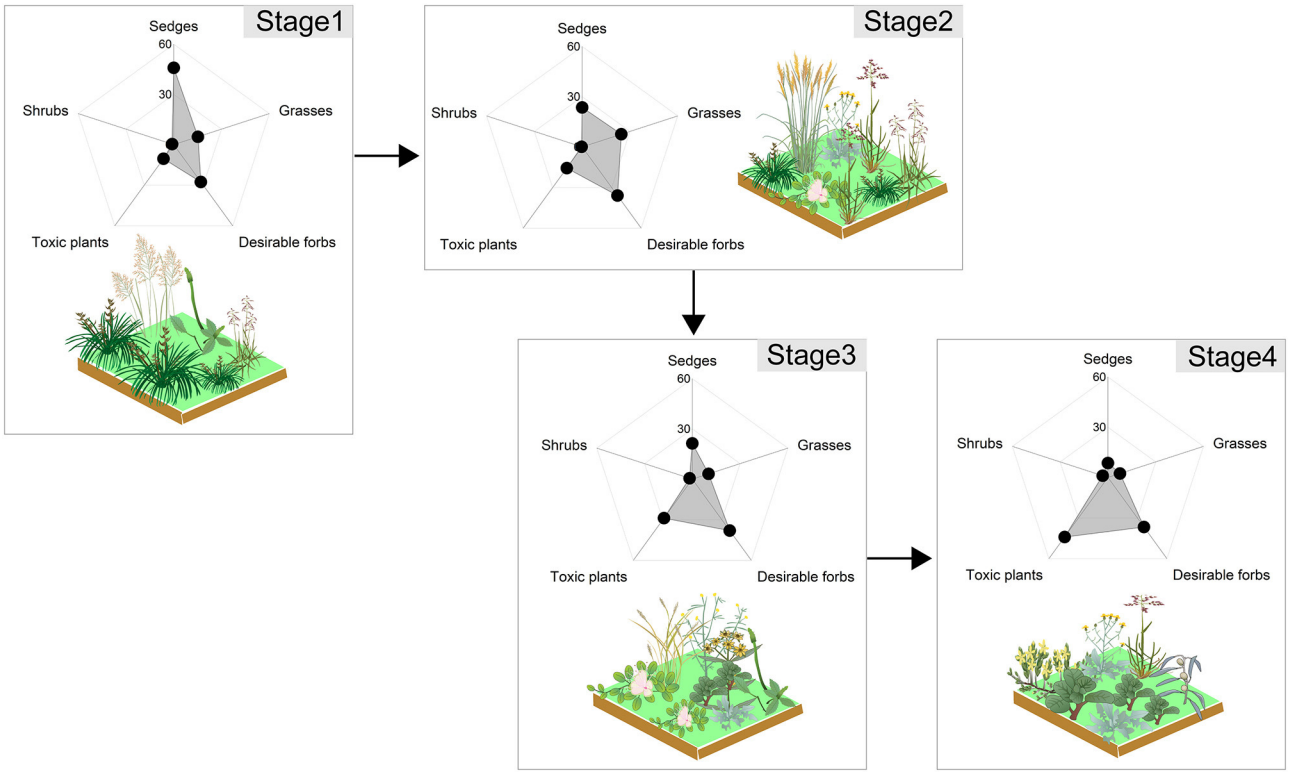

FIGURE 1 | The plant community succession of an alpine meadow of the Tibetan Plateau as a result of grazing. Dominant sedge genera included *Kobresia* and *Carex*; dominant grass genera included *Elymus* and *Poa*; dominant desirable forb genera included *Saussurea* and *Potentilla*; dominant toxic plant genera included *Gentianaceae*, *Ranunculaceae*, and *Euphorbiaceae*; and dominant shrub species consisted of *Berberis wilsonii* and *Potentilla fruticosa*.

years to complete (Porensky et al., 2017). Generally, using a space series to replace a time course is an accepted method for analyzing community succession (Duan et al., 2008; Hu et al., 2016). Plant functional group (PFG) pathway could eliminate the disadvantages of individual plant species approach because of each PFG has its specific and vital role in the grassland ecosystem by altering the stability and functions (Bermejo et al., 2012; Sun and Wang, 2016). Accordingly, we recommend using the biomass proportion of plant functional groups as an effective and integrated index for evaluating the succession trajectory of alpine meadows. Our results demonstrated that the community successional series of alpine meadow were divided into four stages with a trend over time from tall erect-growth sedges community (e.g., *Kobresia*) to short prostrate-growth undesirable toxic forbs community (e.g., *Gentianaceae*, *Ranunculacese*) (**Figure 2**). These findings were also consistent with the actual situation determined by experienced observation of the field work (Zhang Z. et al., 2021) and can be viewed as a general degenerate community succession series for alpine meadows for restoration practices. The succession series can contribute to restoration practices in three aspects as following: (i) further clarification of community structure development, (ii) more cognition of species interactions and of nutrient dynamics, and (iii) better understanding of the species transformation between successional stages and of how these stages fit together into successional trajectories (Walker and del Moral, 2009; Zhang et al., 2015).

Types and Drivers of Plant Composition to Plant Succession

During the process of plant succession induced by grazing, the structure and function of an alpine meadow are affected by changes in the species composition and richness, soil nutrient availability, and a number of abiotic factors including environmental filtering and dispersal mechanisms (Niu et al., 2016). In this study, the changes in across the successional stages can be categorized into the three following types: (i) The decay type is characterized by a decrease in the dominance of a given species or dominance in conjunction with an increase in grazing intensity, as exemplified by *Kobresia graminifolia*, *Gramineae* species (*Poa pratensis*, *Stipa aliena*, and *Festuca sinensis*), and *Fritillaria cirrhosa*; (ii) The growth type is characterized by an increase in the dominance of a given species in conjunction with increased grazing intensity. This was noted for *Anemone rivularis*, *Gentiana macrophylla*, and *Anaphalis lacteal* and (iii) The fluctuating type, which included *Carex thibetica*, *Scirpus pumilus*, *Elymus nutans*, and *Potentilla fragarioides*, undergoes changes that are not consistent across the stages (**Figure 2**).

In a system such as this alpine meadow, the grazing intensity, and selective foraging of the yaks should be the major factors

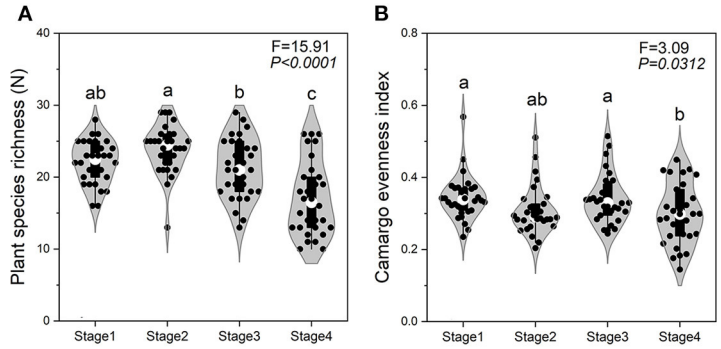

C

Family	Genus	Species	Stage 1	2	3	4
	Kobresia	*Kobresia graminifolia*				
Cyperaceae	*Carex*	*Carex thibetica*				
	Scirpus	*Scirpus pumilus*				
	Elymus	*Elymus nutans*				
	Poa	*Poa pratensis*				
	Agrostis	*Agrostis hugoniana*				
Gramineae	*Stipa*	*Stipa aliena*				
	Festuca	*Festuca sinensis*				
		Festuca elata				
	Koeleria	*Koeleria litvinowii*				
	Allium	*Gramineae*				
Liliaceae	*Fritillaria*	*Fritillaria cirrhosa*				
		Anemone rivularis				
	Anemone	*Anemone obtusiloba*				
		Anemone trullifolia				
Ranunculaceae	*Trollius*	*Trollius farreri*				
	Ranunculus	*Ranunculus tanguticus*				
	Delphinium	*Delphinium grandiflorum*				
	Thalictrum	*Thalictrum alpinum*				
	Oxytropis	*Oxytropis kansuensis*				
Leguminosae	*Tibetia*	*Tibetia himalaica*				
	Astragalus	*Astragalus polycladus*				
	Pedicularis	*Pedicularis szetschuanica*				
		Pedicularis chinensis				
Scrophulariaceae	*Euphrasia*	*Euphrasia pectinata*				
	Lancea	*Lancea tibetica*				
	Veronica	*Veronica eriogyne*				
	Gentianopsis	*Gentianopsis barbata*				
	Halenia	*Halenia corniculata*				
	Swertia	*Swertia mussotii*				
Gentianaceae		*Gentiana macrophylla*				
	Gentiana	*Gentiana sino-ornata*				
		Gentiana stipitata				
		Gentiana spathulifolia				
Labiatae	*Lamiophlomis*	*Lamiophlomis rotata*				
Euphorbiaceae	*Euphorbia*	*Euphorbia esula*				
	Ligularia	*Ligularia virgaurea*				
	Aster L.	*Aster tataricus*				
	Saussurea	*Saussurea hieracioides*				
		Saussurea stella				
Compositae	*Cremanthodium*	*Cremanthodium lineare*				
	Taraxacum	*Taraxacum lugubre*				
	Artemisia	*Artemisia mongolica*				
	Leontopodium	*Leontopodium leontopodioides*				
	Anaphalis	*Anaphalis lactea*				
	Pleurospermum	*Pleurospermum camtschaticum*				
	Heracleum	*Heracleum millefolium*				
Umbelliferae	*Foeniculum*	*Carumcarvi*				
	Bupleurum	*Bupleuri radix*				
	Angelica	*Angelica sinensis*				
	Arenaria	*Arenaria serpyllifolia*				
Caryophyllaceae	*Cerastium*	*Cerastium fontanum*				
	Silene	*Silene fortunei*				
Geraniaceae	*Geranium*	*Geranium wilfordii*				
Equisetaceae	*Equisetum*	*Equisetum arvense*				
	Potentilla	*Potentilla fragarioides*				
Rosaceae		*Potentilla anserina*				
	Geum	*Geum aleppicum*				
Polygonaceae	*Polygonum*	*Polygonum viviparum*				
		Polygonum sibiricum				
Violaceae	*Viola*	*Viola verecunda*				
Orchidaceae	*Herminium*	*Herminium monorchis*				
Plantaginaceae	*Plantago*	*Plantago asiatica*				
Saxifragaceae	*Parnassia*	*Parnassia palustris*				
	Saxifraga	*Saxifraga stolonifera*				
Berberidaceae	*Berberis*	*Berberis wilsonii*				
Thymelaeaceae	*Stellera*	*Stellera chamaejasme*				
		Species numbers	61	55	47	49

FIGURE 2 | Changes characteristics across the four stages of succession. Plant species richness **(A)**, Camargo evenness index **(B)**, and plant composition **(C)** across the successional stages. In Stage 1, the dominant plant species were *Kobresia graminifolia*, *Elymus nutans*, *Poa pratensis*, *Anemone rivularis*, and

(Continued)

FIGURE 2 | *Tibetia himalaica*; in Stage 2, the dominant plant species were *Elymus nutans*, *Scirpus pumilus*, *Pleurospermum camtschaticum*, *Saussurea hieracioides*, and *Potentilla fragarioides*; in Stage 3, the dominant plant species were *Anaphalis lacteal*, *Saussurea hieracioides*, *Anemone trullifolia*, and *Aster tataricus*; in Stage 4, the dominant species were *Gentiana macrophylla*, *Anemone rivularis*, *Saussurea hieracioides*, and *Oxytropis kansuensis*). The color in **(C)** means the relative biomass of each plant species at different plant successions. The value of relative biomass was higher when the color was darker.

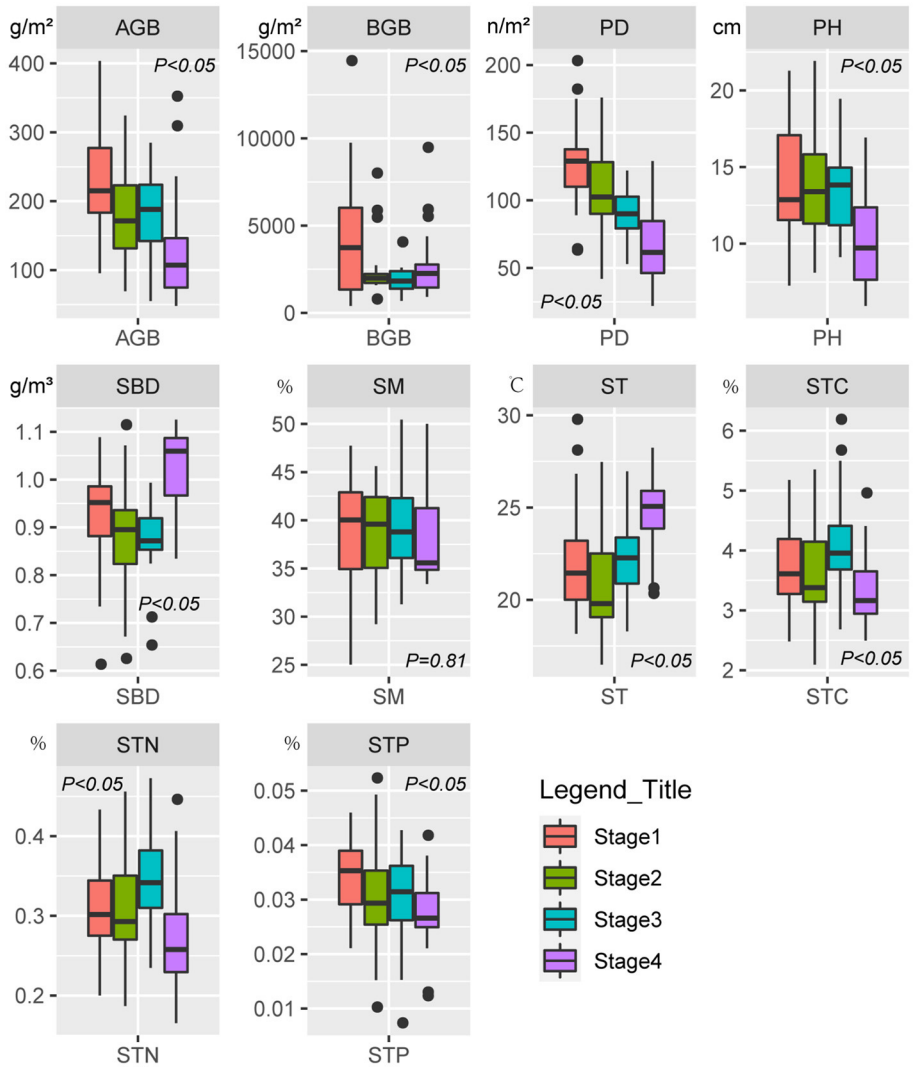

FIGURE 3 | Box plots showing changes in the aboveground biomass (AGB), belowground biomass (BGB), plant density (PD), plant height (PH), soil bulk density (SBD), soil moisture (SM), soil temperature (ST), soil total carbon (STC), soil total nitrogen (STN), and soil total phosphorus (STP) in different successional stages.

driving change in the species composition (Dong et al., 2015). Rational grazing can promote the regeneration and development of erect bunch grasses (e.g., *Scirpus pumilus*, *Elymus nutans*, and *Poa pratensis*) by the fragmentation of tussocks, deposition of manure, removal of standing dead plant tissues, and the stimulation of soil water and nutrient transformation and utilization (Sun et al., 2017; Wang et al., 2018). Also, toxic plants and therophyte are easily germinate and become dominant in the open space among the tussocks resulted from livestock trampling or at excrement patches (Zhang et al., 2020), which is consistent with their dominance under heavy grazing practices (i.e., Stage 4 in this study). During early succession stages, there is no selective advantage for livestock to specialize on specific species, for most of them are edible and desirable. Hence, more plenty of rapid growth plant species with low defense chemicals would be dominant owing to the low consumption of resources to herbivory (Wang et al., 2010; Milchunas and Vandever, 2013). In contrast, resource availability is relatively at low level in the late succession. Given these conditions, slow-growing, well-defended toxic weeds should dominate due to the great cost of resources to herbivory (Bosc and Pauw, 2020).

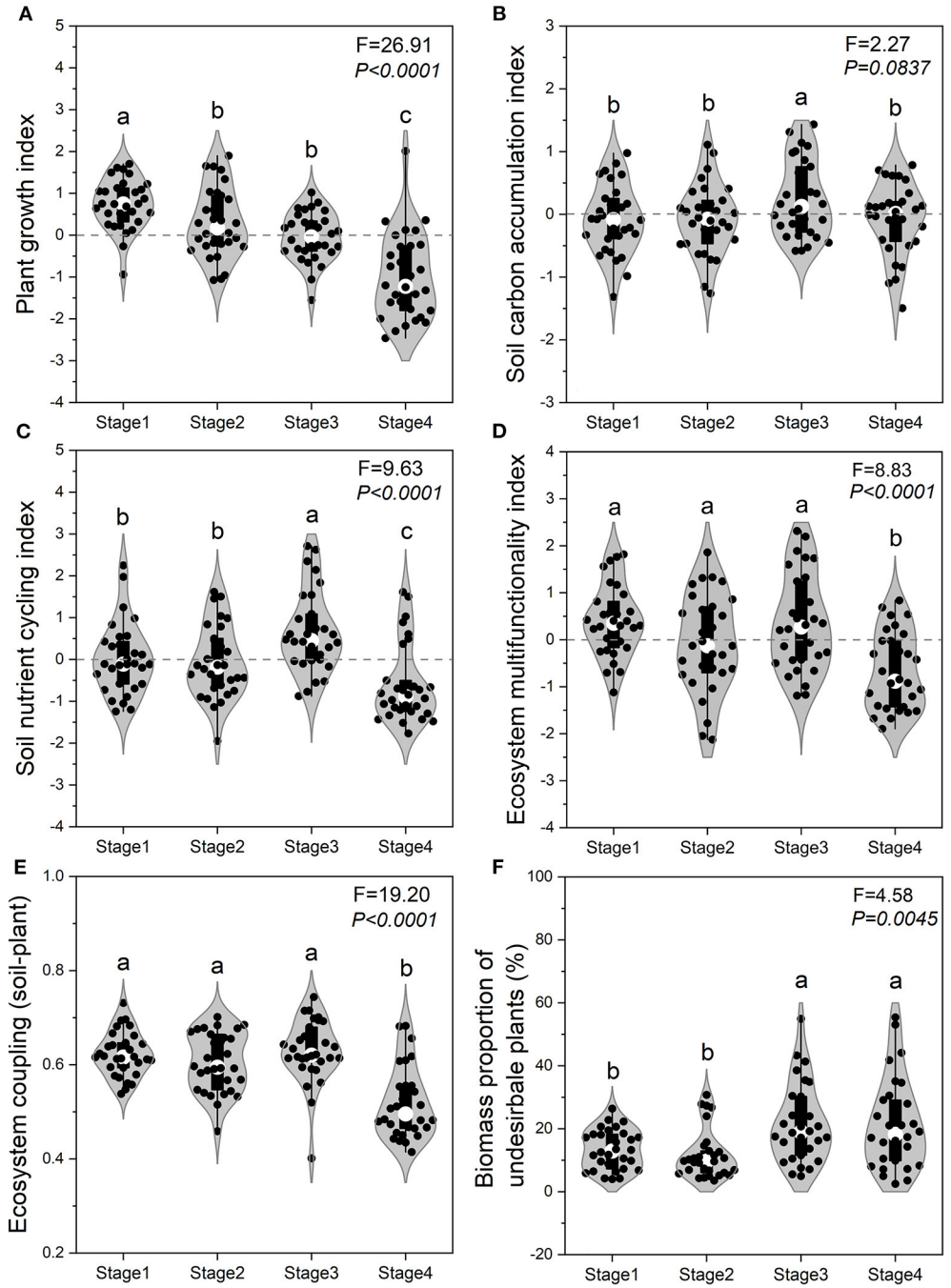

FIGURE 4 | Ecosystem functions across the four stages of succession. Plant growth index **(A)**, soil carbon accumulation index **(B)**, soil nutrient cycling index **(C)**, ecosystem multifunctionality index **(D)**, ecosystem coupling (soil-plant) **(E)**, and biomass proportion of toxic weeds **(F)** across the successional stages. Different lowercase letters above each violin plot indicate statistically significant differences between different succession stages.

Driving Mechanism of Ecosystem Coupling and Ecosystem Multifunctionality to Plant Succession

Plant regressive succession weakens the nutrient cycle and energy flow of ecosystem, ultimately leading to discordance between two dominant components (i.e., soil and plant), as well as in maladjustment of ecosystem multifunctionality in alpine meadow (Wang et al., 2020a). Special standards for grassland restoration emphasize the need for comprehensive evaluations (Gann et al., 2019), yet, plant–soil feedback studies

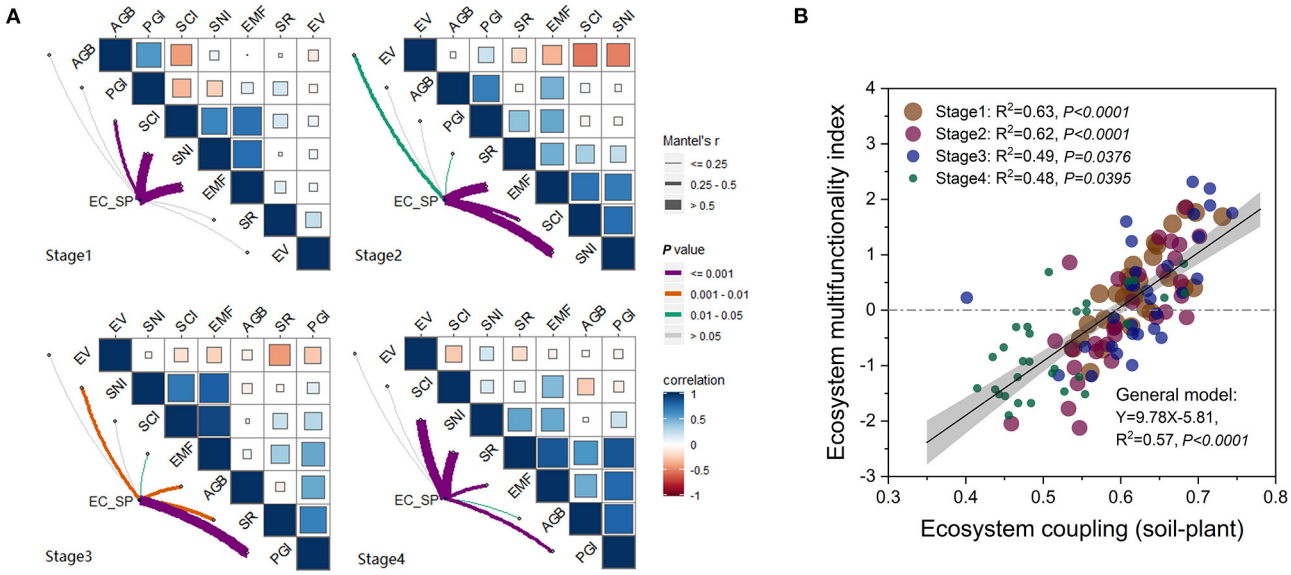

FIGURE 5 | (A,B) Correlations between ecosystem coupling and functionality in each successional stage of alpine meadow. AGB, aboveground biomass; SR, plant species richness; EV, Camargo evenness index; PGI, plant growth index; SCI, soil carbon accumulation index; SNI, soil nutrient index; EMF, ecosystem multifunctionality index; EC_SP, extent of ecosystem coupling (soil-plant).

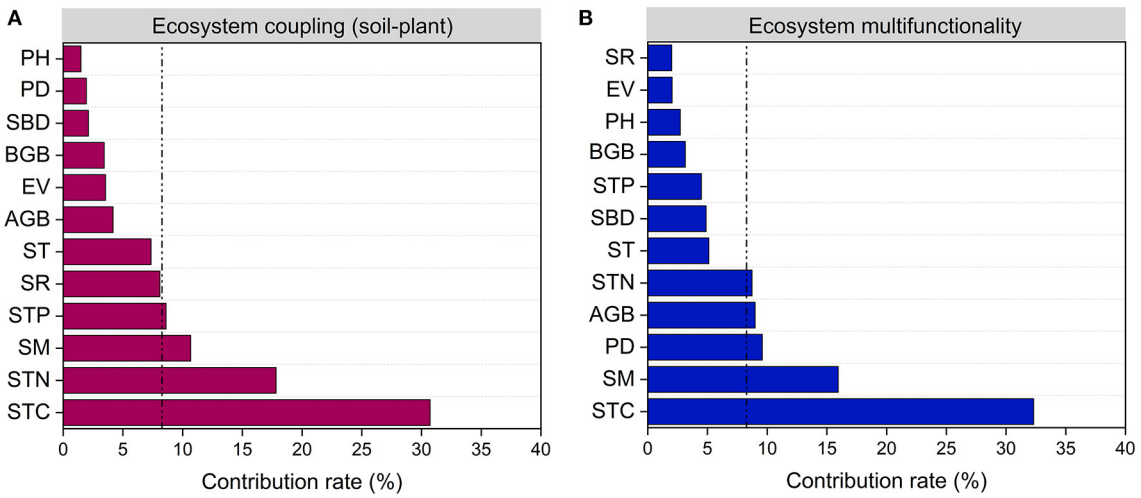

FIGURE 6 | Relative importance of environmental and biological factors explaining ecosystem coupling **(A)** and ecosystem multifunctionality **(B)**. AGB, aboveground biomass; SR, plant species richness; EV, Camargo evenness index; BGB, belowground biomass; PD, plant density; PH, plant height; SBD, soil bulk density; SM, soil moisture; ST, soil temperature; STC, soil total carbon; STN, soil total nitrogen; STP, soil total phosphorus.

in grassland degradation succession remains controversial and how successions stages shape ecosystem multifunction is still unclear. In consequence, using comprehensive indicators such as the extent of ecosystem coupling, ecosystem multifunctionality, and their relationships should provide a broader understanding and sight of the succession process and mechanism induced by grazing.

The difference in EC_SP, EMF and their relationships may reflect the differences in comprehensive changes of plant succession (**Figure 5**; **Supplementary Figure S2**). In this study, the values of EC_SP and EMF in Stage 4 were the lowest compared to other three stages (**Figure 4**). This most likely occurred because EC_SP and EMF were driven by different indicators at different stages (Cortois et al., 2016). In the Stage 1 and 2, soil factors (i.e., STC, STN, and SM) played dominant roles in influencing EC_SP and EMF. Meanwhile, both plant (PD and PH) and soil factors (STC, STN, SM, and SBD) determined the performance of EC_SP and EMF. in the Stage 4 (**Supplementary Figure S2**). The site of Stage 3 was associated with the highest values for the SCI and SNI, which may help

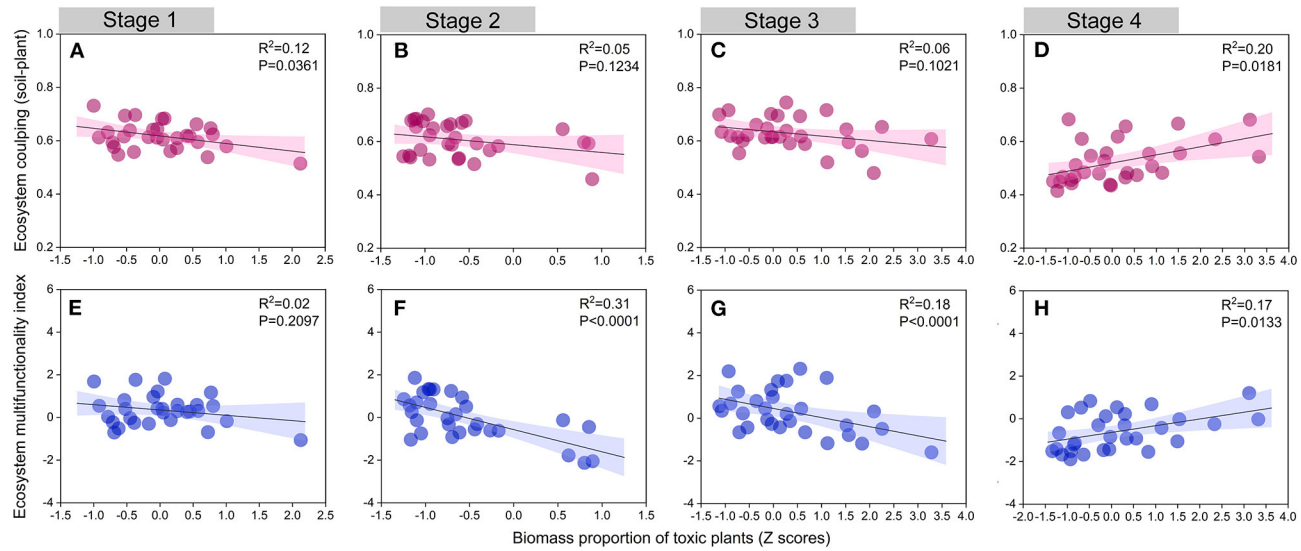

FIGURE 7 | Relationships between ecosystem coupling (soil-plant), ecosystem multifunctionality index, and biomass proportion of toxic weeds (Z scores) in different succession stages. Stage 1, **(A,E)**; Stage 2, **(B,F)**; Stage 3, **(C,G)**; Stage 4, **(D,H)**.

to explain the highest level of EC_SP and EMF (**Figure 5A**). Taken together, high ecosystem coupling may show a higher sensitivity response to STC, STN, SM, and STP (**Figure 6A**). High ecosystem multifunctionality may show a higher sensitivity response to STC, SM, PD, and AGB (**Figure 6B**). Previous studies had used observational data to indicated that ecosystem functions differ in their sensitivity to grazing pressure (Ren et al., 2018) and restoration practices (Wang et al., 2020b). In this case, the lower ecosystem coupling and multifunctionality in Stage 4 induced by grazing may be caused by several mechanisms. First, heavy foraging activity of yak encouraged unpalatable broad-leaved plants (e.g., *Euphorbia esula* and *Gentiana macrophylla*) to invade. Second, overgrazing by yak leads to alpine meadow degeneration which result in rodent infestation and further grassland degeneration. Furthermore, the deeper and nutrient-poor soil was transferred to the ground level and mixed with topsoil through burrowing activity of rodent, which could contribute to the decrease of SOC and STN in the topsoil (Yu et al., 2017). Also, the latest research found that microbes also mediate the shift in ecosystem multifunctionality (Wang et al., 2021). To further illustrate the mechanism, how soil microbe affects ecosystem coupling and ecosystem multifunctionality in each succession stage needs to be further explored. In addition, our results also suggested that coefficients of correlation between ecosystem coupling and the ecosystem multifunctionality in the earlier stages were higher than those in the later stages (**Figure 5B**).

Toxic plants can exhibit self-protective mechanisms in degraded grasslands and promote positive feedback between plants and soil (Zhang et al., 2020). For instance, toxic plants with well-developed root systems can stabilize sand and extract nutrients from the coarser soil (Estapé et al., 2013; Li et al., 2014). Our study also emphasized the critical role of toxic plants during the late stage of succession (Stage 4). We found that both ecosystem coupling and ecosystem multifunctionality showed a significant increase with an increase in the biomass proportion of toxic plants in Stage 4 (**Figure 7**). In the case of this alpine meadow, we suggest that the expansion of toxic plants is a consequence of their greater suitability form a successional perspective. We thus conclude that the heavily degraded region of this alpine meadow needs toxic plant species, and these species are vital for ecological restoration, as well as for maintaining ecosystem function and coupling.

CONCLUSION

Our study quantified the plant succession sequence of alpine meadow induced by grazing with plant functional group approach. The plant succession sequence is from the tall sedge community with erect growth to the short undesirable toxic forbs community with prostrate growth. Ecosystem coupling, ecosystem multifunctionality and their relationships were all the lowest in Stage 4. Our results indicated that the driving factors of ecosystem coupling and ecosystem multifunctionality were soil properties individual in the early succession to plant-soil simultaneously in the late stage. Our results highlight the importance of toxic weeds during the late stage of degraded succession and suggest that the expansion of toxic plants is a consequence of their greater suitability form a successional perspective.

DATA AVAILABILITY STATEMENT

The original contributions presented in the study are included in the article/**Supplementary Material**, further inquiries can be directed to the corresponding author.

AUTHOR CONTRIBUTIONS

YW, ZW, and FH designed the methodology of this study. YW, ZW, and SC conducted the field work and collected the data. YW, YQ, ZW, and JC analyzed the data. YW, ZJ, QZ, and FH wrote the manuscript. All authors contributed substantially to the revision. All authors contributed to the article and approved the submitted version.

FUNDING

This work was supported by the National Natural Science Foundation of China (32161143028 and U21A20242), the Program of National Science and Technology Assistance (KY202002011), the Program for Innovative Research Team of Ministry of Education (IRT17R50), and Lanzhou City's Scientific Research Funding Subsidy to Lanzhou University.

SUPPLEMENTARY MATERIAL

The Supplementary Material for this article can be found online at: https://www.frontiersin.org/articles/10.3389/fpls.2022.839920/full#supplementary-material

Supplementary Figure S1 | (a,b) The cluster dendrogram of sample plot.

Supplementary Figure S2 | Correlations among variables of plant, soil properties and ecosystem coupling and multifunctionality in each succession stage, respectively. The value in the square represents the value of the correlation coefficient. *, **, and *** show the significant correlations at 0.05, 0.01, and 0.001 levels. SR, plant species richness; EV, Camargo evenness index; PGI, plant growth index; SCI, soil carbon accumulation index; SNI, soil nutrient index; EMF, ecosystem multifunctionality index; EC_SP, extent of ecosystem coupling (soil-plant); AGB, aboveground biomass; BGB, belowground biomass; PD, plant density; PH, plant height; SBD, soil bulk density; SM, soil moisture; ST, soil temperature; STC, soil total carbon; STN, soil total nitrogen; STP, soil total phosphorus.

REFERENCES

Abbas, S., Nichol, J. E., Zhang, J., and Fischer, G. A. (2019). The accumulation of species and recovery of species composition along a 70 year succession in a tropical secondary forest. *Ecol. Indic.* 106, 105524. doi: 10.1016/j.ecolind.2019.105524

Ameztegui, A., and Lluí, C. (2015). Herbivory and seedling establishment in Pyrenean forests: influence of micro- and meso-habitat factors on browsing pressure. *Forest Ecol. Manag.* 342, 103–111. doi: 10.1016/j.foreco.2015.01.021

Asquith, N. M., Wright, S. J., and Clauss, M. J. (1997). Does mammal community composition control recruitment in neotropical forests? evidence from Panama. *Ecology* 78, 941–946. doi: 10.1890/0012-9658(1997)078

Avolio, M. L., Pierre, K., Houseman, G. R., Koerner, S. E., Grman, E., Isbell, F., et al. (2015). A framework for quantifying the magnitude and variability of community responses to global change drivers. *Ecosphere* 6, 280. doi: 10.1890/ES15-00317.1

Baeten, L., Hermy, M., Daele, S. V., and Verheyen, K. (2010). Unexpected understorey community development after 30 years in ancient and post-agricultural forests. *J. Ecol.* 98, 1447–1453. doi: 10.1111/j.1365-2745.2010.01711.x

Bagchi, S., Briske, D. D., Bestelmeyer, B. T., and Wu, X. B. (2013). Assessing resilience and state-transition models with historical records of cheatgrass *Bromus tectorum* invasion in North American sagebrush-steppe *J. Appl. Ecol.* 50, 1131–1141. doi: 10.1111/1365-2664.12128

Barnes, A. D., Jochum, M., Lefcheck, J. S., Eisenhauer, N., Scherber, C., O'Connor, M. I., et al. (2018). Energy flux: the link between multitrophic biodiversity and ecosystem functioning. *Trends Ecol. Evol.* 33, 186–197. doi: 10.1016/j.tree.2017.12.007

Barton, K. E., and Hanley, M. E. (2013). Seedling-herbivore interactions: Insights into plant defence and regeneration patterns. *Ann. Bot.* 4, 643–650. doi: 10.1093/aob/mct139

Bermejo, L. A., Nascimento, L. D., Mata, J., Fernández-Lugo, S., Camacho, A., and Arévalo, J. R. (2012). Responses of plant functional groups in grazed and abandoned areas of a natural protected area. *Basic Appl. Ecol.* 13, 312–318. doi: 10.1016/j.baae.2012.05.004

Bestelmeyer, B. T., Khalil, N. I., and Peters, D. (2010). Does shrub invasion indirectly limit grass establishment via seedling herbivory? a test at grassland-shrubland ecotones. *J. Veg. Sci.* 18, 363–370. doi: 10.1111/j.1654-1103.2007.tb02548.x

Bosc, C., and Pauw, A. (2020). Increasing importance of niche versus neutral processes in the assembly of plant-herbivore networks during succession. *Oecologia* 194, 123–134. doi: 10.1007/s00442-020-04740-7

Camargo, J. A. (1993). Must dominance increase with the number of subordinates species in competitive interactions? *J. Theor. Biol.* 161, 537–542. doi: 10.1006/jtbi.1993.1072

Chinese Soil Taxonomy Research Group (1995). *Chinese Soil Taxonomy*. Beijing: Science Press. p. 58–147.

Cortois, R., Schröder-Georgi, T., Weigelt, A., van der Putten, W. H., and De Deyn, G. B. (2016). Plant-soil feedbacks: role of plant functional group and plant traits. *J. Ecol.* 104, 1608–1617. doi: 10.1111/1365-2745.12643

de Mendiburu, F. (2014). *Agricolae: Statistical Procedures for Agricultural Research. R Package Version*, 1.2–1. Available online at: http://CRAN.R-project.org/package=agricolae (accessed November 11, 2019).

Devaney, J. L., Pullen, J., Cook-Patton, S. C., Burghardt, K. T., and Parker, J. D. (2020). Tree diversity promotes growth of late successional species despite increasing deer damage in a restored forest. *Ecology* 101, e03063. doi: 10.1002/ecy.3063

Dong, Q. M., Zhao, X. Q., Wu, G. L., and Chang, X. F. (2015). Optimization yak grazing stocking rate in an alpine grassland of Qinghai-Tibetan Plateau, China. *Environmen. Earth Sci.* 73, 2497–2503. doi: 10.1007/s12665-014-3597-7

Duan, W. J., Ren, H., Fu, S. L., Guo, Q. F., and Wang, J. (2008). Pathways and determinants of early spontaneous vegetation succession in degraded lowland of South China. *J. Integr. Plant Biol.* 50, 147–156. doi: 10.1111/j.1744-7909.2007.00603.x

Duhamel, M., Wan, J., Bogar, L. M., Segnitz, R. M., Duncritts, N. C., and Peay, K. G. (2019). Plant selection initiates alternative successional trajectories in the soil microbial community after disturbance. *Ecol. Monogr.* 89, e01367. doi: 10.1002/ecm.1367

Estapé, S. E. N., Semmartin, M., and Paruelo, J. M. (2013). Refuge effect of an unpalatable forb on community structure and grass morphology in a temperate grassland. *Plant Ecol.* 214, 363–372. doi: 10.1007/s11258-013-0173-2

Gann, G. D., Mcdonald, T., Walder, B., Aronson, J., and Dixon, K. W. (2019). International principles and standards for the practice of ecological restoration. second edition. *Restor. Ecol.* 27, S1–S46. doi: 10.1111/rec.13035

Gilmour, A. R., Gogel, B. J., Cullis, B. R., Welham, S. J., and Thompson, R. (2015). *ASReml User Guide Release 4.1 Functional Specification*. Hemel Hempstead: VSN International Ltd. Retrieved from: www.vsni.co.uk

Hanley, M. E., and Lamont, B. B. (2001). Herbivory, serotiny and seedling defence in western Australian Proteaceae. *Oecologia* 126, 409–417. doi: 10.1007/s004420000538

He, N. P., Liu, C. C., Piao, S. L., Sack, L., Xu, L., Luo, Y. Q., et al. (2019). Ecosystem traits linking functional traits to macroecology. *Trends Ecol. Evol.* 34, 200–210. doi: 10.1016/j.tree.2018.11.004

Howard, M. M., Kao-Kniffin, J., and André, K. (2020). Shifts in plant–microbe interactions over community succession and their effects on plant

resistance to herbivores. *New Phytol*. 226, 1144–1157. doi: 10.1111/nph.16430

Hu, G., Liu, H. Y., Yin, Y., and Song, Z. L. (2016). The role of Legumes in plant community succession of degraded grasslands in northern China. *Land Degrad Dev*. 27, 366–372. doi: 10.1002/ldr.2382

Huang, H. Y. (2019). *ggcor: Extended Tools for Correlation Analysis and Visualization. R package version: 0.7.6*. Available online at: http://CRAN.R-project.org/package=ggcor (accessed November 9, 2019).

Kahmen, S., and Poschlod, P. (2004). Plant functional trait responses to grassland succession over 25 years. *J. Veg. Sci*. 15, 21–32. doi: 10.1111/j.1654-1103.2004.tb02233.x

Kemp, D. R., and King, W. M. (2001). "Plant competition in pastures-implications for management, in *Competition and Succession in Pastures*, eds P. G. Tow and A. Lazenby (Wallingford: CABI Publishing), 85–102. doi: 10.1079/9780851994413.0085

Lavorel, S., and Garnier, E. (2010). Predicting changes in community composition and ecosystem functioning from plant traits: revisiting the holy grail. *Funct. Ecol*. 16, 545–556. doi: 10.1046/j.1365-2435.2002.00664.x

Leizeaga, A., Hicks, L. C., Manoharan, L., Hawkes, C. V., and Rousk, J. (2020). Drought legacy affects microbial community trait distributions related to moisture along a savanna-grassland precipitation gradient. *J. Ecol.* 109, 3195–3210. doi: 10.1111/1365-2745.13550

Li, S. P., Cadotte, M. W., Meiners, S. J., Hua, Z. S., Jiang, L., and Shu, W. S. (2015). Species colonisation, not competitive exclusion, drives community overdispersion over long-term succession. *Ecol. Lett*. 18, 964–973. doi: 10.1111/ele.12476

Li, S. Y., Sun, J., Zhou, T. C., Zhao, M., l., Cong, N., et al. (2021). Biologic and abiotic factors regulate dissolved organic nitrogen with low and high nutrient concentrations on Tibetan Plateau, respectively. *Front. Env. Sci-Switz*. 249, 702713. doi: 10.3389/fenvs.2021.702713

Li, Y. Y., Dong, S. K., Liu, S. L., Wang, X. X., Wen, L., and Wu, Y. (2014). The interaction between poisonous plants and soil quality in response to grassland degradation in the alpine region of the Qinghai-Tibetan Plateau. *Plant Ecol*. 215, 809–819. doi: 10.1007/s11258-014-0333-z

Liu, M., Zhang, Z., Sun, J., Li, Y., Liu, Y., Berihun, M. L., et al. (2020). Restoration efficiency of short-term grazing exclusion is the highest at the stage shifting from light to moderate degradation at Zoige, Tibetan Plateau. *Ecol. Indic.* 114, 106323. doi: 10.1016/j.ecolind.2020.106323

Lusk, C. H., and Kelly, C. K. (2003). Interspecific variation in seed size and safe sites in a temperate rain forest. *New Phytol*. 158, 535–541. doi: 10.1046/j.1469-8137.2003.00760.x

Ma, Z. W., Wang, Y. X., Gu, Y. C., Bowatte, S., and Hou, F. J. (2020). Effects of litter leachate on plant community characteristics of alpine grassland in Qinghai Tibetan Plateau. *Rangeland Ecol. Manag.* 73, 147–155. doi: 10.1016/j.rama.2019.10.003

Maggi, E., Bertocci, I., Vaselli, S., and Benedetti-Cecchi, L. (2011). Connell and slatyer's models of succession in the biodiversity era. *Ecology* 92, 1399–1406. doi: 10.1890/10-1323.1

Marcora, P. I., Renison, D., País-Bosch, A. I., Cabido, M. R., and Tecco, P. A. (2013). The effect of altitude and grazing on seedling establishment of woody species in central Argentina. *Forest Ecol Manag*. 291, 300–307. doi: 10.1016/j.foreco.2012.11.030

Milchunas, D. G., and Vandever, M. W. (2013). Grazing effects on plant community succession of early- and mid-seral seeded grassland compared to shortgrass steppe. *J. Veg. Sci*. 25, 22–35. doi: 10.1111/jvs.12049

Muscarella, R., Uriarte, María, Aide, T. M., Erickson, D. L., Forero-Montaña, J., John Kress, W., Swenson, N. G., et al. (2016). Functional convergence and phylogenetic divergence during secondary succession of subtropical wet forests in Puerto Rico. *J. Veg. Sci*. 27, 283–294. doi: 10.1111/jvs.12354

Nicolai, N. (2019). Ecological engineers' nests benefit plant recovery following fire in a semiarid grassland, New Mexico, USA. *J. Veg. Sci*. 30, 709–719. doi: 10.1111/jvs.12755

Niu, K. C., He, J. S., and Lechowicz, M. J. (2016). Grazing-induced shifts in community functional composition and soil nutrient availability in Tibetan alpine meadows. *J. Appl. Ecol*. 53, 1554–1564. doi: 10.1111/1365-2664.12727

Paterno, G. B., Siqueira Filho, J. A., Ganade, G., and Pugnaire, F. (2016). Species-specific facilitation, ontogenetic shifts and consequences for plant community succession. *J. Veg. Sci*. 27, 606–615. doi: 10.1111/jvs.12382

Pickett, S. (1989). *Space-for-Time Substitution as an Alternative to Long-Term Studies*. New York, NY: Springer. doi: 10.1007/978-1-4615-7358-6_5

Porensky, L. M., Derner, J. D., Augustine, D. J., and Milchunas, D. G. (2017). Plant community composition after 75 yr of sustained grazing intensity treatments in shortgrass steppe. *Rangeland Ecol. Manag*. 70, 456–464. doi: 10.1016/j.rama.2016.12.001

Prugh, L. R., and Sivy, K. J. (2020). Enemies with benefits: integrating positive and negative interactions among terrestrial carnivores: enemies with benefits. *Ecol. Lett*. 23, 902–918. doi: 10.1111/ele.13489

R Core Team (2021). *R: A Language and Environment for Statistical Computing*. R Foundation for Statistical Computing, Vienna, Austria. Available online at: https://www.R-project.org/

Ren, H. Y., Eviner, V. T., Gui, W. Y., Wilson, G. W. T., Cobb, A. B., Yang, G. W., et al. (2018). Livestock grazing regulates ecosystem multifunctionality in semi-arid grassland. *Funct. Ecol.* 32, 2790–2800. doi: 10.1111/1365-2435.13215

Risch, A. C., Ochoa-Hueso, R., van der Putten, W. H., Bump, J. K., Busse, M. D., Frey, B., et al. (2018). Size-dependent loss of aboveground animals differentially affects grassland ecosystem coupling and functions. *Nat. Commun*. 9, 3684. doi: 10.1038/s41467-018-06105-4

Rodríguez, A., and Jansson, G., Henrik Andrén. (2007). Composition of an avian guild in spatially structured habitats supports a competition–colonization trade-off. *P Roy. B-Biol. Sci*. 274, 1403–1411. doi: 10.1098/rspb.2007.0104

Shi, Y., Hu, T. H., Gao, H. J., Luo, Q. Y., and Yu, Y. W. (2019). The community vegetation composition and stability characteristics of alpine meadow under two grazing modes. *Acta Pratacult. Sinica* 28, 1–10. doi: 10.11686/cyxb2018571

Shi, Z., Lin, Y., Wilcox, K. R., Souza, J.iang, L. F., Jiang, J., Gyo Jung, C., et al. (2018). Successional change in species composition alters climate sensitivity of grassland productivity. *Global Change Biol.* 24, 4993–5003. doi: 10.1111/gcb.14333

Song, X. X., Wang, L., Zhao, X., Liu, C., Chang, Q., Wang, Y., et al. (2017). Sheep grazing and local community diversity interact to control litter decomposition of dominant species in grassland ecosystem. *Soil Biol. Biochem*. 115, 364–370. doi: 10.1016/j.soilbio.2017.09.003

Sun, J., and Wang, H. (2016). Soil nitrogen and carbon determine the trade-off of the above- and below-ground biomass across alpine grasslands, Tibetan Plateau. *Ecol. Indic*. 60, 1070–1076. doi: 10.1016/j.ecolind.2015.08.038

Sun, J., Zhan, T., Liu, M., Zhang, Z., Wang, Y., Liu, S., et al. (2020). Verification of the biomass transfer hypothesis under moderate grazing across the Tibetan Plateau: a meta-analysis. *Plant Soil* 458, 139–150. doi: 10.1007/s11104-019-04380-8

Sun, Y., He, X. Z., Hou, F. J., Wang, Z. F., and Chang, S. H. (2017). Grazing increases litter decomposition rate but decreases nitrogen release rate in an alpine meadow. *Biogeosci*. 15, 4233–4243. doi: 10.5194/bg-15-4233-2018

Tang, C. Q., Zhao, M. H., Li, X. S., Ohsawa, M., and Ou, X. K. (2010). Secondary succession of plant communities in a subtropical mountainous region of SW China. *Ecol. Res*. 25, 149–161. doi: 10.1007/s11284-009-0644-z

Tang, Z. (2015). An integrated approach to evaluating the coupling coordination between tourism and the environment. *Tourism Manage*. 46, 11e19. doi: 10.1016/j.tourman.2014.06.001

Walker, L. R., and del Moral, R. (2009). Lessons from primary succession for restoration of severely damaged habitats. *Appl. Veg. Sci*. 12, 55–67. doi: 10.1111/j.1654-109X.2009.01002.x

Wang, L., Delgado-Baquerizob, M., Wang, DL., Isbell, F., Liu, J., Feng, C., et al. (2019). Diversifying livestock promotes multidiversity and multifunctionality in managed grasslands. *PNAS*. 116, 6187–6192. doi: 10.1073/pnas.1807354116

Wang, L., Wang, D., He, Z. B., Liu, G. F., and Hodgkinson, K. C. (2010). Mechanisms linking plant species richness to foraging of a large herbivore. *J. Appl. Ecol*. 47, 868–875. doi: 10.1111/j.1365-2664.2010.01837.x

Wang, Y., Liu, M., Chen, Y, C., Zeng, T., Lu X. Y., Yang, B., et al. (2021). Plants and microbes mediate the shift in ecosystem multifunctionality from low to high patterns across alpine grasslands on the Tibetan Plateau. *Front. Plant Sci.* 12, 760599. doi: 10.3389/fpls.2021.760599

Wang, Y. X., Sun, Y., Chang, S. H., Wang, Z. F., Fu, H., Zhang, W. G., et al. (2020a). Restoration practices affect alpine meadow ecosystem coupling and functions. *Rangeland Ecol. Manag*. 73, 441–451. doi: 10.1016/j.rama.2020.01.004

Wang, Y. X., Sun, Y., Wang, Z. F., Chang, S. H., and Hou, F. J. (2018). Grazing management options for restoration of alpine grasslands on the Qinghai-Tibet Plateau. *Ecosphere* 9, e02515. doi: 10.1002/ecs2.2515

Wang, Y. X., Zhang, X. L., Sun, Y., Chang, S. H., Wang, Z. F., Li, G., et al. (2020b). Pika burrow and zokor mound density and their relationship with grazing management and sheep production in alpine meadow. *Ecosphere* 11, e03088. doi: 10.1002/ecs2.3088

Wu, J. S., Yang, P. W., Zhang, X. Z., Shen, Z. X., and Yu, C. Q. (2015). Spatial and climatic patterns of the relative abundance of poisonous vs. non-poisonous plants across the Northern Tibetan Plateau. *Environmen Monit Assess*. 187, 491. doi: 10.1007/s10661-015-4707-z

Yu, C., Zhang, J., Pang, X. P., Wang, Q., Zhou, Y. P., and Guo, Z. G. (2017). Soil disturbance and disturbance intensity: response of soil nutrient concentrations of alpine meadow to plateau pika bioturbation in the Qinghai-Tibetan Plateau, China. *Geoderma* 307, 98–106. doi: 10.1016/j.geoderma.2017.07.041

Zhang, H., Qi, W., John, R., Wang, W. B., Song, F. F., and Zhou, S. R. (2015). Using functional trait diversity to evaluate the contribution of multiple ecological processes to community assembly during succession. *Ecography*. 38, 1176–1186. doi: 10.1111/ecog.01123

Zhang, R., and Tielbrger, K. (2019). Facilitation from an intraspecific perspective – stress tolerance determines facilitative effect and response in plants. *New Phytol*. 221, 2203–2212. doi: 10.1111/nph.15528

Zhang, R. Y., Wang, J., and Niu, S. L. (2021). Toward a sustainable grazing management based on biodiversity and ecosystem multifunctionality in drylands. *Curr. Opin. Env. Sust*. 48, 36–43. doi: 10.1016/j.cosust.2020.09.005

Zhang, Z., Liu, Y., Sun, J., and Wu, G. L. (2021). Suitable duration of grazing exclusion for restoration of a degraded alpine meadow on the eastern Qinghai-Tibetan Plateau. *Catena* 207, 105582. doi: 10.1016/j.catena.2021.105582

Zhang, Z. C., Sun, J., Liu, M., Xu, M., Wang, Y., Wu, G. L., et al. (2020). Don't judge toxic weeds on whether they are native but on their ecological effects. *Ecol Evol*. 10, 9014–9025. doi: 10.1002/ece3.6609

Zhao, X., Zhu, H. S., Dong, K. H., and Li, D. Y. (2017). Plant community and succession in lowland grasslands under Saline-Alkali conditions with grazing exclusion. *Agron. J*. 109, 2428–2437. doi: 10.2134/agronj2016.12.0734

Conflict of Interest: The authors declare that the research was conducted in the absence of any commercial or financial relationships that could be construed as a potential conflict of interest.

Publisher's Note: All claims expressed in this article are solely those of the authors and do not necessarily represent those of their affiliated organizations, or those of the publisher, the editors and the reviewers. Any product that may be evaluated in this article, or claim that may be made by its manufacturer, is not guaranteed or endorsed by the publisher.

Copyright © 2022 Wang, Wu, Wang, Chang, Qian, Chu, Jia, Zhou and Hou. This is an open-access article distributed under the terms of the Creative Commons Attribution License (CC BY). The use, distribution or reproduction in other forums is permitted, provided the original author(s) and the copyright owner(s) are credited and that the original publication in this journal is cited, in accordance with accepted academic practice. No use, distribution or reproduction is permitted which does not comply with these terms.

frontiers in Plant Science

ORIGINAL RESEARCH
published: 18 March 2022
doi: 10.3389/fpls.2022.847680

Experimental Warming Has Not Affected the Changes in Soil Organic Carbon During the Growing Season in an Alpine Meadow Ecosystem on the Qinghai–Tibet Plateau

Yue Yang[1†‡], Guoxi Shi[2,3‡], Yongjun Liu[1], Li Ma[3], Zhonghua Zhang[3], Shengjing Jiang[4], Jianbin Pan[1], Qi Zhang[1], Buqing Yao[2], Huakun Zhou[3] and Huyuan Feng[1*†]*

[1]Ministry of Education Key Laboratory of Cell Activities and Stress Adaptations, School of Life Sciences, Lanzhou University, Lanzhou, China, [2]Key Laboratory of Utilization of Agriculture Solid Waste Resources in Gansu Province, College of Bioengineering and Biotechnology, Tianshui Normal University, Tianshui, China, [3]Key Laboratory of Restoration Ecology of Cold Area in Qinghai Province, Northwest Institute of Plateau Biology, Chinese Academy of Sciences, Xining, China, [4]State Key Laboratory of Grassland and Agro-Ecosystems, College of Pastoral Agriculture Science and Technology, Lanzhou University, Lanzhou, China

The effects of climate warming and season on soil organic carbon (SOC) have received widespread attention, but how climate warming affects the seasonal changes of SOC remains unclear. Here, we established a gradient warming experiment to investigate plant attributes and soil physicochemical and microbial properties that were potentially associated with changes in SOC at the beginning (May) and end (August) of the growing season in an alpine meadow ecosystem on the Qinghai–Tibet Plateau. The SOC of August was lower than that of May, and the storage of SOC in August decreased by an average of 18.53 million grams of carbon per hectare. Warming not only failed to alter the content of SOC regardless of the season but also did not affect the change in SOC during the growing season. Among all the variables measured, microbial biomass carbon was highly coupled to the change in SOC. These findings indicate that alpine meadow soil is a source of carbon during the growing season, but climate warming has no significant impact on it. This study highlights that in the regulation of carbon source or pool in alpine meadow ecosystem, more attention should be paid to changes in SOC during the growing season, rather than climate warming.

Keywords: climate warming, seasonal differences, dynamic of soil organic carbon, soil microbiota, the growing season

OPEN ACCESS

Edited by:
Ming Dong,
Hangzhou Normal University, China

Reviewed by:
Huajun Yin,
Chengdu Institute of Biology (CAS), China
Xuehua Ye,
Institute of Botany (CAS), China

***Correspondence:**
Huakun Zhou
hkzhou@nwipb.cas.cn
Huyuan Feng
fenghy@lzu.edu.cn

***ORCID:**
Yue Yang
orcid.org/0000-0001-7120-1959
Huyuan Feng
orcid.org/0000-0001-5704-3384

These authors have contributed equally to this work

Specialty section:
This article was submitted to Functional Plant Ecology, a section of the journal Frontiers in Plant Science

Received: *03 January 2022*
Accepted: *23 February 2022*
Published: *18 March 2022*

Citation:
Yang Y, Shi G, Liu Y, Ma L, Zhang Z, Jiang S, Pan J, Zhang Q, Yao B, Zhou H and Feng H (2022) Experimental Warming Has Not Affected the Changes in Soil Organic Carbon During the Growing Season in an Alpine Meadow Ecosystem on the Qinghai–Tibet Plateau. Front. Plant Sci. 13:847680. doi: 10.3389/fpls.2022.847680

INTRODUCTION

Since the 1850s, the global surface temperature has increased by approximately 1.09°C (IPCC, 2021). Climate warming is one of the detrimental aspects of climate change (Lippmann et al., 2019), and it has a strong impact on ecosystem processes (Singh et al., 2010; Scheffers et al., 2016). Numerous studies have focused on the effects of climate warming on the aboveground

ecosystem (Klein et al., 2004; Post and Pedersen, 2008; Elmendorf et al., 2012; Zhang et al., 2017). However, compared with the key role of belowground part of an ecosystem in the regulation of material and energy flows between the aboveground and belowground parts of an ecosystem (Peng et al., 2021; Zhang et al., 2021), research on the impacts of climate warming on the belowground part of an ecosystem is still lacking. This greatly limits the accuracy of predictions of the ecological consequences of climate warming.

As the largest repository of organic carbon in the world, the soil stores approximately 2 trillion tons of carbon (Hutchins et al., 2019). This is approximately twice the carbon storage of the atmosphere and three times that of terrestrial plants (Lal, 2004; Schmidt et al., 2011). The annual carbon flux out of the soil is as high as 6–8 billion tons, which is 6- to 8-fold higher than the carbon emissions produced by human activities (Schlesinger and Andrews, 2000; Bond-Lamberty and Thomson, 2010). Thus, any slight change in the soil carbon pool can lead to an increase in the concentration of carbon dioxide in the atmosphere, which will further accelerate climate warming *via* positive feedback (García-Palacios et al., 2021; Zhu et al., 2021). In view of the important regulatory role of the soil carbon pool in the global carbon cycle, numerous evidence has shown that experimental warming has demonstrated negative (Feng et al., 2017; Wang et al., 2019), neutral (Zhang et al., 2016; Jia et al., 2017; Guan et al., 2018; Ding et al., 2019; Wang et al., 2019; Tian et al., 2021), and positive effects on the content of soil organic carbon (SOC; Xu et al., 2015; Zheng et al., 2020; Tian et al., 2021). Such controversy indicates that the responses of the content of SOC to warming are complex and merit further investigation (Zhang et al., 2020; Craig et al., 2021).

Although the responses of content of SOC to warming have been widely documented, the mechanisms of how elevated temperatures impact SOC remain unclear. The soil carbon cycle model is included in the Earth System Models, which will be used to predict the turnover of SOC (Campbell and Paustian, 2015; Zhang et al., 2020; Fan et al., 2021). In one aspect of this model, warming will affect plant growth by changing the availability of soil nutrients, thereby affecting the input of plants to the SOC pool; alternatively, the temperature increase caused by the warming treatment will accelerate the loss of SOC by changing the metabolism of soil microorganisms (Luo et al., 2001; Luo, 2007; Conant et al., 2011; Campbell and Paustian, 2015). These potential pathways indicate that the effect of elevated temperatures on the content of SOC can approximately be classified into direct, that is, they affect soil microbial metabolism, or indirect, that is, they change the plant biomass or soil properties. Therefore, there is still an urgent need for a more systematic study to determine the potential impact of classified temperature on SOC and its underlying mechanism.

The Qinghai–Tibet Plateau, with an average altitude that exceeds 4,000 m, is known as "the roof of the world" and has experienced striking warming at the rate of 0.4°C per decade over the past 50 years, which is double that of the global mean (Gao et al., 2014; Fu et al., 2021). The dominant ecosystem of the region is composed of alpine meadows (Wang et al., 2014). The combination of alpine meadows and alpine steppes contributes 2.32 billion tons of carbon (69.3%) to the soil total organic carbon stock on the Qinghai–Tibetan Plateau, and alpine meadows had the highest content of carbon in this region (Wang et al., 2002; Guan et al., 2018). Since the SOC in high-altitude regions is extremely sensitive to climate warming (García-Palacios et al., 2021), alpine meadows are ideal places to study the response of terrestrial ecosystems to climate warming (Zhang et al., 2016). Currently, a large number of studies have been conducted to examine the impact of climate warming (Xu et al., 2015; Jia et al., 2017; Ding et al., 2019; Chen et al., 2020) or seasons (Luo and Weng, 2011) on the content of SOC. Nevertheless, to our knowledge, few studies have focused on changes in the content of SOC between the beginning and the end of the growing season along a temperature gradient in an alpine meadow ecosystem. This substantially limits our understanding of the driving mechanism of changes in SOC during the growth season under the warming scenario because both plant and soil microbial communities in alpine meadow ecosystems are highly vital during the growing season, and the effects of warming on SOC are always coupled with seasonal changes. Therefore, to explore the impact of climate warming on the changes of organic carbon during the growing season, we conducted an 8-year warming gradient experiment with open-top chambers (OTCs) to reveal the impact of experimental warming on the differences of SOC between the beginning (May) and end (August) of the growing season. Previous studies have confirmed that warming can facilitate plant growth and increase soil microbial activity and soil respiration (Conant et al., 2011; Luo and Weng, 2011). Thus, we hypothesized that warming could facilitate the loss of SOC regardless of the season (H1). In addition, since the end of the growing season has a higher soil temperature than the beginning of the growing season in alpine meadow ecosystems, we also predicted that the content of SOC at the end of the growing season would be lower than that at the beginning of the growing season (H2). Moreover, warming can reduce the differences in soil temperature between the beginning and end of the growing season by prolonging the growing season (Luo and Weng, 2011). We also hypothesized that as the temperature increased, the seasonal difference of SOC would gradually decrease (H3).

MATERIALS AND METHODS

Field Site Description and Experimental Setup

This study was conducted at the Haibei Research Station of the Chinese Academy of Sciences (37°29′N, 101°12′E; 3,220 ma.s.l.), China. This region has a typical continental semi-humid plateau climate with long cold dry winters and short warm wet summers. The average annual temperature is −1.7°C and ranges from −15.2°C in January to 9.9°C in July. The average annual precipitation is 561 mm, and more than 80% of the annual precipitation is concentrated during the growing season. The growing season in this region is from May to August. The vegetation of this region

is dominated by graminoids and forbs, such as *Kobresia humilis* Sergiev., *Stipa aliena* Keng., *Elymus nutans* Griseb., *Poa pratensis* L., *Oxytropis ochrocephala* Bunge., *Medicago ruthenica* (L.) Trautv., and *Gentiana straminea* Maxim.

The field experiment was established in July 2011 in a fenced $50 \times 50\,m^2$ flat area that was previously used as a winter pasture to examine how the alpine meadow ecosystem responds to gradient warming. Twenty-five plots composed of five temperature treatments (ambient temperature and four warming treatments) with five repetitions were distributed into subplots divided into five rows and five columns based on a random block design (**Supplementary Figure S1A**). These four warming treatments were achieved with open-top chambers that were designed as four types of sample rounds from large to small, corresponding to the magnitude of warming from weak to strong (**Supplementary Figure S1A**). These OTCs were constructed with 1 mm thick fiberglass and were 40 cm high. The diameters of the bottom/top of the chambers were 2.05 m/1.60 m for W1, 1.75 m/1.30 m for W2, 1.45 m/1.00 m for W3, and 1.15 m/0.70 m for W4. During the experiment, all the open-top chambers were maintained at the plots throughout the year (**Supplementary Figure S1**). Decagon ECT sensors (Decagon Devices, Pullman, WA, United States) were used to record the daily air temperature at 20 cm high and 10 cm aboveground and soil temperature at a depth of 15 cm belowground. After monitoring, these four types of OTC treatments (W1–W4) successfully produced increased soil temperature gradients. The mean increase in soil temperature at the beginning of growing season (May) was 0.73°C, 1.60°C, 1.73°C, and 2.25°C in W1 to W4, respectively, while the mean increase in soil temperature at the end of growing season (August) was 0.52°C, 0.97°C, 1.49°C, and 1.57°C, respectively (**Supplementary Table S1**). Compared with the beginning of the growing season (May), the soil temperature at the end of the growing season (August) increased by 5.82°C (W0), 5.61°C (W1), 5.19°C (W2), 5.58°C (W3) and 5.14°C (W4; **Supplementary Table S1**).

Soil Sampling and the Plant Community Survey

Soil samples were collected at the beginning (on May 3) and end of the growing season (August 28) in 2019, respectively. Three soil cores (5.0 cm in diameter and 25 cm deep) were randomly collected in each plot and homogenized into one composite sample (2 seasons × 5 treatments × 5 repetitions = 50 soil samples). Each soil composite sample was then divided into two subsamples. One was used to extract DNA, and the other was used to determine the soil physicochemical and microbial properties. All the soil samples were stored at 4°C during the sampling process (within 48 h) and were transferred into −20°C storage once they had been transported to the laboratory. The plant community survey was only performed at the end of growing season because it was difficult to identify plant species when the plant community had just turned green at the beginning of growing season. The plant community in each plot was surveyed using a $50 \times 50\,cm^2$ sample quadrat. All the shoots in each quadrat were cut at the ground surface and grouped by plant species. The shoots of each species were then weighed after drying at 80°C for 48 h, and aboveground biomass of plant community was calculated as sum of shoot biomass of each species.

Analysis of Soil Properties

The soil moisture was measured gravimetrically after drying at 105°C for 12 h. The soil pH was measured with a pH electrode (Sartorius PB-10; Sartorius AG, Göttingen, Germany). SOC, dissolved organic carbon (DOC), and nitrogen were measured using an Elementar analysis system (CHNS; Elementar Analysensysteme GmbH, Langenselbold, Germany; Cabrera and Beare, 1993; Jones and Willett, 2006; Makarov et al., 2013). Both soil available nitrogen (as ammonia and nitrate) and available phosphorus were measured using FIAstar analyzer 5,000 (FOSS, Hillerød, Denmark). The rate of soil respiration for each warming treatment was measured 10 days per month with an LI-8100A Automated Soil CO_2 Flux System (LICOR, Inc., Lincoln, NE, United States) throughout the growing season (from May to August; Ren et al., 2021). SOC storage was calculated based on the SOC, bulk density, and soil sampling depth (Emde et al., 2021). Both microbial biomass carbon (MBC) and microbial biomass nitrogen (MBN) were measured using the chloroform fumigation direct extraction method (Brookes et al., 1985; Vance et al., 1987). The activities of four soil extracellular enzymes that decompose SOC, including the labile carbon decomposing enzymes amylase and sucrase and the recalcitrant carbon decomposing enzymes cellulase and peroxidase, were assayed as described by Xun et al. (2018), Yin et al. (2014), and Jiang et al. (2021).

Soil DNA Extraction, Real-Time Quantitative PCR, and Amplicon Sequencing

Total DNA was extracted from 0.5 g of each soil sample using an E.Z.N.A.® Soil DNA Kit (Omega Bio-tek, Norcross, GA, United States) following the manufacturer's instructions. The primer pair combination of ITS1F (5'-CTTGGTCATTTAGA GGAAGTAA-3')-ITS2R (5'-GCTGCGTTCTTCATCGATGC-3') was then used to determine the number of gene copies of fungal DNA (ITS), while the primer pair combination of 338F (5'-ACTCCTACGGGAGGCAGCAG-3')-806R (5'-GGACTACH VGGGTWTCTAAT-3') were used to determine the number of gene copies of bacteria (16S rRNA) using a QuantStudio™ 6 Flex Real-Time PCR System (Applied Biosystems, Waltham, MA, United States; Majorbio Bio-Pharm Technology Co., Ltd., Shanghai, China). The target fragment of the primer combination ITS1F-ITS2R was ~300 bp that targeted the ITS1 region (White et al., 1900), while the target fragment of the primer combination 338F-806R was ~468 bp in the V3-V4 region (Mori et al., 2014). The primers used for high-throughput sequencing of fungi (ITS) and bacteria (16S rRNA) were the same as the primers for qPCR. The amplification with primer pair ITS1F-ITS2R was conducted in a 20 µl reaction that consisted of 10 ng for the total DNA template, 0.8 µl of each primer (5 µM), 2 µl 10 × TransStart FastPfu buffer, 2 µl dNTPs (2.5 mM), and 0.2 µl TaKaRa rTaq DNA Polymerase. The thermal cycling conditions were as follows: 95°C for 3 min, 27 cycles of 95°C for 30 s, 55°C for 30 s 72°C for 45 s, and 72°C

for 10 min. The amplification with primer pair 338F-806R was similar to those of the ITS1F-ITS2R amplifications with the exception of the use of 0.4 μl TransStart FastPfu DNA Polymerase. The PCR reactions were performed in triplicate. The sizes of both fungal and bacterial amplicons were confirmed separately using 2% agarose gel electrophoresis, purified using an AxyPrep DNA Gel Extraction Kit (Axygen Biosciences, Union City, CA, United States), and quantified using a Quantus™ Fluorometer (Promega, Madison, WI, United States). Purified amplicons were pooled in equimolar amounts and paired-end sequenced on an Illumina MiSeq PE300 platform (Illumina, San Diego, CA, United States) by Majorbio Bio-Pharm Technology Co., Ltd. (Shanghai, China) using a NEXTFLEX® Rapid DNA-Seq Kit (Bioo Scientific Corporation, Austin, TX, United States) for library construction. All the raw sequencing reads were quality-filtered by FASTP (ver. 0.20.0; Chen et al., 2018) and merged by FLASH (ver. 1.2.7; Magoc and Salzberg, 2011). Operational taxonomic units (OTUs) with a 97% similarity cutoff (Stackebrandt and Goebel, 1994; Edgar, 2013) were clustered using UPARSE (ver. 7.1; Edgar, 2013). The taxonomy of each representative OTU sequence was analyzed using RDP Classifier (ver. 2.2; Wang et al., 2007) against the ITS database (UNITE ver. 7,[1] for fungal OTUs) and the 16S rRNA database (Silva ver. 138,[2] for bacterial OTUs) using a confidence threshold of 0.7. The sequence raw datasets in this study were deposited in the NCBI Sequence Read Archive (SRA) with accession numbers: PRJNA719774 (ITS-BioProject) and PRJNA719776 (16S rRNA-BioProject).

Statistical Analyses

The statistical analyses were primarily conducted using R 4.0.5.[3] A linear mixed-effects (LME) model ("lme" model) was applied to analyze the individual effects of warming and season on soil, plant, and microbial variables using the "nlme" and "nlme" functions in R (Pinheiro et al., 2019), in which both warming and season were treated as fixed effects and block as a random effect. Significant differences between treatments were tested using the *post-hoc* multiple comparisons Tukey method at a 95% significance level ($p \leq 0.05$). A rarefaction curve of microbial species richness was estimated using the "rarecurve" function of the "vegan" package in R (Oksanen et al., 2019). A taxonomy Circlize of microbial community composition at the phylum level was summarized using the "tax_circlize" function of the "amplicon" package in R.[4] Dissimilarities of the plant or microbial community were depicted with principal coordinate analysis (PCoA) ordination based on the Bray–Curtis dissimilarity index using the "cmdscale" function of the "stats" package in R (Oksanen et al., 2007). A permutational multivariate analysis of variance (PERMANOVA) was used to determine the effects of warming or season on both plant and microbial communities using the "adonis" function of the "vegan" package in R (Oksanen et al., 2019). Linear discriminant analysis (LDA) effect size (LEfSe ver. 1.0)[5] was performed to assess significant differences of the fungal and bacterial taxa from Kingdom; Domain, not Kingdom, was used as the basic classification level for bacteria to genus levels (Segata et al., 2011).

The natural logarithm ratio was used to interpret the rate of change of all the variables measured during the growing season. For example, the rate of change of SOC during the growing season was calculated as $\Delta SOC_{content}(\%) = \left(e^{\ln\left(\frac{SOC_{Aug}}{SOC_{May}}\right)} - 1 \right) \times 100$, where SOC_{Aug} and SOC_{May} represent the content of SOC in August and May, respectively (Emde et al., 2021). Considering that the score values of the PCoA axis of the plant or microbial communities cannot be characterized by the natural logarithm owing to a negative value, we applied the ratio of γ-diversity to α-diversity to characterize the rate of change of the composition of plant or microbial community during the growing season using the "diversity" function of the "vegan" package in R (Oksanen et al., 2019).

Linear regression analysis was performed to assess the relationships between the content of SOC or the rates of change of SOC with all plant, soil, and microbial variables using the linear mixed-effects regression with block as a random effect. A random forest test was performed to predict response variables that are significantly related to the content of SOC (or the rate of change of SOC) using the "rfPermute" function of the "rfPermute" package in R (Archer, 2013). A structural equation model (SEM) was also constructed using SPSS AMOS 21.0 (IBM, Inc., Armonk, NY, United States).

RESULTS

Soil Properties and Plant Community

Warming had no significant effect on all the soil variables measured, but the season had significant effects on other soil physical and chemical properties except for soil ammonium nitrogen and nitrate nitrogen (**Figure 1**). The soil moisture and available phosphorus in May were lower than those in August, while the contents of SOC, DOC, dissolved organic nitrogen, and soil carbon storage in May were higher than those in August (**Figure 1**). Moreover, warming significantly reduced the aboveground biomass and species richness of the plant communities but did not affect the species composition of these communities (**Supplementary Figure S2**).

Soil Microbial Biomass, Soil Respiration Rate, and Soil Extracellular Enzyme Activity

Except for W1, both the MBC and MBN of May were higher than those of August (**Figures 2A,B**). There was no significant difference in the ratio of MBC/MBN and MBC/SOC among the treatments (**Figures 2C,D**). The rates of soil respiration in

[1]https://unite.ut.ee/
[2]http://www.arb-silva.de
[3]http://www.r-project.org/
[4]https://github.com/microbiota/amplicon
[5]http://huttenhower.sph.harvard.edu/galaxy/

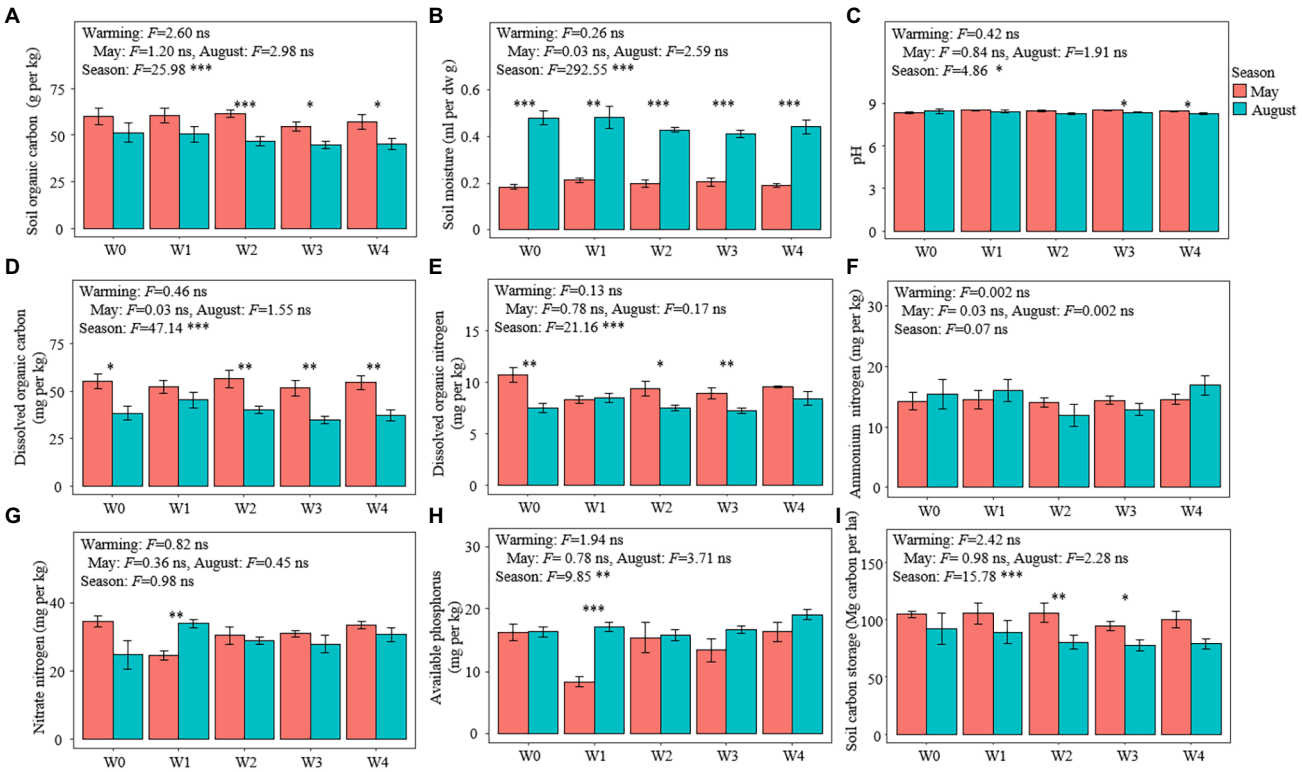

FIGURE 1 | Soil characteristics in the different treatments. **(A)** Soil organic carbon content, **(B)** soil moisture, **(C)** pH, **(D)** dissolved organic carbon content, **(E)** dissolved organic nitrogen content, **(F)** ammonium nitrogen content, **(G)** nitrate nitrogen content, **(H)** available phosphorus content, and **(I)** soil carbon storage. Bars represent the means ± SE ($n = 5$). Significant differences among the treatments were tested using Tukey's honest significant difference test ($p \leq 0.05$). The F-values and significance shown correspond to the linear mixed-effects model. *$p < 0.05$, **$p < 0.01$, ***$p < 0.001$. SE, standard error.

May were lower than those in August under all the warming treatments (**Figure 2E**). The activity of amylase in May was lower than that in August, and the activity of sucrase in May was higher than that in August under the W0 treatment (**Figures 2F,G**). The activity of cellulase in both W0 and W3 in May was lower than that in August, while there were no significant differences in the activity of peroxidase between May and August under all the warming treatments (**Figures 2H,I**).

Microbial Community Diversity

Warming had no significant effect on the fungal (ITS) gene copy number (**Figure 2J**), bacterial gene copy number (**Figure 2K**), and the ratio of fungal/bacterial gene copy number (**Figure 2L**), while seasons significantly affected the gene copy number of fungi (**Figure 2J**). The gene copy number of fungi in May under all the warming treatments (except for W4) was higher than that in August (**Figure 2J**). Rarefaction curves showed that the high-throughput sequencing effectively identified the species richness of both fungal and bacterial communities (**Supplementary Figure S3**). A total of 307 genera of 36 classes of fungi were detected in 13 phyla, and 407 genera of 81 classes of bacteria were detected in 36 phyla (**Supplementary Table S2**). Ascomycetes were the dominant fungal taxon, comprising 65.27% of the total number of reads, while Proteobacteria was the dominant taxon of bacteria, comprising 30.90% of the total number of bacterial reads (**Supplementary Figure S4**).

Warming had no significant effect on the species richness of fungal and bacterial communities (**Figures 3A,B**). The season had a significant effect on the richness of fungal species but had no significant effect on the richness of bacterial species (**Figures 3A,B**). The richness of fungal species was higher in May than that in August (except for W4) under all the warming treatments, while the richness of bacterial species in May was significantly lower than that in August under the W0 treatment (**Figures 3A,B**). In addition, warming had no significant effect on the taxonomic composition of fungal and bacterial communities, while season had a significant effect on them (**Figures 3C,D**). The relative abundances of 21 fungal OTUs and 310 bacterial OTUs were higher in May than in August, while the relative abundances of only four bacterial OTUs were lower in May than in August (**Supplementary Figure S5**).

Relationships of Plant Attributes, Soil Properties, and Microbial Properties With the Content of SOC

Soil organic carbon positively correlated with the DOC, MBC, MBN, and sucrase activity but negatively correlated with the

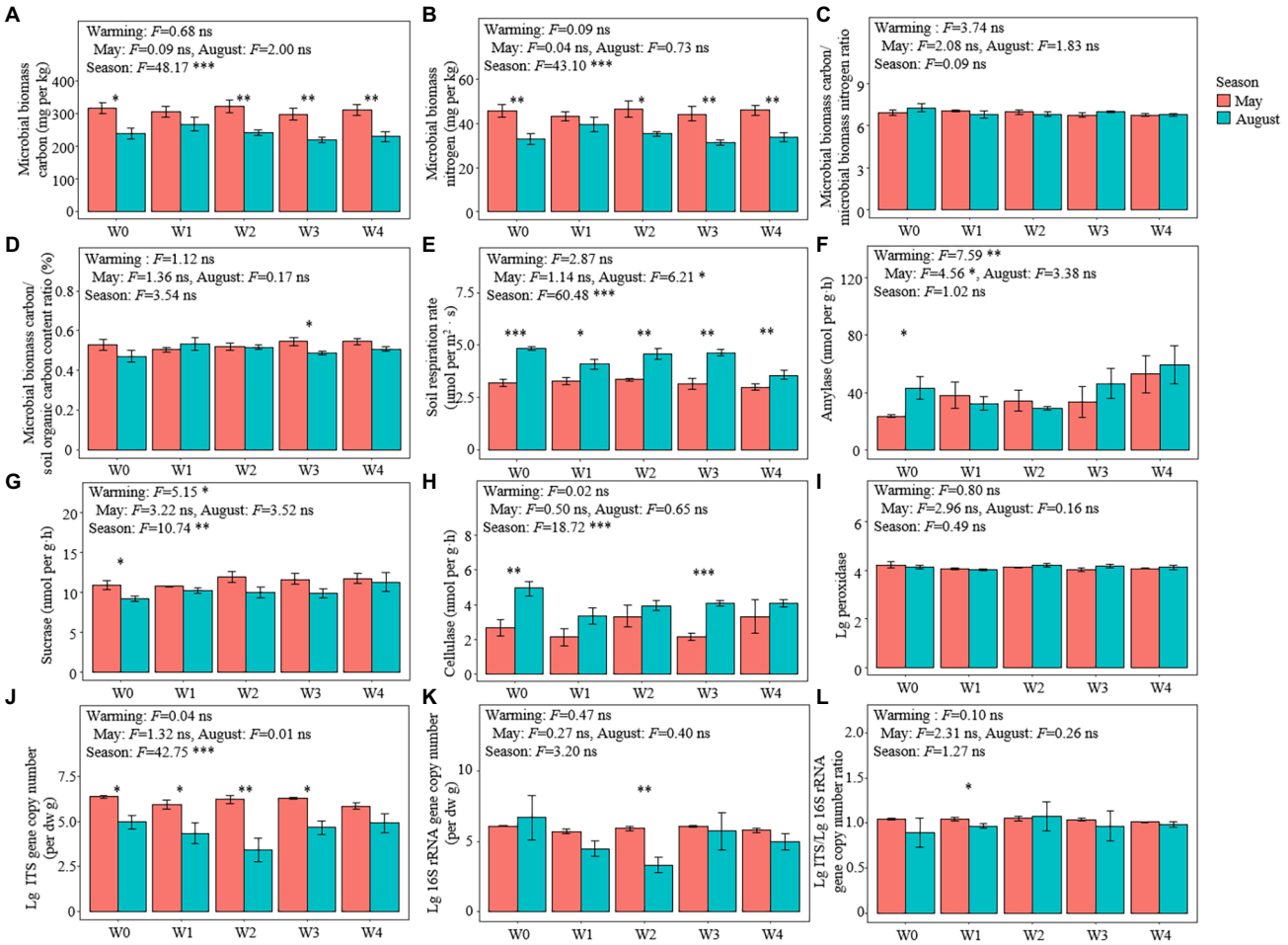

FIGURE 2 | Microbial properties in the different treatments. **(A)** microbial biomass carbon (MBC) content, **(B)** microbial biomass nitrogen (MBN) content, **(C)** MBC/MBN ratio, **(D)** MBC/SOC ratio (%), **(E)** soil respiration rate, **(F)** amylase activities, **(G)** sucrase activities, **(H)** cellulase activities, **(I)** lg_{10} transformed peroxidase activities (lg peroxidase), gene copy numbers of **(J)** eukaryotic (lg ITS) and **(K)** bacteria (lg 16S rRNA), and **(L)** lg ITS/lg 16S rRNA ratio. Bars represent the means ± SE ($n = 5$). Significant differences among the treatments were tested using Tukey's honest significant difference test ($p \leq 0.05$). The *F*-values and significance shown correspond to the linear mixed-effects model. *$p < 0.05$, **$p < 0.01$, ***$p < 0.001$. SE, standard error.

soil temperature, aboveground biomass, rate of soil respiration, and cellulase activity (**Table 1**). The random forest analysis confirmed that MBC, DOC, MBC/MBN, and microbial biomass nitrogen were response variables that highly correlated with changes in the SOC (**Figure 4A**). The structural equation models also showed that the season, but not warming, mediated changes in the SOC through MBC (**Figure 5A**).

Relationships of the Change in Plant Attributes and Soil and Microbial Properties With the Change in Content of SOC During the Growing Season

The rate of change of soil and microbial properties were not significantly different among the warming treatments (**Supplementary Figure S6**). The rates of change of the SOC were positively related to the rates of seasonal change of DOC, MBC, and MBC/MBN (**Table 2**). Although warming had no significant effect on the rates of change of SOC, the SOC decreased significantly during the growing season only under the warming treatments (W2, W3, and W4; **Supplementary Figure S6**). The random forest analysis also confirmed that the rates of change of MBC, MBC/MBN, and DOC were variables that were associated with the change of SOC during the growing season (**Figure 4B**). The structural equation model that was conducted to measure the causal effect of warming on the change of SOC had also shown that warming failed to alter the change of SOC by the seasonal changes in soil temperature, but the change of MBC had a significant effect on it (**Figure 5B**).

DISCUSSION

Season, Rather Than Warming, Dominates the Change of SOC

Regardless of season, warming had no significant effect on the SOC (**Figure 1A**). This result does not support hypothesis

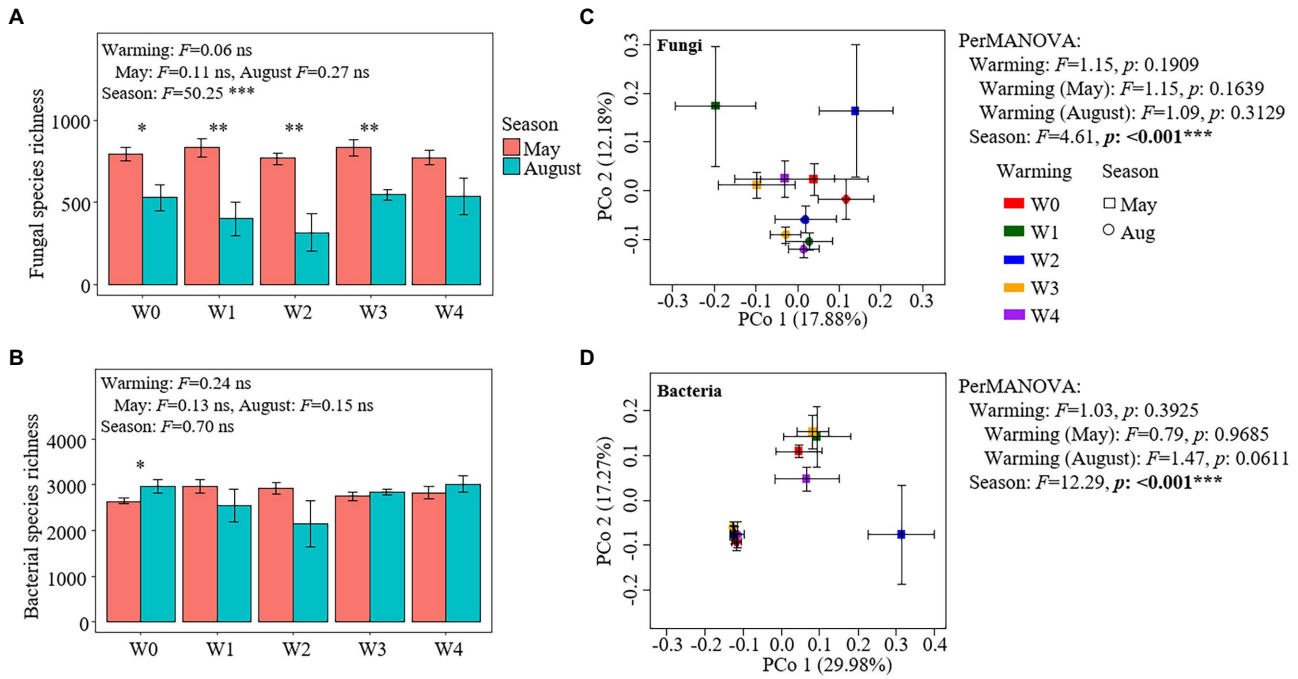

FIGURE 3 | Species richness and the results of principal coordinate analysis (PCoA) and permutational multivariate analysis of variance of fungal **(A,C)** and bacterial communities **(B,D)**.

I (H1) and is consistent with the findings of other studies (Yue et al., 2015; Zhang et al., 2016; Jia et al., 2017; Guan et al., 2018; Jia et al., 2019; Wang et al., 2019; Chen et al., 2021) that indicated that warming did not dominate the change of SOC. Unlike the warming treatments, the content of SOC in August was significantly lower than that in May (**Figure 1A**), and the storage of SOC of August decreased by an average of 18.53 million grams of carbon per hectare (**Figure 1I**), indicating that alpine meadow soil is a carbon source rather than a carbon pool during the growing season. This result supports hypothesis 2 (H2) and is similar to that of another study in a grassland ecosystem (Yang et al., 2021), suggesting that the season, rather than warming, dominated the change in SOC (Gavazov et al., 2017). Since a study has confirmed that the soil carbon flow is higher than that in the non-growing season, we hypothesize that there is an "interannual cycle" process. In the "interannual cycle" process, the content of SOC changes from a "loss state" of the growing season to an "increase state" of the non-growing season and finally returns to the original level at the beginning of the growing season in the following year. In this study, warming reduced the aboveground biomass of plants, which in turn reduced the return of plant litter to the soil during the non-growing season. Therefore, warming did not cause the loss of SOC under the current experimental conditions, but it was expected that the alpine meadow SOC could be lost in future long-term climate warming.

Temperature is a key limiting factor for high-altitude ecosystems (Duan et al., 2019). In this study, the negative correlation between the soil temperature and SOC further confirmed that changes in soil temperature induced by warming or seasons could be used to explain the change in SOC (**Supplementary Table S1**). In particular, the maximum increase in temperature produced by the warming treatment in May and August was 2.25°C and 1.57°C, respectively. This is well below the increase in temperature caused by the season (5.14–5.82°C), which also indicated that the insignificant effect of warming on SOC could be because the increase in soil temperature caused by warming did not reach the temperature threshold of organic carbon change (Feng et al., 2022). Structural equation modeling also confirmed this (**Figure 5**). However, since the seasonal changes of SOC are likely to be a cumulative process, whether this inference is suitable for this study still merits further exploration.

Warming Has Not Affected the Change of SOC During the Growing Season

The rate of change of SOC during the growing season was not significantly related to the rate of change of soil temperature (**Table 2**). This was inconsistent with the third hypothesis (H3) but confirms the conclusions of other studies (Classen et al., 2015; Yue et al., 2015), which found that the inter-seasonal temperature difference caused by the warming treatment did not impact microbiota, and thus, failed to alter the seasonal dynamic changes of SOC. However, this result is inconsistent with the results of some studies (Xu et al., 2018; Tian et al., 2021). Tian et al. (2021) and Xu et al. (2018) found that elevated soil temperatures indirectly affected the seasonal dynamics of the content of SOC by altering soil nutrition,

TABLE 1 | Relationships between soil organic carbon content and plant attributes and soil and microbial properties.

Variable	Slope	*F*	*p*-Adjusted
Plant attributes			
Aboveground biomass	−0.02	19.79	**0.0003*****
Plant richness	−0.47	18.80	**0.0003*****
Plant composition	−12.77	28.26	**<0.0001*****
Soil properties			
Soil temperature	−2.08	30.57	**<0.0001*****
Soil moisture	−35.02	16.34	**0.0005*****
pH	13.04	2.12	0.1799
Dissolved organic carbon	0.72	90.21	**<0.0001*****
Dissolved organic nitrogen	4.20	31.21	**<0.0001*****
Ammonia	0.41	1.02	0.3599
Nitrate	0.08	0.10	0.7536
Available phosphorus	−0.57	2.68	0.1404
Microbial properties			
Soi respiration rate	−5.32	11.27	**0.003****
Microbial biomass carbon (MBC)	0.16	129.15	**<0.0001*****
Microbial biomass nitrogen (MBN)	0.83	40.09	**<0.0001*****
MBC/MBN ratio	12.27	16.54	**0.0005****
Lg ITS gene copy number	3.65	14.00	**0.001****
Lg 16S rRNA gene copy number	0.40	0.26	0.6603
Lg ITS/Lg 16S rRNA gene copy number	12.98	3.50	0.0974
Fungal richness	0.02	10.90	**0.0031****
Bacterial richness	0.00	3.11	0.1151
Fungal composition	−12.98	14.00	**0.001****
Bacterial composition	−22.52	9.14	**0.0065****
Amylase activity	−0.03	0.15	0.7296
Sucrase activity	1.91	5.11	**0.0434***
Cellulase activity	−3.60	15.98	**0.0005*****
Peroxidase activity	12.98	2.23	0.1754

Values of p correspond to the linear mixed-effects model regression.
Significant correlations (p <0.05) are formatted in bold.
**p<0.05; **p<0.01; ***p<0.001.*

physical protection, and microbial biomass. Plant biomass (Classen et al., 2015), soil respiration (Tian et al., 2021), and microbiota (Classen et al., 2015; Xu et al., 2018, 2021) are often used to explain the seasonal changes of SOC. In this study, the aboveground biomass gradually decreased with increasing temperature (**Supplementary Figure S2A**). Since the aboveground biomass of all the treatments was close to zero at the beginning of the growing season, the reduction in aboveground biomass caused by warming also illustrates the decrease in the seasonal difference of aboveground biomass under warming treatments. This also indicates that the seasonal difference of aboveground biomass had decreased as the temperature increased. Thus, we inferred that owing to the small input of plant aboveground carbon, the seasonal difference of SOC should be reduced as the temperature increases. However, this inference was inconsistent with the results of this study (**Figure 1A**), indicating that it was unreasonable to only use the plant aboveground biomass to predict the changes in SOC. Considering that belowground biomass and root exudates also play an important role in driving the change of SOC (Jansson and Hofmockel, 2020), further research needs to comprehensively consider belowground biomass and root exudates to explore the effect of warming on the seasonal changes of SOC. In addition to plant biomass, soil respiration is highly sensitive to temperature, and an increase in the temperature will activate soil respiration and accelerate its rate (García-Palacios et al., 2021). Since warming led to a gradual decrease in the seasonal temperature difference in this study (**Supplementary Table S1**), the seasonal difference of SOC will decrease as the temperature increases. However, we had not observed a decrease in the seasonal difference of SOC across a temperature gradient (**Supplementary Figure S6**), indicating that the seasonal change of SOC in this study cannot also be explained by the seasonal change of soil respiration. The insignificant correlation between the rate of change of soil respiration and that of the SOC effectively supported this (**Table 2**). Moreover, the decomposition of soil microbiota was another important reason for the seasonal change in SOC (Chen et al., 2015; García-Palacios et al., 2021; Tian et al., 2021). On the one hand, changes in the soil microbial community composition will affect the SOC by changing the activity of soil extracellular enzymes (Tian et al., 2021). In this study, warming did not have a significant effect on the seasonal differences of fungal and bacterial communities and the activities of soil extracellular enzymes. In addition, there was no significant correlation between the rate of change of the soil microbial community and the rate of change of the soil enzyme activity and that of SOC (**Table 2**). These results indicate that changes in soil microbial communities and soil enzyme activities in this study cannot explain the insignificant effect of warming on the seasonal differences of SOC. Alternatively, MBC, as an internal component of SOC, directly or indirectly affects the change in content of SOC (**Table 2**). In this study, the rate of change of MBC was significantly related to the rate of change of SOC. In addition, the SEM models also showed that warming failed to mediate seasonal changes in SOC by altering the changes in MBC (**Figures 4B, 5B**), indicating that the insignificant seasonal changes in soil temperature on microbial biomass caused by warming in this study could be an important reason for the insignificant effect of warming on the seasonal changes in SOC.

MBC Was Highly Coupled to the Change of SOC

Although MBC comprises a small proportion of SOC (**Figure 2D**), both the random forest analysis and structural equation model all showed that MBC significantly correlated with the change in SOC, indicating a high degree of coupling of MBC to the change in SOC (**Figures 4A, 5A**). This is consistent with the findings of another study (Wang et al., 2021). This occurs because MBC, as an internal component of soil carbon (Mcdaniel et al., 2014; Ogle, 2018; Huang et al., 2021), has been regarded to be the liable carbon fraction of SOC that is closely related to the availability of soil nutrients (Guan et al., 2018) and indirectly participates in the key process of the soil carbon cycle (Ma et al., 2020). In addition, our results had shown that neither season nor warming had a significant effect on the ratio of MBC/MBN. This was also confirmed by another study on an alpine meadow ecosystem

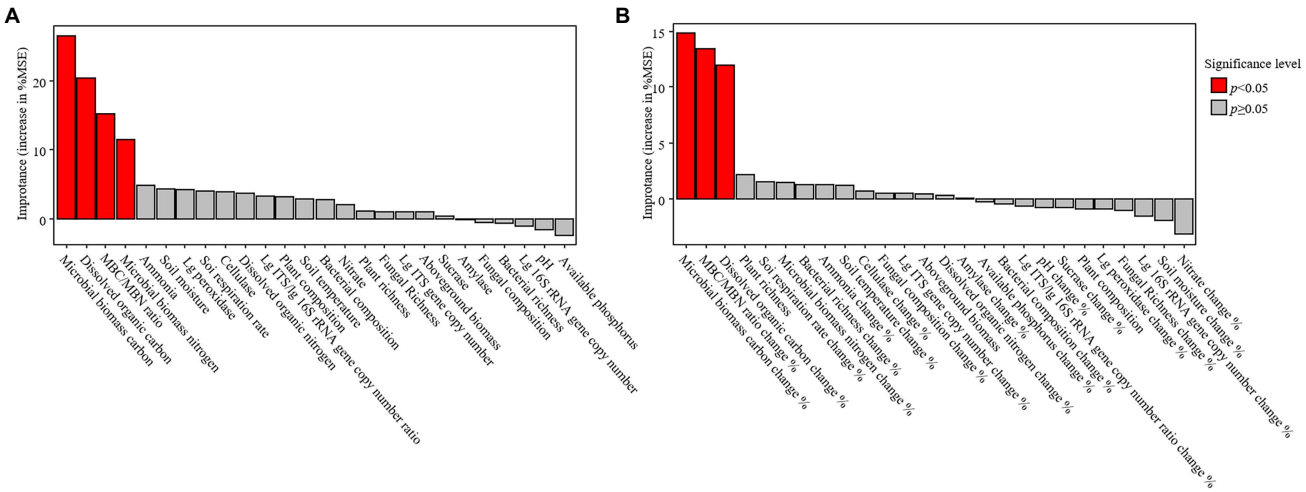

FIGURE 4 | Results of the random forest analysis for soil organic carbon **(A)** and the changes in soil organic carbon during the growing season **(B)**. Variables that significantly correlated with changes of the independent variable are represented by red bars. MSE, mean square error. Lg, $\log_{10}$ transformed.

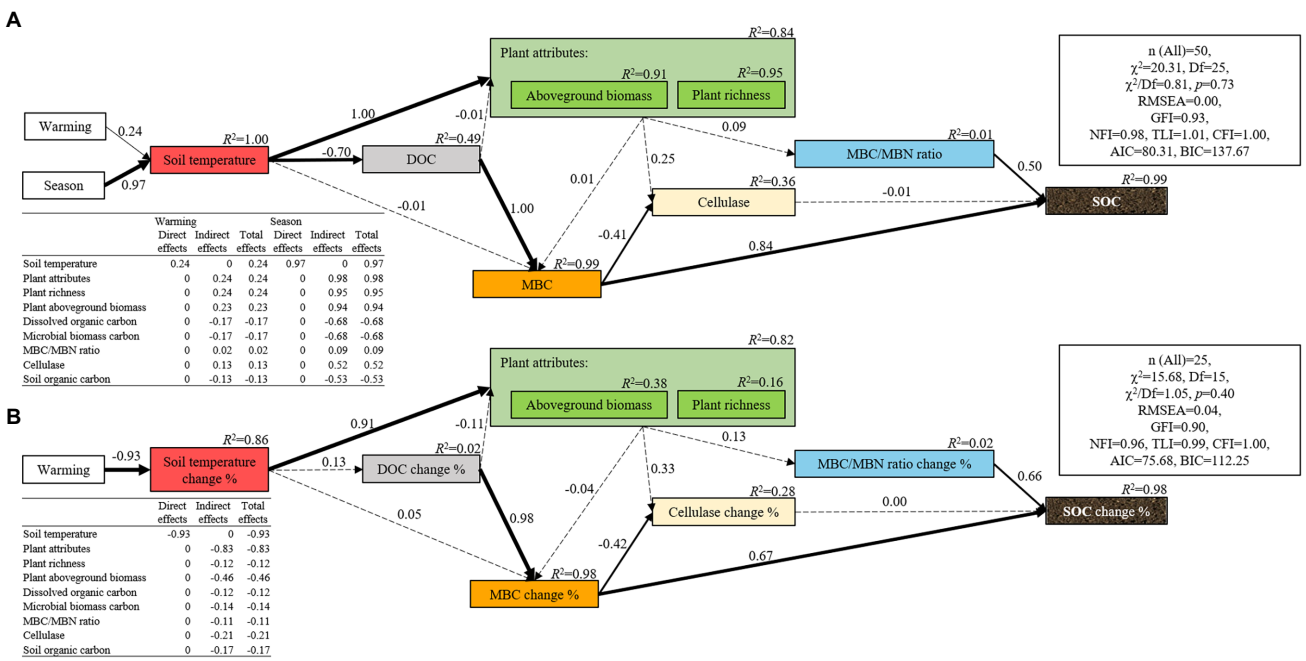

	Warming			Season		
	Direct effects	Indirect effects	Total effects	Direct effects	Indirect effects	Total effects
Soil temperature	0.24	0	0.24	0.97	0	0.97
Plant attributes	0	0.24	0.24	0	0.98	0.98
Plant richness	0	0.24	0.24	0	0.95	0.95
Plant aboveground biomass	0	0.23	0.23	0	0.94	0.94
Dissolved organic carbon	0	-0.17	-0.17	0	-0.68	-0.68
Microbial biomass carbon	0	-0.17	-0.17	0	-0.68	-0.68
MBC/MBN ratio	0	0.02	0.02	0	0.09	0.09
Cellulase	0	0.13	0.13	0	0.52	0.52
Soil organic carbon	0	-0.13	-0.13	0	-0.53	-0.53

	Direct effects	Indirect effects	Total effects
Soil temperature	-0.93	0	-0.93
Plant attributes	0	-0.83	-0.83
Plant richness	0	-0.12	-0.12
Plant aboveground biomass	0	-0.46	-0.46
Dissolved organic carbon	0	-0.12	-0.12
Microbial biomass carbon	0	-0.14	-0.14
MBC/MBN ratio	0	-0.11	-0.11
Cellulase	0	-0.21	-0.21
Soil organic carbon	0	-0.17	-0.17

FIGURE 5 | Structural equation model for soil organic carbon **(A)** and the change of soil organic carbon during the growing season **(B)**. The thickness of the arrows indicates the strength of the effect, and the number along each arrow represents the coefficient of the path. The dotted lines indicate paths that are not significant. The R^2 value represents the proportion of variance that each variable can explain.

on the Qinghai–Tibet Plateau, in which the MBC/MBN remained stable under the warming treatment (Wang et al., 2014). However, this result contradicts another study in a subtropical ecosystem that confirmed that warming produces positive effects on MBC/MBN by increasing the decomposition of soil organic matter (Gao et al., 2017). This inconsistency is primarily determined by the climate characteristics of the two types of ecosystems. In particular, the characteristic cold climates of alpine meadows do not facilitate the decomposition of organic matter, but the opposite is true for subtropical climates. In addition to the decomposition of organic matter, the microbial community dominated by fungi (or bacteria) should not be confirmed to be associated with a high (or low) ratio of MBC/MBN (Gao et al., 2021). However, the ratio of l g ITS/l g 16S rRNA gene copy numbers was always approximately equal to 1 under all the treatments, suggesting a co-dominance of

TABLE 2 | Relationships between the change of soil organic carbon with the change of plant attributes and soil and microbial properties during the growing season.

Variable	Slope	*F*	*p*-Adjusted
Plant attributes			
Aboveground biomass	−0.01	0.12	0.8485
Plant richness	0.07	0.01	0.9403
Plant composition	−26.32	0.53	0.7806
Soil properties			
Soil temperature change %	0.38	1.06	0.6784
Soil moisture change %	−0.02	0.06	0.8485
pH change %	1.72	0.75	0.7806
Dissolved organic carbon change %	0.81	23.48	**0.0009*****
Dissolved organic nitrogen change %	0.52	6.31	0.1128
Ammonia change %	0.19	2.10	0.4640
Nitrate change %	−0.08	0.32	0.8272
Available phosphorus change %	0.05	0.42	0.7971
Microbial properties			
Soi respiration rate change %	−0.10	0.28	0.8272
Microbial biomass carbon (MBC) change %	1.06	39.39	**<0.0001*****
Microbial biomass nitrogen (MBN) change %	0.55	5.01	0.1595
MBC/MBN ratio change %	1.70	33.90	**<0.0001*****
Lg ITS gene copy number change %	0.24	1.70	0.5340
Lg 16S rRNA gene copy number change %	−0.03	0.09	0.8485
Lg ITS/Lg 16S rRNA gene copy number change %	0.17	1.20	0.6736
Fungal richness change %	0.07	0.21	0.8477
Bacterial richness change %	0.24	2.73	0.3637
Fungal composition change %	−0.11	0.51	0.7806
Bacterial composition change %	−0.09	0.60	0.7806
Amylase activity change %	−0.01	0.06	0.8485
Sucrase activity change %	0.06	0.08	0.8485
Cellulase activity change %	−0.10	6.16	0.1128
Peroxidase activity change %	1.25	3.01	0.3577

*Values of p shown correspond to the linear mixed-effects model regression. Significant correlations ($p < 0.05$) are formatted in bold. ***$p < 0.001$.*

fungi and bacteria. This also explained the stability of MBC/MBN ratio under every treatment in this study. However, what was anomalous was that although the MBC/MBN ratio changed owing to warming or season, it was shown to be another variable that was closely associated with the rate of change of SOC. However, both the random forest analysis and the structural equation model also showed that the rate of change of the content of SOC was determined by the rate of change of MBC rather than MBN (**Figure 5**). Therefore, we inferred that the contribution of MBC/MBN to the change in SOC is just another manifestation of the contribution of MBC and is not really driven by the ratio of MBC/MBN, indicating that the microbiological properties of soil that were related to the carbon cycle were "carbon-related" rather than "nitrogen-related."

In addition, warming had no significant effect on the content of DOC regardless of season (**Figure 1D**). This result contradicts those of other studies (Six et al., 2004; Li et al., 2016; Tian et al., 2021). One of these studies found that warming can increase the content of DOC by increasing the dissolved organic compounds produced by plants or microbiota (Bai et al., 2020). However, other studies have found that warming can reduce the organic carbon content dissolved in the soil by promoting the formation of aggregates to solidify the DOC (Six et al., 2004; Li et al., 2016; Tian et al., 2021). In addition, the rate of change of DOC can mediate the rate of change of the SOC by changing the rate of change of MBC during the growing season (**Figure 5B**). These results are consistent with those of other studies (Zhang et al., 2015; Xiong et al., 2016; Bhople et al., 2019; Deltedesco et al., 2020) that further confirm that the DOC participates in the process of regulation of soil carbon cycle by affecting MBC-derived carbon as described in the carbon cycle model by Fan et al. (2021). However, since the content of DOC makes only minor contributions to the variation in the content of SOC (Chen et al., 2015), its impact on SOC stability was likely to be achieved only through its impact on MBC. Integrating this analysis, MBC, the ratio of MBC/MBN, and DOC are all variables that are significantly associated with the change in the content of SOC, but the effects of both MBC/MBN and DOC are essentially mediated by MBC. There was a high degree of coupling between MBC and soil organic carbon. In addition, MBC is more sensitive to temperature than SOC (Walker et al., 2018). Thus, strengthening the research on the temperature sensitivity of MBC can improve our ability to predict changes in SOC under climate warming.

CONCLUSION

This study found that SOC at the end of the growing season was lower than that at the beginning of the growing season, and this seasonal change of SOC during the growing season remained unchanged following warming treatments (**Figure 6**). These findings indicate that alpine meadow soil was a source of carbon during the growing season, but climate warming had no significant impact on it. Our findings have important implications for improving our understanding of the effects of climate warming on the change in SOC during the growing season, suggesting that in the regulation of carbon source or pool in alpine meadow ecosystem, more attention should be paid to changes in SOC during the growing season, rather than climate warming.

DATA AVAILABILITY STATEMENT

The datasets presented in this study can be found in online repositories. The names of the repository/repositories and accession number(s) can be found at: https://www.ncbi.nlm.nih.gov/, PRJNA719774; https://www.ncbi.nlm.nih.gov/, PRJNA719776.

AUTHOR CONTRIBUTIONS

GS, YL, HZ, and HF designed the study. GS, LM, ZZ, and SJ performed field work and done experiments with the help

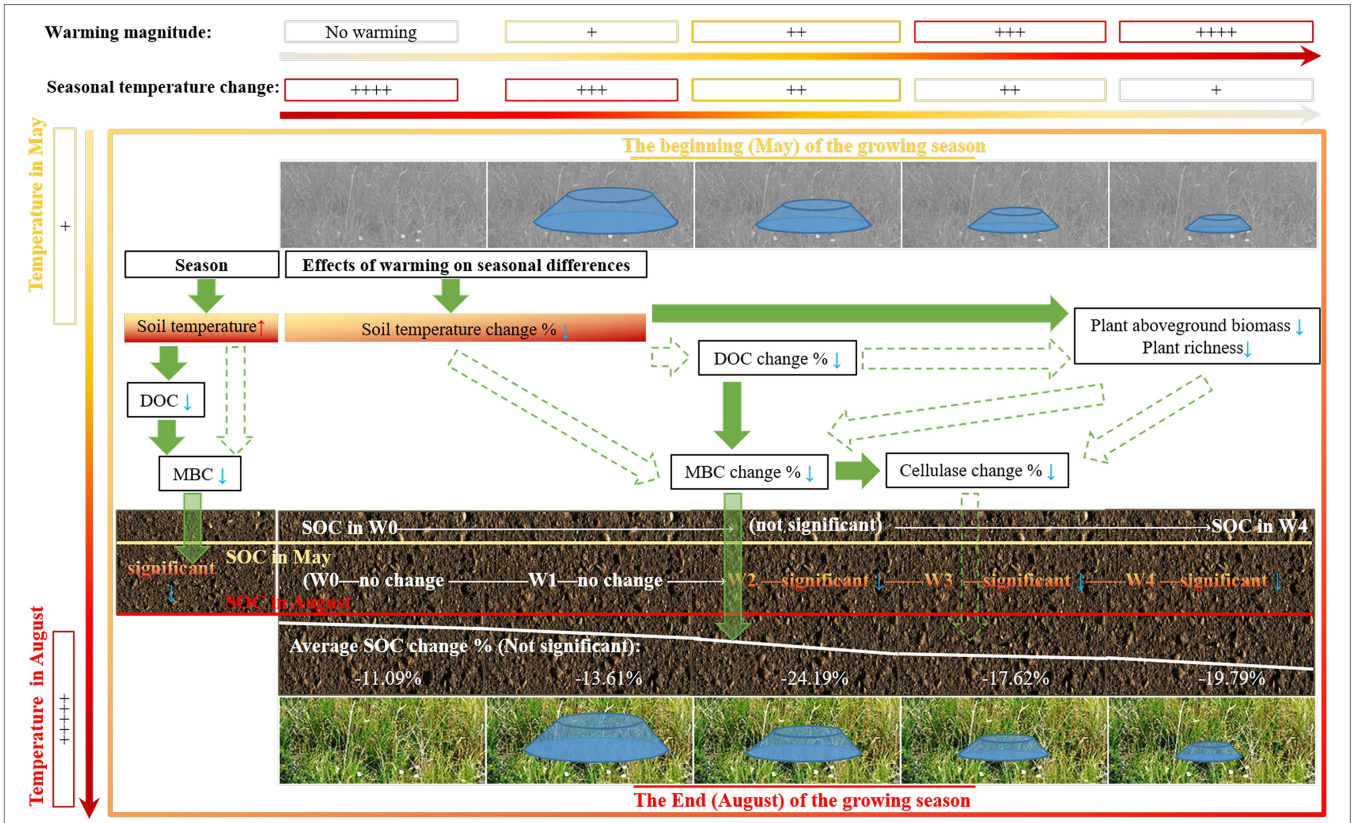

FIGURE 6 | Schematic representation of the effect of experimental warming on the change of soil organic carbon during the growing season.

of YY and JP. YY carried out statistical and bioinformatics analysis, prepared figures and tables, and done results interpretations and wrote the manuscript with help from GS and YL. GS, YL, QZ, BY, HZ, and HF reviewed and edited the manuscript. GS, YL, HZ, and HF acquired the funds for the study. All authors contributed to the article and approved the submitted version.

FUNDING

This research was funded financially by the Second Tibetan Plateau Scientific Expedition and Research (STEP) program (Nos. 2019QZKK0301 and 2019QZKK0302), the National Natural Science Foundation of China (Nos. 31860146; 31971445; 31870494; 32171579 and U21A20186), the Outstanding Youth Foundation of Gansu Province (No. 20JR5RA500), the CAS "Light of West China" Program, "Qinghai Provincial Natural Science Foundation Innovation Team Project (2021-ZJ-902)," and the Joint Research Project of Three-River-Resource National Park (No. LHZX-2020-08).

ACKNOWLEDGMENTS

YY and GS thank the National Field Scientific Observation and Research Station of Alpine Grassland Ecosystem in Haibei, Qinghai for providing the site access and allowing to harvest the samples from their field trial. We are thankful to the editors and reviewers for their valuable suggestions and comments.

SUPPLEMENTARY MATERIAL

The Supplementary Material for this article can be found online at: https://www.frontiersin.org/articles/10.3389/fpls.2022.847680/full#supplementary-material

REFERENCES

Archer, E. (2013). rfPermute: Estimate permutation p-values for importance metrics. Available at: https://github.com/EricArcher/rfPermute (Accessed January 15, 2022).

Bai, T., Wang, P., Hall, S. J., Li, Z., Li, S., Zhou, L., et al. (2020). Interactive global change factors mitigate soil aggregation and carbon change in a semi-arid grassland. *Glob. Chang. Biol.* 26, 5320–5332. doi: 10.1111/gcb.15220

Bhople, P., Djukic, I., Keiblinger, K., Zehetner, F., Liu, D., Bierbaumer, M., et al. (2019). Variations in soil and microbial biomass C, N and fungal biomass ergosterol along elevation and depth gradients in alpine ecosystems. *Geoderma* 345, 93–103. doi: 10.1016/j.geoderma.2019.03.022

Bond-Lamberty, B., and Thomson, A. (2010). A global database of soil respiration data. *Biogeosciences* 7, 1915–1926. doi: 10.5194/bg-7-1915-2010

Brookes, P. C., Landman, A., Pruden, G., and Jenkinson, D. S. (1985). Chloroform fumigation and the release of soil nitrogen: a rapid direct extraction method to measure microbial biomass nitrogen in soil. *Soil Biol. Biochem.* 17, 837–842. doi: 10.1016/0038-0717(85)90144-0

Cabrera, M. L., and Beare, M. H. (1993). Alkaline persulfate oxidation for determining total nitrogen in microbial biomass extracts. *Soil Sci. Soc. Am. J.* 57, 1007–1012. doi: 10.2136/sssaj1993.03615995005700040021x

Campbell, E. E., and Paustian, K. (2015). Current developments in soil organic matter modeling and the expansion of model applications: a review. *Environ. Res. Lett.* 10:123004. doi: 10.1088/1748-9326/10/12/123004

Chen, Y., Han, M., Yuan, X., Hou, Y., Qin, W., Zhou, H., et al. (2021). Warming has a minor effect on surface soil organic carbon in alpine meadow ecosystems on the Qinghai-Tibetan plateau. *Glob. Chang. Biol.* 28, 1618–1629. doi: 10.1111/gcb.15984

Chen, H., Li, D., Gurmesa, G. A., Yu, G., Li, L., Zhang, W., et al. (2015). Effects of nitrogen deposition on carbon cycle in terrestrial ecosystems of China: a meta-analysis. *Environ. Pollut.* 206, 352–360. doi: 10.1016/j.envpol.2015.07.033

Chen, Q., Niu, B., Hu, Y., Luo, T., and Zhang, G. (2020). Warming and increased precipitation indirectly affect the composition and turnover of labile-fraction soil organic matter by directly affecting vegetation and microorganisms. *Sci. Total Environ.* 714:136787. doi: 10.1016/j.scitotenv.2020.136787

Chen, S., Zhou, Y., Chen, Y., and Gu, J. (2018). Fastp: an ultra-fast all-in-one FASTQ preprocessor. *Bioinformatics* 34, i884–i890. doi: 10.1093/bioinformatics/bty560

Classen, A. T., Sundqvist, M. K., Henning, J. A., Newman, G. S., Moore, J. A. M., Cregger, M. A., et al. (2015). Direct and indirect effects of climate change on soil microbial and soil microbial-plant interactions: what lies ahead? *Ecosphere* 6, art130. doi: 10.1890/es15-00217.1

Conant, R. T., Ryan, M. G., Ågren, G. I., Birge, H. E., Davidson, E. A., Eliasson, P. E., et al. (2011). Temperature and soil organic matter decomposition rates-synthesis of current knowledge and a way forward. *Glob. Chang. Biol.* 17, 3392–3404. doi: 10.1111/j.1365-2486.2011.02496.x

Craig, M. E., Mayes, M. A., Sulman, B. N., and Walker, A. P. (2021). Biological mechanisms may contribute to soil carbon saturation patterns. *Glob. Chang. Biol.* 27, 2633–2644. doi: 10.1111/gcb.15584

Deltedesco, E., Keiblinger, K. M., Piepho, H.-P., Antonielli, L., Pötsch, E. M., Zechmeister-Boltenstern, S., et al. (2020). Soil microbial community structure and function mainly respond to indirect effects in a multifactorial climate manipulation experiment. *Soil Biol. Biochem.* 142:107704. doi: 10.1016/j.soilbio.2020.107704

Ding, X., Chen, S., Zhang, B., Liang, C., He, H., and Horwath, W. R. (2019). Warming increases microbial residue contribution to soil organic carbon in an alpine meadow. *Soil Biol. Biochem.* 135, 13–19. doi: 10.1016/j.soilbio.2019.04.004

Duan, M., Li, A., Wu, Y., Zhao, Z., Peng, C., DeLuca, T. H., et al. (2019). Differences of soil CO2 flux in two contrasting subalpine ecosystems on the eastern edge of the Qinghai-Tibetan plateau: a four-year study. *Atmos. Environ.* 198, 166–174. doi: 10.1016/j.atmosenv.2018.10.067

Edgar, R. C. (2013). UPARSE: highly accurate OTU sequences from microbial amplicon reads. *Nat. Methods* 10, 996–998. doi: 10.1038/nmeth.2604

Elmendorf, S. C., Henry, G. H., Hollister, R. D., Bjork, R. G., Bjorkman, A. D., Callaghan, T. V., et al. (2012). Global assessment of experimental climate warming on tundra vegetation: heterogeneity over space and time. *Ecol. Lett.* 15, 164–175. doi: 10.1111/j.1461-0248.2011.01716.x

Emde, D., Hannam, K. D., Most, I., Nelson, L. M., and Jones, M. D. (2021). Soil organic carbon in irrigated agricultural systems: A meta-analysis. *Glob. Chang. Biol.* 27, 3898–3910. doi: 10.1111/gcb.15680

Fan, X., Gao, D., Zhao, C., Wang, C., Qu, Y., Zhang, J., et al. (2021). Improved model simulation of soil carbon cycling by representing the microbially derived organic carbon pool. *ISME J.* 15, 2248–2263. doi: 10.1038/s41396-021-00914-0

Feng, W., Liang, J., Hale, L. E., Jung, C. G., Chen, J., Zhou, J., et al. (2017). Enhanced decomposition of stable soil organic carbon and microbial catabolic potentials by long-term field warming. *Glob. Chang. Biol.* 23, 4765–4776. doi: 10.1111/gcb.13755

Feng, Y., Zhang, J., Berdugo, M., Guirado, E., Guerra, C. A., Egidi, E., et al. (2022). Temperature thresholds drive the global distribution of soil fungal decomposers. *Glob. Chang. Biol.* doi: 10.1111/gcb.16096 [Epub ahead of print].

Fu, Y., Gao, X., Zhu, Y., and Guo, D. (2021). Climate change projection over the Tibetan plateau based on a set of RCM simulations. *Adv. Clim. Chang. Res.* 12, 313–321. doi: 10.1016/j.accre.2021.01.004

Gao, D., Bai, E., Yang, Y., Zong, S., and Hagedorn, F. (2021). A global meta-analysis on freeze-thaw effects on soil carbon and phosphorus cycling. *Soil Biol. Biochem.* 159:108283. doi: 10.1016/j.soilbio.2021.108283

Gao, Q., Li, Y., Xu, H., Wan, Y., and Jiangcun, W. (2014). Adaptation strategies of climate variability impacts on alpine grassland ecosystems in Tibetan plateau. *Mitig. Adapt. Strateg. Glob. Chang.* 19, 199–209. doi: 10.1007/s11027-012-9434-y

Gao, J., Wang, E., Ren, W., Liu, X., Chen, Y., Shi, Y., et al. (2017). Effects of simulated climate change on soil microbial biomass and enzyme activities in young Chinese fir (Cunninghamia lanceolata) in subtropical China. *Acta Ecol. Sin.* 37, 272–278. doi: 10.1016/j.chnaes.2017.02.007

García-Palacios, P., Crowther, T. W., Dacal, M., Hartley, I. P., Reinsch, S., Rinnan, R., et al. (2021). Evidence for large microbial-mediated losses of soil carbon under anthropogenic warming. *Nat. Rev. Earth Environ.* 2, 507–517. doi: 10.1038/s43017-021-00178-4

Gavazov, K., Ingrisch, J., Hasibeder, R., Mills, R. T. E., Buttler, A., Gleixner, G., et al. (2017). Winter ecology of a subalpine grassland: effects of snow removal on soil respiration, microbial structure and function. *Sci. Total Environ.* 590-591, 316–324. doi: 10.1016/j.scitotenv.2017.03.010

Guan, S., An, N., Zong, N., He, Y., Shi, P., Zhang, J., et al. (2018). Climate warming impacts on soil organic carbon fractions and aggregate stability in a Tibetan alpine meadow. *Soil Biol. Biochem.* 116, 224–236. doi: 10.1016/j.soilbio.2017.10.011

Huang, J., Liu, W., Yang, S., Yang, L., Peng, Z., Deng, M., et al. (2021). Plant carbon inputs through shoot, root, and mycorrhizal pathways affect soil organic carbon turnover differently. *Soil Biol. Biochem.* 160:108322. doi: 10.1016/j.soilbio.2021.108322

Hutchins, D. A., Jansson, J. K., Remais, J. V., Rich, V. I., Singh, B. K., and Trivedi, P. (2019). Climate change microbiology-problems and perspectives. *Nat. Rev. Microbiol.* 17, 391–396. doi: 10.1038/s41579-019-0178-5

IPCC (2021). "Summary for policymakers," in *Climate Change 2021: The Physical Science Basis. Contribution of Working Group I to the Sixth Assessment Report of the Intergovernmental Panel on Climate Change* . eds. V. Masson-Delmotte, P. Zhai, A. Pirani, S. L. Connors, C. Péan, S. Berger et al. (Cambridge & New York: Cambridge University Press).

Jansson, J. K., and Hofmockel, K. S. (2020). Soil microbiomes and climate change. *Nat. Rev. Microbiol.* 18, 35–46. doi: 10.1038/s41579-019-0265-7

Jia, J., Cao, Z., Liu, C., Zhang, Z., Lin, L., Wang, Y., et al. (2019). Climate warming alters subsoil but not topsoil carbon dynamics in alpine grassland. *Glob. Chang. Biol.* 25, 4383–4393. doi: 10.1111/gcb.14823

Jia, J., Feng, X., He, J.-S., He, H., Lin, L., and Liu, Z. (2017). Comparing microbial carbon sequestration and priming in the subsoil versus topsoil of a Qinghai-Tibetan alpine grassland. *Soil Biol. Biochem.* 104, 141–151. doi: 10.1016/j.soilbio.2016.10.018

Jiang, X., Xu, D., Rong, J., Ai, X., Ai, S., Su, X., et al. (2021). Landslide and aspect effects on artificial soil organic carbon fractions and the carbon pool management index on road-cut slopes in an alpine region. *Catena* 199, 105094. doi: 10.1016/j.catena.2020.105094

Jones, D., and Willett, V. (2006). Experimental evaluation of methods to quantify dissolved organic nitrogen (DON) and dissolved organic carbon (DOC) in soil. *Soil Biol. Biochem.* 38, 991–999. doi: 10.1016/j.soilbio.2005.08.012

Klein, J. A., Harte, J., and Zhao, X. Q. (2004). Experimental warming causes large and rapid species loss, dampened by simulated grazing, on the Tibetan plateau. *Ecol. Lett.* 7, 1170–1179. doi: 10.1111/j.1461-0248.2004.00677.x

Lal, R. (2004). Soil carbon sequestration impacts on global climate change and food security. *Science* 304, 1623–1627. doi: 10.1126/science.1097396

Li, L., Vogel, J., He, Z., Zou, X., Ruan, H., Huang, W., et al. (2016). Association of Soil Aggregation with the distribution and quality of organic carbon in soil along an elevation gradient on Wuyi Mountain in China. *PLoS One* 11:e0150898. doi: 10.1371/journal.pone.0150898

Lippmann, R., Babben, S., Menger, A., Delker, C., and Quint, M. (2019). Development of wild and cultivated plants under global warming conditions. *Curr. Biol.* 29, R1326–R1338. doi: 10.1016/j.cub.2019.10.016

Luo, Y. (2007). Terrestrial carbon–cycle feedback to climate warming. *Annu. Rev. Ecol. Evol. Syst.* 38, 683–712. doi: 10.1146/annurev.ecolsys.38.091206.095808

Luo, Y., Wan, S., Hui, D., and Wallace, L. L. (2001). Acclimatization of soil respiration to warming in a tall grass prairie. *Nature* 413, 622–625. doi: 10.1038/35098065

Luo, Y., and Weng, E. (2011). Dynamic disequilibrium of the terrestrial carbon cycle under global change. *Trends Ecol. Evol.* 26, 96–104. doi: 10.1016/j.tree.2010.11.003

Ma, W., Li, G., Wu, J., Xu, G., and Wu, J. (2020). Response of soil labile organic carbon fractions and carbon-cycle enzyme activities to vegetation degradation in a wet meadow on the Qinghai–Tibet Plateau. *Geoderma* 377:114565. doi: 10.1016/j.geoderma.2020.114565

Magoc, T., and Salzberg, S. L. (2011). FLASH: fast length adjustment of short reads to improve genome assemblies. *Bioinformatics* 27, 2957–2963. doi: 10.1093/bioinformatics/btr507

Makarov, M. I., Shuleva, M. S., Malysheva, T. I., and Menyailo, O. V. (2013). Solubility of the labile forms of soil carbon and nitrogen in K2SO4 of different concentrations. *Eur. J. Soil Sci.* 46, 369–374. doi: 10.1134/s1064229313040091

Mcdaniel, M. D., Tiemann, L. K., and Grandy, A. S. (2014). Does agricultural crop diversity enhance soil microbial biomass and organic matter dynamics? A meta-analysis. *Ecol. Appl.* 24, 560–570. doi: 10.1890/13-0616.1

Mori, H., Maruyama, F., Kato, H., Toyoda, A., Dozono, A., Ohtsubo, Y., et al. (2014). Design and experimental application of a novel non-degenerate universal primer set that amplifies prokaryotic 16S rRNA genes with a low possibility to amplify eukaryotic rRNA genes. *DNA Res.* 21, 217–227. doi: 10.1093/dnares/dst052

Ogle, K. (2018). Microbes weaken soil carbon sink. *Nature* 560, 32–33. doi: 10.1038/d41586-018-05842-2

Oksanen, J., Blanchet, F.G., Friendly, M., Kindt, R., Legendre, P., McGlinn, D., et al. (2019). Vegan: community ecology package. R Package Version 2.5-6. Available at: https://cran.r-project.org/web/packages/vegan/vegan.pdf (Accessed January 15, 2022).

Oksanen, J., Kindt, R., Legendre, P., O'Hara, B., Stevens, M., Oksanen, M., et al. (2007). Vegan: community ecology package. Available at: http://vegan.r-forge.r-project.org/ (Accessed January 15, 2022).

Peng, F., Zhang, W., Lai, C., Li, C., You, Q., Xue, X., et al. (2021). Legacy effect of warming on the heterotrophic respiration of alpine grassland on the Qinghai-Tibet plateau. *Appl. Soil Ecol.* 166:104093. doi: 10.1016/j.apsoil.2021.104093

Pinheiro, J., Bates, D., DebRoy, S., and Sarkar, D.R Core Team (2019). nlme: Linear and nonlinear mixed effects models. R package version 3.1–141. Available at: https://cran.r-project.org/package=nlme (Accessed January 15, 2022).

Post, E., and Pedersen, C. (2008). Opposing plant community responses to warming with and without herbivores. *Proc. Natl. Acad. Sci. U. S. A.* 105, 12353–12358. doi: 10.1073/pnas.0802421105

Ren, C., Wang, J., Bastida, F., Delgado-Baquerizo, M., Yang, Y., Wang, J., et al. (2021). Microbial traits determine soil C emission in response to fresh carbon inputs in forests across biomes. *Glob. Chang. Biol.* 28, 1516–1528. doi: 10.1111/gcb.16004

Scheffers, B. R., Meester, L. D., Bridge, T. C. L., Hoffmann, A. A., Pandolfi, J. M., Corlett, R. T., et al. (2016). The broad footprint of climate change from genes to biomes to people. *Science* 354:aaf7671. doi: 10.1126/science.aaf7671

Schlesinger, W. H., and Andrews, J. A. (2000). Soil respiration and the global carbon cycle. *Biogeochemistry* 48, 7–20. doi: 10.1023/A:1006247623877

Schmidt, M. W., Torn, M. S., Abiven, S., Dittmar, T., Guggenberger, G., Janssens, I. A., et al. (2011). Persistence of soil organic matter as an ecosystem property. *Nature* 478, 49–56. doi: 10.1038/nature10386

Segata, N., Izard, J., Waldron, L., Gevers, D., Miropolsky, L., Garrett, W. S., et al. (2011). Metagenomic biomarker discovery and explanation. *Genome Biol.* 12:R60. doi: 10.1186/gb-2011-12-6-r60

Singh, B. K., Bardgett, R. D., Smith, P., and Reay, D. S. (2010). Microorganisms and climate change: terrestrial feedbacks and mitigation options. *Nat. Rev. Microbiol.* 8, 779–790. doi: 10.1038/nrmicro2439

Six, J., Bossuyt, H., Degryze, S., and Denef, K. (2004). A history of research on the link between (micro) aggregates, soil biota, and soil organic matter dynamics. *Soil Tillage Res.* 79, 7–31. doi: 10.1016/j.still.2004.03.008

Stackebrandt, E., and Goebel, B. M. (1994). Taxonomic note: a place for DNA-DNA reassociation and 16S rRNA sequence analysis in the present species definition in bacteriology. *Int. J. Syst. Bacteriol.* 44, 846–849. doi: 10.1099/00207713-44-4-846

Tian, J., Zong, N., Hartley, I. P., He, N., Zhang, J., Powlson, D., et al. (2021). Microbial metabolic response to winter warming stabilizes soil carbon. *Glob. Chang. Biol.* 27, 2011–2028. doi: 10.1111/gcb.15538

Vance, E. D., Brggkes, P. C., and Jenkinson, D. S. (1987). An extraction method for measuring soil microbial biomass C. *Soil Biol. Biochem.* 19, 703–707. doi: 10.1016/0038-0717(87)90052-6

Walker, T. W. N., Kaiser, C., Strasser, F., Herbold, C. W., Leblans, N. I. W., Woebken, D., et al. (2018). Microbial temperature sensitivity and biomass change explain soil carbon loss with warming. *Nat. Clim. Chang.* 8, 885–889. doi: 10.1038/s41558-018-0259-x

Wang, X., Dong, S., Gao, Q., Zhou, H., Liu, S., Su, X., et al. (2014). Effects of short-term and long-term warming on soil nutrients, microbial biomass and enzyme activities in an alpine meadow on the Qinghai-Tibet plateau of China. *Soil Biol. Biochem.* 76, 140–142. doi: 10.1016/j.soilbio.2014.05.014

Wang, Q., Garrity, G. M., Tiedje, J. M., and Cole, J. R. (2007). Naive Bayesian classifier for rapid assignment of rRNA sequences into the new bacterial taxonomy. *Appl. Environ. Microbiol.* 73, 5261–5267. doi: 10.1128/AEM.00062-07

Wang, H., Liu, S., Schindlbacher, A., Wang, J., Yang, Y., Song, Z., et al. (2019). Experimental warming reduced topsoil carbon content and increased soil bacterial diversity in a subtropical planted forest. *Soil Biol. Biochem.* 133, 155–164. doi: 10.1016/j.soilbio.2019.03.004

Wang, G., Qian, J., Cheng, G., and Lai, Y. (2002). Soil organic carbon pool of grassland soils on the Qinghai-Tibetan plateau and its global implication. *Sci. Total Environ.* 291, 207–217. doi: 10.1016/S0048-9697(01)01100-7

Wang, C., Xiao, R., Guo, Y., Wang, Q., Cui, Y., Xiu, Y., et al. (2021). Changes in soil microbial community composition during Phragmites australis straw decomposition in salt marshes with freshwater pumping. *Sci. Total Environ.* 762:143996. doi: 10.1016/j.scitotenv.2020.143996

White, T. J., Bruns, T., Lee, S., and Taylor, J. (1900). "Amplification and direct sequencing of fungal ribosomal RNA genes for phylogenetics," in *PCR Protocols a Guide to Methods and Applications*. eds. M. A. Innis, D. H. Gelfand, J. J. Sninsky and T. J. White (San Diego: Academic Press), 315–322.

Xiong, Q. L., Pan, K. W., Zhang, L., Wang, Y. J., Li, W., He, X. J., et al. (2016). Warming and nitrogen deposition are interactive in shaping surface soil microbial communities near the alpine timberline zone on the eastern Qinghai–Tibet Plateau, southwestern China. *Appl. Soil Ecol.* 101, 72–83. doi: 10.1016/j.apsoil.2016.01.011

Xu, G., Chen, J., Berninger, F., Pumpanen, J., Bai, J., Yu, L., et al. (2015). Labile, recalcitrant, microbial carbon and nitrogen and the microbial community composition at two Abies faxoniana forest elevations under elevated temperatures. *Soil Biol. Biochem.* 91, 1–13. doi: 10.1016/j.soilbio.2015.08.016

Xu, M., Li, X., Kuyper, T. W., Xu, M., Li, X., and Zhang, J. (2021). High microbial diversity stabilizes the responses of soil organic carbon decomposition to warming in the subsoil on the Tibetan plateau. *Glob. Chang. Biol.* 27, 2061–2075. doi: 10.1111/gcb.15553

Xu, B., Wang, J., Wu, N., Wu, Y., and Shi, F. (2018). Seasonal and interannual dynamics of soil microbial biomass and available nitrogen in an alpine meadow in the eastern part of Qinghai–Tibet Plateau, China. *Biogeosciences* 15, 567–579. doi: 10.5194/bg-15-567-2018

Xun, W., Yan, R., Ren, Y., Jin, D., Xiong, W., Zhang, G., et al. (2018). Grazing-induced microbiome alterations drive soil organic carbon turnover and productivity in meadow steppe. *Microbiome* 6, 170. doi: 10.1186/s40168-018-0544-y

Yang, Y., Shi, Y., Sun, W., Chang, J., Zhu, J., Chen, L., et al. (2021). Terrestrial carbon sinks in China and around the world and their contribution to carbon neutrality. *Sci. China Life Sci.* 1–73. doi: 10.1007/s11427-021-2045-5

Yin, H., Wheeler, E., and Phillips, R. P. (2014). Root-induced changes in nutrient cycling in forests depend on exudation rates. *Soil Biol. Biochem.* 78, 213–221. doi: 10.1016/j.soilbio.2014.07.022

Yue, H., Wang, M., Wang, S., Gilber, J. A., Sun, X., Wu, L., et al. (2015). The microbe-mediated mechanisms affecting topsoil carbon stock in Tibetan grasslands. *ISME J.* 9, 2012–2020. doi: 10.1038/ismej.2015.19

Zhang, B., Chen, S. Y., Zhang, J. F., He, X. Y., Liu, W. J., Zhao, Q., et al. (2015). Depth-related responses of soil microbial communities to experimental

warming in an alpine meadow on the Qinghai-Tibet plateau. *Eur. J. Soil Sci.* 66, 496–504. doi: 10.1111/ejss.12240

Zhang, H., Goll, D. S., Wang, Y. P., Ciais, P., Wieder, W. R., Abramoff, R., et al. (2020). Microbial dynamics and soil physicochemical properties explain large-scale variations in soil organic carbon. *Glob. Chang. Biol.* 26, 2668–2685. doi: 10.1111/gcb.14994

Zhang, Z., Qiao, M., Li, D., Yin, H., and Liu, Q. (2016). Do warming-induced changes in quantity and stoichiometry of root exudation promote soil N transformations via stimulation of soil nitrifiers, denitrifiers and ammonifiers? *Eur. J. Soil Biol.* 74, 60–68. doi: 10.1016/j.ejsobi.2016.03.007

Zhang, G., Shen, Z., and Fu, G. (2021). Function diversity of soil fungal community has little exclusive effects on the response of aboveground plant production to experimental warming in alpine grasslands. *Appl. Soil Ecol.* 168, 104153. doi: 10.1016/j.apsoil.2021.104153

Zhang, C., Willis, C. G., Klein, J. A., Ma, Z., Li, J., Zhou, H., et al. (2017). Recovery of plant species diversity during long-term experimental warming of a species-rich alpine meadow community on the Qinghai-Tibet plateau. *Biol. Conserv.* 213, 218–224. doi: 10.1016/j.biocon.2017.07.019

Zheng, H., Liu, Y., Chen, Y., Zhang, J., Li, H., Wang, L., et al. (2020). Short-term warming shifts microbial nutrient limitation without changing the bacterial community structure in an alpine timberline of the eastern Tibetan plateau. *Geoderma* 360:113985. doi: 10.1016/j.geoderma.2019.113985

Zhu, E., Cao, Z., Jia, J., Liu, C., Zhang, Z., Wang, H., et al. (2021). Inactive and inefficient: warming and drought effect on microbial carbon processing in alpine grassland at depth. *Glob. Chang. Biol.* 27, 2241–2253. doi: 10.1111/gcb.15541

Conflict of Interest: The authors declare that the research was conducted in the absence of any commercial or financial relationships that could be construed as a potential conflict of interest.

Publisher's Note: All claims expressed in this article are solely those of the authors and do not necessarily represent those of their affiliated organizations, or those of the publisher, the editors and the reviewers. Any product that may be evaluated in this article, or claim that may be made by its manufacturer, is not guaranteed or endorsed by the publisher.

Copyright © 2022 Yang, Shi, Liu, Ma, Zhang, Jiang, Pan, Zhang, Yao, Zhou and Feng. This is an open-access article distributed under the terms of the Creative Commons Attribution License (CC BY). The use, distribution or reproduction in other forums is permitted, provided the original author(s) and the copyright owner(s) are credited and that the original publication in this journal is cited, in accordance with accepted academic practice. No use, distribution or reproduction is permitted which does not comply with these terms.

frontiers in Plant Science

ORIGINAL RESEARCH
published: 21 March 2022
doi: 10.3389/fpls.2022.850854

The Plant Interspecific Association in the Revegetated Alpine Grasslands Determines the Productivity Stability of Plant Community Across Restoration Time on Qinghai–Tibetan Plateau

Shengnan Wu[1], Lu Wen[2], Shikui Dong[1]*, Xiaoxia Gao[3], Yudan Xu[4], Shuai Li[5], Quanming Dong[6] and Kelly Wessell[7]*

[1] School of Grassland Science, Beijing Forestry University, Beijing, China, [2] Ministry of Education Key Laboratory of Ecology and Resource Use of the Mongolian Plateau and Inner Mongolia Key Laboratory of Grassland Ecology, School of Ecology and Environment, Inner Mongolia University, Hohhot, China, [3] State Key Laboratory of Vegetation and Environmental Change, Institute of Botany, Chinese Academy of Sciences, Beijing, China, [4] College of Grassland Science, Shanxi Agricultural University, Jinzhong, China, [5] College of Resources and Environment, Shanxi Agricultural University, Jinzhong, China, [6] Qinghai Academy of Animal and Veterinary Sciences, Qinghai University, Xining, China, [7] Tompkins Cortland Community College, Dryden, NY, United States

OPEN ACCESS

Edited by:
Shiliang Liu,
Beijing Normal University, China

Reviewed by:
Xukun Su,
Research Center for Eco-Environmental Sciences (CAS), China
Yuanyuan Li,
Ministry of Ecology and Environment, China

***Correspondence:**
Lu Wen
wenlu5210@126.com
Shikui Dong
dongshikui@bjfu.edu.cn

Specialty section:
This article was submitted to Functional Plant Ecology, a section of the journal Frontiers in Plant Science

Received: *08 January 2022*
Accepted: *22 February 2022*
Published: *21 March 2022*

Citation:
Wu S, Wen L, Dong S, Gao X, Xu Y, Li S, Dong Q and Wessell K (2022) The Plant Interspecific Association in the Revegetated Alpine Grasslands Determines the Productivity Stability of Plant Community Across Restoration Time on Qinghai–Tibetan Plateau. Front. Plant Sci. 13:850854. doi: 10.3389/fpls.2022.850854

Grassland cultivation is the key measure for restoring "Black Beach," the extremely degraded alpine meadow in the Three River Headwater Area of the Qinghai–Tibetan Plateau. In this study, we examined the inter-specific relationship in the vegetation community of cultivated grasslands with different restoration times through the network analysis method. The results showed that with the extension of restoration time, the development of cultivated grassland would lead to increasing neutral interactions among the plant species. The proportion of species with positive and negative associations in the community decreased, while the number of species-independent pairs increased significantly. The complexity of plant interspecific association (species network density) had more influence on community stability with the extension of recovery time, which can be used to quantify the characteristics of community structure.

Keywords: cultivated grasslands, stability, interspecific association, Qinghai–Tibet Plateau, restoration

INTRODUCTION

At present, grassland ecosystems, the typical human-managed ecosystem through grazing, are the focus of terrestrial ecosystems studies in the field of ecosystem function of biodiversity (Isbell, 2010). On the Qinghai–Tibetan Plateau (QTP), the "Third Pole of Earth," alpine grassland is the largest ecosystem and provides critically important functions and services such as water regulation, carbon sequestration, biodiversity conservation, livestock production, and pastoral culture (Dong et al., 2013; Liu B. et al., 2018; Xu et al., 2019). However, natural and human factors such as climate change and livestock overgrazing have resulted in massive grassland degradation on the QTP (Zeng et al., 2015). In the past decade, approximately 26% of the alpine grasslands in the Three River Headwater Area in the central QTP have been severely degraded as "Black Beach" or "Black Soil Land," which is defined as the bare land in winter and the sparsely covered land with annual weeds

or poisonous plants in summer (Li et al., 2014). Caused mainly by overgrazing, "Black Beach" is an area that has little grazing value and degraded ecosystem services (Dong et al., 2013; Shang et al., 2018). Grassland degradation has not only dramatically reduced ecosystem service functions, but also seriously affected the social adaptability of local herdsmen (Liu S.B. et al., 2018; Shen et al., 2019), limiting sustainable development of these coupled human–natural systems at local and regional levels (Dong et al., 2012). To alleviate the negative effects of grassland degradation on natural ecosystems and social–economic systems, governments and researchers of various countries have made large-scale efforts to restore degraded grassland. Developing cultivated grasslands is one of the effective measures to alleviate the serious degradation of alpine grasslands (Wang et al., 2015). A large number of experimental studies have shown that the establishment of artificial vegetation is one of the quick and effective ways to restore the production and ecological functions of extremely degraded alpine meadow, but this method also has the problem of re-degradation, so it is necessary to fully understand the restoration of artificial grassland habitat and explore suitable artificial grassland reconstruction techniques (Feng et al., 2010; Shang et al., 2018).

The relationship between stability and biodiversity has been the focus of much ecological research and is key to understanding trends in global biodiversity (Isbell et al., 2009; Liu B. et al., 2018); however, the explanatory model and mechanism of the relationship between stability and biodiversity are still controversial (Loreau and De Mazancourt, 2013). Species play a vital role in the ecosystem, as well as in the function of the ecosystem (Cleland, 2011). Previous studies exploring the relationship between diversity and stability have emphasized the important role of species, functional group composition, and inter-specific relationships in productivity (Klanderud, 2010; Wang et al., 2013). Isbell et al. (2009) proposed that the interaction between species could promote biodiversity and stability. Recently, worldwide scientists have begun to use networks to help analyze ecological consequences of various types of species interactions (Zhou et al., 2011). According to Pellissier et al. (2018), it is necessary to study species composition and their interactions in the form of a network. Little is known about plant interspecific association and its relationship with community stability. However, a few scholars have recorded the stability of plant productivity and its relationships with species composition and interactions during the long-term recovery of grasslands on the QTP. Plant productivity is crucial to the restoration and sustainable management of grassland ecosystems (Maselli et al., 2013; Pallett et al., 2016; Yang et al., 2018; Zeeman et al., 2019). Species composition and functional group representation are the key factors to affect the aboveground or belowground biomass of the community (Cortois et al., 2017). For a long time, scholars have paid more attention to the effects of nutrients such as nitrogen, phosphorus, or organic carbon concentration on the plant community structure and productivity (Byrne and Jones, 2002; Zhao et al., 2018). Although some scholars have documented the changes in the diversity and stability of cultivated grassland with different restoration years (Li et al., 2014), a few researchers have examined the species composition and interactions on the stability of the artificial grassland plant community. In the field of succession research, it is often emphasized that the dynamics of plant community composition and structures related to species interactions should be studied (Bai et al., 2004). However, a few scholars have studied how the stability of alpine grassland productivity changes with time and whether this change depends on biodiversity or community composition. Heterogeneity plays an important role in the function and processes of ecosystems at different scales, and its coefficients of variation and time repetition are indicators of the stability of ecosystems (Eisenhauer et al., 2011; Lv et al., 2020). Exploring the community structure and composition is of great significance for research on ecosystems (Johnson et al., 2008).

We hope to explore the structure and relationship of the ecosystem through as many methods and indicators as possible. Social network analysis methods based on inter-specific relationships may provide a quantitative means for exploring the characteristics of community structure. Therefore, we conducted this study to examine species composition and interaction dynamics of alpine grassland communities planted on "Black Beach" during the restoration process and its influence on grassland ecosystem stability.

The objectives of this study are to address the following questions: (1) How do plant species composition and diversity of cultivated grassland change in the restoration time? (2) How do plant inter-specific relationships change in the cultivated grasslands following restoration? (3) How do the plant species diversity and the complexity of plant interspecific association affect the plant stability of cultivated grasslands in the restoration process?

MATERIALS AND METHODS

Study Site

The study site is located in the town of Dawu, Maqin County of Qinghai Province, China, the core zone of the Three Rivers Headwater Area (**Figure 1**). The geographical position of the study site is 32°31′–35°37′N in latitude, 96°54′–101°51′E in longitude, and the average elevation is over 4,000 m. The annual average temperature is 0.54°C (from 1997 to 2017 statistics) and the annual average precipitation is 518.2 mm (The coefficient of variation of the inter-divisional dynamics is 24%). The average temperature in the coldest month (January) is −11.1°C, and the average temperature in the hottest month (July) is 10.7°C. The soil type is loam (Gao et al., 2019). The primary vegetation type in the study area is an alpine meadow with *Kobresia pgymaea* as the dominant species, and *Kobresia humilis*, *Stipa aliena*, *Festuca ovina*, *Poa pratensis*, *Elymus nutans*, and *Leontopodium nanum*, as companion species. Harsh environments make alpine meadow habitats sensitive and fragile to climate change and human disturbances. Around one-quarter of the alpine meadow in the study sites have been degraded as "Black Beach" with severe soil erosion due to lowered coverage of pioneer plants such as *Aconitum flavum*, *Ligularia virgaurea*, *Pedicularis kansuensis*, and *Potentilla anserina* (Shang et al., 2018).

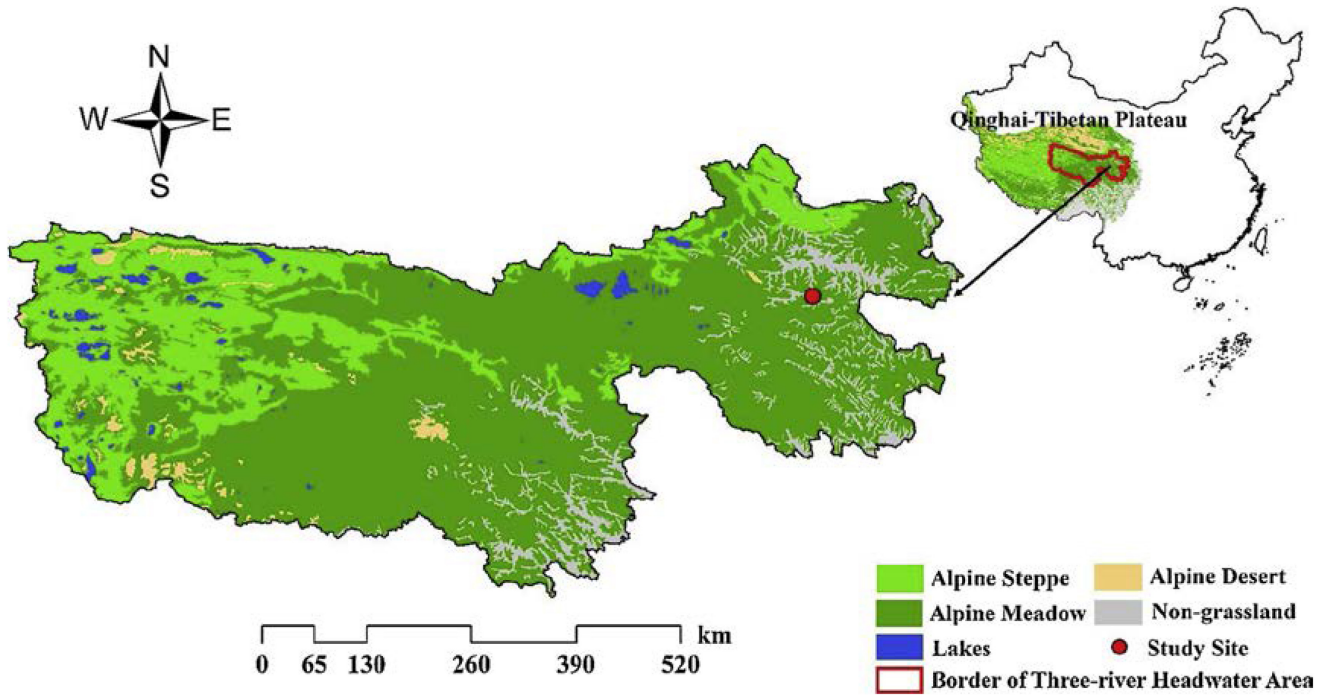

FIGURE 1 | Distribution of the study sites in the three river headwater area of Qinghai–Tibetan Plateau (Gao et al., 2019).

The severely degraded alpine meadow, "Black Beach" has been largely rebuilt with revegetated grasslands. Cultivated grassland (also called artificial grassland) is a new grassland community formed by planting one or more plants on the completely degraded grassland by using comprehensive agricultural technology. Over past decades, large areas of the "Black Beach" degraded grasslands have been restored with cultivated grassland under the governmental programs "Returning Grazing Land into Grassland" and "Grazing Ban" (Dong et al., 2013). With the support of a series of these restoration projects, numerous demonstration sites of cultivated grasslands with different restoration times have been established in the study area (Gao et al., 2019).

According to relevant information and as reported in the literature, in this study, we did the samplings based on the chronosequence/space-for-time approach in the cultivated grasslands, which were established in 2000 (A1), 2002 (A3), 2004 (A4), 2006 (A6), 2008 (A8), 2010 (A10), 2012 (A12), 2014 (A14), 2015 (A16), and 2017 (A18) and severely degraded alpine meadow (Black Beach, A0), and non-degraded healthy alpine meadow (ND). All the sampling plots in this study were located in the same demonstration study sample area accompanied by similar topography and geographical location. The planting area of each cultivated grassland was 50 hm^2. The cultivated grasslands by sowing *E. nutans* were all degraded grasslands on "Black Beach" and were built through deep turning, harrowing, fertilizing [45 kg/hm^2 of diammonium phosphate (NH_3HPO_4)], sowing (sowing amount was 45 kg/hm^2 local seed), covering soil, crushing, fencing, and other agronomic measures.

Field Survey

In mid-August 2017, five quadrats with an area of 1 m × 1 m were randomly selected from each plot for plant sampling and species identification. According to the classification method on the functional groups of alpine grassland plants (Wang et al., 2004), and in combination with the morphological and physiological characteristics of alpine grassland plants, we divided the species into four functional groups: Grass, Cyperaceae, Leguminosae, and the remaining species were classified as Forb (Yu et al., 2017; Zhao et al., 2017). The number of species, density, height, coverage, and frequency of individual species were estimated. In each plot, one subplot in the size of 0.5 m × 0.5 m was selected for sampling aboveground plant biomass, which was brought back to the laboratory and dried in an oven at 65°C to constant weight for measurement. After plant sampling, soil core samples were taken to a depth of 20 cm in each subplot.

Based on commonly used soil properties analysis test theory in the laboratory, we conducted experiments on the measurement of the following soil properties for each soil sample: total organic carbon (TC) and nitrogen content (TN) were tested by the elemental analyzer (Euro EA 3000, Italy), available phosphorus (AP) and available potassium (AK) were tested by an Inductive Coupled Plasma Emission Spectrometer (Germany). We also quantified soil moisture.

Data Analysis

We used the variables related to diversity, stability, and the plant interspecific association (network analysis) mentioned above for data analysis. In detail, for characterization of species

diversity and dominance structure, Pielou's evenness index (E), Shannon–Wiener diversity index (H), and Simpson's dominance (λ) index were calculated. Associated coefficient (AC) was used to characterize the degree of association among species (Fang et al., 2012). The range of AC is from -1 to 1. The closer the AC value is to 1, the stronger the positive association between species is. The closer the AC value is to -1, the stronger the negative association between species is. When the AC value is 0, the species are completely independent. So, we classified the inter-species relationships into three trends, positive inter-species association, negative inter-species association, and random inter-species association, respectively. The calculation of the above indices was conducted in R using the "vegan" package.

Stability (PS) was calculated as the inverse coefficient of variation, which was calculated *via* the ratio of the average biomass to the standard deviation (Strecker et al., 2016; Zhou et al., 2019). The importance value (IV) of individual species was calculated *via* the formula of IV = (C′+H′+P′)/3, where IV is the important value of each species, C′ is relative coverage, H′ is relative height, and P′ is relative frequency.

The network analysis method was used to identify the species connection in the plant community. In the network, each species was considered as a node. We used the SPAA package in R to calculate the inter-species relationship matrix, which was treated as the basic data of sub-group analysis. The modular analysis was performed to build the block model and simplify through the CONCER algorithm (convergent correlation) (Xie et al., 2019). Before drawing two complete sub-networks, we obtained the simplest network diagram that maintained the integrity of the network using UCINET 6.5 software, which is a social network analysis program containing a graphical illustration tool called Net-Draw, a program used widely to obtain the simplest network diagram of the plant community (Johnson, 1987; Thomas et al., 2007). The density is an indicator of the closeness of membership and betweenness centrality represented the ability of a member to act as an intermediary, that is, to what extent a node is located in the middle of other nodes in the network (Qin and Li, 2009). In the network of vegetation communities, the density reflects the closeness of the inter-species relationship in a vegetation community. The networks of interacting species are usually described in terms of hardiness and stability (Kleyer et al., 2018). Network density (*D*) was calculated as the ratio between the total actual lines presented in the network graphics and the potential lines (Wolfe, 1995). Betweenness Centrality (C_B) in the network was calculated *via* the formula (Wolfe, 1995):

$$C_B = 2\sum_{i=1}^{g}[C_B(n^8) - C_B(n_i)]/[(g-1)^2 - (g-2)],\ C_B(n_i) = \sum_{j<k} n_i/g_{iK}$$

Where *g* represents the number of nodes in the network diagram, g_{ik} represents the shortcut of member *i* to member *k*, $C_B(n_i)$ is the intermediary of node n_i, and $C_B(n^*)$ is the maximum node intermediation. Based on this, we calculated the network density (SND) and betweenness centrality (SNB) of the plant interspecific linkage network.

Statistical Analysis

The data were processed and analyzed using Microsoft Excel 2016, SPSS 22.0, R version 3.5.1, and R Studio version 1.1.456. Network analysis was performed using UCINET 6.5 software. Network analysis graphs were drawn with Net Draw.

We used 28 indicators including density (*D*), network indexes containing the complexity of plant interspecific association (network density: SND) and betweenness of plant interspecific linkage network (SNB), diversity indexes, which include the evenness indexes of the total community (E-T), Grass (E-G), Cyperaceae (E-C), Legume (E-L), and Forb (E-F); the diversity of whole community (H-T), Grass (H-G), Cyperaceae (H-C), Legume (H-L), and Forb (H-F); the proportional dominance of Grass (G_λ), Cyperaceae (C_λ), Legume (L_λ), and Fords(F_λ); the proportion of inter-specific associations of plant community containing positive inter-species associations (Positive); negative inter-species associations (Negative); random inter-species associations (Random); and stability indices which include the stability of the whole community (T-PS), Grass (G-PS), Cyperaceae (C-PS), Legume (L-PS), and Forb (F-PS) and soil properties containing the carbon (C) and nitrogen (N), available phosphorus (AP), available potassium (AK), and soil moisture of the soil samples.

To test the above-mentioned indicators as the influence of independent variables on the overall stability and to avoid redundancy, we used correlation analysis to filter the variables. For the same type of indicators with a correlation coefficient greater than 0.70, one of them was retained (Zhou et al., 2019). Finally, a structural equation model (SEM) was adopted to test the hypothetical model, which was established and tested using AMOS 4.0.

RESULTS

Plant Community Composition and Diversity Over Restoration Time

In each plot, the species with a 100% probability of occurrence are the grass *E. nutans*, the legume *Astragalus membranaceus* var. *membranaceus*, and the Forb *Potentilla multifida*. The dominant species was *E. nutans* (an indigenous grass planted) along restoration years except for the 8th year. The sub-dominant species changed greatly with the restoration time and the range of average species number of each plot (**Table 1**). Compared with "Black Beach," the species richness of cultivated grassland decreased by 9.2% in the first recovery year and increased from the second restoration year until the 8th restoration year. Over 10 years of restoration, plant species richness in the cultivated grassland tended to continuously increase. Through all restoration years, the number of species in the plant community of artificial grassland increased. Over 16 years, there was a high similarity of species composition between the cultivated grasslands at different restoration years and the non-degraded native grassland, and low similarity of species composition

TABLE 1 | Important species of the plot and their important values and proportion of comprehensive dominance of species in different functional groups.

Grassland types	Important value of species			Proportion of comprehensive dominance of species in different functional groups				Species richness
				Grass (G_λ)	Cyperaceae (C_λ)	Leguminosae (L_λ)	Fords (F_λ)	
Black Soil Beach A0	*Ligularia virgaurea* 3.2	*Artemisia hedinii* 2.5	*Oplopanax elatus* 2.0	0.19	0.43	0.17	0.20	30
1-year-old cultivated grassland A1	*Elymus nutans* 2.4	*Polygonum viviparum* 1.5	*Nepeta coerulescens* 1.4	0.45	0.00	0.35	0.20	23
3-year-old cultivated grassland A3	*Elymus nutans* 3.1	*Poa pratensis* 2.3	*Koeleria cristata* 2.1	0.19	0.00	0.51	0.29	32
4-year-old cultivated grassland A4	*Elymus nutans* 3.0	*Koeleria cristata* 1.9	*Poa pratensis* 1.9	0.36	0.22	0.30	0.12	33
6-year-old cultivated grassland A6	*Elymus nutans* 2.1	*Koeleria cristata* 2.0	*Poa pratensis* 1.8	0.19	0.41	0.23	0.17	34
8-year-old cultivated grassland A8	*Poa pratensis* 2.8	*Koeleria cristata* 2.0	*Elymus nutans* 1.9	0.30	0.32	0.26	0.12	39
10-year-old cultivated grassland A10	*Elymus nutans* 2.5	*Koeleria cristata* 2.2	*Poa pratensis* 1.9	0.17	0.38	0.32	0.12	37
12-year-old cultivated grassland A12	*Elymus nutans* 2.2	*Poa pratensis* 2.1	*Poa crymophila* 1.8	0.20	0.23	0.46	0.12	35
14-year-old cultivated grassland A14	*Elymus nutans* 3.1	*Koeleria cristata* 1.7	*Poa pratensis* 1.5	0.20	0.13	0.41	0.25	29
16-year-old cultivated grassland A16	*Elymus nutans* 2.7	*Pedicularis kansuensis* 2.0	*Poa crymophila* 1.8	0.30	0.08	0.41	0.21	32
18-year-old cultivated grassland A18	*Elymus nutans* 3.2	*Poa pratensis* 1.8	*Koeleria cristata* 1.8	0.27	0.35	0.26	0.13	35
Non-degraded grassland ND	*Elymus nutans* 2.3	*Poa pratensis* 1.5	*Ligularia virgaurea* 1.3	0.29	0.31	0.33	0.07	41

G_λ, C_λ, L_λ, and F_λ, respectively, represent the proportion of comprehensive dominance of Grass, Cyperaceae, Legume, and Forb in the sampling plots.

between the cultivated grasslands at different restoration years and the "Black Beach."

In the first 3 years after the cultivated grassland was built to replace the extremely degraded grassland, the proportion of comprehensive dominance of other functional groups except Cyperaceae increased. In the next 7 years, the proportion of dominance in Cyperaceae increased, while the proportion of other functional groups showed a fluctuating decrease trend. With the increase of recovery time, the dominance of Forb was close to 10%, while the dominance proportion of the other three functional groups was close to 30%, respectively (**Table 1**).

Inter-Specific Association of Plant Communities Over Restoration Time

We classified the inter-species relationships into three categories, positive inter-species association, negative inter-species association, and random inter-species association (**Figure 2A**). The proportion of species with random associations was higher than those of species with positive and negative associations in the plant community of all types of grasslands except "Black Beach." The proportion of species with positive associations was slightly greater than those with negative associations in all types of grasslands. Throughout the restoration time, the proportions of species with both positive and negative associations generally tended to decrease and those of species with random associations tended to increase, although there were great fluctuations of inter-species relations after 4 and 10 restoration years.

The SNB of extremely degraded grasslands and cultivated grasslands planted for 1 year was greater than 4. The SNB values of other cultivated grasslands were all about 2–3, while the value of non-degraded grasslands was the minimum of 1.268. The complexity of plant interspecific association (species network density) was positive for non-degraded alpine meadow and cultivated grassland communities were positive in the 6th, 12th, and 16th years, while in the "Black Beach" degraded grassland it was negative. Plant interspecific association indicated that a few species highly influenced the entire network (**Table 2**).

Internal Driving Forces of Plant Community Stability Over Restoration Time

In the first 3 years of grassland restoration, the plant stability in the revegetated areas was significantly lower than that of the "Black Beach" degraded grassland (**Figure 2B**). The stability of Grass was increased after 6 years of restoration. The change in the productivity of the Forb was quite low. The similarity coefficients between the stability of Grass, Cyperaceae, Leguminosae, Forb,

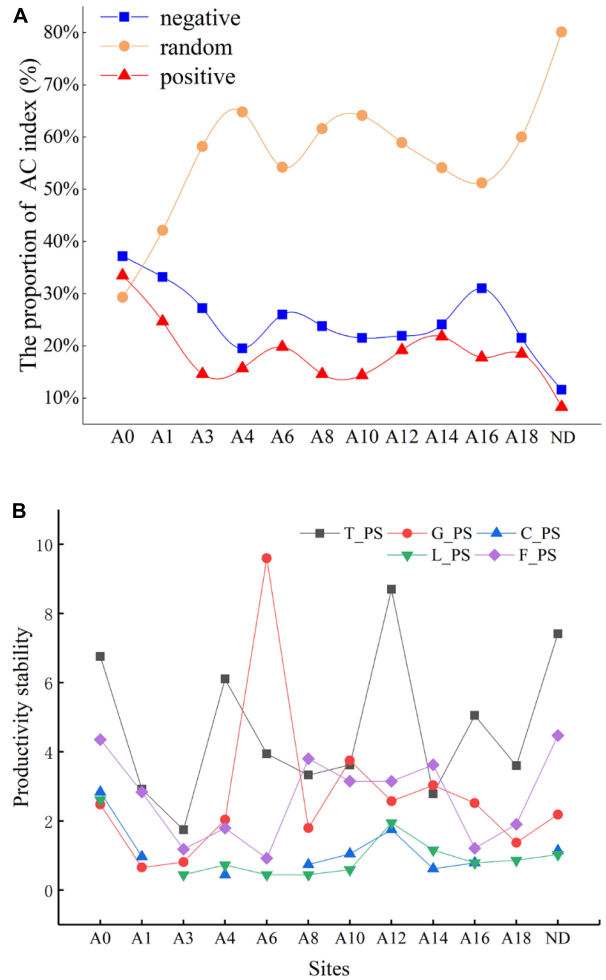

FIGURE 2 | Changes in the proportion of inter-specific associations of the plant community **(A)** and stability index of artificial grassland productivity **(B)** in different years of construction. T_PS, G_PS, C_PS, L_PS, and F_PS, respectively, represent the stability of the total community, Grass stability, Cyperaceae stability, Leguminosae stability, and Forb stability. The number after the letter "A" indicates the restoration period of artificial grassland, A0 represents "black beach" and ND represents a non-degraded healthy alpine meadow.

TABLE 2 | Network structure characteristics of cultivated grassland in different growing years.

Sites	SND	SNB
A0	−0.030	4.392
A1	−0.041	5.138
A3	−0.027	3.038
A4	−0.020	3.782
A6	0.011	3.03
A8	−0.021	2.706
A10	−0.019	2.501
A12	0.022	3.041
A14	−0.030	3.841
A16	0.000	2.708
A18	−0.003	3.214
ND	0.046	1.268

SND, the complexity of plant interspecific association (network density); SNB, betweenness of plant interspecific linkage network (simplest network betweenness). The number after the letter "A" indicates the restoration period of artificial grassland, A0 represents "black beach," and ND represents a non-degraded healthy alpine meadow.

TABLE 3 | The score matrix of the principal component analysis of the diversity of each functional group.

	Principal component			
	Legume	Cyperaceae	Grass	Forb
H_G				0.966
H_C		0.968		
H_L	0.972			
H_F			0.973	
E_G				0.979
E_C		0.984		
E_L	0.980			
E_F			0.985	
Factor	D-L	D-C	D-G	D-F

H-G, H-C, H-L, H-F, respectively, represent Shannon–Wiener diversity index of Grass, Cyperaceae, Legume, and Forb in the sampling plots; E-G, E-C, E-L, E-F, respectively, represent Pielou's evenness index of Grass, Cyperaceae, Legume, and Forb in the sampling plots; D-L, D-C, D-G, D-F, respectively, represent the diversity information of these four plant functional groups (Legume, Cyperaceae, Grass, Forb).

and the whole community were -0.158, 0.531, 0.659, and 0.368 respectively. The trend of stability of the whole community was similar to that of legumes, which was reflected by the greatest correlation among all plant groups.

The structural equation model was used to test the relationship and mediation between variables to study the influence mechanisms of plant community composition and diversity on grassland stability during the restoration process of alpine grassland. Since there was strong collinearity in the evenness and diversity of plant communities in different functional groups, eight factors including the evenness index of Grass (E-G), Cyperaceae (E-C), Leguminosae (E-L), Forb (E-F), Grass (H-G), Cyperaceae (H-C), Legumes (H-L), and Forb (H-F) were extracted and expressed as four principal components. We defined them as D-L, D-C, D-G, D-F, respectively, representing the diversity information of these four plant functional groups (Legume, Cyperaceae, Grass, Forb) (**Table 3**). Similarly, using the same analytical method, the total soil carbon (TC) and total soil nitrogen (TN), available phosphorus (AP), available potassium (AK), and soil moisture were extracted as two principal components. We defined them as soil nutrient and moisture, respectively (**Table 4**).

The results of the structural equation model indicated that compared with other functional groups, grass diversity had a more significant effect on the stability of the whole community during the restoration process of artificial grasslands (**Figure 3**). The restoration process of artificial grassland can directly affect or indirectly affect the species composition characteristics of the

TABLE 4 | Principal component analysis score matrix of each soil property index.

	Principal component	
	Soil nutrients	**Moisture**
AP	0.830	
AK	0.894	
C	0.921	
N	0.872	
Soil moisture		0.983

C, N, AP, and AK, respectively, represent the total soil carbon and total soil nitrogen, available phosphorus (AP), available potassium (AK), and soil moisture.

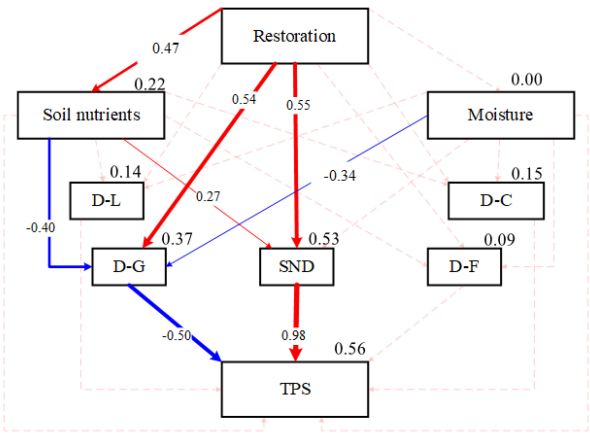

FIGURE 3 | Structural equation model analysis results of community composition, network structure, and community stability path for the recovery years. D-L, D-C, D-G, and D-F, respectively, represent the diversity information of these four plant functional groups (Legume, Cyperaceae, Grass, Forb); TPS, stability of whole community; SND, the complexity of plant interspecific association (network density); Restoration represents human-induced revegetated grassland restoration. The boxes are the variables of the model. The solid line indicates a significant effect ($P < 0.05$); the dotted line indicates an insignificant effect ($P > 0.05$); Chi_square = 8.40 ($P = 0.40$); GF1 = 0.97; RMSEA = 0.03.

community (i.e., the network structure based on the interspecific relationship) by changing the soil nutrient conditions, and thus significantly affect the overall stability of the community.

DISCUSSION

Revegetation with cultivated grassland has been widely accepted as the best way to improve "Black Beach" degraded alpine grassland (Li et al., 2018), as it can improve the vegetation and soil of extremely degraded grassland in a short period (Li et al., 2014; Xu et al., 2019). We also found in this study that "Black Beach" can be intuitively changed within 3 years of plantation, and the proportion of excellent forages increased with restoration. From this perspective, we may conclude that the development of cultivated grassland can effectively curb the expansion of "Black Beach" on the QTP.

Interspecific association reflects the relationship between species pairs and their adaptability to the environment (Liu et al., 2019). In this study, we found that the proportion of species with positive and negative correlations was reduced in the cultivated grasslands over the restoration time. Identifying the positive or negative association of inter-species associations was meaningful to interpret the inter-specific relationships of different species in the plant community (Lou and Zhao, 2008). Although the mechanisms that regulate species interactions have not been fully elucidated, Bulleri et al. (2014) reported that the increase of time fluctuation in environmental stressors can enhance the absolute pressure level perceived by the interacting species. Some scholars found that inter-specific competition usually plays a destabilizing role (Loreau and De Mazancourt, 2013; Michalet and Pugnaire, 2016), while we can deduce that the relationship between species interactions will tend to be neutral as restoration proceeds in the cultivated grassland. Our findings are supported by Lou and Zhao's (2008) study that mutual dependence and mutual competition in the plant community are greatly reduced and weakened in the long-term succession process. In later stages of restoration, each species occupies a narrower niche, so the plant community is stable with the harmonious coexistence of species. With the increase of restoration time, the inter-specific association of most species in cultivated grassland tends to be zero, which was highly related to the natural performance of plant communities. After 4 years of restoration, the number of unconnected species in the community decreased, indicating that the community was susceptible to external interferences (such as human disturbance and livestock feeding) and tended to reverse succession.

Plant composition is the most intuitive feature that determines the appearance, structure, and function of the grassland community, and even its successional direction (Wei et al., 2011; Guo et al., 2019). We hypothesize that the composition and structure of species may be the internal driving force for the change of community stability. Most experiments showed that exaggerated species diversity can promote increased stability of productivity over time (Hautier et al., 2014), for example, Río et al. (2017) reported from a study on European forests that changes in community composition can change the temporal stability of community productivity, and external and internal factors affecting the species composition may impact the stability of community productivity (Gross et al., 2014). With the progress of related research, scientists have also emphasized the important role of species composition and inter-specific relationships (Isbell et al., 2009; Klanderud, 2010; Loreau and De Mazancourt, 2013; de Mazancourt et al., 2013). In theoretical ecology, traditional research based on dynamic stability and numerical simulation has not found a unified answer to explain the impact of network architecture on community persistence (Rohr et al., 2014). All of these can be used as evidence to support the importance of species composition and interspecific relationships in influencing community stability and even ecosystem services and functions (Johnson et al., 2008; Maselli et al., 2013; Pellissier et al., 2018; Zeeman et al., 2019). Social network analysis methods based on interspecies relationships may provide a quantitative means for exploring the characteristics of community structure for future studies of grassland communities on the QTP.

CONCLUSION

With the extension of planting time, the relationship between species interactions of cultivated grasslands for replacing "Black Beach" on the QTP will become more neutral. In the present study, we found that the complexity of plant interspecific association (species network density) had more influence on community stability with the extension of recovery time. The novel method of quantifying the structural characteristics of a community for gauging its stability can provide a quantitative way to explore the characteristics of community structure. The plant species network that is based on species interaction is needed to support the applicable and efficient revegetation actions, for which restoring the severely degraded alpine grasslands on the QTP and even worldwide is essential.

DATA AVAILABILITY STATEMENT

The original contributions presented in the study are included in the article/supplementary material, further inquiries can be directed to the corresponding authors.

AUTHOR CONTRIBUTIONS

SW and SL: conceptualization. SW: methodology, software, validation, formal analysis, resources, data curation, writing—original draft preparation, and visualization. SW, XG, and YX: investigation. SD and LW: writing—review and editing and funding acquisition. SD and KW: supervision. SD and QD: project administration. All authors contributed to the article and approved the submitted version.

FUNDING

This research was financially supported by the Second Tibetan Plateau Scientific Expedition and Research Program (2019QZKK0307), the National Key R&D Program of China (2021FED1124000), the Key R&D Program of Qinghai Province (2018-NK-A2), the Qinghai innovation platform construction project (2017-ZJ-Y20), and the National Scientific Foundation of China (31960249 and 31400391).

REFERENCES

Bai, Y. F., Han, X. G., Wu, J. G., Chen, Z. Z., and Li, L. H. (2004). Ecosystem stability and compensatory effects in the Inner Mongolia grassland. *Nature* 431, 181–184. doi: 10.1038/nature02850

Bulleri, F., Xiao, S., Maggi, E., and Benedetti-Cecchi, L. (2014). Intensity and temporal variability as components of stress gradients: implications for the balance between competition and facilitation. *Oikos* 123, 47–55. doi: 10.1111/j.1600-0706.2013.00604.x

Byrne, C., and Jones, M. B. (2002). Effects of elevated CO_2 and Nitrogen fertiliser on biomass productivity, community structure and species diversity of a semi–natural grassland in Ireland. *Biol. Environ. Proc. R. Irish Acad.* 102B, 141–150. doi: 10.1353/bae.2002.0005

Cleland, E. (2011). Biodiversity and ecosystem stability. *Nat. Educ. Knowledge* 3:14.

Cortois, R., Veen, G. F., Duyts, H., Abbas, M., Strecker, T., Kostenko, O., et al. (2017). Possible mechanisms underlying abundance and diversity responses of nematode communities to plant diversity. *Ecosphere* 8:e01719. doi: 10.1002/ecs2.1719

de Mazancourt, C., Isbell, F., Larocque, A., Berendse, F., De Luca, E., Grace, J. B., et al. (2013). Predicting ecosystem stability from community composition and biodiversity. *Ecol. Lett.* 16, 617–625. doi: 10.1111/ele.12088

Dong, Q. M., Zhao, X. Q., Wu, G. L., Shi, J. J., and Ren, G. H. (2013). A review of formation mechanism and restoration measures of "black-soil-type" degraded grassland in the Qinghai-Tibetan Plateau. *Environ. Earth Sci.* 70, 2359–2370.doi10.1007/s12665-013-2338-7

Dong, S. K., Lassoie, J., Wen, L., Zhu, L., Li, X. Y., Li, J. P., et al. (2012). Degradation of rangeland ecosystems in the developing world: tragedy of breaking coupled human-natural systems. *Int. J. Soc. Robot.* 4, 357–371. doi: 10.1007/s12369-012-0155-x

Eisenhauer, N., Milcu, A., Allan, E., Nitschke, N., Scherber, C., Temperton, V., et al. (2011). Impact of above- and below-ground invertebrates on temporal and spatial stability of grassland of different diversity. *J. Ecol.* 99, 572–582. doi: 10.1111/j.1365-2745.2010.01783.x

Fang, F., Hu, Y. K., Zhang, W., Gong, Y. M., Liu, Y. Y., and Yang, X. J. (2012). Numerical analysis of inter-specific relationships in Alpine steppe community in Bayanbulak. *Acta Ecol. Sin.* 32, 1898–1907. doi: 10.5846/stxb201102170182

Feng, R. Z., Long, R. J., Shang, Z. H., Ma, Y. Z., Dong, S. K., and Wang, Y. L. (2010). Establishment of Elymus natans improves soil quality of a heavily degraded alpine meadow in Qinghai-Tibetan Plateau, China. *Plant Soil* 327, 403–411. doi: 10.1007/s11104-009-0065-3

Gao, X. X., Dong, S. K., Xu, Y. D., Wu, S. N., Wu, X. H., Zhang, X., et al. (2019). Resilience of revegetated grassland for restoring severely degraded alpine meadows is driven by plant and soil quality along recovery time: a case study from the Three-river Headwater Area of Qinghai-Tibetan Plateau. *Agric. Ecosyst. Environ.* 279, 169–177. doi: 10.1016/j.agee.2019.01.010

Gross, K., Cardinale, B. J., Fox, J. W., Gonzalez, A., Loreau, M., Polley, H. W., et al. (2014). Species richness and the temporal stability of biomass production: a new analysis of recent biodiversity experiments. *Am. Nat.* 183, 1–12. doi: 10.1086/673915

Guo, N., Degen, A. A., Deng, B., Shi, F., Bai, Y., Zhang, T., et al. (2019). Changes in vegetation parameters and soil nutrients along degradation and recovery successions on alpine grasslands of the Tibetan plateau. *Agric. Ecosyst. Environ.* 284:106593. doi: 10.1016/j.agee.2019.106593

Hautier, Y., Seabloom, E. W., Borer, E. T., Adler, P. B., Harpole, W. S., Hillebrand, H., et al. (2014). Eutrophication weakens stabilizing effects of diversity in natural grasslands. *Nature* 508, 521–525. doi: 10.1038/nature13014

Isbell, F. I, Polley, H. W., and Wilsey, B. J. (2009). Biodiversity, productivity and the temporal stability of productivity: patterns and processes. *Ecol. Lett.* 12, 443–451. doi: 10.1111/j.1461-0248.2009.01299.x

Isbell, F. I. (2010). *Processes that Influence Biodiversity, Ecosystem Functioning, and Stability in Grasslands*. Ann Arbor, MI: Iowa State University.

Johnson, D., Phoenix, G. K., and Grime, J. P. (2008). Plant community composition, not diversity, regulates soil respiration in grasslands. *Biol. Lett.* 4, 345–348. doi: 10.1098/rsbl.2008.0121

Johnson, J. D. (1987). UCINET - A software tool for network analysis. *Commun. Educ.* 36, 92–94. doi: 10.1080/03634528709378647

Klanderud, K. (2010). Species recruitment in alpine plant communities: the role of species interactions and productivity. *J. Ecol.* 98, 1128–1133. doi: 10.1111/j.1365-2745.2010.01703.x

Kleyer, M., Trinogga, J., Cebrián-Piqueras, M. A., Trenkamp, A., Fløjgaard, C., Ejrnæs, R., et al. (2018). Trait correlation network analysis identifies biomass allocation traits and stem specific length as hub traits in herbaceous perennial plants. *J. Ecol.* 107, 1–14. doi: 10.1111/1365-2745.13066

Li, W., Wang, J. L., Zhang, X. J., Shi, S. L., and Cao, W. X. (2018). Effect of degradation and rebuilding of artificial grasslands on soil respiration and carbon and nitrogen pools on an alpine meadow of the Qinghai-Tibetan Plateau. *Ecol. Eng.* 111, 134–142. doi: 10.1016/j.ecoleng.2017.10.013

Li, X. L., Perry, G. L. W., Brierley, G., Sun, H. Q., Li, C. H., and Lu, G. X. (2014). Quantitative assessment of degradation classifications for degraded

alpine meadows (heitutan), SanJiangYuan, western China. *Land Degrad. Dev.* 25, 417–427. doi: 10.1002/ldr.2154

Liu, B., Zhao, W. Z., and Meng, Y. Y. (2018). Biodiversity, productivity, and temporal stability in a natural grassland ecosystem of China. *Sci. Cold Arid Regions* 10, 293–304.

Liu, J. H., Wang, Z. W., Han, G. D., and Environment, R. A. (2019). Effects of heavy grazing on the interspecific relationship of main plant species and community stability in a desert steppe. *Chin. J. Ecol.* 38, 2595–2602.

Liu, S. B., Zamanian, K., Schleuss, P., Zarebanadkouki, M., and Kuzyakov, Y. (2018). Degradation of Tibetan grasslands: consequences for carbon and nutrient cycles. *Agric. Ecosyst. Environ.* 252, 93–104. doi: 10.1016/j.agee.2017.10.011

Loreau, M., and De Mazancourt, C. (2013). Biodiversity and ecosystem stability: a synthesis of underlying mechanisms. *Ecol. Lett.* 16, 106–115. doi: 10.1111/ele.12073

Lou, Y. J., and Zhao, K. Y. (2008). Analysis of inter-specific associations of *Carex lasiocarpa* community in recent 30-year succession in Sanjiang Plain. *Chin. J. Ecol.* 27, 509–513.

Lv, S. J., Yan, B. L., Wang, Z. W., Wang, Z. W., and Han, G. D. (2020). Dominant species' dominant role and spatial stability are enhanced with increasing stocking rate. *Sci. Total Environ.* 730:138900. doi: 10.1016/j.scitotenv.2020.138900

Maselli, F., Argenti, G., Chiesi, M., Angeli, L., and Papale, D. (2013). Simulation of grassland productivity by the combination of ground and satellite data. *Agric. Ecosyst. Environ.* 165, 163–172. doi: 10.1016/j.agee.2012.11.006

Michalet, R., and Pugnaire, F. I. (2016). Facilitation in communities: underlying mechanisms, community and ecosystem implications. *Funct. Ecol.* 30, 3–9. doi: 10.1111/1365-2435.12602

Pallett, D. W., Pescott, O. L., and Schäfer, S. M. (2016). Changes in plant species richness and productivity in response to decreased nitrogen inputs in grassland in southern England. *Ecol. Indic.* 68, 73–81. doi: 10.1016/j.ecolind.2015.12.024

Pellissier, L., Albouy, C., Bascompte, J., Farwig, N., Graham, C., Loreau, M., et al. (2018). Comparing species interaction networks along environmental gradients. *Biol. Rev.* 93, 785–800. doi: 10.1111/brv.12366

Qin, X. J., and Li, C. B. (2009). Social network analysis research of virtual learning community. *Mod. Educ. Technol.* 19, 26–29.

Río, M. D., Pretzsch, H., Ruíz-Peinado, R., Ampoorter, E., and Bravo-Oviedo, A. (2017). Species interactions increase the temporal stability of community productivity in *Pinus sylvestris-Fagus sylvatica* mixtures across Europe. *J. Ecol.* 105, 1032–1043. doi: 10.1111/1365-2745.12727

Rohr, R. P., Saavedra, S., and Bascompte, J. (2014). On the structural stability of mutualistic systems. *Science.* 345:1253497. doi: 10.1126/science.1253497

Shang, Z. H., Dong, Q. M., Shi, J. J., Zhou, H. K., Dong, S. K., Shao, X. Q., et al. (2018). Research progress in recent ten years of ecological restoration for 'Black Soil Land' degraded grassland on Tibetan Plateau——Concurrently discuss of ecological restoration in Sangjiangyuan Region. *Acta Agrestia Sin.* 26, 1–21.

Shen, H., Dong, S. K., Li, S., Xiao, J. N., Han, Y. H., Yang, M. Y., et al. (2019). Grazing enhances plant photosynthetic capacity by altering soil nitrogen in alpine grasslands on the Qinghai-Tibetan plateau. *Agric. Ecosyst. Environ.* 280, 161–168. doi: 10.1016/j.agee.2019.04.029

Strecker, T., Macé, O. G., Scheu, S., and Eisenhauer, N. (2016). Functional composition of plant communities determines the spatial and temporal stability of soil microbial properties in a long-term plant diversity experiment. *Oikos.* 125, 1743–1754. doi: 10.1111/oik.03181

Thomas, J. C., Isler, M. R., Carter, C., and Torrone, E. (2007). An interagency network perspective on HIV prevention. *Sex. Transm. Dis.* 34, 71–75. doi: 10.1097/01.olq.0000223281.30734.b1

Wang, C. T., Long, R. J., and Ding, L. M. (2004). The effects of differences in functional group diversity and composition on plant community productivity in four types of alpine meadow communities. *Biodiv. Sci.* 12, 403–409. doi: 10.17520/biods.2004049

Wang, C. T., Wang, G. X., Liu, W., Wang, Y., Hu, L., and Ma, L. (2013). Effects of establishing an artificial grassland on vegetation characteristics and soil quality in a degraded meadow. *Isr. J. Ecol. Evol.* 59, 141–153. doi: 10.1080/15659801.2013.863669

Wang, X. X., Dong, S. K., Sherman, R., Liu, Q. R., Liu, S. L., Li, Y. Y., et al. (2015). A comparison of biodiversity–ecosystem function relationships in alpine grasslands across a degradation gradient on the Qinghai–Tibetan Plateau. *Rangeland J.* 37, 44–45. doi: 10.1071/RJ14081

Wei, Z. J., Li, X., Liu, H. M., Wu, Q. Q., and Lv, S. J. (2011). Response of meadow steppe community characteristics to different grazing systems in Hulunbeir. *Chin. J. Grassland* 33, 65–70.

Wolfe, A. W. (1995). Social network analysis: methods and applications. *Contemp. Sociol. J. Rev.* 24, 219–220. doi: 10.1525/ae.1997.24.1.219

Xie, Y. X., Zeng, W. H., and Ma, B. R. (2019). Social network analysis of governance types of global protected areas. *Acta Ecol. Sin.* 39, 1394–1406. doi: 10.5846/stxb201808261827

Xu, Y. D., Dong, S. K., Gao, X. X., Yang, M. Y., Li, S., Shen, H., et al. (2019). Trade-offs and cost-benefit of ecosystem services of revegetated degraded alpine meadows over time on the Qinghai-Tibetan Plateau. *Agric. Ecosyst. Environ.* 279, 130–138. doi: 10.1016/j.agee.2019.04.015

Yang, S., Feng, Q., Liang, T., Liu, B., Zhang, W., and Xie, H. (2018). Modeling grassland above-ground biomass based on artificial neural network and remote sensing in the Three-River Headwaters Region. *Agric. Ecosyst. Environ.* 204, 448–455. doi: 10.1016/j.rse.2017.10.011

Yu, H. L., Fan, W. J., Zhong, H. P., and Li, Y. Z. (2017). Characteristics of N and P stoichiometry of plants in different functional groups in the Qinghai-Tibet Plateau regions. *Acta Ecol. Sin.* 37, 3755–3764. doi: 10.5846/stxb201604040609

Zeeman, M. J., Shupe, H., Baessler, C., and Ruehr, N. K. (2019). Productivity and vegetation structure of three differently managed temperate grasslands. *Agric. Ecosyst. Environ.* 27, 129–148. doi: 10.1016/j.agee.2018.10.003

Zeng, C. X., Wu, J. S., and Zhang, X. Z. (2015). Effects of grazing on above- vs. below-ground biomass allocation of Alpine Grasslands on the Northern Tibetan Plateau. *PLoS One* 10:e0135173. doi: 10.1371/journal.pone.0135173

Zhao, G. S., Shi, P. L., Wu, J. S., Xiong, D. P., Zong, N., and Zhang, X. Z. (2017). Foliar nutrient resorption patterns of four functional plants along a precipitation gradient on the Tibetan Changtang Plateau. *Ecol. Evol.* 7, 7201–7212. doi: 10.1002/ece3.3283

Zhao, Y. N., Yang, B., Li, M. X., Xiao, R. Q., Rao, K. Y., Wang, J. Q., et al. (2018). Community composition, structure and productivity in response to nitrogen and phosphorus additions in a temperate meadow. *Sci. Total Environ.* 654, 863. doi: 10.1016/j.scitotenv.2018.11.155

Zhou, B. G., Li, S., Li, F., Dong, S. K., Ma, F. L., Zhu, S. C., et al. (2019). Plant functional groups asynchrony keep the community biomass stability along with the climate change- a 20-year experimental observation of alpine meadow in eastern Qinghai-Tibet Plateau. *Agr. Eco. Env.* 282, 49–57. doi: 10.1016/j.agee.2019.06.002

Zhou, J., Deng, Y., Luo, F., He, Z., and Yang, Y. (2011). Phylogenetic molecular ecological network of soil microbial communities in response to elevated CO_2. *MBio* 2, 534–544. doi: 10.1128/mBio.00122-11

Conflict of Interest: The authors declare that the research was conducted in the absence of any commercial or financial relationships that could be construed as a potential conflict of interest.

Publisher's Note: All claims expressed in this article are solely those of the authors and do not necessarily represent those of their affiliated organizations, or those of the publisher, the editors and the reviewers. Any product that may be evaluated in this article, or claim that may be made by its manufacturer, is not guaranteed or endorsed by the publisher.

Copyright © 2022 Wu, Wen, Dong, Gao, Xu, Li, Dong and Wessell. This is an open-access article distributed under the terms of the Creative Commons Attribution License (CC BY). The use, distribution or reproduction in other forums is permitted, provided the original author(s) and the copyright owner(s) are credited and that the original publication in this journal is cited, in accordance with accepted academic practice. No use, distribution or reproduction is permitted which does not comply with these terms.

frontiers in Plant Science

ORIGINAL RESEARCH
published: 23 March 2022
doi: 10.3389/fpls.2022.848691

Phosphorus Shapes Soil Microbial Community Composition and Network Properties During Grassland Expansion Into Shrubs in Tibetan Dry Valleys

Hanchang Zhou[1,2], Anzhou Ma[1,2], Xiaorong Zhou[1,2], Xianke Chen[1,2], Jiejie Zhang[1,2], Qinwei Zhang[1,2], Xiangning Qi[1,2], Guohua Liu[1,2] and Guoqiang Zhuang[1,2]**

[1] Research Centre for Eco-Environmental Sciences, Chinese Academy of Sciences, Beijing, China, [2] College of Resources and Environment, University of Chinese Academy of Sciences, Beijing, China

OPEN ACCESS

Edited by:
Jian Sun,
Institute of Tibetan Plateau Research (CAS), China

Reviewed by:
Gengxin Zhang,
Institute of Tibetan Plateau Research (CAS), China
He Yixin,
Key Laboratory of Mountain Ecological Rehabilitation and Biological Resource Utilization, Chengdu Institute of Biology (CAS), China

***Correspondence:**
Anzhou Ma
azma@rcees.ac.cn
Guoqiang Zhuang
gqzhuang@rcees.ac.cn

Specialty section:
This article was submitted to Functional Plant Ecology, a section of the journal Frontiers in Plant Science

Received: 04 January 2022
Accepted: 11 February 2022
Published: 23 March 2022

Citation:
Zhou H, Ma A, Zhou X, Chen X, Zhang J, Zhang Q, Qi X, Liu G and Zhuang G (2022) Phosphorus Shapes Soil Microbial Community Composition and Network Properties During Grassland Expansion Into Shrubs in Tibetan Dry Valleys. Front. Plant Sci. 13:848691. doi: 10.3389/fpls.2022.848691

Alpine ecosystem stability and biodiversity of the Tibetan plateau are facing threat from dry valley vegetation uplift expansion, a process which is highly connected to variations in the soil microbial community and soil nutrients. However, the variation of microbial community properties and their relationship to soil nutrients have scarcely been explored in Tibetan dry valleys, which is a gap that hampers understanding the dry valley ecosystem's response to vegetation change. In this study, we sampled grasslands (G), a grass-shrub transition area (T), and shrublands (S) along an uplift expansion gradient and investigated the link between microbial community properties and soil nutrients. The results showed that shrub degradation by grass expansion in Tibetan dry valley was accompanied by increasing relative phosphorus (P) limitation, which was the main driver for bacterial and fungal composition variation as it offered highest total effect on PC1 (0.38 and 0.63, respectively). Total phosphorus (TP) was in the center module of bacterial and fungal network under shrub soil and even acted as key nodes in fungal networks. During the replacement by grass, TP was gradually marginalized from both bacterial and fungal center network module and finally disappeared in networks, with ammonia and nitrate gradually appearing in the bacterial network. However, TC and total nitrogen (TN) were always present in the center modules of both fungal and bacterial network. These support that a TP variation-induced compositional and network functional shift in the microbial community was a potential reason for vegetation uplift expansion in Tibetan dry valley. This study highlighted the effect of TP on microbial community properties during dry valley vegetation uplift expansion and offered basic information on Tibetan alpine dry valley ecosystem's response to climate change.

Keywords: phosphorus, composition, network, Tibetan dry valleys, soil microbial community

INTRODUCTION

Dry valleys are important components of the Tibetan plateau alpine ecosystem (Li, 2001; Zhao et al., 2015). Compared with other alpine ecosystems, the main vegetation of Tibetan dry valley is grass and shrub (Li, 2001; Zhao et al., 2015), in which the relatively lower biodiversity leads dry valley vegetation sensitive to climate change (Li, 2001; Zhao et al., 2015). Since the 1930s, the dry valley

vegetation in Tibet plateau has shown an uplift expansion of over 300 m (Li, 2001; Zhao et al., 2015), with continued invasion and replacement of other alpine ecosystems, severely threatening the stability and biodiversity of the entire Tibetan plateau (Liu and Zhu, 2016). Unfortunately, very little research has focused on dry valley ecosystems as compared with other alpine ecosystems, especially on the aspect of lower grass uplift expansion into higher shrub (Qiong et al., 2010; Liu and Zhu, 2016), which deeply hampers the comprehensive understanding to the reasons and mechanisms of dry valley ecosystem's response to current vegetation change, as well for local biodiversity conservation (Lindenmayer and Fischer, 2007; Harris et al., 2018).

The vegetation expansion between shrub and grass is always accompanied by the change in phosphorus (P) and the chemical stoichiometry (Yong et al., 2018; Gao et al., 2021), as shrub commonly had higher P content in biomass and higher P demand than grass (Yang et al., 2016; Carrillo et al., 2017). In nature terrestrial ecosystem, P originates from slow weathering of parental material and atmosphere ash deposition, cycles in different nutrient pools, and relocates in soil profiles (Walker and Syers, 1976; Canfield et al., 2005). To meet the higher P demand, shrubs uptake deep soil layer P into biomass *via* the root and release P as litters, which lead P accumulate in topsoil (Yong et al., 2018; Gao et al., 2021). Then, rain water moves the topsoil P downward into deeper active root area, and the P can be absorbed by shrub again (Walker and Syers, 1976; Canfield et al., 2005). Thus, a rapid, high-mobile P fraction-containing cycling was formed to benefit shrub dominance (Dinh et al., 2017).

The soil microbial community plays an irreplaceable role in accelerating the P cycle and improving high-mobile P fraction (Walker and Syers, 1976; Canfield et al., 2005). Microorganisms release extracellular enzymes and organic compounds to dissolute P-containing minerals and to mineralize litter organic P, thus enhancing the soil phosphate content (Walker and Syers, 1976; Canfield et al., 2005). Microorganisms also act as a temporally available P sink through microbial uptake and anabolism (Turner et al., 2013; Dinh et al., 2017). As a high richness system comprised fast reproductive potential members, the composition and function of the microbial community are sensitive to moisture and temperature variation, which makes it a contributor to soil nutrient content variation under climate change (Curtis, 2006; Singh et al., 2010; de Vries and Ashley, 2013). For example, frequent dry-wet cycling under an increasing irregular precipitation pattern stimulated microbial nitrification and denitrification, accelerating soil nitrogen loss as N_2O and N_2 (Kuypers et al., 2018). Rising temperature directly stimulates microbial community respiration and reduces soil carbon storage (Dong and Somero, 2009; Crowther et al., 2016). Thus, the P -related microbial community's composition and functional changes are potential reasons for the grass-shrub expansion happened in Tibetan alpine dry valley. However, till present, there is still scarce research that had elucidated the microbial community change under such situation.

To fill the gap mentioned above, topsoil along the grass-shrub expansion gradient was sampled from a typical dry valley ecosystem located in the eastern edge of Tibetan plateau, and the soil microbial community's property variations were explored. We hypothesized that (1) shrub degradation caused by grass uplift expansion is accompanied by decreasing topsoil P; (2) the P change is correlated with soil microbial composition; and (3) the microbial network in shrub soil tends to focus more on P.

MATERIALS AND METHODS

Site Description and Sampling

Photos of the sampling sites are shown in **Supplementary Figure 1**, from low elevation to high elevation; grassland (G) (28°40′58.05″N, 101°12′8.56″E, 2,212 m), transition area of grass and shrubs (T) (28°40′59.38″N, 101°12′1.91″E, 2,340 m), and shrubland (S) (28°41′0.18″N, 101°11′55.16″E, 2,450 m) were sampled, respectively. The sites were located on an eastern facing slope above the Yalong River, near Bowo village (Sichuan Province); the slope degree ranged from ∼10°–45°. The mean annual temperature was about 11.59°C, and the mean annual precipitation was about 820 mm; climatic data were extracted from the "WorldClim-Global Climate Data"[1]. The soil samples were collected in August 2020. Ten composite samples (minimum of 10 m between samples) were collected uniformly at each site from 1 m × 1 m square to cover the within-site variability. For each composite sample, approximately 500 g top soil (0–10 cm) of each sampling spots were cored from 4 corners and the center of the square and thoroughly mixed. After roughly removing plant debris, small rocks, and animal bodies, ∼500 g was packed and stored in an ice box. The samples were transported at 4°C to the laboratory as soon as possible, after which, all samples were passed through the 2 mm sieves and divided into two parts, with one portion stored at −80°C for molecular analyses and the other portion stored at 4°C for the analysis of soil physicochemical property.

Basic Soil Abiotic Properties Measurement

Soil pH was measured using a pH meter (FE20-FiveEasyTM pH, MettlerToledo, Germany) after shaking a soil water (1:2.5 w/v) suspension for 30 min (Guo et al., 2017; Zhou et al., 2022). Soil moisture was measured gravimetrically (Guo et al., 2017; Zhou et al., 2022). Total carbon (TC) and total nitrogen (TN) contents were measured using an elemental analyzer (VarioMAX, Elementar, Germany) (Guo et al., 2017; Zhou et al., 2022). Ammonium (NH_4^+-N) and nitrate (NO_3^--N) were extracted at a ratio of 10 g fresh soil to 50 ml 2 mol L^{-1} KCl. After shaking under 180 r min^{-1} for 1 h, NH_4^+-N and NO_3^--N contents in the filtered extracts were analyzed using a continuous flow analytical system (San^{++} System, Skalar, Holland) (Guo et al., 2017; Zhou et al., 2022). Total phosphorus (TP) content was measured using the alkali fusion-Mo-Sb antispectrophotometric method (Guo et al., 2017; Zhou et al., 2022).

DNA Extraction and Sequencing

Soil DNA was extracted according to the manufacturer's protocol using the FastDNA^{TM} SPIN kit (MP Biomedicals);

[1]http://www.worldclim.org/

the DNA concentrations and quality were checked using a Nano-100 NanoDrop spectrophotometer. Primers for 16S rRNA gene amplification targeted the V3-V4 hypervariable region and included 338F 5′-ACTCCTACGGGAGGCAGCA-3′ and 806R 5′-GGACTACHVGGGTWTCTAAT-3′ (Mori et al., 2014). The primers for ITS2 region amplification included 3F 5′-GCATCGATGAAGAACGCAGC-3′ and 4R 5′-TCCTCCGCTTATTGATATGC-3′ (Toju et al., 2012). PCR amplification was performed in 50.0 μl reaction systems containing 25.0 μl of Premix Taq DNA polymerase, 0.5 μl of the forward primer (20 mM), 0.5 μl of the reverse primer (20 mM), 23.0 μl of double-distilled water (ddH_2O), and 1.0 μl of the DNA template (20 ng total DNA) (Liu et al., 2021). Amplicons were pooled in equimolar ratios and paired-end sequenced on the Illumina Nova6000 platform (Majorbio Company, Shanghai). Majorbio Cloud Platform[2] was used to conduct all of the sequence bioinformatic scripts; sequences were merged with a minimum overlap length of 20 bp into full-length sequences by FLASH after removing barcodes and primers (Magoč and Salzberg, 2011; Kai et al., 2017). UPARSE was used to remove chimeras and cluster operational taxonomic units (OTUs) defined at the 97% similarity level (Edgar, 2013). The bacterial OTUs were annotated according to the Sliva-138 database, while the fungal OTUs were annotated according to the UNITE-8.0 database. Reads number of 26,349 (bacterial) and 101,210 (fungal) sequences were randomly selected from each sample to form an evenly resampled OTU table for further analysis. The raw sequences were uploaded onto NCBI, and the project numbers are listed in **Supplementary Table 1**.

Data Analysis

Network analyses were conducted according to the molecular ecological network analysis pipeline (MENA[3]) protocols. The top 1,000 relative abundance bacterial OTUs (BOTUs) and all fungal OTUs (FOTUs) were selected for bacterial and fungal network construction, respectively, as they covered over 90% of the total reads and appeared in every sample, which meant they could provide meaningful information for network construction. The construction parameters for the bacterial network were set as majority = 10, missing fill = fill paired (0.0100), logarithm = y, and similarity = pcc. The construction parameters for the fungal network were set as majority = 8, missing fill = fill paired (0.0100), logarithm = y, and similarity = pcc. The threshold values ranging from 0.01 to 0.99 over 0.01 intervals were applied to the Pearson correlation matrix for all three sites to scan for plausible network models, and cutoff threshold values of 0.92 ± 0.01 for bacterial network and 0.75 for fungal network were used to maintain a similar interaction strength comparison among the three different elevation sites ($p > 0.05$). Nodes with Pi (among-module connectivity) > 0.625 were divided into connectors, nodes of Zi (within-module connectivity) > 2.5 were divided into module hubs, and nodes of both Pi > 0.625 and Zi > 2.5 were divided into network hubs or were peripherals (Deng and Zhou, 2015; Xie et al., 2020). The constructed networks were visualized using the Cytoscape 3.3.0 software. Nearly, all parameters between the empirical networks and their corresponding random networks had significant differences, which indicated a plausible network construction and analysis (**Supplementary Table 2**). The statistically significant differences in basic soil properties and diversity indices among sites were measured using one-way ANOVA (Tamhane's T2 test and Tukey's HSD according to normality and homoscedasticity of data). Calculations of richness, Shannon index, and principal coordinates analysis (PCoA) based on Bray-Curtis distances at the OTU level were conducted with the online platform https://cloud.majorbio.com using R base (Edwards et al., 2015). The coordinates of the main axes, PC1 and PC2, from the PCoA analysis results for bacterial and fungal community were selected as community structure indicators to conduct further analysis, and the analysis of similarities (ANOISM) test was adopted to check the composition differences among the three sites; the $p < 0.001$ indicated significant compositional differences among sites (He and Xie, 2020). The scanning electron microscopic (SEM) analysis was conducted using the Amos software (Kline et al., 2011). Factor extractions were conducted using a Pearson correlation matrix in the SPSS software suite (version 24) (Ramette, 2007; Xie et al., 2020). In SEM, P limitation was extracted from C:P and N:P (molar ratio), two common indicators for measuring relative P limitation. The previous research has reported that global soil C:N:P stoichiometry averaged around 186:13:1 and soil microbial C:N:P stoichiometry averaged around 60:7:1 (Cleveland and Liptzin, 2007). The overly high C:P and N:P values are signs of soil P limitation, and the increasing C:P and N:P values indicate the enhanced relative P limitation to carbon and nitrogen (Cleveland and Liptzin, 2007). The variation from C:P and N:P was 0.96, and in total, they offered 91.42% explanation power. N resources were extracted from nitrate and ammonia; the variation from them was 0.84, and they offered 71.20% explanation power in total. Diversity was represented by bacterial or fungal Shannon indices in the corresponding SEMs. Composition was represented by bacterial or fungal PC1 of the PCoA analysis results in the corresponding SEM.

RESULTS

Basic Abiotic and Biotic Properties Variation

During replacement of shrubland by grassland, the relative P limitation (C:P and N:P) gradually increased due to the significant change in TP and TN. TP in S was about 0.8 times higher than T and G ($p < 0.05$). On the contrary, TN showed an increasing trend from S (0.10% ± 0.04%) to T (0.12% ± 0.02%) and G (0.15% ± 0.06%), and S was significantly lower than G ($p < 0.05$). Thus, N:P ratios increased from 4.76 ± 0.91 (S) to 10.55 ± 1.85 (T) and 12.11 ± 4.09 (G), which indicated a decreasing relative N limitation and increasing P limitation. Compared with TN, TC showed no significant differences among the S, G, and T stages ($p > 0.05$), which were lowest in T (1.52% ± 0.18%), which was about 75% of the highest S (**Figure 1A**). However, due to the decreasing of TP, C:P also

[2]www.majorbio.com

[3]http://ieg2.ou.edu/MENA/

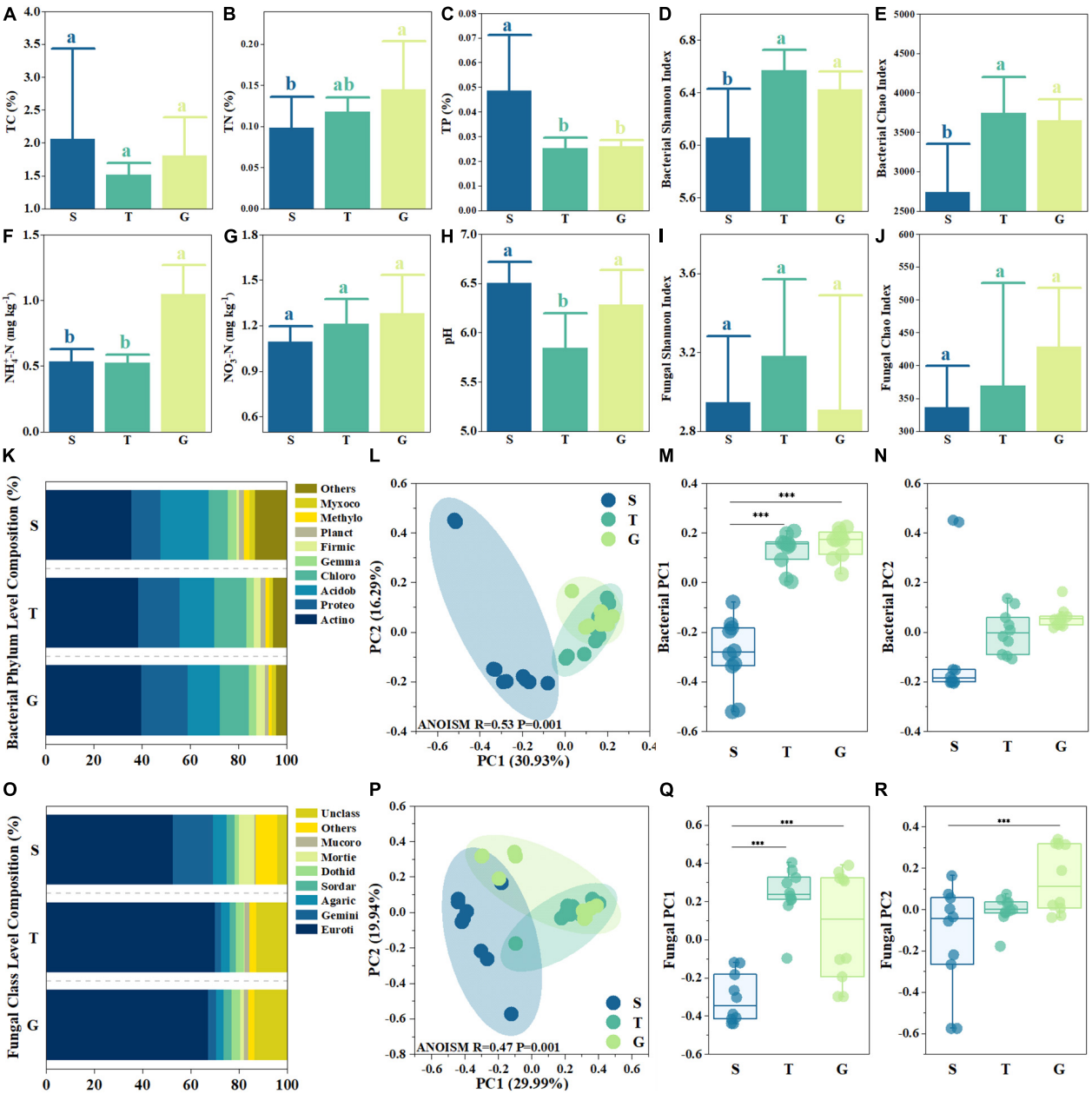

FIGURE 1 | Basic abiotic and biotic site properties. Shrubland (S), transitional (T), and Grass (G) in each sub-figures indicate shrub, transition, and grassland. Subfigures **(A–J)** depict soil total carbon (TC), total nitrogen (TN), total phosphorus (TP), ammonia content, nitrate content, pH, bacterial and fungal community Shannon index, and Chao index. The bars in the histogram indicate the average, and the error bars indicate standard deviation (n = 10). The different letters inside subfigures **(A–J)** indicate significant differences between groups ($p < 0.05$, one-way ANOVA Tukey's test). **(K,O)** depict the bacterial phylum composition and fungal class composition, respectively, with six letter abbreviations adopted for bacterial phylum and fungal class names. **(L,P)** depict principal coordinates analysis (PcoA) analysis for bacterial community and fungal community at the OUT level, respectively. The *** in subfigures **(M,N,Q,R)** indicate significant differences between groups ($p < 0.05$, one-way ANOVA Tamhaney's T2 test).

increased from 111.77 ± 31.67 (S) to finally 176.99 ± 48.18 (G), which indicated increasing relative P limitation and decreasing relative C limitation. Similar to TN, ammonia also showed an increasing trend from S to G. The highest ammonia nitrogen content was observed in G (1.05 ± 0.23 mg kg^{-1}), which was about two times that of S and T ($p < 0.05$) (**Figure 1F**). Nitrate nitrogen increased from 1.10 ± 0.10 mg kg^{-1} (S) to 1.28 ± 0.25 mg kg^{-1} (G), although no significant differences were found among the three sites (**Figure 1G**). These indicated that G possessed a higher labile nitrogen content pool rather than S. The pH in T was 5.84 ± 0.35, which was significantly lower ($p < 0.05$) than S (6.50 ± 0.21) and G (6.28 ± 0.35) (**Figure 1H**).

The bacterial Shannon and Chao indices increased significantly ($p < 0.05$) from S (6.06 ± 0.00 and 2,739 ± 616,

respectively) to T (6.57 ± 0.16 and 3,743 ± 453, respectively) and then displayed a slight but non-significant decrease ($p > 0.05$) (**Figures 1D,E**). The fungal Shannon index was highest in T (3.18 ± 0.39) (**Figure 1I**), while non-significant differences were found among the three stages ($p > 0.05$). The fungal Chao index also displayed a non-significant ($p > 0.05$) increase from S (336 ± 63) to G (429 ± 89) (**Figure 1J**).

From S to G, most bacterial phyla showed linear changes in relative abundance (RA) (**Figure 1K**). For example, the RA of *Proteobacteria* in G (19.19%) was 0.6 times higher than S (11.98%), the RA of *Chloroflexi* also increased from 8.17% (S) to 12.17% (G) and 13.44% (T). Instead of the increasing trend, the RA of Acidobacteriota decreased from 20.03% (S) to 13.36% (G), and RA of "Others," a group composed by rare species (less than 2% RA), was 13.14% in S and only 4.41% in G, decreased even nearly 70%. However, the most abundant phylum, Actinobacteriota, shared similar RA among three sites, which only slightly increased from S (36.65%) to G (39.77%). The most dominant fungal Class was Eurotiomycetes (**Figure 1O**), for which RA increased from 52.59% (S) to 70.01% (T) and 67.17% (G). The second most dominant fungal Class was Geminibasidiomycetes (RA 16.62% in S), whose RA shrank to 2.53% (T) and 3.30% (G). However, the RA of group "Unclassified" was 4.02% in S but 13.41% in G, while other groups also showed several differences among the three stages, like Dothideomycetes, whose RA at G and T was about twice that of S (1.61%).

The PCoA analysis of bacterial and fungal community composition at the OUT level found that there were significant differences in the community structure among the three stages (ANOISM $p < 0.001$). PC1 and PC2 of the bacterial community were 30.93 and 16.29%, respectively, while PC1 and PC2 of the fungal community were 29.99 and 19.94%, respectively (**Figures 1L,P**). Significant differences were found between bacterial PC1 of S and T and of S and G ($p < 0.05$), but not between T and G ($p > 0.05$) (**Figure 1M**). Fungal PC1 showed a similar trend (**Figure 1Q**). However, there were no significant differences among bacterial PC2 of the three stages ($p > 0.05$) (**Figure 1N**), while fungal PC2 of S and G was significantly different ($p < 0.05$) (**Figure 1R**). These results indicated that the variation in microbial composition during vegetation uplift expansion mainly occurred during the first stage of expansion (S to T) rather than the final stage of expansion (T to G).

Structure Equation Modeling on Microbial Composition

The null model construction is depicted in detail in **Supplementary Figure 2**. The SEM showed that P limitation offered the highest total effect (0.38), direct effect (0.64), and indirect effect (−0.26) on fungal composition. Although the total effect was only 0.04 higher than pH and N resources, direct effect was almost four times and three times of pH and N resources, respectively. Indirect effect was 17.8% higher than pH and 48% higher than N resources, respectively (**Figure 2C**). The total effect of P limitation on bacterial composition was as high as 0.63, which was about 2.4 times that of pH (total effect, −0.26) and three times of N resources (0.21). Its direct effect was also as high as 0.47, while pH was 0.02 and N resources was 0.22 (**Figure 2D**). These results indicated that P limitation was the greatest contributor to microbial composition during vegetation variation.

Network Analysis on Microbial Community

While the bacterial network grew in size during the transition from shrubland (S) to grassland (G), it became less interactive, with the number of nodes increasing from 163 (S) to 375 (T) and 333 (G) but links decreasing from 607 (S) to 532 (T) and 411 (G). The corresponding average degrees (avgK) decreased from 7.45 (S) to 2.84 (T) and 2.47 (G). As the nodes were less clustered, the clustering coefficient (avgCC) decreased from 0.41 (S) to 0.19 (T) and 0.20 (G) (**Figure 3** and **Supplementary Table 2**). Most importantly, TP gradually disappeared from the large central network modules, while ammonia and nitrate gradually appeared in the network modules (**Figure 3**). At the S stage, TP was present in a module with 15 (12 microbial) nodes and 26 links, while at the T stage, TP was in a module with only seven nodes and six links, and by the G stage, TP was not present in any of the modules, which indicated a shrinking TP-related functional module in the bacterial community network during shrub degradation. On the contrary, nitrate was not present in any module of network at the S stage but was in a peripheral module at T stage and a mid-sized module at G stage (10 nodes and 13 links) (**Figure 3**). Ammonia also appeared in a peripheral module at the G stage, which indicated a potential concentration on labile nitrogen formation of bacterial community during shrub degradation. However, the TC and TN were present in S, T, and G stages, which indicated relatively fixed bacterial TC, TN engaged functional modules during shrub degradation. The number of key network nodes increased from S to G. S had only 1 module hub (BOTU6475), while T and G had 3 and 2 module hubs, respectively, and each had 1 connector closely linking different modules, which indicated an increasing functional module interaction in bacterial network during shrub degradation.

On the contrary to the bacterial network, the fungal network became less member participated, shrinking from S (89 nodes) to T and G (68 and 79 nodes, respectively). S had 324 links, while T and G decreased to 188 and 222 links, respectively (**Figure 4** and **Supplementary Table 2**). However, the fungal network also showed decreased interactivity as avgK changed from 7.28 (S) to 5.53 (T) and 5.62 (G), in a manner similar to the bacterial networks. The fungal network clustering state displayed no great variation among the three stages, as avgCC ranged between 0.39 (S) and 0.35 (T). Interestingly, TP also gradually disappeared in fungal network modules during shrub degradation, from a large central module in the S stage (30 nodes and 148 links) to a mid-sized module in the T stage (16 nodes and 35 links), and by G stage, it was not present in any modules (**Figure 4**). Moreover, TP acted as a connector at S, which indicated it had a strong effect on network organization at the S stage (**Figure 4**). Similar to bacterial networks, TC and TN were also present

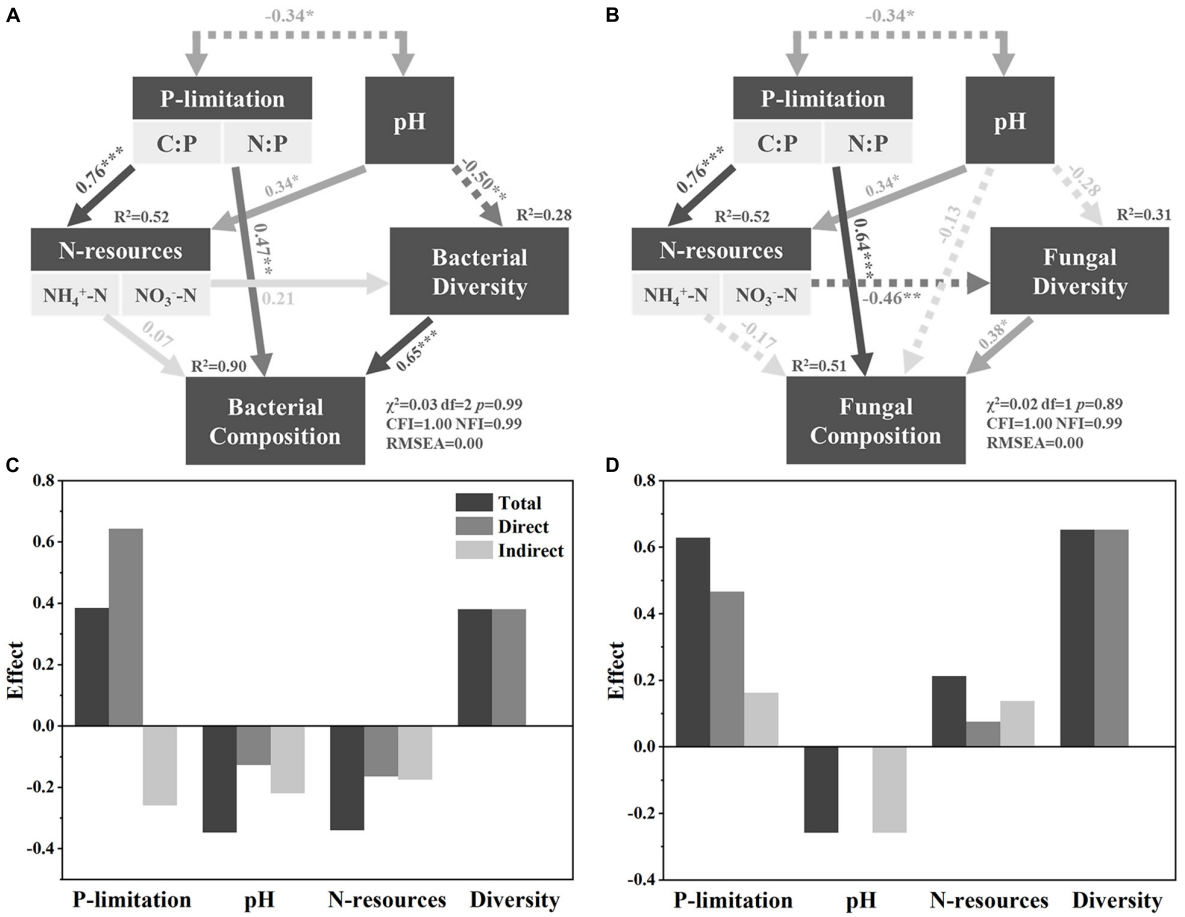

FIGURE 2 | SEM resolving bacterial composition and fungal composition. Panels **(A,B)** are detailed SEMs for bacterial and fungal composition, respectively, while panels **(C,D)** show the effects of different factors on composition accordingly. Solid and dashed lines indicate positive and negative correlations, respectively. *, **, and *** indicate significant correlated under $p < 0.05$, $p < 0.01$, and $p < 0.001$, respectively.

in S, T, and G stages, which indicated that the fungal network was also functionally constant about TC and TN during shrub degradation. However, different to bacterial network, key nodes of the fungal network had five connectors at S but only 1 connector each at T and G stages, displaying a decreasing trend, which indicated a decreasing functional module interaction in the fungal network during shrub degradation.

The results showed that the shrub site had a more member-participated fungal network and a less member-participated bacterial network than the other two stages. During the shrubland degradation by grass expansion, both bacterial and fungal network become less interactive and less focused on TP, with the bacterial network becoming more focused on nitrate and ammonia.

DISCUSSION

TP, TN, and Shrub Degradation

In this study, shrubland degradation by grass expansion was accompanied by a decreasing TP and increasing TN, ammonia, and nitrate, which indicated an increase in relative P limitation (**Figure 1C**). This is unfavorable for shrub dominance as its higher P demand than grass needs to waste extra energy and material to uptake adequate P under P-limited condition (Yang et al., 2016; Carrillo et al., 2017). TP primarily decreased at the beginning of grass expansion (from S to T), while the further decrease during T to G was not as significant as during S to T, which indicated that the variation in TP was potentially the first step for shrub degradation. In the recent decade, Yalong dry valley tends to possess an increasing mean annual temperature, a drier wet season, and a wetter dry season (Sun et al., 2019). The drought-induced death of microbes stimulated the releasing of microbial organic P, and the following rewetting accelerated the leaching (Dinh et al., 2017; Brödlin et al., 2019). Since P leaching with precipitation is a major way for topsoil TP loss, the increasing frequency of dry-wet alteration might be a contributor to enhanced P limitation. In this research, TN, ammonia, and nitrate increased from S to G, which also enhanced relative P limitation indirectly. This is consistent to the conclusion from other ecosystems. Recent research found that nitrogen deposition released relative N limitation but increased P limitation and

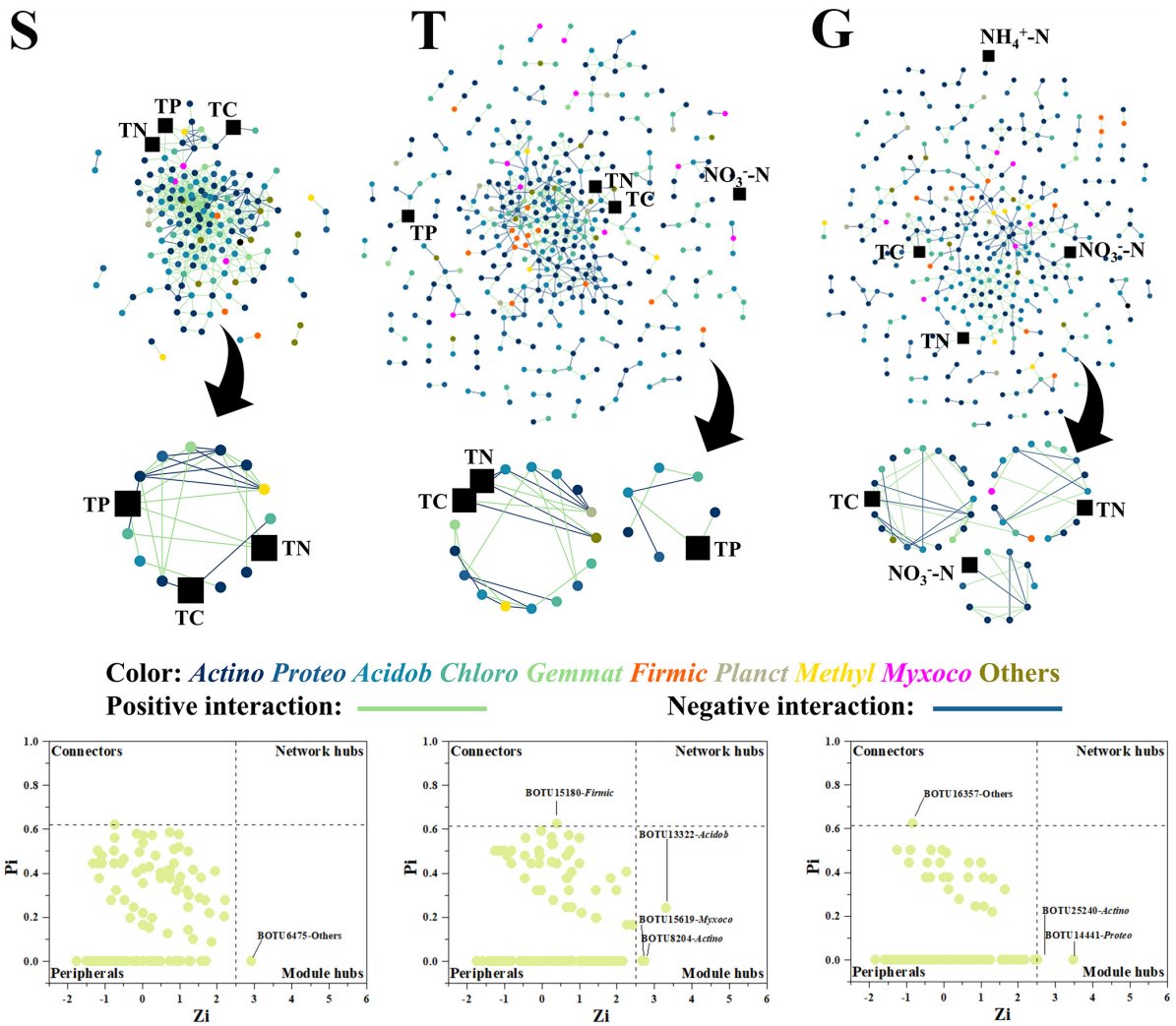

FIGURE 3 | The bacterial network, with functional modules and key node composition. The phylogenetic identity (phylum level) of nodes is depicted by different colors; positive and negative interactions are depicted as green and blue lines, respectively. The environmental factors are depicted as black squares. The "*Actino*" is the abbreviation for "Actinobacteria" and similarly to other bacterial phylum.

lead significant higher grass biomass increase rather than other species (Wang et al., 2021). Research on subalpine grassland also reported nitrogen deposition benefited grasses to a greater degree than shrub (Blanke et al., 2012). In this study, ammonia increased mostly during the later stage of expansion (from T to G) (**Figures 1B,F,G**), indicating that the final grass dominance over shrub was potentially linked to a more active nitrogen cycle. Compared with perennial shrubs, annual grass species tend to have faster growing rate (Uddin et al., 2020); fast-growing species had higher efficient in transporting water, in acquiring and using nutrients and in fixing carbon (Reich, 2014). Ammonia is released from the decomposition of organic nitrogen, a process conducted by microbes (Galloway et al., 2004). Moreover, ammonia is easily to be assimilated by fast-growing grass plants (Uddin et al., 2020), which could meet the higher nitrogen demand of grass species and enhance their dominance over shrubs (Galloway et al., 2004). Thus, our results support that enhanced relative P limitation, accompanied by the decreasing TP and increasing TN, potentially altered the relative competence of grass and shrub in this research.

P Limitation Acts as a Main Driver of Microbial Community Composition Variation During Shrub Degradation

In this research, the SEM showed that P limitation exerted the highest total effect on both bacterial and fungal communities (**Figures 2A,B**), indicating that P limitation was the main driver of microbial community composition during grassland expansion of Tibetan dry valleys. This is possibly because the sampling site was mainly P-limited. The C:P in this research ranged from 111.77 ± 31.67 (S) to 176.99 ± 48.18 (G), according to global average soil microbial C:P (60:1); the microbial community in Tibetan dry valley tends to be more P-limited

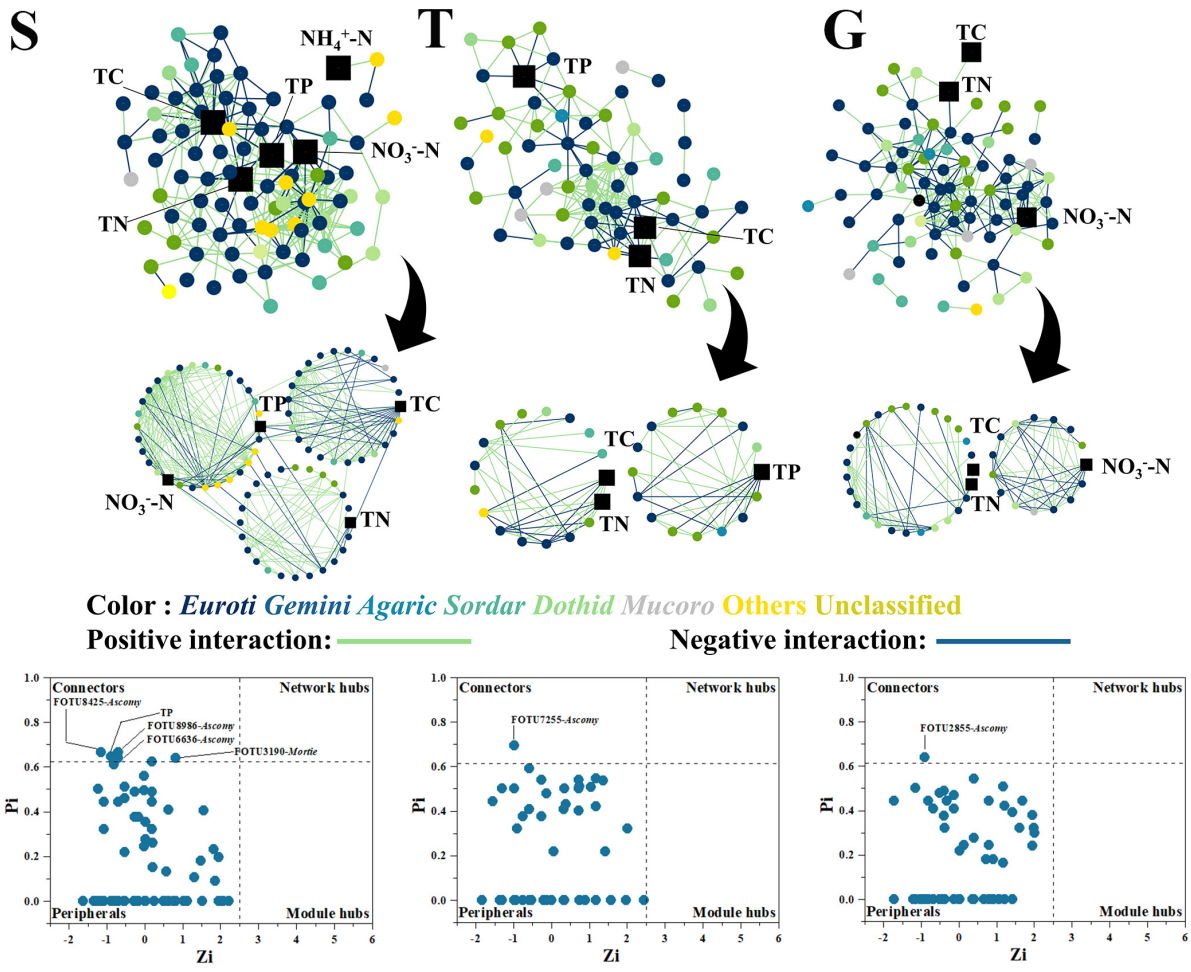

FIGURE 4 | The fungal network, with functional modules and key node composition. The phylogenetic identity of nodes (class level) is depicted by different colors; network positive and negative interactions are depicted as green and blue lines, respectively. The environmental factors are depicted as black squares. The "*Euroti*" is the abbreviation for "Eurotiomycetes" and similarly to other fungal class.

rather than C-limited as the field C:P offered less ratio P than microbes physiologically required (Cleveland and Liptzin, 2007). Similarly, global average soil microbial N:P was about 7:1, which was higher than 4.76 ± 0.91 (S) but lower than 10.55 ± 1.85 (T) and 12.11 ± 4.09 (G). These indicated that the microbial community faced a switch from less P-limited in S to a more P-limited state in T and G. As one of the basic nutrients to microorganisms, P was widely reported a driver to the variation on soil microbial community's composition and function, especially under the P-limiting condition, including agricultural field (Su et al., 2015), grassland (Widdig et al., 2020a,b), and forest (Liu et al., 2012; Spohn et al., 2018). Thus, the microbial community composition in P-limited Tibetan dry valley was also mostly influenced by P limitation rather than pH and N resources.

However, the driver of microbial community composition during shrub-grass expansion varied in previous reports, and no congruent conclusions can be found. An Inner Mongolian grassland field investigation reported that TC and plant litter chemical composition played the most important role in regulating microbial composition (Zhou et al., 2017), and a subtropical marsh grassland study found that shrubs significantly altered microbial nitrogen cycle function, indicating nitrogen was the main driver of microbial community composition (Ho and Chambers, 2019). A separate report on Sayeret Shaked Park found that TC and TN were the main factors contributing to heterotrophic microbial composition change after the death of shrubs, while autotrophic microbial composition was controlled by soil moisture (Nejidat et al., 2016). This indicates that the detailed main driver of soil microbial community under shrub-grass change varies with climatic background, ecosystem types, microbial functional group concerned, etc. For example, a recent sub-continental investigation revealed that under dryer conditions, enhanced precipitation would release P limitation by accelerating rocky P mineralization. But under humid conditions, enhanced precipitation would increase P limitation by accelerating leaching (Li et al., 2022). Considering around 820 mm mean annual precipitation (relatively humid) in our

sampling sites, P limitation tended to be amplified due to the higher precipitation in wet season. Moreover, P limitation would act as a main driver to microbial community's composition in the climate change background in near future in Tibetan dry valley.

The Change of Microbial Network Properties During Shrub Degradation

Our result showed that with the expansion of grass into shrub, both bacterial and fungal networks marginalized, then excluded TP from the central modules, and the bacterial network integrated nitrate and ammonia into mid-size (G) and peripheral modules (G), respectively (**Figures 3**, **4**). A network module is a collection of microbial members that conduct highly linked functions (Deng and Zhou, 2015), and our results indicated a functional shift from a more P cycle-centered network to more nitrogen cycle-centered network. This was consistent with previous discussion that shrubs dominate under higher P content conditions, where the corresponding microbial community helps to turn over litter organic P into available soil phosphate (Yong et al., 2018; Gao et al., 2019, 2021), while grasses dominate under higher nitrogen conditions, where the corresponding microbial community accelerates nitrogen cycling and plant nitrogen assimilation (Galloway et al., 2004). Plant and soil microbial communities have been reported to select each other and mutually create a functional system that favors both sides (Veen et al., 2015). The plants were reported to be capable of shaping the soil community by altering the composition of their root exudates and litter falls to help obtain the nutrients they most require (Berendsen et al., 2012; Bruggen et al., 2019). In this study, shrubland soils had a more member-participated fungal network and a less member-participated bacterial network than transitional and grassland soils (**Figures 3**, **4**), and the shrubland fungal network contained more key network nodes than the other sites, while the bacterial networks of transitional and grassland zones had more key network nodes than shrubland (**Figures 3**, **4**), which indicated fungi played a greater role in S networks, while bacteria were more important in T and G networks. This is possibly due to the ecological function preference between bacterial members and fungal members. Compared with bacteria, fungi were reported to play a more important role in P cycling, as several members (mycorrhizal fungi) are strong P mineralizers (Smith et al., 2003). While bacteria play a more central roles in N cycling, as N fixation, nitrification and denitrification are mainly conducted by bacteria rather than fungi (Kuypers et al., 2018). Thus, higher P -demanding shrubs are prone to shape a more fungal member-participated network, while grasses shape a more member-participated bacterial network. Moreover, TP even acted as a connector in the S fungal network. Connectors are special nodes that link modules conduct different functions (Deng and Zhou, 2015). This indicated that the shrubland fungal community had several functions highly connected to TP. During further grass expansion, TP and the microbial community were not significantly changed, thus highlighting the disappearance of TP in the microbial network, a sign of functional change on the microbial network and a potential reason for further shrub degradation, as the microbial network changed to a state that could not support the P turnover rates to meet shrub demands. However, this requires further research on soil P component analysis and relative enzyme activities to confirm (Canfield et al., 2005; Chen et al., 2016).

CONCLUSION

In this study, a grassland, a grass-shrub transitional field, and a shrubland from a Tibetan dry valley were chosen to investigate the microbial community variation change under a vegetation uplift expansion background. Consistent to our hypothesis, we found that during invasion by lower elevation grasses into higher elevation shrubs, P limitation was the main driver of both bacterial and fungal community composition. The soil network in shrubland was originally more P cycling-centered with a greater number of fungal members participating but gradually changed to a state that was less P cycling-centered and more bacterial members participating, which indicated that composition and network functional module change is a potential reason for shrub degradation. This research provides a microbial ecology mechanism to vegetation uplift expansion in Tibetan dry valleys and offers valuable information for dry valley ecosystem bioconservation and vegetation change response.

DATA AVAILABILITY STATEMENT

The datasets presented in this study can be found in online repositories. The names of the repository/repositories and accession number(s) can be found below: https://www.ncbi.nlm.nih.gov/, SAMN17245059.

AUTHOR CONTRIBUTIONS

HZ, AM, and GZ: design. HZ, JZ, XZ, and QZ: methodology. XC and HZ: software. HZ, JZ, and XQ: validation. HZ, JZ, and XC: formal analysis. HZ, JZ, QZ, and XC: investigation and resources. HZ: writing of the manuscript with help from AM, GL, and GZ. All authors involved in revising this manuscript, contributed intellectual input and assistance to this study, and manuscript preparation.

FUNDING

This work was supported by the Second Tibetan Plateau Scientific Expedition and Research Program (2019QZKK0402 and 2019QZKK0307); the National Key Research and Development Program of China (2018YFA0901200); and the National Natural Science Foundation of China (41671270 and 41673082).

SUPPLEMENTARY MATERIAL

The Supplementary Material for this article can be found online at: https://www.frontiersin.org/articles/10.3389/fpls.2022.848691/full#supplementary-material

REFERENCES

Berendsen, R. L., Pieterse, C. M. J., and Bakker, P. A. H. M. (2012). The rhizosphere microbiome and plant health. *Trends Plant Sci.* 17, 478–486. doi: 10.1016/j.tplants.2012.04.001

Blanke, V., Bassin, S., Volk, M., and Fuhrer, J. (2012). Nitrogen deposition effects on subalpine grassland: The role of nutrient limitations and changes in mycorrhizal abundance. *Acta. Oecologica* 45, 57–65. doi: 10.1016/j.actao.2012.09.002

Brödlin, D., Kaiser, K., Kessler, A., and Hagedorn, F. (2019). Drying and rewetting foster phosphorus depletion of forest soils. *Soil Biol. Biochem.* 128, 22–34. doi: 10.1016/j.soilbio.2018.10.001

Bruggen, A. H. C., Goss, E. M., Havelaar, A., van Diepeningen, A. D., Finckh, M. R., and Morris, J. G. Jr. (2019). One Health - Cycling of diverse microbial communities as a connecting force for soil, plant, animal, human and ecosystem health. *Sci. Total Environ.* 664, 927–937. doi: 10.1016/j.scitotenv.2019.02.091

Canfield, D. E., Kristensen, E., and Thamdrup, B. (2005). Aquatic geomicrobiology. *Adv. Mar. Biol.* 48, 1–599. doi: 10.1080/01490451.2021.1983670

Carrillo, Y., Bell, C., Koyama, A., Canarini, A., Boot, C. M., Wallenstein, M., et al. (2017). Plant traits, stoichiometry and microbes as drivers of decomposition in the rhizosphere in a temperate grassland. *J. Ecol.* 105, 1750–1765. doi: 10.1111/1365-2745.12772

Chen, Y., Sun, T. T., Qian, H. Y., Fan, J. B., He, Y. Q., and Sun, B. (2016). Nitrogen mineralization as a result of phosphorus supplementation in long-term phosphate deficient soil. *Appl. Soil Ecol.* 106, 24–32. doi: 10.1016/j.apsoil.2016.04.019

Cleveland, C. C., and Liptzin, D. (2007). C:N:P stoichiometry in soil: is there a "Redfield ratio" for the microbial biomass? *Biogeochemistry* 85, 235–252. doi: 10.1007/s10533-007-9132-0

Crowther, T. W., Todd-Brown, K. E. O., Rowe, C. W., et al. (2016). Quantifying global soil carbon losses in response to warming. *Nature* 540, 104–108. doi: 10.1038/nature20150

Curtis, T. (2006). Microbial ecologists: it's time to 'go large'. *Nat. Rev. Microbiol.* 4, 488–488. doi: 10.1038/nrmicro1455

de Vries, F., and Ashley, S. (2013). Controls on soil microbial community stability under climate change. *Front. Microbiol.* 4:265. doi: 10.3389/fmicb.2013.00265

Deng, Y., and Zhou, J. (2015). *Molecular Ecological Network of Microbial Communities. Encyclopedia of Metagenomics: Genes, Genomes and Metagenomes: Basics, Methods, Databases and Tools,*(Nelson KE, ed.) p. Boston, MA: Springer US, 504–510. doi: 10.1007/978-1-4899-7478-5_758

Dinh, M.-V., Guhr, A., Spohn, M., and Matzner, E. (2017). Release of phosphorus from soil bacterial and fungal biomass following drying/rewetting. *Soil Biol. Biochem.* 110, 1–7. doi: 10.1016/j.soilbio.2017.02.014

Dong, Y., and Somero, G. N. (2009). Temperature adaptation of cytosolic malate dehydrogenases of limpets (genus Lottia): differences in stability and function due to minor changes in sequence correlate with biogeographic and vertical distributions. *J. Exp. Biol.* 212, 169–177. doi: 10.1242/jeb.024505

Edgar, R. C. (2013). UPARSE: highly accurate OTU sequences from microbial amplicon reads. *Nat. Methods* 10:996. doi: 10.1038/nmeth.2604

Edwards, J., Johnson, C., Santos-Medellín, C., Lurie, E., Podishetty, N. K., Bhatnagar, S., et al. (2015). Structure, variation, and assembly of the root-associated microbiomes of rice. *Proc. Natl. Acad. Sci. U.S.A.* 112, E911–E920. doi: 10.1073/pnas.1414592112

Galloway, J. N., Dentener, F. J., Capone, D. G., Boyer, E. W., Howarth, R. W., Seitzinger, S. P., et al. (2004). Nitrogen Cycles: Past, Present, and Future. *Biogeochemistry* 70, 153–226. doi: 10.1007/s10533-004-0370-0

Gao, X., Li, X., Zhao, L., and Kuzyakov, Y. (2021). Shrubs magnify soil phosphorus depletion in Tibetan meadows: Conclusions from C:N:P stoichiometry and deep soil profiles. *Sci. Total Environ.* 785:147320. doi: 10.1016/j.scitotenv.2021.147320

Gao, X.-L., Li, X. G., Zhao, L., and Kuzyakov, Y. (2019). Regulation of soil phosphorus cycling in grasslands by shrubs. *Soil Biol. Biochem.* 133, 1–11. doi: 10.1016/j.soilbio.2019.02.012

Guo, H., Ye, C., Zhang, H., Pan, S., Ji, Y., Li, Z., et al. (2017). Long-term nitrogen & phosphorus additions reduce soil microbial respiration but increase its temperature sensitivity in a Tibetan alpine meadow. *Soil Biol. Biochem.* 113, 26–34. doi: 10.1016/j.soilbio.2017.05.024

Harris, R. M. B., Beaumont, L. J., Vance, T. R., et al. (2018). Biological responses to the press and pulse of climate trends and extreme events. *Nat. Clim. Change* 8, 579–587. doi: 10.1038/s41558-018-0187-9

He, H., and Xie, Y. (2020). Effect of different hemodialysis methods on microbiota in uremic patients. *BioMed Res. Int.* 2020:6739762. doi: 10.1155/2020/6739762

Ho, J., and Chambers, L. G. (2019). Altered soil microbial community composition and function in two shrub-encroached marshes with different physicochemical gradients. *Soil Biol. Biochem.* 130, 122–131. doi: 10.1016/j.soilbio.2018.12.004

Kai, F., Zhang, Z., Cai, W., Liu, W., Xu, M., Yin, H., et al. (2017). Biodiversity and species competition regulate the resilience of microbial biofilm community. *Mol. Ecol.* 26, 6170–6182. doi: 10.1111/mec.14356

Kline, R., Kline, R. B., and Kline, R. (2011). Principles and Practice of Structural Equation Modeling.

Kuypers, M. M. M., Marchant, H. K., and Kartal, B. (2018). The microbial nitrogen-cycling network. *Nat. Rev. Microbiol.* 16, 263–276. doi: 10.1038/nrmicro.2018.9

Li, C. (2001). Strategy on Sustainable Development of Eco- fragile Area of Xerothermic Valley in Southwest China. *China Soft Sci.* 6, 95–99.

Li, J., Dong, L., Liu, Y., Wu, J., Wang, J., Shangguan, Z., et al. (2022). Soil organic carbon variation determined by biogeographic patterns of microbial carbon and nutrient limitations across a 3, 000-km humidity gradient in China. *CATENA* 209:105849. doi: 10.1016/j.catena.2021.105849

Lindenmayer, D., and Fischer, J. (2007). Habitat Fragmentation and Landscape Change: An Ecological and Conservation Synthesis. Washington: Island Press

Liu, L., Gundersen, P., Zhang, T., and Mo, J. (2012). Effects of phosphorus addition on soil microbial biomass and community composition in three forest types in tropical China. *Soil Biol. Biochem.* 44, 31–38. doi: 10.1016/j.soilbio.2011.08.017

Liu, Y., Yang, H., Liu, Q., Zhao, X., Xie, S., Wang, Z., et al. (2021). Effect of Two Different Sugarcane Cultivars on Rhizosphere Bacterial Communities of Sugarcane and Soybean Upon Intercropping. *Front. Microbiol.* 11:596472. doi: 10.3389/fmicb.2020.596472

Liu, Y., and Zhu, X. (2016). Flora compositions and spatial differentiations of vegetation in dry valleys of Southwest China. *Biodivers. Sci.* 24, 367–377. doi: 10.17520/biods.2015240

Magoč, T., and Salzberg, S. (2011). FLASH: fast length adjustment of short reads to improve genome assemblies. *Bioinformatics* 27, 2957–2963. doi: 10.1093/bioinformatics/btr507

Mori, H., Maruyama, F., Kato, H., Toyoda, A., Dozono, A., Ohtsubo, Y., et al. (2014). Design and Experimental Application of a Novel Non-Degenerate Universal Primer Set that Amplifies Prokaryotic 16S rRNA Genes with a Low Possibility to Amplify Eukaryotic rRNA Genes. *DNA Res.* 21, 217–227. doi: 10.1093/dnares/dst052

Nejidat, A., Potrafka, R. M., and Zaady, E. (2016). Successional biocrust stages on dead shrub soil mounds after severe drought: Effect of micro-geomorphology on microbial community structure and ecosystem recovery. *Soil Biol. Biochem.* 103, 213–220. doi: 10.1016/j.soilbio.2016.08.028

Qiong, L., Grytnes, J.-A., and Birks, H. J. B. (2010). Alpine vegetation and species-richness patterns along two altitudinal gradients in the Gyama Valley, southcentral Tibet, China. *Trans. Bot. Soc. Edinb.* 3, 235–247. doi: 10.1080/17550874.2010.542782

Ramette, A. (2007). Multivariate analyses in microbial ecology. *FEMS Microbiol. Ecol.* 62, 142–160. doi: 10.1111/j.1574-6941.2007.00375.x

Reich, P. B. (2014). The world-wide 'fast-slow' plant economics spectrum: a traits manifesto. *J. Ecol.* 102, 275–301. doi: 10.1111/1365-2745.12211

Singh, B. K., Bardgett, R. D., Smith, P., and Reay, D. S. (2010). Microorganisms and climate change: terrestrial feedbacks and mitigation options. *Nat. Rev. Microbiol.* 8, 779–790. doi: 10.1038/nrmicro2439

Smith, S. E., Smith, F. A., and Jakobsen, I. (2003). Mycorrhizal Fungi Can Dominate Phospate Supply to Plants Irrespective of Growth Responses. *Plant Physiol.* 133, 16–20. doi: 10.1104/pp.103.024380

Spohn, M., Zavišić, A., Nassal, P., Bergkemper, F., Schulz, S., Marhan, S., et al. (2018). Temporal variations of phosphorus uptake by soil microbial biomass and young beech trees in two forest soils with contrasting phosphorus stocks. *Soil Biol. Biochem.* 117, 191–202. doi: 10.1016/j.soilbio.2017.10.019

Su, J.-Q., Ding, L.-J., Xue, K., et al. (2015). Long-term balanced fertilization increases the soil microbial functional diversity in a phosphorus-limited paddy soil. *Mol. Ecol.* 24, 136–150. doi: 10.1111/mec.13010

Sun, L., Cai, Y., Yang, W., Yi, Y., and Yang, Z. (2019). Climatic variations within the dry valleys in southwestern China and the influences of artificial reservoirs. *Clim. Change* 155, 111–125. doi: 10.1007/s10584-019-02457-y

Toju, H., Tanabe, A. S., Yamamoto, S., and Sato, H. (2012). High-Coverage ITS Primers for the DNA-Based Identification of Ascomycetes and Basidiomycetes in Environmental Samples. *Plos One* 7:e40863. doi: 10.1371/journal.pone.0040863

Turner, B. L., Lambers, H., Condron, L. M., Cramer, M. D., Leake, J. R., Richardson, A. E., et al. (2013). Soil microbial biomass and the fate of phosphorus during long-term ecosystem development. *Plant Soil* 367, 225–234. doi: 10.1007/s11104-012-1493-z

Uddin, M. N., Robinson, R. W., and Asaeda, T. (2020). Nitrogen immobilization may reduce invasibility of nutrient enriched plant community invaded by Phragmites australis. *Sci. Rep.* 10:1601. doi: 10.1038/s41598-020-58523-4

Veen, G. F., Freschet, G. T., Ordonez, A., and Wardle, D. A. (2015). Litter quality and environmental controls of home-field advantage effects on litter decomposition. *Oikos* 124, 187–195. doi: 10.1111/oik.01374

Walker, T. W., and Syers, J. K. (1976). The fate of phosphorus during pedogenesis. *Geoderma* 15, 1–19. doi: 10.3390/ijerph14121475

Wang, X., Wang, M., Tao, Y., Fang, N., Yang, G., Cai, J., et al. (2021). Beneficial effects of nitrogen deposition on carbon and nitrogen accumulation in grasses over other species in Inner Mongolian grasslands. *Global Ecol. Conserv.* 26:e01507. doi: 10.1016/j.gecco.2021.e01507

Widdig, M., Heintz-Buschart, A., Schleuss, P.-M., Guhr, A., Borer, E. T., Seabloom, E. W., et al. (2020a). Effects of nitrogen and phosphorus addition on microbial community composition and element cycling in a grassland soil. *Soil Biol. Biochem.* 151:108041. doi: 10.1016/j.soilbio.2020.108041

Widdig, M., Schleuss, P.-M., Biederman, L. A., Borer, E. T., Crawley, M. J., Kirkman, K. P., et al. (2020b). Microbial carbon use efficiency in grassland soils subjected to nitrogen and phosphorus additions. *Soil Biol. Biochem.* 146:107815.

Xie, F., Ma, A., Zhou, H., Liang, Y., Yin, J., Ma, K., et al. (2020). Niche differentiation of denitrifying anaerobic methane oxidizing bacteria and archaea leads to effective methane filtration in a Tibetan alpine wetland. *Environ. Int.* 140:105764. doi: 10.1016/j.envint.2020.105764

Yang, X., Chi, X., Ji, C., et al. (2016). Variations of leaf N and P concentrations in shrubland biomes across northern China: phylogeny, climate, and soil. *Biogeosciences* 13, 4429–4438. doi: 10.5194/bg-13-4429-2016

Yong, Z., Boutton, T. W., and Ben, W. X. (2018). Soil C:N:P stoichiometry responds to vegetation change from grassland to woodland. *Biogeochemistry* 140, 341–357. doi: 10.1007/s10533-018-0495-1

Zhao, O. U., Zhu, Q. K., Sun, Y. Y., Ecotourism, S. O., and University, S. F. (2015). Research Progress in the Landcape Pattern of Dry-hot valley in Southwest China. *J. West China Forestr. Sci.* 2015, 1672-8246

Zhou, H., Ma, A., Zhou, X., Chen, X., Zhang, J., Gen, P., et al. (2022). Soil phosphorus accumulation in mountainous alpine grassland contributes to positive climate change feedback *via* nitrifier and denitrifier community. *Sci. Total Environ.* 804:150032. doi: 10.1016/j.scitotenv.2021.150032

Zhou, L., Li, H., Shen, H., Xu, Y., Wang, Y., Xing, A., et al. (2017). Shrub encroachment induced alterations in input chemistry and soil microbial community affect topsoil organic carbon in an Inner Mongolian grassland. *Biogeochemistry* 136, 311–324. doi: 10.1007/s10533-017-0396-8

Conflict of Interest: The authors declare that the research was conducted in the absence of any commercial or financial relationships that could be construed as a potential conflict of interest.

Publisher's Note: All claims expressed in this article are solely those of the authors and do not necessarily represent those of their affiliated organizations, or those of the publisher, the editors and the reviewers. Any product that may be evaluated in this article, or claim that may be made by its manufacturer, is not guaranteed or endorsed by the publisher.

Copyright © 2022 Zhou, Ma, Zhou, Chen, Zhang, Zhang, Qi, Liu and Zhuang. This is an open-access article distributed under the terms of the Creative Commons Attribution License (CC BY). The use, distribution or reproduction in other forums is permitted, provided the original author(s) and the copyright owner(s) are credited and that the original publication in this journal is cited, in accordance with accepted academic practice. No use, distribution or reproduction is permitted which does not comply with these terms.

frontiers in Plant Science

ORIGINAL RESEARCH
published: 25 March 2022
doi: 10.3389/fpls.2022.757077

Context-Dependency in Relationships Between Herbaceous Plant Leaf Traits and Abiotic Factors

Zhenchao Zhang[1,2], Jian Sun[2], Miao Liu[3], Hua Shang[4], Jinniu Wang[5], Jinsong Wang[6], Huakun Zhou[7], Yong Li[8], Yi Wang[2] and Wanjie Chen[9]*

[1] Key Laboratory of National Forestry and Grassland Administration on Grassland Resources and Ecology in the Yellow River Delta, College of Grassland Science, Qingdao Agricultural University, Qingdao, China, [2] State Key Laboratory of Tibetan Plateau Earth System, Resources and Environment, Institute of Tibetan Plateau Research, Chinese Academy of Sciences, Beijing, China, [3] College of Grassland Science and Technology, China Agricultural University, Beijing, China, [4] Department of Ecology, Evolution and Natural Resources, Rutgers, The State University of New Jersey, New Brunswick, NJ, United States, [5] Chengdu Institute of Biology, Chinese Academy of Sciences, Chengdu, China, [6] Key Laboratory of Ecosystem Network Observation and Modelling, Institute of Geographic Sciences and Natural Resources Research, Chinese Academy of Sciences, Beijing, China, [7] Key Laboratory of Restoration Ecology for Cold Regions in Qinghai, Northwest Institute of Plateau Biology, Chinese Academy of Sciences, Xining, China, [8] Beijing Key Laboratory of Wetland Services and Restoration, Institute of Wetland Research, Chinese Academy of Forestry, Beijing, China, [9] State Key Laboratory of Vegetation and Environmental Change, Institute of Botany, Chinese Academy of Sciences, Beijing, China

Leaf traits are important indicators of plants' adaptive strategy to environmental changes. It is an established fact that leaf traits are jointly regulated by climatic and edaphic factors besides genetic factors. However, the relative importance of these abiotic forces in determining the general patterns of herbaceous plant leaf traits across different climatic regions in China is far from clear. We collected 1,653 observations of 542 species of herbaceous plant leaf traits including leaf mass per area, leaf nitrogen, and leaf phosphorus from 316 sampling sites across four climatic regions. We found that the leaf mass per area in the arid region was apparently larger than the others, whereas the smallest mass-based leaf nitrogen and mass-based leaf phosphorus were found in the humid region. Increased growing season temperature and evapotranspiration consistently promoted a conservative growth strategy indicated by higher relative benefit of leaf mass per area, especially in the arid region. Solar radiation in growing season promoted an acquisitive growth strategy indicated by higher relative benefits of mass-based leaf nitrogen and phosphorus in the humid region, but opposite patterns were found in the arid region and semi-humid region. Of all the soil nutrients including soil organic matter, total nitrogen, total phosphorus, and available nitrogen, soil available nitrogen was the strongest predictor of relative benefits of leaf traits associated with a nutrient acquisitive strategy, except in the nutrient-rich semi-humid region. There was a relatively larger number of abiotic factors contributing to relative benefits of leaf traits in the arid and humid regions. We concluded that plant functionality could respond divergently to the same factor facing different habitat conditions. Moreover, the relative benefits of leaf traits tended to be more vulnerable to abiotic filtering in more stressful conditions. Our findings have important implications for understanding the context-dependency of plant functionality to environmental filtering and further improving the predictability of plant dynamics under global change.

Keywords: herbaceous plant, leaf trait, growth strategy, abiotic filtering, environmental stress, climatic region

OPEN ACCESS

Edited by:
Boris Rewald, University of Natural Resources and Life Sciences Vienna, Austria

Reviewed by:
Amber Churchill, University of Minnesota, United States
Gabriela Woźniak, University of Silesia in Katowice, Poland

***Correspondence:**
Jian Sun
sunjian@iptcas.ac.cn

Specialty section:
This article was submitted to Functional Plant Ecology, a section of the journal Frontiers in Plant Science

Received: *11 August 2021*
Accepted: *21 February 2022*
Published: *25 March 2022*

Citation:
Zhang Z, Sun J, Liu M, Shang H, Wang J, Wang J, Zhou H, Li Y, Wang Y and Chen W (2022) Context-Dependency in Relationships Between Herbaceous Plant Leaf Traits and Abiotic Factors. Front. Plant Sci. 13:757077. doi: 10.3389/fpls.2022.757077

INTRODUCTION

Leaf traits are important predictors of evolved plant adaptations to particular inhabiting environments (Violle et al., 2014). They are related to numerous ecological functions: the leaf mass per area (LMA) indicates the investment of photosynthesis and nutrients acquired per unit leaf area; the leaf nitrogen (N) is an essential component of proteins for photosynthesis; and the leaf phosphorus (P) is integral to the nucleic acids and bioenergetics molecules fundamental for metabolism (Wright et al., 2004). Generally, a higher LMA with denser mesophyll tissues and thicker-walled cells allows for a longer leaf lifespan (Wright et al., 2006; Wright and Suttongrier, 2012), whereas higher leaf N and *P*-values, which are associated with higher photosynthetic rates, are observed in leaves with shorter longevity (Gusewell and Koerselman, 2002; Han et al., 2005). The trait-based ecology theory states that environmental changes shape leaf traits (Wang, 2007), which in turn affect ecosystem processes (Van Bodegom et al., 2007; Pearson et al., 2013; Bjorkman et al., 2018), and then soil quality (Buzzard et al., 2019). Variability of leaf traits allows individual plants to adapt to new environmental conditions. The plasticity of traits provides a mechanism for selection by altered environmental conditions that will drive future ecosystem processes.

The adaption and evolution of the leaf traits regulate plant survival and growth under a given set of conditions (Reichstein et al., 2014; Asner et al., 2016). There are two strategies reflecting the trade-off between plant persistence and productivity, and with contrary investment-return patterns, i.e., a slow-growing versus a fast-growing strategy. The former corresponds to greater resource conservation indicated by high relative benefit of LMA, low relative benefit of leaf N and leaf P under a stressful environment (Reich et al., 2003; Carvajal et al., 2019), whereas the latter refers to a quick investment-return pattern that is often associated with rapid resource acquisition indicated by low relative benefit of LMA, high relative benefits of leaf N and leaf P in optimal conditions (Shipley et al., 2006; Wright and Suttongrier, 2012). These strategies provide the most promising methods for determining how an ecosystem functions, such as indicating how the primary productivity and carbon/N cycling vary when facing different environmental conditions. Therefore, obtaining knowledge of leaf traits is a high priority for understanding terrestrial ecosystem adaptations to changing environments, and predicting how ecological processes shift with rapid climate change.

In the past decades, a compelling number of studies have attempted to reveal the relationships between leaf trait and its drivers (Wright et al., 2005; Ordonez and Olff, 2013; Carvajal et al., 2019). Both natural selection (Asner et al., 2016) and genetic constraints (Lusk et al., 2008) control the strength and direction of leaf trait evolution, and the given genetic constraints might play a relatively weaker role in shaping the leaf traits (Reich et al., 2003). In fact, the leaf traits may vary with the plant growth form (Simova et al., 2018; Gong and Gao, 2019), climate (Moles et al., 2014), soil fertility (Asner et al., 2016), taxonomy and phylogeny (He et al., 2009), and sampling scale (Borgy et al., 2017). Thus, no consistent patterns were found from the different studies. For instance, the trait-based ecology theory considers temperature as the central driver of leaf trait variation (Michaletz et al., 2016; Buzzard et al., 2019), but leaf N has been observed to significantly increase (Ordonez et al., 2009; Swenson et al., 2012) or decrease with increasing temperature (Moles et al., 2014; Simova et al., 2017); the soil nutrient supply may play a minor (Bowman et al., 2003) or influential (Ordonez et al., 2009; Reich et al., 2009) role in shaping the leaf traits; and precipitation also shows either strong (Swenson et al., 2012; Asner et al., 2016) or weak (Moles et al., 2014) relationships with leaf traits. To date, there has been no general pattern for the drivers of leaf traits, challenging its universality and predictability (Shipley et al., 2016).

Water and heat availability greatly affect nutrient cycling (Schuur and Matson, 2001), and play crucial roles in mediating plant growth (Sun and Du, 2017; Sun et al., 2020). The favourability hypothesis in biogeography suggests that species in a temperate zone with temperature seasonality should closely follow environmental filtering rules (Fischer, 1960). Previous studies have revealed that species with a narrow geographical range often adapt an extreme drought habitat, with stress-tolerant leaf traits (Thuiller et al., 2004; Geng et al., 2012). Long-term specific water and heat patterns would induce shifts in plant functional compositions (Griffinnolan et al., 2019). That is, the water and heat regime can shape the plant adaptations to the environment, and thereby affect the spatial distribution of the leaf traits (Schwinning and Ehleringer, 2001; Zhang et al., 2017). Though winter climate can affect plant growth especially in more northern latitudes and for cold climate systems, the climatic conditions in growing season play important roles in the growth of plants and thereby their leaf traits.

China has an east-to-west precipitation and temperature gradient as the dominant basis of the climate-region divisions (Zhang and Shen, 2008; Zhang et al., 2016). Meanwhile, herbaceous plants in China cover the broadest geographic range, from a hot arid desert steppe at the lowlands to a cold humid alpine meadow with a $\geq$4,000 m altitude (Chen et al., 2013), offering an ideal macrocosm for evaluating the spatial pattern of the leaf traits and interpreting plant adaptations to environmental gradients (Westoby and Wright, 2006). However, early studies focusing on the leaf trait response to environmental gradients were mostly performed at small scales (Stubbs and Wilson, 2004; He et al., 2006; Wang, 2007; Werden et al., 2018; Zhang X. L. et al., 2019), and a large-scale leaf trait pattern across China has not been previously reported. We hypothesised that the leaf traits might be divergent and mediated in different ways among different climatic regions across China. In this study, we aimed to address two questions. First, how does China's herbaceous plant leaf trait change along climatic regions? Second, how do edaphic and climatic factors regulate the leaf traits, specifically in different climatic regions? The answers will advance our knowledge of the ecological filtering and evolution shaping the leaf traits. Moreover, they will help in developing more quantitative and predictive ecological models for incorporating leaf functional traits applicable for China's terrestrial ecosystems under climate change and anthropogenic activities.

MATERIALS AND METHODS

Data Collection

The raw data were either obtained from tables or figures (extracted by using the GetData Graph Digitizer, version 2.24)[1], and a list of all contributing papers were included in **Supplementary 2** (**Supplementary Material**). For each publication, we recorded the following data: site location (longitude and latitude) as well as herbaceous plant LMA, leaf N concentration per mass (N_{mass}), and leaf P concentration per mass (P_{mass}) as three key leaf functional traits associated with the leaf traits and growing strategies (Diaz et al., 2016). Finally, our database consists of 1,653 observations of 542 species of herbaceous plant from 316 sampling sites across China [shown in **Supplementary 3** (**Supplementary Material**)], with longitude ranging from 74.93°E to 123.92°E, and latitude ranging from 19.10°N to 50.19°N (**Figure 1**). According to the dry and wet climate-region division in China[2] (Thornthwaite, 1948), our sampling sites are distributed in four climatic regions: arid, semi-arid, semi-humid, and humid regions in China (**Figure 1**).

The climate (precipitation, temperature, evapotranspiration, and solar radiation) data were derived from the database of WorldClime 2.0 Beta version 1 (June 2016), as downloaded from http://worldclim.org. They represent average monthly climate data for 1970–2000. The soil attributes [soil organic matter (SOM); total N (STN) and available N (SAN); and total P (STP)] were extracted from a Chinese dataset of soil properties, which was constructed based on a 1:1,000,000 soil map of China and 8,595 soil profiles (Shangguan et al., 2013). Due to the constraint based on data availability and accuracy, there are many measurements of leaf traits at the same soil property level especially for STP. To explore the effects of climatic factors on plant functional traits, we used the mean values from May to September, the growing season, for temperate zone where our sites are mostly located, including the mean growing season precipitation (GSP), mean growing season temperature (GST), mean growing season evapotranspiration (GSE), and mean growing season solar radiation (GSR). Abbreviations of these variables are shown in **Table 1**. The edaphic and climatic information of the sampling sites were extracted according to

[1]http://www.getdata-graph-digitizer.com/

[2]http://www.resdc.cn/data.aspx?DATAID=125

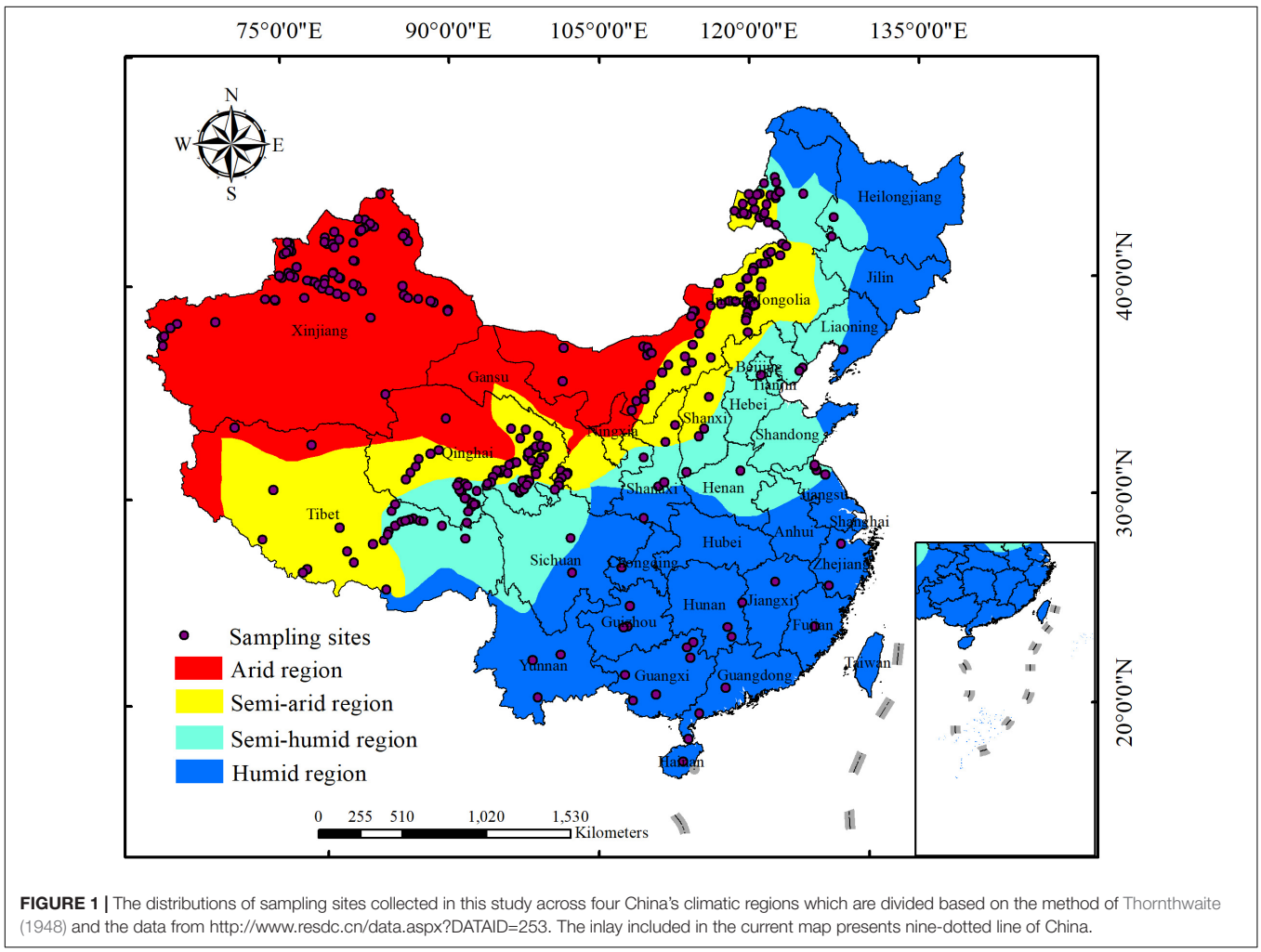

FIGURE 1 | The distributions of sampling sites collected in this study across four China's climatic regions which are divided based on the method of Thornthwaite (1948) and the data from http://www.resdc.cn/data.aspx?DATAID=253. The inlay included in the current map presents nine-dotted line of China.

geographical location (latitude and longitude) through ArcGIS 10.1 (ESRI, Inc., Redlands, CA, United States). The frequency distributions of the leaf traits (LMA, N_{mass}, and P_{mass}) were used to ensure the normality of the distribution (Zhou et al., 2019).

Statistical Analysis

The benefit for a single objective leaf trait is defined as the relative deviation from the mean of a given observation. The relative benefit for the objective leaf trait (LMA, N_{mass}, or P_{mass}) indicates the relative magnitude of the values of these leaf traits, and is calculated as follows (Bradford and Damato, 2012; Sun et al., 2018):

$$Bi = \frac{xi - x_{\min}}{x_{\max} - x_{\min}} \quad (1)$$

where i is a certain leaf trait (LMA, N_{mass}, or P_{mass}), B_i is the magnitude of the relative benefit for objective leaf trait i, x_i, x_{min}, and x_{max} are the observed value of i, minimum, and maximum values for all measured i, respectively. A three-dimensional (3D) relative benefit method was used to describe the leaf traits (relative benefits among LMA, N_{mass}, or P_{mass}) (Li et al., 2019). As shown in **Supplementary Figure 1**, the vertical distance (l) from the 3D point to the 1:1:1 line represents the magnitude of benefit for the three objective leaf traits, forming 3D coordinates in the LMA-N_{mass}-P_{mass} economic spectrum. The relative benefit was decomposed into the LMA (a), N_{mass} (c), and P_{mass} (b) directions, whose values could reflect a plant's growing strategy (**Supplementary Figure 1**): a low relative benefit of LMA combined with high relative benefits of N_{mass} and P_{mass} implied a quick investment-return growth strategy; in contrast, a slow investment-return growth strategy was indicated by a high relative benefit of the LMA combined with low relative benefits of N_{mass} and P_{mass}.

A principal component analysis (PCA) was performed with all the potential explanatory variables pooled together, to determine the explanatory powers of variance in the leaf functional traits, soil properties, and climatic factors among different climatic regions. The packages of "*FactoMineR*," "*factoextra*," and "*corrplot*" in R software (R Core Team, 2016) were used for the PCA. A one-way analysis of variance was performed with SPSS 19.0 software (SPSS Inc., Chicago, IL, United States) to detect differences in the plant, soil, and climate variables among the four climatic regions, using the least significant difference (LSD) as *post hoc* analysis. Regression and correlation analyses were conducted with R Version 3.3.2 (R Core Team, 2016) and SigmaPlot 14.0 software (Systat Software, Inc., Chicago, IL, United States) in each climatic region, to explore the correlations of leaf traits with edaphic and climatic variables. Besides, the correlogram of intercorrelations among relative benefits of leaf traits, soil properties, and climate factors was graphed by "*mgcv*" package in software R (R Core Team, 2016).

TABLE 1 | Abbreviations of leaf traits, climatic factors, and soil chemical properties.

Variable name	Abbreviation	Unit
Leaf mass per area	LMA	$g\ m^{-2}$
Leaf nitrogen concentration per mass	N_{mass}	$mg\ g^{-1}$
Leaf phosphorus concentration per mass	P_{mass}	$mg\ g^{-1}$
Growing season temperature	GST	°C
Growing season precipitation	GSP	mm
Growing season evapotranspiration	GSE	mm
Growing season solar radiation	GSR	$MJ\ m^{-2}$
Soil organic matter	SOM	$g\ kg^{-1}$
Soil total nitrogen	STN	$g\ kg^{-1}$
Soil total phosphorus	STP	$g\ kg^{-1}$
Soil available nitrogen	SAN	$mg\ kg^{-1}$

RESULTS

Variations of Leaf Traits Among the Climatic Regions

The LMA in the arid region, with a mean value of 124.34 $g\ m^{-2}$, was significantly higher than the mean values of 97.64, 81.90, and 79.73 $g\ m^{-2}$ for the semi-arid, semi-humid, and humid regions, respectively ($P < 0.05$, **Figure 2A**). N_{mass} and P_{mass} tended to initially increase and then decrease from arid to humid regions. The average values of N_{mass} were 23.51, 24.82, 25.92, and 16.64 $mg\ g^{-1}$ for the arid, semi-arid, semi-humid, and humid regions, respectively (**Figure 2B**). P_{mass} was significantly different among the four climatic regions ($P < 0.05$), with mean values of 1.52, 1.70, 1.86, and 1.27 $mg\ g^{-1}$ for the arid, semi-arid, semi-humid, and humid regions, respectively (**Figure 2C**). The LMA was negatively associated with N_{mass} and P_{mass}, with the deepest slope in the arid region (**Figures 2D,E**), whereas N_{mass} was positively correlated with P_{mass} (**Figure 2F**).

Variations of Edaphic and Climatic Factors in Different Climatic Regions

The PCA results indicated that two components explained 57.4% of the total variance (**Supplementary Figure 2**). Specifically, the first principal component (PC1) was highly relevant to the GSP, GSE, GSR, N_{mass}, and P_{mass}; the second principal component (PC2) was highly relevant to the SOM, STN, SAN, SAP, and LMA (**Supplementary Figure 2**). For the soil properties, SOM, STN, STP, and SAN presented a unimodal pattern along climatic regions, and peaked in the semi-humid region, with average values of 4.77, 0.23, 0.08, and 173.65 $mg\ kg^{-1}$, respectively (**Supplementary Table 1**). For the climatic variables, from arid to humid region, the GST initially decreased, and then increased with a minimum value of 9.55°C in the semi-humid region, while there was a significant decrease in the GSR (**Supplementary Table 1**).

Effects of Edaphic and Climatic Variables on Leaf Traits in Different Climatic Regions

In regard to the climatic factors, GST, GSE, and GSR positively affected the relative benefit of the LMA, but negatively influenced the relative benefits of N_{mass} and P_{mass} in the arid and semi-humid regions, similar to the effect of GST in the humid region ($P < 0.05$, **Figures 3A1–C1, A3–C3, A4–C4** and **Table 2**). However, the relationship patterns of the GSR with the leaf

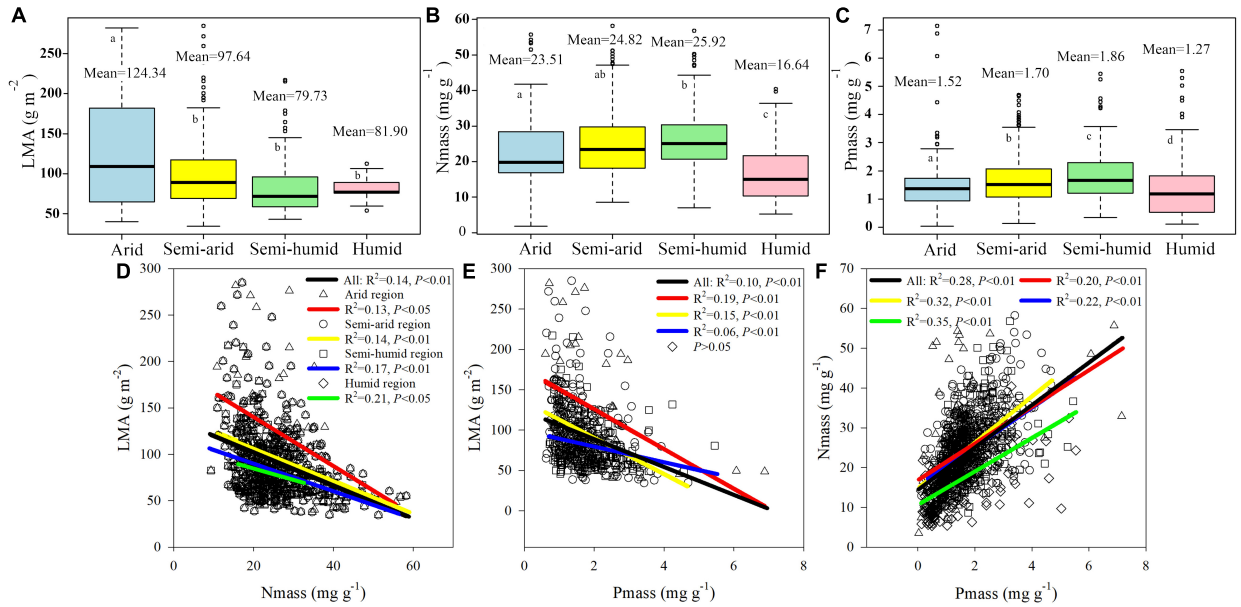

FIGURE 2 | The boxplot **(A–C)** and linear regression relationship **(D–F)** of herbaceous plant LMA, N_{mass}, P_{mass} among four China's climatic regions. The different letters in **(A–C)** represent significance at the 5% confidence level. The black line in **(D–F)** indicates the linear regression of the total data. LMA, N_{mass}, and P_{mass} represent leaf mass per area, mass-based leaf nitrogen, and mass-based leaf phosphorus, respectively.

traits in the humid region were converse to those in the arid and semi-arid regions (**Figures 3A4–C4**). The GSP showed weak negative correlations with the relative benefits of the LMA but was positively associated with the relative benefits of N_{mass} and P_{mass} in the semi-arid and semi-humid regions (**Figures 3A2–C2**).

For the edaphic factors, SOM, STN, and STP were negatively related to the relative benefit of the LMA, but positively affected the relative benefits of N_{mass} and P_{mass} in the semi-arid regions (**Figures 4A1–C2** and **Supplementary Figure 7**). Similar correlations were observed between the SAN with the relative benefits of the LMA, N_{mass}, and P_{mass}, except in the semi-humid region (**Figures 4A3–C3**). The number of key edaphic and climatic factors driving the leaf traits in the arid and humid regions was greater than those in the semi-arid and semi-humid regions (**Figure 5**).

DISCUSSION

Variations of Leaf Traits in Different Intervals Across Climatic Regions

Our study showed that the LMA in the arid region was drastically higher than those in other regions (**Figure 2A**), indicating that plants in hyper-arid conditions invest more photosynthate per unit leaf area. This result is in agreement with many previous studies indicating that plants inhabiting arid areas have a high LMA as manifested by thicker leaves with denser mesophyll (Fonseca et al., 2000; Niinemets, 2001; Wright et al., 2001), often combined with smaller and thicker-walled cells for reducing water loss (Wright et al., 2006). As the maximum photosynthetic rate of plants in a dry environment is relatively lower at the same level of leaf N content, the high LMA increases the photosynthetic tissue per unit area supporting photosynthesis, and allows for continued leaf function in arid conditions (Evans and Poorter, 2001). In addition, the SOM, STN, STP, and SAN in the arid region are significantly lower than those in other regions (**Supplementary Table 1**), and the low available water decreases the soil nutrient availability (Sardans and Penuelas, 2004) and further restricts plant nutrient absorption (Farooq et al., 2009). Consequently, survival is the primary goal for plants, which tend to select a relatively conservative investment strategy. The higher LMA in the arid region should be interpreted as an adaptive strategy of plants against extreme environmental stress, which was alleviated in other climatic regions, and the LMA was relatively smaller.

The leaf N and P values play pivotal roles in photosynthesis and protein synthesis, respectively (Niklas et al., 2005; Westoby and Wright, 2006). The N_{mass} and P_{mass} values in the humid region were dramatically lower than those in the other regions (**Figures 2B,C**), indicating a small carbon gain rate. This is probably because frequent strong precipitations accelerated the soil erosion and nutrient losses in the humid region, indicated by that the soil nutrients were significantly lower than those in the semi-humid region (**Supplementary Table 1**). Moreover, the soils were often waterlogged and anoxic, depressing the oxidative metabolic processes of the roots and microbes in the mesic lands, where the plant growth rates were greatly inhibited by excessive rainfall (Zhang S. S. et al., 2019; Zheng Q. et al., 2019).

We observed significantly negative correlations of the LMA with N_{mass} and P_{mass} (**Figures 2D,E**), which agrees with previous studies demonstrating that a higher LMA is often associated with

TABLE 2 | Statistical information of linear regression relationships between the relative benefits of leaf traits and climatic factors.

Climatic variables	Climatic region	Relative benefit of LMA				Relative benefit of N_{mass}				Relative benefit of P_{mass}			
		R	Slope	Intercept	*P*	*R*	Slope	Intercept	*P*	*R*	Slope	Intercept	*P*
Growing season temperature	Arid	0.25	0.02	–0.27	*	0.18	–0.01	0.16	*	0.24	–0.01	0.11	*
	Semi-arid				0.93				0.30				0.19
	Semi-humid	0.19	0.009	–0.11	**				0.15	0.19	–0.005	–0.02	**
	Humid	0.63	0.03	–0.19	*	0.45	–0.02	0.20	*				0.46
Growing season precipitation	Arid				0.87				0.41				0.32
	Semi-arid	0.09	–0.0003	0.08	*	0.14	0.0004	–0.007	*				0.60
	Semi-humid	0.17	–0.0008	0.21	*				0.16	0.15	0.0004	–0.18	*
	Humid				0.08				0.31				0.35
Growing season evapotransp-iration	Arid	0.36	0.003	–0.32	*	0.46	–0.002	0.28	**	0.17	–0.001	0.04	*
	Semi-arid				0.28				0.20				0.38
	Semi-humid	0.16	0.001	–0.16	*				0.16	0.14	–0.0006	0.004	*
	Humid				0.09				0.35				0.35
Growing season solar radiation	Arid	0.39	0.0002	–3.04	***	0.48	–0.0001	2.18	***				0.22
	Semi-arid				0.42				0.20				0.77
	Semi-humid	0.19	0.00006	–0.77	**				0.15	0.18	–0.00003	0.35	**
	Humid	0.57	–0.0003	3.39	*				0.23				0.36

*$P < 0.05$, **$P < 0.01$, ***$P < 0.001$.

lower leaf N and P concentrations, indicating slow growth rates (Santiago and Wright, 2007; Donovan et al., 2011). Nevertheless, the leaves with a high LMA and low N_{mass} and P_{mass} are more tolerant to unfavourable growing conditions. In contrast, plants would be vulnerable to damages from environmental stress if a high LMA was combined with high N_{mass} and P_{mass}, as it would accelerate energy losses *via* respiration (Wright et al., 2004). This might explain why negative-relationship slopes were the deepest in the arid region (**Figures 2D,E**).

Edaphic and Climatic Variables Regulating Leaf Traits

The favourability hypothesis suggests that plants tend to choose certain optimum trait assemblages when facing particular inhabiting conditions, either through trait plasticity within a species or via species turnover in community composition (Swenson et al., 2012; Simova et al., 2015). Temperature which influences plant hydraulics, nutrient utilization, and leaf energy balance, is a central controller of leaf trait variation (Fonseca et al., 2000; Michaletz et al., 2016). In the present study, it was obvious that the orientations of GST and LMA exhibited the smallest angle (**Supplementary Figure 2**), indicating that the GST tended to promote an increase in the LMA, which conflicts with prior studies (Swenson et al., 2012; Simova et al., 2015; Simova et al., 2018). We propose two probable explanations for the contradictory results. First, the sampling sites in our study covered a relatively narrower GST range (from –1 to 28.63°C) than the former studies. The plant growth form was mainly herbaceous plant species in the temperate zone, unlike, e.g., boreal coniferous species, with higher LMAs in cold conditions for modulating the temperatures of leaves (Michaletz et al., 2016). Second, the soil nutrients such as SOM, STN, STP, and SAN apparently decreased with increases in GST (**Supplementary Figure 4**). Plants exhibited low potential for resource capture and a slow photosynthetic rate under the more unfavourable inhabiting conditions (Wright et al., 2010; Swenson et al., 2012). They can also explain why the GST negatively influences P_{mass} and thereby affects the photosynthesis-N relationship (Reich et al., 2009), in accordance with previous studies (Kerkhoff et al., 2005; Sun et al., 2019). In addition, the negative correlation of the GST with N_{mass} (**Supplementary Figure 2**) provides evidence for the temperature–plant physiological hypothesis, i.e., leaf N would increase with decreasing temperature, as a high N concentration could compensate for physiological inefficiency in a cold environment (Reich and Oleksyn, 2004).

In this study, we used the benefit metrics for leaf traits to determine changes in plant growth strategy by analysing their relationship with different environmental drivers. Specifically, low relative benefits of LMA, high relative benefits of N_{mass} and P_{mass} implied an acquisitive growth strategy; conversely, a conservative growth strategy. Consistent with previous studies indicating that the responses of plant physiological processes to the same factor and underlying rules may be largely divergent in face of different environments (Quan et al., 2019), we found that the relative benefit of LMA was distinctly elevated, while the relative benefits of N_{mass} and P_{mass} decreased with increasing GSR in the arid and semi-humid regions, whereas in the humid region, the leaf traits showed the opposite pattern (**Figures 3A4–C4**). In that regard, the GSR is strongly positively associated with the GST and GSE in the arid and semi-humid

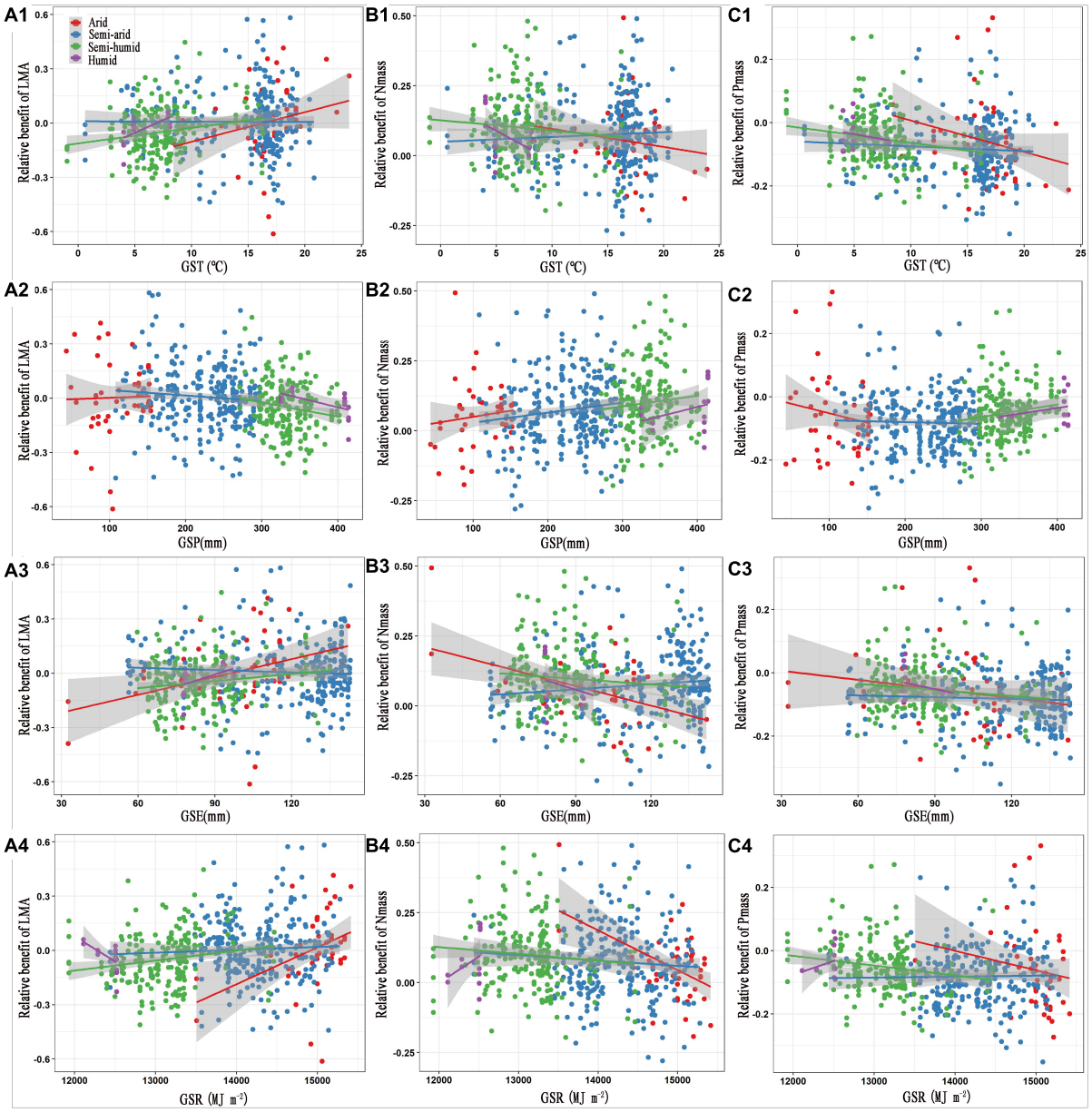

FIGURE 3 | Relationships between the relative benefits of leaf traits with growing season temperature **(A1–C1)**, precipitation **(A2–C2)**, evapotranspiration **(A3–C3)** and solar radiation **(A4–C4)**. The red, blue, green, and purple colours represent the arid, semi-arid, semi-humid, and humid climatic regions, respectively. LMA, leaf mass per area; N_{mass}, mass-based leaf nitrogen; P_{mass}, mass-based leaf phosphorus; GST, growing season temperature; GSP, growing season precipitation; GSE, growing season evapotranspiration; GSR, growing season solar radiation. The statistical information of linear regression are shown in **Table 2**.

regions and displays a significantly negative relation to the GSP in the semi-humid region (**Supplementary Figures 3D–F**). The radiation-induced warming leads to the reduction of soil water through intensifying evaporation (Wang et al., 2009), thereby aggravating the negative influences of drought in the arid area (Quan et al., 2019). Moreover, an increase in the GSE with increasing GSR accelerates the water consumption from transpiration (Decker et al., 2013). As the GSR increases, plants are expected to adopt conservative investment-return strategies with slow growth rates and higher LMAs with smaller areas exposed to solar radiation per gram leaf, to reduce radiative heating and water loss (Wright et al., 2004; Chen et al., 2013; Moles et al., 2014).

However, for the humid region, the overall relationships of the GIR with the GST, GSP, and GSR are considerably weaker than those in the other regions (**Supplementary Figure 3**). Indeed, the GIR is the lowest in this region (**Supplementary Table 1**), implying a relatively limited light resource availability. As a vital factor directly influencing plant growth, solar radiation plays crucial roles in many plant physiological processes, such as leaf

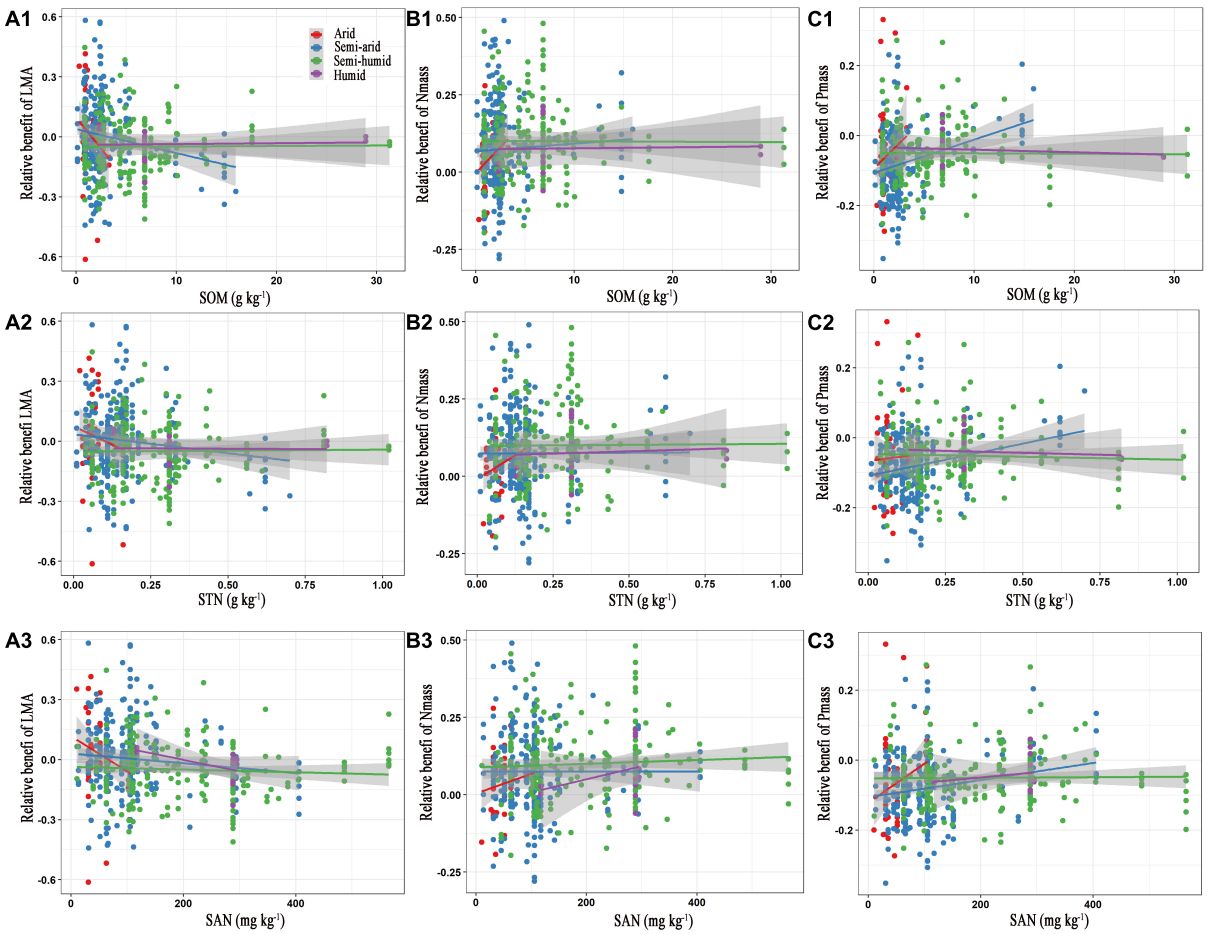

FIGURE 4 | Relationships between the relative benefits of leaf traits with soil organic matter **(A1–C1)**, total nitrogen **(A2–C2)** and available nitrogen **(A3–C3)**. The red, blue, green, and purple colours represent the arid, semi-arid, semi-humid, and humid climatic region, respectively. LMA, leaf mass per area; N_{mass}, mass-based leaf nitrogen; P_{mass}, mass-based leaf phosphorus; SOM, soil organic matter; STN, soil total nitrogen; SAN, soil available nitrogen. The statistical information of linear regression are shown in **Table 3**.

N and P accumulations (Takashima et al., 2004; Sun et al., 2019), photosynthesis (Waite and Sack, 2010), and protein synthesis (Xu, 2003). Consistent with Wright et al. (2006), who revealed that plants in higher-irradiance regions had a lower LMA and higher photosynthetic capacity than those in lower-irradiance areas, we observed that the GSR presented a negative impact on the relative benefit of LMA, but remarkably positively affected the relative benefits of N_{mass} and P_{mass} in the radiation-lacking region. This indicated that the plant growing strategy shifted from slow to fast as the GSR increased.

Unexpectedly, the GSP showed no significant effect on the relative benefit of leaf traits in the arid region (**Figures 3A2–C2**). The following several mechanisms might contribute to this. First, although precipitation data are relatively easier to obtain, they are not always sufficient proxies for soil water availability (Hickler et al., 2009), especially in hyper-arid grassland mostly belonging to desert steppe, where the soil water holding capacity are small. Thus, the soil available water is still limited, even if there is relatively high rainfall (Li et al., 2008; Xie, 2011). Second, it may be attributed to the inherent characteristics of plant species evolutionarily adapted to the hyper-arid conditions, with corresponding trait syndromes such as a high LMA and small stature (Wellstein et al., 2017), thereby inducing the plant community to be relatively less sensitive to rainfall (White et al., 2000). Finally, the low soil nutrient contents in this region (**Supplementary Table 1**) greatly restrict plant growth, which might weaken the relative importance of the GSP in mediating the leaf traits.

Soil nutrients play positive roles in multiple plant physiological activities. For example, the SOM provides energy for heterotrophic N-fixing microbes, and further facilitates plant N fixation (Reed et al., 2011; Zheng M. H. et al., 2019); the soil N can strongly affect the leaf N and plant photosynthesis (Lu et al., 2011; Yue et al., 2019); and a low soil P may lead to a lower leaf P and thus limit plant function (Han et al., 2005; Quesada et al., 2009; Sun et al., 2019). Plants invest more energy for resource acquisition in nutrient-insufficient soil

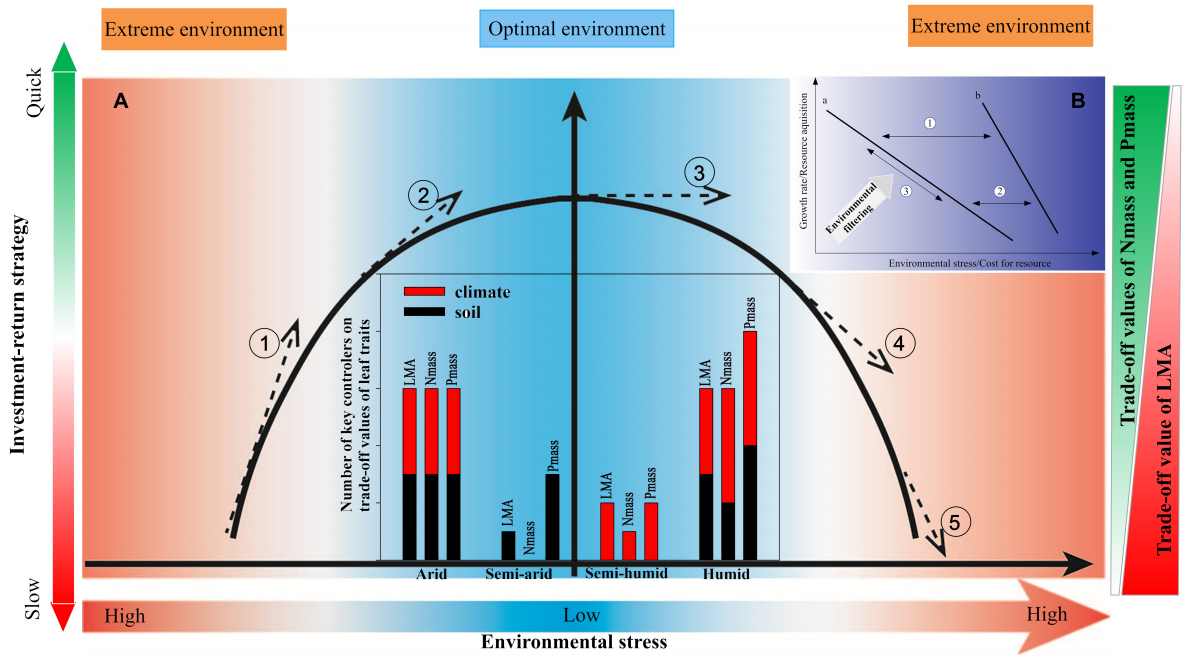

FIGURE 5 | Conceptual frameworks of relationship between leaf traits and environment reflect changes in the responses of plant growing strategies to environmental conditions. Subgraph **(A)** the relative benefit of LMA decreases while relative benefits of N_{mass} and P_{mass} increase when the environmental stress weakens, indicating an investment-return strategy changing from slow to quick (① and ②), ④ and ⑤ represent opposite trends from optimal to extreme environmental conditions; the leaf traits are more sensitive to environmental drivers with steeper slopes (① and ⑤) in an extreme environment than in an optimal environment (②, ③, and ④). The bar chart shows the numbers of the key climatic and edaphic factors controlling the relative benefits of leaf traits, with R square values no less than 0.20 according to the correlogram of intercorrelations (**Supplementary Figure 5**); the red and black colours represent climatic and edaphic factors, respectively. LMA, leaf mass per area; N_{mass}, mass-based leaf nitrogen; P_{mass}, mass-based leaf phosphorus. The shades of the colours represent the investment-return rate, the extent of environmental stress, and the magnitude of relative benefits of LMA, N_{mass}, and P_{mass}, respectively. Subgraph **(B)** a conceptual framework of environmental stress and cost for resource-regulating plant growth rate and resource acquisition indicated by leaf traits. Arrow ① and ②: the relationship curve turns but keeps a downward sloping trend when the environmental stress and costs for resources shift. The slope of curve b under high environmental stress is generally steeper than that of curve a in a less stressful environment. Arrow ③: plant growth rate and resource acquisition slide along curve a or b driven by environmental filtering. For example, as the environmental stress characterised by low resource availability strengthens, the cost for resources increases, so that the plants select a conservative strategy with a slow growth rate and long-life span.

(Nasto et al., 2014). Soil nutrient changes can induce species turnover, by influencing plant facilitation and competitive exclusion (Marriott et al., 2002; Guo, 2003). The regression relation between relative benefits of each leaf trait and soil nutrients indicated that the SOM, STN, and STP consistently presented significant promotion of an acquisitive growth strategy in the semi-arid region (**Figure 4**, **Table 3**, and **Supplementary Figure 7**). This may be ascribed to the poorer soil quality in this region (**Supplementary Table 1**). In contrast, the soils in the semi-humid region were relatively more fertile, providing plentiful nutrients for plant growth. In that regard, the leaf traits will not respond to the nutrient supply after the soil fertility fully meets the plant demand (**Figure 5**③; Bowman et al., 2003).

We found no evidence that the SOM, STN, and STP caused variations of relative benefits of leaf traits in the arid region with insufficient soil nutrients (**Figure 4** and **Supplementary Figure 7**). This may be owing to the narrow ranges of the SOM, STN, and STP content. Moreover, drought constrains the effectiveness of soil fertility on plant growth, and thus the sensitivity of the leaf traits to nutrients in the hyper-arid area (Sardans and Penuelas, 2004; Farooq et al., 2009). Additionally, the SAN presented negative effects on the relative benefit of LMA, but positively affected the relative benefits of N_{mass} and P_{mass}, promoting an acquisitive investment strategy except in the SAN-rich semi-humid region (**Figures 4A3–C3**). This agrees with early studies, i.e., that the leaf traits are more related to the N supply at a global scale (Ordonez et al., 2009).

Overall, our results confirm that abiotic filtering shapes the leaf trait pattern, i.e., higher costs for resources and environmental stress lead to a slow-growing strategy with conservative leaf traits, whereas optimal conditions result in a fast tissue turnover with acquisitive leaf traits across climatic regions in China (**Figure 5**). This supports the favourability hypothesis, i.e., that the plant leaf traits should be governed mainly via environmental filtering in a climatically harsh temperate zone (Fischer, 1960). Furthermore, more key environmental drivers and steeper leaf-trait-environment relationship slopes were found in the arid and humid regions (**Figure 5**), suggesting

TABLE 3 | Statistical information of linear regression relationships between the relative benefits of leaf traits and edaphic factors.

Edaphic variables	Climatic region	Relative benefit of LMA				Relative benefit of N_{mass}				Relative benefit of P_{mass}			
		R	Slope	Intercept	*P*	*R*	Slope	Intercept	*P*	*R*	Slope	Intercept	*P*
Soil organic matter	Arid				0.16				0.11				0.33
	Semi-arid	0.19	–0.01	0.039	**				0.38	0.29	0.01	–0.11	***
	Semi-humid				0.90				0.94				0.92
	Humid				0.88				0.91				0.67
Soil total nitrogen	Arid				0.33				0.08				0.82
	Semi-arid	0.13	–0.19	0.04	*				0.95	0.24	0.18	–0.11	***
	Semi-humid				0.84				0.88				0.57
	Humid				0.95				0.81				0.76
Soil total phosphorus	Arid				0.44				0.11				0.96
	Semi-arid	0.16	–1.42	0.10	**	0.12	81	0.02	*	0.14	0.61	–0.12	*
	Semi-humid				0.38				0.50				0.59
	Humid				0.97				0.82				0.74
Soil available nitrogen	Arid	0.26	–0.002	0.12	*	0.2	0.0006	0.004	*	0.25	0.001	–0.12	*
	Semi-arid	0.10	–0.0002	0.03	*				0.99	0.20	0.0002	–0.11	***
	Semi-humid				0.36				0.35				0.84
	Humid	0.48	–0.0006	0.11	*				0.27				0.52

*$P < 0.05$, **$P < 0.01$, ***$P < 0.001$.

that the degree of abiotic filtering is stronger in more stressful environments characterised by e.g., nutrient limitations or drought or over-wet conditions, in line with previous studies (Swenson et al., 2012; Simova et al., 2015). In that regard, the more stressful ecosystems are commonly inhabited by stress-tolerant species with a narrow geographical range size owing to natural selection (Thuiller et al., 2004), which respond more sensitively to environmental changes than wide-ranging species (Geng et al., 2012). Together with the finding that the environmental signal for the leaf traits would be relatively weaker in the optimal environmental conditions represented by the semi-humid region (**Supplementary Figure 6**), we conclude that an extreme environment elicits extreme ecological responses (Zhang F. Y. et al., 2019) and predict that frequent extreme climatic events caused by future climate change may enhance the fluctuations of the leaf traits in the terrestrial ecosystems (Jentsch and Beierkuhnlein, 2008; Stott et al., 2016).

CONCLUSION

Our findings provide valuable information for the emerging field of functional biogeography, particularly across the different climatic regions in China. First, the large LMA and small N_{mass} and P_{mass} were observed in the arid region, implying that plants under environmental stress as characterised by drought and low nutrient availability are slow-growing, with a conservative investment-return strategy. In contrast, acquisitive leaf traits were found in the semi-humid region, which presented optimal inhabiting conditions. Second, the GST and GSE consistently promoted conservative leaf traits, especially in the arid region. However, the GSR induced an opposite leaf trait pattern between the humid region and the others, confirming that plant functionality could respond divergently to the same factor in the face of different habitat conditions. Of all the studied soil nutrients, the SAN was the best indicator of a large-scale leaf trait pattern. Finally, we revealed that the leaf-trait-environment relationships were stronger under more stressful environmental conditions. These findings will help in refining ecological models and improving their applicability for China's ecosystems, further enabling us to evaluate the influence of global change. Owing to limited data availability, we only focused on the spatial patterns of the leaf traits and environmental controls with all herbaceous species pooled together; the influences of biotic interactions were not examined in the current study. Further in-depth systematic studies to evaluate the co-effects of abiotic and biotic factors on the leaf traits while considering the plant growth form are therefore highly desirable.

DATA AVAILABILITY STATEMENT

The raw data supporting the conclusions of this article will be made available by the authors, without undue reservation.

AUTHOR CONTRIBUTIONS

ZZ and JS conceived the study and wrote the manuscript. ZZ, JS, ML, HS, JNW, and JSW collected and analysed the data. ZZ, JS, ML, JNW, HZ, and YW drew the graphs. All authors reviewed and revised the manuscript.

FUNDING

This work was financially supported by the National Science Foundation of China (Grant No. 41871040), the Second Tibetan Plateau Scientific Expedition and Research (Grant No. 2019QZKK0405), the Open Project of the Qinghai Provincial Key Laboratory of Restoration Ecology in Cold Area (2020-KF-05), the China Postdoctoral Science Foundation (2021M702682), the Agricultural Research System of China (CARS-34), and the First Class Grassland Science Discipline Programme in Shandong Province of China.

ACKNOWLEDGMENTS

The authors thank Tiancai Zhou and the anonymous referees for their constructive suggestions on this manuscript.

SUPPLEMENTARY MATERIAL

The Supplementary Material for this article can be found online at: https://www.frontiersin.org/articles/10.3389/fpls.2022.757077/full#supplementary-material

REFERENCES

Asner, G. P., Knapp, D. E., Anderson, C. B., Martin, R. E., and Vaughn, N. R. (2016). Large-scale climatic and geophysical controls on the leaf economics spectrum. *Proc. Natl. Acad. Sci. U.S.A.* 113:201604863. doi: 10.1073/pnas.1604863113

Bjorkman, A. D., Myerssmith, I. H., Elmendorf, S. C., Normand, S., Ruger, N., Beck, P. S. A., et al. (2018). Plant functional trait change across a warming tundra biome. *Nature* 562, 57–62. doi: 10.1038/s41586-018-0563-7

Borgy, B., Violle, C., Choler, P., Garnier, E., Kattge, J., Loranger, J., et al. (2017). Sensitivity of community-level trait–environment relationships to data representativeness: a test for functional biogeography. *Glob. Ecol. Biogeogr.* 26, 729–739. doi: 10.1111/geb.12573

Bowman, W. D., Bahn, L., and Damm, M. (2003). Alpine landscape variation in foliar nitrogen and phosphorus concentrations and the relation to soil nitrogen and phosphorus availability. *Arct. Antarct. Alp. Res.* 35, 144–149. doi: 10.1657/1523-04302003035

Bradford, J. B., and Damato, A. W. (2012). Recognizing trade-offs in multi-objective land management. *Front. Ecol. Environ.* 10:210–216. doi: 10.1890/110031

Buzzard, V., Michaletz, S. T., Deng, Y., He, Z., Ning, D., Shen, L., et al. (2019). Continental scale structuring of forest and soil diversity via functional traits. *Nat. Ecol. Evol.* 3, 1298–1308. doi: 10.1038/s41559-019-0954-7

Carvajal, D. E., Loayza, A. P., Rios, R. S., Delpiano, C. A., and Squeo, F. A. (2019). A hyper-arid environment shapes an inverse pattern of the fast–slow plant economics spectrum for above-, but not below-ground resource acquisition strategies. *J. Ecol.* 107, 1079–1092. doi: 10.1111/1365-2745.13092

Chen, L. T., Niu, K. C., Wu, Y., Geng, Y., Mi, Z. R., Flynn, D. F. B., et al. (2013). UV radiation is the primary factor driving the variation in leaf phenolics across Chinese grasslands. *Ecol. Evol.* 3, 4696–4710. doi: 10.1002/ece3.862

Decker, M., Pitman, A. J., and Evans, J. P. (2013). Groundwater constraints on simulated transpiration variability over southeastern Australian forests. *J. Hydrometeorol.* 14, 543–559. doi: 10.1175/JHM-D-12-058.1

Diaz, S., Kattge, J., Cornelissen, J. H. C., Wright, I. J., Lavorel, S., Dray, S., et al. (2016). The global spectrum of plant form and function. *Nature* 529, 167–171. doi: 10.1038/nature16489

Donovan, L. A., Maherali, H., Caruso, C. M., Huber, H., and De Kroon, H. (2011). The evolution of the worldwide leaf economics spectrum. *Trends Ecol. Evol.* 26, 88–95. doi: 10.1016/j.tree.2010.11.011

Evans, J. R., and Poorter, H. (2001). Photosynthetic acclimation of plants to growth irradiance: the relative importance of specific leaf area and nitrogen partitioning in maximizing carbon gain. *Plant Cell Environ.* 24, 755–767. doi: 10.1046/j.1365-3040.2001.00724.x

Farooq, M., Wahid, A., Kobayashi, N., Fujita, D., and Basra, S. M. A. (2009). Plant drought stress: effects, mechanisms and management. *Agron. Sustain. Dev.* 29, 185–212. doi: 10.1051/agro:2008021

Fischer, A. G. (1960). Latitudinal variation in organic diversity. *Evolution* 14, 64–81. doi: 10.1111/j.1558-5646.1960.tb03057.x

Fonseca, C. R., Overton, J. M., Collins, B., and Westoby, M. (2000). Shifts in trait-combinations along rainfall and phosphorus gradients. *J. Ecol.* 88, 964–977. doi: 10.1046/j.1365-2745.2000.00506.x

Geng, Y., Wang, Z. H., Liang, C. Z., Fang, J. Y., Baumann, F., Kuhn, P., et al. (2012). Effect of geographical range size on plant functional traits and the relationships between plant, soil and climate in Chinese grasslands. *Glob. Ecol. Biogeogr.* 21, 416–427. doi: 10.1111/j.1466-8238.2011.00692.x

Gong, H. D., and Gao, J. (2019). Soil and climatic drivers of plant SLA (specific leaf area). *Glob. Ecol. Conserv.* 20:e00696. doi: 10.1016/j.gecco.2019.e00696

Griffinnolan, R. J., Blumenthal, D. M., Collins, S. L., Farkas, T. E., Hoffman, A. M., Mueller, K. E., et al. (2019). Shifts in plant functional composition following long-term drought in grasslands. *J. Ecol.* 107, 2133–2148. doi: 10.1111/1365-2745.13252

Guo, Q. F. (2003). Temporal species richness-biomass relationships along successional gradients. *J. Veg. Sci.* 14, 121–128. doi: 10.1658/1100-92332003014

Gusewell, S., and Koerselman, W. (2002). Variation in nitrogen and phosphorus concentrations of wetland plants. *Perspect. Plant Ecol. Evol. Syst.* 5, 37–61. doi: 10.1078/1433-8319-0000022

Han, W. X., Fang, J. Y., Guo, D., and Zhang, Y. (2005). Leaf nitrogen and phosphorus stoichiometry across 753 terrestrial plant species in China. *New Phytol.* 168, 377–385. doi: 10.1111/j.1469-8137.2005.01530.x

He, J. S., Wang, X. P., Flynn, D. F. B., Wang, L., Schmid, B., and Fang, J. Y. (2009). Taxonomic, phylogenetic, and environmental trade-offs between leaf productivity and persistence. *Ecology* 90, 2779–2791. doi: 10.1890/08-1126.1

He, J. S., Wang, Z. H., Wang, X. P., Schmid, B., Zuo, W., Zhou, M., et al. (2006). A test of the generality of leaf trait relationships on the Tibetan Plateau. *New Phytol.* 170, 835–848. doi: 10.1111/j.1469-8137.2006.01704.x

Hickler, T., Fronzek, S., Araujo, M. B., Schweiger, O., Thuiller, W., and Sykes, M. T. (2009). An ecosystem model-based estimate of changes in water availability differs from water proxies that are commonly used in species distribution models. *Glob. Ecol. Biogeogr.* 18, 304–313. doi: 10.1111/j.1466-8238.2009.00455.x

Jentsch, A., and Beierkuhnlein, C. (2008). Research frontiers in climate change : effects of extreme meteorological events on ecosystems. *C. R. Geosci.* 340, 621–628. doi: 10.1016/j.crte.2008.07.002

Kerkhoff, A. J., Enquist, B. J., Elser, J. J., and Fagan, W. F. (2005). Plant allometry, stoichiometry and the temperature-dependence of primary productivity. *Glob. Ecol. Biogeogr.* 14, 585–598. doi: 10.1111/j.1466-822X.2005.00187.x

Li, C. L., Hao, X. Y., Zhao, M. L., Han, G. D., and Willms, W. D. (2008). Influence of historic sheep grazing on vegetation and soil properties of a Desert Steppe in Inner Mongolia. *Agric. Ecosyst. Environ.* 128, 109–116. doi: 10.1016/j.agee.2008.05.008

Li, P., Deng, W., Zhang, H., Sun, J., and Xiong, J. N. (2019). Focus on economy or ecology? A three-dimensional trade-off based on ecological carrying capacity in southwest China. *Nat. Resour. Model.* 32:e12201. doi: 10.1111/nrm.12201

Lu, M., Yang, Y. H., Luo, Y. Q., Fang, C. M., Zhou, X. H., Chen, J. K., et al. (2011). Responses of ecosystem nitrogen cycle to nitrogen addition: a meta-analysis. *New Phytol.* 189, 1040–1050. doi: 10.1111/j.1469-8137.2010.03563.x

Lusk, C. H., Reich, P. B., Montgomery, R. A., Ackerly, D. D., and Cavenderbares, J. M. (2008). Why are evergreen leaves so contrary about shade. *Trends Ecol. Evol.* 23, 299–303. doi: 10.1016/j.tree.2008.02.006

Marriott, C. A., Bolton, G. R., Barthram, G. T., Fisher, J. M., and Hood, K. (2002). Early changes in species composition of upland sown grassland under extensive grazing management. *Appl. Veg. Sci.* 5, 87–98. doi: 10.1111/j.1654-109X.2002.tb00538.x

Michaletz, S. T., Weiser, M. D., Mcdowell, N. G., Zhou, J., Kaspari, M., Helliker, B. R., et al. (2016). The energetic and carbon economic origins of leaf thermoregulation. *Nat. Plants* 2:16129. doi: 10.1038/nplants.2016.129

Moles, A. T., Perkins, S., Laffan, S. W., Floresmoreno, H., Awasthy, M., Tindall, M. L., et al. (2014). Which is a better predictor of plant traits: temperature or precipitation? *J. Veg. Sci.* 25, 1167–1180. doi: 10.1111/jvs.12190

Nasto, M. K., Alvarezclare, S., Lekberg, Y., Sullivan, B. W., Townsend, A. R., and Cleveland, C. C. (2014). Interactions among nitrogen fixation and soil phosphorus acquisition strategies in lowland tropical rain forests. *Ecol. Lett.* 17, 1282–1289. doi: 10.1111/ele.12335

Niinemets, U. (2001). Global-scale climatic controls of leaf dry mass per area, density, and thickness in trees and shrubs. *Ecology* 82, 453–469.

Niklas, K. J., Owens, T. G., Reich, P. B., and Cobb, E. D. (2005). Nitrogen/phosphorus leaf stoichiometry and the scaling of plant growth. *Ecol. Lett.* 8, 636–642. doi: 10.1111/j.1461-0248.2005.00759.x

Ordonez, A., and Olff, H. (2013). Do alien plant species profit more from high resource supply than natives? A trait-based analysis. *Glob. Ecol. Biogeogr.* 22, 648–658. doi: 10.1111/geb.12019

Ordonez, J. C., Van Bodegom, P. M., Witte, J. P. M., Wright, I. J., Reich, P. B., and Aerts, R. (2009). A global study of relationships between leaf traits, climate and soil measures of nutrient fertility. *Glob. Ecol. Biogeogr.* 18, 137–149. doi: 10.1111/j.1466-8238.2008.00441.x

Pearson, R. G., Phillips, S. J., Loranty, M. M., Beck, P. S. A., Damoulas, T., Knight, S. J., et al. (2013). Shifts in Arctic vegetation and associated feedbacks under climate change. *Nat. Clim. Chang.* 3, 673–677. doi: 10.1038/nclimate1858

Quan, Q., Tian, D. S., Luo, Y. Q., Zhang, F. Y., Crowther, T. W., Zhu, K., et al. (2019). Water scaling of ecosystem carbon cycle feedback to climate warming. *Sci. Adv.* 5:eaav1131. doi: 10.1126/sciadv.aav1131

Quesada, C. A., Lloyd, J., Schwarz, M., Baker, T. R., Phillips, O. L., Patino, S., et al. (2009). Regional and large-scale patterns in Amazon forest structure and function are mediated by variations in soil physical and chemical properties. *Biog. Disc.* 6, 3993–4057. doi: 10.5194/bgd-6-3993-2009

R Core Team (2016). *R: A language and Environment for Statistical Computing*. Vienna: R Foundation for Statistical Computing.

Reed, S. C., Cleveland, C. C., and Townsend, A. R. (2011). Functional ecology of free-living nitrogen fixation: a contemporary perspective. *Annu. Rev. Ecol. Evol. Syst.* 42, 489–512. doi: 10.1146/annurev-ecolsys-102710-145034

Reich, P. B., and Oleksyn, J. (2004). Global patterns of plant leaf N and P in relation to temperature and latitude. *Proc. Natl. Acad. Sci. U.S.A.* 101, 11001–11006. doi: 10.1073/pnas.0403588101

Reich, P. B., Oleksyn, J., and Wright, I. J. (2009). Leaf phosphorus influences the photosynthesis–nitrogen relation: a cross-biome analysis of 314 species. *Oecologia* 160, 207–212. doi: 10.1007/s00442-009-1291-3

Reich, P. B., Wright, I. J., Cavenderbares, J. M., Craine, J. M., Oleksyn, J., Westoby, M., et al. (2003). The evolution of plant functional variation: traits, spectra, and strategies. *Int. J. Plant Sci.* 164, 143–164. doi: 10.1086/374368

Reichstein, M., Bahn, M., Mahecha, M. D., Kattge, J., and Baldocchi, D. D. (2014). Linking plant and ecosystem functional biogeography. *Proc. Natl. Acad. Sci. U.S.A.* 111, 13697–13702. doi: 10.1073/pnas.1216065111

Santiago, L. S., and Wright, S. J. (2007). Leaf functional traits of tropical forest plants in relation to growth form. *Funct. Ecol.* 21, 19–27. doi: 10.1111/j.1365-2435.2006.01218.x

Sardans, J., and Penuelas, J. (2004). Increasing drought decreases phosphorus availability in an evergreen Mediterranean forest. *Plant Soil* 267, 367–377. doi: 10.1007/s11104-005-0172-8

Schuur, E. A. G., and Matson, P. A. (2001). Net primary productivity and nutrient cycling across a mesic to wet precipitation gradient in Hawaiian montane forest. *Oecologia* 128, 431–442. doi: 10.2307/4223025

Schwinning, S., and Ehleringer, J. R. (2001). Water use trade-offs and optimal adaptations to pulse-driven arid ecosystems. *J. Ecol.* 89, 464–480. doi: 10.1046/j.1365-2745.2001.00576.x

Shangguan, W., Dai, Y. J., Liu, B. Y., Zhu, A. X., Duan, Q. Y., Wu, L. Z., et al. (2013). A China data set of soil properties for land surface modeling. *J. Adv. Model. Earth Syst.* 5, 212–224. doi: 10.1002/jame.20026

Shipley, B., De Bello, F., Cornelissen, J. H. C., Laliberte, E., Laughlin, D. C., and Reich, P. B. (2016). Reinforcing loose foundation stones in trait-based plant ecology. *Oecologia* 180, 923–931. doi: 10.1007/s00442-016-3549-x

Shipley, B., Lechowicz, M. J., Wright, I. J., and Reich, P. B. (2006). Fundamental trade-offs generating the worldwide leaf economics spectrum. *Ecology* 87, 535–541. doi: 10.2307/20068973

Simova, I., Rueda, M., and Hawkins, B. A. (2017). Stress from cold and drought as drivers of functional trait spectra in North American angiosperm tree assemblages. *Ecol. Evol.* 7, 7548–7559. doi: 10.1002/ece3.3297

Simova, I., Violle, C., Kraft, N. J. B., Storch, D., Svenning, J., Boyle, B., et al. (2015). Shifts in trait means and variances in North American tree assemblages: species richness patterns are loosely related to the functional space. *Ecography* 38, 649–658. doi: 10.1111/ecog.00867

Simova, I., Violle, C., Svenning, J., Kattge, J., Engemann, K., Sandel, B., et al. (2018). Spatial patterns and climate relationships of major plant traits in the New World differ between woody and herbaceous species. *J. Biogeogr.* 45, 895–916. doi: 10.1111/jbi.13171

Stott, P. A., Christidis, N., Otto, F. E. L., Sun, Y., Vanderlinden, J., Van Oldenborgh, G. J., et al. (2016). Attribution of extreme weather and climate-related events. *Wiley Interdiscip. Rev. Clim. Chang.* 7, 23–41. doi: 10.1002/wcc.380

Stubbs, W. J., and Wilson, J. B. (2004). Evidence for limiting similarity in a sand dune community. *J. Ecol.* 92, 557–567. doi: 10.1111/j.0022-0477.2004.00898.x

Sun, J., and Du, W. P. (2017). Effects of precipitation and temperature on net primary productivity and precipitation use efficiency across China's grasslands. *GISci. Remote Sens.* 54, 881–897. doi: 10.1080/15481603.2017.1351147

Sun, J., Liu, B. Y., You, Y., Li, W. P., Liu, M., Shang, H., et al. (2019). Solar radiation regulates the leaf nitrogen and phosphorus stoichiometry across alpine meadows of the Tibetan Plateau. *Agr. For. Meteorol.* 271, 92–101. doi: 10.1016/j.agrformet.2019.02.041

Sun, J., Ma, B. B., and Lu, X. Y. (2018). Grazing enhances soil nutrient effects: trade-offs between aboveground and belowground biomass in alpine grasslands of the Tibetan Plateau. *Land Degrad. Dev.* 29, 337–348. doi: 10.1002/ldr.2822

Sun, J., Zhou, T. C., Liu, M., Chen, Y., Liu, G., Xu, M., et al. (2020). Water and heat availability are drivers of the aboveground plant carbon accumulation rate in alpine grasslands on the Tibetan Plateau. *Glob. Ecol. Biogeogr.* 29, 50–64. doi: 10.1111/geb.13006

Swenson, N. G., Enquist, B. J., Pither, J., Kerkhoff, A. J., Boyle, B., Weiser, M. D., et al. (2012). The biogeography and filtering of woody plant functional diversity in North and South America. *Glob. Ecol. Biogeogr.* 21, 798–808. doi: 10.1111/j.1466-8238.2011.00727.x

Takashima, T., Hikosaka, K., and Hirose, T. (2004). Photosynthesis or persistence: nitrogen allocation in leaves of evergreen and deciduous Quercus species. *Plant Cell Environ.* 27, 1047–1054. doi: 10.1111/j.1365-3040.2004.01209.x

Thornthwaite, C. W. (1948). An approach toward a rational classification of climate. *Geogr. Rev.* 38, 55–94. doi: 10.1111/10.2307/210739

Thuiller, W., Lavorel, S., Midgley, G. F., Lavergne, S., and Rebelo, T. (2004). Relating plant traits and species distributions along bioclimatic gradients for 88 *Leucadendron* taxa. *Ecology* 85, 1688–1699. doi: 10.1890/03-0148

Van Bodegom, P. M., Callaghan, T. V., Chapin, F. S., Gerdol, R., Gwynn, D., Hartley, A. E., et al. (2007). Global negative vegetation feedback to climate warming responses of leaf litter decomposition rates in cold biomes. *Ecol. Lett.* 10, 619–627. doi: 10.1111/j.1461-0248.2007.01051.x

Violle, C., Reich, P. B., Pacala, S. W., Enquist, B. J., and Kattge, J. (2014). The emergence and promise of functional biogeography. *Proc. Natl. Acad. Sci. U.S.A.* 111, 13690–13696. doi: 10.1073/pnas.1415442111

Waite, M., and Sack, L. (2010). How does moss photosynthesis relate to leaf and canopy structure? Trait relationships for 10 Hawaiian species of contrasting light habitats. *New Phytol.* 185, 156–172. doi: 10.1111/j.1469-8137.2009.03061.x

Wang, C. T., Long, R. J., Wang, Q. L., Jing, Z. C., and Shi, J. J. (2009). Changes in plant diversity, biomass and soil C, in alpine meadows at different degradation stages in the headwater region of three rivers, China. *Land Degrad. Dev.* 20, 187–198. doi: 10.1002/ldr.879

Wang, G. H. (2007). Leaf trait co-variation, response and effect in a chronosequence. *J. Veg. Sci.* 18, 563–570. doi: 10.1111/j.1654-1103.2007.tb02570.x

Wellstein, C., Poschlod, P., Gohlke, A., Chelli, S., Campetella, G., Rosbakh, S., et al. (2017). Effects of extreme drought on specific leaf area of grassland species: a meta-analysis of experimental studies in temperate and sub-Mediterranean systems. *Glob. Chang. Biol.* 23, 2473–2481. doi: 10.1111/gcb.13662

Werden, L. K., Waring, B. G., Smithmartin, C. M., and Powers, J. S. (2018). Tropical dry forest trees and lianas differ in leaf economic spectrum traits but have overlapping water-use strategies. *Tree Physiol.* 38, 517–530. doi: 10.1093/treephys/tpx135

Westoby, M., and Wright, I. J. (2006). Land-plant ecology on the basis of functional traits. *Trends Ecol. Evol.* 21, 261–268. doi: 10.1016/j.tree.2006.02.004

White, T. A., Campbell, B. D., Kemp, P. D., and Hunt, C. L. (2000). Sensitivity of three grassland communities to simulated extreme temperature and rainfall events. *Glob. Chang. Biol.* 6, 671–684. doi: 10.1046/j.1365-2486.2000.00344.x

Wright, I. J., Reich, P. B., Atkin, O. K., Lusk, C. H., Tjoelker, M. G., and Westoby, M. (2006). Irradiance, temperature and rainfall influence leaf dark respiration in woody plants: evidence from comparisons across 20 sites. *New Phytol.* 169, 309–319. doi: 10.1111/j.1469-8137.2005.01590.x

Wright, I. J., Reich, P. B., Cornelissen, J. H. C., Falster, D. S., Groom, P. K., Hikosaka, K., et al. (2005). Modulation of leaf economic traits and trait relationships by climate. *Glob. Ecol. Biogeogr.* 14, 411–421. doi: 10.1111/j.1466-822x.2005.00172.x

Wright, I. J., Reich, P. B., and Westoby, M. (2001). Strategy shifts in leaf physiology, structure and nutrient content between species of high- and low-rainfall and high- and low-nutrient habitats. *Funct. Ecol.* 15, 423–434. doi: 10.2307/826662

Wright, I. J., Reich, P. B., Westoby, M., Ackerly, D. D., Baruch, Z., Bongers, F., et al. (2004). The worldwide leaf economics spectrum. *Nature* 428, 821–827. doi: 10.1038/nature02403

Wright, J. P., and Suttongrier, A. E. (2012). Does the leaf economic spectrum hold within local species pools across varying environmental conditions. *Funct. Ecol.* 26, 1390–1398. doi: 10.1111/1365-2435.12001

Wright, S. J., Kitajima, K., Kraft, N. J. B., Reich, P. B., Wright, I. J., Bunker, D. E., et al. (2010). Functional traits and the growth-mortality trade-off in tropical trees. *Ecology* 91, 3664–3674. doi: 10.1890/09-2335.1

Xie, Y. Z. (2011). Water Holding Capacity and Capita Storage of Plant Community Litter in Representative Desert Steppe. *J. Soil Water Conserv.* 25, 144–147.

Xu, J. W. (2003). Effect of low-light stress on nitrogen accumulation, distribution and grains protein content of Indica hybrid. *Plant Nutr. Fert. Sci.* 9, 288–293.

Yue, K., Peng, Y., Fornara, D. A., Van Meerbeek, K., Vesterdal, L., Yang, W. Q., et al. (2019). Responses of nitrogen concentrations and pools to multiple environmental change drivers: a meta-analysis across terrestrial ecosystems. *Glob. Ecol. Biogeogr.* 28, 690–724. doi: 10.1111/geb.12884

Zhang, C. C., Li, X. Y., Wu, H. W., Wang, P., Wang, Y., Wu, X. C., et al. (2017). Differences in water-use strategies along an aridity gradient between two coexisting desert shrubs (*Reaumuria soongorica* and *Nitraria sphaerocarpa*): isotopic approaches with physiological evidence. *Plant Soil* 419, 169–187. doi: 10.1007/s11104-017-3332-8

Zhang, C. J., Liao, Y. M., Duan, J. Q., Song, Y. L., Huang, D. P., Sheng, W., et al. (2016). The Progresses of Dry-Wet Climate Divisional Research in China. *Clim. Chang. Res.* 12, 261–267.

Zhang, F. M., and Shen, S. H. (2008). A Study on Dry/Wet Conditions and Changes of Dry/Wet Climate Boundary in China. *J. Nanj. Inst. Met.* 31, 574–579. doi: 10.3724/SP.J.1047.2008.00014

Zhang, F. Y., Quan, Q., Ma, F. F., Tian, D. S., Hoover, D. L., Zhou, Q. P., et al. (2019). When does extreme drought elicit extreme ecological responses. *J. Ecol.* 107, 2553–2563. doi: 10.1111/1365-2745.13226

Zhang, S. S., Zheng, Q., Noll, L., Hu, Y. T., and Wanek, W. (2019). Environmental effects on soil microbial nitrogen use efficiency are controlled by allocation of organic nitrogen to microbial growth and regulate gross N mineralization. *Soil Biol. Biochem.* 135, 304–315. doi: 10.1016/j.soilbio.2019.05.019

Zhang, X. L., Zhou, J. H., Guan, T. Y., Cai, W. T., Jiang, L. H., Lai, L. M., et al. (2019). Spatial variation in leaf nutrient traits of dominant desert riparian plant species in an arid inland river basin of China. *Ecol. Evol.* 9, 1523–1531. doi: 10.1002/ece3.4877

Zheng, M. H., Chen, H., Li, D. J., Luo, Y. Q., and Mo, J. M. (2019). Substrate stoichiometry determines nitrogen fixation throughout succession in southern Chinese forests. *Ecol. Lett.* 23, 336–347. doi: 10.1111/ele.13437

Zheng, Q., Hu, Y. T., Zhang, S. S., Noll, L., Bockle, T., Richter, A., et al. (2019). Growth explains microbial carbon use efficiency across soils differing in land use and geology. *Soil Biol. Biochem.* 128, 45–55. doi: 10.1016/j.soilbio.2018.10.006

Zhou, T. C., Sun, J., Liu, M., Shi, P. L., Zhang, X. B., Sun, W., et al. (2019). Coupling between plant nitrogen and phosphorus along water and heat gradients in alpine grassland. *Sci. Total Environ.* 701:134660. doi: 10.1016/j.scitotenv.2019.134660

Conflict of Interest: The authors declare that the research was conducted in the absence of any commercial or financial relationships that could be construed as a potential conflict of interest.

Publisher's Note: All claims expressed in this article are solely those of the authors and do not necessarily represent those of their affiliated organizations, or those of the publisher, the editors and the reviewers. Any product that may be evaluated in this article, or claim that may be made by its manufacturer, is not guaranteed or endorsed by the publisher.

Copyright © 2022 Zhang, Sun, Liu, Shang, Wang, Wang, Zhou, Li, Wang and Chen. This is an open-access article distributed under the terms of the Creative Commons Attribution License (CC BY). The use, distribution or reproduction in other forums is permitted, provided the original author(s) and the copyright owner(s) are credited and that the original publication in this journal is cited, in accordance with accepted academic practice. No use, distribution or reproduction is permitted which does not comply with these terms.

frontiers | Frontiers in Plant Science

ORIGINAL RESEARCH
published: 06 April 2022
doi: 10.3389/fpls.2022.854152

Soil Moisture Variations in Response to Precipitation Across Different Vegetation Types on the Northeastern Qinghai-Tibet Plateau

Licong Dai[1,2,3], Ruiyu Fu[4], Xiaowei Guo[2,3], Yangong Du[2,3], Fawei Zhang[2,3] and Guangmin Cao[2,3]*

[1] College of Ecology and Environment, Hainan University, Haikou, China, [2] Qinghai Provincial Key Laboratory of Restoration Ecology for Cold Regions, Northwest Institute of Plateau Biology, Chinese Academy of Sciences, Xining, China, [3] Key Laboratory of Adaptation and Evolution of Plateau Biota, Northwest Institute of Plateau Biology, Chinese Academy of Sciences, Xining, China, [4] Hainan Academy of Forestry, Haikou, China

An understanding of soil moisture conditions is crucial for hydrological modeling and hydrological processes. However, few studies have compared the differences between the dynamics of soil moisture content and soil moisture response to precipitation infiltration under different types of vegetation on the Qinghai-Tibet Plateau (QTP). In this study, a soil moisture sensor was used for continuous volumetric soil moisture measurements during 2015 and 2016, with the aim of exploring variations in soil moisture and its response to precipitation infiltration across two vegetation types (alpine meadow and alpine shrub). Our results showed that temporal variations in soil moisture at the surface (0–20 cm) and middle soil layers (40–60 cm) were consistent with precipitation patterns for both vegetation types. However, there was a clear lag in the soil moisture response to precipitation for the deep soil layers (80–100 cm). Soil moisture content was found to be significantly positively related to precipitation and negatively related to air temperature. Aboveground biomass was significantly negatively associated with the surface soil moisture content (0–20 cm) during the growing season. Statistically significant differences were observed between the soil water content of the surface, middle, and deep soil layers for the two vegetation types ($p < 0.05$). Soil moisture (19.81%) in the surface soil layer was significantly lower than that in the deep soil layer (24.75%) for alpine shrubs, and the opposite trend was observed for alpine meadows. The maximum infiltration depth of alpine shrubs was greater than that of alpine meadows under extremely high-precipitation events, which indicates that alpine shrubs might be less susceptible to surface runoff under extreme precipitation events. Furthermore, low precipitation amounts did not affect precipitation infiltration for either vegetation type, whereas the infiltration depth increased with precipitation for both vegetation types. Our results suggest that a series of small precipitation events may not have the same effect on soil moisture as a single large precipitation event that produces the equivalent total rainfall.

Keywords: soil moisture, Qinghai-Tibet Plateau, precipitation infiltration, temporal variations, vegetation type

OPEN ACCESS

Edited by:
Gao-Lin Wu,
Northwest A&F University, China

Reviewed by:
Lafe Conner,
Utah Valley University, United States
Furong Niu,
University of Arizona, United States

***Correspondence:**
Xiaowei Guo
xwguo1206@163.com

Specialty section:
This article was submitted to Functional Plant Ecology, a section of the journal Frontiers in Plant Science

Received: *13 January 2022*
Accepted: *25 February 2022*
Published: *06 April 2022*

Citation:
Dai L, Fu R, Guo X, Du Y, Zhang F and Cao G (2022) Soil Moisture Variations in Response to Precipitation Across Different Vegetation Types on the Northeastern Qinghai-Tibet Plateau. Front. Plant Sci. 13:854152. doi: 10.3389/fpls.2022.854152

INTRODUCTION

Soil moisture is a key component of the hydrological cycle of terrestrial ecosystems (Schwinning and Sala, 2004; Song et al., 2007) and provides an important link between soil properties and plants, which play critical roles in vegetation restoration and hydrological processes, such as infiltration, evaporation, and the uptake of groundwater and root water (Puri et al., 2011). However, soil moisture is often heterogeneous in both temporal and spatial dimensions, even at small scales (Gómez-Plaza et al., 2000), and is affected by factors such as vegetation (Vivoni et al., 2010), topography (Svetlitchnyi et al., 2003; Yang et al., 2012), soil type (Tomer and Anderson, 1995), and land use (Biro et al., 2013). Characterizing soil moisture and its spatial and temporal variability is, therefore, a key focus area for research into water resource management and hydrological processes.

Many studies have investigated the dynamics and magnitude of temporal and spatial changes to soil moisture distribution driven by land-use change (Gómez-Plaza et al., 2000; Chen et al., 2007), and previous studies have focused on understanding the dominant influences on soil moisture variability at a catchment scale and at larger scales (Deng et al., 2016; Mei et al., 2018). For example, Niu et al. (2015) analyzed soil moisture conditions under different land uses in an arid region of Horqin Sandy Land in northern China and found that soil moisture was sensitive to differences in land use. They also showed that temporal variability in soil moisture did not always agree with rainfall events. Other studies have suggested that vegetation type and precipitation characteristics have the strongest influence on soil moisture across soil profiles (Chen et al., 2007; Duan et al., 2016). Moreover, surface soil moisture is greatly affected by the amount and intensity of precipitation, whereas the moisture content of deeper soil layers is mainly determined by vegetation type (Cheng et al., 2020). For instance, Yao et al. (2013) found that surface soil moisture is more sensitive to precipitation than soil moisture in deeper soil layers.

In addition to different land uses and precipitation patterns, soil moisture is also affected by vegetation cover and topography. A previous study found that vegetation cover is negatively related to soil moisture because the plant canopy intercepts rainfall, and plant growth can consume soil water (Yang et al., 2018). In comparison with soil moisture, slope position and aspect may affect shallow soil moisture more than deep layers, whereas slope gradient considerably affects both shallow and deep soil moisture (Yang et al., 2012). Furthermore, precipitation patterns and vegetation cover also affect soil infiltration processes, as well as antecedent soil water content (Guo et al., 2015; Dai et al., 2019a) and soil properties (Neris et al., 2012). Several studies have shown that soil infiltration is significantly affected by precipitation intensity and that infiltration depth increases with precipitation amount (Yao et al., 2013; Niu et al., 2015). Overall, the previous research has mostly been conducted in temperate, semiarid, and arid regions such as the Loess Plateau and Inner Mongolia in China (Yao et al., 2013; Cheng et al., 2020). The dynamics that control soil moisture in alpine ecosystems have received less attention, and the effects of different vegetation types have been neglected. The assessment of soil moisture dynamics for different vegetation types in an alpine ecosystem can provide much-needed insights into the effective use of water resources in alpine environments.

The 2.5 million km^2 of alpine grassland, which covers nearly 60% of the Qinghai-Tibet Plateau (QTP), is the largest area of alpine grassland in the world (Dong et al., 2020). Streams in the surrounding regions are important water resources for China and Southeast Asia (Dai et al., 2019a) and most originate in the QTP. The previous studies in this region have focused on the effects of alpine meadow degradation on soil water retention (Zeng et al., 2013; Pan et al., 2016; Dai et al., 2020a,b), rather than assessing soil moisture dynamics and responses to precipitation infiltration under different vegetation types. In this study, we aimed to describe how soil moisture responds to precipitation across different vegetation types in the QTP. The objectives were to explore (1) the dynamics that control soil moisture for two types of vegetation, (2) the response of soil moisture to different precipitation events under different vegetation types, and (3) differences in the vertical soil moisture distribution under different vegetation types.

MATERIALS AND METHODS

Study Area

This study was conducted at the Haibei National Field Research Station, Qinghai, China (37°37N, 101°19E), at an elevation of 3,200 m ASL on the northeastern QTP (**Figure 1**). This region has a plateau continental monsoon climate with an average annual temperature of −1.7°C and monthly mean temperatures ranging from −15.0°C in January to 10.1°C in July. The annual precipitation is 580 mm, of which 80% falls between May and September (the growing season), and the annual pan evaporation is approximately 1,191.4 mm. Two vegetation types were selected for this region: alpine shrub and alpine meadow (**Figure 1**). The alpine shrubs and alpine meadows were mainly dominated by *Potentilla fruticosa* and *Kobresia humilis*, respectively. Both vegetation types were close to the meteorological station at Haibei National Field Research Station. Seasonally frozen ground is well developed in this region, and the groundwater level is approximately 3–5 m (Dai et al., 2019b). For the alpine meadow, there was a thick mattic epipedon layer in the topsoil at a depth of 10–30 cm. The mattic epipedon has a relatively high water-holding capacity and low heat conductivity. The basic soil properties of the two vegetation types are presented in **Table 1**.

Experimental Design

Three research plots (25 m × 25 m) were selected for each vegetation type and were located on flat terrain where no runoff occurred. To explore the soil water content variation under different soil layers, we defined soil layers of 0–20, 40–60, and 80–100 cm to represent the surface horizon, middle soil layer, and deep soil layer, respectively (Yao et al., 2013). In this study, the mean surface soil water content (0–20 cm) was sampled at 5-, 10-, 15-, and 20-cm depths, the mean middle soil water content (40–60 cm) was sampled at 40- and 60-cm depths and

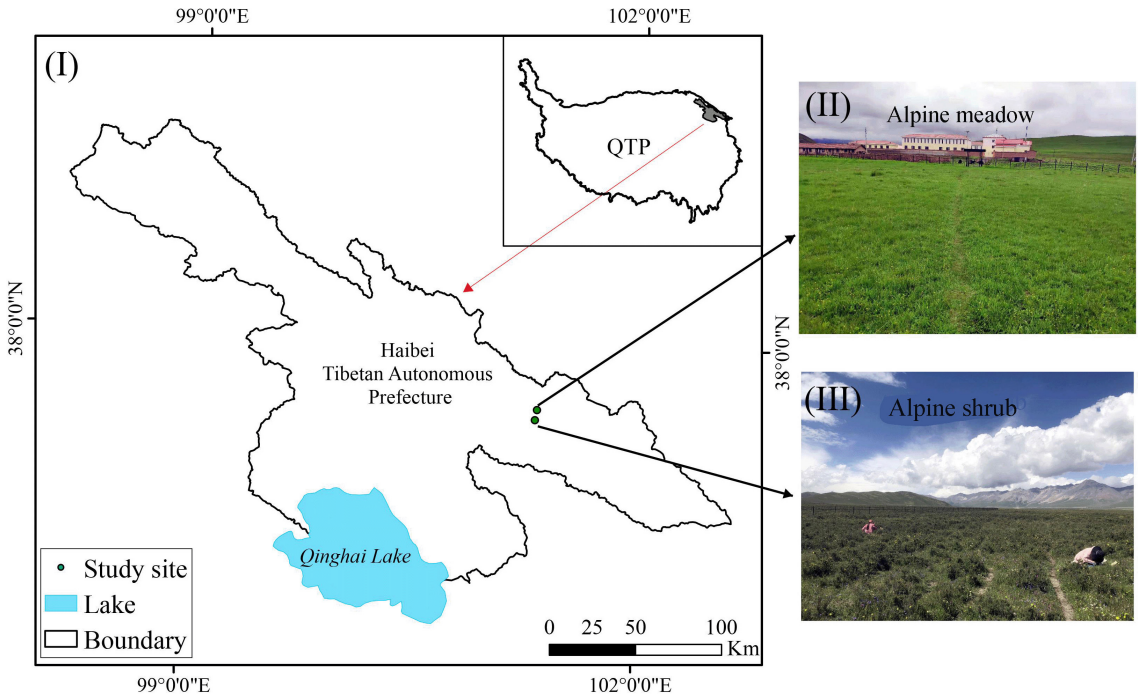

FIGURE 1 | The location of study area **(I)**, alpine meadow **(II)**, and alpine shrub **(III)**.

TABLE 1 | Vegetation and soil characteristics at 0–40 cm across two vegetation types in the study area.

Vegetation type	Dominant species	Soil depth (cm)	Soil bulk density (g cm^{-3})	Soil organic matter (g kg^{-1})	Clay content (%)	Silt content (%)	Sand content (%)	Saturated water (%, v/v)	Field water (%,v/v)
Alpine meadow	*Kobresia humilis*	0–20	0.90	91.22	4.66	47.22	48.12	56.50	38.47
		20–40	1.06	60.97	7.58	60.54	31.88	53.38	34.15
Alpine shrub	*Potentilla fruticosa*	0–20	0.72	118.35	6.81	67.06	26.13	72.40	42.96
		20–40	0.98	75.65	6.23	60.17	33.60	63.17	43.44

the mean deep layer soil water content (80–100 cm) was sampled at 80- and 100-cm depths.

To investigate the soil moisture response to precipitation infiltration under different vegetation types, we measured the soil moisture content 1–2 days before precipitation events, 1–2 days after precipitation events, and before the next precipitation event. We selected four different precipitation events in 2016 to assess changes in the vertical soil water distribution following each event (Gao et al., 2014). A low precipitation event (2.6 mm) occurred on April 24, a medium precipitation event (16.5 mm) occurred on June 13 and 14, a high-precipitation event (37.4 mm) lasted from August 12 to 14, and an extremely high-precipitation event (68.1 mm) lasted from June 19 to 25.

Soil Properties and Biomass Measurement

The volumetric soil moisture was measured from 2015 to 2016 using the soil moisture sensor for the two vegetation types at depths of 5, 10, 15, 20, 40, 60, 80, and 100 cm, with three sensors per depth. This probe continuously measures soil moisture and updates a data logger (CR10X, Campbell Scientific, Logan, UT, United States) every 30 min. To avoid the effect of soil properties on the accuracy of soil water content measured by a soil moisture sensor, we adopted a manual field measurement method to calibrate the soil water content. This was done using a cutting-ring sampler to obtain an undisturbed soil sample at the same depth around the buried soil moisture sensors each month, repeated four times at each depth. The manually measured soil moisture was analyzed using linear regression with the soil moisture measured using a soil moisture sensor to obtain the calibration coefficient. Meteorological data for the study period, which include precipitation, air temperature, and wind velocity, were obtained from an automatic meteorological station located less than 60 m from the study site. To examine the effects of soil properties on soil moisture, we collected soil samples at depths of 0–20 and 20–40 cm, with three replicates. Soil organic matter was determined using the Walkley–Black method (Nelson and Sommers, 1996), and the soil particle distribution was measured using a MasterSizer 2000 (Malvern Instruments Ltd., United Kingdom) to obtain the clay (<0.002 mm), silt (0.002–0.02 mm), and sand (0.02–2 mm) contents. The soil bulk

density was calculated as the ratio of the oven-dried soil mass to the core volume, and saturated water and field water were obtained using the cutting-ring method (Dai et al., 2020a).

Furthermore, the aboveground biomass was also obtained monthly during the growing season (i.e., from May to September) in 2015–2016, with the aim of exploring the effect of vegetation coverage on soil moisture content. The aboveground biomass was obtained using the standard harvesting method in 10 randomly selected quadrats (25 cm × 25 cm) and then oven-dried at 65°C to a constant weight.

Data Analysis

First, a one-way analysis of variance (ANOVA) was used to test the effects of vegetation type on soil moisture content, followed by Tukey's HSD test to compare differences in the mean water content for different land uses and soil layers when the results of the ANOVA were significant at $p < 0.05$. Second, Pearson's correlation analysis was used to examine the relationship between meteorological factors and soil moisture. All analyses were conducted using R version 3.4.3 (R Development Core Team, 2006).

RESULTS

Precipitation Patterns

From January 2015 to December 2016, 208 precipitation events were recorded, amounting to a cumulative total of 908.9 mm during the research period (**Figure 2B**). The minimum precipitation for any individual event within the 208 events was 0.1 mm and the maximum was 27.2 mm. The most prevalent precipitation event was a small precipitation event (<3.0 mm of precipitation), which accounted for almost 58% of all precipitation events (**Figure 2A**). Other precipitation event types, corresponding to 3.1–6 mm, 6.1, 10, and 10–20 mm precipitation, accounted for 15, 14, and 11% of all precipitation events, respectively (**Figure 2A**). Precipitation events >20 mm accounted for 2% of all the precipitation events (**Figure 2A**). Almost 86% of the precipitation occurred during the growing season (from May to September) when most of the greater precipitation (>3 mm) events occurred (**Figure 3**).

Temporal Variations in Soil Moisture for the Two Vegetation Types

In general, the daily variations in 0–100-cm soil moisture for the two vegetation types were consistent with the temporal variations in precipitation, and soil moisture increased sharply after each precipitation event, particularly after a heavy precipitation event (**Figure 3A**). Surface soil moisture was more sensitive to precipitation events, whereas there was a clear lag in the moisture response for the deep soil layers (**Figures 3B,D**). The soil moisture content in the surface and middle layers was higher for alpine meadows than for alpine shrubs, whereas the soil moisture content in the deep soil layer was lower for alpine meadows than for alpine shrubs (**Figures 3B,C**). There was a clear seasonal pattern in soil moisture for the two vegetation types, which was characterized by two peaks for the upper soil layers in both 2015 and 2016 (**Figure 4**). The peaks for the surface soil water content occurred in May and September, with a much higher content in May than in September (**Figure 4B**). There was a single peak in the deeper soil layers for both vegetation types in July (**Figure 4D**).

Comparisons Between the Vertical Soil Moisture Distributions for the Two Vegetation Types

Significant differences were observed between the three soil layers for the two vegetation types (**Figure 5**). The soil moisture content was significantly ($p < 0.05$) higher for alpine meadows than for alpine shrubs in the surface and middle soil layers, whereas the deep soil moisture content of alpine shrubs was significantly higher than that of alpine meadows, which ultimately leads to no significant difference in 0–100 cm between the two vegetation types (**Figure 5**). There was an increasing trend in soil moisture from the surface to deep soil layers for alpine shrubs, whereas the soil water content for alpine meadows first increased and then decreased from the surface to deep soil layers, with maximum moisture occurring in the middle soil layer (**Figure 5**).

Determining Factors of Soil Moisture Content for the Two Vegetation Types

Pearson's correlation coefficient (r) was calculated between the monthly mean soil moisture in each soil layer and meteorological observations (**Table 2**). The results showed a significant positive correlation ($p < 0.01$) between soil moisture and precipitation for alpine shrubs for all soil layers, except for the 80–100-cm soil layer, whereas the average air temperature was significantly negatively correlated with soil moisture (**Table 2**). For alpine meadows, we observed a significant positive correlation ($p < 0.01$) between soil moisture and precipitation at all soil depths, whereas average air temperature only had a significant negative impact at depths of 0–80 cm (**Table 2**). In addition to these meteorological factors, aboveground biomass had a significant negative effect on the monthly average surface soil moisture content in both alpine meadows and alpine shrubs during the growing season (**Figure 6**).

Response of Soil Moisture to Precipitation Patterns

To analyze variations in soil moisture and relate them to different precipitation amounts, we examined the differences between soil moisture before and after precipitation for four precipitation events (**Figure 7**). We found that the low precipitation event (2.6 mm) had no effect on precipitation infiltration for either vegetation type (**Figures 7A**, **8A**), whereas the medium precipitation event (16.5 mm) replenished the soil moisture content of the uppermost 15 cm for the soil under the alpine meadow (**Figure 7B**) and replenished the moisture at depths up to 40 cm for the soil under the alpine shrub (**Figure 8B**). When the precipitation amount was high (47.4 mm), the maximum infiltration depth was 60 cm for the alpine meadows (**Figure 7C**) and 80 cm for the alpine shrubs (**Figure 8C**). When

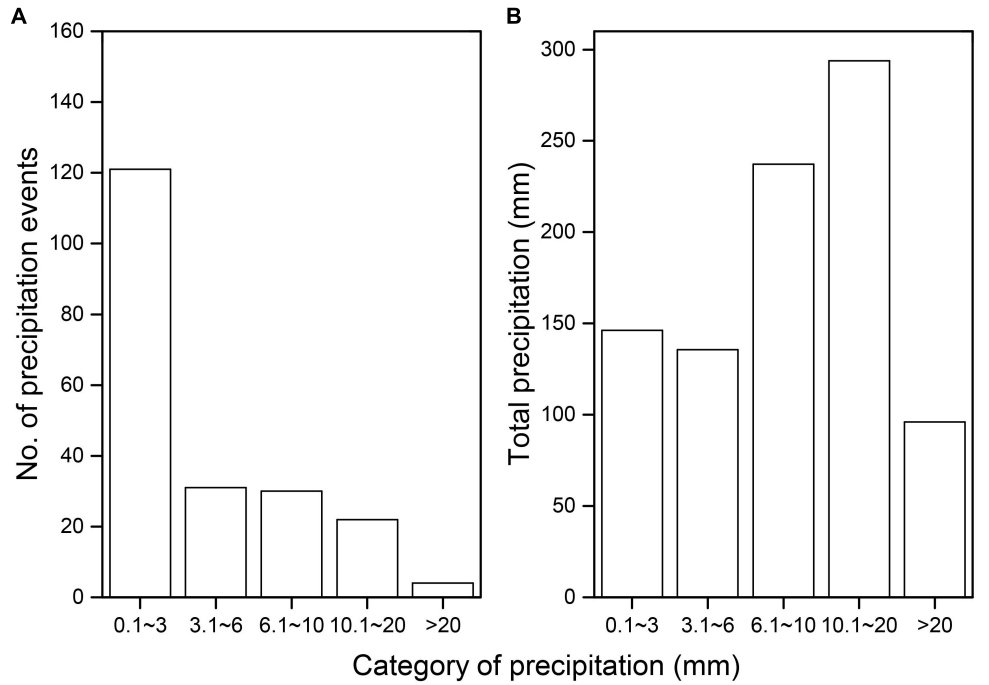

FIGURE 2 | Number of precipitation event **(A)** and total precipitation **(B)** amount across different category precipitation.

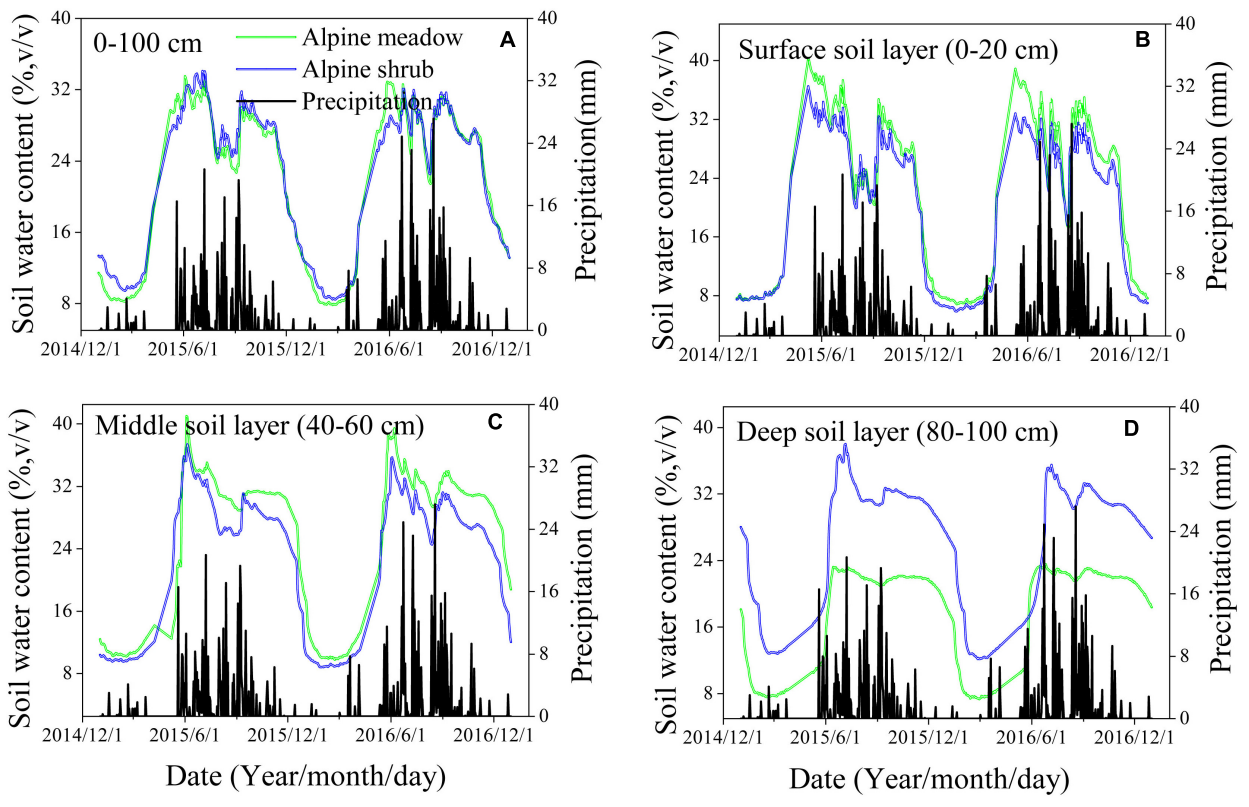

FIGURE 3 | Daily variations of soil water content for 0–100 cm **(A)**, surface soil layer **(B)**, middle soil layer **(C)**, and deep soil layer **(D)** across two vegetation types.

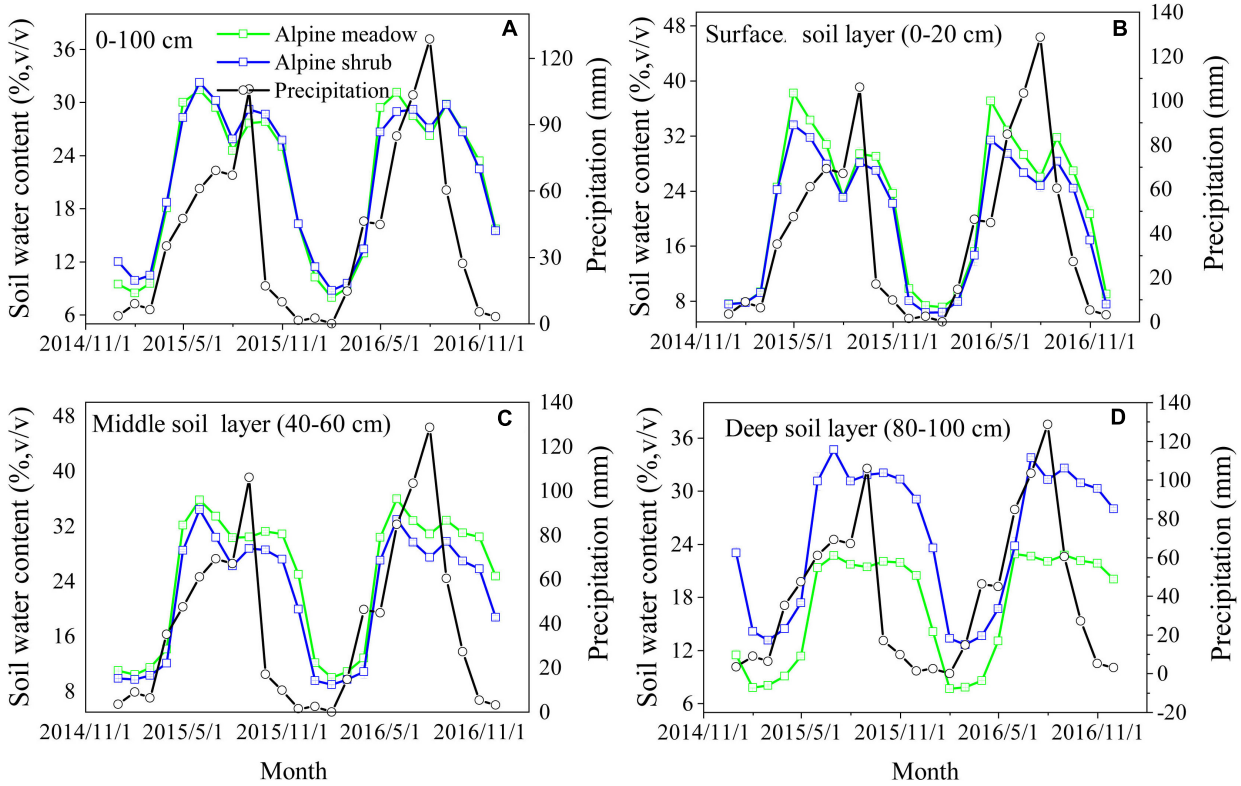

FIGURE 4 | Monthly variations of soil water content for 0–100 cm **(A)**, surface soil layer **(B)**, middle soil layer **(C)**, and deep soil layer **(D)** across two vegetation types.

the precipitation amount was extremely high (68.1 mm), the maximum infiltration depth was 60 cm for alpine meadows (**Figure 7D**) and >100 cm for alpine shrubs (**Figure 8D**).

DISCUSSION

Temporal Variability and Controlling Factors for Soil Moisture for the Two Vegetation Types

Soil moisture variability is a key process in the hydrological cycle of terrestrial ecosystems and is affected by many factors such as soil properties, precipitation patterns, groundwater levels, and the characteristics of the overlying vegetation (Yang et al., 2012; Niu et al., 2015). In this study, the groundwater level was relatively shallow (3–5 m); therefore, precipitation was the primary controlling factor for soil moisture variability in the shallow and middle soil layers. For these layers, we found that the variations in soil moisture were consistent with the temporal variations in precipitation for both vegetation types (**Figure 3**). The soil moisture increased sharply after precipitation events, particularly following heavy precipitation events. This result concurs with the findings of the previous studies conducted in different precipitation regions, which found that higher soil water content is always accompanied by higher precipitation (Zhao et al., 2017; Mei et al., 2018). Precipitation patterns, therefore, determine the observed temporal variations in soil moisture, and the substantial seasonal variations resulting from the uneven distribution of precipitation. In our study region, almost 86% of the total annual precipitation falls during the growing season (**Figure 3**), which results in highly observed soil moisture levels which drive plant growth. However, the soil moisture during the non-growing season was relatively low owing to less precipitation, and most of the liquid water was frozen in the ground (Dai et al., 2019b). Precipitation in our study area was characterized by small events (<3.0 mm of precipitation), which accounted for almost 58% of all precipitation events, whereas events with more than 20 mm of precipitation accounted for only 2% of all precipitation events (**Figure 2**). We found that small precipitation events did not lead to an increase in soil moisture, and some cases, there was a slight reduction where evaporative demands were high (**Figure 3**). Our results suggest that the effect of a series of small rainfall events is not necessarily equivalent to the effect of the same total rainfall amount from a single large event, because the water from most small rainfall events quickly evaporates into the atmosphere instead of being absorbed by the plant. In contrast, larger rainfall events could immediately increase soil moisture, subsequently enhancing soil moisture storage and infiltration, which provides abundant nutrients for plants.

Furthermore, we found that the soil moisture content in the surface and middle soil layers was more sensitive to

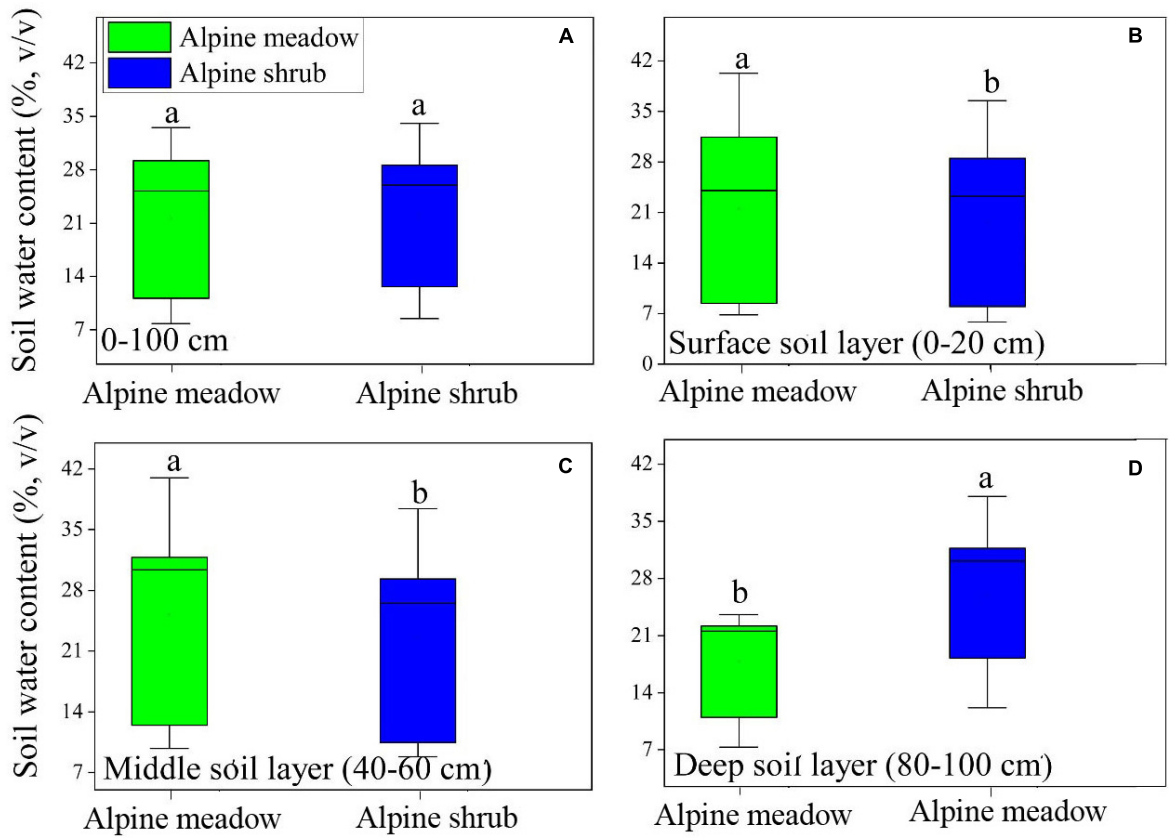

FIGURE 5 | Comparison of soil water content for 0–100 cm **(A)**, surface soil layer **(B)**, middle soil layer **(C)**, and deep soil layer **(D)** across two vegetation types.

precipitation events than the deep soil moisture content. When the precipitation amounts reached their maximum, the surface soil moisture content also reached its maximum (**Figure 3**), whereas the soil moisture content for the deep soil layer displayed a smooth temporal change and exhibited a clear lag in response to precipitation (**Figure 3D**). Moreover, the same temporal variations in soil moisture were observed for the two vegetation types in the surface, middle, and deep soil layers; however, the vertical distribution of soil moisture was different for the two vegetation types. Therefore, we conclude that precipitation was the dominant factor that affects the temporal trends of soil moisture, whereas vegetation type was the dominant factor that affects the spatial distribution of soil moisture. These results are consistent with the previous findings by Yao et al. (2012). The effect of precipitation on soil moisture in alpine ecosystems is complex and is affected by dynamic processes such as the amount, intensity, and duration of precipitation (Niu et al., 2015). In addition to the sensitivity of soil moisture to precipitation, we found a significant negative correlation between soil moisture content and air temperature (**Table 2**). This agrees with the previous studies that demonstrated that temperature drives a decrease in soil moisture under high moisture conditions because soil moisture loss after a rainfall event is primarily driven by atmospheric demand or energy (Wang et al., 2011). We also observed that soil moisture content was affected by vegetation characteristics, such as vegetation biomass (**Figure 6**). The previous studies have found that increasing aboveground biomass leads to a decrease in soil moisture because canopy interception and root water consumption reduce rainfall recharge to the soil (Chen et al., 2008), and this was corroborated by our findings that soil moisture was negatively related to aboveground

TABLE 2 | Pearson's correlation between precipitation and soil moisture at different soil layers for alpine shrub and alpine meadow.

Correlation coefficient	Alpine shrub		Alpine meadow	
	PPT	T_{ave}	PPT	T_{ave}
5 cm SWC	0.71***	−0.86***	0.58***	−0.76***
10 cm SWC	0.68***	−0.86***	0.68***	−0.85***
15 cm SWC	0.67***	−0.84***	0.66***	−0.82***
20 cm SWC	0.65***	−0.81***	0.63***	−0.78***
40 cm SWC	0.63**	−0.76***	0.59**	−0.72***
60 cm SWC	0.60**	−0.68***	0.55**	−0.62**
80 cm SWC	0.46*	−0.44*	0.47*	−0.47*
100 cm SWC	0.34	−0.28	0.44*	−0.41

SWC, soil water content; PPT, precipitation; T_{ave}, average air temperature.
**Indicates that the correlation is significant at $p < 0.05$.*
***Indicates that the correlation is significant at $p < 0.01$.*
****Indicates that the correlation is significant at $p < 0.001$.*

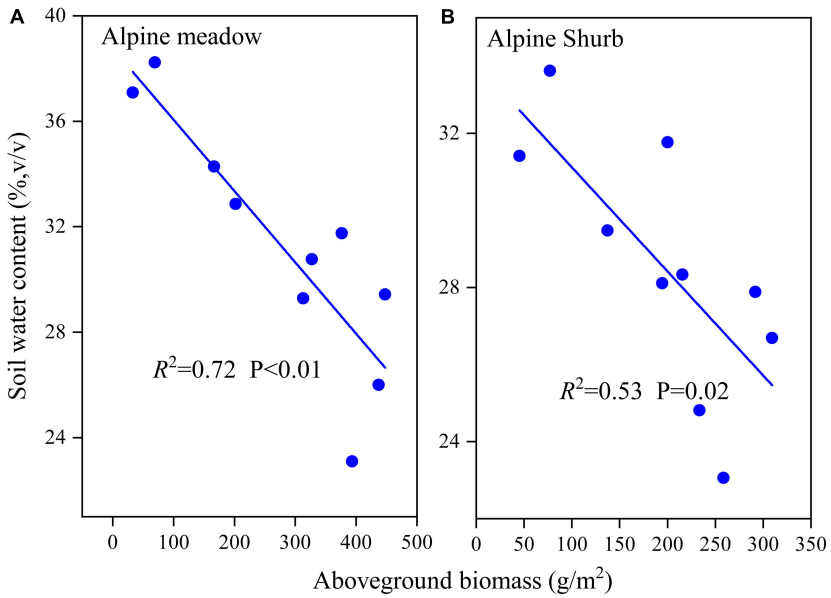

FIGURE 6 | The relationship between aboveground biomass and soil water content for alpine meadow **(A)** and alpine shrub **(B)**.

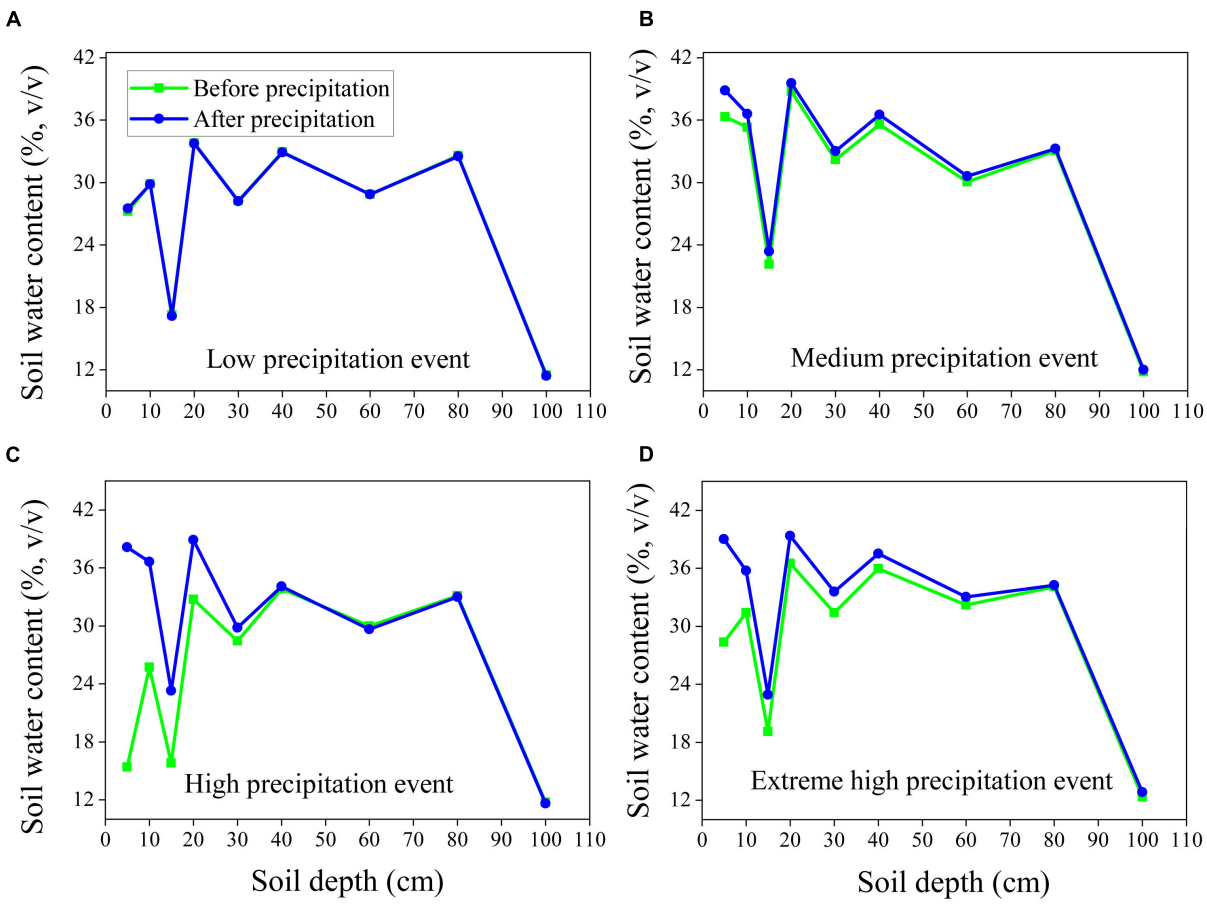

FIGURE 7 | The depth of soil water infiltration of alpine meadow at low precipitation event **(A)**, medium precipitation event **(B)**, high-precipitation event **(C)** and extremely high-precipitation event **(D)**.

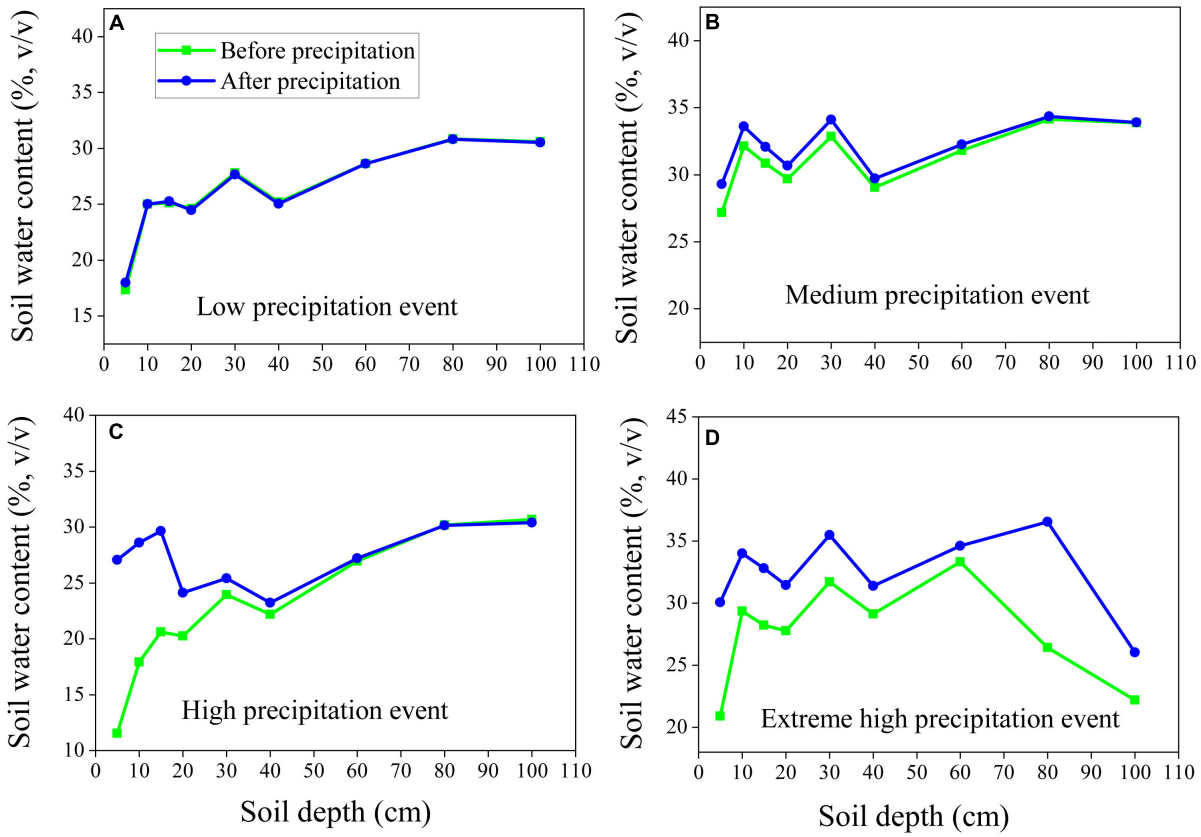

FIGURE 8 | The depth of soil water infiltration of alpine shrub at low precipitation event **(A)**, medium precipitation event **(B)**, high-precipitation event **(C)** and extremely high-precipitation event **(D)**.

biomass during the growing season (**Figure 6**). In general, higher aboveground biomass leads to higher canopy coverage and leaf area index, which promotes the interception of precipitation and subsequent evapotranspiration of soil water, thereby reducing soil moisture (Zhang et al., 2020). Nevertheless, increased canopy coverage can impact the local soil moisture in arid regions because wind speed and temperature are decreased *via* shading, thereby reducing evaporation.

Differences in Soil Moisture Content and Infiltration Processes for Two Vegetation Types

Infiltration processes are complex and affected by factors such as precipitation patterns, ground cover, soil characteristics, topography, and initial soil moisture (Gabarrón-Galeote et al., 2013; Wang et al., 2013). In this study, we found that low amounts of precipitation did not affect the soil moisture for the two vegetation types, possibly because moisture in the soil surface layer was rapidly lost through direct evaporation and transpiration, as no surface runoff occurred during the study period (Wang et al., 2012). The medium precipitation event affected only the uppermost 15 cm of the alpine meadow soil but reached the uppermost 40 cm of the alpine shrub soil. The deeper infiltration depth for alpine shrubs compared to alpine meadows may be related to the low bulk density and thus higher soil porosity for alpine shrubs (**Table 1**). In addition, alpine shrubs have a deeper root system that favors precipitation infiltration because root channels increase soil macroporosity, which leads to higher infiltration and preferential soil flow (Wu et al., 2017). Overall, the infiltration depth increased with precipitation amount for both alpine meadows and alpine shrubs, but the maximum infiltration depth of alpine shrubs was higher than that of alpine meadows under extreme high-precipitation events. This suggests that alpine shrubs might be less susceptible to surface runoff from increasing precipitation variability due to future climate change. Furthermore, alpine meadows have been experiencing rapid shrub encroachment on the QTP, which could favor precipitation infiltration and reduce the occurrence of surface runoff. It should be noted that, although a positive correlation between precipitation and infiltration depth has been widely reported in the previous studies (Yao et al., 2013), it remains difficult to quantify the relationship because of the differences in initial soil moisture, rainfall intensity, and vegetation cover among different precipitation events (Gao et al., 2014). Furthermore, only one measurement point for each soil depth before and after a precipitation event might be insufficient to draw a conclusion on infiltration depth; thus, adding more points should yield more accurate measurements of infiltration

depth in future studies. In addition, seasonally frozen ground is well developed in this region, and the infiltration processes are greatly affected by the freeze-thaw cycle (Dai et al., 2019b). For instance, soil water infiltration was reduced during the soil freezing phase, whereas soil water infiltration was promoted during the soil thawing phase, which was confirmed after observing lower soil moisture during the non-growing season but higher moisture during the growing season (**Figure 3**). Further studies are needed for elucidating the relationship between the processes of soil moisture infiltration and soil freeze-thaw to attain a more comprehensive understanding of soil moisture infiltration processes.

Furthermore, we found that the surface moisture content of alpine meadows was higher than that of alpine shrubs (**Figure 5**). This difference may be attributable to differences in evapotranspiration due to the different root distributions and soil physical properties of the two vegetation types (Fu et al., 2003). The surface soil moisture content was higher in alpine meadows than in alpine shrubs, which may be explained by the following arguments. First, alpine shrubs have higher canopy heights than alpine meadows, which can intercept a greater proportion of incident precipitation *via* its thick branches and luxuriant foliage (Gao et al., 2014), as well as increased water evaporation, and reduced topsoil water content. A previous study found that the alpine shrub community canopy intercepts 11.7% of precipitation (Wang et al., 2005). Second, alpine shrubs have a deeper root system than alpine meadows, which leads to higher infiltration and preferential soil flow owing to higher soil macroporosity, which reduces surface soil water content but increases soil water content. Third, the alpine meadow has a thick mattic epipedon layer in the topsoil at 10–30 cm, which has a relatively higher water holding capacity, thus leading to higher surface soil moisture levels of alpine meadows (Dai et al., 2019a).

CONCLUSION

Temporal variations in surface soil moisture for the two vegetation types were predominately controlled by temporal variations in precipitation and aboveground biomass, whereas there was a clear lag in the soil moisture response to precipitation events in deeper soil layers (80–100 cm). Spatial variability in soil moisture was explained by the differences between the two types of overlying vegetation. There were significant differences in the soil water content for the surface (0–20 cm), middle (40–60 cm), and deep (80–100 cm) soil layers in both alpine meadows and alpine shrubs. Soil moisture content was significantly positively correlated with precipitation, but the correlation coefficient decreased with soil depth. Air temperature and aboveground biomass were significantly negatively correlated with SM. Alpine shrubs had a deeper infiltration depth than alpine meadows under extreme high-precipitation events, which indicates that alpine shrubs might be less susceptible to surface runoff under these events. Furthermore, we found that the impact of a series of small rainfall events was not necessarily equivalent to the impact of the same total rainfall amount provided in a single large event.

DATA AVAILABILITY STATEMENT

The original contributions presented in the study are included in the article/supplementary material, further inquiries can be directed to the corresponding author.

AUTHOR CONTRIBUTIONS

LD and XG performed the research, analyzed the data, and wrote the manuscript. FZ, RF, and YD analyzed the data. GC conceived the study. All authors contributed to the article and approved the submitted version.

FUNDING

This study was supported by the National Natural Science Foundation of China (41730752) and Natural Science Foundation of Qinghai (2021-HZ-811).

REFERENCES

Biro, K., Pradhan, B., Buchroithner, M., and Makeschin, F. (2013). land use/land cover change analysis and its impact on soil properties in the northern part of Gadarif region, Sudan. *Land Degrad. Dev.* 24, 90–102. doi: 10.1002/ldr.1116

Chen, H., Shao, M., and Li, Y. (2008). The characteristics of soil water cycle and water balance on steep grassland under natural and simulated rainfall conditions in the Loess Plateau of China. *J. Hydrol.* 360, 242–251. doi: 10.1016/j.jhydrol.2008.07.037

Chen, L., Huang, Z., Gong, J., Fu, B., and Huang, Y. (2007). The effect of land cover/vegetation on soil water dynamic in the hilly area of the loess plateau, China. *Catena* 70, 200–208. doi: 10.1016/j.catena.2006.08.007

Cheng, R. R., Chen, Q., Zhang, J., Shi, W., Li, G., and Du, S. (2020). Soil moisture variations in response to precipitation in different vegetation types: a multi-year study in the loess hilly region in China. *Ecohydrology* 13, e2196.

Dai, L., Guo, X., Zhang, F., Du, Y., Ke, X., Li, Y., et al. (2019a). Seasonal dynamics and controls of deep soil water infiltration in the seasonally-frozen region of the Qinghai-Tibet plateau. *J. Hydrol.* 571, 740–748. doi: 10.1016/j.jhydrol.2019.02.021

Dai, L., Guo, X., Du, Y., Zhang, F., Ke, X., Cao, Y., et al. (2019b). The response of shallow groundwater levels to soil freeze–thaw process on the Qinghai-Tibet plateau. *Groundwater* 57, 602–611. doi: 10.1111/gwat.12832

Dai, L., Guo, X., Ke, X., Du, Y., Zhang, F., and Cao, G. (2020a). The variation in soil water retention of alpine shrub meadow under different degrees of degradation on northeastern Qinghai-Tibetan plateau. *Plant Soil* 458, 231–244. doi: 10.1007/s11104-020-04522-3

Dai, L., Yuan, Y., Guo, X., Du, Y., Ke, X., Zhang, F., et al. (2020b). Soil water retention in alpine meadows under different degradation stages on the northeastern Qinghai-Tibet Plateau. *J. Hydrol.* 590:125397. doi: 10.1016/j.jhydrol.2020.125397

Deng, L., Yan, W., Zhang, Y., and Shangguan, Z. (2016). Severe depletion of soil moisture following land-use changes for ecological restoration: evidence from northern China. *For. Ecol. Manag.* 366, 1–10. doi: 10.1016/j.foreco.2016.01.026

Dong, S., Shang, Z., Gao, J., and Boone, R. B. (2020). Enhancing sustainability of grassland ecosystems through ecological restoration and grazing management in an era of climate change on Qinghai-Tibetan Plateau. *Agric. Ecosyst. Environ.* 287:106684. doi: 10.1016/j.agee.2019.106684

Duan, L., Huang, M., and Zhang, L. (2016). Differences in hydrological responses for different vegetation types on a steep slope on the Loess Plateau, China. *J. Hydrol.* 537, 356–366. doi: 10.1016/j.jhydrol.2016.03.057

Fu, B., Wang, J., Chen, L., and Qiu, Y. (2003). The effects of land use on soil moisture variation in the Danangou catchment of the Loess Plateau, China. *Catena* 54, 197–213. doi: 10.1016/s0341-8162(03)00065-1

Gabarrón-Galeote, M. A., Martínez-Murillo, J. F., Quesada, M. A., and Ruiz-Sinoga, J. D. (2013). Seasonal changes in the soil hydrological and erosive response depending on aspect, vegetation type and soil water repellency in different Mediterranean microenvironments. *Solid Earth* 4, 497–509. doi: 10.5194/se-4-497-2013

Gao, X., Wu, P., Zhao, X., Wang, J., and Shi, Y. (2014). Effects of land use on soil moisture variations in a semi-arid catchment: implications for land and agricultural water management. *Land Degrad. Dev.* 25, 163–172. doi: 10.1002/ldr.1156

Gómez-Plaza, A., Alvarez-Rogel, J., Albaladejo, J., and Castillo, V. (2000). Spatial patterns and temporal stability of soil moisture across a range of scales in a semi-arid environment. *Hydrol. Process.* 14, 1261–1277. doi: 10.1002/(sici)1099-1085(200005)14:7<1261::aid-hyp40>3.0.co;2-d

Guo, L., Chen, J., and Lin, H. (2015). Subsurface lateral preferential flow network revealed by time-lapse ground-penetrating radar in a hillslope. *Water Resour. Res.* 50, 9127–9147. doi: 10.1002/2013wr014603

Mei, X., Zhu, Q., Ma, L., Zhang, D., Liu, H., and Xue, M. (2018). The spatial variability of soil water storage and its controlling factors during dry and wet periods on loess hillslopes. *Catena* 162, 333–344. doi: 10.1016/j.catena.2017.10.029

Nelson, D. W., and Sommers, L. E. (1996). Total carbon, organic carbon, and organic matter. *Methods Soil Analys. Part 3 Chem. Methods* 5, 961–1010. doi: 10.2136/sssabookser5.3.c34

Neris, J., Jiménez, C., Fuentes, J., Morillas, G., and Tejedor, M. (2012). Vegetation and land-use effects on soil properties and water infiltration of Andisols in Tenerife (Canary Islands, Spain). *Catena* 98, 55–62. doi: 10.1016/j.catena.2012.06.006

Niu, C. Y., Musa, A., and Liu, Y. (2015). Analysis of soil moisture condition under different land uses in the arid region of Horqin sandy land, northern China. *Solid Earth* 7, 1979–2009.

Pan, T., Hou, S., Wu, S., Liu, Y., Liu, Y., Zou, X., et al. (2016). Variation of soil hydraulic properties with alpine grassland degradation in the Eastern Tibetan Plateau. *Hydrol. Earth Syst. Sci.* 21, 2249–2261. doi: 10.5194/hess-21-2249-2017

Puri, S., Stephen, H., and Ahmad, S. (2011). Relating TRMM precipitation radar land surface backscatter response to soil moisture in the Southern United States. *J. Hydrol.* 402, 115–125. doi: 10.1016/j.jhydrol.2011.03.012

R Development Core Team (2006). *R: A Language and Environment for Statistical Computing*. Vienna: R foundation for statistical computing.

Schwinning, S., and Sala, O. E. (2004). Hierarchy of responses to resource pulses in arid and semi-arid ecosystems. *Oecologia* 141, 211–220. doi: 10.1007/s00442-004-1520-8

Song, D., Kai, Z., and Zhi, G. (2007). Advances in Research on Soil Moisture by Microwave Remote Sensing in China. *Chin. Geogr. Sci.* 17, 186–191. doi: 10.1007/s11769-007-0186-7

Svetlitchnyi, A. A., Plotnitskiy, S. V., and Stepovaya, O. Y. (2003). Spatial distribution of soil moisture content within catchments and its modelling on the basis of topographic data. *J. Hydrol.* 277, 50–60. doi: 10.1016/s0022-1694(03)00083-0

Tomer, M. D., and Anderson, J. L. (1995). Variation of soil water storage across a Sand Plain Hillslope. *Soil Sci. Soc. Am. J.* 59, 1091–1100. doi: 10.2136/sssaj1995.03615995005900040021x

Vivoni, E. R., Rinehart, A. J., Méndez-Barroso, L. A., Aragón, C. A., Bisht, G., Cardenas, M. B., et al. (2010). Vegetation controls on soil moisture distribution in the Valles Caldera, New Mexico, during the North American monsoon. *Ecohydrology* 1, 225–238. doi: 10.1002/eco.11

Wang, S., Fu, B. J., He, C. S., Sun, G., and Gao, G. Y. (2011). A comparative analysis of forest cover and catchment water yield relationships in northern China. *For. Ecol. Manag.* 262, 1189–1198. doi: 10.1016/j.foreco.2011.06.013

Wang, S., Fu, B., Gao, G., and Zhou, J. (2012). The hydrological responses of different land cover types in a re-vegetation catchment area of the Loess Plateau, China. *Hydrol. Earth Syst. Sci. Discuss.* 9, 5809–5835.

Wang, S., Fu, B., Gao, G., Liu, Y., and Zhou, J. (2013). Responses of soil moisture in different land cover types to rainfall events in a re-vegetation catchment area of the Loess Plateau, China. *Catena* 101, 122–128. doi: 10.1016/j.catena.2012.10.006

Wang, X.-P., Li, X.-R., Zhang, J.-G., Zhang, Z.-S., and Berndtsson, R. (2005). Measurement of rainfall interception by xerophytic shrubs in re-vegetated sand dunes/Mesure de l'interception de la pluie par des arbustes xérophiles sur des dunes de sable replantées. *Hydrol. Sci. J.* 50:910.

Wu, G., Liu, Y., Yang, Z., Cui, Z., Deng, L., Chang, X., et al. (2017). Root channels to indicate the increase in soil matrix water infiltration capacity of arid reclaimed mine soils. *J. Hydrol.* 546, 133–139. doi: 10.1016/j.jhydrol.2016.12.047

Yang, L., Wei, W., Chen, L., Jia, F., and Mo, B. (2012). Spatial variations of shallow and deep soil moisture in the semi-arid Loess Plateau, China. *Hydrol. Earth Syst. Sci.* 16, 3199–3217. doi: 10.5194/hess-16-3199-2012

Yang, T., Ala, M., Zhang, Y., Wu, J., Wang, A., and Guan, D. (2018). Characteristics of soil moisture under different vegetation coverage in Horqin Sandy Land, northern China. *PLoS One* 13:e0198805. doi: 10.1371/journal.pone.0198805

Yao, S. X., Zhao, C. C., Zhang, T. H., and Liu, X. P. (2013). Response of the soil water content of mobile dunes to precipitation patterns in Inner Mongolia, northern China. *J. Arid Environ.* 97, 92–98. doi: 10.1016/j.jaridenv.2013.06.003

Yao, S., Zhang, T., Liu, X., and Ma, Y. (2012). Feature of soil saturated hydraulic conductivity in various lands of Horqin Sandy Land. *J. Arid Land Resour. Environ.* 4, 123–126.

Zeng, C., Zhang, F., Wang, Q., Chen, Y., and Joswiak, D. R. (2013). Impact of alpine meadow degradation on soil hydraulic properties over the Qinghai-Tibetan Plateau. *J. Hydrol.* 478, 148–156. doi: 10.1016/j.scitotenv.2020.142338

Zhang, Q., Wei, W., Chen, L., Yang, L., Luo, Y., and Cai, A. (2020). Plant traits in influencing soil moisture in semiarid grasslands of the Loess Plateau, China. *Sci. Total Environ.* 718, 137355. doi: 10.1016/j.scitotenv.2020.137355

Zhao, Y., Wang, Y., Wang, L., Fu, Z., Zhang, X., and Cui, B. (2017). Soil-water storage to a depth of 5 m along a 500-km transect on the Chinese Loess Plateau. *Catena* 150, 71–78. doi: 10.1016/j.catena.2016.11.008

Conflict of Interest: The authors declare that the research was conducted in the absence of any commercial or financial relationships that could be construed as a potential conflict of interest.

Publisher's Note: All claims expressed in this article are solely those of the authors and do not necessarily represent those of their affiliated organizations, or those of the publisher, the editors and the reviewers. Any product that may be evaluated in this article, or claim that may be made by its manufacturer, is not guaranteed or endorsed by the publisher.

Copyright © 2022 Dai, Fu, Guo, Du, Zhang and Cao. This is an open-access article distributed under the terms of the Creative Commons Attribution License (CC BY). The use, distribution or reproduction in other forums is permitted, provided the original author(s) and the copyright owner(s) are credited and that the original publication in this journal is cited, in accordance with accepted academic practice. No use, distribution or reproduction is permitted which does not comply with these terms.

frontiers | Frontiers in Plant Science

ORIGINAL RESEARCH
published: 08 April 2022
doi: 10.3389/fpls.2022.861231

Alpine Treeline Dynamics and the Special Exposure Effect in the Hengduan Mountains

Fuyan Zou[1], Chengyi Tu[1,2], Dongmei Liu[3], Chaoying Yang[1], Wenli Wang[1] and Zhiming Zhang[1]*

[1] Yunnan Key Laboratory of Plant Reproductive Adaptation and Evolutionary Ecology, School of Ecology and Environmental Sciences, Yunnan University, Kunming, China, [2] Department of Environmental Science, Policy, and Management, University of California, Berkeley, Berkeley, CA, United States, [3] Chinese Research Academy of Environmental Sciences, Beijing, China

Alpine treeline is highly sensitive to climate change, but there remains a lack of research on the spatiotemporal heterogeneity of treeline and their relationships with climate change at the landscape scale. We extracted positions of alpine treeline from high-resolution Google Earth images from three periods (2000, 2010, and 2020) and analyzed the elevation patterns and dynamics of treeline positions in the Hengduan Mountains. Based on the treeline positions in 2020, a buffer zone of 300 m is established as the treeline transition zone, and the changing trend of the fraction vegetation cover (*FVC*) from 2000 to 2020 and its relationship with climate are also analyzed. Due to the special geographical and climatic environment, the treeline in the Hengduan Mountains area is high in the middle but lower in the surrounding areas. We found that over the past 20 years, the treeline position did not change significantly but that the *FVC* increased in 80.3% of the treeline areas. The increase in *FVC* was related to the decrease in precipitation in the growing season. The results also revealed a special exposure effect on the alpine treeline in the Hengduan Mountains. Because of the lower treeline, isotherm position caused by the monsoon climate, the treeline position on south-facing slopes is lower than that on slopes with other exposures. Our results confirmed that the pattern and dynamics of the alpine treeline are driven by the regional monsoon climate regime.

Keywords: treeline dynamics, fraction vegetation cover, landscape scale, exposure effect, the Hengduan mountains

OPEN ACCESS

Edited by:
Jian Sun,
Institute of Tibetan Plateau Research (CAS), China

Reviewed by:
Baiping Zhang,
State Key Laboratory of Resources and Environmental Information System, Institute of Geographic Sciences and Natural Resources Research (CAS), China
Yafeng Wang,
Nanjing Forestry University, China

****Correspondence:***
Wenli Wang
wwl@ynu.edu.cn

Specialty section:
This article was submitted to Functional Plant Ecology, a section of the journal Frontiers in Plant Science

Received: *24 January 2022*
Accepted: *07 March 2022*
Published: *08 April 2022*

Citation:
Zou F, Tu C, Liu D, Yang C, Wang W and Zhang Z (2022) Alpine Treeline Dynamics and the Special Exposure Effect in the Hengduan Mountains. Front. Plant Sci. 13:861231. doi: 10.3389/fpls.2022.861231

INTRODUCTION

Alpine treeline is a sensitive indicator of the responses of terrestrial ecosystems to climate change (Lenoir et al., 2008; Hagedorn et al., 2019) and provides early warnings of global climate change (Alatalo and Ferrarini, 2017; Du et al., 2018). The treeline ecotone is expected to expand to higher latitudes and elevations because of rapid climate warming (Scuderi et al., 1993; Chen et al., 2011; Malanson, 2013). A global study showed that the treelines at only 52% of all 166 global treeline sites have advanced upslope over the past 100 years (Harsch et al., 2009). Recently, Lu et al. (2020) conducted a meta-analysis of the annual shift rate of treelines in the Northern Hemisphere and revealed that the treelines have shifted upward at 127 out of 143 sites (88.8%) since 1901. This

shows that the trend of upward treeline movement is becoming increasingly obvious at most sites around the world. However, it has been suggested that the sensitivity of treeline ecotones depends more on changes in tree density than on the position of the treeline (Camarero and Gutierrez, 2004). Sigdel et al. (2020) quantified the changes in density and the spatial patterns of 17 treeline sites in the central Himalayas. The results suggested that younger trees showed clustering near the treeline. The method of historical reconstructions of tree positions has provided numerous examples of forest infilling in some alpine regions (Payette and Filion, 1985; Lyu et al., 2016; Wang et al., 2016). However, regardless of whether the treeline position shifts upward or the tree density increases (La Sorte and Jetz, 2010; Hagedorn et al., 2019; Rees et al., 2020), the area of tundra and meadow ecosystems at higher elevations will be reduced, resulting in the loss of biodiversity and ecosystem services (Thuiller et al., 2005; Feurdean et al., 2016; Pecl et al., 2017). Therefore, it is necessary to pay attention to these two aspects simultaneously while discussing the treeline pattern and its dynamic change.

Treeline exhibits a scale effect (Körner, 2012; Singh et al., 2015), which also determines the diversity of treeline research scales (Holtmeier and Broll, 2019). At the local scale, researchers usually focus on ecological processes, tree density changes, species distribution, and composition of the treeline transition zone (Liang et al., 2016; Sigdel et al., 2020). An increasing number of studies have analyzed position and spatial pattern changes in treeline on relatively large scales (global, regional, or landscape) (Guo et al., 2014; Mohapatra et al., 2019; Wei et al., 2020). However, there are differences in treeline patterns and their dynamics from local to global scales (Holtmeier and Broll, 2012; Marc and Johnson, 2013; Bader et al., 2020). For example, Gaire et al. (2014) found that the treeline in the central Nepal Himalaya is moving upward at a rate of 2.61 m/year at the sample plot scale. Mohapatra et al. (2019) found that the Himalayan treeline is moving upward at a rate of 11.3 m/year at the landscape scale. However, a meta-analysis of annual treeline shift rates in the Northern Hemisphere showed that the mean shift rate was only 0.354 m/year (Lu et al., 2020). This shows that many research results are controversial due to the influence of different scales.

How to choose an appropriate treeline scale to evaluate and predict the relationship between treeline change and climate change more comprehensively and accurately is a key problem. There are great differences among treelines in different climatic zones and biogeographic regions, but the influence of topographic factors on the spatial pattern of treeline is often ignored (Yirdaw et al., 2015; Bader et al., 2020). However, the treeline pattern on a fine scale is usually described as the relative position between trees (Sigdel et al., 2020), but this pattern cannot be applied to other areas. In addition, different scales will also affect the response of treeline to climate. On a fine scale, physical and biological factors may interfere with the response of tree growth to climate (Hellmann et al., 2016), and the position of treeline might be inconsistent with the climate conditions (Marc and Johnson, 2013). On the global scale, local differences will be ignored, and it may be easy to overemphasize coarse drivers such as temperature (Harsch et al., 2009; Moyes et al., 2015). The landscape scale may better reflect the relationship between treeline dynamics and climate (Batllori and Gutiérrez, 2008; Case and Duncan, 2014; Singh et al., 2015). However, how to obtain large-scale and high-precision treeline data is also a problem to be solved in the current research.

The Hengduan Mountains provide an extensive longitudinal, latitudinal, and topographical framework for studying the landscape pattern and dynamics of treeline. The objective of this study was to characterize the responses of treeline dynamics (treeline position and vegetation cover) to changes in climate at the landscape scale. Specifically, high-resolution Google Earth images were used to extract the alpine treeline in the Hengduan Mountains area in different periods, and then the changes in treeline position and vegetation coverage, and also their relationships with climate, were assessed. The results of this study provide new insights into the factors driving treeline dynamics at the landscape scale, and these insights could aid in the evaluation of the risks faced by alpine ecosystems and species in the alpine regions under future climate change.

MATERIALS AND METHODS

Study Area

The Hengduan Mountains (24°39′N–33°34′N, 96°58′E–104°27′E) are composed of a series of north–south-trending parallel mountains and rivers (Li, 1987). The terrain of this region fluctuates greatly, with high terrain in the north and low terrain in the south; there are many high mountains and deep valleys (Wen, 1989). The climate conditions are complex, and the temperature and precipitation in the region vary greatly (Bai et al., 2019). The mean annual temperature ranges from 5 to 13°C, and the total annual precipitation ranges from 500 to 1,000 mm (Dai et al., 2020). Since the 1960s, the mean annual temperature of the Hengduan Mountains area has increased, and the rate of increase has increased significantly since 2000 (Li et al., 2010). This region is also one of the most biodiverse regions worldwide, with high species diversity and endemism (Myers et al., 2000; Sun et al., 2017). Natural treelines are abundant and are ideal for studying the dynamic responses of treelines to climate (Miehe et al., 2007; Kramer et al., 2010).

The forest ecosystem in the Hengduan Mountains is mainly distributed in the south. We choose 9 mountains at different longitudes and latitudes in this region (**Figure 1**), each of which features a large number of undisturbed treelines. The nine main mountains are the Boshulaling Mountain (BSLL), Meili Snow Mountain (ML), Baima Snow Mountain (BM), Gezong Snow Mountain (GZ), Haba Snow Mountain (HB), Gongga Mountain (GG), Sanshen Mountain (SS), Yulong Snow Mountain (YL), and Jinping Mountain (JP). These mountains are national nature reserves, provincial nature reserves, or major mountains in the region.

Extraction of the Treeline

Generally, the alpine treeline is located between the tree species line (upper limit of seedlings or young trees) and the forest line (upper limit of closed forest) and roughly corresponds to the line

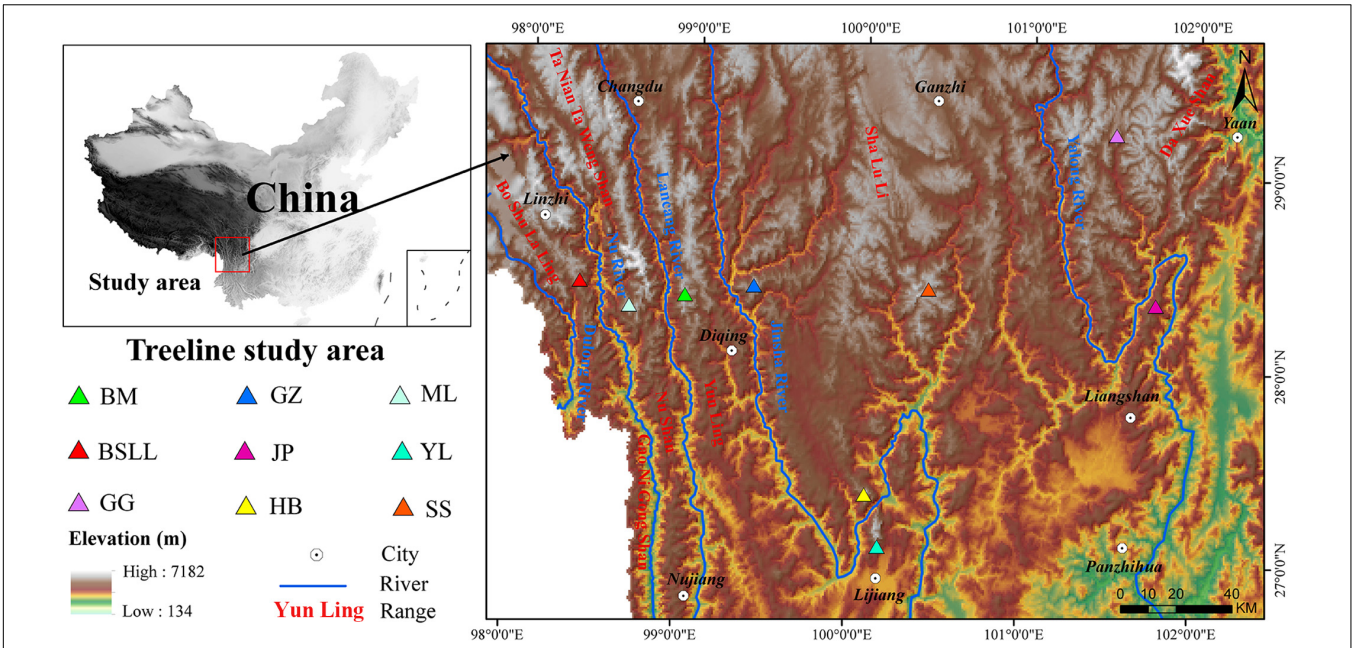

FIGURE 1 | Location of the studied treeline sites in Hengduan Mountains area. BSLL, Boshulaling Mountain; ML, Meili Snow Mountain; BM, Baima Snow Mountain; GZ, Gezong Snow Mountain; HB, Haba Snow Mountain; GG, Gongga Mountain; SS, Sanshen Mountain; YL, Yulong Snow Mountain; JP, Jinping Mountain.

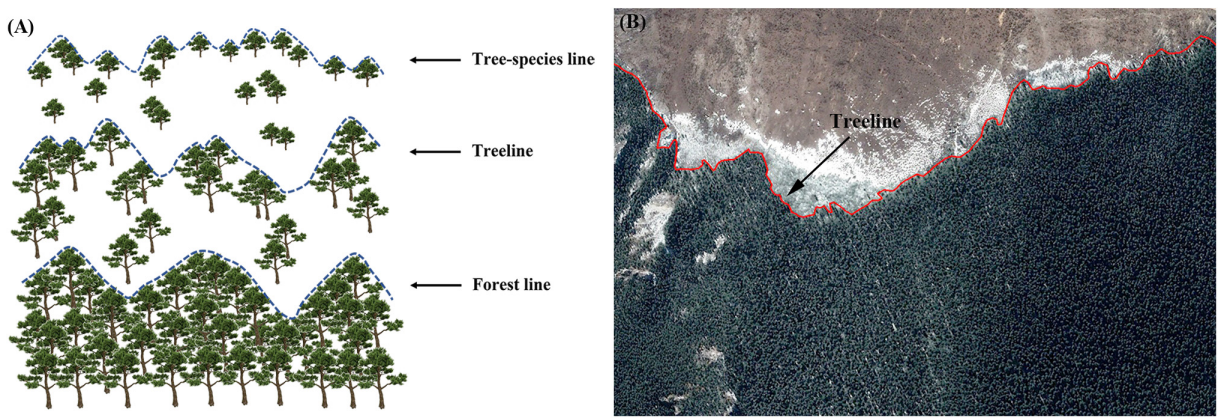

FIGURE 2 | (A) The position of treeline. **(B)** Extraction of treeline from Google Earth images.

linking the densest patches of trees >3 m in height (Körner, 2012; Singh et al., 2015), as shown in **Figure 2A**.

In this study, the alpine treeline is defined as the line representing the physical boundary between forest and alpine vegetation. Treeline data were extracted using remote-sensing images in Google Earth software (**Figure 2B**). Elevation is an important variable for distinguishing the climatic treeline from a disturbance treeline (Holtmeier and Broll, 2005; Leonelli et al., 2013). According to the previous research, the climatic treeline in the study area is greater than 3,800 m (Wang et al., 2013). However, the elevation of disturbed treelines is often lower than that of climatic treelines (Holtmeier and Broll, 2005; Leonelli et al., 2013). To account for the effect of interference factors on the obtained treeline data, the canopy boundary formed by natural interference factors, such as topography, snow cover, landslides, and gullies and human interference factors, including road construction, mining, and grazing, was removed. Google Earth images from 2000, 2010, and 2020 were used to extract treeline data, and the treeline data obtained from Google Earth were imported into ArcGIS software and converted into grid data.

Extraction of the Fraction Vegetation Cover

Extraction of Normalized Difference Vegetation Index

Landsat images with 30-m resolution in the study area were used to extract the normalized difference vegetation index (NDVI),

and then the vegetation coverage was extracted (Wilson and Norman, 2018). The formula is as follows:

$$NDVI = \frac{\rho_{NIR} - \rho_{RED}}{\rho_{NIR} + \rho_{RED}}$$

where ρ_{NIR} is the reflectivity of the near infrared band and ρ_{RED} is the reflectivity of visible light in the red band.

Calculation of the Fraction Vegetation Cover

The fraction vegetation cover (FVC) was calculated based on the NDVI (Gu et al., 2009), and the formula is as follows:

$$FVC = \frac{NDVI - NDVI_{min}}{NDVI_{max} - NDVI_{min}}$$

where $NDVI_{min}$ is the minimum value of the vegetation index, which is the NDVI value of bare or non-vegetated areas on the remote sensing images, and $NDVI_{max}$ is the maximum value of the vegetation index, which is the NDVI value of an area completely covered by vegetation, that is, the NDVI value of pure vegetation pixels.

Extraction of Climatic and Topographic Factors

Climate Data

Climate data with a 1-km resolution were downloaded from the monthly precipitation and temperature data of China from 1961 to 2020 from the National System Earth Science Data Center, National Science and Technology Infrastructure of China.[1] Then, the monthly climate grid data were clipped, projected, and calculated by ArcGIS software to obtain gridded data of spring mean temperature, summer mean temperature, autumn mean temperature, winter mean temperature, spring precipitation, summer precipitation, autumn precipitation, and winter precipitation in the study area.

The precipitation and mean temperature of the growing season (PGS and MTGS) were extracted from the monthly precipitation and mean temperature layer data following the method of Wang et al. (2013). The mean temperature of the growing season was defined as the mean value of the monthly mean temperature ≥5°C (Walther and Linderholm, 2006). The raster calculator tool in ArcGIS was used for processing; the formula is as follows:

$$MTGS = \frac{\sum_1^{12} T_i \geq 5 \times Float\ (\mathbf{T_i})}{\sum_1^{12} \mathbf{T_i} \geq 5}$$

$$PGS = \frac{\sum_1^{12} P_i \times \sum_1^{12} T_i \geq 5}{\sum_1^{12} \mathbf{T_i} \geq 5}$$

where *Ti* and *Pi* refer to the mean monthly temperatures, and the float (*Ti*) function represents the conversion factor for converting integer data to floating-point data.

Geographic Data

The Hengduan Mountains is located in the southeastern part of the Qinghai-Tibet Plateau, and its topography is extremely complex. Terrain factors were considered in the analysis of the treeline formation mechanism, and digital elevation data with 12.5-m resolution was used.[2] The surface tools in ArcGIS were used to extract aspect and slope data.

Data Analysis

The Extract Multi Values to Points module in the ArcGIS Spatial Analyst toolbox was then used to associate the treeline data with temperature, precipitation, aspect, and other information. A total of 777,649 treeline grids were obtained (**Table 1**), and then Excel was used to export the data for data analysis. The average alpine treeline distribution at different latitudes, longitudes, slope angles and aspects, and the proportions of the treeline on different slopes in the Hengduan Mountains area were analyzed.

The factors potentially affecting the elevation of the treeline were analyzed using convergent cross mapping (CCM). The basic idea of CCM is to use prediction between variables as a test for causality. If variable X has a causal effect on variable Y, then causal information of variable X should be present in Y; thus, the attractor recovered for variable Y should be able to predict the states of variable X. In practice, the Pearson correlation coefficient between the original time series Y and its estimate from the CCM by another time series X is used as a criterion for establishing causality (ρ_{ccm}). ρ_{ccm} is positively related to the degree to which X can reconstruct Y; thus, the

[1] http://www.geodata.cn/

[2] https://search.asf.alaska.edu/

TABLE 1 | Numerical statistics of treeline grids in each slope direction.

Aspect	Count	2000		2010		2020	
		Elevation ± SD (m)	MTGS ± SD (°C)	Elevation ± SD (m)	MTGS ± SD (°C)	Elevation ± SD (m)	MTGS ± SD (°C)
N	81416	4205 ± 140	7.49 ± 0.93	4208 ± 144	7.45 ± 0.93	4212 ± 144	7.44 ± 0.94
NE	100548	4194 ± 148	7.47 ± 0.97	4199 ± 152	7.47 ± 0.97	4203 ± 151	7.45 ± 0.97
E	107981	4153 ± 137	7.57 ± 0.98	4165 ± 139	7.54 ± 0.98	4168 ± 139	7.52 ± 0.99
SE	100713	4127 ± 130	7.61 ± 0.97	4132 ± 135	7.58 ± 0.97	4137 ± 135	7.58 ± 0.97
S	94092	4132 ± 138	7.56 ± 0.95	4136 ± 140	7.57 ± 0.95	4143 ± 141	7.54 ± 0.96
SW	109680	4128 ± 139	7.69 ± 0.89	4130 ± 139	7.69 ± 0.89	4138 ± 141	7.67 ± 0.9
W	102017	4152 ± 138	7.75 ± 0.85	4155 ± 136	7.73 ± 0.85	4164 ± 137	7.72 ± 0.85
NW	81202	4185 ± 141	7.68 ± 0.88	4188 ± 143	7.66 ± 0.88	4198 ± 142	7.62 ± 0.88

TABLE 2 | Variables used for the impact factors analysis.

Variable types	Abbreviation	Full name
Climatic variables	MGTS	Mean temperature of growing season
	WinterMT	Winter mean temperature
	AutumnMT	Autumn mean temperature
	SummerMT	Summer mean temperature
	SpringMT	Spring mean temperature
	PGS	Precipitation of growing season
	WinterP	Winter precipitation
	AutumnP	Autumn precipitation
	SummerP	Summer precipitation
	SpringP	Spring precipitation
Terrain variables	—	Slope
	—	Elevation
	—	Longitude
	—	Latitude

causal effect is stronger as ρ_{ccm} increases (Sugihara et al., 2012; Lin et al., 2020). The focus of our study was on a more specific problem: distinguishing the effects (causes) of variation in the elevation of treeline from different types of climatic factors. We used a spatial version of CCM to detect the causality between the response variable (result) and putative drivers (**Table 2**). For each possible pair (one putative variable and one response variable), we randomly permuted the indices of the paired variables and then calculated their correlations with ρ_{ccm}. If the correlation with$\rho_{ccm} \to 1$, then the climatic variable is a driver of treeline elevation; if $\rho_{ccm} \to 0$, then the climatic variable is not causally related to treeline elevation. The shuffling procedure was repeated 100 times. A Wilcoxon signed-rank test was used to determine whether the median was significantly greater than zero. A small p-value suggests that it is unlikely that the environmental variable affects treeline elevation. The analysis was carried out in R 3.6.1.

The Theil-Sen median trend analysis method is a robust non-parametric statistical trend calculation method (Sen and Kumar, 1968; Theil, 1992), and its formula can be written as follows:

$$S_{FVC} = median\left(\frac{FVC_j - FVC_i}{j - i}\right),\ 2000 \le i < j \le 2020;$$

S_{FVC}, which is used to quantify a monotonic trend, is the median of the slope of the $n(n\text{-}1)/2$ data combinations, and FVC_j and FVC_i represent the FVC values in years i and j.

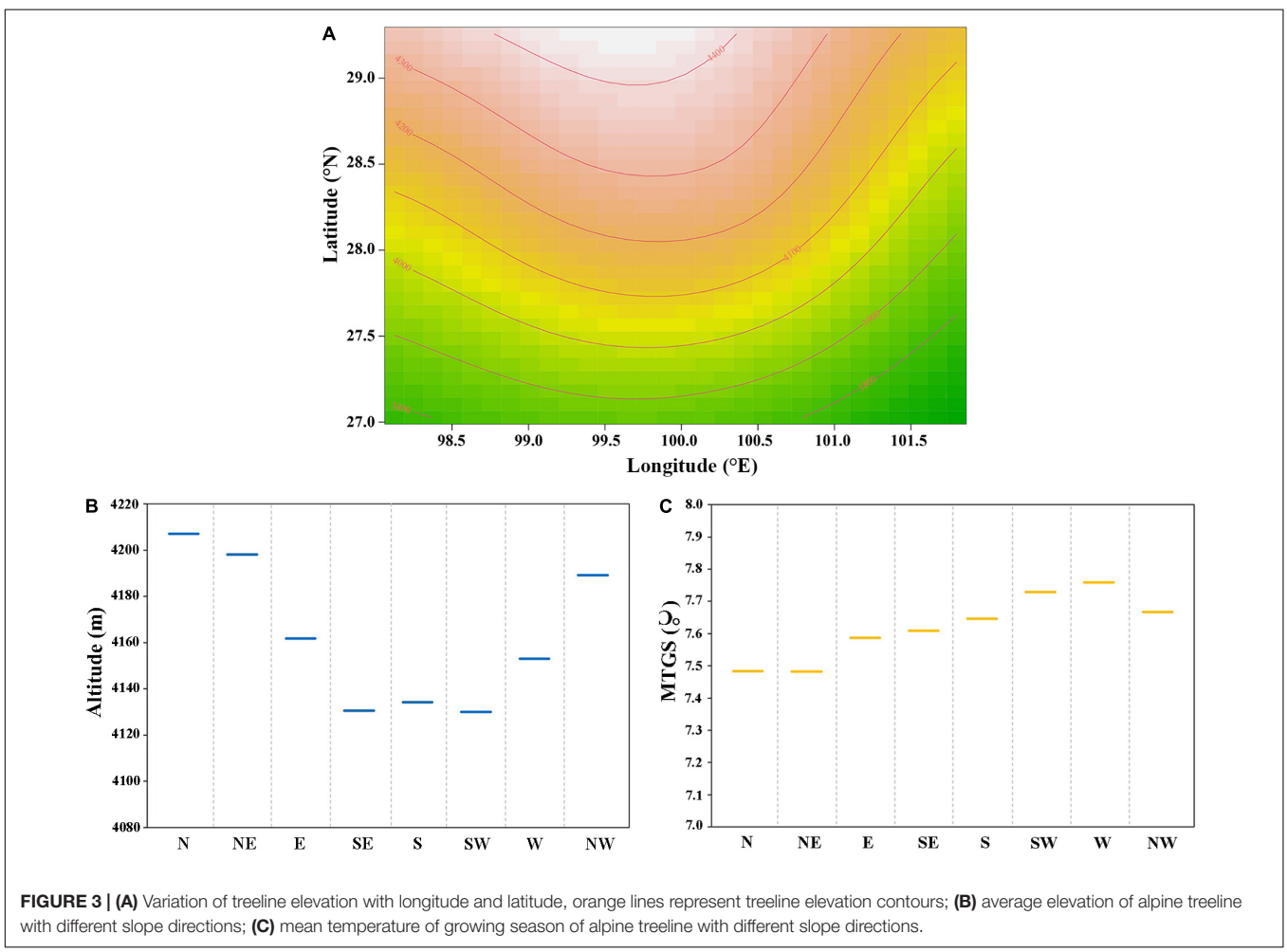

FIGURE 3 | (A) Variation of treeline elevation with longitude and latitude, orange lines represent treeline elevation contours; **(B)** average elevation of alpine treeline with different slope directions; **(C)** mean temperature of growing season of alpine treeline with different slope directions.

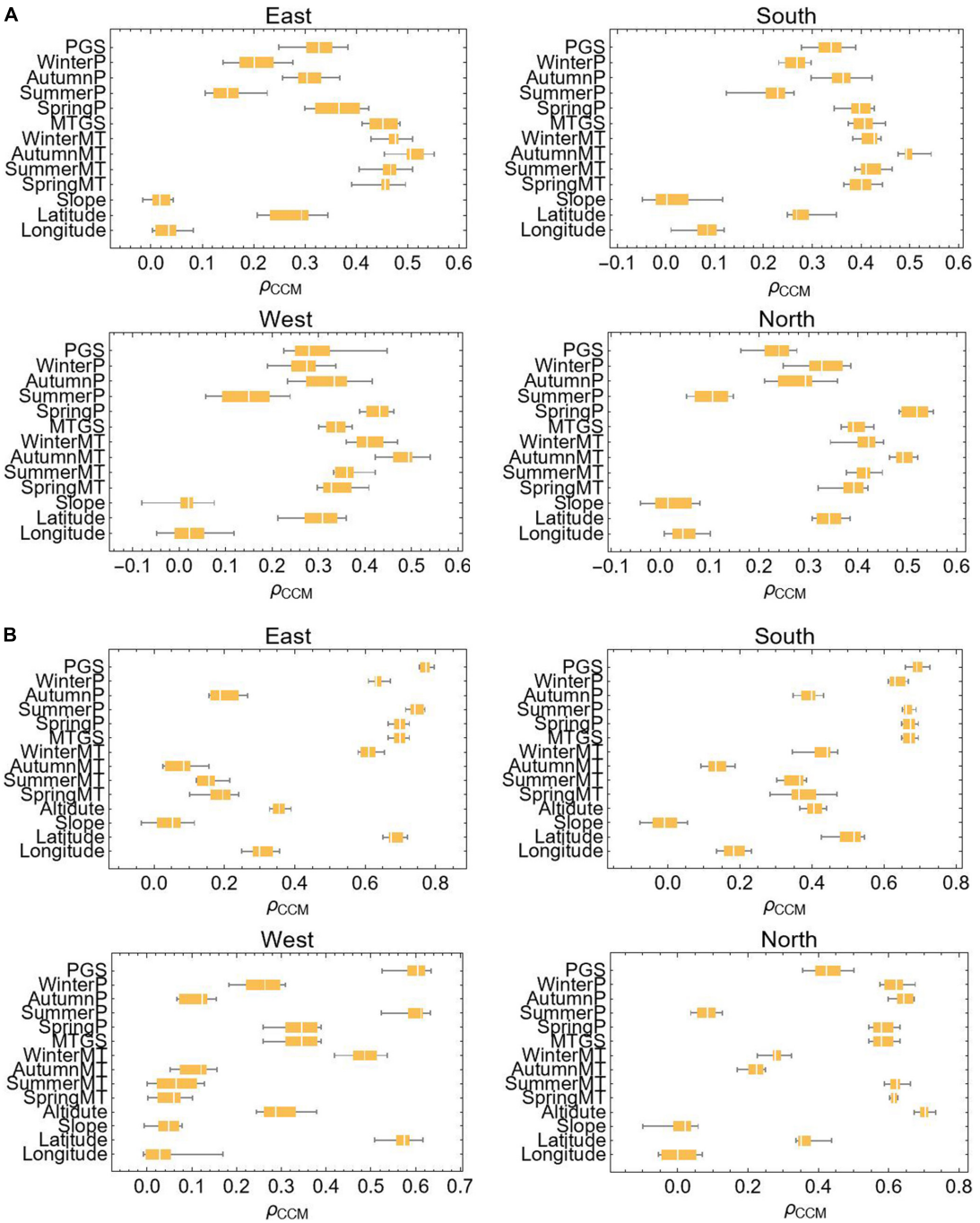

FIGURE 4 | Causality test of factors affecting treeline elevation. **(A)** Treeline elevation; **(B)** the fraction vegetation cover; ρ_{CCM} represents the strength of causality.

When *S*FVC >0, the *FVC* of the time series shows an increasing trend; when S_{FVC} <0, the FVC of the time series shows a decreasing trend.

The Mann–Kendall test (Kendall, 1938; Mann, 1945) is a non-parametric statistical test that measures the significance of a trend. When the Mann-Kendall method is applied to the *FVC* trend, the value of a certain time series is regarded as a set of independently distributed sample data, and the parameter *Xc* is used as the pixel *FVC* attenuation index. The calculation formula is as follows:

$$X_c = \begin{cases} \dfrac{M-1}{\sqrt{var\,(M)}} & M > 0 \\ 0 & M = 0 \\ \dfrac{M+1}{\sqrt{var\,(M)}} & M < 0 \end{cases}$$

Where

$$M = \sum_{i=1}^{n-1} \sum_{k=i+1}^{n} sign\ (FVC_k - FVC_i)$$

$$var\ (M) = \frac{n(n-1)(2n+5)}{18}$$

$$sign\ (FVC_k - FVC_i) = \begin{cases} 1 & FVC_k - FVC_i > 0 \\ 0 & FVC_k - FVC_i = 0 \\ -1 & FVC_k - FVC_i < 0 \end{cases}$$

Where FVC_k and FVC_i are sample time series datasets, n is the dataset length, and sign is a symbol function. At a given significance level a, when $|Xc| > \mu_1$-a/2, the time series data of the study represents a significant change in the α level, where $\pm X_1$-a/2 is the standard normal deviation. In this study, we take $a = 0.05$, and when $|Xc| \geq 1.96$, the time series confidence level is $a < 0.05$ and *vice versa*. We not only use Theil Sen median trend analysis to test the change of fraction vegetation cover, but also make corresponding analysis on temperature and precipitation, and obtain S_{FVC}, S_{tem}, and S_{pre} values, respectively.

We calculated the Pearson correlation coefficient among temperature change, precipitation change, and FVC change. The Pearson partial correlation coefficient reflects the relationship between one climate factor and vegetation coverage after controlling for the influence of another climate factor (after eliminating the influence of this factor). According to the difference between the correlation coefficient and partial correlation coefficient, the correlation degree among temperature change, precipitation change, and vegetation coverage change is described.

RESULTS

Treeline Elevation

The distribution of alpine treeline in the region spans approximately 4° of longitude (98.1–101.7°E) and approximately 3° of latitude (27–29.2°N) (**Figure 3A**). The treeline elevation in high-latitude areas is higher than that in low-latitude areas, and the treeline elevation in the middle is higher than that in the east and west. The treeline elevation difference reaches 600 m. Overall, the elevation of alpine treeline in the region is higher in the middle and lower in the surrounding areas.

The distribution of the treeline is also affected by the aspect. The treeline elevation is significantly lower on southern, southeastern, and southwestern slopes than on northern, northeastern, and northwestern slopes, and the average aspect-dependent elevation difference reaches 84 m (**Figure 3B**). However, there is little difference in temperature in the growing season among the different aspects (**Figure 3C**), which indicates that the average temperature isotherm in the growing season of the treeline on south-facing slopes is lower than that on slopes with other aspects.

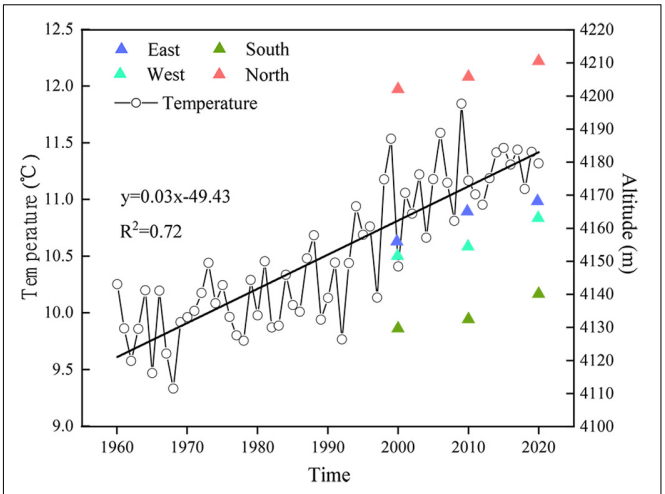

FIGURE 5 | Relationship between temperature change and treeline shift.

Impact Factors for Treeline Elevation and the Fraction Vegetation Cover

To facilitate the analysis, we combined the eight slope directions with few differences in treeline elevation, and divided them into four slope directions (east, south, west, and north). Because climatic factors such as temperature and precipitation vary in their effects on the treeline elevation, the relative importance of these factors needs to be parsed carefully. We thus subdivided climatic and terrain factors into several categories to explore their relative importance in determining treeline elevation (**Table 2**). Generally, climatic factors were more important than terrain factors in predicting treeline elevation (**Figure 4A**). Among the various climatic variables, temperature was the most important ($\rho_{ccm} > 0.5$). However, there was a weak linear relationship or no relationship between treeline elevation and various terrain factors.

Similarly, to understand the potential main driving factors of vegetation coverage in the treeline transition zone, we also use the corresponding methods for analysis, where the terrain factor is added to the elevation. When predicting vegetation coverage, the influencing factors of different slope directions vary (**Figure 4B**). On the east slope, south slope, and west slope, the key factor affecting vegetation cover is precipitation ($\rho_{ccm} > 0.7$, $\rho_{ccm} > 0.7$, and $\rho_{ccm} > 0.6$), and on the north slope, in addition to precipitation, elevation is also an important factor ($\rho_{ccm} > 0.7$).

Treeline Dynamics and Climate Change

Treeline Elevation Change and Climate Change

The relationships between different temperature variables and treeline elevation in 2000, 2010, and 2020 are shown in **Figure 5**. From 2000 to 2020, the temperature increased, and the treeline shifted. The elevations of treelines on the east, south, west, and north slopes shifted by 12, 10, 1, and 8 m, respectively. Since the resolution of the digital elevation model (DEM) data used in the study area is 12.5 m and the change in treeline elevation is within

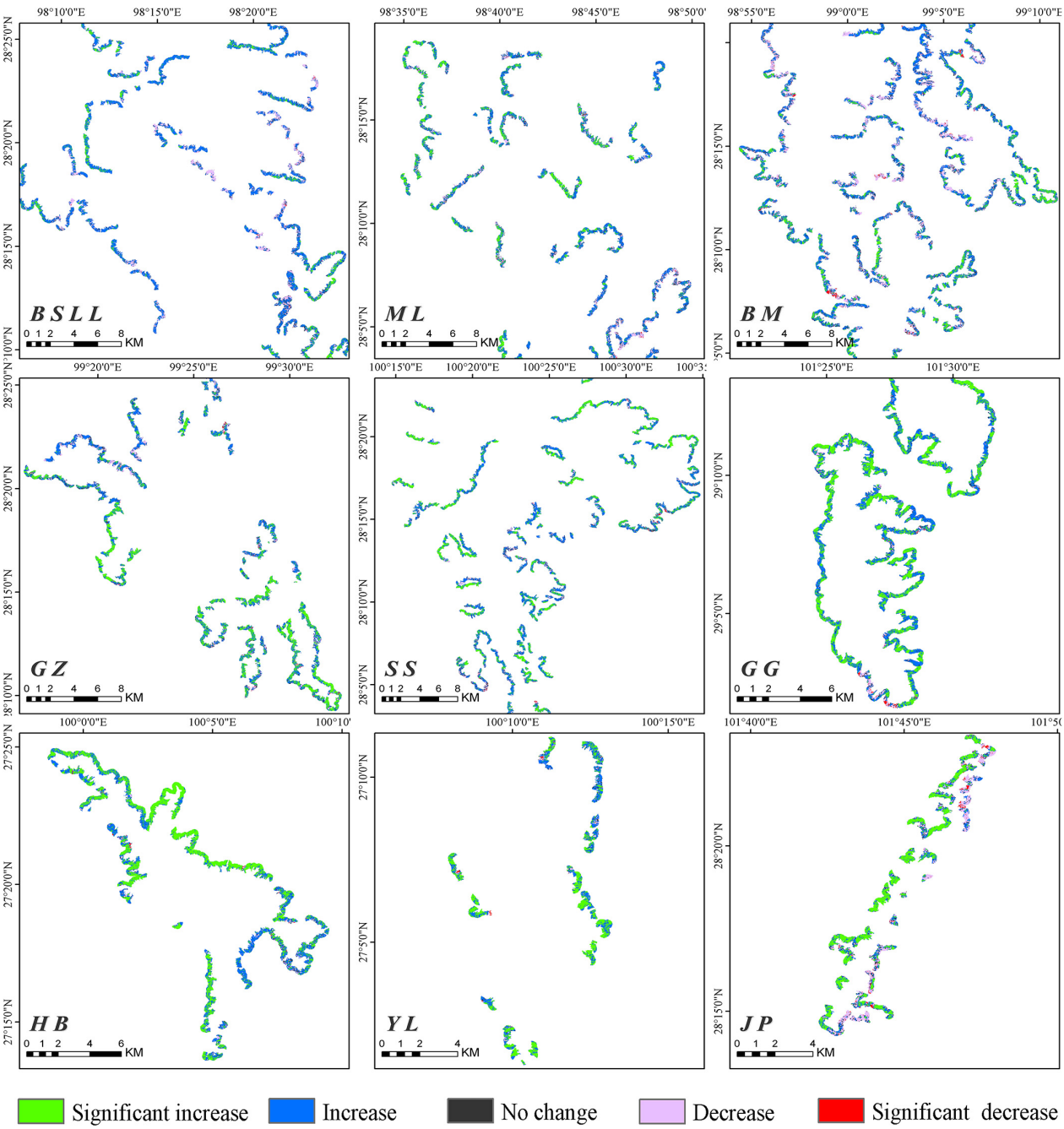

FIGURE 6 | Spatial variation trend analysis of fraction vegetation cover on the main mountains in the Hengduan Mountains from 2000 to 2020.

this resolution range, we believe that there has been no significant change in the treeline elevation over the last 20 years.

The Fraction Vegetation Cover Change and Climate Change

Based on the FVC raster data from 2000 to 2020, the 21-year FVC of each pixel and the slope (S_{FVC}) with significance were calculated. The purpose was to illustrate the spatial distribution of the FVC in the treeline transition zone and the characteristics of the spatial changes over time. In ArcGIS software, we used the buffer zone established by the treeline, and then the change trend of the FVC in the treeline transition zone was obtained (**Figure 6**).

A comparison of 2000 and 2020 shows that the FVC in the treeline transition zone of each mountain range increased significantly (**Figure 7**). Overall, during 2000–2020, the *increase in FVC* in the treeline transition zone (80.30%) was much larger than the decrease (13.37%), with areas of significant increases, slight increases, significant decreases, slight decreases and no

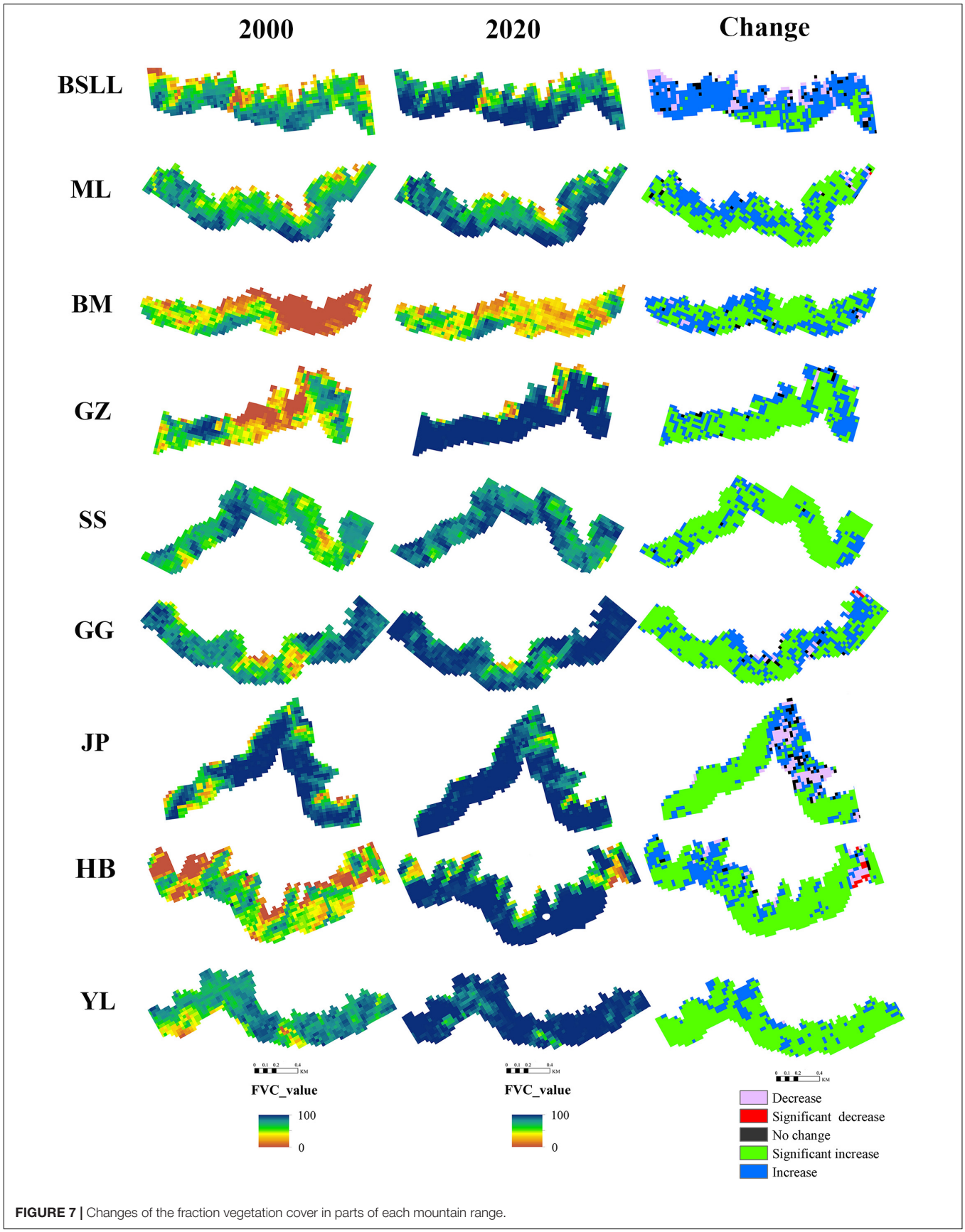

FIGURE 7 | Changes of the fraction vegetation cover in parts of each mountain range.

TABLE 3 | Statistical analysis results of *FVC* trends in treeline transition zone.

Slope of *FVC*	Significance	*FVC* trend	Area percentage (/%)
$S_{FVC} > 0$	$P < 0.05$	Significant increase	30.17
$S_{FVC} > 0$	$P > 0.05$	Increase	50.13
$S_{FVC} = 0$	—	No change	6.33
$S_{FVC} < 0$	$P < 0.05$	Significant decrease	0.69
$S_{FVC} < 0$	$P > 0.05$	Decrease	12.68

changes accounting for 30.17, 50.13, 0.69, 12.68, and 6.33%, respectively (**Table 3**). These results indicate that the tree density in the *treeline transition zone* has significantly increased in the last 20 years.

The difference between zero-order and partial correlations indicated the degree of dependence of the correlation between the climatic variables and the FVC (**Figure 8**). The dependence between one climatic factor and vegetation coverage changed after removing the effect of another climatic factor; for example, temperature affects the relationship between precipitation and FVC change. The FVC change associated with different slope directions is significantly affected by temperature and precipitation. The dependence degree between FVC change and temperature change on the east and south slopes (Pearson's $r = 0.062$ and 0.087, $P < 0.01$) is higher than that between FVC change and precipitation change (Pearson's $r = -0.027$ and 0.071, $P < 0.01$). However, the dependence degree between FVC change and temperature change and precipitation change on the west and north slopes (Pearson's $r = 0.062$ and 0.087, $P < 0.01$) is significantly higher than that between FVC change and temperature change alone (Pearson's $r = -0.027$ and 0.071, $P < 0.01$).

DISCUSSION

The treeline elevation in the Hengduan Mountains area is high in the middle but lower in the surrounding areas. This may be caused by the mass elevation effect and the unique monsoon climate. Compared with the edges of the mountain at similar elevations, the interior part of the mountain range experiences higher solar radiation input and higher temperatures (Holtmeier, 2009; Han et al., 2020). This temperature difference is consistent with the difference in the elevation of the treeline between the inner and outer parts of the mountain range (Wang et al., 2017). The study area is also affected by the southwestern monsoon and the southeastern monsoon; precipitation decreases from

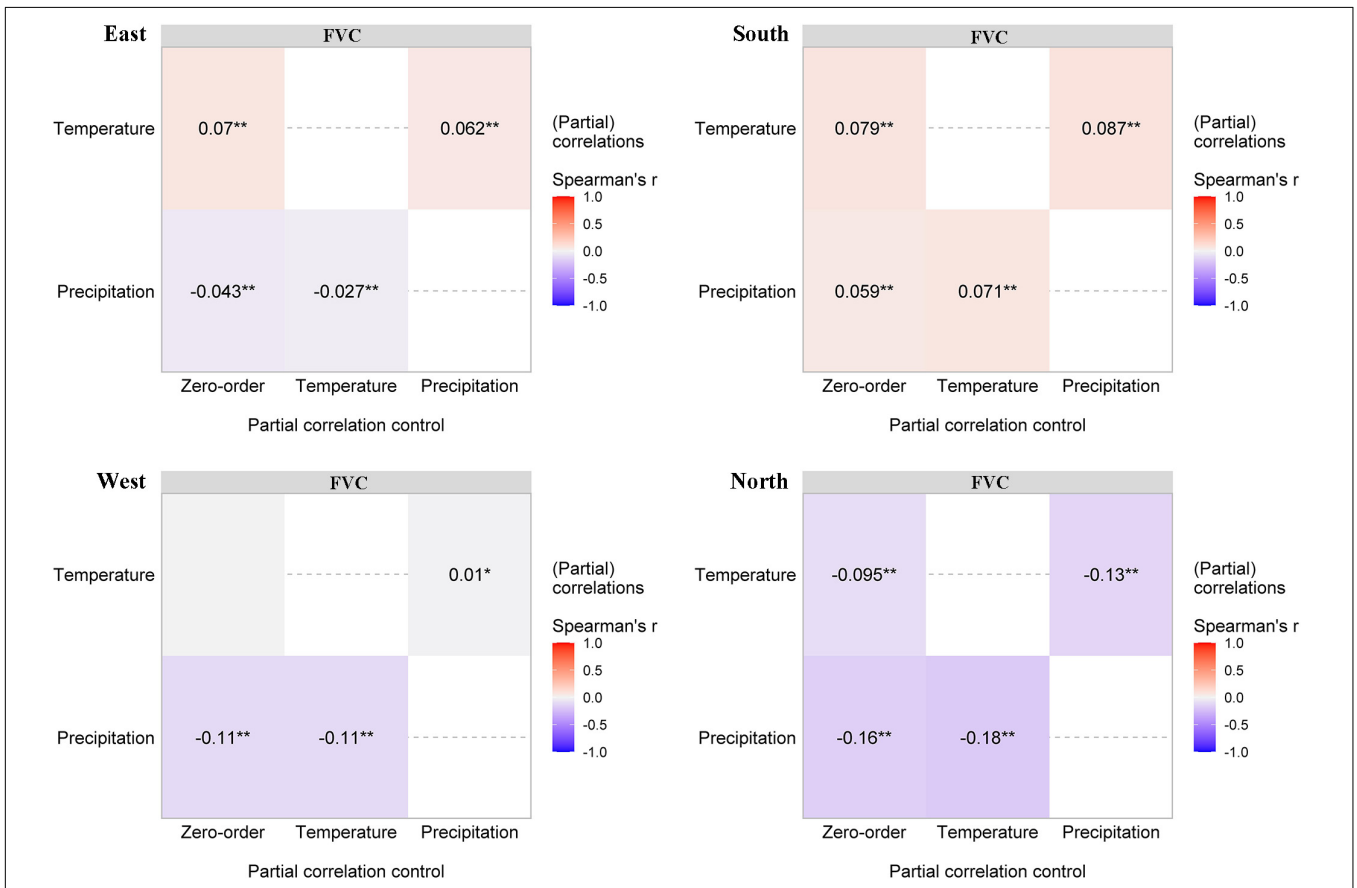

FIGURE 8 | Partial correlations (Pearson's *r*) between fraction vegetation cover and the two climatic variables. The intensity of colors and numbers indicate the strength of the correlation. Significant levels are: $^{*}P < 0.05$; $^{**}P < 0.01$.

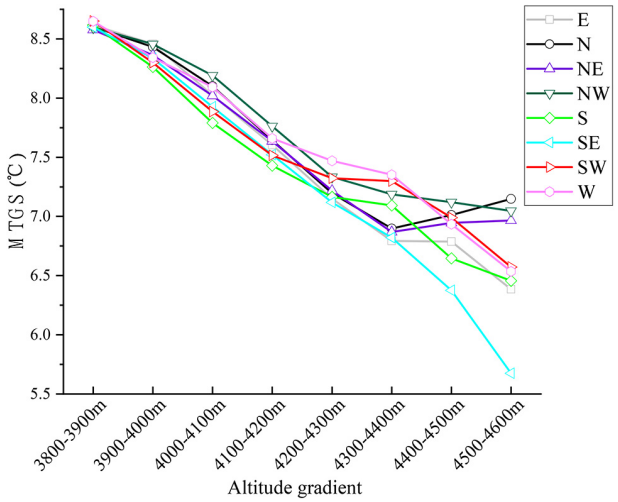

FIGURE 9 | The variation of mean temperature in growing season along the elevation gradient of treeline in different slope directions.

southwest to northeast and from southeast to northwest (Li et al., 2010; Yao et al., 2012). The elevation of the treeline also increases along the direction of seasonal winds (Wang et al., 2013; Yao and Zhang, 2015).

In general, the treeline can reach greater heights on warm southern slopes compared with cold northern slopes (Malyshev and Nimis, 1997). Our study found that the elevation of the treeline is generally lower on the southern slope of the Hengduan Mountains than on the northern slope, but there is no difference in the mean temperature during the growing season. This shows that the growing season temperature at the treeline is consistent, while the isotherm distribution of the treeline on the southern slope is lower than that on the slopes with other aspects. To further support our conclusion, we calculated statistics for the mean growing season temperature of different aspects at different elevations and found that the mean growing season temperature of the southern slope at a given elevation is lower than that of the northern slope (**Figure 9**). These findings are consistent with a study in the Mediterranean region showing that treeline elevation on southern slopes may be limited by summer drought, which reduces the elevation of the treeline (Piper et al., 2016; Bonanomi et al., 2018). Different from the previous conclusions, the low elevation of the treeline on the southern slope of the Hengduan Mountains is not caused by drought but by the low temperatures induced by the special regional monsoon climate. This stems from the formation of a large number of clouds on the southern and western slopes of the Hengduan Mountains after noon, and the blocking of solar radiation and the low temperatures caused by rainfall decrease the elevation of the treeline (Poveda et al., 2005; Körner, 2012; Wang et al., 2013). In addition, the south-facing slopes are steeper and barren, making it very difficult for seedlings to colonize and grow.

Treeline location has a time lag in terms of reflecting climate (Holtmeier and Broll, 2019). In this study, we calculated the multiyear mean seasonal temperature to analyze the relationships between treeline elevation and various climate factors. Since there are obvious differences in the treeline elevation among each aspect, we use CCM to test the causal relationships between the treeline elevation of each aspect and climate variables and topographic variables. Compared with topography and precipitation, temperature has a stronger driving effect on treeline elevation. Although the range of the temperature threshold for tree growth is not clearly defined, it is widely accepted that the treeline position is closely related to temperature (Case and Duncan, 2014). The upper limit of the treeline is thought to be determined by the effect of temperature on the ability of trees to form new tissue rather than by a lack of photosynthesis (Körner, 1998). Both biogeographic and physiological evidence strongly suggests that low temperatures are the most important factor limiting the upslope advance of the treeline (Cieraad, 2011; Case and Duncan, 2014). Temperature is a critical factor limiting the production and differentiation of xylem cells in cold climates, and thermal conditions below a certain temperature can inhibit xylem growth (Rossi et al., 2008). Immature trees are unable to survive in alpine areas with low air temperatures (Li and Yang, 2004). Thus, under undisturbed natural conditions, as long as there is soil and sufficient moisture, trees can grow until a low temperature limit is reached, forming a natural climatic treeline (Körner, 2020).

Due to the impact of global warming, the growth of trees in most treeline sites has responded positively to the rise in temperature (Harsch et al., 2009; Camarero et al., 2021). A temperature increase gradually alleviates physiological limitations associated with low temperatures in alpine trees (Körner and Paulsen, 2004; Pandey et al., 2020). Most global treeline advances correspond to strong winter warming (Harsch et al., 2009). Due to the obvious differences in the degree of seasonal warming experienced by different regions, the treeline position is greatly affected by the local climatic and topographic conditions (Armbruster et al., 2007; Bonanomi et al., 2020). Since 1960, the temperature in the Hengduan Mountains has increased at a rate of 0.03°C/year, and in recent decades, the temperature has increased by approximately 1.8°C. According to the IPCC (2018) assessment report, the global temperature has increased by nearly 1°C during the past century (1906–2017). Although the speed of the temperature increase in the Hengduan Mountains area is much higher than the global average, the position of the treeline has not obviously moved upward. Based on a previous treeline study in the central Hengduan Mountains, the larch and fir trees required averages of 18 ± 2 ($n = 150$) and 33 ± 5 ($n = 30$) years to reach 2 m in height, respectively (Wang et al., 2019). This means that a seedling may require 27–50 years to reach 3 m in height (treeline trees), so 20 years is still too short to recognize a treeline advance.

Although there was no obvious upward trend in treeline elevation in the Hengduan Mountains over the past 20 years, the trend of increasing vegetation coverage was significant. In this study, 80.3% of the regional FVC showed an upward trend, of which 30.17% showed a significant upward trend. The FVC was strongly affected by precipitation in the growing season. A warm-growing season and adequate moisture are favorable for seedling emergence and growth (Körner, 2012; Han et al., 2018).

In some drought-prone areas, tree recruitment also showed a gradual decrease in the treeline transition zone (Camarero and Gutierrez, 2004; Liang et al., 2014). However, our study shows that the increase in the FVC is related to a decrease in precipitation. Because precipitation decreases with increasing elevation, considering the impact of water availability (Liang et al., 2014), trees may not become established at higher elevations that are seasonally dry. In this context, trees tend to gather (Moyes et al., 2015; Treml and Chuman, 2018). Sigdel et al. (2020) showed a higher clustering tendency in dry treelines than in wet treelines. In high-elevation areas with high abiotic stress, plants can have a positive impact on each other, reduce the negative impact of adverse environmental conditions and improve the species richness of adjacent areas (Callaway et al., 2002; Smith et al., 2003; Chen et al., 2020). The FVC in 13.37% of the treeline areas showed a decreasing trend, and only 0.69% showed a significant decrease. Although this study carefully removed disturbed treeline areas in the process of treeline extraction in the early stage, the damage to vegetation in the alpine areas caused by natural interference factors (avalanches, landslides, gullies, etc.) and human interference factors (road construction, mining, grazing, fire, etc.) cannot be ignored (Ameztegui et al., 2016; Holtmeier and Broll, 2019; Wang et al., 2019).

CONCLUSION

The rate of the temperature increase in the Hengduan Mountains is much higher than the global average. Under this background, the treeline position has not changed significantly, but the FVC in the treeline area has markedly increased. The results also revealed a special exposure effect of alpine treeline in the Hengduan Mountains. Because of the lower treeline isotherm position caused by the monsoon climate, the treeline position on south-facing slopes is lower than that on the slopes with other exposures. The aforementioned results are helpful for understanding the dynamic changes in treeline under the background of climate warming at the landscape scale and provide a reference for predicting and evaluating the threats faced by alpine ecosystems in the future.

DATA AVAILABILITY STATEMENT

The original contributions presented in the study are included in the article/supplementary material, further inquiries can be directed to the corresponding author.

AUTHOR CONTRIBUTIONS

WW designed the study. FZ and CY collected and processed data. CT and FZ conducted the statistical analyses. FZ wrote the manuscript. ZZ and DL revised the manuscript. All authors commented upon and contributed to the final version of the manuscript.

FUNDING

This study was funded by the second comprehensive scientific investigation and research subproject of the Ministry of Science and Technology "Investigation and assessment of the main ecological problems and risks in the Qinghai Tibet Plateau" (2019QZKK0308), the Ministry of Ecology and Environment for its biodiversity survey and assessment project: "Analysis and protection assessment of the ecosystem pattern of the priority areas in the southern end of Hengduan Mountain"' (2019HB2096001006), and Yunnan University Graduate Research and Innovation Fund (2020242), and Microsoft AI for the Earth and Yunnan University project C176210103 (to CT).

REFERENCES

Alatalo, J. M., and Ferrarini, A. (2017). Braking effect of climate and topography on global change-induced upslope forest expansion. *Int. J. Biometeorol.* 61, 541–548. doi: 10.1007/s00484-016-1231-y

Ameztegui, A., Coll, L., Brotons, L., and Ninot, J. M. (2016). Land-use legacies rather than climate change are driving the recent upward shift of the mountain tree line in the Pyrenees. *Glob. Ecol. Biogeogr.* 25, 263–273. doi: 10.1111/geb.12407

Armbruster, S. W., Rae, D. A., and Edwards, M. E. (2007). "Topographic complexity and terrestrial biotic response to highlatitude climate change: Variance is as important as the mean," in *Arctic Alpine Ecosystems and People in a Changing Environment*, eds J. B. Ørbæk, R. Kallenborn, I. Tombre, E. N. Hegseth, S. Falk-Petersen, and A. H. Hoel (Berlin: Springer), 105–121.

Bader, M. Y., Llambí, L. D., Case, B. S., Buckley, H. L., Toivonen, J. M., Camarero, J. J., et al. (2020). A global framework for linking alpine-treeline ecotone patterns to underlying processes. *Ecography* 44, 265–292. doi: 10.1111/ecog.05285

Bai, W., Chen, X., Tang, Y., He, Y., and Zheng, Y. (2019). Temporal and spatial changes of soil moisture and its response to temperature and precipitation over the Tibetan Plateau. *Hydrol. Sci. J.* 64, 1370–1384. doi: 10.1080/02626667.2019.1632459

Batllori, E., and Gutiérrez, E. (2008). Regional tree line dynamics in response to global change in the Pyrenees. *J. Ecol.* 96, 1275–1288. doi: 10.1111/j.1365-2745.2008.01429.x

Bonanomi, G., Rita, A., Allevato, E., Cesarano, G., Saulino, L., Di Pasquale, G., et al. (2018). Anthropogenic and environmental factors affect the tree line position of Fagus sylvatica along the Apennines (Italy). *J. Biogeogr.* 45, 2595–2608. doi: 10.1111/jbi.13408

Bonanomi, G., Zotti, M., Mogavero, V., Cesarano, G., Saulino, L., Rita, A., et al. (2020). Climatic and anthropogenic factors explain the variability of Fagus sylvatica treeline elevation in fifteen mountain groups across the Apennines. *Forest Ecosyst.* 7:5 doi: 10.1186/s40663-020-0217-8

Callaway, R. M., Brooker, R. W., Choler, P., Kikvidze, Z., Lortie, C. J., Michalet, R., et al. (2002). Positive interactions among alpine plants increase with stress. *Nature* 417, 844–848. doi: 10.1038/nature00812

Camarero, J. J., Gazol, A., Sanchez-Salguero, R., Fajardo, A., McIntire, E. J. B., Gutierrez, E., et al. (2021). Global fading of the temperature-growth coupling at alpine and polar treelines. *Glob. Chang. Biol.* 27, 1879–1889. doi: 10.1111/gcb.15530

Camarero, J. J., and Gutierrez, E. (2004). Pace and pattern of recent treeline dynamics: Response of ecotones to climatic variability in the Spanish Pyrenees. *Clim. Chang.* 63, 181–200.

Case, B. S., and Duncan, R. P. (2014). A novel framework for disentangling the scale-dependent influences of abiotic factors on alpine treeline position. *Ecography* 37, 838–851. doi: 10.1111/ecog.00280

Chen, I. C., Hill, J. K., Ohlemuller, R., Roy, D. B., and Thomas, C. D. (2011). Rapid range shifts of species associated with high levels of climate warming. *Science* 333, 1024–1026. doi: 10.1126/science.1206432

Chen, J., Yang, Y., Wang, S., Sun, H., and Schob, C. (2020). Shrub facilitation promotes selective tree establishment beyond the climatic treeline. *Sci. Total Environ.* 708:134618. doi: 10.1016/j.scitotenv.2019.134618

Cieraad, E. (2011). "*Temperate oceanic Treelines"-Low Temperature Effects on Photosynthesis and Growth*.[Ph.D thesis] England: Durham University.

Dai, E., Yin, L., Wang, Y., Ma, L., and Tong, M. (2020). Quantitative assessment of the relative impacts of land use and climate change on the key ecosystem services in the Hengduan Mountain region. *China. Sustainabil.* 12:4100. doi: 10.3390/su12104100

Du, H., Liu, J., Li, M. H., Buntgen, U., Yang, Y., Wang, L., et al. (2018). Warming-induced upward migration of the alpine treeline in the Changbai Mountains, northeast China. *Glob. Chang. Biol.* 24, 1256–1266. doi: 10.1111/gcb.13963

Feurdean, A., Gałka, M., Tanţău, I., Geantă, A., Hutchinson, S. M., and Hickler, T. (2016). Tree and timberline shifts in the northern Romanian Carpathians during the Holocene and the responses to environmental changes. *Q. Sci. Rev.* 134, 100–113. doi: 10.1016/j.quascirev.2015.12.020

Gaire, N. P., Koirala, M., Bhuju, D. R., and Borgaonkar, H. P. (2014). Treeline dynamics with climate change at the central Nepal Himalaya. *Clim. Past* 10, 1277–1290. doi: 10.5194/cp-10-1277-2014

Gu, Z. J., Zeng, Z. Y., Shi, X. Z., Li, L., Yu, D. S., Zheng, W., et al. (2009). Assessing factors influencing vegetation coverage calculation with remote sensing imagery. *Int. J. Remote Sensing* 30:2489.

Guo, D., Zhang, H. Y., Hou, G. L., Zhao, J. J., Liu, D. Y., and Guo, X. Y. (2014). Topographic controls on alpine treeline patterns on Changbai Mountain. *China. J. Mount. Sci.* 11, 429–441. doi: 10.1007/s11629-013-2706-5

Hagedorn, F., Gavazov, K., and Alexander, J. M. (2019). Above- and belowground linkages shape responses of mountain vegetation to climate change. *Science* 365, 1119–1123. doi: 10.1126/science.aax4737

Han, F., Wan, L., Wu, H. Z., Zhang, B. P., Gao, L., and Song, G. (2020). What factors determine the mass elevation effect of the Tibetan Plateau? *J. Mount. Sci.* 17, 2742–2749. doi: 10.1007/s11629-020-6011-9

Han, F., Zhang, B. P., Zhao, F., Wan, L., Tan, J., and Liang, T. (2018). Characterizing the Mass Elevation Effect across the Tibetan Plateau. *J. Mount. Sci.* 15, 2651–2665. doi: 10.1007/s11629-018-4978-2

Harsch, M. A., Hulme, P. E., McGlone, M. S., and Duncan, R. P. (2009). Are treelines advancing? A global meta-analysis of treeline response to climate warming. *Ecol. Lett.* 12, 1040–1049. doi: 10.1111/j.1461-0248.2009.01355.x

Hellmann, L., Agafonov, L., Ljungqvist, F. C., Churakova, O., Duethorn, E., Esper, J., et al. (2016). Diverse growth trends and climate responses across Eurasia's boreal forest. *Environ. Res. Lett.* 11:074021. doi: 10.1088/1748-9326/11/7/074021

Holtmeier, F. K., and Broll, G. (2019). Treeline research-from the roots of the past to present time. A review. *Forests* 11:38. doi: 10.3390/f11010038

Holtmeier, F. K. (2009). *Mountain Timberline Ecology, Patchiness, And Dynamics*. Berlin: Springer.

Holtmeier, F. K., and Broll, G. (2005). Sensitivity and response of northern hemisphere altitudinal and polar treelines to environmental change at landscape and local scales. *Glob. Ecol. Biogeogr.* 14, 395–410. doi: 10.1111/j.1466-822X.2005.00168.x

Holtmeier, F. K., and Broll, G. (2012). Landform influences on treeline patchiness and dynamics in a changing climate. *Phys. Geogr.* 33, 403–437. doi: 10.2747/0272-3646.33.5.403

IPCC (2018). "Global warming of 1.5°C," in *An IPCC Special Report on the Impacts of Global Warming of 1.5°C Above Pre-Industrial Levels and Related Global Greenhouse gas Emission Pathways, in the Context of Strengthening the Global Response to the Threat of Climate Change, Sustainable Development, and Efforts to Eradicate Poverty*, eds V. Masson-Delmotte, P. Zhai, H. O. Pörtner, D. Roberts, J. Skea, P. R. Shukla, et al. (Geneva: IPCC).

Kendall, M. (1938). A new measure of rank correlation. *Biometrika* 30, 81–93.

Körner, C. (1998). A re-assessment of high elevation treeline positions and their explanation. *Oecologia* 115, 445–459. doi: 10.1007/s004420050540

Körner, C. (2012). *Alpine Treelines: Functional Ecology of the Global High Elevation Tree Limits*. Basel: Springer.

Körner, C. (2020). "*Climatic controls of the global high elevation treelines*," *in Encyclopedia of the World's Biomes*. Berlin: Elsevier. 275–281.

Körner, C., and Paulsen, J. (2004). A world-wide study of high altitude treeline temperatures. *J. Biogeogr.* 31, 713–732.

Kramer, A., Herzschuh, U., Mischke, S., and Zhang, C. (2010). Holocene treeline shifts and monsoon variability in the Hengduan Mountains (southeastern Tibetan Plateau), implications from palynological investigations. *Palaeogeogr. Palaeoclimatol. Palaeoecol.* 286, 23–41. doi: 10.1016/j.palaeo.2009.12.001

La Sorte, F. A., and Jetz, W. (2010). Projected range contractions of montane biodiversity under global warming. *Proc. Biol. Sci. U.S.A.* 277, 3401–3410. doi: 10.1098/rspb.2010.0612

Lenoir, J., Gegout, J. C., Marquet, P. A., de Ruffray, P., and Brisse, H. (2008). A significant upward shift in plant species optimum elevation during the 20th century. *Science* 320, 1768–1771. doi: 10.1126/science.1156831

Leonelli, G., Pelfini, M., and di Cella, U. M. (2013). Detecting climatic treelines in the Italian Alps: the influence of geomorphological factors and human impacts. *Phys. Geogr.* 30, 338–352. doi: 10.2747/0272-3646.30.4.338

Li, B. (1987). On the boundaries of the Hengduan Mountains. *Mount. Res.* 5, 74–82.

Li, M. H., and Yang, J. (2004). Effects of microsite on growth of Pinus cembrain the subalpine zone of the Austrian Alps. *Ann. Forest Sci.* 61, 319–325. doi: 10.1051/forest:2004025

Li, Z. S., He, Y. Q., Xing, H. Y., Wang, C. F., Jia, W. X., Zhang, W., et al. (2010). Spatio-temporal variations of temperature and precipitation in Mts. Hengduan region during 1960-2008. *Acta Geographica Sinica* 65, 563–579.

Liang, E., Dawadi, B., Pederson, N., and Eckstein, D. (2014). Is the growth of birch at the upper timberline in the Himalayas limited by moisture or by temperature? *Ecology* 95, 2453–2465. doi: 10.1890/13-1904.1

Liang, E. Y., Wang, Y. F., Piao, S. L., Lu, X. M., Camarero, J. J., Zhu, H. F., et al. (2016). Species interactions slow warming-induced upward shifts of treelines on the Tibetan Plateau. *Proc. Natl. Acad. Sci. U.S.A.* 113, 4380–4385. doi: 10.1073/pnas.1520582113

Lin, H., Tu, C., Fang, J., Gioli, B., Loubet, B., Gruening, C., et al. (2020). Forests buffer thermal fluctuation better than non-forests. *Agricult. Forest Meteorol.* 288–289. doi: 10.1016/j.agrformet.2020.107994

Lu, X., Liang, E., Wang, Y., Babst, F., Camarero, J. J., and Grytnes, J. A. (2020). Mountain treelines climb slowly despite rapid climate warming. *Glob. Ecol. Biogeogr.* 30, 305–315. doi: 10.1111/geb.13214

Lyu, L. X., Zhang, Q. B., Deng, X., and Mäkinen, H. (2016). Fine-scale distribution of treeline trees and the nurse plant facilitation on the eastern Tibetan Plateau. *Ecol. Indic.* 66, 251–258. doi: 10.1016/j.ecolind.2016.01.041

Malanson, G. P. (2013). Complex responses to global change at alpine treeline. *Phys. Geogr.* 22, 333–342. doi: 10.1080/02723646.2001.10642747

Malyshev, L., and Nimis, P. L. (1997). Climatic dependence of the ecotone between alpine and forest orobiomes in southern Siberia. *Flora* 192, 109–120. doi: 10.1016/s0367-2530(17)30765-x

Mann, H. B. (1945). Nonparametric test against trend. *Econometrica* 13, 245–259.

Marc, M. F., and Johnson, E. A. (2013). Warming-induced upslope advance of subalpine forest is severely limited by geomorphic processes. *Proc. Natl. Acad. Sci. U.S.A.* 110, 8117–8122. doi: 10.1073/pnas.1221278110

Miehe, G., Miehe, S., Vogel, J., Co, S., and La, D. (2007). Highest treeline in the northern hemisphere found in southern Tibet. *Mount. Res. Dev.* 27, 169–173. doi: 10.1659/mrd.0792

Mohapatra, J., Singh, C. P., Tripathi, O. P., and Pandya, H. A. (2019). Remote sensing of alpine treeline ecotone dynamics and phenology in Arunachal Pradesh Himalaya. *Int. J. Remote Sensing* 40, 7986–8009. doi: 10.1080/01431161.2019.1608383

Moyes, A. B., Germino, M. J., and Kueppers, L. M. (2015). Moisture rivals temperature in limiting photosynthesis by trees establishing beyond their cold-edge range limit under ambient and warmed conditions. *New Phytol.* 207, 1005–1014. doi: 10.1111/nph.13422

Myers, N., Mittermeier, R. A., Mittermeier, C. G., da Fonseca, G. A. B., and Kent, J. (2000). Biodiversity hotspots for conservation priorities. *Nature* 403, 853–858. doi: 10.1038/35002501

Pandey, S., Cherubini, P., Saurer, M., Carrer, M., Petit, G., and Wildi, O. (2020). Effects of climate change on treeline trees in Sagarmatha (Mt. Everest, Central Himalaya). *J. Veg. Sci.* 31, 1146–1155. doi: 10.1111/jvs.12921

Payette, S., and Filion, L. (1985). White spruce expansion at the tree line and recent climatic change. *Can. J. Forest Res.* 15:251. doi: 10.1890/06-0265

Pecl, G. T., Araujo, M. B., Bell, J. D., Blanchard, J., Bonebrake, T. C., Chen, I. C., et al. (2017). Biodiversity redistribution under climate change: Impacts on ecosystems and human well-being. *Science* 355:9. doi: 10.1126/science.aai9214

Piper, F. I., Vinegla, B., Linares, J. C., Camarero, J. J., Cavieres, L. A., and Fajardo, A. (2016). Mediterranean and temperate treelines are controlled by different environmental drivers. *J. Ecol.* 104, 691–702. doi: 10.1111/1365-2745.12555

Poveda, G., Mesa, O. J., Salazar, L. F., Arias, P. A., Moreno, H. A., Vieira, S. C., et al. (2005). The diurnal cycle of precipitation in the tropical Andes of Colombia. *Monthly Weather Rev.* 133, 228–240. doi: 10.1175/mwr-2853.1

Rees, W. G., Hofgaard, A., Boudreau, S., Cairns, D. M., Harper, K., Mamet, S., et al. (2020). Is subarctic forest advance able to keep pace with climate change? *Glob. Chang. Biol.* 26, 3965–3977. doi: 10.1111/gcb.15113

Rossi, S., Deslauriers, A., Griçar, J., Seo, J. W., Rathgeber, C. B. K., Anfodillo, T., et al. (2008). Critical temperatures for xylogenesis in conifers of cold climates. *Glob. Ecol. Biogeogr.* 17, 696–707. doi: 10.1111/j.1466-8238.2008.00417.x

Scuderi, L. A., Schaaf, C. B., Orth, K. U., and Band, L. E. (1993). Alpine treeline growth variability - simulation using an ecosystem process model. *Arctic Alpine Res.* 25, 175–182. doi: 10.2307/1551810

Sen, and Kumar, P. (1968). Estimates of the Regression Coefficient Based on Kendall's Tau. *Publications Am. Stat. Assoc.* 63, 1379–1389.

Sigdel, S. R., Liang, E., Wang, Y., Dawadi, B., and Camarero, J. J. (2020). Tree-to-tree interactions slow down Himalayan treeline shifts as inferred from tree spatial patterns. *J. Biogeogr.* 47, 1816–1826. doi: 10.1111/jbi.13840

Singh, C. P., Mohapatra, J., and Dharaiya, N. (2015). Remote sensing of alpine treeline dynamics. *Int. J. Remote Sensing* 21:8. doi: 10.1016/j.scitotenv.2020.141344

Smith, W. K., Germino, M. J., Hancock, T. E., and Johnson, D. M. J. T. P. (2003). Another perspective on altitudinal limits of alpine timberlines. *Tree Physiol* 23, 1101–1112. doi: 10.1093/treephys/23.16.1101

Sugihara, G., May, R., Ye, H., Hsieh, C. H., Deyle, E., Fogarty, M., et al. (2012). Detecting causality in complex ecosystems. *Science* 338, 496–500. doi: 10.1126/science.1227079

Sun, H., Zhang, J., Deng, T., and Boufford, D. E. (2017). Origins and evolution of plant diversity in the Hengduan Mountains. *China. Plant Divers.* 39, 161–166. doi: 10.1016/j.pld.2017.09.004

Theil, H. (1992). *A Rank-Invariant Method of Linear and Polynomial Regression Analysis*.Amsterdam: Springer. 23.

Thuiller, W., Lavorel, S., Araujo, M. B., Sykes, M. T., and Prentice, I. C. (2005). Climate change threats to plant diversity in Europe. *Proc. Natl. Acad. Sci. U.S.A.* 102, 8245–8250. doi: 10.1073/pnas.0409902102

Treml, V., and Chuman, T. (2018). Ecotonal dynamics of the altitudinal forest limit are affected by terrain and vegetation structure variables: an example from the sudetes mountains in Central Europe. *Arctic Antarctic Alpine Res.* 47, 133–146. doi: 10.1657/aaar0013-108

Walther, A., and Linderholm, H. W. (2006). A comparison of growing season indices for the Greater Baltic Area. *Int. J. Biometeorol.* 51, 107–118. doi: 10.1007/s00484-006-0048-5

Wang, J., Zhang, B., He, W., Yao, Y., Zhang, W., and Zhao, C. (2017). A quantitative study on the mass elevation effect of the Rocky Mountains and its significance for treeline distribution. *Physical. Geogr.* 38, 231–247. doi: 10.1080/02723646.2017.1281013

Wang, W., Körner, C., Zhang, Z., Wu, R., Geng, Y., Shi, W., et al. (2013). No slope exposure effect on alpine treeline position in the Three Parallel Rivers Region. *SW China. Alpine Bot.* 123, 87–95. doi: 10.1007/s00035-013-0118-3

Wang, Y., Case, B., Lu, X., Ellison, A. M., Peñuelas, J., Zhu, H., et al. (2019). Fire facilitates warming-induced upward shifts of alpine treelines by altering interspecific interactions. *Trees* 33, 1051–1061. doi: 10.1007/s00468-019-01841-6

Wang, Y. F., Pederson, N., Ellison, A. M., Buckley, H. L., Case, B. S., Iang, E. L., et al. (2016). Increased stem density and competition may diminish the positive effects of warming at alpine treeline. *Ecology* 97, 1668–1679. doi: 10.1890/15-1264.1

Wei, C., Karger, D. N., and Wilson, A. M. (2020). Spatial detection of alpine treeline ecotones in the Western United States. *Remote Sensing Environ.* 240:111672. doi: 10.1016/j.rse.2020.111672

Wen, C. (1989). Influence of the relief on conditions of water and heat in the Hengduan Mountains region. *Mount. Res.* 7, 65–73.

Wilson, N. R., and Norman, L. M. (2018). Analysis of vegetation recovery surrounding a restored wetland using the normalized difference infrared index (NDII) and normalized difference vegetation index (NDVI). *Int. J. Remote Sensing* 39:3274.

Yao, T., Thompson, L., Yang, W., Yu, W., Gao, Y., Guo, X., et al. (2012). Different glacier status with atmospheric circulations in Tibetan Plateau and surroundings. *Nat. Clim. Chang.* 2, 663–667. doi: 10.1038/nclimate1580

Yao, Y., and Zhang, B. (2015). The mass elevation effect of the Tibetan Plateau and its implications for Alpine treelines. *Int. J. Climatol.* 35, 1833–1846. doi: 10.1002/joc.4123

Yirdaw, E., Starr, M., Negash, M., and Yimer, F. (2015). Influence of topographic aspect on floristic diversity, structure and treeline of afromontane cloud forests in the Bale Mountains, Ethiopia. *J. For. Res.* 26, 919–931. doi: 10.1007/s11676-015-0155-4

Conflict of Interest: The authors declare that the research was conducted in the absence of any commercial or financial relationships that could be construed as a potential conflict of interest.

Publisher's Note: All claims expressed in this article are solely those of the authors and do not necessarily represent those of their affiliated organizations, or those of the publisher, the editors and the reviewers. Any product that may be evaluated in this article, or claim that may be made by its manufacturer, is not guaranteed or endorsed by the publisher.

Copyright © 2022 Zou, Tu, Liu, Yang, Wang and Zhang. This is an open-access article distributed under the terms of the Creative Commons Attribution License (CC BY). The use, distribution or reproduction in other forums is permitted, provided the original author(s) and the copyright owner(s) are credited and that the original publication in this journal is cited, in accordance with accepted academic practice. No use, distribution or reproduction is permitted which does not comply with these terms.

Frontiers in
Plant Science

Cultivates the science of plant biology and its applications

The most cited plant science journal, which advances our understanding of plant biology for sustainable food security, functional ecosystems and human health.

Discover the latest Research Topics

See more →

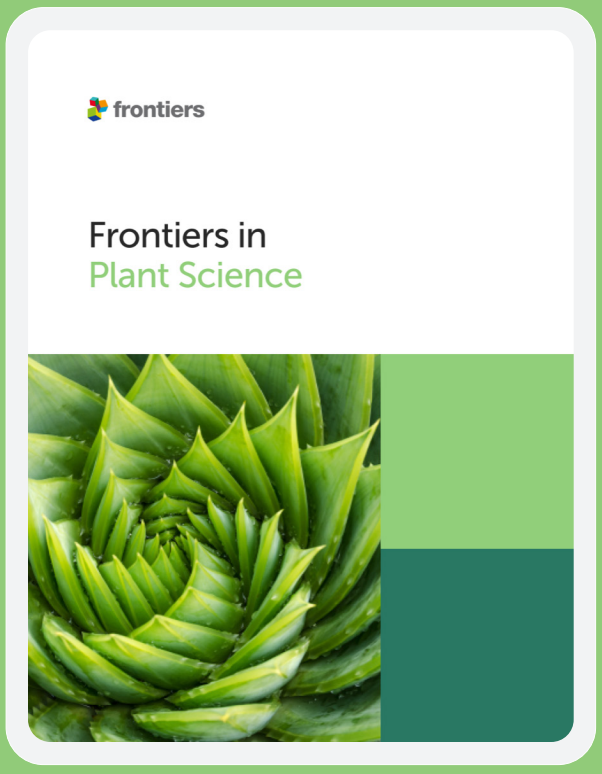

Frontiers

Avenue du Tribunal-Fédéral 34
1005 Lausanne, Switzerland
frontiersin.org

Contact us

+41 (0)21 510 17 00
frontiersin.org/about/contact